HANS J. TEN DONKELAAR
MARTIN LAMMENS
AKIRA HORI

CLINICAL NEURO-EMBRYOLOGY

Development and
Developmental Disorders
of the
Human Central Nervous System

Springer

Hans J. ten Donkelaar, Martin Lammens, Akira Hori

Clinical Neuroembryology

**Development and Developmental Disorders
of the Human Central Nervous System**

Hans J. ten Donkelaar
Martin Lammens
Akira Hori

Clinical Neuroembryology

**Development and Developmental Disorders
of the Human Central Nervous System**

In co-operation with:
Cor W.R.J. Cremers
Johannes R.M. Cruysberg
Ben Hamel
Reinier Mullaart
Willy O. Renier
Kohei Shiota
Ton van der Vliet

Gerard van Noort
John M.G. van Vugt
Berit Verbist
Christl Vermeij-Keers
Pieter Wesseling
Michèl Willemsen

Illustrated by Marlu de Leeuw and Ad Gruter

With 405 Figures in 1222 parts, Mostly in Colour,
and 51 Tables

Springer

Hans J. ten Donkelaar, MD, PhD
935 Department of Neurology
Radboud University Nijmegen Medical Centre
P.O. Box 9101
6500 HB Nijmegen
The Netherlands

Martin Lammens, MD, PhD
812 Department of Pathology
Radboud University Nijmegen Medical Centre
P.O. Box 9101
6500 HB Nijmegen
The Netherlands

Akira Hori, MD, PhD
Research Institute for Longevity Medicine
Fukushimura Hospital, Noyori-Yamanaka 19–14
Toyohashi 441-8124
Japan

Preface

The spectacular progress in developmental neurobiology, the tremendous advances in (neuro)genetics and the high resolution of the modern imaging techniques applicable to developmental disorders of the human brain and spinal cord have created a growing interest in the developmental history of the central nervous system (CNS). This new book provides a comprehensive overview of the development of the human CNS in the context of its many developmental disorders due to genetic, environmental and hypoxic/ischemic causes. The book contains three general, introductory chapters in which an overview of the development of the human brain and spinal cord, a summary of mechanisms of development as obtained in experimental studies in various invertebrates and vertebrates, and an overview of the causes of congenital malformations with some notes on prenatal diagnosis, are presented. The developmental disorders of the human brain and spinal cord are presented in a regional, more or less segmental way, starting with neurulation and the neural tube defects, and ending with developmental disorders of the cerebral cortex. These chapters are abundantly illustrated with clinical case studies with imaging data and, when available, postmortem verification of the developmental disorders involved. The book is intended for advanced medical students, and all those clinicians working with children and adults with developmental disorders of the CNS.

This book would not have been possible without the help of many colleagues in The Netherlands and from abroad. Their help is gratefully acknowledged. Most of the neuropathological material comes from the extensive collections of Drs. Akira Hori and Martin Lammens. Many cases were kindly provided by Drs. Pieter Wesseling (Nijmegen), Gerard van Noort (Enschede), and Kohei Shiota (Kyoto). Photographical assistance was provided by Mrs. Roelie de Boer-van Huizen (Nijmegen), Mrs. Chigako Uwabe (Kyoto) and Richard Rieksen (Enschede). Material for the clinical case studies was provided by many clinical colleagues, including Drs. Ellsworth C. Alvord Jr (Seattle), Harm-Gerd Blaas (Trondheim), Cor Cremers and Hans Cruysberg (Nijmegen), Mark D'hooghe (Bruges), Jennian Geddes (London), Ben Hamel (Nijmegen), Frans Hoevenaars (Nijmegen), Nomdo Jansonius (Groningen), Akiyoshi Kakita (Niigata), Max Kros (Rotterdam), Hajime Miyata (Tottori), Masashi Mizuguchi (Tokyo), Reinier Mullaart, Willy Renier and Jan Rotteveel (Nijmegen), Harvey B. Sarnat (Calgary), Ben Semmekrot (Nijmegen), Waney Squier (Oxford), Sachio Takashima (Fukuoka), Rudy van Coster and Caroline Van den Broecke (Gent), Christl Vermeij-Keers (Rotterdam), Michèl Willemsen (Nijmegen), and Mieko Yoshioka (Kobe). Imaging data were kindly provided by Drs. Harm-Gerd Blaas (Trondheim), Berit Verbist (Leiden), John van Vugt and collaborators (Amsterdam), Henk Thijssen and Ton van der Vliet (Nijmegen), and Guido Wilms (Leuven). Several figures were contributed by Drs. Jo Curfs (Nijmegen), Marieke de Heer and Jeannette Hoogeboom (Rotterdam), Raoul Hennekam (Amsterdam), Jan E. Jirásek (Prague), Enrico Marani (Leiden), Loreta Medina (Murcia), Zoltán Molnár (Oxford), Ronan O'Rahilly (Villlars-sur-Glâne), Annemieke Potters (Deventer), Kohei Shiota (Kyoto), Henny van Straaten (Maastricht), Michiel Vaandrager (Rotterdam), Jan Voogd (Oegstgeest), and Shigehito Yamada (Kyoto). Most of the drawings were made by Mrs. Marlu de Leeuw and Mr. Ad Gruter. Financial support was generously provided by the "Stichting Neurologie en Wetenschap" of the Department of Neurology (Head: Prof. Dr. George W.A.M. Padberg) and the Department of Pathology (Head: Prof. Dr. Han van Krieken), both of the Radboud University Nijmegen Medical Centre, supporting the costs of the drawings. The Japan Society for the Promotion of Science granted the first author a short-term fellowship in May 2004 at the Congenital Anomaly Research Centre (Head: Prof. Dr. Kohei Shiota) of Kyoto University.

Hans J. ten Donkelaar, Nijmegen

Martin Lammens, Nijmegen

Akira Hori, Toyohashi

Contents

Contributors

Cor W.J.R. Cremers
377 Department of Otorhinolaryngology
Radboud University Nijmegen Medical Centre
P.O. Box 9101
6500 HB Nijmegen, The Netherlands

Johannes R.M. Cruysberg
409 Department of Ophthalmology
Radboud University Nijmegen Medical Centre
P.O. Box 9101
6500 HB Nijmegen, The Netherlands

Ben Hamel
849 Department of Human Genetics
Radboud University Nijmegen Medical Centre
P.O. Box 9101
6500 HB Nijmegen, The Netherlands

Akira Hori
Research Institute for Longevity Medicine
Fukushimura Hospital
Noyori-Yamanaka 19-14
Toyohashi 441-8124, Japan

Martin Lammens
812 Department of Pathology
Radboud University Nijmegen Medical Centre
P.O. Box 9101
6500 HB Nijmegen, The Netherlands

Reinier A. Mullaart
820 Department of Child Neurology
Radboud University Nijmegen Medical Centre
P.O. Box 9101
6500 HB Nijmegen, The Netherlands

Willy O. Renier
935 Department of Neurology
Radboud University Nijmegen Medical Centre
P.O. Box 9101
6500 HB Nijmegen, The Netherlands

Kohei Shiota
Congenital Anomaly Research Center
Department of Anatomy and Developmental Biology
Kyoto University Graduate School of Medicine
Kyoto 606-8501, Japan

Hans J. ten Donkelaar
935 Department of Neurology
Radboud University Nijmegen Medical Centre
P.O. Box 9101
6500 HB Nijmegen, The Netherlands

Ton van der Vliet
667 Department of Radiology
Radboud University Nijmegen Medical Centre
P.O. Box 9101
6500 HB Nijmegen, The Netherlands

Gerard van Noort
Laboratory for Pathology East-Netherlands
P.O. Box 377
7500 AJ Enschede, The Netherlands

John M.G. van Vugt
Department of Obstetrics and Gynaecology
VU University Medical Centre
P.O. Box 7057
1007 MB Amsterdam, The Netherlands

Berit Verbist
Department of Radiology
Leiden University Medical Centre
P.O. Box 9600
2300 RC Leiden, The Netherlands

Christl Vermeij-Keers
van Beuningenlaan 8
2344 CC Leiden, The Netherlands

Pieter Wesseling
812 Department of Pathology
Radboud University Nijmegen Medical Centre
P.O. Box 9101
6500 HB Nijmegen, The Netherlands

Michèl Willemsen
820 Department of Child Neurology
Radboud University Nijmegen Medical Centre
P.O. Box 9101
6500 HB Nijmegen, The Netherlands

Overview of the Development of the Human Brain and Spinal Cord

Hans J. ten Donkelaar and Ton van der Vliet

1.1 Introduction

The development of the human brain and spinal cord may be divided into several phases, each of which is characterized by particular developmental disorders (Volpe 1987; van der Knaap and Valk 1988; Aicardi 1992; Table 1.3). After implantation, formation and separation of the germ layers occur, followed by dorsal and ventral induction phases, and phases of neurogenesis, migration, organization and myelination. With the transvaginal ultrasound technique a detailed description of the living embryo has become possible. Fetal development of the brain can now be studied in detail from about the beginning of the second half of pregnancy (Garel 2004). In recent years, much progress has been made in elucidating the mechanisms by which the CNS develops, and also in our understanding of its major developmental disorders, such as neural tube defects, holoprosencephaly, microcephaly and neuronal migration disorders. Molecular genetic data, that explain programming of development aetiologically, can now be incorporated (Sarnat 2000; Barkovich et al. 2001). In this chapter an overview is presented of (1) major stages in the development of the human CNS, (2) the first 3 weeks of development, (3) neurulation, (4) pattern formation, (5) early development of the brain, (6) fetal development of the brain, (7) the development of the blood supply of the brain, and (8) the development of major fibre tracts including the development of myelination. Mechanisms of development are discussed in Chap. 2, and an overview of the causes of developmental malformations and their molecular genetic basis is presented in Chap. 3. In the second, specialized part of this book the development of the CNS and its disorders are discussed in more detail.

1.2 Major Stages in the Development of the Human Brain and Spinal Cord

The **embryonic period** in man, i.e. the first 8 weeks of development, can be divided into 23 stages, the **Carnegie stages** (O'Rahilly and Müller 1987), originally described as developmental horizons (XI–XXIII) by Streeter (1951), and completed by Heuser and Corner (1957; developmental horizon X) and O'Rahilly (1973; developmental stages 1–9). Impor-

tant contributions to the description of human embryos were also made by Nishimura et al. (1977) and Jirásek (1983, 2001, 2004). Examples of human embryos are shown in Figs. 1.1 and 1.2. In the embryonic period, **postfertilization** or **postconceptional age** is estimated by assigning an embryo to a developmental stage using a table of norms, going back to the first *Normentafeln* by Keibel and Elze (1908). The term **gestational age** is commonly used in clinical practice, beginning with the first day of the last menstrual period. Usually, the number of **menstrual** or **gestational weeks** exceeds the number of postfertilization weeks by 2. During week 1 (stages 2–4) the blastocyst is formed, during week 2 (stages 5 and 6) implantation occurs and the primitive streak is formed, followed by the formation of the notochordal process and the beginning of neurulation (stages 7–10). Somites first appear at stage 9. The neural folds begin to fuse at stage 10, and the rostral and caudal neuropores close at stages 11 and 12, respectively. Gradually, the pharyngeal bars, the optic and otic vesicles and the limb buds appear. The main external and internal features of human embryos are summarized in Table 1.1. The first four embryonic weeks are also described as the period of *blastogenesis*, and the fifth to eighth weeks as the period of *organogenesis* (Opitz 1993; Opitz et al. 1997). The **fetal period** cannot be divided into a series of morphologically defined stages. It is the period of *phenogenesis* (Opitz 1993; Opitz et al. 1997). In the clinical literature a subdivision of the prenatal period into three trimesters of 13 weeks each is commonly used. At the junction of trimesters 1 and 2, the fetus of about 90 days has a greatest length of 90 mm, whereas at the junction of trimesters 2 and 3, the fetus is about 250 mm in length and weighs approximately 1,000 g (O'Rahilly and Müller 2001; Table 1.2). The newborn brain weighs 300–400 g at full term. Male brains weigh slightly more than those of females but, in either case, the brain constitutes 10% of the body weight (Crelin 1973).

The brain and spinal cord arise from an area of the ectoderm known as the neural plate. The folding of the neural plate, leading to successively the neural groove and the neural tube, is called primary neurulation. The caudal part of the neural tube does not arise by fusion of the neural folds but develops from the so-called caudal eminence. This process is called secondary neurulation (Chap. 4). Before and after the

Fig. 1.1 Dorsal views of staged early human embryos (Carnegie stages 6, 7, 9–11; from the Kyoto Collection of Human Embryos; kindly provided by Kohei Shiota)

surface ectoderm of the two sides fuses, the fusing neuroectodermal cells of the neural folds give off the neural crest cells. The neural crest is a transient structure and gives rise to the spinal and cranial ganglia. Moreover, the whole viscerocranium and part of the neurocranium are formed from the neural crest (Le Douarin and Kalcheim 1999; Wilkie and Morriss-Kay 2001; Chap. 5).

The embryonic period includes three in time overlapping phases: formation and separation of the germ layers, dorsal and ventral induction phases (Table 1.3). During the first phase, the neural plate is formed. In the **dorsal induction phase**, the neural tube is formed and closed, and the three primary divisions or neuromeres of the brain (the prosencephalon, mesencephalon and rhombencephalon) appear. In the **ventral induction phase** (*telencephalization*), the cerebral hemispheres, the eye vesicles, the olfactory bulbs and tracts, the pituitary gland and

part of the face are formed. In the sixth week of development strong proliferation of the ventral walls of the telencephalic vesicles gives rise to the ganglionic or ventricular eminences. These elevations do not only form the basal ganglia but, in addition, give rise to many neurons that migrate tangentially to the cerebral cortex. **Neurogenesis** starts in the spinal cord and the brain stem. Neurogenesis in the cerebellum and the cerebral cortex occurs largely in the fetal period. In man, the **fetal period** extends from the ninth week of development to the time of birth. With regard to the prenatal ontogenesis of the cerebral cortex, Marín-Padilla (1990) suggested dividing this long developmental period into two separate ones: (1) the **fetal period proper** (9–24 gestational weeks), characterized by the formation of the cortical plate; and (2) the **perinatal period**, extending from the 24th week of gestation to the time of birth. This period is characterized by neuronal maturation. The separation be-

Table 1.1 Developmental stages and features of human embryos (after O'Rahilly; Müller 1987, 2001)

Carnegie stages	Length (mm)	Age (days)	External features	Internal features (with emphasis on the nervous system)
1		1	Fertilization	
2		2–3	From 2 to about 16 cells	
3		4–5	Free blastocyst	Inner cell mass and trophoblast
4		6	Attaching blastocyst	Cytotrophoblast and syncytiotrophoblast distinguishable
5	0.1–0.2	7–12	Implantation; embryonic disc circular	Amniotic cavity; primary yolk sac; extra-embryonic mesoderm
6	0.2	17	Embryonic disc elongated	Chorionic villi; primitive streak and node; prechordal plate appears; secondary yolk sac
7	0.4	19	Embryonic disc oval	Notochordal process visible; haematopoiesis starts
8	1.0–1.5	23	Primitive pit appears; neural folds may begin to form	Notochordal and neurenteric canals detectable
9	1.5–2.5	25	First somites appear; mesencephalic flexure begins; otic disc forms	Neural groove evident; 3 major subdivisions of brain distinguishable; heart begins to develop
10	2–3.5	28	Neural folds begin to fuse; otic pit develops; 4–12 somites; pharyngeal arches 1 and 2 visible	Optic primordium begins to develop; cardiac loop appears; intermediate mesoderm
11	2.5–4.5	29	Rostral neuropore closes; 13–20 somites	Optic vesicles develop
12	3–5	30	Caudal neuropore closes; 21–29 somites; 4 pharyngeal arches visible; upper limb buds appearing	Secondary neurulation starts
13	4–6	32	Otic vesicle closed; lens disc not yet indented; 30 or more somites; 4 limb buds visible	Retinal and lens discs develop; primordium of cerebellum
14	5–7	33	Lens pit appears; upper limb buds elongated	Future cerebral hemispheres; pontine flexure; optic cup develops; adenohypophysial pouch defined
15	7–9	36	Lens pit closed; nasal pit appearing; hand plate forming	Future cerebral hemispheres become defined; retinal pigment visible
16	8–11	38	Retinal pigment visible; nasal sacs face ventrally; auricular hillocks beginning; foot plate appears	Epiphysis cerebri develops; neurohypophysial evagination; olfactory tubercle
17	11–14	41	Head relatively larger; trunk straighter; auricular hillocks distinct; finger rays	Internal and external cerebellar swellings; chondrification begins in humerus, radius and some vertebral centra
18	13–17	44	Body more cuboidal; elbow region and toe rays appearing	Oronasal membrane develops; 1–3 semicircular ducts in internal ear
19	16–18	46	Trunk elongating and straightening	Olfactory bulb develops; cartilaginous otic capsule; choroid plexus of fourth ventricle
20	18–22	49	Upper limbs longer and bent at elbows	Optic fibres reach optic chiasm; choroid plexus of lateral ventricle
21	22–24	51	Fingers longer; hands approach each other, feet likewise	Cortical plate becomes visible; optic tract and lateral geniculate body
22	23–28	53	Eyelids and external ear more developed	Olfactory tract; internal capsule; adenohypophysial stalk incomplete
23	27–31	56	Head more rounded; limbs longer and more developed	Insula indented; caudate nucleus and putamen recognizable; humerus presents all cartilaginous stages
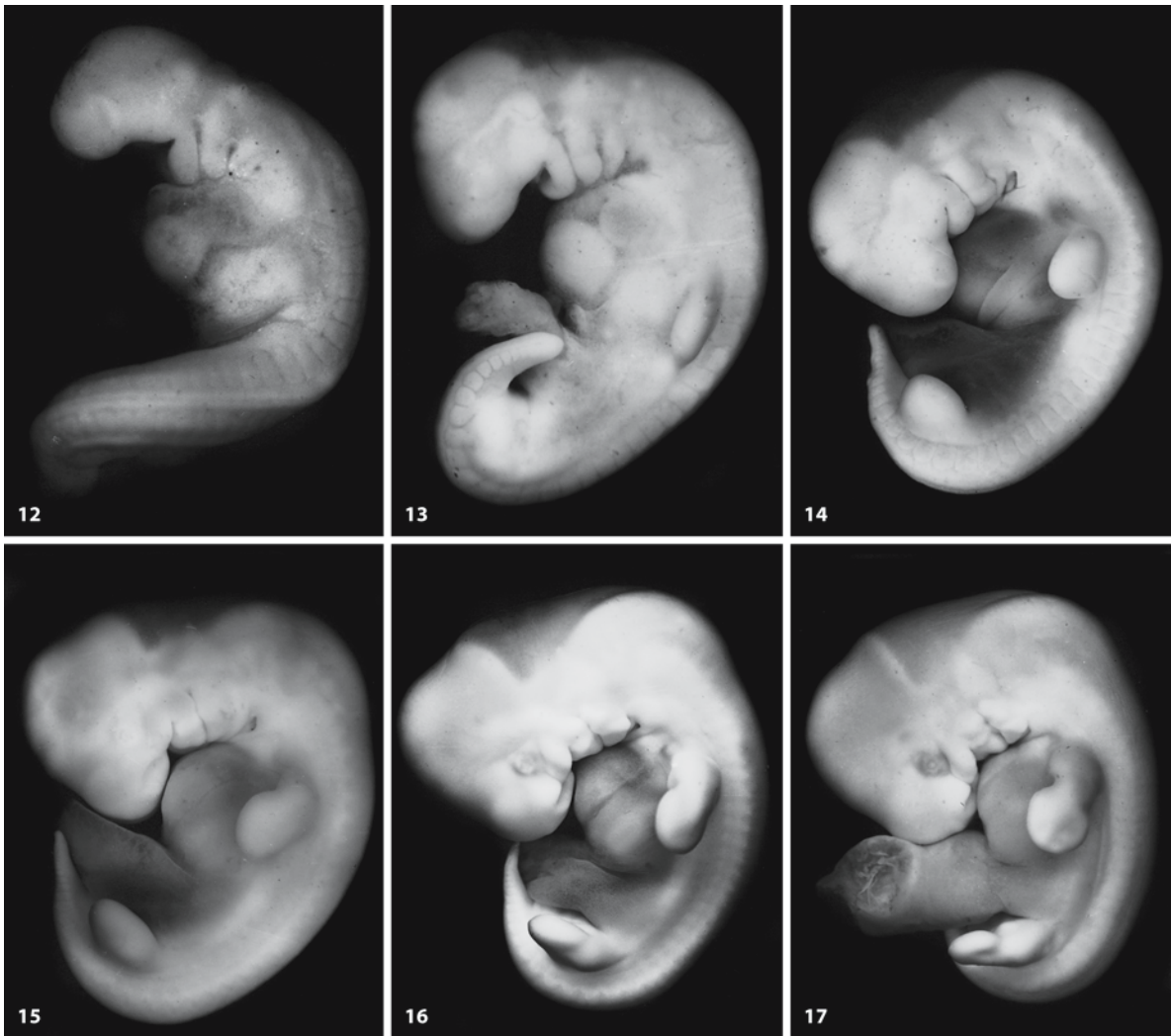
Fig. 1.2 Lateral views of staged human embryos (Carnegie stages 12–23; from the Kyoto Collection of Human Embryos; kindly provided by Kohei Shiota)

tween these two periods at the 24th week of gestation is somewhat arbitrary but may be clinically relevant. The 24th week of gestation approximates roughly the lower limit for possible survival of the prematurely born infant. Disorders of migration are more likely to occur in the fetal period, whereas abnormalities affecting the architectonic organization of the cerebral cortex are more likely to occur in the perinatal period (Chap. 10).

Each of the developmental phases of the brain is characterized by particular **developmental disorders** (Table 1.3). During the separation of the germ layers, enterogenous cysts and fistulae may occur. In the dorsal induction phase, neural tube defects (Chap. 4)

occur. Developmental disorders in the ventral induction phase, in which the prosencephalon is normally divided into the diencephalon and the two cerebral hemispheres, are characterized by a single, incompletely divided forebrain (holoprosencephaly; Chap. 9). This very heterogeneous disorder may be due to disorders of ventralization of the neural tube (Sarnat 2000) such as underexpression of the strong ventralizing gene *Sonic hedgehog* (*SHH*). During neurogenesis of the forebrain, malformations due to abnormal neuronal proliferation or apoptosis may occur, leading to microcephaly or megalocephaly. During the migration of the cortical neurons, malformations due to abnormal neuronal migration may

Fig. 1.2 *(Continued)*

appear, varying from classic lissencephaly ('smooth brain'), several types of neuronal heterotopia, polymicrogyria to minor cortical dysplasias. For many of these malformations, disorders of secretory molecules and genes that mediate migration have been found (Chap. 10). Many of these malformations are characterized by the presence of mental retardation and epilepsy. Cerebellar disorders are more difficult to fit into this scheme. The Dandy–Walker malformation is thought to arise late in the embryonic period, whereas cerebellar hypoplasia presumably occurs in the fetal period. These malformations are discussed in Chap. 8.

1.3   The First 3 Weeks of Development

During the first 3 weeks of development, the three germ layers (ectoderm, mesoderm and endoderm), the basis of the various organs and systems of the body, are established. During the first week of development (stages 2–4), the embryo develops from a solid mass of totipotent cells or blastomeres (the **morula**) into the blastocyst. This occurs when 16–32 cells are present. The **blastocyst** is composed of an inner cell mass or **embryoblast**, giving rise to the embryo, and the **trophoblast**, the peripherally situated cells, surrounding the blastocystic cavity and forming the developmental adnexa (Fig. 1.3). Embryoblast cells

Table 1.2 Criteria for estimating age during the fetal period (after Moore et al. 2000)

Age (post-conceptional weeks)	Average crown–rump length (mm)	Average foot length (mm)	Average weight (g)	Main external characteristics
Previable fetuses				
9	50	7	8	Eyes closing or closed; head large and more rounded; external genital not distinguishable as male or female; intestines in proximal part of umbilical cord; low-set ears
10	61	9	14	Intestines returned to abdomen; early fingernail development
12	87	14	45	Sex distinguishable externally; well-defined neck
14	120	20	110	Head erect; eyes face anteriorly; ears close to their definitive position; lower limbs well-developed; early toenail development
16	140	27	200	External ears stand out from head
18	160	33	320	Vernix caseosa covers skin; quickening felt by mother
20	190	39	460	Head and body hair (lanugo) visible
Viable fetuses				
22	210	45	630	Skin wrinkled, translucent, pink to red
24	230	50	820	Fingernails present; lean body
26	250	55	1,000	Eyes partially open; eyelashes present
28	270	59	1,300	Eyes wide open; good head of hair may be present; skin slightly wrinkled
30	280	63	1,700	Toenails present; body filling out; testes descending
32	300	68	2,100	Fingernails reach finger tips; skin pink and smooth
36	340	79	2,900	Body usually plump; lanugo hairs almost absent; toenails reach toe tips; flexed limbs; firm grasp
38	360	83	3,400	Prominent chest; breasts protrude; testes in scrotum or palpable in inguinal canals; fingernails extend beyond finger tips

adjacent to this cavity form a new layer of flat cells, the **hypoblast.** This cell layer covers the blastocystic cavity from inside what is now called the **primitive umbilical vesicle** or **yolk sac.** The rest of the inner cell mass remains relatively undifferentiated and is known as the **epiblast.** Duplication of the inner cell mass is probably the basis for most cases of monozygotic twinning. Possibly, such divisions arise during 'hatching', the emergence of the blastocyst from the zona pellucida (O'Rahilly and Müller 2001). At approximately 6 days (stage 4b), the blastocyst becomes attached to the endometrium of the uterus.

1.3.1　Implantation

The second week is characterized by **implantation** (stage 5) and the formation of the primitive streak (stage 6). The trophoblast differentiates into the **cytotrophoblast** and the more peripherally situated **syncytiotrophoblast** that invades the endometrium. Blood-filled spaces, the **lacunae,** soon develop within

the syncytiotrophoblast and communicate with endometrial vessels, laying the basis for the placental circulation. Between the epiblast and the cytotrophoblast, the **amniotic cavity** appears. The embryonic disc is now known as the **bilaminar embryo.** Only the cylindric epiblast cells adjacent to the hypoblast form the embryo. The remaining flattened epithelial cells participate in the formation of the amnion (Fig. 1.3). The amniotic cavity is bounded ventrally by the epiblast and dorsally by a layer of amniotic ectoderm.

1.3.2　Gastrulation

During stage 6, in the slightly elongated embryonic disc caudally situated cells of the epiblast migrate ventralwards along the median plane, and form the **primitive streak** (Fig. 1.4). It probably appears between days 12 and 17 (Jirásek 1983, 2001; Moore et al. 2000; O'Rahilly and Müller 2001). The rostral, usually distinct part of the primitive streak is known as the

Table 1.3 Major stages of human CNS development (based on Aicardi 1992)

Stage	Time of occurrence (weeks)	Major morphological events in brain	Main corresponding disorders
Embryonic period			
Formation and separation of germ layers	2	Neural plate	Enterogenous cysts and fistulas; split notochord syndrome
Dorsal induction: primary neurulation	3–4	Neural tube, neural crest and derivatives; closure of rostral and caudal neuropores; paired alar plates	Anencephaly, encephalocele, myeloschisis; myelomeningocele, Chiari malformations
Ventral induction: telencephalization	4–6	Development of forebrain and face; formation of cerebral vesicles; optic and olfactory placodes; rhombic lips appear; 'fusion' of cerebellar plates	Holoprosencephaly; Dandy–Walker malformation; craniosynostosis
Fetal period			
Neuronal and glial proliferation	6–16	Cellular proliferation in ventricular and subventricular zones; early differentiation of neuroblasts and glioblasts; cellular death (apoptosis); migration of Purkinje cells and external granular layer in cerebellum	Microcephaly, megalencephaly
Migration	12–24	Migration of cortical neurons; formation of corpus callosum	Neuronal migration disorders (lissencephalies, polymicrogyria, schizencephaly, heterotopia)
Perinatal period			
Organization	24 to postnatal	Late migration; organization and maturation of cerebral cortex; synaptogenesis; formation of internal granular layer in cerebellum	Minor cortical dysplasias
Myelination	24 to 2 years postnatally		Myelination disorders, destructive lesions (secondarily acquired injury of normally formed structures)

primitive node of Hensen. The primitive streak is a way of entrance whereby cells invaginate, proliferate and migrate to subsequently form the extra-embryonic mesoderm, the endoderm and the intra-embryonic mesoderm. Remnants of the primitive streak may give rise to *sacrococcygeal teratomas* (Chap. 6). The **endoderm** replaces the hypoblast. The remaining part of the epiblast is the **ectoderm**. For this process the term **gastrulation** is frequently used. Originally, the term referred to the invagination of a monolayered blastula to form a bilayered gastrula, containing an endoderm-lined archenteron as found in amphibians (Chap. 2). Nowadays, the term gastrulation is more generally used to delimit the phase of development from the end of cleavage until the formation of an embryo possessing a defined axial structure (Collins and Billett 1995).

Rostral to the primitive streak and node, the endoderm appears thicker and is called the **prechordal plate**. Caudally, the epiblast is closely related to the endoderm, giving rise to the **cloacal membrane** (Fig. 1.4). The primitive streak is the first clear-cut in-

dication of bilaterality, so the embryo now, apart from rostral and caudal ends, also has right and left sides. Genetic mutations expressed in the primitive streak may lead to duplication of the neural tube (Chap. 6) or its partial or complete agenesis (Sarnat 2000).

The **extra-embryonic mesoderm** soon covers the trophoblast, the amniotic ectoderm and the yolk sac (Fig. 1.3). Extra-embryonic mesoderm at the caudal part of the embryo forms the **connecting** or **umbilical stalk** that anchors the embryo to the **chorion**. The chorion is composed of the trophoblast and the covering extra-embryonic mesoderm. Hypoblast cells and the covering extra-embryonic mesoderm form the wall of the yolk sac, whereas the amniotic epithelium and its mesodermal layer form the **amnion**. The **secondary umbilical vesicle** or **yolk sac** develops from the primary one, probably by collapse and disintegration of the latter (Luckett 1978). The yolk sac is involved in active and passive transport to the embryo, and is possibly associated with the relationship between metabolic disorders such as diabetes melli-
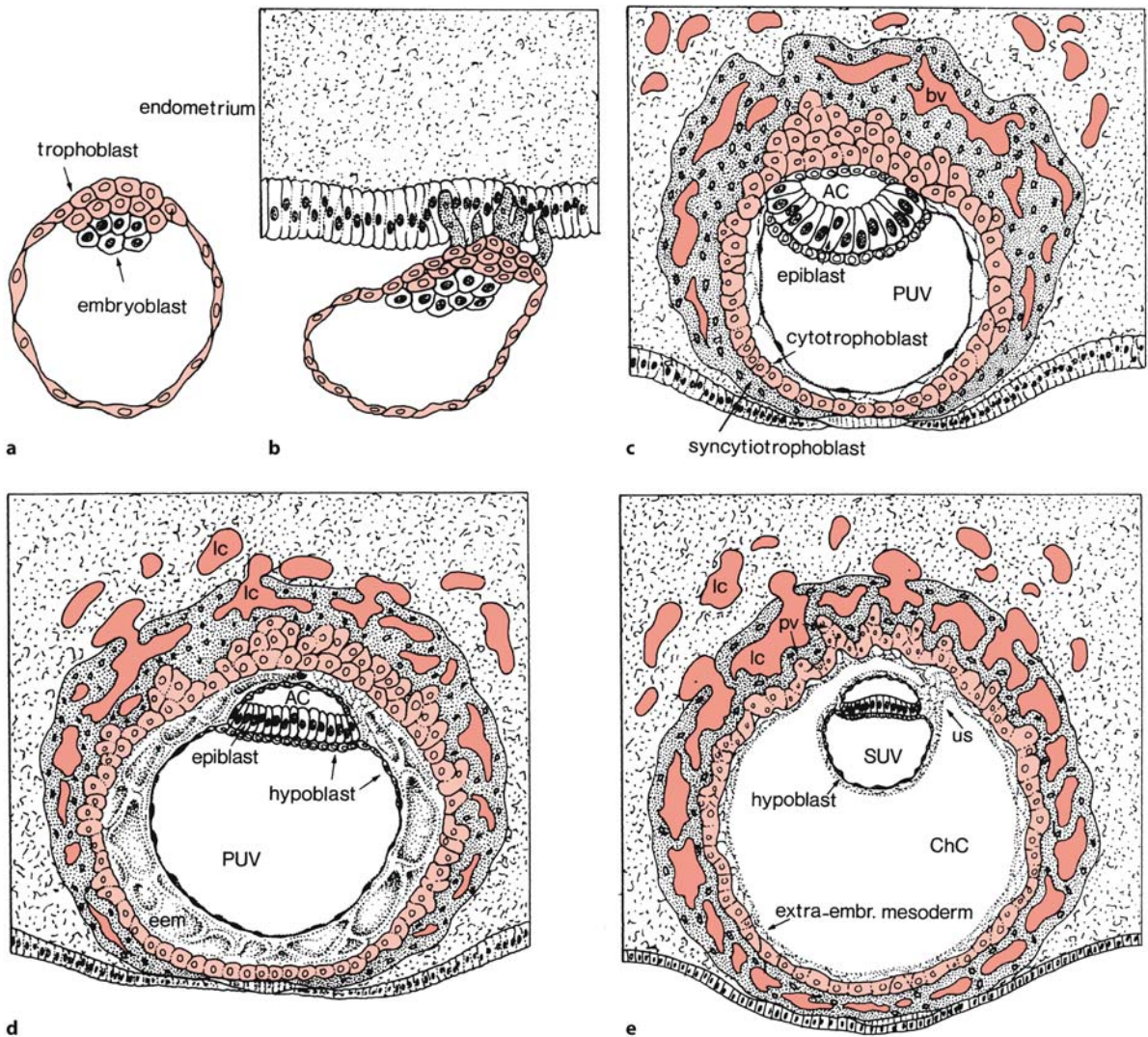
Fig. 1.3 Implantation and the formation of the bilaminar embryo: **a** 107-cell blastocyst; **b–e** blastocysts of approximately 4.5, 9, 12 and 13 days, respectively. The trophoblast and the cytotrophoblast are indicated in *light red*, the syncytiotrophoblast is *stippled* and maternal blood in lacunae is shown in *red*. *AC* amniotic cavity, *ChC* chorionic cavity, *eem* extra-embryonic mesoderm, *lc* lacuna, *PUV* primary umbilical vesicle, *pv* primary villi, *SUV* secondary umbilical vesicle (yolk sac), *us* umbilical stalk. (After Langman 1963)

tus and congenital malformations (O'Rahilly and Müller 2001). The chorion encloses the **chorionic cavity**, in which the embryonic disc, now a **trilaminar embryo**, is located.

During the third and the fourth weeks, the somites, the heart, the neural folds, the three major divisions of the brain, the neural crest and the beginnings of the internal ear and the eye develop. At approximately 19 days (stage 7), rostral to the primitive streak, a prolongation below the ectoderm, the **notochordal process**, arises from the primitive node, and extends rostrally as far as the prechordal plate (Fig. 1.4). The floor of the notochordal process breaks down at stage 8, giving rise to the notochordal plate.

The embryonic disc is now broader rostrally, and a shallow neural groove appears, which is the first morphological indication of the nervous system (O'Rahilly 1973; O'Rahilly and Gardner 1979; O'Rahilly and Müller 1981; Jirásek 2001, 2004). The primitive node may be hollowed by a **primitive pit**, which extends into the notochordal process as the **notochordal canal** (O'Rahilly 1973). The channel becomes intercalated in the endoderm, and its floor begins to disintegrate at once, allowing temporary communication between the amniotic cavity and the umbilical vesicle. The remnant of the notochordal canal at the level of the primitive pit is known as the **neurenteric canal** (Fig. 1.5a). It may be involved in
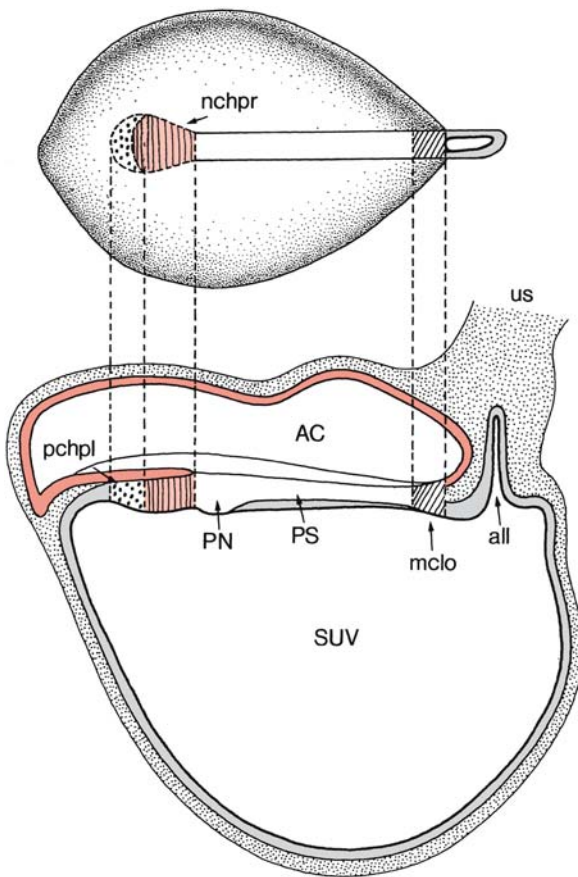
Fig. 1.4 Dorsal (*top*) and medial (*bottom*) views of a stage 7 embryo. The ectoderm is indicated in *red*, the notochordal process (*nchpr*) in *light red* and the endoderm in *grey*. *AC* amniotic cavity, *all* allantois, *mclo* membrana cloacalis, *pchpl* prechordal plate, *PN* primitive node, *PS* primitive streak, *SUV* secondary umbilical vesicle (yolk sac), *us* umbilical stalk. (After O'Rahilly 1973)

the pathogenesis of *enterogenous cysts* (Chap. 6). The **prechordal plate** is wider than the notochordal process, and is in close contact with the floor of the future forebrain. The prechordal plate is derived from the prechordal mesendoderm (de Souza and Niehrs 2000) and it is essential for the induction of the forebrain. The prechordal plate is usually defined as mesendodermal tissue underlying the medial aspect of the anterior neural plate just anterior to the rostral end of the notochord.

1.3.3   Folding of the Embryo

At approximately 25 days (stage 9), **folding** of the **embryo** becomes evident. Rostral or cephalic and caudal folds overlie the beginning foregut and hindgut, re-

spectively (Fig. 1.5). Caudal to the cloacal membrane, the allantois arises as a dorsal diverticle of the umbilical vesicle. On each side the mesoderm is arranged into three components (Fig. 1.5 e): (1) a longitudinal, **paraxial** band adjacent to the notochord, forming the somites; (2) **intermediate** mesoderm, giving rise to the urogenital system; and (3) a **lateral plate**, giving rise to two layers covering the body wall and the viscera, respectively. The first layer is known as the **somatopleure**, the other as the **splanchnopleure**. In the Anglo-Saxon literature, however, the terms somatopleure and splanchnopleure include the covering ectoderm and endoderm, respectively (O'Rahilly and Müller 2001). The space between the somatopleure and the splanchnopleure is the **coelom**. At first it is found outside the embryo (the *extra-embryonic coelom*), later also within the embryo. This is the *intra-embryonic coelom* or body cavity, which develops in the lateral plate mesoderm (Fig. 1.5 e, f).

Somites arise at stage 9 in longitudinal rows on each side of the neural groove. The first four pairs of somites belong to the occipital region. Within the next 10 days subsequently 8 cervical, 12 thoracic, 5 lumbar, 5 sacral and some 3–6 coccygeal somites are formed, but they are never visible together at one stage of development. Each somite divides into a ventromedial **sclerotome**, participating in the formation of the vertebral column (Chap. 6), and a dorsolateral **dermamyotome** that forms a myotome and the overlying dermis (**dermatome**). Each **myotome** divides into two parts: (1) a dorsal *epimere*, giving rise to the erector spinae, and (2) a ventral *hypomere*, from which the ventral vertebral muscles (*epaxial* muscles), the muscles of the lateral and ventral body wall (*hypaxial* muscles) and the muscles of the extremities arise. The derivatives of the epimeres become innervated by the dorsal rami of the spinal nerves, those of the hypomeres by the ventral rami (Chap. 6).

The primitive streak becomes confined to a region known as the **caudal eminence**, or end-bud, which gives rise to the hindgut, adjacent notochord and somites, and the most caudal part of the spinal cord (O'Rahilly and Müller 2001). Malformations in this region may lead to the still poorly understood *caudal regression syndrome* that is discussed in Chap. 4. Rostrally, the ectoderm and the endoderm come together as the **oropharyngeal membrane**, which temporarily separates the gut from the amniotic cavity. Pharyngeal arches, clefts and pouches become visible. The **pharyngeal arches** are separated by the **pharyngeal clefts**, and appear ventrolaterally on the head and neck between 4 and 5 weeks. Four pairs are visible at stage 13 (Fig. 1.2). More caudally, no clear-cut arrangement is found, but it is customary to distinguish a fifth and a sixth arch. The externally situated clefts have internal counterparts, the **pharyngeal pouches**. The development of the pharyngeal arches
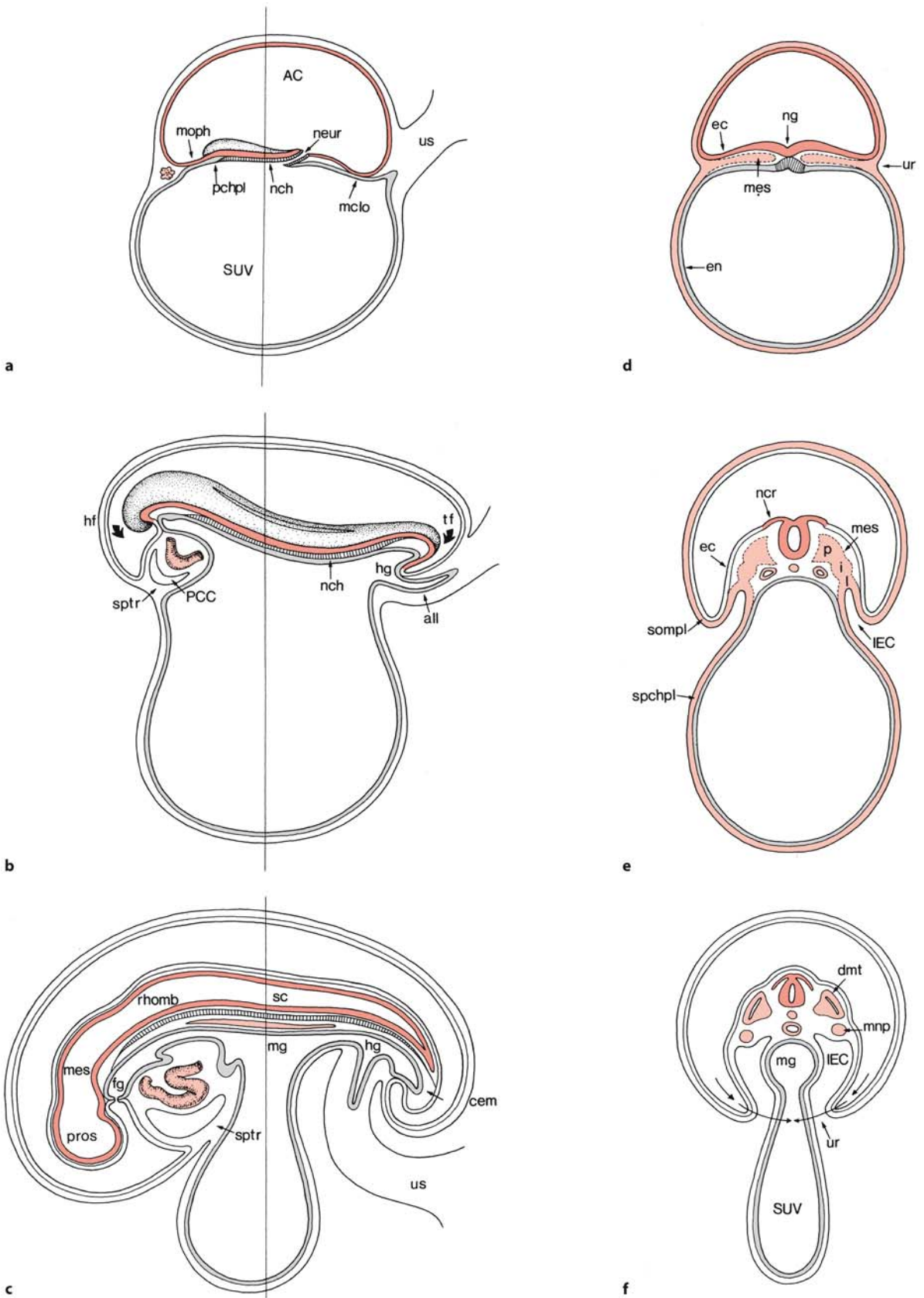
Fig. 1.5

Fig. 1.5 The folding of the embryo: **a**, **d** Carnegie stage 8; **b**, **e** Carnegie stage 10; **c**, **f** Carnegie stage 11/12. The ectoderm (*ec*) and its derivates are indicated in *red*, derivates of the mesoderm (*mes*) in *light red* and the endoderm (*en*) in *grey*. *AC* amniotic cavity, *all* allantois, *cem* caudal eminence, *dmt* dermamyotome, *fg* foregut, *hf* head fold, *hg* hindgut, *i* intermediate mesoderm, *IEC* intra-embryonic coelom, *l* lateral plate of mesoderm, *mclo* membrana cloacalis, *mes* mesencephalon, *mg* midgut, *mnp* mesonephros, *moph* membrana oropharyngealis, *nch* notochord, *ncr* neural crest, *neur* neurenteric canal, *ng* neural groove, *p* paraxial mesoderm, *PCC* pericardiac cavity, *pchpl* prechordal plate, *pros* prosencephalon, *rhomb* rhombencephalon, *sc* spinal cord, *sompl* somatopleure, *spchpl* splanchnopleure, *sptr* septum transversum, *SUV* secondary umbilical vesicle (yolk sac), *tf* tail fold, *ur* umbilical ring, *us* umbilical stalk. (After Streeter 1951; Hamilton and Mossman 1972)

is closely related to that of the rhombomeres and the neural crest, and is controlled by *Hox* genes (Favier and Dollé 1997; Rijli et al. 1998). Each pharyngeal arch is characterized by a unique combination of *Hox* genes. Rostral to the somites, the paraxial mesoderm forms the **somitomeres** from which the external eye musculature and the muscles of the pharyngeal bars arise (Noden 1991). These aspects and developmental disorders of the pharyngeal arches are discussed in

Chap. 5. The major sensory organs of the head develop from the interactions of the neural tube with a series of epidermal thickenings called the **cranial ectodermal placodes**. The olfactory placode forms the olfactory epithelium, the trigeminal placode the trigeminal ganglion, the otic placode or disc forms the inner ear, and the epibranchial placodes the distal ganglia of the VIIth, IXth and Xth nerves. The lens placode forms the lens and induces the overlying ectoderm to form the transparent cornea.

1.4 Neurulation

The first indication of the neural plate in human embryos is a median sulcus around 23 days of development. At approximately 25 days (stage 9), this **neural groove** is deeper and longer. Its rostral half represents the forebrain, its caudal half mainly the hindbrain (Fig. 1.6). The **neural folds** of the forebrain are conspicuous. The **mesencephalic flexure** appears, and allows a first subdivision of the brain into three major divisions in the still unfused neural folds (O'Rahilly 1973; O'Rahilly and Gardner 1979; Müller and O'Rahilly 1983, 1997; Jirásek 2001, 2004): the forebrain or **prosencephalon**, the midbrain or **mesencephalon**, and the hindbrain or **rhombencephalon** (Figs. 1.7, 1.8). The otic discs, the first indication of the internal ears, can also be recognized. At stage 10, the two subdivisions of the forebrain, the **telen-**
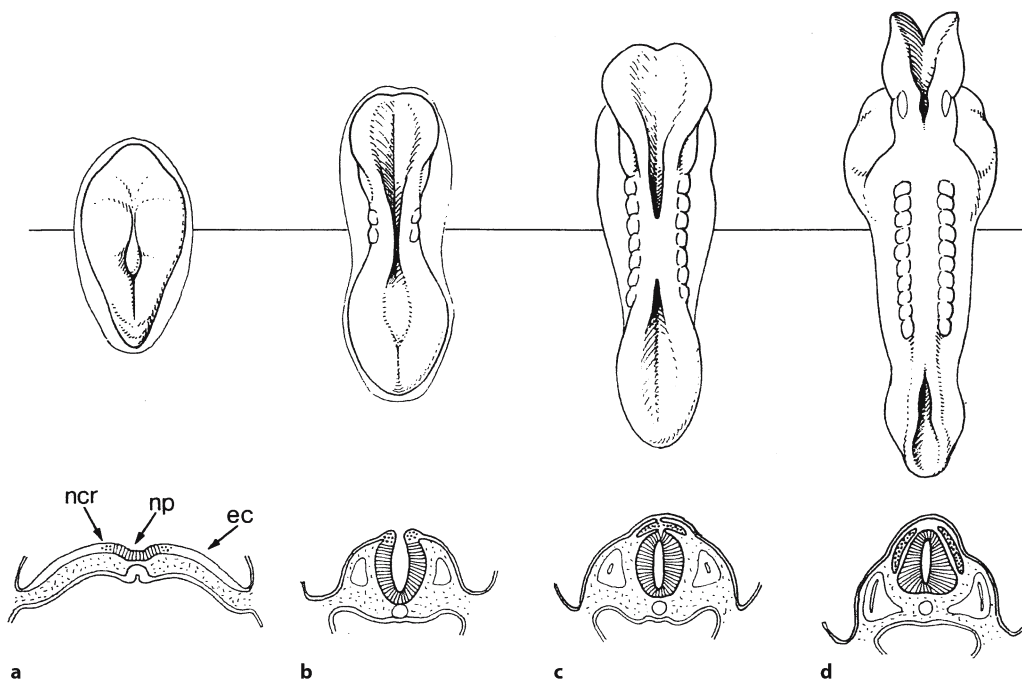
Fig. 1.6 The formation of the neural tube and neural crest. Dorsal views and transverse sections are shown for human embryos of stages 8 (**a**), 9 (**b**), 10 (**c**, seven somites) and 10 (**d**, ten somites). *ec* ectoderm, *ncr* neural crest, *np* neural plate

a　　　　　　　　　　　　　　　　　　　　　　b
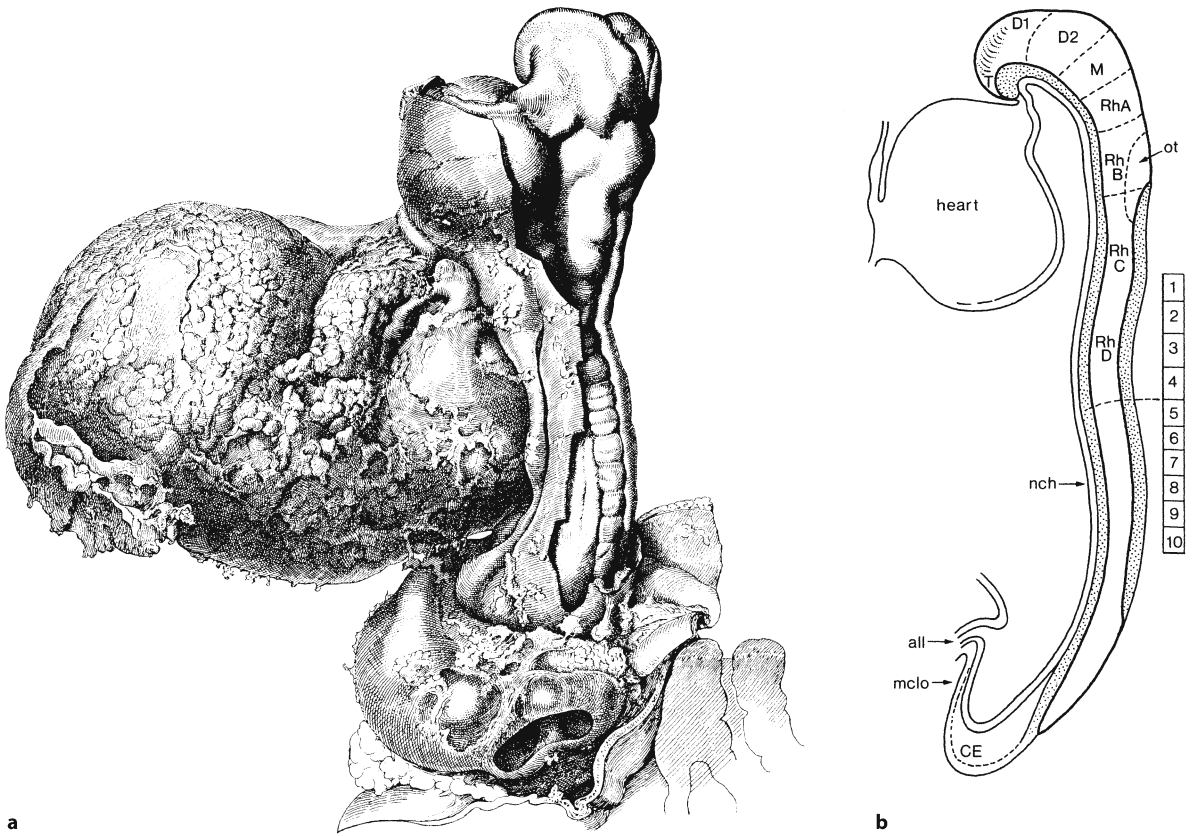
Fig. 1.7 Corner's ten-somite embryo (**a**). **b** A median section, showing the subdivision of the brain into the primary neuromeres. *all* allantois, *CE* caudal eminence, *D1*, *D2* diencephalic neuromeres, *M* mesomere, *mclo* membrana cloacalis, *nch* notochord, *ot* otocyst, *RhA–RhD* primary rhombomeres, *T* telencephalic neuromere *1–10* first ten somites. (**a** Illustrated by James Didusch, from Corner 1929, with permission; **b** after O'Rahilly and Müller 1987)
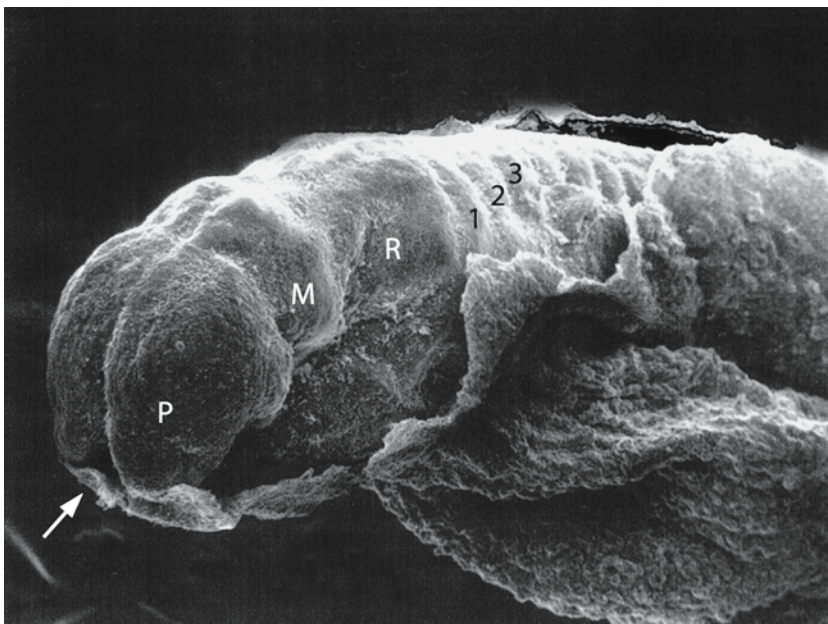
Fig. 1.8 Scanning electron micrograph of a 26–27-day-old, 2.5-mm embryo with 14 paired somites (stage 11). The *arrow* indicates the rostral neuropore. *P* prosencephalon, *M* mesencephalon, *R* rhombencephalon, *1–3* first three somites. (From Jirásek 2004, with permission)

cephalon and the **diencephalon**, become evident (Müller and O'Rahilly 1985). An **optic sulcus** is the first indication of the developing eye. Closure of the neural groove begins near the junction between the future brain and the spinal cord. Rostrally and caudally, the cavity of the developing neural tube communicates via the **rostral** and **caudal neuropores** with the amniotic cavity. The rostral neuropore closes at about 30 days (stage 11), and the caudal neuropore about 1 day later (stage 12). The site of final closure of the rostral neuropore is at the site of the embryonic lamina terminalis (O'Rahilly and Müller 1999). The closure of the neural tube in human embryos is generally described as a continuous process that begins at the level of the future cervical region, and proceeds both rostrally and caudally (O'Rahilly and Müller 1999, 2001). Nakatsu et al. (2000), however, provided evidence that neural tube closure in humans may be initiated at multiple sites as in mice and other animals. *Neural tube defects* are among the most common of human malformations (Chap. 4).

When the surface ectodermal cells of both sides fuse, the similarly fusing neuroectodermal cells of the neural folds give off neural crest cells (Fig. 1.6). These cells arise at the neurosomatic junction. The **neural crest** cells migrate extensively to generate a large diversity of differentiated cell types (Le Douarin and Kalcheim 1999; Chap. 5), including (1) the spinal, cranial and autonomic ganglia, (2) the medulla of the adrenal gland, (3) the melanocytes, the pigment-containing cells of the epidermis, and (4) many of the skeletal and connective tissues of the head. The final phase of primary neurulation is the separation of neural and surface ectoderm by mesenchyme. Failure to do so may lead to an encephalocele, at least in rats (O'Rahilly and Müller 2001). Malformations of the neural crest (*neurocristopathies*) may be accompanied by developmental disorders of the CNS (Chap. 5).

Detailed **fate map** studies are available for amphibians and birds (Chap. 2). The organization of vertebrate neural plates appears to be highly conserved. This conservation probably extends to mammals, for which detailed fate maps are more difficult to obtain. Nevertheless, available data (Rubinstein and Beachy 1998; Rubinstein et al. 1998; Inoue et al. 2000) show that in mice ventral parts of the forebrain such as the hypothalamus and the eye vesicles arise from the medial part of the rostral or prosencephalic part of the neural plate (Fig. 1.10c). Pallial as well as subpallial parts of the telencephalon arise from the lateral parts of the prosencephalic neural plate. The lateral border of this part of the neural plate forms the dorsal, median part of the telencephalon and the commissural plate from which the anterior commissure and the corpus callosum arise.

Initially, the wall of the neural tube consists of a single layer of neuroepithelial cells, the **germinal neuroepithelium** or **matrix layer**. As this layer thickens, it gradually acquires the configuration of a pseudostratified epithelium. Its nuclei become arranged in more and more layers, but all elements remain in contact with the external and internal surface. Mitosis occurs on the internal, ventricular side of the cell layer only (Figs. 2.18, 2.19), and migrating cells form a second layer around the original neural tube. This layer, the **mantle layer** or **intermediate zone**, becomes progressively thicker as more cells are added to it from the germinal neuroepithelium that is now called the **ventricular zone**. The cells of the intermediate zone differentiate into neurons and glial cells. Radial glial cells are present during early stages of neurogenesis. Most radial glial cells transform into astrocytes (Chap. 2). The neurons send axons into an outer layer, the **marginal zone**. The mantle layer, containing the cell bodies, becomes the **grey matter**, and the axonal, marginal layer forms the **white matter**. In the spinal cord, this three-zone pattern is retained throughout development.

Secondary proliferative compartments are found elsewhere in the brain. The **external germinal** or **granular layer** is confined to the cerebellum. It develops from the ventricular zone of the rhombic lip, a thickened germinal zone in the rhombencephalic alar plate, and gives rise to the granule cells of the cerebellum. The **subventricular zone** is found in the lateral and basal walls of the telencephalon. This zone gives rise to a large population of glial cells and to the granule cells of the olfactory bulb.

1.5   Development of the Spinal Cord

After neurulation, the **spinal cord** can be divided into dorsal **alar plates** derived from lateral parts of the neural plate, and ventral **basal plates** derived from its medial parts (Fig. 1.9). The alar and basal plates are separated by the **sulcus limitans** of His (1880). The alar plates are united by a small roof plate, and the basal plates by a thin floor plate. The alar plates and incoming dorsal roots form the afferent or sensory part of the spinal cord, whereas the basal plate and its exiting ventral root form the efferent or motor part. The spinal ganglia arise from the neural crest. The development of the alar and basal plates is induced by **extracellular signalling molecules**, secreted by the notochord and the adjacent ectoderm (Fig. 1.9). The protein SHH of the *SHH* gene in the notochord induces the formation of the floor plate. In its turn, the floor plate induces the formation of motoneurons in the basal plate. Bone morphogenetic proteins (BMPs) from the ectoderm induce the formation of the alar and roof plates and of the neural crest. BMP4 and
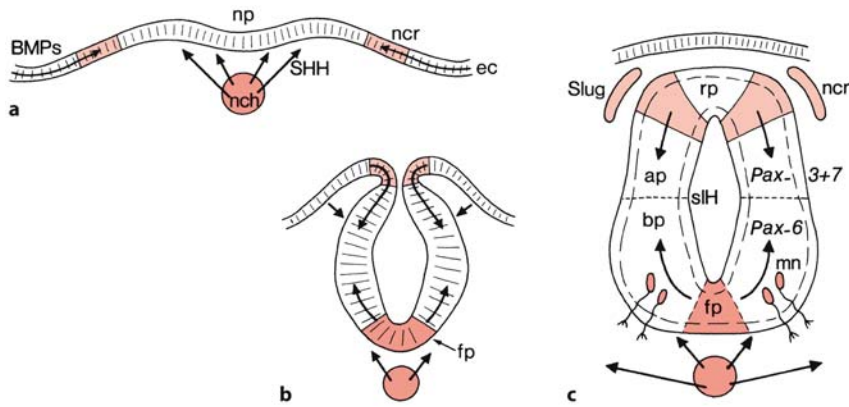
Fig. 1.9 The development of the spinal cord and the dorsalizing (bone morphogenetic proteins, *BMPs*) and ventralizing (Sonic hedgehog, *SHH*) factors involved. **a** SHH in the notochord (*nch*,*red*) induces the formation of the floor plate (*fp*), after which SHH in the floor plate induces the formation of motoneurons (**b**,**c**).BMP4 and BMP7 (*light red*) from the ectoderm

(*ec*) induce Slug in the neural crest (*ncr*) and support the expression of *Pax3* and *Pax7* in the dorsal part of the spinal cord. SHH suppresses the expression of these transcription factors. *ap* alar plate, *bp* basal plate, *mn* motoneurons, *np* neural plate, *rp* roof plate, *slH* sulcus limitans of His. (After Carlson 1999)

BMP7 induce the expression of the transcription factor 'Slug' in the neural crest and the expression of certain *Pax* transcription factors in the alar plates. SHH suppresses these dorsal *Pax* genes in the ventral half of the spinal cord. Many other genes are involved in the specification of the various types of neurons in the spinal cord (Chap. 6). Motoneurons are the first neurons to develop (Windle and Fitzgerald 1937; Bayer and Altman 2002). They appear in the uppermost spinal segments at approximately embryonic day 27 (about Carnegie stage 13/14). At this time of development also dorsal root ganglion cells are present. Dorsal root fibres enter the spinal grey matter very early in development (Windle and Fitzgerald 1937; Konstantinidou et al. 1995; Chap. 6). The first synapses between primary afferent fibres and spinal motoneurons were found in a stage 17 embryo (Okado et al. 1979; Okado 1981). Ascending fibres in the dorsal funiculus have reached the brain stem at stage 16, i.e. at about 37 postovulatory days (Müller and O'Rahilly 1989). The first descending supraspinal fibres from the brain stem have extended into the spinal cord at stage 14 (Müller and O'Rahilly 1988b). Even the late developing pyramidal tract extends as far caudally as the spinomedullary junction at the end of the embryonic period (Müller and O'Rahilly 1990c; ten Donkelaar 2000). The spinal cord then still reaches the end of the vertebral canal. During the fetal period, it 'ascends' to sacral and later lumbar levels (Chap. 6).

1.6 Pattern Formation of the Brain

Prospective subdivisions of the brain are specified through **pattern formation** which takes place in two directions: from medial to lateral, and from rostral to caudal (Lumsden and Krumlauf 1996; Rubinstein and Beachy 1998; Fig. 1.10). Mediolateral or ventrodorsal pattern formation generates longitudinal areas such as the alar and basal plates, and rostrocaudal pattern formation generates transverse zones (one or more neuromeres). Most likely, the rostrocaudal regionalization of the neural plate is induced already during gastrulation (Nieuwkoop and Albers 1990). In amphibians, the first mesoderm to ingress gives rise to the anterior head mesoderm. The mesoderm that follows will form the chordamesoderm and more lateral mesodermal structures. The anterior mesoderm differs from the chordamesoderm also in the genes that it expresses. Signals from both the anterior mesoderm and the chordamesoderm initiate neural development by inducing neural tissue of an anterior type, i.e. forebrain and midbrain, in the overlying ectoderm along its entire anteroposterior length. A second signal from chordamesoderm alone converts the overlying neuroectoderm induced by the first signal into a posterior type of neural tissue, i.e. hindbrain and spinal cord (Chap. 2). Endodermal signalling molecules also play an important role in the induction of the rostral part of the CNS (de Souza and Niehrs 2000).

Developmental gene expression studies show that the vertebrate CNS can be divided into three regions. The anterior region comprises the forebrain and most of the midbrain, and is characterized by expres-
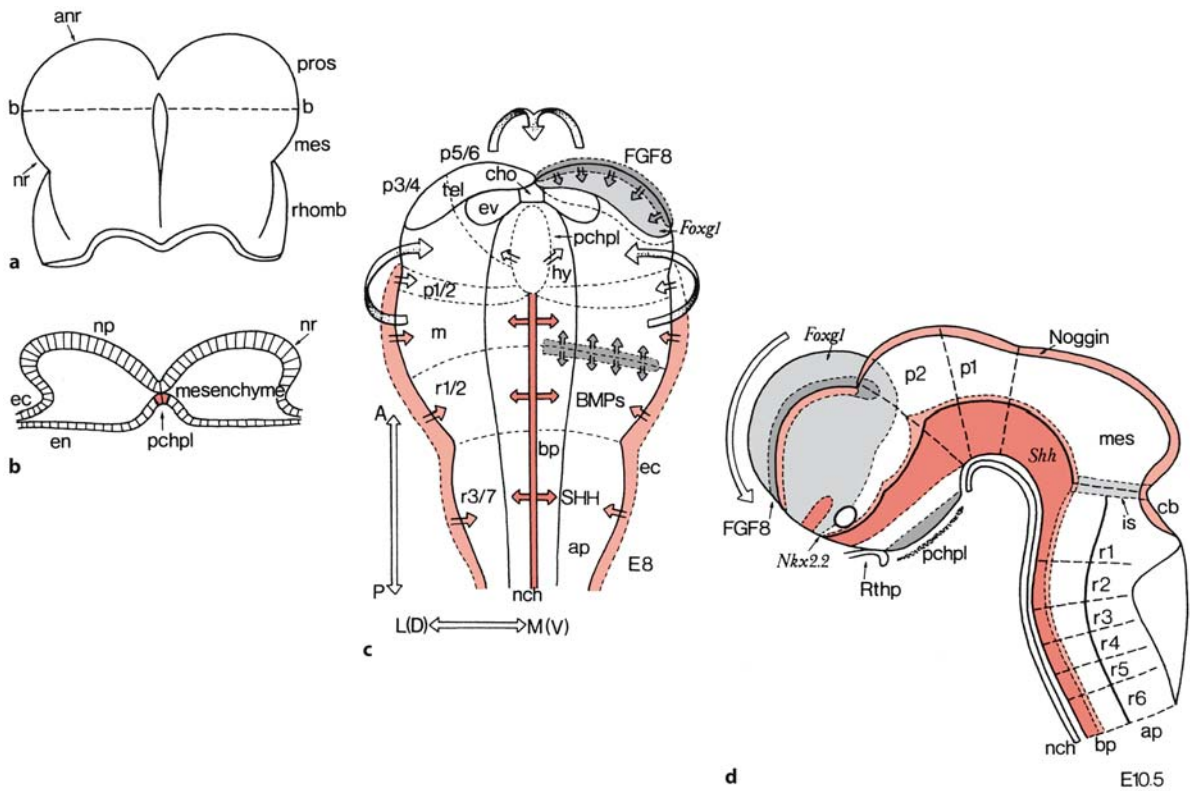
Fig. 1.10 Bauplan and pattern formation of the mouse brain. **a** The dorsal view of the rostral part of the neural plate (*np*) shows the approximate locations of the prosencephalon (*pros*), mesencephalon (*mes*) and rhombencephalon (*rhomb*), and **b** the the transverse section shows the structures involved. The expression of some genes involved in the patterning of the brain is shown in a dorsal view of the neural plate of an E8 mouse (**c**) and in a median section through the neural tube at E10.5 (**d**). The *arrows* indicate the morphogenetic processes involved in the closure of the neural tube. The expression of lateralizing (*L*) or dorsalizing (*D*) signalling molecules such as BMPs is indicated in *light red*, the medializing (*M*) or ventralizing (*V*) factor SHH in *red*, the fibroblast growth factor 8 (*FGF8*) in *dark grey* and brain factor 1 (*Foxg1*) in *grey*. Medial signals induce the basal plate (*bp*), whereas lateral signals induce the alar plate (*ap*). *anr* anterior neural ridge, *cb* cerebellum, *cho* chiasma opticum, *ec* ectoderm, *en* endoderm, *ev* eye vesicle, *hy* hypothalamus, *is* isthmus, *m* mesencephalon, *nch* notochord, *nr* neural ridge, *pchpl* prechordal plate, *p1*, *p6* prosomeres, *Rthp* Rathke's pouch, *r1–r7* rhombomeres, *tel* telencephalon. (After Rubinstein and Beachy 1998; Rubinstein et al. 1998)

sion of the **homeobox genes** *Emx* and *Otx*. The middle division comprises the posterior part of the midbrain and most of the first rhombomere. It is known as the midbrain–hindbrain boundary (MHB) or isthmocerebellar region. The third region comprises the rhombencephalon and spinal cord, and is characterized by *Hox* gene expression.

Longitudinal patterning centres are present along the ventral (notochord and prechordal plate, and later the floor plate) and dorsal (epidermal–neuroectodermal junction, and later the roof plate) aspects of the neural plate and early neural tube. Medial, i.e. **ventralizing,** signals such as SHH play an important role during the formation of the primordia of the basal plate. SHH induces the formation of motoneurons in the spinal cord and brain stem (Chap. 6). Lateral, i.e. **dorsalizing,** signals such as BMPs from the adjacent ectoderm induce the formation of the alar plate and the dorsal part of the forebrain. SHH is not only responsible for dorsoventral patterning in the CNS, but also plays a role during the specification of oligodendrocytes, the proliferation of neural precursors and the control of axon growth (Marti and Bovolenta 2002). The BMPs also have a variety of functions (Mehler et al. 1997). *Holoprosencephaly*, a defect in brain patterning, is the most common structural anomaly of the developing forebrain (Golden 1998; Muenke and Beachy 2000; Sarnat and Flores-Sarnat 2001; Chap. 9).

Specialized, **transverse patterning centres** are present at specific anteroposterior locations of the neural plate such as the anterior neural ridge and the
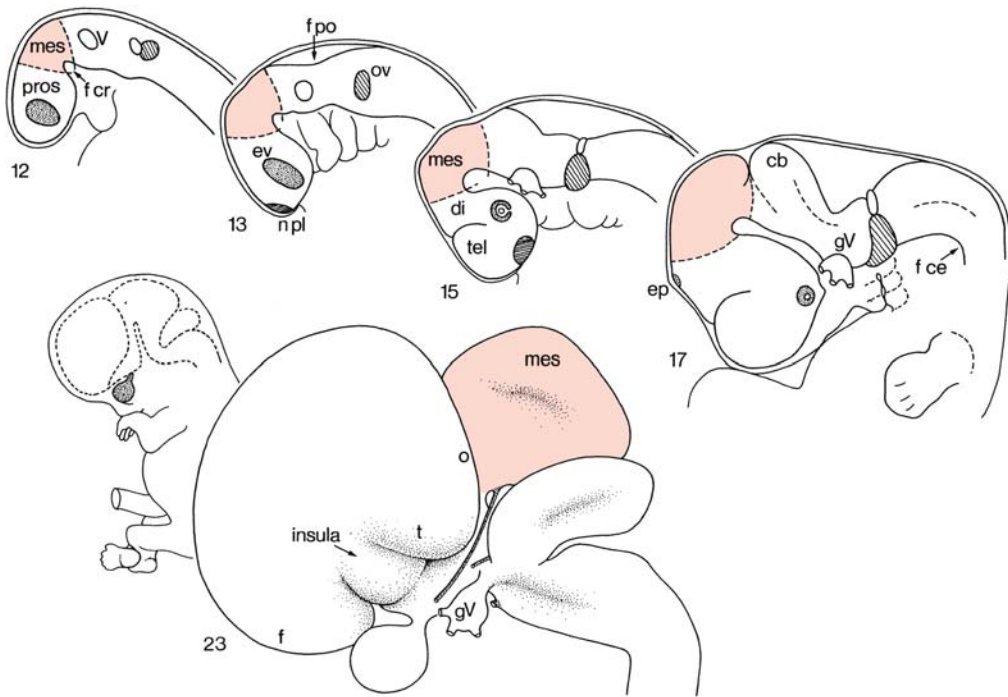
Fig. 1.11 Lateral views of the developing brain in Carnegie stages 12, 13, 15, 17 and 23. The mesencephalon is indicated in *light red*. *cb* cerebellum, *di* diencephalon, *ep* epiphysis, *ev* eye vesicle, *f* frontal lobe, *f ce* flexura cervicalis, *f cr* flexura cranialis, *f po* flexura pontina, *gV*, *V* trigeminal ganglion, *mes* mesencephalon, *n pl* nasal placode, *o* occipital lobe, *pros* prosencephalon, *t* temporal lobe, *tel* telencephalon. (After O'Rahilly and Müller 1999)

already mentioned MHB (Fig. 1.10). They provide a source of secreted factors that establish the regional identity in adjacent domains of the neural tube. The posterior limit of *Otx2* expression marks the anterior limit of the MHB, whereas the anterior limit of *Gbx2* expression marks its posterior limit. In *Otx2* knockout mice, the rostral neuroectoderm is not formed, leading to the absence of the prosencephalon and the rostral part of the brain stem (Acampora et al. 2001; Wurst and Bally-Cuif 2001). In *Gbx2* knockouts, all structures arising from the first three rhombomeres, such as the cerebellum, are absent. Cells in the MHB (the **isthmic organizer**) secrete fibroblast growth factor (FGFs) and *Wnt* proteins which are required for the differentiation and patterning of the midbrain and hindbrain (Rhinn and Brand 2001). Signals from the **anterior neural ridge** including FGF8 regulate the expression of *Foxg1* (earlier known as *brain factor 1*, *BF1*), a transcription factor that is required for normal telencephalic and cortical morphogenesis (Rubinstein and Beachy 1998; Monuki and Walsh 2001). Although much of our insight into these patterning mechanisms relies on studies in mice, humans are subject to a wide variety of naturally occurring mutations (Chap. 9).

1.7   Early Development of the Brain

Lateral and medial views of the developing brain are shown in Figs. 1.11 and 1.12. The neural tube becomes bent by three flexures: (1) the **mesencephalic flexure** at the midbrain level, already evident before fusion of the neural folds; (2) the **cervical flexure**, situated at the junction between the rhombencephalon and the spinal cord, and (3) the **pontine flexure** in the hindbrain. The three main divisions of the brain (prosencephalon, mesencephalon and rhombencephalon) can already be recognized when the neural tube is not yet closed. The forebrain soon divides into an end portion, the **telencephalon**, and the **diencephalon** that can be identified because it gives rise to the optic vesicles (Fig. 1.12). With the development of the **cerebellum**, the pons and the trigeminal nerve, the division of the hindbrain into a rostral part, the **metencephalon**, and a caudal part, the **medulla oblongata** or **myelencephalon**, becomes evident. The junction between the hindbrain and midbrain is relatively narrow and is known as the **isthmus rhombencephali**. The first part of the telencephalon that can be recognized is the **telencephalon medium** or **impar**. By stage 15, the future cerebral hemispheres can be recognized. The **cerebral hemispheres**
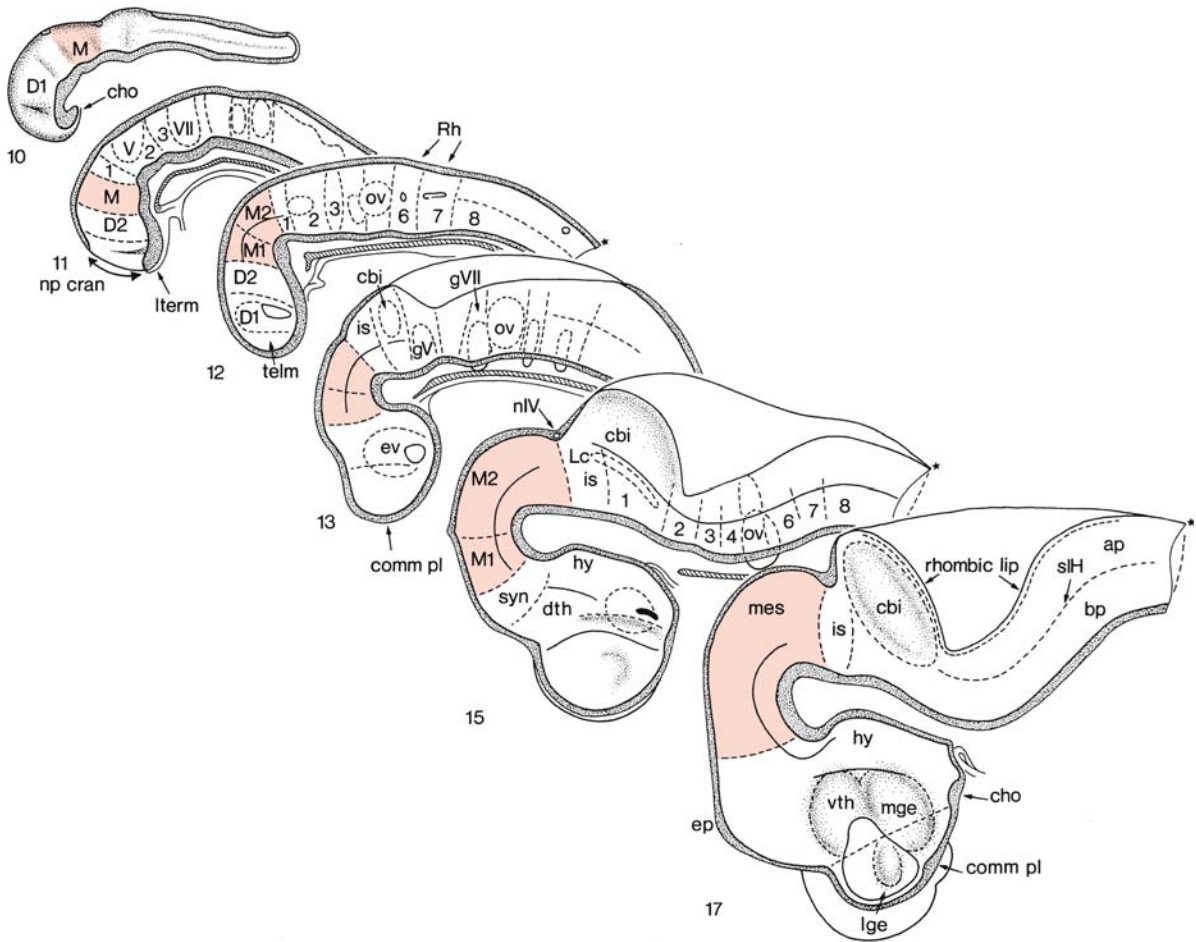
Fig. 1.12 Medial views of the developing brain in Carnegie stages 10–13, 15 and 17. The mesomeres (*M*, *M1*, *M2*) and the mesencephalon (*mes*) are indicated in *light red*. *Asterisks* indicate the spinomedullary junction. *ap* alar plate, *bp* basal plate, *cbi* internal cerebellar bulge, *cho* chiasma opticum, *comm pl* commissural plate, *D1*, *D2* diencephalic neuromeres, *dth* dorsal thalamus, *ep* epiphysis, *ev* eye vesicle, *gV* trigeminal ganglion, *gVII* facial ganglion, *hy* hypothalamus, *is* isthmus, *Lc* locus coeruleus, *lge* lateral ganglionic eminence, *lterm* lamina terminalis, *mge* medial ganglionic eminence, *np cran* cranial neuropore *nIV* nervus trochlearis, *ov* otic vesicle, *1–8* rhombomeres, *slH* sulcus limitans of His, *syn* synencephalon, *telm* telencephalon medium, *vth* ventral thalamus. (After O'Rahilly and Müller 1999)

enlarge rapidly so that by the end of the embryonic period they completely cover the diencephalon. Frontal, temporal and occipital poles and the insula become recognizable (Fig. 1.11), whereas an olfactory bulb becomes visible on the ventral surface.

1.7.1 Imaging of the Embryonic Brain

The introduction of the ultrasound method has opened new possibilities for studying the human embryonic brain. The use of the transvaginal route has so greatly improved the image quality that a detailed description of the living embryo and early fetus has become possible (Fig. 1.13). Ultrasound data show agreement with the developmental time schedule described in the Carnegie staging system (Blaas et al. 1994, 1995a, b; Blaas and Eik-Nes 1996; van Zalen-Sprock et al. 1996; Blaas 1999; Pooh et al. 2003). Human development and possible maldevelopment can be followed in time. The extension of the ultrasound techniques to three dimensions has made it possible to reconstruct the shape of the brain ventricles and to measure their volumes (Blaas et al. 1995a, b; Blaas 1999; Blaas and Eik-Nes 2002). Anomalies of the ventricular system such as diverticula are rare (Hori et al. 1983, 1984a). Accessory ventricles of the posterior horn are relatively common and develop postnatally (Hori et al. 1984b; Tsuboi et al. 1984).
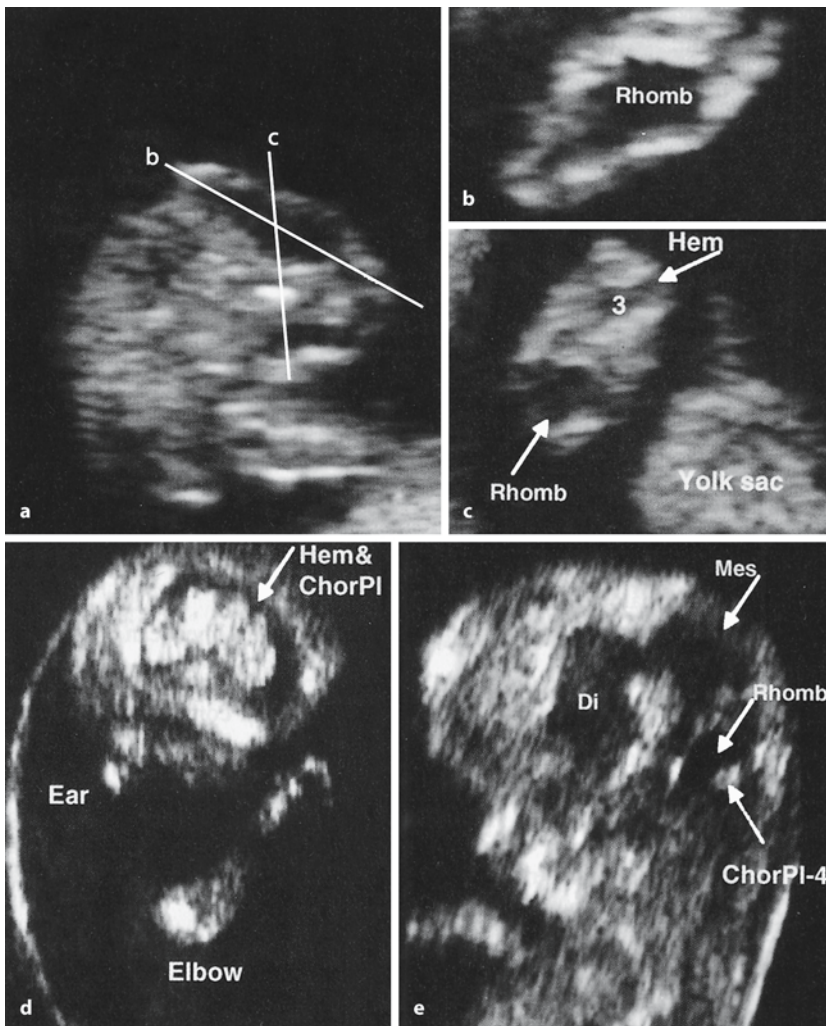
Fig. 1.13 Ultrasound images in human embryos of 7.5 (**a**–**c**), 9.5 (**d**) and 10 (**e**) weeks of gestation with crown–rump lengths of 11, 29 and 33 mm, respectively. *ChorP1-4* choroid plexuses of lateral and fourth ventricles, *Di* diencephalon, *Hem* cerebral hemisphere, *Mes* mesencephalon, *Rhomb* rhombencephalon, *3* third ventricle. (Kindly provided by Harm-Gerd K. Blaas, Trondheim)

1.7.2   Neuromeres

Morphological segments or neuromeres of the brain were already known to von Baer (1828), and were described for the human brain by Bartelmez (1923) and Bergquist (1952), and for many other vertebrates (Nieuwenhuys 1998). **Neuromeres** are segmentally arranged transverse bulges along the neural tube, particularly evident in the hindbrain (Fig. 1.14). Only recently, interest in neuromeres was greatly renewed owing to the advent of gene-expression studies on development, starting with the homeobox genes. The expression of *HOX* genes in the developing human brain stem is directly comparable to that of *Hox* genes in mice (Vieille-Grosjean et al. 1997). Each rhombomere is characterized by a unique combination of *Hox* genes, its *Hox* code. The timing and sequence of appearance of neuromeres and their derivatives were studied in staged human embryos (Müller and O'Rahilly 1997; Fig. 1.15). The neuromeres of the forebrain, midbrain and hindbrain were determined morphologically on the basis of sulci, mitotic activity in the walls and fibre tracts. Six **primary neuromeres** appear already at stage 9 when the neural folds are not fused (Fig. 1.7b): prosencephalon, mesencephalon and four rhombomeres (A–D). Sixteen **secondary neuromeres** can be recognized from about stage 11. They gradually fade after stage 15 (Fig. 1.12). Eight **rhombomeres (Rh1–Rh8)**, an **isthmic neuromere (I)**, two **mesomeres (M1, M2)** of the midbrain, two **diencephalic neuromeres (D1, D2)** and one **telencephalic neuromere (T)** can be distinguished. The diencephalic neuromere D2 can be further subdivided into the **synencephalon,** the **parencephalon caudalis** and the **parencephalon rostralis.** Neuromere D1 gives rise to the eye vesicles and the medial ganglionic eminences (Müller and O'Rahilly 1997).

Each neuromere has **alar** (dorsal) and **basal** (ventral) components. In the developing spinal cord and brain stem, the **sulcus limitans** divides the proliferative compartments into alar and basal plates. The

Fig. 1.14 Dorsal view of a malformed embryo (Carnegie stage 14) showing the bulging of several rhombomeres (kindly provided by Kohei Shiota, Kyoto)

mesencephalic part of the sulcus is not continuous with a more rostral, diencephalic sulcus (Keyser 1972; Gribnau and Geijsberts 1985; Müller and O'Rahilly 1997; Fig. 1.12). Studies in mice (Bulfone et al. 1993; Puelles and Rubinstein 1993; Shimamura et al. 1995; Rubinstein et al. 1998) show that some genes are expressed in the alar plate only, others only in the basal plate (Fig. 1.10). One gene, *Nkx2.2*, is expressed along the longitudinal axis of the brain, ending in the chiasmatic region. On the basis of these findings, in all murine prosomeres alar and basal parts are distinguished (Rubinstein et al. 1998; Puelles et al. 2000; Puelles and Rubinstein 2003).

In mice (Fig. 2.9b), the prosencephalon has been divided into six **prosomeres**, numbered P1–P6 from caudal to rostral. Prosomeres P1–P3 form the diencephalon: P1 is the synencephalon, P2 the parencephalon caudalis and P3 the parencephalon rostralis. The alar component of the synencephalon forms the pretectum, that of the caudal parencephalon the dorsal thalamus and epithalamus and that of the rostral parencephalon the ventral thalamus. The basal components jointly form the prerubral tegmentum. Prosomeres P4–P6, together known as a protosegment, form the **secondary prosencephalon** (Rubinstein et al. 1998; Puelles et al. 2000; Puelles and Rubinstein 2003), from which the hypothalamus, both optic vesicles and the telencephalon arise. The basal parts of the secondary prosencephalon give rise to the various subdivisions of the hypothalamus, whereas from the alar parts prethalamic areas and the entire telencephalon, i.e. the cerebral cortex and the subcortical centers such as the basal ganglia, arise. The main differences between human and murine neuromeres concern the prosomeres. Puelles and Verney (1998) applied the prosomeric subdivision to the human forebrain.

Fig. 1.15 Median section of a stage 13 embryo. Rhombomeres *2, 4* and *6* can be recognized by ventral bulges. *cb* cerebellum, *is* isthmus, *M1, M2* mesomeres, *Rp* Rathke's pouch, *syn* synencephalon, *tel* telencephalon, *v4* fourth ventricle. (From O'Rahilly 1975, with permission)
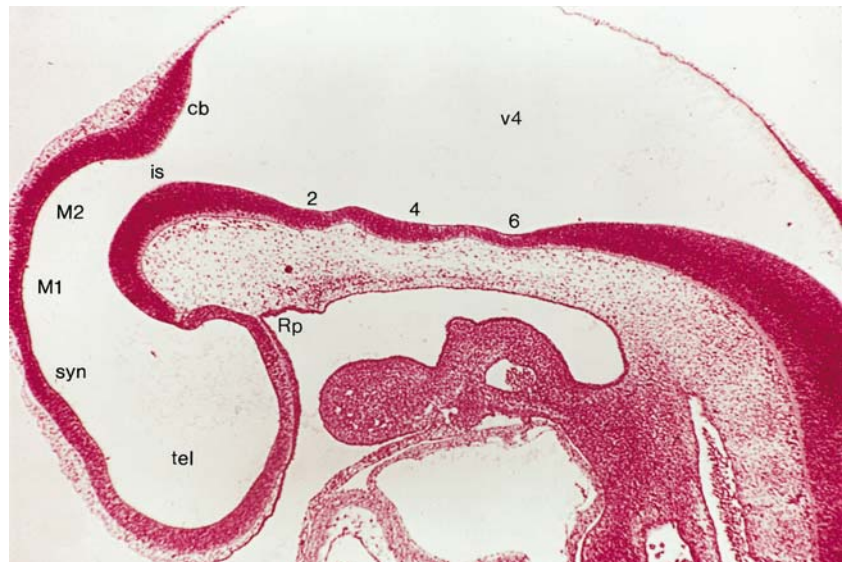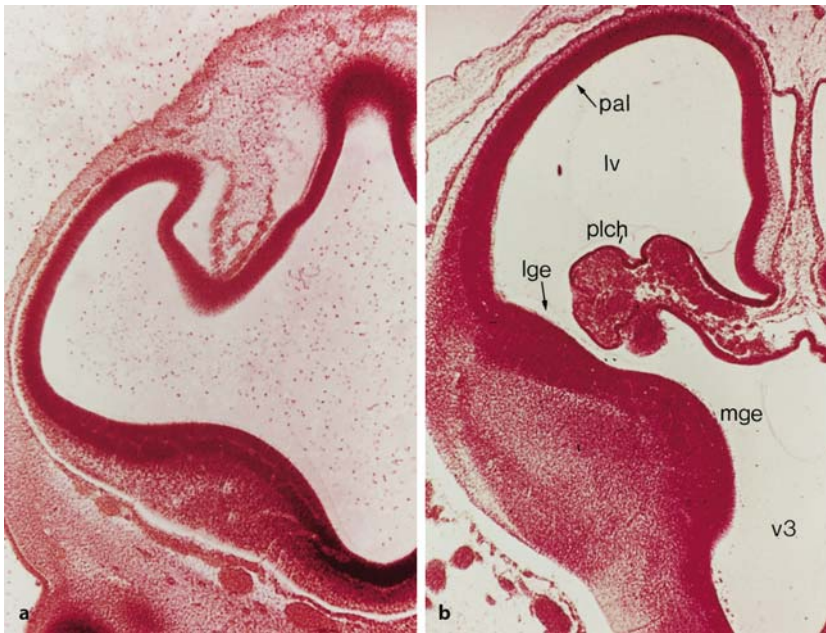
Fig. 1.16 Transverse sections through the human forebrain, showing the developing ganglionic or ventricular eminences at stages 17 (**a**) and 20 (**b**), respectively. *lge* lateral ganglionic eminence, *lv* lateral ventricle, *mge* medial ganglionic eminence, *pal* pallium, *plch* plexus choroideus, *v3* third ventricle. (From O'Rahilly 1975, with permission)

1.7.3   The Ganglionic Eminences

At first, each cerebral hemisphere consists of a thick basal part, the **subpallium**, giving rise to the basal ganglia, and a thin part, the **pallium**, that becomes the future cerebral cortex. The subpallium appears as medial and lateral elevations, known as the **ganglionic** (*Ganglionhügel* of His 1889) or **ventricular eminences** (Fig. 1.16). The caudal part of the ventricular eminences is also known as the **caudal ganglionic eminence**, and primarily gives rise to parts of the amygdala. The **medial ganglionic eminence** is derived from the diencephalon, and is involved in the formation of the globus pallidus. The larger **lateral ganglionic eminence** is derived from the telencephalon, and gives rise to the caudate nucleus and the putamen. As the internal capsule develops, its fibres separate the caudate nucleus from the putamen, and the thalamus and the subthalamus from the globus pallidus. Both the lateral and the medial ventricular eminences are also involved in the formation of the cerebral cortex. The pyramidal cells of the cerebral cortex arise from the ventricular zone of the pallium, but the cortical GABAergic interneurons arise from both ganglionic eminences, the medial eminence in particular (Parnavelas 2000; Anderson et al. 2001; Marín and Rubinstein 2001; Chap. 9). The caudal part of the ganglionic eminence also gives rise to a contingent of GABAergic neurons for dorsal thalamic association nuclei such as the pulvinar through a transient fetal structure, the **gangliothalamic body** (Rakić and Sidman 1969; Letinić and Kostović 1997; Letinić and Rakic 2001).

1.8   Fetal Development of the Brain

The most obvious changes in the fetal period are (1) the outgrowth of the cerebellar hemispheres and the formation of its median part, the vermis, (2) the continuous expansion of the cerebral hemispheres, the formation of the temporal lobe and the formation of sulci and gyri and (3) the formation of commissural connections, the corpus callosum in particular.

1.8.1   The Cerebellum

The development of the **cerebellum** takes place largely in the fetal period (Fig. 1.17). The cerebellum arises bilaterally from the alar layers of the first rhombomere (Fig. 1.12). Early in the fetal period, the two cerebellar primordia are said to unite dorsally to form the vermis. Sidman and Rakic (1982), however, advocated Hochstetter's (1929) view that such a fusion does not take place, and suggested one cerebellar primordium (the **tuberculum cerebelli**). The tuberculum cerebelli consists of a band of tissue in the dorsolateral part of the alar plate that straddles the midline in the shape of an inverted V. The arms of the V are directed caudally as well as laterally, and thicken enormously, accounting for most of the early growth of the cerebellum. The rostral, midline part of the V, however, remains small and relatively inconspicuous. The further morphogenesis of the cerebellum can be summarized as follows: (1) the caudally and laterally directed limbs of the tuberculum cerebelli thicken rapidly during the sixth postovulatory week and bulge downwards into the fourth ventricle
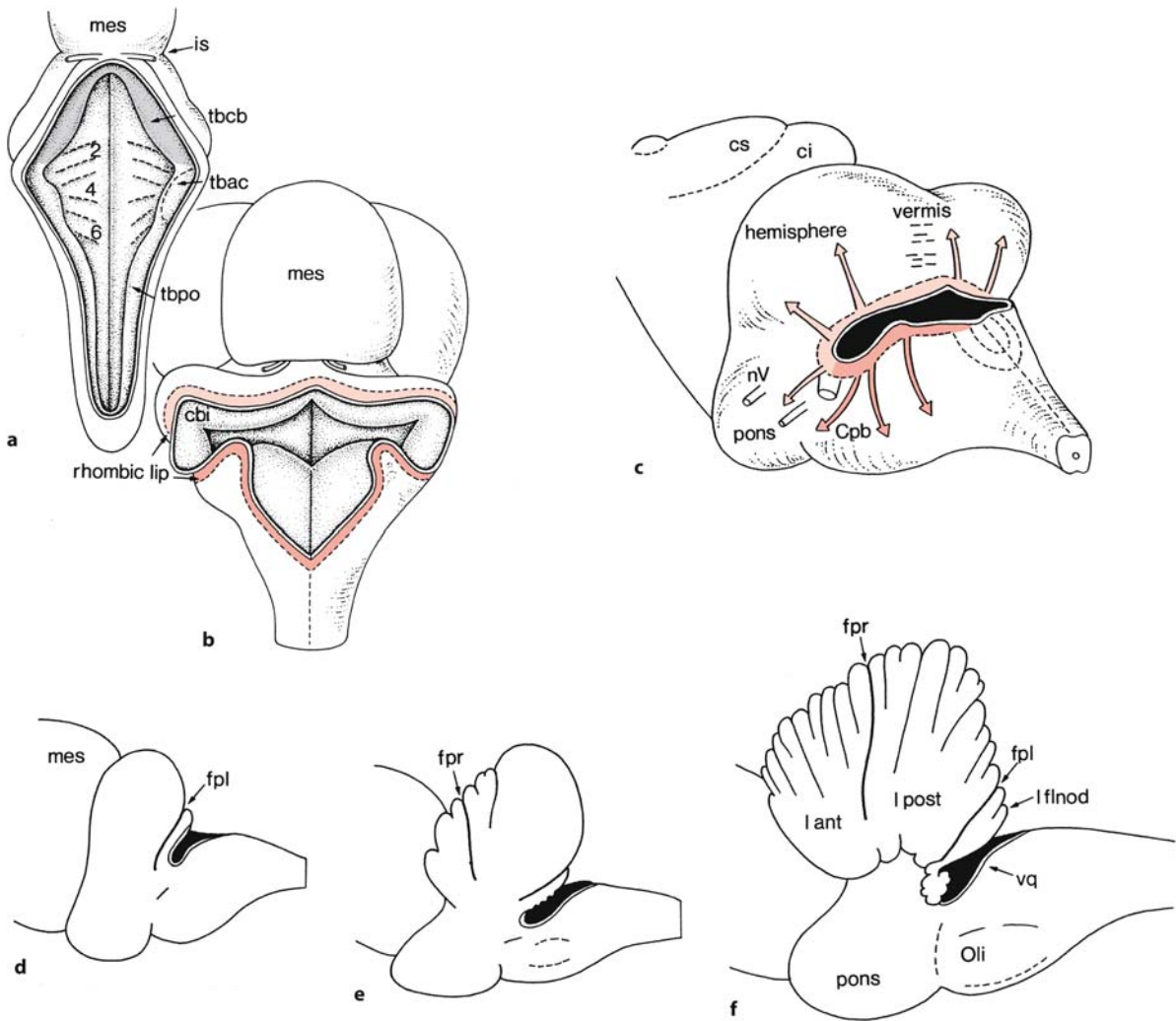
Fig. 1.17 Embryonic (**a**, **b**) and fetal (**c**–**f**) development of the human cerebellum: **a** at approximately 4 weeks; **b** at the end of the embryonic period; **c**–**f** at 13 weeks (**c**, **d**), and 4 (**e**) and 5 (**f**) months of development. The V-shaped tuberculum cerebelli (*tbcb*) is indicated in *grey*, and the upper and lower rhombic lips in *light red* and *red*, respectively. *cbi* internal cerebellar bulge, *ci* colliculus inferior, *Cpb* corpus pontobulbare, *cs* colliculus superior, *fpl* fissura posterolateralis, *fpr* fissura prima, *is* isthmus, *l ant* lobus anterior, *l flnod* lobus flocculonodularis, *l post* lobus posterior, *mes* mesencephalon, *nV* trigeminal nerve, *Oli* oliva inferior, *tbac* tuberculum acusticum, *tbpo* tuberculum ponto-olivare, *vq* ventriculus quartus, *2*, *4*, *6* rhombomeres. (**a** After Streeter 1911, 1912; Jakob 1928; **b** after Hochstetter 1929; **c**–**f** after Streeter 1911, 1912)

(on each side the internal cerebellar bulge or *innerer Kleinhirnwulst* of Hochstetter which together form the **corpus cerebelli**); (2) during the seventh week, the rapidly growing cerebellum bulges outwards as the external cerebellar bulges (*äusserer Kleinhirnwulst* of Hochstetter) which represent the **flocculi**, which are delineated by the posterolateral fissures; (3) during the third month of development, i.e. early in the fetal period, growth of the midline component accelerates and begins to fill the gap between the limbs of the V, thereby forming the **vermis**; and (4) by the 12th to 13th weeks of development, outward, lateral and rostral growth processes have reshaped the cerebellum to a transversely oriented bar of tissue overriding the fourth ventricle. At the 12th week, fissures begin to form transverse to the longitudinal axis of the brain, first on the vermis and then spreading laterally into the hemispheres. By stage 18 (approximately 44 days), the internal cerebellar swellings contain the dentate nuclei, the first sign of the superior cerebellar peduncles can be seen around stage 19 (about 48 days) and the cerebellar commissures appear at the end of the embryonic period (Müller and O'Rahilly 1990b).
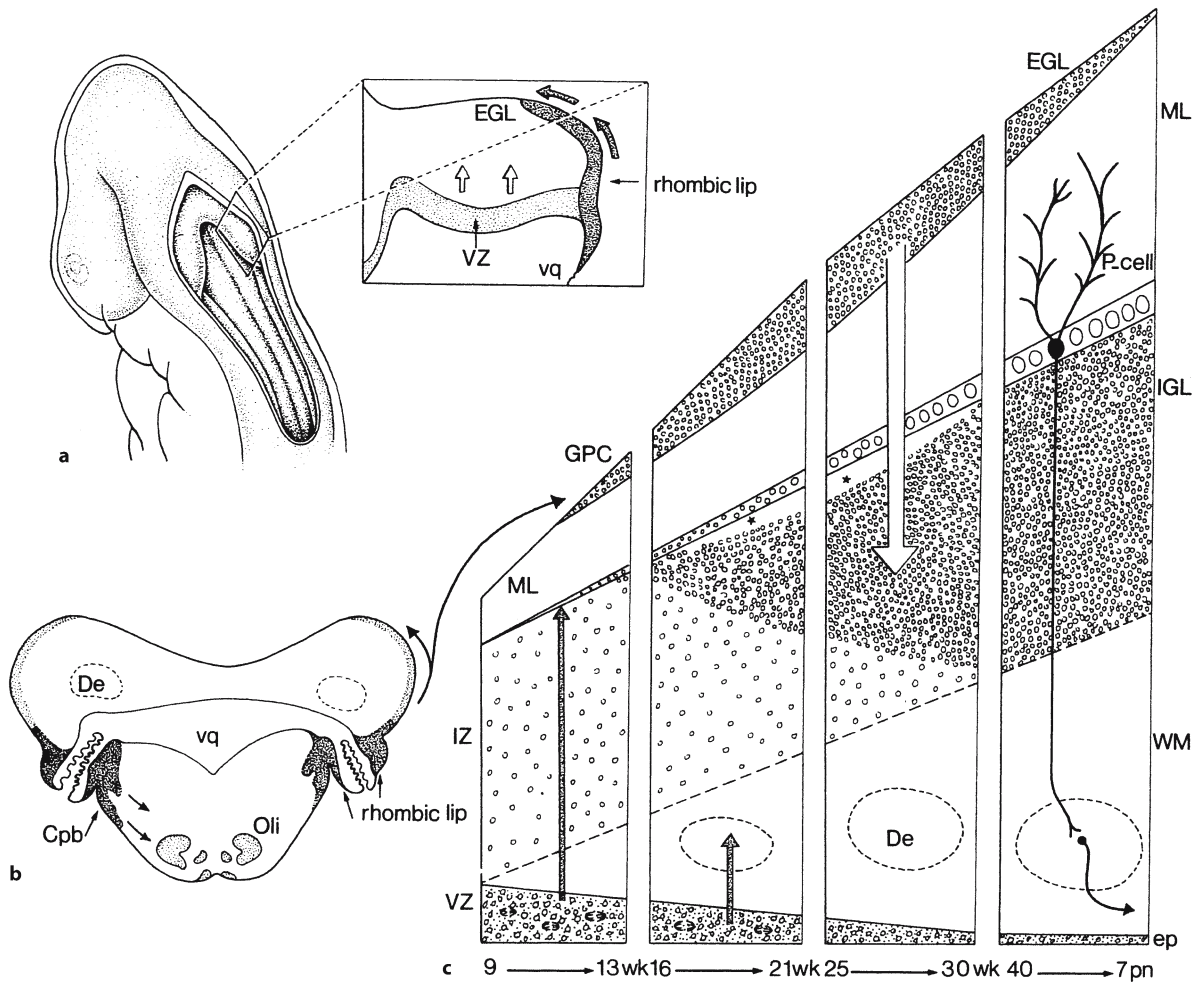
Fig. 1.18 Overview of the histogenesis of the cerebellum. **a** A dorsolateral view of a human embryo and part of the tuberculum cerebelli enlarged, showing the two proliferative compartments: the ventricular zone (*VZ*), giving rise to Purkinje cells and the deep cerebellar nuclei, and the external germinal or granular layer (*EGL*), giving rise to the granule cells. **b** The position of the rhombic lip in a transverse section at the level of the lateral recess of the fourth ventricle. The upper rhombic lip is found lateral to the lateral recess, and the lower rhombic lip medial to the recess. **c** The formation of the layers of the cerebellum in four periods from the early fetal period until 7 weeks postnatally. The lamina dissecans is indicated with *asterisks*. The *arrows* in **a**–**c** show the migration paths. *Cpb* corpus pontobulbare, *De* dentate nucleus, *ep* ependyma, *GPC* granule precursor cells, *IGL* internal granular layer, *IZ* intermediate zone, *ML* molecular layer, *Oli* oliva inferior, *P-cell* Purkinje cell, *vq* ventriculus quartus, *WM* white matter. (After Sidman and Rakic 1982; Hatten et al. 1997; O'Rahilly and Müller 2001; from ten Donkelaar et al. 2003, with permission)

The **histogenesis** of the cerebellum is summarized in Fig. 1.18. The main cell types of the cerebellum arise at different times of development and at different locations. The Purkinje cells and the deep cerebellar nuclei arise from the ventricular zone of the metencephalic alar plates. Bayer et al. (1995) estimated that in man the deep cerebellar nuclei as well as the Purkinje cells are generated from the early fifth to sixth weeks of development. Towards the end of the embryonic period, granule cells are added from the rhombic lip. The **rhombic lip** (*Rautenleiste* of His 1890) is the dorsolateral part of the alar plate, and it forms a proliferative zone along the length of the hindbrain. Cells from its rostral part, the **upper rhombic lip**, reach the superficial part of the cerebellum, and form the **external germinal** or **granular layer** at the end of the embryonic period. Granule cells are formed in the external germinal layer. The granule cells that arise from it migrate along the processes of Bergmann glia cells to their deeper, definitive site. Adhesion molecules such as TAG1, L1 and astrotactin play a role in this migration (Hatten et al.
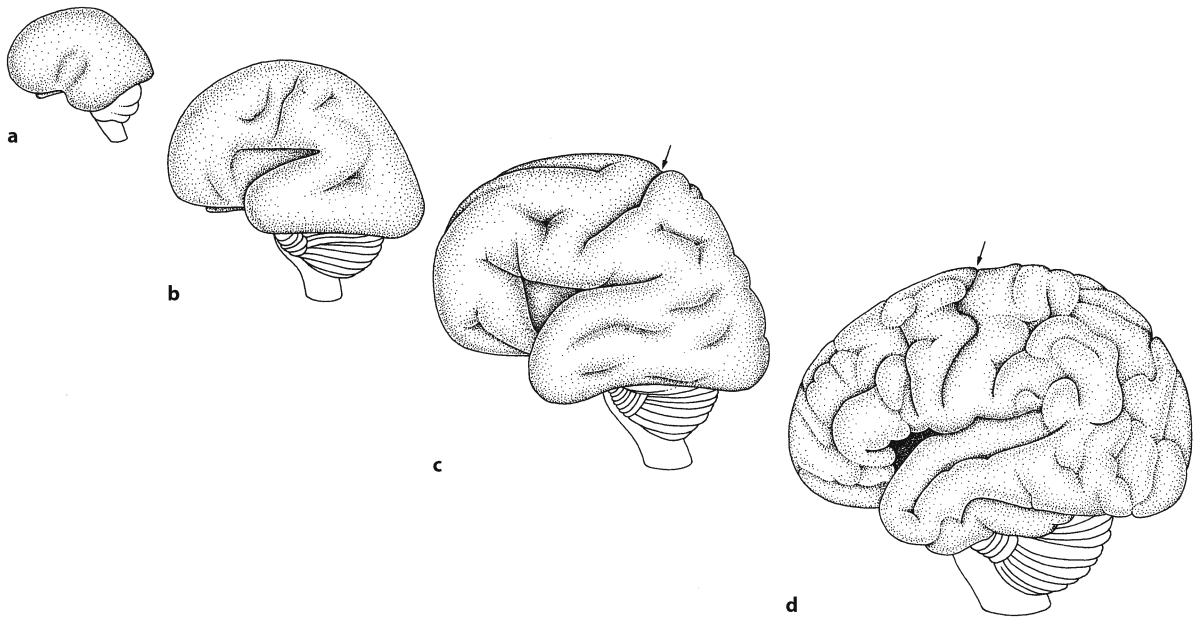
Fig. 1.19 Lateral views of the developing human brain in the fourth (**a**), sixth (**b**) and eighth (**c**) gestational months, and in a neonate (**d**). The *arrows* indicate the central sulcus. (After Kahle 1969; O'Rahilly and Müller 1999)

1997). In the fetal period, the **internal granular layer** is formed by further proliferation and migration of the external germinal cells. This layer, situated below the layer of Purkinje cells, is the definitive granular layer of the cerebellar cortex. A transient layer, the **lamina dissecans**, separates the internal granular layer from the Purkinje cells. Ultimately, it is filled by migrating granular cells and disappears (Rakic and Sidman 1970). At the same time as the postmitotic granule cells migrate inwards (16–25 weeks), the Purkinje cells enlarge and develop dendritic trees. In man, the external germinal layer appears at the end of the embryonic period and persists for several months to 1–2 years after birth (Lemire et al. 1975). The caudal part of the rhombic lip, the **lower rhombic lip**, gives rise to the pontine nuclei and the inferior olivary nucleus (Essick 1912; Wingate 2001; Fig. 1.17 c). Neurons of these precerebellar nuclei migrate along various pathways, the **corpus pontobulbare** in particular, to their ultimate position in the brain stem (Altman and Bayer 1997).

Several genes have a marked impact upon cerebellar development. In mice, knockouts of the *Wnt1* and *En1* genes largely or totally eliminate the cerebellum, whereas in *En2* knockouts the lobular pattern of the posterior vermis is disrupted (Hatten et al. 1997; Millen et al. 1999; Wang and Zoghbi 2001). The *Math1* (mouse atonal homologue) gene is expressed in the rhombic lip (Ben-Arie et al. 1997). In *Math1* knockout mice, no granular layer is formed. SHH is expressed in migrating and settled Purkinje cells, and acts as a potent mitogenic signal to expand the granule cell progenitor population (Wechsler-Reya and Scott 1999). *Medulloblastoma*, a brain stem tumour of childhood, is thought to originate in malignant external granule cells. **Developmental malformations** of the cerebellum are mostly bilateral and may be divided into (1) malformations of the vermis and (2) malformations of the vermis as well as of the hemispheres (Norman et al. 1995; Kollias and Ball 1997; Ramaeckers et al. 1997; Barkovich 2000; ten Donkelaar et al. 2003). *Agenesis* or *hypoplasia* of the *vermis* may occur in a great variety of disorders, most frequently in the *Dandy–Walker malformation* (Chap. 8). *Pontocerebellar hypoplasia* forms a large group of disorders, characterized by a small pons and a varying degree of hypoplasia of the cerebellum (Barth 1993; Ramaeckers et al. 1997), up to its near-total absence (Gardner et al. 2001).

1.8.2   The Cerebral Cortex

The outgrowth of the **cerebral cortex** and the proliferation and migration of cortical neurons largely takes place in the fetal period. Each hemisphere first grows caudalwards, and then bends to grow in ventral and rostral directions (Figs. 1.19, 1.20). In this way the temporal lobe arises. The outgrowth of the caudate nucleus, the amygdala, the hippocampus and the lateral ventricle occurs in a similar, C-shaped way. During the fetal period, the complex pattern of sulci
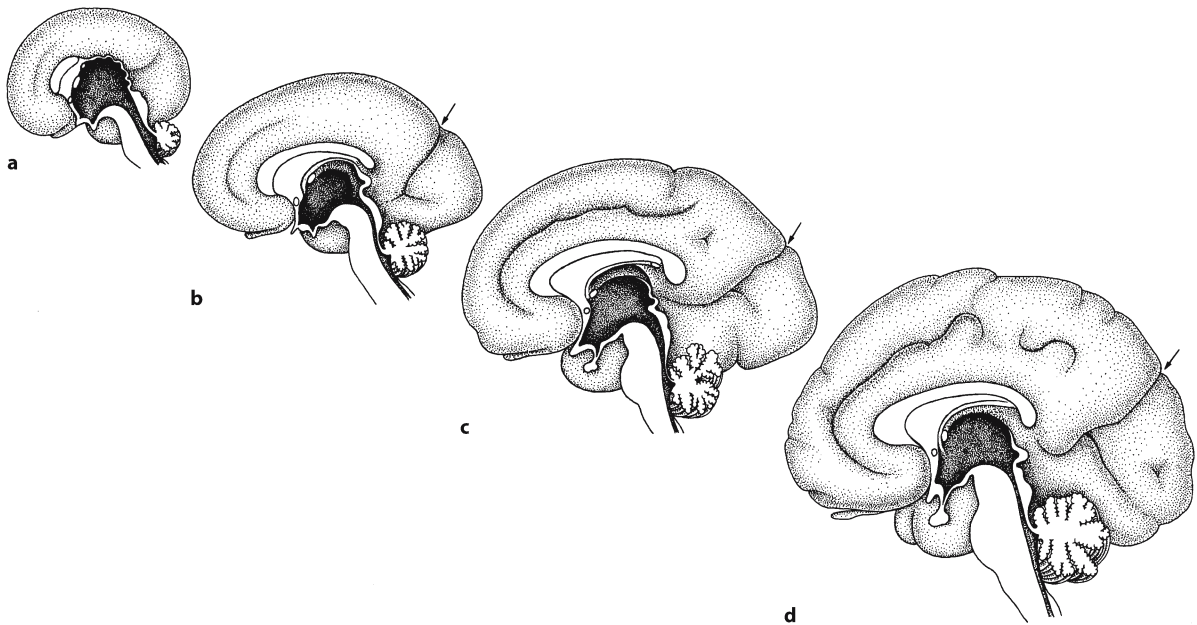
Fig. 1.20 Medial views of the developing human brain at the end of the fourth (**a**), sixth (**b**) and eighth (**c**) gestational months, and in a neonate (**d**). The *arrows* indicate the sulcus parieto-occipitalis. (After Macchi 1951, Kahle 1969 and Feess-Higgins and Larroche 1987)

and gyri arises. On the lateral surface of the brain the **sulcus lateralis** and the **sulcus centralis** can be recognized from 4 months onwards. Owing to the development of the prefrontal cortex, the sulcus centralis gradually moves caudalwards. On its medial surface first the parieto-occipital and cingulate sulci appear, followed by the calcarine and central sulci. The formation of sulci and gyri in the right hemisphere usually preceeds that in the left one. The **plexus choroideus** of the lateral ventricle arises in the lower part of the medial wall of the telencephalic vesicle (Fig. 1.16).

Usually, the **pallium** is divided into a **medial pallium** or **archipallium**, a **dorsal pallium** or **neopallium** and a **lateral pallium** or **paleopallium** (Fig. 1.21). Recently, an additional **ventral pallium** was added (Puelles et al. 2000; Marín and Rubinstein 2002; Schuurmans and Guillemot 2002). The medial pallium forms the hippocampal cortex, the three-layered allocortex. Parts of the surrounding transitional cingulate and entorhinal cortex, the four-to-five-layered mesocortex, may have the same origin. The dorsal pallium forms the six-layered isocortex. The lateral pallium forms the olfactory cortex and the ventral pallium the claustroamygdaloid complex. The **subpallium** consists of two progenitor domains, the lat-

eral and medial ganglionic eminences, generating the striatum and the pallidum, respectively. Dorsal and ventral domains of the developing telencephalon are distinguished by distinct patterns of gene expression, reflecting the initial acquisition of regional identity by progenitor populations (Puelles et al. 2000; Schuurmans and Guillemot 2002; Chap. 9).

The **hippocampal formation** or **formatio hippocampi** comprises the dentate gyrus, the hippocampus, the subiculum and the parahippocampal gyrus. These structures develop from the medial pallium and are originally adjacent cortical areas (Fig. 1.22). During the outgrowth of the cerebral hemispheres, first caudalwards and subsequently ventralwards and rostralwards, the *retrocommissural part* of the hippocampal formation becomes situated in the temporal lobe (Stephan 1975; Duvernoy 1998). Rudiments of the *supracommissural part* of the hippocampus can be found on the medial side of the hemisphere on top of the corpus callosum: the *indusium griseum*, a thin cell layer, flanked by the *stria longitudinalis medialis* and *lateralis* of Lancisi (Chap. 10). At the beginning of the fetal period, the hippocampal formation contains four layers (Humphrey 1966; Kahle 1969; Arnold and Trojanowski 1996): a ventricular zone, an intermediate layer, a hippocampal plate comprised of

Fig. 1.21 Subdivision of the forebrain into the medial pallium (*MP*), dorsal pallium (*DP*), lateral pallium (*LP*) and ventral pallium (*VP*), and subpallium. *AEP/POA* anterior entopeduncular/preoptic area, *CH* cortical hem, *dLGE* dorsal part of lateral ganglionic eminence, *MGE* medial ganglionic eminence, *vLGE* ventral part of lateral ganglionic eminence. (After Puelles et al. 2000; Schuurmans and Guillemot 2002)
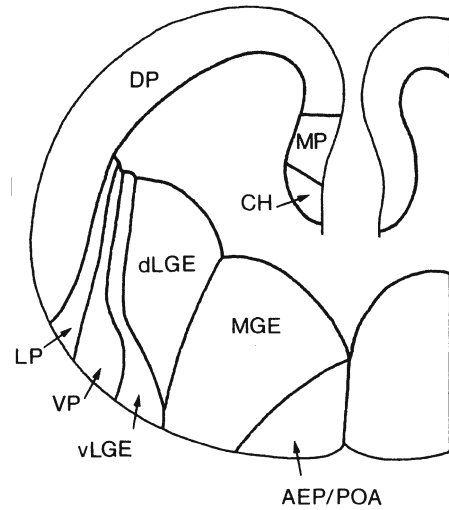
Fig. 1.22 Development (**a**–**c**) and structure (**d**) of the human hippocampal formation. The cornu Ammonis (*CA*) is indicated in *light red*, the dentate gyrus (*GD*) in *red* and the entorhinal cortex (*EC*) in *grey*. *CA1–CA3* cornu Ammonis subfields, *ffor* fimbria fornicis, *GPh* gyrus parahippocampalis, *ship* sulcus hippocampi, *Sub* subiculum
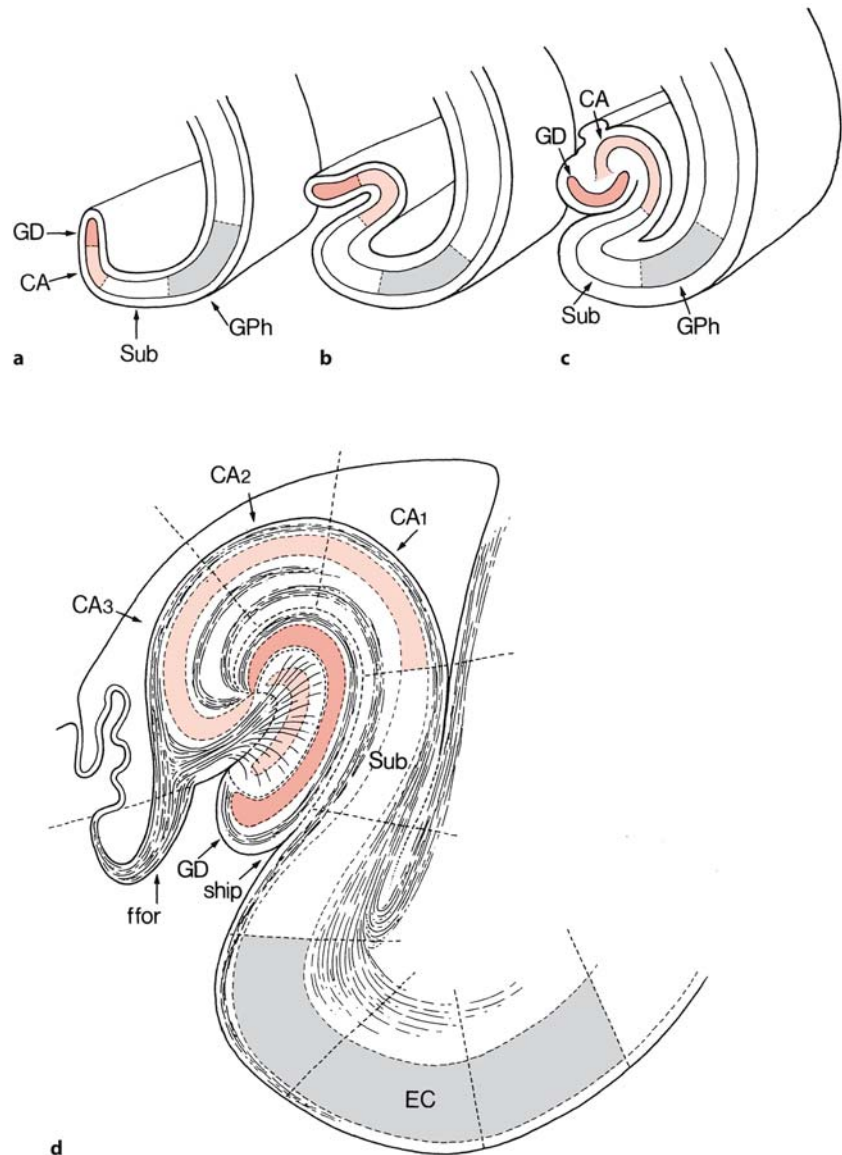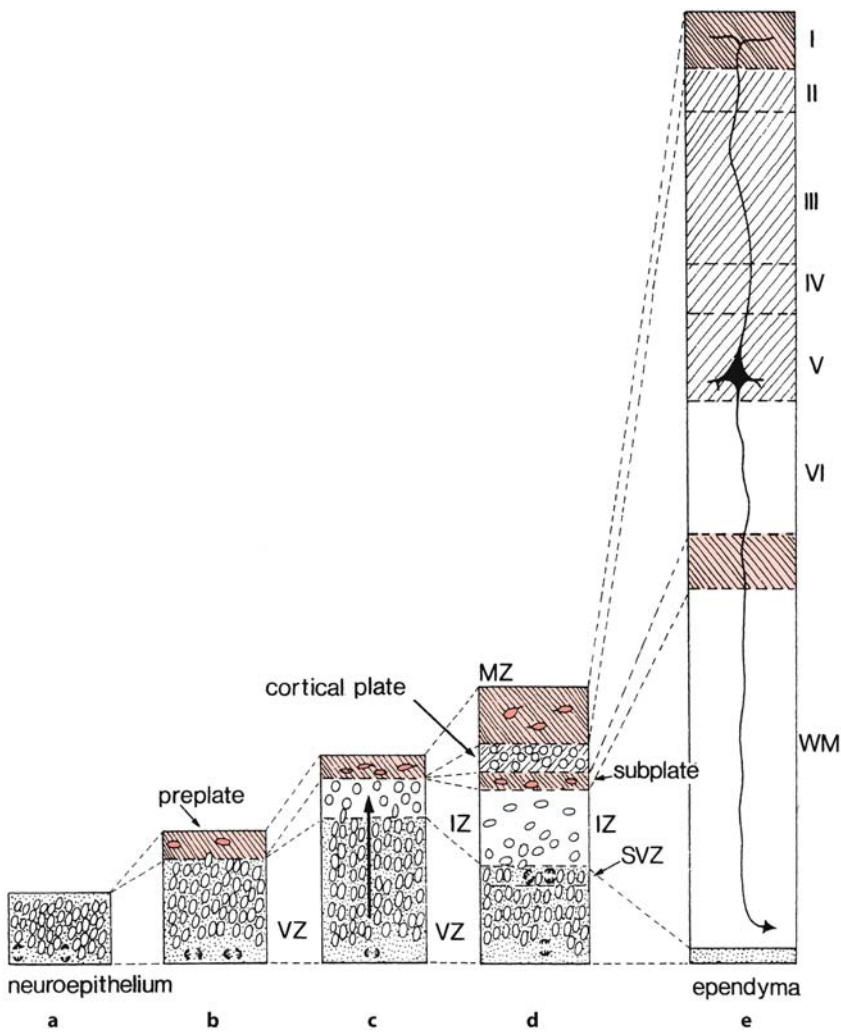
Fig. 1.23 Histogenesis of the cerebral cortex. **a**–**c** The neuroepithelium forms three zones, the ventricular zone (*VZ*), the intermediate zone (*IZ*) and the preplate. During the eighth to 18th weeks of development, neurons migrate from the ventricular zone and form the cortical plate (**d**). The preplate becomes divided into the marginal zone (*MZ*) and the subplate. A second compartment for cell division, the subventricular zone (*SVZ*), is mainly involved in the production of glial cells. Finally (**e**), the marginal zone forms the molecular layer (layer *I*) and the cortical plate layers *II–VI*. The intermediate zone forms the subcortical white matter (*WM*). The subplate disappears. (After O'Rahilly and Müller 1999)

bipolar-shaped neurons, and a marginal zone. At 15–19 weeks of gestation, individual subfields can be distinguished. A distal-to-proximal gradient of cytoarchitectonic and neuronal maturity is found, with the subiculum appearing more developed than the ammonic subfields (CA1–CA3). The dentate gyrus is the latest area to develop. Most pyramidal cells in the cornu Ammonis fields are generated in the first half of pregnancy and no pyramidal neurons are formed after the 24th gestational week (Seress et al. 2001). Granule cells of the dentate gyrus proliferate at a decreasing rate during the second half of pregnancy and after birth but still occur at a low percentage during the first postnatal year (Seress et al. 2001). Reciprocal entorhinal–hippocampal connections are established by fetal midgestation (Hevner and Kinney 1996). Fibres connecting the entorhinal cortex, hippocampus and subiculum are present by about 19 weeks of gestation. The perforant path, connecting the entorhinal cortex with the dentate gyrus, and all connections with the neocortex are only beginning at 22 weeks of gestation.

The **histogenesis** of the six-layered cerebral cortex is shown in Fig. 1.23. The developing cerebral wall contains several transient embryonic zones: (1) the ventricular zone, which is composed of dividing neural progenitor cells; (2) the subventricular zone, which acts early in corticogenesis as a secondary neuronal progenitor compartment and later in development as the major source of glial cells; (3) the intermediate zone, through which migrating neurons traverse along radial glial processes; (4) the subplate, thought to be essential in orchestrating thalamocortical connectivity and pioneering corticofugal projections (Chap. 2); (5) the cortical plate, the initial condensation of postmitotic neurons that will become layers II–VI of the mature cortex; and (6) the marginal zone, the superficial, cell-sparse layer that is important in the establishment of the laminar organization of the cortex.
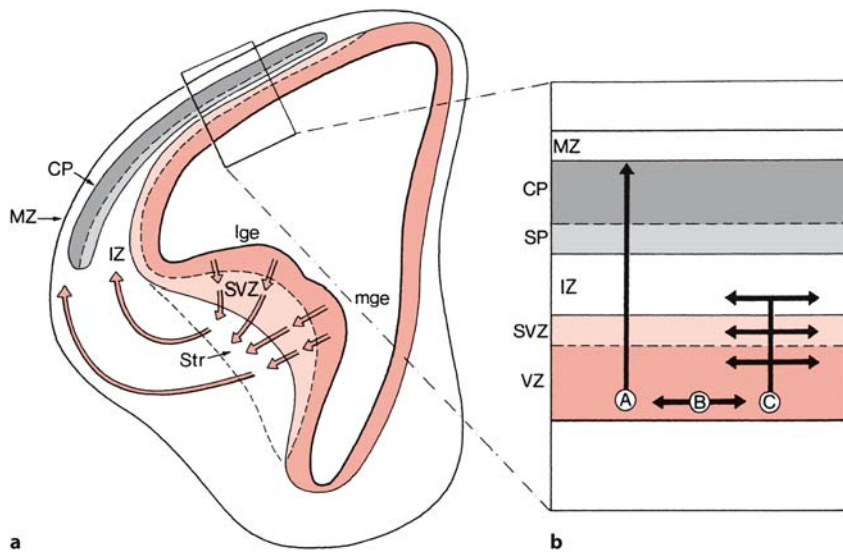
Fig. 1.24 Radial and tangential migration of cortical neurons. **a** The proliferative compartments of the murine telencephalon: the ventricular zone (*VZ*, *red*) and the subventricular zone (*SVZ*, *light red*). Postmitotic GABAergic neurons leave the lateral (*lge*) and medial (*mge*) ganglionic eminences and reach the striatum (*Str*) and through tangential migration the marginal zone (*MZ*) and the intermediate zone (*IZ*). **b** Part of the cortex is enlarged in which radial migration of neurons (*A*) through the subplate (*SP*) to the cortical plate (*CP*) and tangential migration, occurring in the ventricular, subventricular and intermediate zones (*B*, *C*), is indicated. (After Pearlman et al. 1998)

Cortical neurons are generated in the ventricular zones of the cortical walls and ganglionic eminences, and reach their destination by radial and tangential migration, respectively. The first postmitotic cells form the **preplate** or **primordial plexiform layer** (Marín-Padilla 1998; Meyer and Goffinet 1998; Supèr et al. 1998; Zecevic et al. 1999; Meyer et al. 2000). Then, cells from the ventricular zone migrate to form an **intermediate zone** and, towards the end of the embryonic period, the **cortical plate**. This plate develops within the preplate, thereby dividing the preplate into a minor superficial component, the **marginal zone** and a large deep component, the **subplate**. The marginal zone is composed largely of **Cajal–Retzius neurons** (Meyer et al. 1999), secreting the extracellular protein Reelin, and the subplate contains pioneer projection neurons. Reelin is required for the normal inside-to-outside positioning of cells as they migrate from the ventricular zone. The formation of the cortical plate takes place from approximately 7 to 16 weeks. The first cells to arrive will reside in the future layer VI. Cells born later migrate past the already present cortical cells to reside in progressively more superficial layers. In this way, cortical layers VI–II are subsequently formed. The marginal zone becomes layer I, i.e. the molecular or plexiform layer. The subplate gradually disappears. The ventricular zone becomes the ependyma and the intermediate zone

the subcortical white matter. A transient cell layer, the **subpial granular layer** (SGL) of Ranke (1910), originates from the basal periolfactory subventricular zone (Brun 1965; Gadisseux et al. 1992; Meyer and Wahle 1999). It migrates tangentially beneath the pia to cover the neocortical marginal zone from the 14th gestational week onwards. The SGL provides a constant supply of Reelin-producing cells during the critical period of cortical migration, keeping pace with the dramatic growth and surface expansion during corticogenesis. Naturally occurring cell death is an active mechanism contributing to the disappearance of the SGL (Spreafico et al. 1999).

In the telencephalon, **radial migration** is the primary mechanism by which developing neurons arrive at their final position (Rakic 1972). The newly born neuroblasts associate with specialized glial cells known as the radial glial cells. Radial glial cells are bipolar cells with one short process extended to the adjacent ventricular surface and a second projecting to the pial surface (Chap. 2). A two-way signalling process between the migrating neuron and the radial glial fibre permits the neuroblast to migrate, and provides a signal to maintain the structure of the radial glial fibre (Hatten 1999). This process requires known receptors and ligands such as neuregulin and Erb4, cell adhesion molecules, putative ligands with unknown receptors such as astrotactin, and extracellu-

lar matrix molecules and their surface receptors. Blocking any of these components can slow or prevent radial cell migration (Pilz et al. 2002). Cell migration perpendicular to the radial axis, i.e. **tangential migration** (Fig. 1.24), differs from radial cell migration in the direction of movement and in the mechanism of cell guidance. Instead of radial glia, axons appear to be the substrate for at least some nonradial cell migration (Pearlman et al. 1998). Non-radial cell migration provides most, if not all, GABAergic interneurons of the cerebral cortex. This population of cortical neurons migrates from the ganglionic eminences along non-radial routes to reach the cerebral cortex (Anderson et al. 1999, 2001; Lavdas et al. 1999; Marín and Rubinstein 2001). The medial ganglionic eminence is the source of most cortical interneurons, and is also a major source of striatal interneurons (Marín et al. 2000). The tangential migration of postmitotic interneurons from the ganglionic eminences to the neocortex occurs along multiple paths, and is directed in part by members of the Slit and semaphorin families of guidance molecules (Marín et al. 2001).

Malformation of cortical development may be divided into several categories, based on the stage of development (cell proliferation, neuronal migration, cortical organization) at which cortical development was first affected (Barkovich et al. 2001; Chap. 10). Malformations due to abnormal proliferation or apoptosis may lead to extreme microcephaly. Malformations due to abnormal migration, i.e. *neuronal migration disorders* (*NMDs*) have been extensively studied (Gleeson and Walsh 2000; Barkovich et al. 2001; Olson and Walsh 2002; Pilz et al. 2002). Malformations due to abnormal cortical organization include the polymicrogyrias and schizencephalies (Barkovich et al. 2001).

The **olfactory bulbs** evaginate after olfactory fibres penetrate the cerebral wall at the ventrorostral part of the hemispheric vesicles (Pearson 1941). By the end of the sixth week, several bundles of fibres arising in the olfactory placodes have reached the forebrain vesicles. A few days later, a shallow protrusion appears at the site of contact, and between 8 and 13 weeks, the cavity of the evagination enlarges and becomes the olfactory ventricle. The olfactory bulbs gradually elongate rostralwards along the base of the telencephalon. Mitral cells arise from the surrounding ventricular zone. As the olfactory bulbs form, future granule and preglomerular cells are generated in the subventricular zone of the lateral ganglionic eminences, and migrate into each bulb along a rostral migratory stream (Hatten 1999). These neurons move rapidly along one another in chain formations, independent of radial glia or axonal processes. In rats and primates, this migration persists into adulthood

(Doetsch et al. 1997; Kornack and Rakic 2001; Brazel et al. 2003). Numerous cells of the **piriform cortex** originate in a region close to the corticostriatal boundary (Bayer and Altman 1991). They reach the rostrolateral telencephalon via a lateral cortical stream (de Carlos et al. 1996).

1.8.3 Cerebral Commissures

Cerebral commissures arise in a thin plate, the **embryonic lamina terminalis**, i.e. the median wall of the telencephalon rostral to the chiasmatic plate. It is also known as the lamina reuniens or *Schlussplatte* (His 1889, 1904; Hochstetter 1919; Rakic and Yakovlev 1968). At approximately 5 weeks (stage 16), the **commissural plate** appears as a thickening in the embryonic lamina terminalis. The remainder of the lamina then constitutes the adult lamina terminalis (*Endplatte* of His 1889, 1904). The commissural plate gives rise to (Fig. 1.25) (1) the anterior commissure, which appears at the end of the embryonic period and connects the future temporal lobes, (2) the hippocampal commissure, which appears several weeks later and connects the crura of the fornix, and (3) the corpus callosum, which appears early in the fetal period and connects the cerebral hemispheres. The **corpus callosum** is first identified at 11–12 weeks after ovulation, and gradually extends considerably caudalwards. The overlying part of the commissural plate becomes thinned to form the septum pellucidum. Within the septum a narrow cavity appears, the cavum septi pellucidi. The corpus callosum appears to be fully formed by the middle of prenatal life. Partial or complete *absence* of the *corpus callosum* is not uncommon (Aicardi 1992; Norman et al. 1995; Kollias and Ball 1997; Barkovich 2000). Every disorder that influences the development of the commissural plate may lead to this malformation. Dysgenesis of the corpus callosum occurs in approximately 20% of cases as an isolated disorder, but in about 80% of cases in combination with other disorders of the brain (Chap. 10).

1.8.4 Imaging of the Fetal Brain

Fetal magnetic resonance images at 20 and 35 weeks of development are shown in Figs. 1.26 and 1.27, respectively. At 20 weeks of development, cortical layers, the hypodense subplate in particular, can be easily distinguished in the smooth cerebral cortex. Germinal zones are hyperdense. A 35-week-old brain shows the extensive changes that appear in the cerebrum in the second half of pregnancy. Garel's (2004) MRI atlas presents the fetal brain in detail from 20 weeks of development until birth.
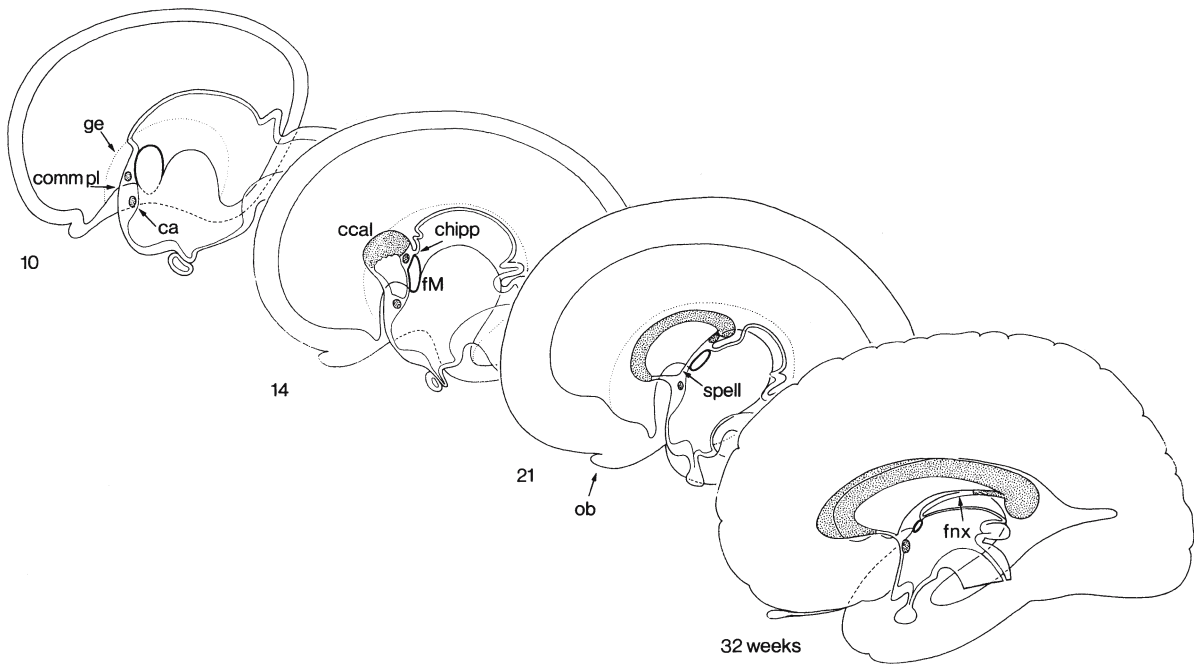
Fig. 1.25 Development of the cerebral commissures at the 10th, 14th, 21st and 32rd weeks of development. *ca* commissura anterior, *ccal* corpus callosum, *chipp* commissura hippocampi, *comm pl* commissural plate, *fM* foramen of Monro, *fnx* fornix, *ge* ganglionic eminence, *ob* olfactory bulb, *spell* septum pellucidum. (After Streeter 1911, 1912)
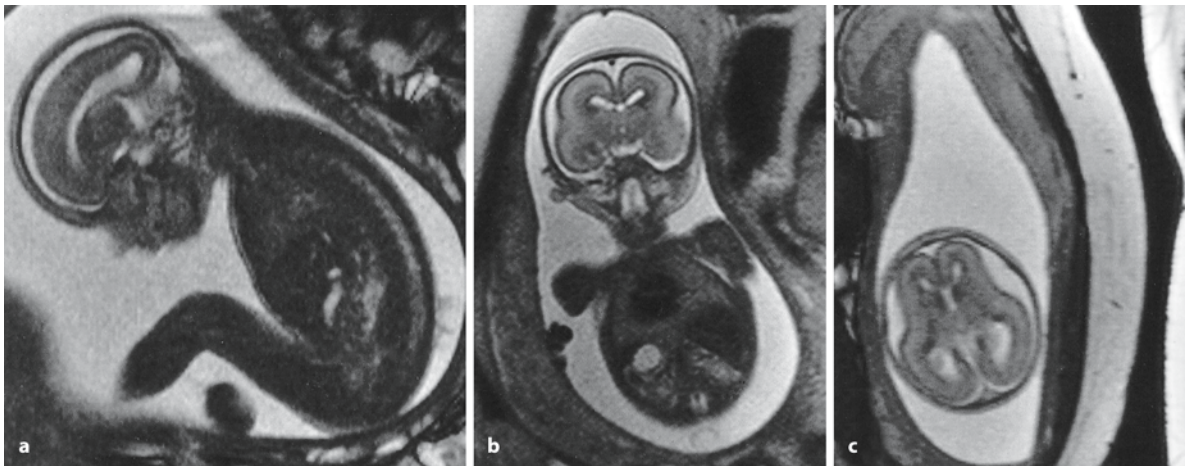
Fig. 1.26 Fetal T2-weighted MRI taken at the 20th week of development: **a** sagittal section; **b** frontal (or coronal) section; and **c** horizontal (or axial) section. There is a smooth cerebral surface without gyration. The thick periventricular germinal layer has a low-signal intensity. A thin cortical layer is present, below which the large subplate can be recognized
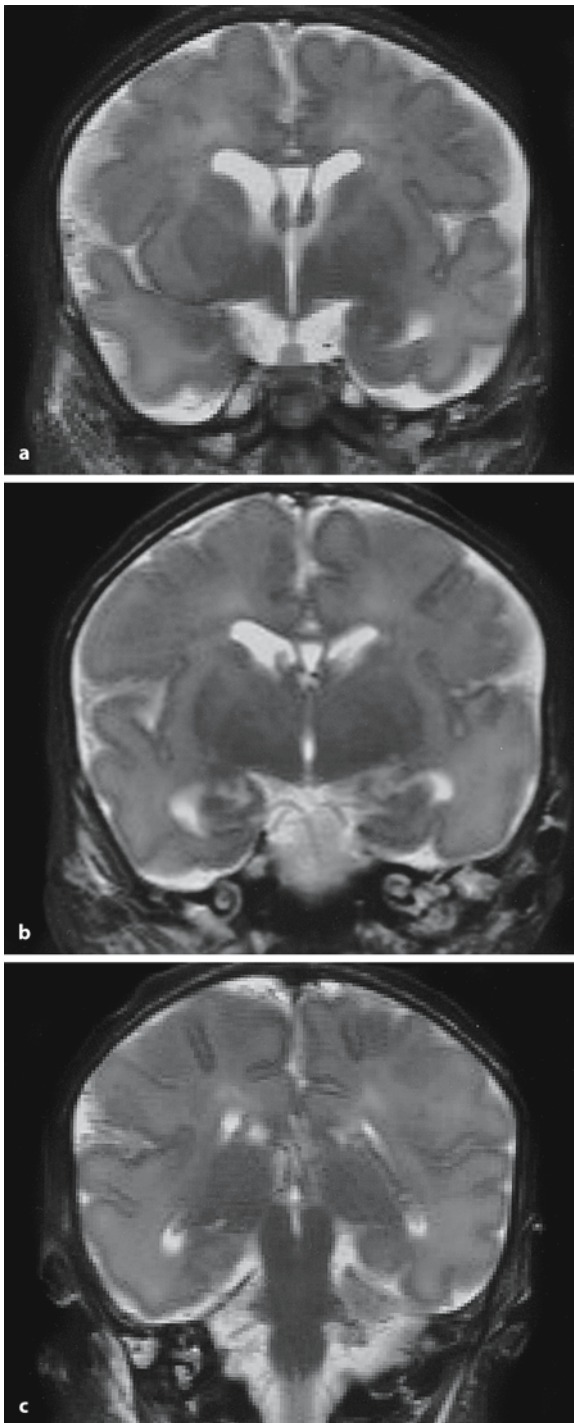
Fig. 1.27 Fetal T2-weighted MRI taken at the 35th week of development. The three frontal (or coronal) sections show increasing development of the insulae and lateral fissures, and an increasing number of gyri and sulci. The basal ganglia (in **a**), the amygdala (in **a**) and the hippocampal region (in **b**) are easily recognized. Note the large cavum septi pellucidi and the prominent fornices (in **a** and **b**). The corpus callosum is visible in **a** and **b**

1.9   Development of the Meninges and Choroid Plexuses

The **cranial meninges** originate from several sources such as the prechordal plate, the parachordal mesoderm and the neural crest (O'Rahilly and Müller 1986). The loose mesenchyme around most of the brain at 5 weeks of development (stage 15) forms the primary meninx. At 6 weeks (stage 17), the dural limiting layer is found basally and the skeletogenous layer of the head becomes visible. At 7 weeks (stage 19), the cranial pachymeninx and leptomeninx are distinguishable. Hochstetter (1939) showed that, as the dural reflections develop, the posterior point of attachment between the tentorium cerebelli and the falx cerebri gradually moves to a more caudal position in the skull, thereby producing a continual reduction in the size of the posterior cranial fossa relative to that of the supratentorial fossae. Increases of supratentorial volume relative to infratentorial volume affect such an inferoposterior rotation of the human fetal tentorium cerebelli (Jeffery 2002). Klintworth (1967) found the tentorium cerebelli at stage 20 as a bilateral, three-layered structure. The two tentorial precursors were visible macroscopically by stage 23. They fuse at 55-mm crown–rump length (CRL) to create the straight sinus (Streeter 1915).

The development of the **spinal meninges** has been studied by Hochstetter (1934) and Sensenig (1951). The future pia mater appears as neural crest cells by stage 11, and at 5 weeks (stage 15) the primary meninx is represented by a loose zone between the developing vertebrae and the neural tube. After 6 weeks (stage 18), the mesenchyme adjacent to the vertebrae becomes condensed to form the dural lamella. At the end of the embryonic period (stage 23), the dura completely lines the wall of the vertebral canal. The spinal arachnoid, however, does not appear until either the third trimester or postnatally (O'Rahilly and Müller 1999).

A **choroid plexus** first appears in the roof of the fourth ventricle at stage 18, in the lateral ventricles at stage 19, and in the third ventricle at stage 21 (Ariëns Kappers 1958; Bartelmez and Dekaban 1962). The primordia appear as simple or club-shaped folds protruding into the ventricles. During stage 21, the choroid plexuses become vascularized. The early choroid plexus of the lateral ventricle is lobulated with vessels running in the mesenchymal stroma and forming capillary nets under the single-layered ependyma. The embryonic choroid plexus is converted into the fetal type during the ninth week of development as the embryonic capillary net is replaced by elongated loops of wavy capillaries that lie under regular longitudinal epithelial folds (Kraus and Jirásek 2002). The stroma of the plexus originates from ex-

tensions of the arachnoid into the interior of the brain that form the **vela interposita**. This may explain the origin of the sporadically occurring intraventricular meningiomas, most commonly found in the trigone of the third ventricle (Nakamura et al. 2003).

1.10   Development of the Blood Supply of the Brain

The brain is supplied by two pairs of internal carotid and vertebral arteries, connected by the circle of Willis. During the closure of the neural tube, primordial endothelial blood-containing channels are established. From these all other vessels, arteries, veins and capillaries are derived. At stage 12, capital venous plexuses, the capital vein and three aortic arches are present (Streeter 1918; Congdon 1922; Padget 1948, 1957; Fig. 1.28). The internal carotids develop early (stages 11–13), followed by the posterior communicating artery, the caudal branch of the internal carotid at stage 14, the basilar and vertebral arteries (stage 16), the main cerebral arteries (stage 17) and finally the anterior communicating artery, thereby completing the circle of Willis (Evans 1911, 1912; Padget 1948; Gillilan 1972). Bilaterally, longitudinal arteries are established at stage 13 and are connected with the internal carotids by temporary trigeminal, otic and hypoglossal arteries. At first, the posterior communicating artery provides the major blood supply of the brain stem. Anastomotic channels unite the two longitudinal arteries, thereby initiating the formation of the basilar artery. The temporary arteries are gradually eliminated, but each of them may persist. The primitive trigeminal artery is the most common of the primitive carotid–basilar anastomoses that persist into adulthood, with an incidence of 0.1–1.0% (Wollschlaeger and Wollschlaeger 1964; Lie 1968; Salas et al. 1998; Suttner et al. 2000; Fig. 1.29). The persistence of a primitive otic artery is shown in Fig. 1.30.

Capillaries at the level of the cerebral hemispheres begin to appear at 5 weeks, and probably earlier in the brain stem (Padget 1948; O'Rahilly and Müller 1999). By 5 weeks (stage 16), many of the definitive arteries are present and are being transformed into the definitive pattern. At the end of the embryonic period, an anular network of **leptomeningeal arteries** arises from each middle cerebral artery and extends over each developing hemisphere (Van den Bergh and Vander Eecken 1968). Similar meningeal branches, originating from the vertebral and basilar arteries, embrace the brain stem and cerebellum. From these gradually muscularizing leptomeningeal artery branches grow into the brain. Both supratentorially and infratentorially, **paramedian**, **short circumferential** and **long circumferential arteries** can be distin-

guished. The first vessels penetrate the telencephalon in the seventh week of gestation, form a subventricular plexus at about 12 weeks of gestation (Duckett 1971) and also gradually muscularize. The paramedian branches of the anterior cerebral artery have a short course before they penetrate the cerebral parenchyma, whereas the short circumferential arteries such as the striate artery have a slightly longer course and the long circumferential arteries may reach the dorsal surface of the cerebral hemispheres. At 16 weeks of gestation, the anterior, middle and posterior cerebral arteries, contributing to the formation of the circle of Willis, are well established (Padget 1948; Van den Bergh and Vander Eecken 1968). During the further fetal period the relatively simple leptomeningeal arteries increase in tortuosity, size and number of branches. Their branching pattern is completed by 28 weeks of gestation (Takashima and Tanaka 1978).

The leptomeningeal perforating branches pass into the cerebral parenchyma as **cortical, medullary** and **striate branches** (Fig. 1.31). The cortical vessels supply the cortex via short branches, whereas the medullary branches supply the underlying white matter. The striate branches penetrate into the brain via the anterior perforate substance and supply the basal ganglia and internal capsule. The cortical and medullary branches supply cone-shaped areas along the periphery of the cerebrum and are called **ventriculopetal arteries**. Striate branches arborize close to the ventricle and supply a more central part of the cerebrum. Together with branches of the tela choroidea, they were supposed to give rise to **ventriculofugal arteries**, supplying the ventricular zone or germinal matrix (Van den Bergh and Vander Eecken 1968; De Reuck et al. 1972). The presence of such arteries could not be confirmed by Gilles and coworkers (Kuban and Gilles 1985; Nelson et al. 1991). More likely, the central parts are supplied by deep penetrating branches (Rorke 1982). Smooth muscle is present at the basal ends of striatal arteries by midgestation and extends well into the vessels in the caudate nucleus by the end of the second trimester (Kuban and Gilles 1985). The intracortical vessels also develop gradually (Allsop and Gamble 1979). From the 13th to 15th weeks, radial arteries without side branches course through the cortex. By 20 weeks of gestation, horizontal side branches and recurrent collaterals appear, and from 27 weeks to term, shorter radial arteries increase in number. Growth of the intracortical capillaries continues well after birth (Norman and O'Kusky 1986). In the fetal brain, the density of capillaries is much higher in the ventricular zone than in the cortical plate until 17 weeks (Duckett 1971; Allsopp and Gamble 1979; Norman and O'Kusky 1986). After 25 weeks, increasing vascularization of the cortical areas occurs.
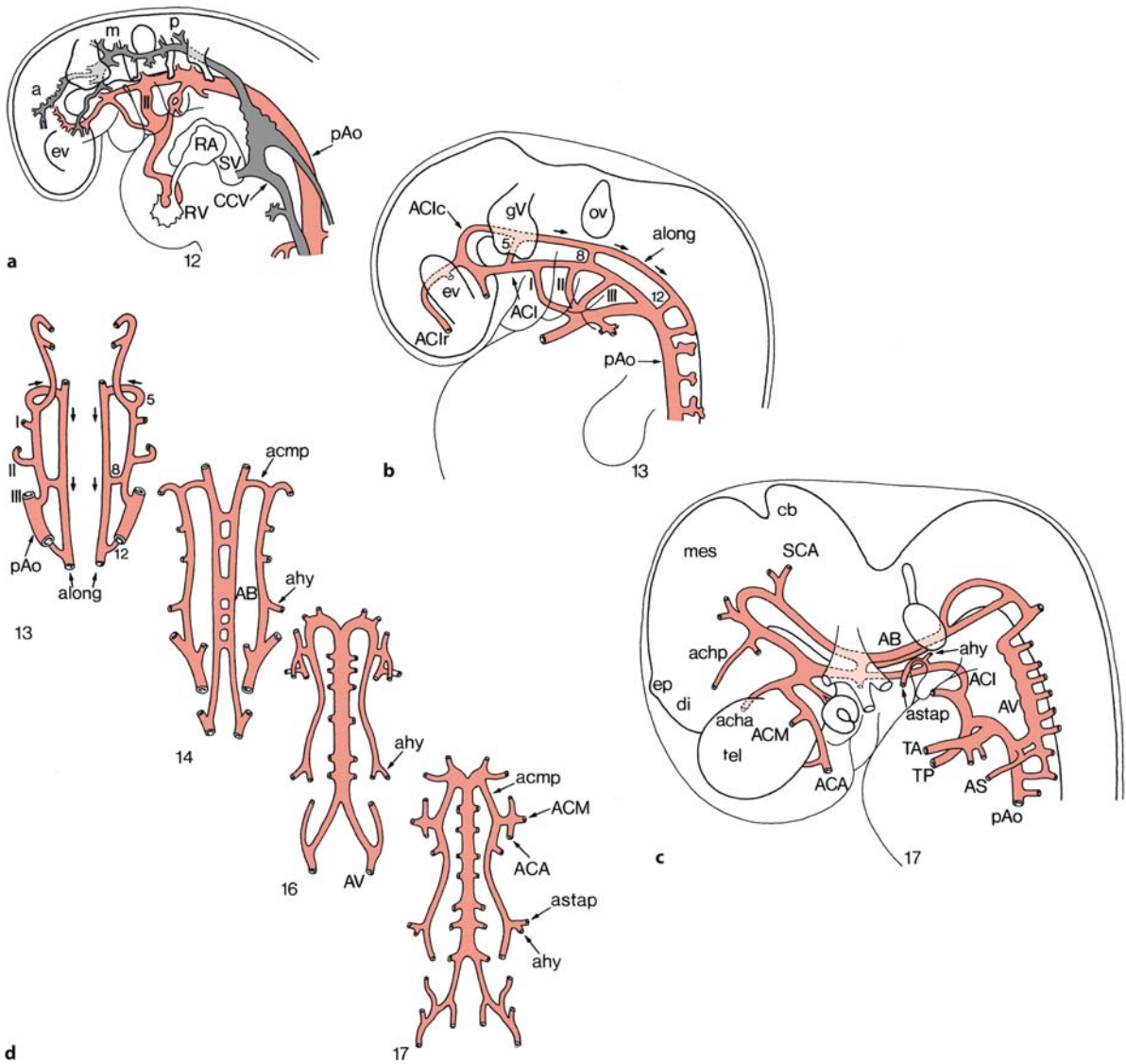
Fig. 1.28 Overview of the development of the blood supply of the human brain from stage 12 until the neonatal period. Arteries are in *red*, veins in *grey*. *a* anterior capital plexus, *AA* aortic arch, *AB* a. basilaris, *ACA* a. cerebri anterior, *ACE* a. carotis externa, *acha* anterior choroidal artery, *achp* posterior choroidal artery, *ACI* a. carotis interna, *ACIc* caudal branch of a. carotis interna, *ACIr* rostral branch of a. carotis interna, *ACM* a. cerebri media, *acmp* a. communicans posterior, *ACP* a. cerebri posterior, *ahy* hyoid artery, *AICA* anterior inferior cerebellar artery, *along* a. longitudinalis, *AS* a. subclavia, *astap* a. stapedia, *AV* a. vertebralis, *cb* cerebellum, *cc* corpus callosum, *CCV* com-mon cardinal vein, *DA* ductus arteriosus, *di* diencephalon, *ep* epiphysis, *ev* eye vesicle, *gV* trigeminal ganglion, *m* middle capital plexus, *mes* mesencephalon, *OA* ophthalmic artery, *ov* otic vesicle, *p* posterior capital plexus, *pAo* posterior aorta, *PICA* posterior inferior artery, *plch* plexus choroideus, *RA* right atrium, *RV* right ventricle, *SCA* superior cerebellar artery, *SV* sinus venosus, *TA* truncus arteriosus, *tel* telencephalon, *TP* truncus pulmonalis, *I–III* aortic branches, *5, 8, 12* temporary trigeminal, otic and hypoglossal arteries. (After Padget 1948; O'Rahilly and Müller 1999)
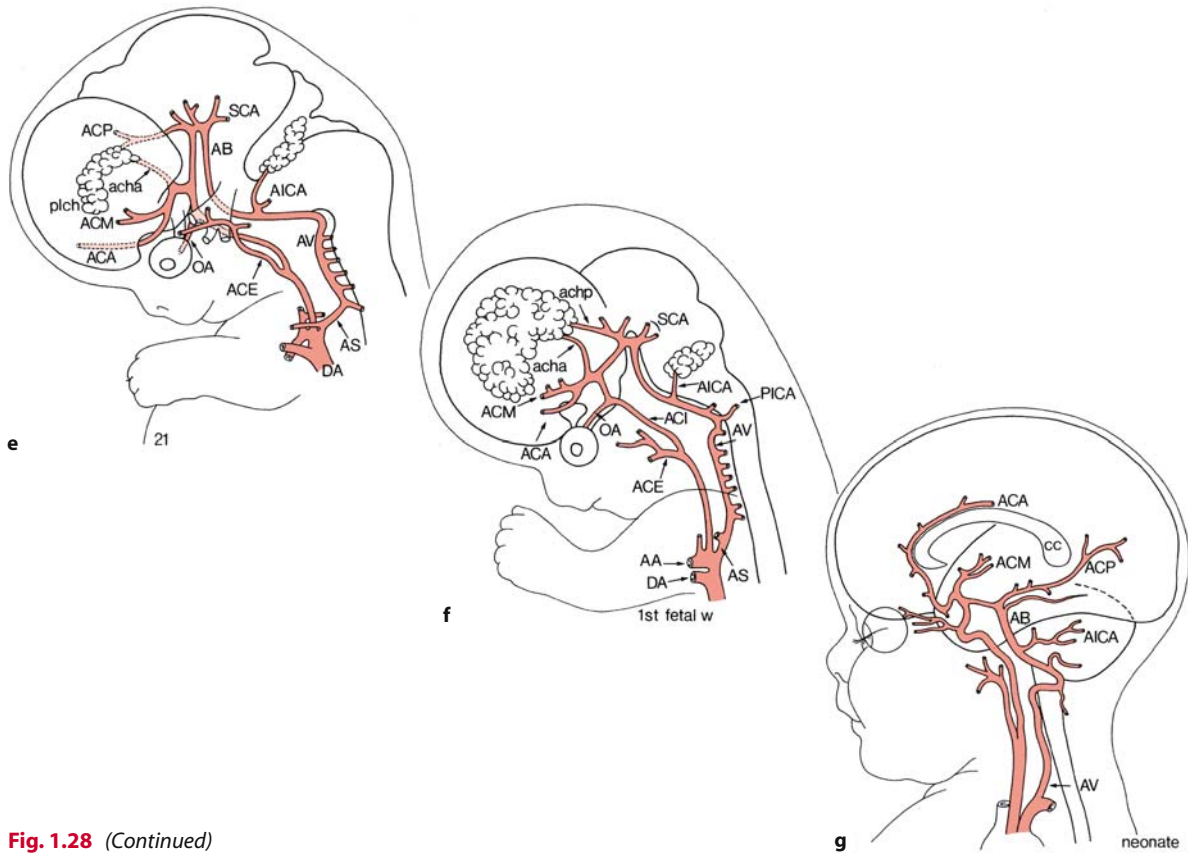
Fig. 1.28 *(Continued)*

Fig. 1.29 Persistence of the primitive trigeminal artery. Occasional autopsy finding by Akira Hori in a 42-year-old woman
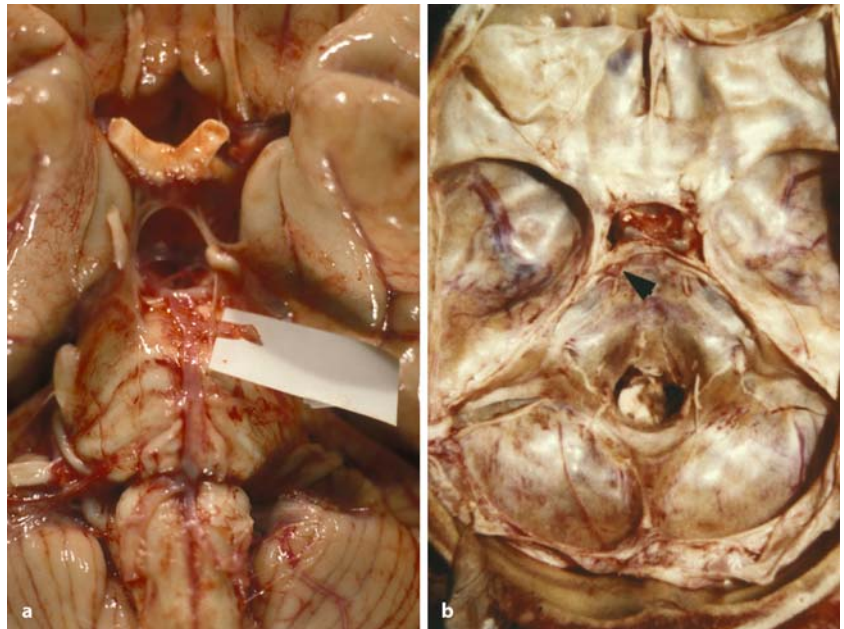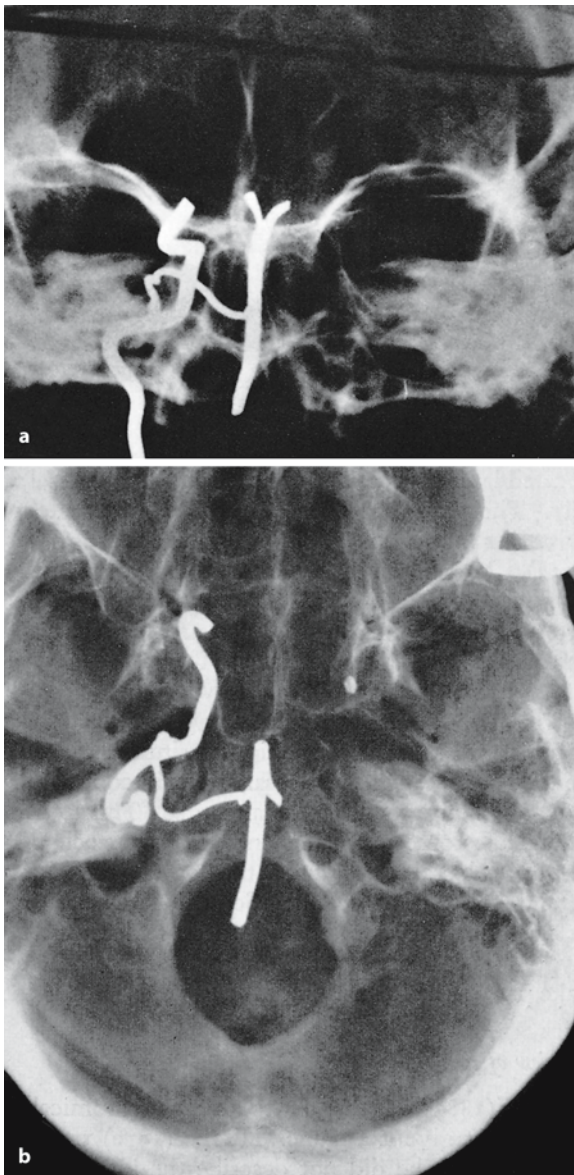
Fig. 1.30 Persistence of the primitive otic artery (from Lie 1968)

At 24 weeks of gestation, a large part of the basal ganglia and internal capsule is supplied by a prominent **Heubner's artery**, arising from the anterior cerebral artery (Hambleton and Wigglesworth 1976). The capillary bed in the ventricular zone is supplied mainly by Heubner's artery and terminal branches of the lateral striate arteries from the middle cerebral artery (Wigglesworth and Pape 1980). The cortex and the underlying white matter are rather poorly vascularized at this stage of development. Gradually, the area supplied by the middle cerebral artery becomes predominant when compared with the territories supplied by the anterior and posterior cerebral arter-

ies (Okudera et al. 1988). Early arterial anastomoses appear around 16 weeks of gestation. The sites of arterial anastomoses between the middle and the anterior cerebral arteries move from the convexity of the brain towards the superior sagittal sinus and those between the middle and posterior cerebral arteries move towards the basal aspect of the brain. By 32–34 weeks of gestation, the ventricular zone involutes and the cerebral cortex acquires its complex gyral pattern with an increased vascular supply. The ventricular zone capillaries blend with the capillaries of the caudate nucleus and the territory of Heubner's artery becomes reduced to only a small medial part of the caudate nucleus. In the cortex, there is progressive elaboration of the cortical blood vessels (Van den Bergh and Vander Eecken 1968; Hambleton and Wigglesworth 1976; Weindling 2002). Towards the end of the third trimester, the balance of cerebral circulation shifts from a central, ventricular zone oriented circulation to a circulation predominant in the cerebral cortex and white matter. These changes in the pattern of cerebral circulation are of major importance in the pathogenesis and distribution of hypoxic/ischemic lesions in the developing human brain.

Cerebrovascular density correlates with regional metabolic demand (Pearce 2002). Correspondingly, cerebrovascular conductance in the vertebrobasilar and carotid systems increases more slowly than brain weight, particularly during the postnatal period of rapid cerebral growth, myelination and differentiation. As part of normal development, most immature human cerebral arteries appear to have regions of weakened media near vessel bifurcations. These weakened areas are reinforced during maturation via the deposition of additional smooth muscle, but can comprise areas of heightened vulnerability to rupture during early postnatal development (Pearce 2002).

In younger premature infants (22–30 weeks old), the blood vessels of the germinal, periventricular zone and the perforating ventriculopetal vessels are particularly vulnerable to **perinatal asphyxia** (Marín-Padilla 1996; Volpe 1998; Weindling 2002). Damage to these vessels often causes focal haemorrhagic lesions. In older premature infants (30–34 weeks), the fetal white matter seems to be particularly vulnerable to hypoxic-ischemic injury, leading to **periventricular leukomalacia** or **PVL** (Chap. 3), and often resulting in infarction (necrosis) and cavitation (Banker and Larroche 1962; Marín-Padilla 1997, 1999; Volpe 2001; Squier 2002; Weindling 2002). PVL refers to necrosis of white matter in a characteristic distribution, i.e. in the white matter dorsal and lateral to the external angles of the lateral ventricles. The corticospinal tracts run through the periventricular region. Therefore, impaired motor function is
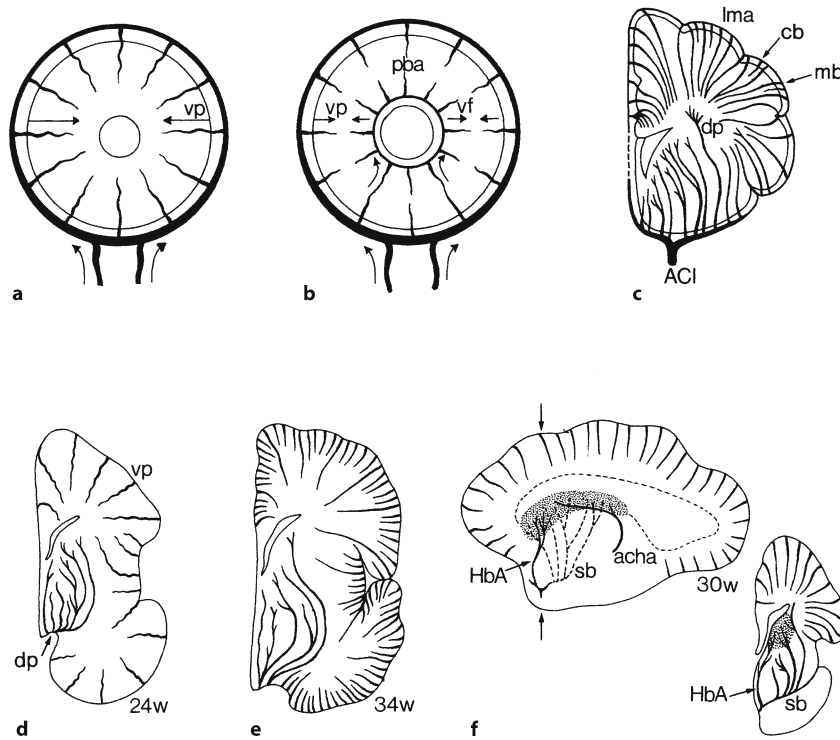
Fig. 1.31 Development of cerebral blood vessels. The brain is surrounded by a system of leptomeningeal arteries, which is supplied by afferent trunks at the base of the brain, and gives off ventriculopetal arteries (*vp*) towards the lateral ventricle (**a**). A few deep-penetrating arteries supply periventricular parts of the brain and were supposed to send ventriculofugal arteries (*vf*) towards the ventriculopetal vessels, without making anastomoses (**b**). Between these two systems there may be a periventricular border area. Deep penetrators (*dp*) more likely supply the periventricular parts of the brain. **c** The arrangement of both types of vessels around a cerebral hemisphere. **d**, **e** Changes in the arterial pattern of the cerebrum between 24 and 34 weeks of gestation. **f** Blood supply to the basal ganglia at 20 weeks of gestation. *acha* anterior choroidal artery, *ACI* internal carotid artery, *cb* cortical branches, *HbA* Heubner's artery, *lma* leptomeningeal arteries, *mb* medullary branches, *pba* periventricular border area, *sb* striate branches of middle cerebral artery. (After Van den Bergh and Vander Eecken 1968; Hambleton and Wigglesworth 1976)

the most common neurologic sequela of periventricular white matter injury (Banker and Larroche 1962; Aida et al. 1998; Staudt et al. 2000). Periventricular white matter lesions account for the pathogenesis of a large number of children with spastic hemiparesis (Niemann et al. 1994).

Dural plexuses associated with the precardinal veins become modified to form the various dural sinuses around the brain (Streeter 1915, 1918; Lindenberg 1956; Padget 1957). Definitive venous channels emerge from the primitive vascular net later than the arteries do. Moreover, the complicated venous anastomoses are essential to facilitate a greater adjustment to the changing needs of their environment over a considerably longer period (Padget 1957). The development of the human **cranial venous system** is summarized in Fig. 1.32. During Padget's venous stage 1 (Carnegie stage 12), **capital venous plexuses** and the **capital vein** are forming (Fig. 1.32 a). By venous stage 2 (Carnegie stage 14), three relatively constant **dural stems**, anterior, middle and posterior, are present draining into a **primary head sinus** (capital or 'head' vein) that is continuous with the anterior cardinal vein. During venous stages 3 and 4 (Carnegie stages 16 and 17), the dural venous channels come to lie more laterally as the cerebral hemispheres and the cerebellar anlage expand and the otic vesicles enlarge (Fig. 1.32 c). The head sinus and the primitive internal jugular vein also migrate laterally. By venous stage 5 (Carnegie stage 19), the head sinus is replaced by a secondary anastomosis, the **sigmoid sinus**. Moreover, more cranially the **primitive transverse sinus** is formed. During venous stage 6 (Carnegie stage 21), the external jugular system arises (Fig. 1.32 d). Most parts of the brain, except for the medulla, drain into the junction of the sigmoid sinus with the primitive transverse sinus. Meanwhile, the Galenic system of intracerebral drainage emerges as

a

b

c

d

e
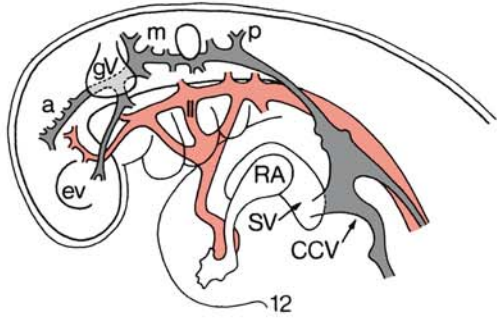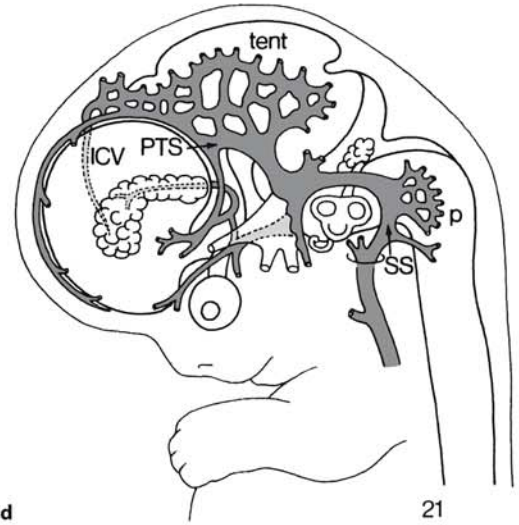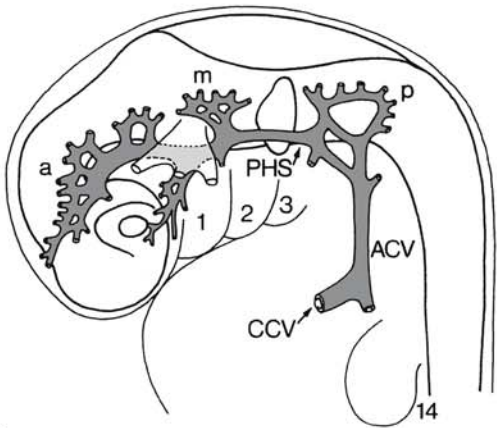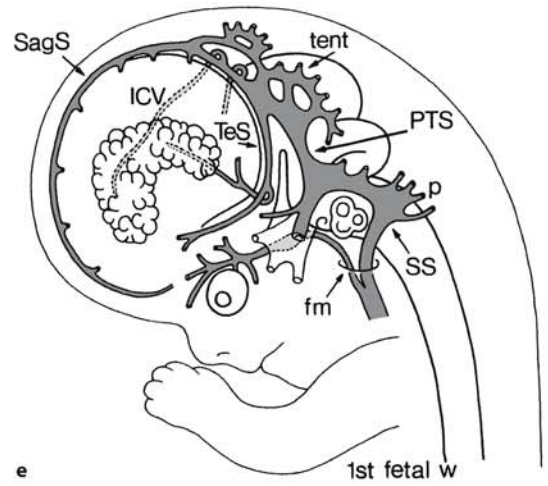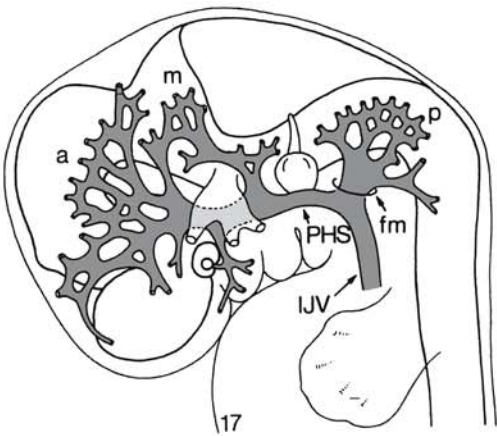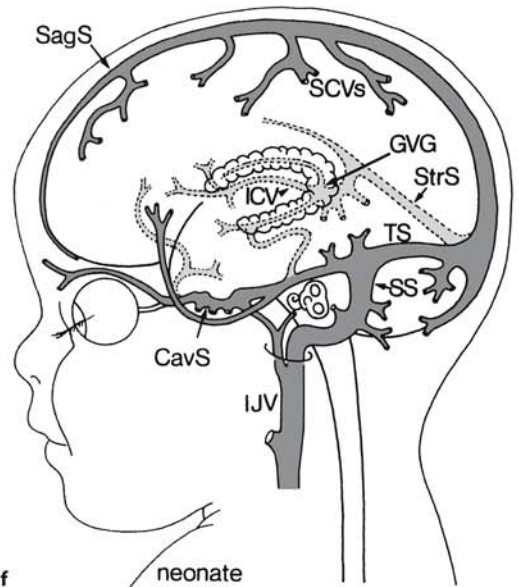
f

Fig. 1.32 Development of the venous system of the human brain from stage 12 until the neonatal period. Veins are in *grey*, early arteries in *red*. *a* anterior capital plexus, *ACV* anterior cardinal vein, *CavS* cavernous sinus, *CCV* common cardinal vein, *ev* eye vesicle, *fm* foramen magnum, *GVG* great vein of Galen, *ICV* internal cerebral vein, *IJV* internal jugular vein, *m* middle capital plexus, *p* posterior capital plexus, *PHS* primary head sinus, *PTS* primitive transverse sinus, *RA* right atrium, *SagS* sagittal sinus, *SCVs* superior cerebral veins, *SS* sigmoid sinus, *StrS* straight sinus, *SV* sinus venosus, *tent* tentorial plexus, *TeS* tentorial sinus, *TS* transverse sinus, *II* second aortic branch *1*, *2*, *3* pharyngeal arches. (After Streeter 1918; Padget 1957)
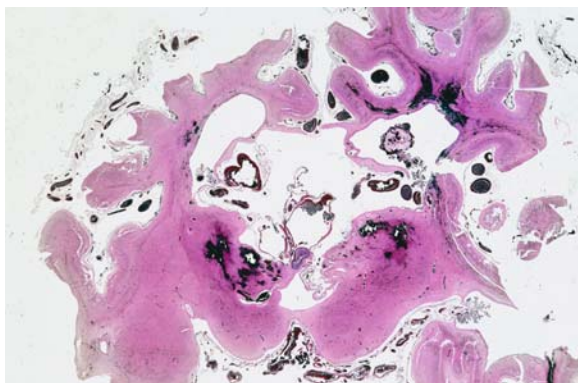
Fig. 1.33 Vein of Galen aneurysm in a 3-day-old female baby, accompanied by an aneurysm of the internal cerebral veins (from Akira Hori's archives)

Fig. 1.34 The outgrowth of the human corticospinal tracts (after Humphrey 1960)

the result of accelerated growth of the ganglionic eminences. Subsequent venous changes depend largely upon the expansion of the cerebral and cerebellar hemispheres and the relatively late ossification of the skull (Fig. 1.32 e, f). One of the most common malformations of the cerebral venous system is the **vein of Galen malformation** (Fig. 1.33).

1.11 Development of Fibre Tracts (Including Development of Myelination)

Early generated, 'pioneer' neurons lay down an axonal scaffold, containing guidance cues that are available to later outgrowing axons (Chap. 2). The first descending brain stem projections to the spinal cord can be viewed as pioneer fibres. They arise in the interstitial nucleus of the fasciculus longitudinalis medialis (flm) and in the reticular formation (Müller and O'Rahilly 1988 a, b). At early developmental stages (from stage 11/12 onwards), in the brain stem a ventral longitudinal tract can be distinguished, followed by lateral and medial longitudinal fasciculi at stage 13. Descending fibres from the medullary

reticular formation reach the spinal cord in embryos of 10–12-mm CRL (Windle and Fitzgerald 1937). Interstitiospinal fibres from the interstitial nucleus of the flm start to descend at stage 13, i. e. at 28 days. In 12-mm-CRL embryos (about stage 17/18), vestibulospinal projections were found (Windle 1970). At the end of the embryonic period, the flm is well developed, and receives ascending and descending (the medial vestibulospinal tract) components from the vestibular nuclear complex (Müller and O'Rahilly 1990c). The lateral vestibulospinal tract arises from the lateral vestibular nucleus. Windle and Fitzgerald (1937) also followed the ingrowth of dorsal root projections and the development of commissural, ascending and descending spinal pathways (Chap. 6). Ascending fibres in the dorsal funiculus have reached the brain stem at stage 16 (Müller and O'Rahilly 1989). Decussating fibres, forming the medial lemniscus, were first noted at stage 20 (Müller and O'Rahilly 1990a, b; Chap. 7).

The **corticospinal tract** is one of the latest developing descending pathways (ten Donkelaar 2000). At stage 21, the cortical plate starts to develop, whereas a definite internal capsule is present by stage 22 (Müller and O'Rahilly 1990b). Hewitt (1961) found
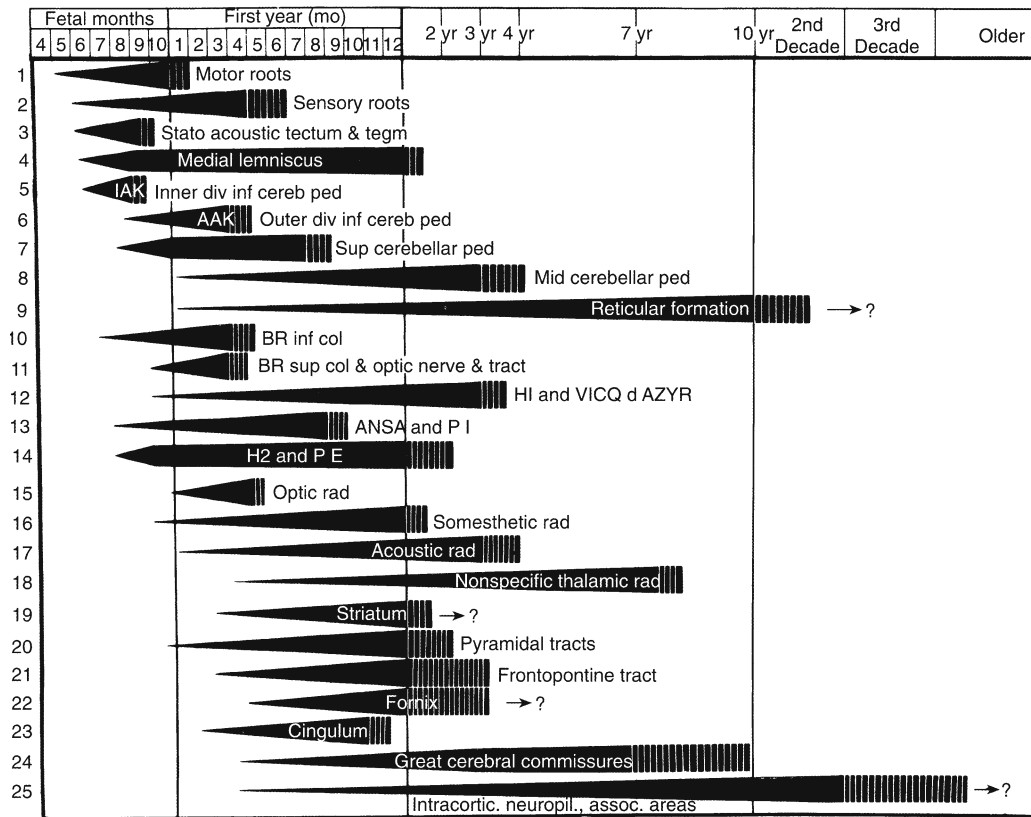
Fig. 1.35 Development of myelination of the main fibre tracts in the human CNS (from Yakovlev and Lecours 1967)

the earliest sign of the internal capsule (probably the thalamocortical component; Yamadori 1965) in stage 18 (13–17-mm CRL). Humphrey (1960) studied the ingrowth of the corticospinal tract into the brain stem and spinal cord with a silver technique (Fig. 1.34). The pyramidal tract reaches the level of the pyramidal decussation at the end of the embryonic period, i.e. at 8 weeks of development (Müller and O'Rahilly 1990c). Pyramidal decussation is complete by 17 weeks of gestation, and the rest of the spinal cord is invaded by 19 weeks (lower thoracic cord) and 29 weeks (lumbosacral cord) of gestation (Humphrey 1960). Owing to this long, protracted development, *developmental disorders* of *the pyramidal tract* may occur over almost the entire prenatal period, and may include aplasia, hypoplasia, hyperplasia, secondary malformations due to destructive lesions, anomalies of crossing and disorders of myelination (ten Donkelaar et al. 2004). Aplasia of the pyramidal tracts is characterized by the absence of the pyramids (Chap. 6).

Fibre tracts that appear early in development generally undergo myelination before later-appearing tracts (Flechsig 1920; Yakovlev and Lecours 1967; Gilles et al. 1983; Brody et al. 1987; Kinney et al. 1988; Fig. 1.35). **Myelination** in the CNS is undertaken by

oligodendrocytes, and is a very slow process. The presence of myelin has been noted in the spinal cord at the end of the first trimester and proceeds caudorostrally. The motor roots preceed the dorsal roots slightly. In the CNS the afferent tracts become myelinated earlier than the motor pathways. In the brain stem, myelination starts in the flm at eight postovulatory weeks. The vestibulospinal tracts become myelinated at the end of the second trimester, whereas the pyramidal tracts begin very late (at the end of the third trimester), and myelination is not completed in them until about 2 years. Cortical association fibres are the last to become myelinated. The appearance of myelin in MRI lags about 1 month behind the histological timetables (van der Knaap and Valk 1995; Ruggieri 1997). As judged from relative signal intensities, myelin is present at 30–34 weeks of development in the following structures (Sie et al. 1997; van Wezel-Meijler et al. 1998): the medial lemniscus, the superior and inferior colliculi, the decussation of the superior cerebellar peduncles, the crus cerebri, the ventrolateral thalamus, the lateral globus pallidus and dorsolateral putamen, the dentate nucleus, the middle and superior cerebellar peduncles, the vermis, the cortex around the central sulcus and the hippocampus. Between 34 and 46 weeks, myelin appears
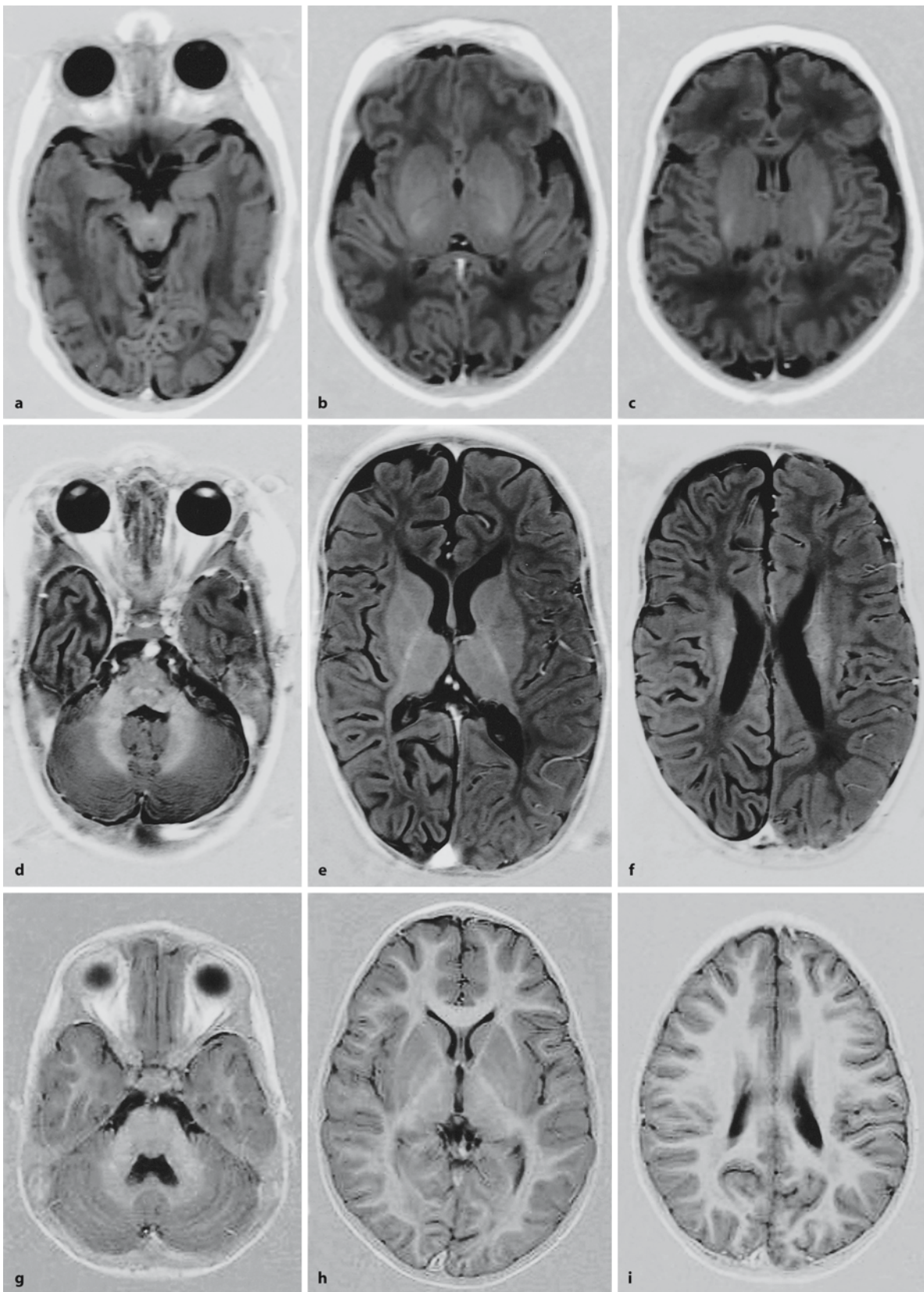
Fig. 1.36 Myelination in T1-weighted horizontal (or axial) images of a newborn (**a**–**c**), a child of 1.5 years of age (**d**–**f**) and a young adult (**g**–**i**). In **a** myelination is visible in the decussation of the brachia conjunctiva, and in **b** and **c** in the posterior limb of the internal capsule. Myelination is far more advanced in the pictures of the infant (**d**–**f**)

in the lateral part of the posterior limb of the internal capsule and the central part of the corona radiata; therefore, at birth the human brain is rather immature in regard to the extent of its myelination. The rate of deposition of myelin is greatest during the first two postnatal years (van der Knaap and Valk 1990, 1995). On magnetic resonance images, a significant decrease in water content leads to a decrease in longitudinal relaxation times (T1) and transverse relaxation times (T2). Consequently, 'adult-like' appearance of T1-weighted and T2-weighted images becomes evident towards the end of the first year of life. Age-related changes in white matter myelination continue during childhood and adolescence (Paus et al. 2001). The pattern of myelination around birth is illustrated in Fig. 1.36.

Prenatal motor behaviour has been analysed in ultrasound studies. The first, just discernable movements emerge at 6–7 weeks' postmenstrual age (Ianniruberto and Tajani 1981; de Vries et al. 1982). About 2 weeks later, movements involving all parts of the body appear. Two major forms of such movements can be distinguished, the startle and the general movement (Hadders-Algra and Forssberg 2002). The first movements appear prior to the formation of the spinal reflex arc, which is completed at 8 weeks' postmenstrual age (Okado and Kojima 1984). This means that the first human movements, just like those of chick embryos (Hamburger et al. 1966), are generated in the absence of afferent information. During the following weeks, new movements are added to the fetal repertoire, such as isolated arm and leg movements, various movements of the head, stretches, periodic breathing movements and sucking and swallowing movements (de Vries et al. 1982). Arm and leg movements, just like the palmar and plantar grasp reflexes, develop at 9–12 weeks, suggesting that fetal motility develops without a clear craniocaudal sequence. The age at which the various movements develop shows considerable interindividual variation, but at about 16 weeks' postmenstrual age all fetuses exhibit the entire fetal repertoire. The repertoire continues to be present throughout gestation (Hadders-Algra and Forrsberg 2002). If these movements are diminished or even absent owing to cerebral, spinal, nervous or muscular defects, the *fetal akinesia deformation sequence* occurs (Moessinger 1983), the phenotype of which was first described as Pena–Shokeir phenotype. This phenotype is characterized by multiple joint contractures, limb pterygia, lung hypoplasia, short umbilical cord, craniofacial deformities, growth retardation, hydrops and polyhydramnion (Hall 1986). The fetal akinesia sequence has been detected by ultrasound as early as 13 weeks of gestation owing to cerebral deformities leading to hydranencephaly (Witters et al. 2002) and at 16 weeks of gestation in a case of muscular origin (Lammens et al. 1997).

References

Acampora D, Gulisano M, Broccoli V, Simeone A (2001) *Otx* genes in brain morphogenesis. Prog Neurobiol 64:69–95

Aicardi J (1992) Diseases of the Nervous System in Childhood. Clinics in Developmental Medicine. Nr 115/118. Mac Keith, London

Aida N, Nishimura G, Hachiya Y, Matsui K, Takeuchi M, Itani Y (1998) MR imaging of perinatal brain damage: Comparison of clinical outcome with initial and follow-up MR findings. AJNR Am J Neuroradiol 19:1909–1921

Allsop G, Gamble HJ (1979) Light and electron microscopic observations on the development of the blood vascular system of the human brain. J Anat (Lond) 128:461–477

Altman J, Bayer SA (1997) Development of the Cerebellar System: In relation to its evolution, structure and functions. CRC, Boca Raton, FL

Anderson SA, Mione M, Yun K, Rubinstein JLR (1999) Differential origins of neocortical projection and local circuit neurons: Role of Dlx genes in neocortical interneuronogenesis. Cereb Cortex 9:646–654

Anderson SA, Marín O, Horn C, Jennings K, Rubinstein JLR (2001) Distinct cortical migrations from the medial and lateral ganglionic eminences. Development 128:353–363

Ariëns Kappers JA (1958) Structural and functional changes in the telencephalic choroid plexus during brain ontogenesis. In: Wolstenholme GEW, O'Connor CM (eds) The Cerebrospinal Fluid. Little, Brown, Boston, MA, pp 3–25

Arnold SE, Trojanowski JQ (1996) Human fetal hippocampal development: I. Cytoarchitecture, myeloarchitecture, and neuronal morphologic features. J Comp Neurol 367:274–292

Banker BQ, Larroche JC (1962) Periventricular leukomalacia of infancy. Arch Neurol 7:386–410

Barkovich AJ (2000) Pediatric Neuroimaging, 3rd ed. Lippincott, Philadelphia, PA

Barkovich AJ, Kuzniecky RI, Jackson GD, Guerrini R, Dobyns WB (2001) Classification system for malformations of cortical development. Update 2001. Neurology 57:2168–2178

Bartelmez GW (1923) The subdivisions of the neural folds in man. J Comp Neurol 35:231–295

Bartelmez GW, Dekaban AS (1962) The early development of the human brain. Contrib Embryol Carnegie Instn 37:13–32

Barth PG (1993) Pontocerebellar hypoplasias. An overview of a group of inherited neurodegenerative disorders with fetal onset. Brain Dev 15:411–422

Bayer SA, Altman J (1991) Neocortical Development. Raven, New York

Bayer SA, Altman J (2002) The Spinal Cord from Gestational Week 4 to the 4th Postnatal Month. CRC, Boca Raton, FL

Bayer SA, Altman J, Russo RJ, Zhang X (1995) Embryology. In: Duckett S (ed) Pediatric Neuropathology. Williams & Wilkins, Baltimore, MD, pp 54–107

Ben-Arie N, Bellen HJ, Armstrong DL, McCall AE, Gordadze PR, Guo Q, Matzuk MM, Zoghbi HY (1997) *Math1* is essential for genesis of cerebellar granule neurons. Nature 390:169–172

Bergquist H (1952) The formation of neuromeres in Homo. Acta Soc Med Ups 57:23–32

Blaas H-GK (1999) The Embryonic Examination. Ultrasound studies on the development of the human embryo. Thesis, Norwegian University of Science and Technology, Trondheim. TAPIR, Trondheim, Norway

Blaas H-GK, Eik-Nes SH (1996) Ultrasound assessment of early brain development. In: Jurkovic D, Jauniaux E (eds) Ultrasound and Early Pregnancy. Parthenon, New York, pp 3–18

Blaas H-G, Eik-Nes SH (2002) The description of the early development of the human central nervous system using two-dimensional and three-dimensional ultrasound. In: Lagercrantz H, Hanson M, Evrard P, Rodeck CH (eds) The Newborn Brain–Neuroscience and clinical applications. Cambridge University Press, Cambridge, pp 278–288

Blaas H-G, Eik-Nes SH, Kiserud T, Hellevik LR (1994) Early development of the forebrain and midbrain: A longitudinal ultrasound study from 7 to 12 weeks of gestation. Ultrasound Obstet Gynecol 4:183–192

Blaas H-G, Eik-Nes SH, Kiserud T, Berg S, Angelsen B, Olstad B (1995a) Three-dimensional imaging of the brain cavities in human embryos. Ultrasound Obstet Gynecol 5:228–232

Blaas H-G, Eik-Nes SH, Kiserud T, Hellevik LR (1995b) Early development of the hindbrain: A longitudinal ultrasound study from 7 to 12 weeks of gestation. Ultrasound Obstet Gynecol 5:151–160

Brazel CY, Romanko MJ, Rothstein RP, Levison SW (2003) Roles of the mammalian subventricular zone in brain development. Prog Neurobiol 69:49–69

Brody BA, Kinney HC, Kloman AS, Gilles FH (1987) Sequence of central nervous system myelination in human infancy. I. An autopsy study of myelination. J Neuropathol Exp Neurol 46:283–301

Brun A (1965) The subpial granular layer of the foetal cerebral cortex in man. Its ontogeny and significance in congenital cortical malformations. Acta Pathol Microbiol Scand 179(Suppl):1–98

Bulfone A, Puelles L, Porteus MH, Frohman MA, Martin GR, Rubinstein JLR (1993) Spatially restricted expression of Dlx-1, Dlx-2, (Tes-1), Gbx-2, and Wnt-3 in the embryonic day 12.5 mouse forebrain defines potential transverse and longitudinal boundaries. J Neurosci 13:3155–3172

Carlson BM (1999) Human Embryology & Development, 2nd ed. Mosby, St. Louis, MO

Collins P, Billett FS (1995) The terminology of early development. Clin Anat 8:418–425

Congdon ED (1922) Transformation of the aortic-arch system during the development of the human embryo. Contrib Embryol Carnegie Instn 14:47–110

Corner GW (1929) A well-preserved human embryo of 10 somites. Contrib Embryol Carnegie Instn 20:81–102

Crelin EA (1973) Functional Anatomy of the Newborn. Yale University Press, London

de Carlos JA, Lopez-Mascaraque L, Valverde F (1996) Dynamics of cell migration from the lateral ganglionic eminence in the rat. J Neurosci 16:6146–6156

de Souza FSJ, Niehrs C (2000) Anterior endoderm and head induction in early vertebrate embryos. Cell Tissue Res 300:207–217

De Reuck J, Chattha AS, Richardson EPJ (1972) Pathogenesis and evolution of periventricular leukomalacia in infancy. Arch Neurol 27:229–236

de Vries JIP, Visser GHA, Prechtl HFR (1982) The emergence of fetal behaviour. I. Qualitative aspects. Early Hum Dev 7:301–322

Doetsch F, García-Verdugo JM, Alvarez-Buylla A (1997) Cellular composition and three-dimensional organization of the subventricular germinal zone in the adult mammalian brain. J Neurosci 17:5046–5061

Duckett S (1971) The establishment of internal vascularization in the human telencephalon. Acta Anat (Basel) 80:107–113

Duvernoy HM (1998) The Human Hippocampus. Functional anatomy, vascularization and serial sections with MRI, 2nd ed. Springer, Berlin Heidelberg New York

Essick CR (1912) The development of the nuclei pontis and the nucleus arcuatus in man. Am J Anat 13:25–54

Evans HM (1911) Die Entwicklung des Blutgefäßsystems. In: Keibel F, Mall FP (Hrsg) Handbuch der Entwicklungsgeschichte des Menschen, Zweiter Band. Hirzel, Leipzig, pp 551–688

Evans HM (1912) The development of the vascular system. In: Keibel F, Mall FP (eds) Manual of Human Embryology, Vol 2. Lippincott, Philadelphia, PA, pp 570–709

Favier B, Dollé P (1997) Developmental functions of mammalian Hox genes. Mol Hum Reprod 3:115–131

Feess-Higgins A, Larroche J-C (1987) Le développement du cerveau foetal humain. Atlas anatomique. Masson, Paris

Flechsig PE (1920) Anatomie des menschlichen Gehirns und Rückenmarks auf myelogenetischer Grundlage. Thieme, Leipzig

Gadisseux J-F, Goffinet AM, Lyon G, Evrard P (1992) The human transient subpial granular layer: An optical, immunohistochemical, and ultrastructural analysis. J Comp Neurol 324:94–114

Garel C (2004) MRI of the Fetal Brain. Normal development and cerebral pathologies. Springer, Berlin Heidelberg New York

Gardner RJM, Coleman LT, Mitchell LA, Smith LJ, Harvey AS, Scheffer IE, Storey E, Nowotny MJ, Sloane RA, Lubitz L (2001) Near-total absence of the cerebellum. Neuropediatrics 32:62–68

Gilles FH, Shankle W, Dooling EC (1983) Myelinated tracts. In: Gilles FH, Leviton A, Dooling EC (eds) The Developing Human Brain. Wright, Bristol, pp 117–183

Gillilan LA (1972) Anatomy and embryology of the arterial system of the brain stem and cerebellum. Handb Clin Neurol 11:24–44

Gleeson JG, Walsh CA (2000) Neuronal migration disorders: From genetic diseases to developmental mechanisms. Trends Neurosci 23:352–359

Golden JA (1998) Holoprosencephaly: A defect in brain patterning. J Neuropathol Exp Neurol 57:991–999

Gribnau AAM, Geijsberts LGM (1985) Morphogenesis of the brain in staged rhesus monkey embryos. Adv Anat Embryol Cell Biol 91:1–69

Hadders-Algra M, Forssberg H (2002) Development of motor functions in health and disease. In: Lagercrantz H, Hanson M, Evrard P, Rodeck CH (eds) The Newborn Brain–Neuroscience and clinical applications. Cambridge University Press, Cambridge, pp 479–507

Hall JG (1986) Analysis of Pena Shokeir phenotype. Am J Med Genet 25:99–117

Hambleton G, Wigglesworth JS (1976) Origin of intraventricular haemorrhage in the preterm infant. Arch Child Dis 51:651–659

Hamburger V, Wenger E, Oppenheim RW (1966) Motility in the chick embryo in the absence of sensory input. J Exp Zool 162:133–160

Hamilton WJ, Mossman HW (1972) Hamilton, Boyd and Mossman's Human Embryology. Prenatal development of form and function, 4th ed. Heffer, Cambridge

Hatten ME (1999) Central nervous system neuronal migration. Annu Rev Neurosci 22:511–539

Hatten ME, Alder J, Zimmerman K, Heintz N (1997) Genes involved in cerebellar cell specification and differentiation. Curr Opin Neurobiol 7:40–47

Heuser CH, Corner GW (1957) Developmental horizons in human embryos. Description of age group X, 4 to 12 somites. Contrib Embryol Carnegie Instn 36:29–39

Hevner RF, Kinney HC (1996) Reciprocal entorhinal-hippocampal connections established by human fetal midgestation. J Comp Neurol 372:384–394

Hewitt W (1961) The development of the human internal capsule and lentiform nucleus. J Anat (Lond) 95:191–199

His W (1880) Anatomie menschlicher Embryonen. I. Embryonen des ersten Monats. Vogel, Leipzig

His W (1889) Die Formentwickelung des menschlichen Vorder-
hirns vom Ende des ersten bis zum Beginn des dritten Monats.
Abh Kön Sächs Ges Wiss, Math Phys Kl 15:675–735

His W (1890) Die Entwickelung des menschlichen Rautenhirns
vom Ende des ersten bis zum Beginn des dritten Monats. I. Ver-
längertes Mark. Abh Kön Sächs Ges Wiss, Math Phys Kl 29:1–74

His W (1904) Die Entwickelung des menschlichen Gehirns
während der ersten Monate. Hirzel, Leipzig

Hochstetter F (1919) Beiträge zur Entwicklungsgeschichte des
menschlichen Gehirns, I. Teil. Deuticke, Vienna

Hochstetter F (1929) Beiträge zur Entwicklungsgeschichte des
menschlichen Gehirns, II. Teil, 3. Lieferung. Die Entwicklung des
Mittel- und Rautenhirns. Deuticke, Vienna

Hochstetter F (1934) Über die Entwicklung und Differenzierung
der Hüllen des Rückenmarkes beim Menschen. Morphol Jahrb
74:1–104

Hochstetter F (1939) Über die Entwicklung und Differenzierung
der Hüllen des menschlichen Gehirns. Morphol Jahrb 83:359–
494

Hori A, Friede RL, Fischer G (1983) Ventricular diverticles with local-
ized dysgenesis of the temporal lobe in a cloverleaf skull
anomaly. Acta Neuropathol (Berl) 60:132–136

Hori A, Eubel R, Ulbrich R (1984a) Congenital ventricular diverticu-
lum in the brainstem. Report of four cases. Acta Neuropathol
(Berl) 63:330–333

Hori A, Bardosi A, Tsuboi K, Maki Y (1984b) Accessory cerebral ven-
tricle of the occipital lobe. Morphogenesis and clinical and
pathological appearance. J Neurosurg 61:767–771

Humphrey T (1960) The development of the pyramidal tracts in
human fetuses, correlated with cortical differentiation. In: Tow-
er DB, Schadé JP (eds) Structure and Function of the Cerebral
Cortex. Elsevier, Amsterdam, pp 93–103

Humphrey T (1966) The development of the human hippocampal
formation correlated with some aspects of its phylogenetic
history. In: Hassler R, Stephan H (eds) Evolution of the Fore-
brain. Thieme, Stuttgart, pp 104–116

Ianniruberto A, Tajani E (1981) Ultrasonographic study of fetal
movements. Sem Perinatol 5:175–181

Inoue T, Nakamura S, Osumi N (2000) Fate mapping of the mouse
prosencephalic neural plate. Dev Biol 219:373–383

Jakob A (1928) Das Kleinhirn. In: von Möllendorf W (ed) Handbuch
der mikroskopischen Anatomie des Menschen, Vol 4, Teil 1.
Springer, Berlin Heidelberg New York, pp 674–916

Jeffery N (2002) Differential regional brain growth and rotation of
the prenatal human tentorium cerebelli. J Anat (Lond)
200:135–144

Jirásek JE (1983) Atlas of Human Prenatal Morphogenesis. Nijhoff,
Baltimore, MD

Jirásek JE (2001) An Atlas of the Human Embryo and Fetus.
Parthenon, New York

Jirásek JE (2004) An Atlas of Human Prenatal Developmental
Mechanisms. Anatomy and staging. Taylor & Francis, London,
New York

Kahle W (1969) Die Entwicklung der menschlichen Grosshirn-
hemisphäre. Schriftenr Neurol 1:1–116

Keibel F, Elze C (1908) Normentafeln zur Entwicklungsgeschichte
des Menschen. Hirzel, Leipzig

Keyser AJM (1972) The development of the diencephalon of the
Chinese hamster. Acta Anat (Basel) 83(Suppl 59):1–178

Kinney HC, Brody BA, Kloman AS, Gilles FH (1988) Sequence of
central nervous system myelination in human infancy. II. Pat-
terns of myelination in autopsied infants. J Neuropathol Exp
Neurol 47:217–234

Klintworth GK (1967) The ontogeny and growth of the human ten-
torium cerebelli. Anat Rec 158:433–442

Kollias SS, Ball WS (1997) Congenital malformations of the brain.
In: Ball WS (ed) Pediatric Neuroradiology. Lippincott, Philadel-
phia, PA, pp 91–174

Konstantinidou AD, Silos-Santiago I, Flaris N, Snider WD (1995) De-
velopment of the primary afferent projection in human spinal
cord. J Comp Neurol 354:1–12

Kornack DR, Rakic P (2001) The generation, migration, and differ-
entiation of olfactory neurons in the adult primate brain. Proc
Natl Acad Sci USA 98:4752–4757

Kraus I, Jirásek JE (2002) Some observations of the structure of the
choroid plexus and its cysts. Prenat Diagn 22:1223–1228

Kuban KCK, Gilles FH (1985) Human telencephalic angiogenesis.
Ann Neurol 17:539–548

Lammens M, Moerman P, Fryns JP, Lemmens F, van de Kamp GM,
Goemans N, Dom R (1997) Fetal akinesia sequence caused by
nemaline myopathy. Neuropediatrics 28:116–119

Langman J (1963) Medical Embryology. Williams & Wilkins, Balti-
more, MD

Lavdas AA, Grigoriou M, Pachnis V, Parnavelas JG (1999) The medi-
al ganglionic eminence gives rise to a population of early neu-
rons in the developing cerebral cortex. J Neurosci 19:7881–
7888

Le Douarin NM, Kalcheim C (1999) The Neural Crest, 2nd ed.
Cambridge University Press, Cambridge

Lemire RJ, Loeser JD, Leech RW, Alvord EC (1975) Normal and Ab-
normal Development of the Human Nervous System. Harper &
Row, Hagerstown, MD

Letinić K, Kostović I (1997) Transient fetal structure, the ganglio-
thalamic body, connects telencephalic germinal zone with all
thalamic regions in the developing human brain.
J Comp Neurol 384:373–395

Letinić K, Rakic P (2001) Telencephalic origin of human thalamic
GABAergic neurons. Nat Neurosci 9:931–936

Lie KTA (1968) Congenital Anomalies of the Carotid Arteries.
Thesis, University of Amsterdam. Excerpta Medica Foundation,
Amsterdam

Lindenberg R (1956) Die Gefässversorgung und ihre Bedeutung
für Art und Ort von kreislaufgedingten Gewebsschäden und
Gefässprozessen. In: Lubarsch-Henke-Rössle's Handbuch der
speziellen pathologischen Anatomie und Histologie, Vol 13
(Scholz W, Hrsg), Teil 1B. Springer, Berlin Heidelberg New York,
pp 1071–1164

Luckett WP (1978) Origin and differentiation of the yolk sac and
extraembryonic mesoderm in presomite human and rhesus
monkey embryos. Am J Anat 152:59–97

Lumsden A, Krumlauf AR (1996) Patterning the vertebrate neu-
raxis. Science 274:1109–1115

Macchi G (1951) The ontogenetic development of the olfactory
telencephalon in man. J Comp Neurol 95:245–305

Marín O, Rubinstein JLR (2001) A long, remarkable journey: Tan-
gential migration in the telencephalon. Nat Rev Neurosci
2:780–790

Marín O, Rubinstein JLR (2002) Patterning, regionalization, and cell
differentiation in the forebrain. In: Rossant J, Tam PPL (eds)
Mouse Development–Patterning, Morphogenesis, and Organo-
genesis. Academic, San Diego CA, pp 75–106

Marín O, Anderson SA, Rubinstein JLR (2000) Origin and molecular
specification of striatal interneurons. J Neurosci 20:6063–6076

Marín O, Yaron A, Bagri A, Tessier-Lavigne M, Rubinstein JLR (2001)
Sorting of striatal and cortical interneurons regulated by sem-
aphorin-neuropilin interactions. Science 293:872–875

Marín-Padilla M (1990) Origin, formation, and prenatal maturation
of the human cerebral cortex: An overview. J Craniofac Genet
Dev Biol 10:137–146

Marín-Padilla M (1996) Developmental neuropathology and impact of perinatal brain damage. I. Hemorrhagic lesions of neocortex. J Neuropathol Exp Neurol 55:758–773

Marín-Padilla M (1997) Developmental neuropathology and impact of perinatal brain damage. II. White matter lesions of the neocortex. J Neuropathol Exp Neurol 56:219–235

Marín-Padilla M (1998) Cajal-Retzius cells and the development of the neocortex. Trends Neurosci 21:64–71

Marín-Padilla M (1999) Developmental neuropathology and impact of perinatal brain damage. III. Gray matter lesions of the neocortex. J Neuropathol Exp Neurol 58:407–429

Marti E, Bovolenta P (2002) Sonic hedgehog in CNS development: One signal, multiple outputs. Trends Neurosci 25:89–96

Mehler MF, Mabie PC, Zhang D, Kessler JA (1997) Bone morphogenetic proteins in the nervous system. Trends Neurosci 20:309–317

Meyer G, Goffinet AM (1998) Prenatal development of reelin-immunoreactive neurons in the human neocortex. J Comp Neurol 397:29–40

Meyer G, Wahle P (1999) The paleocortical ventricle is the origin of reelin-expressing neurons in the marginal zone of the foetal human neocortex. Eur J Neurosci 11:3937–3944

Meyer G, Goffinet AM, Fairén A (1999) What is a Cajal-Retzius cell? A reassessment of a classical cell type based on recent observations in the developing neocortex. Cereb Cortex 9:765–775

Meyer G, Schaaps JP, Moreau L, Goffinet AM (2000) Embryonic and early fetal development of the human neocortex. J Neurosci 20:1858–1868

Millen KJ, Millonig JH, Wingate RJT, Alder J, Hatten ME (1999) Neurogenetics of the cerebellar system. J Child Neurol 14:574–582

Moessinger AC (1983) Fetal akinesia deformation sequence: An animal model. Pediatrics 72:857–863

Monuki ES, Walsh CA (2001) Mechanisms of cerebral cortical patterning in mice and human. Nat Neurosci 4:1199–1206

Moore KL, Persaud TVN, Shiota K (2000) Color Atlas of Clinical Embryology, 2nd ed. Saunders, Philadelphia, PA

Muenke M, Beachy PA (2000) Genetics of ventral forebrain development and holoprosencephaly. Curr Opin Genet Dev 10:262–269

Müller F, O'Rahilly R (1983) The first appearance of the major divisions of the human brain at stage 9. Anat Embryol (Berl) 168:419–432

Müller F, O'Rahilly R (1985) The first appearance of the neural tube and optic primordium in the human embryo at stage 10. Anat Embryol (Berl) 172:157–169

Müller F, O'Rahilly R (1988a) The development of the human brain from a closed neural tube at stage 13. Anat Embryol (Berl) 177:203–224

Müller F, O'Rahilly R (1988b) The first appearance of the future cerebral hemispheres in the human embryo at stage 14. Anat Embryol (Berl) 177:495–511

Müller F, O'Rahilly R (1989) The human brain at stage 16, including the initial evagination of the neurohypophysis. Anat Embryol (Berl) 179:551–569

Müller F, O'Rahilly R (1990a) The human brain at stages 18–20, including the choroid plexuses and the amygdaloid and septal nuclei. Anat Embryol (Berl) 182:285–306

Müller F, O'Rahilly R (1990b) The human brain at stages 21–23, with particular reference to the cerebral cortical plate and to the development of the cerebellum. Anat Embryol (Berl) 182:375–400

Müller F, O'Rahilly R (1990c) The human rhombencephalon at the end of the embryonic period proper. Am J Anat 189:127–145

Müller F, O'Rahilly R (1997) The timing and sequence of appearance of neuromeres and their derivatives in staged human embryos. Acta Anat (Basel) 158:83–99

Nakamura M, Roser F, Rundschuh O, Vorkapic P, Samii M (2003) Intraventricular meningiomas: A review of 16 cases with reference to the literature. Surg Neurol 59:491–503

Nakatsu T, Uwabe C, Shiota K (2000) Neural tube closure in humans initiates at multiple sites: Evidence from human embryos and implications for the pathogenesis of neural tube defects. Anat Embryol (Berl) 201:455–466

Nelson MD, Gonzalez-Gomez I, Gilles FH (1991) The search for human telencephalic ventriculofugal arteries. Am J Neuroradiol 12:215–222

Niemann G, Wakat JP, Krägeloh-Mann I, Grodd W, Michaelis R (1994) Congenital hemiparesis and periventricular leukomalacia: Pathogenetic aspects on magnetic resonance imaging. Dev Med Child Neurol 36:943–950

Nieuwenhuys R (1998) Morphogenesis and general structure. In: Nieuwenhuys R, ten Donkelaar HJ, Nicholson C The Central Nervous System of Vertebrates. Springer, Berlin Heidelberg New York, pp 159–228

Nieuwkoop PD, Albers B (1990) The role of competence in the craniocaudal segregation of the central nervous system. Dev Growth Diff 32:23–31

Nishimura H, Semba R, Tanimura T, Tanaka O (1977) Prenatal Development of the Human with Special Reference to Craniofacial Structures. An atlas. Department of Health, Education & Welfare, National Institute of Health, Bethesda, MD

Noden DM (1991) Cell movements and control of patterned tissue assembly during craniofacial development. J Craniofac Genet Dev Biol 11:192–213

Norman MG, O'Kusky JR (1986) The growth and development of microvasculature in human cerebral cortex. J Neuropathol Exp Neurol 45:222–232

Norman MG, McGillivray BC, Kalousek DK, Hill A, Poskitt KJ (1995) Congenital Malformations of the Brain. Pathological, embryological, clinical, radiological and genetic aspects. Oxford University Press, New York

Okado N (1981) Onset of synapse formation in the human spinal cord. J Comp Neurol 201:211–219

Okado N, Kojima T (1984) Ontogeny of the central nervous system: Neurogenesis, fibre connections, synaptogenesis and myelination in the spinal cord. In: Prechtl HFR (ed) Continuity of Neural Functions from Prenatal to Postnatal Life. Blackwell, Oxford, pp 31–45

Okado N, Kahimi S, Kojima T (1979) Synaptogenesis in the cervical cord of the human embryo: Sequence of synapse formation in a spinal reflex pathway. J Comp Neurol 184:491–517

Okudera T, Ohta T, Huang YP, Yokota A (1988) Development and radiological anatomy of the superficial cerebral convexity vessels in the human fetus. J Neuroradiol 15:205–224

Olson EC, Walsh CA (2002) Smooth, rough and upside-down neocortical development. Curr Opin Genet Dev 12:320–327

Opitz JM (1993) Blastogenesis and the "primary field" in human development. Birth Defects 29:3–37

Opitz JM, Wilson GN, Gilbert-Barness E (1997) Abnormalities of blastogenesis, organogenesis, and phenogenesis. In: Gilbert-Barness E (ed) Potter's Pathology of the Fetus and Infant. Mosby, St. Louis, pp 65–105

O'Rahilly R (1973) Developmental Stages in Human Embryos. Part A: Embryos of the first three weeks (stages 1 to 9). Carnegie Institution of Washington Publication 631, Washington, DC

O'Rahilly R (1975) A Color Atlas of Human Embryology. A slide presentation. Saunders, Philadelphia, PA

O'Rahilly R, Gardner E (1979) The initial development of the human brain. Acta Anat (Basel) 104:123–133

O'Rahilly R, Müller F (1981) The first appearance of the human nervous system at stage 8. Anat Embryol (Berl) 163:1–13

O'Rahilly R, Müller F (1986) The meninges in human development. J Neuropathol Exp Neurol 45:588–608

O'Rahilly R, Müller F (1987) Developmental Stages in Human Embryos. Carnegie Institution of Washington Publication 637, Washington, DC

O'Rahilly R, Müller F (1999) The Embryonic Human Brain. An atlas of developmental stages, 2nd ed. Wiley-Liss, New York

O'Rahilly R, Müller F (2001) Human Embryology & Teratology, 3rd ed. Wiley-Liss, New York

Padget DH (1948) The development of the cranial arteries in the human embryo. Contrib Embryol Carnegie Instn 32:205–261

Padget DH (1957) The development of the cranial venous system in man, from the viewpoint of comparative anatomy. Contrib Embryol Carnegie Instn 36:79–140

Parnavelas JG (2000) The origin and migration of cortical neurones: New vistas. Trends Neurosci 23:126–131

Paus T, Collins DL, Evans AC, Leonard G, Pike B, Zijdenbos A (2001) Maturation of white matter in the human brain: A review of magnetic resonance studies. Brain Res Bull 54:255–266

Pearce WJ (2002) Cerebrovascular regulation in the neonate. In: Lagercrantz H, Hanson M, Evrard P, Rodeck CH (eds) The Newborn Brain–Neuroscience and clinical applications. Cambridge University Press, Cambridge, pp 252–277

Pearlman AL, Faust PL, Hatten ME, Brunstrom JE (1998) New directions for neuronal migration. Curr Opin Neurobiol 8:45–54

Pearson AA (1941) The development of the olfactory nerve in man. J Comp Neurol 75:199–217

Pilz D, Stoodley N, Golden JA (2002) Neuronal migration, cerebral cortical development, and cerebral cortical anomalies. J Neuropathol Exp Neurol 61:1–11

Pooh RK, Maeda K, Pooh K (2003) An Atlas of Fetal Central Nervous System Diseases. Diagnosis and treatment. Parthenon, Boca Raton, FL

Puelles L, Rubinstein JLR (1993) Expression patterns of homeobox and other putative regulatory genes in the embryonic forebrain suggest a neuromeric organization. Trends Neurosci 16:472–479

Puelles L, Rubinstein JLR (2003) Forebrain gene expression domains and the evolving prosomeric model. Trends Neurosci 26:469–476

Puelles L, Verney C (1998) Early neuromeric distribution of tyrosine-hydroxylase-immunoreactive neurons in human embryos. J Comp Neurol 394:283–308

Puelles L, Kuwana E, Puelles E, Bulfone A, Shimamura K, Keleher J, Smiga S, Rubinstein JLR (2000) Pallial and subpallial derivatives in the embryonic chick and mouse telencephalon, traced by the expression of the genes Dlx-2, Emx-1, Nkx-2.1, Pax-6, and Tbr-1. J Comp Neurol 424:409–438

Rakic P (1972) Mode of cell migration to the superficial layers of fetal monkey neocortex. J Comp Neurol 145:61–84

Rakić P, Sidman RL (1969) Telencephalic origin of pulvinar neurons in the fetal human brain. Z Anat Entw Gesch 129:53–82

Rakic P, Sidman RL (1970) Histogenesis of cortical layers in human cerebellum, particularly the lamina dissecans. J Comp Neurol 139:473–500

Rakic P, Yakovlev PI (1968) Development of the corpus callosum and cavum septi in man. J Comp Neurol 132:45–72

Ramaekers VT, Heimann G, Reul J, Thron A, Jaeken J (1997) Genetic disorders and cerebellar structural abnormalities in childhood. Brain 120:1739–1751

Ranke G (1910) Beiträge zur Kenntnis der normalen und pathologischen Hirnrindenbildung. Ziegl Beitr Path Anat 47:51–125

Rhinn M, Brand M (2001) The midbrain-hindbrain boundary organizer. Curr Opin Neurobiol 11:34–42

Rijli FM, Gavalas A, Chambon P (1998) Segmentation and specification in the branchial region of the head: The role of the *Hox* selector genes. Int J Dev Biol 42:393–401

Rorke LB (1992) Anatomical features of the developing brain implicated in pathogenesis of hypoxic-ischemic injury. Brain Pathol 2:211–221

Rubinstein JLR, Beachy PA (1998) Patterning of the embryonic forebrain. Curr Opin Neurobiol 8:18–26

Rubinstein JLR, Shimamura K, Martinez S, Puelles L (1998) Regionalization of the prosencephalic neural plate. Annu Rev Neurosci 21:445–477

Ruggieri PM (1997) Metabolic and neurodegenerative disorders and disorders with abnormal myelination. In: Ball WS (ed) Pediatric Neuroradiology. Lippincott, Philadelphia, PA, pp 175–237

Salas E, Ziyal IM, Sekhar LN, Wright DC (1998) Persistent trigeminal artery: An anatomic study. Neurosurgery 43:557–562

Sarnat HB (2000) Molecular genetic classification of central nervous system malformations. J Child Neurol 15:675–687

Sarnat HB, Flores-Sarnat L (2001) Neuropathologic research strategies in holoprosencephaly. J Child Neurol 16:918–931

Schuurmans C, Guillemot F (2002) Molecular mechanisms underlying cell fate specification in the developing telencephalon. Curr Opin Neurobiol 12:26–34

Sensenig EC (1951) The early development of the meninges of the spinal cord in human embryos. Contrib Embryol Carnegie Instn 34:145–157

Seress L, Ábrahám H, Tornóczky T, Kosztolányi G (2001) Cell formation in the human hippocampal formation from mid-gestation to the late postnatal period. Neuroscience 105:831–843

Shimamura K, Hartigan DJ, Martinez S, Puelles L, Rubinstein JLR (1995) Longitudinal organization of the anterior neural plate and neural tube. Development 121:3923–3933

Sidman RL, Rakic P (1982) Development of the human central nervous system. In: Haymaker W, Adams RD (eds) Histology and Histopathology of the Nervous System. Thomas, Springfield, IL, pp 3–145

Sie LTL, van der Knaap MS, van Wezel-Meijler G, Valk J (1997) MRI assessment of myelination of motor and sensory pathways in the brain of preterm and term-born infants. Neuropediatrics 28:97–105

Spreafico R, Arcelli P, Frassoni C, Canetti P, Giaccone G, Rizzutti T, Mastrangelo M, Bentivoglio M (1999) Development of layer I of the human cerebral cortex after midgestation: Architectonic findings, immunocytochemical identification of neurons and glia, and in situ labeling of apoptotic cells. J Comp Neurol 410:126–142

Squier W (2002) Pathology of fetal and neonatal brain development: Identifying the timing. In: Squier W (ed) Acquired Damage to the Developing Brain: Timing and causation. Arnold, London, pp 110–127

Staudt M, Niemann G, Grodd W, Krägeloh-Mann I (2000) The pyramidal tract in congenital hemiparesis: Relationship between morphology and function in periventricular lesions. Neuropediatrics 31:257–264

Stephan H (1975) Allocortex. Handbuch der mikroskopischen Anatomie des Menschen, Band 4, Teil 9. Springer, Berlin Heidelberg New York

Streeter GL (1911) Die Entwicklung des Nervensystems. In: Keibel F, Mall FP (Hrsg) Handbuch der Entwicklungsgeschichte des Menschen, Zweiter Band. Hirzel, Leipzig, pp 1–156

Streeter GL (1912) The development of the nervous system. In: Keibel F, Mall FP (eds) Manual of Human Embryology, Vol 2. Lippincott, Philadelphia, PA, pp 1–156

Streeter GL (1915) The development of the venous sinuses in the dura mater in the human embryo. Am J Anat 18:145–178

Streeter GL (1918) The developmental alterations in the vascular system of the brain of the human embryo. Contrib Embryol Carnegie Instn 8:5–38

Streeter GL (1951) Developmental Horizons in Human Embryos. Age groups XI to XXIII. Carnegie Institution of Washington, Washington, DC

Supèr H, Soriano E, Uylings HBM (1998) The functions of the preplate in development and evolution of the neocortex and hippocampus. Brain Res Rev 27:40–64

Suttner N, Mura J, Tedeschi H, Ferreira MAT, Wen HT, de Oliveira E, Rhoton AL Jr (2000) Persistent trigeminal artery: A unique anatomic specimen–Analysis and therapeutic implications. Neurosurgery 47:428–434

Takashima S, Tanaka K (1978) Development of cerebrovascular architecture and its relationship to periventricular leukomalacia. Arch Neurol 35:11–16

ten Donkelaar HJ (2000) Development and regenerative capacity of descending supraspinal pathways in tetrapods: A comparative approach. Adv Anat Embryol Cell Biol 154:1–145

ten Donkelaar HJ, Lammens M, Wesseling P, Thijssen HOM, Renier WO (2003) Development and developmental disorders of the human cerebellum. J Neurol 250:1025–1036

ten Donkelaar HJ, Lammens M, Wesseling P, Hori A, Keyser A, Rotteveel J (2004) Development and malformations of the human pyramidal tract. J Neurol 251:1429–1442

Tsuboi K, Maki Y, Hori A, Ebihara R (1984) Accessory ventricles of the posterior horn. Prog Comp Tomogr 6:529–534

Van den Bergh R, Vander Eecken H (1968) Anatomy and embryology of cerebral circulation. Prog Brain Res 30:1–25

van der Knaap MS, Valk J (1988) Classification of congenital abnormalities of the CNS. AJNR Am J Neuroradiol 9:315–326

van der Knaap MS, Valk J (1990) MR imaging of the various stages of normal myelination during the first year of life. Neuroradiology 31:459–470

van der Knaap MS, Valk J (1995) Magnetic Resonance of Myelin, Myelination and Myelin Disorders, 2nd ed. Springer, Berlin Heidelberg New York

van Wezel-Meijler G, van der Knaap MS, Sie LTL, Oosting J, Taets van Amerongen AHM, Cranendonk A, Lafeber HN (1998) Magnetic resonance imaging of the brain in premature infants during the neonatal period. Normal phenomena and reflection of mild ultrasound abnormalities. Neuropediatrics 29:89–96

van Zalen-Sprock RM, van Vugt JMG, van Geijn HPM (1996) First-trimester sonographic detection of neurodevelopmental abnormalities in some single-gene defects. Prenat Diagn 16:199–202

Vieille-Grosjean I, Hunt P, Gulisano M, Boncinelli E, Thorogood P (1997) Branchial HOX gene expression and human craniofacial development. Dev Biol 183:49–60

Volpe JJ (1987) Neurology of the Newborn, 2nd ed. Saunders, Philadelphia, PA

Volpe JJ (1998) Neurologic outcome of prematurity. Arch Neurol 55:297–300

Volpe JJ (2001) Neurobiology of periventricular leukomalacia in the premature infant. Pediatr Res 50:553–562

von Baer KE (1828) Über die Entwickelungsgeschichte der Thiere, Beobachtung und Reflexion. Bornträger, Königsberg

Wang VY, Zoghbi HY (2001) Genetic regulation of cerebellar development. Nat Rev Neurosci 2:484–491

Wechsler-Reya RJ, Scott MP (1999) Control of neuronal precursor proliferation in the cerebellum by sonic hedgehog. Neuron 22:103–114

Weindling M (2002) Clinical aspects of brain injury of the preterm brain. In: Lagercrantz H, Hanson M, Evrard P, Rodeck CH (eds) The Newborn Brain – Neuroscience and clinical applications. Cambridge University Press, Cambridge, pp 443–478

Wigglesworth JS, Pape KE (1980) Pathophysiology of intracranial haemorrhage in the newborn. J Perinat Med 8:119–133

Wilkie AOM, Morriss-Kay GM (2001) Genetics of craniofacial development and malformation. Nat Rev Genet 2:458–468

Windle WF (1970) Development of neural elements in human embryos of four to seven weeks gestation. Exp Neurol Suppl 5:44–83

Windle WF, Fitzgerald JE (1937) Development of the spinal reflex mechanism in human embryos. J Comp Neurol 67:493–509

Wingate RJT (2001) The rhombic lip and early cerebellar development. Curr Opin Neurobiol 11:82–88

Witters I, Moerman P, Devriendt K, Braet P, Van Schoubroeck D, Van Assche FA, Fryns JP (2002) Two siblings with early onset fetal akinesia deformation wequence and hydranencephaly: Further evidence for autosomal recessive inheritance of hydranencephaly, Fowler type. Am J Med Genet 108:41–44

Wollschlaeger G, Wollschlaeger PB (1964) The primitive trigeminal artery as seen angiographically and at postmortem examination. AJR Am J Roentgenol 92:761–768

Wurst W, Bally-Cuif L (2001) Neural plate patterning: Upstream and downstream of the isthmic organizer. Nat Rev Neurosci 2:99–108

Yakovlev PI, Lecours AR (1967) The myelogenetic cycles of regional maturation of the brain. In: Minkowski A (ed) Regional Development of the Brain in Early Life. Blackwell, Oxford, pp 3–70

Yamadori T (1965) Die Entwicklung des Thalamuskerns mit ihren ersten Fasersystemen bei menschlichen Embryonen. J Hirnforsch 7:393–413

Zecevic N, Milosevic A, Rakic S, Marín-Padilla M (1999) Early development and composition of the human primordial plexiform layer: An immunohistochemical study. J Comp Neurol 412:241–254

Mechanisms of Development

Hans J. ten Donkelaar

2.1   Introduction

Many of the mechanisms underlying neural development are basically similar in vertebrates and invertebrates. Among invertebrates the nematode *Caenorhabditis elegans*, the grasshopper, *Schistocerca americana*, and the fruitfly, *Drosophila melanogaster*, are favourite species for research on general principles of neural development. *C. elegans* is a powerful experimental system for lineage studies and for the analysis of programmed cell death (Sulston et al. 1983; Wood 1988). The large cells of the grasshopper embryo can also be readily labelled with dyes, after which their lineal descendants and differentiating axons can be followed during subsequent development (Bate 1976; Goodman and Bate 1983). The grasshopper and the fruitfly have a common plan for neuronal development (Thomas et al. 1984; Goodman and Doe 1993; Campos-Ortega and Hartenstein 1997). The well-advanced molecular genetics of *Drosophila* (Nüsslein-Volhard et al. 1987; Ashburner 1989; Lawrence 1992) makes it possible to carry out large-scale mutant screens, subsequently clone the relevant genes and analyse their function in vivo by gene perturbation experiments.

Among vertebrates, popular species for experimental studies on neural development are the zebrafish, *Danio rerio*, the South African clawed toad, *Xenopus laevis*, the chick embryo (*Gallus domesticus*) and mice. Like *Drosophila*, the zebrafish provides the ability to carry out large-scale mutant screens, and cloning and functional analysis of novel genes (Westerfield 1995; Postlethwait and Talbot 1997; Schier 1997, 2001; Driever 1999). The large eggs of *X. laevis* have been extensively used for lineage and neural induction studies (Kay and Peng 1991; Keller et al. 1999). For their easy accessibility chick embryos are widely used for surgical manipulation and grafting experiments. The transplantation of cells and tissues from the Japanese quail embryo into the chick embryo has provided an excellent model for lineage studies and for constructing regional fate maps (Le Douarin 1973). In mice, many spontaneously occurring mutations affecting the cerebral cortex and the cerebellum have been described (Mullen et al. 1997; Rice and Curran 1999). Their molecular analysis, combined with transgenic technology to achieve ectopic gene expression and targeted gene ablation, has made the mouse the mammal of choice for molecular

genetic studies of early development (Rossant and Tam 2002).

In this chapter mechanisms of development will be discussed with emphasis on neural induction, pattern formation, neurogenesis, migration, and axon outgrowth and guidance. Examples of some key experiments will be illustrated.

2.2   Neural Induction

Early events in the development of the vertebrate CNS have been most intensively studied in amphibians, first in urodeles (Spemann 1936, 1938; Holtfreter 1938; Nieuwkoop 1973), and more recently particularly in the clawed toad, *X. laevis* (Kay and Peng 1991). Since our understanding of neural induction in amniotes is rudimentary (Gilbert 2000; Wolpert et al. 2002), this section will deal mostly with amphibian development. The extensive data recently obtained on induction mechanisms in zebrafish have been reviewed by Fraser (1999), Appel (2000) and Schier (2001).

2.2.1   The Spemann–Mangold Organizer

The nervous system has its origin in the blastula stage of development, when the amphibian embryo consists of a ball of cells that surrounds a fluid-filled cavity, the blastocoel (Fig. 2.1). Although nearly spherical in shape, the **blastula** has recognizable anteroposterior and dorsoventral axes. The **blastocoel** lies in the **anterior** or **animal hemisphere** and is surrounded by small cells that will later form the ectoderm and the neurectoderm. The **posterior** or **vegetal hemisphere** consists of large, yolk-laden cells that will contribute to the endoderm. Between these two regions is an equatorial belt of cells that is known as the **marginal zone**. The dorsoventral axis is marked by a small depression on the outside at the future dorsal midline, the **blastopore**. This is the starting point for extensive cell movements during the subsequent gastrula stage that result in the internalization of cells from around the equator and posterior half of the embryo. **Gastrulation** is a complex process of crucial importance in embryogenesis. The layers of future endoderm and mesoderm in the marginal zone move inside through the dorsal lip of the blastopore and extend along the anteroposterior
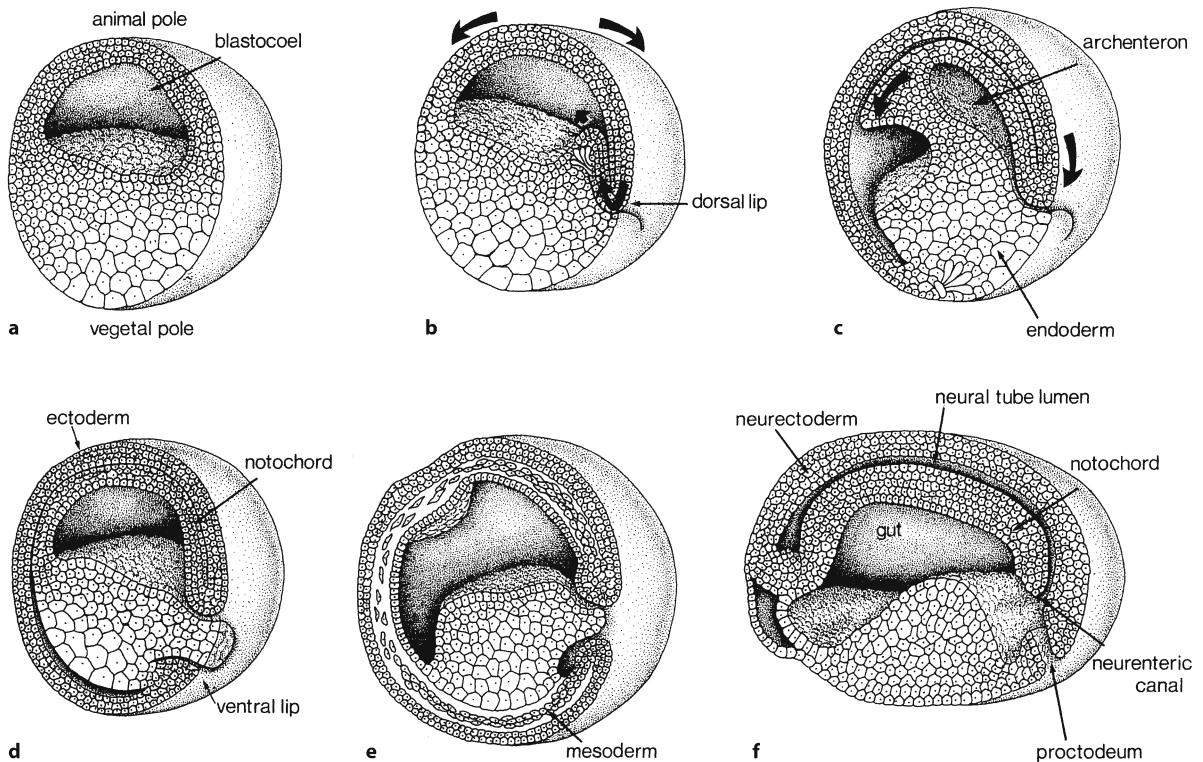
Fig. 2.1 Cell movements during gastrulation in a frog embryo. The major cell movements (*arrows*) are indicated. During early gastrulation (**a**, **b**), bottle cells of the margin move inwards to form the dorsal lip of the blastopore and mesodermal cells involute under the roof of the blastocoel. During midgastrulation (**c**, **d**), the archenteron forms and displaces the blastocoel. Cells migrate from the lateral and ventral blastopore lips into the embryo. Towards the end of gastrulation (**d**, **e**), the blastocoel becomes obliterated, the embryo is surrounded by ectoderm, the endoderm becomes internalized and mesodermal cells are found between the ectoderm and the entoderm. During the early tadpole stage (**f**), cells lining the blastopore form the neurenteric canal, part of which becomes the lumen of the secondary neural tube. (After Balinsky 1965; Gilbert 2000)

axis beneath the ectoderm, while the ectoderm spreads downwards to cover the whole embryo (Fig. 2.1 b–d). The layer of dorsal endoderm is closely applied to the mesoderm. Between this endodermal layer and the yolk-laden vegetal cells the **archenteron**, the precursor of the gut cavity, is formed. The cell movements of gastrulation transform the blastula into a bilateral, trilaminar embryo with head and tail ends, and three distinct layers, the germ layers: the ectoderm on the entire outside, enclosing the mesoderm and endoderm (Keller 1975; Keller et al. 1991). The nervous system arises from the ectoderm on the dorsal surface of the blastula. During gastrulation, tissue interactions between the ingressing dorsal cells (prospective pharyngeal endoderm and dorsal mesoderm, together referred to as mesendoderm) and the overlying ectoderm define the region of the ectoderm that will form the nervous system and establish principal axes, and direct cells within this region towards a neural fate. This process is known as neural induction.

Neural induction was discovered in the 1920s by Hans Spemann and Hilde Mangold (Spemann 1921; Spemann and Mangold 1924), during the course of grafting experiments on urodele blastulas. They transplanted a small region from the dorsal blastopore lip of a darkly pigmented *Triturus taeniatus* embryo to the ventral side of a non-pigmented *T. cristatus* embryo, and found that the host responded by forming an additional embryonic axis (Fig. 2.2) with a virtually complete CNS. The only tissues in the secondary axis that were contributed by the transplant were those that are normally derived from the dorsal mesoderm, such as the prechordal mesoderm and the notochord. The neural tissue arose from the ventral ectoderm of the host, a region that normally differentiates into epidermis. This experiment demonstrated that the nervous system forms in response to inductive signals. Subsequently, Waddington (1933) showed that the anterior end of the primitive streak in avian embryos, known as Hensen's node, can also duplicate the dorsal axis, including an induced ner-
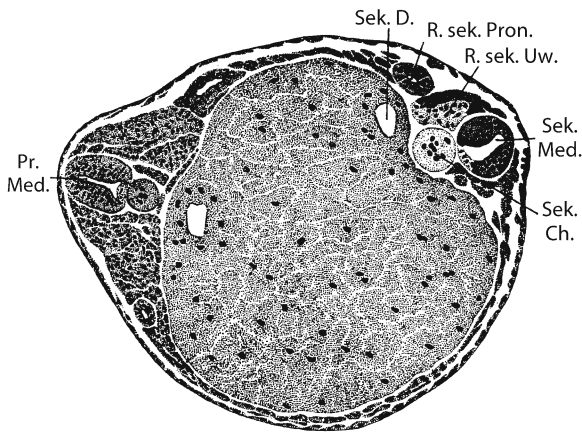
Fig. 2.2 The 'organizer' experiment carried out in the early 1920s by Hilde Mangold and Hans Spemann. Transplantation of the upper lip of the blastopore from one gastrula of a darkly pigmented newt to another lightly pigmented host often led to the induction of a second nervous system. *Pr.Med.* primary neural tube, *R.sek.Pron.* secondary pronephric duct, *R.sek.Uw.* secondary somite, *Sek.Ch.* secondary notochord, *Sek.D.* secondary endoderm, *Sek.Med.* secondary neural tube. (From Spemann and Mangold 1924)
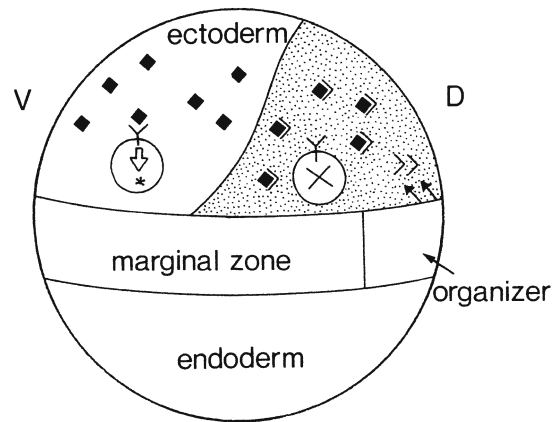
Fig. 2.3 The 'neural default' model for neural induction in *Xenopus laevis*. The ectoderm of the *Xenopus* gastrula contains a high local concentration of a soluble epidermal inducer (diamonds). Binding of this factor to its receptor (*Y*) in the ventral ectoderm initiates the programme for epidermal induction (marked with an *asterisk*), whereas in the dorsal ectoderm (*stippled*) antagonists of the epidermal inducer (>) are secreted from the organizer. These factors bind the epidermal inducer, prevent interaction with its receptor, and epidermal induction is not initiated (*X*). (After Weinstein and Hemmati-Brivanlou 1997)

vous system, and a similar role was attributed to the embryonic shield in fish embryos (Oppenheimer 1936; Driever 1999). Transplantation of the mouse node to an ectopic location can induce secondary axes, but they lack the anterior CNS (Beddington 1994). Therefore, vertebrate embryos contain a region, called the **Spemann–Mangold organizer**, which is necessary for inducing dorsal ectoderm to form neural tissue (De Robertis et al. 2000). The organizer is itself induced by the Nieuwkoop centre that in amphibians is located in the dorsalmost vegetal cells (Nieuwkoop 1973, 1977; Kessler 1999; Gilbert 2000; Wolpert et al. 2002). The posterior marginal zone of the chick embryo has Nieuwkoop-centre-like properties (Skromne and Stern 2001; Wittler and Kessel 2004).

2.2.2 The Molecular Basis of Neural Induction

Cells of the organizer contribute to the pharyngeal endoderm, the head mesoderm (the prechordal plate), the notochord and the dorsal blastopore lip (Keller 1976). The **pharyngeal endoderm** and the **prechordal plate** lead the migration of the organizer tissue, and induce the forebrain and the midbrain. The prechordal mesendoderm is essential for correct development of the optic stalks and the hypothala-

mus (Chap. 9). The **notochord** induces the hindbrain and the spinal cord. The early transplantation experiments showed that the organizer produces a soluble, neural-inducing factor that could neuralize competent ectoderm. Several soluble factors that can neuralize ectoderm in explant cultures have been isolated (Harland and Gerhart 1997; Weinstein and Hemmati-Brivanlou 1997; Streit and Stern 1999). Experiments with dissociated animal cap cells in *X. laevis* showed that ectodermal cells have a natural tendency to differentiate into neural tissue (Grunz and Tacke 1989), but are inhibited from doing so under the influence of BMP signalling (Hemmati-Brivanlou and Melton 1992, 1997). Bone morphogenetic protein 4 (BMP4), a member of the transforming growth factor β (TGFβ) ligand superfamily, is a potent neural inhibitor and epidermal inducer, and may represent the endogenous epidermis-inducing factor (Weinstein and Hemmati-Brivanlou 1997, 1999; Wilson and Edlund 2001; Muñoz-Sanjuán and Hemmati-Brivanlou 2002). The nervous system develops from that region of the ectoderm that is protected from epidermal induction. The inhibition of the BMP signalling pathway in the ectoderm is the hallmark of neural-fate acquisition, and forms the basis of the **default model** of neural induction (Fig. 2.3). Organizer proteins such as Noggin, Chordin, and Follistatin block the action of BMP4. Comparable data were obtained for zebrafish (Schier 2001). In mice, genetic knockouts of

chordin and *noggin* do not result in dramatic early embryonic phenotypes, but a compound knockout for both genes yields mice with severe defects in forebrain development (Bachiller et al. 2000). Another class of neural inhibitors are the Wnts, glycoproteins related to the *Drosophila* wingless proteins, which are required for a number of developmental processes, including midbrain and neural crest development. The inhibition of Wnt signalling by soluble Wnt antagonists leads to the induction of anterior neural markers in animal cap explants (Itoh et al. 1995; Leyns et al. 1997). Recently, the default model has been challenged (Wilson and Edlund 2001; Muñoz-Sanjuán and Hemmati-Brivanlou 2002; Stern 2002; Bally-Cuif and Hammerschmidt 2003). Various proteins, including Wnts, Fgfs and Igfs, are proposed to be positive inducers of the neural state.

2.2.3 Polarity and the Establishment of the Neuraxis

Initial polarity of the vertebrate CNS is established at about the same time as neural induction, through interactions between the ectoderm and the organizer or its derivatives (Gilbert 2000; Brown et al. 2001; Wolpert et al. 2002). Otto Mangold (1933) found that dorsal lip grafts from early gastrulae induced head structures, sometimes even a complete additional embryo, but that grafts from later gastrulae could induce only trunk and tail structures. These experiments suggested that the organizer consists of two components: (1) a **'head' organizer**, which induces the anterior part of the neuraxis (the forebrain), and (2) a **'tail' organizer**, which induces the caudal part (the rest of the brain and the spinal cord). In the 1950s, Nieuwkoop (Nieuwkoop and Nigtevecht 1954; Nieuwkoop and Albers 1990) and Saxén and Toivonen (Toivonen and Saxén 1955; Saxén and Toivonen 1962; Saxén 1989) proposed the two-step or **two-signal model** to explain results from their experiments on newt embryos. They proposed that the anteroposterior neural pattern is induced by the combined action of two signals produced by the dorsal mesoderm. The first signal, described by Nieuwkoop as the activator and as the neuralizing inducer by Saxén and Toivonen, initiates neural development by inducing neural tissue of an anterior type (forebrain and midbrain). This inducer was proposed to be produced by both the head mesoderm and the chordamesoderm. The second signal, the transformer (Nieuwkoop) or mesodermalizing inducer (Saxén and Toivonen), converts the neural tissue induced by the first signal into progressively more posterior types of neural tissue (hindbrain and spinal cord) with increasing concentration, and was proposed to be produced in a gradient by chordamesoderm. Mangold's experi-

ments suggested that each of the major regions of the neural tube is specified by signals secreted by at least two separate organizers, one for the head, one for trunk and tail. Nieuwkoop's activation–transformation model is the more attractive because it accounts for the generation of more than two regions with a smaller number of signals (Stern 2001, 2002).

Candidate anteriorizing signals include Cerberus and Dickkopf, expressed by the deep layer cells of the organizer in amphibians, by the prechordal mesendoderm in birds and by the **anterior visceral endoderm** (AVE) in mammals (Beddington and Robertson 1998; de Souza and Niehrs 2000; Kiecker and Niehrs 2001; Lu et al. 2001; Wittler and Kessel 2004). **Candidate posteriorizing signals** include retinoic acid, members of the fibroblast growth factor (FGF) and Wnt families and members of the TGFβ superfamily. These molecules are produced by the organizer and its mesodermal derivatives, and they can posteriorize induced neural tissue in animal cap assays and other experimental situations. If *Xenopus* neurulae are treated with retinoic acid, their forebrain and midbrain development is impaired in a concentration-dependent fashion (Durston et al. 1989; Papalopulu et al. 1991; Sharpe 1991; Maden 2002).

2.2.4 Neural Induction in Amniote Embryos

In amniotes, neural induction shows some differences compared with amphibians. In birds, the invagination of the cells of the blastula occurs along the **primitive streak**, a groove on the surface of the blastula (Fig. 2.4). Gastrulation results in the transformation of the pluripotent epiblast to three germ layers. In the chick embryo, the primitive ectoderm from which the nervous system arises has to be induced to form a neural plate, presumably through the inactivation of neural inhibitors, by signals from the mesendoderm. Grafts of Hensen's node, the avian organizer, can induce neural differentiation, and early nodes induce the expression of anterior neural genes, whereas later nodes induce posterior gene expression (Storey et al. 1992; Darnell et al. 1999). Avian forebrain expression appears to be a specialized property of the prechordal plate mesendoderm (Pera and Kessel 1997).

Gastrulation in mammals is generally similar to that in birds (Balinsky 1965). The early **mouse gastrula** has a cylindrical shape and consists of an outer and an inner epithelial layer (Fig. 2.5). All embryonic structures are derived from the inner layer (epiblast), while the outer layer, the visceral endoderm, does not contribute to the embryo proper (Tam and Behringer 1997; Beddington and Robertson 1998, 1999; Davidson et al. 1999; Lu et al. 2001). Gastrulation begins at the posterior side with the formation of the primitive

Fig. 2.4 Ingression of mesoderm and entoderm (*arrows*) during gastrulation in the chick embryo. Gastrulation begins with the formation of the primitive streak, a region of proliferating and migrating cells. Future mesodermal and endodermal cells migrate through the primitive streak into the interior of the embryo. The endodermal cells replace the hypoblast. At the rostral end of the primitive streak, Hensen's node forms. (After Balinsky 1965)
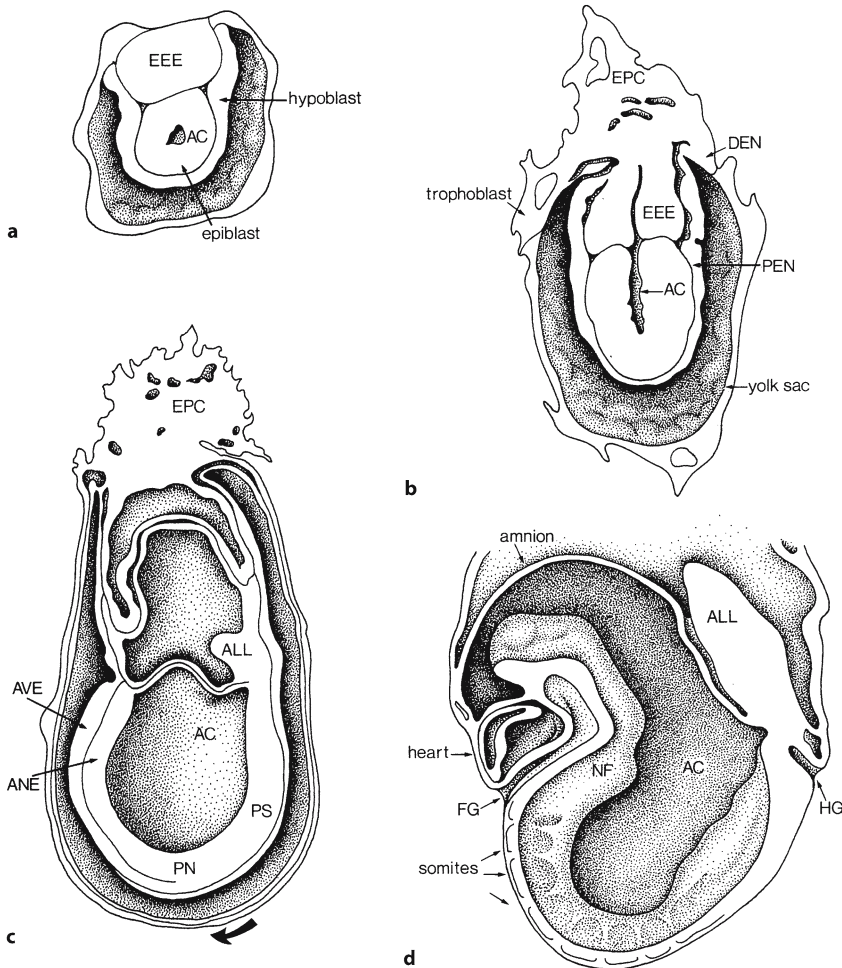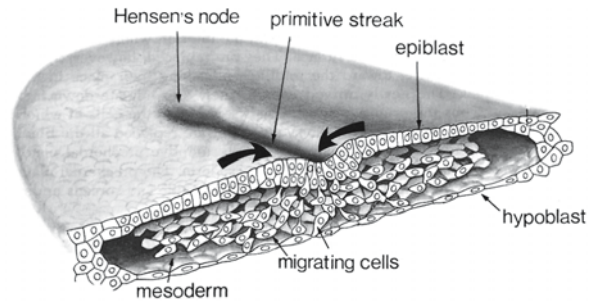
Fig. 2.5 Four stages of development of the mouse embryo. In the early egg cylinder stage (**a**), the inner cell mass is composed of the rudiment of the embryo proper (epiblast) around the amniotic cavity (*AC*), and the extraembryonic ectoderm (*EEE*). The hypoblast surrounds the epiblast. In the later egg cylinder stage (**b**), the extraembryonic ectoderm gives rise to the ectoplacental cone (*EPC*) which invades the maternal tissues. The endoderm spreads and covers the inner surface of the trophoblast (distal endoderm, *DEN*), whereas its proximal part (*PEN*) still surrounds the epiblast. In the primitive streak (*PS*) stage (**c**), the cavity inside the embryo has become subdivided into the amniotic cavity proper and the cavity of the ectoplacental cavity. The endoderm now completely surrounds both walls of the yolk sac cavity. The anterior visceral endoderm (*AVE*) covers the anterior neurectoderm (*ANE*). In a neural plate stage embryo (**d**), the embryo is curved around the amniotic cavity and is concave dorsally. *ALL* allantois, *FG* foregut, *HG* hindgut, *NF* neural fold, *PN* primitive node. (After Snell 1941; Theiler 1972; de Souza and Niehrs 2000)

streak and the node, a structure equivalent to the amphibian organizer. Axial mesendoderm derived from the node (pharyngeal endoderm, prechordal mesendoderm, chordamesoderm) migrates anteriorly and displaces the visceral endoderm. The AVE, which contacts the future anterior CNS during early gastrulation, induces the forebrain and midbrain (Thomas and Beddington 1996; Bouwmeester and Leyns 1997; Beddington and Robertson 1998). Initially, it was thought that the AVE could correspond to Mangold's 'head organizer', but more recently it has been shown that the AVE can only induce neural fates when combined both with the node and with responsive ectoderm (Tam and Steiner 1999; Stern 2002). The anterior endoderm of the *X. laevis* organizer and the mouse AVE express homologous genes (Beddington and Robertson 1998; de Souza and Niehrs 2000). Expression of *Otx2*, *Lhx1*, *Hex* and *Cerberus-like* genes in the AVE precedes the onset of gastrulation by half a day or more (Acampora et al. 1995; Belo et al. 1997; Biben et al. 1998; Thomas et al. 1998). In fact, in mice anterior identity is established before gastrulation starts.

2.2.5   Specific Pathways for Head Induction

In addition to the action of the neuralizing factors on ectoderm with prespecified anterior competence, other molecular signals are required for complete head induction (Beddington and Robertson 1998; de Souza and Niehrs 2000; Kiecker and Niehrs 2001; Stern 2001, 2002). Candidate effector molecules in pathways crucial to anterior head formation include the secreted molecules Cerberus, Frzb and Dickkopf (Dkk1). They block the Wnt signal from the lateral and ventral mesoderm. **Cerberus**, named after the mythological three-headed dog that guarded the entrance to Hades, can induce multiple heads without tails when injected as messenger RNA (mRNA) into early *Xenopus* embryos (Bouwmeester et al. 1996). It is expressed in the deep cells of the organizer that, during gastrulation, form the leading edge of the extending mesendoderm. These cells move ahead of the prechordal plate and are the first to contact the ectoderm from beneath. The heads induced by *cerberus* overexpression are not complete as they have only one eye (cyclopia), suggesting that Cerberus alone is not sufficient as a head inducer. **Frzb** is a small, soluble form of Frizzled, the Wnt receptor. It is synthesized predominantly in mesendodermal cells beneath the head (Leyns et al. 1997). Microinjection of *frzb* mRNA into the marginal zone leads to inhibition of trunk formation; the embryos become solely heads. The **Dickkopf** protein is normally expressed in the presumptive prechordal plate region of the organizer. Its mRNA induces the formation of complete
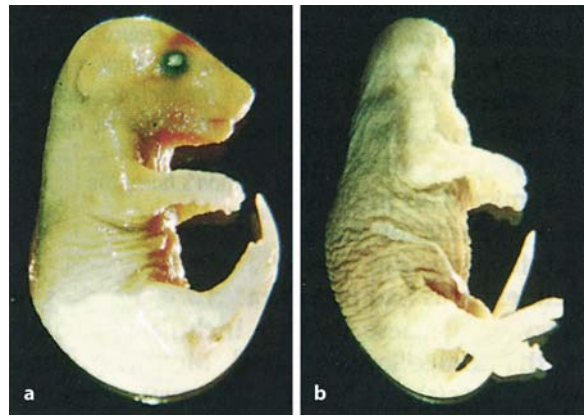
Fig. 2.6 Phenotype of a wild-type mouse with maintenance of anterior patterning (**a**), and a hOtx1²/hOtx1²-mouse (**b**) with failure in maintenance of anterior patterning (reproduced with permission from Acampora and Simeone 1999, *Trends Neurosci.* 22:116–122; copyright 1999, Elsevier)

heads with two eyes when co-injected with BMP inhibitors into early embryos (Glinka et al. 1998). Moreover, the injection of blocking antibodies to Dickkopf leads to microcephaly, showing that this molecule, in cooperation with BMP inhibitors, is necessary as well as sufficient for head induction. Dickkopf is thought to act as an antagonist of Wnt signaling in a double inhibitory mechanism reminiscent of that involving Noggin and BMPs. Comparable data were obtained for zebrafish (Schier 2001). *Dickkopf1* appears to be essential for forebrain development in mice (Mukhopadhyay et al. 2001).

In *Xenopus* and chick embryos, the prechordal mesendoderm is the dominant source of head-inducing signals during early gastrulation. In mammals, head induction needs a combination of signals from anterior primitive endoderm, prechordal plate and anterior ectoderm (Beddington and Robertson 1998; de Souza and Niehrs 2000). This suggests that, despite the homology of vertebrate anterior primitive endoderm, its role in head induction does not seem well-conserved. The principle role of the murine AVE appears to be to direct cell movements of the adjacent epiblast, to 'protect' portions of the prospective neural plate against the caudalizing (posteriorizing) influence of the node (Stern 2002). *Otx2* expression in the AVE is required for the normal movements of this layer (Kimura et al. 2000; Perea-Gómez et al. 2001). Like in the avian hypoblast (Foley et al. 2000; Stern 2002), movement of the AVE (Fig. 2.5) seems to be required for head development by distancing prospective forebrain cells from the caudalizing influence of the organizer.

Loss of function by targeted mutation of *Otx2* results in head deletion, an abnormal body plan, and in lack of the forebrain, midbrain and rostral hindbrain
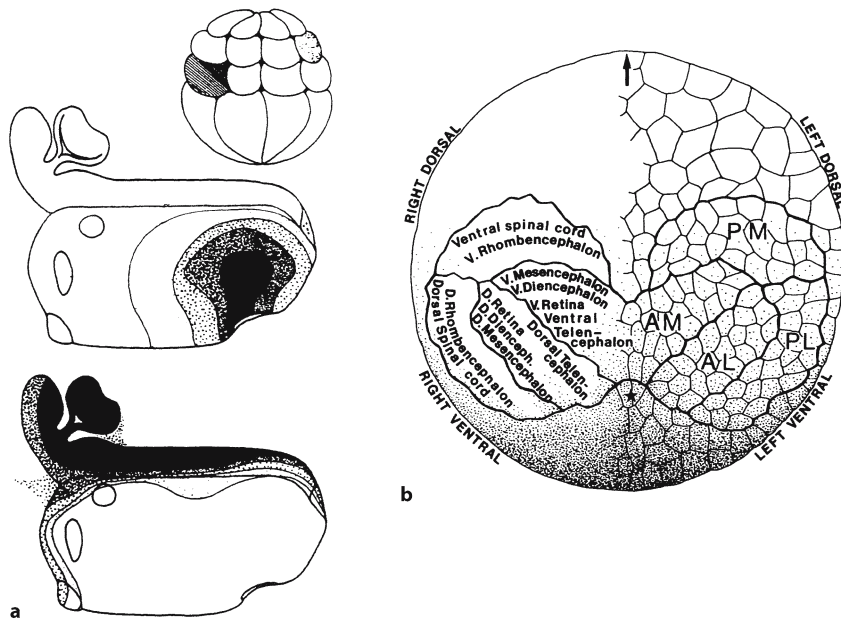
Fig. 2.7 Cell lineage studies in *X. laevis*. **a** The distribution of the neurectodermal descendants of V3 and D3 blastomeres after injection of a vital dye is shown at stages 28–30. **b** The locations and relative positions of the founder cell groups and the compartments of the CNS which they give rise to in a 512-cell embryo. The anteromedial founder cell group (*AM*) gives rise to the ventral parts of the retina, telencephalon, diencephalon and mesencephalon, and the anterolateral founder cell group (*AL*) gives rise to the dorsal parts of the retina, telencephalon, diencephalon and mesencephalon. The posteromedial (*PM*) and posterolateral (*PL*) founder cell groups give rise to ventral and dorsal parts of the rhombenephalon and spinal cord, respectively. (**a** After Gimlich and Cooke 1983; **b** after Jacobson 1982)

(Acampora and Simeone 1999; Acampora et al. 2001; Fig. 2.6). Probably, *Otx2* plays two separate roles in head development. Early expression in the AVE suggests an involvement in either the specification of anterior competence or induction, whereas later expression in the forebrain and midbrain suggests a subsequent role in the maintenance of the region. Straightforward loss of *Otx2* function by targeted mutation in mice deletes the entire head rostral to the middle of the hindbrain. The replacement of *Otx2* by the closely related gene *Otx1*, which is normally expressed late in forebrain development and not in the AVE, allows the embryo to escape the early gastrulation phenotype of *Otx2–/–* mutants. *Otx1* functionally substitutes for *Otx2* in the visceral endoderm. Mutants that lack other genes that are normally expressed in the AVE such as *Hex* and *Lhx1* also fail to develop anterior structures, including the forebrain (Beddington and Robertson 1999).

2.3 Cell Lineage Studies and Fate Mapping

Lineage analysis has been widely used to determine the phenotype and location of the progeny of a progenitor cell or group of progenitors. In animals with large, accessible cells, such as the nematode *C. elegans*, the grasshopper, *S. americana*, and the clawed toad, *X. laevis*, cells can readily be labelled with dyes like horseradish peroxidase (HRP) or fluorescent markers (Bate 1976; Sulston and Horvitz 1977; Goodman 1982; Jacobson 1982, 1985; Stent and Weisblat 1985). In this way, lineal descendants and differentiating axons can be followed during subsequent development. In *C. elegans*, the lineage of each of its cells is known (Sulston and Horvitz 1977; Sulston et al. 1983), and the pattern of cell lineage is completely invariant from animal to animal.

In *X. laevis*, Jacobson and co-workers (Hirose and Jacobson 1979; Jacobson and Hirose 1981; Jacobson 1983; Jacobson and Moody 1984; see also Gimlich and Cooke 1983; Moody 1987a, b, 1989; Moody and Kline 1990; Sullivan et al. 1999) studied the **clonal organization** of the CNS. They obtained highly consistent **fate maps** by injecting HRP or fluorescein dextran into individual ancestral cells that contribute progeny to the CNS in a large series of embryos at successive stages from the two-cell to the 512-cell stage (Fig. 2.7). The organization of the zebrafish fate map is similar to that of *Xenopus* (Kimmel et al. 1990; Driever 1999; Fraser 1999). In *Xenopus*, the brain and spinal cord are formed from seven compartments, and the ancestry of all cells in each compartment
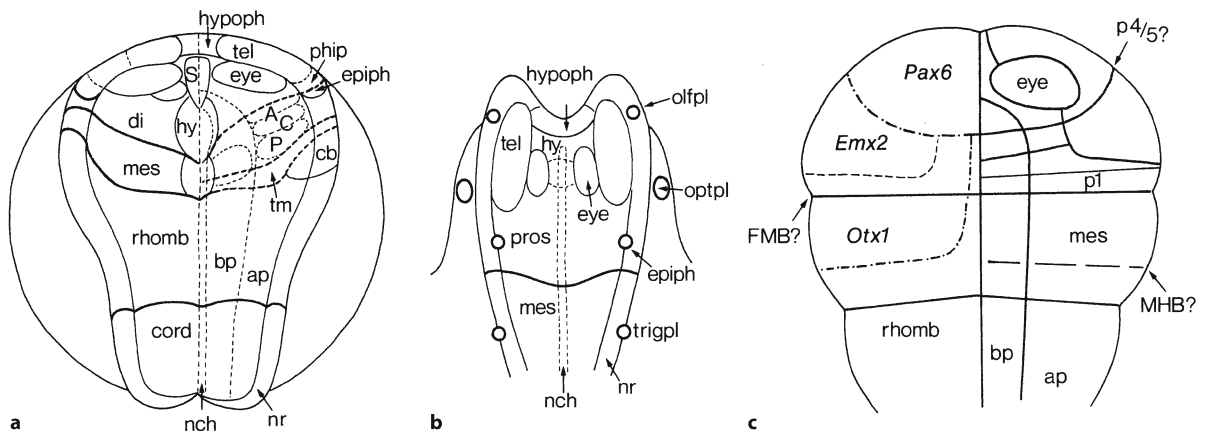
Fig. 2.8 Fate maps of: **a** *X. laevis* (stage 15); **b** the chick embryo (three to four somite stage) and **c** the mouse prosencephalic neural plate (after Inoue et al. 2000). For the mouse the distribution of the *Emx2*, *Otx1* and *Pax6* genes is also shown. *A, C, P* anterior, central and posterior thalamic nuclei, *ap* alar plate, *bp* basal plate, *cb* cerebellum, *di* diencephalon, *epiph* epiphysis, *FMB* forebrain–midbrain boundary, *hy* hypothalamus, *hypoph* hypophysis, *mes* mesencephalon, *MHB* mid-brain–hindbrain boundary, *nch* notochord, *nr* neural ridge, *olfpl* olfactory placode, *optpl* optic placode, *phip* primordium hippocampi, *pros* prosencephalon *rhomb* rhombencephalon, *S* suprachiasmatic nucleus, *tel* telencephalon, *tm* tectum mesencephali, *trigpl* tigeminal placode, *p1*, *p4/5* prosomeres. (**a** After Eagleson and Harris 1990; **b** after Couly and Le Douarin 1987)

could be traced back to a small group of founder cells in the 512-cell blastula (Hirose and Jacobson 1979). The outgrowth of labelled axons from neurons that received their label from progenitor cells could also be traced, at least for early differentiating neurons such as Rohon–Beard cells and primary motoneurons (Jacobson and Huang 1985; Hartenstein 1989). After injection of HRP into a single blastomere, the tracer is transmitted during mitosis to all descendants and can be seen up to a week later in well-developed cells, including neurons and their peripheral targets. All types of nerve fibres studied grew by the most direct pathway, apparently without errors of initial outgrowth, pathway selection or target selection (Jacobson and Huang 1985).

Unfortunately, single cell injections can hardly be used to label entire populations of the much smaller cells in the neural plate; therefore, Eagleson and Harris (1990) applied fluorescent dyes as vital markers to the neural plate and ridge of *X. laevis*. Most areas of the brain derive from the neural plate in a fate map (Fig. 2.8a) that is consistent with the topology of a sheet rolling into a tube, i.e. neighbouring areas are maintained as neighbours. Much of the telencephalon, ventral forebrain and dorsal brain stem appear to derive from the neural ridge and not from the neural plate (Eagleson and Harris 1990; Eagleson et al. 1995). The anterior pituitary arises from the median part of the anterior neural ridge, whereas the hypothalamus originates from the midline parts of the anterior neural plate (Fig. 2.8a).

To study the lineal relationships in the avian central and peripheral nervous system, Le Douarin (1973) pioneered the **chimera method.** By combining chick and quail tissue and following the cells of each species through distinctive nuclear staining patterns, Couly and Le Douarin (1987) produced a fate map of the three to four somite stage chick embryo (Fig. 2.8b). In chick embryos, the telencephalon arises from the lateral (future dorsal or alar) regions of the anterior neural plate, whereas the medial (later ventral or basal) region gives rise to the diencephalon (Couly and Le Douarin 1987; Rubinstein et al. 1998; Le Douarin and Kalcheim 1999; Cobos et al. 2001). In a mouse whole-embryo culture system, Inoue et al. (2000) labeled neuroepithelial cells with vital dyes and traced their siblings for 1 or 2 days. The fate map of the mouse prosencephalic neural plate appears to be rather similar to the fate maps of other vertebrates (Fig. 2.8c).

In mammalian embryos, **retroviral vectors** are increasingly used to study clonal patterns of proliferation, migration and dispersal in the CNS (Cepko 1988; Sanes 1989; Cepko et al. 1997). A retrovirus vector is an infectious virus that transduces a non-viral gene into mitotic cells in vivo or in vitro. Modified viral vectors are passed to all daughter cells of the originally infected progenitor cell. Retroviruses have been used for lineage analysis in the mouse, chicken, rat, ferret and primate CNS (McConnell 1995; Cepko et al. 1997). Examples of such clonal analysis will be discussed in the chapters on the spinal cord, brain stem, cerebellum and cerebral cortex.

2.4   Pattern Formation

Pattern formation is the spatial ordering of cell differentiation. Patterning of all regions of the neural plate involves two general sets of mechanisms, one that patterns along the anteroposterior axis and the other that patterns along the mediolateral axis. **Anteroposterior patterning** generates transverse subdivisions of the neural plate. During an early phase, regions and subregions are specified, later followed by the acquisition of individual identity. The principle brain regions are characterized by the expression of region-specific transcription factors. A prominent signalling centre at the midbrain–hindbrain boundary (MHB; the isthmus) is responsible for specifying the fate of the midbrain and cerebellum. Hindbrain development is characterized by a process of segmentation, setting up a modular organization of brain stem nuclei. **Mediolateral patterning** induces the primordia of the principal longitudinal columns or domains of the CNS, the floor, basal, alar and roof plates. Within the neural plate mediolateral regional identities are specified in part by molecules produced by adjacent non-neural tissues. At spinal and brain stem levels of the neural plate, medial cell fates are specified by the notochord (Placzek 1995; Tanabe and Jessell 1996). Lateral cell fates are specified by the adjacent non-neural ectoderm (Dickinson et al. 1995; Liem et al. 1995; Lee and Jessell 1999).

The **neuromeric organization** of the brain is shown in Fig. 2.9. Bergquist and Källén (Bergquist 1932, 1952; Bergquist and Källén 1954; Källén 1951a, b) extensively studied the segmentation of the vertebrate brain. They clearly showed that neuromeres are present during a certain developmental period in all vertebrates, and that they coincide topographically with zones of high mitotic rate, i.e. centres of proliferation (for further discussion see Nieuwenhuys 1998a). The topography of the neuromeres and the different migration areas in a generalized vertebrate brain is shown in Fig. 2.9a. Each neuromere has alar (dorsal) and basal (ventral) components, divided by the sulcus limitans of His, at least in the spinal cord and brain stem (His 1888). In the spinal cord and brain stem, the basal plate contains the motor centres and the alar plate the sensory centres. Gene expression studies in mice (Bulfone et al. 1993; Puelles and Rubinstein 1993; Shimamura et al. 1995; Rubinstein et al. 1998) show that some genes are expressed in the alar plate only, others only in the basal plate (Fig. 2.13). One gene, *Nkx2.2*, is expressed along the longitudinal axis of the brain, ending in the chiasmatic region (Figs. 2.9b, 2.13c, d). On the basis of these findings, in all murine prosomeres alar and basal parts are distinguished (Rubinstein et al. 1998; Puelles et al. 2000; Puelles and Rubinstein 2003).
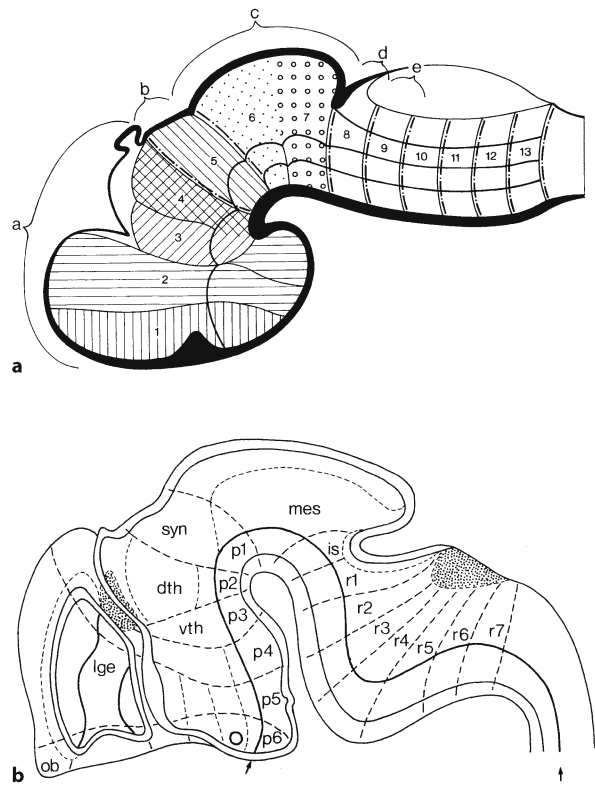
Fig. 2.9 Neuromeric organization of the brain: **a** Bergquist and Källén's view of a generalized vertebrate brain; **b** recent view according to Puelles and co-workers (Puelles 1995; Rubinstein et al. 1998). In **a**, the neuromeres are marked *a–e*; areas that form transverse bands are marked *1–13*. The *arrows* in **b** mark the longitudinal axis of the brain. *dth* dorsal thalamus, *is* isthmus, *lge* lateral ganglionic eminence, *mes* mesencephalon, *ob* olfactory bulb, *p1–p6* prosomeres, *r1–r7* rhombomeres *syn* synencephalon (pretectum), *vth* ventral thalamus. (**a** After Bergquist and Källén 1954; from Nieuwenhuys 1998a)

Figure 2.10 shows an overview of inductive signals and regional patterning of the neural tube. Specialized, transverse patterning centres found along the rostrocaudal axis of the neural tube, such as the anterior neural ridge, the zona limitans interthalamica and the isthmus rhombencephali, provide sources of secreted factors that establish regional identity and neuronal fate in adjacent parts of the neural tube. Cells in the isthmus secrete FGFs and Wnts, both of which are required for the differentiation of the midbrain and hindbrain. FGF8 is also expressed in the future basal forebrain and the anterior neural ridge. The rostral part of the brain (forebrain and midbrain) is characterized by the expression of the Otx genes. The engrailed genes mark the midbrain and first rhombomere, whereas the identity of the other rhombomeres is controlled by Hox genes. Medial
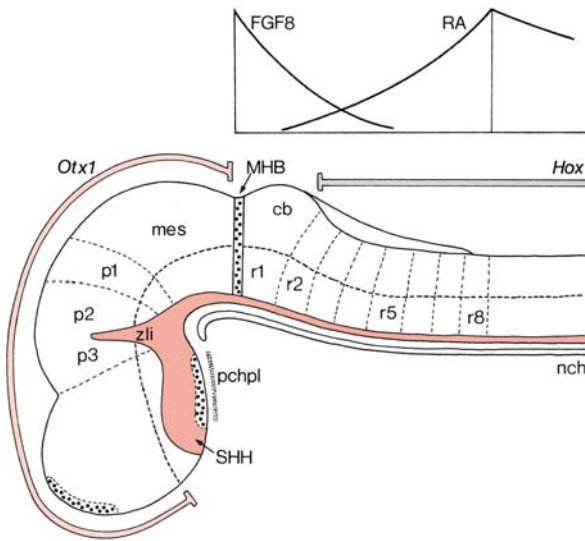
Fig. 2.10 Overview of inductive signals and regional patterning of the neural tube (fibroblast growth factor 8, *FGF8/* retinoic acid, *RA* data from Gavalas and Krumlauf 2000). FGF expression is shown by *dots*. The high point of the RA morphogen occurs at the spinal cord–hindbrain boundary with gradual decreasing levels both rostrally and caudally. The FGF8 highpoint occurs at the level of the isthmus. *cb* cerebellum, *Hox* expression of *Hox* genes, *mes* mesencephalon, *MHB* midbrain–hindbrain boundary, *nch* notochord, *p1–p3* prosomeres, *Otx1* expression of the *Otx1* gene, *pchpl* prechordal plate, *r1–r8* rhombomeres, *SHH* Sonic hedgehog expression, *zli* zona limitans interthalamica. (After Jessell and Sanes 2000)

signalling is regulated by Sonic hedgehog (SHH; Echelard et al. 1993; Roelink et al. 1994, 1995; Chiang et al. 1996), whereas lateral signalling is regulated by bone morphogenetic proteins (Dickinson et al. 1995; Liem et al. 1995; Tanabe and Jessell 1996; Lee and Jessell 1999).

The anatomical **bauplan** of early brain development is remarkably similar in insects and vertebrates (Reichert and Boyan 1997; Arendt and Nübler-Jung 1999; Brown et al. 2001). This is evident in the regional expression of homologous pattern-controlling genes (Fig. 2.11) as well as in the arrangement of the first axonal pathways to appear (Fig. 2.26). The three main clusters of neuroblasts, proto-, deuto- and tritocerebrum, forming the anterior part of the insect brain (the future supraoesophageal ganglion), may be equivalent to the vertebrate forebrain and midbrain regions. Moreover, the paired ganglia of the gnathal segments (the future suboesophageal ganglion) and the vertebrate rhombomeres express particular combinations of *Hox* genes. The molecules that regulate the development of the brain may be divided into (1) **transcription factors** (Table 2.1), coded by the homeobox genes such as the *Dlx*, *Emx*,
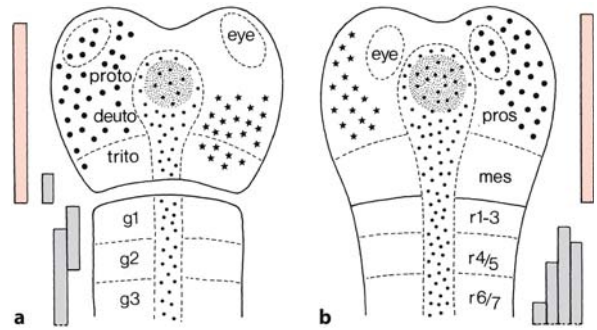
Fig. 2.11 Comparison of *Drosophila* (**a**) and mouse (**b**) data on similar patterns of nerve cell groupings and expression of orthologous genes. *Large dots* indicate the expression of *tailless* and *Tlx*, *asterisks* that of *empty spiracles* and *Emx2*, medium-sized dots that of *forkhead* and *HNF3″*, and small dots that of *decapentaplegic* and *Bmp4*. The *red bars* show the expression domains of *orthodenticle* and *Otx2* and the *grey bars* show the expression domains of *HOM-C* and *Hoxa* genes. *deuto* deutocerebrum, *g1–g3* suboesophageal ganglia, *mes* mesencephalon, *pros* prosencephalon, *proto* protocerebrum, *r1–r7* rhombomeres, *trito* tritocerebrum. (After Arendt and Nübler-Jung 1999)
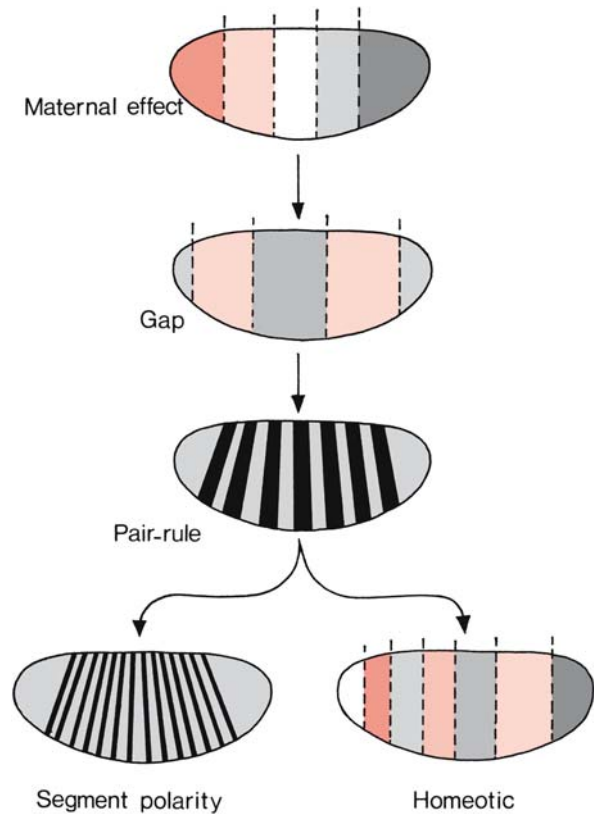
Fig. 2.12 Generalized model of *Drosophila* pattern formation: maternal effect, segmentation and homeotic selector genes (see text for explanation) (after Wilkinson and Krumlauf 1990; Gilbert 2000)

Table 2.1 Some regulatory genes encoding transcription factors expressed in the developing murine brain (after Price and Willshaw 2000)

Gene	Expression	Function
Ascl1	Telencephalon	Regulates differentiation of ventral telencephalon
Dlx genes		Family of homeobox-containing genes with homology to *Drosophila* distal-less
Dlx1/Dlx2	Subpallium	Subcortical neuroblast migration; interneuron migration from ganglionic eminences to cerebral cortex
Dlx5	Diencephalon and ganglionic eminences, olfactory bulb	
Emx genes		Mouse homologues of *Drosophila* genes (empty spiracles) that regulate its head development
Emx1	Telencephalon	Cell proliferation
Emx2	Cerebral hemispheres	Neuroblast migration
En genes		Mouse homologues of *Drosophila* engrailed genes
En1	Mesencephalon, rhombomere 1	Formation of mesencephalon and metencephalon, including cerebellar cortex
En2	Mesencephalon, rhombomere 1	Formation of mesencephalon and metencephalon, including cerebellar cortex
Hox genes		
Lhx genes		Members of a family of genes each encoding two LIM domains and a homeodomain. LIM domains may modulate the functions of the homeodomain
Lhx1	Forebrain	
Lhx2	Cerebral cortex	
Lhx5	Forebrain	
Math1	Rhombomere 1, cerebellum	Differentiation of cerebellar granule cells
Nkx genes		Members of homeobox-containing genes, expressed in restricted regions of developing forebrain
Nkx2.1	Striatum	
Nkx2.2		
Otx genes		Mouse homologues of *Drosophila* orthodenticle gene, involved in head development
Otx1	Forebrain, midbrain	
Otx2	Forebrain, midbrain	
Pax genes		Members of a family that contain a paired-box. Most *Pax* genes are expressed in the CNS in temporally and spatially restricted patterns
Pax3	Spinal cord, rhombomeres 1 and 8; cerebellum, forebrain	Identity of Bergmann glia; spinal cord dorsalizing gradient
Pax6	Spinal cord, rhombomeres 1 and 8, cerebral cortex	Identity of cerebellar granule cells; spinal cord dorsalizing gradient; neuroblast migration to cerebral cortex; iris

Hox, *Lhx*, *Otx* and *Pax* families, which act intracellularly and, by binding to DNA, control the expression of other genes, and (2) **extracellular signalling molecules** (Table 2.2), which are either released by a cell or are anchored on its cell surface, and act upon other cells. This category includes secreted proteins involved in early neural induction, the BMPs, the secreted proteins of the *Wnt* and *hedgehog* families, the FGFs, molecules involved in axon guidance, and neurotrophic factors. Such morphogens may play multiple roles in CNS development. SHH was initially described as a protein secreted from the notochord, the prechordal plate and the floor plate. Subsequently, it was identified as a morphogen that is directly responsible for dorsoventral patterning of the CNS. Later, additional sites of SHH expression were identified. Multiple actions of SHH during CNS development were discovered, including the specification of oligodendrocytes, proliferation of neural precursors and control of axon growth (Marti and Bovolenta 2002).

A generalized model of *Drosophila* pattern formation is shown in Fig. 2.12. This pattern is established by **maternal effect genes** that form gradients and regions of morphogenetic proteins (Wilkinson and Krumlauf 1990; Gilbert 2000; Wolpert et al. 2002). One of these proteins, bicoid, regulates the production of anterior structures, whereas another maternally specified protein, nanos, is involved in the formation of the posterior part of the embryo. These morphogenetic determinants create a gradient of the hunchback protein that differentially activates the **gap genes** (mutations in them cause gaps in the segmentation pattern). The gap genes enable the expression of **pair-rule genes**, each of which divides the embryo into regions of about two segment primordia.

Table 2.2 Some of the extracellular signalling molecules that regulate brain development (after Price and Willshaw 2000)

Extracellular signalling molecules	Function
Proteins	
Members of the transforming growth factor beta superfamily	The bone morphogenetic proteins form a large subgroup that regulates diverse developmental processes including proliferation, cell death, cell migration, cell differentiation and morphogenesis
Members of the Wnt family	These glycoproteins have multiple roles in development. Wnt is a fusion of the name of the *Drosophila* segment polarity gene wingless with that of one of its vertebrate homologues, integrated
Members of the hedgehog family	Vertebrates have at least three homologues of the hedgehog proteins: Sonic hedgehog (SHH), Desert hedgehog (DHH) and Indian hedgehog (IHH). Of these, SHH is the most important for CNS development. It is produced by the notochord and induces floor plate cells
Fibroblast growth factors	Fibroblast growth factors are associated with angiogenesis, mesoderm formation, induction of specific neural structures (anterior neural ridge, isthmus organizer), axonal extension and cell survival
Epidermal growth factor	Implicated in fate determination in the developing cerebral cortex, the generation of glial cells in particular
Neuroregulins	Implicated in glial-guided migration of neuronal precursors. These secreted growth factors act on ErbB receptors
Notch and Delta	Regulators of neural induction, bound to the cell surface. The Notch receptor protein on one cell binds to the Delta protein on another cell when the cells are juxtaposed
Cerberus, Chordin, Follistatin, Noggin	Secreted proteins involved in early neural induction by mesodermal and endodermal tissues
Neurotransmitters	Glutamate, GABA and serotonin have been implicated in the regulation of cortical developmental processes, such as proliferation, migration and thalamocortical innervation
Molecules involved in axon guidance	These molecules include (1) cell adhesion molecules and receptors of the immunoglobulin superfamily, and (2) diffusable and membrane-bound molecules of the netrin and semaphorin families
Neurotrophic factors	Neurotrophic factors include (1) growth factors such as the neurotrophins and fibroblast growth factors and (2) cytokines

The **segment polarity genes** in their turn divide the embryo into 14 segment-sized units along the antero-posterior axis. Interaction of proteins of the gap, pair-rule and segment polarity genes regulates the **homeotic genes,** whose description determines the developmental fate of each segment.

2.4.1   Regionalization of the Forebrain

Fate mapping experiments suggest that the telen-cephalic vesicles derive from the anterolateral neural plate (Couly and Le Douarin 1987; Eagleson and Harris 1990; Inoue et al. 2000; Cobos et al. 2001). This region includes the lateral part of the anterior neural ridge (Figs. 2.8, 2.13a). When the neural plate is formed, anteroposterior patterning within the forebrain appears to be controlled by the **anterior neural ridge** (Shimamura and Rubinstein 1997; Houart et al. 1998, 2002; Marín and Rubinstein 2002; Schuurmans

and Guillemot 2002; Zaki et al. 2003). Its patterning properties may be mediated by FGF8. Reduction in the expression of *Fgf8* in the anterior neural ridge leads to rostral midline defects in the forebrain (Shanmugalingam et al. 2000), similar to that described in mice lacking the brain factor *BF1* (*Foxg1*) gene (Xuan et al. 1995; Dou et al. 1999). *BF1* is activated by FGF8 (Shimamura et al. 1995; Shimamura and Rubinstein 1997). FGF signalling is also required for olfactory bulb morphogenesis (Hébert et al. 2003).

    Mediolateral patterning of the forebrain involves signals from the axial mesendoderm and non-neural ectoderm (Rubinstein and Beachy 1998; Lee and Jessell 1999). **Medial patterning** of the anterior forebrain is primarily regulated by the prechordal plate, whereas medial patterning of more posterior parts of the forebrain may be controlled by the rostral notochord (Dale et al. 1997; Pera and Kessell 1997; Shimamura and Rubinstein 1997). The medial patterning activity of the prechordal plate and notochord is me-
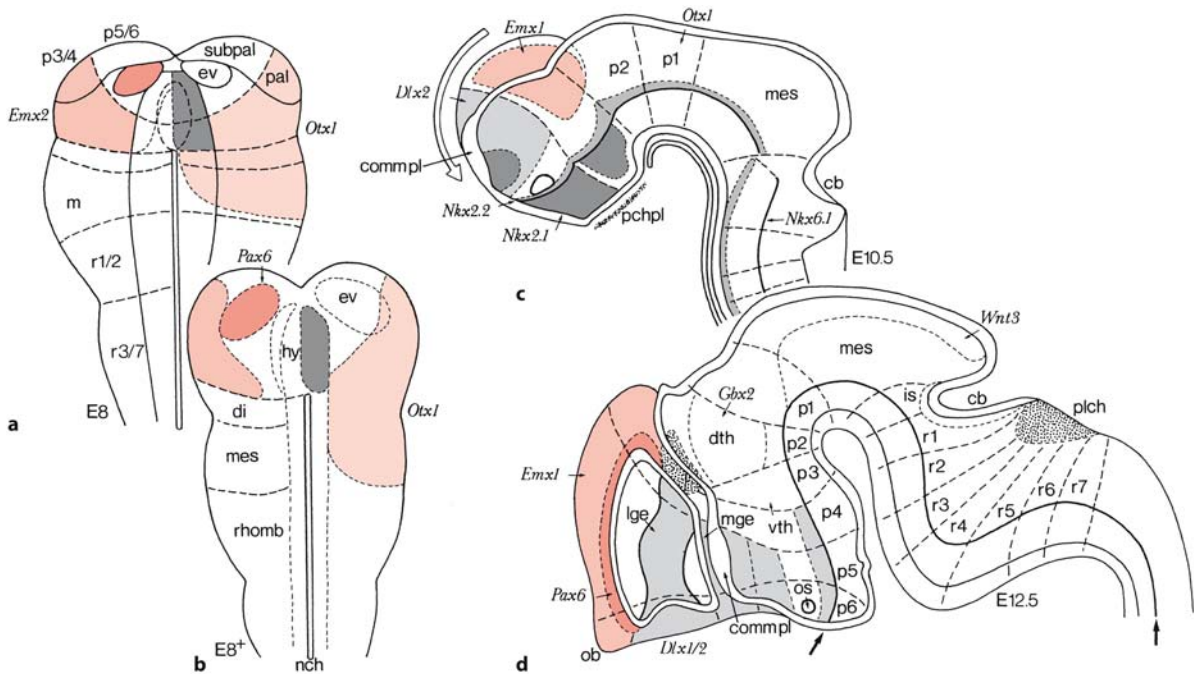
Fig. 2.13 Gene expression patterns in the developing murine forebrain. The *arrows* indicate the longitudinal axis of the brain. *cb* cerebellum, *comm pl* commissural plate, *di* diencephalon, *dth* dorsal thalamus, *ev* eye vesicle, *hy* hypothalamus, *is* isthmus, *lge* lateral ganglionic eminence, *m* mesomere, *mes* mesencephalon, *mge* medial ganglionic eminence, *nch* notochord, *ob* olfactory bulb, *os* optic stalk, *p1–p6* prosomeres, *pal* pallium, *pchpl* prechordal plate, *r1–r7* rhombomeres, *rhomb* rhombencephalon, *subpal* subpallium, *vth* ventral thalamus. (After Bulfone et al. 1993; Puelles and Rubinstein 1993; Shimamura et al. 1995; Rubinstein et al. 1998)

diated by the secreted molecule SHH (Echelard et al. 1993; Litingtung and Chiang 2000; Marti and Bovolenta 2002). Defects that affect the formation or differentiation of the axial mesendoderm or that directly disrupt the production or signal transduction of SHH affect medial patterning of the forebrain. Severe defects in medial patterning lead to the loss of the prosencephalic basal plate and also affect craniofacial development. Cyclopia and holoprosencephaly may result from defective patterning of the median eye-field structures and the basal telencephalon, respectively (Chap. 9). **Lateral patterning** of the anterior neural plate is mediated by members of the TGFβ superfamily, such as BMPs and growth differentiating factors, largely derived from the neural ridge and non-neural ectoderm flanking the anterior neural plate (Fig. 1.10). BMP activity appears to be required for the specification of all dorsal (lateral) cell fates (Mehler et al. 1997; Barth et al. 1999; Lee and Jessell 1999). The entire cerebral cortex (the pallium) as well as the basal ganglia (the subpallium) appear to be derived from the alar plate territory (Fig. 2.13).

2.4.2 The Midbrain–Hindbrain Boundary Organizer

The **midbrain–hindbrain boundary organizer** (MHB organizer) or **isthmic organizer** was identified through transplantation experiments in chick embryos. When MHB tissue was transplanted into the caudal forebrain of chick embryos, the surrounding host tissue adopted an isthmic or midbrain character (Martínez et al. 1991; Marín and Puelles 1994; Wassef and Joyner 1997). Moreover, in the hindbrain transplanted MHB tissue induced cerebellar fate (Martínez et al. 1995). Several genes, encoding transcription factors such as the *Engrailed* (*En*), *Pax*, *Otx* and *Gbx* families or secreted proteins (Wnt and Fgf families), are expressed within the MHB at early embryonic stages (Wassef and Joyner 1997; Rhinn and Brand 2001; Liu and Joyner 2001; Wurst and Bally-Cuif 2001; Joyner 2002; Raible and Brand 2004). The isthmus organizer itself is set up by the expression of a complex array of genes, two of which are central to its development (Fig. 2.13). The first, *Otx2* (one of the mouse homologues of the *Drosophila* gene orthodenticle), is expressed in the prosencephalon and mesencephalon. Its posterior limit of expression marks the anterior
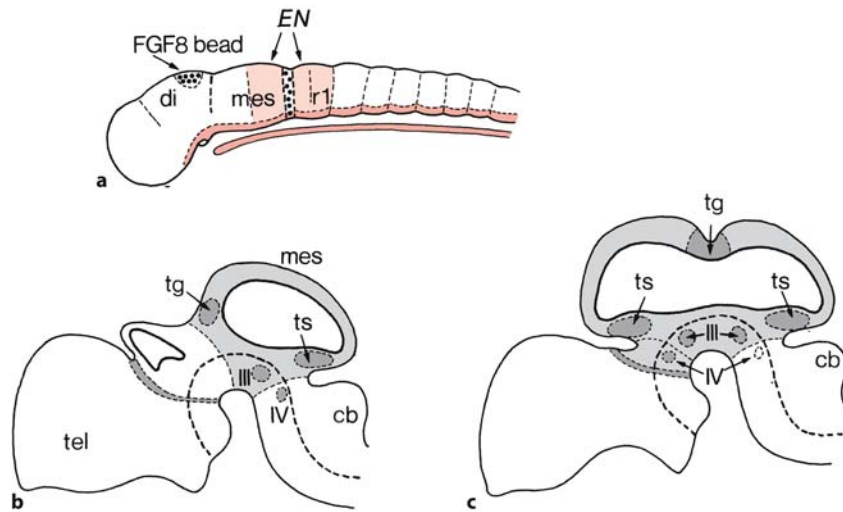
Fig. 2.14 Effects of implantation of an FGF8-containing bead into the posterior diencephalon (**a**). The normal situation (**b**) is transformed in such a way that the posterior diencephalon is replaced by a second set of midbrain structures (**c**), laid out in reverse anteroposterior polarity to the normal midbrain, and thought to be due to the ectopic expression of *Engrailed* (*EN*). *cb* cerebellum, *di* diencephalon, *mes* mesencephalon, *r1* first rhombomere, *tg* tectal grey, *tel* telencephalon, *ts* torus semicircularis (auditory midbrain), *III*, *IV* oculomotor and trochlear nuclei. (After Crossley et al. 1996; Brown et al. 2001)

limit of the MHB. A second gene, *Gbx2* (a homologue of the *Drosophila* gene unplugged), is expressed in the rostral part of the hindbrain. Its anterior limit of expression marks the posterior limit of the MHB. In *Otx2* knockout mice, the rostral neuroectoderm is not formed, leading to the absence of the prosencephalon and the rostral part of the brain stem (Acampora et al. 2001; Wurst and Bally-Cuif 2001). MHB cells secrete FGFs and *Wnt* (mouse homologues of the *Drosophila* gene wingless) proteins which are required for the differentiation and patterning of the midbrain and hindbrain (Nakamura 2001; Rhinn and Brand 2001; Joyner 2002; Raible and Brand 2004). The isthmic organizer signal FGF8 is required for cell survival in the prospective midbrain and cerebellum (Chi et al. 2003). Elimination of murine *Fgf8* during early somitogenesis leads to progressive loss of the midbrain. Two other FGF ligands, FGF17b and FGF18, are likely to be involved in the midbrain-directed signal (Raible and Brand 2004). In *Wnt1* knockout mice, the mesencephalon is malformed and a cerebellum is hardly present (McMahon et al. 1992; Mastick et al. 1996).

A number of homeobox-containing transcription factors are expressed across the isthmus, including the homeobox genes *En1* and *En2* (homologues of the *Drosophila* gene engrailed) and the paired box genes *Pax2*, *Pax5* and *Pax8*. Expression of the two *En* genes is the earliest known marker for mesencephalic polarity (Joyner 1996). They are expressed in almost similar domains in a gradient that decreases anteriorly through the mesencephalon and posteriorly

through the first rhombomere. Graded expression of the *En* genes appears to be regulated by signalling from the isthmus. Mutations in these genes cause deletions of mesencephalic and cerebellar structures (Millen et al. 1994; Wurst et al. 1994; Kuemerle et al. 1997; Chap. 7). FGF8 is expressed immediately posterior to expression of *Wnt1*, and has midbrain-inducing and polarizing abilities (Crossley et al. 1996). Implantation of a bead, releasing FGF8 protein, into the posterior diencephalon of a 1.5-day-old chick embryo results in the transformation of the diencephalon into midbrain (Fig. 2.14). This is thought to be due to the induction of *En* expression by FGF8 and the formation of a novel anteroposterior gradient of EN protein in the diencephalon that is the mirror image of the endogenous EN gradient in the midbrain. *Pax2*, *Pax5*, and *Pax8* are also required for specification of the isthmus. The isthmus is deleted in *Pax5–/–* mice (Urbanek et al. 1994). Mutations in at least three zebrafish genes, *no isthmus* (*noi*; lacking functional *Pax2/5/8*), *acerebellar* (*ace*) and *spiel ohne grenzen* (*spg*), lead to defects in the development of the MHB region (Brand et al. 1996; Schier et al. 1996; Schier 1997; Reifers et al. 1998; Belting et al. 2001; Burgess et al. 2002; Reim and Brand 2002; Jászai et al. 2003; Raible and Brand 2004). Whereas *noi* is involved in the development of both prospective tectum and cerebellum, the effect of *ace* is mostly restricted to the cerebellum, and the phenotype of *spg* resembles that of *ace/fgf8* mutants in that both lack an isthmus and have brain patterning defects.

2.4.3   Segmentation of the Hindbrain

Hindbrain development is characterized by the process of segmentation. A modular organization (**compartments**) of neuronal subtypes and nuclei in the hindbrain is set up by its early transverse subdivision into eight rhombomeres (Lumsden and Keynes 1989; Lumsden 1990, 2004; Guthrie 1996; Moens and Prince 2002; Pasini and Wilkinson 2002). Rhombomere identity is controlled by *Hox* genes. Signalling by FGF8 from the isthmus patterns anterior hindbrain and establishes the anterior limit of *Hox* gene expression (Irving and Mason 2000). Rhombomere 1 is the only hindbrain segment in which no *Hox* genes are expressed. It gives rise to the entire cerebellum (Chap. 8). The neuronal organization of the posterior hindbrain is less overtly segmental than that of the anterior hindbrain. The segmentation and patterning of the hindbrain and pharyngeal arches are intimately linked (Rijli et al. 1998; Trainor and Krumlauf 2000; Graham and Smith 2001).

In the avian embryo, rhombomeres become apparent immediately following neural tube closure as a series of constrictions, the interrhombomeric boundaries, progressively subdivide the developing hindbrain. The pattern of eight rhombomeres is complete at the onset of neurogenesis. Two patterns of **metameric cellular organization** are found in the embryonic hindbrain. Like in zebrafish (Kimmel et al. 1988), the first is a repeat pattern through every segment involving eight identified types of reticulospinal neurons (Glover and Petursdottir 1991; Clarke and Lumsden 1993; for rodent data see Auclair et al. 1999). More or less the same holds for vestibular projection neurons (Díaz et al. 1998; Díaz and Glover 2002; for frog data see Straka et al. 2001, 2002). The second is a two-segment repeat pattern involving the branchial motoneurons. They first appear in the even-numbered rhombomeres, r2 (trigeminal), r4 (facial) and r6 (glossopharyngeal), containing the respective exit sites of these cranial nerves in the alar plate. Thereafter, further neurons are formed in the intervening odd-numbered rhombomeres, each in association with the cluster of motoneurons in the rostrally adjacent rhombomere (Lumsden and Keynes 1989). Later in development, the segmental origins of the branchiomotor neurons become obscured as the motor nuclei condense and migrate to new positions. This two-segment periodicity of the early hindbrain is also found in the migration of neural crest cells to the branchial arches: neural crest cells migrate from r2, r4 and r6 into the first, second and third arches, respectively (Lumsden et al. 1991; Le Douarin and Kalcheim 1999; Chap. 5). Each rhombomere is unique owing to differences in the size, number and projections of reticulospinal neurons. Rhombomere 1 is distinct by lacking branchiomotor
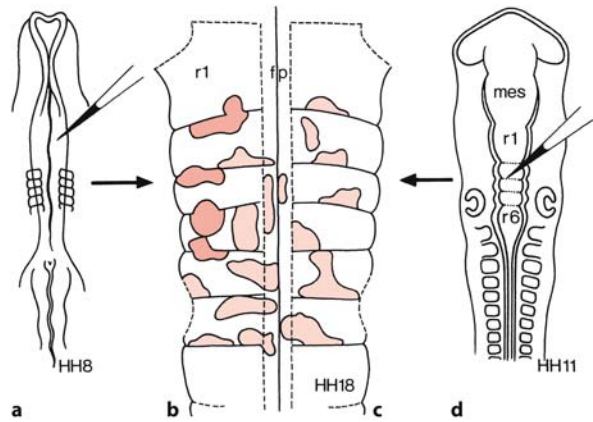
Fig. 2.15 Cell lineage restriction in the segmented avian hindbrain. Single cells labelled with a fluorescent tracer in neural plate (**a**) or neural tube (**d**) stages divide several times over a period of 2 days to form clones that are detectable in a flat-mounted E3.5 hindbrain (**b**, **c**). Clones marked before boundary formation (**a**) may pass a boundary (*red patches* in **b**). Clones marked near an already formed boundary (**c**) are always restricted from spreading into an adjacent rhombomere. *fp* floor plate, *HH8, HH11, HH18* Hamburger–Hamilton stages, *mes* mesencephalon, *r1, r6* rhombomeres. (After Fraser et al. 1990)

neurons and being the precursor region of the cerebellum. Vaage (1969) suggested that the first rhombomere is composed of two distinct domains, r0, or the so-called isthmic rhombomere anteriorly, and a narrower r1 posteriorly (Puelles 1995). In the chick, no molecular markers of this r0/r1 boundary have been identified, but data for zebrafish suggest that anterior and posterior parts of r1 are patterned independently (Moens and Prince 2002).

Compartmental restriction of cell mingling begins at the time rhombomeres become delineated and persists while the ventricular zone is predominantly germinative (Fraser et al. 1990; Guthrie and Lumsden 1991). Rhombomeric domains of the ventricular zone remain lineage-restricted up to late stages (Fig. 2.15), when neurogenesis is almost complete (Wingate and Lumsden 1996). Two-segment periodicity has also been found in the expression of Eph-like receptor tyrosine kinases and their ephrin ligands (Nieto et al. 1992; Flanagan and Vanderhaeghen 1998; Cooke and Moens 2002): three receptors (EphA4, EphB2, EphB3) are expressed in r3 and r5, whereas their ephrin-B ligands are expressed in r2, r4 and r6. Eph–ephrin interaction mediates repulsive interactions that serve to sharpen rhombomeric borders and, moreover, prevent cell mixing between adjacent rhombomeres (Xu et al. 1999).

Rhombomeres are thought to acquire their individual identities under the influence of *Hox* genes
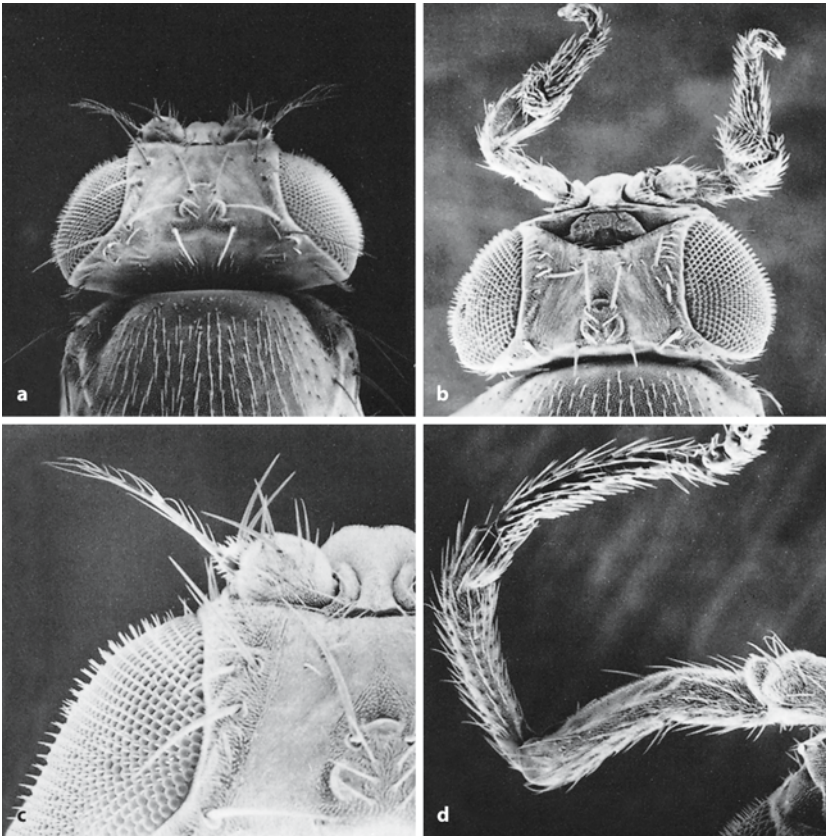
Fig. 2.16 Homeotic transformation of the head of *Drosophila*: **a** dorsal view of the head of a wild-type fly; **b** dorsal view of the head of an *Antennapedia* fly (*Antp–/–*); **c** higher magnification of the eye and normal antenna; **d** higher magnification of the homeotic appendage, a well-formed mesothoracic leg (from Palka 1982, with permission)

that are expressed in overlapping, or nested, domains (Wilkinson et al. 1989; Krumlauf 1994; Lumsden and Krumlauf 1996; Moens and Prince 2002). *Hox* gene expression precedes rhombomere foundation but becomes progressively sharpened such that the borders of their expression domains coincide with the emerging rhombomere boundaries. In the fully segmented hindbrain, many *Hox* genes show a two-rhombomere periodicity. Superimposed on this pattern are rhombomere-specific variations in expression levels. There is a striking correspondence of the expression of the *Hox* clusters of flies and vertebrates (Favier and Dollé 1997; Hirth et al. 1998; Arendt and Nübler-Jung 1999). In mice and men, there are four *Hox* clusters (A–D), each lying on a different chromosome. The genes fall into 13 paralog groups, but no individual cluster has representatives on all 13 paralogs owing to multiple gene losses during evolution. The paralog groups 1–4 are expressed in the developing hindbrain and migratory cranial neural crest cells, whereas the paralog groups 5–13 are expressed in the developing vertebral column, extremities, alimentary canal and urogenital system. The total number of *Hox* genes for mice and men is 39. Teleost fishes such as the zebrafish have a seven *Hox* cluster arrangement with a total of 48 *Hox* genes (Amores et al. 1998). Each rhombomere and pharyngeal or branchial arch is characterized by a unique combination of *Hox* genes,

its *Hox* code (for human data see Vieille-Grosjean et al. 1997). In mice, spontaneous and targeted (knockouts) mutations in these genes result in specific, rhombomere-restricted disruptions in the development of the cranial motor nuclei (Chap. 7).

Hindbrain patterning involves graded responses to **retinoic acid signalling** (Dupé et al. 1999; Morriss-Kay and Ward 1999; Gavalas and Krumlauf 2000; Dupé and Lumsden 2001; Wendling et al. 2001; Maden 2002). More posterior rhombomeres need progressively higher amounts of retinoic acid. Reducing retinoic signalling, whether by mutation of genes for biosynthetic enzymes or receptors, by dietary intervention or by pharmacological inhibition of receptor function, results in hindbrain patterning defects, ranging from partial transformations of hindbrain rhombomere identity to a severe loss of posterior hindbrain and anterior spinal cord (Gavalas and Krumlauf 2000; Wendling et al. 2001; Maden 2002). These phenotypes reflect the direct role that retinoic acid plays in regulating *Hox* gene expression in the hindbrain. Enhancers of several *Hox* genes contain retinoic acid response elements that are essential for the onset of expression within the mouse hindbrain (Gavalas 2002).

Among the most bizarre developmental perturbations in *Drosophila* are those asociated with **homeotic mutations**, which have the capacity to transform a

specific part of one body segment into the homologous part of another (Palka 1982). These mutations include rearrangement of the *Antennapedia* (*Antp*) locus which, through ectopic expression of the Antp protein, transform antennae into legs (Fig. 2,16), and certain loss-of-function mutations at the *bithorax* (*bx*) locus, which transform the third thoracic segment into a duplicate of the second one, leading to mutant flies with two pairs of wings.

2.5   Neurogenesis, Gliogenesis and Migration

The CNS uses several strategies to generate distinct classes of neurons during development (Jacobson 1991; McConnell 1995; Nieuwenhuys 1998b): dorsal–ventral polarization in the spinal cord, segmentation in the brain stem and lamination in the cerebral cortex. Most types of neurons are generated in the primary proliferative compartment (the ventricular zone), but several cell types arise from secondary proliferative compartments, including the subventricular zone and the external granular or germinal layer.

2.5.1   Neurogenesis: Primary and Secondary Proliferative Compartments

The neural plate and early neural tube consist of a single layer of columnar cells, the **neuroepithelium**. Through thickening, this layer gradually forms a pseudostratified epithelium, i.e. its nuclei become arranged in more and more layers, but all elements remain in contact with the outer and inner surfaces (Fig. 2.17). Mitotic figures are only found along the ventricular surface (Fig. 2.18). Early students of the developing neural tube, like His (1889), thought that these mitoses belong to cells which form a ventricular layer of germinal cells (*Keimzellen*), and that the more peripherally located cells represent spongioblasts, primordial glial cells, forming a syncytial meshwork (*Markgerüst*). Neuroblasts arising from the germinal cells were supposed to migrate peripherally in the intercellular spaces of this meshwork. Although Schaper (1897a, b) already challenged His's concept of neurogenesis, it was Sauer (1935a, b) who proved that the neural tube is composed of discrete cells that do not form a syncytium. In fact, His's radially arranged columnar cells (spongioblasts) and the rounded cells near the lumen, passing through mitosis, are not two types of cells, but are the interkinetic and mitotic stages of the same cell (Figs. 2.18a, 2.21). Thus, the early neural tube is composed of a single type of epithelial cell in various stages of the mitotic cycle: the resting cells reside in the outer part of the
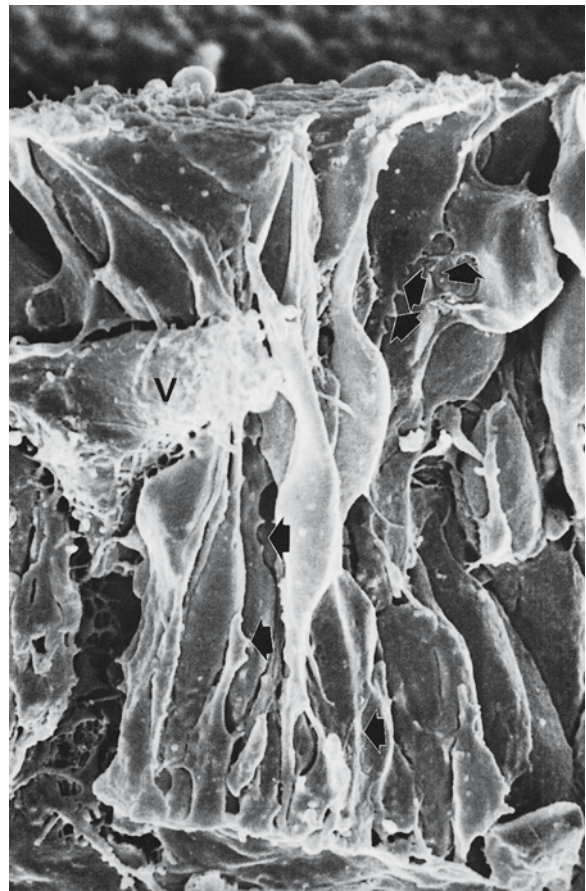
Fig. 2.17 Scanning electron micrograph of the developing forebrain wall. The sagittal fracture of a cerebral hemisphere of an E10 mouse embryo shows the undulating membranes of the different cell types (*arrows*); *V* marks a blood vessel. (From Meller and Tetzlaff 1975, with permission)

wall, and the nuclei of the cells that are going to divide are moving towards the ventricular surface. At the end of this migration phase, the peripheral processes lose their contacts with the outer surface and retract. The cells round up and divide into two daughter cells each. Each daughter cell produces a new peripheral process, and their nuclei move away from the ventricle. Sauer's cytological studies were confirmed by numerous studies using [³H]thymidine autoradiography (Fujita 1963, 1966), and electron microscopy (Hinds and Ruffett 1971; Meller and Tetzlaff 1975).

At a certain developmental stage the nuclei of the elongated neuroepithelial cells withdraw from the most superficial layer of the neural tube (Fig. 2.19). The outer, anuclear zone, or **marginal layer**, first consists of the external processes of the neuroepithelial cells, but is soon invaded by the axonal processes of maturing neuroblasts. The inner zone is known as the **matrix layer** (Kahle 1951; Fujita 1963, 1966; Keyser
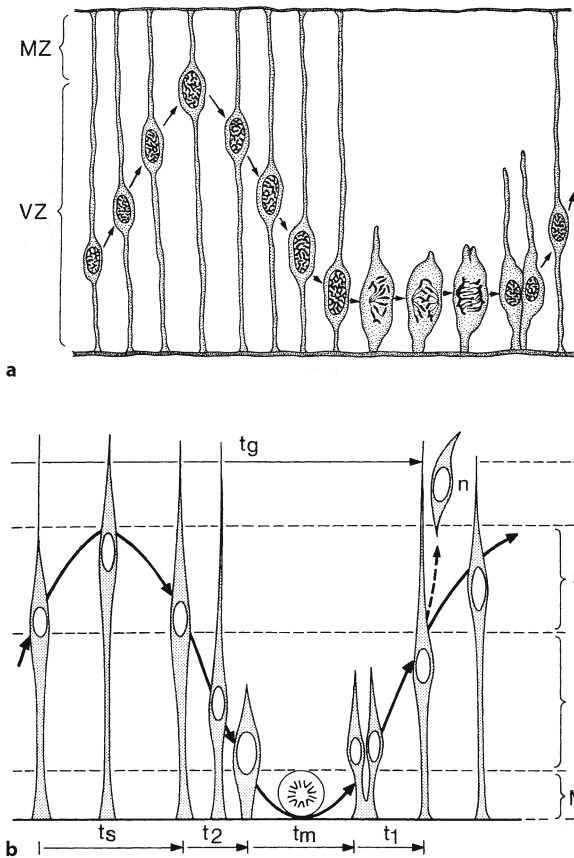
Fig. 2.18 Cell division in the wall of the neural tube. *S, I* and *M* mark the synthetic, intermediate and mitotic periods of the elevator movement in the ventricular zone (*VZ*). *MZ* marginal zone, t_g generation time of a cell, t_m mitotic time, t_s DNA-synthesis time, t_1 postmitotic resting time, t_2 premitotic resting time. (**a** After Sauer 1935b; **b** Fujita's data on the 'elevator movement'; after Fujita 1966, from Nieuwenhuys 1998b, with permission)

1972) or **ventricular zone** (Boulder Committee 1969). It contains the densely crowded nuclei of homogeneous cell population, all elements of which participate in the proliferation process. The matrix cells are the precursors of all neuronal and macroglial cells of the CNS. The matrix layer may be divided into three zones, the M or mitotic zone, the I or intermediate zone and the S or synthetic zone, in line with the subdivision of the mitotic cycle into M, G_1, S and G_2 phases (Fig. 2.18b). Fujita (1963, 1966) characterized the translocation of the nuclei of the matrix or germinal cells during a generation cycle as an '**elevator movement**'. At the time of DNA synthesis (S phase), the nuclei are located in the S zone, and when DNA synthesis is complete, they descend during a postsynthetic or premitotic period (G_2 phase) through the I zone to enter the M zone. Here, the matrix cells divide and, after mitotic time (M phase), both nuclei of the daughter cells pass to the I zone for their postmitotic or presynthetic period (G_1 phase). Finally, they enter the S zone again, where a new generation cycle starts. The G_1 and G_2 phases are important control points in passage of cells through the mitotic cycle. Normally, neurons are permanently arrested in the G_1 phase, whereas glial cells may be temporarily suspended in either the G_1 or the G_2 phase (Jacobson 1991). Radiation, excess of thymidine and other experimental conditions arrest cells in the G_1 or G_2 phases (Pardee et al. 1978).

At first, the matrix layer is a purely proliferative compartment. Progenitor cells produce more progenitor cells, with the surface area as well as the thickness of the neural tube increasing steadily. This period of **symmetrical division** of progenitor cells is followed by a period of **asymmetrical division**, in which one of the daughter cells resulting from each mitosis withdraws from the mitotic cycle and migrates out from the matrix layer. These postmitotic elements or
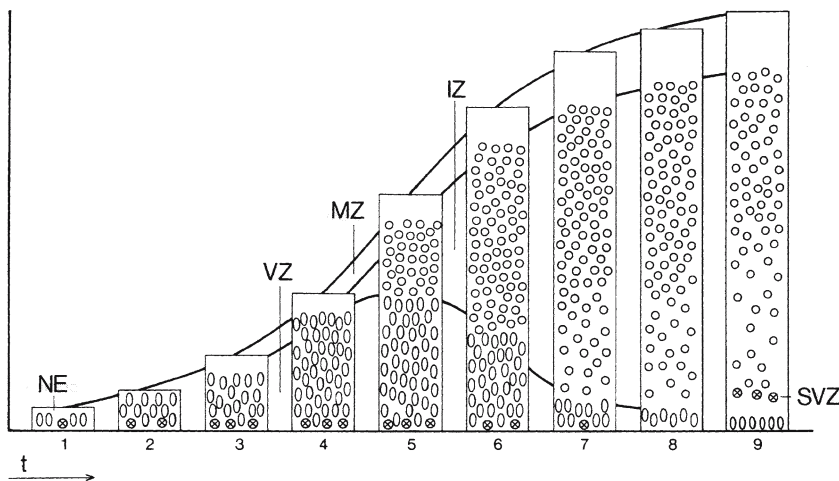
Fig. 2.19 Histogenesis of the CNS divided into nine phases. *IZ* intermediate zone, *MZ* marginal zone, *NE* neuroepithelium, *SVZ* subventricular zone, *VZ* ventricular zone, *t* time. (After Kahle 1951; Keyser 1972)

1
Rückenmark
Vorderhorn

1   2   3   4
Rückenmark
Hinterhorn

1   2   3   4
Mittelhirn
Tegmentum

1   2   3   4
Mittelhirn
Tectum

1   2   3   4
Zwischenhirn
Subthalamus

1   2   3   4
Zwischenhirn
Thalamus

1   2   3   4
Endhirn
Ganglienhügel

1   2   3   4
Endhirn
Pallium

Matrixbildung   Matrixanstieg   Matrixaufbrauch   Ependym
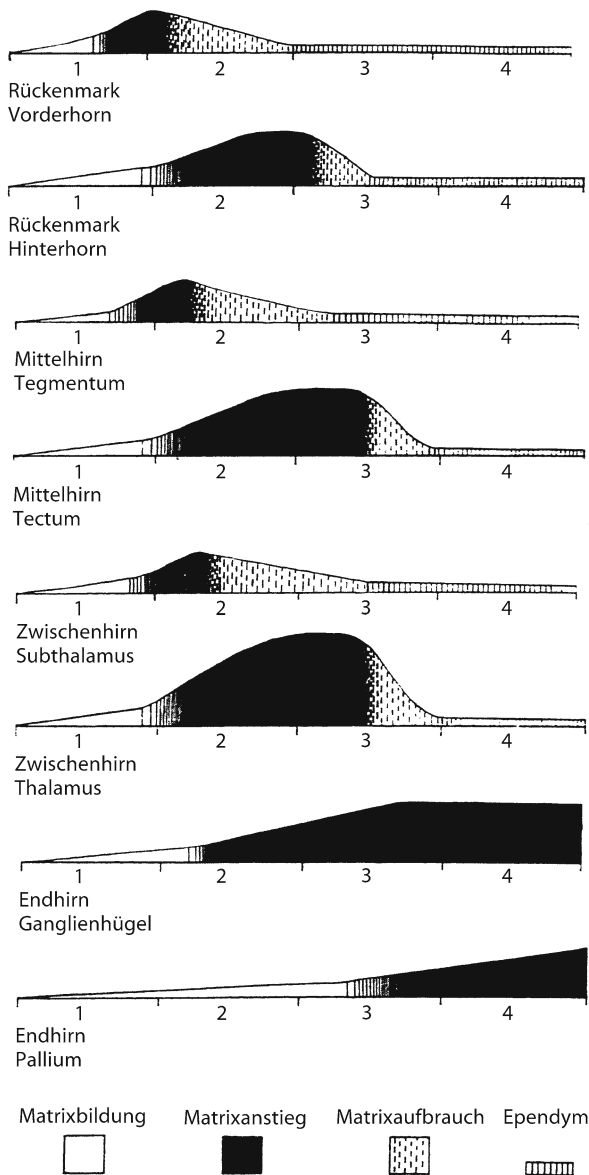
Fig. 2.20 Development of the matrix layer in various parts of the human brain during the first four intrauterine months. This development is subdivided into four phases: formation (*Matrixbildung*), increase (*Matrixanstieg*), decrease (*Matrixaufbrauch*) and complete depletion and formation of the ependyma (*Ependym*). (After Kahle 1951)

neuroblasts form a third compartment, the **mantle layer** or **intermediate zone**, between the matrix and marginal layers. The elements giving rise to one postmitotic and one proliferative daughter cell are the **stem cells**. When stem cells appear in the matrix layer, the period of pure proliferation ends. More and more dividing neuroepithelial cells switch to the presumptive stem cell mode and begin to generate postmitotic daughter cells, leading to the rapid thickening of the mantle layer (Fig. 2.19). During this phase, pro-

liferation and stem cells coexist in the matrix layer. Later, matrix cells start to produce two postmitotic cells, thereby gradually depleting the matrix layer.

The development of the matrix layer is spatially and temporally patterned. The proliferative activity in the neural tube shows local maxima that coincide with the formation of neuromeres and of the later-appearing migration areas (Bergquist and Källén 1954). Moreover, the development of the matrix layer shows profound differences among the various parts of the CNS (Kahle 1951; Fig. 2.20). [^{3}H]Thymidine autoradiography studies on the time of origin of neuronal populations throughout the CNS, in particular by Altman and Bayer (reveiwed in Bayer and Altman 1995 a, b; Bayer et al. 1995), revealed that neurons assemble either by stacking in laminar structures or by packing into nuclear regions in regular **spatiotemporal gradients**. Such gradients are described as '**inside out**' when the neurons that originate at successively later times migrate past those formed earlier and take up successively more external positions. This inside-out pattern of assembly of neurons is generally characteristic for laminar structures such as the cerebral cortex and the superior colliculus. Exceptions are the granular layers of the cerebellar cortex and dentate gyrus. Here, the granule cells arise in an '**outside-in**' pattern from displaced germinal zones and not directly from the ventricular germinal zone. In many other regions of the CNS such as the thalamus, basal forebrain and amygdala, neurons assemble in an outside-in or a lateral-to-medial gradient. In general, large neurons are produced before small ones in the same region of the CNS, and the neurons produced last are granule cells or local circuit neurons.

Apart from the ventricular zone, two **secondary proliferative compartments**, i.e. the subventricular zone and the external granular or germinal layer, are found in the developing CNS (Smart 1961; Altman 1966; Rakic 1971, 1974; Sturrock and Smart 1980). The **subventricular zone**, also known as the subependymal layer or plate, has been found mainly in the lateral and basal walls of the mammalian telencephalon (Fig. 2.26). The subventricular cell population expands exponentially during the last third of prenatal development. In the E16 mouse, over 90% of the subventricular cells are dividing, whereas the majority of the cells in the ventricular zone are leaving the cell cycle (Takahashi et al. 1995). The subventricular zone persists after birth and, in a vestigial manner, into adult life and even senescence (Doetsch et al. 1997, 1999; Temple and Alvarez-Buylla 1999; Brazel et al. 2003). The number of cells in the subventricular zone peaks during the first week after birth in rodents (Lewis and Lai 1974; Bayer and Altman 1991; Takahashi et al. 1995) and at approximately the 35th week of gestation in humans (Kershman 1938;
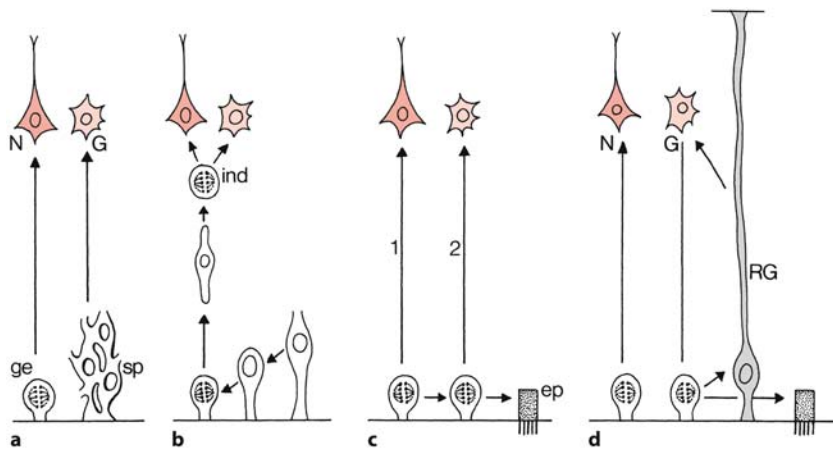
Fig. 2.21 Theories about the origin of neuronal and glial cell lines. His (1889) recognized two major cell varieties in the ventricular zone (**a**): spheroidal, proliferative, germinal cells (*ge*), their progeny giving rise to neuroblasts (*N*), and neighbouring spongioblasts (*sp*) forming glioblasts (*G*). Schaper (1897a, b) held that mitoses in the ventricular zone led to indifferent cells (*ind*), to be further divided into neuroblasts, glioblasts, or both (**b**). Using autoradiography, Fujita (1963) suggested that a single proliferative matrix cell gave rise to several migratory generations (**c**), first neuroblasts, and later glioblasts, the remaining cells forming the ependymal layer (*ep*). With immunohistochemical techniques, at least two distinct cell varieties were found in the ventricular zone (**d**), a glial fibrillary acidic protein (*GFAP*) positive and a GFAP-negative population. The GFAP-negative cells gave rise to migrating neuroblasts (*dark red*), whereas the GFAP-positive cells first gave rise to radial glioblasts (*RG*, *grey*), and later to glioblasts (*light red*), both directly as well as indirectly. (After Rakic 1981; Fishell and Kriegstein 2003)

Globus and Kuhlenbeck 1944), after which the subventricular zone begins to decrease in size (Thomaidou et al. 1997). The subventricular zone gives rise to special classes of neurons and to all types of macroglial elements (Miller 2002; Brazel et al. 2003). The cells of the perinatal and adult subventricular zone have the capacity to replace neurons and glia after ischemic and traumatic brain injuries (Romanenko et al. 2004). The **external germinal layer** is confined to the cerebellum. This layer develops from the ventricular zone in the upper rhombic lip (Hatten and Heintz 1995; Altman and Bayer 1997; Wingate 2001). The rhombic lip is a thickened germinal zone in the rhombencephalic alar plate, situated directly adjacent to the attachment of the roof of the fourth ventricle (Chap. 8). From this zone, the layer spreads by tangential migration of its elements over the entire outer surface of the cerebellar anlage. This transitory germinal zone gives rise to the cerebellar granule cells.

Seasonal plasticity of structure and function is a fundamental feature of the nervous system in a wide variety of animals that occupy seasonal environments (Tramontin and Brenowitz 2000). The best studied is the avian song system. In songbirds, Alvarez-Buylla et al. (1988) showed that neurons originating in the subventricular zone migrate into the cortex during the season when new neurons are added to the hippocampus and vocal nuclei. Adult mammals contain two active CNS germinal zones, the subgranular zone of the dentate gyrus which generates hippocampal interneurons (Altman 1970; Kaplan and Hinds 1977), and the forebrain subventricular zone which generates interneurons that migrate to the olfactory bulb (Luskin 1993; Lois and Alvarez-Buylla 1994). Here, neuron incorporation continues into childhood (Altman 1970; Bayer 1983; for human data see Johansson et al. 1999).

2.5.2   Gliogenesis

In general, gliogenesis follows neurogenesis but overlaps neurogenesis in several brain regions (Jacobson 1991). Gliogenesis persists long after neurogenesis has ceased, and astrocyte generation may persist throughout life (Altman 1966; Sturrock 1982; Lee et al. 2000). Radial glia are the first identified glial population to develop (Rakic 1972, 1981; Schmechel and Rakic 1979; Bentivoglio and Mazzarello 1999), followed by oligodendrocyte precursors, astrocytes and oligodendrocytes (Lee et al. 2000; Gaiano and Fishell 2002; Miller 2002). In general, oligodendrocyte precursors are generated in ventral regions of the neural tube, and astrocytes from dorsal regions (Ono et al. 1995; Miller 1996; Miller and Ono 1998; Pringle et al. 1996, 2003; Lee et al. 2000). Successively held theories about the origin of neuronal and glial cell lines are shown in Fig. 2.21. His (1889) originally proposed

that neural and glial cell lines were entirely separate. Schaper (1897a, b) held that these two cell types arise from a single class of precursors that divide after migrating away from the ventricular zone. Magini (1888) observed varicosities along the filaments of the radial neuroglial cells and suggested that these represented immature neurons. Using autoradiography, Fujita (1963) concluded that dividing cells first give rise to neurons and then, after neurogenesis has ceased, produce glial cells. The ability to demonstrate glial fibrillary acidic protein (GFAP), a specific glial marker, provides evidence for the currently held view that neuronal and glial cell precursors coexist in the ventricular zone from early embryonic stages (Choi and Lapham 1978; Levitt and Rakic 1980). Recent data suggest that radial glial cells represent many, if not most, of the neuronal progenitors in the developing cerebral cortex (Miyata et al. 2001; Noctor et al. 2001; Fishell and Kriegstein 2003). Asymmetric cell division of radial glia may result in the self-renewal of the radial glial cell and the birth of a neuron.

Radial glial cells are specialized cells that radially span the entire wall of the neuraxis from the ventricular to the meningeal surface. In most non-mammalian species, radial glial cells persist in many regions throughout life, but in mammals they represent a transient class of cells, which gradually disappears from most regions (Nieuwenhuys 1998b). The classical Golgi studies of von Lenhossék (1895) and Ramón y Cajal (1909) as well as more recent GFAP data (Choi 1981; Choi and Kim 1984; Hirano and Goldmann 1988; Voight 1989) have shown that in mammals most radial glial cells transform into astrocytes. Type 1 astrocytes originate from ventricular zone neurons and subsequently migrate into the parenchyme of the CNS where they associate with blood vessels and contribute to the formation of the blood–brain barrier (reviewed in Jacobson 1991). Type 1 astrocytes release mitogenic growth factors that promote proliferation and differentiation of oligodendrocytes and type 2 astrocytes. Type 2 astrocytes and oligodendrocytes arise from a common precursor, the O-2A cell, that migrates into all regions of the CNS containing nerve fibres (Raff 1989; Lee et al. 2000; Miller 2002). Microglial cells originate from a specific population of mononuclear leucocytes which penetrate the blood–brain barrier and transform into microglia. Recent studies indicate that radial glia are multipurpose cells for vertebrate brain development (Parnavelas and Nadarajah 2001; Lemke 2001; Campbell and Götz 2002). Apart from guiding the radial migration of newborn neurons from the ventricular zone to their ultimate positions, further roles for these cells as ubiquitous precursors that generate neurons and glia, and as key elements in patterning and region-specific differences of the CNS have been suggested.
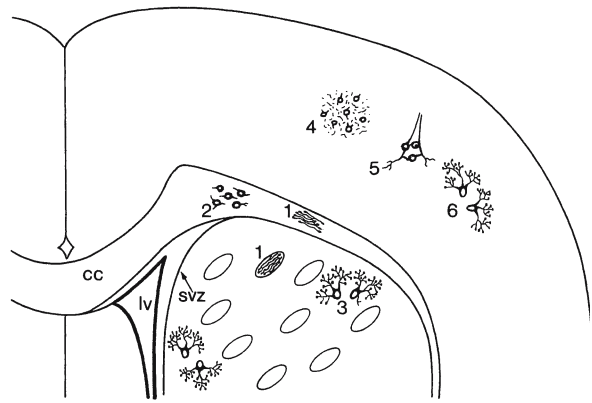
Fig. 2.22 Descendants of the perinatal dorsolateral part of the subventricular zone (*SVZ*). Progenitors that leave this part of the subventricular zone and differentiate within the subcortical white matter become either myelinating (*1*) or nonmyelinating (*2*) oligodendrocytes. Few become astrocytes (*3*). Those progenitor cells that differentiate within the neocortex become myelinating oligodendrocytes (*4*) as well as satellite oligodendrocytes (*5*). Some progenitors that make contact with naked cerebral endothelial cells become protoplasmic astrocytes (*6*). *cc* corpus callosum, *lv* lateral ventricle. (After Brazel et al. 2003)

At least part of the **oligodendrocytes** is also derived from radial glial cells. Oligodendrocytes are responsible for the formation of myelin in the CNS (Lemke 1993; Compston et al. 1997). Oligodendrocytes develop relatively late and always after completion of axonal outgrowth in the CNS. The founder cells of the oligodendrocyte lineage initially arise in distinct regions of the ventricular zone during early CNS development as the result of local signals including SHH (Nery et al. 2001; Marti and Bovolenta 2002; Miller 2002). In the spinal cord, oligodendrocyte precursors are located ventrally (Warf et al. 1991; Ono et al. 1995; Pringle et al. 1996, 2003). In more rostral areas of the CNS, the earliest oligodendrocyte precursors are also generated in special domains of the ventricular and subventricular zones. The telencephalic oligodendrocytes are derived from the ganglionic eminences and later migrate to the cerebral cortex (Spassky et al. 1998, 2001; He et al. 2001; Brazel et al. 2003; Fig. 2.22). In chick embryos, all telencephalic oligodendrocytes arise from the anterior entopeduncular area (Olivier et al. 2001). In mouse mutants, in which the medial ganglionic eminence is converted into the lateral one, there is a significant loss of oligodendrocytes, suggesting that the medial ganglionic eminence is the major source of oligodendrocytes (Sussel et al. 1999; Nery et al. 2001). Immature oligodendrocyte precursors are highly migratory. They reach the developing white matter using a variety of guidance molecules, including diffusible

chemorepellents such as netrin-1 and semaphorin-3a (Sugimoto et al. 2001; Miller 2002).

The majority of oligodendrocyte precursor proliferation occurs in developing white matter as a result of the local expression of mitogenic signals such as PDGF-A, the platelet-derived growth factor A (Noble et al. 1988; Miller 2002). Oligodendrocyte precursor proliferation is regulated by a number of distinct growth factors, including PDGFs and FGFs (reviewed in Miller 2002). The final matching of oligodendrocyte and axon number is accomplished through a combination of local regulation of cell proliferation, differentiation and cell death (Barres and Raff 1994). The adult CNS still contains a significant population of precursors. *Olig* genes, which encode the basic helix–loop–helix Olig transcription factors, are essential for the development of oligodendrocytes (Rowitch et al. 2002). Proneural genes such as *neurogenin-1* (*Ngn1*) suppress gliogenesis (Schuurmans and Guillemot 2002).

Oligodendrocytes in the CNS and Schwann cells in the peripheral nervous system (PNS) ensheath axons, and provide the **myelin sheath** that greatly improves the electrical cable properties of the axon, resulting in considerable gain of speed of impulses. Myelin is formed by these glial cells inserting successive layers of their cell membranes around axons, adding each new layer from the inside (Wood and Bunge 1984; Jacobson 1991; Campagnoni 1995). Oligodendrocytes exert a strong inhibition on axonal growth and regeneration (Schwab and Caroni 1988). During their differentiation into myelin-forming cells, oligodendrocytes and Schwann cells activate expression of a group of myelin-specific genes, encoding proteins that play roles in the induction of myelination, in the initial deposition of myelin sheathes, and in wrapping and subsequent compaction of these around axons. The major group of myelin-specific genes includes three genes, encoding protein zero (P_0), the proteolipid protein (PLP) and myelin basic protein (MBP). P_0 is the major structural protein of PNS myelin and its expression is restricted to myelin-forming Schwann cells. PLP is the major structural protein of CNS myelin and is largely restricted to oligodendrocytes. MBP is present in both CNS and PNS myelin. MBP plays an essential role in CNS myelin formation. Myelination starts after cellular proliferation and migration in the CNS have virtually ceased, and continues until at least the 16th postnatal week in rats and well into the first decade in humans (Chap. 1).

Glial mutations in mice, known as *jimpy*, *shiverer* and *trembler*, affect genes encoding proteins expressed in Schwann cells or oligodendrocytes which are necessary for the formation of compact myelin (Griffiths 1996; Kamiguchi et al. 1998; Campagnoni and Skoff 2001; Poliak and Peles 2003). The outcome is impaired myelin formation with consequent defects in nerve conduction and motor performance. The *jimpy* mutation is found in the gene coding for PLP (Nave et al. 1987; Koeppen et al. 1988) and in its human equivalent, Pelizaeus–Merzbacher disease (Koeppen et al. 1987; van der Knaap and Valk 1995; Ruggieri 1997; Koeppen and Robitaille 2002). Targeted PLP knockout mice make virtually normal compact CNS myelin, which suggests that dysmyelination seen in Pelizaeus–Merzbacher disease is due to a long-term requirement for PLP in stabilizing myelin (Klugmann et al. 1997). *Shiverer* mutants fail to produce normal myelin basic protein (Kimura et al. 1985; Readhead et al. 1987), whereas *trembler* mice have a deficiency in PMP22, the peripheral myelin protein 22 (Suter and Snipes 1995). Charcot–Marie–Tooth disease (type 1), in which there is progressive onset of weakness starting in the distal parts of the limbs, is also due to mutations affecting PMP22 (Suter et al. 1993; Harding 1995; Hanemann and Müller 1998; Nelis et al. 1999). Most cases result from a duplication of the gene, leading to axonal atrophy and demyelination (Gabreëls-Festen et al. 1995). Other patients with Charcot–Marie–Tooth disease have mutations in the gene coding for the major peripheral myelin-associated protein, P_0 (Hayasaka et al. 1993; Gabreëls-Festen et al. 1996; Kamiguchi et al. 1998).

2.5.3 Migration

In anamniotes, most postmitotic cells settle just peripheral to the ventricular zone and form a periventricular zone of grey matter. In amniotes, most neurons migrate over a considerable distance from the ventricular zone to their final position. Two main modes of migration can be recognized: radial and tangential. During **radial migration**, the predominant pathway, the neuroblasts move from the ventricular zone to the meningeal surface. In the telencephalon of the North American opossum, Morest (1970) showed in Golgi material that neuroblasts maintain central and peripheral primitive processes that extend to the ventricular and meningeal surfaces, respectively. Not the cells per se, but rather their nuclei and perikaryal regions move through their peripheral primitive processes outwards (**somal displacement**). This translocation is accompanied or followed by a loss of the central primitive process, and the cell later detaches itself also from the meningeal surface. On the basis of extensive Golgi and electron microscopic studies of the cerebellar and cerebral cortices (Rakic 1971, 1972; Sidman and Rakic 1973; Schmechel and Rakic 1979), Rakic proposed that radially oriented glial fibres provide contact guidance paths for migrating neuroblasts. In the developing pallium the neuroblasts generated in the

Fig. 2.23 Patterns of radial alignment and neuroblast migration in medial (*M*), dorsal (*D*) and lateral (*L*) pallial regions. *CP* cortical plate, *VZ* ventricular zone. (After Misson et al. 1991)
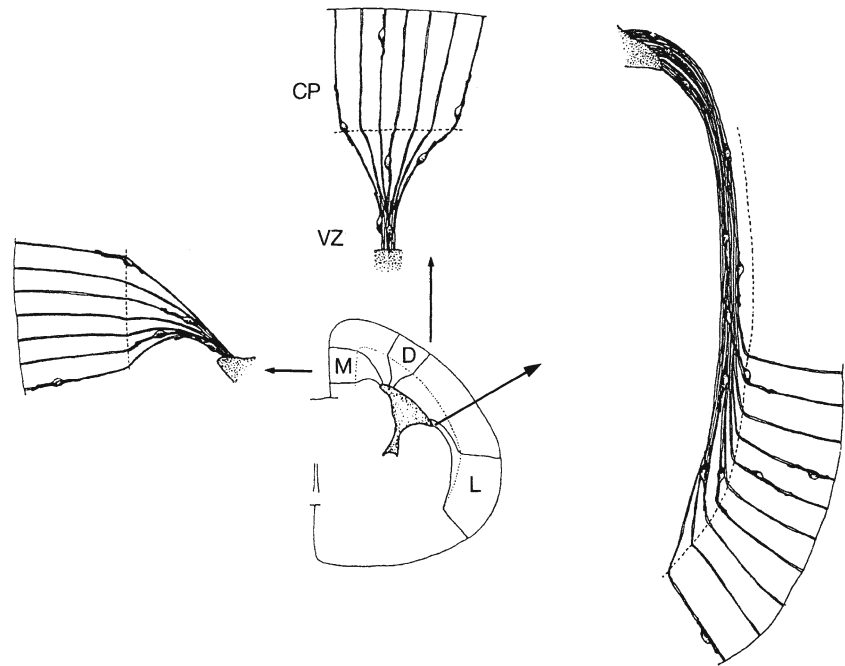
ventricular zone were supposed to travel to the anlage of the cerebral cortex along transient glial elements that span the full thickness of the pallial wall. Using retroviral labelling of cortical neuroblasts, Misson et al. (1991) found three patterns of alignment of neuroblasts and glial fibres (Fig. 2.23): *radial divergent*, observed in the dorsal pallial region, *curving divergent* in the medial pallial region, and *curving convergent*, then *divergent*, occurring in the lateral pallial region. Cortical cell migration can be monitored in embryonic (rodent) brain slices through time-lapse videography (Nadarajah et al. 2002). In the developing cerebellum postmitotic elements from the external granular layer were thought to migrate inwards along Bergmann fibres, i.e. the radially oriented peripheral processes of the Golgi epithelial cells. Several molecules have been shown to function in glial guided migration (Hatten 1999; Lemke 2001).

Since the investigations of His (1890) on the rhombic lip (Fig. 2.24) it has been known that neuroblasts in the CNS may migrate tangentially over considerable distances. His's observations have been confirmed by many authors (Essick 1912; Hayashi 1924; Harkmark 1954; Taber Pierce 1966; Altman and Bayer 1987 a–d). Different sectors of the rhombic lip give rise to different structures (Hayashi 1924; Taber Pierce 1966; Altman and Bayer 1987a–d; Hatten and Heintz 1995; Wingate 2001; Chap. 8). Neurons generated in the rhombic lip assume a bipolar shape and migrate closely apposed to the neuronal surface provided by fibre tracts that run parallel to the brain surface (Ono and Kawamura 1989, 1990; Rakic 1990). Bourrat and Sotelo (1988, 1990) showed that rhombic
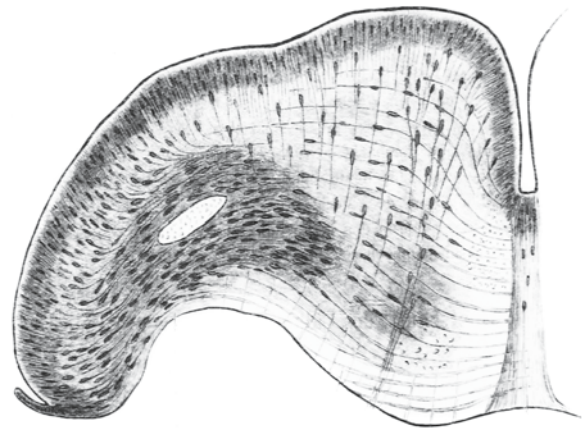
Fig. 2.24 His's (1890) figure on tangential migration in the brain stem of a human embryo

lip neuroblasts first develop an axon, and that the soma subsequently moves down this process. **Tangential migration** of neuroblasts has also been found in the spinal cord (Leber and Sanes 1995) and especially from the ganglionic eminences to the cerebral cortex and olfactory bulb (Luskin 1993; O'Rourke 1996; Hatten 1999; Corbin et al. 2001; Marín and Rubinstein 2001, 2002; Kriegstein and Noctor 2004; Chap. 9). A unique population of tangentially migrating neurons was found to originate in the subventricular zone of the rostral telencephalon (Fig. 2.25). These cells migrate further rostrally in 'chains' (**chain migration**) as the rostral migratory stream parallel to the pial surface to the developing olfactory bulb (Lois
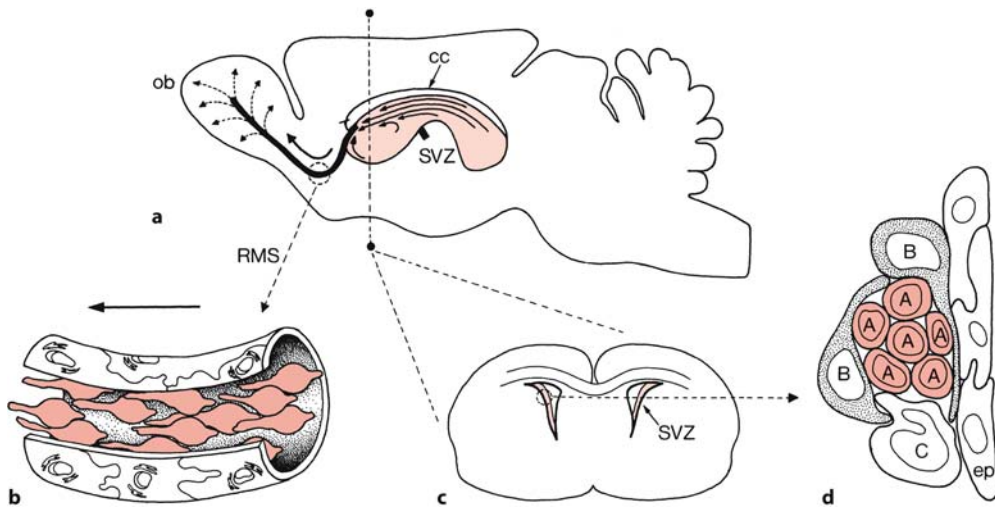
Fig. 2.25 Neurogenesis and migration in the subventricular zone (*SVZ*) of adult rodents. The sagittal section (**a**) shows the extent of the subventricular zone (*red*). Large numbers of neuroblasts are continually generated in the subventricular zone. Neuroblasts (type A cells in *dark red*) migrate as chains through the subventricular zone (*arrows* in **a**; transverse sections in **c** and **d**), join the rostral migratory stream (*RMS*; see longitudinal section in **b**) and differentiate into local interneurons in the olfactory bulb (*ob*). The neuroblasts (A cells in **d**) are surrounded by subventricular zone astrocytes (B cells) and are adjacent to clusters of immature precursors (C cells). *cc* corpus callosum, *ep* ependymal cells. (After Doetsch et al. 1997; Temple and Alvarez-Buylla 1999; Brazel et al. 2003)

et al. 1996; O'Rourke 1996; Doetsch et al. 1997, 1999; Temple and Alvarez-Buylla 1999; Brazel et al. 2003). Here they migrate radially and differentiate into interneurons. The rostral migratory stream is absent in the adult human brain (Weickert et al. 2000; Sanai et al. 2004).

2.6   Axon Outgrowth and Guidance

The complex pattern of axonal pathways found in mature animals requires a special set of mechanisms to develop properly. These mechanisms involve recognition of environmental cues by growing axons (Goodman 1996; Goodman and Tessier-Lavigne 1997; Cook et al. 1998; Sanes and Jessell 2000; Brown et al. 2001). The pathways along which axons grow provide a large number of diverse molecular cues to guide axons to their targets, and the growth cones of axons possess specific receptors to recognize these cues. Axon trajectories are often subdivided into shorter segments, interrupted by intermediate targets or choice points where growth cones have to make critical guidance decisions. A first set of axon bundles forms a precise, stereotyped scaffold of axonal bundles or pioneer fibres. Late-developing axons often grow along these pioneer fibres by fasciculation. Various attractive and repellent factors that guide the growth cones to their targets have been studied in particular at choice points such as the ven-tral midline and the optic chiasm. Examples of axon outgrowth and guidance will be illustrated for some major fibre systems, including the thalamocortical and corticofugal projections. The formation of topographic maps in the CNS is particularly evident in sensory systems and will be discussed for the retino-tectal projection.

2.6.1   Pioneer Fibres

The **earliest-appearing**, **'pioneer' axon growth cones** in the developing brain navigate a precise scaffold of initial tracts that show a strikingly similar overall pattern in insects and vertebrates (Fig. 2.26). Early-generated, **'pioneer' neurons** lay down an axonal scaffold, containing guidance cues that are available to later-generated growth cones. This axonal scaffold has been labeled with immunohistochemical techniques such as staining against axonal glycoproteins of the Fasciclin family in the developing grasshopper (Bastiani et al. 1987; Boyan et al. 1995) and in embryonic *Drosophila* brain (Goodman and Doe 1993; Therianos et al. 1995; Nassif et al. 1998). The adhesion molecule Fasciclin II (Fas II) is expressed in a large number of early-differentiating neurons. The Fas II antigen is present on the surface of clusters of neuronal somata prior to axon outgrowth. These **'fibre tract founder'** clusters (Nassif et al. 1998) are laid out in a linear pattern. After expressing Fas II on their so-
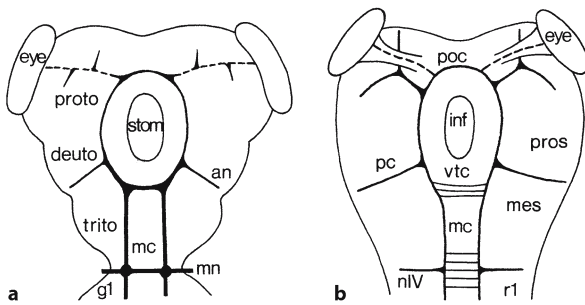
Fig. 2.26 Comparison of early pattern of axon scaffolds in **a** the grasshopper and **b** the zebrafish. *an* antennal nerve, *deuto* deutocerebrum, *g1* anterior pair of suboesophageal ganglia, *inf* infundibulum, *mc* midline cells, *mes* mesencephalon, *mn* mandibular nerve, *nIV* trochlear nerve, *pc* posterior commissure, *poc* postoptic commissure, *pros* prosencephalon, *proto* protocerebrum, *r1* first rhombomere, *stom* stomodeum, *trito* tritocerebrum, *vtc* ventral tegmental commissure. (After Brown et al. 2001)

adult brain become evident, it is possible to trace the development of several embryonic pioneer tracts fairly clearly into the corresponding adult pathways. Pioneer axons in the *Drosophila* embryo may be guided by multiple cues including glial cells (Jacobs and Goodman 1989; Hartenstein et al. 1998; Araújo and Tear 2003). The removal of one of these cues, for instance the neuropile glial cells, does not necessarily lead to the total disability of axons to reach their target, but enhances the frequency of error in pathfinding. There is now enough evidence that similar mechanisms may operate in vertebrates (Easter et al. 1994; Goodman and Tessier-Lavigne 1997; Chotard and Salecker 2004).

In *Drosophila*, a prominent **axonal circle** forms in the anterior part of the brain (the future supraoesophageal ganglion), enclosing the developing foregut (Fig. 2.26a). In vertebrate embryos (Fig. 2.26b), using antibodies against acetylated tubulin and HNK-1, such an axonal circle encloses the future hypothalamus and infundibulum (Chitnis and Kuwada 1990; Wilson et al. 1990; Easter et al. 1993, 1994; Chédotal et al. 1995). In both cases, this axonal ring is connected laterally with the developing eye. More posteriorly, axons in the insect brain navigate segmental commissural axon bundles and two prominent **longitudinal bundles** that run immediately lateral to the midline cells. In vertebrate embryos, these

ma, neurons of the fibre tract founder clusters extend axons that grow along the surface of the founder clusters and form a simple system of pioneer tracts for each of the components of the brain neuropile. Moreover, since Fas II expression goes on into the larval period, when the first features of the reorganizing

Fig. 2.27 Initial tract formation in the avian brain as found in silver impregnation studies and by applying specific antibodies. The early developing tracts are shown for Hamburger–Hamilton stages 11/12 (**a**), about 13 (**b**), about 17 (**c**) and 20 (**d**). *flm* fasciculus longitudinalis medialis, *mes* mesencephalon, *ov* otic vesicle, *pa* anterior parencephalon, *pc* posterior commissure, *poc* postoptic commissure, *pp* posterior parencephalon, *resp* reticulospinal neurons, *rmesV* mesencephalic root of the trigeminal nerve, *syn* synencephalon, *tb* tectobulbar neurons. (**a**–**c** After Windle and Austin 1936; **d** after Chédotal et al. 1995; from ten Donkelaar 2000)
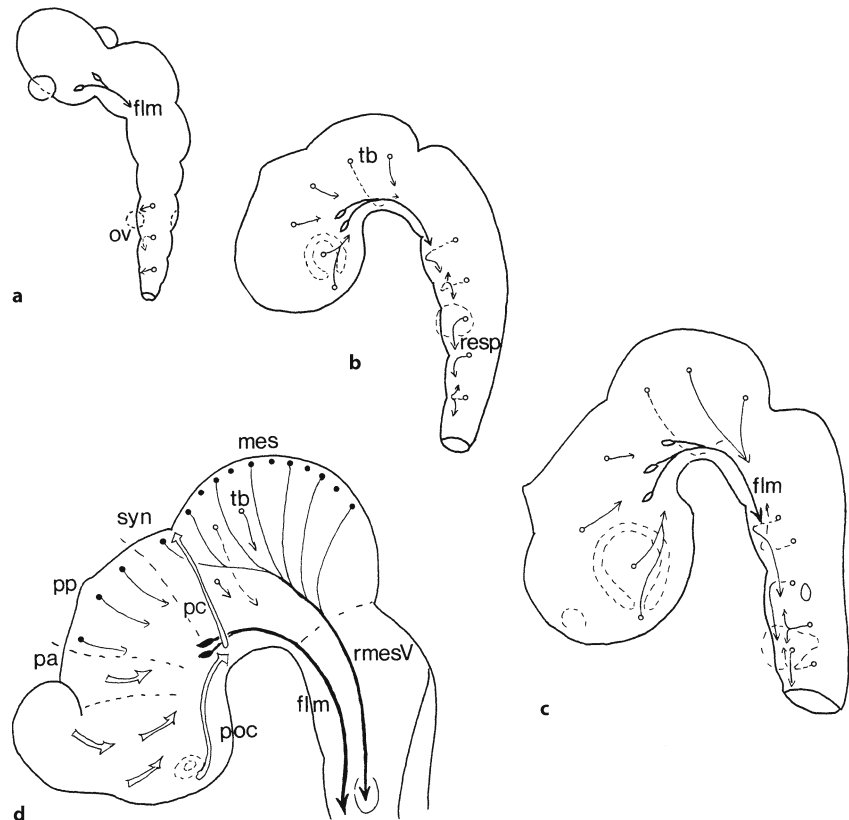
longitudinal bundles form the **medial longitudinal fasciculi** alongside the floor plate. Commissural axons course preferentially at rhombomere boundaries. The pattern of early axonal tracts in vertebrates, however, was in fact already described by Herrick (1937, 1938) and Windle and co-workers (Windle 1935; Windle and Austin 1936; Windle and Baxter 1936), using reduced silver staining techniques (Fig. 2.27).

2.6.2 The Guidance of Axons to their Targets

Axonal pathfinding is a highly directed process. Ramón y Cajal (1890) first discovered the motile, ameboid-shaped tips of growing axons, named them **growth cones** and suggested that growth cones play an attractive role in pathfinding. With an innovative tissue culture technique, Harrison (1910) confirmed that growth cones are active, mobile and adaptable structures. Ideas concerning specific axon pathfinding fell out of fashion in the 1930s and 1940s, largely due to Weiss's (1941) alternative that specificity of connections would arise from selective retention of connections that initially formed at random. On the basis of regeneration experiments on retinotectal projections in frogs, Sperry (1943) suggested that axon-target recognition relied on chemical matching rather than functional validation of randomly formed connections. Sperry's (1963) **chemoaffinity hypothesis** initiated an intensive search for recognition molecules, first in invertebrate embryos but soon thereafter in vertebrate embryos. In the grasshopper embryo, growth cones were found to follow specific pathways (Bate 1976; Goodman and Bate 1983). These initial studies were followed by detailed studies in *Drosophila* (reviewed in Goodman and Doe 1993) and on axonal pathfinding in the PNS of chick and zebrafish embryos (Landmesser 1978; Lance-Jones and Landmesser 1981a, b; Tosney and Landmesser 1985a, b; Eisen et al. 1986, 1989). The retinotectal system became one of the best studied pathways, especially in the zebrafish (Karlstrom et al. 1997; Hutson and Chien 2002).

Growth cones advancing to their synaptic targets encounter a variety of guidance cues (Fig. 2.28). Axons interact with growth-promoting molecules in the extracellular matrix such as laminin, fibronectin and tenascin. Adhesive cell-surface molecules such as the cadherins, neural cell adhesion molecule (NCAM), the vertebrate homologue of Fas II, L1 and TAG1, on neuroepithelial cells promote the axon's growth. On encountering other axons or pioneer bundles, axons fasciculate. Soluble chemoattractant molecules such as the netrins direct axons (Cook et al. 1998; Yu and Bargmann 2001; Guan and Rao 2003). Guidance is also provided by molecules that prevent axon advance in particular directions (Kolodkin 1996; Cook et al. 1998; Brose and Tessier-Lavigne 2000; Raper 2000; Yu and Bargmann 2001; Pasterkamp and Kolodkin 2003). These may be surface-bound (contact inhibition or repulsion) or diffusable (chemorepulsion by semaphorins, ephrins and Slits). Finally, after contacting the synaptic target the growth cone stops elongating and begins to form its terminal arborization.

A large number of molecules have been found that control axon growth by acting as attractants or repellents. **NCAM** was the first adhesion molecule to be characterized (Edelman 1983). Despite the wide distribution of NCAM in neurons, only defasciculation and errors of targeting in the hippocampal mossy fibre system were found in NCAM knockout mice (Cremer et al. 1997). In vertebrates, **L1-type molecules** comprise L1, NrCAM and NgCAM. They are expressed in various neurons and glia during development. **TAG1** is found on commissural axons crossing the midline floor plate. Recently, morphogens for embryonic patterning, including the BMPs, WNTs and SHH, have also been implicated in axon guidance (Augsburger et al. 1999; Marti and Bovolenta 2002; Charron et al. 2003; Guan and Rao 2003; Yoshikawa et al. 2003; Butler and Dodd 2003; Yoshikawa and Thomas 2004). SHH acts as a chemoattractant for commissural neurons, and certain BMPs and WNTs act as chemorepellents; therefore, morphogen gradients, initially used for specifying cell fates, may be reused to guide axons.

To reach their proper target, axons rely upon the actions of highly conserved families of attractive (the netrins) and repulsive (the Slits, semaphorins and ephrins) guidance molecules. The **netrins** were isolated as floor-plate chemoattractants in chick embryos (Kennedy et al. 1994; Serafini et al. 1994) and are homologous to UNC6, a laminin-related protein required for circumferential growth of axons in the body wall of *C. elegans*. A human homologue was found encoded by the *NTN2L* gene on chromosome 16p13.3 (van Raay et al. 1997). Netrin-1 is important for axon guidance to the midline in the brain. Netrin-1 deficient mice do not only show abnormal spinal commissural axon projections, but also defects in the corpus callosum, and the hippocampal and anterior commissures (Serafini et al. 1996). A netrin receptor has been identified in mammals and is encoded by the *deleted in colon carcinoma* (*DCC*) gene, originally described as a tumour-suppressor gene lost in patients with colorectal cancer (Keino-Masu et al. 1996). The **semaphorins** are defined by the presence of a 'sema' domain at their amino-terminal end and form one of the largest families of repulsive and attractive growth cone guidance proteins (Cook et al. 1998; Raper 2000; Pasterkamp and Kolodkin 2003). They affect the growth cone's actin cytoskeleton
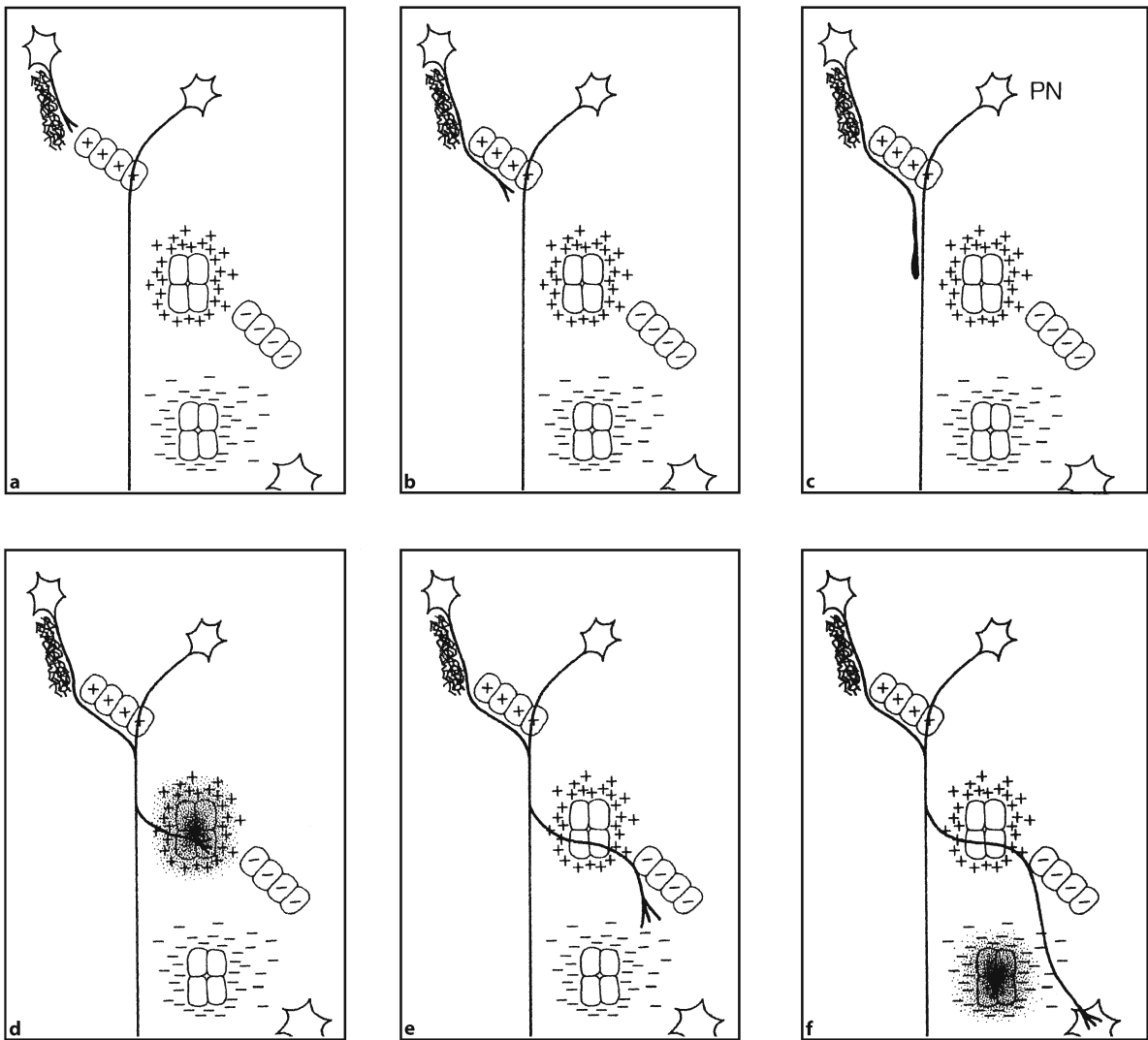
Fig. 2.28 Axons encounter a variety of guidance cues on their way to their synaptic targets: **a** the axon interacts with growth-promoting molecules in the extracellular matrix; **b** adhesive cell surface molecules on neuroepithelial cells promote the growth of axons; **c** the axon encounters an axon of a pioneer neuron (*PN*) and fasciculates with it; **d** a soluble chemoattractant molecule directs the axon; **e** an intermediate target with a repellent cue on its surface makes the axon turn; and **f** a soluble inhibitory molecule directs the axon to the right. After contacting the synaptic target, the growth cone stops elongating and begins to form terminal arborizations. (After Sanes and Jessell 2000)

through interactions with receptor complexes composed of ligand-binding, signal-transducing and modulatory subunits. Two receptor families have been implicated in mediating many semaphorin functions: plexins and neuropilins. At least 19 identified members are found, several of which act as axonal guidance molecules.

A variety of **ephrins** and their **Eph receptors** have been implicated in guiding axons to and from choice points, axon fasciculation and target selection (Orioli and Klein 1997; Cook et al. 1998; Wilkinson 2001). This signalling system is involved in the repulsive guidance of retinal axons during the formation of an ordered topographic map between the retina and the midbrain roof as well as in the development of forebrain commissures (Orioli and Klein 1997; Knöll and Drescher 2002). In EphB2 knockout mice, axons fail to navigate the anterior commissure and grow aberrantly into the ipsilateral part of the ventral forebrain (Henkemeyer et al. 1996). The recently discovered **Slit proteins** are key regulators of axon guidance, axonal branching and cell migration (Brose and Tessier-Lavigne 2000). Proteins of the Roundabout (Robo) family are the receptors. Robo was originally described in

Drosophila as a gene required to prevent aberrant crossing of the midline. Slit was identified as a repellent ligand for Robo. In mice, three homologues of *Drosophila* Robo, Robo1, Robo2 and Rig1 (Kidd et al. 1998; Brose et al. 1999; S.S. Yuan et al. 1999) and three Slit homologues, Slit1, Slit2 and Slit3, have been identified (Kidd et al. 1998; Brose et al. 1999; W. Yuan et al. 1999). Slit proteins prevent midline crossing and determine the dorsoventral position of major axonal pathways in the mammalian forebrain (Bagri et al. 2002).

2.6.3 Axon Guidance at Choice Points

In grasshopper embryos, Bate (1976) noted that pioneering growth cones migrate along a pathway marked by the presence of special cells, termed 'stepping stones' or **guidepost cells**. In vertebrates, the floor plate, a group of cells at the ventral midline of the CNS, presents a variety of different guidance cues with profound influences on the direction of migration of different classes of axons that navigate the midline (Colamarino and Tessier-Lavigne 1995; Goodman and Tessier-Lavigne 1997; Stoeckli and Landmesser 1998; Kaprielian et al. 2001). Another example of midline cells that may function as an important intermediate target is the optic chiasm (Silver 1993; Godement and Mason 1993; Sretavan 1993; Mason and Sretavan 1997). Other intermediate targets were described in the ventral forebrain. Such intermediate targets might be considered the vertebrate analogues of the insect guidepost cells.

Ventral midline structures in nematodes, fruitflies and vertebrates provide a variety of different guidance signals (Fig. 2.29). The vertebrate **floor plate** is a source of netrin-1 (Kennedy et al. 1994; Serafini et al. 1994), a long-range guidance cue. To be able to cross the midline, commissural axons also require an additional set of short-range guidance cues such as axonin-1, a TAG1 homologue, and NrCAM, an L1-type molecule, providing a positive signal for commissural axons to enter the floor plate (Yaginuma et al. 1994; Stoeckli and Landmesser 1995; Stoeckli et al. 1997). In the chick embryo, spinal commissural axons and growth cones express axonin-1, whereas the floor-plate cells express NrCAM. Commissural axons experience a prevalence of positive cues upon contact with the floor plate, causing them to enter, whereas ipsilaterally projecting fibres fail to enter, presumably because negative cues predominate (Stoeckli and Landmesser 1998). In *Drosophila*, large-scale mutant screens revealed two mutants with dramatic alterations in axonal growth across the midline (Seeger et al. 1993; Tear et al. 1996; Kidd et al. 1998). In *commissureless* (*comm*), axons do not cross the midline, resulting in the absence of commissures. In
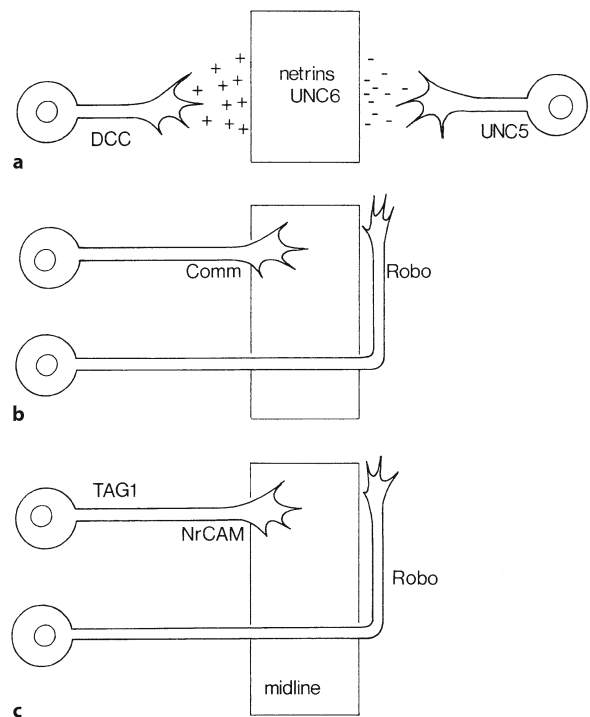
Fig. 2.29 Long-range and short-range guidance at the ventral midline in **a** *Caenorhabditis elegans*, **b** *Drosophila* and **c** the chick embryo. The netrins function as both long-range chemoattractants and long-range chemorepellents for different classes of axons. Attraction of growth cones by netrins appears to involve the DCC/UNC-40/Frazzled receptor, whereas repulsion of growth cones by netrins involves the UNC-5 receptor. In chick embryos, crossing of the midline requires interaction of TAG1/axonin-1 with NrCAM on the surface of midline cells. In *Drosophila*, it also requires the midline expression of commissureless (*Comm*). Moreover, many commissural growth cones turn longitudinally along the midline after crossing, expressing the Robo receptor. (After Goodman and Tessier-Lavigne 1997)

contrast, excessive numbers of axons crossed the midline in *roundabout* (*robo*) mutants. Slit proteins appear to be midline repellents (Brose and Tessier-Lavigne 2000; Kaprielian et al. 2001; Wong et al. 2002). Robo and Slit proteins interact with another signalling pair, netrin and its receptor DCC. Robo1 and Robo2 inhibit the midline attractant netrin through interaction of specific cytoplasmic domains of Robo proteins with DCC, thus blocking DCC's response to netrin (Stein and Tessier-Lavigne 2001). By preventing midline attraction through silencing of netrin, Robo1 and Robo2 help to keep axons on one side of the midline. Another Robo protein, Robo3, differs from other Robo proteins in that it acts as a chemoattractant and not as a repellent to axons trying to cross the midline. Robo3 promotes crossing of the midline by pyramidal tract axons (Sabatier et al. 2004).
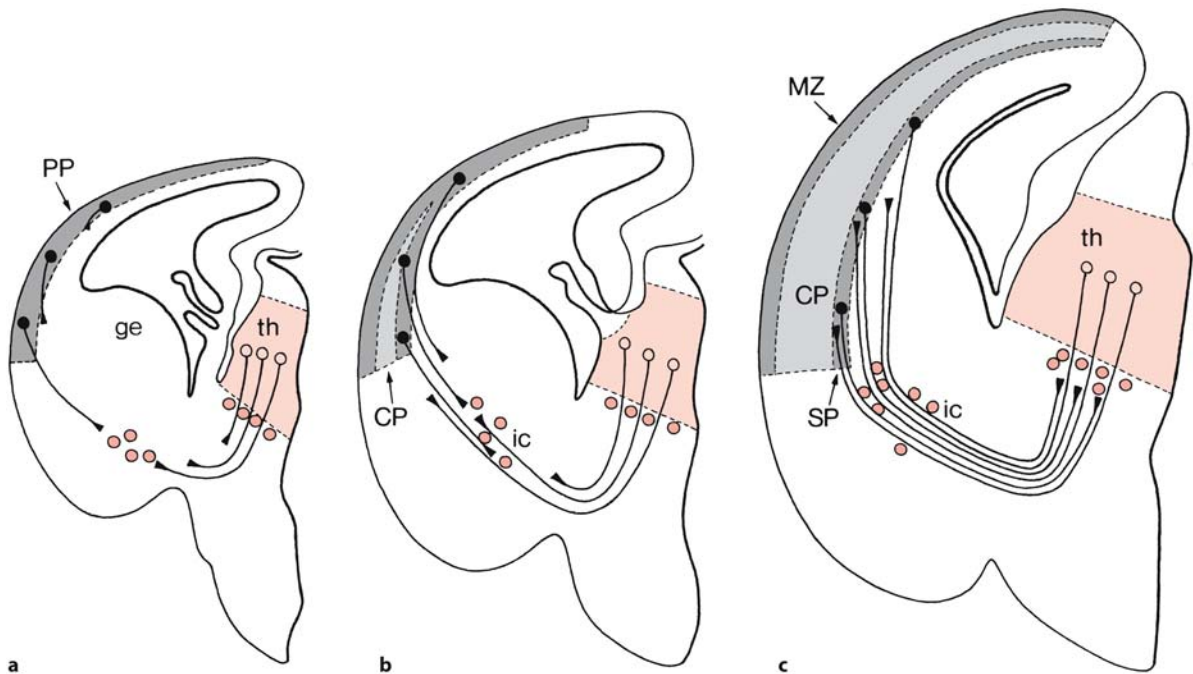
Fig. 2.30 'Handshake' hypothesis (see text for explanation). *CP* cortical plate, *ge* ganglionic eminence, *ic* internal capsule, *MZ* marginal zone, *PP* preplate, *SP* subplate, *th* thalamus. (After Molnár and Blakemore 1995)

At the vertebrate **optic chiasm**, one population of retinal ganglion cell (RGC) axons crosses the midline to project contralaterally, whereas a population of uncrossed axons is deflected at the midline, projecting ipsilaterally. Interactions between RGC axons and specific glial and neuronal populations in the embryonic forebrain appear to be involved in determining the position of the optic chiasm and RGC axon patterning (Mason and Sretavan 1997; Williams et al. 2004). In the optic chiasm of *Xenopus* and mice, ephrin-B regulates the ipsilateral routing of RGC axons (Nakagawa et al. 2000; Williams et al. 2004). In mice, Slit proteins cooperate to prevent premature midline crossing of RGC axons (Plump et al. 2002). Mice deficient in *Slit1* or *Slit2* showed few RGC axon guidance defects, but double mutants display a variety of guidance errors, including the formation of an ectopic chiasm rostral to the true chiasm, and other misprojections of RGC axons into the contralateral optic nerve and around the chiasm. A comparable role for Slit proteins was found in zebrafish embryos (Hutson and Chien 2002). The same 'channelling mechanism' is found in the forebrain. In *Slit1/Slit2* double mutants, corticofugal and thalamocortical axons deviate within the internal capsule and form an ectopic commissure at the level of the anterior commissure (Bagri et al. 2002). In the developing **corpus callosum**, Slit expression may provide a repulsive signal that forms a barrier, keeping axons within the corpus callosum (Shu and Richards 2001).

2.6.4   Formation of Thalamocortical and Corticofugal Projections

The development of thalamocortical and corticofugal projections is closely related. A cascade of simple mechanisms influences **thalamic innervation** of the cerebral cortex (Blakemore and Molnár 1990; Molnár and Blakemore 1995; Métin and Godement 1996; Molnár et al. 1998; Braisted et al. 1999; Tuttle et al. 1999; Auladell et al. 2000; López-Bendito and Molnár 2003; Vanderhaeghen and Polleux 2004). The cortex exerts a remote growth-promoting influence on thalamocortical axons when they start to grow out, becomes growth-permissive when the axons begin to invade, and later expresses a 'stop signal', causing termination of thalamocortical fibres in layer 4. In culture, any part of the thalamus will innervate any region of developing cortex (Molnár and Blakemore 1999), and the precise topographic distribution of thalamocortical fibres in vivo is unlikely to depend exclusively on regional chemoaffinity. Axons of preplate cells may pioneer the pathway from the cerebral cortex into the diencephalon (Blakemore and Molnár 1990; de Carlos and O'Leary 1992; Molnár and Blakemore 1995) as originally described in fetal cats (McConnell et al. 1989, 1994). Molnár and Blakemore (1995) proposed the '**handshake hypothesis**', implicating that axons from the thalamus and from early-born cortical preplate cells meet and intermingle in the basal telencephalon (Fig. 2.30). Later, thalamic
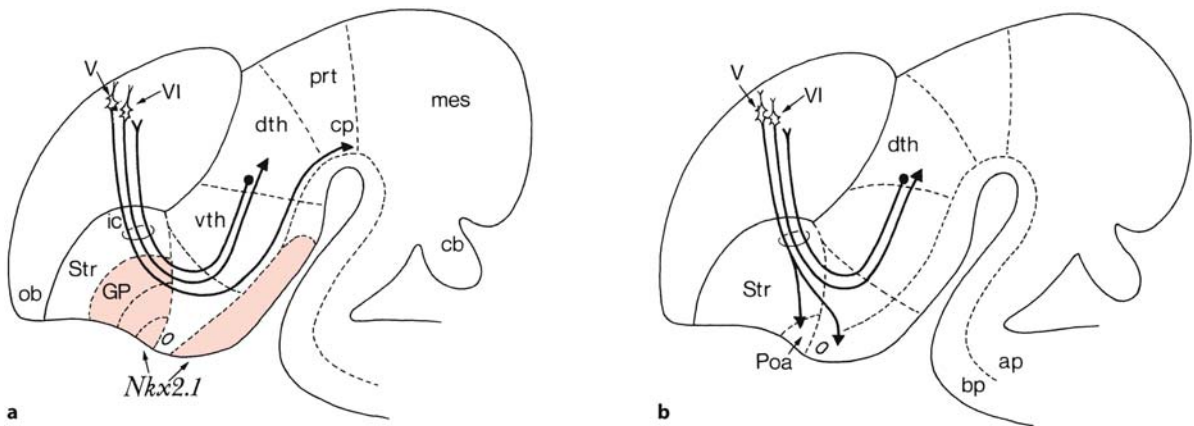
Fig. 2.31 Guidance of corticofugal projections at the telencephalic–diencephalic boundary. The paths followed by corticospinal and corticothalamic axons are shown for wild-type (**a**) and *Nkx2.1* mutant (**b**) mice. The *red areas* in **a** show the normal expression domain of *Nkx2.1* in the forebrain. *ap* alar plate, *bp* basal plate, *cb* cerebellum, *cp* cerebral peduncle,

dth dorsal thalamus, *GP* globus pallidus, *ic* internal capsule, *mes* mesencephalon, *ob* olfactory bulb, *Poa* preoptic area, *prt* pretectum, *Str* striatum, *vth* ventral thalamus, *V, VI* layer V and layer VI cortical neurons, respectively. (After Marín et al. 2002; Bagri et al. 2002)

axons grow over the scaffold of preplate axons, and become 'captured' for a waiting period in the subplate below the corresponding part of the cortex. The bizarre pattern of development of thalamocortical innervation in mouse mutants such as reeler and in *Tbr1*-knockouts provides strong evidence that thalamic axons are guided by preplate axons (Molnár and Hannan 2000; Hevner et al. 2001; López-Bendito and Molnár 2003; Chap. 9). Netrin-1 acts in vitro as an attractant and growth promoter for thalamocortical axons and is required for the proper development of the thalamocortical projection in vivo (Braisted et al. 1999, 2000). Netrin-1 is expressed in the ventral telencephalon at the time thalamocortical axons navigate through the developing internal capsule (Serafini et al. 1996; Métin et al. 1997). Ephrins control the establishment of topography of axonal projections between the thalamus and cortex, and later control the mapping of thalamocortical projections (Vanderhaeghen and Polleux 2004).

Corticospinal axon growth cones are set a formidable task in navigating through the internal capsule, cerebral peduncle, pons and medulla to reach their distant targets. This task is simplified by the fragmentation of the journey into shorter steps interrupted by intermediate targets or choice points, at which other cells provide critical guidance cues that direct growth cones on the next stage of their trajectory (Goodman and Tessier-Lavigne 1997). The subpallium appears to play a prominent role in the guidance of corticofugal and thalamocortical axons (de Carlos and O'Leary 1992; Molnár et al. 1998; Molnár and Cordery 1999; Sussel et al. 1999). The initial trajectories of these axons in the subpallium appear to

be pioneered by transient projections from the ganglionic eminences (Métin and Godement 1996; Molnár et al. 1998; Braisted et al. 1999; Molnár and Cordery 1999; Tuttle et al. 1999). The early steps in the guidance of corticofugal axons appear to be controlled by common mechanisms. Semaphorins regulate the initial extension of cortical axons towards the adjacent white matter through a complex mechanism, involving repulsion from the outer, marginal zone and attraction from the inner, ventricular zone (Bagnard et al. 1998; Polleux et al. 1998). Subsequently, netrin-1, prominently expressed in the ganglionic eminences (Métin et al. 1997; Richards et al. 1997), attracts corticofugal axons laterally towards the internal capsule. A critical decision point in the guidance of corticofugal fibres is located at the telencephalic/diencephalic boundary (Marín et al. 2002). Corticofugal fibres enter the cerebral peduncle and subsequently split into the layer VI arising corticothalamic axons and the layer V originating pyramidal tract. Appropriate patterning of the basal telencephalon and hypothalamus is essential for guidance of corticospinal projections (Fig. 2.31). Loss of function of the homeobox gene Nkx2.1 causes molecular transformation of the basal forebrain. In Nkx2.1-deficient mice, layer V cortical projections take an abnormal path when coursing through the basal forebrain. Guidance of corticothalamic and thalamocortical axons is not impaired. The basal telencephalon and the hypothalamus repel the growth of cortical axons. The axon guidance molecule Slit2 may contribute to this activity. In Slit2 mutant mice, corticofugal axons fail to enter the cerebral peduncle normally, and instead follow an abnormal course

velop by delayed interstitial branching off the flank of a spinally directed primary axon; and (3) specific branches and segments of the primary axon are selectively eliminated to yield the mature projections functionally appropriate for the area of cortex in question. The homeodomain transcription factor *Otx1* plays an important role in this elimination process (Weimann et al. 1999). *Otx1* mutants are defective in the refinement of the exuberant, transient projections. The cell adhesion molecule L1 (LICAM) may be involved in fascicle formation of outgrowing later-arriving corticospinal axons (Joosten et al. 1990; Fujimori et al. 2000). In *L1* mutant mice, the *L1* mutation causes a primary pathfinding deficit in the development of the corticospinal decussation (Cohen et al. 1997; Dahme et al. 1997; Castellani et al. 2000). A varying, but reduced number of corticospinal fibres were observed in the posterior columns of the spinal cord of L1-deficient mice and a substantial number of corticospinal axons failed to cross the midline, suggesting that the first corticospinal axons pioneer a path through the pyramidal decussation, independent of L1 function, and that later-arriving axons follow the pioneer fibres by L1-mediated fascicle formation. In *L1* knockout mice, the corpus callosum was reduced in size because of the failure of many callosal axons to cross the midline (Demyanenko et al. 1999). Human *L1* mutations are linked to a set of overlapping hereditary syndromes associated with brain malformations such as aqueduct stenosis, hydrocephalus, hypoplasia of the pyramidal tract, dysgenesis of the corpus callosum, spastic paraplegia and mental retardation (Brümmendorf et al. 1998; Kamiguchi et al. 1998; Chap. 6).

2.6.5   Formation of Topographic Maps

Development of the appropriate functional connections of the CNS requires a series of steps. Axons reach the correct area of the developing nervous system through guidance mechanisms. Many axonal projections within the CNS establish an orderly arrangement of connections in their target field, forming a topographic map. Each sensory system is characterized by **topographic maps** of the receptor array. The retinotectal projection is the dominant model system to study the development of topographic maps (Sanes and Yamagata 1999; Hutson and Chien 2002; McLaughlin et al. 2003). **Retinotectal projections** form on the basis of graded expression of guidance molecules by the projecting axons and the target area. The projections of each eye establish a pattern of interdigitation eye-specific stripes (Fig. 2.33). The tectum mesencephali is the major target of retinal axons in non-mammalian vertebrates. The formation of the retinotectal pathway (Fig. 2.34) in-

Fig. 2.32 Three stages in the development of layer V cortical axons. **a** Layer V axons extend out of the cortex towards the spinal cord, by-passing their subcortical targets. **b** The subcortical targets are exclusively contacted by axon collaterals that develop by branching off a spinally directed primary axon. **c** Specific branches and segments of the primary axon are selectively eliminated to yield the mature projections functionally appropriate for the area of cortex in question. *cb* cerebellum, *ci* colliculus inferior, *cs* colliculus superior, *Cx_{mot}* motor cortex layer V neuron, *Cx_{vis}* visual cortex layer V neuron, *dcn* dorsal column nuclei, *ob* olfactory bulb, *oli* inferior olive, *tegm* mesencephalic tegmentum. (After O'Leary and Koester 1993)

towards the surface of the telencephalon (Bagri et al. 2002).

The further outgrowth of corticospinal axons is shown in Fig. 2.32. O'Leary and co-workers (O'Leary et al. 1990; O'Leary and Koester 1993) distinguished three stages in the development of cortical axons arising in layer V neurons: (1) layer V axons extend out of the cortex towards the spinal cord, bypassing their subcortical targets; (2) the subcortical targets are exclusively contacted by axon collaterals that de-

Fig. 2.33 A double-innervation study in which an eye primordium was transplanted (**a**) into a host embryo (**b**). The projections of each eye establish a pattern of interdigitating eye-specific strips (**c**). (After Constantine-Paton and Law 1982)
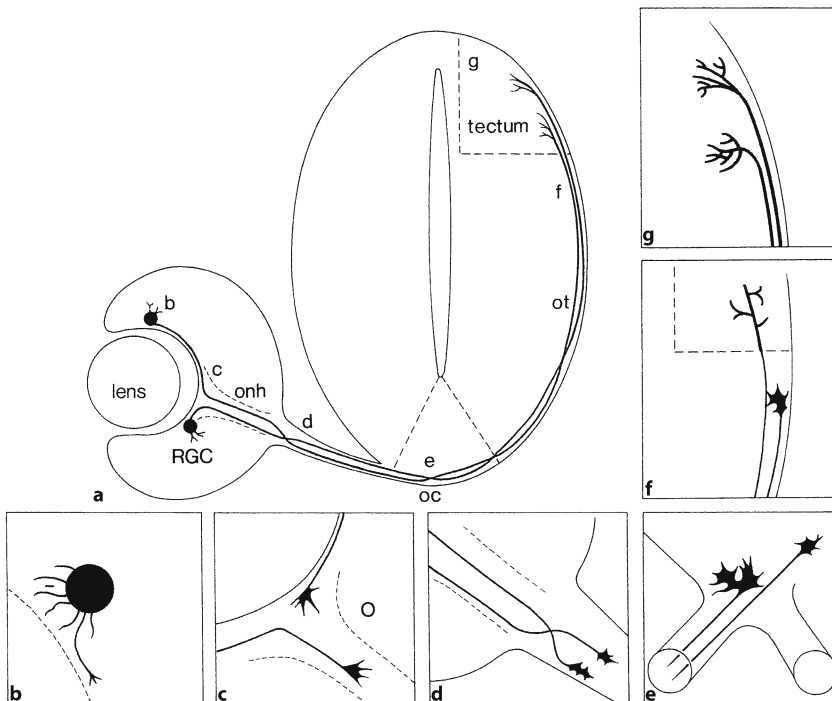
Fig. 2.34 The development of the retinotectal connection: **a** overview; **b**–**g** necessary steps to reach the tectum. Retinal ganglion cells (*RGCs*) send out transient processes including a central axon (**b**). These axons navigate along the vitreal surface of the retina to the optic nerve head (*onh*) where the fibres from younger retinal ganglion cells enter more centrally (**c**). After reorganization (**d**), axons reach the optic chiasm (*oc*) and cross to the other side (**e**). Retinal ganglion cell axons climb the optic tract (*ot*) and change their growth cone morphology (**f**, **g**). (After Johnson and Harris 2000)
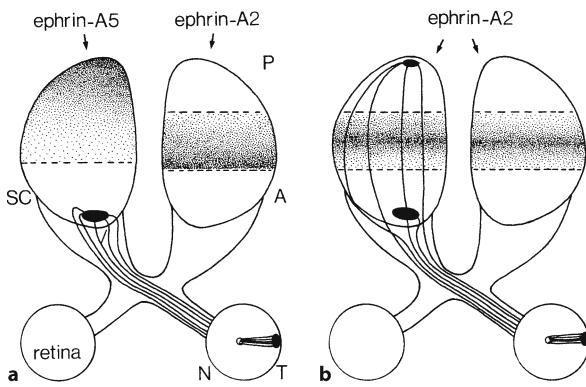
Fig. 2.35 Development of retinotopic projections. Ephrins repel axons from temporal ganglion cells (*T*) of the retina. In wild-type mice (**a**), temporal retinal axons project to the anterior part (*A*) of the superior colliculus (*SC*) only, where ephrin-A5 and ephrin-A2 have their lowest expression. When ephrin-A5 is absent (**b**), temporal axons are no longer constrained to the anterior part of the superior colliculus, and also reach the posterior part (*P*) of the superior colliculus where ephrin-A2 expression is low. (After Frisén et al. 1998; McLaughlin et al. 2003)

volves a series of steps (Holt and Harris 1993; Mason et al. 1996; Mason and Sretavan 1997; Johnson and Harris 2000; van Horck et al. 2004): (1) axonogenesis of RGCs; (2) navigation of RGC axons to the optic nerve head; (3) reorganization of RGC axons in the optic nerve; (4) crossing at the optic chiasm; (5) climbing the optic tract towards the tectum; (6) target recognition; and (7) finding the proper tectal target, resulting in topographic mapping. Many molecules are involved in guiding RGC axons at different points of the retinotectal pathway. Within the retina, RGC axons grow along a rich substrate containing laminin, N-cadherin and NCAM, before turning into the netrin-rich optic nerve head. Upon entering the optic chiasm, RGC axons encounter a set of neurons expressing molecules such as stage-specific embryonic antigen 1 (SSEA1), the cell adhesion receptor CD44 and L1. Ipsilaterally projecting fibres never traverse this set of neurons, but make a sharp turn to enter the ipsilateral optic tract. When RGC axons reach the tectal border, they must change their growth from a substrate rich in bFGF and HSPG1, to a substrate nearly devoid of these growth factors. RGC axons establish a topographic map in the tectum such that more temporal axons project to the anterior tectum, whereas more nasal axons project to the posterior tectum.

In studies using an in vitro assay of the chick tectum, Bonhoeffer and co-workers (Bonhoeffer and Huf 1980, 1982; Drescher et al. 1995) demonstated that this anterior–posterior gradient is due to a repulsive axonal guidance signal (RAGS, currently known

as ephrin-A5). Ephrins play an important role in the establishment of the retinotopic map (Knöll and Drescher 2002; McLaughlin et al. 2003). Ephrins are able to repel axons from temporal RGCs of the retina. In wild-type mice, temporal retinal axons project to anterior superior colliculus only, where the lowest expression of ephrin-A5 and ephrin-A2 is found (Fig. 2.35). In *Ephrin-A5* knockout mice, temporal axons are no longer restrained to the anterior part of the colliculus but also terminate posteriorly where ephrin-A2 expression is low (Frisén et al. 1998; Feldheim et al. 2000; Knöll and Drescher 2002; Yates et al. 2001). Dorsoventral patterning is controlled by ephrin-Bs (Hindges et al. 2002; Mann et al. 2002). Much is known on the genetic analysis of retinotectal mapping in zebrafish (Trowe et al. 1996; Karlstrom et al. 1997; Hutson and Chien 2002). Over 30 genes were found that affect either retinal axon pathfinding to the contralateral tectum or the topographic connection between the eye and the tectum. In midline crossing mutants (*sonic-you*, *you-too*, *smooth-muscle-omitted*), retinal axons project to both the ipsilateral and contralateral optic tecta. In another class of mutants (*noi* and *ace*), retinal axons project anteriorly in the forebrain and to the ipsilateral tectum. In the *astray/robo2* (*ast*) mutant, retinal axons also project into the opposite eye and to the ventral hindbrain, and show extra midline crossing.

The development of subcortical and cortical maps is shaped by a combination of molecular gradients such as shown for retinotectal projections, and of patterns of neural activity that shape important aspects of sensory representations. Sensory representations commonly have visible septa between groups of cells that are activated by separated arrays of peripheral receptors (Kaas and Catania 2002). In the rodent **somatosensory system**, each whisker on the side of the face activates a specific cluster of cells or 'barrel field' in the primary somatosensory cortex (Fig. 2.36). They become apparent at the fourth postnatal day (Rice and Van der Loos 1977). The barrel fields are ovals of tissue densely expressing the metabolic enzyme cytochrome oxidase (CO), separated by CO-light septa (Woolsey et al. 1975; Killackey et al. 1995). In mice with one or two extra or fewer whiskers, Van der Loos and co-workers (Van der Loos and Dörfl 1978; Van der Loos and Welker 1985; Welker 1985; Van der Loos et al. 1986) found the same changes in the number of barrels in the cortex and barreloids at each subcortical relay station. Similar observations were made in the somatosensory cortex in star-nosed moles with an aberrant number of appendages on their tactile nose (Catania and Kaas 1997). The matching changes in the number of whiskers or rays on the nose and the number of related neural structures in further levels of processing in the somatosensory system suggest that a genetic change or envi-
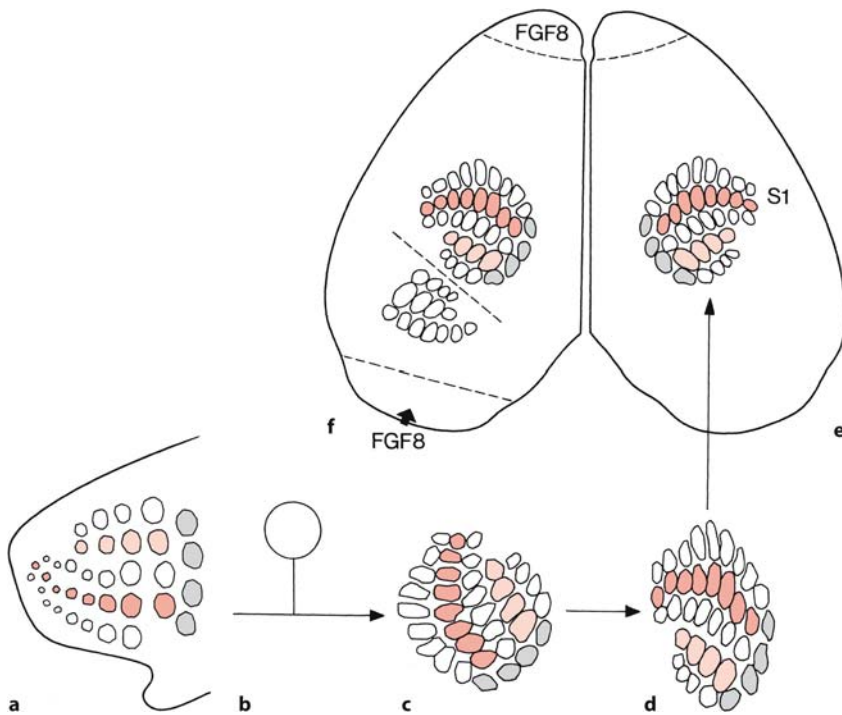
Fig. 2.36 Development of barrel fields in the murine somatosensory area S1. Whiskers-related (**a**) maps are relayed via the trigeminal ganglion (**b**), the trigeminal nuclear complex of the brain stem (**c**), and the contralateral ventroposterior thalamic nucleus (**d**) to the somatosensory area (**e**). When FGF8 was ectopically expressed in the caudal part of the neo-cortical primordium (Fukuchi-Shimogori and Grove 2001), a partial duplication of the S1-barrel field was found (**f**). (After O'Leary and Nakagawa 2002)

ronmental event during development altered the number of whiskers or rays on the face (Kaas and Catania 2002). When FGF8 is ectopically expressed in the caudal part of the embryonic neocortex, a partial duplication of the S1 barrel field (Fig. 2.36) occurs (Fukuchi-Shimogori and Grove 2001).

Similar changes occur in the **visual system.** Siamese cats result from a mutation that changes coat colour and eye colour by reducing pigmentation in parts of the body with normal body temperature. The reduced pigment in the retina has the unexplained developmental consequence of misdirecting axons from the temporal half of the retina that project abnormally to the contralateral lateral geniculate nucleus (LGN), instead of to the ipsilateral LGN (Guillery and Kaas 1971; Guillery 1996). The LGN is the major target of retinal axons in most mammals. In rhesus monkeys, Rakic (1976) showed that projections from both eyes initially overlap in the LGN, with eye-specific laminae forming from the initially different projection late in embryogenesis (Chap. 9). The development of lamina-specific connections in the spinal cord and in the cerebral cortex will be discussed in Chaps. 6 and 10, respectively.

2.7   Programmed Cell Death

Programmed cell death (**apoptosis**) is an important mechanism for determining the size and shape of the nervous system (Kerr et al. 1972; Wyllie et al. 1980; Oppenheim 1991; Lo et al. 1995; Haydar et al. 1999).

Apoptosis can be divided into four phases (Kerr et al. 1972, 1995; Clarke 1990; Oppenheim 1991): (1) activation of the cell death programme by apoptotic triggers such as deprivation or trophic support, occurring when too many neurons attempt to innervate a target population, the wrong targets are innervated or if there is inadequate incoming innervation; (2) metabolic changes such as decreased glucose uptake and reduced protein and RNA synthesis; (3) these changes appear irreversible and the cell reaches the point of 'no return', characterized by stereotypic morphological changes in cell structure; and (4) the execution phase, characterized by lysis of the cell. Removal of apoptotic cells by adjacent cells or macrophages takes place in a relatively short period without invoking an inflammatory response from the surrounding tissue as occurs during necrosis (Kerr et al. 1972; Wyllie et al. 1980). The differences between apoptosis and necrosis of a cell are shown in Fig. 2.37. Homologues of the cell-death pathway in the nematode *C. elegans* have analogous functions in apoptosis in the developing vertebrate brain (Wyllie 1997; Huppertz et al. 1999; Kuan et al. 2000). During the development of a *C. elegans* hermaphrodite, 131 out of 1,090 cells undergo programmed cell death in a lineage-specific and mostly cell autonomous manner (Sulston and Horvitz 1977; Ellis and Horvitz 1986; Yuan and Horvitz 1990; Ellis et al. 1991). A large number of cell death (*ced*) genes have been identified (Metzstein et al. 1998). Structural homologues of the genes involved in the execution phase of cell death in *C. elegans* have been identified in mammals. The
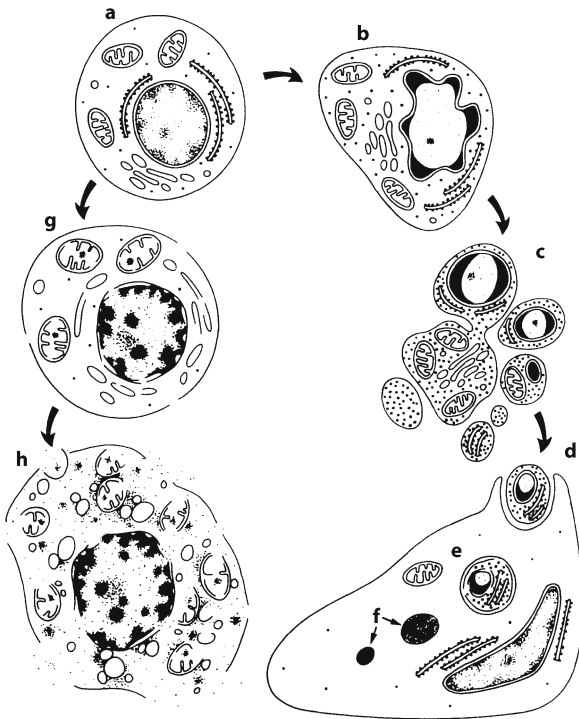
Fig. 2.37 Sequence of ultrastructural changes in apoptosis (**b**–**f**) and necrosis (**g**, **h**) occurring in a normal cell (**a**). Early apoptosis (**b**) is characterized by compaction and segregation of chromatin in sharply circumscribed masses that abut on the inner side of the nuclear envelope with convolution of the nuclear outline and condensation of the cytoplasm. In the next phase (**c**), the nucleus fragments and further condensation of the cytoplasm is associated with extensive cell surface protrusion, followed by the formation of membrane-bound apoptotic bodies. These apoptotic bodies are phagocytosed (**d**) by nearby cells, are degraded by lysosomal enzymes (**e**) and are rapidly reduced to non-descript residues (**f**). In an irreversibly injured cell, the onset of necrosis (**g**) manifests itself as irregular clumping of chromatin, gross swelling of mitochondria, dissolution of ribosomes and focal rupture of membranes. At a more advanced stage (**h**), all cellular components disintegrate. (After Kerr et al. 1995)

Fig. 2.38 The apoptosis cascade (after Huppertz et al. 1999)

mammalian homologues of *ced3* comprise a large family of cysteine-containing, aspartate-specific proteases called **caspases** (Salvesen and Dixit 1997; Wyllie 1997; Thornberry and Lazebnik 1998; Boonstra and Isacson 1999). Once activated, caspases cleave other caspases and various cellular substrates, leading to the ultrastructural changes that characterize apoptosis (Jacobson et al. 1996, 1997; Salvesen and Dixit 1997; Wyllie 1997; Fig. 2.38). Null mutants of *Casp3* (CPP32) and *Casp9* showed severe defects in the nervous system (Kuida et al. 1996, 1998; Hakem et al. 1998). By preventing normal selected apoptotic cell death in the early forebrain progenitor cell lin-

eage, caspase deletion causes an increase in forebrain founder cells. In caspase-3 deficient mice, the entire brain is larger, with hyperplastic, ectopic cell masses in the cerebral cortex, the cerebellum, the striatum and the hippocampus (Kuida et al. 1996). Instead of a normal smooth brain, the increase in forebrain founder cells leads to a large expansion of the cerebral wall and a convoluted cerebrum of larger surface area (Kuida et al. 1996; Haydar et al. 1999). Caspase-3 deficient mice have a high prenatal lethality and are not fertile. Most caspase-9 deficient mice die perinatally with a markedly enlarged and malformed brain, most severe in the cerebral cortex as a result of reduced apoptosis during development (Kuida et al. 1998). The Jnk1 and Jnk2 protein kinases are also required for regional specific apoptosis during early brain development (Kuan et al. 1999, 2000).

Neuron death during normal development was first noted by Vogt (1842), who reported cell death in the notochord and adjacent cartilage of metamorphosing toads (Clarke and Clarke 1996). Ernst (1926) was one of the first to recognize that overproduction of neurons was followed by death of a significant fraction of neurons in many regions of the nervous system of vertebrates. He suggested three main types of cell death during normal development: the first occurring during regression of vestigial organs such as the pronephros and mesonephros; the second occurring during cavitation, folding or fusion of organ

anlage such as the neural plate and neural tube; the third occurring as part of the process of remodelling of tissues such as cartilage, bone and various cell groups in the CNS. Glücksmann (1940, 1951) introduced the terms phylogenetic, morphogenetic and histogenetic cell death for Ernst's types. Hughes (1961), Prestige (1965) and Cowan and Wenger (1968) showed that the number of neurons produced (motoneurons, spinal ganglion cells and ciliary ganglion cells, respectively) is matched to the size of the targets as a result of reciprocal trophic interactions between nerves and their peripheral innervation fields. Cell death was initially detected by classic histological staining techniques. New sensitive techniques such as the terminal deoxynucleotidyl transferase-mediated dUTP-biotin nick end-labelling (TUNEL) method (Gavrieli et al. 1992) and markers such as annexin V (van den Eijnde et al. 1997, 1999) greatly improved the study of apoptosis.

Programmed degeneration of Rohon–Beard cells is an example of **phylogenetic cell death**. Rohon–Beard cells are derived from the neural crest and form a transient primary sensory system linking the ectoderm with the neural tube in fish and amphibian embryos. They degenerate as their place is taken by spinal dorsal root ganglia (Beard 1896; Hughes 1957; Lamborghini 1987). During insect metamorphosis, phylogenetic cell death occurs of neurons such as those innervating larval musculature (Bate 1976). **Morphogenetic cell death** occurs in many developing structures such as the limbs, the face, and in many parts of the developing nervous system during cavitation, fusion, folding and bending of organ anlage such as the neural plate and tube and during formation of the optic and otic vesicles. Programmed cell death plays an essential role in sculpting parts of the body such as the face and the formation of the digits (Vermeij-Keers 1972; Mori et al. 1994, 1995; Kimura and Shiota 1996; van den Eijnde et al. 1997; van den Eijnde 1999). Caspase inhibitors block digit formation (Jacobson et al. 1996, 1997). Similarly, programmed cell death is involved in hollowing out solid structures to create lumina for the nasolacrimal, parotid and other glandular ducts (van den Eijnde et al. 1997; van den Eijnde 1999).

Histogenetic cell death occurs during histogenesis and remodelling of tissues. This is the common type of cell death during development of the nervous system. There are several mechanisms known to cause histogenetic neuronal death (Clarke 1990; Jacobson 1991). Cell death during normal development of the vertebrate nervous system has been demonstrated for many locations, ranging from the ciliary, sympathetic, spinal and cranial ganglia, through motoneurons to the cerebral cortex. Widespread apoptosis occurs in proliferative and postmitotic regions of the fetal cerebral cortex and thalamus of rodents

(Spreafico et al. 1995; Blaschke et al. 1996, 1998; Thomaidou et al. 1997) and the human basal ganglia (Itoh et al. 2001). Apoptosis in the cerebral cortex may be associated with neuronal proliferation and may be linked with phenotype selection of clonally expanding neurons and the initiation of postmitotic neuron generation (Blaschke et al. 1996, 1998). Moreover, it may serve to delete cells carrying mutations and/or helps to regulate cell numbers (Thomaidou et al. 1997).

References

Acampora D, Simeone A (1999) Understanding the role of *Otx1* and *Otx2* in the control of brain morphogenesis. Trends Neurosci 22:116–122

Acampora D, Mazan S, Lallemand Y, Avantaggiato V, Maury M, Simeone A, Brûlet P (1995) Forebrain and midbrain regions are deleted in *Otx2*–/– mutants due to a defective anterior neuroectoderm specification during gastrulation. Development 121:3279–3290

Acampora D, Gulisano M, Broccoli V, Simeone A (2001) *Otx* genes in brain morphogenesis. Prog Neurobiol 64:69–95

Altman J (1966) Proliferation and migration of undifferentiated precursor cells in the rat during postnatal gliogenesis. Exp Neurol 16:263–278

Altman J (1970) Postnatal neurogenesis and the problem of neural plasticity. In: Himwich WA (ed) Developmental Neurobiology. Thomas, Springfield, IL, pp 197–237

Altman J, Bayer SA (1987a) Development of the precerebellar nuclei in the rat. I. The precerebellar neuroepithelium of the rhombencephalon. J Comp Neurol 257:477–489

Altman J, Bayer SA (1987b) Development of the precerebellar nuclei in the rat. II. The intramural olivary migratory stream and the neurogenetic organization of the inferior olive. J Comp Neurol 257:490–512

Altman J, Bayer SA (1987c) Development of the precerebellar nuclei in the rat. III. The posterior precerebellar extramural migratory stream and the lateral reticular and external cuneate nuclei. J Comp Neurol 257:513–528

Altman J, Bayer SA (1987d) Development of the precerebellar nuclei in the rat. IV. The anterior precerebellar extramural migratory stream and the nucleus reticularis tegmenti pontis and the basal pontine gray. J Comp Neurol 257:529–552

Altman J, Bayer SA (1997) Development of the Cerebellar System: In relation to its evolution, structure and function. CRC, Boca Raton, FL

Alvarez-Buylla A, Theelen M, Nottebohm F (1988) Mapping of radial glia and of a new cell type in adult canary brain. J Neurosci 8:2707–2712

Amores A, Force A, Yan Y-L, Amemiya C, Fritz A, Ho RK, Joly L, Langeland J, Prince V, Wang Y-L, et al. (1998) Genome duplications in vertebrate evolution: Evidence from zebrafish *Hox* clusters. Science 282:1711–1714

Appel B (2000) Zebrafish neural induction and patterning. Dev Dyn 203:155–168

Arendt D, Nübler-Jung K (1999) Comparison of early nerve cord development in insects and vertebrates. Development 126:2309–2325

Araújo SJ, Tear G (2003) Axon guidance mechanisms and molecules: Lessons from invertebrates. Nat Rev Neurosci 4:910–922

Ashburner M (1989) *Drosophila*: A Laboratory Handbook. Cold Spring Harbor Laboratory Press, Cold Spring Harbor, NY

Auclair F, Marchand R, Glover JC (1999) Regional patterning of reticulospinal and vestibulospinal neurons in the hindbrain of mouse and rat embryos. J Comp Neurol 411:288–300

Auladell C, Pérez-Sust P, Supèr H, Soriano E (2000) The early development of thalamocortical and corticothalamic projections in the mouse. Anat Embryol (Berl) 201:169–179

Augsburger A, Schuchardt A, Hoslins S, Dodd J, Butler S (1999) BMPs as mediators of roof plate repulsion of commissural neurons. Neuron 24:127–141

Bachiller D, Klingensmith J, Kemp C, Belo JA, Anderson RM, May SR, McMahon JA, McMahon AP, Harland RM, Rossant J, De Robertis EM (2000) The organizer factors Chordin and Noggin are required for mouse forebrain development. Nature 403:658–661

Bagnard D, Lohrum M, Uziel D, Puschel AW, Bolz J (1998) Semaphorins act as attractive and repulsive guidance signals during the development of cortical projections. Development 125:5043–5053

Bagri A, Marín O, Plump AS, Mak Y, Pleasure SJ, Rubinstein JLR, Tessier-Lavigne M (2002) Slit proteins prevent midline crossing and determine the dorsoventral position of major axonal pathways in the mammalian forebrain. Neuron 33:233–248

Balinsky BI (1965) An Introduction to Embryology, 2nd ed. Saunders, Philadelphia, PA

Bally-Cuif L, Hammerschmidt M (2003) Induction and patterning of neuronal development, and its connections to cell cycle control. Curr Opin Neurobiol 13:16–25

Barres BA, Raff MC (1994) Control of oligodendrocyte number in the developing rat optic nerve. Neuron 12:935–942

Barth KA, Kishimoto Y, Rohr KB, Seydler C, Schulte-Merker S, Wilson SW (1999) Bmp activity establishes a gradient of positional information throughout the entire neural plate. Development 126:4977–4987

Bastiani MJ, Harrelson AL, Snow PM, Goodman CS (1987) Expression of fasciclin I and II glycoproteins on subsets of axon pathways during neuronal development in the grasshopper. Cell 48:745–755

Bate CM (1976) Embryogenesis of an insect nervous system. I. A map of the thoracic and abdominal neuroblasts in *Locusta migratoria*. J Embryol Exp Morphol 35:107–123

Bayer SA (1983) 3H-Thymidine-radiographic studies of neurogenesis in the rat olfactory bulb. Exp Brain Res 50:329–340

Bayer SA, Altman J (1991) Neocortical Development. Raven, New York

Bayer SA, Altman J (1995a) Neurogenesis and neuronal migration. In: Paxinos G (ed) The Rat Nervous System, 2nd ed. Academic, San Diego, CA, pp 1041–1078

Bayer SA, Altman J (1995b) Principles of neurogenesis, neuronal migration and neural circuit formation. In: Paxinos G (ed) The Rat Nervous System, 2nd ed. Academic, San Diego, CA, pp 1079–1098

Bayer SA, Altman J, Russo RJ, Zhang X (1995) Embryology. In: Duckett S (ed) Pediatric Neuropathology. Williams & Wilkins, Baltimore, MD, pp 54–107

Beard J (1896) The history of a transient nervous apparatus in certain Ichthyopsida. An account of the development and regeneration of ganglion cells and nerve fibres. I. Raja batis. Zool Jahrb 9:319–426

Beddington RSP (1994) Induction of a second neural axis by the mouse node. Development 120:613–620

Beddington RSP, Robertson EJ (1998) Anterior patterning in mouse. Trends Genet 14:277–284

Beddington RSP, Robertson EJ (1999) Axis development and early asymmetry in mammals. Cell 96:195–209

Belo JA, Bouwmeester T, Leyns L, Kertesz N, Gallo M, Gollettie M, De Robertis EM (1997) Cerberus-like is a secreted factor with neuralizing activity expressed in the anterior primitive endoderm of the mouse gastrula. Mech Dev 68:45–57

Belting HG, Hauptmann G, Meyer D, Abdelilah-Seyfried S, Chitnis A, Eschbach C, Söll I, Thisse C, Thisse B, Artinger KB, et al. (2001) *spiel ohne grenzen/pou2* is required during establishment of the zebrafish midbrain-hindbrain boundary organizer. Development 128:4165–4176

Bentivoglio M, Mazzarello P (1999) The history of radial glia. Brain Res Bull 49:305–315

Bergquist H (1932) Zur Morphologie des Zwischenhirns bei niederen Wirbeltieren. Acta Zool (Stockh) 13:57–303

Bergquist H (1952) Studies on the cerebral tube in vertebrates. Acta Zool (Stockh) 33:117–187

Bergquist H, Källén B (1954) Notes on the early histogenesis and morphogenesis of the central nervous system in vertebrates. J Comp Neurol 100:627–659

Biben C, Stanley E, Fabri L, Kotecha S, Rhinn M, Drinkwater C, Lah M, Wang CC, Nash A, Hilton D, et al. (1998) Murine cerberus homologue mCer-1: A candidate anterior patterning molecule. Dev Biol 194:135–151

Blakemore C, Molnár Z (1990) Factors involved in the establishment of specific interconnections between thalamus and cerebral cortex. Cold Spring Harbor Symp Quant Biol 55:491–504

Blaschke AJ, Staley K, Chun J (1996) Widespread programmed cell death in proliferative and postmitotic regions of the fetal cerebral cortex. Development 122:1165–1174

Blaschke AJ, Weiner JA, Chun J (1998) Programmed cell death is a universal feature of embryonic and postnatal neuroproliferative regions throughout the central nervous system. J Comp Neurol 396:39–50

Bonhoeffer F, Huf J (1980) Recognition of cell types by axonal growth cones in vitro. Nature 288:162–164

Bonhoeffer F, Huf J (1982) In vitro experiments on axon guidance demonstrating an anterior-posterior gradient on the tectum. EMBO J 1:427–431

Boonstra Z, Isacson O (1999) Apoptosis in neuronal development and transplantation: Role of caspases and trophic factors. Exp Neurol 156:1–15

Boulder Committee (1969) Embryonic vertebrate central nervous system: Revised terminology. Anat Rec 166:257–262

Bourrat F, Sotelo C (1988) Migratory pathways and neuritic differentiation of inferior olivary neurons in rat embryo. Axonal tracing study using the in vitro slab technique. Brain Res 467:19–37

Bourrat F, Sotelo C (1990) Early development of the rat precerebellar system: Migratory routes, selective aggregation and neuritic differentiation of the inferior olive and lateral reticular nucleus neurons. An overview. Arch Ital Biol 128:151–170

Bouwmeester T, Leyns L (1997) Vertebrate head induction by anterior primitive endoderm. BioEssays 19:855–863

Bouwmeester T, Kim S-H, Sasai Y, Lu B, De Robertis EM (1996) Cerberus is a head-inducing secreted factor expressed in the anterior endoderm of Spemann's organizer. Nature 382:595–601

Boyan G, Therianos S, Williams JLD, Reichert H (1995) Axonogenesis in the embryonic brain of the grasshopper *Schistocerca gregaria*: An identified cell analysis of early brain development. Development 121:75–86

Braisted JE, Tuttle R, O'Leary DDM (1999) Thalamocortical axons are influenced by chemorepellent and chemoattractant activities localized to decision points along their path. Dev Biol 208:430–440

Braisted JE, Catalano SM, Stimac R, Kennedy TE, Tessier-Lavigne M, Shatz CJ, O'Leary DDM (2000) Netrin-1 promotes thalamic axon growth and is required for proper development of the thalamocortical projection. J Neurosci 20:5792–5801

Brand M, Heisenberg CP, Jiang YJ, Beuchle D, Lun K, Furutani-Seiki M, Granato M, Haffter P, Hammerschmidt M, Kane DA, et al. (1996) Mutations in zebrafish genes affecting the formation of the boundary between midbrain and hindbrain. Development 123:179–190

Brazel CY, Romanko MJ, Rothstein RP, Levison SW (2003) Roles of the mammalian subventricular zone in brain development. Prog Neurobiol 69:49–69

Brose K, Tessier-Lavigne M (2000) Slit proteins: Key regulators of axon guidance, axonal branching, and cell migration. Curr Opin Neurobiol 10:95–102

Brose K, Bland KS, Wang KH, Arnott D, Henzel W, Goodman CS, Tessier-Lavigne M, Kidd T (1999) Slit proteins bind Robo receptors and have an evolutionary conserved role in repulsive axon guidance. Cell 96:795–806

Brown M, Keynes R, Lumsden A (2001) The Developing Brain. Oxford University Press, Oxford

Brümmendorf T, Kenwrick S, Rathjen FG (1998) Neural cell recognition molecule L1: From cell biology to human hereditary brain malformations. Curr Opin Neurobiol 8:87–97

Bulfone A, Puelles L, Porteus MH, Frohman MA, Martin GR, Rubinstein JLR (1993) Spatially restricted expression of *Dlx-1*, *Dlx-2*, (*Tes-1*), *Gbx-2*, and *Wnt-3* in the embryonic day 12.5 mouse forebrain defines potential transverse and longitudinal boundaries. J Neurosci 13:3155–3172

Burgess S, Reim G, Chen W, Hopkins N, Brand M (2002) The zebrafish *spiel-ohne-grenzen (spg)* gene encodes the POU domain protein Pou2 related to mammalian *Oct4* and is essential for formation of the midbrain and hindbrain, and for pre-gastrula morphogenesis. Development 129:905–916

Butler SJ, Dodd J (2003) A role for BMP heterodimers in roof plate-mediated repulsion of commissural axons. Neuron 38:389–401

Campagnoni AT (1995) Molecular Biology of Myelination. Oxford University Press, New York

Campagnoni AT, Skoff RP (2001) The pathobiology of myelin mutants reveals novel biological functions of the MBP and PLP genes. Brain Pathol 11:74–91

Campbell K, Götz M (2002) Radial glia: Multi-purpose cells for vertebrate brain development. Trends Neurosci 25:235–238

Campos-Ortega JA, Hartenstein V (1997) The Embryonic Development of *Drosophila melanogaster*, 2nd ed. Springer, Berlin Heidelberg New York

Castellani V, Chédotal A, Schachner M, Faivre-Sarrailh C, Rougon G (2000) Analysis of the L1-deficient mouse phenotype reveals cross-talk between Sema3A and L1 signaling pathways in axonal guidance. Neuron 27:237–249

Catania KC, Kaas JH (1997) The mole nose instructs the brain. Somatosens Motor Res 14:56–58

Cepko C (1988) Retrovirus vectors and their applications in neurobiology. Neuron 1:345–353

Cepko CL, Golden JA, Szele FG, Lin JC (1997) Lineage analysis in the vertebrate central nervous system. In: Cowan WM, Jessell TM, Zipursky SL (eds) Molecular and Cellular Approaches to Neural Development. Oxford University Press, New York, pp 391–439

Charron F, Stein E, Jeong J, McMahon AP, Tessier-Lavigne M (2003) The morhogen sonic hedgehog is an axonal chemoattractant that collaborates with netrin-1 in midline axonguidance. Cell 113:11–23

Chédotal A, Pourquié O, Sotelo C (1995) Initial tract formation in the brain of the chick embryo: Selective expression of the BEN/SC1/DM-GRASP cell adhesion molecule. Eur J Neurosci 7:198–212

Chi CL, Martinez S, Wurst W, Martin GR (2003) The isthmic organizer signal FGF8 is required for cell survival in the prospective midbrain and cerebellum. Development 130:2633–2644

Chiang C, Litingtung Y, Lee E, Young KE, Corden JL, Westphal H, Beachy PA (1996) Cyclopia and defective axial patterning in mice lacking *Sonic hedgehog* gene function. Nature 383:407–413

Chitnis AB, Kuwada JY (1990) Axonogenesis in the brain of zebrafish embryos. J Neurosci 10:1892–1905

Choi BH (1981) Radial glia of developing human fetal spinal cord: Golgi, immunohistochemical and electron microscopic study. Dev Brain Res 1:249–267

Choi BH, Kim RC (1984) Expression of glial fibrillary acidic protein in immature oligodendroglia. Science 223:407–409

Choi BH, Lapham LW (1978) Radial glia in the human fetal cerebrum: A combined Golgi, immunofluorescence and electron microscope study. Brain Res 148:295–311

Chotard C, Salecker I (2004) Neurons and glia: Team players in axon guidance. Trends Neurosci 27:655–661

Clarke JD, Lumsden A (1993) Segmental repetition of neuronal phenotype sets in the chick embryo hindbrain. Development 118:151–162

Clarke PGH (1990) Developmental cell death: Morphological diversity and multiple mechanisms. Anat Embryol (Berl) 181:195–213

Clarke PGH, Clarke S (1996) Nineteenth century research on naturally occurring cell death and related phenomena. Anat Embryol (Berl) 193:81–99

Cobos I, Shimamura K, Rubinstein JLR, Martínez S, Puelles L (2001) Fate maps of the avian anterior forebrain at the four-somite stage, based on the analysis of quail-chick chimeras. Dev Biol 239:46–67

Cohen NR, Taylor JSH, Scott LB, Guillery RW, Soriano P, Furley AJ (1997) Errors in corticospinal axon guidance in mice lacking the neural cell adhesion molecule L1. Curr Biol 8:26–33

Colamarino SA, Tessier-Lavigne M (1995) The role of the floor plate in axon guidance. Annu Rev Neurosci 18:497–529

Compston A, Zajicek J, Sussman J, Webb A, Hall G, Muir D, Shaw C, Wood A, Scolding N (1997) Glial lineages and myelination in the central nervous system. J Anat (Lond) 190:161–200

Constantine-Paton M, Law MI (1982) The development of maps and stripes in the brain. Sci Am 247:54–62

Cook G, Tannahill D, Keynes R (1998) Axon guidance to and from choice points. Curr Opin Neurobiol 8:64–72

Cooke JE, Moens CB (2002) Boundary formation in the hindbrain: *Eph* only it were simple. Trends Neurosci 25:260–267

Corbin JG, Nery S, Fishell G (2001) Telencephalic cells take a tangent: Non-radial migration in the mammalian forebrain. Nat Neurosci 4(Suppl):1177–1182

Couly GF, Le Douarin NM (1987) Mapping of the early neural primordium in quail-chick chimeras. II. The prosencephalic neural plate and neural folds: Implications for the genesis of cephalic human congenital abnormalities. Dev Biol 120:198–214

Cowan WM, Wenger E (1968) Degeneration in the nucleus of origin of the preganglionic fibers to the chick ciliary ganglion following early removal of the optic vesicle. J Exp Zool 168:105–124

Cremer H, Chazal G, Goridis C, Represa A (1997) NCAM is essential for axonal growth and fasciculation in the hippocampus. Mol Cell Neurosci 8:323–335

Crossley PH, Martínez S, Martin GR (1996) Midbrain development induced by FGF8 in the chick embryo. Nature 380:66–68

Dahme M, Bartsch U, Martini R, Anliker B, Schachner M, Mantei N (1997) Disruption of the mouse L1 gene leads to malformations of the nervous system. Nat Genet 17:346–349

Dale JK, Vesque C, Lints TJ, Sampath TK, Furley A, Dodd J, Placzek M (1997) Cooperation of BMP7 and SHH in the induction of forebrain ventral midline cells by prechordal mesoderm. Cell 90:257–269

Darnell DK, Stark MR, Schoenwolf GC (1999) Timing and cell interactions underlying neural induction in the chick embryo. Development 126:2505–2514

Davidson BP, Camus A, Tam PPL (1999) Cell fate and lineage specification in the gastrulating mouse embryo. In: Moody SA (ed) Cell Lineage and Determination. Academic, San Diego, CA, pp 491–504

de Carlos JA, O'Leary DDM (1992) Growth and targeting of subplate axons and establishment of major cortical pathways. J Neurosci 12:1194–1211

Demyanenko GP, Tsai AY, Maness PF (1999) Abnormalities in neural process extension, hippocampal development, and the ventricular system of L1 knockout mice. J Neurosci 19:4907–4920

De Robertis EM, Larrain J, Oelgeschlager M, Wessely O (2000) The establishment of Spemann's organizer and patterning of the vertebrate embryo. Nat Rev Genet 1:171–181

de Souza FSJ, Niehrs C (2000) Anterior endoderm and head induction in early vertebrate embryos. Cell Tissue Res 300:207–217

Díaz C, Glover JC (2002) Comparative aspects of the hodological organization of the vestibular nuclear complex and related neuron populations. Brain Res Bull 57:307–312

Díaz C, Puelles L, Marín F, Glover JC (1998) The relationship between rhombomeres and vestibular neuron populations as assessed in quail-chicken chimeras. Dev Biol 202:14–28

Dickinson ME, Selleck MA, McMahon AP, Bronner-Fraser M (1995) Dorsalization of the neural tube by the non-neural ectoderm. Development 121:2099–2106

Doetsch F, García-Verdugo JM, Alvarez-Buylla A (1997) Cellular comparison in three-dimensional organization of the subventricular germinal zone in the adult mammalian brain. J Neurosci 17:5046–5061

Doetsch F, Caillé I, Lim DA, García-Verdugo JM, Alvarez-Buylla A (1999) Subventricular zone astrocytes are neural stem cells in the adult mammalian brain. Cell 97:703–716

Dou CL, Li S, Lai E (1999) Dual role of brain factor-1 in regulating growth and patterning of the cerebral hemispheres. Cereb Cortex 9:543–550

Drescher U, Kremoser C, Handwerker C, Loschinger J, Noda M, Bonhoeffer F (1995) In vitro guidance of retinal ganglion cell axons by RAGS, a 25 kDa tectal protein related to ligands for Eph receptor tyrosine kinases. Cell 82:359–370

Driever W (1999) Introduction to the zebrafish. In: Moody SA (ed) Cell Lineage and Fate Determination. Academic, San Diego, CA, pp 383–398

Dupé V, Lumsden A (2001) Hindbrain patterning involves graded responses to retinoic acid signalling. Development 128:2199–2208

Dupé V, Ghyselinck NB, Wendling O, Chambon P, Mark M (1999) Key roles of retinoic acid receptors alpha and beta in the patterning of the caudal hindbrain, pharyngeal arches and otocyst in the mouse. Development 126:5051–5059

Durston AJ, Timmermans JPM, Hage WJ, Hendricks HFJ, de Vries NJ, Heideveld M, Nieuwkoop PD (1989) Retinoic acid causes an anteroposterior transformation in the developing central nervous system. Nature 340:140–147

Eagleson GW, Harris WA (1990) Mapping of the presumptive brain regions in the neural plate of Xenopus laevis. J Neurobiol 21:427–440

Eagleson GW, Ferreiro B, Harris WA (1995) Fate of the anterior neural ridge and the morphogenesis of the Xenopus forebrain. J Neurobiol 28:146–158

Easter SS Jr, Ross LS, Frankfurter A (1993) Initial tract formation in the mouse brain. J Neurosci 13:285–299

Easter SS Jr, Burrill J, Marcus RC, Ross LS, Taylor JSH, Wilson SW (1994) Initial tract formation in the vertebrate brain. Prog Brain Res 102:79–93

Echelard Y, Epstein DJ, St-Jacques B, Shen L, Mohler J, McMahon JA, McMahon AP (1993) Sonic hedgehog, a member of a family of putative signalling molecules, is implicated in the regulation of CNS polarity. Cell 75:1417–1430

Edelman GM (1983) Cell adhesion molecules. Science 219:450–457

Eisen JS, Myers PZ, Westerfield M (1986) Pathway selection by growth cones of identified motoneurones in live zebrafish embryos. Nature 320:269–271

Eisen JS, Pike SH, Debu B (1989) The growth cones of identified motoneurons in embryonic zebrafish select appropriate pathways in the absence of specific cellular interactions. Neuron 2:1097–1104

Ellis HM, Horvitz HR (1986) Genetic control of programmed cell death in the nematode C. elegans. Cell 44:817–829

Ellis HM, Yuan JY, Horvitz HR (1991) Mechanisms and function of cell death. Annu Rev Cell Biol 7:663–698

Ernst M (1926) Über Untergang von Zellen während der normalen Entwicklung bei Wirbeltieren. Z Anat Entw Gesch 79:228–262

Essick CR (1912) The development of the nuclei pontis and the nucleus arcuatus in man. Am J Anat 13:25–54

Favier B, Dollé P (1997) Developmental functions of mammalian Hox genes. Mol Hum Reprod 3:115–131

Feldheim DA, Kim YI, Bergemann AD, Frisén J, Barbacid M, Flanagan JG (2000) Genetic analysis of ephrin-A2 and ephrin-A5 shows their requirement in the multiple aspects of retinocollicular mapping. Neuron 25:563–574

Fishell G, Kriegstein AR (2003) Neurons from radial glia: The consequences of asymmetric inheritance. Curr Opin Neurobiol 13:34–41

Flanagan JG, Vanderhaeghen P (1998) The ephrins and Eph receptors in neural development. Annu Rev Neurosci 21:309–345

Foley AC, Skromne IS, Stern CD (2000) Reconciling different models of forebrain induction and patterning: A dual role for the hypoblast. Development 127:3839–3854

Fraser S, Keynes R, Lumsden A (1990) Segmentation in the chick embryo hindbrain is defined by cell lineage restrictions. Nature 344:431–435

Fraser SE (1999) Cell interactions and morphogenetic motions pattern the zebrafish nervous system. In: Moody SA (ed) Cell Lineage and Fate Determination. Academic, San Diego, CA, pp 371–382

Frisén J, Yates PA, McLaughlin T, Friedman GC, O'Leary DDM, Barbacid M (1998) Ephrin-A5 (AL-1/RAGS) is essential for proper retinal axon guidance and topographic mapping in the mammalian visual system. Neuron 20:235–243

Fujimori KE, Takeuchi K, Yazaki T, Uyemura K, Nojyo Y, Tamamaki N (2000) Expression of L1 and TAG-1 in the corticospinal, callosal, and hippocampal commissural neurons in the developing rat telencephalon as revealed by retrograde and in situ hybridization double labeling. J Comp Neurol 417:275–288

Fujita S (1963) The matrix cell and cytogenesis in the developing central nervous system. J Comp Neurol 120:37–42

Fujita S (1966) Application of light and electron microscopic autoradiography in the study of cytogenesis of the forebrain. In: Hassler R, Stephan H (eds) Evolution of the Forebrain. Thieme, Stuttgart, pp 180–196

Fukuchi-Shimogori T, Grove EA (2001) Neocortex patterning by the secreted signaling molecule FGF8. Science 294:1071–1074

Gabreëls-Festen AAWM, Bolhuis PA, Hoogendijk JE, Valentijn LJ, Eshuis EJHM, Gabreëls FJM (1995) Charcot-Marie-Tooth disease type 1A: Morphological phenotype of the 17p duplication versus PMP22 point mutations. Acta Neuropathol (Berl) 90:645–649

Gabreëls-Festen AAWM, Hoogendijk JE, Meijerink PHS, Gabreëls FJM, Bolhuis PA, van Beersum S, Kulkens T, Nelis E, Jennekens FGI, de Visser M, et al. (1996) Two different types of nerve pathology in patients with different P0 mutations in Charcot-Marie-Tooth disease. Neurology 47:761–765

Gaiano N, Fishell G (2002) The role of Notch in promoting glial and neural stem cell fates. Annu Rev Neurosci 25:471–490

Gavalas A (2002) ArRAnging the hindbrain. Trends Neurosci 25:61–64

Gavalas A, Krumlauf R (2000) Retinoid signalling and hindbrain patterning. Curr Opin Genet Dev 10:380–386

Gavrieli Y, Sherman Y, Ben-Sasson SA (1992) Identification of programmed cell death in situ via specific labeling of nuclear DNA fragmentation. J Cell Biol 119:493–501

Gilbert SF (2000) Developmental Biology, 6th ed. Sinauer, Sunderland, MA

Gimlich RL, Cooke J (1983) Cell lineage and the induction of second nervous systems in amphibian development. Nature 306:471–473

Glinka A, Wu W, Delius H, Monaghan PA, Blumenstock C, Niehrs C (1998) Dickkopf-1 is a member of a new family of secreted proteins and functions in head induction. Nature 391:357–362

Globus JH, Kuhlenbeck H (1944) Subependymal cell plate (matrix) and its relation to brain tumors of ependymal type. J Neuropathol 3:1–35

Glover JC, Petursdottir G (1991) Regional specificity of developing reticulospinal, vestibulospinal, and vestibulo-ocular projections of the chicken embryo. J Neurobiol 22:353–376

Glücksmann A (1940) Development and differentiation of the tadpole eye. Br J Ophthalmol 24:153–178

Glücksmann A (1951) Cell deaths in normal vertebrate ontogeny. Biol Rev 26:59–86

Godement P, Mason CA (1993) Guidance of retinal fibers in the optic chiasm. Perspect Dev Neurobiol 1:217–225

Goodman CS (1982) Embryonic development of identified neurons in the grasshopper. In: Spitzer NC (ed) Neuronal Development. Plenum, New York, pp 171–212

Goodman CS (1996) Mechanisms and axon molecules that control growth cone guidance. Annu Rev Neurosci 19:341–377

Goodman CS, Bate M (1983) Neuronal development of the grasshopper. Trends Neurosci 4:163–169

Goodman CS, Doe CQ (1993) Embryonic development of the *Drosophila* central nervous system. In: Bate M, Martinez-Arias A (eds) The Development of *Drosophila*. Cold Spring Harbor Laboratory Press, Cold Spring Harbor, NY, pp 1131–1206

Goodman CS, Tessier-Lavigne M (1997) Molecular mechanisms of axon guidance and target recognition. In: Cowan WM, Jessell TM, Zipursky SL (eds) Molecular and Cellular Approaches to Neural Development. Oxford University Press, New York, pp 108–176

Graham A, Smith A (2001) Patterning the pharyngeal arches. BioEssays 23:54–61

Griffiths IR (1996) Myelin mutants: Model systems for the study of normal and abnormal myelination. BioEssays 18:789–797

Grunz H, Tacke L (1989) Neural differentiation of *Xenopus laevis* ectoderm takes place after disintegration and delayed reaggregation without inducer. Cell Diff Dev 28:211–217

Guan K-L, Rao Y (2003) Signalling mechanisms mediating neuronal responses to guidance cues. Nat Rev Neurosci 4:941–956

Guillery RW (1996) Why do albinos and other hypopigmented mutants lack normal binocular vision, and what else is abnormal in their central visual pathways. Eye 10:217–221

Guillery RW, Kaas JH (1971) A study of normal and congenitally abnormal retinogeniculate terminations in cats. J Comp Neurol 143:71–100

Guthrie S (1996) Patterning the hindbrain. Curr Opin Neurobiol 6:41–48

Guthrie S, Lumsden A (1991) Formation and regeneration of rhombomere boundaries in the developing chick hindbrain. Development 112:221–229

Hakem R, Hakem A, Duncan GS, Henderson JT, Woo M, Soengas MS, Elia A, de la Pompa JL, Kagi D, Khoo W, et al. (1998) Differential requirement for caspase 9 in apoptotic pathways *in vivo*. Cell 94:339–352

Hanemann CO, Müller HW (1998) Pathogenesis of Charcot-Marie-Tooth 1A (CMT1A) neuropathy. Trends Neurosci 21:282–286

Harding AE (1995) From the syndrome of Charcot, Marie and Tooth to disorders of peripheral myelin proteins. Brain 118:809–818

Harkmark W (1954) Cell migration from the rhombic lip to the inferior olive, the nucleus raphe and the pons. A morphological and experimental investigation on chick embryos. J Comp Neurol 100:115–210

Harland R, Gerhart J (1997) Formation and function of Spemann's organizer. Annu Rev Cell Dev Biol 13:611–667

Harrison RG (1910) The outgrowth of the nerve fiber as a mode of protoplasmic movements. J Exp Zool 9:787–846

Hartenstein V (1989) Early neurogenesis in Xenopus: The spatiotemporal pattern of proliferation and cell lineages in the embryonic spinal cord. Neuron 3:399–411

Hartenstein V, Nassif C, Lekven A (1998) Embryonic development of the *Drosophila* brain. II. Pattern of glial cells. J Comp Neurol 402:32–47

Hatten ME (1999) Central nervous system neuronal migration. Annu Rev Neurosci 22:511–539

Hatten ME, Heintz N (1995) Mechanisms of neural patterning and specification in the developing cerebellum. Annu Rev Neurosci 18:385–408

Hayasaka K, Himoro M, Sato W, Takada G, Uyemura K, Shimizu N, Bird TD, Conneally PM, Chance PF (1993) Charcot-Marie-Tooth neuropathy type 1B is associated with mutations of the myelin P0 gene. Nat Genet 5:31–34

Hayashi M (1924) Einige wichtige Tatsachen aus der ontogenetischen Entwicklung des menschlichen Kleinhirns. Dtsch Z Nervenheilkd 81:74–82

Haydar TF, Kuan C-Y, Flavell RA, Rakic P (1999) The role of cell death in regulating the size and shape of the mammalian forebrain. Cereb Cortex 9:621–626

He W, Ingraham C, Rising L, Goderie S, Temple S (2001) Multipotent stem cells from the basal forebrain contribute GABAergic neurons and oligodendrocytes to the cerebral cortex during development. J Neurosci 21:8854–8863

Hébert JM, Lin M, Partanen J, Rossant J, McConnell SK (2003) FGF signaling through FGFR1 is required for olfactory bulb morphogenesis. Development 130:1101–1111

Hemmati-Brivanlou A, Melton D (1992) A truncated activin receptor inhibits mesoderm induction and formation of axial structures in *Xenopus* embryos. Nature 359:609–614

Hemmati-Brivanlou A, Melton D (1997) Vertebrate embryonic cells will become nerve cells unless told otherwise. Cell 88:13–17

Henkemeyer M, Orioli D, Henderson JT, Saxton TM, Roder J, Pawson T, Klein R (1996) Nuk controls pathfinding of commissural axons in the mammalian central nervous system. Cell 86:35–46

Herrick CJ (1937) Development of the brain of Amblystoma in early functional stages. J Comp Neurol 67:381–422

Herrick CJ (1938) Development of the brain of Amblystoma during early swimming stages. J Comp Neurol 68:203–241

Hevner RF, Shi L, Justice N, Hsueh Y, Sheng M, Smiga S, Bulfone A, Goffinet AM, Campagnoni AT, Rubinstein JLR (2001) *Tbr1* regulates differentiation of the preplate and layer 6. Neuron 29:353–366

Hindges R, McLaughlin T, Geroud N, Henkemeyer M, O'Leary DDM (2002) EphB forward signaling controls directional branch extension and arborization required for dorsal-ventral retinotopic mapping. Neuron 35:475–487

Hinds JW, Ruffett TL (1971) Cell proliferation in the neural tube: An electron microscopic and Golgi analysis in the mouse cerebral vesicle. Z Zellforsch 115:226–264

Hirano M, Goldmann JE (1988) Gliogenesis in rat spinal cord: Evidence of origin of astrocytes and oligodendrocytes from radial precursors. J Neurosci Res 21:155–167

Hirose G, Jacobson M (1979) Clonal organization of the central nervous system of the frog. I. Clones stemming from individual blastomeres of the 16-cell and earlier stages. Dev Biol 71:191–202

Hirth F, Hartmann B, Reichert H (1998) Homeotic gene action in embryonic brain development of *Drosophila*. Development 125:1579–1589

His W (1888) Zur Geschichte des Gehirns sowie der centralen und peripherischen Nervenbahnen beim menschlichen Embryo. Abh Kön Sächs Ges Wiss Math Phys Kl 14:339–393

His W (1889) Die Neuroblasten und deren Entstehung im embryonalen Mark. Abh Kön Sächs Ges Wiss Math Phys Kl 15:313–372

His W (1890) Die Entwickelung des menschlichen Rautenhirns vom Ende des ersten bis zum Beginn des dritten Monats. I. Verlängertes Mark. Abh Kön Sächs Ges Wiss Math Phys Kl 17:1–74

Holt CE, Harris WA (1993) Position, guidance, and mapping in the developing visual system. J Neurobiol 24:1400–1422

Holtfreter J (1938) Differenzierungspotenzen isolierter Teile der Urodelengastrula. Roux Arch Entw Mech Org 138:522–656

Houart C, Westerfield M, Wilson SW (1998) A small population of anterior cells patterns the forebrain during zebrafish gastrulation. Nature 391:788–792

Houart C, Caneparo L, Heisenberg C-P, Take-Uchi M, Wilson SW (2002) Establishment of the telencephalon during gastrulation by local antagonism of Wnt signaling. Neuron 35:255–265

Hughes AF (1957) The development of the primary sensory system in *Xenopus laevis* (Daudin). J Anat (Lond) 91:323–338

Hughes AF (1961) Cell degeneration in the larval ventral horn of *Xenopus laevis* (Daudin). J Embryol Exp Morphol 9:269–284

Huppertz B, Frank H-G, Kaufmann P (1999) The apoptosis cascade–morphological and immunohistochemical methods for its visualization. Anat Embryol (Berl) 200:1–18

Hutson LD, Chien C-B (2002) Wiring the zebrafish: Axon guidance and synaptogenesis. Curr Opin Neurobiol 12:87–92

Inoue T, Nakamura S, Osumi N (2000) Fate mapping of the mouse prosencephalic neural plate. Dev Biol 219:373–383

Irving C, Mason I (2000) Signalling by FGF8 from the isthmus patterns anterior hindbrain and establishes the anterior limit of Hox gene expression. Development 127:177–186

Itoh K, Tang TL, Neel BG, Sokol SY (1995) Specific modulation of ectodermal cell fates in *Xenopus* embryos by glycogen synthase kinase. Development 121:3979–3988

Itoh K, Suzuki K, Bise K, Itoh H, Mehraein P, Weis S (2001) Apoptosis in the basal ganglia of the developing human nervous system. Acta Neuropathol (Berl) 101:92–100

Jacobs JR, Goodman CS (1989) Embryonic development of axon pathways in the *Drosophila* CNS. I. A glial scaffold appears before the first growth cones. J Neurosci 9:2402–2411

Jacobson M (1982) Origins of the nervous system in amphibians. In: Spitzer NC (ed) Neuronal Development. Plenum, New York, pp 45–99

Jacobson M (1983) Clonal organization of the central nervous system of the frog. III. Clones stemming from individual blastomeres of the 128-, 256-, and 512-cell stages. J Neurosci 3:1019–1038

Jacobson M (1985) Clonal analysis and cell lineages of the vertebrate central nervous system. Annu Rev Neurosci 8:71–102

Jacobson M (1991) Developmental Neurobiology, 3rd ed. Plenum, New York

Jacobson M, Hirose G (1981) Clonal organization of the central nervous system of the frog. II. Clones stemming from individual blastomeres of the 32- and 64-cell stages. J Neurosci 1:271–284

Jacobson M, Huang S (1985) Neurite outgrowth traced by means of horseradish peroxidase inherited from neuronal ancestral cells in frog embryos. Dev Biol 110:102–113

Jacobson M, Moody SA (1984) Quantitative lineage analysis of the frog's nervous system. I. Lineages of Rohon-Beard neurons and primary motoneurons. J Neurosci 4:1361–1369

Jacobson MD, Weil M, Raff RC (1996) Role of Ced-3/ICE family proteases in staurosporine-induced programmed cell death. J Cell Biol 133:1041–1051

Jacobson MD, Weil M, Raff MC (1997) Programmed cell death in animal development. Neuron 88:347–354

Jászai J, Reifers F, Picker A, Langenberg T, Brand M (2003) Isthmus-to-midbrain transformation in the absence of midbrain-hindbrain organizer activity. Development 130:6611–6623

Jessell TM, Sanes JR (2000) Development–The decade of the developing brain. Curr Opin Neurobiol 10:599–601

Johansson CB, Svensson M, Wallstedt L, Janson AM, Frisén J (1999) Neural stem cells in the adult human brain. Exp Cell Res 253:733–736

Johnson KG, Harris WA (2000) Connecting the eye with the brain: The formation of the retinotectal pathway. In: Fini ME (ed) Vertebrate Eye Development. Springer, Berlin Heidelberg New York, pp 157–177

Joosten EAJ, Gribnau AAM, Gorgels TGMF (1990) Immunoelectron microscopic localization of cell adhesion molecule L1 in developing rat pyramidal tract. Neuroscience 38:675–686

Joyner AL (1996) *Engrailed, Wnt* and *Pax* genes regulate midbrain-hindbrain development. Trends Genet 12:15–20

Joyner AL (2002) Establishment of anterior-posterior and dorsal-ventral pattern in the early central nervous system. In: Rossant J, Tam PPL (eds) Mouse Development. Patterning, morphogenesis, and organogenesis. Academic, San Diego, CA, pp 107–126

Kaas JH, Catania KC (2002) How do features of sensory representations develop? BioEssays 24:334–343

Kahle W (1951) Studien über die Matrixphasen und die örtliche Reifungsunterschiede im embryonalen menschlichen Gehirn. Dtsch Z Nervenheilkd 166:273–302

Källén B (1951a) Contributions to the ontogeny of the nuclei and the ventricular sulci in the vertebrate forebrain. Kgl Fysiogr Sällsk Lund Handl NF 62:Nr 3

Källén B (1951b) Embryological studies on the nuclei and their homologization in the vertebrate forebrain. Kgl Fysiogr Sällsk Lund Handl NF 62:Nr 5

Kamiguchi H, Hlavin ML, Yamasaki M, Lemmon V (1998) Adhesion molecules and inherited diseases of the human nervous system. Annu Rev Neurosci 21:97–125

Kaplan MS, Hinds JW (1977) Neurogenesis in the adult rat: Electron microscopic analysis of light radioautographs. Science 197:1092–1094

Kaprielian Z, Runko E, Imondi R (2001) Axon guidance at the midline choice point. Dev Dyn 221:154–181

Karlstrom RO, Trowe T, Bonhoeffer F (1997) Genetic analysis of axon guidance and mapping in the zebrafish. Trends Neurosci 20:3–8

Kay BK, Peng HB, eds (1991) Xenopus laevis: Practical Uses in Cell and Molecular Biology. Methods in Cell Biology, Vol 36. Academic, San Diego, CA

Keino-Masu K, Masu M, Hinck L, Leonardo ED, Chan SSY, Culotti JG, Tessier-Lavigne M (1996) Deleted in Colorectal Cancer (DCC) encodes a netrin receeotor. Cell 87:175–195

Keller R, Shih J, Wilson P (1991) Cell motility, control and function of convergence and extension during gastrulation of *Xenopus*. In: Keller R, Clark W, Griffin F (eds) Gastrulation: Movements, patterns, and molecules. Plenum, New York, pp 101–119

Keller R, Poznanski A, Elul T (1999) Experimental embryological methods for analysis of neural induction in the amphibian. In: Sharpe PI, Mason I (eds) Molecular Embryology: Methods and Protocols. Methods in Molecular Biology, Vol 97. Humana, Totowa, NJ, pp 351–392

Keller RE (1975) Vital dye mapping of the gastrula and neurula of *Xenopus laevis*. I. Prospective areas and morphogenetic movements of the superficial layer. Dev Biol 42:222–241

Keller RE (1976) Vital dye mapping of the gastrula and neurula of *Xenopus laevis*. II. Prospective areas and morphogenetic movements of the deep layers. Dev Biol 51:118–137

Kennedy TE, Serafini T, de la Torre JR, Tessier-Lavigne M (1994) Netrins are diffusible chemotrophic factors for commissural axons in the embryonic spinal cord. Cell 78:425–435

Kerr JF, Wyllie AH, Currie AR (1972) Apoptosis: A basic biological phenomenon with wide-ranging implications in tissue kinetics. Br J Cancer 26:239–257

Kerr JFR, Gobé GC, Winterford CM, Harman BV (1995) Anatomical methods in cell death. Meth Cell Biol 46:1–27

Kershman J (1938) The medulloblast and the medulloblastoma. Arch Neurol Psychiatr 40:937–967

Kessler DS (1999) Maternal signaling pathways and the regulation of cell fate. In: Moody SA (ed) Cell Lineage and Fate Determination. Academic, San Diego, CA, pp 323–340

Keyser AJM (1972) The development of the diencephalon of the Chinese hamster. Acta Anat (Basel) 83(Suppl 59):1–181

Kidd T, Brose K, Mitchell KJ, Fetter RD, Tessier-Lavigne M, Goodman CS (1998) Roundabout controls axon crossing of the CNS midline and defines a new subfamily of evolutionary conserved guidance receptors. Cell 92:205–215

Kiecker C, Niehrs C (2001) The role of prechordal mesendoderm in neural patterning. Curr Opin Neurobiol 11:27–33

Killackey HP, Rhoades RW, Bennett-Clarke CA (1995) The formation of a cortical somatotopic map. Trends Neurosci 18:402–407

Kimmel CB, Sepich DS, Trevarrow B (1988) Development of segmentation in zebrafish. Development 104(Suppl):197–207

Kimmel CB, Warga RM, Schilling TF (1990) Origin and organization of the zebrafish fate map. Development 108:581–594

Kimura C, Yoshinaga K, Tian E, Suzuki M, Aizawa S, Matsuo I (2000) Visceral endoderm mediates forebrain development by suppressing posteriorizing signals. Dev Biol 225:304–321

Kimura M, Inoko H, Katsuki M, Ando A, Sato T, Hirose T, Takashima T, Inayama S, Okano H, Takamatsu K, et al. (1985) Molecular genetic analysis of myelin-deficient mice: Shiverer mutant mice show deletion in gene(s) coding for myelin basic protein. J Neurochem 44:692–696

Kimura S, Shiota K (1996) Sequential changes of programmed cell death in developing fetal mouse limbs and its morphogenesis. J Morphol 229:337–346

Klugmann M, Schwab MH, Pühlhofer A, Schneider A, Zimmermann F, Griffiths IR, Nave K-A (1997) Assembly of CNS myelin in the absence of proteolipid protein. Neuron 19:205–218

Knöll B, Drescher U (2002) Ephrin-As as receptors in topographic projections. Trends Neurosci 25:145–149

Koeppen AH, Robitaille Y (2002) Pelizaeus-Merzbacher disease. J Neuropathol Exp Neurol 61:747–759

Koeppen AH, Ronca NA, Greenfield EA, Hans MB (1987) Defective biosynthesis of proteolipid protein in Pelizaeus-Merzbacher disease. Ann Neurol 21:159–170

Koeppen AH, Barron KD, Csiza CK, Greenfield EA (1988) Comparative immunocytochemistry of Pelizaeus-Merzbacher disease, the jimpy mouse, and the myelin-deficient rat. J Neurol Sci 84:315–327

Kolodkin AL (1996) Growth cones and the cues that repel them. Trends Neurosci 19:507–513

Kriegstein AR, Noctor SC (2004) Patterns of neuronal migration in the embryonic cortex. Trends Neurosci 27:392–399

Krumlauf R (1994) *Hox* genes in vertebrate development. Cell 78:191–201

Kuan C-Y, Yang DD, Samanta Roy DR, Davis RJ, Rakic P, Flavell RA (1999) Jnk1 and Jnk2 protein kinases are required for regional specific apoptosis during early brain development. Neuron 22:667–676

Kuan C-Y, Roth KA, Flavell RA, Rakic P (2000) Mechanisms of programmed cell death in the developing brain. Trends Neurosci 23:291–297

Kuemerle B, Zanjani H, Joyner A, Herrup K (1997) Pattern deformities and cell loss in *Engrailed-2* mutant mice suggest two separate patterning events during cerebellar development. J Neurosci 17:7881–7889

Kuida K, Zheng TS, Na S, Kuan C-Y, Yang D, Karasuyama H, Rakic P, Flavell RA (1996) Decreased apoptosis in the brain and premature lethality in CPP32-deficient mice. Nature 384:368–372

Kuida K, Haydar TF, Kuan C-Y, Gu Y, Taya C, Karasuyama H, Su MS, Rakic P, Flavell RA (1998) Reduced apoptosis and cytochrome c-mediated caspase activation in mice lacking caspase 9. Cell 94:325–337

Lamborghini JE (1987) Disappearance of Rohon-Beard neurons from the spinal cord of larval *Xenopus laevis*. J Comp Neurol 264:47–55

Lance-Jones C, Landmesser L (1981a) Pathway selection by chick lumbosacral motoneurones during normal development. Proc R Soc Lond B 214:1–18

Lance-Jones C, Landmesser L (1981b) Pathway selection by embryonic chick motoneurones in an experimentally altered environment. Proc R Soc Lond B 214:19–52

Landmesser LT (1978) The development of motor projection patterns in the chick hind limb. J Physiol (Lond) 284:391–414

Lawrence PA (1992) The Making of a Fly. Blackwell, Oxford

Leber SM, Sanes JR (1995) Migratory paths of neurons and glia in the embryonic chick spinal cord. J Neurosci 15:1236–1248

Le Douarin N (1973) A biological cell labeling technique and its use in experimental embryology. Dev Biol 30:217–222

Le Douarin NM, Kalcheim C (1999) The Neural Crest, 2nd ed. Cambridge University Press, Cambridge

Lee JC, Mayer-Proschel M, Rao MS (2000) Gliogenesis in the central nervous system. Glia 30:105–121

Lee KJ, Jessell TM (1999) The specification of dorsal fates in the vertebrate central nervous system. Annu Rev Neurosci 22:261–294

Lemke G (1993) The molecular genetics of myelination: An update. Glia 7:263–271

Lemke G (2001) Glial control of neuronal development. Annu Rev Neurosci 24:87–105

Levitt P, Rakic P (1980) Immunoperoxidase localization of glial fibrillary acidic protein in radial glial cells and astrocytes of the developing rhesus monkey brain. J Comp Neurol 193:815–840

Lewis PD, Lai M (1974) Cell generation in the subependymal layer of the rat brain during the early postnatal period. Brain Res 77:520–525

Leyns L, Bouwmeester T, Kim S-H, Piccolo S, De Robertis EM (1997) Frzβ-1 is a secreted antagonist of Wnt signaling expressed in the Spemann organizer. Cell 88:747–756

Liem KF, Tremml G, Roelink H, Jessell TM (1995) Dorsal differentiation of neural plate cells induced by BMP-mediated signals from epidermal ectoderm. Cell 82:969–979

Litingtung Y, Chiang C (2000) Control of Shh activity and signaling in the neural tube. Dev Dyn 219:143–154

Liu A, Joyner AL (2001) Early anterior/posterior patterning of the midbrain and cerebellum. Annu Rev Neurosci 24:869–896

Lo AC, Houenou LJ, Oppenheim RW (1995) Apoptosis in the nervous system: Morphological features, methods, pathology, and prevention. Arch Histol Cytol 58:139–149

Lois C, Alvarez-Buylla A (1994) Long-distance neuronal migration in the adult mammalian brain. Science 264:1145–1148

Lois C, Garcia-Verdugo JM, Alvarez-Buylla A (1996) Chain migration of neuronal precursors. Science 271:978–981

López-Bendito G, Molnár Z (2003) Thalamocortical development: How are we going to get there? Nat Rev Neurosci 4:276–289

Lu CC, Brennan J, Robertson EJ (2001) From fertilization to gastrulation: Axis formation in the mouse embryo. Curr Opin Genet Dev 11:384–392

Lumsden A (1990) The cellular basis of segmentation in the developing hindbrain. Trends Neurosci 13:329–335

Lumsden A (2004) Segmentation and compartition in the early avian hindbrain. Mech Dev 121:1081–1088

Lumsden A, Keynes R (1989) Segmental patterns of neuronal development in the chick hindbrain. Nature 337:424–428

Lumsden A, Krumlauf R (1996) Patterning the vertebrate neuraxis. Science 274:1109–1115

Lumsden A, Sprawson N, Graham A (1991) Segmental origin and migration of neural crest cells in the hindbrain region of a chick embryo. Development 113:1281–1291

Luskin MB (1993) Restricted proliferation and migration of postnatally generated neurons derived from the forebrain subventricular zone. Neuron 11:173–189

Maden M (2002) Retinoid signalling in the development of the central nervous system. Nat Rev Neurosci 3:843–853

Magini G (1888) Ulteriori richerche istologiche sul cervello fetale. Rend R Accad Lincei 4:760–763 (quoted from Fishell and Kriegstein 2003)

Mangold O (1933) Über die Induktionsfähigkeit der verschiedenen Bezirke der Neurula von Urodelen. Naturwissenschaften 21:761–766

Mann F, Ray S, Harris W, Holt C (2002) Topographic mapping in dorsoventral axis of Xenopus retinotectal system depends on signaling through ephrin-B ligands. Neuron 35:461–473

Marín F, Puelles L (1994) Patterning of the embryonic avian midbrain after experimental inversions: A polarizing activity from the isthmus. Dev Biol 163:19–37

Marín O, Rubinstein JLR (2001) A long, remarkable journey: Tangential migration in the telencephalon. Nat Rev Neurosci 2:780–790

Marín O, Rubinstein JLR (2002) Patterning, regionalization, and cell differentiation in the forebrain. In: Rossant J, Tam PPL (eds) Mouse Development. Patterning, morphogenesis, and organogenesis. Academic, San Diego, CA, pp 75–106

Marín O, Baker J, Puelles L, Rubinstein JLR (2002) Patterning of the basal telencephalon and hypothalamus is essential for guidance of cortical projections. Development 129:761–773

Marti E, Bovolenta P (2002) Sonic hedgehog in cell development: One signal, multiple outputs. Trends Neurosci 25:89–96

Martínez S, Wassef M, Alvarado-Mallart RM (1991) Induction of a mesencephalic phenotype in the 2-day-old chick prosencephalon is preceded by the early expression of the homeobox gene En. Neuron 6:971–981

Martínez S, Marín F, Nieto MA, Puelles L (1995) Induction of ectopic engrailed expression and fate change in avian rhombomeres: Intersegmental boundaries as barriers. Mech Dev 51:289–303

Mason CA, Sretavan DW (1997) Glia, neurons, and axon pathfinding during optic chiasm development. Curr Opin Neurobiol 7:647–653

Mason CA, Marcus RC, Wang LC (1996) Retinal axon divergence in the optic chiasm: Growth cone behaviors and signalling cells. Prog Brain Res 108:95–107

Mastick GS, Fan C-M, Tessier-Lavigne M, Serbedzija GN, McMahon AP, Easter SS Jr (1996) Early detection of neuromeres in Wnt-1–/– mutant mice: Evaluation by morphological and molecular markers. J Comp Neurol 374:246–258

McConnell SK (1995) Strategies for the generation of neuronal diversity in the developing central nervous system. J Neurosci 15:6987–6998

McConnell SK, Ghosh A, Shatz CJ (1989) Subplate neurons pioneer the first axon pathway from the cerebral cortex. Science 245:978–982

McConnell SK, Ghosh A, Shatz CJ (1994) Subplate pioneers and the formation of descending connections from cerebral cortex. J Neurosci 14:1892–1907

McLaughlin T, Hindges R, O'Leary DDM (2003) Regulation of axial patterning of the retina and its topographic mapping in the brain. Curr Opin Neurobiol 13:57–69

McMahon AP, Joyner AL, Bradley A, McMahon JA (1992) The midbrain-hindbrain phenotype of Wnt-1-/Wnt-1- mice results from stepwise deletion of engrailed-expressing cells by 9.5 days postcoitum. Cell 69:581–595

Mehler MF, Mabie PC, Zhang D, Kessler JA (1997) Bone morphogenetic proteins in the nervous system. Trends Neurosci 20:309–317

Meller K, Tetzlaff W (1975) Neuronal migration during the early development of the cerebral cortex – A scanning electron microscopic study. Cell Tissue Res 163:313–325

Métin C, Godement P (1996) The ganglionic eminence may be an intermediate target for corticofugal and thalamocortical axons. J Neurosci 16:3219–3235

Métin C, Deléglise D, Serafini T, Kennedy TE, Tessier-Lavigne M (1997) A role for netrin-1 in the guidance of cortical effenets. Development 12:5063–5074

Metzstein MM, Stanfield GM, Horvitz HR (1998) Genetics of programmed cell death in C. elegans: Past, present and future. Trends Genet 14:410–414

Millen KJ, Wurst W, Herrup K, Joyner AL (1994) Abnormal embryonic cerebellar development and patterning of postnatal foliation in two mouse Engrailed-2 mutants. Development 120:695–706

Miller RH (1996) Oligodendrocyte origins. Trends Neurosci 19: 92–96

Miller RH (2002) Regulation of oligodendrocyte development in the vertebrate CNS. Prog Neurobiol 67:451–467

Miller RH, Ono K (1998) Morphological analysis of the early stages of oligodendrocyte development in the vertebrate central nervous system. Microsc Res Tech 41:441–453

Misson J-P, Austin CP, Takahashi T, Cepko CL, Caviness VS Jr (1991) The alignment of migrating neural cells in relation to the murine neopallial radial glial fiber system. Cereb Cortex 1:221–229

Miyata T, Kawaguchi A, Okano H, Ogawa M (2001) Asymmetric inheritance of radial glial fibers by cortical neurons. Neuron 31:727–741

Moens CB, Prince VE (2002) Constructing the hindbrain: Insights from the zebrafish. Dev Dyn 224:1–17

Molnár Z, Blakemore C (1995) How do thalamic axons find their way to the cortex? Trends Neurosci 18:389–397

Molnár Z, Blakemore C (1999) Development of signals influencing the growth and termination of thalamocortical axons in organotypic culture. Exp Neurol 156:363–393

Molnár Z, Cordery P (1999) Connections between cells of the internal capsule, thalamus, and cerebral cortex in embryonic rat. J Comp Neurol 413:1–25

Molnár Z, Hannan AJ (2000) Development of thalamocortical projections in normal and mutant mice. In: Goffinet AM, Rakic P (eds) Mouse Brain Development. Springer, Berlin Heidelberg New York, pp 293–332

Molnár Z, Adams R, Blakemore C (1998) Mechanisms underlying the early establishment of thalamocortical connections in the rat. J Neurosci 18:5723–5745

Moody SA (1987a) Fates of the blastomeres of the 16-cell *Xenopus* embryo. Dev Biol 119:560–578

Moody SA (1987b) Fates of the blastomeres of the 32-cell *Xenopus embryo*. Dev Biol 122:300–319

Moody SA (1989) Quantitative lineage analysis of the origin of frog primary motor and sensory neurons from cleavage stage blastomeres. J Neurosci 9:2919–2930

Moody SA, Kline MJ (1990) Segregation of fate during cleavage of frog (*Xenopus laevis*) blastomeres. Anat Embryol (Berl) 182: 347–362

Morest DK (1970) A study of neurogenesis in the forebrain of opossum pouch young. Z Anat Entw Gesch 130:265–305

Mori C, Nakamura N, Okamoto Y, Osawa M, Shiota K (1994) Cytochemical identification of programmed cell death in the fusing fetal mouse palate by specific labelling of DNA fragmentation. Anat Embryol (Berl) 190:21–28

Mori C, Nakamura N, Kimura S, Irie H, Takigawa T, Shiota K (1995) Programmed cell death in the interdigital tissue of fetal mouse limb is apoptosis with DNA fragmentation. Anat Rec 242: 103–110

Morriss-Kay GM, Ward SJ (1999) Retinoids and mammalian development. Int Rev Cytol 188:73–131

Mukhopadhyay M, Shtrom S, Rodriguez-Esteban C, Chen L, Tsukui T, Gomer L, Dorward DW, Glinka A, Grinsberg A, Huang SP, et al. (2001) Dickkopf1 is required for embryonic head induction and limb morphogenesis in the mouse. Dev Cell 1:423–434

Mullen RJ, Hamre KM, Goldowitz D (1997) Cerebellar mutant mice and chimeras revisited. Persp Dev Neurobiol 5:43–55

Muñoz-Sanjuán I, Hemmati-Brivanlou AH (2002) Neural induction, the default model and embryonic stem cells. Nat Neurosci Rev 3:271–280

Nadararajah B, Alifragis P, Wong RO, Parnavelas JG (2002) Ventricle-directed migration in the developing cerebral cortex. A novel method of labeling and characterizing migrating neurons in the developing central nervous system. Nat Neurosci 5:218–224

Nakagawa S, Brennan C, Johnson KG, Shewan D, Harris WA, Holt CE (2000) Ephrin-B regulates the ipsilateral routing of retinal axons at the optic chiasm. Neuron 25:599–610

Nakamura H (2001) Regionalization of the optic tectum: Combinations of gene expression that define the tectum. Trends Neurosci 24:32–39

Nassif C, Noveen A, Hartenstein V (1998) Embryonic development of the *Drosophila* brain. J Comp Neurol 402:10–31

Nave K-A, Bloom FE, Milner RJ (1987) A single nucleotide difference in the gene for myelin proteolipid protein defines the *jimpy* mutation in the mouse. J Neurochem 49:1873–1877

Nelis E, Haites N, Van Broeckhoven C (1999) Mutations in the peripheral myelin genes and associated genes in inherited peripheral neuropathies. Hum Mut 13:1–28

Nery S, Wichterle H, Fishell G (2001) Sonic hedgehog contributes to oligodendrocyte specification in the mammalian forebrain. Development 128:527–540

Nieto MA, Gilardi HP, Charnay P, Wilkinson DG (1992) A receptor protein tyrosine kinase implicated in the segmental patterning of the hindbrain and mesoderm. Development 116: 1137–1150

Nieuwenhuys R (1998a) Morphogenesis and general structure. In: Nieuwenhuys R, ten Donkelaar HJ, Nicholson C The Central Nervous System of Vertebrates. Springer, Berlin Heidelberg New York, pp 159–228

Nieuwenhuys R (1998b) Histogenesis. In: Nieuwenhuys R, ten Donkelaar HJ, Nicholson C The Central Nervous System of Vertebrates. Springer, Berlin Heidelberg New York, pp 229–271

Nieuwkoop PD (1973) The "organisation center" of the amphibian embryo: Its origin, spatial organisation and morphogenetic action. Adv Morphogenet 10:1–310

Nieuwkoop PD (1977) Origin and establishment of embryonic polar axes in amphibian development. Curr Top Dev Biol 11:115–132

Nieuwkoop PD, Albers B (1990) The role of competence in the craniocaudal segregation of the central nervous system. Dev Growth Diff 32:23–31

Nieuwkoop PD, Nigtevecht GV (1954) Neural activation and transformation in explants of competent ectoderm under the influence of fragments of anterior notochord in urodeles. J Embryol Exp Morphol 2:175–193

Noble M, Murray K, Stroobant P, Waterfield MD, Riddle P (1988) Platelet-derived growth factor promotes division and motility and inhibits premature differentiation of the oligodendrocyte-type-2 astrocyte progenitor cell. Nature 333:550–562

Noctor SC, Flint AC, Weissman TA, Dammerman RS, Kriegstein AR (2001) Neurons derived from radial glial cells establish radial units in neocortex. Nature 409:714–720

Nüsslein-Volhard C, Fronhöfer C, Lehmann R (1987) Determination of anteroposterior polarity in *Drosophila*. Science 238:1675–1681

O'Leary DDM, Koester SE (1993) Development of projection neuron types, axon pathways, and patterned projections of the mammalian cortex. Neuron 10:991–1006

O'Leary DDM, Nakagawa Y (2002) Patterning centers, regulatory genes and extrinsic mechanisms controlling arealization of the neocortex. Curr Opin Neurobiol 12:14–25

O'Leary DDM, Bicknese AR, de Carlos JA, Heffner CD, Koester SE, Kutka LJ, Terashima T (1990) Target selection by cortical axons: Alternative mechanisms to establish axonal connections in the developing brain. Cold Spring Harb Symp Quant Biol 55:453–480

Olivier C, Cobos I, Perez Villegas EM, Spassky N, Zalc B, Martinez S, Thomas J-L (2001) Monofocal origin of telencephalic oligodendrocytes in the anterior entopeduncular area of the chick embryo. Development 128:1757–1769

Ono K, Kawamura K (1989) Migration of immature neurons along tangentially oriented fibers in the subpial part of the fetal mouse medulla oblongata. Exp Brain Res 78:290–300

Ono K, Kawamura K (1990) Mode of neuronal migration of the pontine stream in fetal mice. Anat Embryol (Berl) 182:11–19

Ono K, Bansal R, Payne J, Rutishauser U, Miller RH (1995) Early development and dispersal of oligodendrocyte precursors in the embryonic chick spinal cord. Development 121:1743–1754

Oppenheim RW (1991) Cell death during development of the nervous system. Annu Rev Neurosci 14:453–501

Oppenheimer JM (1936) Structures developed in amphibians by implantation of living fish organizer. Proc Soc Exp Biol Med 34:461–463

Orioli D, Klein R (1997) The Eph receptor family: Axonal guidance by contact repulsion. Trends Genet 13:354–359

O'Rourke NA (1996) Neuronal chain gangs: Homotypic contacts support migration into the olfactory bulb. Neuron 16:1061–1064

Palka J (1982) Genetic manipulation of sensory pathways in Drosophila. In: Spitzer NC (ed) Neuronal Development. Plenum, New York, pp 121–170

Papalopulu N, Clarke JDW, Bradlet D, Wilkinson D, Krumlauf R, Holder N (1991) Retinoic acid causes abnormal development and segmental patterning of the anterior hindbrain in Xenopus embryos. Development 113:1145–1158

Pardee AB, Dubrow R, Hamlin JL, Kletzien RF (1978) Animal cell cycle. Annu Rev Biochem 47:715–750

Parnavelas JG, Nadarajah B (2001) Radial glial cells: Are they really glia? Neuron 31:881–884

Pasini A, Wilkinson DG (2002) Stabilizing the regionalisation of the developing vertebrate central nervous system. BioEssays 24:427–438

Pasterkamp RJ, Kolodkin AL (2003) Semaphorin junction: Making tracks towards neural connectivity. Curr Opin Neurobiol 13:79–89

Pera E, Kessel M (1997) Patterning of the chick forebrain anlage by the prechordal plate. Development 124:4153–4162

Perea-Gómez A, Lawson KA, Rhinn M, Zakin L, Brûlet P, Mazan S, Ang SL (2001) Otx2 is required for visceral endoderm movement and for the restriction of posteriorizing signals in the epiblast of the mouse embryo. Development 128:753–765

Placzek M (1995) The role of the notochord and floor plate in inductive interactions. Curr Opin Genet Dev 5:499–506

Plump AS, Erskine L, Sabatier C, Brose K, Epstein CJ, Goodman CS, Mason CA, Tessier-Lavigne M (2002) Slit1 and Slit2 cooperate to prevent premature midline crossing of retinal axons in the mouse visual system. Neuron 33:219–232

Poliak S, Peles E (2003) The local differentiation of myelinated axons at nodes of Ranvier. Nat Rev Neurosci 4:968–980

Polleux F, Giger RJ, Ginty DD, Kolodkin AL, Ghosh A (1998) Patterning of cortical efferent projections by semaphorin-neuropilin interactions. Science 282:1904–1906

Postlethwait JH, Talbot W (1997) Zebrafish genomics: From mutants to genes. Trends Genet 13:183–190

Prestige MC (1965) Cell turnover in the spinal ganglia of Xenopus laevis tadpoles. J Embryol Exp Morphol 13:63–72

Price DJ, Willshaw DJ (2000) Mechanisms of Cortical Development. Monographs of the Physiological Society, Vol 48. Oxford University Press, Oxford

Pringle NP, Yu W, Guthrie S, Roelink H, Lumsden A, Peterson AC, Richardson WD (1996) Determination of neuroepithelial cell fate: Induction of the oligodendrocyte lineage by ventral midline cells and sonic hedgehog. Dev Biol 177:30–42

Pringle NP, Yu W-P, Howell M, Colvin JS, Ornitz DM, Richardson WD (2003) Fgfr3 expression by astrocytes and their precursors: Evidence that astrocytes and oligodendrocytes originate in distinct neuroepithelial domains. Development 130:93–102

Puelles L (1995) A segmental morphological paradigm for understanding vertebrate forebrains. Brain Behav Evol 46:319–337

Puelles L, Rubinstein JLR (1993) Expression patterns of homeobox and other putative regulatory genes in the embryonic forebrain suggests a neuromeric organization. Trends Neurosci 16:472–479

Puelles L, Rubinstein JLR (2003) Forebrain gene expression domains and the evolving prosomeric model. Trends Neurosci 26:469–476

Puelles L, Kuwana E, Puelles E, Bulfone A, Shimamura K, Keleher J, Smiga S, Rubinstein JLR (2000) Pallial and subpallial derivatives in the embryonic chick and mouse telencephalon, traced by the expression of the genes Dlx-2, Emx-1, Nkx-2.1, Pax-6, and Tbr-1. J Comp Neurol 424:409–438

Raff MC (1989) Glial cell diversification in the rat optic nerve. Science 243:1450–1455

Raible F, Brand M (2004) Divide et Impera – the midbrain-hindbrain boundary and its organizer. Trends Neurosci 27:727–734

Rakic P (1971) Neuron-glia relationship during granule cell migration in developing cerebellar cortex. A Golgi and electronmicroscopic study in Macacus rhesus. J Comp Neurol 141:283–312

Rakic P (1972) Mode of cell migration to the superficial layers of fetal monkey neocortex. J Comp Neurol 145:61–84

Rakic P (1974) Neurons in rhesus monkey visual cortex: Systemic relation between time of origin and eventual disposition. Science 183:425–427

Rakic P (1976) Prenatal genesis of connections subserving ocular dominance in the rhesus monkey. Nature 261:467–471

Rakic P (1981) Neuronal-glial interaction during brain development. Trends Neurosci 4:184–187

Rakic P (1990) Principles of neural cell migration. Experientia 46:883–891

Ramón y Cajal S (1890) A quelle époque apparaissent les expansions des cellules nerveuses de la moëlle épinière du poulet? Anat Anz 5:631–639

Ramón y Cajal S (1909) Histologie du Système Nerveux de l'Homme et des Vertébrés, Vol I. Masson, Paris

Raper JA (2000) Semaphorins and their receptors in vertebrates and invertebrates. Curr Opin Neurobiol 10:88–94

Readhead C, Popko B, Takahashi N, Shine HD, Saavedra RA, Sidman RL, Hood L (1987) Expression of a myelin basic protein gene in transgenic shiverer mice: Correction of the dysmyelinating phenotype. Cell 48:703–712

Reichert H, Boyan G (1997) Building a brain: Developmental insights in insects. Trends Neurosci 20:258–264

Reifers F, Böhli H, Walsh EC, Crossley PH, Stainier DYR, Brand M (1998) Fgf8 is mutated in zebrafish acerebellar (ace) mutanys and is required for maintenance of midbrain-hindbrain boundary development and somitogenesis. Development 125:2381–2395

Reim G, Brand M (2002) spiel-ohne-grenzen/pou2 mediates regional competence to respond to Fgf8 during zebrafish early neural development. Development 129:917–933

Rhinn M, Brand M (2001) The midbrain-hindbrain organizer. Curr Opin Neurobiol 11:34–42

Rice DS, Curran T (1999) Mutant mice with scrambled brains: Understanding the signaling pathways that control cell positioning in the CNS. Genes Dev 13:2758–2773

Rice FL, Van der Loos H (1977) Development of the barrels and barrel fields in the somatosensory cortex of the mouse. J Comp Neurol 171:545–560

Richards LJ, Koester SE, Tuttle R, O'Leary DDM (1997) Directed growth of early cortical axons is influenced by a chemoattractant released from an intermediate target. J Neurosci 17:2445–2458

Rijli FM, Gavalas A, Chambon P (1998) Segmentation and specification in the branchial region of the head: The role of the *Hox* selector genes. Int J Dev Biol 42:393–401

Roelink H, Augsburger A, Heemskerk J, Korzh V, Norlin S, Ruiz i Altaba A, Tanabe Y, Placzek M, Edlund T, Jessell TM, Dodd J (1994) Floor plate and motor neuron induction by *vhh-1*, a vertebrate homolog of *hedgehog* expressed by the notochord. Cell 76:761–775

Roelink H, Porter JA, Chiang C, Tanabe Y, Chang DT, Beachy PA, Jessell TM (1995) Floor plate and motor neuron induction by different concentrations of the amino-terminal cleavage product of sonic hedgehog autoproteolysis. Cell 81:445–455

Romanenko MJ, Rola R, Fike JR, Szele FG, Dizon MLV, Felling RJ, Brazel CY, Levison SW (2004) Role of the mammalian subventricular zone in cell replacement after brain injury. Prog Neurobiol 74:77–99

Rossant J, Tam PPL, eds (2002) Mouse Development. Patterning, Morphogenesis, and Organogenesis. Academic, San Diego, CA

Rowitch DH, Lu QR, Kessaris N, Richardson WD (2002) An 'oligarchy' rules neural development. Trends Neurosci 25:417–422

Rubinstein JLR, Beachy PA (1998) Patterning of the embryonic forebrain. Curr Opin Neurobiol 8:18–26

Rubinstein JLR, Shimamura K, Martínez S, Puelles L (1998) Regionalization of the prosencephalic neural plate. Annu Rev Neurosci 21:445–477

Ruggieri PM (1997) Metabolic and neurodegenerative disorders and disorders with abnormal myelination. In: Ball WS (ed) Pediatric Neuroradiology. Lippincott, Philadelphia, PA, pp 175–237

Sabatier C, Plump AS, Ma L, Brose K, Tamada A, Murakami F, Lee EY-HP, Tessier-Lavigne M (2004) The divergent Robo family protein Rig-1/Robo3 is a negative regulator of Slit responsiveness required for midline crossing by commissural axons. Cell 117:157–169

Salvesen GS, Dixit VM (1997) Caspases: Intracellular signaling by proteolysis. Cell 91:443–446

Sanai N, Tramontin AD, Quinones-Hinojosa A, Barbaro NM, Gupta N, Kunwar S, Lawton MT, McDermott MW, Parsa AT, Manuel-Garcia Verdugo J, et al. (2004) Unique astrocyte ribbon in adult human brain contains neural stem cells but lacks chain migration. Nature 427:740–744

Sanes JR (1989) Analysing cell lineage with a recombinant retrovirus. Trends Neurosci 12:21–28

Sanes JR, Jessell TM (2000) Guidance of axons to their targets. In: Kandel E, Schwartz JH, Jessell TM (eds) Principles of Neural Science, 4th ed. McGraw-Hill, New York, pp 1063–1086

Sanes JR, Yamagata M (1999) Formation of lamina-specific synaptic connections. Curr Opin Neurobiol 9:79–87

Sauer F (1935a) Mitosis in the neural tube. J Comp Neurol 62:377–407

Sauer F (1935b) Cellular structure of the neural tube. J Comp Neurol 63:13–23

Saxén L (1989) Neural induction. Int J Dev Biol 33:21–48

Saxén L, Toivonen S (1962) Primary Embryonic Induction. Logos, London

Schaper A (1897a) Die frühesten Differenzierungsvorgänge im Centralnervensystem. Arch Entw-Mech Organ 5:81–132

Schaper A (1897b) The earliest differentiation in the central nervous system of vertebrates. Science 5:430–431

Schier AF (1997) Genetics of neural development in zebrafish. Curr Opin Neurobiol 7:119–126

Schier AF (2001) Axis formation and patterning in zebrafish. Curr Opin Genet Dev 11:393–404

Schier AF, Neuhaus SC, Harvey M, Malicki J, Solnica-Krezel L, Stainier DY, Zwartkruis F, Abdelilah S, Stemple DL, Rangini Z, et al. (1996) Mutations affecting the development of the embryonic zebrafish brain. Development 123:165–178

Schmechel DE, Rakic P (1979) A Golgi study of radial glial cells in developing monkey telencephalon: Morphogenesis and transformation into astrocytes. Anat Embryol (Berl) 156:115–152

Schuurmans C, Guillemot F (2002) Molecular mechanisms underlying cell fate specification in the developing telencephalon. Curr Opin Neurobiol 12:26–34

Schwab ME, Caroni P (1988) Oligodendrocytes and CNS myelin are non-permissive substrates for neurite growth and fibroblast spreading *in vitro*. J Neurosci 8:2381–2393

Seeger M, Tear G, Ferres-Marco D, Goodman CS (1993) Mutations affecting growth cone guidance in *Drosophila*: Genes necessary for guidance toward or away from the midline. Neuron 10:409–426

Serafini T, Kennedy TE, Galko MJ, Mirzayan C, Jessell TM, Tessier-Lavigne M (1994) The netrins define a family of axon outgrowth-promoting proteins homologous to C. elegans UNC-6. Cell 78:409–424

Serafini T, Colamarino SA, Leonardo ED, Wang H, Beddington R, Skarnes WC, Tessier-Lavigne M (1996) Netrin-1 is required for commissural axon guidance in the developing vertebrate nervous system. Cell 87:1001–1014

Shanmugalingam S, Houart C, Picker A, Reifers F, Macdonald R, Barth A, Griffin K, Brandt M, Wilson SW (2000) Ace/Fgf8 is required for forebrain commissure formation and patterning of the telencephalon. Development 127:2549–2561

Sharpe CR (1991) Retinoic acid can mimic endogenous signals involved in transformation of the *Xenopus* nervous system. Neuron 7:239–247

Shimamura K, Rubinstein JLR (1997) Inductive interactions direct early regionalization of the mouse forebrain. Development 124:2709–2718

Shimamura K, Hartigan DJ, Martinez S, Puelles L, Rubinstein JLR (1995) Longitudinal organization of the anterior neural plate and neural tube. Development 121:3923–3933

Shu T, Richards LJ (2001) Cortical axon guidance by the glial wedge during the development of the corpus callosum. J Neurosci 21:2749–2758

Sidman RL, Rakic P (1973) Neuronal migration, with special reference to developing human brain. Brain Res 62:1–35

Silver J (1993) Glia-neuron interactions at the midline of the developing mammalian brain and spinal cord. Perspect Dev Neurobiol 1:227–236

Skromne I, Stern CD (2001) Interactions between Wnt and Vg1 signalling pathways initiate primitive streak formation in the chick embryo. Development 128:2915–2927

Smart IHM (1961) The subependymal layer of the mouse brain and its cellular production as shown by radioautography after thymidine-H^3 injection. J Comp Neurol 116:325–349

Snell JD, ed (1941) Biology of the Laboratory Mouse. Dover, New York

Spassky N, Goujet-Zalc C, Parmantier E, Olivier C, Martinez S, Ivanova A, Ikenaka K, Macklin W, Cerruti I, Zalc B, Thomas J-L (1998) Multiple restricted origins of oligodendrocytes. J Neurosci 18:8331–8343

Spassky N, Heydon K, Mangatal A, Jankovski A, Olivier C, Queraud-Lesaux F, Goujet-Zalc C, Thomas J-L, Zalc B (2001) Sonic hedgehog-dependent emergence of oligodendrocytes in the telencephalon: Evidence for a source of oligodendrocytes in the olfactory bulb that is independent of PDGF2α signaling. Development 128:4993–5004

Spemann H (1921) Die Erzeugung tierischer Chimären durch heteroplastische embryonale Transplantation zwischen *Triton cristatus* und *Triton taeniatus*. Roux Arch Entw Mech Org 48:533–570

Spemann H (1936) Experimentelle Beiträge zu einer Theorie der Entwicklung. Springer, Berlin Heidelberg New York

Spemann H (1938) Embryonic Development and Induction. Yale University Press, New Haven, CT

Spemann H, Mangold H (1924) Über Induktion von Embryonalanlagen durch Implantation artfremder Organisatoren. Roux Arch Entw Mech Org 100:599–638

Sperry RW (1943) Effects of 180 degree rotation of the retinal fields on visuomotor coordination. J Exp Zool 92:263–279

Sperry RW (1963) Chemoaffinity in the orderly growth of nerve fibre patterns and connections. Proc Natl Acad Sci USA 50:703–710

Spreafico R, Frassoni C, Arcelli P, Selvaggio M, de Biasi S (1995) In situ labeling of apoptotic cell death in the cerebral cortex and thalamus of rats during development. J Comp Neurol 363:281–295

Sretavan DW (1993) Pathfinding at the mammalian optic chiasm. Curr Opin Neurobiol 3:45–52

Stein E, Tessier-Lavigne M (2001) Hierarchical organization of guidance receptors: Silencing of netrin attraction by Slit through a Robo/DCC receptor complex. Science 291:1928–1938

Stent GS, Weisblat DA (1985) Cell lineage in the development of invertebrate nervous systems. Annu Rev Neurosci 8:45–70

Stern CD (2001) Initial patterning of the central nervous system: How many organizers? Nat Rev Neurosci 2:92–98

Stern CD (2002) Induction and initial patterning of the nervous system – the chick embryo enters the scene. Curr Opin Genet Dev 12:447–451

Stoeckli ET, Landmesser LT (1995) Axonin-1, NrCAM, and NgCAM play different roles in the *in vivo* guidance of chick commissural neurons. Neuron 14:1165–1179

Stoeckli ET, Landmesser LT (1998) Axon guidance at choice points. Curr Opin Neurobiol 8:73–79

Stoeckli ET, Sonderegger P, Pollerberg GE, Landmesser LT (1997) Interference with axonin-1 and NrCAM interactions unmasks a floor-plate activity inhibitory for commissural axons. Neuron 18:209–221

Storey KG, Crossley JM, De Robertis EM, Norris WE, Stern CD (1992) Neural induction and regionalisation in the chick embryo. Development 114:729–741

Straka H, Baker R, Gilland E (2001) Rhombomeric organization of vestibular pathways in larval frogs. J Comp Neurol 437:42–55

Straka H, Baker R, Gilland E (2002) The frog as a unique vertebrate model for studying the rhombomeric organization of functionally identified hindbrain neurons. Brain Res Bull 57:301–305

Streit A, Stern CD (1999) Neural induction – a bird's eye view. Trends Genet 15:20–24

Sturrock RR (1982) Gliogenesis in the prenatal rabbit spinal cord. J Anat (Lond) 134:771–793

Sturrock RR, Smart IHM (1980) A morphological study of the mouse subependymal layer from embryonic life to old age. J Anat (Lond) 130:391–415

Sugimoto Y, Taniguchi M, Yagi T, Akagi Y, Nojyo Y (2001) Guidance of glial precursor cell migration by secreted cues in the developing optic nerve. Development 128:3321–3330

Sullivan SA, Moore KB, Moody SA (1999) Early events in frog blastomere fate determination. In: Moody SA (ed) Cell Lineage and Fate Determination. Academic, San Diego, CA, pp 297–321

Sulston JE, Horvitz HR (1977) Post-embryonic cell lineages of the nematode *Caenorhabditis elegans*. Dev Biol 56:110–156

Sulston JE, Schierenberg E, White JG, Thomson JN (1983) The embryonic cell lineage of the nematode *Caenorhabditis elegans*. Dev Biol 100:64–119

Sussel L, Marín O, Kimura S, Rubinstein J (1999) Loss of Nkx2.1 homeobox gene function results in a ventral to dorsal molecular respecification within the basal telencephalon: Evidence for a transformation of the pallidum into the striatum. Development 126:3359–3370

Suter U, Snipes GJ (1995) Biology and genetics of hereditary motor and sensory neuropathies. Annu Rev Neurosci 18:45–75

Suter U, Welcher AA, Snipes GJ (1993) Progress in the molecular understanding of hereditary peripheral neuropathies reveals new insights into the biology of the peripheral nervous system. Trends Neurosci 16:50–56

Taber Pierce E (1966) Histogenesis of the nuclei griseum pontis, corporis pontobulbariss and reticularis tegmenti pontis (Bechterew) in the mouse. An autoradiographic study. J Comp Neurol 126:219–240

Takahashi T, Nowakowski RS, Caviness VS Jr (1995) Early ontogeny of the secondary proliferative population of the embryonic murine cerebral wall. J Neurosci 15:6058–6068

Tam PP, Behringer RR (1997) Mouse gastrulation: The formation of a mammalian body plan. Mech Dev 68:3–23

Tam PPL, Steiner KA (1999) Anterior patterning by synergistic activity of the early gastrula organizer and the anterior germ layer tissues of the mouse embryo. Development 126:5171–5179

Tanabe Y, Jessell TM (1996) Diversity and pattern in the developing spinal cord. Science 274:1115–1123

Tear G, Harris R, Sutaria S, Kilomanski K, Goodman CS, Seeger MA (1996) *Commissureless* controls growth cone guidance across the CNS midline in *Drosophila* and encodes a novel membrane protein. Neuron 16:501–514

Temple S, Alvarez-Buylla A (1999) Stem cells in the adult mammalian central nervous system. Curr Opin Neurobiol 9:135–141

ten Donkelaar HJ (2000) Development and regenerative capacity of descending supraspinal pathways in tetrapods: A comparative approach. Adv Anat Embryol Cell Biol 154:1–145

Theiler K (1972) The House Mouse – Development and normal stages from fertilization to 4 weeks of age. Springer, Berlin Heidelberg New York

Therianos S, Leuzinger S, Hirth F, Goodman CS, Reichert H (1995) Embryonic development of the *Drosophila* brain: Formation of commissural and descending pathways. Development 121:3849–3860

Thomaidou D, Mione MC, Cavanagh JFR, Parnavelas JC (1997) Apoptosis and its relation to the cell cycle in the developing cerebral cortex. J Neurosci 17:1075–1085

Thomas JB, Bastiani MJ, Bate M, Goodman CS (1984) From grasshopper to *Drosophila*: A common plan for neuronal development. Nature 310:203–207

Thomas P, Beddington R (1996) Anterior primitive endoderm may be responsible for patterning the anterior neural plate in the mouse embryo. Curr Biol 6:1487–1496

Thomas PQ, Brown A, Beddington RSP (1998) *Hex*: A homeobox gene revealing peri-implantation asymmetry in the mouse embryo and an early transient marker of endothelial cell precursors. Development 125:85–94

Thornberry NA, Lazebnik Y (1998) Caspases: Enemies within. Science 281:1312–1316

Toivonen S, Saxén L (1955) The simultaneous inducing action of liver and bone marrow of the guinea pig in implantation and explantation experiments with embryos of *Triturus*. Exp Cell Res (Suppl) 3:346–357

Tosney KW, Landmesser LT (1985a) Specificity of early motoneuron growth cone outgrowth in the chick embryo. J Neurosci 5:2336–2344

Tosney KW, Landmesser LT (1985b) Growth cone morphology and trajectory in the lumbosacral region of the chick embryo. J Neurosci 5:2345–2358

Trainor PA, Krumlauf R (2000) Patterning the cranial neural crest: Hindbrain segmentation and *Hox* gene plasticity. Nat Rev Neurosci 1:116–124

Tramontin AD, Brenowitz EA (2000) Seasonal plasticity in the adult brain. Trends Neurosci 23:251–258

Trowe T, Klostermann S, Baier H, Crawford AD, Grunewald B, Hoffmann H, Karlstrom RO, Meyer SU, Muller B, Richter S, et al. (1996) Mutations disrupting the ordering and topographic mapping of axons in the retinotectal projection of the zebrafish, Danio rerio. Development 123:439–450

Tuttle R, Nakagawa Y, Johnson JE, O'Leary DDM (1999) Defects in thalamocortical axon pathfinding correlate with altered cell domains in *Math-1*-deficient mice. Development 126:1903–1916

Urbanek P, Wang ZQ, Fetka L, Wagner EF, Busslinger M (1994) Complete block of early B cell differentiation and altered patterning of the posterior midbrain in mice lacking Pax5/BSAP. Cell 79:901–912

Vaage S (1969) The segmentation of the primitive neural tube in chick embryos (Gallus domesticus). Ergebn Anat Entw Gesch 41:1–88

van den Eijnde SM (1999) Apoptosis and Annexin V. Thesis, Erasmus University, Rotterdam

van den Eijnde SM, Luijsterburg AJM, Boshart L, de Zeeuw CI, Reutelingsperger CPM, Vermeij-Keers C (1997) *In situ* detection of apoptosis during embryogenesis with annexin V: From whole mount to ultrastructure. Cytometry 29:313–320

van den Eijnde SM, Lips J, Boshart L, Vermeij-Keers C, Marani E, Reutelingsperger CPM, de Zeeuw CI (1999) Spatiotemporal distribution of dying neurons during early mouse development. Eur J Neurosci 11:712–724

Vanderhaeghen P, Polleux F (2004) Developmental mechanisms patterning thalamocortical projections: Intrinsic, extrinsic and in between. Trends Neurosci 27:364–391

van der Knaap MS, Valk J (1995) Magnetic Resonance of Myelin, Myelination and Myelin Disorders, 2nd ed. Springer, Berlin Heidelberg New York

Van der Loos H, Dörfl J (1978) Does the skin tell the somatosensory cortex how to construct a map of the periphery? Neurosci Lett 7:23–30

Van der Loos H, Welker E (1985) Development and plasticity of somatosensory brain maps. In: Rowe MJ, Willis WD (eds) Development, Organization, and Processing in Somatosensory Pathways. Liss, New York, pp 53–67

Van der Loos H, Welker E, Dörfl J, Rumo G (1986) Selective breeding for variations in patterns of mystacial vibrissae of mice. Bilaterally symmetrical strains derived from ICR stock. J Hered 77:66–82

van Horck FPG, Weinl C, Holt CE (2004) Retinal axon guidance: Novel mexchanisms for steering. Curr Opin Neurobiol 14:61–66

van Raay TJ, Foskett SM, Connors TD, Klinger KW, Landes GM, Burn TC (1997) The NTN2L gene encoding a novel human netrin maps to the autosomal dominant polycystic kidney disease region on chromosome 16p13.3. Genomics 41:279–282

Vermeij-Keers C (1972) Degeneration in the epithelial plate of Hochstetter in the mouse: A light and electron microscopic study. Acta Morphol Neerl-Scand 9:386–387

Vieille-Grosjean I, Hunt P, Gulisano M, Boncinelli E, Thorogood P (1997) Branchial HOX gene expression and human craniofacial development. Dev Biol 183:49–60

Vogt C (1842) Untersuchungen über die Entwicklungsgeschichte der Geburtshelferkröte (*Alytes obstetricans*). Jent und Gassmann, Solothurn (quoted from Clarke and Clarke 1996)

Voight T (1989) Development of glial cells in the cerebral wall of ferrets: Direct tracing of their transformation from radial glia into astrocytes. J Comp Neurol 289:74–88

von Lenhossék M (1895) Die feinere Bau des Nervensystems im Lichte neuester Forschungen. Fischer, Berlin

Waddington CH (1933) Induction by the primitive streak and its derivatives. J Exp Biol 10:38–46

Warf BC, Fok-Seang J, Miller RH (1991) Evidence for the ventral origin of oligodendrocyte precursors in the rat spinal cord. J Neurosci 11:2477–2488

Wassef M, Joyner AL (1997) Early mesencephalon/metencephalon patterning and development of the cerebellum. Persp Dev Neurobiol 5:3–16

Weickert CS, Webster MJ, Calvin SM, Herman MM, Hyde TM, Weinberger DR, Kleinman JE (2000) Localization of epidermal growth factor receptors and putative neuroblasts in human subependymal zone. J Comp Neurol 423:359–372

Weimann JM, Zhang YA, Levin ME, Devine WP, Brûlet P, McConnell SK (1999) Cortical neurons require Otx1 for the refinement of exuberant axonal projections to subcortical targets. Neuron 24:819–831

Weinstein DC, Hemmati-Brivanlou A (1997) Neural induction in *Xenopus laevis*: Evidence for the default model. Curr Opin Neurobiol 7:7–12

Weinstein DC, Hemmati-Brivanlou A (1999) Neural induction. Annu Rev Cell Dev Biol 15:411–433

Weiss P (1941) Nerve patterns: The mechanisms of nerve growth. Growth 5(Suppl):163–203

Welker E (1985) Brain Maps and Patterns of Sensory Organs; A genetical and experimental analysis of the whisker-to-barrel pathway in mice (*Mus musculus*). Thesis, Free University, Amsterdam

Wendling O, Ghyselinck NB, Chambon P, Mark M (2001) Roles of retinoic acid receptors in early embryonic morphogenesis and hinbrain patterning. Development 128:2031–2038

Westerfield M, ed (1995) The Zebrafish Book, 3rd ed. University of Oregon Press, Eugene, OR

Wilkinson DG (2001) Multiple roles of EPH receptors and ephrins in neural development. Nat Rev Neurosci 2:155–164

Wilkinson DG, Krumlauf R (1990) Molecular approaches to the segmentation of the hindbrain. Trends Neurosci 13:335–339

Wilkinson DG, Bhatt S, Cook M, Boncinelli E, Krumlauf R (1989) Segmental expression of Hox-2 homeobox-containing genes in the developing mouse hindbrain. Nature 341:405–409

Williams SE, Mason CA, Herrera A (2004) The optic chiasm as a midline choice point. Curr Opin Neurobiol 14:51–60

Wilson SI, Edlund T (2001) Neural induction: Toward a unifying mechanism. Nat Neurosci 4(Suppl):1161–1168

Wilson SW, Ross LS, Parrett T, Easter SS Jr (1990) The development of a simple scaffold of axon tracts in the brain of the embryonic zebrafish *Brachydanio rerio*. Development 108:121–145

Windle WF (1935) Neurofibrillar development of cat embryos: Extent of development in the telencephalon and diencephalon up to 15 mm. J Comp Neurol 63:139–171

Windle WF, Austin MF (1936) Neurofibrillar development in the central nervous system of chick embryos up to 5 days incubation. J Comp Neurol 63:431–463

Windle WF, Baxter RE (1936) The first neurofibrillar development in albino rat embryos. J Comp Neurol 63:173–199

Wingate RJT (2001) The rhombic lip and early cerebellar development. Curr Opin Neurobiol 11:82–88

Wingate R, Lumsden A (1996) Persistence of rhombomeric organisation in the postsegmental avian hindbrain. Development 122:2143–2152

Wittler L, Kessel M (2004) The acquisition of neural fate in the chick. Mech Dev 121:1031–1042

Wolpert L, Beddington R, Jessell T, Lawrence P, Meyerowitz E, Smith J (2002) Principles of Development, 2nd ed. Current Biology, London

Wong K, Park HT, Wu JY, Rao Y (2002) Slit proteins: Molecular guidance cues for cells ranging from neurons to leukocytes. Curr Opin Genet Dev 12:583–591

Wood P, Bunge RP (1984) The biology of the oligodendrocyte. In: Norton WT (ed) Oligodendroglia. Adv Neurochem, Vol 5. Plenum, New York, pp 1–46

Wood WB, ed (1988) The Nematode *Caenorhabditis elegans*. Cold Spring Harbor Laboratory Press, Cold Spring Harbor, NY

Woolsey TA, Welker C, Schwartz RH (1975) Comparative anatomical studies of the Sm1 face cortex with special reference to the occurrence of 'barrels' in layer IV. J Comp Neurol 164:79–94

Wurst W, Bally-Cuif L (2001) Neural plate patterning: Upstream and downstream of the isthmic organizer. Nat Rev Neurosci 2:99–108

Wurst W, Auerbach AB, Joyner AL (1994) Multiple developmental defects in Engrailed-1 mutant mice: An early mid-hindbrain deletion and patterning defects in forelimbs and sternum. Development 120:2065–2075

Wyllie AH (1997) Apoptosis: An overview. Br Med Bull 53:451–465

Wyllie AH, Kerr J, Currie A (1980) Cell death: The significance of apoptosis. Int Rev Cytol 68:251–306

Xu Q, Mellitzer G, Robinson V, Wilkinson DG (1999) *In vivo* cell sorting in complementary segmental domains mediated by Eph receptors and ephrins. Nature 400:267–271

Xuan S, Baptista CA, Balas G, Tao W, Soares VC, Lai E (1995) Winged helix transcription factor BF-1 is essential for the development of the cerebral hemispheres. Neuron 14:1141–1152

Yaginuma H, Shiga T, Oppenheim RW (1994) Early developmental patterns and mechanisms of axonal guidance of spinal interneurons in the chick embryo spinal cord. Prog Neurobiol 44:249–278

Yates PA, Roskies AL, McLaughlin T, O'Leary DDM (2001) Topographic-specific axon branching controlled by ephrin-As is the critical event in retinotectal map development. J Neurosci 21:8548–8563

Yoshikawa S, Thomas JB (2004) Secreted cell signaling molecules in axon guidance. Curr Opin Neurobiol 14:45–50

Yoshikawa S, McKinnon RD, Kokel M, Thomas JB (2003) Wnt-mediated axon guidance via the *Drosophila* derailed receptor. Nature 422:583–588

Yu TW, Bargmann CI (2001) Dynamic regulation of axon guidance. Nat Neurosci 4(Suppl):1169–1176

Yuan J, Horvitz HR (1990) The *Caenorhabditis elegans* genes *ced-3* and *ced-4* act cell autonomously to cause programmed cell death. Dev Biol 138:33–41

Yuan SS, Cox LA, Dasika GK, Lee EY (1999) Cloning and functional studies of a novel gene aberrantly expressed in RB-deficient embryos. Dev Biol 207:62–75

Yuan W, Zhou L, Chen J, Rao Y, Ornitz D (1999) The mouse Slit family: Secreted ligands for ROBO expression in patterns that suggest a role in morphogenesis and axon guidance. Dev Biol 212:290–306

Zaki PA, Quinn JC, Price DJ (2003) Mouse models of telencephalic development. Curr Opin Genet Dev 13:423–437

Causes of Congenital Malformations

Martin Lammens, Hans J. ten Donkelaar, John M.G. van Vugt, Gerard van Noort,
Michèl Willemsen and Ben Hamel

3.1   Introduction

Congenital malformations are structural abnormalities due to faulty development, present at birth, and are among the major causes of prenatal, perinatal and infant mortality and morbidity. They include gross and microscopic malformations, inborn errors of metabolism, mental retardation and cellular and molecular abnormalities. About 2–3% of newborns have a single major malformation, and 0.7% have multiple major defects (Norman et al. 1995; Opitz and Wilson 1997; Aicardi 1998; Volpe 2001a). The frequency is much higher prenatally, the majority aborting spontaneously (Shiota 1991, 1993; Kalousek 1997). More than 80% of malformed conceptuses are lost during the embryonic period, and more than 90% before birth. The importance of congenital malformations as a cause of perinatal mortality has increased as deaths from intrapartum problems and infectious diseases have declined, and better neonatal care has improved the survival of normally developed low-birthweight babies. During the last few decades, there has been a rapid expansion of methods for detecting many different types of disorders prenatally. In this introductory chapter the known causes of congenital CNS malformations, and possibilities to detect them prenatally, will be outlined. Some emphasis will be given to the increasing group of inborn errors of metabolism affecting the CNS (neurometabolic disorders), myelination disorders, and vascular disorders, the last being the major cause of acquired damage to the developing nervous system.

3.2   Causes of Congenital Malformations

The causes of congenital malformations may be divided into five broad groups (Warkany 1971; Norman et al. 1995; Jones 1997; Opitz and Wilson 1997; Keeling and Boyd 2001): (1) single gene defects (mutant genes); (2) chromosome abnormalities; (3) multifactorial disorders which are the result of interaction between genetic predisposition and presumed environmental factors; (4) teratogenic factors; and (5) those of unknown cause. Despite the tremendous advances in genetics over the last decade, the aetiology of more than 50% of malformations is still unknown (Opitz

and Wilson 1997; Moore et al. 2000; Keeling and Boyd 2001). Mutant genes, chromosome abnormalities and known teratogens can each be identified in about 7–8% of malformations, and a further 20–25% of malformations fall into the group of multifactorial disorders. A broad subdivision of malformations includes abnormalities of **pregenesis** (gonadogenesis, gametogenesis), **blastogenesis** (the first four embryonic weeks), **organogenesis** (the fifth to eighth embryonic weeks) and **phenogenesis** (roughly the fetal period; Opitz 1993; Opitz et al. 1997). Some essential and widely used terms and concepts relating to malformations are summarized in Table 3.1 (Spranger et al. 1982; Opitz 1993; Opitz et al. 1997). A glossary of genetic terms is included as Table 3.2 (Anderson 1995; Strachan and Read 2004).

3.2.1   Genetic Disorders

Chromosomal Abnormalities

Human development is dependent on the correct chromosome complement, usually 22 homologous pairs of autosomes and one pair of sex chromosomes (Fig. 3.1a). In general, one member of each pair of chromosomes is inherited from each parent. Each chromosome can be easily recognized by banding technology and, more recently, with fluorescence in situ hybridization (FISH; Fig. 3.2). Chromosome malformations are due to either excess or deficiency of chromosomal material including unbalanced rearrangements (Fig. 3.4). Approximately 1 in 200 live newborns will have a chromosome abnormality (Gilbert-Barness 1997; Miller and Therman 2001). In perinatal deaths, the frequency varies between 5 and 10%, and is estimated to be more than 60% in first-trimester miscarriages (Shiota 1993; Kalousek 1997; Keeling and Boyd 2001). Excess or deficiency of chromosomal material can arise through a change in either chromosome number or structure. Changes in chromosome number are of two types: (1) **polyploidy**, an abnormal multiple of the haploid number 23, such as triploidy with 69 chromosomes; and (2) **aneuploidy**, the loss or gain of a whole chromosome (monosomy and trisomy, respectively). A given aberration may be present in all body cells, or in two or more cell lines (**mosaicism**; Hall 1988; Youssoufian and Pyeritz 2002). **Triploidy** occurs in approximately 6% of recognized pregnancies (Keeling and Boyd

Table 3.1 Terms and concepts relating to malformations (based on Spranger et al. 1982; Opitz and Wilson 1997)

Individual alterations of form and structure	
Malformation	A morphological defect of an organ, part of an organ or a larger region of the body resulting from an intrinsically abnormal developmental process
Disruption	A morphological defect of an organ, part of an organ or a larger region of the body resulting from the extrinsic breakdown of, or interference with, an originally normal developmental process
Deformation	An abnormal form, shape or position of a part of the body caused by mechanical forces
Dysplasia	An abnormal organization of cells into tissue(s) and its morphological result(s)
General terminology	
Hypoplasia, hyperplasia	Underdevelopment and overdevelopment of an organism, organ or tissue resulting from a decreased or increased number of cells, respectively
Hypotrophy, hypertrophy	A decrease or increase in the size of cells, tissues or organs, respectively
Agenesis	Absence of a part of the body caused by an absent anlage (primordium)
Aplasia	Absence of a part of the body resulting from a failure of the anlage to develop
Atrophy	Decrease of a normally developed mass of tissue(s) or organ(s) because of a decrease in cell size and/or cell number
Patterns of morphological defects	
Polytopic field defect	A pattern of anomalies derived from the disturbance of a single developmental field
Sequence	A pattern of multiple anomalies derived from a single known or presumed prior anomaly or mechanical factor
Syndrome	A pattern of multiple anomalies thought to be pathogenetically related and not known to represent a single sequence or a polytopic field defect
Association	A non-random occurrence in two or more individuals of multiple anomalies not known to be a polytopic field defect, sequence or syndrome

2001), and is usually due to an error of fertilization: an ovum being fertilized by two spermatozoa. Both polyploidy and monosomy (with the exception of a small proportion of monosomy X: Turner syndrome) are virtually lethal in man. An additional chromosome is much more common than chromosome loss. *Autosomal trisomy* has been recorded for most autosomes, but the incidence varies enormously. Trisomy of chromosome 16 is the most common, but the usual result of this anomaly is spontaneous or missed abortion in the first trimester (Kalousek et al. 1990; Warburton et al. 1991; Kalousek 1997). The most common liveborn example is Down syndrome (trisomy 21; Fig. 3.1b), followed by trisomy 18 (Edwards syndrome) and trisomy 13 (Patau syndrome); first described by Down (1866), Edwards et al. (1960) and Patau et al. (1960) (Table 3.3). Even amongst these karyotypes, miscarriage is the most common outcome (Kalousek et al. 1990; Kalousek 1997).

Down syndrome is characterized by mental deficiency, a characteristic facial expression that results from the upward slanting of the eyes and the prominent skin folds extending from the base of the nose to the inner aspect of the eyebrows and other anomalies of body form. Frequently, there are also congenital heart malformations. Down syndrome is due to three categories of chromosomal abnormalities: (1) trisomy 21, secondary to non-disjunction during meiosis (95% of affected individuals); (2) translocation type or partial trisomy 21; and (3) mosaicism for trisomy 21. The extra chromosome 21 is maternal in origin in some 95% of cases (Antonarakis 1991). In less than 5% of the cases with Down syndrome, the trisomy 21 occurs as a result of an unbalanced translocation. Mosaicism for trisomy 21 is the rarest, less than 1–2% of cases. Trisomy 21 is the most common of all age-related chromosomal abnormalities, constituting about half the overall maternal age-related risk (Laxova 1997): at ages 35, 40 and 45, the risk is about 1 in 270, 1 in 135, and 1 in 50, respectively. Cytogenetic prenatal diagnosis of Down syndrome is established by chorion villus sampling (between 10 and 12 gestational weeks) or amniocentesis (between 14 and 16 weeks). Screening by measuring nuchal translucency thickness (Fig. 3.3), an early ultrasound marker for Down syndrome (Nicolaides et al. 1992, 1999; Snijders and Nicolaides 1996; Pajkrt et al. 1998a, b), carried out in the first trimester of pregnancy has a higher detection rate than invasive methods. Brains of patients with Down syndrome are characteristically small, rounded, foreshortened and exhibit a steep rise of the occipital lobes, extreme

Table 3.2 Glossary of genetic terms (after Anderson 1995; Strachan and Read 2004)

Alleles	Alternative forms of genes occupying an identical site (locus), e.g. the A and B alleles of the ABO blood group gene
Aneuploidy	Deviations by an integral number (rather than a multiple) from the normal diploid complement ($2\times23=46$) of chromosomes
Association	The occurrence together in the population of two genes or phenotypic traits in a frequency greater than would be predicted on the chance basis of their individual frequencies
Autosomes	Non-sex chromosomes in the nucleus (pairs 1–22)
Carrier	A person who is carrying one copy of a gene, which causes symptoms only when present in double dose, and therefore the person is unaffected
Centromere	A construction connecting the chromatids in mitosis, separating the two arms
Codon	The unit of the genetic code, i.e. 3 bases in either DNA or RNA, that specifies a single amino acid to be incorporated into a protein
Dominant	One copy of a gene out of the normal pair produces a phenotypic effect
Exon	The portion of the gene that is transcribed into messenger RNA, usually containing coding information
Fragile site	A specific region on a chromosome that is prone to breakage, usually appearing as a non-staining gap or constriction in one or both chromatids in a metaphase chromosome
Gene	The unit of inheritance for one characteristic or trait, i.e. usually one localized DNA sequence coding for one protein
Haploid	The chromosome number usually found in a normal gamete with only one copy of each pair (in humans, the haploid complement is 23)
Insertion	A structural abnormality in which a sequence of DNA is introduced into another sequence, either at the DNA level or at the chromosome level
Intron	A sequence of DNA that is initially transcribed into messenger RNA, but is then removed from the trancsript by 'splicing' together the exon sequences on either side of it. It is the portion of DNA that usually does not contain coding information
Inversion	A structural chromosomal abnormality in which a segment of a chromosome is reversed, each end reattached to where the other end had previously been attached
Linkage	The location of two genes near enough to one another on the same chromosome that they are coinherited through a meiotic event more than 50% of the time
Locus	A location on the chromosome, usually implying the position of a gene
Mosaic	A person with cells with more than one genetic makeup
Multifactorial	A pattern of inheritance determined by the interaction of multiple genes with others and with the environment
Mutation	A permanent and inheritable change in genetic material.
Oligonucleotide	A short piece of DNA, usually 5–50 nucleotides
Phenotype	Characteristics observed in a person that reflect the gene and/or (to varying degrees) interaction with the environment
Polymorphism	An inherited characteristic present in the population at a frequency great enough that the rarest allele is not maintained by recurrence mutation alone
Recessive	The mechanism of single-gene inheritance that requires 2 doses of a mutant gene in order for the phenotype to manifest
Ring chromosome	A structural chromosomal abnormality with deletions of the terminal portions of the arms of the chromosome and the broken sticky arms rejoining to form a ring
Sex chromosome	The chromosomes that are different in the sexes (usually XX in women and XY in men)
Telomere	The tip of a chromosome
Translocation	The exchange of chromosomal material between two different chromosomes, either 'balanced' (no loss or gain of genetic material) or 'unbalaned'
Trisomy	3, rather than 2, copies of a given chromosome are present
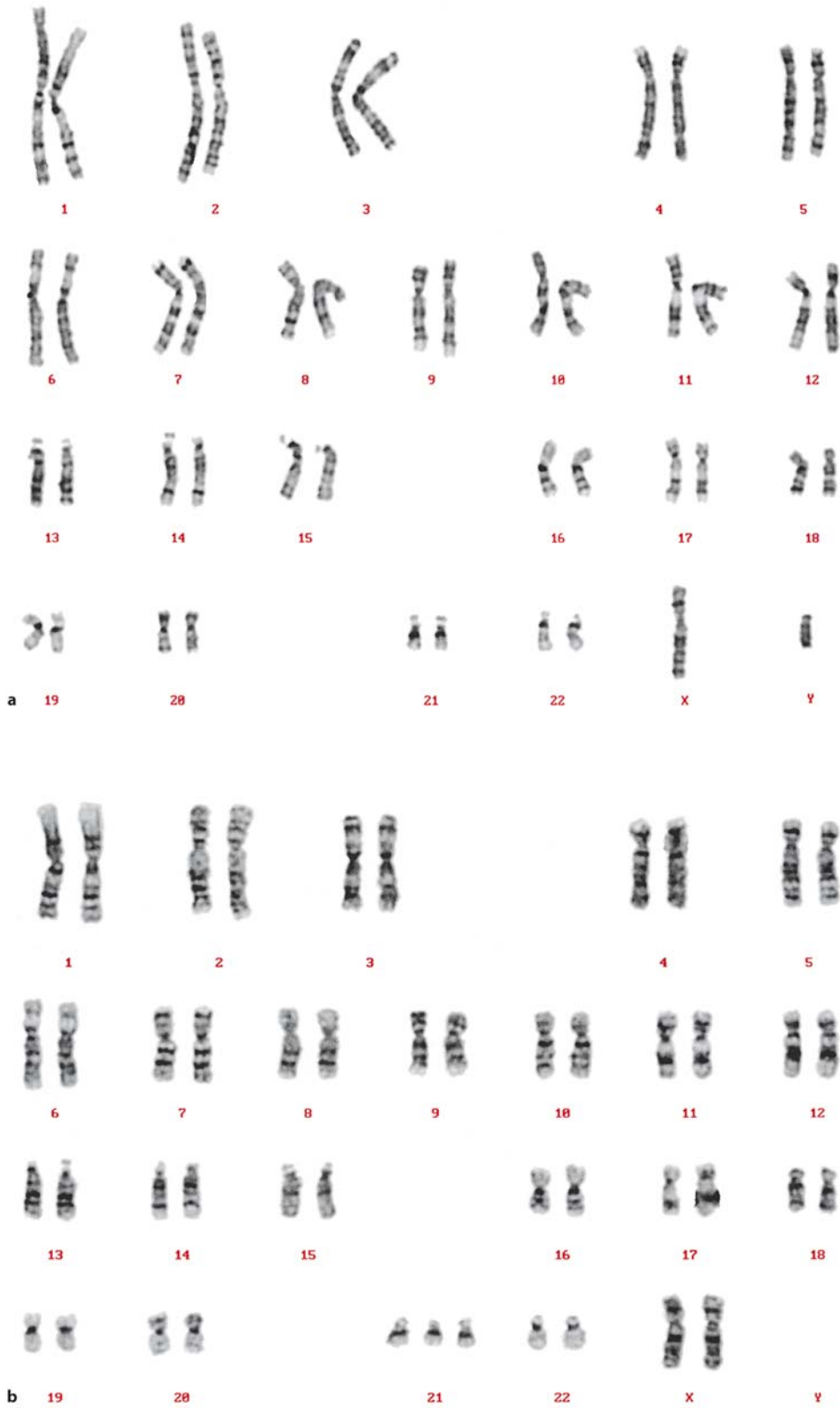
Fig. 3.1 G-banding pattern of human chromosomes: **a** normal; **b** in trisomy 21
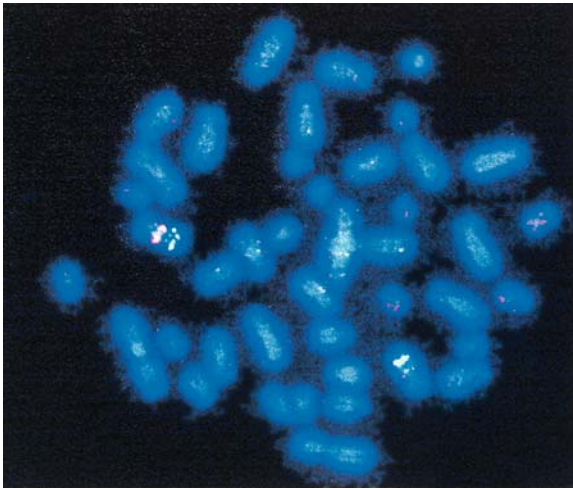
Fig. 3.2 Fluorescence in situ hybridization: example of micro-deletion syndrome (Williams syndrome). The *light-blue* probe is a marker for the chromosome of interest (chromosome 7). The *pink* probe is a marker for the region of interest on that chromosome (7q11.23). The absence of a signal of the pink probe on one of the two chromosomes 7 proves that region 7q11.23 is deleted and supports the clinical diagnosis of Williams syndrome
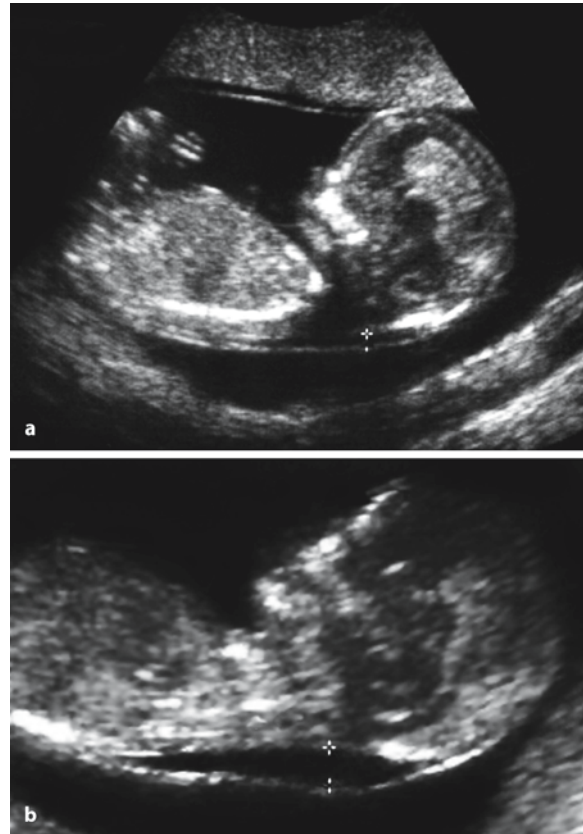
Fig. 3.3 Normal (**a**) and thickened (**b**) nuchal translucency associated with Down syndrome

Table 3.3 Autosomal trisomy syndromes (after Moore et al. 2000)

Chromosome aberration/syndrome	Incidence	Clinical manifestations
Trisomy 13 (Patau syndrome)	1:25,000	Mental deficiency; severe CNS malformations; sloping forehead; malformed ears; scalp defects; microphthalmia; bilateral cleft lip and/or palate; polydactyly; posterior prominence of heels
Trisomy 18 (Edwards syndrome)	1:8,000	Mental deficiency; growth retardation; prominent occiput; short sternum; ventricular septal defect; micrognathia; low-set, malformed ears, flexed digits with hypoplastic nails; rocker-bottom feet
Trisomy 21 (Down syndrome)	1:800	Mental deficiency; brachycephaly; flat nasal bridge; upward slant topalpebral fissures; protruding tongue; simian crease, clinodactyly of the 5th digit; congenital heart defects

narrowing of the superior temporal gyri, incomplete opercularization with exposure of the insular cortex and reduced secondary sulcal development (Källén et al. 1996; Cairns 1999; de la Monte 1999). These abnormalities are largely due to diminished and malformed growth of the frontal and temporal lobes secondary to impaired neuronal differentiation (Lubec and Engidawork 2002). Brain weight is usually in the low normal range, whereas the brain stem and cerebellum are small in relation to the cerebral hemispheres (Scott et al. 1983; Weis et al. 1991). Histological changes include abnormalities in cortical lamination, irregular clustering of neurons, muted dendritic arborization and proliferation of dystrophic neurites (Marín-Padilla 1972, 1976; de la Monte 1999; Chap. 10). Virtually all Down syndrome patients develop Alzheimer-like pathology by the fourth decade of life (Mann 1988).

Structural chromosome abnormalities may involve translocations (exchange of material between chromosomes), inversions, deletions or duplications (Gardner and Sutherland 1996; Fig. 3.4). They may
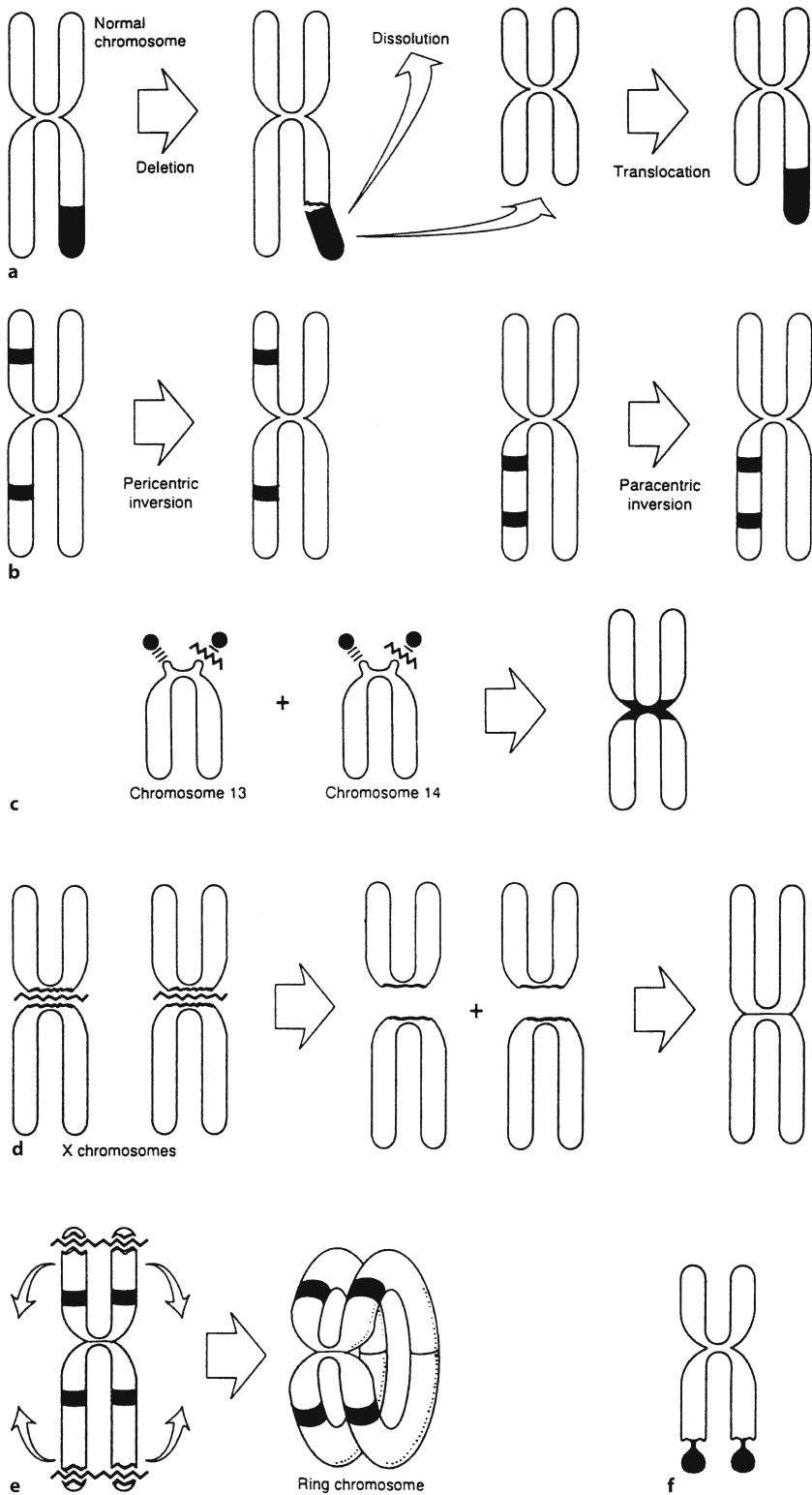
Fig. 3.4 Structural chromosomal abnormalities: **a** deletion and translocation; **b** inversion; **c** Robertsonian translocation; **d** isoschromosomal translocation; **e** ring formation; **f** fragile site (after Anderson 1995)

arise de novo or as a result of a parental chromosome rearrangement. Fusion at or near the centromere of the five acrocentric chromosomes, known as Robertsonian translocation, is one of the most common balanced structural rearrangements. Simple reciprocal translocations involve exchange of material between two chromosomes. Balanced carriers are entirely normal, but they are at risk of having chromosomally unbalanced offspring or miscarriages due to malsegregation at meiosis. Unbalanced structural

Table 3.4 Microdeletion syndromes with CNS manifestations

Syndrome	Location	Parental origin	Symptoms
Angelmann syndrome	15q11-13	Maternal	Mental retardation; macrostomia; prognathia; paroxysmal laughter
DiGeorge syndrome	22q11	Either parent	Aplasia of thymus and parathyroids; malformations great vessels/heart
Velocardiofacial (Shprintzen) syndrome	22q11	Either parent	Palatoschizis; heart malformations; growth retardation; sometimes mental retardation
Miller–Dieker syndrome	17p13	Either parent	Mental retardation; lissencephaly
Prader–Willi syndrome	15q11-13	Paternal	Mental retardation; hypotonia; adipositas
Rubinstein–Taybi syndrome	16p13.3		Mental retardation; broad thumbs and great toes
Smith–Magenis syndrome	17p11.2	Either parent	Mental retardation; deafness; eye malformations
Williams syndrome	7q11.23	Either parent	Mental retardation; typical facies; cardiovascular malformations
Wilms tumour and aniridia genitourinary anomalies and mental retardation	11p13		Urogenital malformations; mental retardation

chromosome rearrangements result in deletions (partial monosomy) and duplications (partial trisomy). *Microdeletion syndromes*, such as Prader–Willi and Angelmann syndromes (chromosome 15), DiGeorge and Shprintzen syndromes (chromosome 22), and Miller–Dieker syndrome (chromosome 17; Chap. 10), are being recognized with increasing frequency (Malcolm 1996; Strachan and Read 2004; Table 3.4). Deletion of chromosome 22q11 (del22q11) is associated with a wide variety of clinical phenotypes (Chap. 5). In certain microdeletion syndromes, *genomic imprinting* is important. The female and male parent confer a sex-specific mark on a chromosome subregion so that only the paternal or maternal allele of a gene is active in the offspring. Therefore, the sex of the transmitting parent will influence the expression or non-expression of certain genes in the offspring. In Prader–Willi and Angelmann syndromes, the phenotype is determined by whether the microdeletion is transmitted by the father (Prader–Willi syndrome) or the mother (Angelmann syndrome).

Single Gene Defects

These disorders are the result of a single mutant gene and follow the Mendelian rules, either as autosomal dominant, autosomal recessive or X-linked traits. Many of the more than 8,000 disorders identified are rare and others may not show morphological defects (McKusick 1998; OMIM). Known single gene defects account for approximately 8% of congenital malformations at term. **Autosomal dominant gene defects** give rise to recognizable effects in heterozygous individuals, usually with an equal sex distribution in about 50% of the offspring. Some of these disorders, such as Huntington disease and some of the autosomal dominant cerebellar ataxias, do not produce rec-

ognizable disease before adult life, whereas others, such as achondroplasia and thanatophoric dysplasia, are recognizable at birth and may be detected prenatally by ultrasound examination. When an autosomal disorder occurs with unaffected parents, a new mutation is not likely to recur in siblings. Gonadal mosaicism, reduced penetrance and variable expression may represent a small but real recurrence rate. Small deletions, responsible for contiguous gene syndromes, may segregate as dominant mutations. For example, velocardiofacial syndrome (VCFS) is due to deletion of 22q11, but with sufficient extensive deletion a more severe condition arises, including DiGeorge sequence (Chap. 5).

Autosomal recessive gene defects occur equally in males and females, and are only clinically manifest in homozygotes with a recurrence risk of 25%. Therefore, affected individuals have healthy, heterozygous parents. Unless an autosomal recessive disorder is common in a certain population, such as Tay–Sachs disease in Ashkenazi Jews, there is often a history of consanguineous marriage. An example of a recessive inherited disorder, affecting the CNS, is Meckel–Gruber syndrome, a triad of CNS malformations, consisting of prosencephalic dysgenesis, occipital encephalocele and rhombic roof dysgenesis, combined with multicystic, dysplastic kidneys and polydactyly (Hori et al. 1980; Ahdab-Barmada and Claassen 1990; Clinical Case 3.1).

X-linked recessive gene defects usually affect only males in 50% of cases if the mother is a carrier. The disorder is usually transmitted by healthy female carriers and their daughters have a similar chance of carrying the gene. Since the father, in general, does not pass an X chromosome to his sons, he will never pass the X-linked recessive trait to his male offspring. Examples are Duchenne muscular dystrophy and

Clinical Case 3.1
Meckel–Gruber Syndrome

Originally described by Meckel (1822) and labelled ***dysencephalia splanchnocystica*** by Gruber (1934), the autosomal recessive ***Meckel–Gruber syndrome*** is a lethal multiple malformation syndrome that is characterized by a posterior encephalocele, by cysts of the kidneys, pancreas and liver and by polydactyly (Opitz and Howe 1969; Ahdab-Barmada and Claassen 1990). Additionally, aplasia of the olfactory tracts, microphthalmia, talipes and incomplete development of the external and/or internal genitalia may be found. Hori et al. (1980) presented a case of a male infant with multiple malformations (see Case Report).

Case Report. A 40-year-old mother with a history of three abortions and one child with multiple malformations including cheilopalatoschisis, cardiac anomalies and cleft bladder who died shortly after birth gave birth to a macrosomic male infant (4,650 g body weight) with multiple malformations. The infant survived for 4 days. External dysplasias comprised macrocephaly (head circumference 42 cm), cheilopalatoschisis, auricular anomalies and unilateral hexadactyly. Internal dysplasias were cysts of the kidneys and pancreas and a patent foramen ovale. The child had frequent generalized convulsions and died of bronchopneumonia. Chromosomal analysis was normal. The main neuropathological findings were a cleft foramen magnum, micropolygyria and heterotopia of the cerebral cortex, hypoplasia of the vermis and central white matter of the cerebellum, diffuse heterotopia of Purkinje cells and unique heterotopic grey matter in the central part of the cervical spinal cord (Fig. 3.5). The infant's disorder was classified as Gruber syndrome (Hori et al. 1980).
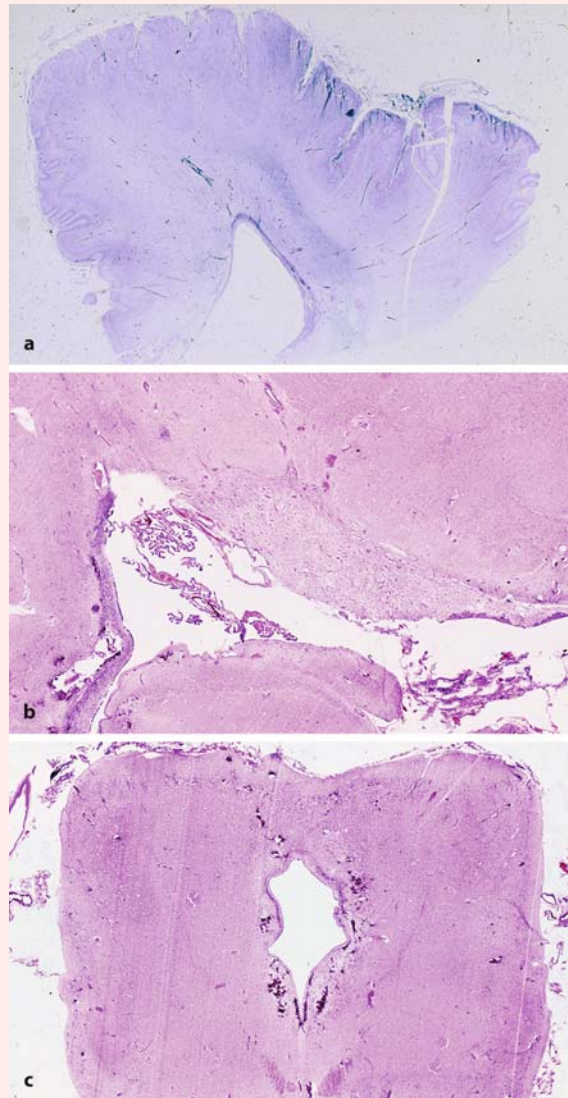
Fig. 3.5 Meckel–Gruber syndrome, showing various malformations of the brain: **a** micropolygyria of the cerebral cortex; **b** gliomesenchymal dysgenesis of the basal forebrain; **c** subependymal and tegmental calcifications in the mesencephalon

References

Ahdab-Barmada M, Claassen D (1990) A distinctive triad of malformations of the central nervous system in the Meckel-Gruber syndrome. J Neuropathol Exp Neurol 49:610–620

Gruber GB (1934) Beiträge zur Frage "gekoppelter" Mißbildungen (Akrocephalo-Syndactylie und Dysencephalia splanchnocystica). Beitr Pathol Anat Alg Pathol 93:459–476

Hori A, Orthner H, Kohlschütter A, Schott KM, Hirabayashi K, Shimokawa K (1980) CNS dysplasia in dysencephalia splanchnocystica (Gruber's syndrome). Acta Neuropathol (Berl) 51:93–97

Meckel JF (1822) Beschreibung zweier, durch sehr ähnliche Bildungsabweichungen entstellter Geschwister. Dtsch Arch Physiol 7:99–172

Opitz JM, Howe JJ (1969) The Meckel syndrome (dysencephalia splanchnocystica, the Gruber syndrome). Birth Defects Orig Art Ser 5:167–179
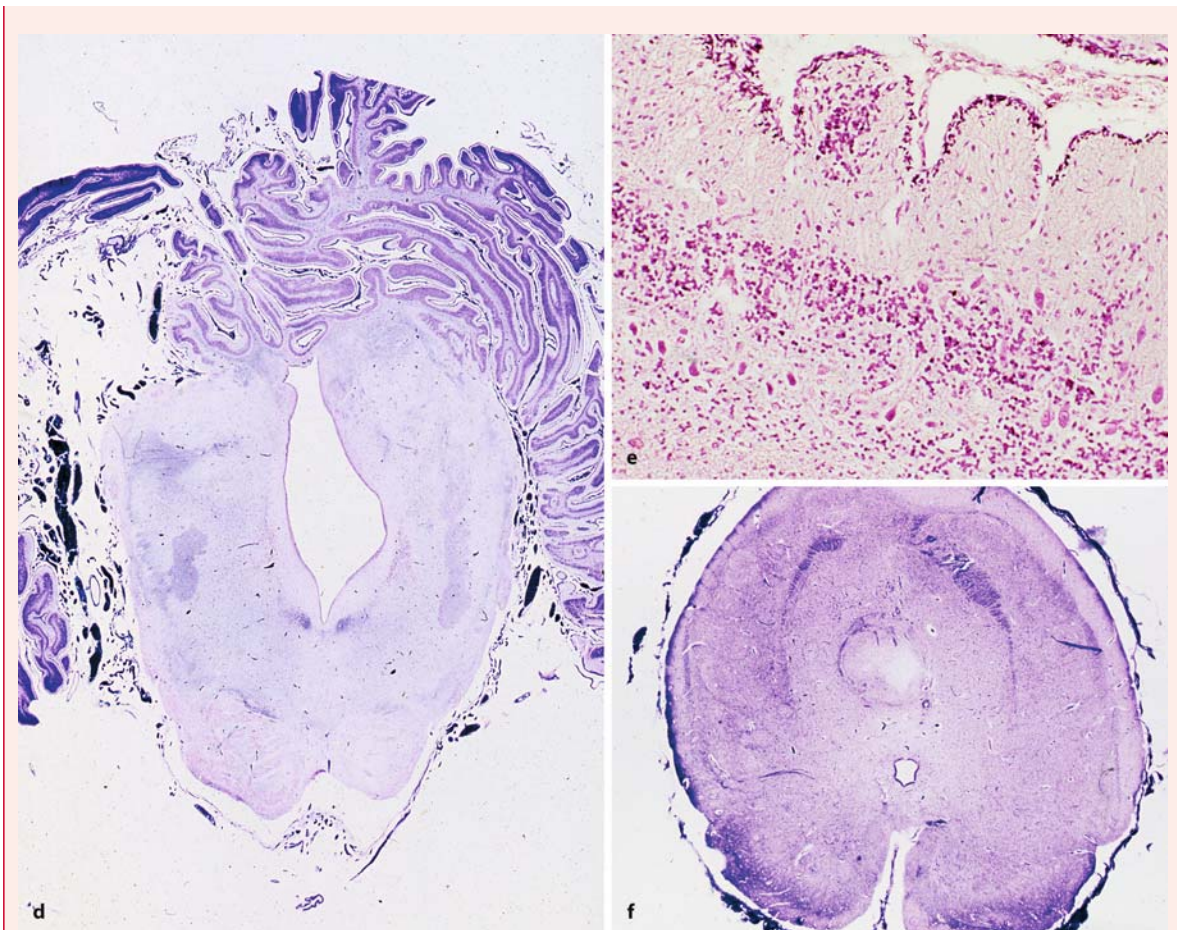
Fig. 3.5 *(Continued)* **d** displacement of cerebellar and vestibular nuclei, enlarged fourth ventricle and pontine hypoplasia; **e** reversed Purkinje cell layer; **f** heterotopia above the central canal and misplaced dorsal roots in upper cervical cord (mostly Luxol Fast Blue staining; from the Department of Neuropathology, Medizinische Hochschule Hannover; courtesy Akira Hori)

haemophilia. The fragile X mental retardation syndrome is not straightforwardly X-linked (Gardner and Sutherland 1996; Hamel 1999; Warren and Sherman 2001; O'Donnell and Warren 2002). It is the most common form of inherited mental retardation, affecting 1 in 4,000–6,000 males and 1 in 8–10,000 females. The *FMR1* gene on the long arm of the X chromosome causes an instable, fragile site at Xq27.3, where these chromosomes are easily broken. The sites can be detected by DNA analysis.

Mitochondrial DNA mutations

The known effects of mitochondrial DNA (mtDNA) mutations, transmitted by the mother, are mostly metabolic and apparently degenerative diseases. Since mitochondria are present in all cells with nuclei, every tissue or organ may be involved in mtDNA mutations. Most frequently, the brain, the heart and skeletal muscles are affected; therefore, these disorders are usually described as *mitochondrial encephalomyopathies*. A better term may be *defects* of *oxidative phosphorylation* (*OXPHOS defects*), since all tissues and organs may be affected (Zeviani et al. 1998; Smeitink and van den Heuvel 1999). Many patients present the first symptoms before the age of 2 years. In general, OXPHOS defects are progressive and fatal disorders. The clinical features in patients suffering from OXPHOS defects are highly variable, but a well-recognized phenotype and in fact prototype of this large group of disorders is Leigh syndrome. *Leigh syndrome* (Leigh 1951) or subacute necrotizing encephalomyopathy is a progressive subcortical disorder, characterized by multifocal, bilateral areas of subtotal necrosis in the basal ganglia, the brain stem tegmentum, the cerebellum and to some extent the spinal cord (Chap. 9). Movement disorders of any type, including hypokinetic-rigid syndrome, chorea, myoclonus or dystonia, may be most obvious.
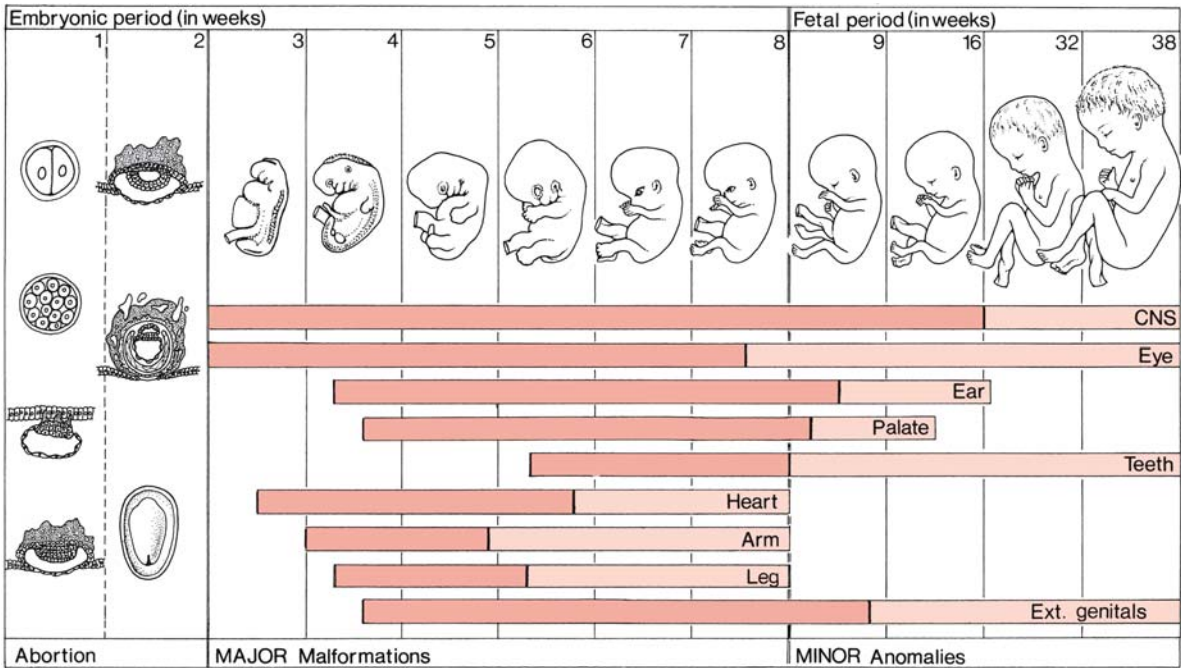
Fig. 3.6 Critical periods in human development and the site of action of teratogens. During the first 2 weeks of development, teratogenic factors destroy most cells of the embryo, resulting in the death of the embryo and spontaneous abortion. Alternatively, only a few cells are destroyed, the embryo recovers, and does not show malformations afterwards. In the *horizontal columns*, the period of major complications is shown in *red*, that of minor anomalies in *light red*. (After Moore and Persaud 1998)

Multifactorial Disorders

Common congenital malformations such as cleft lip with or without cleft palate and neural tube defects have a familial distribution consistent with **multifactorial inheritance**, suggesting that the disease is due to the interaction of different genes and environmental factors. Such disorders occur with increased frequency among family members of an affected individual in an inverse frequency to their relationship. A mathemathical 'liability' model invoking a threshold effect can be constructed and recurrence risks in the offspring of family members calculated. The recurrence risks used for genetic counselling of families with congenital anomalies determined by multifactorial inheritance are empirical risks based on the frequency of the anomaly in the general population and in different categories of relatives. In individual families, such estimates may be inaccurate, because they are usually averages from the population rather than precise probabilities for the individual family. **Digenic inheritance** in human diseases has been demonstrated in an increasing number of diseases (Ming and Muenke 2002), including retinitis pigmentosa, deafness, Hirschsprung disease, Usher syndrome, Waardenburg syndrome type 2 and holoprosencephaly.

3.2.2   Environmental Causes

Teratogenic factors have an adverse, disruptive effect on an embryo or a fetus between fertilization and birth. The term teratogen is usually limited to environmental agents, such as drugs, radiation and viruses. The disruptive effects include congenital abnormalities, embryonic and fetal death, intrauterine growth retardation (IUGR) and mental dysfunction. Critical periods in human development and the site of action are shown in Fig. 3.6. The fetus is less sensitive to morphological alterations than the embryo, but changes in functional capacity, intellect, reproduction or renal function may occur. Mechanical effects may be due to vascular disruptions and the amnion disruption sequence.

Chemicals, Drugs, Hormones and Vitamins

Drugs with a known teratogenic effect are relatively few (Gilbert-Barness and Van Allen 1997; Laxova 1997; Shepard 1998; Moore et al. 2000). Examples include alcohol, cocaine, thalidomide, lithium, retinoic acid, warfarin and anticonvulsant drugs (Table 3.5). *Retinoic acid syndrome* malformations first appeared after the introduction of Accutane (13-*cis*-retinoic

Table 3.5 Some drugs and infectious agents with teratogenic effects (after Gilbert-Barness and Van Allen 1997; Laxova 1997; Moore et al. 2000)

Agent	Mechanism of action	Most common congenital anomalies	Prenatal detection
Drugs			
Alcohol	Increased cell death	Fetal alcohol syndrome: IUGR; CNS abnormalities; characteristic facial expression	Ultrasound for growth, anomalies
Aminopterin and antifolates	Disrupted cell division	IUGR; skeletal defects; malformations of the CNS, notably meroanencephaly	Ultrasound for anomalies
Cocaine	Vasoconstriction	IUGR; prematurity; microcephaly; cerebral infarction; neurobehavioural disorders	High-risk care
Isotretinoin (13-*cis*-retinoic acid or Accutane)	Excessive cell death	Retinoic acid syndrome: craniofacial malformations; NTDs; cardiovascular defects	Ultrasound
Lithium carbonate		Right heart defects; increased incidence of NTDs	Fetal echo-cardography
Methotrexate	Increased cell death	Multiple anomalies, especially skeletal (face, skull, limbs, vertebral column); hydocephalus; meningomyelocele; cleft palate	Ultrasound
Phenytoin (Dilantin)	Increased cell death	Fetal hydantoin syndrome: IUGR; microcephaly; mental retardation; cleft lip/palate	Ultrasound
Thalidomide	Abnormal cell division	Abnormal development limbs (meromelia, amelia)	Ultrasound
Valproic acid		Craniofacial anomalies; NTDs; often hydrocephalus	
Warfarin	Impaired calcium and vitamin K metabolism	Fetal warfarin syndrome: nasal hypoplasia; stippled epiphyses; eye anomalies; mental retardation	Ultrasound
Chemicals			
Methylmercury		Minimata disease: cerebral palsy; microcephaly; mental retardation; blindness	
Polychlorated biphenyls		IUGR; skin discoloration	
Infections			
Cytomegalovirus		Microcephaly; hydrocephaly; cerebral palsy; chorioretinitis; sensorineural loss; psychomotor/mental retardation	Ultrasound
Herpes simplex virus		Chorioretinitis; hydranencephaly	
Human immuno-deficiency virus		Growth failure; microcephaly; prominent forehead; flattened nasal bridge; hypertelorism	Ultrasound
Rubella virus		IUGR; heart abnormalities; eye defects; hearing loss	
Toxoplasma gondii		Microcephaly; mental retardation	
Treponema pallidum		Hydrocephalus; congenital deafness; mental retardation	Ultrasound
Varicella virus		Hydrocephalus; limb paresis; seizures; eye malformations; mental retardation	Ultrasound

IUGR intrauterine growth retardation, *NTDs* neural tube defects

acid), a drug used for the treatment of severe cystic acne (Lammer et al. 1985). Although the retinoids (the normal biologically active retinoic acid and related compounds such as vitamin A, the dietary precursor of retinoic acid) had been long known to be potent teratogens, and the drug Accutane was not to be taken during pregnancy, in the USA many accidental exposures occurred, resulting in a surprising-ly high incidence of severe craniofacial malformations (Lammer et al. 1985; Jones 1997; Gorlin et al. 2001; Chap. 5). Maternal chronic or excessive alcohol consumption, in particular during the first trimester of pregnancy, may lead to the *fetal alcohol syndrome* (Clarren et al. 1978; Gilbert-Barness and Van Allen 1997). The newborn baby is small and may show craniofacial anomalies. Brain anomalies are variable

and unspecific, in contrast to the more common craniofacial anomalies. Hydrocephalus, agenesis of the corpus callosum, neural tube defects and porencephaly may be found (Gilbert-Barness and Van Allen 1997), and even holoprosencephaly has been noted (Bonnemann and Meinecke 1990).

Maternal Conditions

A variety of maternal diseases, either genetic or acquired, and deficiency states may affect the developing embryo. In other disorders, such as epilepsy, the therapy is most likely damaging. *Maternal phenylketonuria* (*PKU*) is the best documented example of a genetic disorder in the mother affecting her offspring when her serum phenylalanine level is elevated during pregnancy. Without a strict diet throughout pregnancy, the children of women with PKU have severe mental retardation, microcephaly and heart defects (Scriver and Kaufman 2001). *Maternal diabetes mellitus type 1* is a risk factor for all sorts of congenital anomalies. Good control can prevent birth defects, however. A high incidence of Down syndrome (Narchi and Kulaylat 1997) and caudal regression syndrome (Passarge and Lenz 1966; Williamson 1970) have been noted. Maternal connective tissue disorders, such as osteogenesis imperfecta and Ehlers–Danlos syndrome, are risk factors for early amnion disruption sequence. *Radiation effects* on the developing brain were extensively studied after the atomic bombings of Hiroshima and Nagasaki (UNSCEAR 1986; Otake et al. 1989, 1991; Schull et al. 1992). The most conspicuous effect on brain development is an increased occurrence of severe mental retardation, with or without microcephaly at specific gestational ages. The period between 8 and 15 weeks following fertilization appeared to be the most vulnerable. Schull et al. (1992) studied brain abnormalities in five of these mentally retarded individuals, using MRI. In the two patients exposed at the eighth or ninth week following fertilization, large areas of ectopic grey matter were seen, due to failure of neurons to migrate properly. The two individuals exposed in the 12th or 13th week showed no readily recognized ectopic grey areas but did show mild macrogyria, which implies some impairment in the development of the cortical zone. The one individual who was exposed in the 15th week did not show such changes. The brain was small with an apparently normal architecture. *Hyperthermia* during pregnancy can cause embryonic death, abortion, growth retardation and developmental defects (Edwards et al. 1995, 2003). Cell proliferation, migration, differentiation and apoptosis are all adversely affected by elevated maternal temperature, showing some similarity to the effects of ionizing radiation. The development of the CNS is especially vulnerable: a 2.5 °C elevation for 1 h during early

neural tube closure in rats resulted in an increased incidence of craniofacial defects, whereas 2–2.5 °C elevation for 1 h during early neurogenesis in guinea pigs caused an increase in the incidence of microcephaly (Edwards et al. 1995). In general, thresholds and dose–response relationships vary between species. In humans, epidemiological studies suggest that an elevation of maternal body temperature by 2 °C for at least 24 h during fever can cause a range of developmental defects, but there is little information on the threshold for shorter exposures (Chambers et al. 1998; Edwards et al. 2003).

Infectious Agents

A number of infectious agents can affect the fetus, producing a range of effects from structural anomalies to mental retardation (Table 3.5). Classically, the TORCH group of infections (toxoplasmosis, rubella virus, cytomegalovirus and herpes/varicella virus) are screened for in the case of permanent cerebral impairment in the neonate (Becker 1992; Stray-Pedersen 1993; Sunderland 1993). But also infections with human immunodeficiency virus (HIV) and other agents may lead to permanent fetal injury. Microcephaly, hydrocephalus, hydranencephaly and cerebral calcifications are the sequelae most often found in the TORCH group of infections (Fig. 3.7), and lead to developmental delay, psychomotor retardation and seizures. Microphthalmia is also often noted in toxoplasmosis, rubella and HIV infection. Often the infection ultimately leads to destruction of cerebral tissue with the formation of cystic spaces in the brain. They have been described as porencephaly (Tominaga et al. 1996) and schizencephaly (Iannetti et al. 1998). When the border of cystic lesions is formed by dysplastic cortex such as polymicrogyria, cytomegalovirus infection should be suspected (Barth 2003). In all instances the nature and the degree of the brain disturbances is a function of the time of the infection. Early infections may lead to intrauterine death, lissencephaly may result from cytomegalovirus onset between 16 and 18 weeks of gestation, whereas polymicrogyria may be due to onset of infection between 18 and 24 weeks of gestation (Barkovich and Linden 1994; de Vries et al. 2004). If the fetus is aborted early, the lesions may be restricted to foci of macrophages around glial or neuronal cells with classical intranuclear viral inclusions. The CNS malformations observed in a case of cytomegalovirus infection are illustrated in Clinical Case 3.2. Rubella virus is embryopathic but also has a recognizable fetopathic effect. Its features are cardiac defects, congenital cataract and deafness. Intracerebral calcifications, visible on ultrasound and CT examination, should raise suspicion for an intrauterine infection.
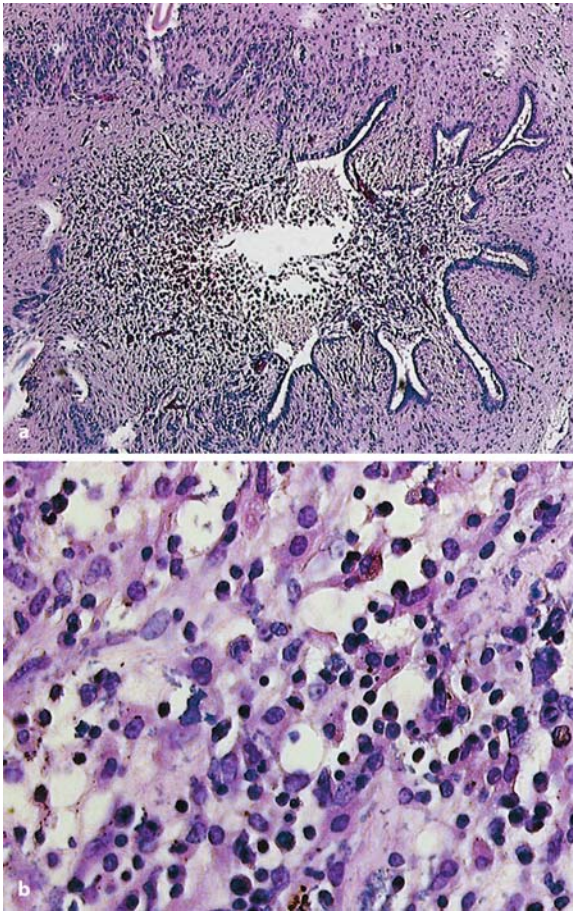
Fig. 3.7 Toxoplasmosis encephalopathy: **a** obstruction of the aqueduct by gliotic and inflamed tissue in intrauterine toxoplasmosis infection in a neonate; **b** detail of inflamed white matter (courtesy Caroline Van den Broecke, University Hospital Gent)

Mechanical Effects

Disruptions of the developing embryo and fetus are rather frequent (Gilbert-Barness and Van Allen 1997), and may arise as a result of vascular disruptions (e.g. Poland sequence), amnion rupture sequence (Van Allen et al. 1987a, b; Bamforth 1992; Moerman et al. 1992; Clinical Case 3.3) and less frequent mechanical effects due to invasive procedures for prenatal diagnosis (Squier et al. 2000; Squier 2002; Clinical Case 3.4) or pregnancy reduction. *Amnion rupture sequence* is a disruption sequence characterized by major anomalies of the craniofacial region, body wall, and limbs. The pathogenesis of these defects is unknown, but it is probably heterogeneous. Mechanisms involved may be vascular disruption (Van Allen et al. 1987a, b), mechanical disruption (Torpin 1965; Higginbottom et al. 1979), genetic disruption (Donnai and Winter 1989) and germ disc disruption (Streeter 1930).

3.3   Prenatal Diagnosis

Suspicion of a congenital malformation may arise on clinical grounds or because of an abnormal result from a routine prenatal investigation. A pregnancy may be at high risk of abnormality because of a particular family history or the advanced age of the mother. Higher-risk groups for chromosome abnormalities include older mothers, those with a previous chromosomally abnormal child, and when one parent is a translocation carrier. Usually, these women are offered chorion villus sampling or amniocentesis routinely. An increasing number of single gene disorders and chromosome abnormalities can now be identified at the molecular level. Population screening programmes may identify women at increased risk of fetal abnormalities (Brock et al. 1992; Laxova 1997; Nicolaides et al. 1992, 1999): second trimester serum test (triple test), first trimester serum test (double test) combined with nuchal translucency measurement on ultrasound examination, and the standard anomaly scan at 18–20 weeks of gestation. For instance, α-fetoprotein (AFP) escapes from the circulation into the amniotic fluid from fetuses with open neural tube defects and open ventral wall defects (gastroschisis, omphalocele). Measuring the level of AFP in amniotic fluid was first carried out for the prenatal diagnosis of neural tube defects. The various imaging methods for prenatal diagnosis will be briefly discussed.

3.3.1   Ultrasound and Magnetic Resonance Examination

High-frequency ultrasonography allows visualization of the normal and abnormal development of the embryo or fetus. However, detailed knowledge about early development of the embryo and fetus is a prerequisite for evaluation of the pregnancy at risk for genetic diseases of the fetus, or when abnormal development of the embryo or fetus is suspected (Blaas et al. 1994; Amin et al. 1999; Blaas and Eik-Nes 1999; Garel 2004; Chap. 1).

Ultrasound Examination of the Normal Spine

In normally developing embryos, the spine can be visualized from the eighth week of gestation onwards (van Zalen-Sprock et al. 1995). It is recognizable as two lines representing the not yet ossified vertebrae (Fig. 3.10a). Primary ossification of the vertebrae starts in the cervical spine and gradually extends caudally. Complete mineralization of the vertebrae is achieved between the 12th and 14th weeks of gestation; therefore, evaluation of the spine with ultrasound is possible from the 13th of gestation onwards.

Cytomegalovirus Encephalopathy

Cytomegalovirus (CMV) infection affects the fetus and results in structural anomalies such as destruction of cerebral tissue with the formation of cystic spaces in the brain. Early CMV infections may lead to intrauterine death, lissencephaly may result from onset between 16 and 18 weeks of gestation, whereas polymicrogyria may be due to onset of infection between 18 and 24 weeks of gestation (Barkovich and Linden 1994; Tominaga et al. 1996; de Vries et al. 2004). The Case Report concerns an intrauterine fetal death at 33 weeks of gestation.

Case Report. The neuropathological findings in a case of intrauterine fetal death at 33 weeks of gestation from a 21-year-old mother are shown in Fig. 3.8. Intrauterine growth retardation was confirmed with ultrasound examination which further revealed ascites and oligohydramnios. A CMV infection was suggested. At autopsy, a male fetus of 793-g weight, 35-cm total length, 4.5-cm foot length and 4.5-cm femur diaphysis length, data comparable to those at 26 weeks of development, was examined. There was fetal hydrops and strong maceration. Generalized CMV infection was found of the lungs, kidneys, pancreas, thyroid, brain and placenta. Viral inclusions were easily recognized. The small placenta (250 g) showed a chronic villitis. The heart showed a perimembranous ventricular septal defect, a wide pulmonary trunk and interruption of the aortic arch between the left carotid and brachial arteries. The descending part of the aorta was continuous with the pulmonary trunk via the ductus arteriosus. The leptomeninges were thickened (Fig. 3.8 a, b). In the brain, polymicrogyria (Fig. 3.8 c) and periventricular necrosis with calcifications (Fig. 3.8 d) were found. Immunoperoxidase staining showed the viral organisms.

This case was kindly provided by Gerard van Noort (Laboratory for Pathology East-Netherlands, Enschede, The Netherlands).
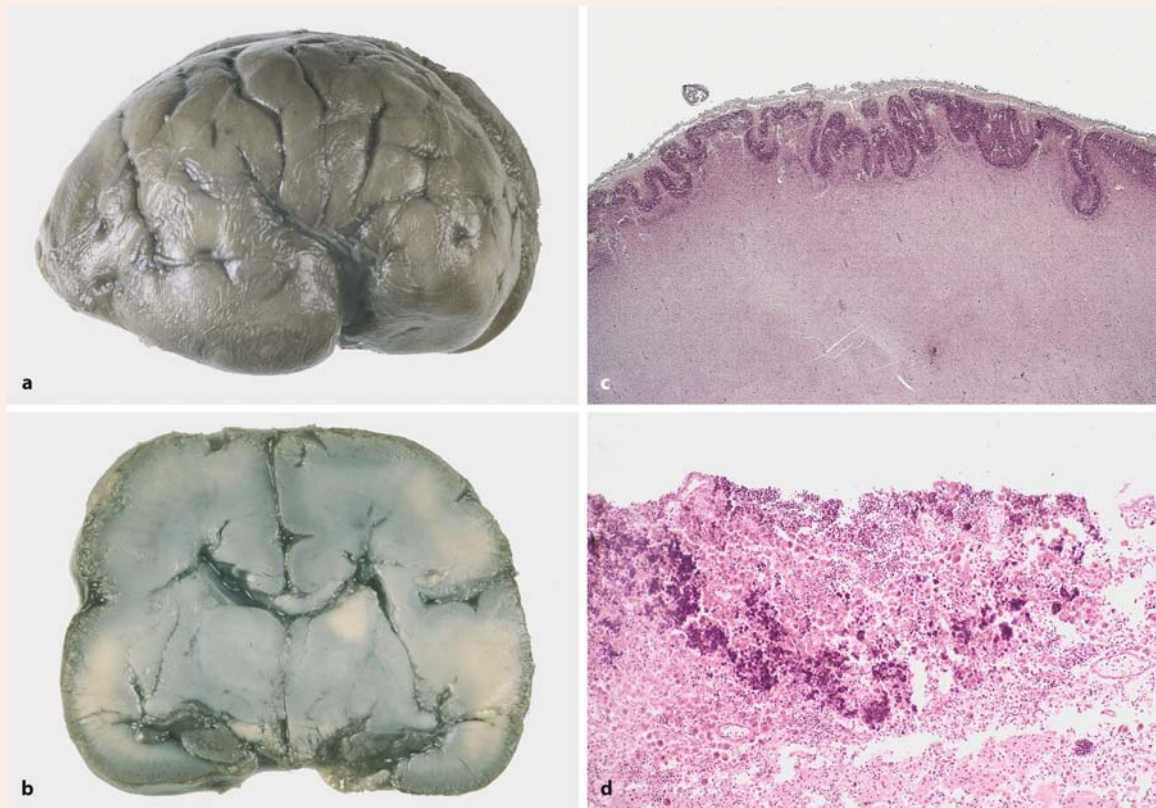
Fig. 3.8 Cytomegalovirus encephalopathy in a case of intrauterine fetal death at 33 weeks of gestation: **a**, **b** lateral view and frontal section of the brain showing thickened lerptomeninges; **c** polymicrogyria of the cerebral cortex; **d** periventricular necrosis with calcifications (courtesy Gerard van Noort, Enschede)

References

Barkovich AJ, Linden CL (1994) Congenital cytomegalovirus infection of the brain: Imaging analysis and embryonic considerations. AJNR Am J Neuroradiol 15:703–715

de Vries LS, Gunardi H, Barth PG, Bok LA, Verboon-Maciolek MA, Groenendaal F (2004) The spectrum of cranial ultrasound and magnetic resonance imaginig abnormalities in congenital cytomegalovirus infection. Neuropediatrics 35:113–119

Tominaga I, Kaihou M, Kimura T, Onaya M, Kashima H, Kato Y, Tamagawa K (1996) Infection foetale par le cytomégalovirus. Porencéphalie avec polymicrogyrie chez un garçon de 15 ans. Rev Neurol (Paris) 152:479–482

The curled position of the embryo in the first trimester requires consecutive scanning planes to visualize the entire spine. In the second trimester of pregnancy, the vertebrae and spinous processes are visible in the sagittal plane as a double row of elements, converging caudally into the sacrum (Fig. 3.10 b). In the transverse plane the neural canal appears as a closed circle, which is lined anteriorly by the vertebral body and posteriorly by the two ossification centres of the laminae. A coronal scan shows the typical three-lined appearance of the vertebrae (Fig. 3.10 c).

Ultrasound Examination of the Normal Brain

At 6 weeks of gestation, when the secondary brain vesicles are being formed, the embryonic cephalic pole is clearly visible and distinguishable from the embryonic torso (Achiron and Achiron 1991). The cavity of the rhombencephalon is one of the first 'structures' of the embryonic CNS that can be visualized with transvaginal ultrasound (Fig. 3.10 e). The rhombencephalic cavity is no longer recognizable after 10–12 weeks of gestation. From 10 weeks onwards, in the fetal head a symmetric, butterfly-like structure (the choroid plexuses) can be seen (Fig. 3.10 f), divided by a thin straight hyperechogenic line (the falx cerebri). The choroid plexuses become considerably reduced in size from the 18th week of gestation onwards. From 15–16 weeks of gestation onwards, the central parts (the atria) and the frontal horns of the lateral ventricles are clearly visible. The brain parenchyma is still translucent and hardly distinguishable. From 26 weeks of gestation, the brain parenchyma becomes more hyperechogenic (Fig. 3.11 a). In the posterior cranial fossa, the hypoechogenic cerebellar hemispheres can easily be seen on each side of the echogenic midline vermis, rostral to the cisterna magna (Fig. 3.11 b). The cerebellum is detectable from 14 weeks of gestation onwards. Imaging of the posterior fossa is important for exclusion of nearly all open spinal defects (see also Chap. 4).

Ultrasound Examination of the Abnormal Spine and Brain

The incidence of abnormalities of the fetal CNS has been estimated at approximately 5–6 per 1,000 births. Overall, the best detection rates by ultrasound are found for CNS abnormalities. The sensitivity of detecting CNS abnormalities by ultrasound is about 90 % (Chitty et al. 1991; Levi 1998; Grandjean et al. 1999). *Neural tube defects* are the most common CNS abnormalities likely to be diagnosed by ultrasound. *Anencephaly* can be recognized by failure of development of the fetal skull vault with secondary degeneration of the brain (Fig. 3.11 c). In the first trimester of pregnancy, the fetus shows acrania with the brain being either normal or disorganized and often incompletely formed (Fig. 3.11 d). The malformation progresses through exencephaly into anencephaly in the second and third trimesters of pregnancy (Wilkins-Haug and Freedman 1991; Chap. 4). The facial bones, brain stem and portions of the occipital bone and midbrain are usually present. Associated spinal defects are found in about 50 % of cases. A high detection rate of up to 99 % is reported for anencephaly (Levi 1998). In *spina bifida*, the neural arch is incomplete with secondary damage to the exposed spinal cord (Fig. 3.10 d). Most lesions occur in the lumbosacral and sacral region, fewer in the thoracolumbar region and only a few in the cervical region (Van den Hof et al. 1990). The effectiveness of ultrasound in diagnosing spinal defects has been greatly improved by the recognition of associated intracranial abnormalities: (1) the changing shape of the skull vault from egg-shaped to lemon-shaped (Fig. 3.11 e) with indentation of the frontal lobes bilaterally (Nicolaides et al. 1986); (2) changes that can be seen in the posterior fossa with an alteration of the shape of the cerebellum from a typical dumbbell shape to a 'banana' shape, owing to compression of the cerebellum in the posterior fossa (Fig. 3.11 f); and (3) the possible presence of ventriculomegaly. The 'lemon' and 'banana' signs are seen in cases with an open spina bifida before 24 weeks of gestation. With the transvaginal ultrasound technique, spina bifida can already be diagnosed by the end of the embryonic period (Blaas et al. 2000). An *encephalocele* is characterized by a defect in the skull and dura through which

Clinical Case 3.3
Amnion Rupture Sequence

Amnion rupture causes constrictive bands with subsequent entanglement of fetal parts (mostly the limbs) by amniotic strands (Jones et al. 1974). Adhesive bands are the result of a broad fusion between disrupted fetal parts (mostly craniofacial) and an intact amniotic membrane. Most of the craniofacial defects, such as encephaloceles and/or facial clefts, that are found in these fetuses are not caused by constrictive amniotic bands but are due to a vascular disruption sequence with or without cephalo-amniotic adhesion (Bamforth 1992; Moerman et al. 1992). The combination of complex, atypical facial clefts, not strictly following embryogenetic patterns, and unusually large asymmetric encephaloceles should raise suspicion for amnion rupture sequence (see Case Report).

Case Report. Ultrasound examination of the first pregnancy of a 27-year-old mother revealed multiple malformations at 23 weeks of gestation; therefore, abortion was induced. Owing to the large size of the occipital encephalocele, some 30 ml of haemorrhagic brain tissue had to be extruded before a female fetus was born. Apart from the occipital encephalocele that was partly attached to the umbilical cord, an asymmetric face with cheilognathopalatoschisis, contractures of both ankle joints, an inverted flexed right foot and a hyperextended left foot were found (Fig. 3.9). Asymmetric hypertelorism was present with normal eyes and a single nostril on the left. Above the right eye there was a defect of 6 mm in diameter in the frontal and ethmoid bones through which some brain tissue protruded. A large, partly collapsed occipital encephalocele contained the larger part of the right cerebral hemisphere with the hippocampus and basal ganglia. The tentorium cerebelli could not be found. Infratentorial tissue was absent, probably lost during the difficult birth. The medial side of the right hemisphere showed some neuronal migration disturbances. Otherwise the brain was normally structured. Despite the extensive midline defects, there were no signs of holoprosencephaly. The other viscera were without gross malformations. The placenta was, apart from a small infarction, normally structured. The umbilical cord contained two arteries and one umbilical vein. At places, the umbilical cord was covered with multiple folds of fibrotic and focally calcified amniotic bands.

References

Bamforth JS (1992) Amniotic band sequence: Streeter's hypothesis re-examined. Am J Med Genet 44:280–287

Jones KL, Smith DW, Hall BD, Hall JG, Ebbin AJ, Massoud H, Golbus MS (1974) A pattern of craniofacial and limb defects secondary to aberrant tissue bands. J Pediatr 84:90–95

Moerman P, Fryns J-P, Vandenberghe K, Lauweryns JM (1992) Constrictive amniotic bands, amniotic adhesions, and limb-body wall complex: Discrete disruption sequences with pathogenetic overlap. Am J Med Genet 42:470–479

the meninges herniate with or without skin covering (Chap. 4). The meningeal sac can contain brain tissue (an encephalocele) or only cerebrospinal fluid (a meningocele). In the majority of cases a bone defect of the skull can be recognized (Fig. 3.12a).

Malformations of the *cerebrum* that can be visualized by ultrasound include ventriculomegaly, holoprosencephaly, schizencephaly and porencephaly. *Ventriculomegaly* means enlargement of the intracranial ventricular system. It is distinct from hydrocephalus in which not only enlargement but also raised pressure within the ventricular system is found (Nyberg et al. 1987). Ventriculomegaly is defined as dilatated central parts (atria) of the lateral ventricles of 10 mm or more, at any gestation time, measured in a transverse plane at the level of the cavum septi pellucidi (Cardoza et al. 1988; Fig. 3.12b). In most cases, ventriculomegaly is caused by an obstruction of the circulation of the cerebrospinal fluid. Associated sonographic features such as a 'dangling choroid plexus' and an enlarged third ventricle may be present. Ventriculomegaly may not be apparent until the second or third trimester of pregnancy. The corpus callosum can be visualized on ultrasound, but it should be emphasized that it forms rather late in development and has not formed entirely before 20 weeks of gestation (Chaps. 1, 10); therefore, accurate diagnosis of *agenesis* of the *corpus callosum* can only be made after that time. In routine scanning, agenesis of the corpus callosum is suspected by detection of focal dilatation of the posterior horns of the lateral ventricles (teardrop configuration), absence of the cavum septi pellucidi and a high-riding third ventricle (Parrish et al. 1979).

Holoprosencephaly is a failure of the development of midline forebrain structures that is usually classified into alobar, semilobar and lobar forms (Chap. 9). In the alobar form, a monoventricle and non-separation of the thalami are found (Fig. 3.12c), whereas the non-separation of these structures declines in the
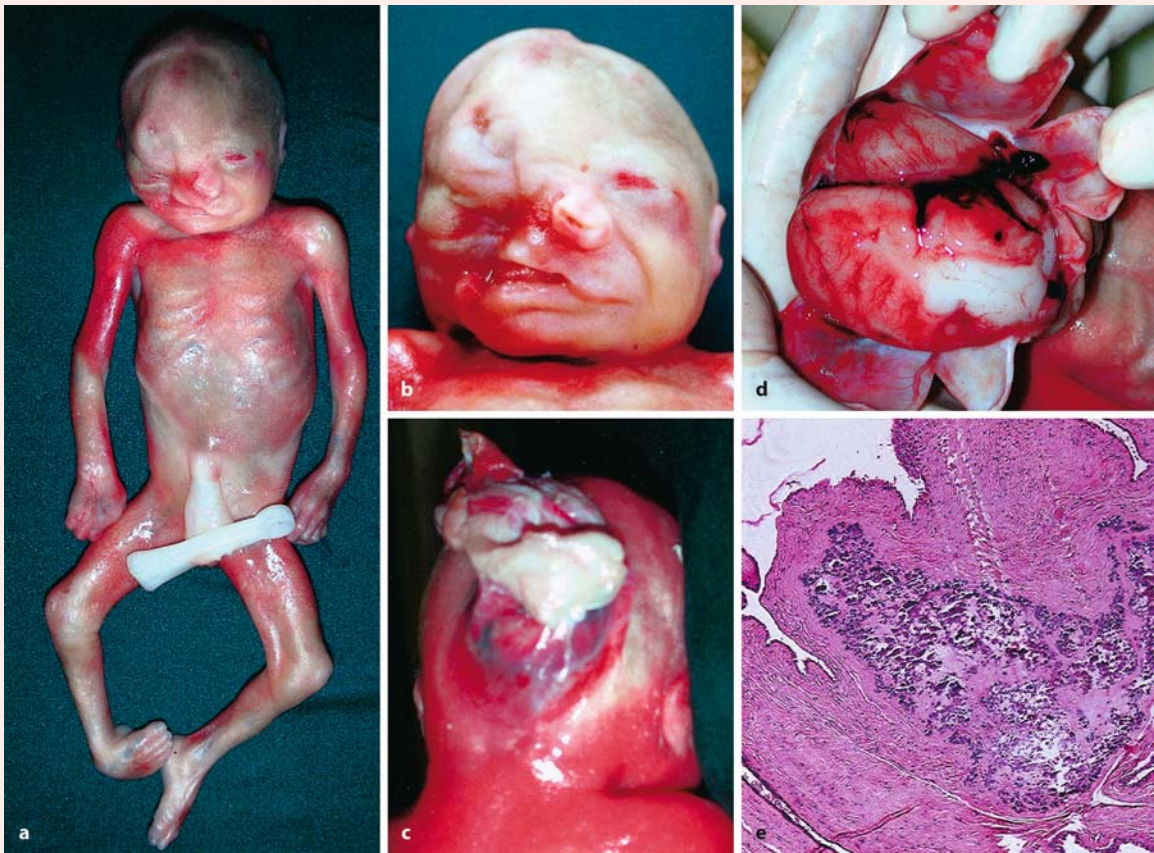
Fig. 3.9 Amnion rupture sequence in a fetus of 23 gestational weeks: **a** overview of malformations; **b** malformed craniofacial region; **c** occipital encephalocele; **d** the brain after opening of the skull; **e** detail of calcified amniotic band (courtesy Martin Lammens, Nijmegen)

semilobar and lobar forms (Chap. 9). Holoprosencephaly is usually associated with craniofacial malformations such as brachycephaly, microcephaly and abnormal facial development (Chap. 5). The detection rate by routine fetal anomaly scan is high for both the alobar and semilobar forms of holoprosencephaly, even in the first trimester (Blaas et al. 2002). In *schizencephaly*, mostly bilateral clefts can be seen as translucent areas extending from the dilatated lateral ventricles to the subarachnoid space.

Malformations of the *cerebellum* detectable by ultrasound include the Dandy–Walker complex and cerebellar hypoplasias (Chap. 8). The *Dandy–Walker complex* refers to a spectrum of abnormalities of the cerebellar vermis, cystic dilatation of the fourth ventricle and enlargement of the cisterna magna (Barkovich et al. 1989; Chap. 8). The *Dandy–Walker malformation* is characterized by failure of development of the cerebellar vermis with a midline cyst-like appearance in the posterior fossa with communica-

tion between the fourth ventricle and the enlarged cisterna magna (Fig. 3.12 d).

Anomalies of the *choroid plexuses* detectable by ultrasound are rather common. *Choroid plexus cysts* are found in approximately 1–2 % of fetuses in a low-risk population (Chitty et al. 1998) and in 1 in 150–200 fetuses of 16–18 gestational weeks (Kraus and Jirásek 2002). On ultrasound, choroid plexus cysts with a variable diameter are detected as hypoechoic structures within the body of the choroid plexus (Fig. 3.12 e). The majority will resolve by 24–28 weeks of gestation (Chitkara et al. 1988; Chitty et al. 1998). It is generally accepted that such cysts reflect a normal variation of the intracranial anatomy. An *aneurysm* of the *vein* of *Galen* is a rare vascular malformation of the choroid plexus within the roof of the third ventricle. Arteriovenous fistulas from the choroidal, anterior cerebral and other arteries to the vein of Galen lead to the aneurysmal dilatation of the vein (Fig. 3.12 f). On ultrasound, a large midline
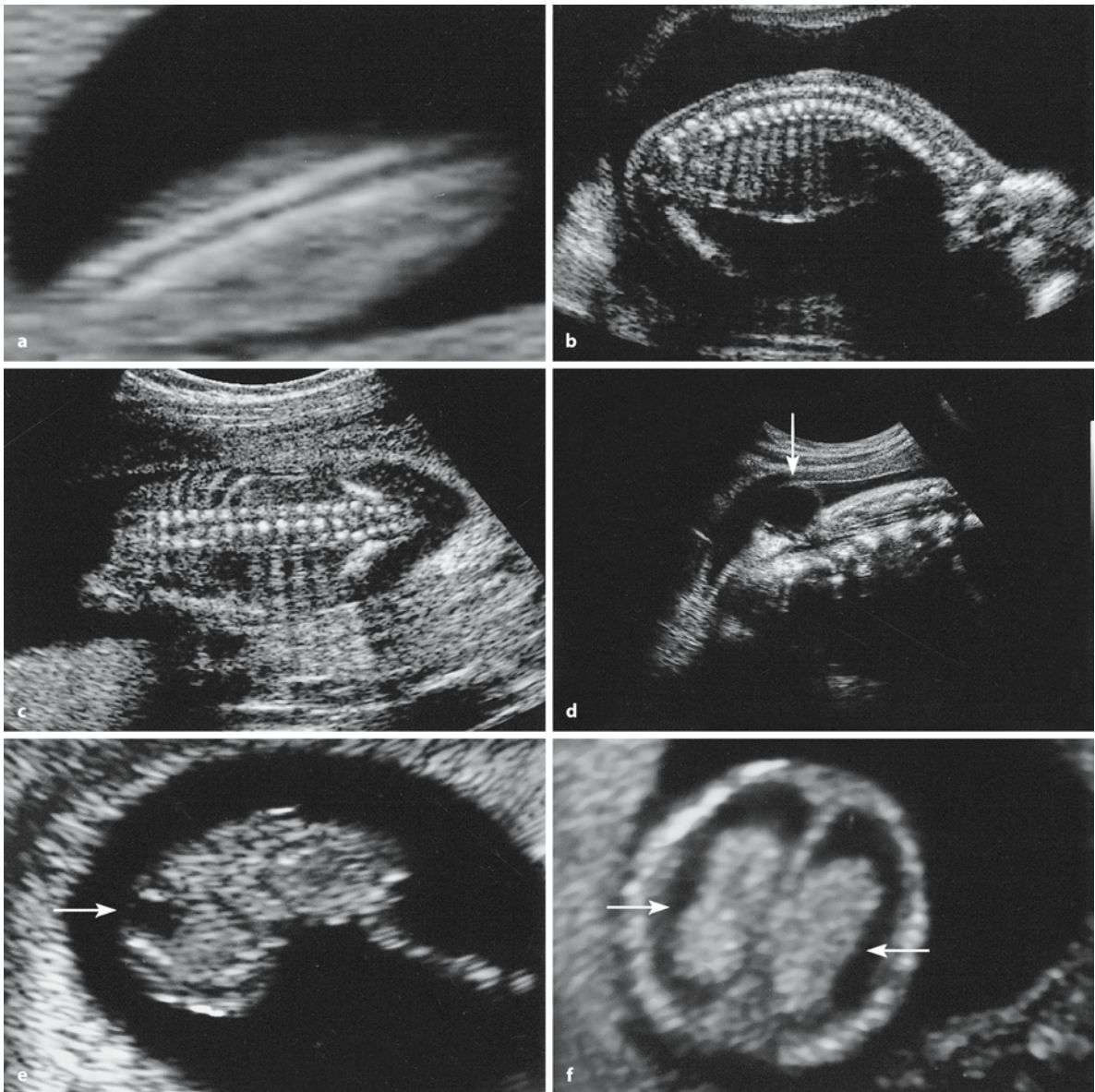
Fig. 3.10 Normal and abnormal ultrasound scans: **a** transvaginal ultrasound of 11-week-old fetal spine; **b** sagittal view of second-trimester normal fetal spine; **c** coronal view of second-trimester normal fetal spine; **d** spina bifida with meningocele (*arrow*) in lumbosacral region; **e** cavity of the rhombencephalon (*arrow*) in a 6-week-old embryo; **f** normal choroid plexuses (*arrows*) in an 11-week-old fetus (**b**, **c** courtesy Monique Haak; **d** courtesy Mireille Bekker, Amsterdam)

cystic structure above the thalamus can be seen. With colour Doppler investigation a turbulent blood flow can be demonstated (Gerards et al. 2003).

Three-Dimensional Ultrasound

Three-dimensional ultrasound can be used for surface reconstruction, multiplanar image analysis and volume calculation (Blaas 1999; Pooh et al. 2003). The surface mode shows not only fetal head anomalies such as acrania but also the normal structure of cra-

nial bones and sutures. Rotation of brain volume image and multiplanar analysis enable tomographic visualization as MRI. The planes obtained are comparable to sections obtained by CT or MRI (Montteagudo et al. 2000). Three-dimensional ultrasound provides the ability to simultaneously view a brain volume in all three scanning planes. In spinal defects, the three orthogonal planes proved to be most helpful in delineating the exact nature and level of the defect.
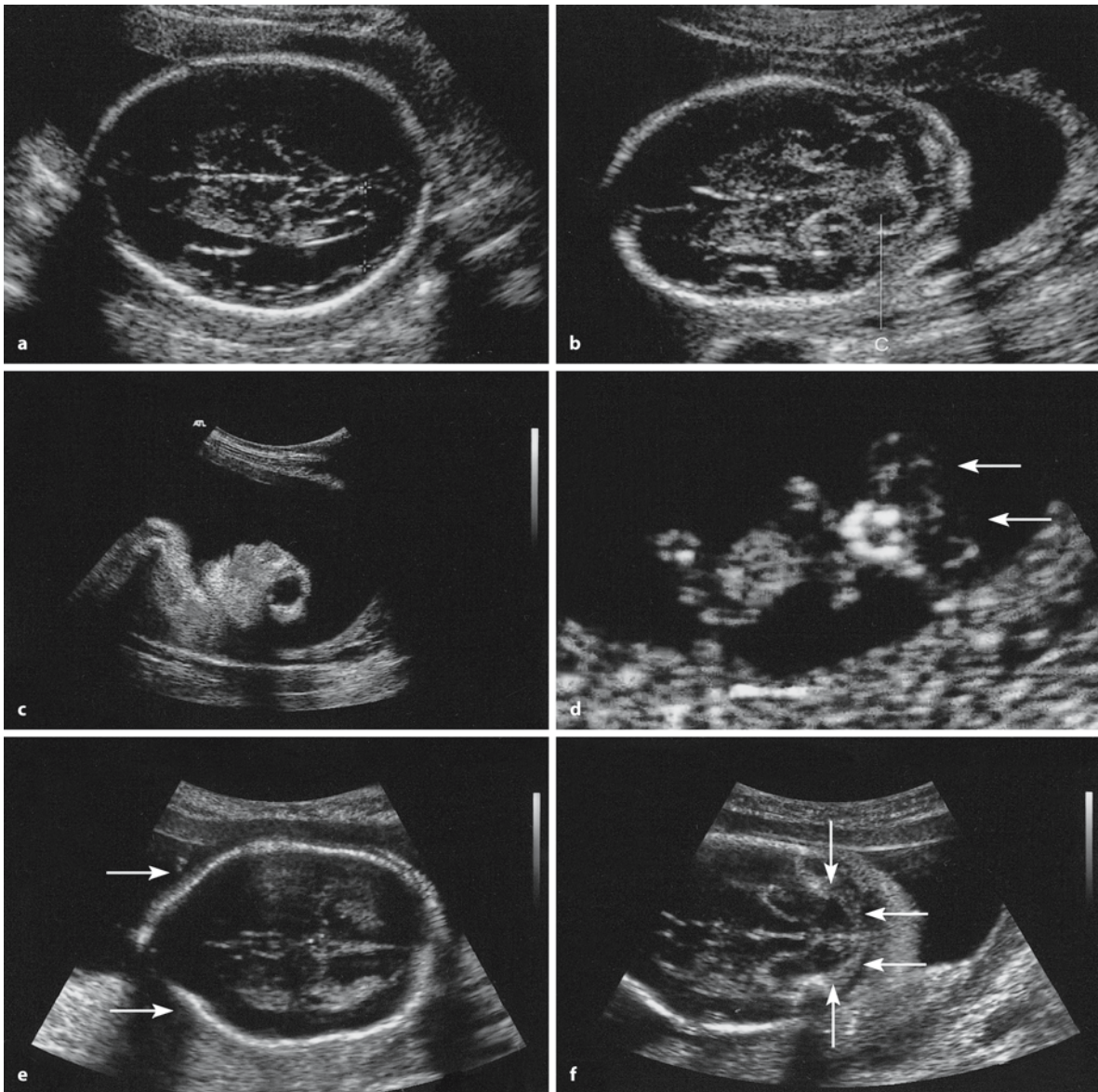
Fig. 3.11 Normal and abnormal ultrasound scans: **a** transverse plane with view of normal brain parenchyma in a second-trimester fetus; **b** transverse plane with view of the cerebellum; **c** fetus with anencephaly; **d** first-trimester fetus with exencephaly (*arrows*); **e** frontal denting: 'lemon' sign (*arrows*) in fetus with spina bifida in the lumbosacral region; **f** Chiari II malformation: 'banana' sign (*arrows*) in fetus with spina bifida (**a**, **b** courtesy Monique Haak, Amsterdam; **e**, **f** courtesy Mireille Bekker, Amsterdam)

Magnetic Resonance Imaging

Ultrasonography is the method of choice for prenatal scanning of fetal anomalies; however, there remain circumstances in which ultrasound data obtained are limited or technically difficult, for example in maternal obesity, oligohydramnios and unfavourable position of the fetus. Moreover, ultrasound examination of the fetal CNS is limited because of the non-specific appearance of some abnormalities and ossification of the fetal skull. Some subtle parenchymal abnor-

malities cannot be seen on ultrasound (Poutamo et al. 1999). MRI may be a useful adjuvant when ultrasound examination is indeterminate. Fetal MRI is hindered by fetal motion and long acquisition times, but ultrafast MRI with scan times of less then 1 s greatly decreases motion artefacts. MRI has proved to be especially useful in the evaluation of the fetal CNS (Levine et al. 1999; Garel 2004; Chap. 1).

MRI is especially useful in cases in which fetal ventriculomegaly (Fig. 3.13a) is associated with other
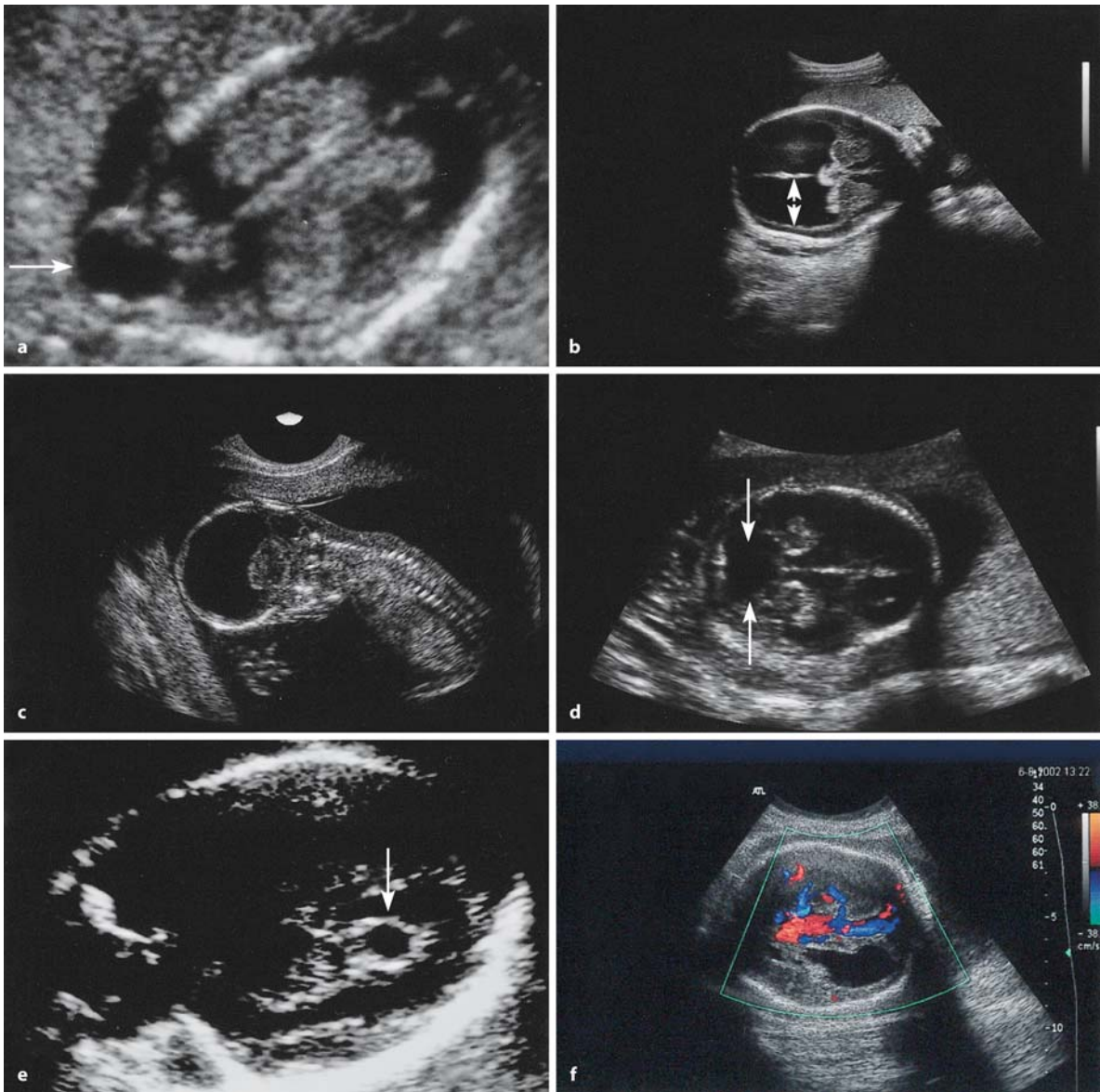
Fig. 3.12 Normal and abnormal ultrasound scans: **a** 12-week-old fetus with encephalocele (*arrow*); **b** second-trimester fetus with ventriculomegaly (*arrows*); **c** fetus with alobar form of holoprosencephaly; **d** Dandy–Walker malformation (*arrows*; **e** choroid plexus cyst (*arrow*); **f** colour Doppler of vein of Galen malformation (**b**–**d** courtesy Melanie Engels, Amsterdam; **f** courtesy Franca Gerards, Amsterdam)

CNS malformations and anomalies outside the CNS (Wagenvoort et al. 2000). Agenesis of the corpus callosum is also such an anomaly easily missed on ultrasound examination, although it is often suspected by indirect signs, that can be visualized with MRI (Levine et al. 1997; Fig. 3.14). In fetuses with arachnoid or other cerebral cysts, MRI contributes to defining the extent of the cyst and its relationship to surrounding structures (Fig. 3.13b). With ultrasound it may be difficult to distinguish between hydrocephalus and mild forms of holoprosencephaly. With MRI (Fig. 3.13c), all forms of holoprosencephaly can be visualized (Hubbard et al. 1999). MRI evaluation of the posterior cranial fossa is not hindered by the engagement of the fetal head, especially not in the third trimester. Other anomalies such as lissencephaly and schizencephaly, and also more subtle parenchymal migration disorders such as heterotopia and polymicrogyria have been visualized with MRI (Levine and Barnes 1999; Garel 2004). Fetal intracranial haemorrhage can be detected with MRI (Fig. 3.13d). The signal intensity of the bleeding varies with its duration (Zanders et al. 2003). Recently developed techniques such as diffusion-weighted imaging, which makes it
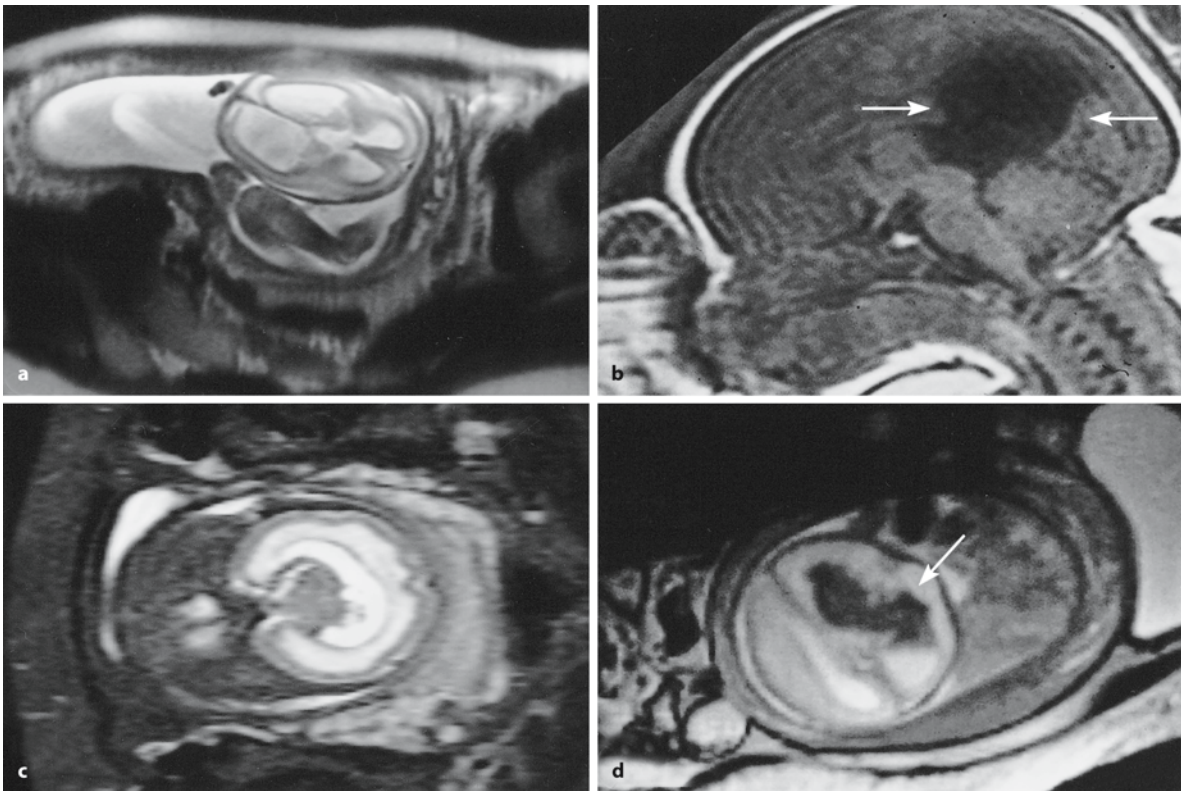
Fig. 3.13 Fetal MRI: **a** ventriculomegaly; **b** arachnoid cyst (between *arrows*); **c** holoprosencephaly; **d** intracranial haemorrhage (*arrow*)
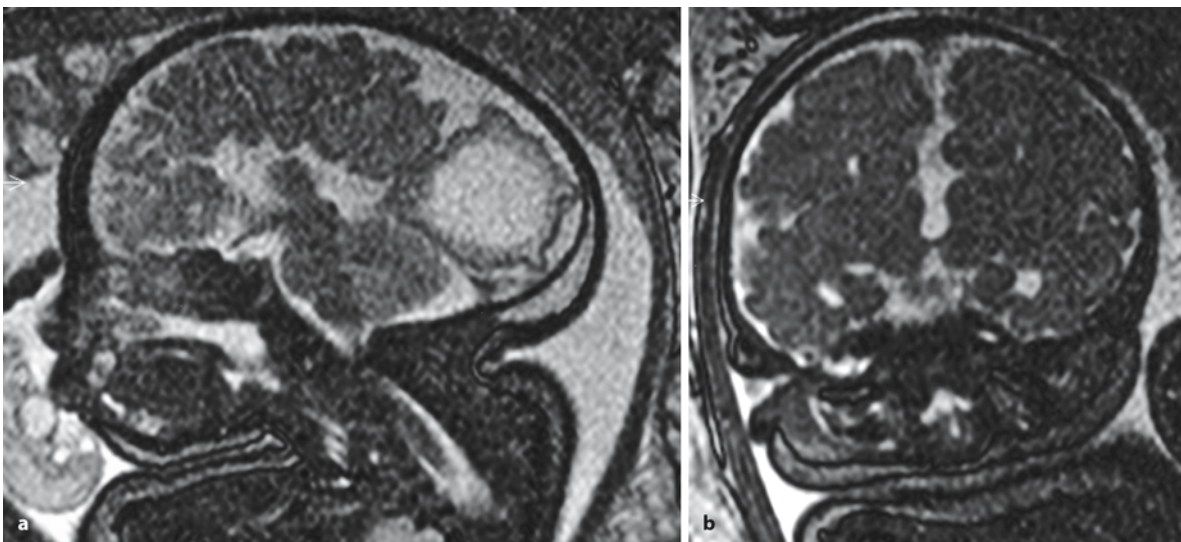
Fig. 3.14 MRI of callosal agenesis in a fetus of 36 gestational weeks: **a** sagittal view showing a high third ventricle, colpocephaly (dilatation of occipital horn) and radial patterning of medial cortex; **b** frontal section (courtesy Berit Verbist, Leiden)

Fig. 3.15 Invasive sampling tests: **a** chorion villus sampling, **b** amniocentesis; **c** fetal blood sampling from the umbilical cord

possible to detect hypoxic brain regions, provide the opportunity to assess fetuses at risk from intrauterine growth restriction, pre-eclampsia of the mother or the twin-to-twin transfusion syndrome. MRI is also helpful in cases with spinal defects to delineate the precise defect and therefore may play a role in fetal surgery for such defects (Sutton et al. 2001).

3.3.2 Invasive Tests

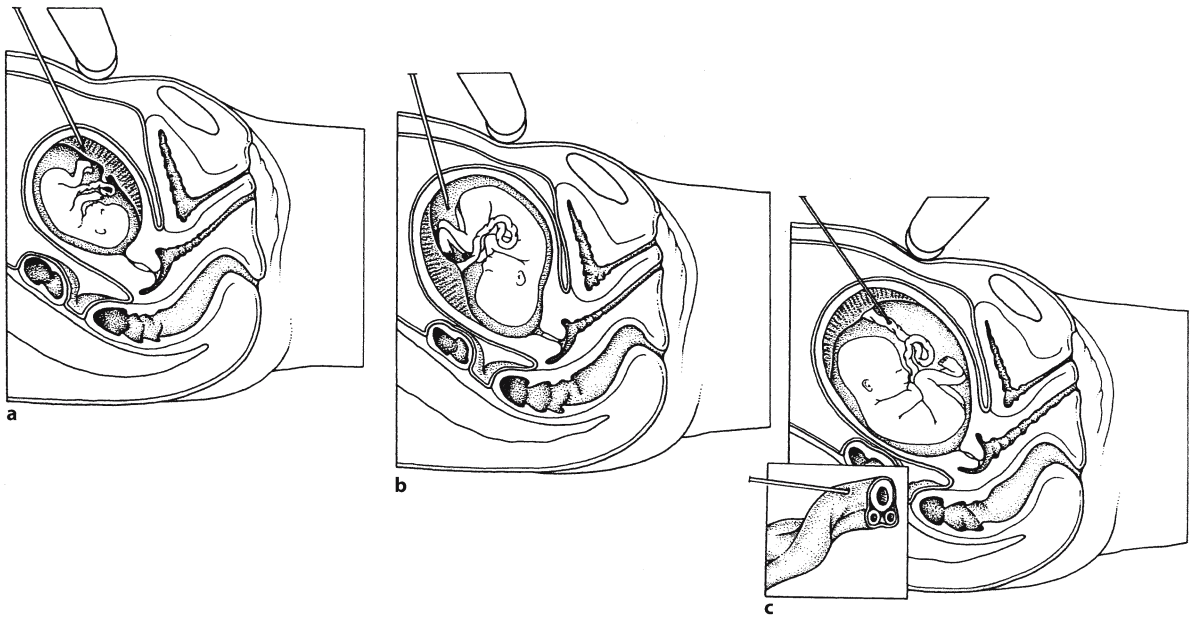Various invasive sampling techniques for prenatal diagnosis are available (Fig. 3.15): chorion villus sampling, amniocentesis and fetal blood sampling. *Chorion villus sampling* can be carried out during the first trimester and presents the possibility of an early termination of pregnancy. Biopsies of chorionic villi may be obtained by a transcervical or a transabdominal approach (Fig. 3.15a). For safety chorion villus sampling is usually carried out after 11 weeks of gestation. It is used for detecting chromosomal abnormalities, DNA analysis, inborn errors of metabolism and X-linked disorders. Karyotyping of aspirated/biopsied chorionic villi can be performed both from direct examination or from short-term culture of the cytotrophoblast and/or long-term culture of fibroblasts from the core of the villus. Complications of chorion villus sampling are, apart from reliability, maternal cell contamination and confined placental mosaicism, increased miscarriage risk and fetal injury, especially oromandibular/limb hypogenesis syndrome and transverse limb reduction defects, the latter when chorion villus sampling is carried out before 10 weeks of gestation (Boyd et al. 1990; Quintero et al. 1992; Firth 1997; Keeling and Boyd 2001).

Amniocentesis has been performed for much longer than chorion villus sampling and is the most common invasive prenatal diagnostic procedure (Fig. 3.15b). A 15–20-ml aliquot of amniotic fluid is taken transabdominally under ultrasound guidance, usually between 14 and 16 weeks of gestation. Indications for amniocentesis are similar to those for chorion villus sampling, but amniocentesis provides also the possibility to analyse AFP in the amniotic fluid as an indicator for neural tube defects. The vast majority of amniocenteses are performed because of increased risk of Down syndrome in women aged over 35 years or in younger women with a positive result from biochemical (AFP) screening or those with a suspicion of abnormality on ultrasound examination. The reliability of amniocentesis is very accurate. A miscarriage risk of 0.5–1.4% has been found in large studies but it may be higher (Nicolaides et al. 1999). Fetal damage is rare, but documented (Squier et al. 2000; Squier 2002; Clinical Case 3.4). *Fetal blood sampling* may be used at about 20 weeks of gestation for chromosomal analysis when ultrasound or other invasive tests have shown a fetal anomaly. It is carried out transabdominally from the umbilical cord (Fig. 3.15c) or a transplacental route into an umbilical cord vessel at the placental insertion if the placenta is anterior. Fetal blood sampling is not routinely done but miscarriage risk in experienced hands is in the order of 1.5%.

References

Squier W (2002) Pathology of fetal and neonatal brain damage: Identifying the timing. In: Squier W (ed) Acquired Damage to the Fetal Brain: Timing and Causation. Arnold, London, pp 110–127

Squier W, Chamberlain P, Zaiwalla Z, Anslow P, Oxbury J, Gould S, McShane MA (2000) Five cases of brain injury following amniocentesis in midterm pregnancy. Dev Med Child Neurol 42:554–560
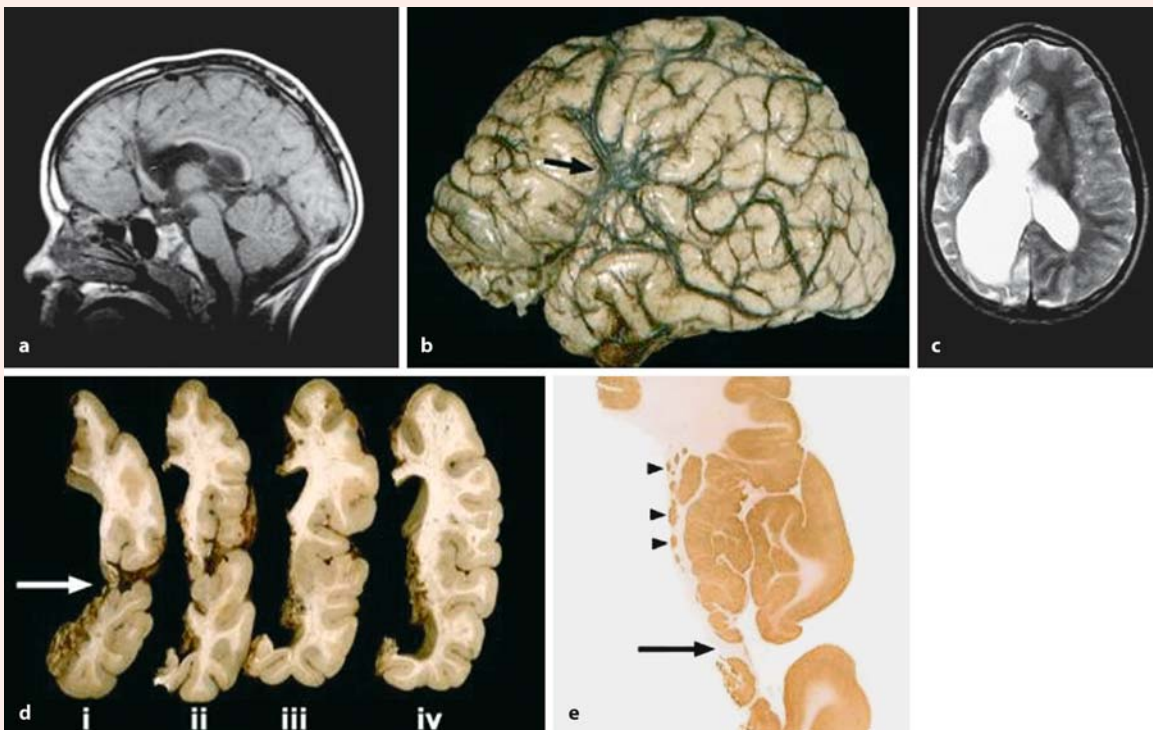
Fig. 3.16 Traumatic amniocentesis: **a** sagittal MRI showing a defect in the anterior part of the corpus callosum; **b** lateral surface of the hemisphere; the *arrow* indicates a cortical scar; **c** horizontal MRI showing atrophy of the left cerebral hemisphere; **d** coronal slices through the affected hemisphere showing a cortical defect (*arrow*) and a thin corpus callosum; **e** section of part of the hemisphere, stained to show neurons, illustrating the cortical defect (*arrow*) and several nodular heterotopia (*small arrows*) due to lack of normal migration (from Squier 2002, with permission; courtesy Waney Squier, Oxford)

3.3.3 Genetic Diagnosis

Karyotyping

Chromosome analysis can be performed on any tissue with living nucleated cells which undergo division. Circulating lymphocytes from peripheral blood are most commonly used, but also skin, bone marrow, chorionic villi or amniocytes are often used. After culturing and a technical preparation, different staining methods can be used in order to identify the individual chromosomes by their banding pattern such as G (Giemsa) banding, which gives each chromosome a characteristic and reproducable pattern of light and dark bands. **G banding** is the most widely used banding technique with up to 400–500 bands. High-resolution banding provides greater sensitivity with up to 800 bands, but is much more time consuming. Usually 10–15 cells are microscopically analysed. If mosaicism is suspected 30 or more cells are examined. The karyotype is the end result of the analysis whereby each chromosome is pairwise represented in descending order of size (Fig. 3.1a). **Fluorescent in situ hybridization** (FISH) combines chromosome analysis with a molecular technique that allows a piece of single-stranded DNA (probe) with known genomic localization to hybridize with its complementary target sequence. The probe is fixed to a fluorescent label which gives a visible signal after hybridization (Fig. 3.2). FISH technology is particularly useful for the detection of submicroscopic deletions such as 22q11 deletion in VCFS and DiGeorge syndrome, 7q11 deletion in Williams syndrome, 15q11 maternal deletion in Angelmann syndrome and 15q11 paternal deletion in Prader–Willi syndrome. In these examples the clinical suspicion is highly relevant: only when VCFS is suspected, 22q11 FISH will be performed. Newer techniques have been developed–and are being improved–to detect even smaller deletions and/or duplications in a systematic way (multiplex amplifiable probe hybridization, multiplex ligation-dependent probe amplification, microarray-based comparative genomic hybridization; Sismani et al. 2001; Schouten et al. 2002; Vissers et al. 2003; Strachan and Read 2004).

Identifying the Genes for Human Developmental Anomalies

The most commonly used way to initiate the identification of genes involved in monogenic disorders is linkage analysis; its aim is to map the locus where the putative gene, mutated in the involved monogenic disease, is located. **Linkage analysis** is based on the fact that when two loci are sufficiently close together on a chromosome, alleles at these loci are very likely to stay together in meiosis, or in other words are very unlikely to be separated by crossover or recombination in meiosis. It involves study of the segregation of a monogenic disease in large families with a set of polymorphic markers from each chromosome. In families with an X-linked disorder only X-chromosomal polymorphic markers will be used. Eventually a marker can be identified which cosegregates with the disease or in other words the marker locus and the disease locus are linked. The likelihood of linkage can be calculated and is expressed in a Lod score. Since usually many markers are used, it is possible to construct a linked haplotype: a set of alleles of linked markers with on each side a recombined non-linked marker, so defining the linkage interval or the linked chromosomal region. The size of such a region is expressed in centimorgan: the smaller the region, the better the chances to identify a gene.

Positional gene cloning uses two strategies. The first is based on linkage studies: if the linkage interval is very small, techniques are available to identify one or more genes in the interval and to test these for the presence of pathogenic mutations. In this way, for instance, the cystic fibrosis gene was found. The second is based on the identification of patients with a monogenic disease and a chromosomal rearrangement: the hypothesis is that the chromosomal rearrangement disrupts the gene involved in that monogenic disease. Again techniques are available to identify that gene. When subsequently in other patients with that monogenic disease mutations in the so-identified gene are found the hypothesis becomes true. The X-chromosomal gene for the Duchenne muscular dystrophy was detected in this way. **Candidate gene mapping** is another method. From animal models and the human genome project information about genes and the gene content of a given linkage interval can be retrieved. Very often information about the function and/or the expression pattern of the genes is available and this allows for the selection of one or more candidate genes for a given disorder. Finally, identifying pathogenic mutations in patients confirms that this candidate gene is in fact the disease gene. In this way p63 was found to be the gene involved in the ectrodactyly–ectodermal dysplasia-clefting (EEC) syndrome.

DNA Diagnosis

DNA diagnosis in monogenic diseases can be done in two ways: the indirect and the direct way. In indirect DNA diagnosis linkage analysis is performed. This gives reliable results, though never 100 % reliable, provided the disease locus is known, the clinical diagnosis is correct, the disease is homogeneous, a sufficient number of family members are available and recombination does not occur. Direct DNA diagnosis is presently the more commonly used method and is based on mutation analysis in the known disease gene. This gives usually 100 % reliable results, though not finding the mutation does not necessarily

exclude the disease owing to genetic heterogeneity and/or technical shortcomings. For hundreds of monogenic disorders DNA diagnosis is possible both pre- and postnatally. Also carrier testing is reliably possible for autosomal and X-linked recessive disorders. Presymptomatic DNA diagnosis involves the genetic testing of healthy individuals in families with an usually late onset hereditary disease and in which the pathogenic mutation is known. Examples are Huntington disease and hereditary breast/ovary cancer. Obviously, adequate pre- and posttest genetic counselling and where relevant psychosocial support are required.

Preimplantation Genetic Diagnosis

Preimplantation genetic diagnosis (PGD) is the combination of in vitro fertilization (IVF) and genetic testing (Braude et al. 2002). After IVF early embryos are allowed to develop into the eight-cell stage. Then one to two cells are biopsied and examined while the rest are set aside in the deep freezer. After the results are known only the healthy embryos are implanted in the uterus. This is still a fairly experimental method with as its most serious drawback the relatively low chance of an ongoing pregnancy. Examples in which it is performed are cystic fibrosis, spinal muscular atrophy, haemophilia and fragile X syndrome.

3.4 Inborn Errors of Metabolism Affecting the CNS

Inborn errors of metabolism present a large group of genetic metabolic disorders, the common feature of which is a genetically determined interruption in one or several related metabolic pathways (Fitzpatrick 2001; Scriver et al. 2001; Epstein et al. 2004). In general, metabolic diseases are recessive disorders without clinical symptoms in heterozygous individuals. However, involved genes may also be located on the X chromosome and on the mtDNA, leading to different modes of inheritance. Many metabolic diseases are caused by mutations in genes encoding proteins with a single enzymatic function. Most conditions are individually rare, but collectively metabolic diseases are rather common. The complexity and vulnerability of the CNS is illustrated by the presence of neurological signs and symptoms in the majority of inborn errors of metabolism. CNS malformations may occur in almost all types of inborn errors of metabolism, including disorders of oxidative phosphorylation, aminoacidopathies, organic acidurias, fatty acid oxidation disorders, lysosomal storage disorders, peroxisomal disorders, congenital disorders of glycosylation and disorders of cholesterol biosynthesis. From a clinical point of view, the following three categories can be distinguished:

1) *Inborn errors of metabolism that primarily are located in other organs, whereby the CNS is secondarily involved*. In such cases, the CNS is generally threatened by energy deficiency or intoxication. Examples are disorders of carbohydrate metabolism and fatty acid oxidation that primarily involve the liver but lead to acute energy crises of the CNS owing to hypoglycemia or CNS intoxication (e.g. in galactosemia and PKU), respectively. In propionic and methylmalonic acidurias and urea cycle defects, the CNS is threatened by energy defects as well as intoxication. Many disorders in this category exhibit acute neurological manifestations like coma and seizures.

2) *Inborn errors of metabolism that mainly affect the CNS*. In this category, the involved metabolic pathway is located in the CNS. For such disorders, the term *neurometabolic diseases* is increasingly used (Moser 1998). The pathophysiological mechanisms of these disorders include energy failure, substrate deficiency, intoxication, or combinations of these. Pattern recognition via MRI is very helpful in the classification of neurometabolic diseases (Barkovich 2000). An important decision to be made is whether the disorder is primarily in the grey matter, primarily in the white matter or a combination of both. Examples of neurometabolic disorders are:

   a) Some lysosomal storage disorders (Tay–Sachs disease and the neuronal ceroid lipofuscinoses, classic examples of 'grey matter' disorders; and metachromic leukodystrophy, a typical 'white matter' disorder)

   b) Cerebral organic acid disorders such as glutaric aciduria types 1 and 2, and L-2-hydroxyglutaric aciduria and D-2-hydroxyglutaric aciduria

   c) Neurotransmitter synthesis disorders (e.g. tyrosine hydroxylase deficiency)

   d) Neurotransmitter degradation defects (e.g. succinic semialdehyde dehydrogenase deficiency)

   e) CNS disorders of energy production due to defective substrate availability (e.g. glucose transporter type 1 deficiency) or defective substrate intoxication (e.g. mitochondrial encephalopathies). Most neurometabolic disorders show progressive neurological features such as mental retardation, motor disturbances and epilepsy.

Table 3.6 Some inborn errors of metabolism that mainly affect the CNS

Group of disorders	Disorder	Defective gene/protein	CNS malformations	References
Amino acids	Non-ketotic hyper-glycinemia		Dysgenetic corpus callosum	Dobyns (1989); Hamosh and Johnston (2001)
Organic acids	Pyruvate dehydrogenase deficiency		Dysgenetic corpus callosum	Brown et al. (1989); Robinson (2001)
	Fumarase deficiency		Agenesis corpus callosum; polymicrogyria; hydrocephalus See Chap. 9	Remes et al. (1992); Kerrigan et al. (2000)
	Glutaric aciduria type 1 Glutaric aciduria type 2		Pachygyria; heterotopia; hypoplastic corpus callosum; dysplastic cerebellum	Goodman and Frerman (2001)
Purines, pyrimidines	Lesch–Nyhan syndrome	Purine salvage enzyme hypo-xanthine–guanine phosphoribosyl-transferase	Neurobehavioural syndrome with motor dysfunction and self-injurious behaviour	Jinnah and Friedmann (2001)

3) ***Inborn errors of metabolism that present as multisystem disorders with mild, moderate, or severe CNS involvement.*** Many inborn errors of metabolism fall into this category. Striking examples of multisystem disorders are:
   a) Congenital disorders of N- and O-linked glycosylation
   b) Mitochondrial encephalomyopathies
   c) Lysosomal storage disorders
   d) Peroxisomal disorders
   e) Cholesterol biosynthesis disorders

The clinical approach to metabolic diseases of the CNS involves careful history-taking, MRI pattern recognition, ophthalmological investigation (some disorders are accompanied by highly typical forms of cataract or retinopathy) and appropriate laboratory analyses at the metabolite, enzyme or DNA level.

3.4.1   Inborn Errors of Metabolism that Mainly Affect the CNS

Some of the inborn errors of metabolism that cause isolated CNS malformations are summarized in Table 3.6. Pachygyria or microgyria appear to be the most common malformations, followed by agenesis of the corpus callosum, hydrocephalus and (ponto)cerebellar hypoplasia. Pyruvate dehydrogenase deficiency is the best studied neurometabolic disorder (Brown et al. 1989; Brown and Squier 1996; Robinson 2001), with partial or total agenesis of the corpus callosum as the dominant feature. Other examples of disorders in the metabolism of organic acids are fumarase deficiency (Remes et al. 1992; Kerrigan et al. 2000) and glutaric aciduria type 1 (Chap. 9) and type 2 (Goodman and Frerman 2001).

The best known disorder of amino acid metabolism is non-ketotic hyperglycinemia (Hamosh and Johnston 2001), clinically characterized by a severe neonatal epileptic encephalopathy. In many patients, the corpus callosum is absent (Dobyns 1989). In Lesch–Nyhan syndrome, hyperuricemia and a characteristic neurobehavioural syndrome with motor dysfunction and self-injurious behaviour is found (Jinnah and Friedmann 2001). This syndrome and its variants are due to inherited deficiency of the purine salvage enzyme hypo-xanthine–guanine phosphoribosyltransferase (HPRT).

3.4.2   Multisystem Disorders with CNS Involvement

Under this heading the following inborn errors of metabolism will be briefly discussed: (1) congenital disorders of glycosylation (the CDG syndromes); (2) inherited disorders of cholesterol biosynthesis; and (3) disorders of peroxisomal structure and function, Zellweger's cerebrohepatorenal syndrome in particular (Table 3.7).

Congenital Disorders of Glycosylation

Congenital disorders of glycosylation (the *CDG syndromes*) are a rapidly growing family of genetic diseases caused by defects in the synthesis of the glycan moiety of glycoconjugates or in the attachment of glycans to macromolecules (Jaeken and Carchon 2001; Jaeken and Matthijs 2001; Jaeken et al. 2001; Marquardt and Denecke 2003). In addition to many other organs, the brain is affected in 10 of the 11 known congenital disorders of N-linked glycosylation, mostly to a severe degree. Because a large number of enzymes, transporters and other proteins

Table 3.7 Some multisystem disorders with CNS involvement

Group of disorders	Disorder	Defective gene/protein	CNS malformations	References
Cholesterol biosynthesis	Smith–Lemli–Opitz syndrome	*DHCR7*; 7-dehydrochol-esterol reductase	Holoprosencephaly; periventricular nodes; dysplasia cerebellum and corpus callosum	Cunniff et al. (1997); Haas et al. (2001)
	Mevalonic aciduria	*MVK*; mevalonate kinase	Cerebellar atrophy	Hoffmann et al. (1993)
	CHILD syndrome	Sterol-4-demethylase	Unilateral hypoplasia brain stem and spinal cord	Happle et al. (1980)
	Desmosterolosis	Sterol-Δ24-reductase	Variable phenotype, ranging from macrocephaly to microcephaly	FitzPatrick et al. (1998); Haas et al. (2001); Waterham et al. (2001)
Congenital disorders of N-glycosylation	CDG-1a	*PMM2*; phospho-mannomutase	Olivopontocerebellar atrophy	Jaeken and Carchon (2001); Chap. 8
Congenital disorders of O-glycosylation defects	Walker–Warburg syndrome	*POMT*; *O*-mannosyl-transferase	Cobblestone lissencephaly; encephalocele; pontocerebellar hypoplasia	Barkovich et al. (2001); Beltrán-Valero de B et al. (2002); Chap. 10
	Fukuyama type of congenital muscular dystrophy	*Fukutin*/Fukutin	Cobblestone lissencephaly; mental retardation; congenital muscular dystrophy	Kobayashi et al. (1998); Toda et al. (2003)
	Muscle–eye–brain disease	POMGnT1 (a glysosyltransferase)	Pachygyria; pontocerebellar hypoplasia	Barkovich et al. (2001); Yoshida et al. (2001); Chap. 10
Peroxisomes	Zellweger syndrome		Polymicrogyria; pachygyria; hypoplasia corpus callosum, cerebellar dysplasia	Zellweger (1987); Gould et al. (2001); Wanders et al. (2001)
	X-linked adreno-leukodystrophy	ALD protein gene		Moser et al. (2001)

are involved in glycosylation (both N-linked and O-linked), it is expected that the great majority of congenital disorders of glycosylation are yet to be identified (Jaeken and Carchon 2001). An example of an N-linked glycosylation disorder (CDG-1a), leading to pontocerebellar hypoplasia, is shown in Clinical Case 3.5. O-linked glycosylation defects form the underlying mechanism of certain lissencephalies such as Walker–Warburg syndrome, Fukuyama congenital muscular dystrophy and muscle–eye–brain disease (Barkovich et al. 2001; Chap. 10).

Disorders of Cholesterol Biosynthesis

Defects of cholesterol biosynthesis (Fig. 3.18) comprise a heterogeneous group of disorders, most of which have only recently been described. More are likely to follow in the near future (Haas et al. 2001; Kelley and Herman 2001). In general, there are two mechanisms by which aberrant cholesterol biosynthesis may cause developmental disorders: (1) a relative deficiency of cholesterol; and (2) a relative excess of the sterol precursor. Abnormal sterols are known to alter membrane fluidity, which may alter both the movement of embryonic cells and cell–cell interaction. Altering the sterol content of membranes may also lead to the aberrant functioning or mistargeting of some proteins. Perturbations in cholesterol homeostasis may result from a defect in the normal Sonic hedgehog signalling network and cholesterol biosynthesis (Cohen and Shiota 2002; Chap. 9). *Mevalonic aciduria*, caused by deficiency of mevalonate kinase, an enzyme located proximally in the cholesterol pathway, was the first reported disorder of cholesterol (Hoffmann et al. 1986). The patient showed profound psychomotor retardation, ataxia, a dysmorphic appearance, cataract, hepatosplenomegaly and recurrent febrile attacks. Later, several patients with milder forms were described (Hoffmann et al. 1993; Gibson et al. 1997). The other recognized defects of cholesterol biosynthesis, such as CHILD syndrome, desmosterolosis and Smith–Lemli–Opitz syndrome, are due to enzyme defects located distally in the cholesterol pathway (Fig. 3.18). Patients with these disorders all show complex malformation syndromes

**Congenital Disorders
of Glycosylation**

Congenital disorders of glycosylation (the CDG syndromes) are genetic diseases caused by defects in the synthesis of the glycoconjugates or in the attachment of glycans to macromolecules (Jaeken and Matthijs 2001; Jaeken et al. 2001). Apart from the brain, many other organs are usually severely involved in disorders of N-linked glycosylation (Strømme et al. 1991). The best known N-linked CDG syndrome, CDG-1a, leads to pontocerebellar hypoplasia (see Case Report). The defective gene and protein are *PMM2* and the enzyme phosphomannomutase, respectively.

Case Report. A 15-year-old boy, with psychomotor retardation of unknown aetiology and severe scoliosis, died after a severe bronchopneumonia. At autopsy, an extensive necrotic bronchopneumonia and signs of aspiration were found. The endocard showed fibrosis and the liver was steatotic and mildly fibrotic (Fig. 3.17 f). Cystically enlarged tubules were present in the kidneys (Fig. 3.17 g) and a calyceal vein was occluded by thrombotic material. Brain examination showed no obvious malformations of the cerebrum but extensive olivopontocerebellar atrophy (Fig. 3.17 a–c). The cerebellar atrophy was present in the vermis as well as in the hemispheres. A reduced number of small folia were present. Microscopic examination of the brain stem revealed severe atrophy of the inferior olives (Fig. 3.17 d). No accessory olives and arcuate nuclei were present. In the cerebellar cortex, small molecular and granular layers could be distinguished, but no Purkinje cells. Distinct dentate nuclei were found. The pontine nuclei were small. In the cerebrum, some nodular heterotopia were found along the lateral ventricles. These characteristic findings at autopsy permitted the diagnosis of CDG type 1a, a diagnosis that was confirmed by deficient enzymatic phosphomannomutase activity in cultured fibroblasts (0.06 mU/mg protein; normal range 1.27–4.53).

This case was kindly provided by Gerard van Noort (Laboratory for Pathology East-Netherlands, Enschede, The Netherlands).

References

Jaeken J, Matthijs G (2001) Congenital disorders of glycosylation. Annu Rev Genomics Hum Genet 2:129–152

Jaeken J, Matthijs G, Carchon H, Van Schaftingen E (2001) Defects of N-glycan synthesis. In: Scriver CR, Beaudet AL, Sly WS, Valle D (eds) The Metabolic & Molecular Bases of Inherited Disease, 8th ed. McGraw-Hill, New York, pp 1601–1622

Strømme P, Maehlen J, Strøm EH, Torvik A (1991) Postmortem findings in two patients with the carbohydrate-deficient glycoprotein syndrome. Acta Paediatr Scand Suppl 375:55–62
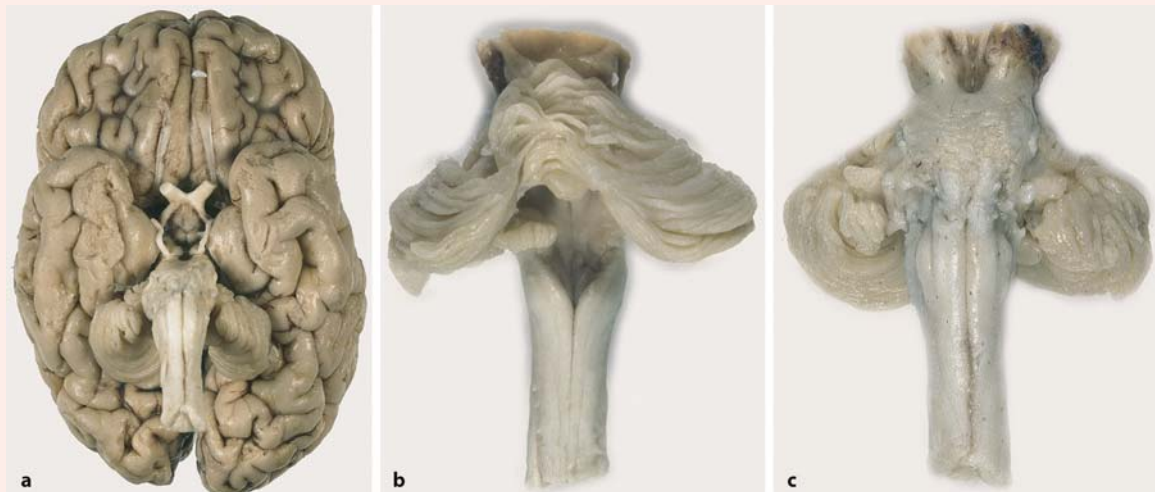
Fig. 3.17 CDG-1a case in a 15-year-old boy: **a** basal view of the brain; **b, c** dorsal and ventral views of the brain stem and cerebellum
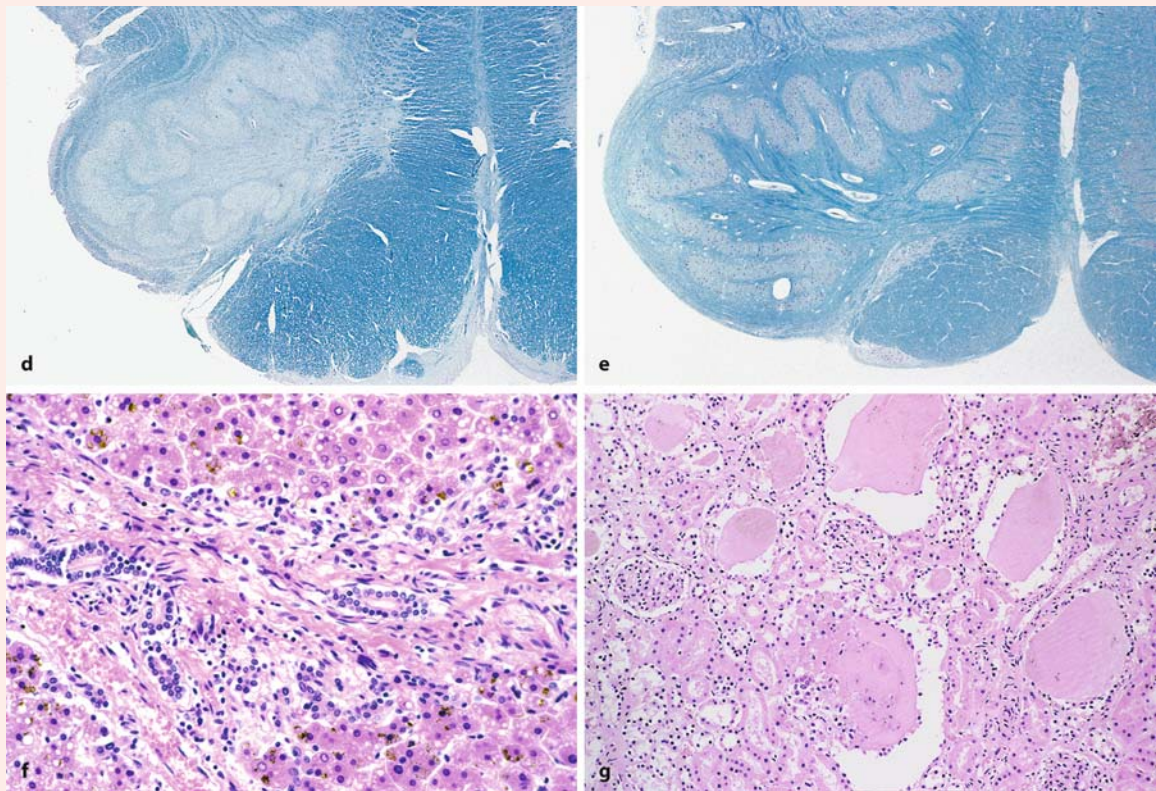
Fig. 3.17 *(Continued)* **d**, **e** Luxol Fast Blue stained sections of the inferior olive in this case and a control, respectively; **f** steatotic and mildly fibrotic liver; **g** cystically enlarged tubuli in the kidney (courtesy Gerard van Noort, Enschede)

involving different organ systems. *CHILD syndrome*, an acronym for congenital hemidysplasia, ichthyosiform erythroderma and limb defects, is characterized by unilateral ichthyotic skin lesions with a sharp demarcation at the midline of the trunk (Happle et al. 1980). *Desmosterolosis* shows a variable phenotype ranging from macrocephaly to microcephaly with facial and limb malformations (FitzPatrick et al. 1998; Haas et al. 2001; Waterham et al. 2001). *Smith–Lemli–Opitz syndrome* (*SLOS*) is an autosomal recessively inherited, multiple malformation syndrome, characterized by retardation, syndactyly and hypogenitalism (Smith et al. 1964; Opitz et al. 1969; Cunniff et al. 1997; Kelley and Hennekam 2000). The face of SLOS patients is distinct and characterized by microcephaly, bitemporal narrowing, hypertelorism, ptosis, a short nasal root, anteverted nares and micrognathia. Characteristic skeletal abnormalities include postaxial polydactyly and syndactyly of the second and third toes, and limb shortness. Hypogenitalism

ranges from cryptorchidism to apparent complete sex reversal. Cardiac malformations are common (Liu et al. 1997). Common CNS malformations include hypoplasia or aplasia of the corpus callosum, hypoplasia of the frontal lobes, and cerebellar hypoplasia, especially of the vermis (Cherstvoy et al. 1975; Fierro et al. 1977; Marion et al. 1987). Congenital sensorineural hearing deficits may affect about 10% of patients (Ryan et al. 1998), and some form of holoprosencephaly, from a small midline notch of the upper lip to semilobar holoprosencephaly, occurs in about 5% of patients (Kelley et al. 1996). Irons et al. (1993) noted that patients with SLOS had a more than a 100-fold increase in the plasma level of 7-dehydrocholesterol, the immediate precursor of cholesterol. A few years later, Moebius et al. (1998) cloned the human DHCR7 gene, localized it to chromosome 11q12-13, and subsequently mutations of DHCR7 causing SLOS were found (Fitzky et al. 1998; Moebius et al. 1998; Wassif et al. 1998; Waterham et al. 1998).
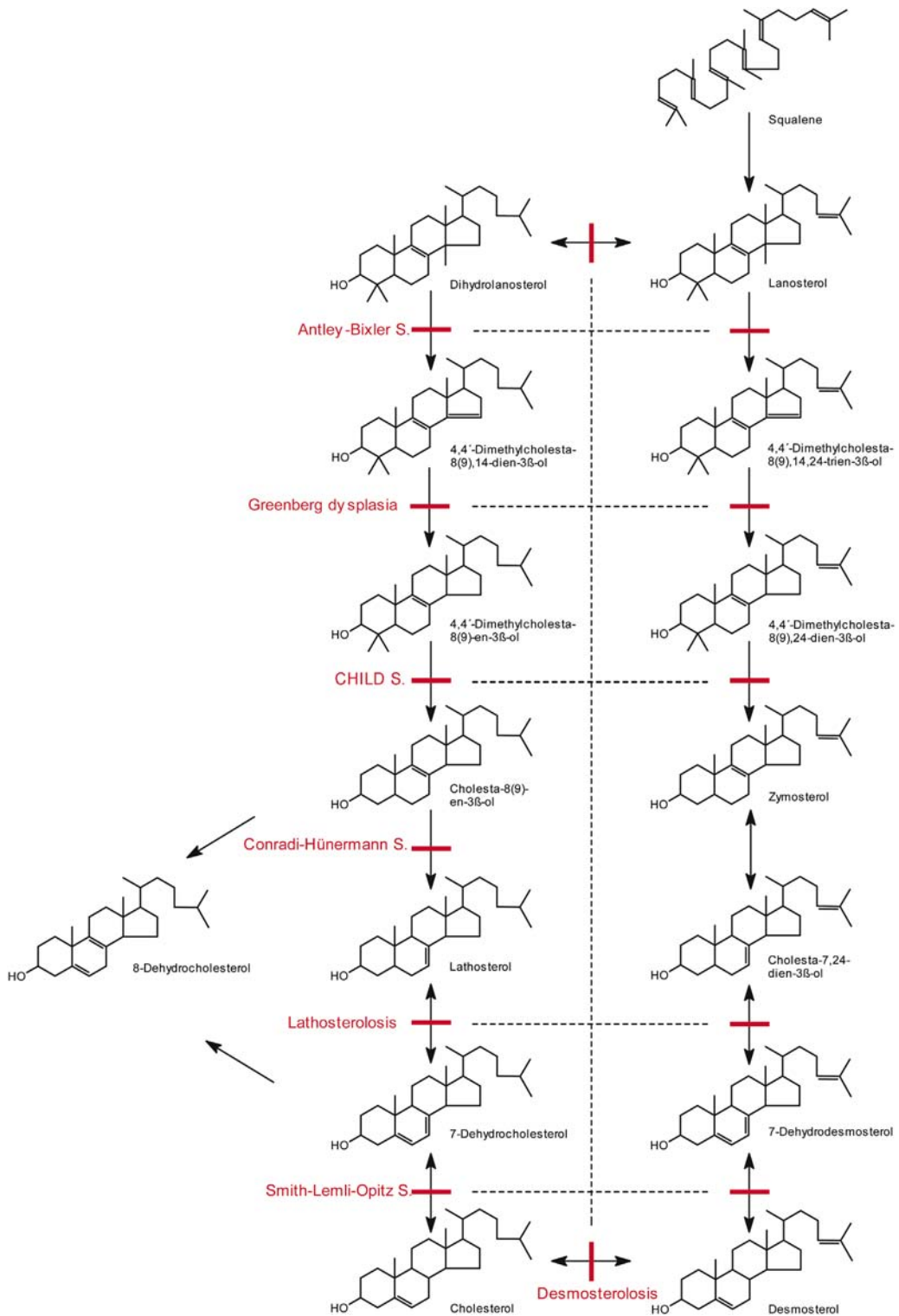
Fig. 3.18 Pathway of cholesterol biosynthesis. This pathway is used with informed agreement of Drs. D. Haas, J.G. Okun (both of the University Children's Hospital Heidelberg, Germany), and R.I. Kelley (Johns Hopkins University, Kennedy Krieger Institute, Baltimore, USA)

Disorders of Peroxisomal Structure and Function

Peroxisomes are roughly spherical organelles bound by a single lipid bilayer to the intracellular membrane. Their enzymatic abilities include roles as oxidases, in ether lipid synthesis, and in cholesterol and dolichol biosynthesis. The disorders of peroxisome biosynthesis have been divided into 11 complementation groups (Moser et al. 1995). Groups 1–10 are associated with the phenotypes of *Zellweger syndrome* (Gould et al. 2001; Wanders et al. 2001; Clinical Case 3.6), neonatal adrenoleukodystrophy or infantile Refsum disease, which are now thought to represent variants with different severity of the same disorder (Moser et al. 1995). Group 11 is associated with the rare rhizomelic chondrodysplasia punctata phenotype.

3.5   Myelination Disorders

Myelination is the final phase in the development of the cerebral white matter. In the CNS, myelin is produced by oligodendrocytes. Flat processes, extending outwards from the oligodendrocyte cell body, are being wrapped around axons in a spiral fashion and so form myelin. As a rule myelination in the CNS occurs along a caudal to rostral gradient (Chap. 1). Most of the myelination of the forebrain takes place after birth. MRI assessment of myelination patterns in children can be performed to score functional maturity of the brain (van der Knaap and Valk 1990, 1995; Sie et al. 1997). Primary absence of central myelination has not been described so far. Even patients with a null mutation of the major CNS myelin protein, the proteolipid protein 1, as found in Pelizaeus–Merzbacher disease, do show light microscopical presence of myelin even at adult age (Koeppen and Robitaille 2002). *Pelizaeus–Merzbacher disease* is the prototype of a central hypomyelinating disorder (Fig. 3.20), and is due to mutations of the *proteolipid protein* (*PLP*) gene on chromosome Xq22 (Inoue et al. 1996; Koeppen and Robitaille 2002; Chap. 2).

Several inherited metabolic diseases have their principal target in the cerebral white matter and are generally called *leukodystrophies*. They include diseases such as globoid cell leukodystrophy (Krabbe disease), metachromic leukodystrophy and adrenoleukodystrophy (Ruggieri 1997; Aicardi 1998). Early in the disease course, their clinical picture is generally dominated by bilateral and slowly progressive motor manifestations such as spasticity and ataxia. Cognitive and behavioural deterioration and epileptic phenomena usually appear at a later time and remain overshadowed by motor disturbances for a long time. *Congenital white matter hypoplasia* has also been reported without evidence of demyelination, dysmyeli-nation or degeneration of cortical neurons (Chattha and Richardson 1977; Lyon et al. 1990), and may possibly be due to a primary defect of axonal development. Recently, the so-called *vanishing white matter disease*, originally descibed as occurring only in children older than 1 year of age and in adults (van der Knaap et al. 1997), has been found to start prenatally (van der Knaap et al. 2003). Autopsy of one of the nine patients originally described confirmed MRI findings (van der Knaap et al. 1997) of extensive cystic degeneration of the cerebral white matter with reactive changes and a preserved cortex. Moreover, typical involvement of the pontine tegmental white matter was observed. This autosomal recessive disorder is due to mutations in one of the five subunits of the translation initiation factor eIF2B, located on chromosome 3q27 (Leegwater et al. 1999, 2001; van der Knaap et al. 2002; Clinical Case 3.7). The neurological signs of vanishing white matter disease include cerebellar ataxia, spasticity, inconstant optic atrophy and a usually relatively mild mental decline. The disease is chronically progressive, with in most patients episodes of rapid deterioration following febrile infections and minor head trauma. Death occurs after a variable period of a few months to a few decades. MRI findings are diagnostic, showing a diffuse abnormality of the cerebral white matter (van der Knaap 1997, 2002).

3.6   Vascular Disorders

The developing brain is vulnerable to various vascular disturbances during pregnancy. The resulting brain lesions are not only dependent on the severity of the particular disturbance but correlate also with the developmental state of the brain. The cause of ischemia or hypoxia may be maternal, placental, fetal or a combination of these factors. Early in gestation, general hypoxia may lead to very severe brain malformations such as porencephaly and hydranencephaly. *Porencephaly* was originally defined as a smooth-walled cyst with communication between the ventricle and the subarachnoid space due to circumscribed hemispheric necrosis that occurs in utero or before the adult features of the hemisphere are manifest (Friede 1989; Norman et al. 1995; Clinical Case 3.8). This term is often used more widely, particularly by neuroradiologists, who include unilateral enlargement of the lateral ventricles. *Hydranencephaly* means the destruction of the cerebral hemispheres, usually the bilateral territories of supply of the internal carotid arteries, combined with hydrocephalus due to aqueduct stenosis (Fig. 3.23). In both types of brain injury a varying part of the basal ganglia and the thalamus are also involved (Norman et al. 1995). When the fetus survives such serious

Clinical Case 3.6
Zellweger Syndrome

Zellweger syndrome is an early lethal multisystem disorder with deficient peroxisomes, and is characterized by cerebrohepatorenal malformations due to defective β-oxidation of very long chain fatty acids (Moser et al. 1984). Definitive diagnosis is made by demonstration of increased levels of very long chain fatty acids in plasma or cultivated fibroblasts (Gould et al. 2001; Wanders et al. 2001). Clinical features include dysmorphic facies, deafness, congenital cataract, hepatomegaly, gastrointestinal bleeding, hypotonia and seizures (see Case Report).

Case Report. The girl was the first child of nonconsanguineous parents, born at 40.5 weeks of gestation. Her weight was 2,500 g (P5), and her head circumference was 33 cm (P3). There were dysmorphic signs: a broad nasal bridge, low-set ears, a high forehead, a small chin, Simian crease, joint contractures of the lower limbs and bilateral congenital cataract. The baby was hypotonic. There was hepatomegaly. X-ray examination of the knees showed stippled patellar calcifications. Abdominal ultrasound examination showed renal cortical cysts. There was severe epilepsy and poor psychomotor development. The clinical diagnosis of Zellweger syndrome was confirmed by the demonstration of deficiency of per-
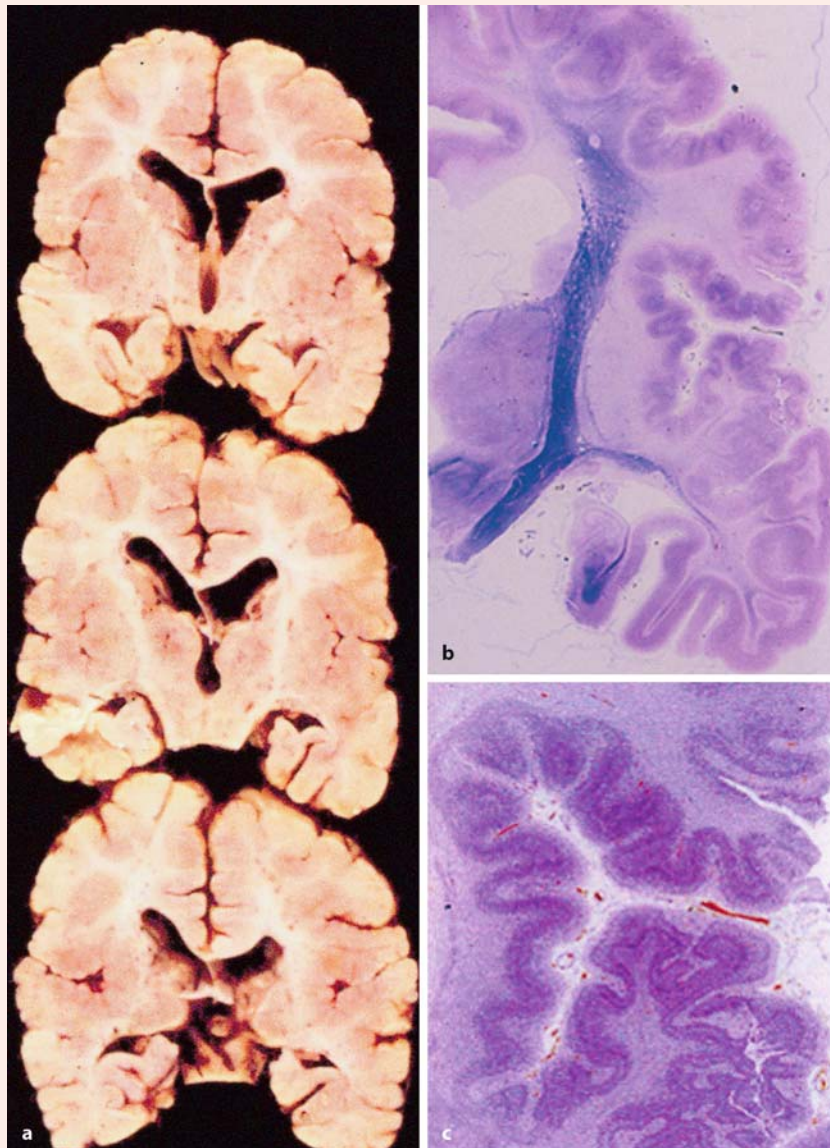
Fig. 3.19 Zellweger syndrome, showing bilateral polymicrogyria in frontal sections of the brain:
a overview of three slices; note hypoplastic corpus callosum and periventricular cavity on the left side;
b, **c** Luxol Fast Blue stained sections of the insular region (courtesy Martin Lammens, Nijmegen)

oxisomal enzymes such as palmitoylcoenzyme A oxidase and glycolate oxidase, by the presence of phytanic acid (1.21 Ìg/ml), by the increase of very long chain fatty acids and by electron microscopic examination of the liver which revealed absence of peroxisomes. The child died at 9 months of age. The neuropathological findings are shown in Fig. 3.19. Brain weight was 940 g (range 820±49 g). The cerebrum showed bilateral polymicrogyria, especially pronounced in the insular region of the temporal lobe, whereas the middle and lower temporal gyri were normal. The corpus callosum was hypoplastic. A periventricular cavity was found on the left side. On microscopy, there was hypomyelination and widespread gliosis of the white matter. The polymicrogyric cortex showed some vertical lamination, with vertically oriented strands of neurons present in the underlying white matter. A few glioneuronal ectopia were present in the insular leptomeninges. The plump inferior olives showed an abnormal gyration pattern with very sparse undulations. Material for further molecular biological examination was not available.

This case was kindly provided by Mark D'hooghe (General Hospital St. Jan, Bruges, Belgium).

References

Gould SJ, Raymond GV, Valle D (2001) The peroxisome biogenesis disorders. In: Scriver CR, Beaudet AL, Sly WS, Valle D (eds) The Metabolic & Molecular Bases of Inherited Disease, 8th ed. McGraw-Hill, New York, pp 3181–3218

Moser AE, Singh I, Brown FR, Solish GI, Kelley RI, Benke PJ, Moser HW (1984) The cerebro-hepato-renal (Zellweger) syndrome. Increased level and impaired degradation of very-long-chain fatty acids and their use in prenatal diagnosis. N Engl J Med 310:1141–1146

Wanders RJA, Barth PG, Heymans HSA (2001) Single peroxisomal enzyme deficiencies. In: Scriver CR, Beaudet AL, Sly WS, Valle D (eds) The Metabolic & Molecular Bases of Inherited Disease, 8th ed. McGraw-Hill, New York, pp 3219–3256

Fig. 3.20 MRI (T2-weighted) of **a** a normal 2-year-old child and **b** a child with Pelizaeus–Merzbacher disease (courtesy Henk O.M. Thijssen, Nijmegen)
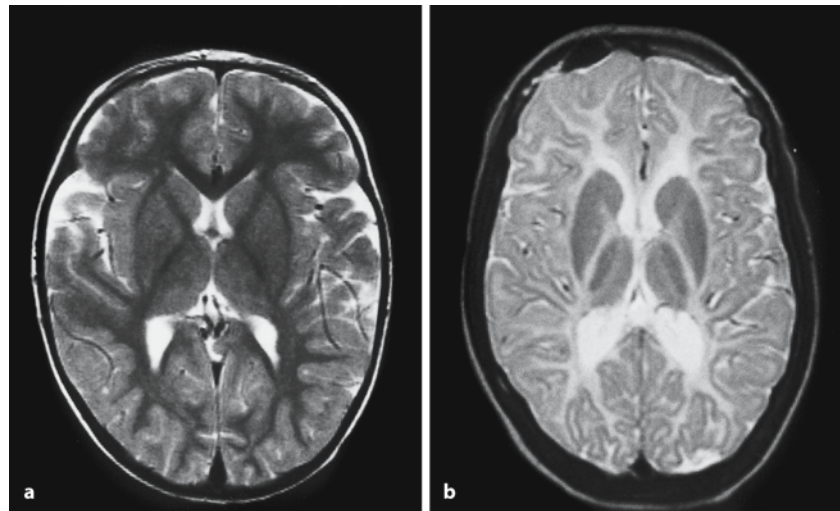
lesions, additionally polymicrogyria and other malformations may be seen, the extent of the lesion again is dependent on the developmental state of the fetus.

An important cause of intrauterine ischemic cerebral damage may be seen in monochorionic twins in which, owing to placental shunting (Arts and Lohman 1971; Eberle et al. 1993; Benirschke and Kaufman 1995), *twin-to-twin transfusion* leads to shortage of blood in one fetus and surplus of blood in the other (Clinical Case 3.9). There are several reports of polymicrogyria in monozygotic twins (Norman 1980; Barth and van der Harten 1985; Larroche et al. 1994). In their cases, Barth and van der Harten (1985) dated the appearance of polymicrogyria in monozygotic twins to the 13th to 16th weeks of gestation. Bordarier and Robain (1995) described a case of dizygotic twins in which both parts showed cerebral damage.

Periventricular haemorrhage, most often synonymous to germinal matrix haemorrhage, represents an important midterm pathology (Fig. 3.25 a). Although classically seen in very low birthweight infants with less than 24 weeks of gestation or in sick premature neonates owing to disturbed autoregulation of cerebral blood flow, it may also occur during intrauterine life (de Vries et al. 1998a) and may be associated with

Clinical Case 3.7
Vanishing White Matter Disease

In two MRI-defined white matter disorders, megalocephalic leukoencephalopathy with subcortical cysts and vanishing white matter, the gene defects have been identified (Leegwater et al. 2001; van der Knaap et al. 2002, 2003). ***Vanishing white matter disease*** (***VWMD***) usually has its onset in late infancy or early childhood, but onsets in early infancy, have also been described. The youngest case reported so far is presented as the Case Report. Mutations in each of the five subunits of the translation initiation factor eIF2B can cause VWMD.

Case Report. The second child, a girl, of a consanguineous Turkish family was born at 38 gestational weeks after a prenatal history of severe and progressive intrauterine growth retardation since the 26th gestational week. At birth, there was microcephaly and the infant had a drop hand. The neurological status of the baby deteriorated progressively with loss of most neurological functions. She died at 3 months of age. MRI showed severe hypomyelination. Autopsy confirmed the diagnosis vanishing white matter disease. The first child in this family, a boy, had a comparable clinical history and died at 4 months of age. In both infants, a homozygous mutation in the delta subunit of eIF2B4 was found. At autopsy, the microcephalic brain showed a normal gyral pattern and a hypoplastic cerebellum. The white matter of the cerebral hemispheres had a grey colour, it was diffusely very weak and focally cystic (Fig. 3.21). The central white matter of the cerebellum was less affected. On microscopic examination, there was severe diffuse degeneration of the myelin in the centrum semiovale and to a lesser degree in the cerebral hemispheres, the pyramidal tracts and the cerebellar hemispheres. Mild degeneration was found in the basal ganglia and the brain stem. In the severely affected parts of the brain, complete absence of myelin with relatively little myelin debris was observed.

This case was kindly provided by Caroline Van den Broecke and Rudy Van Coster (University Hospital, Gent, Belgium).

References

Leegwater PAJ, Vermeulen G, Könst AAM, Naidu S, Mulders J, Visser A, Kersbergen P, Mobach D, Fonds D, van Berkel CGM, et al. (2001) Subunits of the translation initiation factor eIF2B are mutated in leukoencephalopathy with vanishing white matter. Nat Genet 29:383–388

van der Knaap MS, Leegwater PAJ, Könst AAM, Visser A, Naidu S, Oudejans CBM, Schutgens RBH, Pronk JC (2002) Mutations in each of the five subunits of translation initiation factor eIF2B can cause leukoencephalopathy with vanishing white matter. Ann Neurol 51:264–270

van der Knaap MS, van der Voorn P, Barkhof F, Van Coster R, Krägeloh-Mann I, Feigenbaum A, Blaser S, Vles JSH, Rieckmann P, Pouwels PJW (2003) A new leukodystrophy with brain stem and spinal cord involvement and high lactate. Ann Neurol 53:252–258
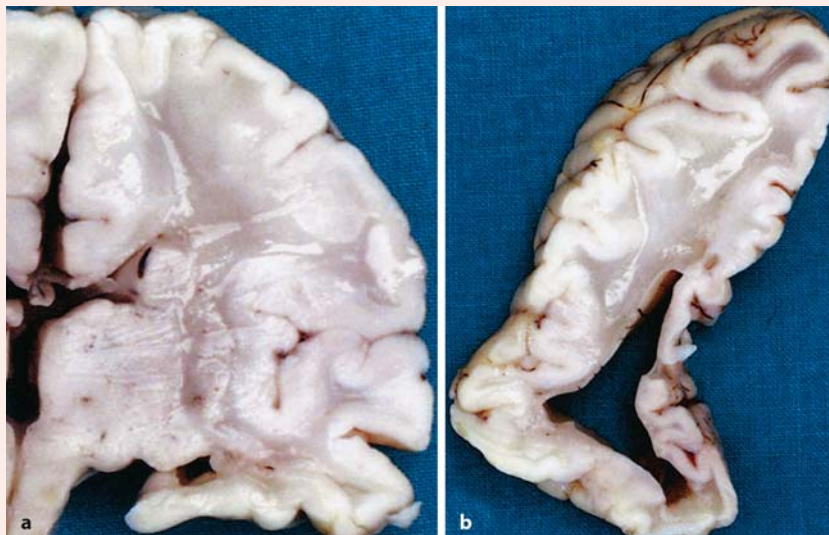
Fig. 3.21 Frontal sections through the frontal and temporal lobes (**a**) and the occipital lobe (**b**) in a fetal case of vanishing white matter disease (courtesy Caroline Van den Broecke, Gent)

Porencephaly

Porencephaly is a severe brain malformation, usually occurring early in gestation owing to general hypoxia (see Case Report).

Case Report. The second child of healthy parents with a normal first child presented with a severe encephalopathy. MRI made in the third week after birth showed extensive defects in both cerebral hemispheres, particularly of the frontoparietal lobes, dilatated lateral ventricles and severe cerebellar hypoplasia (Fig. 3.22 a–d). No cerebral aqueduct could be identified. The boy died at the age of 3 months. At autopsy, brain weight was 280 g. Both hemispheres showed large defects, especially in the insular region, with polymicrogyria around the borders of the defects (Fig. 3.22 e). Aqueduct stenosis, a small, artificially torn corpus callosum, extremely reduced cerebellar hemispheres and absent pyramids (Fig. 6.35 e) were found.
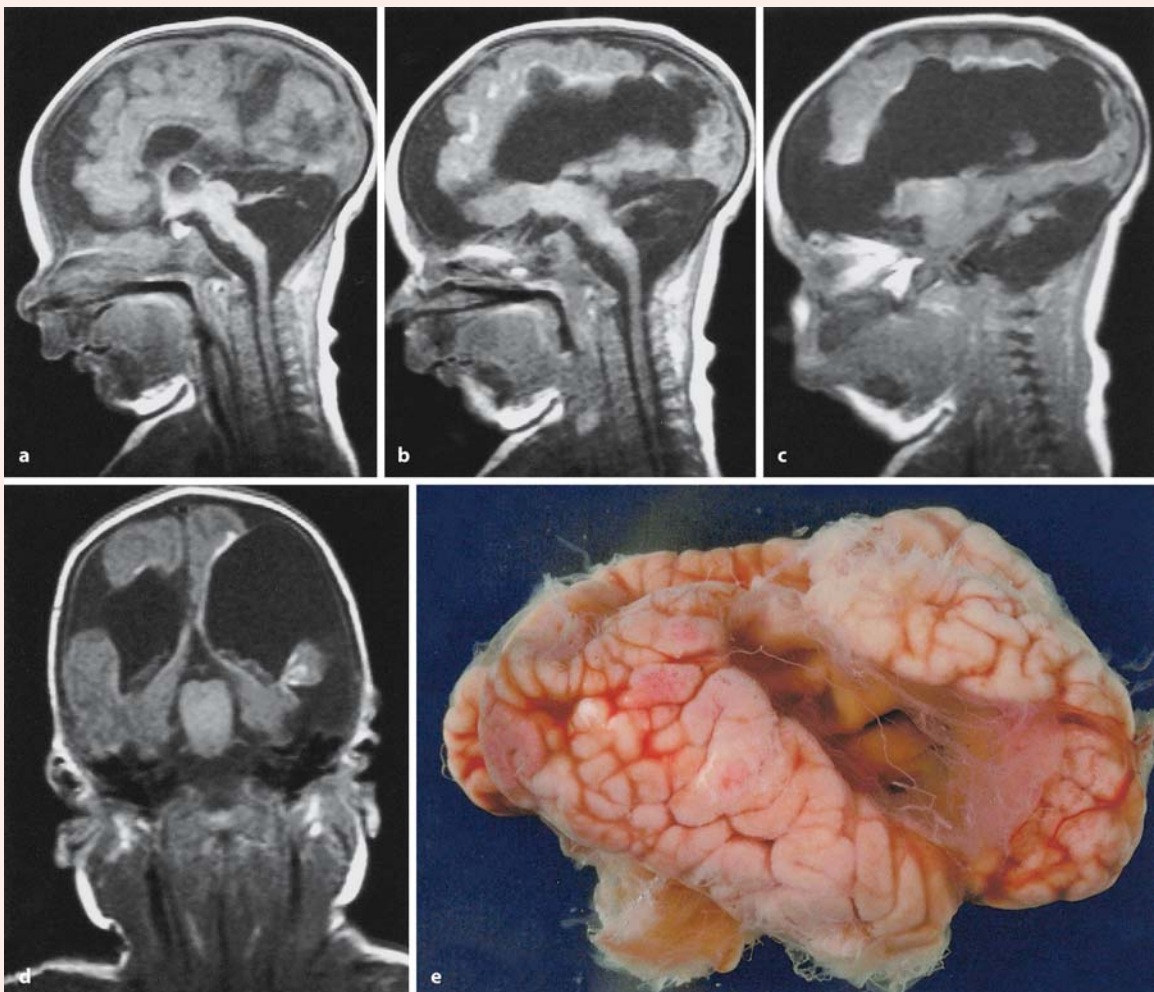
Fig. 3.22 Porencephaly in a 3-month-old male infant: **a**–**c**, sagittal MRI; **d** coronal MRI; **e** lateral view of the brain (courtesy Michèl Willemsen and Pieter Wesseling, Nijmegen)

Fig. 3.23 Hydranencephaly due to intracranial haemorrhage in a term baby who survived 4 days: **a** basal view of brain; **b** coronal section of the cerebrum; **c** section through the cere-bral cortex (from the Department of Neuropathology, Medizinische Hochschule Hannover; courtesy Akira Hori)

amniotic sac inflammation (Hansen and Snyder 1998). Other risk factors are clotting disorders. The periventricular haemorrhage may extend into the ventricle and ultimately give rise to hydrocephalus by blocking the narrow ventricular and arachnoidal pathways for CSF (Jackson and Blumhagen 1983; Hill and Rozdilsky 1984; Weindling 2002). It may also extend into the brain parenchyma and even give rise to infarction of the adjacent white matter. The latter will usually be haemorrhagic by obstruction of the draining veins (de Vries et al. 2001; Volpe 2001b). This is referred to as *periventricular venous infarction* (*PVI*). It provokes intraparenchymatous echodensity (IPE). In 10–15% of all preterm infants with a germinal matrix-intraventricular haemorrhage, a unilateral IPE occurs which leads to contralateral hemiplegia in two thirds of these patients (de Vries et al. 1998b). Recently, Takanashi et al. (2003) described five children born at term with congenital hemiplegia whose magnetic resonance images were compatible with PVI. This suggests that a clinically silent PVI in utero can lead to congenital hemiplegia at term. In contrast to *periventricular leukomalacia* (*PVL*), congenital hemiplegia is usually unilateral.

During the last trimester of pregnancy (26–36 weeks of gestation), the developing white matter is especially vulnerable to hypoxic–ischemic injuries.

The resulting lesions are known as *periventricular white matter disease.* The term periventricular leukomalacia is used for the state in which the periventricular white matter is destroyed and resorbed during the perinatal period in premature infants. The ischemia may be aggravated by the specific anatomical and physiological circumstances of the premature infant. Studies on the anatomy of the vascular supply to the white matter suggested that the deep white matter represented a watershed territory in this period (De Reuck et al. 1972). In a detailed anatomic study, Kuban and Gilles (1985) failed to demonstrate such a watershed zone (Nelson et al. 1991; Rorke 1992). Blood-flow studies showed that arterial flow to the white matter is low at this developmental period (Borch and Greisen 1998; Weindling 2002), and that blood vessel density in the white matter is lower between 28 and 36 weeks than in earlier or later periods of development (Miyawaki et al. 1998; Weindling 2002). More recently, the importance of intrauterine infection, resulting in elevation of proinflammatory cytokines, such as interleukin-6, interleukin-1β and tumour necrosis factor-α, has been emphasized (Kadhim et al. 2001). Another important factor, contributing to the vulnerability of the prenatal white matter, may be the intrinsic vulnerability of the developing oligodendroglial cells. Oligodendroglia

Clinical Case 3.9
Twin-to-Twin Transfusion

Twin-to-twin transfusion may lead to serious defects in the brain of one of the twins (see Case Report). Owing to abnormal blood shunting between the placentae in monochorionic biamniotic twins, perfusion failure may occur. This may result in cerebral damage, the extent of which is dependent on the state of development of the fetus. Polymicrogyria is commonly one of the characteristic malformations (Barth and van der Harten 1985; Larroche et al. 1994).

Case Report. This was the second pregnancy of nonsanguineous parents with one healthy child of 1 year old. Of the monozygotic twins, the female patient was severely affected, the second twin was completely normal. During pregnancy, disproportionate growth was noted and fetal movements were almost absent. At 27 weeks of gestation, polyhydramnios was recognized on ultrasound examination, and 2,000 ml of amniotic fluid was removed through amnion punctures in two sessions. The patient was born at 29 weeks of gestation and died a few minutes after birth owing to lung hypoplasia. The second of the twins was briefly admitted to the neonatal intensive care unit, but did well and showed no congenital malformations. The placenta was monochorionic and biamniotic. There was only one umbilical artery in the first twin and a velamentous insertion of its umbilical cord.

The weight of the girl was 730 g (less than P3). There was hyperextension of the neck and multiple joint contractures were evident. The elbows were fixed in flexion, whereas the hips were fixed in extension. There was clinodactyly and camptodactyly, the knees were extended with genua recurvata. On the left side a pes equinovarus was present, and on the right side a pes calcaneovarus. There was severe scoliosis. The lungs were very hypoplastic (5.6 g). General autopsy further revealed a small stomach, multiple renal cortical cysts and hepatomegaly. Brain weight was 120 g (normal range 174±38 g). On the lateral surface of the brain bilateral polymicrogyria was noted (Fig. 3.24). Microscopic examination showed that the polymicrogyric cortex was severely disrupted. No layering of neurons whatsoever could be observed. Ectopic groups of neuroglial cells were found in the meninges. The brain stem was quite normal. There was no dysplasia of either the inferior olives or the dentate nuclei.
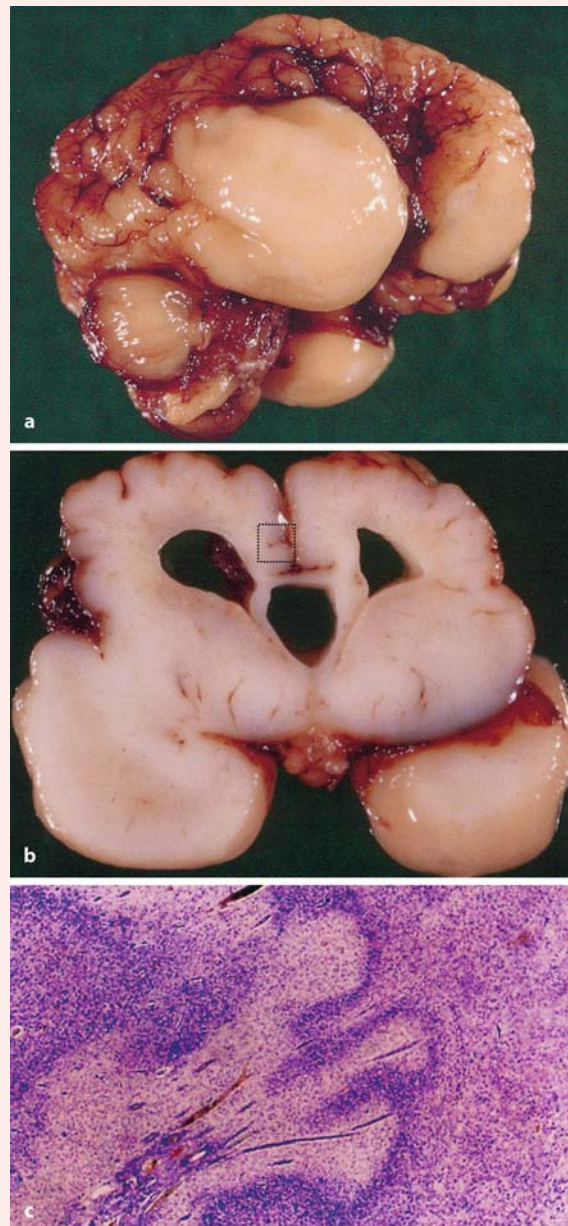
Fig. 3.24 Lateral view (**a**), frontal section (**b**) and detail of polymicrogyric cortex (**c**) in a case of twin-to-twin transfusion (courtesy Martin Lammens, Nijmegen).

References

Barth PG, van der Harten JJ (1985) Parabiotic twin syndromes with topical isocortical disruption and gastroschisis. Acta Neuropathol (Berl) 67:345–349

Larroche JC, Girard N, Narcy F, Gallet C (1994) Abnormal cortical plate (polymicrogyria), heterotopias and brain damage in monozygous twins. Biol Neonate 65:343–352

have glutamate receptors and may be damaged by excess glutamate release when neural tissue is damaged by ischemia (Kinney and Back 1998; McDonald et al. 1998; Volpe 2001a, b). Three patterns of white matter damage, PVL, telencephalic leukoencephalopathy, and multicystic leukoencephalopathy, represent a spectrum of severity of damage (Volpe 2001a, b; Squier 2002). Macroscopically, PVL is characterized by small areas of necrosis in the deep white matter (Fig. 3.25b). The lesions appear yellow owing to calcium deposition and may become cavitated and cystic. Microscopically, in PVL widespread glial proliferation and capillary reactive changes are found. There is often axonal damage adjacent to areas of infarction. The term *telencephalic leukoencephalopathy* is used to describe diffuse reactive changes throughout the white matter of the cerebral hemispheres without focal infarction or cyst formation. In *multicystic leukoencephalopathy*, the white matter contains many large cysts which may almost completely replace it (Clinical Case 3.10).

In neonates, haemorrhages are frequently found in the brain. The most frequent is subventricular haemorrhage, but if isolated it most often has no consequences (Volpe 2001a). An extensive isolated subarachnoidal bleeding in a neonate should raise suspicion for additional factors such as clotting disorders, of which *neonatal alloimmune thrombocytopenia* (*NAIT*) is the most frequent at this age (Clinical Case 3.11). This form of neonatal thrombocytopenia affects 1 per 1,000–2,000 deliveries (Müller-Eckhardt et al. 1989) with a mortality up to 14% (Smith 2001). Infants may present with porencephaly or postdelivery intracranial haemorrhage. The cause of NAIT is incompatibility of the human platelet antigen-1 (HPA1) system in 80% of European women, with a negative mother carrying a positive fetus expressing the antigen inherited from the father. Alloantibody to HPA-5b represents a relatively common cause of NAIT in Europe but results in less severe disease, and only rarely in intracranial haemorrhage and death (Herrero et al. 2003). HPA-4a induced NAIT is often severe but occurs almost exclusively among Asian populations (Glade-Bender et al. 2001). HPA-3a incompatibility represents less than 1% of documented cases of NAIT but is similar in severity to disease caused by incompatibility of HPA-1a (Glade-Bender et al. 2001). Unlike Rhesus-incompatibility pregnancies, the first pregnancy is often affected. Isolated plexus haemorrhages most often are of no consequence.

Vascular malformations such as an *aneurysm* of the *vein* of *Galen* are rare and other arteriovenous malformations only rarely provoke intrauterine problems. Besides rare haemorrhages, malformation of the vein of Galen may also lead to important cerebral damage and ultimately brain atrophy due to is-
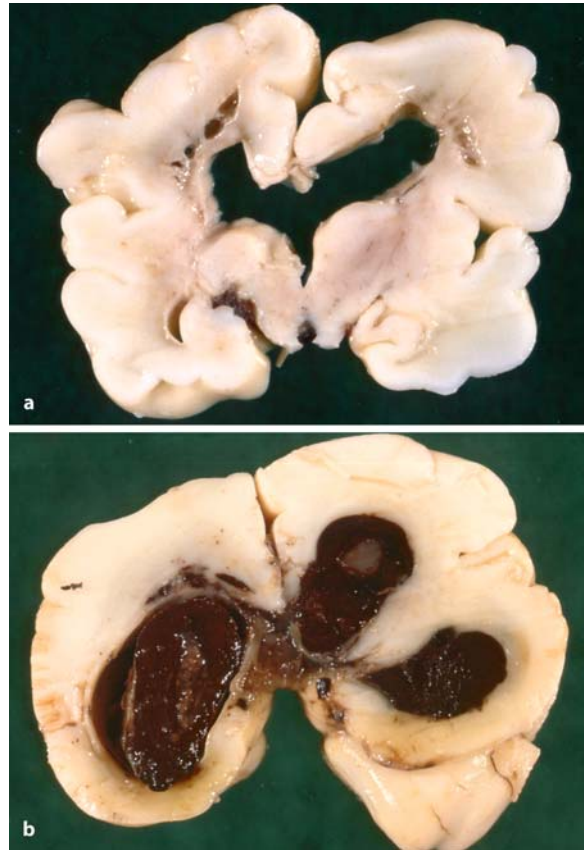
Fig. 3.25 Periventricular leukomalacia (**a**) and periventricular haemorrhage (**b**). See text for explanation

chemic complications (Norman and Becker 1974). They are most likely due to steal phenomena, leading to hypoperfusion in some adjacent or even remote parts of the brain (Grossman et al. 1984; Raybaud et al. 1989).

Focal arterial infarctions due to obstruction of a single cerebral artery are a rare phenomenon early in life. Estimates from brain imaging suggest an incidence of 0.2–0.35 per 1,000 neonates (Govaert et al. 2000). *Perinatal ischemic stroke*, defined as a cerebrovascular event around the time of birth with pathological or radiological evidence of focal arterial infarction, is largely a disorder of term or near-term infants (de Vries et al. 1997; Govaert et al. 2000; Nelson and Lynch 2004). The middle cerebral artery is most often involved. The left hemisphere is more frequently affected than the right, probably owing to haemodynamic differences from a patent ductus arteriosus (Trauner et al. 1993). Perinatal-stroke risk factors include cardiac, blood, homocystein and lipid disorders, infections, maternal and placental diseases, and iatrogenic interventions such as catheterization and extracorporeal membrane oxygenation (Nelson and Lynch 2004). Although rare, perinatal stroke can also

Clinical Case 3.10
Multicystic Leukoencephalopathy

Multicystic leukoencephalopathy is the most severe form of white matter damage (Volpe 2001; Squier 2002), in which the white matter is largely replaced by cysts (see Case Report). The lesions of the grey matter in this case are typical for an episode of complete asphyxia in a full-term neonate. They consist of severe necrosis of the deep brain nuclei, the neocortex and the hippocampus. The reason for the perinatal asphyxia was not entirely clear, but was probably placental in origin.

Case Report. After an uneventful pregnancy, birth at full term at home presented unexpected difficulties. Deteriorating heart tones resulted in the transport of the mother to the hospital. Owing to traffic problems, transport took more than 1 h, after which a boy was born with low Apgar scores. Epileptic fits were present from the first day but no spontaneous movements were noted. MRI after 1 month showed severe leukomalacia. The infant died after 1 week of fluid refusal at 6 weeks of age. At autopsy, brain weight was 300 g. There was complete neuronal loss of the deep nuclei (Fig. 3.26 a), including the basal ganglia and the thalamus, with severe gliosis and partial pseudocystic necrosis of these nuclei. Large parts of the neocortex were also severely necrotic with sparing of the occipital lobes. The top of each sulcus affected was always better preserved than its base. Ultimately, this necrosis would result in ulegyria. On both sides, the hippocampus and the subiculum were almost completely necrotic. In the cerebellum partial loss of Purkinje cells and of some cells in the dentate nuclei was found. The supratentorial white matter was almost completely necrotic except for part of the occipital white matter, leading to porencephaly. The white matter of the cerebellum and the brain stem was partly gliotic, but better preserved than the supratentorial parts. The meningeal arteries showed distinct intima fibrosis and calcification of the inner part of the media (Fig. 3.26 b).

References

Squier W (2002) Pathology of fetal and neonatal brain damage: Identifying the timing. In: Squier W (ed) Acquired Damage to the Developing Brain: Timing and causation. Arnold, London, pp 110–127

Volpe JJ (2001) Neurology of the Newborn, 4th ed. Saunders, Philadelphia, PA
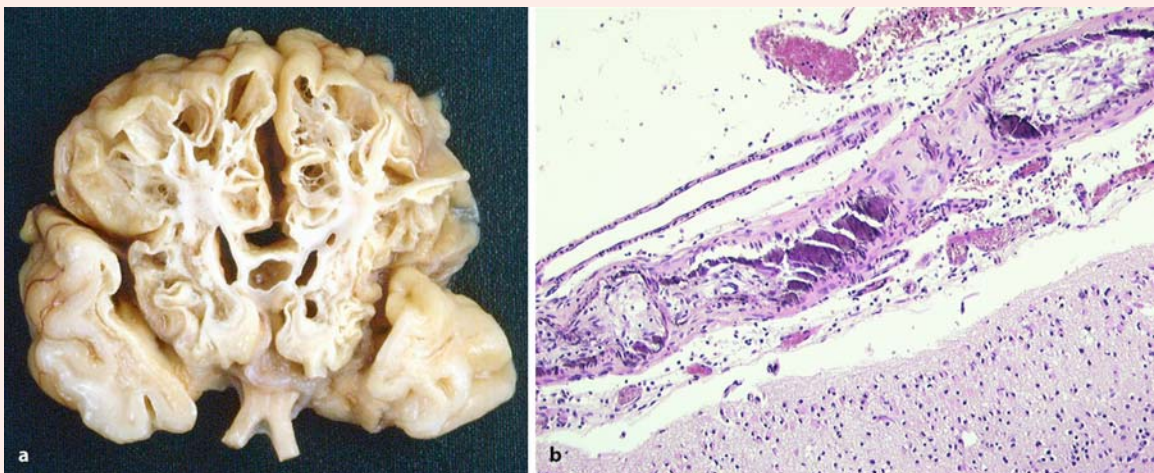
Fig. 3.26 Multicystic leukoencephalopathy: **a** frontal section through the frontal and temporal lobes; **b** intima fibrosis and media calcification of meningeal arteries (courtesy Martin Lammens, Nijmegen)

occur in term infants with neonatal encephalopathy, owing to underlying infections or endocrine disorders of the mother (Ramaswamy et al. 2004).

Generalized ischemic or perfusion failure may lead to *selective necrosis* of particular groups of neurons. The selective vulnerability of neuronal groups is dependent on regional vascular and metabolic factors (Volpe 2001b). The so-called *watershed infarct*, in which neuronal injury is more prominent in border zones between vascular territories, is the most prominent example of regional vascular factors. This may explain the parasagittal cerebral injury at the

Clinical Case 3.11
Neonatal Alloimmune Thrombocytopenia

Extensive isolated subarachnoidal bleeding in a neonate is often due to **neonatal alloimmune thrombocytopenia**. A case of fetomaternal alloimmune thrombocytopenia due to HPA-5b incompatibility came to autopsy (see Case Report).

Case Report. During the first pregnancy of a mother with Sjögren syndrome, intrauterine growth retardation of the fetus was observed at 31 weeks of gestation. Caesarean section was carried out because of a deteriorating cardiotocogram, and a boy of 1,180 g and 39-cm length was born. Apgar scores were 8 and 9, and no meconium-staining of the amniotic fluid was found. The placenta showed no abnormalities. A few hours later, the boy was transferred to a university hospital because of acute respiratory failure. His clinical condition rapidly deteriorated. Ultrasound examination showed a massive intracranial haemorrhage. The boy died 22 h after birth. At autopsy, brain weight was 222 g. Recent massive subarachnoidal haemorrhages were found at the base of both temporal lobes (Fig. 3.27 b) and at the superior surface of the cerebellum. Microscopic haemorrhages were seen in the cerebral white matter, but no large intracerebral bleedings. No other abnormalities were found. In the blood of the mother immunoglobulin G antibodies against thrombocytes were found. The father appeared to be heterozygous for HPA-5a/HPA-5b. Fetomaternal alloimmune thrombocytopenia due to HPA-5b was demonstrated in the fetus and, most probably, caused the unusually large subarachnoidal bleeding.
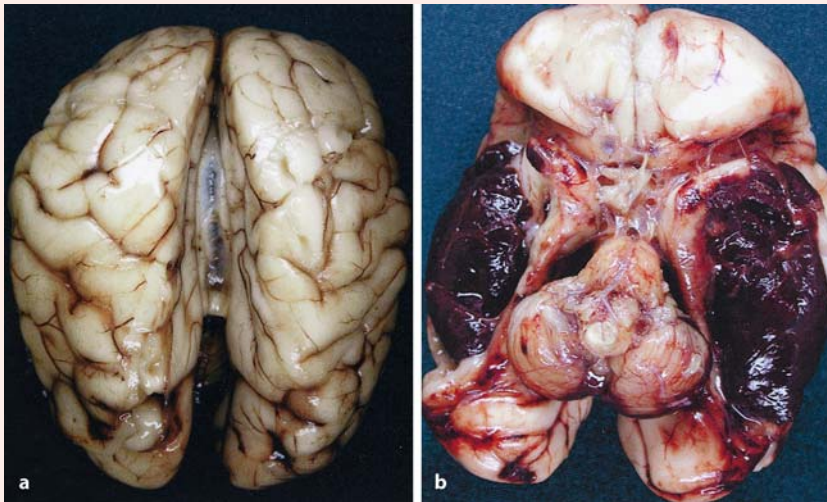
Fig. 3.27 Dorsal (**a**) and ventral (**b**) views of the brain in a case of neonatal alloimmune thrombocytopenia (courtesy Martin Lammens, Nijmegen). Note the massive subarachnoidal haemorrhages at the base of both temporal lobes

border zone between the anterior and middle cerebral artery territories, characterized by a lesion of the cerebral cortex and subcortical white matter on the parasagittal superomedial aspects of the cerebral convexities (Friede 1989; Volpe 2001b). The depths of the sulci are more vulnerable than the tops owing to the fact that they form a relatively avascular area between penetrating meningeal arteries in the near-term infant brain. This leads to ulegyria. Differences in regional distribution of glutamate receptors of the N-methyl-D-aspatate type, in metabolic rate or in NADPH-diaphorase activity are examples of regional metabolic factors which play a role in the selective vulnerability of groups of neurons in the brain stem, the striatum and the hippocampus (Chaps. 7, 9, 10).

3.7 Classifications of CNS Malformations

Traditional schemes of classifying CNS malformations are based on descriptive morphogenesis of the brain and spinal cord. Usually, neural tube defects are discussed separately. Abnormalities of the cerebral hemispheres are grossly subdivided into the prosencephalies and neuronal migration disorders. Other malformations are mostly discussed regionally, such as those of the spinal cord, the brain stem and the cerebellum. Since we discussed the development of the CNS regionally, in this book we have also followed a more or less regional approach for developmental disorders of the CNS. Recently, Sarnat (Sarnat 2000;

Table 3.8 Molecular classification of malformations of early CNS development (after Sarnat 2000)

Proposed molecular genetic classification	Further subdivision	Selected specific disorders
I. Genetic mutations expressed in the primitive streak or node	A. Upregulation of organizer genes	1. Duplication of neural tube
	B. Downregulation of organizer genes	1. Agenesis of neural tube, partial or complete
II. Disorders of ventralizing gradient in the neural tube	A. Overexpression of ventralizing genes	1. Duplication of spinal central canal 2. Duplication of ventral horns of spinal cord 3. Diplomyelia (Clinical Case 6.1) 4. Duplication of neural tube 5. Ventralizing induction of somite (segmental amyoplasia)
	B. Underexpression of ventralizing genes	1. Fusion of ventral horns of spinal cord 2. Sacral (thoracolumbosacral) agenesis (Chap. 3) 3. Arhinencephaly (Chap. 9) 4. Holoprosencephaly (Chap. 9)
III. Disorders of dorsalizing gradient of the neural tube	A. Overexpression of dorsalizing genes	1. Duplication of dorsal horns of spinal cord 2. Duplication of dorsal brain stem structures
	B. Underexpression of dorsalizing genes	1. Fusion of dorsal horns of spinal cord 2. Fusion of midbrain colliculi 3. Rhombencephalosynapsis (Clinical Case 8.1) 4. Septo-optic dysplasia (Clinical Case 9.7)?
IV. Disorders of the rostrocaudal gradient and/or segmentation	A. Increased homeobox domains and/or ectopic expression	1. Chiari II malformation
	B. Decreased homeobox domains and/or neuromere deletion	1. Agenesis of mesencephalon and metencephalon (Clinical Case 7.1) 2. Global cerebellar aplasia or hypoplasia 3. Agenesis of basal telencephalic nuclei (Chap. 9) 4. Agenesis of corpus callosum (some cases)
V. Aberrations in cell lineages by genetic mutation	A. Non-neoplastic	1. Striated muscle in CNS 2. Dysplastic gangliocytoma of cerebellum (Lhermitte–Duclos; Chap. 8) 3. Tuberous sclerosis (Chap. 10)
	B. Neoplastic	1. Myomedulloblastoma 2. Dysembryoplastic neuroepithelial tumours
VI. Disorders of secretory molecules and genes that mediate neuronal migration (Chap. 10)	A. Mediating neuro-blast migration	1. Initial course of neuroblast migration (Filamin-1: X-linked periventricular nodular heterotopia) 2. Middle course of neuroblast migration (subcortical laminar heterotopia or band heterotopia; Miller–Dieker syndrome; Fukuyama muscular dystrophy) 3. Late course of neuroblast migration, differentiation of cortical plate (Reelin and Disabled-related NMDs)
	B. Mediating glioblast migration	
VII. Disorders of secretory molecules and genes that attract and repel axonal growth cones	A. Netrin downregulation	*ROBO3*-deficiency (Chap. 6)
	B. Downregulation of keratan sulfate and other glycosamino-glycans	

Sarnat and Flores-Sarnat 2004) proposed a molecular genetic classification of CNS malformations. His approach is summarized in Table 3.8. The premises of this classification are as follows: (1) genetic expression in the neural tube follows gradients along the axes that are established during gastrulation (Chaps. 1, 2), vertical (dorsoventral or ventrodorsal), rostrocaudal and mediolateral; (2) overexpression in one of these gradients may result in duplication or hypoplasia of structures, or ectopic expression; (3)

underexpression in a gradient generally results in hypoplasia, non-cleavage in the midline of paired structures or segmental deletion of neuromeres. Some examples are shown in clinical cases in other chapters of this book.

References

Achiron R, Achiron A (1991) Transvaginal ultrasonic assessment of the early fetal brain. Ultrasound Obstet Gynecol 1:336–344

Ahdab-Barmada M, Claassen D (1990) A distinct triad of malformations of the central nervous system in the Meckel-Gruber syndrome. J Neuropathol Exp Neurol 49:610–620

Aicardi J (1998) Diseases of the Nervous System in Childhood, 2nd ed. Mac Keith, London

Amin RS, Nikolaidis P, Kawashima A, Kramer LA, Ernst RD (1999) Normal anatomy of the fetus at MR imaging. Radiographics 19:S201–214

Anderson CE (1995) The genetics of disorders of the developing nervous system. In: Duckett S (ed) Pediatric Neuropathology. Williams & Wilkins, Baltimore, MD, pp 41–53

Antonarakis SE (1991) Parental origin of the extra chromosome 21 as indicated by analysis of DNA polymorphisms. Down Syndrome Collaborative Group. N Engl J Med 324:872–876

Arts NFT, Lohman AHM (1971) The vascular anatomy of monochorionic diamniotic twin placenta and the transfusion syndrome. Eur J Obstet Gynecol Reprod Biol 1:85–93

Bamforth JS (1992) Amniotic band sequence: Streeter's hypothesis re-examined. Am J Med Genet 44:280–287

Barkovich AJ (2000) Pediatric Neuroimaging, 3rd ed. Lippincott, Philadelphia, PA

Barkovich AJ, Linden CL (1994) Congenital cytomegalovirus infection of the brain: Imaging analysis and embryonic considerations. AJNR Am J Neuroradiol 15:703–715

Barkovich AJ, Kjos BO, Norman D, Edwards MS (1989) Revised classification of posterior fossa cysts and cystlike malformations based on the results of multiplanar MR imaging. Am J Roentgenol 153:1289–1300

Barkovich AJ, Kuzniecky RI, Jackson GD, Guerrini R, Dobyns WB (2001) Classification system for malformations of cortical development. Update 2001. Neurology 57:2168–2178

Barth PG (2003) Fetal disruption as a cause of neuronal migration defects. In: Barth PG (ed) Disorders of Neuronal Migration. Mac Keith, London, pp 182–194

Barth PG, van der Harten JJ (1985) Parabiotic twin syndromes with topical isocortical disruption and gastroschisis. Acta Neuropathol (Berl) 67:345–349

Becker LE (1992) Infections of the developing brain. AJNR Am J Neuroradiol 13:537–549

Beltrán-Valero de Bernabé D, Currier S, Steinbrecher A, Celli J, van Beusekom E, van der Zwaag B, Kayserili H, Merlini L, Chitayat D, Dobyns WB, et al. (2002) Mutations in the O-mannosyltransferase gene *POMT1* give rise to the severe neuronal migration disorder Walker-Warburg syndrome. Am J Hum Genet 71: 1033–1043

Benirschke K, Kaufman P (1995) Pathology of the Human Placenta. Springer, Berlin Heidelberg New York

Blaas H-GK (1999) The Embryonic Examination. Ultrasound studies on the development of the human embryo. Thesis, Norwegian University of Science and Technology, Trondheim. TAPIR, Trondheim

Blaas H-GK, Eik-Nes SH (1999) First trimester diagnosis of fetal malformations. In: Rodeck CH, Whittle MJ (eds) Fetal Medicine. Churchill Livingstone, London, pp 581–597

Blaas H-GK, Eik-Nes SH, Kiserud T, Hellevik LR (1994) Early development of the forebrain and midbrain: A longitudinal ultrasound study from 7 to 12 weeks of gestation. Ultrasound Obstet Gynecol 4:183–192

Blaas H-GK, Eik-Nes SH, Isaksen CV (2000) The detection of spina bifida before 10 gestational weeks using two- and three-dimensional ultrasound. Ultrasound Obstet Gynecol 16:25–29

Blaas H-GK, Eriksson AG, Salvesen KÅ, Isaksen CV, Christensen B, Møllerløkken G, Eik-Nes SH (2002) Brains and faces in holoprosencephaly: Pre- and postnatal description of 30 cases. Ultrasound Obstet Gynecol 19:24–38

Bonnemann C, Meinecke P (1990) Holoprosencephaly as a possible embryonic alcohol effect: Another observation. Am J Hum Genet 37:431–432

Borch K, Greisen G (1998) Blood flow distribution in the normal human preterm brain. Pediatr Res 43:28–33

Bordarier C, Robain O (1992) Microgyric and necrotic cortical lesions in twin fetuses: Original cerebral damage consecutive to twinning? Brain Dev 14:174–178

Boyd PA, Keeling JW, Selinger M, MacKenzie IZ (1990) Limb reduction and chorion villus sampling. Prenat Diagn 10:437–441

Braude P, Pickering S, Flinter F, Mackie Ogilvie C (2002) Preimplantation genetic diagnosis. Nat Rev Genet 3:941–953

Brock DJH, Rodeck CH, Ferguson Smith MA, eds (1992) Prenatal Diagnosis and Screening. Churchill Livingstone, Edinburgh

Brown GK, Squier MV (1996) Neuropathology and pathogenesis of mitochondrial diseases. J Inher Metab Dis 19:553–572

Brown GK, Brown RM, Scholem RD, Kirby DM, Dahl H-HM (1989) The clinical and biochemical spectrum of human pyruvate dehydrogenase complex deficiency. Ann NY Acad Sci 573: 360–368

Cairns NJ (1999) Neuropathology of Down syndrome. J Neural Transm 57:61–74

Cardoza JD, Goldstein RB, Filly RA (1988) Exclusion of fetal ventriculomegaly with a single measurement: The width of the lateral ventricular atrium. Radiology 163:187–191

Chambers CD, Johnson KA, Dick LM, Felix RJ, Jones KL (1998) Maternal fever and birth outcome: Prospective study. Teratology 58:251–257

Chattha A, Richardson E (1977) Cerebral white matter hypoplasia. Arch Neurol 34:137–140

Cherstvoy ED, Lazjuk GI, Lurie IW, Nedzved MK, Usoev S (1975) The pathological anatomy of Smith-Lemli-Opitz syndrome. Clin Genet 7:382–387

Chitkara U, Cogswell C, Norton K, Wilkins IA, Mehalek K, Berkowitz RL (1988) Choroid plexus cysts in the fetus: A benign anatomic variant or pathological entity? Report of 41 cases and review of the literature. Obstet Gynecol 72:185–189

Chitty LS, Hunt GH, Moore J, Lobb MO (1991) Effectiveness of routine ultrasonography in detecting fetal structural abnormalities in a low risk population. BMJ 303:1165–1169

Chitty LS, Chudleigh P, Wright E, Campbell S, Pembrey M (1998) The significance of choroid plexus cysts in unselected populations: Results of a multicenter study. Ultrasound Obstet Gynecol 12:391–397

Clarren SK, Alvord EC Jr, Sumi SM, Steissguth AP, Smith DW (1978) Brain malformations related to prenatal exposure to ethanol. J Pediatr 92:64–67

Cohen MM Jr, Shiota K (2002) Teratogenesis of holoprosencephaly. Am J Med Genet 109:1–15

Cunniff C, Kratz LE, Moser A, Natowicz MR, Kelley RI (1997) Clinical and biochemical spectrum of patients with RSH/Smith-Lemli-Opitz syndrome and abnormal cholesterol metabolism. Am J Med Genet 68:263–269

de la Monte SM (1999) Molecular abnormalities of the brain in Down syndrome: Relevance to Alzheimer's neurodegeneration. J Neural Transm 57:1–20

De Reuck J, Chattha AS, Richardson EPJ (1972) Pathogenesis and evolution of periventricular leukomalacia in infancy. Arch Neurol 27:229–236

de Vries LS, Groenendaal F, Eken P, van Haastert IC, Rademaker KJ, Meiners LC (1997) Infarcts in the vascular distribution of the middle cerebral artery in preterm and fullterm infants. Neuropediatrics 28:88–96

de Vries LS, Eken P, Groenendaal F, Rademaker KJ, Hoogervorst B, Bruinse HW (1998a) Antenatal onset of haemorrhagic and/or ischaemic lesions in preterm infants: Prevalence and associated obstetric variables. Arch Dis Childh Fetal Neon Ed 78: F51–F56

de Vries LS, Rademaker KJ, Groenendaal F, Eken P, van Haastert IC, Vandertop WP, Gooskens R, Meiners LC (1998b) Correlation between neonatal cranial ultrasound, MRI in infancy and neurodevelopmental outcome in infants with a large intraventricular haemorrhage with or without parenchymal involvement. Neuropediatrics 29:180–188

de Vries LS, Roelants-van Rijn AM, Rademaker KJ, van Haastert IC, Beek FJ, Groenendaal F (2001) Unilateral parenchymal haemorrhagic infarction in the preterm infant. Eur J Paediatr Neurol 5:139–149

de Vries LS, Gunardi H, Barth PG, Bok LA, Verboon-Maciolek MA, Groenendaal F (2004) The spectrum of cranial ultrasound and magnetic resonance imaging abnormalities in congenital cytomegalovirus infection. Neuropediatrics 35:113–119

Dobyns WB (1989) Agenesis of the corpus callosum and gyral malformations are frequent manifestations of nonketotic hyperglycinemia. Neurology 39:817–820

Donnai D, Winter RM (1989) Disorganisation: A model for 'early amnion rupture'? J Med Genet 26:421–425

Down JLH (1866) Observations on the ethnic classification of idiots. Clin Lect Rep Lond Hosp 3:259

Eberle AM, Levesque D, Vintzileos AM, Egan JF, Tsapanos V, Salafia CM (1993) Placental pathology in discordant twins. Am J Obstet Gynecol 169:931–935

Edwards JH, Harnden DG, Cameron AH, Crosse VM, Wolff OH (1960) A new trisomic syndrome. Lancet 1960 (i):787

Edwards MJ, Shiota K, Smith MSR, Walsh DA (1995) Hyperthermia and birth defects. Reprod Toxicol 9:411–425

Edwards MJ, Saunders RD, Shiota K (2003) Effects of heat on embryos and foetuses. Int J Hyperthermia 19:295–324

Epstein CJ, Erickson RP, Wynshaw-Boris A, eds (2004) Inborn Errors of Development. The molecular basis of clinical disorders of morphogenesis. Oxford University Press, Oxford

Fierro M, Martinez AJ, Harbison JW, Hay SH (1977) Smith-Lemli-Opitz syndrome: Neuropathological and ophthalmological observations. Dev Med Child Neurol 19:57–62

Firth HV (1997) Chorion villus sampling and limb deficiency–cause or coincidence? Prenat Diagn 17:1313–1330

Fitzky BU, Witsch-Baumgarten M, Erdel M, Lee JN, Paik YU, Glossmann H, Uterman G, Moebius FF (1998) Mutations in the delta7-sterol reductase gene in patients with the Smith-Lemli-Opitz syndrome. Proc Natl Acad Sci USA 95:8181–8186

Fitzpatrick D (2001) Genetic metabolic disease. In: Keeling JW (ed) Fetal and Neonatal Pathology, 3rd ed. Springer, Berlin Heidelberg New York, pp 153–174

FitzPatrick DR, Keeling JW, Evans MJ, Kan AE, Bell JE, Porteous MEM, Mills K, Winter RM, Clayton PT (1998) Clinical phenotype of desmosterolosis. Am J Med Genet 75:145–152

Friede RL (1989) Developmental Neuropathology, 2nd ed. Springer, Berlin Heidelberg New York

Gardner RJM, Sutherland GR (1996) Chromosome Abnormalities and Genetic Counselling, 2nd ed. Oxford University Press, Oxford

Garel C (2004) MRI of the Fetal Brain. Normal development and cerebral pathologies. Springer, Berlin Heidelberg New York

Gerards FA, Engels MA, Barkhof, van den Dungen FA, Vermeulen RJ, van Vugt JM (2003) Prenatal diagnosis of aneurysms of the vein of Galen (vena magna cerebri) with conventional sonography, three-dimensional sonography, and magnetic resonance imaging: Report of 2 cases. J Ultrasound Med 22:1363–1368

Gilbert-Barness E (1997) Chromosomal abnormalities. In: Gilbert-Barness E (ed) Potter's Pathology of the Fetus and Infant. Mosby, St. Louis, MI, pp 368–432

Gilbert-Barness E, Van Allen MI (1997) Disruptions. In: Gilbert-Barness E (ed) Potter's Pathology of the Fetus and Infant. Mosby, St. Louis, MI, pp 322–387

Gibson KM, Hoffmann GF, Sweetman L, Buckingham B (1997) Mevalonate kinase deficiency in a dizygotic twin with mild mevalonic aciduria. J Inherit Metab Dis 20:391–394

Glade-Bender J, McFarland JG, Kaplan C, Porcelijn L, Bussel JB (2001) Anti-HPA-3A induces severe neonatal alloimmune thrombocytopenia. J Pediatr 138:862–867

Goodman SI, Frerman FE (2001) Organic acidemias due to defects in lysine oxidation: 2-Ketoadipic acidemia and glutaric acidemia. In: Scriver CR, Beaudet AL, Sly WS, Valle D (eds) The Metabolic & Molecular Bases of Inherited Disease, 8th ed. McGraw-Hill, New York, pp 2195–2206

Gorlin RJ, Cohen MM Jr, Hennekam RCM, eds (2001) Syndromes of the Head and Neck, 4th ed. Oxford University Press, Oxford

Gould SJ, Raymond GV, Valle D (2001) The peroxisome biogenesis disorders. In: Scriver CR, Beaudet AL, Sly WS, Valle D (eds) The Metabolic & Molecular Bases of Inherited Disease, 8th ed. McGraw-Hill, New York, pp 3181–3218

Govaert P, Matthys E, Zecic A, Roelens F, Oostra A, Vanzieleghem B (2000) Perinatal cortical infarction within middle cerebral artery trunks. Arch Dis Child Fetal Neonatal Ed 82:F59–F63

Grandjean H, Larroque D, Levi S, and the Eurofetus Study Group (1999) The performance of routine ultrasonographic screening of pregnancies in the Eurofetus Study. Am J Obstet Gynecol 181:446–454

Grossman RI, Bruce DA, Zimmerman RA, Goldberg HI, Bilaniuk LT (1984) Vascular steal associated with vein of Galen aneurysm. Neuroradiology 26:381–386

Haas D, Kelley RI, Hoffmann GF (2001) Inherited disorders of cholesterol biosynthesis. Neuropediatrics 32:113–132

Hall JG (1988) Review and hypotheses: Somatic mosaicism; observations related to clinical genetics. Am J Hum Genet 43:355–363

Hamel BCJ (1999) X-Linked Mental Retardation. A clinical and molecular study. Thesis, University of Nijmegen

Hamosh A, Johnston MV (2001) Nonketotic hyperglycinemia. In: Scriver CR, Beaudet AL, Sly WS, Valle D (eds) The Metabolic & Molecular Bases of Inherited Disease, 8th ed. McGraw-Hill, New York, pp 2065–2078

Hansen AR, Snyder EY (1998) Medical management of neonatal posthemorrhagic hydrocephalus. Neurosurg Clin N Am 9:95–104

Happle R, Koch H, Lenz W (1980) The CHILD syndrome: Congenital hemidysplasia with ichthyosiform erythroderma and limb defects. Eur J Ped Surg 134:27–33

Herrero RJ, Chitrit Y, Caubel P, Lusina D (2003) Feto-maternal alloimmune thrombocytopenia due to HPA-5b incompatibility: A case report. Eur J Obstet Gynecol Reprod Biol 110:240–241

Higginbottom MC, Jones KL, Hall BD, Smith SW (1979) The amniotic band disruption complex: Timing of amniotic rupture and variable spectra of consequent defects. J Pediatr 95:544–549

Hill A, Rozdilsky B (1984) Congenital hydrocephalus secondary to intra-uterine germinal matrix/intraventricular haemorrhage. Dev Med Child Neurol 26:524–527

Hoffmann GF, Gibson KM, Brandt IK, Bader PI, Wappner RS, Sweetman L (1986) Mevalonic aciduria–an inborn error of cholesterol and nonsterol isoprene biosynthesis. N Engl J Med 314:1610–1614

Hoffmann GF, Charpentier C, Mayatepek E, Mancini J, Leichsenring M, Gibson KM, Divry P, Hrebicek M, Lehnert W, Sarton K, et al. (1993) Clinical and biochemical phenotype in eleven patients with mevalonic aciduria. Pediatrics 91:915–921

Hori A, Orthner H, Kohlschütter A, Schott KM, Hirabayashi K, Shimokawa K (1980) CNS dysplasia in dysencephalia splanchnocystica (Gruber's syndrome). Acta Neuropathol (Berl) 51:93–97

Hubbard AM, Harty MP, States LJ (1999) A new tool for prenatal diagnosis: Ultrafast fetal MRI. Semin Perinatol 23:437–447

Iannetti P, Nigro G, Spalice A, Faiella A, Boncinelli E (1998) Cytomegalovirus infection and schizencephaly: Case reports. Ann Neurol 43:123–127

Inoue K, Osaka H, Sugiyama N, Kawanishi C, Onishi H, Nezu A, Kimura K, Kimura S, Yamada Y, Kosaka K (1996) A duplicated PLP causing Pelizaeus-Merzbacher disease detected by comparative multiplex PCR. Am J Hum Genet 59:32–39

Irons M, Elias ER, Salen G, Tint GS, Batta AK (1993) Defective cholesterol biosynthesis in Smith-Lemli-Opitz syndrome. Lancet 1993 (i):1414

Jackson JC, Blumhagen JD (1983) Congenital hydrocephalus due to prenatal intracranial hemorrhage. Pediatrics 72:344–346

Jaeken J, Carchon H (2001) Congenital disorders of glycosylation: The rapidly growing tip of the iceberg. Curr Opin Neurol 14:811–815

Jaeken J, Matthijs G (2001) Congenital disorders of glycosylation. Annu Rev Genomics Hum Genet 2:129–152

Jaeken J, Matthijs G, Carchon H, Van Schaftingen E (2001) Defects of N-glycan synthesis. In: Scriver CR, Beaudet AL, Sly WS, Valle D (eds) The Metabolic & Molecular Bases of Inherited Disease, 8th ed. McGraw-Hill, New York, pp 1601–1622

Jinnah HA, Friedmann T (2001) Lesch-Nyhan disease and its variants. In: Scriver CR, Beaudet AL, Sly WS, Valle D (eds) The Metabolic & Molecular Bases of Inherited Disease, 8th ed. McGraw-Hill, New York, pp 2537–2570

Jones KL (1997) Smith's Recognizable Patterns of Human Malformation, 5th ed. Saunders. Philadelphia, PA

Kadhim H, Tabarki B, Verellen G, de Prez C, Rona AM, Sebire C (2001) Inflammatory cytokines in the pathogenesis of periventricular leukomalacia. Neurology 56:1278–1284

Källén B, Mastroiacovo P, Robert E (1996) Major congenital malformations in Down syndrome. Am J Med Genet 65:160–166

Kalousek DK (1997) Pathology of abortion: The embryo and the previable fetus. In: Gilbert-Barness E (ed) Potter's Pathology of the Fetus and Infant. Mosby, St. Louis, MI, pp 106–127

Kalousek DK, Fitch N, Paradice BA (1990) Pathology of the Human Embryo and Previable Fetus. An atlas. Springer, Berlin Heidelberg New York

Keeling JW, Boyd PA (2001) Congenital abnormalities and the examination of the fetus following prenatal suspicion of congenital abnormality. In: Keeling JW (ed) Fetal and Neonatal Pathology, 3rd ed. Springer, Berlin Heidelberg New York, pp 111–152

Kelley RI, Hennekam RCM (2000) The Smith-Lemli-Opitz syndrome. J Med Genet 37:321–335

Kelley RI, Herman GE (2001) Inborn errors of sterol biosynthesis. Annu Rev Genomics Hum Genet 2:299–341

Kelley RI, Roessler E, Hennekam RCM, Feldman GL, Kosaki K, Jones MC, Palumbos JC, Muenke M (1996) Holoprosencephaly in RSH/Smith-Lemli-Opitz syndrome: Does abnormal cholesterol metabolism affect the function of *Sonic hedgehog*? Am J Med Genet 66:478–484

Kerrigan JF, Aleck KA, Tarby TJ, Bird CR, Heidenreich RA (2000) Fumaric aciduria: Clinical and imaging features. Ann Neurol 47:583–588

Kinney HC, Back SA (1998) Human oligodendroglial development: Relationship to periventricular leukomalacia. Sem Pediatr Neurol 5:180–189

Kobayashi K, Nakahori Y, Miyake M, Matsumura K, Kondo-Iida E, Nomura Y, Segawa M, Yoshioka M, Saito K, Osawa M, et al. (1998) An ancient retrotransposal insertion causes Fukuyama-type congenital muscular dystrophy. Nature 394:388–392

Koeppen AH, Robitaille Y (2002) Pelizaeus-Merzbacher disease. J Neuropathol Exp Neurol 61:747–759

Kraus I, Jirásek JE (2002) Some observations of the structure of the choroid plexus and its cysts. Prenat Diagn 22:1223–1228

Kuban KC, Gilles FH (1985) Human telencephalic angiogenesis. Ann Neurol 17:539–548

Lammens M (1997) Developmental Neuropathology in Etiology and Pathogenesis of Human Malformations: A personal contribution. Thesis, University of Leuven, Belgium (Acta Biomedica Lovaniensia, Vol 154)

Lammer EJ, Chen DT, Hoar RM, Agnish ND, Benke PJ, Braun JT, Curry CJ, Fernhoff PM, Grix AW, Lott IT (1985) Retinoic acid embryopathy. N Engl J Med 313:837–841

Larroche JC, Girard N, Narcy F, Fallet C (1994) Abnormal cortical plate (polymicrogyria), heterotopias and brain damage in monozygous twins. Biol Neonate 65:343–352

Laxova R (1997) Prenatal diagnosis. In: Gilbert-Barness E (ed) Potter's Pathology of the Fetus and Infant. Mosby, St. Louis MI, pp 182–240

Leegwater PAJ, Könst AAM, Kuyt B, Sandkuijl LA, Naidu S, Oudejans CBM, Schutgens RBH, Pronk JC, van der Knaap MS (1999) The gene for leukoencephalopathy with vanishing white matter is located on chromosome 3q27. Am J Hum Genet 65:728–734

Leegwater PAJ, Vermeulen G, Könst AAM, Naidu S, Mulders J, Visser A, Kersbergen P, Mobach D, Fonds D, van Berkel CGM, et al. (2001) Subunits of the translation initiation factor eIF2B are mutated in leukoencephalopathy with vanishing white matter. Nat Genet 29:383–388

Leigh D (1951) Subacute necrotizing encephalomyelopathy in an infant. J Neurol Neurosurg Psychiatr 14:216–221

Levi S (1998) Routine ultrasound screening of congenital anomalies. An overview of the European experience. Ann NY Acad Sci 847:86–98

Levine D, Barnes PD (1999) Cortical maturation in normal and abnormal fetuses as assessed with prenatal MR imaging. Radiology 210:751–758

Levine D, Barnes PD, Madsen JR, Li W, Edelman RR (1997) Fetal central nervous system anomalies: MR imaging augments sonographic diagnosis. Radiology 204:635–642

Levine D, Barnes PD, Madsen JR, Abbott J, Mehta T, Edelman RR (1999) Central nervous system abnormalities assessed with prenatal magnetic resonance imaging. Obstet Gynecol 94:1011–1019

Liu AE, Ardinger HH, Ardinger RH Jr, Cunniff C, Kelley RI (1997) Cardiovascular malformations in Smith-Lemli-Opitz syndrome. Am J Med Genet 68:270–278

Lubec G, Engidawork (2002) The brain in Down syndrome (trisomy 21). J Neurol 249:1347–1356

Lyon G, Arita F, Gallodec EL, Vallée L, Misson J, Ferrière G (1990) A disorder of axonal development, necrotizing myopathy, cardiomyopathy, and cataract: A new familial disease. Ann Neurol 27:193–199

Malcolm S (1996) Microdeletion and microduplication. Prenat Diagn 16:1213–1219

Mann DMA (1988) The pathological association between Down syndrome and Alzheimer's disease. Mech Aging Dev 43:99–136

Marín-Padilla M (1972) Structural abnormalities of the cerebral cortex in human chromosomal aberrations. A Golgi study. Brain Res 44:625–629

Marín-Padilla M (1976) Pyramidal cell abnormalities in the motor cortex of a child with Down's syndrome. A Golgi study. J Comp Neurol 167:63–82

Marion RW, Alvarez LA, Marans ZS, Lantos G, Chitayat D (1987) Computed tomography of the brain in the Smith-Lemli-Opitz syndrome. J Child Neurol 2:198–200

Marquardt T, Denecke J (2003) Congenital disorders of glycosylation: Review of their molecular bases, clinical presentations and specific therapies. Eur J Pediatr 162:359–379

McDonald JW, Althomsons SP, Hyrc KL, Choi DW, Goldberg MPC (1998) Oligodendrocytes from forebrain are highly vulnerable to AMPA/kainate receptor-mediated excitotoxicity. Nat Med 4:291–297

McKusick VA (1998) Mendelian Inheritance in Man. Catalogs of human genes and genetic disorders. 12th ed. Johns Hopkins University Press, Baltimore, MD

Miller OJ, Therman E (2001) Human Chromosomes, 4th ed. Springer, Berlin Heidelberg New York

Ming JE, Muenke M (2002) Multiple hits during early embryonic development: Digenic diseases and holoprosencephaly. Am J Hum Genet 71:1017–1032

Miyawaki T, Matsui K, Takashima S (1998) Developmental characteristics of vessel density in the human fetal and infant brains. Early Hum Dev 53:65–72

Moebius FF, Fitzky BU, Lee JN, Paik YK, Glossmann H (1998) Molecular cloning and expression of the human ¢7-sterol reductase. Proc Natl Acad Sci USA 95:1899–1902

Moerman P, Fryns J-P, Vandenberghe K, Lauweryns JM (1992) Constrictive amniotic bands, amniotic adhesions, and limb-body wall complex: Discrete disruption sequences with pathogenetic overlap. Am J Med Genet 42:470–479

Montteagudo A, Timor-Tritsch IE, Mayberry P (2000) Three-dimensional transvaginal neurosonography of the fetal brain: 'Navigating' in the volume scan. Ultrasound Obstet Gynecol 16:307–313

Moore KL, Persaud TVN (1998) The Developing Human, 6th ed. Saunders, Philadelphia, PA

Moore KL, Persaud TVN, Shiota K (2000) Color Atlas of Clinical Embryology, 2nd ed. Saunders, Philadelphia, PA

Moser AB, Rasmussen M, Naidu S, Watkins PA, McGuinness M, Hajra AK, Chen G, Raymond G, Liu A, Gordon D, et al. (1995) Phenotype of patients with peroxisomal disorders subdivided into 16 complementation groups. J Pediatr 127:13–22

Moser HW (1998) Neurometabolic disease. Curr Opin Neurol 11:91–95

Moser HW, Smith KD, Watkins PA, Powers J, Moser AB (2001) X-linked adrenoleukodystrophy. In: Scriver CR, Beaudet AL, Sly WS, Valle D (eds) The Metabolic & Molecular Bases of Inherited Disease, 8th ed. McGraw-Hill, New York, pp 3257–3302

Müller-Eckhardt C, Kiefel V, Grubert A, Kroll H, Weisheit M, Schmidt S, Müller-Eckhardt G, Santoso S (1989) 348 Cases of suspected neonatal alloimmune thrombocytopenia. Lancet 1989 (i):363–366

Narchi H, Kulayat N (1997) High incidence of Down's syndrome in infants of diabetic mothers. Arch Dis Childh 77:242–244

Nelson KB, Lynch JK (2004) Stroke in newborn infants. Lancet Neurol 3:150–158

Nelson MD, Gonzalez-Gomez I, Gilles FH (1991) The search for human telencephalic ventriculofugal arteries. Am J Neuroradiol 12:215–222

Nicolaides KH, Campbell S, Gabbe SG, Guidetti R (1986) Ultrasound screening for spina bifida: Cranial and cerebellar signs. Lancet (1986) ii):72–74

Nicolaides KH, Azar G, Byrne D, Mansur C, Marks K (1992) Fetal nuchal translucency: Ultrasound screening for chromosomal defects in first trimester of pregnancy. Br Med J 304:867–869

Nicolaides KH, Sebire NJ, Snijders RJM (1999) The 11-14 Week Scan: The diagnosis of fetal abnormalities. Parthenon, London

Norman MG (1980) Bilateral encephaloclastic lesions in a 26 weeks gestation fetus. Can J Neurol Sci 7:191–194

Norman MG, Becker LE (1974) Cerebral damage in neonates resulting from arteriovenous malformation of the vein of Galen. J Neurol Neurosurg Psychiatr 37:252–258

Norman MG, McGillivray BC, Kalousek DK, Hill A, Poskitt KJ (1995) Congenital Malformations of the Brain. Pathological, embryological, clinical, radiological and genetic aspects. Oxford University Press, New York

Nyberg DA, Mack LA, Hirsch J, Pagon RO, Shepard TH (1987) Fetal hydrocephalus: Sonographic detection and clinical significance of associated anomalies. Radiology 163:187–191

O'Donnell WT, Warren ST (2002) A decade of molecular studies of fragile X syndrome. Annu Rev Neurosci 25:315–338

OMIM: Online Mendelian Inheritance in Men. http://www.ncbi.nlm.nih.gov/omim

Opitz JM (1993) Blastogenesis and the "primary field" in human development. Birth Defects 29:3–37

Opitz JM, Wilson GN (1997) Causes and pathogenesis of birth defects. In: Gilbert-Barness E (ed) Potter's Pathology of the Fetus and Infant. Mosby, St. Louis, MI pp 44–64

Opitz JM, Zellweger H, Shannon WR, Ptacek LJ (1969) The RSH syndrome. Birth Defects Orig Artic Ser 5:43–52

Opitz JM, Wilson GN, Gilbert-Barness E (1997) Abnormalities of blastogenesis, organogenesis, and phenogenesis. In: Gilbert-Barness E (ed) Potter's Pathology of the Fetus and Infant. Mosby, St. Louis, MI, pp 65–105

Otake M, Yoshimura H, Schull WJ (1989) Prenatal exposure to atomic radiation and brain damage. Cong Anom 29:309–320

Otake M, Schull WJ, Yoshimura H (1991) Brain damage among the prenatally exposed. J Radiat Res Suppl 249–264

Pajkrt E, Mol BW, van Lith JM, Bleker OP, Bilardo CM (1998a) Screening for Down's syndrome by fetal nuchal translucency measurement in a high-risk population. Ultrasound Obstet Gynecol 12:156–162

Pajkrt E, van Lith JM, Mol BW, Bleker OP, Bilardo CM (1998b) Screening for Down's syndrome by fetal nuchal translucency measurement in a general obstetric population. Ultrasound Obstet Gynecol 12:163–169

Parrish M, Roessmann U, Levinsohn M (1979) Agenesis of the corpus callosum: A study of the frequency of associated malformations. Ann Neurol 6:349–352

Passarge E, Lenz W (1966) Syndrome of caudal regression in infants of diabetic mothers: Observations of further cases. Pediatrics 37:672–675

Patau K, Smith DW, Therman E, Inhorn SL, Wagner HP (1960) Multiple congenital anomaly caused by an extra autosome. Lancet 1960 (i):790–793

Pooh RK, Maeda K, Pooh KH (2003) An Atlas of Fetal Central Nervous System Disease. Diagnosis and management. Parthenon, London

Poutamo J, Vanninen R, Partanen K, Ryyanen M, Kirkinen P (1999) Magnetic resonance imaging supplements ultrasonographic imaging of the posterior fossa, pharynx and neck in malformed fetuses. Ultrasound Obstet Gynecol 13:327–324

Quintero RA, Romero R, Mahonev MJ, Vecchio M, Holden JH, Hobbins JC (1992) Fetal haemorrhagic lesions after chorionic villus sampling (letter). Lancet 1992 (i):193

Ramaswamy V, Miller SP, Barkovich AJ, Partridge JC, Ferreiro DM (2004) Perinatal stroke in term infants with neonatal encephalopathy. Neurology 62:2088–2091

Raybaud CA, Strother CM, Hald JK (1989) Aneurysms of the vein of Galen: Embryonic considerations and anatomical features relating to the pathogenesis of the malformation. Neuroradiology 31:109–128

Remes AM, Rantala H, Hiltunen JK, Leisti J, Ruokonen A (1992) Fumarase deficiency: Two siblings with enlarged cerebral vesicles and polyhydramnios in utero. Pediatrics 89:730–734

Robinson BH (2001) Lactic acidemia: Disorders of pyruvate carboxylase and pyruvate dehydrogenase. In: Scriver CR, Beaudet AL, Sly WS, Valle D (eds) The Metabolic & Molecular Bases of Inherited Disease, 8th ed. McGraw-Hill, New York, pp 2275–2295

Rorke LB (1992) Anatomical features of the developing brain implicated in pathogenesis of hypoxic-ischemic injury. Brain Pathol 2:211–221

Ruggieri PM (1997) Metabolic and neurodegenerative disorders and disorders with abnormal myelination. In: Ball WS (ed) Pediatric Neuroradiology. Lippincott, Philadelphia, PA, pp 175–237

Ryan AK, Bartlett K, Clayton P, Eaton S, Mills L, Donnai D, Winter RM, Burn J (1998) Smith-Lemli-Opitz syndrome: A variable clinical and biochemical phenotype. J Med Genet 35:558–562

Sarnat HB (2000) Molecular genetic classification of central nervous system malformations. J Child Neurol 15:675–687

Sarnat HB, Flores-Sarnat L (2004) Integrative classification of morphology and molecular genetics in central nervous system malformations. Am J Med Genet 126A:386–392

Schouten JP, McElgunn CJ, Waaijer R, Zwijnenburg D, Diepvens F, Pals G (2002) Relative quantification of 40 nucleic acid sequences by multiplex ligation-dependent probe amplification. Nucleic Acids Res 30:e57

Schull WJ, Nishitani H, Hasuo K, Kobayashi T, Goto I, Otake M (1992) Brain abnormalities among the mentally retarded prenatally exposed atomic bomb survivors. Radiation Effects Research Foundation, Technical Report Series 13-91:1–16

Scott BS, Becker LE, Petit TL (1983) Neurobiology of Down's syndrome. Prog Neurobiol 21:199–237

Scriver CR, Kaufman S (2001) Hyperphenylalaninemia: Phenylalanine hydroxylase deficiency. In: Scriver CR, Beaudet AL, Sly WS, Valle D (eds) The Metabolic & Molecular Bases of Inherited Disease, 8th ed. McGraw-Hill, New York, pp 1667–1723

Scriver CR, Beaudet AL, Sly WS, Valle D, eds (2001) The Metabolic & Molecular Bases of Inherited Disease, 8th ed. McGraw-Hill, New York

Shepard TH (1998) Catalog of Teratogenic Agents, 9th ed. Johns Hopkins University Press, Baltimore, MD

Shiota K (1991) Development and intrauterine fate of normal and abnormal human conceptuses. Cong Anom 31:67–80

Shiota K (1993) Teratothanasia: Prenatal loss of abnormal conceptuses and the prevalence of various malformations during human gestation. Birth Defects 29:189–199

Sie LTL, van der Knaap MS, van Wezel-Meijler G, Valk J (1997) MRI assessment of myelination of motor and sensory pathways in the brain of preterm and term-born infants. Neuropediatrics 28:97–105

Sismani C, Armour JA, Flint J, Girgalli C, Regan R, Patsalis PC (2001) Screening for subtelomeric chromosome abnormalities in children with idiopathic mental retardation using multiprobe telomeric FISH and the new MAPH telomeric assay. Eur J Hum Genet 9:527–532

Smeitink J, van den Heuvel L (1999) Human mitochondrial complex in health and disease. Am J Hum Genet 64:1505–1510

Smith DW, Lemli L, Opitz JM (1964) A newly recognized syndrome of multiple congenital anomalies. J Pediatr 64:210–217

Smith NM (2001) The reticuloendothelial system. In: Keeling JW (ed) Fetal and Neonatal Pathology, 3rd ed. Springer, Berlin Heidelberg New York, pp 593–604

Snijders RJM, Nicolaides KH (1996) Ultrasound Markers for Fetal Chromosomal Defects. Parthenon, London

Spranger J, Benirschke K, Hall JG, Lenz W, Lowry RB, Opitz JM, Pinsky L, Schwarzacher HG, Smith DW (1982) Errors of morphogenesis: Concepts and terms. J Pediatr 100:160–165

Squier W (2002) Pathology of fetal and neonatal brain damage: Identifying the timing. In: Squier W (ed) Acquired Damage to the Developing Brain: Timing and causation. Arnold, London, pp 110–127

Squier W, Chamberlain P, Zaiwalla Z, Anslow P, Oxbury J, Gould S, McShane MA (2000) Five cases of brain injury following amniocentesis in midterm pregnancy. Dev Med Child Neurol 42:554–560

Strachan T, Read AP (2004) Human Molecular Genetics, 3rd ed. Garland Science, London

Stray-Pedersen B (1993) Toxoplasmosis in pregnancy. Baillières Clin Obst Gynaecol 7:107–137

Streeter GL (1930) Focal deficiencies in fetal tissues and their relation to intrauterine amputations. Contrib Embryol Carnegie Instn 22:1–46

Sunderland S, ed (1993) TORCH Screening Reassessed. Blackmore, Shaftesbury

Sutton LN, Sun P, Adzick NS (2001) Fetal neurosurgery. Neurosurgery 48:124–144

Takanashi J, Barkovich AJ, Ferreiro DM, Suzuki H, Kohno Y (2003) Widening spectrum of congenital hemiplegia: Periventricular venous infarction in term neonates. Neurology 61:531–533

Toda T, Kobayashi K, Takeda S, Sasaki J, Kurahashi H, Kano H, Tachikawa M, Nagay Y, Taniguchi K, Sunada Y, et al. (2003) Fukuyama-type congenital muscular dystrophy (FCMD) and α-dystroglycanopathy. Cong Anom 43:97–104

Tominaga I, Kaihou M, Kimura T, Onaya M, Kashima H, Kato Y, Tamagawa K (1996) Infection foetale par le cytomégalovirus. Porencéphalie avec polymicrogyrie chez un garçon de 15 ans. Rev Neurol (Paris) 152:479–482

Torpin R (1965) Amniochorionic mesoblastic fibrous strings and amniotic bands. Am J Obstet Gynecol 91:65–75

Trauner DA, Chase C, Walker P, Wulfeck B (1993) Neurologic profiles of infants and children after perinatal stroke. Pediatr Neurol 9:383–386

UNSCEAR (1986) Genetic and Somatic Effects of Ionizing Radiation. Report of United Nations Scientific Committee on Effects of Atomic Radiation to the General Assembly. United Nations, New York

Van Allen MI, Curry C, Gallagher L (1987a) Limb body wall complex. I. Pathogenesis. Am J Med Genet 28:529–548

Van Allen MI, Curry C, Walden CE, Gallagher L, Patten RM (1987b) Limb body wall complex. II. Limb and spine defects. Am J Med Genet 28:549–565

van den Hof MC, Nicolaides KH, Campbell J, Campbell S (1990) Evaluation of the lemon and banana signs in one hundred and thirty fetuses with open spina bifida. Am J Obstet Gynecol 162:322–327

van der Knaap MS, Valk J (1990) MR imaging of the various stages of normal myelination during the first year of life. Neuroradiology 31:459–470

van der Knaap MS, Valk J (1995) Myelination and retarded myelination. In: van der Knaap MS, Valk J (eds) Magnetic Resonance of Myelin, Myelination and Myelin Disorders, 2nd ed. Springer, Berlin Heidelberg New York, pp 31–52

van der Knaap MS, Barth PG, Gabreëls FJM, Franzoni E, Begeer JH, Stroink H, Rotteveel JJ, Valk J (1997) A new leukoencephalopathy with vanishing white matter. Neurology 48:845–855

van der Knaap MS, Leegwater PAJ, Könst AAM, Visser A, Naidu S, Oudejans CBM, Schutgens RBH, Pronk JC (2002) Mutations in each of the five subunits of translation initiation factor eIF2B can cause leukoencephalopathy with vanishing white matter. Ann Neurol 51:264–270

van der Knaap MS, van der Voorn P, Barkhof F, Van Coster R, Krägeloh-Mann I, Feigenbaum A, Blaser S, Vles JSH, Rieckmann P, Pouwels PJW (2003) A new leukodystrophy with brainstem and spinal cord involvement and high lactate. Ann Neurol 53:252–258

van Zalen-Sprock RM, van Vugt JMG, van Geijn HP (1995) First and early second trimester diagnosis of anomalies of the central nervous system. J Ultrasound Med 14:603–610

Vissers LE, de Vries BB, Osoegawa K, Janssen IM, Feuth T, Choy CO, Straatman H, van der Vliet W, Huys EH, van Rijk A, et al. (2003) Array-based comparative genomic hybridization for the genomewide detection of submicroscopic chromosomal abnormalities. Am J Hum Genet 73:1261–1270

Volpe JJ (2001a) Neurology of the Newborn, 4th ed. Saunders, Philadelphia, PA

Volpe JJ (2001b) Neurobiology of periventricular leukomalacia in the premature infant. Pediatr Res 50:553–562

Wagenvoort AM, Bekker MN, Go AT, Vandenbussche FP, van Buchem MA, Valk J, van Vugt JM (2000) Ultrafast scan magnetic resonance in prenatal diagnosis. Fetal Diagn 15:364–372

Wanders RJA, Barth PG, Heymans HSA (2001) Single peroxisomal enzyme deficiencies. In: Scriver CR, Beaudet AL, Sly WS, Valle D (eds) The Metabolic & Molecular Bases of Inherited Disease, 8th ed. McGraw-Hill, New York, pp 3219–3256

Warburton D, Byrne J, Canki N (1991) Chromosome Anomalies and Prenatal Development: An atlas. Oxford University Press, Oxford

Warkany J (1971) Congenital Malformations. Year Book, Chicago, IL

Warren ST, Sherman SL (2001) The fragile X syndrome. In: Scriver CR, Beaudet AL, Sly WS, Valle D (eds) The Metabolic & Molecular Basis of Inherited Disease, 8th ed. McGraw-Hill, New York, pp 1257–1289

Wassif CA, Maslen C, Kachilele-Linjewile S, Lin D, Linck LM, Connor WE, Steiner RD, Porter FD (1998) Mutations in the human sterol delta7-reductase gene at 11q12-13 cause Smith-Lemli-Opitz syndrome. Am J Hum Genet 63:55–62

Waterham HR, Wijburg FA, Hennekam RCM, Vreken P, Poll-The BT, Dorland L, Duran M, Jira PE, Smeitink JAM, Wevers RA, Wanders RJA (1998) Smith-Lemli-Opitz syndrome is caused by mutations in the 7-dehydrocholesterol reductase gene. Am J Hum Genet 63:329–338

Waterham HR, Koster J, Romeijn GJ, Hennekam RCM, Vreken P, Andersson HC, FitzPatrick DR, Kelley RI, Wanders RJA (2001) Mutations in the 3-β-hydroxysterol Δ^{24}-reductase gene cause desmosterolosis, an autosomal recessive disorder of cholesterol biosynthesis. Am J Hum Genet 69:685–694

Weindling M (2002) Clinical aspects of brain injury in the preterm infant. In: Lagercrantz H, Hanson M, Evrard P, Rodeck CH (eds) The Newborn Brain – Neuroscience and clinical applications. Cambridge University Press, Cambridge, pp 443–478

Weis S, Weber G, Neuhold A, Rett A (1991) Down syndrome: MR quantification of brain structures and comparison with normal control subjects. AJNR Am J Neuroradiol 12:1207–1211

Wilkins-Haug L, Freedman W (1991) Progression of exencephaly to anencephaly in the human fetus – an ultrasound perspective. Prenat Diagn 11:227–233

Williamson DA (1970) A syndrome of congenital malformations possibly due to maternal diabetes. Dev Med Child Neurol 12:145–152

Yoshida A, Kobayashi K, Manya H, Taniguchi K, Kano H, Mizuno M, Inazu T, Mitsuhashi H, Takahashi S, Takeuchi M, et al. (2001) Muscular dystrophy and neuronal migration disorders caused by mutations in a glycosyltransferase, POMGnT1. Dev Cell 1:717–724

Youssoufian H, Pyeritz RE (2002) Mechanisms and consequences of somatic mosaicism in humans. Nat Rev Genet 3:748–758

Zanders EH, Buist FC, van Vugt JM (2003) Prenatal diagnosis of fetal intracranial hemorrhage at 25 weeks of gestation. Fetal Diagn Ther 18:327–337

Zellweger H (1987) The cerebro-hepato-renal (Zellweger) syndrome and other peroxisomal disorders. Dev Med Child Neurol 29:821–829

Zeviani M, Tiranti V, Piantadosi C (1998) Mitochondrial disorders. Medicine 77:59–72

Neurulation and Neural Tube Defects

Hans J. ten Donkelaar, Reinier A. Mullaart, Akira Hori and Kohei Shiota

4.1   Introduction

Neurulation is usually described as the developmental process that results in the rolling up of a flat sheet of epithelial cells into an elongated tube (Gilbert 2000; Colas and Schoenwolf 2001). Neurulation has been extensively studied in amphibian, avian and mammalian embryos and occurs in four stages: formation of the neural plate, shaping of the neural plate, bending of the neural plate and closure of the neural groove. The rostral part of the neural tube develops into the brain, whereas the caudal part becomes the spinal cord. This is the **primary type** of **neurulation**. In fish, the neural tube does not form from an infolding of the overlying ectoderm, but instead forms from a solid cord of cells. This cord subsequently becomes cavitated. In birds and mammals, the most caudal part of the neural tube forms by aggregation of cells, as part of the caudal eminence, into a medullary cord which then cavitates and connects to the main neural tube. This process is called **secondary neurulation**.

Neural tube defects (*NTDs*) are among the most common human malformations, with an incidence of 1–5 per 1,000 live births. Striking variation in incidence exists between populations, varying from 1 in 3,000 in the low-risk Finnish population to more than 1 in 300 in high-risk areas in Ireland and the UK (Dolk et al. 1991). Approximately 85 % of NTDs may be the result of a combined influence of environmental and genetic factors, indicating a multifactorial aetiology (Copp and Bernfield 1994). Over the past few decades there has been a worldwide decline in the number of NTD births, due mainly to the introduction of ultrasound screening as part of routine prenatal care, followed by therapeutic termination of pregnancies, and primary prevention through folic acid supplementation during early pregnancy (Czeizel and Dudás 1992). No precise definition of NTDs exists, since they include a very heterogeneous group of defects. Usually, NTDs are defined as a group of defects in which the neural tube has failed to complete neurulation and one or more of the neural tube coverings are incomplete (Norman et al. 1995). In most cases this failure leads to exposure of a portion of the neural tube at the body surface. This definition allows inclusion of encephaloceles, cranial and spinal meningoceles, and myelocystoceles. Most encephaloceles may arise after neural tube closure, owing to non-separation of neural and surface ectoderm, leading to defects in the formation of the skull (Campbell et al. 1986; Vermeij-Keers 1990). The term *dysraphia* is used for malformations appearing prenatally that involve a disturbance of neurulation and/or a defect in the skeletal surroundings. The disturbance of a median seam or raphe, whether neural or skeletal, which normally ensures closure of the CNS from the surface, may affect the cranial or the spinal region, or both. Four main types of NTDs are found at the cranial and spinal level (Norman et al. 1995; Naidich et al. 1996; Aicardi 1998; Barkovich 2000; O'Rahilly and Müller 2001): (1) the neural plate remaining open (anencephaly and myeloschisis, respectively); (2) the neural tube being exteriorized (encephalomeningocele and myelomeningocele); (3) only meninges being exteriorized (cranial and spinal meningoceles); and (4) merely a skeletal defect being evident (cranium bifidum occultum and spina bifida occulta). Spinal lipomas occur with occult spinal dysraphism as well as in cases of open NTDs, and lie dorsal to the defect. Split cord malformations may be associated with NTDs and probably occur before neural tube closure (Pang et al. 1992). They are discussed in Chap. 6.

This chapter presents an overview of primary and secondary neurulation, a discussion of genetic mouse models for NTDs, recognized causes of NTDs and a discussion of the human NTDs, including cranial NTDs, spinal NTDs, the Chiari malformations and caudal dysgenesis syndromes.

4.2   Primary Neurulation

4.2.1   Primary Neurulation in Chick and Mammalian Embryos

The process of primary neurulation appears to be similar in amphibian, avian and mammalian embryos (Balinsky 1965; Karfunkel 1974; Gilbert 2000). With scanning electron microscopy the key events of neural tube formation have been studied. In chick embryos, Schoenwolf and co-workers (Schoenwolf and Smith 1990; Schoenwolf 1994; Smith and Schoenwolf 1997; Colas and Schoenwolf 2001; Lawson et al. 2001) showed four distinct but spatially and temporally overlapping stages of neurulation (Fig. 4.1). First, **formation** of the **neural plate** is induced early in embryogenesis (Chap. 2) and the ectoderm thickens.
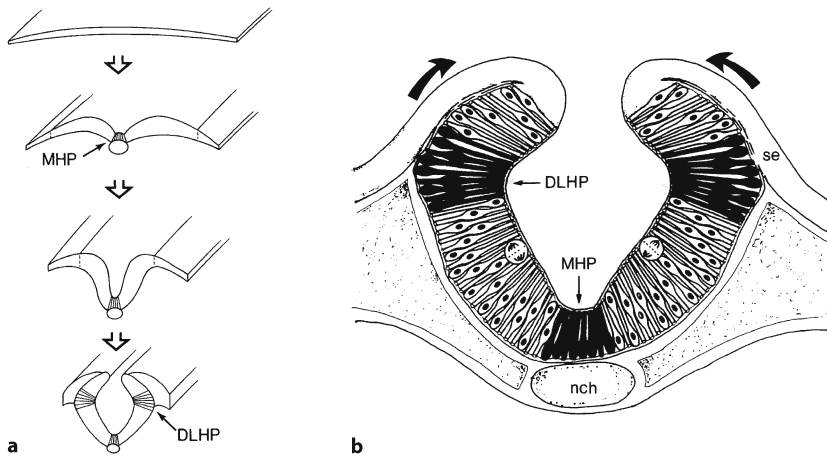
Fig. 4.1 Morphogenetic events during chick neurulation: **a** shaping, folding, elevation and convergence of the neural plate at the future midbrain/hindbrain level; **b** the hinge point model of bending of the chick neural plate. Neuroepithelial cell wedging (*black*) within the dorsolateral and median hinge points is indicated. *Arrows* indicate the mediolateral expansion of the surface ectoderm. *DLHP* dorsolateral hinge point, *MHP* median hinge point, *nch* notochord, *se* surface ectoderm. (After Schoenwolf 1994; Smith and Schoenwolf 1997)

During this stage, the neuroectodermal cells of the forming neural plate increase in height and undergo pseudostratification. Second, **shaping** of the **neural plate** begins, leading to rostrocaudal lengthening, mediolateral narrowing and further apicobasal thickening, except in the midline, where it becomes anchored to the notochord and midline neuroepithelial cells shorten and become wedge-shaped. Together, these form-shaping events modify the original flat neural plate so that subsequent bending produces an elongated neural tube. Third, **bending** of the **neural plate** begins during shaping and involves the following morphogenetic events: (1) formation of hinge points; (2) formation of the neural folds; and (3) folding of the neural plate. The **hinge points**, one median and two dorsolateral, are areas of the neural plate attached to adjacent tissues. The **median hinge point** (MHP) is attached to the underlying prechordal plate rostrally and the notochord caudally. In the avian embryo, the paired **dorsolateral hinge points** (DLHPs) are present only at future brain and rhomboid sinus levels. They are attached to adjacent epidermal ectoderm. Within the hinge points, the neuroepithelial cells become wedge-shaped and the neural plate undergoes longitudinal furrowing. The morphology of the neural folds differs rostrocaudally. At the future brain level, the neural (or head) folds are broad, mediolaterally elongated structures, whereas at the future spinal cord level they are much narrower. Peculiar to avian embryos is the rhomboid sinus, near the closing caudal neuropore, where the neural folds are relatively broad compared with the width of the neural plate. Folding of the neural plate occurs in temporal and spatial relationship to formation of the hinge points (Fig. 4.1). After the MHP has formed, both sides of the neural plate undergo dorsal elevation along the longitudinal axis, resulting in the formation of the neural groove. Continued elevation at the future spinal cord level, where true DLHPs are ab-

sent, brings the lateral walls of the developing neural tube into contact with the midline, leading to a slit-like neural tube lumen. In contrast, at future brain levels, the neural folds undergo a second, convergent, medial folding along the longitudinal axis, which brings them together in the dorsal midline and generates a broad lumen. **Fusion** of the **neural folds** forms the fourth stage of neurulation. During this stage, the non-neural or future surface ectoderm from each fold detaches from the neuroepithelium and fuses with the non-neural ectoderm of the other fold. This process is known as **disjunction**. Both detached neuroepithelial layers fuse deep to the surface ectoderm and form the roof plate of the neural tube. In chick embryos, the first closure of the neural tube occurs in the future mesencephalon, and a second closure is found at the rhombo-cervical level as multiple contacts between the neural folds (van Straaten et al. 1996, 1997).

Neurulation is a **multifactorial process** that requires both extrinsic and intrinsic forces acting in concert (Schoenwolf and Smith 1990). Intrinsic forces arise within the neural plate and drive neural plate shaping and furrowing, whereas extrinsic forces arise outside the neural plate and drive neural plate folding and neural groove closure. The **intrinsic forces** responsible for neural plate shaping and furrowing are generated by fundamental changes in cell shape, position and number of neuroepithelial cells (Schoenwolf and Smith 1990; Smith and Schoenwolf 1997). At the hinge points, the majority of neuroepithelial cells become wedge-shaped (Fig. 4.1b). Neuroepithelial cells also undergo two rounds of rearrangement during neurulation (Schoenwolf and Alvarez 1989). The neural plate undergoes a halving of its width and a corresponding doubling of its length during each round. In amphibian embryos, this rearrangement of neuroepithelial cells probably provides the major intrinsic force for rostrocaudal

lengthening of the neural plate (Jacobson 1994). In birds and mammals, moreover, substantial cell division occurs within the neural plate during neurulation (Tuckett and Morriss-Kay 1985; Smith and Schoenwolf 1987, 1988). Tissue transplantation experiments in chick embryos suggest that neural plate folding is not an autonomous process inherent to the neural plate itself but that it also depends on **extrinsic forces** generated by non-neuroepithelial tissues lateral to the neural plate (Moury and Schoenwolf 1995; Smith and Schoenwolf 1991, 1997). Data from mutant mice also support a role for extrinsic forces in neural plate folding (Copp 1994; Smith and Schoenwolf 1997; Juriloff and Harris 2000). Knockouts for the transcription factor *twist* (Chen and Behringer 1995), the *Cart1* homeobox gene (Zhao et al. 1996) or the transcription factor *AP2* (Schorle et al. 1996; Zhang et al. 1996) show cranial NTDs such as exencephaly. During neurulation, the expression of these genes is restricted to non-neuroepithelial cells, either head mesenchyme (*twist* and *Cart1*) or cranial epidermal ectoderm (*AP2*).

Neurulation in **mammalian embryos** is basically similar to that described for the chick embryo, but considerable variation may be found in the mode of neurulation among different mammals and even among different strains of the same species (Copp et al. 1990; Morriss-Kay et al. 1994; Shum and Copp 1996; Peeters 1998; Peeters et al. 1998a; van Straaten et al. 2000). A relation between the curvature of the longitudinal body axis and the rate of neural tube closure has been suggested (Copp et al. 1990; Brook et al. 1991; van Straaten et al. 1993; Peeters et al. 1996, 1997). **Cranial neural tube closure** is initiated at multiple sites (**multisite closure**). In pig embryos, the rostral neuropore closes in three phases (Fig. 4.2): (1) the dorsal folds slowly align and then close instantaneously, the slow progression being likely due to a counteracting effect of the mesencephalic flexure; (2) the dorsolateral folds close in a zipper-like fashion caudorostralwards; and (3) the remaining round aperture presumably closes by circumferential growth at the stage of 22 somites.

Closure of the neural tube in mice is also initiated at multiple sites (Fig. 4.7a). Separate initiation sites for cranial neural tube closure have been demonstrated (Juriloff et al. 1991; Tom et al. 1991; Golden and Chernoff 1993; Fleming and Copp 2000). The closure sites more or less separate the neural fold elevation zones as defined by Harris and Juriloff (1999). The first contact and fusion of apposed neural folds occurs at the border between the rhombencephalon and the spinal cord (closure 1). This closure proceeds bidirectionally both rostralwards and caudalwards. The second site of closure begins at the border between the prosencephalon and the mesencephalon (closure 2), and also proceeds bidirectionally. A third

initiation site is found at the rostral end of the neural plate (closure 3). Therefore, in mouse embryos at some stage of development, two prominent openings are recognized simultaneously, one over the prosencephalon, rostral to the second closure, and the other over the mesencephalon–rhombencephalon. Neural tube closure spreads bidirectionally, between closures 1 and 2, to complete neurulation at the hindbrain neuropore, and between closures 2 and 3, to complete neurulation at the rostral neuropore. In the SWV/Bc strain, the second initiation site is located further rostrally in the prosencephalon (Juriloff et al. 1991; Fleming and Copp 2000). Multisite closure of the neural tube has also been observed in rats (Christie 1964) and hamsters (Keyser 1972; Shenefelt 1972). Data for mouse embryos suggest that midline bending is not essential for spinal closure (Ybot-Gonzalez et al. 2002; Copp et al. 2003). Midline and dorsolateral bending are regulated by mutually antagonistic signals from the notochord and surface ectoderm. Notochordal signalling induces midline bending and simultaneously inhibits dorsolateral bending through SHH.

The **closure** of the **caudal** or **posterior neuropore** (**PNP**) has received much less attention than that of the rostral one. In the ICR mouse strain, the closure of the caudal neuropore occurs at the caudal end of the neural plate and proceeds rostralwards to meet the extension of the closure initiated at the cervical region (Sakai 1989). Possibly, the closure of the caudal neuropore completes at the future sacrococcygeal level of the spinal cord. In rabbit embryos, the caudal neuropore is at first long and slender, with a tapered cranial part and a wide caudal portion (Peeters et al. 1998a). The groove closes craniocaudally and the caudal neuropore disappears at the caudal end of the neural plate. In pig embryos (Fig. 4.3), the PNP initially closes very fast in the somitic region, but then this process almost stops. Between the stages of eight and 20 somites, the width of the PNP hardly changes. At the stage of 20–22 somites, the PNP suddenly reduces in size, but a small neuropore remains for five somite stages. The closure of the caudal neuropore is completed at the 23-somite stage for the chick and rabbit embryo, at the 25–26-somite stage for rat embryos (Peeters et al. 1998a) and the 28-somite stage in pig embryos (van Straaten et al. 2000). In mouse and human embryos the caudal neuropore closes at the level of the 32nd to 34th somites (Schoenwolf 1984; Nievelstein et al. 1993). The **axial curvature** of the embryo appears to be an important factor in neurulation. The rate of neural tube closure increases as the axial curvature of the embryo decreases (Peeters 1998; Peeters et al. 1998b). In contrast to murine embryos, human and rabbit embryos are flat at younger stages and demonstrate a similarly high rate of neural tube closure.
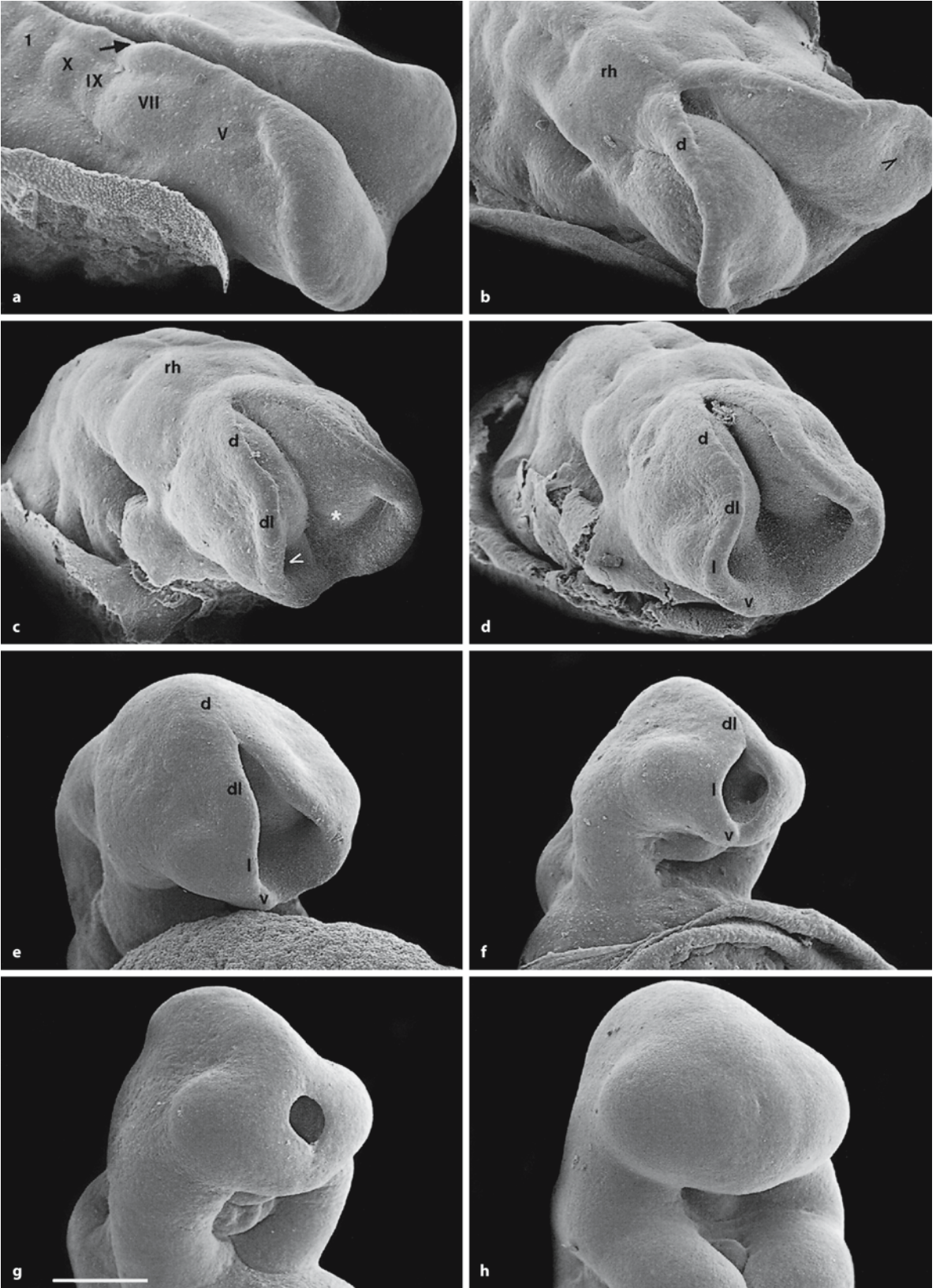
Fig. 4.2 Closure of the rostral neuropore in pig embryos in three phases: **a**–**e** the dorsal folds slowly align and then close instantaneously; **d**–**f** the dorsolateral folds close zipper-like in caudorostral direction; **f**–**h** the final round aperture closes by circumferential growth. The *arrow* in **a** shows the rhombencephalic neuropore; the *arrowheads* in **b** and **c** indicate the optic sulcus. *d* dorsal fold, *dl* dorsolateral fold, *l* lateral fold, *rh* rhombencephalon, *v* ventral fold, *V, VII, IX, X* neural crest swellings, *1* somite 1. (From van Straaten et al. 2000, with permission)

4.2.2 Primary Neurulation in Human Embryos

Primary neurulation has been studied extensively in human embryos (Gardner et al. 1975; O'Rahilly and Müller 1994, 1999, 2001, 2002; Nakatsu et al. 2000). The neural groove and folds can first be observed at stage 8 (approximately 18 days of development). Two days later, at stage 9, the three main divisions of the brain can be distinguished while the neural groove is still completely open (Chap. 1). Another 2 days later, at stage 10, the neural folds begin to fuse near the

Fig. 4.3 Closure of the caudal neuropore in pig embryos. Closure is initiated fast in the somitic region (**a**), subsequently stops, and gradually closes zipper-like in caudal direction with increasing closure rate (**b**–**d**), and stops again (**e**) before definitive closure (**f**). *Arrowheads* indicate raphe where the neural tube is closed already. (From van Straaten et al. 2000, with permission)
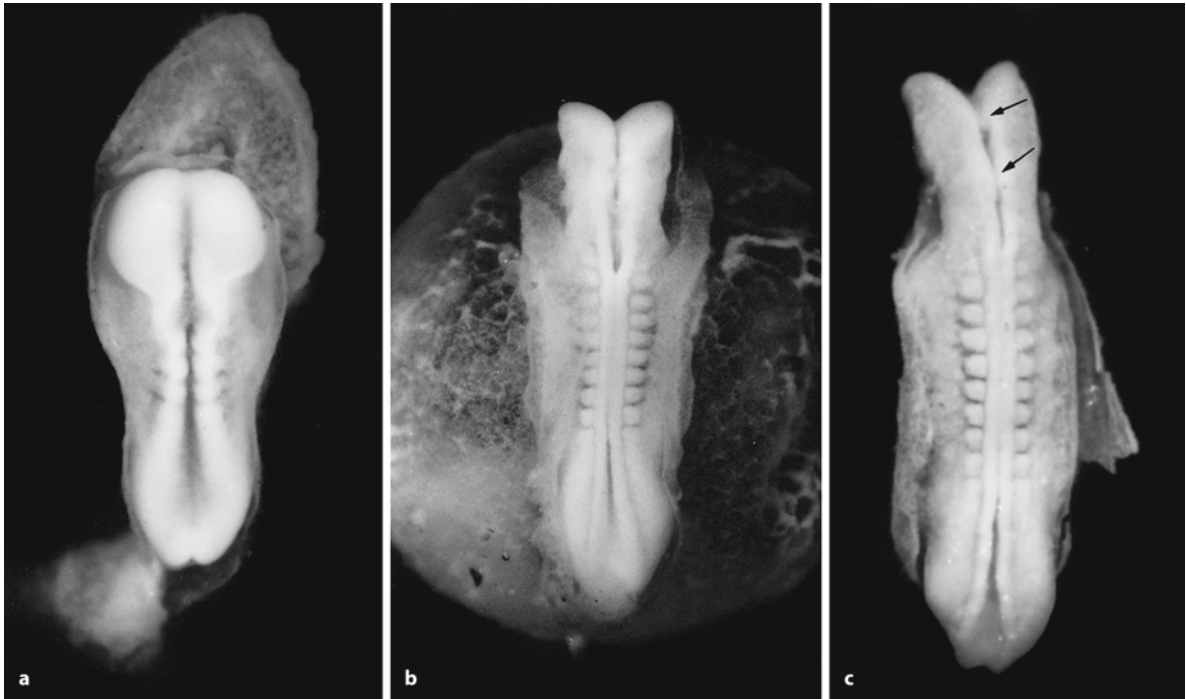
Fig. 4.4 Neurulation in human embryos: **a** a five-somite embryo at Carnegie stage 10; **b** a ten-somite embryo at Carnegie stage 10; **c** a ten-somite embryo at Carnegie stage 10 in which the neural tube has closed at the future cervical level. Another initiation site of neural tube closure can be seen at the mes-encephalic–rhombencephalic junction (*lower arrow*), whereas the medial walls of the mesencephalon appear to make contact with each other (*upper arrow*). (From Nakatsu et al. 2000, with permission)

boundary of the brain stem and spinal cord (Fig. 4.4). The closure of the human neural tube is usually described as a process that begins in the region of the future neck, between the third and sixth somites, and proceeds bidirectionally towards the cranial and caudal ends like a zipper ('**continuous closure model**'). The closure is completed when the rostral and caudal neuropores are closed. The **rostral neuropore** closes within a few hours during stage 11 (about 24 days; Figs. 4.5, 4.6a). This closure is bidirectional (Bartelmez and Dekaban 1962; Müller and O'Rahilly 1986; O'Rahilly and Müller 1989a, 2002; Jirásek 2001, 2004). It takes place from the dorsal lip from the region of the D2 neuromere and from the ventral or terminal lip in the telencephalon, adjacent to the chiasmatic plate. The two lips, however, behave differently. At the dorsal lip, fusion of the surface ectoderm seems to precede that of the neuroectoderm. At the terminal lip, however, fusion of the surface ectoderm and fusion of the neuroectoderm seem to occur simultaneously. The separation of neural and surface ectoderm occurs after the closure of the rostral neuropore in the fourth week of gestation, and forms the final phase of the fusion process of the neural folds. Therefore, a disturbance in the separation between neural and surface ectoderm should be considered as a neu-rulation disorder (Vermeij-Keers 1990; Hoving 1993). Primary non-separation of the neural and surface ectoderm will secondarily cause a mesodermal defect at that site (Sternberg 1927, 1929; Hoving et al. 1990).

The **caudal neuropore** takes a day to close during stage 12 (about 26 days; Fig. 4.6b) and various views on the level of final closure are given. Müller and O'Rahilly (1987) described the localization of final closure at the future somitic pair 31, which corresponds to the second sacral vertebra. On the other hand, Nievelstein et al. (1993), studying mouse and human embryos, found that in both species the final closure of the caudal neuropore occurs at the level of somites 32–34, i.e. at the level of the third to fifth sacral vertebrae. At stage 13 (4 weeks), the neural tube is normally completely closed. In human embryos, an initial fast reduction in caudal neuropore length was found (Peeters et al. 1998b), resembling chick and rabbit embryos. Subsequently, this pattern was shifted towards that of the mouse and rat, with an acceleration at the stages of first caudal neuropore closure.

The continuous closure model of the human neural tube has been challenged by various students of human NTDs. Van Allen et al. (1993) extrapolated the data of murine neural tube closure to human
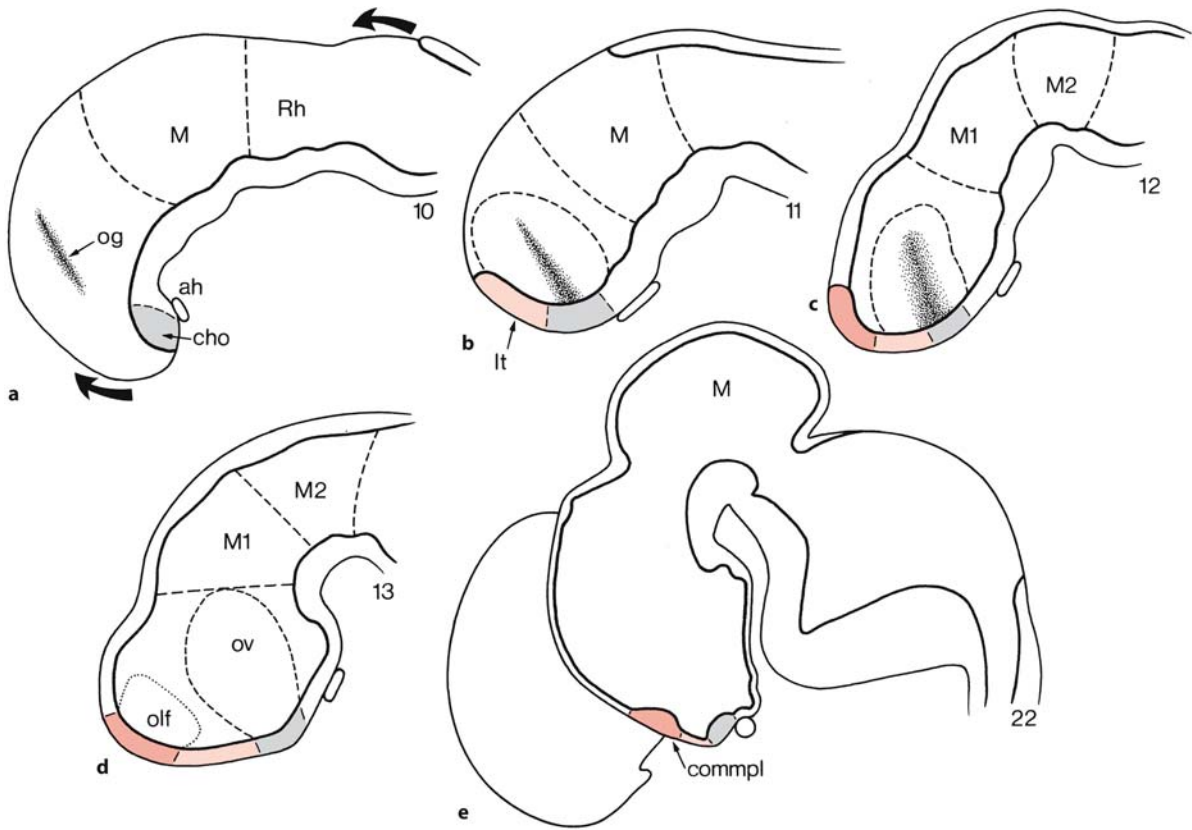
Fig. 4.5 Median reconstructions of the brain at stages 10 (**a**), 11 (**b**), 12 (**c**), 13 (**d**) and 22 (**e**). The *arrows* in **a** indicate the bidirectional progression of the rostral closure of the neural tube. **c** The segment shown in *red* is the closed situs neuroporus, where the future commissural plate arises. The embryonic lamina terminalis is shown in *light red* and the chiasmatic plate in *grey*. **e** The arrangement of the chiasmatic plate, the embryonic lamina terminalis and the commissural plate is clear. (After Bartelmez and Dekaban 1962; Müller and O'Rahilly 1984)

Fig. 4.6 Scanning electron micrographs showing the rostral (**a**) and caudal (**b**) neuropores in human embryos (from Jirásek 2001, 2004, with permission)

a   b   c
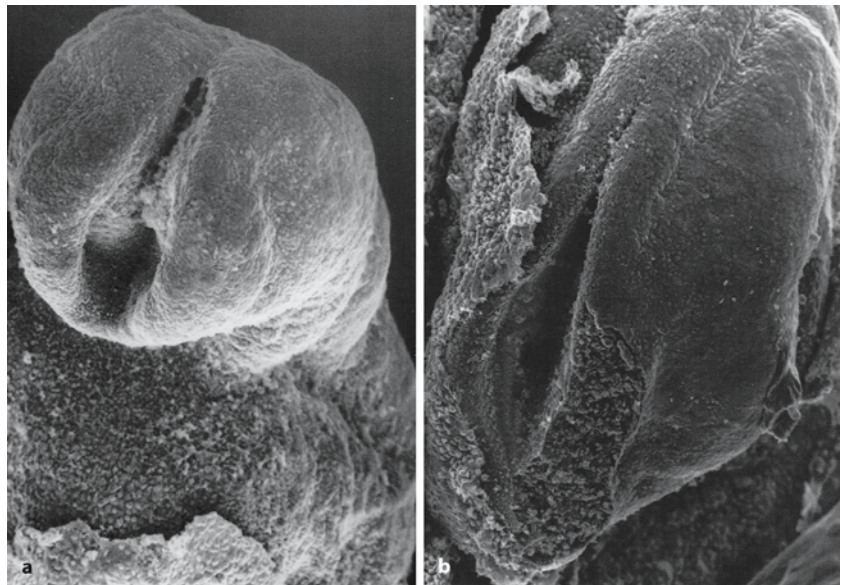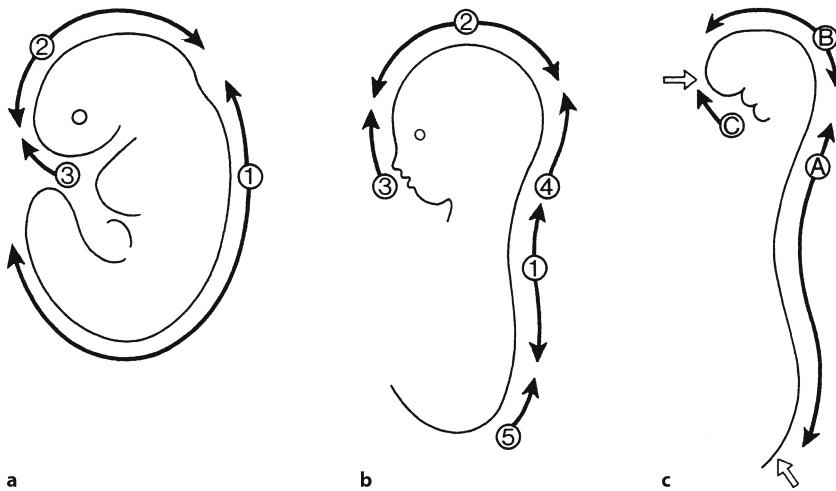
Fig. 4.7 a The rostrocaudal sequence of neurulation events in mouse embryos (after Harding and Copp 1997); **b** the multiclosure model of Van Allen et al. (1993); **c** multisite closure of the neural tube as observed in human embryos (after Nakatsu et al. 2000). Initiation of closure sites is indicated as *1–3*, *1–5* and *A–C*, respectively. The *open arrows* in **c** indicate the rostral and caudal neuropores

embryos and proposed a '**multisite closure model**' with five closures (three in the head and two in the spinal region), occurring during human neural tube closure (Fig. 4.7 b). More recently, Nakatsu et al. (2000) examined 68 embryos of the Kyoto Collection of Human Embryos in which the neural tube was closing (Carnegie stages 10–12) grossly and histologically, and confirmed that neural tube closure in humans initiates at multiple sites. In contrast to Van Allen et al., they concluded that the mode of neural tube closure in human embryos is rather different from that in many other mammalian species, and they suggested the following closure sites for the human neural tube (Fig. 4.7 c): (1) the future cervical region (closure site A); (2) the mesencephalic-rhombencephalic boundary (closure site B); and (3) the rostral end of the neural groove (closure site C). The second closure, beginning at closure site B, extends bidirectionally and its caudal extension meets the first closure from site A over the rhombencephalon, whereas its rostral extension meets the closure extending from the rostral end of the neural tube. The caudal extension of the first closure initiated at site A appeared to extend all the way down to the caudal end of the neural groove where the PNP is formed, suggesting that in human embryos neural tube closure does not initiate at the caudal end of the neural groove as found in mice.

4.3   Secondary Neurulation

In human embryos, secondary neurulation, which begins at stage 12 (about 26 days), is the differentiation of the caudal part of the neural tube from the caudal eminence without the intermediate phase of a neural plate (Müller and O'Rahilly 1987; O'Rahilly and Müller 1989b, 1994, 1999; Nievelstein et al. 1993; Saitsu et al. 2004). The **caudal eminence** is an ecto-

derm-covered mass of pluripotent tissue (Fig. 4.8). It is first recognizable at stage 9 as an elevation of the embryo at the level of the primitive streak. The caudal eminence provides structures comparable to those derived more rostrally from the three germ layers. Its derivatives include the caudal parts of the alimentary canal, coelom, blood vessels, notochord, somites and spinal cord. At stage 12, the caudal eminence forms a solid cellular mass known as the **neural cord**. It is supposed to give rise to the nervous system of the caudal part of the body. The central canal of the spinal cord, which is already present at more rostral levels, extends into the neural cord in continuity. At stage 13, the neural cord extends to the caudal tip of the eminence and is in contact with the clearly delineated surface ectoderm. The caudal eminence gives rise to at least somitic pair 32 and the following pairs, and mesenchyme for the lower limb buds and perineum (O'Rahilly and Müller 1989a; Nievelstein et al. 1993). Caudal to the level of the 32nd somite, the human neural tube shows great similarity with the secondary neural tube in mouse embryos (Schoenwolf 1984; Müller and O'Rahilly 1987; Nievelstein et al. 1993), i.e. a pseudostratified epithelium with two rows of nuclei, surrounding a small round lumen. After closure of the caudal neuropore, formation of spinal ganglia stops in mouse and human embryos. Nievelstein et al. (1993) suggested that, like in mice, secondary neurulation in human embryos also starts below the level of the 32nd to 34th somites, which corresponds to the future third to fifth sacral vertebrae. This view suggests that *primary neurulation leads to the formation of all spinal cord segments and ganglia*, and is supported by observations of myelomeningoceles with and without skin defects in the lower sacral region (Naidich et al. 1983; Copp and Brook 1989; Barkovich 2000). These anomalies may best be explained as defects in the fusion process of the neural walls during primary neurulation.

a

b

c
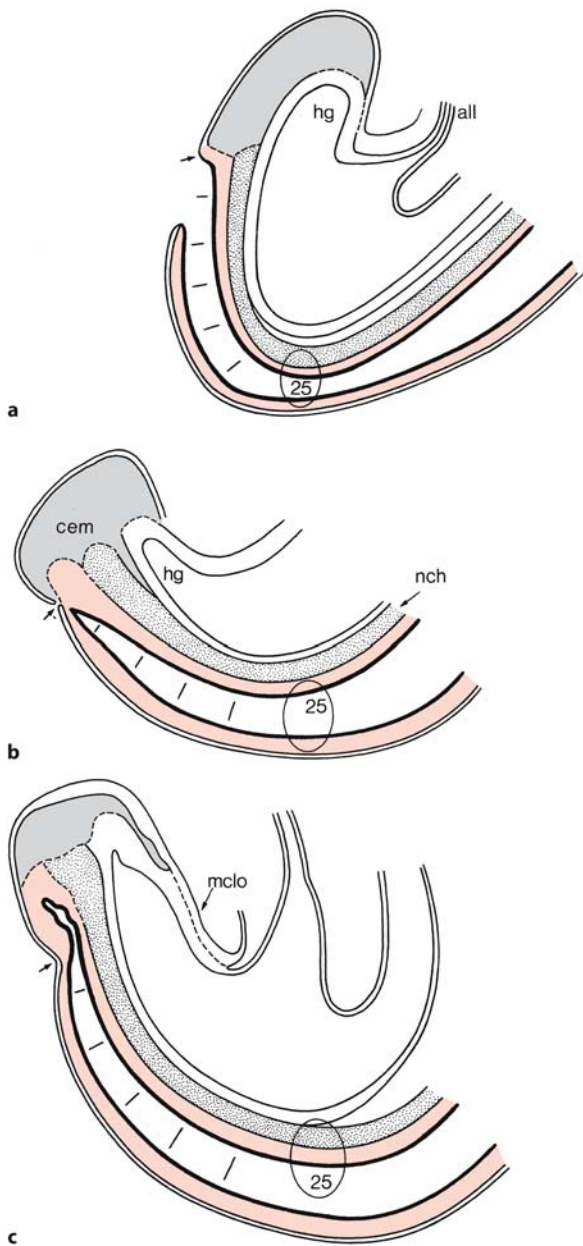
Fig. 4.8 Secondary neurulation in human embryos as observed in the caudal end of embryos of Carnegie stage 12: **a** embryo with still open caudal neuropore; **b** embryo with just closing caudal neuropore; **c** embryo with already closed neuropore. *Arrows* mark the site where the caudal neuropore closes. *all* allantois, *cem* caudal eminence, *hg* hindgut, *mclo* membrana cloacalis, *nch* notochord, *25* somite 25. (After Müller and O'Rahilly 1987)

In human embryos of Carnegie stages 12 and 13, Saitsu et al. (2004) showed that axially condensed mesenchyme intervenes between the neural plate/tube and the notochord in the junctional area of the primary and secondary neural tubes. In the junction-

Fig. 4.9 Collapsed ventriculus terminalis observed at autopsy in an adult (from the Department of Neuropathology, Medizinische Hochschule Hannover; courtesy Akira Hori)

al area, the cavity of the early secondary neural tube is continuous with that of the primary neural tube. When tail-bud mesenchyme cells fail to differentiate into paraxial mesoderm, they follow the process that leads to the formation of the secondary neural tube (Saitsu et al. 2004). In mice deficient for transcriptional factors or signalling molecules which are involved in paraxial mesoderm formation, such as *Fgfr1* (Deng et al. 1997), *Wnt3a* (Yoshikawa et al. 1997), *Tbx6* (Chapman and Papaioannou 1998) and *Lef1/Tcf1* (Galceran et al. 1999), ectopic neural tubes were found where the paraxial mesoderm normally develops. Ectopic expression of *Gcm1* in the developing tail bud downregulates *Tbx6* expression and produces multiple neural tubes in the lumbosacral region (Nait-Oumesmar et al. 2002). Cavities of the secondary neural tube in the caudal region are frequently formed at multiple or isolated sites in the neural cord (Bolli 1966; Lemire 1969; Hughes and Freeman 1974; Saraga-Babic et al. 1995).

The final step in the formation of the distal spinal cord begins around 38 days of gestation, at which time the cell mass and central lumen of the caudal neural tube decrease as a result of apoptosis (Nievelstein et al. 1993). This process has been termed **retrogressive differentiation** (Streeter 1919; Lemire 1988;

Table 4.1 Spontaneous mutations causing neural tube defects (*NTDs*) in mice (after Copp 1994; Juriloff and Harris 2000)

Locus name	Alleles	Chromo-some	Cranial NTD in homozygotes	Spinal NTD in homozygotes	Notes
Loop-tail	*Lp*	1	Craniorachischisis	Craniorachischisis	
Cranioschisis	*Crn*	?	Exencephaly (all?)	–	
Exencephaly	*Xn*	?	Exencephaly in 35–85%	–	
Extra-toes (*Gli3*)	*Xt, Xt^{bph}*	13	Exencephaly (some)	–	
SELH	–	?	Exencephaly	–	SELH is a mouse strain carrying several polymorhic loci that interact additively to produce NTDs (MacDonald et al. 1989)
Bent-tail (*Zic3*)	*Bn*	X	Exencephaly (often)	Spina bifida (often) and tail defect	In man, *ZIC3* mutations are associated with situs abnormalities; occasionally spina bifida
Curly tail	*ct*	4	Exencephaly (1–5%)	Spina bifida (15–20%) and tail defect	
Splotch (*Pax3*)	*Sp, Sp^d, Sp^r, Sp^{1H}, Sp^{2H}, Sp^{4H}*	1	Exencephaly (50–100%)	Spina bifida (25–100%)	In screens of human NTD cases for association with *PAX3* no evidence for its involvement in common NTDs (Chapkupt et al. 1995; Trembath et al. 1999; Melvin et al. 2000)
Axial deformity	*Axd*	?	–	Spina bifida (50–100%)	
Vacuolated lens	*vl*	1	–	Spina bifida (40%)	

McLone and Naidich 1989; Pang 1993). Secondary neurulation involves only the formation of the most caudal part of the conus medullaris, the filum terminale and a focal dilatation of the central canal, known as the **ventriculus terminalis** (Kernohan 1924; Fig. 4.9). The terminal ventricle usually regresses but may persist into adulthood as a normal variation, occasionally found by MRI in adults without any symptoms related to the spinal cord (Lendon and Emery 1970; Sigal et al. 1991; Coleman et al. 1995). A disturbance in secondary neurulation would only result in an abnormal or absent filum terminale and ventriculus terminalis in combination with coccygeal vertebral defects (Nievelstein et al. 1993). Therefore, agenesis of the caudal part of the spinal ganglia and sacral vertebrae found in caudal dysgenesis (Duhamel 1961; Pang 1993; Sect. 4.10) most likely results from a disturbance in the formation and/or differentiation of the caudal part of the primary neural tube and the adjacent neural crest (Nievelstein et al. 1993, 1994).

<h2>4.4   Genetic Mouse Models for Neural Tube Defects</h2>

A large number of genetic mutations have been identified that disrupt normal neurulation and lead to NTDs (Theiler 1988; Copp et al. 1990; Copp 1994; Harris and Juriloff 1999; Juriloff and Harris 2000; Colas and Schoenwolf 2001). In their 1990 review, Copp et al. listed mutations at 13 genetic loci in rodents (12 in mice and one in rats) and three mouse chromosome aberrations. Ten years later, Juriloff and Harris (2000) reviewed more than 60 mouse mutants and strains with NTDs, and in 2001 Harris (2001) counted more than 100 mouse models with NTDs. Spontaneous mutations causing NTDs in mice are summarized in Table 4.1. Several patterns of NTDs were found (Copp et al. 1990; Copp 1994; Harris and Juriloff 1999; Juriloff and Harris 2000; Copp et al. 2003): (1) craniorachischisis beginning in the caudal part of the midbrain and extending along the whole vertebral column (neural fold elevation zones B, C and D as found in *loop tail* mice and *craniomyeloschisis* rats); (2) exencephaly particularly affecting the midbrain (zone B) and also variably involving the forebrain and hindbrain (*curly tail*, SELH, *exencephaly* and *extra toes* mutations, and trisomies of mouse chromosomes 12 and 14); (3) exencephaly specifically affecting the hindbrain (zone C) with variable involvement of the midbrain (*bent tail*, *splotch* and *rib fusions* mutants); and (4) lumbosacral spina bifida (caudal zone D as found in *bent tail*, *curly tail*, *splotch*, *axial deformity* and *vacuolated lens* mutants). The mouse mutants provide a spectrum of conditions that mimic the variation seen among human NTDs. In evolutionary terms, this resemblance
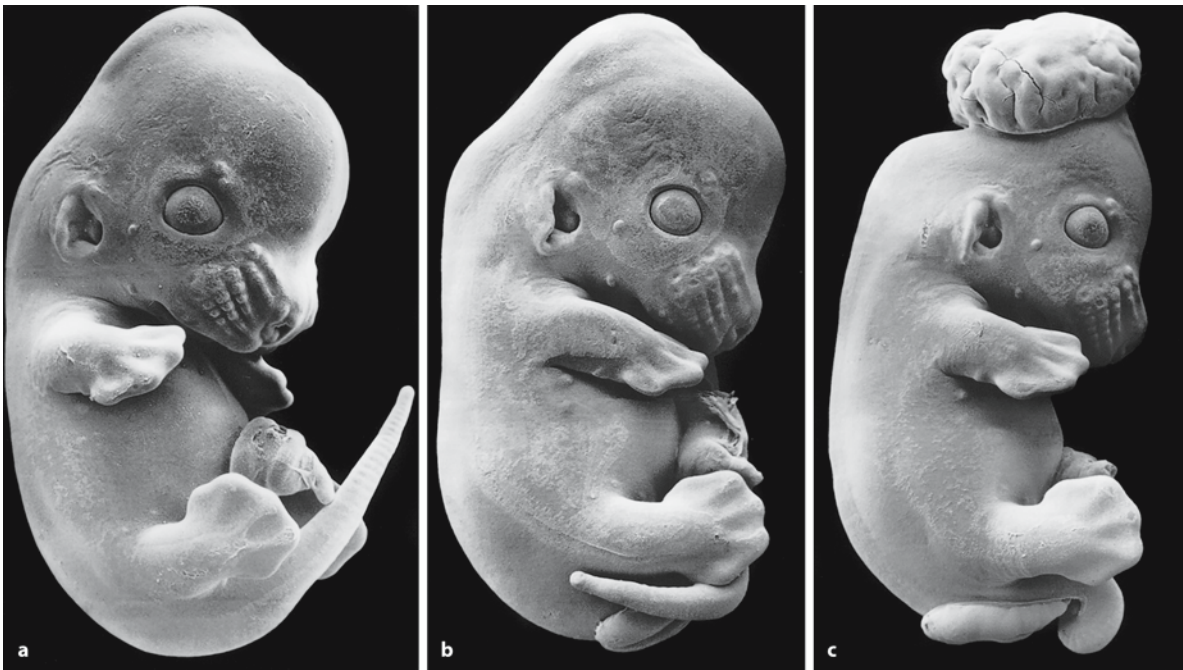
Fig. 4.10 Scanning electron micrographs of E13 *curly tail* mouse embryos: **a** embryo classified as unaffected phenotype; **b** embryo showing spina bifida and a dorsally flexed tail; **c** embryo of the most severely affected phenotype showing exencephaly (from van Straaten and Copp 2001, with permission)

may be convergent, merely reflecting superficial similarities in the mode of formation of mouse and human NTDs, but it may also reflect the action of homologous mechanisms and genes in mice and men (Copp et al. 1990). The gene loci, corresponding to two of the mutations, *splotch* (*Sp*) and *extra toes* (*Xt*), encode the transcription factors Pax3 and Gli3, respectively (Copp 1994). Their human homologues PAX3 and GLI3 are associated with Waardenburg type I syndrome and Greig's cephalopolysyndactyly, respectively. Hol et al. (1995) found a frameshift mutation in the gene for PAX3 in a girl with spina bifida and mild signs of Waardenburg syndrome. *PAX3* mutations are not a major cause of human NTDs, however (Melvin et al. 2000). Numerous gene knockouts have syndromes of multiple severe defects, lethal during embryogenesis, including failure to close the neural tube, in particular of the head (Juriloff and Harris 2000). Similar phenotypes in humans would lead to early spontaneous abortions. Two spontaneously occurring mutants, *curly tail* and *bent tail*, will be discussed briefly.

The *curly tail* (*ct*) mutation arose spontaneously in a litter of inbred GFF mice (Fig. 4.10) in 1950 (Grüneberg 1954). It is the best understood mouse model of NTD pathogenesis. The *curly tail* gene has variable expression and incomplete penetrance, with homozygotes developing exencephaly (approximately 3% of embryos), lumbosacral spina bifida (10%) and a

curled tail (50%); the remaining mice appear unaffected (van Straaten and Copp 2001). Closure of the PNP is delayed, so it remains wide open with everted neural folds, suggesting that elevation and subsequent convergence of the neural folds are failing. The failure of the PNP to close has been traced back to a tissue-specific defect of cell proliferation in the tail bud of the E9.5 embryo. This defect leads to a growth imbalance in the caudal region that generates ventral curvature of the body axis. Neurulation movements are opposed, leading to delayed PNP closure and spina bifida, or tail defects. The *curly tail* phenotype is influenced by several modifier genes and environmental factors (van Straaten and Copp 2001). NTDs in *curly tail* are resistant to folic acid, but they can be prevented by myo-inositol.

Bent tail (*Bn*) mutant mice of the C57B1/6J strain (Garber 1952) are characterized by a short tail with one or more bends. The mutation follows semidominant inheritance with incomplete penetrance in heterozygous females and has been mapped to the proximal part of the X chromosome (Lyon et al. 1987; Klootwijk et al. 2000). Exencephaly occurs in more than 10% of the embryos. Deletion of the *Zic3* gene may play a major role in the congenital malformations of the *bent tail* mice (Carrel et al. 2000; Klootwijk et al. 2000; Franke et al. 2003). The embryonic phenotype is shown in Fig. 4.11. Closure defects of the neural tube occur in the region of the

Fig. 4.11 Scanning electron micrograph of an E13.5 *bent tail* mouse embryo showing exencephaly (kindly provided by Henny W.M. van Straaten, Department of Anatomy and Embryology, University of Maastricht)

rhombencephalic neuropore and comprise the rhombencephalon and the caudal part of the mesencephalon, comparable to the neural fold elevation zones B and C as defined by Harris and Juriloff (1999). At a later stage of development, the defective closure is followed by massive overgrowth of brain tissue in the rhombencephalon and mesencephalon, causing disorganization of these brain structures.

4.5   Aetiology of Human Neural Tube Defects

NTDs are not only very heterogeneous in morphology but also in aetiology (Copp et al. 1990; Copp and Bernfield 1994; Norman et al. 1995; Naidich et al. 1996). Causes include chromosome abnormalities, single mutant genes, teratogens, maternal predisposing factors and multifactorial inheritance (Table 4.2). Several lines of evidence suggest a genetic basis in the majority of human NTDs.

4.5.1   Genetic Basis: Neural Tube Defects as a Multifactorial Trait

Multifactorial diseases are caused by a combination of unfavourable genetic and environmental factors. NTDs form a classic example of a complex disease with multifactorial aetiology (Hall et al. 1988). Family studies reveal that the incidence of NTDs is highest among relatives of the most severely affected patients, presumably because they present individuals with relatively high liabilities. Moreover, an increased risk for NTDs is not only evident for parents of an affected child but also for their first-, second- and third-degree relatives in approximately 4, 1, and less than 0.5% of cases, respectively (Carter 1974; Khoury et al. 1982). If more than one affected close relative is affected, the risk for other relatives is also higher. In spina bifida, if one child is affected, the risk for a subsequent sibling to be affected is around 3%, for newborns with two affected siblings it is about 10%, and for a child with three affected siblings it is as high as 20% (Seller 1994). Several multiple-case families have been described, in most of which no Mendelian pattern of inheritance was found (Drainer et al. 1991; Mariman and Hamel 1992; Chatkupt et al. 1995; Byrne et al. 1996). Apparent monogenic inheritance in some cases suggest that the disease may be caused by single genes, particularly the X gene (Toriello et al. 1980; Baraitser and Burn 1984; Toriello 1984; Jensson et al. 1988). A gene for spina bifida may be present on Xq27 (Fryns et al. 1996).

Females predominate among cases with anencephaly, whereas the sex ratio is equal, or slightly predominantly male, in lumbosacral spina bifida (Cuckle et al. 1993; Seller 1995). An excess of affected individuals among maternal relatives of the patient compared with relatives of the father was found (Byrne et al. 1996). A significant female preponderance was found in multiple-case families (Chapkupt et al. 1992; Mariman and Hamel 1992). Both genomic imprinting and abnormal X inactivation have been proposed as the underlying mechanism by which inherited factors may account for this phenomenon.

In mice, even in strains with apparently monogenic inheritance of the trait, NTDs have a polygenic nature (Copp 1994; Harris and Juriloff 1999; Fleming and Copp 2000). In many mouse mutations, manifestation of the phenotype is greatly influenced by the genetic background of the animal. This suggests that the mouse genome contains modifying genes that are capable of modulating the incidence and severity of mutant phenotypes. Several modifier genes are involved in the severity of the phenotype observed in *curly tail* mice (van Straaten and Copp 2001).

Table 4.2 Recognized causes of NTDs in man (after Copp et al. 1990 and Norman et al. 1995)

Causes	Examples
Chromosome abnormalities	Trisomy 13 Trisomy 18 Various unbalanced chromosome rearrangements, ring chromosomes, triploidy
Single mutant genes: autosomal recessive	Walker–Warburg syndrome Jarco–Levin syndrome Meckel–Gruber syndrome Robert syndrome
Single mutant genes: autosomal dominant	Median cleft face (possible) Syndrome of anterior sacral meningocele and anal stenosis
Probably hereditary	Anterior encephaloceles
Teratogens	Aminopterin/amethopterin Thalidomide Valproic acid Carbamazepine (possible) Hyperthermia (possible)
Maternal predisposing factors	Diabetes mellitus: anencephaly more frequent than spina bifida
Multifactorial inheritance	Anencephaly Meningomyelocele, Chiari II Meningocele, cranial and spinal Encephalocele Myelocystocele
Specific phenotypes without known cause	Amnion rupture sequence Cloacal exstrophy (OEIS) Sacrococcygeal teratoma (includes meningomyelocele) Other, unclassified

OEIS omphalocele, exstrophy of the bladder, imperforate anus and spinal anomalies

4.5.2   Environmental Factors

Many environmental factors have been suggested to play a role in NTD aetiology (Kalter 1968; Warkany 1971; Hall et al. 1988; Copp et al. 1990; Norman et al. 1995). In rodents, most teratogens cause exencephaly, but rarely spina bifida. Socioeconomic status, nutritional deficiency, maternal diabetes and the use of certain therapeutic drugs such as anticonvulsants and insulin are known risk factors (Table 4.2). Periconceptional supplementation of folic acid lowers the occurrence and recurrence risks of human NTDs (Czeizel and Dudás 1992; Berry et al. 1999; Berry and Li 2002). The mechanism involved in NTDs due to a lower maternal folate status may be defective folic acid metabolism in the mother (Steegers-Theunissen et al. 1991, 1994).

4.6   Prenatal Diagnosis

NTDs can be detected prenatally by ultrasound and by analysing the α-fetoprotein level in amniotic fluid or maternal serum (UK Collaborative Study 1977, 1979; Kleyer et al. 1978; Richards et al. 1988; Tidy 1989). α-**Fetoprotein** is produced initially by the yolk sac and subsequently the liver. It enters the amniotic fluid by way of the fetal urine and is removed by fetal swallowing and digestion. In open NTDs, a direct or indirect communication between the CSF and amniotic fluid occurs, leading to increased levels of α-fetoprotein in the amniotic fluid and maternal serum, detectable prenatally. Increased levels of α-fetoprotein are also found in gastroschisis, oesophageal and intestinal atresia, in sacrococcygeal teratoma and in Turner syndrome, but decreased levels are found in trisomies 21 and 18. Moreover, the α-fetoprotein method has a high false-positive rate and a relatively poor sensitivity. **Ultrasound** is the main method for detection of NTDs (Chap. 3). Prenatal diagnosis of a myelomeningocele is usually prompted by recognition of the associated Chiari II malformation. The most efficient sonographic findings, indicating a Chiari II malformation, are the diagnostic 'lemon' and 'banana' signs (Nicolaides et al. 1986; Sebire et al. 1997). The lemon sign of the head has become the diagnostic key for detecting spina bifida in the second trimester. The banana sign represents the cerebellum surrounding the brain stem in a small posterior fossa. The lemon sign is transient and usually not present anymore by the end of the second trimester. It represents an abnormal cranial vault that is narrowed rostrally, and results from low pressure in the ventricular cavity due to loss of CSF through the open NTD to the amniotic cavity. With the introduction of transvaginal ultrasound, detailed diagnosis became
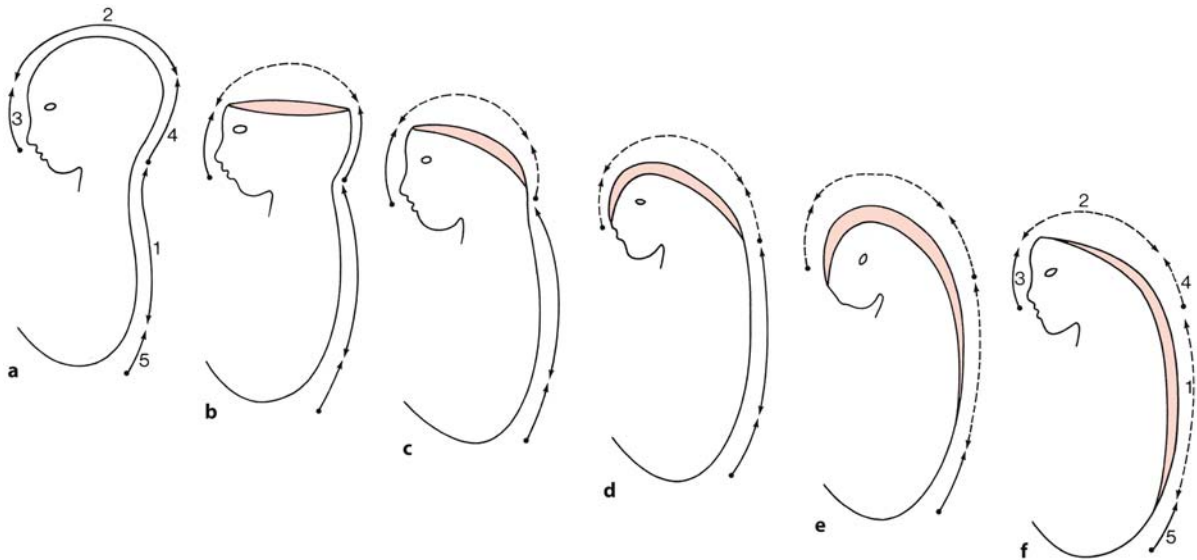
Fig. 4.12 Common neural tube defects (*NTDs*) from errors in multisite closure: **a** normal; **b** meroacrania (closure 2); **c** holoacrania (closures 2 and 4); **d** faciocranioschisis (closures 3, 2 and 4); **e** faciocraniorachischisis (closures 3, 2, 4 and 1); **f** craniorachischisis (closures 2, 4 and 1) (after Van Allen et al. 1993)

possible in the early fetal period and even around the end of the embryonic period (Blaas et al. 2000).

4.7 Cranial Neural Tube Defects

Reviewing their own clinical cases of NTDs and the literature available, Van Allen et al. (1993) recommended classification of human NTDs by closure site. They suggested five separate initiation sites for neural tube fusion, three in the cranial region and two in the spinal area (Fig. 4.12). They hypothesized the following: (1) anencephaly results from failure of closure 2 for meroacrania and closures 2 and 4 for holoacrania; (2) spina bifida cystica results from failure of rostral and/or caudal closure 1 fusion; (3) craniorachischisis results from failure of closures 2, 4 and 1; (4) closure 3 non-fusion is rare, presenting as a midfacial cleft, extending from the upper lip through the frontal area ('facioschisis'); (5) frontal and parietal encephaloceles occur at the sites of the junctions of the cranial closures 3–2 and 2–4 (the prosencephalic and mesencephalic neuropores); (6) occipital encephaloceles result from incomplete membrane fusion of closure 4; (7) the most caudal part of the neural tube may have a fifth closure site, involving L2 to S2; and (8) closure below S2 is by secondary neurulation.

Nakatsu et al. (2000) studied 47 embryos of the Kyoto Collection of Human Embryos that had a NTD at the cranial and/or cervical level. They classified these embryos with cranial NTDs into six groups ac-

cording to the level of the NTD (Fig. 4.13), characterized by the following: (1) an open neural tube at the frontal part of the head (prosencephalon or telencephalon); (2) an opening at the parietal region of the head (prosencephalon or mesencephalon); (3) an open neural tube over the fourth ventricle (rhombencephalon); (4) an open neural tube from the mesencephalon to the rhombencephalon; (5) an open neural tube extending from the frontal part of the head through the cervical region; and (6) total dysraphism, involving the entire length of the brain and spinal cord. Embryos with *total dysraphism* (Figs. 4.13f, 4.15a) were never seen after Carnegie stage 15 (4 weeks of gestation), suggesting that embryos with such extreme NTDs die rather early in utero and are eliminated (Shiota 1991). About two thirds of embryos with NTDs at the rhombencephalon (types 3, 4 and 5) were younger than stage 19 (6.5 weeks of gestation), while about 70% of the cases with prosencephalic NTDs (types 1 and 2) only were older than stage 20 (7.5 weeks of gestation). Therefore, the level and severity of the NTD may affect the intrauterine survival of NTD embryos (Nakatsu et al. 2000).

4.7.1 Anencephaly

Anencephaly is the most severe, usually lethal type of cerebral dysraphia (Figs. 4.14, 4.15), showing partial absence of the brain and the overlying skull (Potter and Craig 1975; Giroud 1977; Lemire et al. 1978;
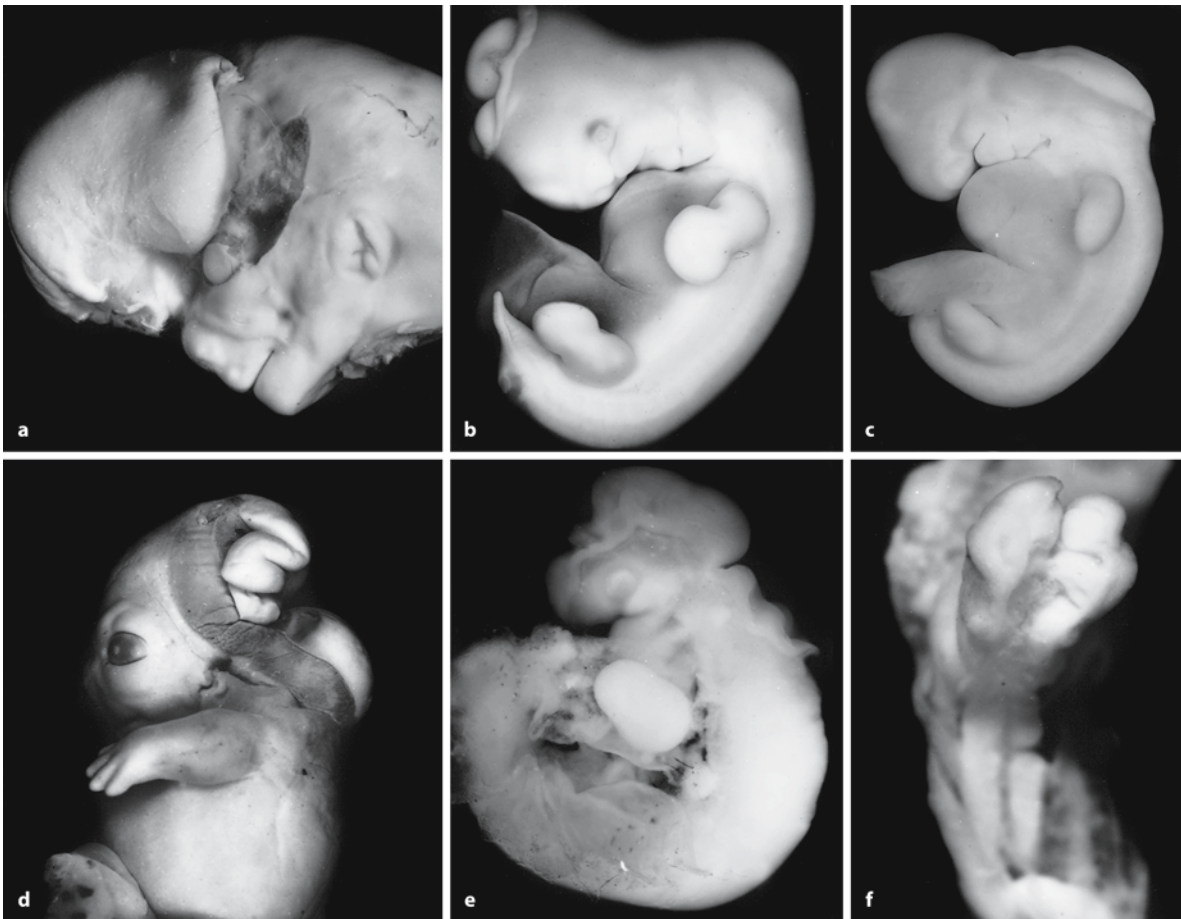
Fig. 4.13 Classification of cranial NTDs in human embryos: **a** type I: the neural tube is open at the frontal part of the head (Carnegie stage 23); **b** type II: the neural tube is open at the parietal region (Carnegie stage 16); **c** type III: the neural tube is open over the fourth ventricle (Carnegie stage 15); **d** type IV: the neural tube is open over the mesencephalon to the rhombencephalon (Carnegie stage 20); **e** type V: the neural tube is open from the frontal part of the head to the cervical region (Carnegie stage 14); **f** type VI: total dysraphism, involving the entire length of the brain and spinal cord (Carnegie stage 11) (from Nakatsu et al. 2000, with permission)

Fig. 4.14 Typical craniofacial features of anencephaly in a fetus born to a 24-year-old gravida by induced abortion (from the Department of Neuropathology, Medizinische Hochschule Hannover; courtesy Akira Hori)

Fig. 4.15 Early fetal dysraphism:
a exencephaly and myeloschisis
in an 18-week-old fetus; **b** sagittal
section of anencephaly in a
16-week-old fetus (from the
Department of Neuropathology,
Medizinische Hochschule
Hannover; courtesy Akira Hori)
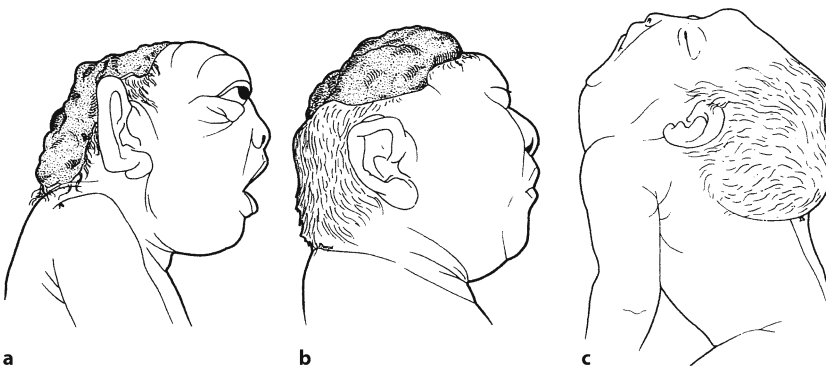
Fig. 4.16 Holoacrania (**a**),
meroacrania (**b**) and inien-
cephaly (**c**) malformations
(after Duhamel 1966)

Lemire 1987; Norman et al. 1995; Larroche et al. 1997). The history of anencephaly includes the finding of an anencephalic Egyptian mummy by the French zoologist Etienne Geoffroy Saint-Hilaire in 1826 and various examples of anencephaly described in Europe since the mid-sixteenth century (Giroud 1977; Lemire et al. 1978). Anencephaly and related dysraphic disorders are complex malformations that may primarily affect the early production of mesenchyme, resulting in failure of the whole neural folds to elevate, thus causing the loss of a buttressing effect to the neuroectoderm, which leads to failure of the neural tube to close and to skeletal defects (Marín-Padilla 1970, 1991). Padget (1970) suggested reopening of the neural tube as a possible mechanism, whereas Gardner (1973) proposed that in some cases anencephaly may be due to rupture of an overdistended neural tube rather than to absence of neural tube closure. Owing to prenatal ultrasound screening and subsequent termination of pregnancies, anencephaly is progressively disappearing from most developed countries. The eyes are usually normal macroscopically and optic nerves are present, suggesting that the forebrain did develop.

In pregnant rats, anencephaly can be produced by hypervitaminosis A (Geelen 1980; Geelen et al. 1980), occurring in three phases: (1) failure of closure of the rostral part of the neural plate (**encephaloschisis**); (2) protrusion of a well-developed brain (**exencephaly**); and (3) degeneration of the exposed portions, resulting in **anencephaly**. Data for human anencephalic embryos suggest that anencephaly in man arises in a similar way in three stages (Müller and O'Rahilly 1984, 1991; Lemire and Siebert 1990): (1) cerebral dysraphia, beginning before or during Carnegie stage 11 (approximately 23–25 days); (2) exposure of the resulting exencephalic but well-differentiated brain during the remainder of the embryonic period; and (3) degeneration of the exposed brain during the fetal period, leading to replacement of the brain by a cerebrovascular mass, the **area cerebrovasculosa** (Figs. 4.15b, 4.16). The area cerebrovasculosa

Fig. 4.17 Iniencephaly in a 33-week-old fetus. The cervical vertebral column was severely retroflexed so that the occipital part of the head was continuous with the inferior thoracic vertebral column. There was extensive rachischisis of the cervical and upper thoracic cord, largely covered by the occiput. (From the Department of Neuropathology, University Hospital Aachen; courtesy Martin Lammens, Nijmegen)

consists of glial and ependymal cells. There are several varieties of anencephaly (Lemire et al. 1978). The most common is *holoacrania*, in which the open defect extends through the level of the foramen magnum (Fig. 4.16a). When the skull defect does not reach the foramen magnum, the anencephaly is classified as *meroacrania* (Fig. 4.16b). The malformations of the CNS in anencephaly are rather variable, depending on the extent of the defect and the age of the case. The cerebral hemispheres are usually disorganized masses of haemorrhagic tissue, and retention of diencephalic and brain stem structures varies. The hypothalamus is missing, but the anterior pituitary can be found in most cases (Lemire et al. 1978; Norman et al. 1995). Cranial nerve nuclei may or may not be present, and the central connections of cranial nerves, the optic nerve in particular, may be interrupted (Lemire et al. 1978). Skeletal malformations are very common in anencephaly. Nearly every bone of the skull is abnormal to some degree (Marín-Padilla 1965a, b, 1970, 1991). Extremely rare are cases of ectopic brain tissue in anencephaly, such as ectopic brain tissue in the submandibular region and lung (Okeda 1978; Rizzuti et al. 1997). Possibly, anencephalic fetuses swallow dysraphic and destroyed brain fragments together with amniotic fluid (Okeda 1978).

Iniencephaly includes deficiency of the occipital bone, cervicothoracic spinal reflexion and rachischisis (Wheeler 1918; Lemire et al. 1972; Nishimura and Okamoto 1977; Aleksic et al. 1983; Friede 1989; Scherrer et al. 1992). Iniencephaly differs from anencephaly in that a cranial cavity is present and skin covers the head and retroflected region (Figs. 4.16c, 4.17). The neural tube lesion is found at the level of the cervical spine and varies from spina bifida with intact skin to myelomeningocele and open rachischisis (Friede 1989). Visceral anomalies are found in 84% of cases (Norman et al. 1995).

4.7.2   Encephaloceles and Cranial Meningoceles

Encephalomeningoceles or *encephaloceles* are protrusions of brain and meninges through an abnormal opening in the skull (Figs. 4.18, 4.19), most commonly in either the occipital or the frontal region (Lemire et al. 1975; Potter and Craig 1975; Naidich et al. 1992; Norman et al. 1995). In Western countries, 85% of encephaloceles are posteriorly located, whereas anterior encephaloceles are more common in southeast Asia, especially in Thailand. *Fronto-ethmoidal encephaloceles* (Figs. 4.18c, 4.19b, c) can be subdivided
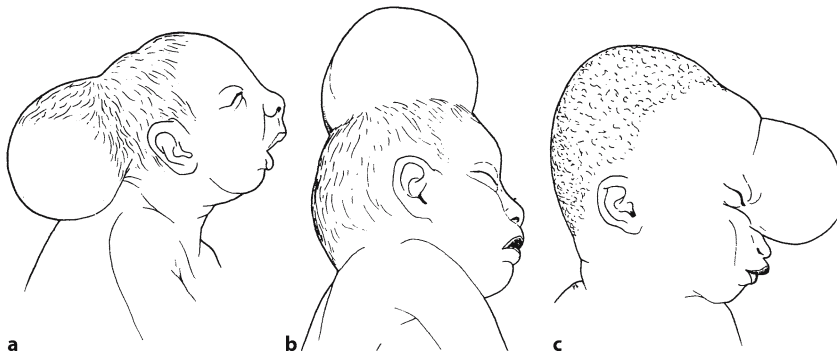
Fig. 4.18 Various forms of encephaloceles: **a** occipital; **b** parietal; **c** frontal encephaloceles (after Duhamel 1966)

Fig. 4.19 Basal and frontal encephaloceles: **a** encephalocele of the skull base, view of a complete cleft secondary palate of a neonate; **b** frontal view of a 10-year-old boy with a nasofrontal encephalocele with hypertelorism; **c** the same patient in profile; note that the skin, covering the encephalocele, did not differentiate properly (kindly provided by Christl Vermeij-Keers, Department of Plastic and Reconstructive Surgery, Erasmus University Medical Centre, Rotterdam)

into nasofrontal, naso-ethmoidal and naso-orbital encephaloceles (Suwanwela et al. 1971; Suwanwela and Suwanwela 1972). They are all characterized by an internal defect of the cranium between the frontal bone and the ethmoid, either in the midline in the anterior cranial fossa, corresponding with the foramen caecum, or on either side of the midline just rostral to the cribriform plate of the ethmoid (Hoving 1993; Fig. 4.20). In early developmental stages, the foramen caecum does not end blindly (Holl 1893). Mesenchyme extends from the intracranial space between the ethmoidal and nasal bones to the fonticulus nasofrontalis. Part of this tissue will differentiate into the nasal process of the frontal bone, thereby closing the bottom of the foramen caecum. The presence of this mesenchymal, i.e. dural opening at the site of the foramen caecum, connecting the intracra-

nial and nasal cavities, may explain the occurrence of ectopic nasal masses such as encephaloceles and gliomas (Gruenwald 1910; Bradley and Singh 1982; Barkovich et al. 1991). Yeoh et al. (1989) considered most nasal gliomas as sequestered encephaloceles, consisting of glial tissue and more rarely neurons and foci of ependyma, choroid plexus and pigmented epithelium. Fronto-ethmoidal encephaloceles may be due to disturbed separation of the neural ectoderm from the surface ectoderm during neurulation at the site of the final closure of the rostral neuropore, *after* the neural folds adhered at Carnegie stage 11 (Sternberg 1927, 1929; Hoving et al. 1990; Hoving 1993). A similar suggestion has been made for basal encephaloceles (Yokota et al. 1986).

Occipital encephaloceles may be found in a large group of syndromes (Table 4.3) such as Meckel–Gru-

Fig. 4.20 Fronto-ethmoidal encephaloceles are characterized by an internal skull defect just anterior to the cribriform plate and crista Galli: **a** nasofrontal; **b** naso-ethmoidal; **c** naso-orbital encephaloceles (after Hoving 1993)
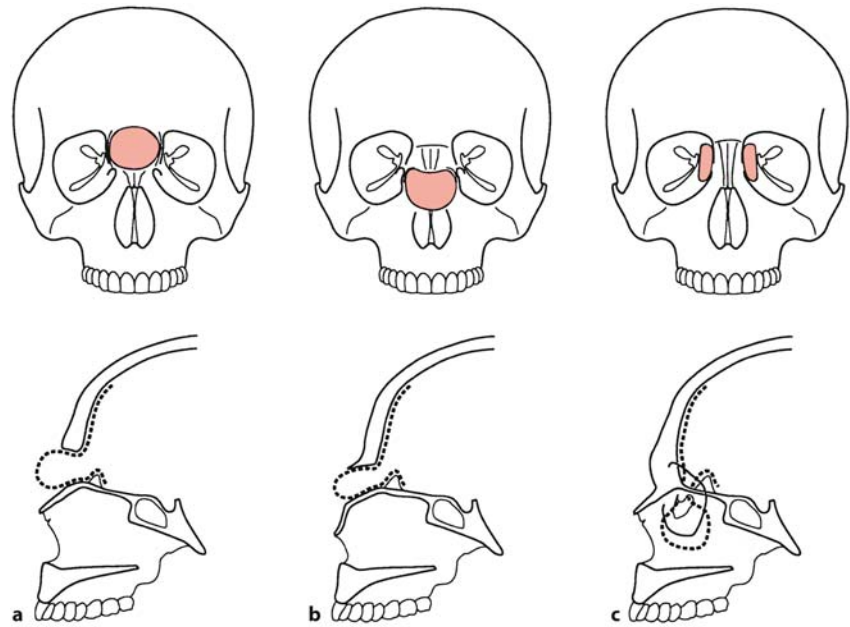
ber syndrome (Meckel 1822; Gruber 1934), which is characterized by prosencephalic dysgenesis, occipital encephalocele, rhombic roof dysgenesis, polycystic kidneys and polydactyly (Opitz and Howe 1969; Hori et al. 1980; Ahdab-Barmada and Claassen 1990; Clinical Case 3.1) and Walker–Warburg syndrome (Clinical Case 10.11). Bassuk et al. (2004) described the clinical and radiographic characteristics of a non-consanguineous Vietnamese with an autosomal dominant form of occipital encephalocele. Unusual encephaloceles should raise suspicion of the amniotic rupture sequence (Moerman et al. 1992; Norman et al. 1995; Clinical Case 3.3). In occipital encephaloceles (Clinical Case 4.1), the primary defect may be non-separation of neural and surface ectoderm, leading to defects in the formation of the occipital bone well before the end of the embryonic period. Subsequent abnormalities of the brain are secondary (Karch and Urich 1972; Chapman et al. 1989; Norman et al. 1995). Although occipital lobes may be found in the encephaloceles, the greatest deformities occur in posterior fossa structures. The clinical picture depends on the site of the encephalocele and its occurrence as part of a specific syndrome. The cerebellum may be absent or may show disorders of neuronal migration. *Tectocerebellar dysraphia* (aplasia of the vermis with occipital encephalocele) may be viewed as a cerebellar malformation (Friede 1978, 1989) or as a subset of occipital encephalocele (Chapman et al. 1989; Hori 1994; Norman et al. 1995). An example is presented in Clinical Case 4.2.

Cranial meningoceles are much less common than encephaloceles. Two cases are shown in Clinical Case 4.3. Isolated cranium bifidum occultum, i.e. a simple skull defect without prolapse of meninges or brain, is rare and clinically insignificant (McLaurin 1977; Aicardi 1998). The skull defect is always situated along the sutures and mostly in the midline. A peculiar case of a rudimentary occipital meningocele is presented in Clinical Case 4.4.

Table 4.3 Main syndromes with encephaloceles (after Norman et al. 1995; Aicardi 1998)

Syndrome	Main features	Inheritance	References
Meckel–Gruber syndrome	Polycystic kidneys, postaxial polydactyly, hydrocephalus, vermis agenesis, cleft lip and palate, clubfoot, genital anomalies, microphthalmia (Clinical Case 3.1)	AR, 1 in 30,000–50,000 births	Hsia et al. (1971); Hori et al. (1980); Paetau et al. (1985)
Walker–Warburg syndrome	Hydrocephalus, vermis agenesis, severe neurological dysfunction from birth, lissencephaly type 2 (Clinical Case 10.11)	AR	Bordarier et al. (1984); Williams et al. (1984)
Dandy–Walker syndrome	Vermis agenesis, hydrocephalus, heterotopia of inferior olive, corpus callosum defects (Clinical Case 8.4)	Sporadic	Hirsch et al. (1984)
Joubert syndrome	Panting respiration and apnoeic pauses from birth, mental retardation, vermis agenesis, retinopathy or optic disc coloboma, cerebellar ataxia (Clinical Case 8.5)	AR	Aicardi et al. (1983); Edwards et al. (1988)
Tectocerebellar dysraphia	Mental retardation (Clinical Case 4.2)	Sporadic	Friede (1989)
Goldenhar–Gorlin syndrome	Orofacial abnormalities, preauricular tags, epibulbar dermoids (Chap. 5)	Sporadic	Aleksic et al. (1984)
Chromosomal syndromes, trisomy 13 in particular		Mainly sporadic	Holmes et al. (1976)
Occipital encephalocele, myopia and retinal dysplasia	Retinal detachment	Unknown	Knobloch and Layer (1971)
Amnion rupture sequence	Congenital amputation of digits or limbs, facial clefts, circumferential scars around limbs (Clinical Case 3.3)	Unknown	Moerman et al. (1992)
Median cleft face syndrome	Anterior encephalocele	AD (possible)	DeMyer (1967)

AD autosomal dominant, *AR* autosomal recessive

Occipital Encephalocele

Most encephaloceles may arise after neural tube closure, owing to non-separation of neural and surface ectoderm, leading to defects in the formation of the skull (Campbell et al. 1986; Vermeij-Keers 1990). In cases in which meninges fail at the site of the defect, continuity of the neuroectoderm and surface ectoderm may be apparent (see Case Report).

Case Report. Prenatally, an *occipital encephalocele* was detected on ultrasound examination, suspicious for Meckel syndrome. Ultrasound examination of the kidneys did not reveal any abnormalities, however. The child died a few hours after birth. In this neonate (total length 48 cm, weight 2,800 g), a large occipital encephalocele was found with a diameter of 15 cm. The brain with the cele were removed from the cranial cavity. The cele consisted of large, cystic, blood-filled spaces and brain tissue (Fig. 4.21). At places, brain tissue was continuous with a thin layer of epidermis, suggesting continuity of neuroectoderm and surface ectoderm. There was no spinal dysraphism. The brain weight was 415 g. The encephalocele was in fact situated at the border of the parietal and occipital lobes. The left half of the cerebrum was malformed. Frontally, small gyri were present, no definite Sylvian sulcus was formed and a central sulcus was only ill-defined. The right cerebral hemisphere showed small gyri in the frontal and parietal lobes. A Sylvian sulcus was present. The dysplastic cerebellum showed two lateral lobes which partly covered the brain stem laterally. The olfactory system did not show abnormalities. Normal olfactory bulbs and tracts were observed.

The encephalocele contained two lobes of dysplastic brain tissue, separated from each other by a septum, continuous with the contents of the cranial cavity. Commissural structures such as the corpus callosum were relatively normally formed. In the cranial cavity, the supratentorially situated brain tissue, i.e. the caudal part of the hemispheres with the corpus callosum, was displaced caudalwards as a whole. Similarly, the upper part of the cerebellum was 'drawn' towards the cele, giving the cerebellum an elongated shape on sagittal section. The brain tissue within the cele appeared to be largely cerebral cortex with choroid plexus. No cerebellar tissue was found in the cele. At some places the dysplastic brain tissue was covered with meningeal tissue in the form of an area cerebrovasculosa.

This case was kindly provided by Max Kros (Department of Pathology, Erasmus University Medical Centre, Rotterdam).

Fig. 4.21 Occipital encephalocele: **a** picture taken before autopsy; **b** median section of the brain and the encephalocele (kindly provided by Max Kros, Department of Pathology, Erasmus University Medical Centre, Rotterdam)

References

Campbell LR, Dayton DH, Sohal GS (1986) Neural tube defects: A review of human and animal studies on the etiology of neural tube defects. Teratology 34:171–187

Vermeij-Keers C (1990) Craniofacial embryology and morphogenesis: Normal and abnormal. In: Stricker M, van der Meulen J, Raphael B, Mazzola D (eds) Craniofacial Malformations. Churchill Livingstone, Edinburgh, pp 21–60

Clinical Case 4.2
Tectocerebellar Dysraphia

Tectocerebellar dysraphia is a rare malformation, consisting of aplasia of the vermis with an occipital encephalocele. Friede (1978) described five cases and introduced the term tectocerebellar dysraphia. Usually, this malformation is viewed as a subset of occipital encephalocele. Hori (1994) reported the youngest case (see Case Report).

Case Report. The mother, a 22-year-old primigravida, had an uneventful pregnancy until Caesarean section was required at term because of hydrocephalus and breech presentation. The baby was, however, stillborn owing to a double twist of the umbilical cord around the neck. The female neonate had a body weight of 2,500 g and a total length of 50 cm. An enormous hydrocephalus (head circumference 43 cm) and a posterior encephalocele with a diameter of 3 cm were found (Fig. 4.22a). The only visceral abnormalities found were hypoplastic and dysplastic kidneys as well as a hypoplastic placenta with several calcifications.

Neuropathologically, the fontanelles were enormously enlarged. The cerebrum showed microgyria over almost its entire surface. On frontal sections, a severe hydrocephalus was observed with very thin cortical ribbons and corpus callosum, and absence of the septum pellucidum (Fig. 4.22b). The fornix was found dorsal to the diencephalon. On the ventricular surface of the hemispheres, numerous small subependymal nodular heterotopia were present. After removing the infratentorial structures from the cerebrum, total agenesis of the vermis was noted (Fig. 4.22c). The cerebellum was very flat and elongated in a posterior direction, reaching the contents of the encephalocele. The stalk of the encephalocele was composed of connective tissue adherent to the tentorium and the leptomeninx. The encephalocele contained soft connective tissue. The midbrain showed a triangular deformation, but the aqueduct was widely patent. There was a dorsal protuberance of the medulla oblongata, giving it a 'kinky' appearance. The spinal canal and cord were grossly normal and the spinal nerve roots showed a normal course. Histologically, the cerebral cortex was, although grossly polygyric in appearance, generally well differentiated. Dysgenetic lesions were generally encountered close to subependymal heterotopia. These heterotopia were also numerous near the ventricular, matrix zone. The cerebellar hemispheres were connected by thin, ventral white matter, containing numerous neuronal heterotopia. Some heterotopia were also observed in the raphe of the lower midbrain. Inside the encephalocele, there were fragments of cerebellar cortical tissue with severe loss of granule cells and cystic necrosis.

The diagnosis of tectocerebellar dysraphia can be made on gross inspection. Awareness of this anomaly will therefore make clinical diagnosis on MRI possible. Furthermore, it should be emphasized that this anomaly tends to affect the first child, whereas the subsequent siblings may be healthy. Both sexes are affected
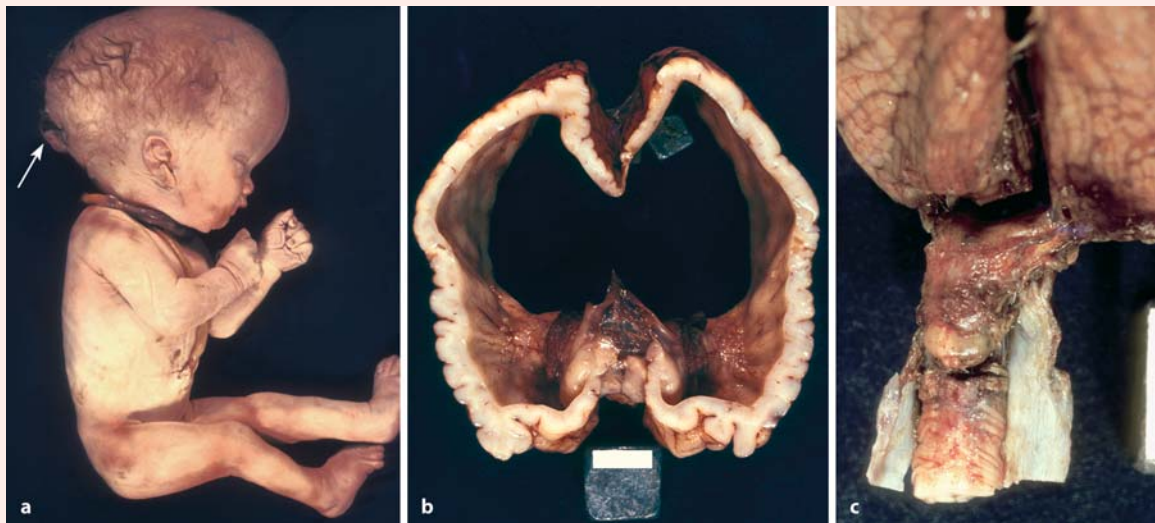
Fig. 4.22 Tectocerebellar dysraphia: **a** enlargement of the head, a posterior encephalocele (*arrow*) and strangulation by the umbilical cord; **b** severe hydrocephalus with absence of the septum pellucidum; **c** dorsal view of infratentorial structures (from Hori 1994, with permission)

with similar frequency. Chromosomal aberrations have not been described. By early, successful neurosurgical resection of the encephalocele and implantation of a ventricular shunt, the psychomotor development of the patient may be favourable (Friede 1978) as in other types of dysraphism with infratentorial malformations.

References

Friede RL (1978) Uncommon syndromes of cerebellar vermis aplasia. II: Tectocerebellar dysraphia with occipital encephalocele. Dev Med Child Neurol 20:764–772

Hori A (1994) Tectocerebellar dysraphia with posterior encephalocele (Friede): Report of the youngest case. Clin Neuropathol 13:216–220

Clinical Case 4.3
Cranial Meningoceles

An encephalocele is a dysraphism with protruding brain tissue in a sac. If the brain tissue is lacking in the sac and the contents consist of leptomeninges, the term cranial meningocele is used. Like encephaloceles, *cranial meningoceles* usually occur along the midline, most frequently in the occipital region and rarely in the frontal region (see Case Reports).

Fig. 4.23 Occipital meningocele (kindly provided by Gerard van Noort, Laboratory for Pathology East-Netherlands, Enschede)

Case Report. The case shown in Fig. 4.23 concerns a male, identical twin pregnancy in a 28-year-old mother. One of the children died in utero around the 19th week of pregnancy. In the other fetus an occipital encephalocele was diagnosed and the pregnancy was terminated at 19 weeks of pregnancy. The placenta was monochorial and bi-amniotic, so the twins were monovular. The first child that died in utero had a growth retardation and was extremely pale, but no obvious congenital malformations were found. Possibly, a transfusion syndrome was present. The second child had a weight of 220 g and a total length of 21.5 cm, in line with a pregnancy duration of 19–20 weeks. This fetus showed an occipital encephalocele with a malformed skull base. The posterior cranial fossa was too small with protruding petrous parts of the temporal bones. In the occipital bone a round opening of 8–9 mm was found, through which the steel of the cele passed. It appeared to be a *ventriculocele* of the fourth ventricle, given its position in the midline and the absence of parts of the occipital lobes. No cerebellar tissue was recognizable, and a small pons was present. The steel was formed by the cerebellar peduncles, the superior peduncle in particular. Possibly, cerebellar tissue was withdrawn secondarily from the sac owing to circulation problems. Other abnormalities noted were as follows: hypoplasia of the cranial nerves, innervating the extra-ocular muscles; a reduced cranial flexure between the mesencephalon and pons; elongated mamillary bodies; and hydromyelia of the spinal cord. The second case was diagnosed as a frontal encephalocele on intrauterine ultrasound examination. At autopsy, however, it appeared to be a meningocele (Fig. 4.24).

Fig. 4.24 Frontal meningocele (reproduced with permission from Hori 1999, *No Shinkei Geka* 27:969–985; copyright 1999, Igaku Shoin Ltd.)

Rudimentary Occipital Meningocele

A peculiar case of a rudimentary occipital meningocele was described by ten Donkelaar et al. (2002) after examination of a surgically removed occipital skin appendix (see Case Report).

Case Report. The occipital skin appendix (Fig. 4.25a) was surgically removed when the infant was 5 months of age. He was born at home after an uneventful pregnancy of duration 38 weeks and 4 days with a birth weight of 3,230 g as the third child of healthy, non-consanguineous parents. Family history was unremarkable, though his mother and two other relatives had a preauricular tag. Congenital hand anomalies and the occipital skin appendage were the reason for hospital admission. Both hands showed constrictions and amputations with fresh, healing wounds (Fig. 4.25 b). The left paramedian, occipital worm-like appendix measured about 2 cm and overlaid a palpable skull defect. At the end of the skin appendage a small ulceration was found. A skull X-ray showed a small round defect in the occipital bone underneath the skin tag with a sclerotic edge. Cerebral MRI showed a normal configuration of the brain and

meninges in the posterior cranial fossa. The child's growth and development were normal. Histological examination of the skin appendage showed that its end contained intestinal tissue including crypts, covered by columnar cells with a brushborder and interspersed goblet cells (Fig. 4.25 c, d). Underneath this intestinal mucosa, a surplus of smooth muscle tissue was present (Fig. 4.25 e). The intestinal tissue was covered with a crusta and sharply demarcated from the orthokeratotic squamous epithelium that covered the rest of the skin tag. The fibrovascular stroma of the skin tag contained clusters of meningothelial cells, staining positive for epithelial membrane antigen (EMA), a marker for meningothelial cells.

The association of congenital scalp defects and distal congenital hand anomalies is relatively rare and one form is known as the Adams–Oliver syndrome (Küster et al. 1988; Keymolen et al. 1999). No comparable cases were found in the literature. Possible explanations for this peculiar situation are as follows: (1) disorganization-like syndrome (Donnai and Winter 1989); (2) homeotic transformations (Slack 1985; Chap. 2); (3) abnormal surface encounter between the epidermis and remnants of the yolk sac or omphaloenteric duct (Blackburn et al. 1997); and (4) endoectodermal adhesion in the presomite embryo (Bremer 1952; Bentley and Smith 1960).

Fig. 4.25 Rudimentary occipital meningocele: **a** skin tag containing a rudimentary occipital meningocele; **b** finger defects of the left hand; **c–e** *(see next page)*
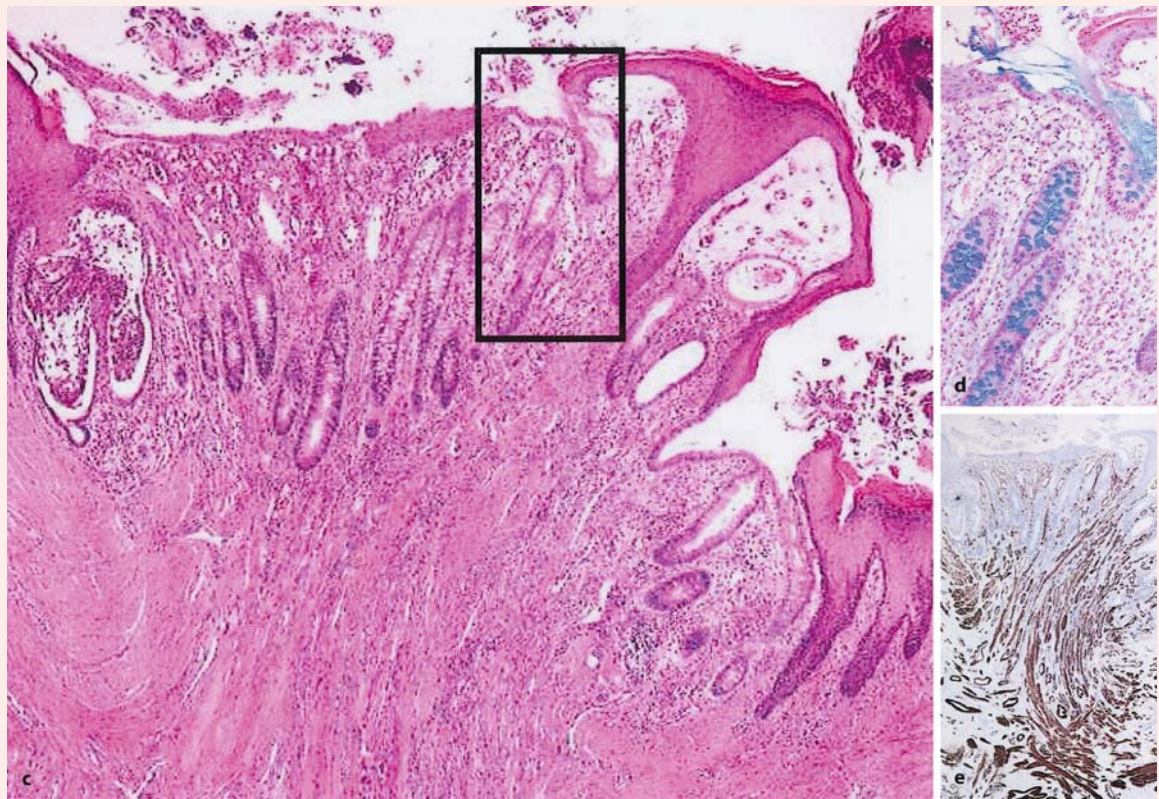
Fig. 4.25 *(Continued)* **c**–**e** histological sections of the top of the occipital appendix: **c** a haematoxylin–eosin stained section in which intestinal mucosa can be seen in its superficial part, the rest of the appendix being covered with epidermis; **d** detail, showing the presence of intestinal mucosa in an Alcian blue staining for acid mucopolysaccharides; the Alcian Blue staining highlights the mucus in the goblet cells of the intestinal mucosa; **e** detail, showing the presence of smooth muscle bundles in the basal part of the mucosa, immunohistochemically stained for α-smooth muscle actin (from ten Donkelaar et al. 2002, with permission)

References

Bentley JFR, Smith JR (1960) Developmental posterior enteric remnants and spinal malformations – The split notochord syndrome. Arch Dis Child 35:76–86

Blackburn W, Stevenson RE, Cooley NR Jr, Stevens CA, Hudson J (1997) An evaluation and classification of the lesions attending abnormal surface encounters within the fetal habitat. Proc Greenw Genet Center 16:81–89

Bremer JL (1952) Dorsal intestinal fistula; accessory neurenteric canal; diastematomyelia. Arch Pathol 54:132–138

Donnai D, Winter RM (1989) Disorganisation: A model for "early amnion rupture"? J Med Genety 26:421–425

Keymolen K, de Smet L, Bracke P, Fryns JP (1999) The concurrence of ring contrictions in Adams-Oliver syndrome: Additional evidence for vascular disruption as common pathogenetic mechanism. Genet Counsel 10:295–300

Küster W, Lenz W, Kääriäinen H, Majewski F (1988) Congenital scalp defect with distal limb anomalies (Adams-Oliver syndrome): Report of ten cases and review of the literature. Am J Med Genet 31:99–115

Slack JMW (1987) Homeotic transformation in man: Implications for the mechanism of embryonic development and for the organization of epithelia. J Theor Biol 114:463–490

ten Donkelaar HJ, Hamel BCJ, Hartman E, van Lier JAC, Wesseling P (2002) Intestinal mucosa on top of a rudimentary occipital meningocele in amniotic rupture sequence: Disorganization-like syndrome, homeotic transformation, abnormal surface encounter or endoectodermal adhesion? Clin Dysmorphol 11:9–13
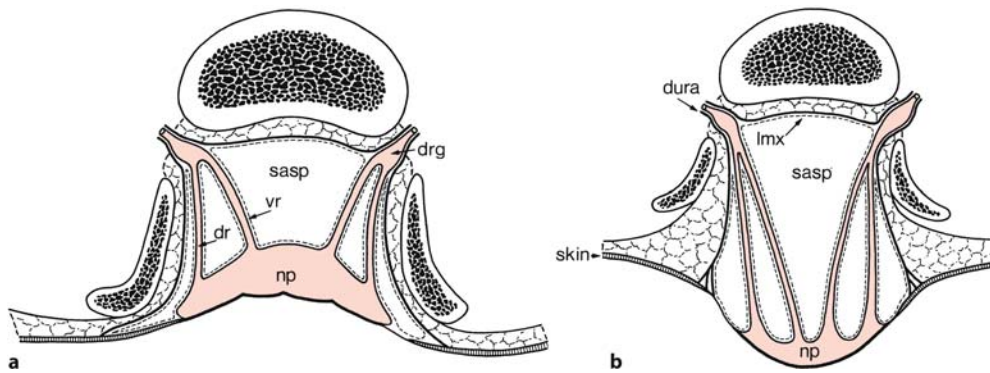
Fig. 4.26 A myelocele and a myelomeningocele. In a myelocele (**a**), the neural tissue has the flat configuration of the unneurulated neural placode. The exposed dorsal surface shows midline and paramedian sulci corresponding to the ventral neural groove and the sulcus limitans. The ventral surface and the dorsal and ventral roots are lined by pia-arachnoid (*stippled lines*). The pia-arachnoid encloses the subarachnoidal space. The dura (*thick lines*) encloses the neural placode with its roots and the subarachnoidal space ventrally and laterally. The laminae of the vertebrae are widely everted. In a myelomeningocele (**b**), the same basic anatomy is found, but expansion of the subarachnoidal space displaces the neural placode dorsally, everts it and elevates it well above the surface. *dr* dorsal root, *drg* dorsal root ganglion, *lmx* leptomeninx, *np* neural placode, *sasp* subarachnoidal space, *vr* ventral root. (After Naidich et al. 1996)

4.8   Spinal Neural Tube Defects

Spinal dysraphism includes a heterogeneous group of spinal abnormalities with imperfect fusion of the midline mesenchymal, bony and neural structures as common feature (Naidich et al. 1996; Aicardi 1998; Tortori-Donati et al. 2000; Rossi et al. 2004.). In *spina bifida aperta*, the overlying skin is deficient and neural tissue and/or meninges are exposed to the environment. The lesion may be covered by a membrane and an underlying cystic mass may protrude as *spina bifida cystica*. Four main types of spina bifida occur, characterized by the following: (1) the neural plate remaining open (myeloschisis or myelocele; Fig. 4.26a); (2) the neural plate or tube being exteriorized (myelomeningocele; Fig. 4.26b), almost always associated with a Chiari II malformation; (3) only meninges protruding (meningocele); and (4) merely a skeletal defect being evident (spina bifida occulta). The last group includes hydromyelia, the split notochord syndrome, dorsal dermal sinuses and diastematomyelia (Naidich et al. 1996; Aicardi 1998; Barkovich 2000; Ikenouchi et al. 2002). Spinal lipomas occur with occult spina bifida as well as in cases of open NTD, and lie dorsal to the neural placode. The clinical importance of spinal lipomas is the cord tethering that is associated with it (Naidich et al. 1983, 1996; Harrison et al. 1990). Encapsulated, ectopic neural tissue has been found in the retroperitoneal region, and is termed 'abdominal brain' (Hori et al. 1998).

4.8.1   Myeloceles, Myelemeningoceles and Spinal Meningoceles

Myeloceles and myelomeningoceles are the two commonest forms of spina bifida aperta, and appear to result from deranged neurulation (Naidich et al. 1996; Clinical Case 4.5). When the neural folds fail to flex and to fuse into a tube, they persist as a flat plate of neural tissue that is known as the **neural placode** (Fig. 4.26a). The superficial ectoderm remains lateral to the neural placode, leaving a midline defect. Mesenchyme also does not reach the midline, so the bony, cartilaginous and ligamentous structures are also deficient in the midline. Some examples found in embryos of the Kyoto Embryology Collection are shown in Figs. 4.27 and 4.28. After birth, the neural tissue appears as a raw, reddish, vascular plate separated into two halves by a midline groove, continuous with the central canal (Fig. 4.29a). The pia-arachnoid membrane may be found as a thin ring encircling the neural tissue. When the subarachnoid space is small, the membranous ring is narrow and the neural plate hardly protrudes (*myelocele*; Fig. 4.26a). When the subarachnoid space is very large, the membranous ring is wide and the neural plate is elevated (*myelomeningocele*; Fig. 4.26b). In both myeloceles and myelomeningoceles, epithelial cells may grow inwards from the skin around the midline defect to cover the membranes and even the neural tissue. The entire site may become epithelialized secondarily by a thin dysplastic skin layer.
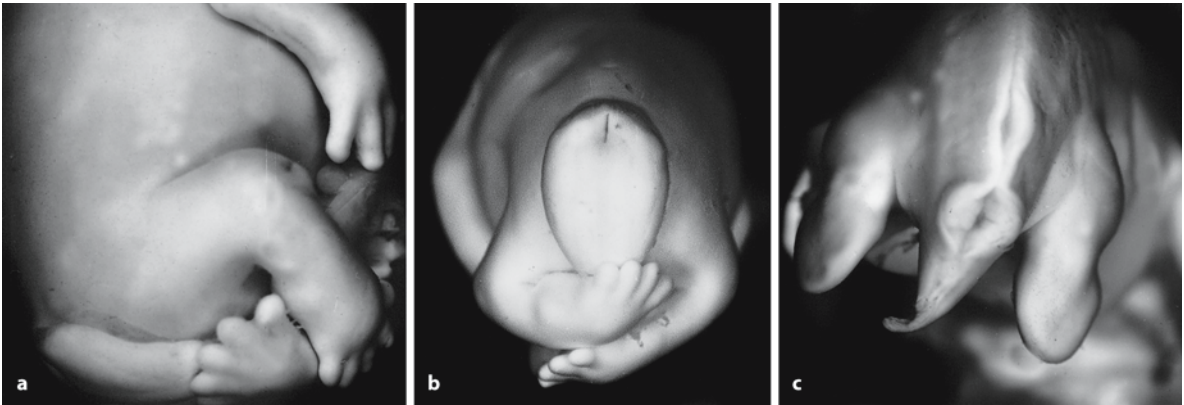
Fig. 4.27 Caudal myeloschisis in human embryos: **a**, **b** a 7-week-old embryo (Carnegie stage 22) with overgrown neural tissue, possibly associated with caudal regression; **c** a 6-week-old embryo (Carnegie stage 17) (from the Kyoto Collection of Human Embryos; courtesy Kohei Shiota)
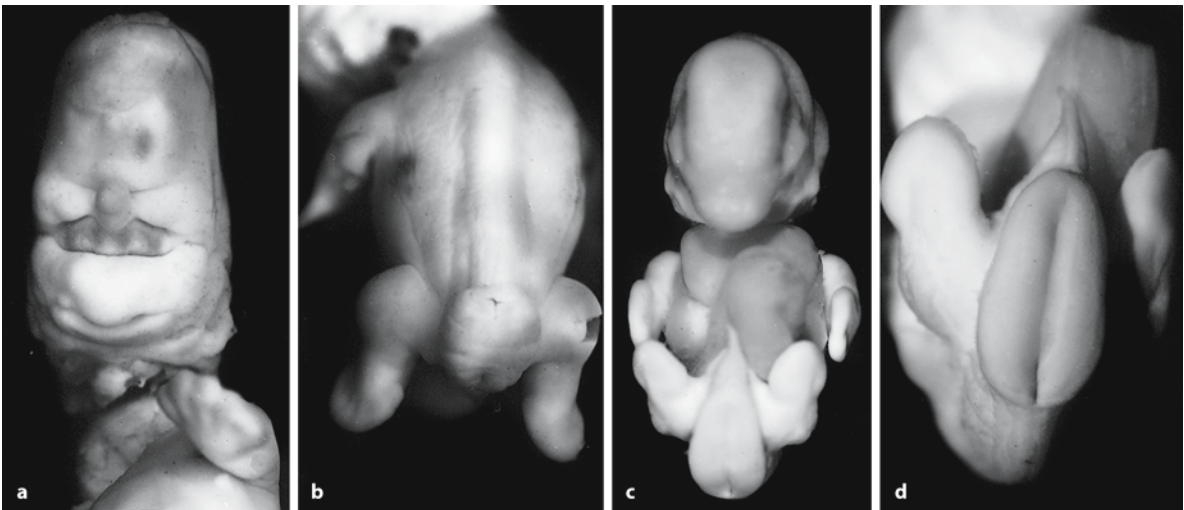
Fig. 4.28 Caudal myeloschisis in human embryos: **a**, **b** a 6-week-old embryo (Carnegie stage 18) with holoprosencephaly (ethmocephaly and proboscis); **c**, **d** a 6-week-old embryo (Carnegie stage 17) with caudal myeloschisis (from the Kyoto Collection of Human Embryos; courtesy Kohei Shiota)

Myelomeningocele is a severe type of spina bifida cystica, involving both neural tissue and the meninges (Figs. 4.26b, 4.29). The neural tissue at the top of the cyst is ectopic, i.e. outside the vertebral canal. At that level it may be merely a neural plate, whereas more rostrally and caudally spinal cord is present. Myelomeningoceles occur mainly in the lumbar region and are almost always associated with the Chiari II malformation (Norman et al. 1995). In fetuses, however, Bell et al. (1980) found the Chiari II malformation in 57.1% of cases with spina bifida, and Hori (1993) found spinal dysraphism in 61.5% of fetal Chiari type II cases. In lipomas and lipo-

myelomeningoceles, the skin also protrudes and the spinal cord lesion may be similar to that in classical myelomeningocele (Aicardi 1998). The clinical manifestations of myelomeningocele include the following: (1) the direct consequences of the spinal malformation such as urinary incontinence; (2) those of hydrocephalus and hindbrain anomalies; and (3) those of associated neural and extraneural abnormalities (McLone and Dias 1991–1992; Aicardi 1998; Naidich et al. 1996).

Spinal meningoceles are much less frequent than myelomeningoceles and involve primarily the arachnoid and dura. The cyst is covered by either intact

Clinical Case 4.5
**The Spectrum
of Deranged Neurulation**

From the perspective of the child neurologist, the clinical presentation of neural tube defects (NTDs) is the most important guiding principle. Ordering criteria for spinal NTDs are the covering and extent of the defect, its composition, involvement of vertebrae, distant CNS co-morbity such as the Chiari II malformation and extra-neurological co-morbity such as anorectal and urogenital malformations in caudal dysgenesis. Usually, spinal NTDs are subdivided into open and closed forms. Complete skin covering and complete defects are easily recognized. The intermediate type in which skin covering is absent but membranes are intact is more problematical. Often there is fusion between membranes and cord tissue, mostly due to scarring. Complete skin covering is considered prognostically favourable and, if detected prenatally, allows normal delivery (Oya et al. 2000). On the basis of the aforementioned criteria, a clinical subdivision is proposed in which the outside (covering of the defect) instead of the inside (contents) is used as a classification criterion (see Case Reports).

Fig. 4.29 The spectrum of deranged neurulation: **a**, **b** dorsal view and MRI of a neonate with a myelocele; **c**, **d** dorsal view and MRI of a neonate with a myelo-meningocele (from the Department of Child Neurology, Radboud University Nijmegen Medical Centre; courtesy Reinier Mullaart)

Case Report. In the first case a spinal NTD was detected by fetal ultrasound at 35 weeks of gestation after an uneventful pregnancy. No periconceptual folic acid intake took place. Besides a back defect, hydrocephalus and a Chiari type II malformation were found. In view of the fetal anomalies and breech position, 3 weeks after the diagnosis, Caesarean section was done and a female baby with a birth weight of 2,595 g was born. Clinical examination at birth revealed a naked neural placode (Fig. 4.29 a), surrounded by a slightly elevated, partly epidermal, partly membranous rim. Spinal MRI showed eventration of the spinal cord above a CSF-containing sac (Fig. 4.29 b). Cranial MRI showed hindbrain herniation, hydrocephalus and dysgenesis of the corpus callosum. This NTD was classified as a *myelocele* with matching cerebral co-morbidity. Spinal surgery took place at 5 days of age. One week after spinal surgery, the hydrocephalus was shunted. At the age of 4 years, the child is wheelchair-dependent but mentally normal.

A case of a *myelomeningocele* is shown in Fig. 4.29 c. After an uneventful pregnancy a boy with a birth weight of 3,960 g and a length of 51 cm was born. No periconceptional folic acid was taken. After birth, a partly skin covered protrusion at the lumbosacral level and a coccygeal dimple were found. Spinal dysfunction ranged from the upper sacral level downwards as suggested by impairment of the function of the legs, the bladder and anorectum. Spinal MRI showed that the lump was mainly fluid-filled and merged with a tethered spinal cord (Fig. 4.29 d). Cranial MRI showed hindbrain herniation but no hydrocephalus and no callosal anomalies. This NTD was classified as a myelomeningocele with cerebral co-

morbidity restricted to the hindbrain. The spinal defect was surgically covered at the age of 2 weeks. One year later, the infant started to stand up straight and spoke a few words.

A multisegmental skin-covered cele, characterized by a spinal-fluid-filled cystic protrusion, complete coverage by skin, and usually present in the lumbar region, may be classified as a *cutaneomyelomeningocele*. Often such an anomaly is accompanied by a vascular nevus. Generally, the cord is slightly involved and cerebral and extra-neurological co-morbidity is rare. A case classified as cutaneomyelomeningocele is shown in Fig. 4.30. After an uneventful pregnancy (without periconceptional folic acid intake), a female baby with a birth weight of 3,500 g was born who presented at birth with an unexpected large, skin-covered sacrococcygeal lump and spinal impairment confined to the lower sacral level. Spinal MRI showed a fluid-filled lump which was largely situated outside the spinal canal, but still merged with the tethered spinal cord (Fig. 4.30 b). Brain co-morbidity was ruled out by clinical examination and MRI. Spinal surgery took place on the tenth day of life. Five years later, the child needs intermittent bladder catheterization and bowel irrigation. Walking and mental functions are normal.

Reference

Oya N, Suzuki Y, Tanemura M, Kojima K, Kajiura S, Murakami I, Yamashita N, Suzumori K (2000) Detection of skin over cysts with spina bifida may be useful not only for preventing neurological damage during labor but also for predicting fetal prognosis. Fetal Diagn Ther 15:156–159
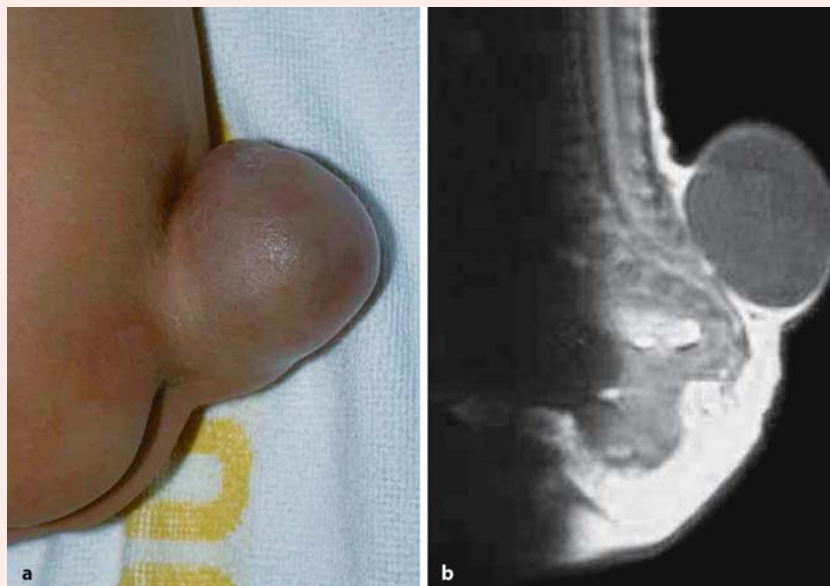
Fig. 4.30 Dorsal view (**a**) and MRI (**b**) of a large, skin-covered cutaneomyelomeningocele (from the Department of Child Neurology, Radboud University Nijmegen Medical Centre; courtesy Reinier Mullaart)
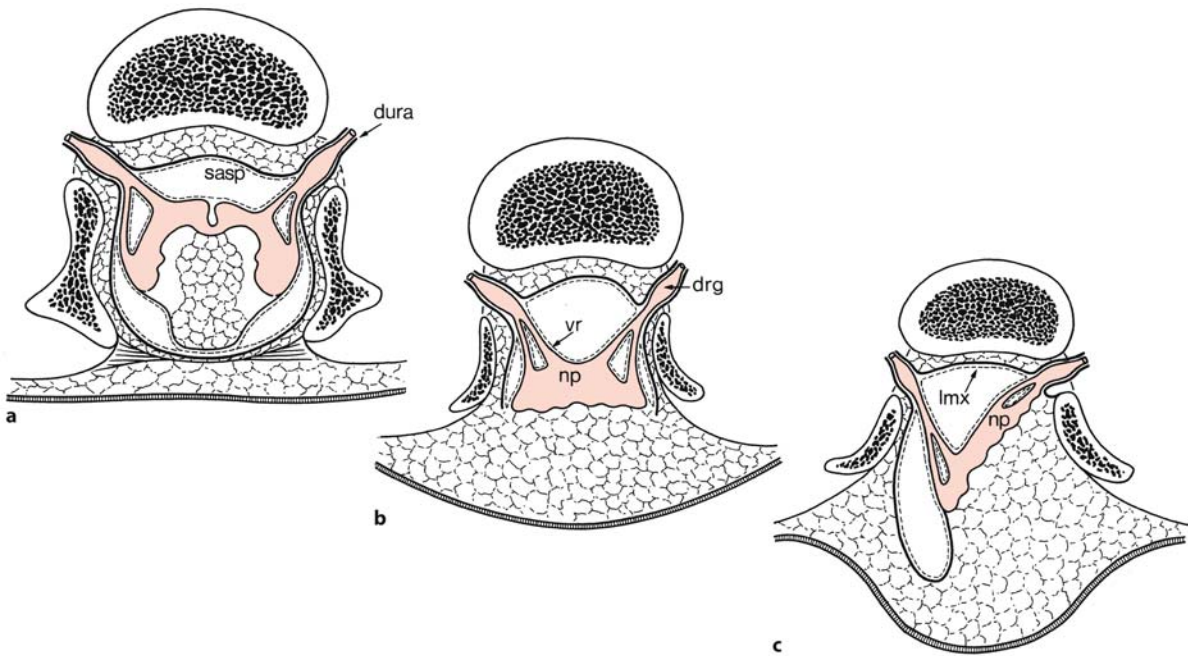
Fig. 4.31 Spinal lipomas: **a** intradural lipoma; **b** lipomyelo-cele; **c** lipomyelomeningocele. The pia-arachnoid is indicated by *stippled lines*, the dura by *thick lines*. *drg* dorsal root gan-glion, *lmx* leptomeninx, *np* neural placode, *sasp* subarach-noidal space, *vr* ventral root. (After Naidich et al. 1996)

skin or a thick, opaque membrane. Since the meninges in the lumbosacral region begin to appear rather late in the embryonic period (stages 17–23; Chap. 1), meningoceles in that area arise probably either late in the embryonic period or early in the fetal period (O'Rahilly and Müller 2001). Osaka et al. (1978) did not find a single case of embryonic meningocele in the Kyoto Collection of Human Embryos.

4.8.2   Spinal Lipomas

Spinal lipomas are the most common type of occult spinal dysraphism (Clinical Case 4.6). They form about 35 % of skin-covered lumbosacral masses and typically lie in the midline just rostral to the inter-gluteal cleft (Naidich et al. 1996). Spinal lipomas are distinct collections of fat and connective tissue that are at least partially encapsulated and connected with the spinal cord (Fig. 4.31). Spinal lipomas are usually subdivided into three groups: spinal lipomas with an intact dura, lipomas with a deficient dura and lipomas of the filum terminale. In *intradural lipomas* (Fig. 4.31 a), the pia-arachnoid encloses the spinal cord and the lipoma. Typically, however, spinal

lipomas are associated with defects in the dura through which the lipoma may extend to the sub-cutaneous tissue (Naidich et al. 1996). Usually, there is a wide spina bifida and segmentation anomalies of the sacrum are found in about 50 % of cases. The spinal cord is split dorsally and resembles the neural plate of a myelomeningocele. The arrangement of the pia-arachnoid and the spinal nerves is similar to that observed in myeloceles and myelomeningo-celes. Therefore, two forms can be distinguished: *lipomyelocele* (Fig. 4.31 b) and *lipomyelomeningocele* (Fig. 4.31 c).

The origin of the cells that form spinal lipomas is controversial. It was suggested that adipocytes arise from spinal vessels (Ehni and Love 1945), astrocytes (Taubner 1887), tail bud (McLone and Naidich 1986) or meningeal tissue of neural crest origin (Virchow 1857). Recently, Catala (1997) postulated that lipomas in spina bifida can result from abnormal develop-ment of the dorsal mesoderm, although the primary defect underlying its abnormal differentiation re-mains to be established. Congenital intraspinal lipo-mas may be simple lipomas similar to those develop-ing elsewhere in the body, or they may be more com-plex, including a variety of unusual ectopic tissues of ectodermal, mesodermal and endodermal origins

Clinical Case 4.6
Spinal Lipomas

The hallmark of spinal lipomas is a skin-covered sacro-coccygeal lipomatous lump. Outside the sacrococ-cygeal region this type of dysraphism is rare. Often this NTD is accompanied by a vascular nevus and of-ten the lipoma merges with the cord (see Case Reports). Usually, a tethered cord is found. Cerebral co-morbidity is exceptional.

Case Report. In the first case, pregnancy was complicated by hypertension and diabetes gravidarum. Fetal distress urged a Caesarean section at term. The newborn girl with a weight of 3,650 g presented with a large sacrococcygeal solid lump, a capillary nevus, a dimple and spinal impairment from the lower sacral level downwards (Fig. 4.32a). On neurological examination spinal impairment was estimated from lower sacral levels downwards. Spinal MRI showed a large subcutaneous **lipoma**, merging with a
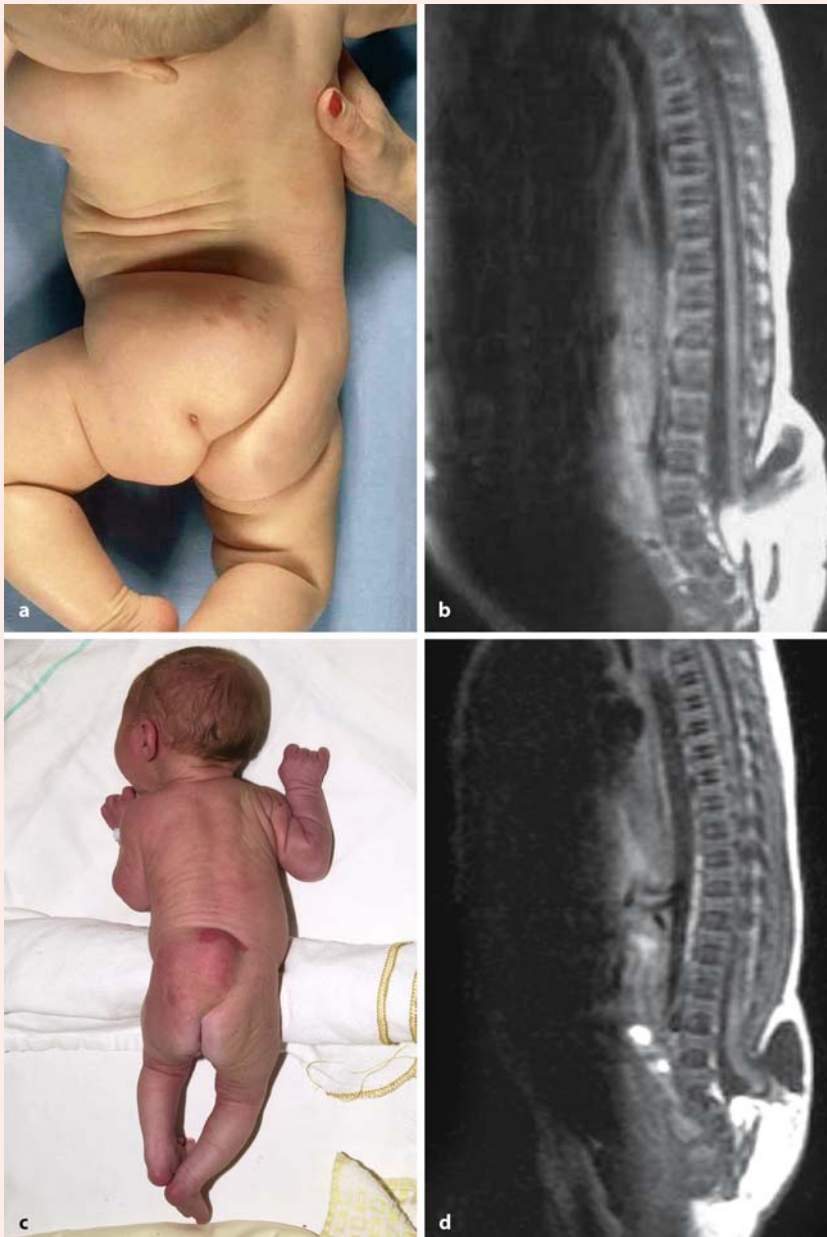
Fig. 4.32 Dorsal views and MRI of two cases of spinal lipomas in neonates (from the Department of Child Neurology, Radboud University Nijmegen Medical Centre; courtesy Reinier Mullaart)

tethered spinal cord (Fig. 4.32 b). Brain co-morbidity was ruled out by clinical examination and cranial MRI. Spinal surgery took place at the age of 5 months. Ten years later, slight foot deformities, slight bladder impairment and subtle sensory defects are found, but the child does not experience any disability at all.

The second case is a *lipomyelomeningocele*. This case also presented at birth. The mother took folic acid beginning 4 weeks before conception. Pregnancy and birth were uneventful. The newborn girl with a birth weight of 3,130 g presented with a partly solid, partly cystic, lumbosacral lump with a capillary nevus on its surface (Fig. 4.32 c). On clinical examination, the upper level of spinal cord dysfunction was estimated as S1. Spinal MRI showed a mixed anomaly composed of a meningocele and a lipoma, both merging with a tethered spinal cord (Fig. 4.30 d). Brain co-morbidity was ruled out by clinical examination and cranial MRI. Spinal surgery took place at the age of 5 months. Three years after surgery, the child needs intermittent bladder catheterization, walks with special aids, but is mentally normal.

(Lellouch-Tubiana et al. 1999). Lellouch-Tubiana et al. (1999) found muscular tissue, cartilage and squamous epithelial tissue in 37, 6 and 2% of cases, respectively, in intraspinal lipomas. On the basis of these findings, they suggested that congenital intraspinal lipomas are at least in part teratomas with pluripotent capacity.

4.8.3   Spina Bifida Occulta and Related Disorders

In *spina bifida occulta*, a defect in one or more vertebral arches occurs without herniation of neural or meningeal structures through the mesenchymal defect. This definition includes hydromyelia, the split notochord syndrome, dorsal dermal sinuses and diastematomyelia (Aicardi 1998; Naidich et al. 1996). A fibrocartilaginous or bony spur in the vertebral canal may be accompanied by a partial splitting of the spinal cord into two halves (*diastematomyelia*; Chap. 6), leading to anomalies of the lower limbs. In *hydromyelia*, overdistention of the central canal may be focal and is often most pronounced in the lumbar region. Isolated hydromyelia is usually asymptomatic and is an incidental finding on MRI (Naidich et al. 1996; Jinkins and Sener 1999) or at autopsy. In about 40% of cases it is associated with the Chiari II malformation (Harding and Copp 1997). *Embryonic hydromyelia* is different from adult hydromyelia (Fig. 4.33). In five cases of the Kyoto Embryology Collection, Ikenouchi et al. (2002) observed abnormal dilatation of the lumbosacral cord. The central canal was enlarged, and the roof plate of the neural tube was extremely thin and expanded, and appeared to be incompletely separated from the surface ectoderm. Mesenchymal tissue was either thin or lacking between the spinal cord and the surface ectoderm. During the fetal period, neural arches are formed around the spinal cord by the surrounding mesenchyme (Chap. 6). If the disjunction between the spinal cord and the surface ectoderm is incomplete and sufficient mesenchymal cells are unable to migrate into the space between them, the formation of neural arches, spinous processes and paraspinal muscles may be inhibited along the posterior midline, resulting in a spina bifida. Gardner (1973) discussed the effects of overdistention of the neural tube on the formation of the surrounding tissue and pointed out that cartilaginous sclerotomes can be displaced laterally and fail to unite because of hydromyelia. Thus, embryonic hydromyelia may represent an early form of spina bifida with a closed neural tube.

If the superficial ectoderm fails to separate from the neural ectoderm, a focal adhesion is created that may give rise to a *dorsal dermal sinus* (Fig. 4.34). Typically, the dermal sinus tract extends inwards from the skin surface for a variable depth. It may end superficial to or deep in the dura, extending into the spinal canal (Wright 1971; Naidich et al. 1996). Rarely, the tract ends in the subarachnoid space. The dermal sinus may also end in a fibrous nodule among the roots of the cauda equina. Lumbosacral dermal sinuses are usually associated with tethering of the spinal cord (McLone and Naidich 1989).
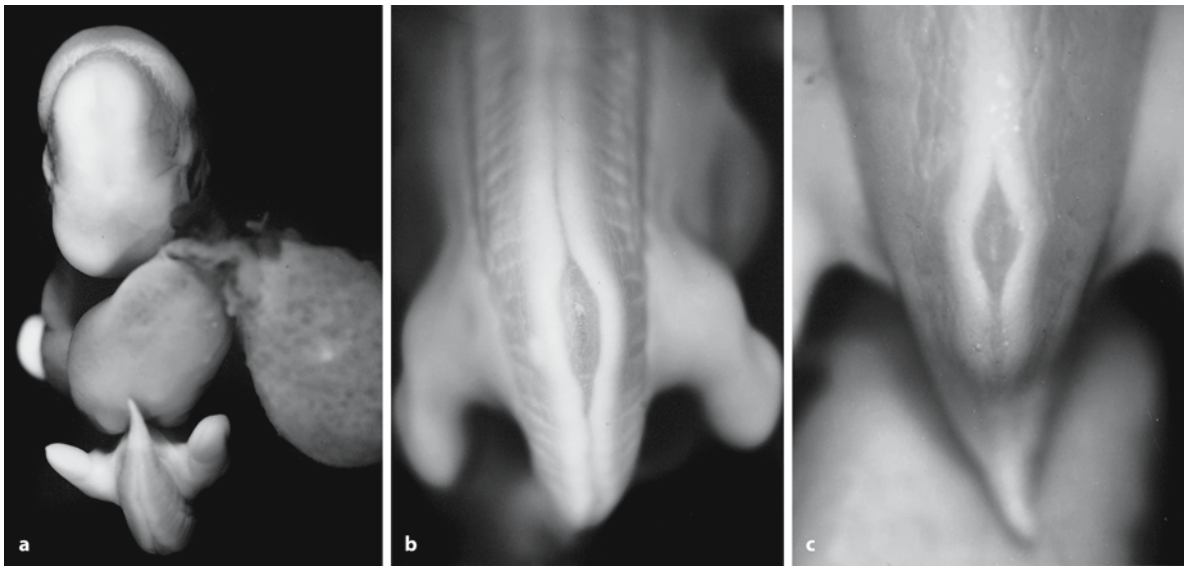
Fig. 4.33 Embryonic hydromyelia: **a**, **b** frontal view and closer look at the caudal part of a Carnegie stage 17 embryo; **c** caudal view of a Carnegie stage 18 embryo with a dilated caudal neural tube (from Ikenouchi et al. 2002; with permission)
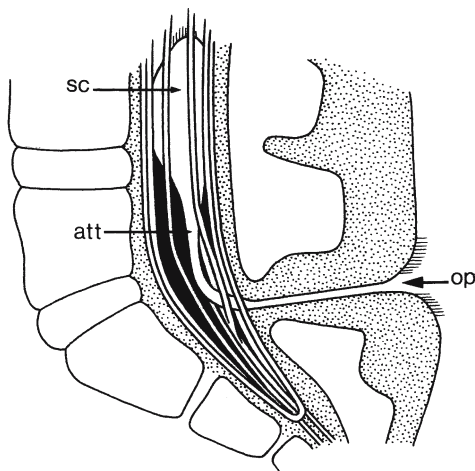
Fig. 4.34 Congenital dermal sinus: the sinus tract ascends for two or more vertebrae and ends on the low-lying spinal cord. *att* attachment of sinus to spinal cord, *op* dermal opening of sinus, *sc* spinal cord. (After Aicardi 1998)

4.9   The Chiari Malformations

Chiari (1891) defined three types of cerebellar deformity associated with hydrocephalus. In a subsequent, extensively illustrated paper he added a fourth type (Chiari 1896). The ***Chiari I malformation*** consists of elongated, peg-like cerebellar tonsils displaced into the upper cervical canal (Fig. 4.35). Friede and Roessmann (1976) introduced the term chronic tonsillar herniation as an alternative to denote tonsillar herni-

ation in the absence of space-occupying lesions. Chiari type I is often asymptomatic but may lead to late-onset hydrocephalus. It is increasingly recognized in young children. In the Chiari II malformation, the vermis, pons, medulla and an elongated fourth ventricle are displaced caudalwards into the cervical canal (Figs. 4.35, 4.36). Type III is very rare and involves an occipitocervical or high cervical bony defect with herniation of cerebellum into the encephalocele. Type IV is a form of cerebellar hypoplasia.

The ***Chiari II malformation*** is also known as Arnold–Chiari malformation. Arnold (1894) described a case of sacrococcygeal teratoma and spina bifida with downwards displacement of the cerebellum but not the brain stem, and without hydrocephalus. In 1907, his collaborators Schwalbe and Gredig reported four additional cases, and suggested the term Arnold–Chiari malformation. In 1883, however, Cleland had already described certain aspects of the Chiari II malformation, and Cleland–Chiari would be more appropriate. The Chiari II malformation is due to a space conflict between the hypoplastic basicranio-cervical mesoderm and the developing hindbrain and spinal cord (Marín-Padilla and Marín-Padilla 1981; Roth 1986; Hori 1998). It consists of inferior cerebellar displacement, elongation of the fourth ventricle and inferior displacement of the pons, medulla oblongata and cervical spinal cord into a widened cervical canal (Figs. 4.35, 4.37). It is associated with cephalocele and myelomeningocele in almost 100 % of cases. Recently, Hori (2003) reported a Chiari anomaly type II without cerebellar herni-
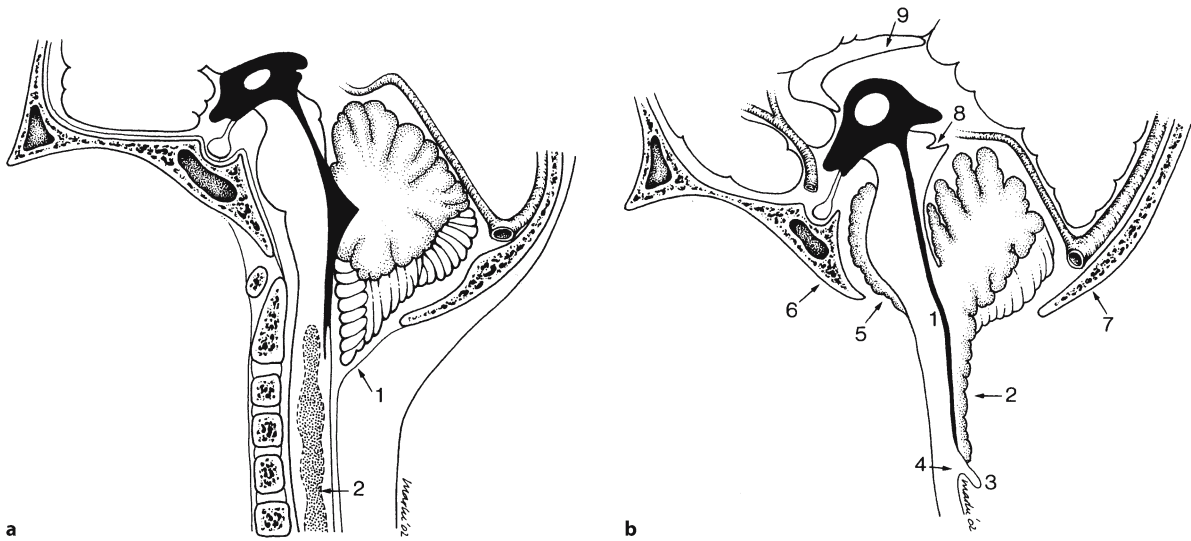
Fig. 4.35 A Chiari I (**a**) and a Chiari II (**b**) malformation. **a** Pointed, low-lying tonsils (*1*) and syringomyelia (*2*) are found. **b** An elongated, tube-like fourth ventricle (*1*), an inferior displaced vermis (*2*), a medullary spur (*3*) and a medullary kink (*4*) are found. The cerebellar hemispheres 'creep' around the brain stem (*5*). Moreover, there are a concave clivus (*6*), a low-lying confluens sinuum (*7*), 'beaked' colliculi (*8*) and partial callosal agenesis (*9*). (After Osborn 1994)
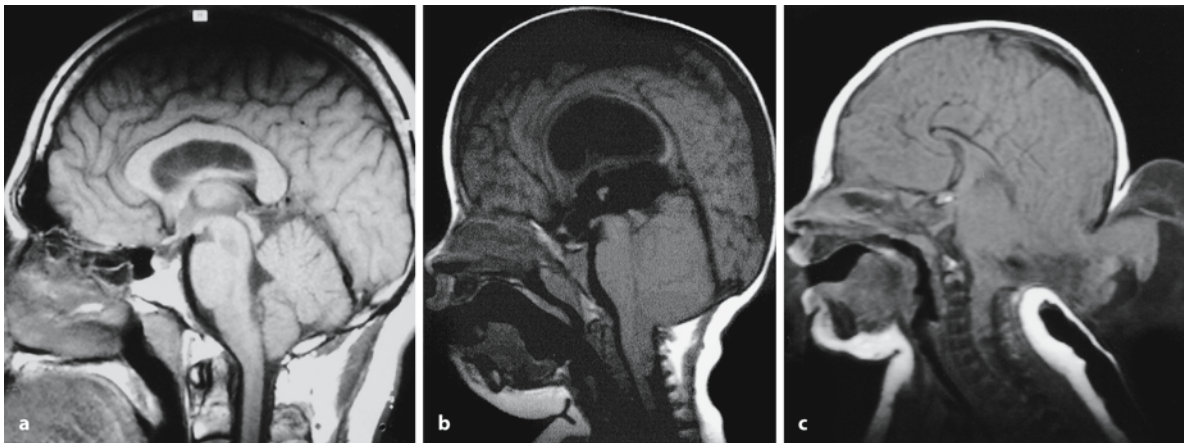
Fig. 4.36 Chiari malformations: MRI of Chiari I (**a**), Chiari II (**b**) and Chiari III (**c**) malformations (kindly provided by Henk O.M. Thijssen, Department of Radiology, Radboud University Nijmegen Medical Centre)

ation in a case of sacral spina bifida. Although the posterior cranial fossa was hypoplastic, the elongated rhomboid fossa was not accompanied by cerebellar herniation.

Several hypotheses for the cause of Chiari II malformation were suggested (McLone and Knepper 1989; Norman et al. 1995). On the basis of their experimental work on the *Splotch* mouse, McLone and Knepper (1989) suggested that a Chiari II malformation could be the result of a delayed or inadequate occlusion of the ventricular system. They attributed both the NTD and failure of occlusion of the neurocele (the fluid-filled space of the developing brain and spinal cord) to a delayed synthesis of glycoconju-

gates on the cell surfaces. Failure of neurocele occlusion leads to failure of the ventricular system to distend normally and to the collapse of the ventricular system. As a result, the neural structures of the posterior fossa are small, which in turn leads to underdevelopment of the neural crest mesenchyme surrounding the brain stem and the cerebellum. Hori (1998) gave a rather simple explanation for the pathogenetic mechanism of cerebellar herniation in Chiari anomalies: if the severe hypoplasia of the posterior cranial fossa already exists during the embryonic/early fetal period, the developing cerebellum, the vermis in particular, would have no other way but to develop into the foramen magnum (Chiari type II
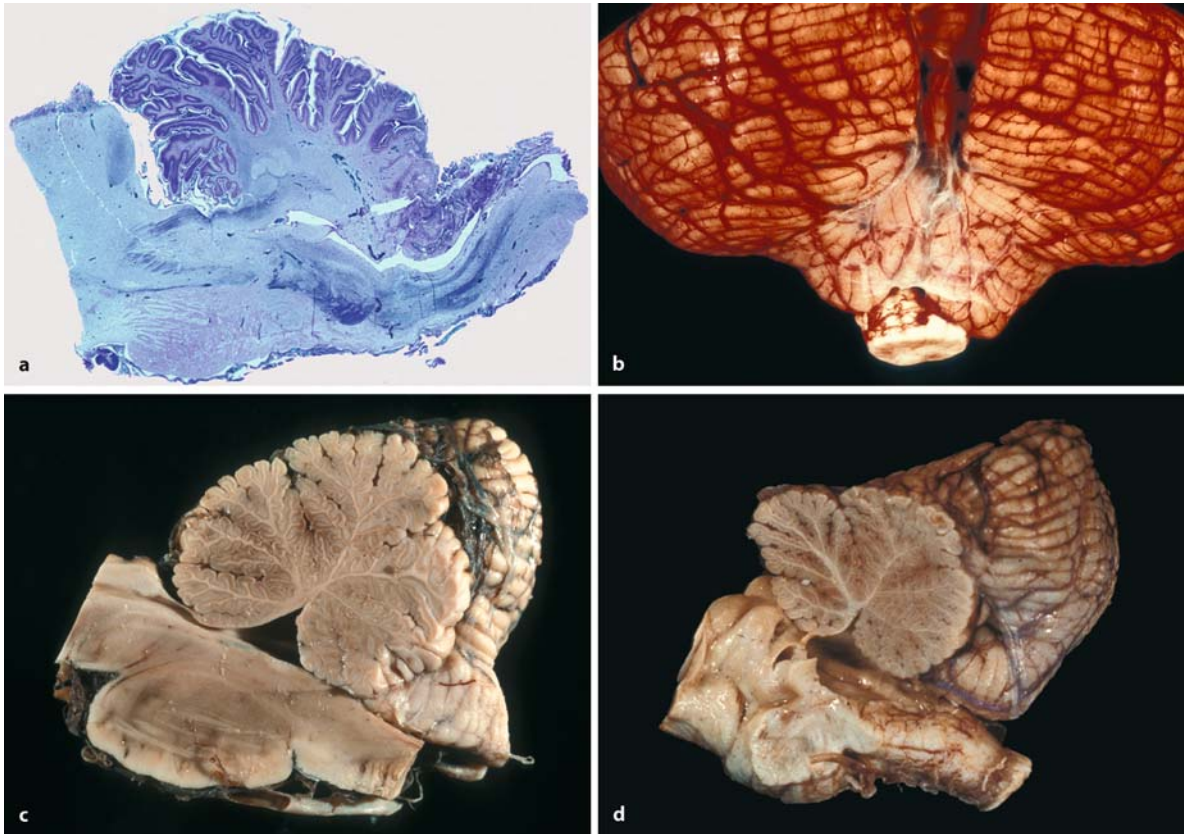
Fig. 4.37 Gross neuropathology of Chiari malformations (from the Department of Neuropathology, Medizinische Hochschule Hannover; courtesy Akira Hori): **a** Chiari II anom-aly, sagittal section of the cerebellum and brain stem; **b**, **c** Chiari I anomaly, dorsal view and sagittal section, showing the herniation of the vermis; **d** normal control

anomaly). If the hypoplasia of the posterior groove is not severe enough, the space will be occupied by the vermis. The later-developing basal neocerebellum (the cerebellar tonsils) must subsequently expand into the foramen magnum (Chiari type I anomaly). The extent of the cerebellar herniation in Chiari type I and II anomalies is shown in Fig. 4.37.

4.10   Caudal Dysgenesis

Several disorders of the caudal spinal cord can be viewed as **disorders** of **deranged canalization** and **retrogressive differentiation** (Naidich et al. 1996). These disorders include the following: (1) the tight filum terminale syndrome, due to failure of complete involution of the spinal cord; (2) lipoma of the filum terminale, probably due to persistence of caudal cells that differentiate to fat cells, found incidentally in 4–6 % of normal adults; (3) sacrococcygeal teratoma; (4) terminal syringomyelia, due to progressive expansion of the terminal ventricle, found in up to 30 % of patients with occult spinal dysraphism; (5) caudal

spinal anomalies with anorectal and urogenital malformations, such as the OEIS (omphalocele, exstrophy of the bladder, imperforate anus and spinal anomalies) complex and the caudal regression syndrome, for which the common term caudal dysgenesis may be used; and (6) anterior sacral meningoceles, diverticula of the thecal sac that protrude anteriorly into the retroperitoneal retrorectal space (Amacher et al. 1968; Naidich et al. 1996).

Sacrococcygeal teratoma, a congenital tumour of the caudal pole of the body, contains by definition tissues derived from all these germ layers (Feldman et al. 1990; Schropp et al. 1992; Naidich et al. 1996). They probably arise from omnipotential cells derived from Hensen's node (Lemire et al. 1975). Sacrococcygeal teratoma is the most common newborn tumour, and occurs in 1 per 35,000–40,000 births with a female predominance (Feldman et al. 1990; Schropp et al. 1992).

The *caudal regression* or *dysgenesis syndrome* was originally defined as a spectrum of lower-limb, vertebral, anorectal and urogenital anomalies, with sirenomelia (Fig. 4.38) and imperforate anus as its
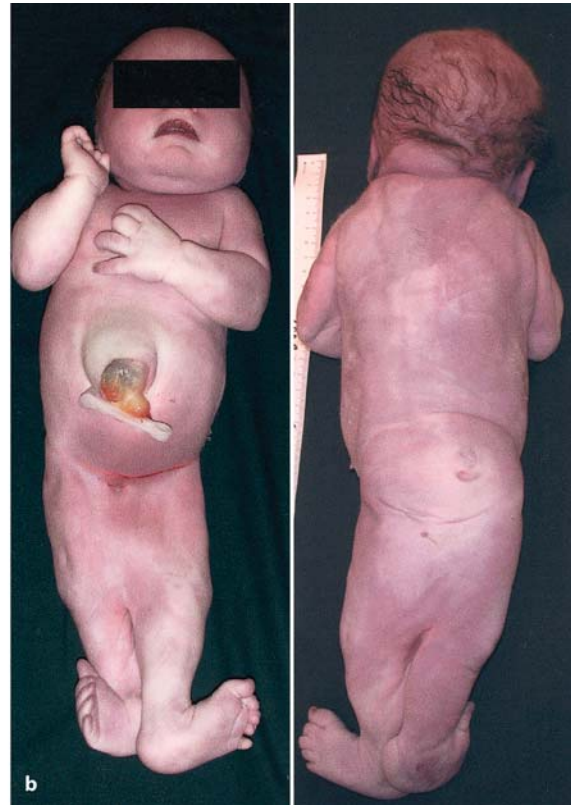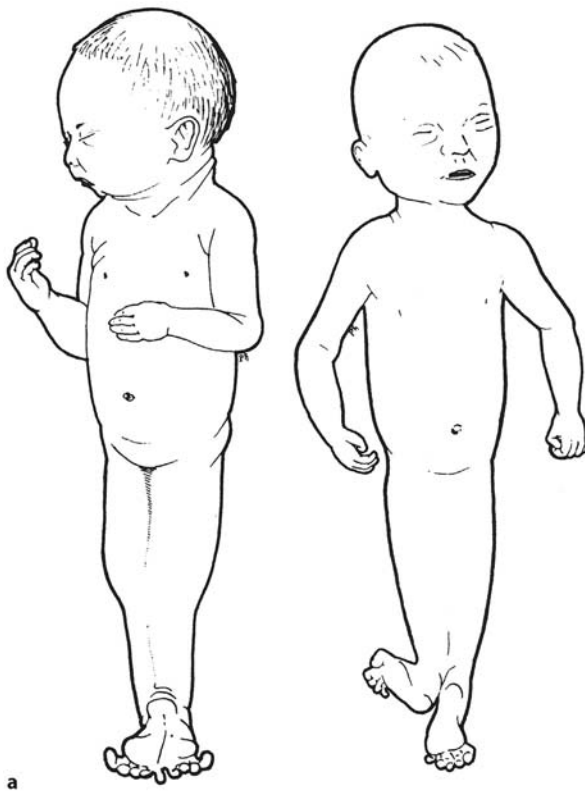
Fig. 4.38 Sirenomelia: **a** two examples shown by Duhamel (1966) with complete and subtotal non-separation of the lower limbs; **b** a comparable autopsy case (from the Department of Pathology, Radboud University Nijmegen Medical Centre; courtesy Pieter Wesseling)

two extremes (Duhamel 1961). Several other terms have been used to describe this combination of syndromes, such as sacral agenesis, caudal agenesis and caudal aplasia or dysplasia (Pang 1993; Hori 1997, 1998). Although the classical postnatal presentation of the caudal regression syndrome is highly variable, the most consistent clinical triad includes agenesis of caudal vertebrae, anorectal malformations and urogenital anomalies (Pang and Hoffman 1980; Pappas et al. 1989; Alles and Sulik 1993; Pang 1993; Nievelstein 1998; Padmanabhan et al. 1999). Its reported incidence varies between approximately 0.01 and 0.05 per 1,000 births, with a slight male preponderance. The severity of expression of the anomaly is variable (Pappas et al. 1989; Pang 1993). In extreme forms, the lower extremities are represented by a median limb with toes turned backwards (symmelia/sirenomelia), giving the appearance of the mythological mermaid ('mermaid anomaly'). The visceral malformations associated with caudal dysgenesis may be incompatible with intrauterine life. Familial occurrence has been reported, but no Mendelian pattern of inheritance has been found. The homeobox gene *HLXB9*

may be involved in dominantly inherited sacral agenesis (Ross et al. 1998).

Maternal diabetes may contribute to sacral dysgenesis (Rusnak and Driscoll 1965; Passarge and Lenz 1966; Williamson 1970; Källén 1987). In addition to diabetes, embryonic trauma, maternal fever, nutritional deficiency, toxic substances and genetic factors have been considered as causes of caudal malformations (Pang and Hoffman 1980). Kampmeier (1927) suggested that an abnormal umbilical artery of vitelline origin could deprive the caudal region of the embryo of essential nutrients, resulting in caudal dysgenesis. This abnormal artery was found in sirenomelic fetuses (Stocker and Heifetz 1987; Kapur et al. 1991). O'Rahilly and Müller (1989b) examined over 100 normal embryos of Carnegie stages 8–18 and four synophthalmic embryos of stages 16–20 and commented on the pathogenesis of several median anomalies including sirenomelia. In mice, vascular disruption precedes caudal dysgenesis (Seller and Wallace 1993; Padmanabhan 1998). Padmanabhan et al. (1999) studied ten embryos of Carnegie stages 16–23 with caudal dysgenesis. Several develop-
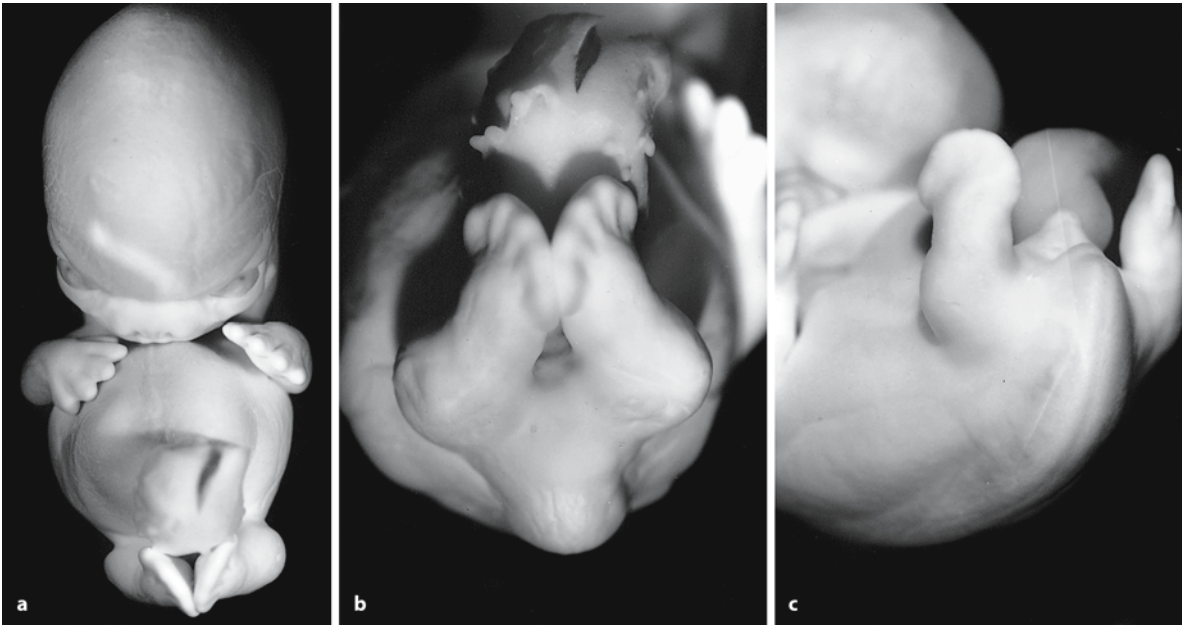
Fig. 4.39 Caudal dysgenesis: external views of embryos of Carnegie stage 19. **a** The hypoplastic hindlimbs are attached to the caudal tip of the trunk with their roots closely positioned in the narrow perineum (**b**) and postaxial borders facing each other. The genital tubercle is either absent (**b**) or adjoins the caudal tip (**c**). (From Padmanabhan et al. 1999, with permission)

mental alterations of the median axis were observed (Fig. 4.39). These included the following: (1) significant reduction in the craniofacial mesenchyme characterized by hypoplasia of the pharyngeal arches, palatal shelves and agenesis of the auricular hillocks; (2) absence of the caudal trunk from midsacral to all coccygeal segments, vertebral fusion or agenesis; (3) defective development of the primary and secondary neural tubes; (4) rectal and urinary tract dysgenesis; and (5) hindlimb malformations such as bilateral agenesis, meromelia and various forms of abnormal rotation. No cases of sirenomelia were present. There was an impressive association between limb malformations and body wall defects. Histological examination revealed caudal vascular deficiency and haemorrhagic lesions in the limbs of the dysplastic embryos. Malformations of the primary and secondary neural tubes are shown in Fig. 4.40.

Pang (1993) studied a large group of patients with sacral agenesis with MRI. Clinically, most patients showed poorly developed trunks with short, shallow intergluteal clefts, poor gluteal musculature, narrow hips, distal leg atrophy and talipes deformities. Approximately 20% had subcutaneous lesions such as skin-covered lipomyelomeningceles, terminal myelocystoceles or limited myeloschisis. Sacral agenesis may be associated with multiple congenital malformations such as the OEIS complex (Keppler-Noreuil 2001; Clinical Case 4.7), the VATER complex and con-

genital heart defects. On the basis of the position of the conus medullaris, Pang (1993) distinguished two groups of patients with sacral agenesis. In the first group (41%), the conus terminates rostral to the lower border of L1. The conus is deformed and ends abruptly at T11 or T12, as if the normal distal tip were missing. In this group with a high conus, the sacral deficit is typically large and the sacrum ends at or above S1. In the second group (59%), the conus ends below L1 and is elongated and tethered by a thick filum terminale, a terminal myelocystocele (McLone and Naidich 1985), a transitional lipoma or an elongated cord with a terminal hydromyelia. The sacrum is relatively well preserved (for neuropathological data see Lemire and Beckwith 1982, Towfighi and Housman 1991 and Hori 1997).

On the basis of MRI examination, Nievelstein (Nievelstein et al. 1994; Nievelstein 1998) suggested a subdivision of caudal dysgenesis into early and late embryonic defects, reminiscent of Pang's two groups. The majority of patients presented with agenesis of parts of the spinal cord, dorsal root ganglia and surrounding vertebrae, all structures derived from the primary neurulation process. Since this process occurs before the end of the seventh week of development, these malformations were regarded as *early embryonic defects*. The second group of patients showed, besides caudal vertebral agenesis, tethered spinal cords with or without agenesis or dysgenesis of
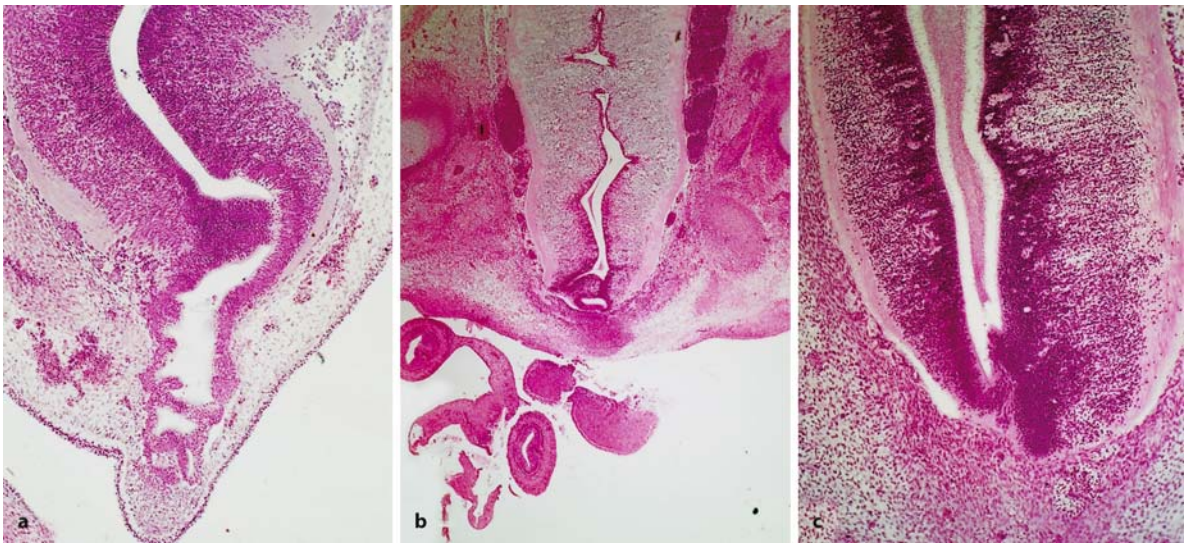
Fig. 4.40 Caudal dysgenesis: transverse sections of embryos of Carnegie stages 21 (**a**) and 22 (**b**, **c**), showing anomalies of the union of the primary and secondary neural tubes. **a** A kinky union between the primary and secondary neural tubes is present. In **b**, duplication of the secondary neural tube is present, whereas in **c**, a vacuolated ventricular zone can be seen. (From Padmanabhan et al. 1999, with permission)

the conus medullaris. This group of malformations may be regarded as *late embryonic defects*, arising after the end of the seventh week of development, and are best explained as resulting from a fault in the process of degeneration and differentiation of initially normally developed primary and secondary neural tubes, in combination with a disturbance of the differentiation of the mesenchymal vertebrae. Combinations of early and late embryonic defects were also found. The anorectal malformations in caudal dysgenesis can also be divided into early and late malformations (Nievelstein et al. 1994; Nievelstein 1998). The majority of patients examined showed early em-

bryonic defects, i.e. anorectal malformations of the communicating type, in which the enteric component opens via fistulae into the urinary or genital tract, or on the perineum (ectopic anal orifice). These malformations are due to a disturbance of the normal development of the dorsal part of the cloacal membrane and cloaca during the early embryonic period. The other group is formed by anorectal malformations with the anus in the normal position. These malformations are caused by a defective recanalization of the secondarily occluded anal orifice during the late embryonic period.

Clinical Case 4.7
OEIS Complex

The **OEIS complex** is characterized by an omphalocele, exstrophy of the bladder, imperforate anus and spinal defects (Carey et al. 1978; Keppler-Noreuil 2001; see Case Report).

Case Report. Ultrasound examination around the 34th gestational week showed a large omphalocele and an extensive NTD (Fig. 4.41). Pregnancy was induced and a child of 1,340 g and a total length of 32 cm was born (Apgar scores 1-1-0). It was the sixth pregnancy of a healthy 34-year-old woman (three normal children, two abortions). At autopsy, the omphalocele (diameter 13 cm) and the lumbosacral, skin-covered cele (diameter 5 cm) were the most obvious malformations. The head, upper extremities and thorax showed no anomalies. The lower extremities were flexed with abnormal position of the feet. Complete atresia ani was present, whereas no external genitals were found. Both lungs were extremely hypoplastic.

Most of the abdominal organs were found within the omphalocele. The small intestine opened into a cloaca. Two blindly ending parts of the colon were found at the level of the cloaca. There was a uterus didelphis with a blindly ending right horn and a left horn opening into the cloaca. Both ovaries and tubae were normal. The kidneys were found cranial to the adrenal glands. Both ureters opened into the lateral walls of the cloaca. There was a bony defect of 1-cm diameter in the dorsal lumbar vertebral column, through which a 3-mm-wide large tail of meningeal and neuroglial tissue extended to form a 5-cm-large meningomyelocele. In the cele, meningeal, neuronal, glial and fat tissues were found. X-ray examination showed malformations of the sacrum.

References

Carey JC, Greenbaum B, Hall BD (1978) The OEIS complex (omphalocele, exstrophy, imperforate anus, spinal defects). Birth Defects Orig Artic Ser 14:255–263

Keppler-Noreuil KM (2001) OEIS complex (omphalocele-exstrophy-imperforate anus-spinal defects): A review of 14 cases. Am J Med Genet 99:271–279

Fig. 4.41 A case of the OEIS complex in which a large omphalocele, exstrophy of the bladder, imperforate anus, and a spina bifida are present (from the Department of Pathology, Radboud University Nijmegen Medical Centre; courtesy Pieter Wesseling)

References

Ahdab-Barmada M, Claassen D (1990) A distinctive triad of malformations of the central nervous system in the Meckel-Gruber syndrome. J Neuropathol Exp Neurol 49:610–620

Aicardi J (1998) Diseases of the Nervous System, 2nd ed. Mac Keith, London

Aicardi J, Castello-Branco ME, Roy C (1983) Le syndrome de Joubert. Arch Franç Pédiatr 40:625–629

Aleksic S, Budzilovich G, Greco MA, Feigin I, Epstein F, Pearson J (1983) Iniencephaly. A neuropathologic study. Clin Neuropathol 2:55–61

Aleksic S, Budzilovich G, Greco MA, McCarthy J, Reuben R, Margolis S, Epstein F, Feigin I, Pearson J (1984) Intracranial lipomas, hydrocephalus and other CNS anomalies in auriculo-vertebral dysplasia (Goldenhar-Gorlin syndrome). Child's Brain 11:285–297

Alles AJ, Sulik KK (1993) A review of caudal dysgenesis and its pathogenesis as illustrated in an animal model. Birth Defects Orig Artic Ser 29:83–102

Amacher AL, Drake CG, McLachin AD (1968) Anterior sacral meningocele. Surg Gynecol Obstet 126:986–994

Arnold J (1894) Myelocyste, Transposition von Gewebskeimen und Sympodie. Ziegl Beitr Path Anat 16:1–28

Balinsky BI (1965) An Introduction to Embryology, 2nd ed. Saunders, Philadelphia, PA

Baraitser M, Burn J (1984) Neural tube defects as an X-linked condition. Am J Med Genet 17:383–385

Barkovich AJ (2000) Congenital anomalies of the spine. In: Barkovich AJ Pediatric Neuroimaging, 3rd ed. Lippincott Williams & Wilkins, Philadelphia, PA, pp 621–683

Barkovich AJ, Vandermarck P, Edwards MSB, Cogen PH (1991) Congenital nasal masses. AJNR Am J Neuroradiol 12:105–116

Bartelmez GW, Dekaban AS (1962) The early development of the human brain. Contrib Embryol Carnegie Instn 37:13–32

Bassuk AG, McLone D, Bowman R, Kessler JA (2004) Autosomal dominant occipital encephalocele. Neurology 62:1888–1890

Bell JE, Gordon A, Maloney AFJ (1980) The association of hydrocephalus and Arnold-Chiari malformation with spina bifida in the fetus. Neuropathol Appl Neurobiol 6:29–39

Berry RJ, Li Z (2002) Folic acid alone prevents neural tube defects: Evidence from the China study. Epidemiology 13:114–116

Berry RJ, Li Z, Erikson JD, Li S, Moore CA, Wang H, Mulinare J, Zhao P, Wong LY, Gindler J, et al. (1999) Prevention of neural tube defects with folic acid in China. N Engl J Med 41:1485–1490

Blaas H-GK, Eik-Nes SH, Isaksen CV (2000) The detection of spina bifida before 10 gestational weeks using two- and three-dimensional ultrasound. Ultrasound Obstet Gynecol 16:25–29

Bolly VP (1966) Sekundäre Lumenbildungen im Neuralrohr und Rückenmark menschlicher Embryonen. Acta Anat (Basel) 64:48–81

Bordarier C, Aicardi J, Goutières F (1984) Congenital hydrocephalus and eye abnormalities with severe developmental brain defects: Warburg syndrome. Ann Neurol 16:60–65

Bradley PJ, Singh SD (1982) Congenital nasal masses: Diagnosis and management. Clin Otolaryngol 7:87–97

Brook FA, Shum ASW, van Straaten HWM, Copp AJ (1991) Curvature of the caudal region is responsible for failure of neural tube closure in the *curly tail* (*ct*) mouse embryo. Development 113:671–678

Byrne J, Cama A, Reilly M, Vigliarolo M, Levato L, Boni L, Lavia N, Andreussi L (1996) Multigeneration maternal transmission in Italian families with neural tube defects. Am J Med Genet 66:303–310

Campbell LR, Dayton DH, Sohal GS (1986) Neural tube defects: A review of human and animal studies on the etiology of neural tube defects. Teratology 34:171–187

Carrel T, Purandare SM, Harrison W, Elder F, Fox T, Casey B, Herman GE (2000) The X-linked mouse mutation Bent tail is associated with a deletion of the Zic3 locus. Hum Mol Genet 9:1937–1942

Carter CO (1974) Clues to the aetiology of neural tube malformations. Dev Med Child Neurol 16(Suppl 32):3–15

Catala M (1997) Why do we need a new explanation for the emergence of a spina bifida with lipoma? Child's Nerv Syst 13:336–340

Chapkupt S, Lucek PR, Koenigsberger MR, Johnson WG (1992) Parental sex in spina bifida: A role for genomic imprinting? Am J Med Genet 44:508–512

Chapkupt S, Hol FA, Shugart YY, Geurds MP, Stenroos ES, Koenigsberger MR, Hamel BCJ, Johnson WG, Mariman ECM (1995) Absence of linkage between familial neural tube defects and PAX3 gene. J Med Genet 32:200–204

Chapman DL, Papaioannou VE (1998) Three neural tubes in mouse embryos with mutations in the T-box gene Tbx6. Nature 391:695–697

Chapman PH, Swearingen B, Caviness VS Jr (1989) Subtorcular occipital encephaloceles: Anatomical considerations relevant to operative management. J Neurosurg 71:375–381

Chen ZF, Behringer RR (1995) twist is required in head mesenchyme for cranial neural tube morphogenesis. Genes Dev 9:686–699

Chiari H (1891) Ueber Veränderungen des Kleinhirns infolge von Hydrocephalie des Grosshirns. Dtsch Med Wochenschr 17:1172–1175

Chiari H (1896) Über Veränderungen des Kleinhirns, des Pons und der Medulla oblongata in Folge von congenitaler Hydrocephalie des Grosshirns. Denkschr Kais Akad Wiss Math-naturwiss Classe 63:71–116

Christie GA (1964) Developmental stages in somite and post-somite rat embryos, based on external appearance, and including some features of the macroscopic development of the oral cavity. J Morphol 114:263–286

Cleland J (1883) Contributions to the study of spina bifida, encephalocele and anencephalus. J Anat Physiol 17:257–292

Colas J-F, Schoenwolf GC (2001) Towards a cellular and molecular understanding of neurulation. Dev Dyn 221:117–145

Coleman LT, Zimmerman RA, Rorke LB (1995) Ventriculus terminalis of the conus medullaris: MR findings in children. AJNR Am J Neuroradiol 16:1421–1426

Copp AJ (1994) Genetic models of mammalian neural tube defects. In: Ciba Foundation Symposium 181. Wiley, Chichester, pp 118–143

Copp AJ, Bernfield M (1994) Etiology and pathogenesis of human neural tube defects: Insights from mouse models. Curr Opin Pediatr 6:624–631

Copp AJ, Brook FA (1989) Does lumbosacral spina bifida arise by failure of neural folding or by defective canalisation? J Med Genet 26:160–166

Copp AJ, Brook FA, Estibeiro JP, Shum ASW, Cockroft DL (1990) The embryonic development of mammalian neural tube defects. Prog Neurobiol 35:363–403

Copp AJ, Greene NDE, Murdoch JN (2003) The genetic basis of mammalian neurulation. Nat Rev Neurosci 4:784–793

Cuckle HS, Wald NJ, Althouse R (1993) Sex differences in the location of a spina bifida lesion. J Med Genet 30:262–263

Czeizel AE, Dudás I (1992) Prevention of the first occurrence of neural tube defects by periconceptional vitamin supplementation. N Engl J Med 327:1832–1835

DeMyer W (1967) The median cleft face syndrome. Differential diagnosis of cranium bifidum, cranium bifidum occultum, hypertelorism, and median cleft nose, lip, and palate. Neurology 17:961–971

Deng C, Bedford M, Li C, Xu X, Jang X, Dunmore J, Leder P (1997) Fibroblast growth factor receptor-1 (FGFR-1) is essential for neural tube and limb development. Dev Biol 185:42–54

Dolk H, de Wals P, Gillerot Y, Lechat MF, Ayme S, Cornel M, Cuschieri A, Garne E, Goujard J, Laurence KM, et al. (1991) Heterogeneity of neural tube defects in Europe: The significance of site of defect and presence of other major anomalies in relation to geographic differences in prevalence. Teratology 44:547–559

Drainer E, May HM, Tolmie JL (1991) Do familial neural tube defects breed true? J Med Genet 28:605–608

Duhamel B (1961) From the mermaid to anal imperforation: The syndrome of caudal regression. Arch Dis Child 36:152–155

Duhamel B (1966) Morphogenèse Pathologique. Masson, Paris

Edwards BO, Fisher AQ, Flannery DB (1988) Joubert syndrome: Early diagnosis by recognition of the behavioral phenotype and confirmation by cranial sonography. J Child Neurol 3:247–249

Ehni G. Love JG (1945) Intraspinal lipomas. Report of cases, review of the literature and clinical and pathological study. Arch Neurol Psychiatry 53:1–28

Feldman M, Byrne P, Johnson MA, Fischer J, Lees G (1990) Neonatal sacrococcygeal teratoma: Multi-imaging modality assessment. J Pediatr Surg 25:675–678

Fleming A, Copp AJ (2000) A genetic risk factor for mouse neural tube defects: Defining the embryonic basis. Hum Mol Genet 9:575–581

Franke B, Klootwijk R, Hekking JWM, de Boer RT, ten Donkelaar HJ, Mariman ECM, van Straaten HWM (2003) Analysis of the embryonic phenotype of bent tail, a mouse model for X-linked neural tube defects. Anat Embryol (Berl) 207:255–262

Friede RL (1978) Developmental Neuropathology. Springer, Berlin Heidelberg New York

Friede RL (1989) Developmental Neuropathology, 2nd ed. Springer, Berlin Heidelberg New York

Friede RL, Roessmann U (1976) Chronic tonsillar herniation. An attempt at classifying chronic herniations at the *foramen magnum*. Acta Neuropathol (Berl) 34:219–235

Fryns JP, Devriendt K, Moerman P (1996) Lumbosacral spina bifida and myeloschizis in a female foetus with *de novo* X/autosomal translation (t(X; 22) (q27; q121)). Genet Couns 7:159–160

Galceran J, Farinas I, Depew MJ, Clevers H, Grosschedl R (1999) Wnt3a–/–like phenotype and limb deficiency in Lef1(–/–)/Tcf1(–/–) mice. Genes Dev 13:709–717

Garber ED (1952) 'Bent-tail', a dominant, sex-linked mutation in the mouse. Proc Natl Acad Sci USA 38:876–879

Gardner E, O'Rahilly R, Prolo D (1975) The Dandy-Walker and Arnold-Chiari malformations. Arch Neurol 32:393–407

Gardner WJ (1973) The Dysraphic States – from syringomyelia to anencephaly. Year Book, Chicago, IL

Geelen JAG (1980) The Teratogenic Effects of Hypervitaminosis A on the Formation of the Neural Tube. Thesis, University of Nijmegen, The Netherlands

Geelen JAG, Langman J, Lowdon JD (1980) The influence of excess vitamin A on neural tube closure in the mouse embryo. Anat Embryol (Berl) 159:223–234

Gilbert SF (2000) Developmental Biology, 6th ed. Sinauer, Sunderland, MA

Giroud A (1977) Anencephaly. Handb Clin Neurol 30:173–208

Golden JA, Chernoff GF (1993) Intermittent pattern of neural tube closure in two strains of mice. Teratology 47:73–80

Gruber GB (1934) Beiträge zur Frage "gekoppelter" Missbildungen (Akrocephalo-syndactylie und Dysencephalia splanchnocystica). Beitr Path Anat Allg Pathol 93:459–476

Gruenwald L (1910) Beiträge zur Kenntnis kongenitaler Geschwülste und Missbildungen an Ohr und Nase. Ztschr Ohrenheilkd 60:270–317

Grüneberg H (1954) Genetical studies on the skeleton of the mouse. VII. Curly tail. J Genet 52:52–67

Hall JG, Friedman JM, Kenna BA, Popkin J, Jawanda M, Arnold W (1988) Clinical, genetic, and epidemiological factors in neural tube defects. Am J Hum Genet 43:827–837

Harding B, Copp AJ (1997) Malformations. In: Graham DI, Lantos PL (eds) Greenfield's Neuropathology, 6th ed. Arnold, London, pp 397–533

Harris MJ (2001) Why are the genes that cause risk of human neural tube defects so hard to find? Teratology 63:165–166

Harris MJ, Juriloff DM (1999) Toward understanding mechanisms of genetic neural tube defects in mice. Teratology 60:292–305

Harrison MJ, Mitnick RJ, Rosenblum BR, Rothmann AS (1990) Leptomyelolipoma: Analysis of 20 cases. J Neurosurg 73:360–367

Hirsch JF, Pierre-Kahn A, Rénier D, Sainte-Rose C, Hoppe-Hirsch E (1984) The Dandy-Walker malformation. J Neurosurg 61:515–522

Hol FA, Hamel BCJ, Geurds MP, Mullaart RA, Barr FG, Macina RA, Mariman ECM (1995) A frameshift mutation in the gene for PAX3 in a girl with spina bifida and mild signs of Waardenburg syndrome. J Med Genet 32:52–56

Holl M (1893) Ueber das Foramen caecum des Schädels. Sitzungsbeitr Kais Akad Wiss Wien 413–436

Holmes LB, Driscoll SG, Atkins L (1976) Etiological heterogeneity of neural tube defects. N Eng J Med 294:365–369

Hori A (1993) A review of the morphology of spinal cord malformations and their relation to neuro-embryology. Neurosurg Rev 16:259–266

Hori A (1994) Tectocerebellar dysraphia with posterior encephalocele (Friede): Report of the youngest case. Clin Neuropathol 13:216–220

Hori A (1997) Sacral agenesis: A case report with pathogenetic considerations. Neuropathology 17:358–361

Hori A (1998) Developmental anomalies of the spinal cord. Neuropathology 18:433–443

Hori A (1999) Morphology of brain malformations: beyond the classification, towards the integration. No Shinkei Geka (Neurol Surg) 27:969–985 (in Japanese)

Hori A (2003) Chiari anomaly type II without cerebellar herniation. Acta Neuropathol (Berl) 105:193–194

Hori A, Orthner H, Kohlschütter A, Schlott KM, Hirabayashi K, Shimokawa K (1980) CNS dysplasia in dysencephalic splanchnocystica (Gruber's syndrome). A case report. Acta Neuropathol (Berl) 51:93–97

Hori A, Brandis A, Walther GF, Petersen C, Massmann J (1998) Retroperitoneal ectopic neural mass: "Abdominal brain" – presentation of two cases and proposal of classification of paraneuraxial neural ectopia. Acta Neuropathol (Berl) 96:301–306

Hoving EW (1993) Frontoethmoidal Encephaloceles. A study of their pathogenesis. Thesis, University of Groningen, The Netherlands

Hoving EW, Vermeij-Keers C, Mommaes-Kienhuis AM, Hartwig NG (1990) Separation of neural and surface ectoderm after closure of the rostral neuropore. Anat Embryol (Berl) 182:455–463

Hsia YE, Bratu M, Herbordt A (1971) Genetics of the Meckel syndrome (dysencephalia splanchnocystica. J Pediatr 48:237–247

Hughes AF, Freeman RB (1974) Comparative remarks on development of the tail cord among higher vertebrates. J Embryol Exp Morphol 32:355–363

Ikenouchi J, Uwabe C, Nakatsu T, Hirose M, Shiota K (2002) Embryonic hydromyelia: Cystic dilatation of the lumbosacral neural tube in human embryos. Acta Neuropathol (Berl) 103:248–254

Jacobson AG (1994) Normal neurulation in amphibians. In: Ciba Foundation Symposium 181. Wiley, Chichester, pp 6–24

Jensson O, Arnason A, Gunnarsdottir H, Petursdottir I, Fossdal R, Hreidarsson S (1988) A family showing apparent X-linked inheritance of both anencephaly and spina bifida. J Med Genet 25:227–229

Jinkins JR, Sener RN (1999) Idiopathic localized hydromyelia: Dilatation of the caudal canal of the spinal cord of probable congenital origin. J Comput Assist Tomogr 23:351–353

Jirásek JE (2001) An Atlas of the Human Embryo and Fetus. Parthenon, New York

Jirásek JE (2004) An Atlas of Human Prenatal Developmental Mechanics. Anatomy and staging. Taylor & Francis, London

Juriloff DM, Harris MJ (2000) Mouse models for neural tube closure defects. Hum Mol Genet 9:993–1000

Juriloff DM, Harris MJ, Tom C, MacDonald KB (1991) Normal mouse strains differ in the site of initiation of closure of the cranial neural tube. Teratology 44:225–233

Källén B (1987) Caudal dysplasia. Handb Clin Neurol 50:509–518

Kalter H (1968) Teratology of the Central Nervous System in Laboratory and Domestic Mammals. University of Chicago Press, Chicago, IL

Kampmeier OF (1927) On sireniform monsters, with a consideration of the causation and the predominance of the male sex among them. Anat Rec 34:365–389

Kapur RP, Mahoney BS, Nyberg DA, Resta RG, Shepard TH (1991) Sirenomelia with a "vanishing twin". Teratology 43:103–108

Karch SB, Urich H (1972) Occipital encephalocele: A morphological study. J Neurol Sci 15:89–112

Karfunkel P (1974) The mechanisms of neural tube formation. Int Rev Cytol 38:245–271

Keppler-Noreuil KM (2001) OEIS complex (omphalocele–exstrophy–imperforate anus–spinal defects): A review of 14 cases. Am J Med Genet 99:271–279

Kernohan JW (1924) The ventriculus terminalis: Its growth and development. J Comp Neurol 38:107–125

Keyser AJM (1972) The development of the diencephalon of the Chinese hamster. Acta Anat (Basel) 83(Suppl 59):1–181

Khoury MJ, Erickson JD, James LM (1982) Etiologic heterogeneity of neural tube defects. II. Clues from family studies. Am J Hum Genet 34:980–987

Kleyer WJ, de Bruin HWA, Leschot NJ (1978) Amniotic fluid alpha-fetoprotein levels and the prenatal diagnosis of neural tube defects: A collaborative study of 2180 pregnancies in the Netherlands. Br J Obstet Gynaecol 85:512–517

Klootwijk R, Franke B, van der Zee CEEM, de Boer RT, Wilms W, Hol FA, Mariman ECM (2000) A deletion encompassing Zic3 in Bent tail, a mouse model for X-linked neural tube defects. Hum Mol Genet 9:1615–1622

Knobloch WH, Layer JM (1971) Retinal detachment and encephalocele. J Pediatr Ophthalmol 8:181–184

Larroche J-C, Encha-Razavi F, de Vries F (1997) Central nervous system. In: Gilbert-Barness E (ed) Potter's Pathology of the Fetus and Infant. Mosby, St. Louis, MI, pp 1045–1056

Lawson A, Anderson H, Schoenwolf GC (2001) Cellular mechanisms of neural fold formation and morphogenesis in the chick embryo. Anat Rec 262:153–168

Lellouch-Tubiana A, Zerah M, Catala M, Brousse N, Kahn A-P (1999) Congenital intraspinal lipomas: Histological analysis of 234 cases and review of the literature. Pediatr Dev Pathol 2:346–352

Lemire RJ (1969) Variations in development in the caudal neural tube in human embryos (Horizons XIV–XXI). Teratology 2:361–369

Lemire RJ (1987) Anencephaly. Handb Clin Neurol 50:71–95

Lemire RJ (1988) Neural tube defects. JAMA 259:558–562

Lemire RJ, Beckwith JB (1982) Pathogenesis of congenital tumors and malformations of the sacrococcygeal region. Teratology 25:201–213

Lemire RJ, Siebert JR (1990) Anencephaly: Its spectrum and relationship to neural tube defects. J Craniofac Genet 10:163–174

Lemire RJ, Beckwith JB, Shepard TH (1972) Iniencephaly and anencephaly with spinal retroflexion. A comparative study of eight human specimens. Teratology 6:27–36

Lemire RJ, Loeser JD, Leech RW, Alvord EC Jr (1975) Normal and Abnormal Development of the Human Nervous System. Harper & Row, Hagerstown, MD

Lemire RJ, Beckwith JB, Warkany J (1978) Anencephaly. Raven, New York

Lendon RG, Emery JL (1970) Forking of the central canal in the equinal cord of children. J Anat (Lond) 106:499–505

Lyon MF, Zenthon J, Burtenshaw MD, Evans EP (1987) Localization of the Hprt locus by in situ hybridization of loci on the mouse X-chromosome. Cytogenet Cell Genet 44:163–166

MacDonald KB, Juriloff DM, Harris MJ (1989) Developmental study of neural tube closure in a mouse stock with a high incidence of exencephaly. Teratology 39:195–213

Mariman ECM, Hamel BCJ (1992) Sex ratios of affected and transmitting members of multiple case families with neural tube defects. J Med Genet 29:695–698

Marín-Padilla M (1965a) Study of the skull in human cranioschisis. Acta Anat (Basel) 62:1–20

Marín-Padilla M (1965b) Study of the sphenoid bone in human cranioschisis and craniorhachischisis. Virchows Arch Pathol Anat Physiol 339:245–253

Marín-Padilla M (1970) Morphogenesis of anencephaly and related malformations. Curr Top Pathol 51:145–174

Marín-Padilla M (1991) Cephalic axial skeletal-neural dysraphic disorders: Embryology and pathology. Can J Neurol Sci 18:153–169

Marín-Padilla M, Marín-Padilla TM (1981) Morphogenesis of experimentally induced Arnold-Chiari malformation. J Neurol Sci 50:29–55

McLaurin RL (1977) Cranium bifidum and cranial cephaloceles. Handb Clin Neurol 30:209–218

McLone DG, Dias MC (1991–1992) Complications of myelomeningocele closure. Pediatr Neurosurg 17:267–273

McLone DG, Knepper PA (1989) The cause of Chiari II malformation: A unified theory. Pediatr Neurosci 15:1–12

McLone DG, Naidich TP (1985) Terminal myelocystocele. Neurosurgery 16:36–43

McLone DG, Naidich TP (1986) Laser resection of 50 spinal lipomas. Neurosurgery 18:611–615

McLone DG, Naidich TP (1989) The tethered spinal cord. In: McLaurin RL, Schut L, Venes JL, Epstein F (eds) Pediatric Neurosurgery, 2nd ed. Saunders, Philadelphia, PA, pp 71–75

Meckel JF (1822) Beschreibung zweier, durch sehr ähnliche Bildungsabweichungen entstellter Geschwister. Dtsch Arch Physiol 7:99–172

Melvin EC, George TM, Worley G, Franklin A, Mackey J, Viles K, Shah N, Drake CR, Enterline DS, McLone D, et al. (2000) Genetic studies in neural tube defects. Pediatr Neurosurg 32:1–9

Moerman P, Fryns JP, Vandenberghe K, Lauweryns JM (1992) Constrictive amniotic bands, amniotic adhesions and limb-body wall complex: Discrete disruption sequences with etiopathogenetic overlap. Am J Med Genet 42:470–479

Morriss-Kay G, Wood H, Chen W-H (1994) Normal neurulation in mammals. In: Ciba Foundation Symposium 181. Wiley, Chichester, pp 51–69

Moury JD, Schoenwolf GC (1995) Cooperative model of epithelial shaping and bending during avian neurulation: Autonomous movements of the neural plate, autonomous movements of the epidermis, and interactions in the neural plate/epidermis transition zone. Dev Dyn 204:323–337

Müller F, O'Rahilly R (1984) Cerebral dysraphia (future anencephaly) in a human twin embryo at stage 13. Teratology 30:167–177

Müller F, O'Rahilly R (1986) The development of the human brain and the closure of the rostral neuropore at stage 11. Anat Embryol (Berl) 175:205–222

Müller F, O'Rahilly R (1987) The development of the human brain, the closure of the caudal neuropore, and the beginning of secondary neurulation at stage 12. Anat Embryol (Berl) 176:413–430

Müller F, O'Rahilly R (1991) The development of anencephaly and its variants. Am J Anat 190:193–218

Naidich TP, McLone DG, Harwood-Nash DC (1983) Spinal dysraphism. In: Newton TH, Potts DG (eds) Modern Neuroradiology, Vol 1: Computed Tomography of the Spine and Spinal Cord. Clavadel, San Anselmo, CA, pp 299–353

Naidich TP, Altman NR, Braffman BH, McLone DG, Zimmerman RA (1992) Cephaloceles and related malformations. AJNR Am J Neuroradiol 12:655–690

Naidich TP, Zimmerman RA, McLone DG, Raybaud CA, Altman NR, Braffman BH (1996) Congenital anomalies of the spine and spinal cord. In: Atlas SW (ed) Magnetic Resonance Imaging of the Brain and Spine, 2nd ed. Lippincott-Raven, New York, pp 1265–1337

Nait-Oumesmar B, Stecca B, Fatterpekar G, Naidich T, Corbin J, Lazzarini RA (2002) Ectopic expression of Gcm1 induces congenital spinal cord abnormalities. Development 129:3957–3964

Nakatsu T, Uwabe C, Shiota K (2000) Neural tube closure in humans initiates at multiple sites: Evidence from human embryos and implications for the pathogenesis of neural tube defects. Anat Embryol (Berl) 201:455–466

Nicolaides KH, Gabbe SG, Campbell S, Guidetti R (1986) Ultrasound screening for spina bifida: Cranial and cerebellar signs. Lancet 1986 (ii):72–74

Nievelstein RAJ (1998) The Caudal Regression Syndrome and Anorectal Malformations. Magnetic resonance imaging and embryological studies. Thesis, Free University of Amsterdam, The Netherlands

Nievelstein RAJ, Hartwig NG, Vermeij-Keers C, Valk J (1993) Embryonic development of the mammalian caudal neural tube. Teratology 48:21–31

Nievelstein RAJ, Valk J, Smit LME, Vermeij-Keers C (1994) MR of the caudal regression syndrome: Embryological implications. AJNR Am J Neuroradiol 15:1021–1029

Nishimura H, Okamoto N (1977) Iniencephaly. Handb Clin Neurol 30:257–268

Norman MG, McGillivray BC, Kalousek DK, Hill A, Poskitt KJ (1995) Congenital Malformations of the Brain. Pathological, embryological, clinical, radiological and genetic aspects. Oxford University Press, New York

Okeda R (1978) Heterotopic brain tissue in the submandibular region and lung. Report of two cases and comments about pathogenesis. Acta Neuropathol (Berl) 43:217–220

Opitz JM, Howe JJ (1969) The Meckel syndrome (dysencephalia splanchnocystica, the Gruber syndrome). Birth Defects Orig Artic Ser 5:167–179

O'Rahilly R, Müller F (1989a) Bidirectional closure of the rostral neuropore in the human embryo. Am J Anat 184:259–268

O'Rahilly R, Müller F (1989b) Interpretation of some median anomalies as illustrated by cyclopia and symmelia. Teratology 40:409–421

O'Rahilly R, Müller F (1994) Neurulation in the normal human embryo. In: Ciba Foundation Symposium 181. Wiley, Chichester, pp 70–89

O'Rahilly R, Müller F (1999) The Embryonic Human Brain. An atlas of developmental stages, 2nd ed. Wiley-Liss, New York

O'Rahilly R, Müller F (2001) Human Embryology & Teratology, 3rd ed. Wiley-Liss, New York

O'Rahilly R, Müller F (2002) The two sites of fusion of the neural folds and the two neuropores in the human embryo. Teratology 65:162–170

Osaka K, Tanimura T, Hirayama A, Matsumoto S (1978) Myelomeningocele before birth. J Neurosurg 49:711–724

Osborn AG (1994) Diagnostic Neuroradiology. Mosby, St. Louis, MI

Padget DH (1970) Neuroschisis and human embryonic maldevelopment. New evidence on anencephaly, spina bifida and diverse mammalian defects. J Neuropathol Exp Neurol 29:192–216

Padmanabhan R (1998) Retinoic acid-induced caudal regression syndrome in the mouse fetus. Reprod Toxicol 12:139–151

Padmanabhan R, Naruse I, Shiota K (1999) Caudal dysgenesis in staged human embryos: Carnegie stages 16-23. Am J Med Genet 87:115–127

Paetau A, Salonen R, Haltia M (1985) Brain pathology in the Meckel syndrome: A study of 59 cases. Clin Neuropathol 4:56–62

Pang D (1993) Sacral agenesis and caudal spinal cord malformations. Neurosurgery 32:755–779

Pang D, Hoffman HJ (1980) Sacral agenesis with progressive neurological deficit. Neurosurgery 7:118–126

Pang D, Dias MS, Ahab-Barmada M (1992) Split cord malformations. Part I. A unified theory of embryogenesis for double spinal cord malformations. Neurosurgery 31:451–480

Pappas CTE, Seaver L, Carrion C, Rekate H (1989) Anatomical evaluation of the caudal regression syndrome (lumboacral agenesis) with magnetic resonance imaging. Neurosurgery 25:462–465

Passarge E, Lenz W (1966) Syndrome of caudal regression in infants of diabetic mothers: Observations of further cases. Pediatrics 37:672–675

Peeters MCE (1998) Embryonic Axial Curvature. Relationships to neuropore closure. Thesis, University of Maastricht, The Netherlands

Peeters MCE, Shum ASW, Hekking JWM, Copp AJ, van Straaten HWM (1996) Relationship between altered axial curvature and neural tube closure in normal and mutant (curly tail) mouse embryos. Anat Embryol (Berl) 193:123–130

Peeters MCE, Hekking JWM, Vainas T, Drukker J, van Straaten HWM (1997) Spatio-temporal curvature pattern of the caudal body axis for non-mutant and curly tail mouse embryos during the period of neural tube closure. Anat Embryol (Berl) 195:259–266

Peeters MCE, Viebahn C, Hekking JWM, van Straaten HWM (1998a) Neurulation in the rabbit embryo. Anat Embryol (Berl) 197:167–175

Peeters MCE, Hekking JWM, Shiota K, Drukker J, van Straaten HWM (1998b) Differences in axial curvature correlate with species-specific rate of neural tube closure in embryos of chick, rabbit, mouse, rat and human. Anat Embryol (Berl) 198:185–194

Potter EL, Craig JM (1975) Pathology of the Fetus & the Infant, 3rd ed. Year Book, Chicago, IL, pp 522–547

Richards DS, Seeds JW, Katz VL, Lingley LH, Albright SG, Cefalo RC (1988) Elevated maternal serum alpha-fetoprotein with normal ultrasound: Is amniocentesis always appropriate? A review of 26,029 screened patients. Obstet Gynecol 71:203–207

Rizzuti T, Ferrarese S, Varesi G, Masini T (1997) Ectopic neuroglial tissue associated with intrapulmonary congenital cystic adenomatoid malformation. Minerva Pediatr 49:89–92

Ross AJ, Ruiz-Perez V, Wang Y, Hagan DM, Scherer S, Lynch SA, Lindsey S, Gustard E, Belloni E, Wilson DI, et al. (1998) A homeobox gene, *HLXB9*, is the major locus for dominantly inherited sacral agenesis. Nat Genet 20:358–361

Rossi A, Biancheri R, Cama A, Piatelli G, Ravegnani M, Tortori-Donati P (2004) Imaging in spine and spinal cord malformations. Eur J Radiol 50:177–200

Roth M (1986) Cranio-cervical growth collision: Another explanation of the Arnold-Chiari malformation and of basilar expression. Neuroradiology 28:187–194

Rusnak SL, Driscoll SG (1965) Congenital spinal anomalies in infants of diabetic mothers. Pediatrics 35:989–995

Saitsu H, Yamada S, Uwabe C, Ishibashi M, Shiota K (2004) Development of the posterior neural tube in human embryos. Anat Embryol (Berl) 209:107–117

Sakai Y (1989) Neurulation in the mouse: Manner and timing of neural tube closure. Anat Rec 223:194–203

Saraga-Babic M, Sapunar D, Wartiovaara J (1995) Variations in the formation of the human caudal spinal cord. J Hirnforsch 36:341–347

Scherrer CC, Hammer F, Schinzel A, Briner J (1992) Brain stem and cervical cord dysraphic lesions in iniencephaly. Pediatr Pathol 12:469–476

Schoenwolf GC (1984) Histological and ultrastructural studies of secondary neurulation in mouse embryos. Am J Anat 169:361–374

Schoenwolf GC (1994) Formation and patterning of the avian neuraxis: One dozen hypotheses. In: Ciba Foundation Symposium 181. Wiley, Chichester, pp 25–50

Schoenwolf GC, Alvarez IS (1989) Roles of neuroepithelial cell rearrangement and division in shaping of the avian neural plate. Development 106:427–439

Schoenwolf GC, Smith JL (1990) Mechanisms of neurulation: Traditional viewpoint and recent advances. Development 109:243–270

Schorle H, Meier P, Buchert M, Jaenisch R, Mitchell PJ (1996) Transcription factor AP-2 essential for cranial closure and craniofacial development. Nature 381:235–238

Schropp KP, Lobe TE, Rao B, Mustabagani K, Kay GA, Gilchrist BF, Philippe PG, Boles ET (1992) Sacrococcygeal teratoma: The experience of four decades. J Pediatr Surg 27:1075–1079

Schwalbe E, Gredig M (1907) Über Entwicklungsstörungen des Kleinhirns, Hirnstamms und Halsmarks bei Spina bifida (Arnold'sche und Chiari'sche Mißbildung). Beitr Pathol Anat Allg Pathol 40:132–194

Sebire NJ, Noble PL, Thorpe-Beeston JG, Snijders RJM, Nicolaides KH (1997) Presence of the 'lemon' sign in fetuses with spina bifida at the 10-14 week scan. Ultrasound Obstet Gynecol 10:403–405

Seller MJ (1994) Risks in spina bifida. Dev Med Child Neurol 36:1021–1025

Seller MJ (1995) Sex, neural tube defects, and multisite closure of the human neural tube. Am J Med Genet 58:332–336

Seller MJ, Wallace ME (1993) Tail short variable: Characterization of a new mouse mutant and its possible analogy to certain human vascular disruption defects. Teratology 48:383–391

Shenefelt RE (1972) Morphogenesis of malformations in hamsters caused by retinioc acid: Relation to dose and stage of treatment. Teratology 5:103–118

Shiota K (1991) Development and intrauterine fate of normal and abnormal human conceptuses. Cong Anom 31:67–80

Shum ASW, Copp AJ (1996) Regional differences in morphogenesis of neuroepithelium suggest multiple mechanisms of spinal neurulation in the mouse. Anat Embryol (Berl) 194:65–73

Sigal R, Denys A, Halimi P, Shapeero L, Doyon D, Boudghène F (1991) Ventriculus terminalis of the conus medullaris: MR imaging in four patients with congenital dilatation. AJNR Am J Neuroradiol 12:733–737

Smith JL, Schoenwolf GC (1987) Cell cycle and neuroepithelial cell shape during bending of the chick neural plate. Anat Rec 218:196–206

Smith JL, Schoenwolf GC (1988) Role of cell-cycle in regulating neuroepithelial cell shape during bending of the chick neural plate. Cell Tissue Res 252:491–500

Smith JL, Schoenwolf GC (1991) Further evidence of extrinsic forces in bending of the neural plate. J Comp Neurol 307:225–236

Smith JL, Schoenwolf GC (1997) Neurulation: Coming to closure. Trends Neurosci 20:510–517

Steegers-Theunissen RP, Boers GH, Trijbels FJ, Eskes TK (1991) Neural tube defects and derangement of homocysteine metabolism. N Engl J Med 324:199–200

Steegers-Theunissen RP, Boers GH, Trijbels FJ, Finkelstein JD, Blom HJ, Thomas CM, Borm GF, Wouters MG, Eskes TK (1994) Maternal hyperhomocysteinemia: A risk factor for neural tube defects? Metabolism 43:1475–1480

Sternberg H (1927) Beiträge zur Kenntniss des vorderen Neuroporus beim Menschen. Ztsch Anat Entwickl-Gesch 82:747–780

Sternberg H (1929) Zur formalen Genese der vorderen Hirnbrüche (Encephalomeningocele anterior). Wien Med Wochenschr 79:462–466

Stocker JT, Heifetz SA (1987) Sirenomelia: A morphological study of 33 cases and review of the literature. Perspect Pediatr Pathol 10:7–50

Streeter GL (1919) Factors involved in the formation of the filum terminale. Am J Anat 25:1–11

Suwanwela C, Suwanwela N (1972) A morphological classification of sincipital encephalomeningoceles. J Neurosurg 36:202–211

Suwanwela C, Sukabote C, Suwanwela N (1971) Frontoethmoidal encephalomeningocele. Surgery 69:617–625

Taubner X (1887) Zur Casuistik und Entwicklung der Hirnlipoma. Virchows Arch Pathol Anat 110:95–101

ten Donkelaar HJ, Hamel BCJ, Hartman E, van Lier JAC, Wesseling P (2002) Intestinal mucosa on top of a rudimentary occipital meningocele in amniotic rupture sequence: Disorganization-like syndrome, homeotic transformation, abnormal surface encounter or endoectodermal adhesion? Clin Dysmorphol 11:9–13

Tidy J (1989) A study of the value of measuring maternal serum alpha-fetoprotein for the antenatal diagnosis of neural tube defects. Arch Gynecol Obstet 244:133–136

Theiler K (1988) Vertebral malformations. Adv Anat Embryol Cell Biol 112:1–99

Tom C, Juriloff DM, Harris MJ (1991) Studies of the effect of retinoic acid on anterior neural tube closure in mice genetically liable to exencephaly. Teratology 43:27–40

Toriello HV (1984) Report of a third kindred with X-linked anencephaly/spina bifida. Am J Med Genet 19:411–412

Toriello HV, Warren ST, Lindstrom JA (1980) Possible X-linked anencephaly and spina bifida – report of a kindred. Am J Med Genet 6:119–121

Tortori-Donati P, Rossi A, Cama A (2000) Spinal dysraphism: A review of neuroradiological features with embryological considerations and proposal for a new classification. Neuroradiology 42:471–491

Towfighi J, Housman C (1991) Spinal cord abnormalities in caudal regression syndrome. Acta Neuropathol (Berl) 81:458–466

Trembath D, Sherbondy AL, Vandyke DC, Shaw GM, Todoroff K, Lammer EJ, Finnell RH, Marker S, Lerner G, Murray JC (1999) Analysis of select folate pathway genes, *PAX3*, and human *T* in a Midwestern neural tube defect population. Teratology 59:331–341

Tuckett F, Morriss-Kay GM (1985) The kinetic behavior of the cranial neural epithelium during neurulation in the rat. J Embryol Exp Morphol 85:111–119

UK Collaborative Study on alpha-fetoprotein in relation to neural tube defects (1977) Maternal serum-alpha-fetoprotein measurement in antenatal screening for anencephaly and spina bifida in early pregnancy. Lancet 1977 (i):1323–1332

UK Collaborative Study on alpha-fetoprotein in relation to neural tube defects (1979) Amniotic-fluid alpha-fetoprotein measurement in antenatal diagnosis of anaencephaly and open spina bifida in early pregnancy. Lancet 1979 (ii):651–661

Van Allen MI, Kalousek DK, Chernoff GF, Juriloff D, Harris M, McGillivray BC, Yong S-L, Langlois S, MacLeod PM, Chitayat D, et al. (1993) Evidence for multi-site closure of the neural tube in humans. Am J Med Genet 47:723–743

van Straaten HWM, Copp AJ (2001) Curly tail: A 50-year history of the mouse spina bifida model. Anat Embryol (Berl) 203:225–237

van Straaten HWM, Hekking JWM, Consten C, Copp AJ (1993) Intrinsic and extrinsic factors in the mechanism of neurulation – effect of curvature of the body axis on closure of the posterior neuropore. Development 117:1163–1172

van Straaten HWM, Janssen HCJP, Peeters MCE, Copp AJ, Hekking JWM (1996) Neural tube closure in the chick embryo is multiphasic. Dev Dyn 307:309–318

van Straaten HWM, Peeters MCE, Szpak KFW, Hekking JWM (1997) Initial closure of the mesencephalic neural groove in the chick embryo involves a releasing zipping-up mechanism. Dev Dyn 209:333–341

van Straaten HWM, Peeters MCE, Hekking JWM, van der Lende T (2000) Neurulation in the pig embryo. Anat Embryol (Berl) 202:75–84

Vermeij-Keers C (1990) Craniofacial embryology and morphogenesis: Normal and abnormal. In: Stricker M, van der Meulen J, Raphael B, Mazzola D (eds) Craniofacial Malformations. Churchill Livingstone, Edinburgh, pp 21–60

Virchow R (1857) Ein Fall von bösartigen, zum Teil in der Form des Neurons auftretenden Fettgeschwülsten. Virchows Arch Pathol Anat 11:281–296

Warkany J (1971) Congenital Malformations. Year Book, Chicago, IL

Wheeler T (1918) Study of a human spina bifida monster with encephaloceles and other abnormalities. Contrib Embryol Carnegie Instn 7:87–110

Williams RS, Swisher CN, Jennings M., Ambler M, Caviness VS Jr (1984) Cerebro-ocular dysgenesis (Walker-Warburg syndrome): Neuropathologic and etiologic analysis. Neurology 34:1531–1541

Williamson DAJ (1970) A syndrome of congenital malformations possibly due to maternal diabetes. Dev Med Child Neurol 12:145–152

Wright RL (1971) Congenital dermal sinuses. Prog Neurol Surg 4:175–191

Ybot-Gonzalez P, Cogram P, Gerrelli D, Copp AJ (2002) Sonic hedgehog and the molecular regulation of mouse naural tube closure. Development 129:2507–2517

Yeoh GPS, Bale PM, de Silva M (1989) Nasal cerebral heterotopia: The so-called nasal glioma or sequestered encephalocele and its variants. Pediatr Pathol 9:531–549

Yokota A, Matsukado Y, Fuwa I, Moroki K, Nagahiro S (1986) Anterior or basal encephalocele of the neonatal and infantile period. Neurosurgery 19:468–478

Yoshikawa Y, Fujimori T, McMahon AP, Takada S (1997) Evidence that absence of Wnt-3a signaling promotes neuralization instead of paraxial mesoderm development in the mouse. Dev Biol 183:234–242

Zhang J, Hagopian-Donaldson S, Serbedzija G, Elsemore J, Plehn-Dujowich D, McMahon AP, Flavell RA, Williams T (1996) Neural tube, skeletal and body wall defects in mice lacking transcription factor AP-2. Nature 381:238–241

Zhao Q, Behringer RR, de Crombrugghe B (1996) Prenatal folic acid treatment suppresses acrania and meoanencephaly in mice mutant for the Cart1 homeobox gene. Nat Genet 13:275–283

The Neural Crest and Craniofacial Malformations

Hans J. ten Donkelaar and Christl Vermeij-Keers

5.1 Introduction

The neural crest is a temporary embryonic structure that is composed of a population of multipotent cells that delaminate from the ectoderm by epitheliomesenchymal tranformation (EMT; Duband et al. 1995; Hay 1995; Le Douarin and Kalcheim 1999; Francis-West et al. 2003). Neural-crest-derived cells are called *mesectodermal* or *ectomesenchymal cells* (mesodermal cells of ectodermal origin) that have arisen through EMT. The neural crest was first described by His (1868) in the chick embryo as a *Zwischenstrang*, a strip of cells lying between the dorsal ectoderm and the neural tube. Classic contributions in amphibians identified interactions between tissues that lead to neural crest formation, and were reviewed by Hörstadius (1950). Cell labelling techniques, particularly the quail-chick chimeric marker (Le Douarin 1969, 1973), showed that the neural crest contributes to a large number of structures in the avian embryo (Le Douarin and Kalcheim 1999; Le Douarin 2004), including the spinal, cranial and autonomic ganglia, the medulla of the adrenal gland, the melanocytes and many of the skeletal and connective tissues of the head. The whole facial and visceral skeleton and part of the neurocranium are formed from the neural crest. Many species-related discrepancies are present in the literature on neural crest cell migration and their targets. In contrast to chick embryos, the neural crest in mammalian embryos is a less distinct structure and can be defined as the transition zone between the neuroectoderm and the presumptive epidermis from neural plate stages onwards (O'Rahilly and Müller 1999). In presomite murine embryos, the whole ectoderm, including the presumptive neural crest, is able to produce mesectodermal cells (Smits-van Prooije 1986; Smits-van Prooije et al. 1988). These EMT cells proliferate shortly after their migration into the mesodermal compartment (Vermeij-Keers and Poelmann 1980). In somite stages during the transformation of the cranial neuroectoderm of the head folds via the neural groove into the neural tube, there is a balance between the outgrowth of the neuroectoderm and the production of EMT cells by the neural crest; therefore, in mammalian embryos, only short-distance migration of EMT cells occurs.

The **cranial neural crest** provides the precursors of cartilage, bone, muscles and connective tissue of the head (Vermeij-Keers 1990; Sulik 1996; LaBonne and Bronner-Fraser 1999; Le Douarin and Kalcheim 1999; Sperber 2002; Knecht and Bronner-Fraser 2002; Francis-West et al. 2003; Santagati and Rijli 2003). In addition, during later developmental stages multiple places of EMT are recognized as well. In the head–neck area, for example, the neurogenic placodes and the optic neural crest are such areas. **Neurogenic placodes**, specialized regions of the embryonic ectoderm, are the major source of primary sensory neurons in the head (Johnston and Bronsky 1995; Graham and Begbie 2000). The vasculature of the head is derived from mesoderm-derived endothelial precursors, while the neural crest provides the pericytes and smooth muscle cells of the vessels of the face and the forebrain (Etchevers et al. 2001).

Deficiencies in migration, proliferation and differentiation of neural-crest-derived tissue account for a wide range of craniofacial malformations, i.e. the so-called *neurocristopathies*, manifested in a variety of syndromes (Jones 1990; Gorlin et al. 2001; Wilkie and Morriss-Kay 2001; Johnston and Bronsky 1995, 2002; Cohen 2002). Abnormalities in form, function or apoptosis of neural crest cells may range from von Recklinghausen's neurofibromatosis through Treacher Collins to DiGeorge and Waardenburg syndromes (Dixon et al. 2000). Neurocristopathies may be accompanied by developmental disorders of the CNS. Recently, however, the idea that neural crest abnormalities underly the pathogenesis of the DiGeorge and Treacher Collins syndromes has been challenged (Sect. 5.5). Major craniofacial malformations are also found in holoprosencephaly (HPE) and the craniosynostoses. *Holoprosencephaly* is an early disorder of pattern formation that may lead to closely related forebrain and facial malformations. In the fetal period, *craniosynostoses* are frequent (approximately one in 2,500 children) craniofacial malformations due to agenesis or premature ossification of the cranial sutures, caused by mutations in *FGFR* and other genes (Wilkie 1997; Cohen and MacLean 2000; Gorlin et al. 2001; Jabs 2002), that may interfere with normal brain development to varying degrees.

In this chapter, the neural crest and its derivatives and craniofacial development will be discussed, followed by an overview of the neurocristopathies, HPE and abnormal development of the skull, leading to CNS malformations. The neuropathology of HPE will be discussed in Chap. 9.

5.2   **Induction of the Neural Crest**

Neural crest cells are induced at the border between the neuroectoderm and the non-neural or surface ectoderm (Fig. 5.1). During the formation of the neural tube in the chick embryo, neural crest progenitors come to lie in or directly adjacent to the dorsal neural tube (Le Douarin and Kalcheim 1999). Depending on the species, neural crest cells leave the neuroepithelium before, during or after neural tube closure, and 'migrate' throughout the body. To leave the neuroepithelium, neural crest cells must lose their epithelial characteristics and take on the properties of migratory mesenchymal cells. Wheat germ agglutinin labelling experiments in mouse embryos (Smits-van Prooije et al. 1988) and 1,1'-dioctadecyl-3,3,3',3'-tetramethylindocarbocyanine perchlorate (DiI) labelling in chick embryos (Kulesa and Fraser 1998) have shown that migration of neural crest cells is random. Other studies have suggested that there are cell-free spaces underneath the neuroectoderm and surface ectoderm resulting in specific pathways for migrating neural crest cells (Le Douarin 1969, 1973). In quail-chick chimeras, however, cell-free spaces may be created artificially. More recent studies suggest a role for chemoattractive signals such as fibroblast growth factor (FGF) in the control of neural crest cell migration (Kubota and Ito 2000; Francis-West et al. 2003).

Induction of the neural crest appears to be a complex multistep process that involves many genes (LaBonne and Bronner-Fraser 1999; Aybar and Mayor 2002; Knecht and Bronner-Fraser 2002; Gammill and Bronner-Fraser 2003; Wu et al. 2003). The **generation** of **neural crest cells** appears to result from inductive interactions shared with the neural plate and the early epidermis. The neural–epidermal boundary can be distinguished by the expression of molecular markers such as the transcription factors of the *Snail* family, Snail and Slug, in *Xenopus*, zebrafish, chick and mouse (Mayor et al. 1995; Sefton et al. 1998; Linker et al. 2000; Aybar et al. 2003). The timing and expression pattern of these markers differs between vertebrates. Bone morphogenetic protein (BMP) signalling specifies the formation of dorsal neural tissues and the neural plate border (Sasai and De Robertis 1997; Weinstein and Hemmati-Brivanlou 1999). Low or absent BMP signalling leads to neural induction, whereas a high level of BMP signalling induces epidermis. An intermediate level of BMP signalling may determine the neural plate border (Wilson et al. 1997; Nguyen et al. 1998, 2000). In zebrafish, BMP signalling is required for the development of the neural crest (Nguyen et al. 2000), but in *Xenopus* intermediate BMP levels alone cannot induce the neural crest. Additional factors, Wnt proteins in particular, are required to induce the neural crest
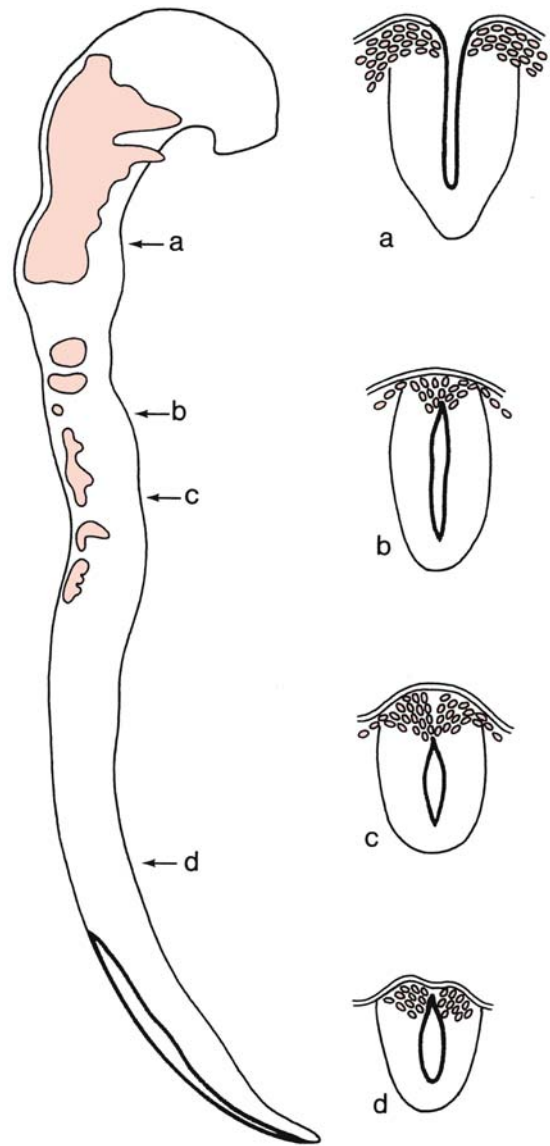
Fig. 5.1 The early development of the human neural crest in a Carnegie stage 10 embryo. At rostral levels (**a**), crest material is formed before closure of the neural groove, whereas at more caudal levels (**b**–**d**) closure of the neural folds preceeds migration of crest material. (After Müller and O'Rahilly 1985)

(LaBonne and Bronner-Fraser 1998; Gammill and Bronner-Fraser 2003; Wu et al. 2003).

The **epitheliomesenchymal tranformation** (**EMT**) of emerging neural crest cells is accompanied by the expression of the zinc-finger transcription factor Slug. In chick and *Xenopus* embryos, its expression is maintained during the phase of crest cell migration (Nieto et al. 1994; LaBonne and Bronner-Fraser 2000). *Slug* mutant mice, however, do not show defects in either neural crest or mesodermal tissues (Jiang et al. 1998). In mice, another family member,

Snail, rather than Slug is expressed in the regions undergoing EMT (Cano et al. 2000; Locascio and Nieto 2001; Knecht and Bronner-Fraser 2002; Gammill and Bronner-Fraser 2003). *Snail* mutant mice die at gastrulation as a result of defects in mesoderm formation arising from deficient EMT.

5.3   Derivatives of the Neural Crest

The neural crest is the major source of mesenchymal cells in the head and neck, and in addition gives rise to sensory ganglia, autonomic and enteric ganglia as well as to pigment cells of the skin. In the postcranial region, mesenchyme forming the connective tissues is mesodermal in origin (Table 5.1). The chick neural crest can be divided into four main domains (Le Douarin and Kalcheim 1999): (1) the **cranial** or **cephalic neural crest**, giving rise to the craniofacial mesenchyme in particular; (2) the **trunk neural crest**, giving rise to the dorsal root and sympathetic ganglia; (3) the **vagal** and **sacral neural crest**, generating the parasympathetic (enteric) ganglia of the gut; and (4) the **cardiac neural crest**, located between the cranial and trunk neural crests. In chick embryos, the cardiac neural crest produces the musculoconnective tissue for the large arteries arising from the heart and contributes to the separation of the truncus arteriosus into the pulmonary artery and aorta (Le Lièvre and Le Douarin 1975; Kirby 1987; Kirby and Waldo 1990). The cranial neural crest is the only part of the neural crest that is able to produce cartilage and bone.

5.3.1   The Cranial Neural Crest

During neural tube closure in the chick embryo, cranial neural crest cells migrate into the underlying tissues as mesenchyme (**ectomesenchyme**), forming a lineage of pluripotential stem cells that give rise to diverse tissues (Le Douarin and Kalcheim 1999). In contrast, in mice the entire ectoderm of early presomite embryos and the ectoderm of the head folds in late presomite and early somite embryos are able to deposit ectomesenchymal cells into mesodermal compartments (Vermeij-Keers and Poelmann 1980; Smits-van Prooije et al. 1985; Tan and Morriss-Kay 1985; Smits-van Prooije 1986; Boshart et al. 2000). From four-somite up to 20-somite murine embryos, i.e. after the closure of the rostral neuropore, the cranial neural crest is active. In human embryos of stage 9 (one to three somites) up to stage 10 (four to 12 somites), ectomesenchymal cells arise from parts of the head folds, probably the rostral and facial crest (Müller and O'Rahilly 1983, 1985; Vermeij-Keers 1990). In chick embryos, however, the embryonic

Table 5.1 Derivatives of neural crest cells (after LeDouarin and Kalcheim 1999; Sperber 2001)

Connective tissues	Ectomesenchyme of facial prominences and pharyngeal arches
	Bones and cartilage of facial and visceral skeleton
	Dermis of face and ventral aspect of neck
	Stroma of salivary, thymus, thyroid, parathyroid and pituitary glands
	Corneal mesenchyme
	Sclera and choroid optic coats
	Blood vessel walls; aortic arch arteries
	Dental papilla; part of periodontal ligament; cementum
Muscle tissues	Ciliary muscles
	Covering connective tissues of pharyngeal-arch muscles (masticatory, facial, faucial, laryngeal)
Nervous tissues	Supporting tissues: leptomeninges of prosencephalon and part of the mesencephalon; glia; Schwann's sheath cells
	Sensory ganglia: spinal dorsal root ganglia; and sensory ganglia of trigeminal, facial, glosso-pharyngeal and vagal nerves
	Autonomic nervous system: sympathetic ganglia and plexuses; parasympathetic ganglia
Endocrine tissues	Adrenomedullary cells and adrenergic paraganglia
	Calcitonin parafollicular cells of thyroid gland
	Carotid body
Pigment cells	Melanocytes in all tissues
	Melanophores of iris

prominences of the face and neck (the so-called frontonasal process and the pharyngeal arches) are dependent on mesencephalic and rhombencephalic neural crest tissue, migrating as ectomesenchyme into ventral regions of the future skull, face and neck (Fig. 5.2; Couly and Le Douarin 1990). In the human head, neural crest cells also arise from the external layer of the optic vesicle, i.e. the optic neural crest (O'Rahilly and Müller 2001).

In chick embryos, cranial neural crest cells migrate from regions rostral to rhombomere 6, taking one of three major **migratory pathways** (Lumsden and Guthrie 1991; Sechrist et al. 1993; Kulesa and Fraser 2000; Fig. 5.3): (1) cells from the first and sec-
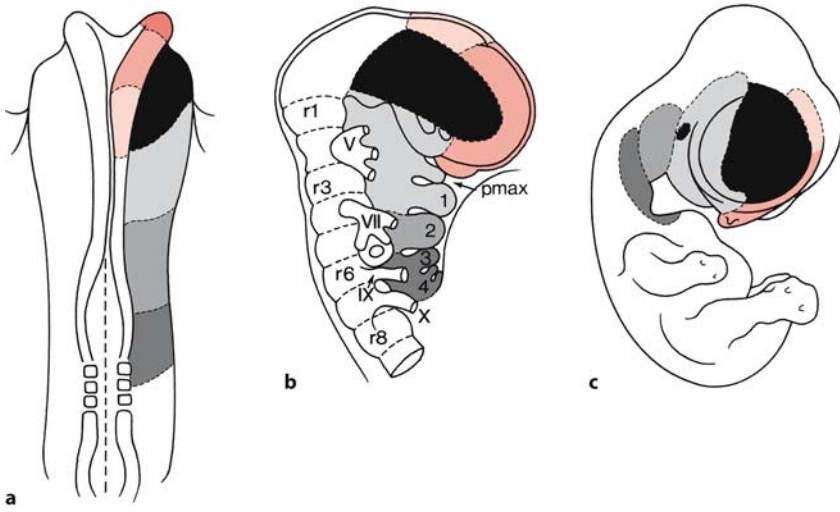
Fig. 5.2 Fate map of the ecto-dermal territories in the chick embryo from the three-somite stage (**a**) to the 8-day embryo (**c**). **b** The rhombomeres (*r1*, *r3*, *r6*, *r8*) and the cranial nerves sup-plying the pharyngeal arches (*1–4*). *pmax* maxillary promi-nence, *V* trigeminal nerve, *VII* facial nerve, *IX* glossopharyn-geal nerve, *X* vagus nerve. (After Couly and Le Douarin 1990)
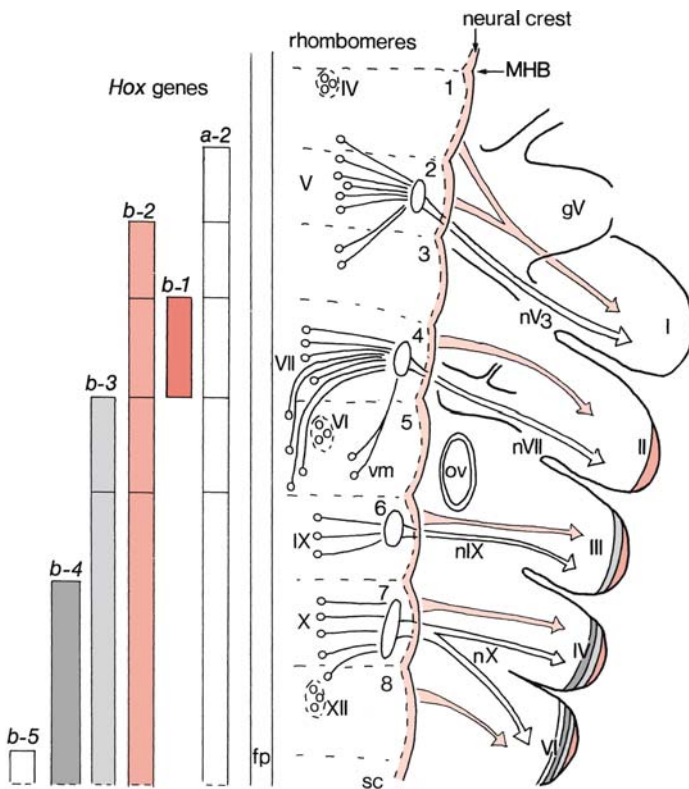
Fig. 5.3 Migratory pathways of cranial neural crest cells to the pharyngeal arches (*I–IV, VI*), and the segmented expression of *Hox* genes in the hindbrain and pharyngeal arches of the chick embryo. *fp* floor plate, *gV* trigem-inal ganglion, *MHB* midbrain–hindbrain boundary, *nV3* mandibular nerve, *nVII* facial nerve, *nIX* glossopharyngeal nerve, *nX* vagus nerve, *ov* otic vesicle, *sc* spinal cord, *vm* vis-ceromotor nucleus of facial nerve, *IV–VII, IX, X, XII* cranial nerve nuclei, *1–8* rhombomeres

ond rhombomeres migrate to the first pharyngeal (mandibular) arch, forming the mandibula, incus and malleus, and contributing to the trigeminal gan-glion; these cells also generate the facial skeleton; (2) cells from the fourth rhombomere invade the second pharyngeal arch and form the hyoid cartilage and the facial and vestibulo-acoustic ganglia; and (3) cells from the sixth rhombomere migrate into the third and fourth pharyngeal arches and pouches to form the thymus, the parathyroid and thyroid glands, and

the superior and jugular ganglia. Neural crest cells from the third and fifth rhombomeres enter the mi-grating streams of neural crest cells of the adjacent rhombomeres. Those that do not enter the various migratory streams will die (Graham et al. 1993, 1994; Sechrist et al. 1993). The apoptotic elimination of neural crest cells in the third and fifth rhombomeres involves the induction of high-level BMP expression in the neural crest, which stimulates expression of the homeobox gene *Msx2* (Graham et al. 1994). In mice, a

similar pattern of neural crest migration pathways has been found (Golding et al. 2000; Trainor et al. 1994, 2002; Trainor and Krumlauf 2000). The separate streams are kept apart by ephrins (Golding et al. 2000; Trainor and Krumlauf 2000).

Experimental studies using transposition of the avian neural folds (Noden 1978a, b, 1983a) led to the concept that the spatial organization of cranial structures is the result of a **prepatterning mechanism** before cells migrate from the neural crest. The ordered domains of *Hox* gene expression in the neural tube and neural crest were later assumed to be a molecular correlate of the prepatterning mechanism. Recently, however, plasticity of *Hox* gene expression has been observed in the hindbrain and postotic neural crest of chick, mouse and zebrafish embryos (Trainor and Krumlauf 2000; Gammill and Bronner-Fraser 2003; Santagati and Rijli 2003). Although the neural crest plays an important role in arch patterning, there are also patterning mechanisms that are established independently in the pharynx. Therefore, the formation of the pharyngeal apparatus must result from an integration between these patterning systems (Graham and Smith 2001; Graham et al. 2004). The neural crest most probably plays a more prominent role in patterning the rostral, preotic arches but a lesser role in the caudal, postotic arches. The development of the branchial arches involves retinoic acid dependent mechanisms. Neural crest cells migrating into branchial arches 3–6, however, are not the primary targets of retinoic acid, but pharyngeal epithelial cells are. Retinoic acid signalling is indispensable for the development of the pharyngeal epithelia of these branchial arches (Niederreither et al. 2003; Mark et al. 2004).

The **segmented expression** of *Hox* **genes** in the hindbrain is reflected in the neural crest cells which express a complement of *Hox* genes characteristic for their level of origin (Hunt et al. 1991; Capecchi 1997; Favier and Dollé 1997; Rijli et al. 1998; Trainor and Krumlauf 2000; Santagati and Rijli 2003; Fig. 5.3). Each rhombomere and pharyngeal arch is characterized by its own complement of *Hox* genes, its **Hox code**. In human embryos, Vieille-Grosjean et al. (1997) showed that the pattern of *HOX* gene expression in the rhombomeres and pharyngeal arches is similar to that observed in mice. The mouse *Hoxb2* gene, which is expressed in the hindbrain up to the boundary between the second and third rhombomeres, has an expression domain that extends caudally from the second pharyngeal arch (Fig. 5.3). *Hoxb3* is expressed as far rostrally as the rhombomere 4–rhombomere 5 boundary and from the third pharyngeal arch caudally. *Hox* genes are required for the normal morphogenesis of arch-derived skeletal elements. Mice with targeted disruptions in the paralogous genes *Hoxa3* and *Hoxd3*, which are expressed in the third and fourth arches,
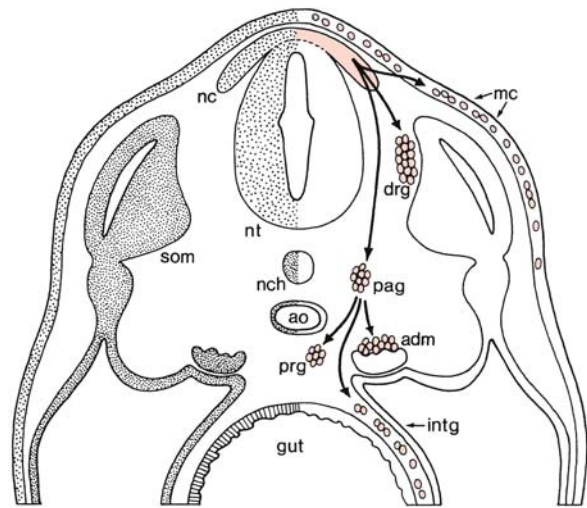
Fig. 5.4 Migratory pathways of chick trunk neural crest cells. *adm* adrenal medulla (chromaffin cells), *ao* aorta, *drg* dorsal root ganglion cells, *intg* intestinal ganglion cells, *mc* melanocytes, *nc* neural crest, *nch* notochord, *nt* neural tube, *pag* paravertebral ganglion cells, *prg* prevertebral ganglion cells, *som* somite

display defects in the laryngeal cartilages (Condie and Capecchi 1994). Mice that lack the *Hoxa2* gene show a transformation of second arch skeletal elements into components of the first arch (Gendron-Maguire et al. 1993; Rijli et al. 1993), suggesting that specification of crest cells to first arch components requires the downregulation of *Hoxa2*. *Hoxa3* knockouts show specific deletions or hypoplasias of structures derived from the third arch, resembling DiGeorge syndrome. They lack a thymus and parathyroid glands, have a reduced thyroid gland and show malformations of the laryngeal cartilages and muscles, and of the heart (Chisaka and Capecchi 1991; Manley and Capecchi 1995). Decreased embryonic retinoic acid synthesis also results in a DiGeorge syndrome phenotype in newborn mice (Vermot et al. 2003; Mark et al. 2004).

5.3.2 The Trunk Neural Crest

The **migratory pathways** of trunk neural crest cells are stereotyped and have been defined by various types of labelling experiments using grafts of Japanese quail crest into chick embryos, immunostaining for cell surface markers such as HNK-1 or fluorescent dyes such as DiI (Le Douarin and Kalcheim 1999) and, more recently, using time-lapse techniques (Kulesa and Fraser 1998, 2000). Two main directions of movement were found (Fig. 5.4): a **dorsolateral pathway** for crest cells that differentiate into

melanocytes, and a **ventral pathway** between neural tube and somites that gives rise to the dorsal root and sympathetic ganglia, to Schwann cells and to chromaffin cells for the adrenal gland. Crest cells pass only via the anterior part of the sclerotome. The migration path taken by trunk neural crest cells is guided by extracellular matrix molecules surrounding the neural tube. Fibronectin, laminin, tenascin and proteoglycans promote their migration (Newgeen et al. 1986), whereas ephrin proteins present in the posterior part of the sclerotome restrict neural crest migration to the anterior part of the sclerotome (O'Leary and Wilkinson 1999). In human embryos, the trunk neural crest participates at stage 12 in the formation of the pia mater, the spinal ganglia and the sympathetic trunk and ganglia. At later stages (13–14), they participate in the formation of the sheaths of the dorsal and ventral roots (O'Rahilly and Müller 1999).

5.4   Craniofacial Development

Prior to a discussion of neurocristopathies and other craniofacial malformations involving the CNS, the development of the face, the pharyngeal arches and the skull will be briefly discussed. Knowledge of the normal developmental events that shape the craniofacial region is necessary for understanding the changes that result in malformations of this region. The following description is largely based on Hinrichsen (1985, 1990) and Vermeij-Keers (1990).

5.4.1   Early Development of the Face

The early development of the forebrain and face is characterized by the formation and subsequent transformation of the so-called head folds (Vermeij-Keers 1990): first, the neural walls with the eye primordia, then the otic disc, the pharyngeal arches and, finally, the lens placode and the nasal placode. These transformations show a rather basic pattern of development, outgrowth of swellings forming and surrounding a cavity or groove that is subsequently closed partly or totally as a result of fusion of the swellings. The first slightly lordotic shape of the human embryo facilitates the initial fusion process of the neural walls transforming the neural groove into the neural tube (Chap. 4). Later, the lordosis changes into a kyphosis, enabling the transformation of the pharyngeal arches and the formation of the neck. The development of the **head** or **cephalic folds** in human and murine embryos is comparable (van Oostrom 1972; Vermeij-Keers 1990; Sulik 1996). In human embryos, the development of the head folds takes place during stages 8–9 (O'Rahilly 1973; O'Rahilly and

Müller 1981; Müller and O'Rahilly 1983), and in mouse embryos around 7.5 days *post coitum* (E7.3–E7.7), at which time the head folds are covered with columnar epithelium (van Oostrom 1972; Smits-van Prooije 1986). The border of the head folds is the transition of the surface ectoderm and the amnion. At stage 8, O'Rahilly and Müller (1981) described the head folds already as **neural folds**. They are the first rostral structures to appear in the embryo, and continue caudally as the neural plate. In four- to seven-somite mouse embryos, the head folds grow out rapidly, and a separation into lateral, thin (surface ectoderm of the head–neck region) and medial, thick (neuroectoderm of the forebrain) parts becomes evident. At the transition of both parts, the **cranial neural crest**, the neuroectoderm produces ectomesenchymal cells.

In amphibians, Adelmann (1936) showed that within the rostral neural plate a median population of cells, the **eye field**, segregates into two lateral primordia, the future optic vesicles. Experimental removal of the prechordal plate resulted in failure of separation of the midline structures of the rostral neural plate, leading to cyclopia as is also found in the most severe forms of HPE. The separation of the eye field is dependent upon interactions with the underlying mesoderm. The resulting degree of bilateralization of the eyes and forebrain has a profound effect on the subsequent morphogenesis of the face. In amphibian and chick embryos, the primordia of the eyes are found in the rostral neural plate, just caudal to the anterior neural ridge (Couly and Le Douarin 1988; Eagleson and Harris 1990; Eagleson et al. 1995; Fig. 2.8). Cyclopic animals such as the zebrafish mutant *cyclops* (Hatta et al. 1991, 1994; Schier 2001) have a defect in the development of the optic stalk and chiasm. Mice lacking the *Shh* gene demonstrate cyclopia and abnormal axial patterning (Chiang et al. 1996). Secreted factors such as Sonic hedgehog (SHH; Chiang et al. 1996) and FGF8 (Sun et al. 1999) play important roles before and during patterning of the neural plate (Chap. 9). In chick embryos, FGF8 and SHH signalling pathways are also required during early morphogenesis of the forebrain and frontonasal process (Schneider et al. 2001). The *Distal-less* related gene *Dlx5* is also required for normal development of the frontonasal process (Acampora et al. 1999). In human embryos, O'Rahilly and Müller (1999) suggested a single eye field at stage 8 that is situated directly above the prechordal plate. The prechordal plate suppresses the median part, so that bilateral optic primordia are formed, presumably still in stage 8 embryos. Instead of a single optic primordium, Vermeij-Keers et al. (1987) found evidence for the existence of bilateral optic primordia in human embryos.

During the transformation of the head folds into the cranial neural walls or neural folds, the **optic pri-**
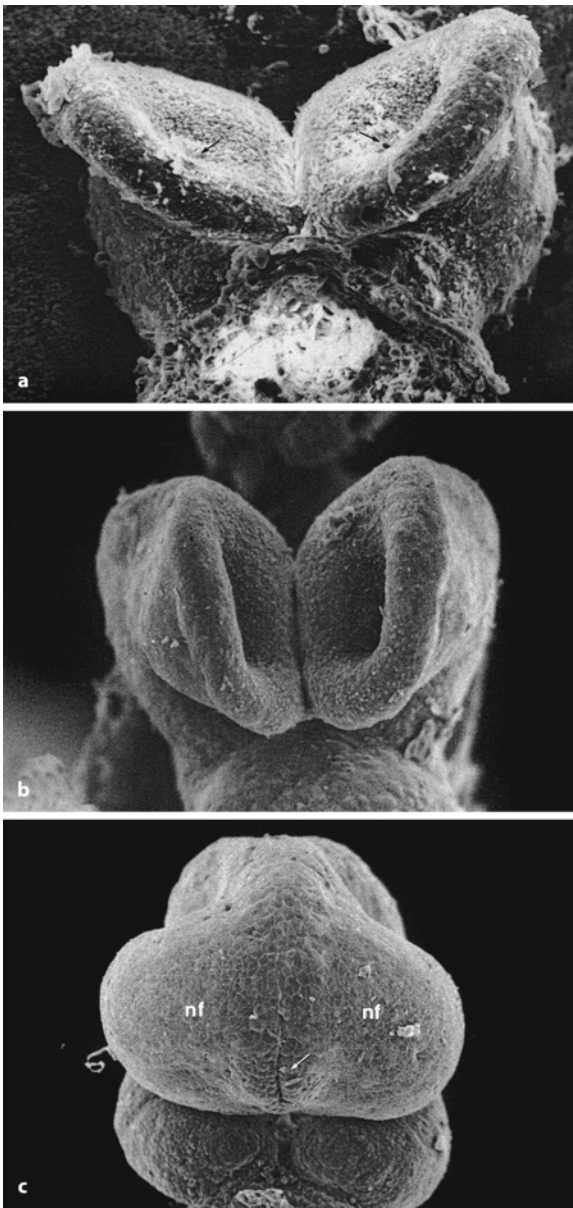
Fig. 5.5 Scanning electron micrographs of the developing face of mouse embryos in frontal view (the heart was removed in **a** and **c**): **a** E8.0 embryo, *arrows* indicate the optic sulci as bilateral grooves in the head folds; **b** E8.3 embryo, showing the prosencephalon with the evaginating optic vesicles; **c** E8.7 embryo in which the prosencephalon is fused except for the rostral neuropore (*arrow*) which separates the two nasal fields (*nf*)

in the surface ectoderm (three-somite mouse embryo: Verwoerd and van Oostrom 1979; man, stage 9: Müller and O'Rahilly 1983). Meanwhile, the caudal part of the neural folds transforms via the neural groove into the neural tube. The initial contact between the neural walls takes place in the caudal part of the rhombencephalic folds or in the upper cervical neural folds (mouse, five-somite embryo: Smits-van Prooije et al. 1985; man, stage 10: Müller and O'Rahilly 1985; Nakatsu et al. 2000). Rostrally, in the head other points of closure occur in the mouse embryo (Geelen and Langman 1977; Sakai 1989; Golden and Chernoff 1993) as well as in the human embryo (Müller and O'Rahilly 1985; Golden and Chernoff 1995; Nakatsu et al. 2000; Chap. 4). The final closure of the rostral neuropore is located between two areas of ectodermal, cuboidal or columnar epithelium, the **nasal fields** (the *Nasenfelder* of His 1885), in mice in 15-somite embryos (Vermeij-Keers et al. 1983; Fig. 5.5 c) and in human embryos at stage 11 (O'Rahilly and Gardner 1971; Müller and O'Rahilly 1986). This location corresponds with the presumptive internasal groove (Vermeij-Keers 1990).

In human embryos, the first visible appearance of the bilateral **optic primordia** is seen in eight-somite embryos (Bartelmez and Blount 1954; O'Rahilly 1966) as a thickened area of each neural wall in which a shallow sulcus is present. Subsequently, each **optic sulcus** widens and changes into an **optic vesicle** after closure of the neural walls. Within each nasal field two local thickenings develop, the **lens placode** (mouse: E8.8, 15–16-somite embryos; stage 13 human embryos: Müller and O'Rahilly 1988a) and the **nasal placode** (mouse: E9.8; stage 14 human embryos: Hinrichsen 1985; Müller and O'Rahilly 1988b). The lens placode is adjacent to the optic vesicle and is transformed into the lens vesicle, whereas the optic vesicle becomes the optic cup. In stage 15 human embryos, the lens vesicle detaches from the surface ectoderm (O'Rahilly 1966). The cavity of the optic vesicle communicates via the lumen of the short optic stalk with that of the forebrain. During the formation of the optic cup, its external layer grows out into the direction of the internal layer. This process is influenced by the lens placode (Chap. 9).

The mesodermal component of the head region is not only supplied by the cranial neural crest but also by cells deposited by the **surface ectoderm** or **neurogenic placodes**: the nasal placodes (Verwoerd and van Oostrom 1979), the acoustic or otic placode (Batten 1958) and the epibranchial placodes of the pharyngeal arches (Adelmann 1925; Graham and Begbie 2000). Neurogenic placodes are specialized regions of the cephalic embryonic ectoderm from which among others neuroblasts for the cranial sensory systems are generated. Neurons in cranial sensory ganglia have a dual origin from the neural crest as well as from pla-

mordia (optic sulci) develop within the neuroectoderm as two separate shallow grooves (Fig. 5.5 a, b; mouse, seven-somite embryo: Smits-van Prooije et al. 1985; man, stage 10: Müller and O'Rahilly 1985). Close to the margin of the neuroectoderm the **otic disc** develops as a concavity of columnar epithelium

codes (Noden 1991a, b; Le Douarin and Kalcheim 1999). The origin of neurogenic precursors and the pattern of expansion of the surrounding surface ectoderm were defined using the quail-chick chimera technique (D'Amico-Martel and Noden 1983; Couly and Le Douarin 1985, 1987, 1990).

The **otic disc** is the first ill-defined appearance of the developing ear (three- to five-somite mouse embryo: Verwoerd and van Oostrom 1979, Smits-van Prooije 1986; stage 9 human embryo: Müller and O'Rahilly 1983). At the end of stage 10, the otic disc becomes incorporated and transforms via the **otic pit** into the **otic vesicle** or **otic cyst** (O'Rahilly 1983; Müller and O'Rahilly 1985; Van De Water et al. 1988). Subsequently, the otic vesicle becomes separated from the surface ectoderm by apoptosis, and induces the condensation of its surrounding mesenchyme into the **otic capsule**. The otic vesicle forms the membranous labyrinth and the otic capsule the osseous labyrinth (Streeter 1906, 1918; Chap. 7). Placodal cells, given off from the walls of the otic vesicle, form the vestibular and possibly the cochlear (spiral) ganglia (O'Rahilly and Müller 2001). The **cavity** of the **middle ear** develops from the **tubotympanic recess** of the first pharyngeal pouch (Kanagasuntheram 1967). The origin of the auditory ossicles is not entirely clear (Anson et al. 1948, 1960; Hanson et al. 1962; O'Rahilly and Müller 2001). Presumably, the head of the malleus and the body and short crus of the incus arise from the first pharyngeal arch, whereas the handle of the malleus, possibly the long crus of the incus and the head and crura of the stapes develop from the second arch. The base of the stapes appears in the lateral wall of the otic capsule. The **external ear** arises from a series of small swellings, the **auricular hillocks**, around the first pharyngeal groove (Streeter 1922).

5.4.2   Development of the Pharyngeal Arches

A prominent feature of human embryos is the presence of a series of bulges on the lateral surface of the head and neck, the **pharyngeal arches** (Fig. 5.6). Each arch has an outer covering of ectoderm, an inner covering of endoderm and a mesenchymal core derived from the neural crest, and most likely the surface ectoderm and mesoderm. Between the arches, the ectoderm and endoderm are in close apposition and form the **pharyngeal membranes**. The externally situated **pharyngeal grooves** have internal counterparts, the **pharyngeal pouches**. During the process of outgrowth of the embryo, the wide lumen of the foregut is transformed into pharyngeal pouches by outgrowing swellings into this lumen. The first pharyngeal pouch develops in the early somite

Fig. 5.6 Scanning electron micrograph of the development of the human pharyngeal arches at stage 15 (from Jirásek 2001, with permission)

stages. Between the first pharyngeal pouch and its complementary pharyngeal groove the first pharyngeal membrane develops. Initially, the groove is shallow and wide but deepens subsequently during the outgrowth of the first pharyngeal arch. The different germ layers generate distinct components of the pharynx. The ectoderm produces the epidermis and the sensory neurons of the arch-associated ganglia (Verwoerd and van Oostrom 1979; D'Amico-Martel and Noden 1983; Couly and Le Douarin 1990), whereas the endoderm gives rise to the epithelial cells lining the pharynx and the endocrine glands that form from the pharyngeal pouches. The neural crest forms the connective and skeletal tissues (Noden 1983b; Couly et al. 1993), whereas the mesoderm forms the musculature and the endothelial cells of the arch arteries (Noden 1983b; Noden et al. 1991a, b; Couly et al. 1992; Trainor et al. 1994; Francis-West et al. 2003). The development of the craniofacial muscles is discussed in Chap. 7.

In human embryos, five **pharyngeal** or **visceral arches** (also known as branchial or aortic arches) develop successively. Four pairs are visible on the outside of the human embryo at 4 weeks and are separated from each other by three grooves (Fig. 5.6). More caudally, their arrangement is less clear-cut but it is customary to label a fifth and even a sixth arch. The first pharyngeal arch is the biggest, develops cranial to the heart primordium of the embryo and forms only the mandibular processes of the facial swellings (Vermeij-Keers et al. 1983). The maxillary prominence expands around the stomodeum below
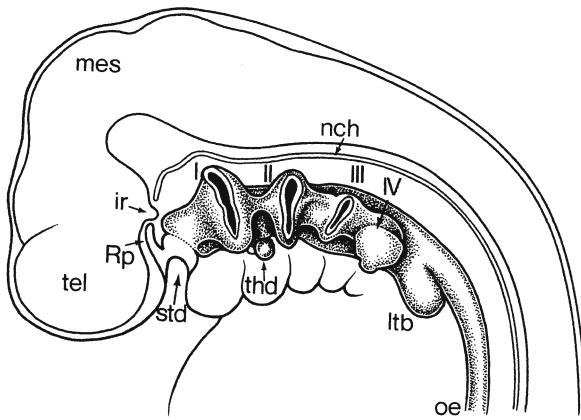
Fig. 5.7 Development of the pharyngeal pouches (*I–IV*) in a 4-week-old human embryo. The *stippled line* caudal to the stomodeal depression (*std*) indicates the position of the buccopharyngeal membrane before its resorption. *ir* infundibular recess, *ltb* laryngotracheal bud, *mes* mesencephalon, *nch* notochord, *oe* oesophagus, *Rp* Rathke's pouch, *tel* telencephalon, *thd* thyroid diverticulum. (After Weller 1933)

the optic vesicle and is unrelated to the pharynx (Vermeij-Keers 1990; Noden 1991 a, b). The mandibular processes keep their positions, grow out and form a groove in the midline between the two swellings. They actually do not fuse but merge because no epithelial plate is formed. The second arch grows caudally and laterally from the side of the second pharyngeal groove, covering the third and fourth arches. The third pharyngeal arch does the same with respect to the fourth. The retrobranchial ridge, incorporating the fifth arch, grows rostrally into the direction of the second arch (Starck 1975). Via contacts with the fourth and third arches this swelling adheres

and fuses with the second pharyngeal arch. Initially, slit-like cavities, remnants of the pharyngeal grooves, remain present between these contact places. Inside the embryo, the slit-like cavities are obliterated and ectodermal epithelial plates are formed at the contact places between the swellings. These plates disappear by apoptosis. The outgrowing pharyngeal arches and their subsequent shifting do not only cause transformations of the pharyngeal grooves but also of their corresponding pouches. The successive organs developing from the pharyngeal pouches (Fig. 5.7; Table 5.2), except for the first one, do not migrate to their definite position but attain their positions during the outgrowth and transformation of the pharyngeal arch system (Vermeij-Keers 1990). Later, they differentiate and form, among others, the thymus (derivative of the third pouch) and the superior (fourth pouch) and inferior (third pouch) parathyroid glands (Weller 1933; Norris 1937, 1938).

5.4.3 Further Development of the Face

The further development of the human face is usually described as a process of merging of five swellings or growth centres surrounding the stomodeum, termed processes or prominences: bilateral maxillary and mandibular processes, and the frontonasal prominence (His 1885; Hochstetter 1891; Bardeen 1910; Politzer 1952; Hinrichsen 1985, 1990; Sulik 1996; Fig. 5.8). The outgrowth of the maxillary processes is not coupled with changes in the shape of the first pharyngeal arch. Therefore, the **maxillary processes** represent *separate swellings* and do not form part of the mandibular arches (Vermeij-Keers 1972, 1990). The term frontonasal prominence is used differently. In some studies it is used as an equivalent for the *mittlere Stirnfortsatz* of His (1885), but in

Table 5.2 Derivatives of the pharyngeal arches, grooves, and pouches (after Sperber 2001)

Pharyngeal arch	Ectodermal groove	Endodermal pouch	Skeleton	Muscles	Nerves
First (mandibular)	External acoustic meatus; ear hillocks; pinna	Auditory tube; tympanic membrane	Meckel's cartilage: malleus, incus, mandibula template	Masticatory, tensor tympani, mylohyoid, anterior belly digastric	nV
Second (hyoid)	Disappears	Tonsillar fossa	Reichert's cartilage: stapes, styloid process; superior part body hyoid	Facial, stapedius, stylohyoid, posterior belly digastric	nVII
Third	Disappears	Inferior parathyroid glands; thymus	Inferior part body hyoid; greater cornu hyoid	Stylopharyngeus	nIX
Fourth	Disappears	Superior parathyroid glands	Thyroid and laryngeal cartilages	Pharyngeal constrictors, palate muscles, cricothyroid	nX
Sixth	Disappears	Ultimopharyngeal body	Cricoid, arytenoid, corniculate cartilages	Laryngeal, pharyngeal constrictors	nX
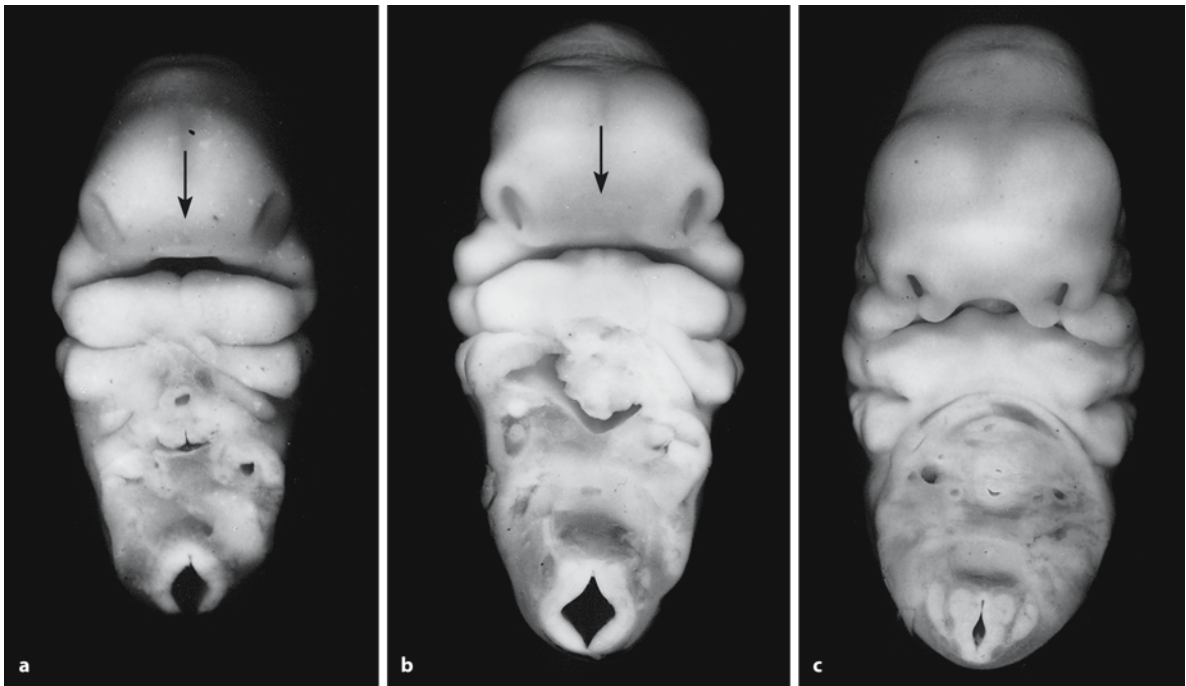
Fig. 5.8 Early development of the human face in Carnegie stages 14 (**a**), 16 (**b**) and 17 (**c**), shown in frontal views. *Arrows* indicate the interplacodal area. (From the Kyoto Collection of Human Embryos; courtesy Kohei Shiota)

many recent textbooks on human embryology the frontonasal prominence covers the nasal fields. In each nasal field a **nasal placode** develops, separated by the **interplacodal area** (Vermeij-Keers et al. 1983; Vermeij-Keers 1990). Around each nasal placode three facial swellings, defined as mesenchymal proliferations covered by ectoderm and separated by grooves, will grow out. At the medial side of each placode the medial nasal process and, laterally, the lateral nasal and maxillary processes develop. The nasal placodes, thereby, evaginate and are turned over by the outgrowth of the lateral nasal and maxillary processes (Vermeij-Keers 1972, 1990). The first contact between the facial swellings is between the maxillary and medial nasal processses. Later, the lateral nasal process will contact the medial process. At the site of contact between the three facial swellings the **epithelial plate** of **Hochstetter** (1891) or nasal fin develops. Cell death occurs before, during and after formation of the epithelial plate. Subsequently, the first disruption of the plate appears halfway, right above the frontally expanded stomodeum that is now called the primitive oral cavity. Cell death continues and gradually the fusion of the three swellings becomes obvious. By 7 weeks of development, the facial processes are no longer separable.

The three facial swellings transform the nasal placode via the nasal groove into the nasal tube, leading to the formation of the primary palate and primitive oral cavity. This transformation is not only accompanied by considerable morphogenetic changes in the developing facial region itself, but also by changes in the nasal lumen and the anlage of the **nasolacrimal duct**. This duct develops from a narrow nasolacrimal groove between the lateral nasal and maxillary prominences. The posterior part of each nasal tube is initially separated from the oral cavity by the oronasal or bucconasal membrane (part of Hochstetter's epithelial plate) at the end of the fifth week, which disintegrates by apoptosis at the end of the seventh week to form the primitive choanae. Failure of membrane disintegration leads to *choanal atresia*, one of the common congenital nasal anomalies (approximately 1 in 8,000 births; Sperber and Gorlin 1997; Sperber 2002). Both medial nasal processes grow out into the interplacodal area, separated by a small groove, the internasal groove (Vermeij-Keers et al. 1983). From these structures, the tip and dorsum of the nose, the nasal septum, the columella and the philtrum are formed. In early developmental stages the nose can be considered as two separate organs, which may develop asymmetrically. This asymmetrical development of the nose is expressed perfectly in the unilateral (in)complete clefting of the lip. Clefting of the upper lip and/or alveolus (*cheilognathoschisis*) is one of the most frequent of all congenital anomalies. The anomaly appears more common in males and has been ascribed to inadequate neural crest tis-
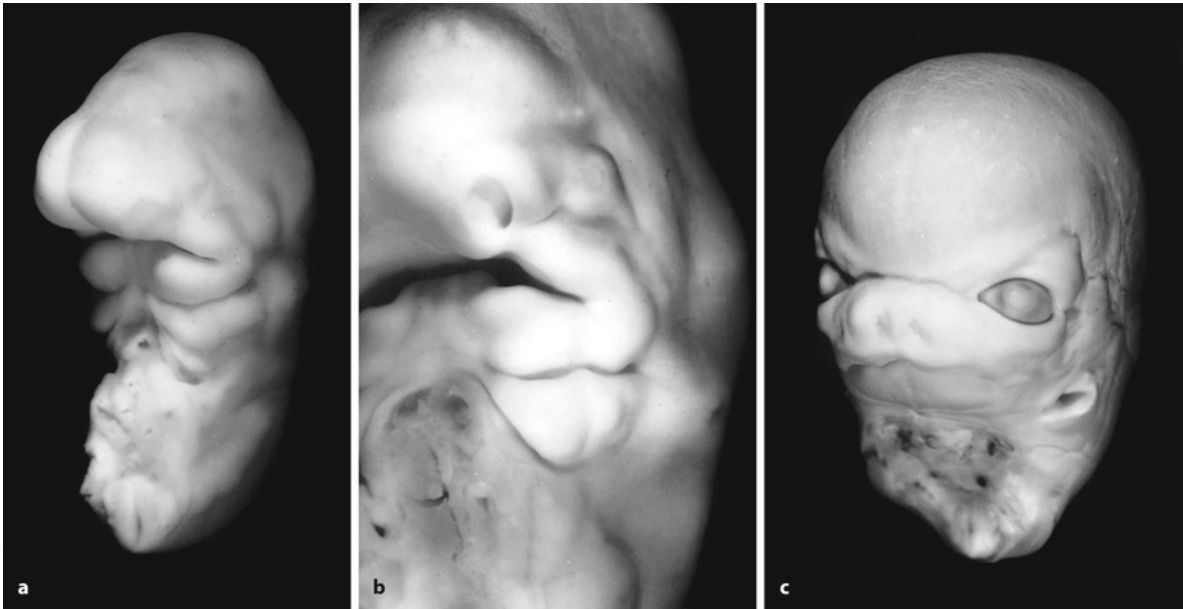
Fig. 5.9 Early development of the human face in Carnegie stages 15 (**a**), 16 (**b**) and 21 (**c**), shown in oblique–lateral views (from the Kyoto Collection of Human Embryos; courtesy Kohei Shiota)

sue migration to the lip/alveolus area. A role for the surface ectoderm including its placodes has also been suggested (Boshart et al. 2000). The degree of clefting varies enormously. Lip/alveolus clefts may coincidentally be associated with cleft palate, which is inherited separately (Wyszinski 2002). Complete or incomplete clefts of the palate concern a defect in the fusion process of the palatine processes with each other and/or the nasal septum and the primary palate. This fusion process of the secondary palate takes place in fronto-occipital direction after formation of the primary palate. Other nasal malformations may vary from a simple depression to complete separation of the nostrils (Sperber and Gorlin 1997; Sperber 2002), and various degrees of aplasia of the wings of the nose and atresia of the nasal cavities (Nishimura 1993).

Severe nasal clefting and abnormal embryonic apoptosis was found in *Alx3/Alx4* double-mutant mice (Beverdam et al. 2001). *Aristaless*-like homeobox genes form a distinct gene family, characterized by a paired-type homeobox and the presence of a small conserved C-terminal domain in the proteins encoded, known as aristaless or OAR domain (Meijlink et al. 1999). During embryogenesis, a subset of these genes, including *Alx3, Alx4, Prx1, Prx2* and *Cart1*, are expressed in neural-crest-derived mesenchyme of developing craniofacial regions and in the mesenchyme of developing limbs (Leussink et al. 1995; Qu et al. 1997; ten Berge et al. 1998a, b). Mice with *Alx4* mutations have strong preaxial polydactyly, and mild craniofacial abnormalities in the rostral

skull base and parietal and frontal bones (Qu et al. 1997). In double *Alx3/Alx4* mutants, most facial bones and many other neural-crest-derived skull elements are malformed, truncated or absent (Beverdam et al. 2001). *Cart1* mutant mice have major cranial defects including acrania and meroanencephaly (Zhao et al. 1996). These severe malformations are discussed in Chap. 4. In man, *ALX4* haploinsufficiency is associated with ossification defects in the parietal bones (Wu et al. 2000; Wuyts et al. 2000a; Mavrogiannis et al. 2001).

After **rupture** of the **buccopharyngeal membrane**, the **stomodeum** communicates with the foregut. The largest part of the primitive oral cavity is derived from the stomodeum. The roof of the stomodeum makes contact with the floor of the prosencephalon, just in front of the still intact buccopharyngeal membrane. After its rupture, initiated by apoptosis, the surrounding tissues grow out into the primitive oral cavity, leading to the formation of **Rathke's pouch** (Chap. 9). Subsequently, the walls of the pouch make contact and form a solid stalk that disappears through apoptosis. The primitive mouth opening becomes reduced by proliferating ectomesenchyme, fusing the maxillary and mandibular prominences to form the corners of the definitive mouth. Inadequate fusion results in *macrostomia* (unilateral or bilateral), whereas tension of the fusion process may produce *microstomia*. The lower lip is rarely defective, but if so, it is clefted in the midline (Oostrom et al. 1996).
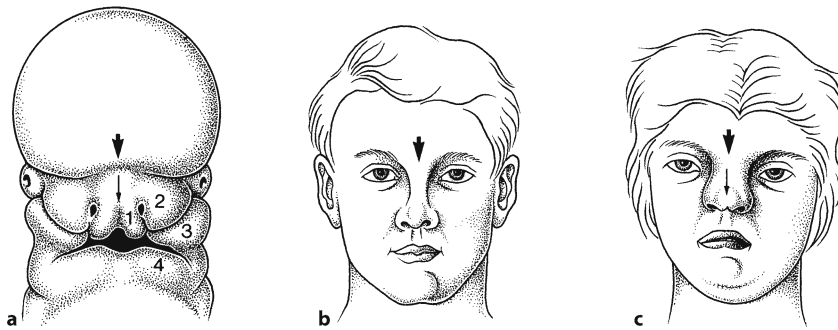
Fig. 5.10 The face of a stage 17/18 human embryo (**a**), an adult face (**b**) and the face of an adolescent with orbital hypertelorism (**c**), showing the relative positions of the eyes and nose components. The internasal groove is indicated by a *small arrow* and the interorbital groove by a *larger arrow*. The facial prominences are numbered: *1* medial nasal process; *2* lateral nasal process; *3* maxillary prominence; *4* mandibular prominence. (From Vermeij-Keers et al. 1984)

Apart from the nasolacrimal and internasal grooves, the interorbital groove develops gradually by outgrowth of the lateral nasal processes and the rapidly growing telencephalic vesicles (Vermeij-Keers 1972; Vermeij-Keers et al. 1984; Fig. 5.9). This groove runs from one eye cup to the other over the now-visible nasal root, and connects the future medial angles of the eyes. The distance between the eyes shows a relative decrease owing to a relative lag in transverse growth. Insufficient relative decrease of the midfacial part leads to *hypertelorism* (Fig. 5.10). The most common form of human hypertelorism is found in *frontonasal dysplasia* or median cleft syndrome (Gorlin et al. 2001). Mutations in the *GLI3* gene cause *Greig cephalopolysyndactyly syndrome*, a rare form of hypertelorism that is associated with polysyndactyly (Mo et al. 1997; Shin et al. 1999; Gorlin et al. 2001).

5.4.4   Development of the Skull

The development of the skull is influenced by environmental as well as genetic factors (Kjaer et al. 1999; Sperber 2001, 2002). Its development is greatly influenced by brain growth. Initial neurocranial development is dependent on the formation of a membrane surrounding the neural tube, whose prior existence is essential for normal development. Persistence of the cranial neural fold stage (*anencephaly*) results in *acalvaria* (Sperber et al. 1986). The surrounding membrane subdivides into an outer **ectomeninx** and an inner **endomeninx**. The ectomeninx produces an outer osteogenic layer, in which bone forms, and an inner dura mater. The endomeninx subdivides into the outer arachnoid and the inner pia mater. The skull consists of the neurocranium, surrounding the brain, and the facial and visceral skeleton, which form the bones of the face and the lower jaw and the

auditory ossicles, respectively. The skull develops from paraxial mesoderm (the sphenoid), the cranial neural crest, occipital somites (parts of the occipital bone) and, presumably, mesenchyme from the prechordal plate. The skull ossifies in part endochondrally and in part intramembranously.

The **neurocranium** comprises the vault of the skull, i.e. the calvaria, and the cranial base (Fig. 5.11). The **chondrocranium** forms the cartilaginous base of the embryonic and fetal skull, in which endochondral ossification occurs. It arises from mesenchymal condensations. At stage 17, the first cartilage of the neurocranium develops around the membranous labyrinth and forms the **otic capsule** (Müller and O'Rahilly 1980). The occipital component of the chondrocranium also arises very early, and corresponds to the first four sclerotomes (Müller and O'Rahilly 1994; O'Rahilly and Müller 2001). Other primary chondrogenic centres are the area of the future clivus (basi-occipital) and the sphenoid, presented by the hypophysial fossa, the dorsum sellae and the greater and lesser wings. The foramen magnum arises at the end of the embryonic period. Intramembranously ossified components of the neurocranium (**desmocranium**) are the bony plates of the skull such as the frontal and parietal bones. The **ossification centres** that develop in the membrane form the frontal, parietal, squamous temporal and squamous occipital bones. In general, each of these bones develops out of one bone centre. The parietal bone, however, develops from two bone centres that fuse with each other and subsequently function as one centre. The intervening areas form fibrous **sutures** and **fontanelles**, termed anterior, posterior, anterolateral and posterolateral. Defects of calvarial intramembranous ossification are recognized as *cranium bifidum* and *foramina parietalia permagna*, and are due to mutations in the *ALX4* and *MSX2* genes (Cargile et al. 2000; Wuyts et al. 2000 a, b). The

Fig. 5.11 Development of the skull base from above: **a** chondrocranium at the end of the embryonic period; **b** the calvaria at birth. *cl* clivus, *cp* (site of) cribriform plate, *d* dens, *eth* ethmoid, *fm* foramen magnum, *fr* frontal bone, *gw* greater wing of sphenoid, *hc* hypoglossal canal, *hf* hypophysial fossa, *iam* internal acoustic meatus, *jf* jugular foramen, *lw* lesser wing of sphenoid, *nc* nasal capsule, *nch* notochord, *ns* nasal septum, *oc* otic capsule, *occ* occipital bone, *opc* optic canal, *par* parietal bone, *pt* petrous part of temporal bone, *so* supra-occipital, *sph* sphenoid, *sqt* squamous part of temporal bone. (After O'Rahilly and Müller 1996)
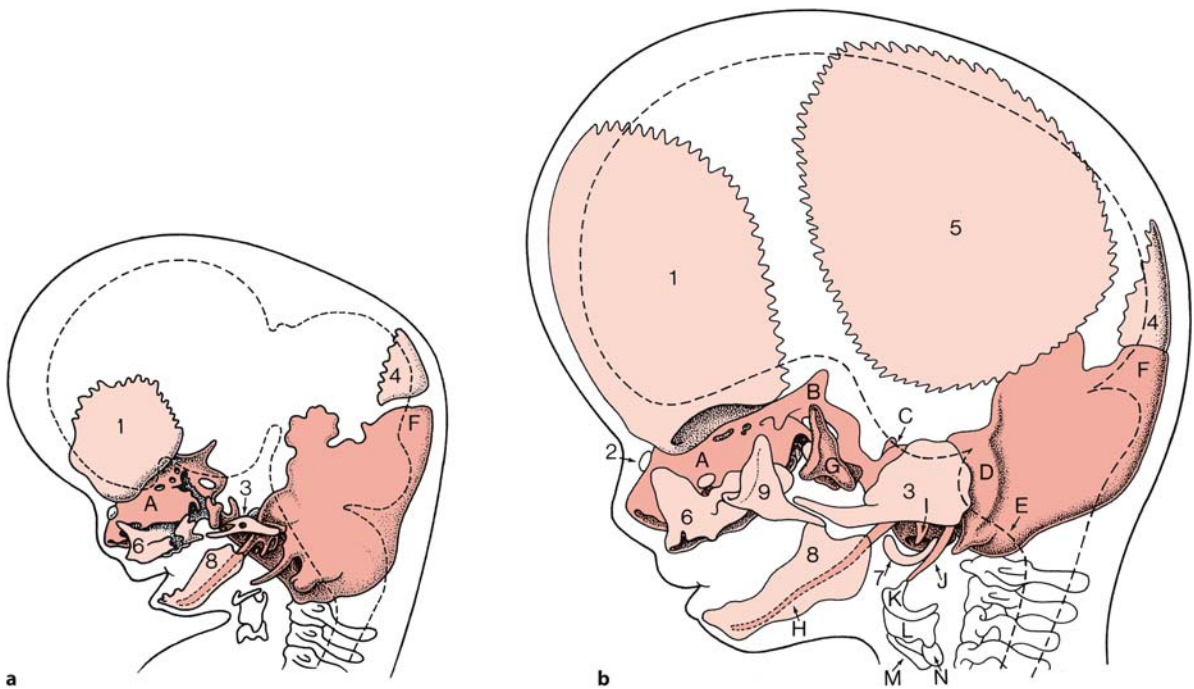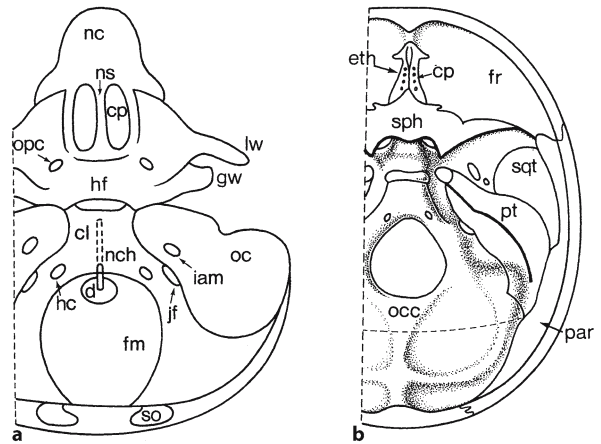
Fig. 5.12 Development of the human desmocranium: **a** a 40-mm embryo; **b** an 80-mm embryo (after *Gray's Anatomy* 1995). The contours of the CNS are indicated by broken lines. Chondral elements (*red*): *A* nasal capsule; *B* orbitosphenoid; *C* postsphenoid; *D* otic capsule; *E* exoccipital; *F* supra-occipital; *G* alisphenoid; *H* Meckel's cartilage; *I* cartilage of malleus; *J* styloid cartilage; *K* hyoid cartilage; *L* thyroid cartilage; *M* cricoid cartilage; *N* arytenoid cartilage. Dermal elements (*light red*): *1* frontal bone; *2* nasal bone; *3* squama of temporal bone; *4* squama of occipital bone; *5* parietal bone; *6* maxilla; *7* tympanic ring; *8* mandibula; *9* zygomatic bone

calvarial sutures are the sites at which the skull expands to accommodate itself to the enlarging brain. Growth takes place in the direction perpendicular to the sutures (Smith and Töndury 1978; Vermeij-Keers 1990; Mathijssen 2000; Opperman 2000). Most volume expansion of the skull occurs in utero and within the first 2 years of life, although most sutures do not ossify before adulthood (Sperber 2001, 2002).

The **facial skeleton** can be subdivided into an upper third, predominantly of neurocranial composition and incorporating the orbita, a middle portion incorporating the nasal complex, maxillae, zygomata and temporal bones, and a lower third, composed of the mandibula, i.e. part of the viscerocranium. The **facial skeleton** develops intramembranously (**desmocranium**) from ossification centres in the ectomesenchyme of the facial prominences (Fig. 5.12). During the third intrauterine month, centres appear for the nasal, lacrimal, palatine, zygomatic and premaxillary bones (Sandikcioglu et al. 1994; Kjaer et al.

1999). Mesenchymal precursors such as those for the auditory ossicles of the visceral skeleton are present early and later become cartilaginous. They are partly replaced by intramembranously ossified bone. The cartilage of the first pharyngeal arch (Meckel's cartilage) is largely replaced by the mandibula. The mandibula ossifies intramembranously from a single centre on each side (Mérida-Velasco et al. 1993). The facial skeleton is largely laid down in mesenchyme at the end of the embryonic period (O'Rahilly and Müller 2001).

Deficient mandibular development (*micrognathia*) is characteristic of the Pierre Robin sequence, and several syndromes such as cri du chat, Treacher Collins and Down syndromes. In the Pierre Robin sequence, the underdeveloped mandibula usually demonstrates catch-up growth in the child. In Treacher Collins syndrome, deficiency of the mandibula is maintained throughout growth (Sperber 2001). Hemifacial microsomia (Goldenhar syndrome) also becomes more severe with retarded growth. The *Prx1/Prx2* genes play a role in mandibular arch morphogenesis (ten Berge et al. 2001). *Agnathia* is found in the *otocephalies*, a series of malformations, ranging from milder forms in which derivatives of the skeletal and dental portions of the first arch are absent to the more severe form in which little more than external ears ('ear head') are apparent (Duhamel 1966; Vermeij-Keers 1990; Fig. 5.17).

Agnathia-otocephaly was described as a lethal developmental field complex, characterized by extreme hypoplasia or absence of the mandibula, astomia, aglossia and synotia (Bixler et al. 1985). It is most likely caused by a persistent buccopharyngeal membrane (Vermeij-Keers 1990) and is frequently associated with HPE (Pauli et al. 1983; Siebert et al. 1990; Cohen and Sulik 1992). In inbred strains of guinea pigs, otocephaly is probably a neural crest problem (Wright and Wagner 1934). In a substrain of C57B1 mice with a balanced chromosomal translocation, Juriloff and co-workers (1985) found that in the less severely affected embryos the first evidence of cell death was in the mesodermal cores of the first pharyngeal arch. The balanced translocation may hasten cell death. In more severe cases, cell death was also found in the mesoderm underlying the neural tube. *Otx2* heterozygous mouse mutants display otocephalic phenotypes, the severity of which is dependent on the genetic background of a C57BL/6 strain (Hide et al. 2002). *Otx2* is not only expressed in the forebrain and the mesencephalon (Acampora et al. 1995, 1998), but also in the cephalic mesenchyme, including mesencephalic neural crest cells which are distributed to the mandibula (Kimura etal. 1997). Therefore, *Otx2* heterozygous mutant defects relate primarily to *Otx2* function in the formation of mesencephalic neural crest (Kimura et al. 1997). Most

Otx2+/– mutant mice also display HPE (Matsuo et al. 1995), but a role for *OTX2* in human HPE has not been found so far.

5.5   Neurocristopathies

A number of craniofacial malformations have major neural crest involvement, and are usually referred to as *neurocristopathies* (Jones 1990; Johnston and Bronsky 1995, 2002). The concept neurocristopathy was introduced by Bolande (1974) to explain the developmental relationships among a number of dysgenetic, hamartomatous and neoplastic disorders, including pheochromocytoma, von Recklinghausen's neurofibromatosis, Hirschsprung's aganglionic megacolon and the multiple endocrine adenomatoses. A neurocristopathy was defined as a condition arising from aberrations in the early migration, growth and differentiation of neural crest cells. Subsequently, an increasing number of disorders such as retinoic acid syndrome (RAS), hemifacial microsomia, Treacher Collins syndrome, DiGeorge sequence, cleft lip and palate, frontonasal dysplasia and Waardenburg syndrome have been included into the neurocristopathies (Table 5.3). Recently, the idea that neural crest abnormalities underlie the pathogenesis of the DiGeorge sequence has been challenged (Sect. 5.5.4). The same holds for Treacher Collins syndrome (Sect. 5.5.3). Two syndromes specifically affect derivatives of the face and the first and second branchial arches. Treacher Collins syndrome affects bilaterally the ear, zygoma, lower eyelid and mandibula. Hemifacial microsomia shows unilateral malformation of nearly the same structures. Some patients who were exposed to thalidomide during a restricted period of development had a malformation similar to mandibulofacial dysostosis and hemifacial microsomia (Kleinsasser and Schlothane 1964; Jacobson and Granström 1997; Gorlin et al. 2001).

5.5.1   Retinoic Acid Syndrome

Retinoic acid syndrome (*RAS*) malformations first appeared shortly after the introduction of Accutane (13-*cis*-retinoic acid), a drug used for the treatment of severe cystic acne (Lammer et al. 1985). Although the retinoids (the normal biologically active retinoic acid and related compounds such as vitamin A, the dietary precursor of retinoic acid) had long been known to be potent teratogens, and the drug Accutane was not to be taken during pregnancy, in the USA many accidental exposures occurred, resulting in a surprisingly high incidence of very severe malformations involving craniofacial structures. Terato-

Table 5.3 Some neurocristopathies and related disorders (after Sperber and Gorlin 1997; Johnston and Bronsky 2002)

Syndrome	Ear abnor-malities	Facial bone malfor-mations	Cardio-vascular malfor-mations	Pharyngeal glands	Facial clefts	Other associated malforma-tions
Retinoic acid syndrome	Microtia/anotia; low-set ears; stenosis external meatus	Mandibular (micrognathia) and other deficiencies	Conotruncal defects	Thymus deficient or absent	Cleft palate (8%)	Brain (particularly cerebellum)
DiGeorge syndrome	Low-set ears	Variable maxillary and mandibular deficiencies (micrognathia)	Conotruncal defects	Thymus deficient or absent	Cleft lip and/or palate (10%)	Brain
Hemifacial microsomia	Microtia; accessory auricles; abnormal ear ossicles	Usually asymmetrical deficiencies of mandibula, squamous temporal and other bones	Conotruncal defects	No reported abnormalities	Cleft lip and/or palate (7–22%)	Eye, brain (in severe cases), vertebrae in oculo-auri-culo-verte-bral variant
Treacher Collins syndrome	Pinna anomalies; abnormal ear ossicles; hypoplasia or atresia external meatus	Symmetrical deficiencies or absence of zygoma, underdevelopment of posterior maxilla and mandibula	No increase in cardiovascular malformations	No reported abnormalities	Cleft palate (35%)	Rarely with limb defects, e.g. Nager syndrome

genic doses of retinoic acid given to mice at early stages of neurulation yielded craniofacial malformations that are strikingly similar to those in children with retinoic acid embryopathy (Webster et al. 1986; Willhite et al. 1986; Sulik et al. 1988; Sulik 1996; Morriss-Kay and Ward 1999). The defects observed in children with RAS include abnormalities of the external and middle ear, sometimes underdevelopment of the mandibula and cleft palate, facial nerve paralysis, cerebellar defects, outflow tract defects of the cardiovascular system, and defects of the thymus and parathyroid glands. Such defects are usually fatal within the first years of life (Johnston and Bronsky 1995, 2002). The unexpectedly severe nature of RAS malformations relates to the very poor ability of humans to clear retinoic acid metabolites (Webster et al. 1986). Teratogenic studies in mice (Goulding and Pratt 1986; Webster et al. 1986; Pratt et al. 1987) suggested that the timing of exposure for the most severe facial malformations coincided with the onset and period of migration of first and second arch crest cells (about day 21 in human embryos), whereas the sensitive period for cardiovascular malformations coincided with the migration of third and fourth arch crest cells (about day 23 in man).

Local retinoid signalling coordinates forebrain and facial morphogenesis by maintaining FGF8 and SHH expression (Schneider et al. 2001). FGF8 and SHH act as survival factors in the brain and facial primordia (Ahlgren and Bronner-Fraser 1999; Helms et al. 1997; Hu and Helms 1999). Experiments in chick embryos (Schneider et al. 2001) show that, in the absence of an intact retinoid signalling pathway, FGF8 and SHH expression is lost, cells fail to proliferate and undergo apoptosis, and the forebrain and frontonasal process cease their morphogenesis. These experiments demonstrate that there is a critical period in which morphogenesis of the forebrain and the frontonasal process is dependent upon retinoid signalling correlated with the timing of retinoic acid production in the frontonasal ectoderm. Forebrain and frontonasal process-derived tissue are sensitive to disruptions in retinoid signalling during early development, but later become insensitive.

5.5.2 Oculoauriculo-vertebral Spectrum

The predominant defects in the non-random association of anomalies known as the *oculoauriculo-vertebral spectrum* are problems in the morphogenesis of the face, the first and second pharyngeal arches, sometimes accompanied by vertebral anomalies (most commonly cervical hemivertebrae or hypoplasia of vertebrae) and/or ocular anomalies (Jones 1997; Gorlin et al. 2001). The association with epibulbar dermoid and vertebral anomaly is known as *Goldenhar syndrome* (Fig. 5.13 a–c), and the predominantly unilateral occurrence is known as *hemifacial microsomia*. The occurrence of various combinations and gradations of these anomalies, both unilateral and bilateral, with or without epibulbar dermoid and

vertebral anomaly, suggested that hemifacial microsomia and the Goldenhar syndrome may simply represent gradations in severity of a similar disorder of morphogenesis. Their frequency of occurrence is estimated to be 1 in 3,000 to 1 in 5,000, with a slight (3:2) male predominance (Jones 1997; Gorlin et al. 2001). CNS malformations include mental deficiency, hydrocephalus, Chiari type II malformation, occipital encephalocele, facial nerve paralysis, agenesis, hypoplasia and lipoma of the corpus callosum, and hypoplasia of the septum pellucidum (Aleksic et al. 1984; Jacobson and Granström 1997). Severe abnormalities of the pons were found in two infants with Goldenhar syndrome (Pane et al. 2004). The syndrome can be detected by prenatal ultrasound examination because of the frequent presence of a lipoma on the corpus callosum (Jeanty et al. 1991; Wong et al. 2001).

The main facial features of **hemifacial microsomia** include a small lower jaw, sometimes with an absent jaw joint, and a malformed or absent external ear with accessory tags and facial clefts (Cousley and Calvert 1997). Experimental studies in rodents suggest that this pattern of malformation is often caused by bleeding in the region of the stapedial artery, transitorily supplying the second pharyngeal arch (Poswillo 1973). Such events are usually sporadic, but genetic predisposition can occur, as shown by the *Hfm* (hemifacial microsomia) mouse, in which a chromosome 10 transgene integration is associated with a small ear or an asymmetric jaw in 25% of progeny heterozygous for the transgene (Naora et al. 1994). At E9.5, rupture of the dorsal vasculature of the second pharyngeal arch has been found in *Hfm+/–* mutants. In man, genetic linkage to chromosome 14q32 was reported in a family with hemifacial microsomia in which first-arch abnormalities segregate with unusually high penetrance (Kelberman et al. 2000).

5.5.3   Treacher Collins Syndrome

Treacher Collins syndrome (Treacher Collins 1900) or *mandibulofacial dysostosis* (Franceschetti and Klein 1949) is an autosomal dominant inherited syndrome that is localized on chromosome 5q32-33.1. Its incidence is approximately 1 in 50,000 live births and its clinical features include the following (Fig. 5.13 d–f): (1) abnormalities of the external ears, atresia of the external auditory canals and malformation of the middle ear ossicles, resulting in bilateral conductive hearing loss (Phelps et al. 1981); (2) lateral downward sloping of the palpebral fissures, frequently with colobomas of the lower eyelids and a paucity of lid lashes medial to the defect; (3) hypoplasia of the mandibula, maxilla and zygoma; and (4) cleft palate (Dixon et al. 1994; Marres et al. 1995; Jacobson and Granström 1997; Jones 1997; Gorlin et al. 2001; Marsh

and Dixon 2001). The Treacher Collins Syndrome Collaborative Group (1996) identified the molecular basis of this rare disorder by positional cloning. Although the causative gene (*TCOF1* after Treacher Collins–Franceschetti syndrome) has a somewhat variable penetrance, malformations are usually very consistent. *TCOF1* appears to be poorly conserved among mammals compared with other developmental genes. Mouse *Tcof1* shows only 62% amino acid identity with the human protein (Dixon et al. 1997). *Tcof1* is widely expressed, most highly at the edges of the neural folds (Dixon et al. 1997). Heterozygous mice show exencephaly associated with extensive apoptosis in the prefusion neural folds (Dixon et al. 2000). The Treacher Collins syndrome has not been associated with neural tube defects. This discrepancy may be due to species-specific differences between mice and man.

Studies on the pathogenesis of RAS defects in mice have also provided data relevant to Treacher Collins syndrome (Poswillo 1975; Wiley et al. 1983; Webster et al. 1986; Sulik et al. 1987; Osumi-Yamachita et al. 1992; Evrard et al. 2000). Treacher Collins syndrome may result from abnormal development of the first and second branchial arch ectodermal placodes rather than as a direct result of primary interference with neural crest cells. Initial abnormalities are largely limited to the distal part of the trigeminal ganglion, which corresponds to that part of the ganglion derived from the ectodermal placodes. Cell death interfered with the development of the surrounding crest cell mesenchyme, which gives rise to the zygoma and posterior parts of the maxillary prominence and mandibular arch, thereby producing defects similar to those in Treacher Collins syndrome; therefore, Treacher Collins syndrome most likely is not a neurocristopathy.

5.5.4   DiGeorge Sequence and Related Disorders

The **DiGeorge sequence** or **syndrome** (DiGeorge 1965) variably includes defects of development of the thymus, parathyroids and great vessels (Conley et al. 1979; Lammer and Opitz 1986; Jones 1997; Gorlin et al. 2001), i.e. tissues of the third and fourth branchial arches, and their associated pouches. Hypoplasia or aplasia of the thymus leads to a deficit in cellular immunity allowing severe infectious diseases. Hypoplasia to absence of the parathyroids results in severe hypocalcemia and seizures in early infancy. Common cardiovascular malformations are aortic arch anomalies, including right aortic arch, interrupted aorta, conotruncal anomalies such as truncus arteriosus and ventricular septal defect, patent ductus arteriosus and tetralogy of Fallot. Specific to partial mono-

Fig. 5.13 Craniofacial dysmorphology syndromes in neuro-cristopathies: **a**–**c** Goldenhar syndrome in a 2-year old boy, showing bilateral microtia (*left* lobar type; *right* concha type), conductive hearing loss, left facial nerve paresis, left-sided mandibular hypoplasia, craniosynostosis, defects of vertebrae and ribs and various heart defects: ventricular septal defect, atrial septal defect, pulmonary stenosis and patent ductus ar-teriosus; **d**–**f**, Treacher Collins syndrome in a 10-year-old boy with the following bilateral craniofacial abnormalities: micro-tia, agenesis of external acoustic meatus, conductive deaf-ness, dysplasia of os petrosum, aplasia of zygoma, hypoplasia and crowding of maxilla and mandibula, hypoplasia of mas-toid and maxillary sinus, and colobomata of lower eyelids. (Courtesy Michiel Vaandrager, Rotterdam)

somy 22q are lateral displacement of inner canthi with short palpebral fissures, short philtrum, microg-nathia and ear anomalies. The DiGeorge sequence is aetiologically heterogeneous. It has been associated with prenatal exposure to alcohol and Accutane, and a variety of chromosome abnormalities (Gorlin et al. 2001; Johnston and Bronsky 2002). The majority of cases, however, result from partial monosomy of the proximal arm of chromosome 22 owing to a mi-crodeletion of 22q11.2 (Fig. 5.14), detectable by mol-ecular or fluorescence in situ hybridization analysis (Lindsay 2001). Therefore, the DiGeorge sequence and related malformations with chromosome 22 deletions such as the velocardiofacial or Shprintzen syndrome (Shprintzen et al. 1978; Goldberg et al.

1993; also known as Sedlacková syndrome: Sed-lacková 1967) and conotruncal anomaly face syn-drome are combined with the chromosome 22 dele-tion (*del22q11*) syndrome (Driscoll et al. 1992a, b; Emanuel et al. 2001; Lindsay 2001). The velocardio-facial syndrome is characterized by hypoplasia or a cleft of the secondary palate, cardiac defects, a typical face, microcephaly and hearing and learning disabil-ities. The occurrence of the *del22q11* syndrome is es-timated as 1 in 4,000 live births (Scambler 1994, 2000; Lindsay 2001). The symptoms of *del22q11* syndrome are diverse. Distinct features can show variable ex-pressivity and incomplete penetrance. Depending on the key symptoms, two phenotypes may be distin-guished (Ryan et al. 1997; Scambler 2000; Lindsay

Fig. 5.14 a–c Craniofacial dysmorphology in a 10-year-old girl with a 22q11 deletion. At birth, the patient showed a flat occiput, short neck, wide but closed palate, tetralogy of Fallot and slight dysmorphic toes. In 1994, a velopharyngeal insufficiency was found, followed by DNA analysis, and the diagnosis of a 22q11 deletion in 1996. Apart from bilateral hearing loss, due to chronic inflammation of the middle ears, no other abnormalities of the derivatives of the pharyngeal arches were found. A general developmental delay of the patient required special education. (Courtesy Jeannette M. Hoogeboom, Rotterdam)

2001). The 'pharyngeal' phenotype encompasses the most characteristic features of *del22q11* syndrome, including congenital cardiovascular defects, craniofacial anomalies and aplasia or hypoplasia of the thymus and parathyroids. The 'neurobehavioural' phenotype becomes manifest in early childhood as learning difficulties, cognitive defects and attention-deficit disorder. In adolescence and adulthood, some patients develop various psychiatric disorders, including schizophrenia, schizoaffective and bipolar disorders. The basis of the neurobehavioural phenotype is unknown. All patients with the *del22q11* syndrome manifest at least some components of the pharyngeal and neurobehavioural phenotypes with varying degrees of severity. In contrast to the clinical heterogeneity of this syndrome, the *del22q11* genetic lesion is remarkably homogeneous in affected individuals. Approximately 90 % of patients have a typical deleted region of some 3 Mb, which encompasses an estimated 30 genes, whereas about 8 % of patients have a smaller deletion of some 1.5 Mb, encompassing 24 genes (Lindsay 2001).

Treatment of pregnant mice with ethanol at the time of migration of the first and second arch crest cells leads to massive cell death, resulting in malformations very similar to those of the DiGeorge sequence (Daft et al. 1986; Sulik et al. 1986). This suggested that the DiGeorge sequence may be secondary to an abnormality in the neural crest (Scambler 1994). A number of gene knockouts produce the DiGeorge sequence. *Hoxa3* knockout mice show some resemblance to the DiGeorge sequence (Chisaka and Capecchi 1991; Manley and Capecchi 1995; Capecchi 1997). They lack a thymus and parathyroid glands, have a reduced thyroid and show malformations of the laryngeal cartilages and muscles, and of the heart. Lindsay and co-workers (Lindsay et al. 1999; Lindsay and Baldini 2001) developed a mouse model heterozygous for the 22q11.2 deletion. Neural crest migration into the pharyngeal arches appeared to be normal but there was severe underdevelopment of the fourth arch aortic vessels in all of the embryos studied. The gene content of the human 22q11 region was found to be highly conserved in a region of mouse chromosome 16. The first mouse deletion generated, *Df1* (Lindsay et al. 1999), encompassing mouse homologues of 18 out of the 24 genes that are deleted in patients with the 1.5-Mb deletion, led to cardiovascular defects similar to those in patients. The T-box transcription factor *Tbx1* plays a crucial role in the fourth arch abnormality in mice (Lindsay 2001; Lindsay et al. 2001). *Tbx1*-null mice die at birth and have a persistent truncus arteriosus, a hypoplastic pharynx, lack a thymus and parathyroids and have ear, jaw and vertebral anomalies. The embryological basis of these abnormalities is maldevelopment of the pharyngeal arches and arch arteries 2–6, and of the pharyngeal pouches 2–4 (Lindsay et al. 2001). The severity and extent of the embryological lesion indicate that *Tbx1* may be required for the segmentation

Fig. 5.15 a, b Waardenburg syndrome in a 32-year-old male patient with a 558-559delCA mutation in exon 4 of the *PAX3* gene, compatible with Waardenburg type 1. The patient shows typical craniofacial dysmorphology, early temporal greying, has severe bilateral congenital hearing loss, mental retardation and no verbal communication. (Courtesy Jeannette M. Hoogeboom, Rotterdam)

of the pharyngeal endoderm, an event that initiates the development of the entire pharyngeal apparatus (Lindsay 2001). Chordin secreted by the mesendoderm is required for the correct expression of *Tbx1* and other transcription factors involved in the development of the pharyngeal region (Bachiller et al. 2003). Chordin mutant mice either die early during development or die perinatally, showing an extensive array of malformations that encompass most features of DiGeorge syndrome and velocardiofacial syndrome in humans. FGF8 is also required for pharyngeal arch and cardiovascular development in mice (Abu-Issa et al. 2002; Frank et al. 2002). *Fgf8* mutants resemble *Tbx1*–/– mouse embryos, probably owing to a common signalling pathway (Vitelli et al. 2002).

The hypothesis that neural crest abnormalities underlie the pathogenesis of the DiGeorge sequence seems unlikely since pharyngeal patterning is not affected in chick embryos in which the neural crest has been ablated (Bockman et al. 1989; Veitch et al. 1999). Moreover, *Tbx1* is not expressed in the neural-crest-derived mesenchyme of the pharyngeal arches. Neural crest cells may, however, play a secondary role in the disorder as targets of *Tbx1*-driven signalling (Lindsay 2001). Recently, Yagi et al. (2003) showed that a *TBX1* mutation is responsible for five major phenotypes in *del22q11* syndrome. In view of these data, the DiGeorge sequence should not be viewed any longer as a neurocristopathy.

5.5.5 Waardenburg Syndrome

The term *Waardenburg syndrome*, originally described by Waardenburg (1951), is used for a heterogeneous set of auditory–pigmentary syndromes, the primary cause of which is a patchy lack of melanocytes in the hair, eyes, skin and stria vascularis (Read 2001; Spritz et al. 2003). Four subtypes can be distinguished: (1) type 1 with dystopia canthorum, caused by mutations in the *PAX3* gene (Fig. 5.15); (2) type 2 without dystopia is heterogeneous, some cases are due to changes in the *MITF* and *SLUG* genes; (3) the rare type 3, resembling type 1 but with additional contractures or hypoplasia of the upper-limb joints and muscles, also results from *PAX3* mutations; and (4) type 4 with Hirschsprung's disease, again heterogeneous and due to mutations in the *EDN3*, *EDNRB* and *SOX10* genes. Most forms are inherited as autosomal dominant traits. The hearing loss in all types is congenital, sensorineural and non-progressive (Chap. 7). Waardenburg syndrome types 1, 3, and 4 are neurocristopathies, affecting more than one neural crest derivative. Type 2 appears to be melanocyte-specific. Auditory–pigmentary syndromes and mouse models are discussed further in Chap. 7.

5.6 Holoprosencephaly

The *holoprosencephalies* encompass a range of phenotypes that vary in severity and involve malformations of the brain and upper face among the midline (DeMyer et al. 1963, 1964; Cohen 1989a, b; Cohen and Sulik 1992; Norman et al. 1995; Golden 1998; Muenke and Beachy 2001; Cohen and Shiota 2002). HPE is aetiologically extremely heterogeneous. Its formation may depend on the interaction of both genetic and environmental factors. Specific teratogens such as maternal diabetes increase the risk for HPE 200-fold (Norman et al. 1995; Cohen and Shiota 2002). About 1–2% of newborn infants of diabetic mothers develop HPE. Numerous other teratogens are known to cause HPE in various animal models (Cohen and

Table 5.4 Aetiology of human holoprosencephaly (after Cohen and Sulik 1992; Norman et al. 1995; Blaas et al. 2002; Cohen and Shiota 2002)

Causes	Examples	Notes
Chromosomal abnormalities	Most frequently involved: Chromosomes 13 and 18 Trisomy 13 Trisomy 18	In 70% HPE (Taylor 1968)
	Numerous deletions, duplications, and ring chromosomes	Examples of deletions and duplications (in order of frequency): del(13)(q22), del(18p), del(7)(q36), dup(3)(p24-pter), del(2)(p21), del(21)(q22.3); for further data see Schinzel (1983), Cohen and Sulik (1992) and Norman et al. (1995)
Identified genes	HPE3 (7q36): *SHH* HPE2 (2p21): *SIX3* HPE5 (13q32): *ZIC2* HPE4 (18p): *TGIF* *Patched/PTCH* *GLI2*	See text for explanation
	DCHR7	Smith–Lemli–Opitz syndrome (Kelley and Hennekam 2001)
Teratogens	Diabetic embryopathy	HPE in 1–2% of newborn infants of diabetic mothers
	Ethyl alcohol (alcohol abuse)	In 28 autopsies of patients with HPE, Jellinger et al. (1981) found 1 case in which the mother had a history of alcohol abuse; Ronen and Andrews (1991) found HPE in 3 such cases
	Retinoic acid	HPE has been noted (Lammer et al. 1985; Rosa et al. 1994)
Syndromes with HPE	Meckel syndrome	May have HPE with median or lateral cleft lip (Hsia et al. 1971)
	Pallister–Hall syndrome	Congenital hypothalamic hamartoblastoma hypopituitarism, other anomalies including HPE (Hall et al. 1980), due to mutations in *GLI3* (Kang et al. 1997)
	Lambotte syndrome	Microcephaly, mental retardation, ocular hypotelorism (Verloes et al. 1990)
	Velocardiofacial syndrome	HPE in 1 out of 61 cases (Wraith et al. 1985)
	Aicardi syndrome	Flexion spasms, mental retardation and agenesis of corpus callosum; arhinencephaly in several instances; rarely HPE (Sato et al. 1987; Donnenfeld et al. 1989)
Associations	Anencephaly	Cases with holoprosencephalic facies (Lemire et al. 1981)
	Frontonasal dysplasia	Median cleft syndrome (DeMyer 1967; Sedano et al. 1970)
	Agnathia-otocephaly	Cyclopia/HPE may occur (Pauli et al. 1983; Siebert et al. 1990)

HPE holoprosencephaly

Sulik 1992; Cohen and Shiota 2002). The incidence of HPE in live-born children with normal chromosomes has been estimated to be 0.48–0.88 per 10,000. In contrast, the rate among human abortuses was estimated at 40 per 10,000, indicating a very high rate of embryonic and fetal loss (Matsunaga and Shiota 1977; Shiota 1993). In a large epidemiologic study in a Californian population, Croen et al. (1996) observed an overall prevalence of 1.2 per 10,000 live births and fetal deaths (121 HPE cases in 1,035,386 live births/fetal death deliveries), whereas the prevalence for live births was 0.88 per 10,000. In another perinatal study from Scotland, Whiteford and Tolmie (1996) found 50 HPE cases in 694,950 live births and still births (a prevalence of 0.7 per 10,000).

Although the majority of HPE cases are sporadic, familial HPE has been described in pedigrees, suggesting autosomal dominant, autosomal recessive, and possibly X-linked inheritance. The clinical variability can be striking even within a single pedigree. In pedigrees with clinically unaffected parents and multiple affected siblings autosomal recessive inheritance is suggested. Since abnormal HPE genes are not fully penetrant and germline mosaicism may happen, some of these cases may actually be autosomal dominant (Nanni et al. 1999). The causes of HPE in man are summarized in Table 5.4. Certain chromosomes, chromosome 13 in particular, display recurrent involvement in HPE. HPE may be present in as many as 70% of trisomy 13 cases (Taylor 1968; Cohen and Sulik 1992; Norman et al. 1995). Cytogenetically verified chromosome abnormalities in perinatal studies range from 34% in Scotland (Whiteford and Tolmie 1996) to 37% in California (Croen et al. 1996). A similar frequency was observed in prenatally diagnosed HPE (Berry et al. 1990; Blaas et al. 2002). Based on non-random cytogenetic rearrangements, genetic studies of HPE have revealed at least 12 putative loci (HPE1-12) on 11 different chromosomes, which may contain genes that play a role in the pathogenesis of

Fig. 5.16 Holoprosencephaly, main types of facial malformation: **a** cyclopia; **b**, **c** single median eye with various degrees of doubling of ocular structures; **d** ethmocephaly; **e** cebocephaly; **f** median cleft lip with arhinencephaly (after Duhamel 1966)
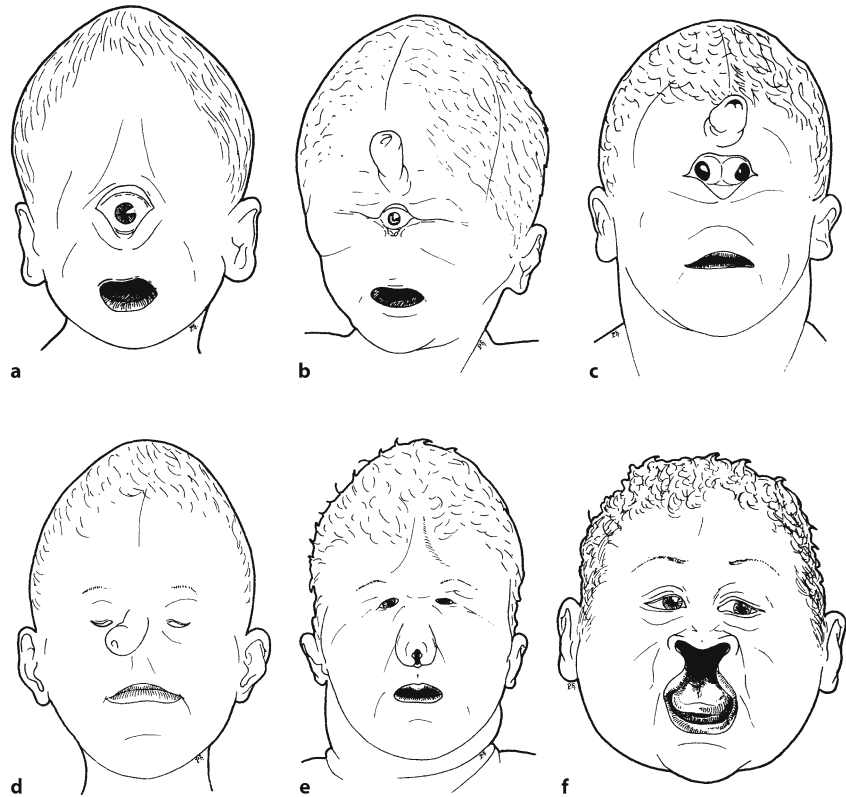
HPE (Roessler and Muenke 1998; Nanni et al. 2000). Identifiable genetic causes account for 15–20% of all cases of HPE. Several HPE genes have been identified: *SHH* (also known as HPE3: Belloni et al. 1996; Roessler et al. 1996; Nanni et al. 1999), *SIX3* (HPE2: Wallis et al. 1999), *ZIC2* (HPE5: Brown et al. 1998), *TGIF* (HPE4: Gripp et al. 2000), *Patched/PTCH* (Ming and Muenke 1998), *GLI2* (Roessler et al. 2003) and *DHCR7* (Kelley et al. 1996). Of these defective genes in human HPE, three exhibit a ventrodorsal gradient of expression (*SHH*, *SIX3* and *TGIF*) and two a dorsoventral gradient (*GLI2* and *ZIC2*). Patients with HPE3 (*SHH*) and HPE2 (*SIX3*) mutations exhibit the HPE spectrum with major facial malformations ((Wallis et al. 1999), whereas *ZIC2* mutations show only minimal facial malformations, such as slanting of the frontal bones as a result of microcephaly (Brown et al. 1998). Heterozygous carriers for mutations in either *SHH* or *SIX3* can appear phenotypically normal, whereas other heterozygous mutation carriers within the same family may be severely affected (Nanni et al. 1999). Nanni and co-workers identified three HPE patients with an *SHH* mutation and an additional *ZIC2* or *TGIF* mutation. The first patient exhibited microcephaly due to semilobar HPE but with normal midfacial dimensions and, therefore, this corresponds best with the *ZIC2* phenotype. The other two cases showed major craniofacial abnormalities matching the *SHH* HPE spectrum. HPE may occur in

a large number of syndromes and associations (Siebert et al. 1990; Cohen and Sulik 1992; Norman et al. 1995; see Table 5.4 for some examples). Syndromal (not chromosomal) conditions with HPE include such diverse disorders as Meckel–Gruber, Pallister–Hall, Smith–Lemli–Opitz and Aicardi syndromes. The *Smith–Lemli–Opitz syndrome* is due to a deficiency in the final step of cholesterol biosynthesis (Tint et al. 1994; Kelley et al. 1996; Kelley and Hennekam 2001; Chap. 3).

The **brain malformations** in HPE will be discussed in Chap. 9. In brief, forebrain malformations range from the *alobar*, *complete form* with one single ventricle, undivided thalami and corpora striata, and absence of the olfactory bulbs and corpus callosum, to the *semilobar*, *incomplete form*, in which hypoplastic cerebral lobes with an interhemispheric posterior fissure and a hypoplastic corpus callosum may be present, to the *lobar type*, in which a distinct interhemispheric fissure is present with some midline continuity and the olfactory bulbs may vary from normal to absent. HPE can be detected prenatally by ultrasound (Kurtz et al. 1980; Blaas et al. 2000, 2002; Clinical Case 5.1). In the Californian study (Croen et al. 1996), 46% of HPEs were of the alobar type, 20% semilobar and 5% lobar.

The **facial anomalies** in HPE are usually categorized into four main types (DeMyer et al. 1964; Cohen and Sulik 1992; Figs. 5.16, 5.17): (1) cyclopia with a

Fig. 5.17 Holoprosencephaly, spectrum of craniofacial malformations. **a** Alobar or complete holoprosencephaly was diagnosed by ultrasound at 22 weeks of gestation, after which pregnancy was terminated at 24 weeks. At autopsy, the female fetus showed agenesis of both eyes and orbits, arhinia and microstomia. **b** Frontal view of a cyclopic face of a female fetus of approximately 35 weeks of gestation. The fetus had a single eye in a single orbit and fused optic nerves, arhinia without proboscis, and agnathia with astomia and synotia. The brain showed a complete holoprosencephaly. **c** Frontal view of a male fetus of 32 weeks of gestation with synorbitism, arhinia with proboscis, agnathia with astomia and synotia. The brain showed a semilobar or incomplete holoprosencephaly with a dorsal sac (Chap. 9). **d** Frontal view of a female fetus of 32 weeks of gestation with hypotelorism, arhinia with a septated proboscis, agnathia with astomia and synotia. The brain showed an incomplete holoprosencephaly. **e** A hypoteloric male fetus of 34 weeks of gestation with a flat nose, cleft palate and agenesis of the premaxillae, the prolabium and the nasal septum. An incomplete holoprosencephaly was found. **f** A case of alobar, complete holoprosencephaly with a normal face. (**a** Courtesy Annemarie Potters, Deventer; **b**–**e** from the collection of the Museum of Anatomy, University of Leiden; courtesy Christl Vermeij-Keers; **f** courtesy Raoul Hennekam, Amsterdam)

single eye or various degrees of doubling of the eye anlage, with or without a proboscis; (2) ethmocephaly with ocular hypotelorism and proboscis located between the eyes; (3) cebocephaly with ocular hypotelorism and a single-nostril nose; and (4) median cleft lip and palate (premaxillary agenesis) and ocular hypotelorism. Less severe facial dysmorphism, microsigns such as a single central incisor and/or ocular hypotelorism, and HPE without facial malformations are also found (DeMyer et al. 1964; Cohen and Sulik 1992; Brown et al. 1998). Five out of the six cases shown in Fig. 5.17 exhibited major facial

malformations, varying from agenesis of the eyes to hypotelorism and were holoprosencephalic and, as a consequence, microcephalic. In these cases the developing forebrain is too narrow, indicating a lack of outgrowth of the ventral neurectoderm during early embryogenesis (Müller and O'Rahilly 1989). As a result the interplacodal area (the area between the nasal placodes) is either absent (resulting in agenesis of the eyes and orbits, cyclopia, synophthalmia, synorbitism, hypotelorism without a nasal septum) or too narrow (hypotelorism with a nasal septum). During normal embryonic development, both medial nasal processes grow out from the interplacodal area, and give rise to the premaxilla, the prolabium, the vomer and other parts of the nasal septum. The mesectoderm of this area originates from the cranial neural crest and surface ectodermal placodes (Smits-van Prooije et al. 1988).

HPE with major facial malformations may be the result of insufficient outgrowth of the prosencephalic neuroectoderm and as a consequence insufficient EMT in presomite stages (Vermeij-Keers 1990). The outcome is an abnormally narrow prosencephalon, particularly along its ventral midline, causing agenesis or non-separation of the eye vesicles, non-separation of the thalami and lack of proper outgrowth of the telencephalic hemispheres, leading to agenesis of the olfactory bulbs and the corpus callosum. This is in keeping with experimental studies in animals on the teratogenic effects of drugs and other chemicals (Cohen and Sulik 1992; Cohen and Shiota 2002) and data from mice lacking *Shh* (Chiang et al. 1996). *Shh* expression has been detected in the mouse prechordal plate and the ventral neuroectoderm. In chick embryos, *Shh* expression in the ectoderm of the craniofacial primordia is essential for outgrowth of the facial swellings (Helms et al. 1997; Hu and Helms 1999). Moreover, *Six3* participates in midline forebrain and eye formation (Bovolenta et al. 1996). In contrast, in mice *Zic2* is expressed along the dorsal neuroectoderm up to the rostral end of the future telencephalon, and reduction of *Zic2* expression causes a neurulation delay and inhibition of EMT, which results in HPE and various neural tube defects (Nagai et al. 1997, 2000). These different expression patterns, *Shh* and *Six3* in the ventral neuroectoderm and *Zic2* in the dorsal neuroectoderm, suggest that these genes affect the outgrowth and differentiation of the forebrain in different ways. Mutations of genes expressed dorsally in the neural tube give rise to either inappropriate division of the prosencephalon into cerebral hemispheres with agenesis of the telencephalic roof plate, resulting in HPE with normal midfacial dimensions (Brown et al. 1998; Fig. 5.17f), or defects in the fusion process of the prosencephalic neural walls, causing exencephaly and anencephaly (Nagai et al. 2000).

5.7   Abnormal Development of the Skull with CNS Manifestations

Developmental defects of the cranial vault and face are relatively common, whereas congenital defects of the skull base and sensory capsules (nasal and otic) are relatively rare (Sperber 2002). During postnatal growth of congenital craniofacial defects, three general patterns of development may occur: maintenance of the defective growth pattern; catch-up growth, minimizing the defect; or marked worsening of the derangement with increasing age. Of great significance to facial development is the normal closing of the **foramen caecum** in the anterior cranial fossa at the fronto-ethmoid junction (Hoving 1993). Abnormal patency of this foramen, due to non-separation of the neuroectoderm and surface ectoderm during neural tube formation, allows a pathway for neural tissue to herniate into the nasal region, providing the basis of encephaloceles, gliomas and dermoid cysts that cause gross disfigurement of facial structures.

5.7.1   The Craniosynostoses

Premature closure of calvarial sutures causes the cessation of growth and leads to isolated and syndromic forms of craniosynostoses. Many ***craniosynostosis syndromes*** are due to genetic mutations of the FGF receptors (FGFRs 1, 2 and 3), and the *TWIST* and *MSX2* genes (Cohen and MacLean 2000; Warren et al. 2001; Jabs 2002; Johnston and Bronsky 2002). FGFRs on mesenchymal cells enhance their differentiation into osteoblasts and increase apoptosis when they bind FGFs, and are repressed by *TWIST*. *MSX2* also enhances the differentiation into osteoblasts and is involved in cell death, which may be important in early suture closure. In mice, *Msx2* and *Twist* cooperatively control the development of the neural-crest-derived skeletogenic mesenchyme of the skull vault (Ishii et al. 2003). Depending on which of the sutures are obliterated prematurely, the skull can develop a characteristic shape (Fig. 5.19). Synostosis of the coronal sutures leads to ***brachycephaly*** or short-headedness. Variant head shapes are ***acrocephaly*** and ***oxycephaly*** (pointed head), or ***turricephaly*** (tower-shaped head). Unilateral coronal synostosis gives rise to ***anterior plagiocephaly***, which is associated with asymmetry of the face and skull. ***Dolichocephaly*** (long-headedness) or ***scaphocephaly*** occurs after premature fusion of the sagittal suture. ***Trigonocephaly*** (triangular-shaped head) results from premature closure of the metopic suture. ***Posterior plagiocephaly*** is mostly non-synostotic and due to abnormal mechanical forces. ***Compound synostosis***, in which two or more sutures are involved, can lead to complex head shapes with severe skull deformities

Clinical Case 5.1
Alobar Holoprosencephaly

Alobar holoprosencephaly (*HPE*) and other forms of HPE can be detected prenatally by ultrasound. Blaas et al. (2000) presented a case of alobar HPE with cyclopia in an embryo with a gestational age of 9 weeks and 2 days with a crown–rump length (CRL) of 22 mm. Three-dimensional ultrasound improved the imaging (see Case Report).

Case Report. A 31-year-old gravida 6 para 1 was referred to a university hospital because of habitual abortion. Her husband had a balanced chromosomal translocation (46,XY,t(8;14)(p21.1;q24.1). At the first examination at the gestational age of 9 weeks and 2 days, ultrasound examination showed an embryo of 22-mm CRL with abnormal development of the brain with a small monoventricular forebrain (Fig. 5.18 a) and a proboscis (Fig. 5.18 b). Seven days later, CRL was 33 mm (Fig. 5.18 d). Three-dimensional
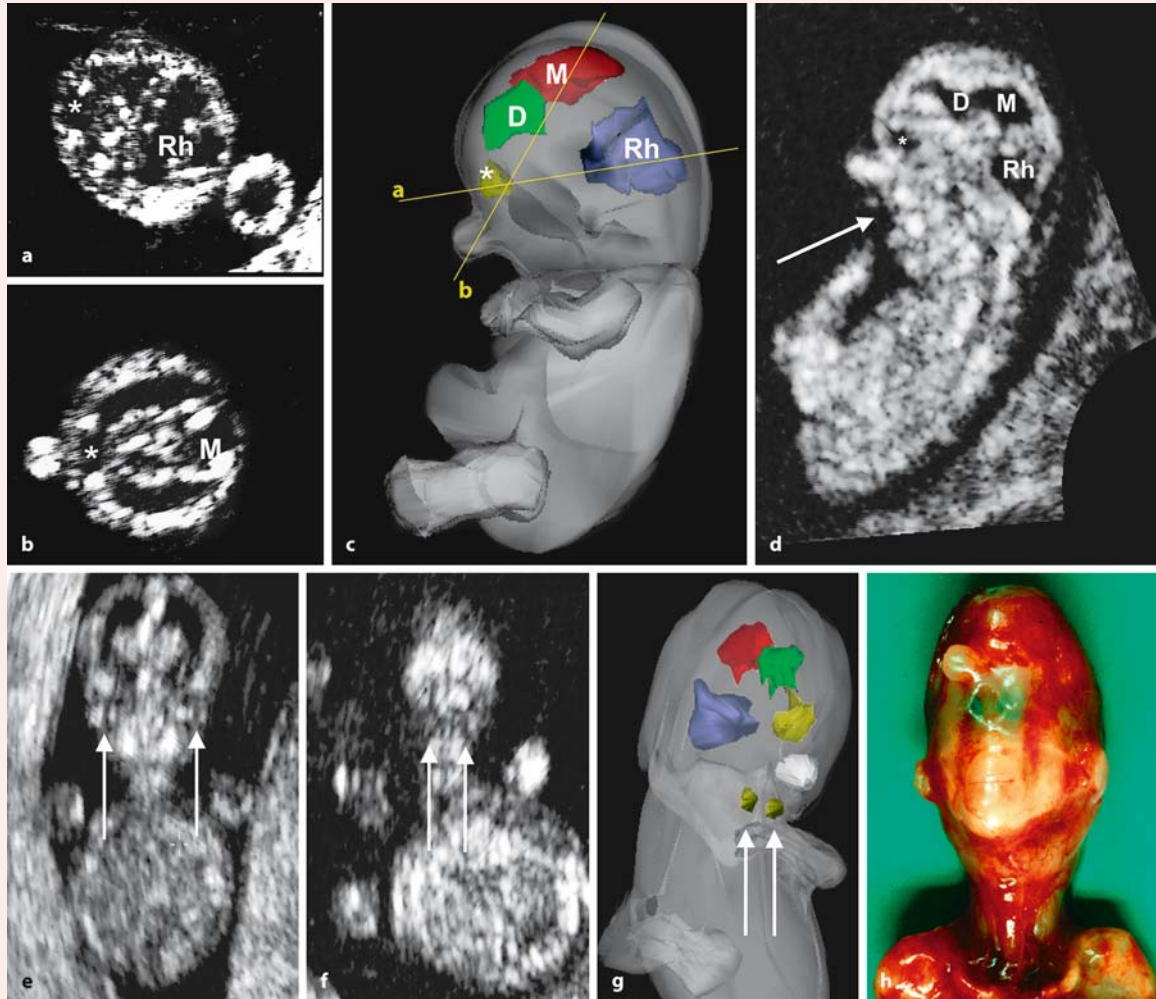
Fig. 5.18 Alobar holoprosencephaly at 9 weeks of gestation visualized by two- and three-dimensional ultrasound: **a**–**c** ultrasound sections showing the non-separation of the forebrain (*asterisks* in **a** and **b**) of the 9-week and 2-day-old embryo (crown–rump length, *CRL*, 22 mm), and three-dimensional reconstruction of the embryo with volume presentation of body and brain cavities (**c**); **d** three-dimensional reconstruction 7 days later, the *arrow* points at the cyclopia; **e** coronal section through the face of a normal fetus (CRL 30 mm), showing the normal hypertelorism of the eyes (*arrows*) at that age; **f** fetus with holoprosencephaly (CRL 33 mm) with the two eye anlagen lying close together (*arrows*); **g** three-dimensional reconstruction of the same fetus with the holosphere (*yellow*) and the cavities of the diencephalon (*D*, *green*), the mesencephalon (*M*, *red*) and the rhombencephalon (*Rh*, *blue*), and the eye anlagen (*yellow*, *arrows*); **h** postabortem photograph of the fetus with cyclopia, two eye anlagen and a proboscis (reproduced with permission from Blaas et al. 2000, *Ultrasound Obstet. Gynecol.* 15:62–65; copyright 2000, John Wiley & Sons Ltd.)

reconstructions were made from both examinations (Fig. 5.18 c, g). The body, including the proboscis and the brain cavities, was outlined by manual segmentation and given different colours. Two eye anlagen, lying closely together below the proboscis, could be identified at 19 weeks of gestation (Fig. 5.18 f). There was a small monoventricular holosphere, connected to the diencephalon by a narrow duct (Fig. 5.18 c, d, f). Chorion villus biopsy at 10.5 weeks revealed the same balanced translocation as that of the father. The patient was informed about the diagnosis of alobar HPE at the first visit. With the informed consent of the patient, the pregnancy continued until 12.5 weeks of gestation before it was terminated. This was done to confirm the diagnosis by ultrasound, by karyotyping

and by postabortem autopsy. The autopsy confirmed the diagnosis of alobar HPE, associated with cyclopia with two eye anlagen, a proboscis and a small monoventricular holosphere (Fig. 5.18h).

References

Blaas H-GK, Eik-Nes SH, Berg S, Torp H (1998) *In-vivo* three-dimensional ultrasound reconstructions of embryos and early fetuses. Lancet 352:1182–1186

Blaas H-GK, Eik-Nes SH, Vainio T, Isaksen CV (2000) Alobar holoprosencephaly at 9 weeks gestational age visualized by two- and three-dimensional ultrasound. Ultrasound Obstet Gynecol 15:62–65
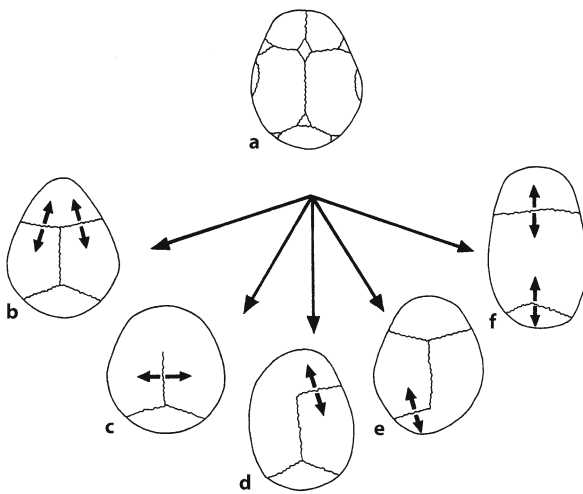
Fig. 5.19 Premature ossification of the cranial sutures leads to an abnormal head shape: **a** normal skull; **b** trigonocephaly; **c** brachycephaly; **d** anterior plagiocephaly; **e** posterior plagiocephaly; **f** dolichocephaly (after Cohen and MacLean 2000)

such as the cloverleaf (*Kleeblattschädel*) malformation found in thanatophoric dysplasia.

Agenesis and premature ossification of one or more cranial sutures are the most common developmental disorders of the skull vault, affecting 1 in 2,500 individuals (Cohen and MacLean 2000; Mathijssen 2000; Muenke and Wilkie 2001; Jabs 2002). These disorders can be associated with increased intracranial pressure, difficulties with vision, hearing and breathing, and facial deformities. In agenesis, direct fusion of bone centres takes place at locations where normally sutures arise. This can be observed in isolated and syndromic forms of craniosynostosis, for example in scaphocephaly and Apert syndrome, respectively (Mathijssen 2000). Non-syndromic cran-

iosynostosis, in which craniosynostosis is an isolated feature, is more frequent than syndromic forms. Sagittal synostosis is the most common of the nonsyndromic synostoses (birth prevalence: 1 in 5,000). In isolated sagittal stenosis, the overall scaphocephalic skull shape is mirrored in anteroposterior expansion of the brain, primarily in a posterior direction (Aldridge et al. 2002). The classical craniosynostosis syndromes are inherited as autosomal dominant traits and include Apert, Pfeiffer, Saethre–Chotzen and Crouzon syndromes (Figs. 5.20, 5.21). Most autosomal dominant craniosynostosis syndromes involve the coronal suture. Syndromic craniosynostoses are usually associated with facial, limb, ear and/or heart malformations. Recently, the molecular bases of these classical craniosynostoses and of several rare craniosynostosis syndromes have been identified. Dominant mutations in one of three FGFR genes (*FGFR1*, *FGFR2* and *FGFR3*) or in the transcription factor *TWIST* account for some 20% of cases of craniosynostosis. Many *FGFR* mutations encode highly recurrent missense substitutions, which arise exclusively from the father and are associated with increased paternal age (Crow 2000; Wilkie and Morriss-Kay 2001). Several different syndromes can be associated with the same mutations in *FGFR* genes (Table 5.5), indicating that the mutations might act by distinct mechanisms. Furthermore, the same syndrome, for example Pfeiffer syndrome, is due to different mutations in *FGFR1* and *FGFR2*. Heterogeneous mutations in *FGFR2* also cause Apert, Crouzon, Jackson–Weiss and Beare–Stevenson syndromes. Muenke syndrome is due to a specific mutation in *FGFR3*. Cytogenetic deletions and translocations involving 7p21.1 and various heterozygous *TWIST* mutations cause Saethre–Chotzen syndrome. A specific heterozygous mutation in the *MSX2* gene, which has been observed in only one family, causes Boston-type craniosynos-

Table 5.5 Overview of the more common syndromic craniosynostoses (after Aicardi 1998; Jabs 2002)

Craniosynostosis syndrome/OMIM number	Main features	Proportion of cases with cranio-synostosis	Inheritance	Gene defect
Apert syndrome/ 101200	Mental retardation, midface deficiency, proptosis, down-slanting palpebral fissures, complex symmetrical syndactyly of hands and feet (either of digits I–V or of digits II–IV)	Almost all (coronal sutures)	AD (most cases new mutations)	*FGFR2*, exons IIIa and IIIc
Crouzon syndrome/ 123500	Hypoplasia of maxilla, shallow orbits, proptosis	Almost all (coronal, then all sutures)	AD	*FGFR2*, exons IIIa and IIIc
Pfeiffer syndrome/ 101600	Strabismus, proptosis, hypertelorism, broad thumbs and toes, mild variable cutaneous syndactyly of fingers and toes	All cases (coronal)	AD	*FGFR1*, *FGFR2*, *FGFR3*, exons IIIa and IIIc
Saethre–Chotzen syndrome/101400	Facial asymmetry, low-set frontal hairline, ptosis, deviated nasal septum, variable brachydactyly and cutaneous syndactyly, mental retardation	All cases (coronal, uni- or bilateral)	AD	*TWIST*
Muenke syndrome/ 602849, 600593	Variable, uni- or bicoronal synostosis, brachydactyly		AD	*FGFR3*, exon IIIa
Boston-type cranio-synostosis/12310.001	Variable craniosynostosis; supraorbital recession; short first metatarsals		AD	*MSX2*
Jackson–Weiss syndrome/123150	Variable craniosynostosis, maxillary hypoplasia, broad great toe and medial deviation, syndactyly, bony fusion		AD	*FGFR1*, exons IIIa and IIIc) *FGFR2*, exon IIIa
Beare–Stevenson syndrome/123790	Variable craniosynostosis, cutis gyrata, acanthosis nigricans		Usually sporadic mutations	*FGFR2*

AD autosomal dominant

tosis. The diagnosis of craniosynostosis syndromes is by clinical examination and imaging of the skull, hands and feet. The more common syndromic craniosynostoses will be briefly discussed.

Apert syndrome or acrocephalosyndactyly (Apert 1906) is characterized by bilateral coronal suture synostosis (Fig. 5.20a, b) due to fusion of bone centres of the frontal and parietal bones, resulting a wide-open gap between the frontal bones instead of the frontal suture at birth, exorbitism, strabismus, midfacial hypoplasia, joint ankylosis and symmetrical complex syndactyly of the hands and feet (Cohen and Kreiborg 1993, 1995). Mental retardation is common and often severe. Deafness and optic atrophy are frequent. Non-progressive ventriculomegaly and agenesis of the corpus callosum are the most frequent CNS malformations (Cohen and Kreiborg 1990; Clinical Case 5.2). Almost all cases with Apert syndrome are associated with either of two *FGFR2* mutations, Ser252Trp or Pro253Ag (Park et al. 1995; Wilkie et al. 1995).

Crouzon syndrome (Crouzon 1912; Kreiborg 1981) is characterized by bicoronal craniosynostosis in which eventually all calvarial sutures can be involved (Fig. 5.20c, d), midfacial hypoplasia, exorbitism,

epilepsy and seemingly unaffected limbs. Subtle radiographic abnormalities such as fusion of carpal bones have been described (Anderson et al. 1997; Murdoch-Kinch and Ward 1997). The gene for Crouzon syndrome has been mapped to 10q25-q26 (Preston et al. 1994) and has been shown to code FGFR2. Several mutations have been demonstrated (Jabs et al. 1994; Reardon et al. 1994; Passos-Bueno et al. 1999). *Pfeiffer syndrome* (Pfeiffer 1964) includes bicoronal synostosis (Fig. 5.20e, f), hypertelorism, and broad and deviated thumbs and halluces (Cohen 1993).

Typical characterics of the *Saethre–Chotzen syndrome* (Saethre 1931; Chotzen 1932) are bilateral coronal synostosis (Fig. 5.21), hypertelorism, unilateral or bilateral ptosis of the eyelids, low-set hairline, hearing loss, brachydactyly and soft-tissue syndactyly. Saethre–Chotzen syndrome has been linked to the *TWIST* gene on chromosome 7p21.1. Mutations in and variably sized deletions of this gene can be found in patients with clinical features of Saethre–Chotzen syndrome. The clinical spectrum of genetic abnormalities of the *TWIST* gene is highly variable. In a large five-generation family with characteristics of Saethre–Chotzen syndrome as well as of the ble-

Fig. 5.20 Dysmorphology of the head in Apert (**a**, **b**), Crouzon (**c**, **d**) and Pfeiffer (**e**, **f**) syndromes (courtesy Michiel Vaandrager, Rotterdam)

Fig. 5.21 a, b Dysmorphology of the head in Saethre–Chotzen syndrome with a *TWIST* mutation (courtesy I. Marieke de Heer, Rotterdam)

Clinical Case 5.2
Apert Syndrome

Apert syndrome, described by Apert (1906) as acrocephalosyndactyly, is characterized by bilateral coronal suture synostosis, related skull malformations, mental retardation, syndactyly of the hands and feet, and frequently deafness and optic atrophy (Apert 1906; Cohen and Kreiborg 1995). The most frequently associated cerebral malformations are hypoplasia of the corpus callosum and the septum pellucidum, and ventricular enlargement (Cohen and Kreiborg 1990; see Case Report).

Case Report. After an uneventful pregnancy, a boy was born as the seventh child in a family with six healthy children. He was born at term with a birth weight of 3,724 g. He had a dysmorphic head with a prominent forehead, retraction of the glabella and upper nose bridge, midfacial hypoplasia and low-implanted ears. There was bilateral choanal atresia. The posterior part of the head was flat with a broad neck. There was symmetric syndactyly of fingers 2–5 of the hands and of toes 1–5. The boy died from severe cardiorespiratory failure due to the following complex malformations of the heart: abnormal venous return of systemic vessels with a persistent left vena cava superior draining through the coronary sinus into the right atrium; hypoplasia of the left ventricle and aorta; bicuspid aortic valve; aortic coarctation, and a persistent patent ductus arteriosus. Head circumference was 36.5 cm (P50) with a shorter-than-normal antero-posterior diameter. This was reflected in a shortened brain with relatively small parieto-occipital lobes (Fig. 5.22 a). There was partial agenesis of the corpus callosum, the posterior part of which was absent. Moreover, the septum pellucidum was absent. The pyramids were hypoplastic, and were flanked by rather large, somewhat plump inferior olives (Fig. 5.22 b).

References

Apert E (1906) De l'acrocéphalosyndactylie. Bull Soc Méd (Paris) 23:1310-1330

Cohen MM Jr, Kreiborg S (1990) The central nervous system in the Apert syndrome. Am J Med Genet 35:36–45

Cohen MM Jr, Kreiborg S (1995) Hands and feet in the Apert syndrome. Am J Med Genet 57:82–96
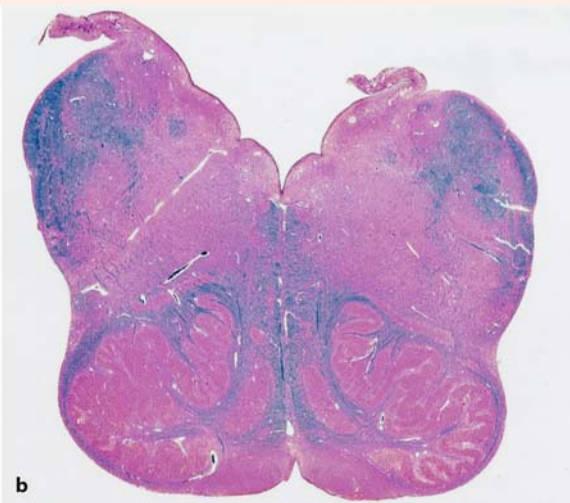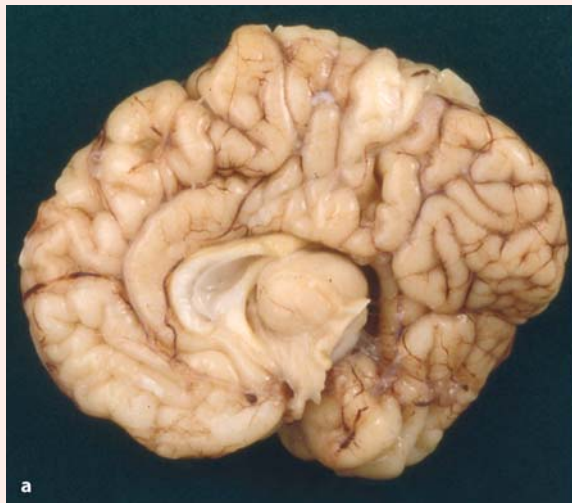
Fig. 5.22 Apert syndrome: **a** medial view of the brain, showing the short anteroposterior diameter of the brain, a relatively small parietal-occipital lobe, incomplete corpus callosum and absent septum pellucidum; **b** Luxol Fast Blue stained section through the medulla oblongata, showing large inferior olives and hypoplastic pyramids (courtesy Pieter Wesseling, Nijmegen)

Clinical Case 5.3
Thanatophoric Dysplasia

Thanatophoric dysplasia is the most common form of lethal skeletal dysplasia. The name is derived from the Greek *thanatus* (death) and *phorus* (seeking). Holtermüller and Wiedemann (1960) described a form of craniosynostosis with trilocular configuration of the skull and severe internal hydrocephalus as *Kleeblattschädel* (cloverleaf skull) as an isolated anomaly but also in combination with generalized skeletal dysplasia. Different mutations at the FGFR3 locus give rise to distinct phenotypes (Cohen 1997; Hall and Lopez-Rangel 1997). Abnormalities in the CNS mainly affect the temporal lobe (see Case Report).

Fig. 5.23 Thanatophoric dysplasia: frontal (**a**) and lateral (**b**) views of the full-term neonate (courtesy Martin Lammens, Nijmegen)
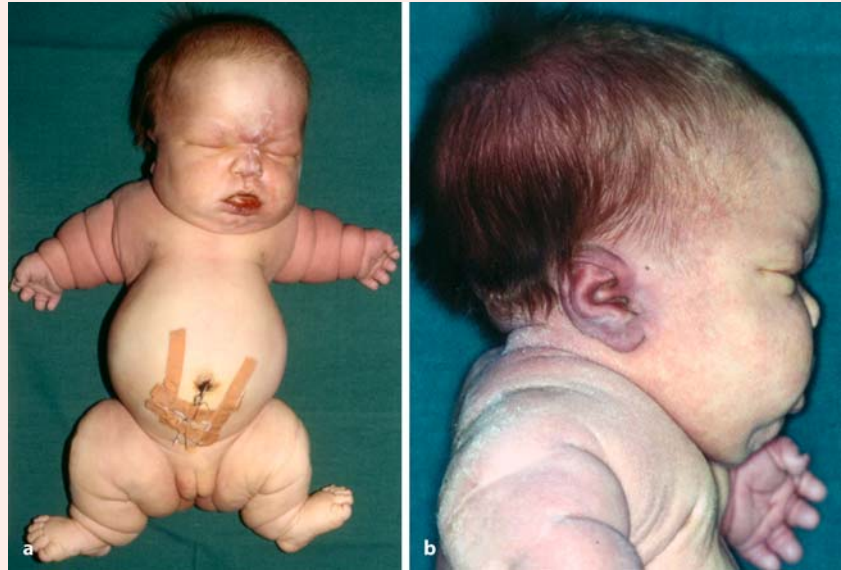
Case Report. This girl was the second child of a 31-year-old healthy mother. After an uneventful pregnancy, apart from breech position, she was born by Caesarean section at 41 weeks of gestation. Birth weight was 4,200 g and crown–heel length was 42 cm (much less than P3). The skull was broad and large with frontal bossing (Fig. 5.23 a, b; head circumference was 40 cm; much greater than P97). There was micromelia with phonehorn-formed long bones, a small and short thorax, and hypoplastic lungs. The baby died after 3 days. The babygram showed the typical configuration of thanatophoric dysplasia. The brain was megalencephalic and weighed 551 g (normal 420±33 g). Both hippocampi lacked normal enrolling (Fig. 5.24). A leptomeningeal neuroglial ectopia was found in the left hippocampal region.
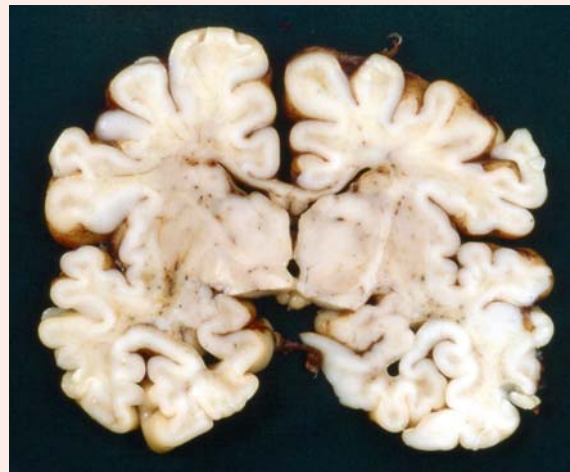
Fig. 5.24 Transverse section through the brain showing the lack of normal enrolling of the hippocampus on both sides (courtesy Martin Lammens, Nijmegen)

References

Cohen MM Jr (1997) Short-limb skeletal dysplasias and craniosynostosis – what do they have in common. Pediatr Radiol 27:442–446

Hall JG, Lopez-Rangel M (1997) Bone dysplasias, nontraditional mechanisms of inheritance and monozygotic twins. Pediatr Radiol 27:422–427

Holtermüller K, Wiedemann HR (1960) Kleeblattschädel Syndrom. Med Monatsschr 14:439–446

pharophimosis–ptosis–epicanthus inversus syndrome, only two patients of the family had craniosynostosis (de Heer et al. 2004). *TWIST* deletions often also include part of the surrounding chromosome 7p and, strikingly, all patients with large *TWIST* deletions suffer from mental retardation, a rare finding in patients with Saethre–Chotzen syndrome (de Heer 2004). In Saethre–Chotzen patients, in whom neither a mutation nor a deletion of *TWIST* has been found, the *FGFR3* P250R mutation was detected in some cases (Muenke et al. 1997; de Heer et al. 2005). This mutation has been specifically linked to **Muenke syndrome,** which is characterized by unicoronal or bicoronal synostosis and slight facial dysmorphology, but a Saethre–Chotzen phenotype can apparently also result from this mutation.

Infants suffering from **thanatophoric dwarfism** or **dysplasia** usually die shortly after birth, at least partially because of respiratory insufficiency. The patients show severe skeletal abnormalities, including a form of craniosynostosis with trilocular configuration of the skull known as cloverleaf skull (*Kleeblattschädel*) and typical facial dysmorphology (Clinical Case 5.3). Temporal lobe abnormalities are a consistent abnormality (Knisely and Ambler 1988; Norman et al. 1995).

5.7.2   Cranial Base Abnormalities

Abnormalities of the cranial base, and of the cervicooccipital junction in particular, account for some serious neurological problems in infants and children (Aicardi 1998). The Chiari malformations are discussed in Chap. 4. Most cases of **basilar impression** are congenital and may be familial (Bull et al. 1955; Coria et al. 1983), but acquired cases occur. The degree of impression is variable. In **platybasia**, the base of the skull is flat. Partial forms exist and are often associated with various abnormalities of the atlas and condylar processes (Bull et al. 1955; Wackenheim 1967). Underlying neural anomalies are hydrosyringomyelia, fibrous bands compressing the lower brain stem, abnormal vessels and kinking of the medulla. Decompression of the posterior fossa can considerably improve the anatomy of the spinal cord (Menezes et al. 1980). A **narrow foramen magnum** is common in achondroplasia (Reid et al. 1987; Nelson et al. 1988). **Cervical vertebral blocks** occur most commonly in Klippel–Feil syndrome (Chap. 6).

References

Abu-Issa R, Smyth G, Smoak I, Yamamura K, Meyers EN (2002) *Fgf8* is required for pharyngeal arch and cardiovascular development in the mouse. Development 129:4613–4625

Acampora D, Mazan S, Lallemand Y, Avantaggiato V, Maury M, Simeone A, Brûlet P (1995) Forebrain and midbrain regions are deleted in *Otx2–/–* mutants due to a defective anterior neuroectoderm specification during gastrulation. Development 121:3279–3290

Acampora D, Avantaggiato V, Tuorte F, Briata P, Corte G, Simeone A (1998) Visceral endoderm-restricted translation of *Otx1* mediates recovery of *Otx2* requirements for specification of anterior neural plate and normal gastrulation. Development 125:5091–5104

Acampora D, Merlo GR, Paleari L, Zerega B, Postiglione MP, Mantero S, Bober E, Barbieri O, Simeone A, Levi S (1999) Craniofacial, vestibular and bone defects in mice lacking the *Distal-less*-related gene *Dlx5*. Development 126:3795–3809

Adelmann HB (1925) The development of the neural folds and cranial ganglia in the rat. J Comp Neurol 39:19–171

Adelmann HB (1936) The problem of cyclopia. Q Rev Biol 11:116–182 and 284–304

Ahlgren SC, Bronner-Fraser M (1999) Inhibition of sonic hedgehog signaling in vivo results in craniofacial neural crest cell death. Curr Biol 9:1304–1314

Aicardi J (1998) Diseases of the Nervous System in Childhood, 2nd ed. Mac Keith, London

Aldridge K, Marsh JL, Govier D, Richtmeier JT (2002) Central nervous system phenotypes in craniosynostosis. J Anat (Lond) 201:31–39

Aleksic S, Budzilovich G, Greco MA, McCarthy J, Reuben R, Margolis S, Epstein F, Feigin I, Pearson J (1984) Intracranial lipomas, hydrocephalus and other CNS anomalies in oculoauriculo-vertebral dysplasia (Goldenhar-Gorlin syndrome). Child's Brain 11:285–297

Anderson PJ, Hall CM, Evans RD, Jones BM, Hayward RD (1997) Hand anomalies in Crouzon syndrome. Skelet Radiol 26:113–115

Anson BJ, Bast TH, Cauldwell EW (1948) The development of the auditory ossicles, the otic capsule and the extracapsular tissues. Ann Otol Rhinol Laryngol 57:603–632

Anson BJ, Hanson JS, Richany SF (1960) Early embryology of the auditory ossicles and associated structures in relation to certain anomalies observed clinically. Ann Otol Rhinol Laryngol 69:427–447

Apert E (1906) De l'acrocéphalosyndactylie. Bull Soc Méd (Paris) 23:1310–1330

Aybar MJ, Mayor R (2002) Early induction of neural crest cells: Lessons learned from frog, fish and chick. Curr Opin Genet Dev 12:452–458

Aybar MJ, Nieto MA, Mayor R (2003) *Snail* precedes *Slug* in the genetic cascade required for the specification and migration of *Xenopus* neural crest. Development 130:483–494

Bachiller D, Klingensmith J, Shneyder N, Tran U, Anderson R, Rossant J, De Robertis EM (2003) The role of chordin/Bmp signals in mammalian pharyngeal development and DiGeorge syndrome. Development 130:3567–3578

Bardeen R (1910) Die Entwicklung des Schädels, des Zungenbeins und des Kehlkopfskeletts. In: Keibel F, Mall FP (Hrsg) Handbuch der Entwicklungsgeschichte des Menschen, I. Band. Hirzel, Leipzig, pp 402–456

Bartelmez GW, Blount MP (1954) The formation of neural crest from the primary optic vesicle in man. Contrib Embryol Carnegie Instn 35:55–91

Batten EH (1958) The origin of the acoustic ganglion in the sheep. J Embryol Exp Morphol 6:597–615

Belloni E, Muenke M, Roessler E, Traverso G, Siegel-Bartelt J, Frumkin A, Mitchell HF, Donis-Keller H, Helms C, Hing AV, et al. (1996) Identification of Sonic hedgehog as a candidate gene responsible for holoprosencephaly. Nat Genet 14:353–356

Berry SM, Gosden C, Snijders RJM, Nicolaides KH (1990) Fetal holoprosencephaly. Associated malformations and chromosomal defects. Fetal Diagn Ther 5:92–99

Beverdam A, Brouwer A, Reijnen M, Korving J, Meijlink F (2001) Severe nasal clefting and abnormal embryonic apoptosis in Alx3/Alx4 double mutant mice. Development 128:3975–3986

Bixler D, Ward R, Gale DD (1985) Agnathia-holoprosencephaly: A developmental field complex involving face and brain. Report of 3 cases. J Craniofac Genet Dev Biol, Suppl1:241–249

Blaas H-GK, Eik-Nes SH, Vainio T, Isaksen CV (2000) Alobar holoprosencephaly at 9 weeks gestational age visualized by two- and three-dimensional ultrasound. Ultrasound Obstet Gynecol 15:62–65

Blaas H-GK, Eriksson AG, Salvesen KÅ, Isaksen CV, Christensen B, Møllerløkken G, Eik-Nes SH (2002) Brains and faces in holoprosencephaly: Pre-and postnatal description of 30 cases. Ultrasound Obstet Gynecol 19:24–38

Bockman DE, Redmond M, Kirby ML (1989) Alteration of early vascular development after ablation of cranial neural crest. Anat Rec 225:209–217

Bolande RP (1974) The neurocristopathies: A unifying concept of disease arising in neural crest development. Hum Pathol 4:409–429

Boshart L, Vlot EA, Vermeij-Keers C (2000) Epithelio-mesenchymal transformation in the embryonic face: Implications for craniofacial malformations. Eur J Plast Surg 23:217–223

Bovolenta P, Mallamaci A, Boncinelli E (1996) Cloning and characterization of two chick homeobox genes, members of the Six/sine oculis family, expressed during eye development. Int J Dev Biol 1(Suppl):738–748

Brown SA, Warburton D, Brown LY, Yu C, Roeder ER, Stengel-Rutkowski S, Hennekam RCM, Muenke M (1998) Holoprosencephaly due to mutation in ZIC2, a homologue of Drosophila odd-paired. Nat Genet 20:180–183

Bull JS, Nixon WL, Pratt RT (1955) Radiological criteria and familial occurrence of primary basilar impression. Brain 78:229–247

Cano A, Perez-Moreno MA, Rodrigo I, Locascio A, Blanco MJ, del Barrio MG, Portillo F, Nieto MA (2000) The transcription factor snail controls epithelial-mesenchymal transitions by repressing E cadherin expression. Nat Cell Biol 2:78–83

Capecchi MR (1997) The role of Hox genes in hindbrain development. In: Cowan WM, Jessell TM, Zipursky SL (eds) Molecular and Cellular Approaches to Neural Development. Oxford University Press, New York, pp 334–355

Cargile CB, McIntosh I, Clough MV, Rutberg J, Yaghmai R, Goodman BK, Chen XN, Korenberg JR, Thomas GH, Geraghty MT (2000) Delayed membranous ossification of the cranium associated with familial translocation (2;3) (p15;q12). Am J Med Genet 92:328–335

Chiang C, Litingtung Y, Lee E, Young KE, Corden JL, Westphal H, Beachy PA (1996) Cyclopia and defective axial patterning in mice lacking Sonic hedgehog gene function. Nature 383:407–413

Chisaka O, Capecchi MR (1991) Regionally restricted developmental defects resulting from targeted disruption of the mouse homeobox gene Hox-1.5. Nature 350:473–479

Chotzen F (1932) Eine eigenartige familiäre Entwicklungsstörung (Akrocephalosyndactylie, Dysostosis craniofacialis und Hypertelorismus). Monatschr Kinderheilk 55:97–122

Cohen MM Jr (1989a) Perspectives on holoprosencephaly: Part I. Epidemiology, genetics, and syndromology. Teratology 40:211–235

Cohen MM Jr (1989b) Perspectives on holoprosencephaly: Part III. Spectra, distinctions, continuities, and discontinuities. Am J Med Genet 34:271–288

Cohen MM Jr (1993) Pfeiffer syndrome update, clinical subtypes, and guidelines for differential diagnosis. Am J Med Genet 45:300–307

Cohen MM Jr (2002) Malformations of the craniofacial region: Evolutionary, embryonic, genetic, and clinical perspectives. Am J Med Genet 115:245–268

Cohen MM Jr, Kreiborg S (1990) The central nervous system in the Apert syndrome. Am J Med Genet 35:36–45

Cohen MM Jr, Kreiborg S (1993) An updated pediatric perspective on the Apert syndrome. Am J Dis Child 147:989–993

Cohen MM Jr, Kreiborg S (1995) Hands and feet in the Apert syndrome. Am J Med Genet 57:82–96

Cohen MM Jr, MacLean RE, eds (2000) Craniosynostosis: Diagnosis, Evaluation, and Management, 2nd ed. Oxford University Press, New York

Cohen MM Jr, Shiota K (2002) Teratogenesis of holoprosencephaly. Am J Med Genet 109:1–15

Cohen MM Jr, Sulik KK (1992) Perspectives on holoprosencephaly: Part II. Central nervous system, craniofacial anatomy, syndrome commentary, diagnostic approach, and experimental studies. J Craniofac Genet Dev Biol 12:196–244

Condie BG, Capecchi MR (1994) Mice with targeted disruptions in the paralogous genes hoxa-3 and hoxd-3 reveal synergistic interactions. Nature 370:304–307

Conley ME, Beckwith JB, Mancer JFK, Tenckhoff L (1979) The spectrum of the DiGeorge syndrome. J Pediatr 94:883–890

Coria F, Quintana F, Rebollo M, Combarras O, Berciano J (1983) Occipital dysplasia and Chiari type I deformity in a family. Clinical and radiological study of three generations. J Neurol Sci 62:147–158

Couly GF, Le Douarin NM (1985) Mapping of the early neural primordium in quail-chick chimeras. I. Developmental relationships between placodes, facial ectoderm, and prosencephalon. Dev Biol 110:422–439

Couly GF, Le Douarin NM (1987) Mapping of the early neural primordium in quail-chick chimeras. II. The prosencephalic neural plate and neural folds: Implications for the genesis of cephalic human congenital abnormalities. Dev Biol 120:198–214

Couly GF, Le Douarin NM (1988) The fate map of the cephalic neural primordium at the presomitic to the 3-somite stage in the avian embryo. Development (Suppl) 103:101–113

Couly GF, Le Douarin NM (1990) Head morphogenesis in embryonic avian chimeras: Evidence for a segmental pattern in the ectoderm corresponding to the neuromeres. Development 108:543–558

Couly GF, Coltey PM, Le Douarin NM (1992) The developmental fate of the cephalic mesoderm in quail-chick chimeras. Development 114:1–15

Couly GF, Coltey PM, Le Douarin NM (1993) The triple origin of skull in higher vertebrates: A study in quail-chick chimeras. Development 117:409–429

Cousley RRJ, Calvert ML (1997) Current concepts in the understanding of hemifacial mocrosomia. Br J Past Surg 50:536–551

Croen LA, Shaw GM, Lammer EJ (1996) Holoprosencephaly: Epidemiologic and clinical characterists of a California population. Am J Med Genet 64:465–472

Crouzon O (1912) Dysostose craniofaciale héréditaire. Bull Med Soc Med Hôp (Paris) 33:545–555

Crow JF (2000) The origins, patterns and implications of human spontaneous mutation. Nat Rev Genet 1:40–47

Daft PA, Johnston MC, Sulik KK (1986) Abnormal heart and great vessel development following acute ethanol exposure in mice. Teratology 33:93–104

D'Amico-Martel A, Noden DM (1983) Contributions of placodal and neural crest cells to avian cranial peripheral ganglia. Am J Anat 66:445–468

de Heer IM (2004) Saethre-Chotzen Syndrome. Craniofacial anomalies caused by genetic changes in the TWIST gene. Thesis, Erasmus University Rotterdam

de Heer IM, Hoogeboom AJM, Eussen HJ, Vaandrager JM, de Klein A (2004) Deletion of the TWIST gene in a large five-generation family. Clin Genet 65:396–399

de Heer IM, de Klein A, van den Ouweland AM, Vermeij-Keers C, Wouters CH, Vaandrager JM, Hovius SER, Hoogeboom AJM (2005) Clinical and genetic analysis of patients with the Saethre-Chotzen syndrome. Plast Reconstr Surg 115:1894–1902

DeMyer WE (1967) The median-cleft syndrome. Differential diagnosis of cranium bifidum occultum, hypertelorism, and median cleft nose, lip, and palate. Neurology 17:961–971

DeMyer WE, Zeman W, Palmer CG (1963) Familial holoprosencephaly (arhinencephaly) with median cleft palate. Neurology 13:913–918

DeMyer WE, Zeman W, Palmer CG (1964) The face predicts the brain: Diagnostic significance of median facial anomalies for holoprosencephaly (arhinencephaly). Pediatrics 34:256–263

DiGeorge AM (1965) Discussion on a new concept of the cellular basis of immunology. J Pediatr 67:907

Dixon J, Hovanes K, Shiang R, Dixon MJ (1997) Sequence analysis, identification of evolutionary conserved motifs and expression analysis of murine tcof1 provide further evidence for a potential function for the gene and its human homologue, TCOF1. Hum Mol Genet 6:727–737

Dixon J, Brakebusch C, Fässler R, Dixon MJ (2000) Increased levels of apoptosis in the prefusion neural folds underlie the craniofacial disorder, Treacher Collins syndrome. Hum Molec Genet 9:1473–1480

Dixon MJ, Marres HAM, Edwards SJ, Dixon J, Cremers CWRJ (1994) Treacher Collins syndrome: Correlation between clinical and genetic linkage studies. Clin Dysmorphol 3:96–103

Donnenfeld AE, Packer RJ, Zackai EH, Chee CM, Sellinger B, Emanuel BS (1989) Clinical, cytogenetic, and pedigree findings in 18 cases of Aicardi syndrome. Am J Med Genet 32:461–467

Driscoll DA, Burdoff ML, Emanuel BS (1992a) A genetic etiology for the DiGeorge syndrome: Consistent deletions and microdeletions of 22q11. Am J Hum Genet 50:924–933

Driscoll DA, Spinner ND, Burdoff ML (1992b) Deletions and microdeletions of 22q11.2 in velo-cardiofacial syndrome. Am J Med Genet 44:261–268

Duband JL, Monier F, Delannet M, Newgreen D (1995) Epithelium-mesenchyme transition during neural cell development. Acta Anat (Basel) 154:63–78

Duhamel B (1966) Morphogenèse Pathologique. Masson, Paris

Eagleson GW, Harris WA (1990) Mapping of the presumptive brain regions in the neural plate of *Xenopus laevis*. J Neurobiol 21:427–440

Eagleson HW, Ferreiro B, Harris WA (1995) Fate of the anterior neural ridge and the morphogenesis of the *Xenopus* brain. J Neurobiol 28:146–158

Emanuel BS, McDonald-McGinn D, Saitta SC, Zackai EH (2001) The 22q11.2 deletion syndrome. Adv Pediatr 48:39–73

Etchevers HC, Vincent C, Le Douarin NM, Couly GF (2001) The cephalic neural crest provides pericytes and smooth muscle cells to all blood vessels of the face and forebrain. Development 128:1059–1068

Evrard L, Vanmuylder N, Dourov N, Hermans C, Biermans J, Werry-Huet A, Rooze M, Louryan S (2000) Correlation of HSP110 expression with all-trans retinoic acid-induced apoptosis. J Craniofac Genet Dev Biol 20:183–192

Favier B, Dollé P (1997) Developmental functions of mammalian *Hox* genes. Mol Hum Reprod 3:115–131

Franceschetti A, Klein D (1949) Mandibulo-facial dysostosis: New hereditary syndrome. Acta Ophthalmol 27:144–224

Francis-West PH, Robson L, Evans DJR (2003) Craniofacial Development: The tissue and molecular interactions that control development of the head. Advances in Anatomy Embryology and Cell Biology, Vol 169. Springer, Berlin Heidelberg New York

Frank DU, Fotheringham LK, Brewer JA, Muglia LJ, Tristani-Firouzi M, Capecchi MR, Moon AM (2002) An *Fgf8* mouse mutant phenocopies human 22q11 deletion syndrome. Development 129:4591–4603

Gammill LS, Bronner-Fraser M (2003) Neural crest specification: Migrating into genomics. Nat Rev Neurosci 4:795–805

Geelen JAG, Langman J (1977) Closure of the neural tube in the cephalic region of the mouse embryo. Anat Rec 189:625–640

Gendron-Maguire M, Mallo M, Zhang M, Gridley T (1993) *Hoxa-2* mutant mice exhibit homeotic transformation of skeletal elements derived from cranial neural crest. Cell 75:1317–1331

Goldberg R, Motzkin B, Marion R, Scambler PJ, Shprintzen RJ (1993) Velocardiofacial syndrome. A review of 120 patients. Am J Med Genet 45:313–319

Golden JA (1998) Holoprosencephaly: A defect in brain patterning. J Neuropathol Exp Neurol 57:991–999

Golden JA, Chernoff GF (1993) Intermittent pattern of neural tube closure in two strains of mice. Teratology 47:73–80

Golden JA, Chernoff GF (1995) Multiple sites of anterior neural tube closure in humans: Evidence from anterior neural tube defects (anencephaly). Pediatrics 95:506–510

Golding J, Trainor P, Krumlauf R, Gassman M (2000) Defects in pathfinding by cranial neural crest cells in mice lacking the Neuregulin receptor ErbB4. Nat Cell Biol 2:103–109

Gorlin RJ, Cohen MM Jr, Hennekam RCM, eds (2001) Syndromes of the Head and Neck, 4th ed. Oxford University Press, Oxford

Goulding EH, Pratt RM (1986) Isotretinoin teratogenicity in mouse whole embryo culture. J Craniofac Genet Dev Biol 6:99–112

Graham A, Begbie J (2000) Neurogenic placodes: A common front. Trends Neurosci 23:313–316

Graham A, Smith A (2001) Patterning the pharyngeal arches. BioEssays 23:54–61

Graham A, Heyman I, Lumsden A (1993) Even-numbered rhombomeres control the apoptotic elimination of neural crest cells from odd-numbered rhombomeres in the chick hindbrain. Development 119:233–245

Graham A, Francis-West P, Brickell P, Lumsden A (1994) The signalling molecule BMP4 mediates apoptosis in the rhombencephalic neural crest. Nature 372:684–686

Graham A, Begbie J, McGonnell I (2004) Significance of the cranial neural crest. Dev Dyn 229:5–13

Gray's Anatomy (1995) 38th Edition (Williams PL et al., eds). Churchill Livingstone, New York

Gripp KW, Wotton D, Edwards MC, Roessler E, Ades L, Meinecke P, Richieri-Costa A, Zackai EH, Massague J, Muenke M, Elledge SJ (2000) Mutations in *TGIF* cause holoprosencephaly and link *NODAL* signalling to human neural axis determination. Nature Genet 25:205–208

Hall JG, Pallister PD, Clarren SK, Beckwith JB, Wiglesworth FW, Fraser FC, Cho S, Benke PJ, Reed SD (1980) Congenital hypothalamic hamartoblastoma, hypopituitarism, imperforate anus, and postaxial polydactyly: A new syndrome? I. Clinical, causal, and pathogenetic considerations. Am J Med Genet 7:47–74

Hanson JR, Anson BJ, Strickland EM (1962) Branchial sources of the auditory ossicles in man. Arch Otolaryngol 76:100–122 and 200–215

Hatta K, Kimmel CB, Ho RK (1991) The cyclops mutation blocks specification on the floor plate of the zebrafish central nervous system. Nature 350:339–341

Hatta K, Puschel AW, Kimmel CB (1994) Midline signaling in the primordium of the zebrafish anterior CNS. Proc Natl Acad Sci USA 91:2061–2065

Hay ED (1995) An overview of epithelio-mesenchymal transformation. Acta Anat (Basel) 154:8–20

Helms JA, Kim CH, Hu D, Minkoff R, Thaller C, Eichele G (1997) Sonic hedgehog participates in craniofacial morphogenesis and is down-regulated by teratogenic doses of retinoic acid. Dev Biol 187:25–35

Hide T, Hatakeyama J, Kimura-Yoshida C, Tian E, Takeda N, Ushio Y, Shinoishi T, Aizawa S, Matsuo I (2002) Genetic modifiers of otocephalic phenotypes in Otx2 heterozygous mutant mice. Development 129:4347–4357

Hinrichsen K (1985) The early development of morphology and patterns of the face in the human embryo. Adv Anat Embryol Cell Biol 98:1–79

Hinrichsen KV (1990) Gesichtsentwicklung. In: Hinrichsen KV (Hrsg) Humanembryologie. Springer, Berlin Heidelberg New York, pp 650–692

His W (1868) Untersuchungen über die erste Anlage des Wirbelthierleibes. Die erste Entwickelung des Hünchens im Ei. Vogel, Leipzig

His W (1885) Anatomie menschlicher Embryonen, III: Zur Geschichte der Organe. Vogel, Leipzig

Hochstetter F (1891) Ueber die Bildung der inneren Nasengänge oder primitiven Choanen. Verh Anat Ges (Anat Anz Suppl) 6:145–151

Hörstadius S (1950) The Neural Crest. Oxford University Press, Oxford

Hoving EW (1993) Frontoethmoidal Encephaloceles. A study of their pathogenesis. Thesis, University of Groningen, The Netherlands

Hsia YE, Bratu M, Herbordt A (1971) Genetics of the Meckel syndrome (dysencephalia splanchnocystica). Pediatrics 48:237–247

Hu D, Helms JA (1999) The role of sonic hedgehog in normal and abnormal craniofacial morphogenesis. Development 126:4873–4884

Hunt P, Gulisano M, Cook M, Sham MH, Faiella A, Wilkinson D, Boncinelli E, Krumlauf R (1991) A distinct Hox code for the branchial region of the vertebrate head. Nature 353:861–864

Ishii M, Merrill AE, Chan Y-S, Gitelman I, Rice DPC, Sucov HM, Maxson RE (2003) Msx2 and Twist cooperatively control the development of the neural crest-derived skeletogenic mesenchyme of the murine skull vault. Development 130:6131–6142

Jabs EW (2002) Genetic etiologies of craniosynostosis. In: Mooney MP, Siegel MI (eds) Understanding Craniofacial Anomalies: The etiopathogenesis of craniosynostoses and facial clefting. Wiley-Liss, New York, pp 125–146

Jabs EW, Li X, Scott AF, Meyers G, Chen W, Eccles M, Mao JI, Charnas LR, Jackson CE, Jayne M (1994) Jackson-Weiss and Crouzon syndromes are allelic with mutations in fibroblast growth factor receptor 2. Nat Genet 8:275–279

Jacobson C, Granström G (1997) Clinical appearance of spontaneous and induced first and second branchial arch syndromes. Scand J Plast Reconstr Hand Surg 31:125–136

Jeanty P, Zaleski W, Fleischer AC (1991) Prenatal sonographic diagnosis of lipoma of the corpus callosum in a fetus with Goldenhar syndrome. Am J Perinatol 8:89–90

Jellinger K, Gross H, Kaltenbäck E, Grisold W (1981) Holoprosencephaly and agenesis of the corpus callosum: Frequency of associated malformations. Acta Neuropathol (Berl) 55:1–10

Jiang R, Lan Y, Norton CR, Sundberg JP, Gridley T (1998) The slug gene is not essential for mesoderm or neural crest development in mice. Dev Biol 198:277–285

Jirásek JE (2001) An Atlas of the Human Embryo and Fetus. Parthenon, New York

Johnston MC, Bronsky PT (1995) Prenatal craniofacial development: New insights on normal and abnormal mechanisms. Crit Rev Oral Biol Med 6:368–422

Johnston MC, Bronsky PT (2002) Craniofacial embryogenesis: Abnormal developmental mechanisms. In: Mooney MP, Siegel MI (eds) Understanding Craniofacial Anomalies: The etiopathogenesis of craniosynostoses and facial clefting. Wiley-Liss, New York, pp 61–124

Jones KL (1997) Smith's Recognizable Patterns of Human Malformation, 5th ed. Saunders, Philadelphia

Jones MC (1990) The neurocristopathies: Reinterpretation based upon the mechanism of abnormal morphogenesis. Cleft Palat J 27:136–140

Juriloff DM, Sulik KK, Roderick TH, Hogan BK (1985) Genetic and developmental studies of a new mouse mutation that produces otocephaly. J Craniofac Genet Dev Biol 5:121–145

Kanagasuntheram R (1967) A note on the development of the tubotympanic recess in the human embryo. J Anat (Lond) 101:731–741

Kang S, Graham JM, Haskins-Olney A, Biesecker LG (1997) Gli3 frameshift mutations cause autosomal dominant Pallister-Hall syndrome. Nat Genet 15:266–268

Kelbermann D, Tyson J, McInemey AM, Malcolm S, Winter RM, Bitner-Glindricz M (2000) Mapping of a locus for autosomal dominant hemifacial microsomia. J Med Genet 37(Suppl 1):S76

Kelley RI, Hennekam RCM (2001) Smith-Lemli-Opitz syndrome. In: Scriver CR, Beaudet AL, Sly WS, Valle D (eds) The Metabolic and Molecular Bases of Inherited Disease, 8th ed. McGraw-Hill, New York, pp 6183–6201

Kelley RI, Roessler E, Hennekam RCM, Feldman GL, Kosaki K, Jones MC, Palumbos JC, Muenke M (1996) Holoprosencephaly in RSH/Smith-Lemli-Opitz syndrome: Does abnormal cholesterol metabolism affect the function of Sonic Hedgehog? Am J Med Genet 66:478–484

Kirby ML (1987) Cardiac morphogenesis: Recent research advances. Pediatr Res 21:219–224

Kirby ML, Waldo KL (1990) Role of neural crest in congenital heart disease. Circulation 82:332–340

Kimura C, Takeda N, Suzuki M, Oshimura M, Aizawa S, Matsuo I (1997) Cis-acting elements conserved between mouse and pufferfish Otx2 genes govern the expression in mesencephalic neural crest cells. Development 124:3929–3941

Kjaer I, Keeling JW, Fischer-Hansen B (1999) The Prenatal Human Cranium – Normal and Pathologic Development. Munksgaard, Copenhagen

Kleinsasser O, Schlothane R (1964) Die Ohrenbildung im Rahmen der Thalidomide-Embryopathie. Z Laryngol Rhinol Otol 43:344–367

Knecht AK, Bronner-Fraser M (2002) Induction of the neural crest: A multigenic process. Nat Rev Genet 3:453–461

Knisely AS, Ambler MW (1988) Temporal-lobe abnormalities in thanatophoric dysplasia. Pediatr Neurosci 14:169–176

Kreiborg S (1981) Crouzon syndrome. A clinical and roentgencephalometric study. Scand J Plast Reconstr Surg 18(Suppl):1–198

Kubota Y, Ito K (2000) Chemotactic migration of mesencephalic neural crest cells in the mouse. Dev Dyn 217:170–179

Kulesa PM, Fraser SE (1998) Neural crest cell dynamics revealed by time-lapse video microscopy of whole embryo chick explant cultures. Dev Biol 204:327–344

Kulesa PM, Fraser SE (2000) In ovo time-lapse analysis after dorsal neural tube ablation shows rerouting of chick hindbrain neural crest. Development 127:2843–2852

Kurtz AB, Wapner RJ, Rubin CS, Cole-Beuglet C, Ross D, Goldberg BB (1980) Ultrasound criteria for in utero diagnosis of microcephaly. J Clin Ultrasound 8:11–16

LaBonne C, Bronner-Fraser M (1998) Neural crest induction in *Xenopus*: Evidence for a two-signal model. Development 125:2403–2414

LaBonne C, Bronner-Fraser M (1999) Molecular mechanisms of neural crest formation. Annu Rev Cell Dev Biol 15:81–112

LaBonne C, Bronner-Fraser M (2000) Snail-related transcriptional repressors are required in *Xenopus* for both the induction of the neural crest and its subsequent migration. Dev Biol 221:195–205

Lammer EJ, Opitz JM (1986) The DiGeorge anomaly as a developmental field defect. Am J Med Genet (Suppl) 2:113–127

Lammer EJ, Chen DT, Hoar RM, Agnish ND, Benke PJ, Braun JT, Curry CJ, Fernhoff PM, Grix AW, Lott IT (1985) Retinoic acid embryopathy. New Engl J Med 313:837–841

Le Douarin NM (1969) Particularités du noyau interphasique chez la caille japonaise (*Coturnix coturnix japonica*). Utilisation de ces particularités comme 'marquage biologique' dans les recherches sur les interactions tissulaires et les migrations cellulaires au cours de l'ontogenèse. Bull Biol Fr Belg 103:435–452

Le Douarin NM (1973) A Feulgen-positive nucleolus. Exp Cell Res 77:459–468

Le Douarin NM (2004) The avian embryo as a model to study the development of the neural crest: a long and still ongoing story. Mech Dev 121:1089–1102

Le Douarin NM, Kalcheim C (1999) The Neural Crest, 2nd ed. Cambridge University Press, Cambridge

Le Lièvre CS, Le Douarin NM (1975) Mesenchymal derivatives of the neural crest: Analysis of chimaeric quail and chick embryos. J Embryol Exp Morphol 34:125–154

Lemire RJ, Cohen MM Jr, Beckwith JB, Kokich VG, Siebert JR (1981) The facial features of holoprosencephaly in anencephalic human specimens. I. Historical review and associated malformations. Teratology 23:297–303

Leussink B, Brouwer A, El Khattabi M, Poelmann RE, Gittenberger-de Groot AC, Meijlink F (1995) Expression patterns of the paired-related homeobox genes MHox/Prx1 and S8/Prx2 suggest roles in development of the heart and the forebrain. Mech Dev 52:51–64

Lindsay EA (2001) Chromosomal microdeletions: Dissecting *del22q11* syndrome. Nat Rev Genet 2:858–868

Lindsay EA, Baldini A (2001) Recovery from arterial growth delay reduces penetrance of cardiovascular defects in mice deleted for the DiGeorge syndrome region. Hum Mol Genet 10:997–1002

Lindsay EA, Botta A, Jurcic V, Carattini-Rivera S, Cheah YC, Rosenblatt HM, Bradley A, Baldini A (1999) Congenital heart disease in mice deficient for the DiGeorge syndrome region. Nature 401:379–383

Lindsay EA, Vitelli F, Su H, Morishima M, Huyuh T, Pramparo T, Jurcic V, Ogunrinu G, Sutherland HF, Scambler PJ, et al. (2001) Tbx1 haploinsufficiency in the DiGeorge syndrome region causes aortic arch defects in mice. Nature 410:97–101

Linker C, Bronner-Fraser M, Mayor R (2000) Relationship between gene expression domains of Xsnail, Xslug and Xtwist and cell movement in the prospective neural crest of *Xenopus*. Dev Biol 224:215–225

Locascio A, Nieto MA (2001) Cell movements during vertebrate development: Integrated tissue behaviour versus individual cell migration. Curr Opin Genet Dev 11:464–469

Lumsden A, Guthrie S (1991) Alternating patterns of cell surface properties and neural crest cell migration during segmentation of the chick embryo. Development (Suppl) 2:9–15

Manley NR, Capecchi MR (1995) The role of *Hoxa-3* in mouse thymus and thyroid development. Development 121:1989–2003

Mark M, Ghyselinck NB, Chambon P (2004) Retinoic acid signalling in the development of branchial arches. Curr Opin Genet Dev 14:591–598

Marres HAM, Cremers CWRJ, Dixon MJ, Huygen PLM, Joosten FBM (1995) The Treacher Collins syndrome: A clinical, radiological and genetic linkage study of two pedigrees. Arch Otolaryngol Head Neck Surg 121:509–514

Marsh KL, Dixon MJ (2001) Treacher Collins syndrome. In: Scriver CR, Beaudet AL, Sly WS, Valle D (eds) The Metabolic & Molecular Bases of Inherited Disease, 8th ed. McGraw-Hill, New York, pp 6147–6152

Mathijssen IMJ (2000) Craniosynostosis: Clinical and fundamental aspects. Thesis, Erasmus University Rotterdam

Matsunaga E, Shiota K (1977) Holoprosencephaly in human embryos: Epidemiologic studies of 150 cases. Teratology 16:261–272

Matsuo I, Kuratani S, Kimura C, Takeda N, Aizawa S (1995) Mouse *Otx2* functions in the formation and patterning of rostral head. Genes Dev 9:2646–2658

Mavrogiannis LA, Antonopoulou I, Baxova A, Kutilek S, Kim C,A, Sugayama SM, Salamanca A, Wall SA, Morriss-Kay GM, Wilkie AO (2001) Haploinsufficiency of the human homeobox gene ALX4 causes skull ossification defects. Nat Genet 27:17–18

Mayor R, Morgan R, Sargent MG (1995) Induction of the prospective neural crest of *Xenopus*. Development 121:767–777

Menezes AH, VanGilder JC, Graf CJ, McDonnell DE (1980) Craniocervical abnormalities: A comprehensive surgical approach. J Neurosurg 53:444–455

Mérida-Velasco JA, Sánchez-Montesinos I, Espín-Ferra J, García-García JD, Roldan-Schilling V (1993) Developmental differences in the ossification process of the human corpus and ramus mandibulae. Anat Rec 235:319–324

Meijlink F, Beverdam A, Brouwer A, Oosterveen TC, ten Berge D (1997) Vertebrate *aristaless*-related genes. Int J Dev Biol 43:651–663

Ming JE, Muenke M (1998) Holoprosencephaly: From Homer to hedgehog. Clin Genet 53:155–163

Mo R, Freer AM, Zinyk DL, Crackower MA, Michaud J, Heng HH, Chik KW, Shi XM, Tsui LC, Cheng SH, et al. (1997) Specific and redundant functions of Gli2 and Gli3 zinc finger genes in skeletal patterning and development. Development 124:113–123

Morriss-Kay GM, Ward SJ (1999) Retinoids and mammalian development. Int Rev Cytol 188:73–131

Muenke M, Beachy PA (2001) Holoprosencephaly. In: Scriver CR, Beaudet AL, Sly WS, Valle D (eds) The Metabolic & Molecular Bases of Inherited Disease, 8th ed. McGraw-Hill, New York, pp 6203–6230

Muenke M, Wilkie AOM (2001) Craniosynostosis syndromes. In: Scriver CR, Beaudet AL, Sly WS, Valle D (eds) The Metabolic & Molecular Bases of Inherited Disease, 8th ed. McGraw-Hill, New York, pp 6117–6146

Muenke M, Gripp KW, McDonald-McGinn DM, Gaudenz K, Whitaker LA, Barlett SP, Markowitz RI, Robin NH, Nwokoro N, Mulvihill JJ, et al. (1997) A unique point mutation in the fibroblast growth factor receptor 3 gene (FGFR3) defines a new craniosynostosis syndrome. Am J Hum Genet 60:555–564

Müller F, O'Rahilly R (1980) The human chondrocranium at the end of the embryonic period, proper, with particular reference to the nervous system. Am J Anat 159:33–58

Müller F, O'Rahilly R (1983) The first appearance of the major divisions of the human brain at stage 9. Anat Embryol (Berl) 168:419–432

Müller F, O'Rahilly R (1985) The first appearance of the neural tube and optic primordium in the human embryo at stage 10. Anat Embryol (Berl) 172:157–169

Müller F, O'Rahilly R (1986) The development of the human brain and the closure of the rostral neuropore at stage 11. Anat Embryol (Berl) 175:205–222

Müller F, O'Rahilly R (1988a) The development of the human brain from a closed neural tube at stage 13. Anat Embryol (Berl) 177:203–224

Müller F, O'Rahilly R (1988b) The first appearance of the future cerebral hemispheres in the human embryo at stage 14. Anat Embryol (Berl) 177:495–511

Müller F, O'Rahilly R (1989) Mediobasal prosencephalic defects, including holoprosencephaly and cyclopia, in relation to the development of the human forebrain. Am J Anat 185:391–414

Müller F, O'Rahilly R (1994) Occipitocervical segmentation in staged human embryos. J Anat (Lond) 185:251–258

Murdoch-Kinch CA, Ward RE (1997) Metacarpophalangeal analysis in Crouzon syndrome: Additional evidence for phenotypic convergence with the acrocephalosyndactyly syndromes. Am J Med Genet 73:61–66

Nagai T, Aruga J, Takada S, Günther T, Spörle R, Shughart K, Mikoshiba K (1997) The expression of the mouse Zic1, Zic2, and Zic3 genes suggests an essential role for Zic genes in body pattern formations. Dev Biol 182:299–313

Nagai T, Aruga J, Minowa O, Sugimoto T, Ohno Y, Noda T, Mikoshiba K (2000) Zic2 regulates the kinetics of neurulation. Proc Nat Acad Sci USA 97:1618–1623

Nakatsu T, Uwabe C, Shiota K (2000) Neural tube closure in humans initiates at multiple sites: Evidence from human embryos and implications for the pathogenesis of neural tube defects. Anat Embryol (Berl) 201:455–466

Nanni L, Ming JE, Bocian M, Steinhaus K, Bianchi DW, de Die-Smulders C, Giannotti A, Imaizumi K, Jones KL, Del Campo M, et al. (1999) The mutational spectrum of the Sonic hedgehog gene in holoprosencephaly: SHH mutations cause a significant proportion of autosomal dominant holoprosencephaly. Hum Mol Genet 8:2479–2488

Nanni L, Croen LA, Lammer EJ, Muenke M (2000) Holoprosencephaly: Molecular study of a Californi population. Am J Med Genet 90:315–319

Naora H, Kimura M, Otani H, Yokoyama M, Koizumi I, Katiuki M, Tanaka O (1994) Transgenic mouse model of hemifacial microsomia: Cloning and characterization of insertional mutation region on chromosome 10. Genomics 23:515–519

Nelson FN, Hecht JT, Horton WA, Butler IJ, Goldie WD, Miner M (1988) Neurological basis of respiratory complications in achondroplasia. Ann Neurol 24:89–93

Newgeen DF, Scheel M, Kaster V (1986) Morphogenesis of sclerotome and neural crest cells in avian embryos: In vivo and in vitro studies on the role of notochordal extracellular material. Cell Tissue Res 244:299–313

Nguyen VH, Schmid B, Trout J, Connors SA, Ekker M, Mullins MC (1998) Ventral and lateral regions of the zebrafish gastrula, including the neural crest progenitors, as established by a bmp2/swirl pathway of genes. Dev Biol 199:103–110

Nguyen VH, Trout J, Connors SA, Andermann P, Weinberg E, Mullins MC (2000) Dorsal and intermediate neuronal cell types of the spinal cord are established by a BMP signaling pathway. Development 127:1209–1220

Niederreither K, Vermot J, Le Roux I, Schuhbaur B, Chambon P, Dollé P (2003) The regional pattern of retinoic acid synthesis by RALDH2 is essential for the development of the posterior pharyngeal arches and the enteric nervous system. Develolment 130:2525–2534

Nieto MA, Sargent MG, Wilkinson DG, Cooke J (1994) Control of cell behavior during vertebrate development by slug, a zinc finger gene. Science 264:835–839

Nishimura Y (1993) Embryological study of nasal cavity development in human embryos with reference to congenital nostril atresia. Acta Anat (Basel) 147:140–144

Noden DM (1978a) The control of avian cephalic neural crest cytodifferentiation. I. Skeletal and connective tissues. Dev Biol 67:296–312

Noden DM (1978b) The control of avian cephalic neural crest cytodifferentiation. II. Neural tissues. Dev Biol 67:313–329

Noden DM (1983a) The role of the neural crest in patterning of avian cranial skeletal, connective, and muscle tissues. Dev Biol 96:144–165

Noden DM (1983b) The embryonic origins of avian craniofacial muscles and associated connective tissues. Am J Anat 186:257–276

Noden DM (1991a) Cell movements and control of patterned tissue assembly during craniofacial development. J Craniofac Genet Dev Biol 11:192–213

Noden DM (1991b) Vertebrate craniofacial development: The relation between ontogenetic process and morphological outcome. Brain Behav Evol 38:190–225

Norman MG, McGillivray BC, Kalousek DK, Hill A, Poskitt PJ (1995) Congenital Malformations of the Brain. Pathologic, embryologic, clinical, radiologic and genetic aspects. Oxford University Press, New York

Norris EH (1937) The parathyroid glands and lateral thyroid in man: Their morphogenesis, histogenesis, topographic anatomy and prenatal growth. Contrib Embryol Carnegie Instn 26:247–294

Norris EH (1938) The morphogenesis and histogenesis of the thymus gland in man: In which the origin of Hassall's corpuscle of the human thymus is discovered. Contrib Embryol Carnegie Instn 27:191–207

O'Leary DDM, Wilkinson DG (1999) Eph receptors and ephrins in neural development. Curr Opin Neurobiol 9:65–73

Oostrom CAM, Vermeij-Keers C, Gilbert PM, van der Meulen JC (1996) Median cleft of the lower lip and mandible: Case reports, a new embryological hypothesis and subdivision. Plast Reconstr Surg 97:313–319

Opperman LA (2000) Cranial sutures as intramembranous growth sites. Dev Dyn 219:472–485

O'Rahilly R (1966) The early development of the eye in staged human embryos. Contrib Embryol Carnegie Instn 38:1–42

O'Rahilly R (1973) Developmental stages in human embryos. Part A: Embryos of the first three weeks (stages 1 to 9). Carnegie Institution of Washington Publication 631, Washington, DC

O'Rahilly R (1983) The timing and sequence of events in the development of the human eye and ear. Anat Embryol (Berl) 168: 87–99

O'Rahilly R, Gardner E (1971) The timing and sequence of events in the development of the human nervous system during the embryonic period proper. Z Anat Entw Gesch 134:1–12

O'Rahilly R, Müller F (1981) The first appearance of the human nervous system at stage 8. Anat Embryol (Berl) 163:1–13

O'Rahilly R, Müller F (1999) The Embryonic Human Brain. An atlas of developmental stages, 2nd ed. Wiley-Liss, New York

O'Rahilly R, Müller F (2001) Human Embryology & Teratology, 3rd ed. Wiley-Liss, New York

Osumi-Yamashita N, Iseki S, Noji S, Nohno T, Koyama E, Taniguchi S, Doi H, Eto K (1992) Retinoic acid treatment induces the ectopic expression of retinoic acid receptor β gene and excessive cell death in the embryonic mouse face. Dev Growth Diff 34:199–209

Pane M, Baranello G, Battaglia D, Donvito V, Carnevale F, Stefanini MC, Guzetta F, Mercuri E, Bertini E (2004) Severe abnormalities of the pons in two infants with Goldenhar syndrome. Neuropediatrics 35:234–238

Park WJ, Theda C, Maestri NE, Meyers GA, Fryburg JS, Dufresne C, Cohen MM Jr, Jabs EW (1995) Analysis of phenotypic features and FGFR2 mutations in Apert syndrome. Am J Hum Genet 57:321–328

Passos-Bueno MR, Wilcox WR, Jabs EW, Sertie AL, Alonso LG, Kitoh H (1999) Clinical spectrum of fibroblast growth factor receptor mutations. Hum Mut 14:115–125

Pauli RM, Pettersen JC, Arya S, Gilbert EF (1983) Familial agnathia-holoprosencephaly. Am J Med Genet 14:677–698

Pfeiffer RA (1964) Dominant erbliche Akrocephalosyndactylie. Z Kinderheilk 90:310–320

Phelps PD, Poswillo D, Lloyd GAS (1981) The ear deformities in mandibulofacial synostosis. Clin Otolaryngol 6:15–28

Politzer G (1952) Zur normalen und abnormen Entwicklung des menschlichen Gesichtes. Z Anat Entw Gesch 116:332–347

Poswillo D (1973) The pathogenesis of the first and second branchial arch syndrome. Oral Surg 35:302–328

Poswillo D (1975) The pathogenesis of the Treacher Collins syndrome (mandibulofacial dysostosis). Br J Oral Surg 13:1–26

Pratt RM, Goulding EH, Abbott BD (1987) Retinoic acid inhibits migration of cranial neural crest cells in the cultured mouse embryo. J Craniofac Genet Dev Biol 7:205–217

Preston RA, Post JC, Keats BJB, Aston CE, Ferrell RE, Priest J, Nouri N, Losken HW, Morris CA, Hurtt MR, et al. (1994) A gene for Crouzon craniofacial dysostosis maps to the long arm of chromosome 10. Nat Genet 7:149–153

Qu S, Niswender KD, Ji QS, van der Meer R, Keeney D, Magnuson MA, Wisdom R (1997) Polydactyly and ectopic ZPA formation in Alx-4 mutant mice. Development 124:3999–4008

Read AP (2001) Waardenburg syndrome. In: Scriver CR, Beaudet AL, Sly WS, Valle D (eds) The Metabolic & Molecular Bases of Inherited Disease. McGraw-Hill, New York, pp 6097–6116

Reardon W, Winter RM, Rutland P, Pulleyn LJ, Jones BM, Malcolm S (1994) Mutations in the fibroblast growth factor receptor 2 gene cause Crouzon syndrome. Nat Genet 8:98–103

Reid CS, Pyeritz RE, Kopits SE, Maria BL, Wang H, McPherson RW, Hurko O, Phillips JA, Rosenbaum AE (1987) Cervicomedullary compression in young patients with achondroplasia: Value of comprehensive neurologic and respiratory evaluation. J Pediatr 110:522–530

Rijli FM, Mark M, Lakharaju S, Dierich A, Dollé P, Chambon P (1993) A homeotic transformation is generated in the rostral branchial region of the head by disruption of *Hoxa-2*, which acts as a selector gene. Cell 75:1333–1349

Rijli FM, Gavalas A, Chambon P (1998) Segmentation and specification in the branchial region of the head: The role of the *Hox* selector genes. Int J Dev Biol 42:393–401

Roessler E, Muenke M (1998) Holoprosencephaly: A paradigm for the complex genetics of brain development. J Inher Metab Dis 21:481–497

Roessler E, Belloni E, Gaudenz K, Jay P, Berta P, Scherer SW, Tsui L-C, Muenke M (1996) Mutations in the human *Sonic Hedgehog* gene cause holoprosencephaly. Nat Genet 14:357–360

Roessler E, Du Y-Z, Muller JL, Casas E, Allen WP, Gillessen-Kaesbach G, Raeder ER, Ming JE, Ruiz i Altaba A, Muenke M (2003) Loss-of-function mutations in the human *GLI2* gene are associated with pituitary anomalies and holoprosencephaly-like features. Proc Nat Acad Sci USA 100:13424–13429

Ronen GM, Andrews WL (1991) Holoprosencephaly as a possible embryonic alcohol effect. Am J Med Genet 40:151–154

Rosa F, Piazza-Hepp T, Goetsch R (1994) Holoprosencephaly with 1st trimester topical isotretinoin. Teratology 49:418–419

Roubicek M, Spranger J, Wende S (1981) Frontonasal dysplasia as an expression of holoprosencephaly. Eur J Pediatr 137:229–231

Ryan AK, Goodship JA, Wilson DI, Philip N, Levy A, Seidel H, Schuffenbauer S, Oechsler H, Belohradsky B, Prieur M, et al. (1997) Spectrum of clinical features associated with interstitial chromosome 22q11 deletions: A European collaborative study. J Med Genet 34:798–804

Saethre H (1931) Ein Beitrag zum Turmschädelproblem (Pathogenese, Erblichkeit, und Symptomologie). Dtsch Z Nervenheilk 117:533–555

Sakai Y (1989) Neurulation in the mouse: Manner and timing of neural tube closure. Anat Rec 223:194–203

Sandikcioglu M, Molsted K, Kjaer I (1994) The prenatal development of the human nasal and vomeronasal bones. J Craniofac Genet Dev Biol 14:124–134

Santagati F, Rijli FM (2003) Cranial neural crest and the building of the vertebrate head. Nat Rev Neurosci 4:806–818

Sasai Y, De Robertis EM (1997) Ectodermal patterning in vertebrate embryos. Dev Biol 182:5–20

Sato N, Matsuishi T, Utsunomiya N, Yamashita Y, Horikoshi T, Okudera T, Hashimoto T (1987) Aicardi syndrome with holoprosencephaly and cleft lip and palate. Pediatr Neurol 3:114–116

Scambler PJ (1994) DiGeorge syndome and related birth defects. Sem Dev Biol 5:303–310

Scambler PJ (2000) The 22q11 deletion syndromes. Hum Mol Genet 9:2421–2426

Schier AF (2001) Axis formation and patterning in zebrafish. Curr Opin Genet Dev 11:393–404

Schinzel A (1983) Catalogue of Unbalanced Chromosome Aberrations in Man. De Gruyter, Berlin

Schneider RA, Hu D, Rubinstein JLR, Maden M, Helms JA (2001) Local retinoid signaling coordinates forebrain and facial morphogenesis by maintaining FGF8 and SHH. Development 128:2755–2767

Sechrist J, Serbedzija GN, Scherson T, Fraser SE, Bronner-Fraser M (1993) Segmental migration of the hindbrain neural crest does not arise from its segmental generation. Development 118:691–703

Sedano HO, Cohen MM Jr, Jirásek JE, Gorlin RJ (1970) Frontonasal dysplasia. J Pediatr 76:906–913

Sedlackova E (1967) The syndrome of the congenitally shortened velum. The dual innervation of the soft palate. Folia Phoniatr Logop 19:441–443

Sefton M, Sánchez S, Nieto MA (1998) Conserved and divergent roles for members of the Snail family of transcription factors in the chick and mouse embryo. Development 125:3111–3121

Shin SH, Kogerman P, Lindstom E, Toftgard R, Biesecker LG (1999) GLI3 mutations in human disorders mimic Drosophila cubitus interruptus protein functions and localization. Proc Nat Acad Sci USA 96:288–304

Shiota K (1993) Teratothanasia: Prenatal loss of abnormal conceptuses and the prevalence of various malformations during human gastrulation. Birth Defects 29:189–199

Shprintzen RJ, Goldberg RB, Lewin HL, Sidoti EJ, Berkman MD, Argamaso RV (1978) A new syndrome involving cleft palate, cardiac anomalies, typical facies, and learning disabilities: Velo-cardio-facial syndrome. Cleft Palate J 15:56–62

Siebert J, Cohen MM Jr, Sulik KK, Shaw C-M, Lemire RJ (1990) Holoprosencephaly: An overview and atlas of cases. Wiley-Liss, New York

Smith DW, Töndury G (1978) Origin of the calvaria and its sutures. Am J Dis Child 132:662–666

Smits-van Prooije AE (1986) Processes Involved in Normal and Abnormal Fusion of the Neural Walls in Murine Embryos. Thesis, University of Leiden

Smits-van Prooije AE, Vermeij-Keers C, Poelmann RE, Mentink MMT, Dubbeldam JA (1985) The neural crest in presomite to 40-somite murine embryos. Acta Morphol Neerl-Scand 23:99–114

Smits-van Prooije AE, Vermeij-Keers C, Poelmann RE, Mentink MMT, Dubbeldam JA (1988) The formation of mesoderm and mesectoderm in 5- to 41-somite rat embryos cultured in vitro, using WGA-Au as a marker. Anat Embryol (Berl) 177:245–256

Sperber GH (2001) Craniofacial Development. Decker, Hamilton

Sperber GH (2002) Craniofacial embryogenesis: Normal developmental mechanisms. In: Mooney MP, Siegel MI (eds) Understanding Craniofacial Anomalies: The etiopathogenesis of craniosynostosis and facial clefting. Wiley-Liss, New York, pp 31–59

Sperber GH, Gorlin RJ (1997) Head and neck. In: Gilbert-Barness E (ed) Potter's Pathology of the Fetus and Infant. Mosby, St. Louis, MI, pp 1541–1579

Sperber GH, Honore LH, Johnson ES (1986) Acalvaria, holoprosencephaly and facial dysmorphia syndrome. In: Melnick M (ed) Current Concepts in Craniofacial Anomalies. Liss, New York, pp 318–329

Spritz RA, Chiang P-W, Oiso N, Alkhateeb A (2003) Human and mouse disorders of pigmentation. Curr Opin Genet Dev 13:284–289

Starck D (1975) Embryologie, 3rd ed. Thieme, Stuttgart

Streeter GL (1906) On the development of the membranous labyrinth and the acoustic and facial nerves in the human embryo. Am J Anat 6:139–165

Streeter GL (1918) The histogenesis and growth of the otic capsule and its contained periotic tissue-spaces in the human embryo. Contrib Embryol Carnegie Instn 7:5–54

Streeter GL (1922) Development of the auricle in the human embryo. Contrib Embryol Carnegie Instn 14:111–138

Sulik KK (1996) Craniofacial development. In: Turvey TA, Vig KWL, Fonseca RJ (eds) Facial Clefts and Synostosis – Principles and Management. Saunders, Philadelphia, PA, pp 3–27

Sulik KK, Johnston MC, Daft PA, Russell WE (1986) Fetal alcohol syndrome and DiGeorge anomaly: Critical ethanol exposure periods for craniofacial malformations as illustrated in an animal model. Am J Med Genet 2:191–194

Sulik KK, Johnston MC, Smiley SJ, Speight HS, Jarvis BE (1987) Mandibulofacial dysostosis (Treacher Collins syndrome): A new proposal for its pathogenesis. Am J Med Genet 27:359–372

Sulik KK, Cook CS, Webster WS (1988) Teratogens and craniofacial malformations: Relationship to cell death. Development 103:213–231

Sun X, Meyers EN, Lewandoski M, Martin GR (1999) Targeted disruption of Fgf8 causes failure of cell migration in the gastrulating mouse embryo. Genes Dev 13:1834–1846

Tan S-S, Morriss-Kay G (1985) The development and distribution of the cranial neural crest in the rat embryo. Cell Tissue Res 240:403–416

Taylor AI (1968) Autosomal trisomy syndrome: A detailed study of 27 cases of Edwards' syndrome and 27 cases of Patau's syndrome. J Med Genet 5:227–252

ten Berge D, Brouwer A, El Bahi S, Guénet JL, Robert B, Meijlink F (1998a) Mouse *Alx3*: an *aristaless*-like homeobox gene expressed during embryogenesis in ectomesenchyme and lateral plate mesoderm. Dev Biol 199:11–25

ten Berge D, Brouwer A, Korving J, Martin JF, Meijlink F (1998b) *Prx1* and *Prx2* in skeletogenesis: Roles in the craniofacial region, inner ear and limbs. Development 125:3831–3842

ten Berge D, Brouwer A, Korving J, Reijnen MJ, van Raaij EJ, Verbeek F, Gaffield W, Meijlink F (2001) *Prx1* and *Prx2* are upstream regulators of sonic hedgehog and control cell proliferation during mandibular arch morphogenesis. Development 128:2929–2938

The Treacher Collins Syndrome Collaborative Group (1996) Positional cloning of a gene involved in the pathogenesis of Treacher Collins syndrome. Nat Genet 12:130–136

Tint OS, Irons M, Elias ER, Batta AK, Frieden R, Chen TS, Salen G (1994) Defective cholesterol biosynthesis associated with Smith-Lemli-Opitz syndrome. N Engl J Med 330:107–113

Trainor PA, Krumlauf R (2000) Patterning the cranial neural crest: Hindbrain segmentation and *Hox* gene plasticity. Nature Rev Neurosci 1:116–124

Trainor PA, Tan S-S, Tam PPL (1994) Cranial paraxial mesoderm: Regionalisation of cell fate and impact on craniofacial development in mouse embryos. Development 120:2397–2408

Trainor PA, Sobieszczuk D, Wilkinson D, Krumlauf R (2002) Signalling between the hindbrain and paraxial tissues dictates neural crest migration pathways. Development 129:433–442

Treacher Collins E (1900) Cases with symmetrical congenital notches in the outer part of each lower lid and defective development of the malar bones. Trans Ophthalmol Soc UK 20: 190–192

Van De Water TR, Noden DM, Maderson PFA (1988) Embryology of the ear: Outer, middle and inner. Otol Med Surg 1:3–27

van Oostrom CG (1972) De initiële regionale ectoderm-ontwikkeling in het kopgebied bij de muis. Thesis, University of Amsterdam (in Dutch)

Veitch E, Begbie J, Schilling TF, Smith MM, Graham A (1999) Pharyngeal arch patterning in the absence of neural crest. Curr Biol 9:1481–1484

Verloes A, Dodinval P, Beco L, Bonnivert J, Lambotte C (1990) Lambotte syndrome: Microcephaly, holoprosencephaly, intrauterine growth retardation, facial anomalies, and early lethality – a new sublethal multiple congenital anomaly/mental retardation syndrome in four sibs. Am J Med Genet 37:119–123

Vermeij-Keers C (1972) Transformations in the facial region of the human embryo. Adv Anat Embryol Cell Biol 46:1–30

Vermeij-Keers C (1990) Craniofacial embryology and morphogenesis: Normal and abnormal. In: Stricker M, van der Meulen JC, Raphael B, Mazzola R, Tolhurst DE (eds) Craniofacial Malformations. Churchill Livingstone, Edinburgh, pp 27–60

Vermeij-Keers C, Poelmann RE (1980) The neural crest: A study on cell degeneration and the improbability of cell migration in mouse embryo. Neth J Zool 30:74–81

Vermeij-Keers C, Mazzola RF, van der Meulen JC, Stricker M, Raphael B (1983) Cerebro-craniofacial and craniofacial malformations: An embryological analysis. Cleft Palate J 20:128–145

Vermeij-Keers C, Poelmann RE, Smits-van Prooije AE, van der Meulen JC (1984) Hypertelorism and the median cleft face syndrome. An embryological analysis. Ophth Pediatr Genet 4:97–105

Vermeij-Keers C, Poelmann RE, Smits-van Prooije AE (1987) 6.5-mm Human embryo with a single nasal placode: Cyclopia or hypotelorism? Teratology 36:1–6

Vermot J, Niederreither K, Garnier JM, Chambon P, Dollé P (2003) Decreased embryonic retinoic acid synthesis results in a DiGeorge syndrome phenotype in newborn mice. Proc Natl Acad Sci USA 100:1763–1768

Verwoerd CDA, van Oostrom CG (1979) Cephalic neural crest and placodes. Adv Anat Embryol Cell Biol 58:1–75

Vieille-Grosjean I, Hunt P, Gulisano M, Boncinelli E, Thorogood P (1997) Branchial HOX gene expression and human craniofacial development. Dev Biol 183:49–60

Vitelli F, Taddei I, Morishima M, Meyers EN, Lindsay Ea, Baldini A (2002) A genetic link between *Tbx1* and fibroblast growth factor signaling. Development 129:4605–4611

Waardenburg PJ (1951) A new syndrome combining developmental anomalies of the eyelids, eyebrows and nose root with pigmentary defects of the iris and head hair and with congenital deafness. Am J Hum Genet 3:195–253

Wackenheim A (1967) Les dysplasies des condyles occipitaux. Ann Radiol 11:535–543

Wallis DE, Roessler E, Hehr U, Nanni L, Wiltshire T, Richieri-Costa A, Gillessen-Kaesbach G, Zackai EH, Rommens J, Muenke M (1999) Mutations in the homeodomain of the human *SIX3* gene cause holoprosencephaly. Nat Genet 22:196–198

Warren SM, Greenwald JA, Spector JA, Bouletreau P, Mehrara BJ, Longaker MT (2001) New developments in cranial suture research. Plast Reconstr Surg 107:523–540

Webster WS, Johnston MC, Lammer EJ, Sulik KK (1986) Isotretinoin embryopathy and the cranial neural crest: An in vivo and in vitro study. J Craniofac Genet Dev Biol 6:211–222

Weinstein DC, Hemmati-Brivanlou A (1999) Neural induction. Annu Rev Cell Dev Biol 15:411–433

Weller GL Jr (1933) Development of the thyroid, parathyroid and thymus glands in man. Contrib Embryol Carnegie Instn 24:93–142

Whiteford ML, Tolmie JL (1996) Holoprosencephaly in the west of Scotland 1975-1994. J Med Genet 33:578–584

Wiley MJ, Cauwenbergs P, Taylor IM (1983) Effects of retinoic acid on the development of the facial skeleton in hamsters; early changes involving neural crest cells. Acta Anat 116:180–192

Wilkie AOM (1997) Craniosynostosis: Genes and mechanisms. Hum Mol Genet 6:1647–1656

Wilkie AOM, Morriss-Kay GM (2001) Genetics of craniofacial development and malformation. Nat Rev Neurosci 2:458–468

Wilkie AO, Slaney SF, Oldridge M, Poole MD, Ashworth GJ, Hockley AD, Hayward RD, David DJ, Pulleyn LJ, Rutland P, et al. (1995) Apert syndrome results from localized mutations of FGFGR2 and is allelic with Crouzon syndrome. Nat Genet 9:165–172

Willhite CC, Hill RM, Irving AW (1986) Isotretinoin-induced craniofacial malformations in humans and hamsters. J Craniofac Genet Dev Biol 6:193–209

Wilson PA, Lagna G, Suzuki A, Hemmati-Brivanlou A (1997) Concentration-dependent patterning of the *Xenopus* ectoderm by BMP4 and its signal transducer Smad1. Development 124:3177–3194

Wong GB, Mulliken JB, Benacerraf BR (2001) Prenatal diagnosis of major craniofacial anomalies. Plast Reconstr Surg 108:1316–1333

Wraith JE, Super M, Watson GH, Phillips M (1985) Velo-cardio-facial syndrome presenting as holoprosencephaly. Clin Genet 27:408–410

Wright S, Wagner K (1934) Types of subnormal development of the head from inbred strains of guinea pigs and their bearing on the classification and interpretation of vertebrate monsters. Am J Anat 54:383

Wu J, Saint-Jeannet J-P, Klein PS (2003) Wnt-frizzled signaling in neural crest formation. Trends Neurosci 26:40–45

Wu YQ, Badano JL, McCaskill C, Vogel H, Potocki L, Shaffer LG (2000) Haploinsufficiency of ALX4 as a potential cause of parietal foramina in the 11p11.2 contiguous gene-deletion syndrome. Am J Hum Genet 67:1327–1332

Wuyts W, Cleiren E, Homfray T, Rasore-Quartino A, Vanhoenacker F, Van Hul W (2000a) The ALX4 homeobox gene is mutated in patients with ossification defects of the skull. J Med Genet 37:916–920

Wuyts W, Reardon W, Preis S, Homfrey T, Rasore-Quartino A, Christians H, Willems PJ, Van Hul W (2000b) Identification of mutations in the *MSX2* homeobox gene in families affected with foramina parietalia permagna. Hum Mol Genet 9:1251–1255

Wyszinski DF, ed (2002) Cleft Lip and Palate: From origin to treatment. Oxford University Press, Oxford

Yagi H, Furutani Y, Hamada H, Sasaki T, Asakawa S, Minoshima S, Ichida F, Joo K, Kimura M, Imamura S-I, et al. (2003) Role of *TBX1* in human del22q11.2 syndrome. Lancet 362:1366–1373

Zhao Q, Behringer RR, DeCrombrugghe B (1996) Prenatal folic acid treatment suppresses acrania and meroanencephaly in mice mutant for the *Cart1* homeobox gene. Nat Genet 13:275–283

Development and Developmental Disorders of the Spinal Cord

Hans J. ten Donkelaar and Akira Hori

6.1 Introduction

Even after its development is complete, the spinal cord remains a rather simple structure with a ventral, motor horn, a dorsal, sensory horn and an intermediate zone in between. Rexed (1952, 1954) introduced a subdivision of the spinal grey matter of the cat into ten layers, laminae I–X. His subdivision is now widely used (for human data see Schoenen and Faull 1990). The dorsal and ventral roots divide the spinal white matter into posterior (dorsal), lateral and anterior (ventral) funiculi. Classic birthdating studies by Altman and Bayer (1984) have demonstrated a ventral-to-dorsal gradient of histogenesis in the spinal cord with motoneurons appearing first, followed by neurons in the intermediate zone and, finally, neurons in the dorsal horn. Recent studies have unraveled many of the molecular mechanisms that specify cell fates in the spinal cord (reviewed in Lee and Jessell 1999; Jessell 2000; Briscoe and Ericson 2001; Caspary and Anderson 2003; Price and Briscoe 2004). A number of homeodomain and basic helix–loop–helix containing transcription factors has been identified that are expressed in the spinal ventricular zone in specific dorsoventral domains. In the spinal cord, the sequential production of motor, relay and interneuron populations is parallelled by the appearance of descending supraspinal, propriospinal and ascending spinal projections around the same time with dorsal root fibres clearly lagging behind. The most frequent developmental disorders of the spinal cord are due to neural tube defects (Chap. 4), but other malformations may also result in developmental anomalies of the spinal cord, such as duplication of the cord, displacement of the cord by neurenteric cysts, syringomyelia and abnormal course or even absence of main fibre tracts.

In this chapter developmental events of spinal neuronal populations, the specification of spinal cell fates, the development of dorsal root, spinal ascending and descending supraspinal projections, and developmental anomalies of the spinal cord other than neural tube defects will be discussed.

6.2 Gross Development of the Spinal Cord

The morphology of the spinal cord in a 5-month-old fetus is shown in Fig. 6.1a. Clearly visible are the cervical and lumbar enlargements, the cauda equina and the dorsal root ganglia. Early development of the human spinal cord is shown in Fig. 6.2. Bayer and Altman (2002) presented an atlas of the human spinal cord from the fourth gestational week to the fourth postnatal month. Since the first description by His (1886) four plates have been distinguished in the developing spinal cord (Fig. 6.2). Lateral to the central canal a dorsal alar plate, giving rise to the neurons of the sensory dorsal horn, and a ventral basal plate, giving rise to the motoneurons of the ventral horn, are found separated by the sulcus limitans. The alar plates are united by a thin roof plate that caps the central canal, whereas the floor plate forms the base of the spinal cord. On the basis of their extensive autoradiographic data, Altman and Bayer (1984, 2001) introduced an intermediate plate, and suggested that the dorsal (alar) neuroepithelium of the spinal cord gives rise to the sensory neurons of the dorsal horn, the ventral (basal) neuroepithelium to the motoneurons, and the intermediate neuroepithelium to the interneurons of the intermediate zone. The dorsal root ganglion (DRG) cells are derived from the neural crest. Their axons form two branches, one towards the periphery, the other towards the alar plate. Except for the occipital region, where ganglia are missing, each spinal ganglion corresponds to one somite. The central branches of the DRG cells form the dorsal roots of the spinal nerves. The developing motoneurons form the ventral roots of the spinal nerves. Between the fifth and sixth weeks of development, a myotome becomes divided into a dorsal epaxial part or epimere and a ventrolateral hypaxial part, the hypomere (Fig. 6.3). The spinal nerves divide into dorsal rami for the dorsal musculature or epimere (mainly the erector spinae) and overlying skin, and ventral rami for the hypomeric ventral musculature, including the muscles of the limbs, and the corresponding skin. The ventral rami of the spinal nerves at cervical and lumbosacral levels soon form the brachial and lumbosacral plexuses for the innervation of the limbs.

Fig. 6.1 a Dorsal view of the spinal cord in a 5-month-old fetus. **b** MRI of a tethered spinal cord in a newborn, due to a spinal lipoma (**a** from the Collection of the Anatomical Museum Nijmegen; kindly provided by Jos Dederen, Nijmegen; **b** kindly provided by Ton van der Vliet, Nijmegen)

Fig. 6.2 Photomicrographs of the human spinal cord at Carnegie stages 13 (**a**) and 16 (**b**) (taken from the Kyoto Collection of Human Embryos)
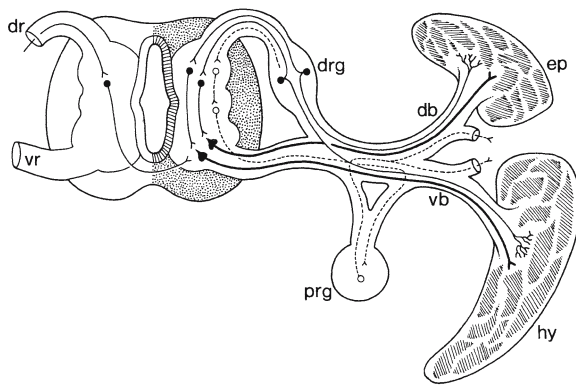
Fig. 6.3 Myotomal derivatives and their innervation. *db* dorsal branch, *dr* dorsal root, *drg* dorsal root ganglion, *ep* epimere, *hy* hypomere, *prg* paravertebral (sympathetic) ganglion, *vb* ventral branch, *vr* ventral root

6.2.1 A Few Notes on the Development of the Vertebral Column

The vertebral column develops from the sclerotomes of the somites (Fig. 6.4). First, an unsegmented perichordal sheath is formed by cells spreading out from the sclerotomes. Second, loose, rostral and dense caudal areas form in a sclerotome. The loose zones of the sclerotomes are traversed by the intersegmental arteries and the spinal nerves. The dense parts form the neural arches of the vertebrae. Third, dense and loose zones also become evident in the cellular sheath of the notochord. The loose rostral zone forms the vertebral centrum, whereas the dense caudal zone becomes the intervertebral disc. Differential proliferation may be the main factor in establishing the alternating pattern of loosely and densely arranged mesenchymal zones (Rickenbacher et al. 1982; Verbout 1985; Christ 1990; O'Rahilly and Müller 2001). Finally, the neural processes will unite and close the neural arch. The sclerotomes from one pair of somites give rise to the caudal and cranial halves of two adjacent vertebrae. The formation of cartilage in the vertebral column begins at six postovulatory weeks and is far advanced at the end of the embryonic period (O'Rahilly and Meyer 1979). Ossification is detectable at about 9 weeks of development. In neonates, most vertebrae consist of cartilage with three ossification centres, one for the centrum and one for each half of the neural arch, giving a typical X-ray image. The transient occipitocervical region develops differently. Its four sclerotomes participate in the formation of the basi-occipital unit of the skull base (Chap. 5).

Variations in number, form and position of vertebrae are rather common (Töndury 1958; O'Rahilly et al. 1980, 1983, 1990a, b; Müller et al. 1986; Theiler 1988). Theiler (1988) studied the development of the vertebral column in 30 mutants of the laboratory mouse. Malformations of the vertebral column may be caused by disturbances of the somites, the notochord, and sclerotome differentiation. The majority of vertebral malformations such as fused and deformed vertebrae are caused by somite disturbances at early stages of development (in mice, embryos of 9–11 days). In the thoracic region, the combined appearance of deformed vertebrae and fused ribs is characteristic for somite disturbances. The human vertebral column usually consists of 24 presacral vertebrae. The last lumbar vertebra may be incorporated into the sacrum (*sacralization*), whereas the first sacral vertebra may be freed (*lumbarization*). Some *vertebral anomalies* are summarized in Fig. 6.5. Most
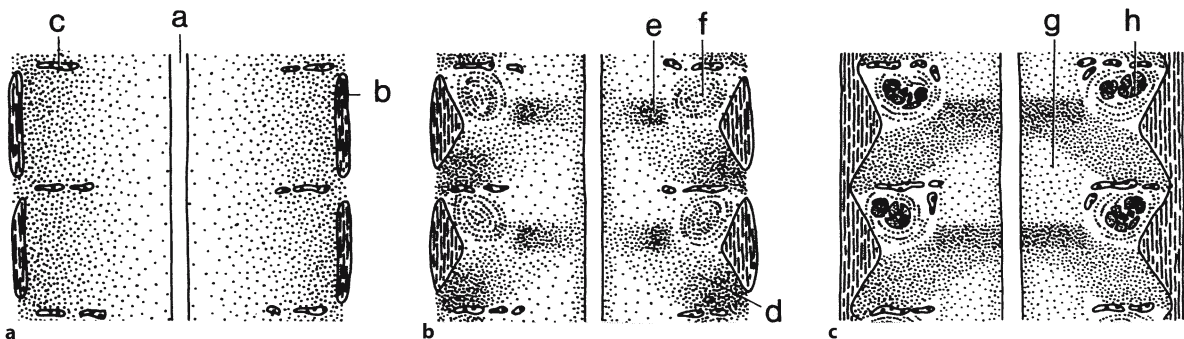
Fig. 6.4 The development of the vertebral column. **a** Around the notochord (*a*) non-segmentally arranged medial sclerotome mesenchyme is found, whereas more lateral parts of the sclerotome, close to the myotome (*b*), are more densely arranged and separated by segmental blood vessels (*c*). **b** The mesenchyme around the notochord is composed of alternating dense zones (*e*) from which the intervertebral discs arise, and looser zones from which the vertebral bodies arise. In the denser caudolateral parts of the sclerotomes (*d*) the vertebral arches and processes are formed, whereas in its less dense rostrolateral parts, the spinal nerves arise (*f*). **c** The contours of the vertebral bodies (*g*) and spinal nerves (*h*) are clearer. (After Verbout 1985, and Christ 1990)
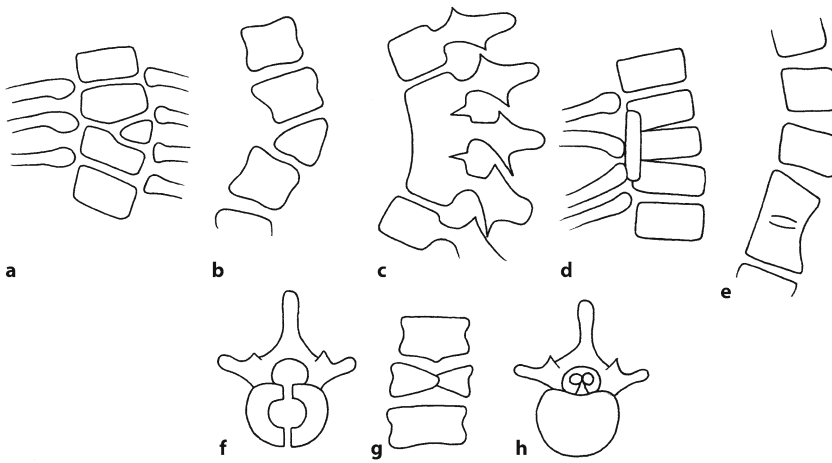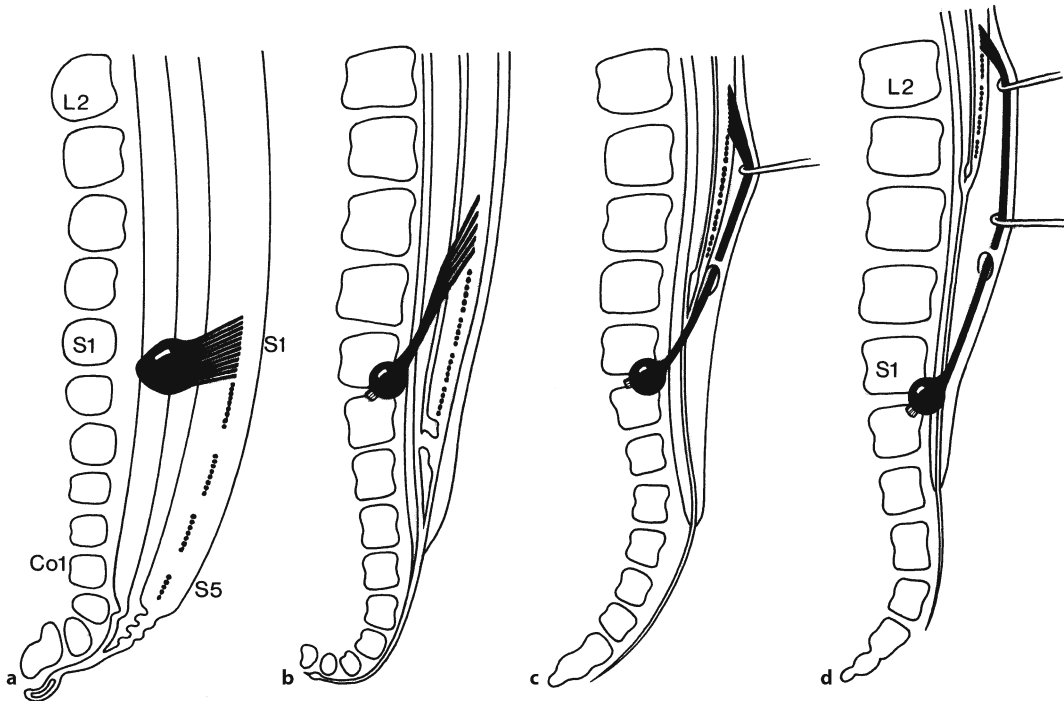
Fig. 6.6 'Ascensus medullae': **a**–**d** four successive stages in the development of the caudal end of the human spinal cord. They show the formation of the filum terminale and the pro-gressive obliquity of the first sacral nerve (*S1*). *L2*, *S1* and *Co1* mark the second lumbar, first sacral and first coccygeal verte-brae. (After Streeter 1919)

common are spina bifida, hemivertebrae, block verte-brae and cleft vertebrae. In *diastematomyelia*, a bony spur may lead to a duplication of the spinal cord (Sect. 6.8.2).

6.2.2   Ascensus Medullae

At the end of the embryonic period, the spinal cord still extends to the end of the vertebral column (Fig. 6.6). During the fetal period, it 'ascends' to lum-bar levels owing to disproportional growth of the spinal cord and the vertebral column. Until the 11th gestational week the length of the spinal cord match-es that of the vertebral column (Streeter 1919). Then, the 'ascensus' starts, the filum terminale is formed and the lower spinal nerves show a progressive obliq-uity caused by the shift between the spinal cord and the vertebral column. Collectively, the lower spinal roots form the cauda equina. In the newborn, the spinal cord ends at the level of the third lumbar ver-tebra, and in adults mostly at the level of the first or second lumbar vertebra. Developmental anomalies may lead to a tethered spinal cord (Fig. 6.1b). The
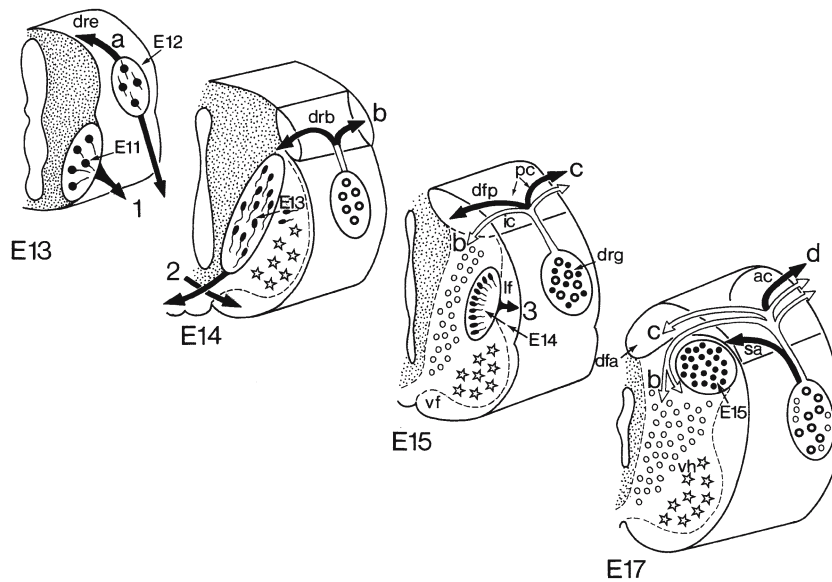
Fig. 6.7 Main developmental events in the rat cervical spinal cord from E13 until E17. At E13, onset of growth of peripheral motor fibres from the early-generated motoneurons (*E11*) and of sensory fibres from the early-generated dorsal root ganglion cells (*E12*) takes place (*1*). At E14, the ventral commissure and ventral funiculi are formed (*2*) by the axons of contralaterally projecting relay neurons that are generated at E13. At E15, lateral migration of the ipsilaterally projecting relay neurons (generated around E14) occurs (*3*), and interneurons in the dorsal horn and small dorsal root ganglion cells are generated. At E17, the dorsal funicular ascending zone is formed.

a–d The ingrowth of dorsal root fibres: **a** arrival of the earliest dorsal root fibres at the dorsal root entrance zone (*dre*); **b** formation of the dorsal root bifurcation zone (*drb*); **c** formation of the dorsal funiculus propriospinal zone (*dfp*) by the ingrowing intersegmental dorsal root collaterals; **d** formation of the dorsal funicular ascending zone (*dfa*) by the growing suprasegmental dorsal root collaterals. *ac* ascending dorsal root collaterals, *ic* intrasegmental collaterals, *lf* lateral funiculus, *pc* propriospinal collaterals, *sa* small-caliber collaterals, *vf* ventral funiculus, *vh* ventral horn. (After Altman and Bayer 1984)

tethered cord syndrome is usually reserved for lumbosacral defects in which there are variable combinations of thickening of the filum terminale, low or dilated conus medullaris, spinal lipoma, dermoid cyst, split cord, hydromyelia and sacral agenesis (Chap. 4). Clinical signs associated with cord tethering include lower limb motor and sensory deficits and neuropathic bladder. The severity of symptoms increases with age and patients are frequently treated surgically by untethering the spinal cord.

6.3 Developmental Events in Spinal Neuronal Populations

In rats, spinal neurons are generated in a sequential order from ventral to dorsal (Altman and Bayer 1984, 2001): first, the basal plate generates the motoneurons, followed by the intermediate plate that generates the relay neurons in the intermediate zone, and finally the alar plate produces the interneurons in the dorsal horn (Fig. 6.7, Table 6.1). Motoneurons are produced over a 2-day period: peak production is at E12 at cervical levels, and at E14 at thoracic and lum-

bar levels. The bulk of DRG cells are produced between E15 and E17. Large ganglion cells are generated before small ones. In general, contralaterally projecting interneurons appear to be generated earlier than the ipsilaterally projecting relay neurons (Nandi et al. 1993). The earliest dorsal root fibres enter the spinal cord at E13 at cervical levels (Altman and Bayer 1984). With carbocyanine dyes, Snider and et al. (1992) traced the outgrowth of dendrites of cervical motoneuron pools and the development of dorsal root projections to these motor pools (Mirnics and Koerber 1995). At E15, the first day at which dorsal root fibres could be seen entering the cervical cord, the lateral motoneurons extend their dendrites medially or dorsomedially into the direction of the incoming dorsal root fibres. Between E15 and E17 dorsal root fascicles converge in the intermediate zone and fan out en route to the motor pools. Between E17 and E19 there is dense branching and bouton formation of muscle (Ia) afferents in the area of the motor pools.

Leber et al. (1989, 1990) used recombinant retroviruses as markers to study the lineage of motoneurons in the chick spinal cord. The descendants of infected cells were not only motoneurons but also in-

Table 6.1 Time of neuron origin data in the rat spinal cord (after Altman and Bayer 1984) and estimated data for the human spinal cord (after Bayer et al. 1995; Altman and Bayer 2001)

Time of neuron origin	Rat	Man
Motoneurons		
Cervical cord	E11–E12	3.5–5.7 weeks of development
Thoracic cord	E12–E13	4.1–5.7 weeks of development
Lumbar cord	E12–E13	4.1–5.7 weeks of development
Intermediate zone	E13–E15	4th to 5th week
Dorsal horn (substantia gelatinosa)	E15–E16	6.7–7.4 weeks of development
Dorsal root ganglion cells	E12–E15	4th to 5th week
Ascending tract neurons		
Contralaterally projecting neurons	E12–E13	4.1–5.7 weeks of development
Ipsilaterally projecting neurons	E14	5.8–6.6 weeks of development

terneurons in the ventral and intermediate parts of the spinal cord and even astrocytes and oligodendrocytes. Clonally related motoneurons were not restricted to a single motor pool. Some clones contained motoneurons in both the medial and the lateral parts of the lateral motor column, known to innervate different groups of limb muscles. Some clones even contained motoneurons in the medial motor column (innervating axial muscles such as the erector spinae) as well as in the lateral motor column.

Several types of interneurons can be distinguished in the spinal cord of rodents (Wentworth 1984b; Silos-Santiago and Snider 1992, 1994). In the rat thoracic cord, Silos-Santiago and Snider (1992) noted seven different types of commissural interneurons, i.e. interneurons with a contralaterally projecting axon, by E13.5. By E15, commissural interneurons were found near their final locations in the dorsal horn, the intermediate zone and the ventral horn. By E19, at least 18 different types of commissural interneurons were found. Also an increasing number of ipsilaterally projecting interneurons was found in the thoracic spinal cord from E14 until E19 (Silos-Santiago and Snider 1994). Therefore, the rat embryonic spinal cord contains a large number of ipsilaterally projecting as well as commissural interneurons. In general, descending supraspinal, propriospinal and ascending spinal projections appear to be formed around the same time, with dorsal root fibres clearly lagging behind. Spinal motoneurons first establish contacts with their target muscles, and subsequently are innervated by propriospinal fibres, descending supraspinal fibres and, finally, dorsal root collaterals.

In mice, motoneurons are generated at E10 and E11, neurons in the intermediate zone from E11 to E14, and dorsal horn neurons from E12 to E14 (Nornes and Carry 1978). Large DRG cells are generated in peak numbers at E10.5, whereas small DRG cells arise in greatest numbers at E12 (Sims and Vaughn 1979). The first axodendritic synaptic contacts on mouse lateral motoneurons, presumably propriospinal in origin, were found on E11 (Vaughn et al. 1977; Wentworth 1984a). Both axodendritic and axosomatic synapses were found at E12. Most of the early-forming, lateral motoneuronal dendrites grow into the lateral marginal zone, where they come into contact with axons of interneurons. The initial trajectories of sensory axons to the spinal cord were studied with carbocyanine tracing (Sect. 6.5). In the human spinal cord, neurons are generated in a similar sequential order as in rodents between the third and sixth weeks of development (Altman and Bayer 2001; Table 6.1).

6.4   The Specification of Cell Fates in the Spinal Cord

In general, neuronal subtypes in the ventral spinal cord, arising from the basal plate, regulate motor output, whereas neurons in the dorsal spinal cord, arising from the alar plate, mediate and integrate sensory input. The development of both sets of neurons is induced by extracellular signalling molecules, secreted by the notochord and the adjacent ectoderm. The Sonic hedgehog (SHH) protein of the *Sonic hedgehog* (*Shh*) gene in the notochord induces the formation of the floor plate (Jessell 2000; Placzek et al. 2000; Patten et al. 2003). In its turn, the floor plate induces the formation of motoneurons and ventral interneurons in the basal plate. Bone morphogenetic proteins from the ectoderm induce the formation of the alar and roof plates. These secreted factors act in opposing gradients to pattern the spinal cord by acting on prepatterning homeodomain and proneural basic helix–loop–helix transcription factor genes (Fig. 6.8). Different sets of prepatterning and proneural genes are involved in the specification of ventral and dorsal spinal cell types (Lee and Jessell 1999; Briscoe and Ericson 2001; Sharma and Peng 2001; Caspary and Anderson 2003; Gómez-Skarmeta et al. 2003; Price and Briscoe 2004).
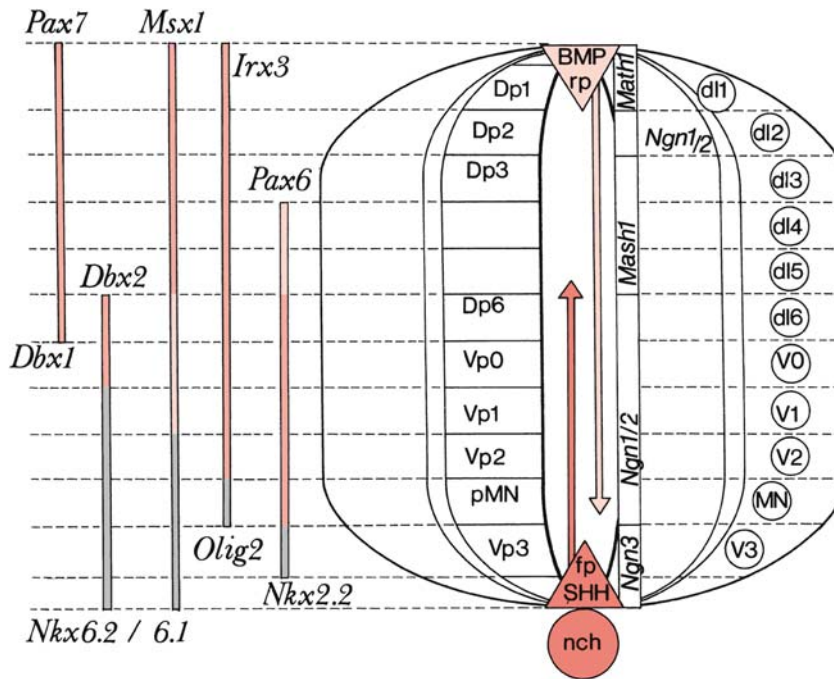
Fig. 6.8 Expression patterns of secreted factors, proneural and dorsoventral prepatterning genes in the vertebrate spinal cord. The secreted factors Sonic hedgehog (*SHH*) from the notochord (*nch*) and the floor plate (*fp*) and bone morphogenetic proteins (*BMP*) from the roof plate (*rp*) act in opposing gradients to pattern the spinal cord by acting on prepattern (at the *left*) and proneural (indicated within the spinal cord) genes in different dorsal/ventral territories. The prepatterning genes *Nkx2.2*, *Nkx6.1* and *Nkx6.2* are expressed in ventral-to-dorsal domains. *Olig2* is expressed in a ventral domain within the *Nkx6.1* territory. *Msx1*, *Pax7*, *Irx3* and *Pax6* are expressed in dorsal-to-ventral domains. *Dbx1* and *Dbx2* are expressed in in-termediate territories. The combinatorial code of these factors specifies different progenitor domains (*Dp1–Dp6*, *Vp0–Vp3* and *pMN*), in which the corresponding neurons (*dl1–dl6* dorsal interneurons, *V0–V3* ventral interneurons *MN* motoneurons) are specified. The proneural gene *Math1* is expressed in a dorsal domain that is complementary to a dorsal domain that expresses *Ngn1* and *Ngn2*. *Mash1* is expressed in an intermediate territory that separates the dorsal and ventral domains of *Ngn1/2*. *Ngn3* is expressed adjacent to the floor plate. (After Diez del Corral and Storey 2001; Marti and Bovolenta 2002; Gómez-Skarmeta et al. 2003)

6.4.1   Specification of Neuronal Fates in the Ventral Spinal Cord

SHH from the notochord is required to pattern the ventral neural tube. Ectopic expression of SHH is capable of inducing ventral spinal cord cell types (Echelard et al. 1993; Roelink et al. 1994), whereas eliminating SHH function by antibody blockade or gene targeting prevents the differentiation of floor plate cells, motoneurons, ventral interneurons and oligodendrocytes (Marti et al. 1995; Chiang et al. 1996; Ericson et al. 1996, 1997; Orentas et al. 1999; Pierani et al. 1999; Litingtung and Chiang 2000; Ruiz i Altaba 2003). The dorsalmost ventral interneurons do not depend on SHH signalling, but can be induced by a parallel, retinoid-mediated pathway (Pierani et al. 1999). In the ventral spinal cord, graded concentrations of SHH set up domains of gene expression along the ventrodorsal axis (Fig. 6.8). Progressively two- to threefold changes in SHH concentration generate five molecularly distinct classes of ventral neurons, the motoneurons and the V0, V1, V2 and V3 types of interneurons. Two classes of homeodomain proteins expressed by these ventral progenitor cells act as intermediary factors in the interpretation of the graded SHH signalling (Pierani et al. 1999; Briscoe et al. 2000; Briscoe and Ericson 2001; Ruiz i Altaba 2003). The expression of each class I protein (Dbx1, Dbx2, Irx3, Pax6, and Pax7) is repressed at a distinct SHH concentration, so that their ventral boundaries of expression delineate progenitor domains. In contrast, the expression of each class II protein (Nkx2.2, Nkx6.1, Nkx6.2 and Olig2) requires SHH signalling and is achieved at a distinct SHH concentration, so that their dorsal boundaries delineate progenitor domains. Postmitotic motoneurons are marked by the expression of *Isl1/Isl2* and *Hb9*, whereas the postmitotic ventral interneurons express the
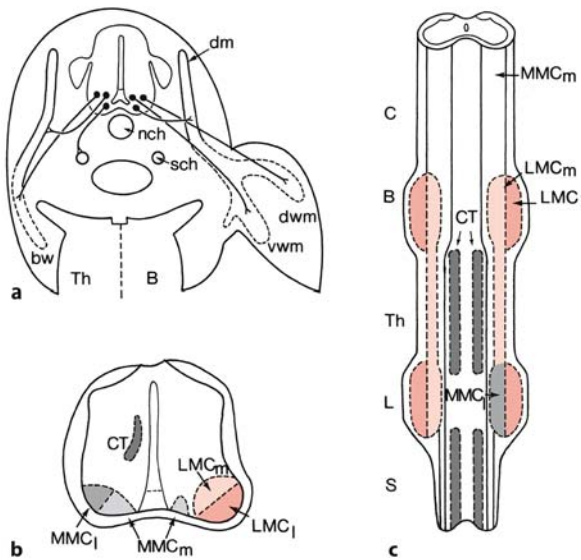
Fig. 6.9 LIM codes in chick spinal motoneurons. A cross section of a E3.5 chick embryo (**a**), a section through the spinal cord of an E8 embryo (**b**) and a ventral view of the spinal cord at E8.5 (**c**). At first (**a**), motoneuron subtypes are intermixed but have distinct pathways in the periphery. Neurons of the medial part of the medial motor column (MMC_m, *grey*) coexpress *Isl1*, *Isl2* and *Lim3* and their axons grow towards the dorsal myotome (*dm*). Neurons of the lateral part of the medial motor column (MMC_l, *dark grey*) coexpress *Isl1* and *Isl2* and grow towards the ventral body wall muscles (*bw*). Axons of neurons of the medial part of the lateral motor column (LMC_m, *light red*) also coexpress *Isl1* and *Isl2* and supply the ventral premuscle mass of the wing (*vwm*). Neurons of the lateral part of the lateral motor column (LMC_l, red) coexpress *Isl2* and *Lim1* and innervate the dorsal premuscle mass (*dwm*). Preganglionic sympathetic neurons of the column of Terni (*CT*, *black*) express *Isl1* and innervate the paravertebral sympathetic chain (*sch*). Later (**b**, **c**), the five motoneuron subtypes, distinguished by their individual *LIM*-homeobox gene codes, have segregated into columns. *C*, *B*, *Th*, *L* and *S* indicate cervical, brachial, thoracic, lumbar and sacral parts of the spinal cord. (After data by Tsuchida et al. 1994)

Fig. 6.10 Organization of motor pools in the chick hindlimb (**a**) and primary motoneurons (**b**) in the zebrafish. **a** Motor pools (*mp*) of the sartorius (*S*), femorotibialis (*F*), adductor (*A*) and ischioflexor (*I*) muscles and their targets are shown in different colours. **b** Primary motoneuron types, characterized by different *LIM3* and *Isl1/2* codes, are shown for one neuromuscular segment. *CaP* caudal primary motoneuron, *dlb* dorsal limb, *MiP* medial primary motoneuron, *RoP* rostral primary motoneuron, *VaP* variable type of primary motoneuron, *vlb* ventral limb. (After Pfaff and Kintner 1998)

Evx1/Evx2, *En1*, *Chx10/Lhx3* and *Sim1* transcription factor genes, respectively (Burrill et al. 1997; Ericson et al. 1997; Matise and Joyner 1997; Arber et al. 1999; Pierani et al. 1999; Briscoe et al. 2000). The initial generation of several neuronal subtypes is only the beginning of the assembly of functional spinal circuits, motor as well as sensory. Spinal motoneurons are further divided into longitudinally organized medial and lateral columns and, subsequently, motoneurons innervating particular muscles are grouped into motor pools. The segregation of spinal motoneurons is correlated with the expression of LIM-homeodomain proteins (Tsuchida et al. 1994; Pfaff and Kintner 1998; Kania et al. 2000). Neurons of the medial part of the medial motor column, innervating dorsal axial muscles such as the erector spinae, coexpress *Isl1*, *Isl2* and *Lim3*, whereas neurons of the lateral part of the medial motor column, innervating ventral axial muscles (ventral body wall muscles), coexpress *Isl1* and *Isl2* only (Fig. 6.9). In a similar way, two parts of the lateral motoneuron column can be characterized by the coexpression of *Isl1* and *Isl2* (a medial part innervating ventral limb muscles) and *Isl2* and *Lim1* (a lateral part innervating dorsal limb muscles), respectively. Examples of the organization of chick motor pools and zebrafish primary motoneurons are shown in Fig. 6.10.

The fate of the various classes of ventral interneurons is only beginning to be unraveled. V1 interneurons appear to be short propriospinal neurons, terminating one to two segments rostrally, close to motoneurons (Saueressig et al. 1999). Possibly, these interneurons represent Renshaw or Ia-inhibiting interneurons (Wenner et al. 1998; Wenner and O'Dono-

van 1999). V0 interneurons are commissural interneurons that project locally over one to four spinal segments (Moran-Divard et al. 2001; Pierani et al. 2001). Throughout vertebrates, certain ventral interneurons are involved in neural networks (central pattern generators) that generate the basic motor patterns underlying rhythmic limb movements. The central pattern generators generate both the rhythm as well as the correct patterns of activities (Grillner 2003; Kiehn and Butt 2003). The ephrin receptor A4 (EphA4) and its ephrin ligand B3 (ephrin-B3) play a role in the construction of the mammalian locomotor network (Kiehn and Butt 2003).

6.4.2 Patterning Cell Types in the Dorsal Spinal Cord

For the proper development of interneurons in the dorsal spinal cord a different set of genes must be expressed (Lee and Jessell 1999; Matise 2002; Caspary and Anderson 2003). In mice, four non-overlapping expression domains of proneural genes define six progenitor types in the dorsal spinal cord at E10 (Gowan et al. 2001). These differentiate into six types of dorsal interneurons (dl1–dl6; Fig. 6.8) which can be characterized by E10 on the basis of the repertoire of the homeodomain transcription factors that they express (Gross et al. 2002; Müller et al. 2002). Proneural genes appear to be required between E9.5 and E12 to initiate the development of distinct neuronal classes. *Math1* is expressed in the dorsalmost cells adjacent to the roof plate (dl1), *neurogenin 1* (*Ngn1*) and *Ngn2* are expressed in domains of the adjacent ventral band of cells (dl2) and *Mash1* is expressed by the progenitors that will become dl3–dl5. The dorsal interneuron subtypes 1–3 (dl1–dl3 cells) migrate ventrally, and the dl4 and a subset of dl5 cells migrate laterally to populate the deep layers of the dorsal horn (laminae IV–V). Another subset of dl5 cells and the dl6 interneurons migrate towards the ventral horn. Three additional populations of interneurons are born later, beginning at E12. Late-born cells, expressing the proneural gene *Math1* and the LIM-homeodomain transcription factor gene *Lhx2a*, settle deep in the dorsal horn near earlier born *Math1*-expressing interneurons. Both cell types may be involved in proprioception. Two other late-born populations derive from dl4 and dl5 cells, and they express either *Pax2* and *Lim1/2*, or *Lmx1b* alone. These cells migrate to the superficial layers of the dorsal horn, where they may mediate pain and temperature. So far, the best understood dorsal interneurons are the dl1 cells which express *Math1*. *Math1*-mutant mice lack dl1 cells (Bermingham et al. 2001; Gowan et al. 2001). The mutants have fewer cells in the population of ventrally projecting commissur-

al neurons, and they show a clear loss of fibres in the spinocerebellar tracts (Arber et al. 2000). Dl2 cells are still present in *Math1*-mutant mice as well as in *Ngn1* mutants, but not in *Ngn1/Ngn2* double-mutant animals (Ma et al. 1999). These mutants lack all dl2 interneurons, and have fewer ventrally projecting commissural neurons, indicating that dl2 cells contribute to this population of propriospinal neurons. The aforementioned data suggest that interneurons derived from *Mash1*-expressing progenitors contribute to both deep and superficial layers of the dorsal horn, whereas *Math1*-expressing cells migrate exclusively to the deep laminae (Caspary and Anderson 2003).

6.5 Development of Dorsal Root Projections

Afferent (sensory) fibres from cutaneous, muscle and joint receptors innervate the spinal cord. After entering the spinal cord, the dorsal root fibres divide into ascending and descending branches. These branches give off collaterals to the dorsal horn. The ascending branches of the thicker fibres reach the dorsal column nuclei in the medulla. The dorsal root fibres vary in thickness. The thickest myelinated fibres (Aα, from muscle spindles and tendon organs) end in the deeper layers of the dorsal horn and partly in the ventral horn (Fig. 6.11). Thick, myelinated fibres from cutaneous receptors (Aβ) end in laminae III–VI of Rexed (Willis and Coggeshall 1991). The thinnest myelinated and unmyelinated dorsal root fibres (Aδ and C), largely from nociceptors, end in laminae I and II and parts of lamina V. With carbocyanine tracers (Fig. 6.12), Snider and co-workers (Snider et al. 1992; Ozaki and Snider 1997) studied the development of the interactions between dorsal root fibres and their targets in the spinal cord of rodents (Kudo and Yamada 1987). In the developing rat spinal cord, Ia axons project towards spinal motoneuron pools in fascicles that exhibit a considerable degree of spatial order. Although motoneuron dendritic projections are well established, the dendrites projecting directly into the path of incoming Ia afferents appear not to guide afferents to appropriate motor pools. The Ia afferents pass over the distal dendrites and grow all the way to the border between grey and developing white matter. Terminal branching and formation of boutons are found in the vicinity of motoneuron somata and proximal dendrites, but hardly on distal dendrites. In mice, Ozaki and Snider (1997) studied the initial trajectories of sensory axons to the thoracic spinal cord. Primary afferent axons reach the thoracic cord at E10.5, and grow rostrocaudally for at least 48 h prior to extending collateral branches into the grey matter. After this 'waiting period', different

classes of murine primary afferent fibres enter the spinal cord in sequence: muscle afferents penetrate the grey matter as early as E13.5, large-caliber sensory afferents first penetrate at E14.5, and most fine cutaneous afferents enter at E15.5. These different classes of sensory axons terminate in different layers of the spinal cord. Apparently, these projections are precise from the entrance of the spinal cord (Ozaki and Snider 1997), and axons are probably guided by intraspinal cues (Sharma and Frank 1998). Candidate ventral cues are the neurotrophin NT-3 and semaphorin-D (Sanes and Yamagata 1999).

In the spinal cord of pyridine silver stained human embryos of 5–8 weeks of estimated menstrual age, i.e. about three to six postovulatory weeks, Windle and Fitzgerald (1937) studied the development of
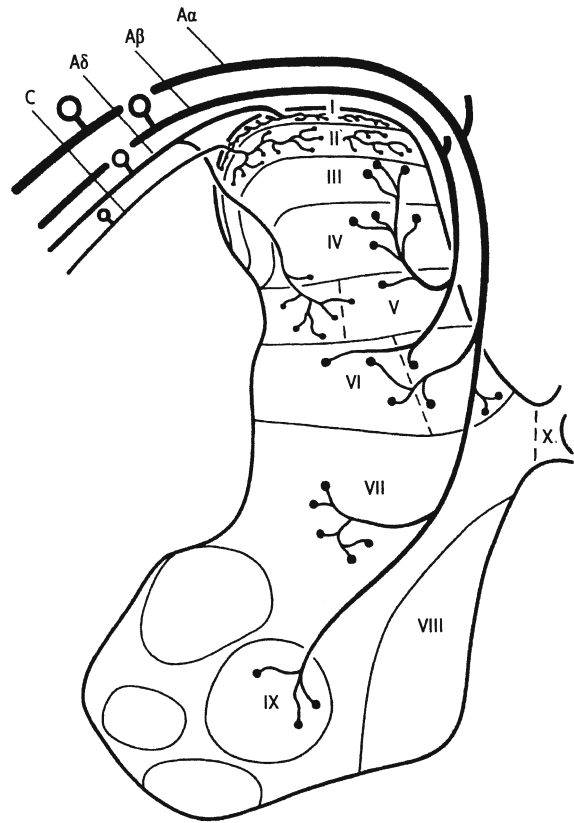
Fig. 6.11 The laminar terminations of dorsal root projections. The thickest myelinated fibres (*Aα*, from muscle spindles and tendon organs) end in the deep parts of the dorsal horn and partly in the ventral horn. Thick, myelinated fibres from cutaneous mechanoreceptors (*Aβ*) end in laminae *III–VI*. The thinnest myelinated (*Aδ*) and unmyelinated (*C*) dorsal root fibres, largely from nociceptors, end in laminae *I* and *II* and in parts of lamina *V*. (After Brodal 1992)
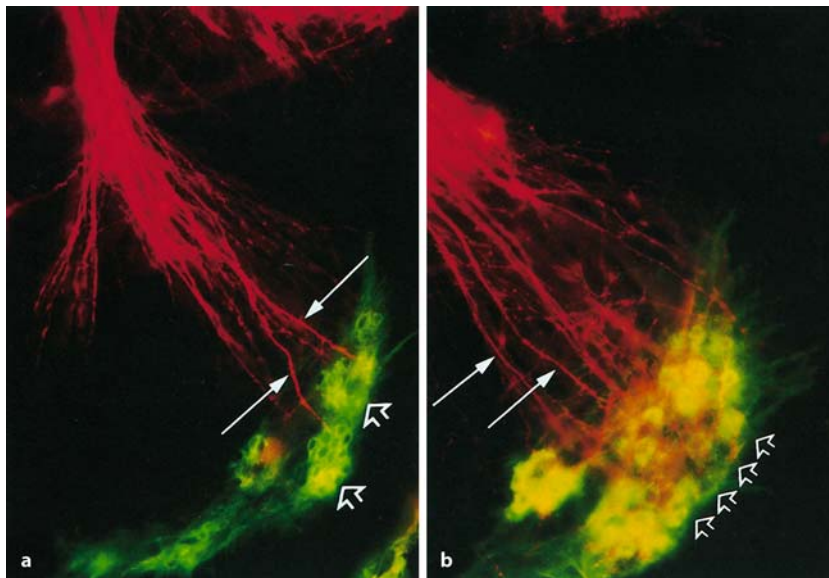
Fig. 6.12 Development of dorsal root projections as found by carbocyanine labelling in rat embryos. Ia-afferent fibres were stained with 1,1′-dioctadecyl-3,3,3′,3′-tetramethylindocarbocyanine perchlorate (*DiI*) and motoneurons with 4,4-dihexadecyl aminostyryl *N*-methylpyridinium iodide (*DiA*). At E17 (**a**), Ia fascicles (*long arrows*) have reached motoneurons somata (*open arrows*). At P2 (**b**), predominantly unbranched Ia fascicles (*long arrows*) reach the motoneuron pool. Terminal branching (*orange*) is on motoneuron somata. *Open arrows* indicate the border between motoneurons and the developing funiculi. (Reproduced with permission from Snider et al. 1992, *J. Neurosci.* 12:3494–3508; copyright 1992, Wiley-Liss Inc, a subsidiary of John Wiley & Sons, Inc.)

Fig. 6.13 a–d Windle and Fitzgerald's data obtained with silver staining in human embryos of 5–8 weeks of gestation. *as* association interneurons, *c* ventral commissure, *col* dorsal root collaterals, *df* dorsal funiculus, *dr* dorsal root, *drg* dorsal root ganglion, *lf*, lateral funiculus, *lmn* lateral motoneurons, *mmn* medial motoneurons, *mn* motoneurons, *sg* substantia gelatinosa, *vf* ventral funiculus, *vr* ventral root. (After Windle and Fitzgerald 1937)
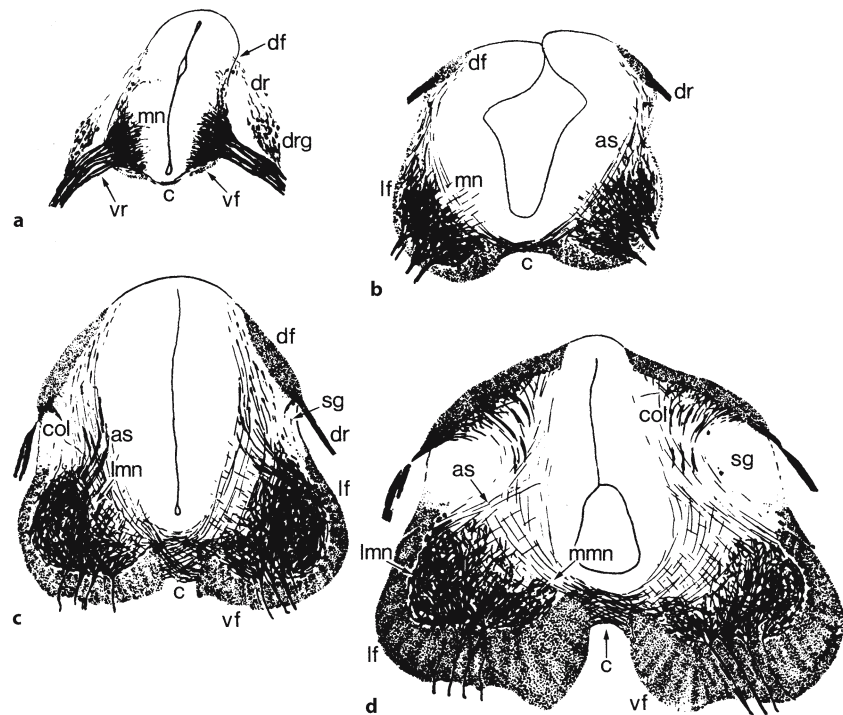
dorsal root projections. At approximately E27 (about Carnegie stage 13/14), DRG cells and motoneurons are present (Fig. 6.13). Central processes of the bipolar ganglion cells reach the spinal cord, where they initiate the formation of the dorsal funiculi. At first, the dorsal funiculi are found only in the cervical spinal cord, and are composed of short fibres, but by stage 15 dorsal funiculi are found throughout most of the spinal cord. At stage 18, collateral branches of primary afferent fibres emerge from the lateral aspect of each dorsal funiculus in the brachial region. A few long collateral branches pass into the lateral division of the ventral horn at stage 20. At this stage of development the ventral funiculus contains descending axons from the brain stem passing via the fasciculus longitudinalis medialis (flm). Most of its other fibres are probably ascending, however (Rhines and Windle 1941). Interneurons with ascending projections send their axons to the floor plate where they cross in the ventral commissure and form contralaterally ascending tracts in the ventrolateral funiculus. Therefore, three components of cutaneous reflex pathways (primary afferent fibres, interneurons and motoneurons) are already found in human embryos of four postovulatory weeks. A rapid differentiation of these components takes place in embryos of six postovulatory weeks (Fig. 6.13 d).

On the basis of extensive analysis of human embryonic material from the Carnegie collection, Altman and Bayer (2001) suggested the following sequence of branching of dorsal root fibres in the cer-

vical spinal cord (Fig. 6.14): (1) following its entry at 5.5 weeks of development, the dorsal root splits into ascending and descending branches; (2) by 7 weeks of development, these branches begin to sprout collaterals in an incipient collateralization zone; (3) by 7.5 weeks, the downwards-growing collaterals form a more definitive collateralization zone; (4) by 8.5 weeks, the continuing outgrowth of local collaterals results in a deepening of the collateralization zone, and ascending branches form the cuneate fascicle; and (5) by 10 weeks of development, ascending axons from caudal segments arrive in the cervical cord and form the gracile fascicle. Konstantinidou et al. (1995) were able to study the development of the dorsal root projections in the fetal human spinal cord between eight and 19 weeks of gestation (about six to 17 postovulatory weeks) using 1,1'-dioctadecyl-3,3,3',3'-tetramethylindocarbocyanine perchlorate (DiI) tracing (Fig. 6.15). Primary afferent fibres were found to enter the spinal grey matter very early in development. By six postovulatory weeks, a few dorsal root axons (presumably muscle spindle afferents) already reached the motor pools. As development progresses, these axons project to the ventral horn and branch in a restricted area in the intermediate zone as well as in the motor pools. Between nine and 17 postovulatory weeks, axon collaterals in the ventral horn form boutons in the proximity of motoneuron somata and their proximal dendrites. Other groups of axons penetrate the spinal grey matter via the mediolateral extent of the dorsal horn to reach

lamina IV, and then turn upwards to terminate in layers III and IV. Probably, these axons arise from DRG cells that innervate low-threshold mechano-receptors.

Okado and co-workers (Okado et al. 1979; Okado 1980, 1981) studied the synaptogenesis in the lateral motor column of the human cervical spinal cord. The first synapses were found in the motor nucleus of the cervical cord in a 10-mm embryo (Carnegie stage 15). Since no dorsal root fibres extend far enough to reach

Fig. 6.14 Hypothetical stages in the sequential branching of dorsal root fibres in the human cervical spinal cord. Following its entry into the spinal cord around 5.5 gestational weeks (**a**), the dorsal root axon splits into ascending and descending branches. By 7 weeks (**b**), the ascending and descending branches begin to sprout local collaterals which form an incipient collateralization zone (*clz*). By 7.5 gestational weeks (**c**), the downwards-growing collaterals form a distinct collateralization zone. By 8.5 weeks (**d**), the cuneate fascicle (*cf*) forms and displaces the collateralization zone laterally. Finally, by ten gestational weeks (**e**), ascending axons from caudal parts of the spinal cord arrive in the cervical cord and form the gracile fascilcle (*gf*). *ab* ascending branch, *bfz* bifurcation zone, *db* descending branch, *dh* dorsal horn. (After Altman and Bayer 2001)
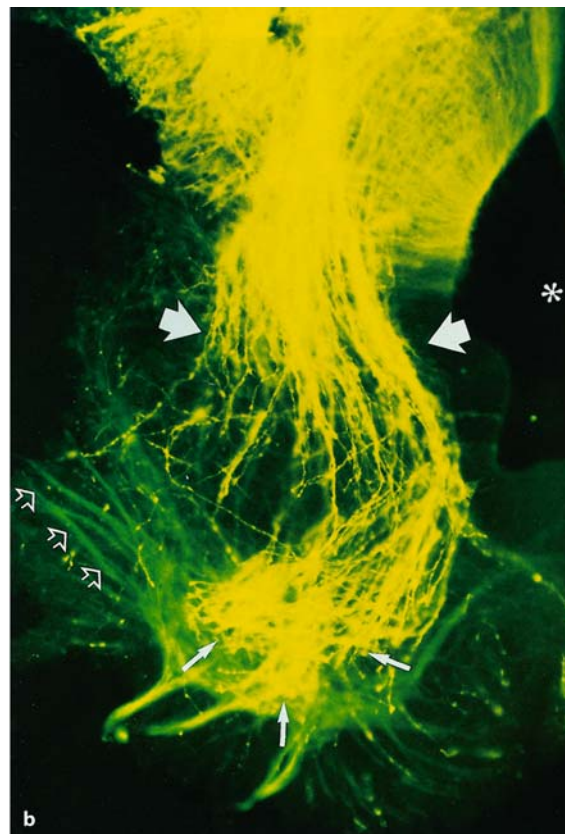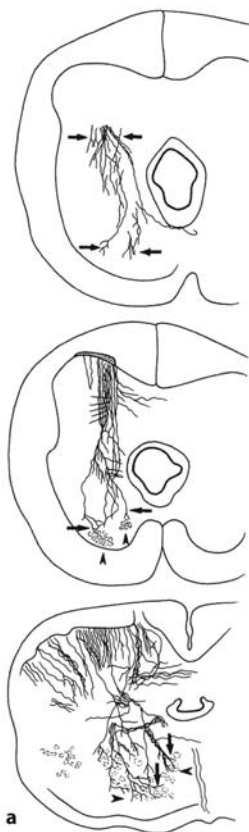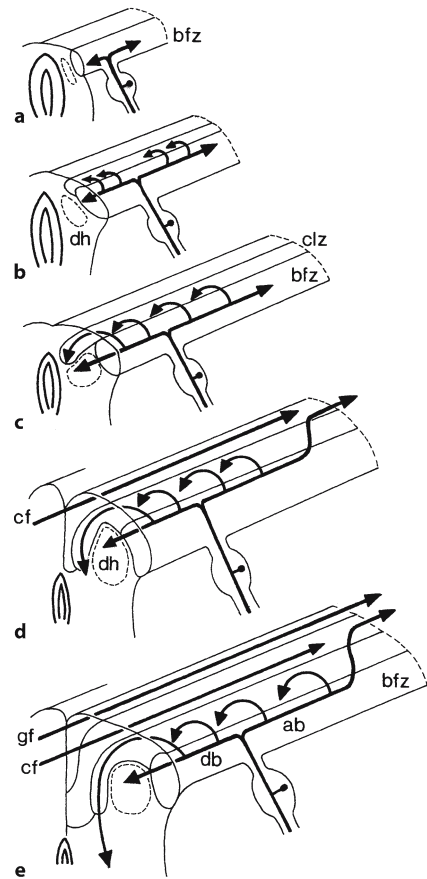
Fig. 6.15 Development of dorsal root projections as found by DiI labelling in the human fetal spinal cord. **a** At 8, 11 and 15 weeks gestational age. A few dorsal root fibres reach the motor pool by 8 weeks. These axons traverse the grey matter in fascicles and defasciculate as they approach the motoneurons (*arrowheads*). These afferents elaborate branches (*arrows*) with increasing complexity. **b** An example of DiI labelling at 11 weeks of gestation. (Reproduced with permission from Konstantinidou et al. 1995, *J. Comp. Neurol.* 354:1–12; copyright 1995, Wiley-Liss Inc, a subsidiary of John Wiley & Sons, Inc.)

Fig. 6.16 Summary of ultrasonic recordings of the first emergence of certain classes of spontaneous movements in human embryos (after de Vries et al. 1982)
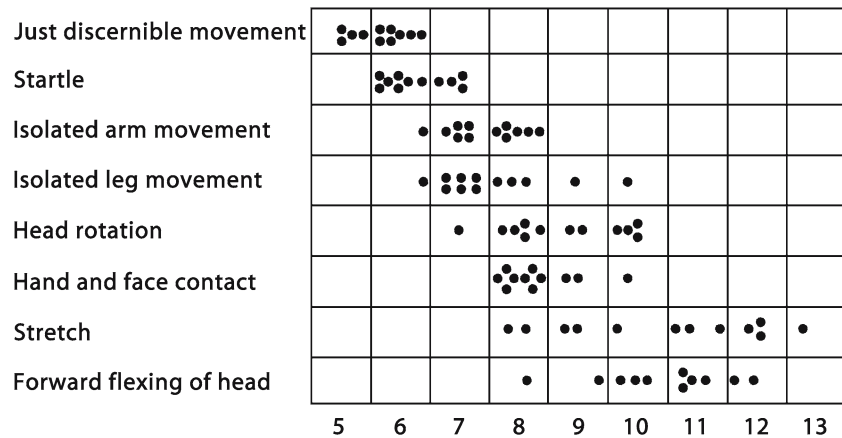
the motor neuropil, these axodendritic synapses probably come from interneurons. The first synapses between dorsal root fibres and interneurons as well as the first axosomatic synapses in the motor neuropil were found at stage 17. During the first 5 months of development there appear to be three critical periods of synaptogenesis coinciding with behavioural changes found in human fetuses (Okado and Kojima 1984): (1) a period of closure of the spinal reflex arc, coinciding with the appearance of spinal reflex activities; (2) a period of rapid increase of axodendritic synapses that corresponds with the onset of local activities (Humphrey 1964); and (3) a period with an increase of axosomatic synapses. Peripheral branches of DRG cells reach the palm of the hand by 8.5 weeks of development (Cauna and Mannon 1961) and contact epithelial cells by about 10.5 weeks (Hogg 1941). Innervation of cutaneous receptors starts between 10.5 and 14.5 weeks (Hogg 1941; Cauna and Mannon 1959).

Using real-time ultrasound, de Vries et al. (1982, 1984) found the first discernible spontaneous movements of the fetus at 7.5 weeks of gestation (about 5.5 postovulatory weeks or approximately stage 16), as already suggested by Hooker's (1938, 1954) experiments on aborted embryos. By the end of the embryonic period, the following types of prenatal movements are discernible by ultrasound (Fig. 6.16): startles, general movements, hiccups, isolated limb movements, head retroflexion and rotation, and hand–face contact. Such movements reflect coordinated motor patterns (de Vries et al. 1982, 1984; Natsuyama 1991). By this time, descending supraspinal pathways arising in the interstitial nucleus of the flm, the reticular formation of the brain stem and the vestibular nuclear complex must have reached the spinal cord (Sect. 6.7).

6.6 Development of Spinal Ascending Projections

The ascending sensory pathways from the spinal cord can be divided into three groups (Willis and Coggeshall 1991): (1) pathways for pain and temperature, i.e. the spinothalamic tract which is accompanied by fibres terminating in the reticular formation (spinoreticular fibres) and fibres to the mesencephalon (spinomesencephalic fibres); (2) pathways for tactile information, vibration and position sense, carried via several pathways, the dorsal funiculus or column in particular; and (3) pathways for somatosensory information to the cerebellum (Fig. 6.17).

Ascending spinal tract neurons begin to differentiate as early as E12 (Altman and Bayer 1984). Waldeyer's cells in the marginal zone, a major source of contralaterally projecting spinothalamic fibres, and several other cells in the intermediate zone giving rise to spinocervical, rostral and ventral spinocerebellar, and some spinothalamic fibres are produced at E12 and E13. The neurons of Clarke's column giving rise to the dorsal spinocerebellar tract are formed at E13. Most neurons of the intermediate zone are generated at E13 and E14. Beal and Bice (1994) showed that lumbar spinothalamic and spinocerebellar neurons are generated between E13 and E15. The primary afferent projections from dorsal root fibres to the dorsal column nuclei also arise prenatally (Chimelli and Scaravilli 1987; Wessels et al. 1991). Projections from the dorsal column nuclei reach the thalamus by the day of birth (Asanuma et al. 1988). Lakke (1997) found the first spinothalamic fibres, anterogradely labelled from cervical injections, in the anterior thalamus at E18.

In human embryos, the dorsal funiculus has reached the caudal brain stem at stage 16, i.e. at about 37 postovulatory days (Müller and O'Rahilly 1989a). Cuneate and gracile decussating fibres forming the
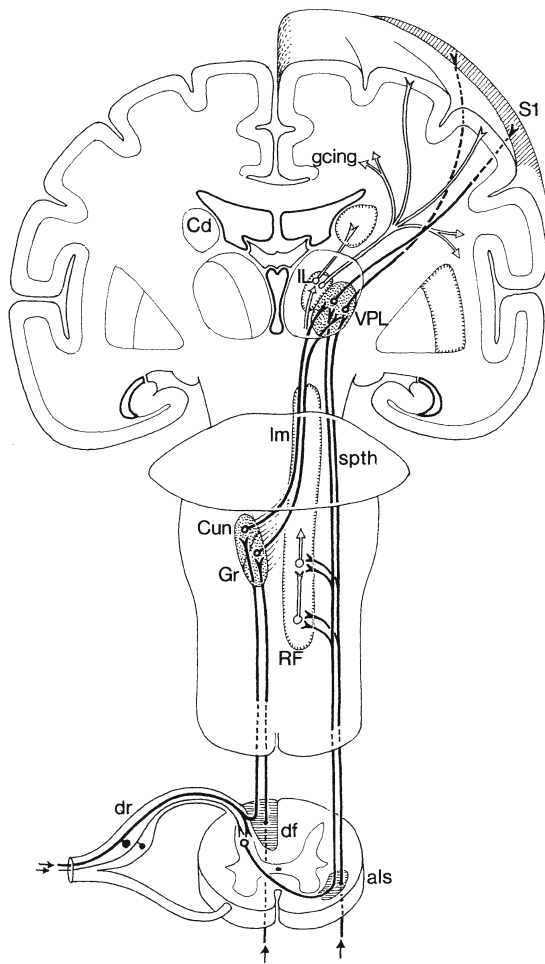
Fig. 6.17 Overview of the human ascending spinal systems for gnostic and vital sensibility. *als* anterolateral system, *Cd* caudate nucleus, *Cun* cuneate nucleus, *df* dorsal funiculus, *dr* dorsal root, *gcing* gyrus cinguli, *Gr* nucleus gracilis, *IL* intralaminar nuclei, *lm* lemniscus medialis, *RF* reticular formation, *S1* primary somatosensory cortex, *spth* spinothalamic tract, *VPL* nucleus ventralis posterolateralis

medial lemniscus are present at stage 20 (Müller and O'Rahilly 1990a,b). Altman and Bayer (2001; Bayer and Altman 2002) studied the growth and maturation of spinal fibre tracts, using the following criteria for maturation: (1) their absence or presence; (2) onset of proliferative gliosis; (3) onset of reactive gliosis; (4) advanced reactive gliosis; (5) onset of myelination; and (6) advanced myelination (Table 6.3). The cuneate and gracile fasciculi become myelinated by the middle of the third trimester, the cuneate before the gracile fascicle. Using, myelin basic protein (MBP) immunohistochemistry, Weidenheim and co-workers (Weidenheim et al. 1992, 1993, 1996; Bodhireddy et al. 1994) showed that in the gracile fascicle

myelination starts at the lumbar level. The dorsal spinocerebellar tract is absent or poorly developed at the beginning of the second trimester (Altman and Bayer 2001). It is present above the lateral corticospinal tract in 20-week-old fetuses. Onset of reactive gliosis in this fibre tract starts in the 26th week of development, and its myelination is evident from 33 weeks onwards. The maturation of the ventral spinocerebellar tract may lag behind that of the dorsal spinocerebellar tract. The spinothalamic tract develops relatively late. It is either absent or very slender in 14-week-old fetuses, and can be delineated from intraspinal tracts by the presence of fewer reactive glia. Reactive gliosis is advanced at 33 weeks and in the perinatal period. Myelination of the spinothalamic tract begins in the late-term neonate.

6.7   Development of Descending Projections to the Spinal Cord

Descending pathways for the control of spinal motor neurons arise in the cerebral cortex, in the hypothalamus and in various brain stem structures, including the reticular formation and the vestibular nuclear complex (Kuypers 1981; Nathan and Smith 1981; Holstege 1991; Nathan et al. 1990, 1996; ten Donkelaar 2000; Fig. 6.18). As regards the course and site of termination of the descending pathways to the spinal cord, a classification can be made into lateral and medial systems (Kuypers 1981). Interstitiospinal, reticulospinal and vestibulospinal pathways from the brain stem pass via the ventral funiculus and ventral parts of the lateral funiculus, and terminate in the mediodorsal parts of the ventral horn and adjacent parts of the intermediate zone. This medial system is functionally related to postural activities and progression, and constitutes a basic system by which the brain exerts control over movements. The lateral system is composed of rubrospinal, some reticulospinal and raphespinal fibres, arising in a rostral, magnocellular part of the medullary raphe nucleus, and the corticospinal tract, all passing via the dorsal part of the lateral funiculus. In vertebrates, the rubrospinal tract terminates in the dorsolateral part of the intermediate zone and plays an important role in the steering of limb movements (ten Donkelaar 2000). The human rubrospinal tract is indistinct (Nathan and Smith 1981) and is superseded by the corticospinal tract. The corticospinal tract arises from layer V pyramidal cells, particularly from rostral, frontal parts of the cerebral cortex (Chap. 10).

The formation of the descending supraspinal pathways occurs according to a developmental sequence. In all tetrapods studied (ten Donkelaar 2000), reticulospinal and interstitiospinal fibres reach the spinal cord first, followed by vestibu-

Fig. 6.18 Overview of human descending supraspinal systems: **a** the pyramidal tract; **b** descending projections from the brain stem. *Cd* caudate nucleus, *cospa* anterior corticospinal tract, *cospl* lateral corticospinal tract, *CS* colliculus superior, *flm* fasciculus longitudinalis medialis, *IC* internal capsule, *INC* interstitial nucleus of Cajal, *Isp* interstitiospinal tract, *M1* primary motor cortex, *resp* reticulospinal tract, *RF* reticular formation, *Rub* nucleus ruber, *rusp* rubrospinal tract, *S1* primary somatosensory cortex, *vespl* lateral vestibulospinal tract, *vespm* medial vestibulospinal tract, *Vest* vestibular nuclei
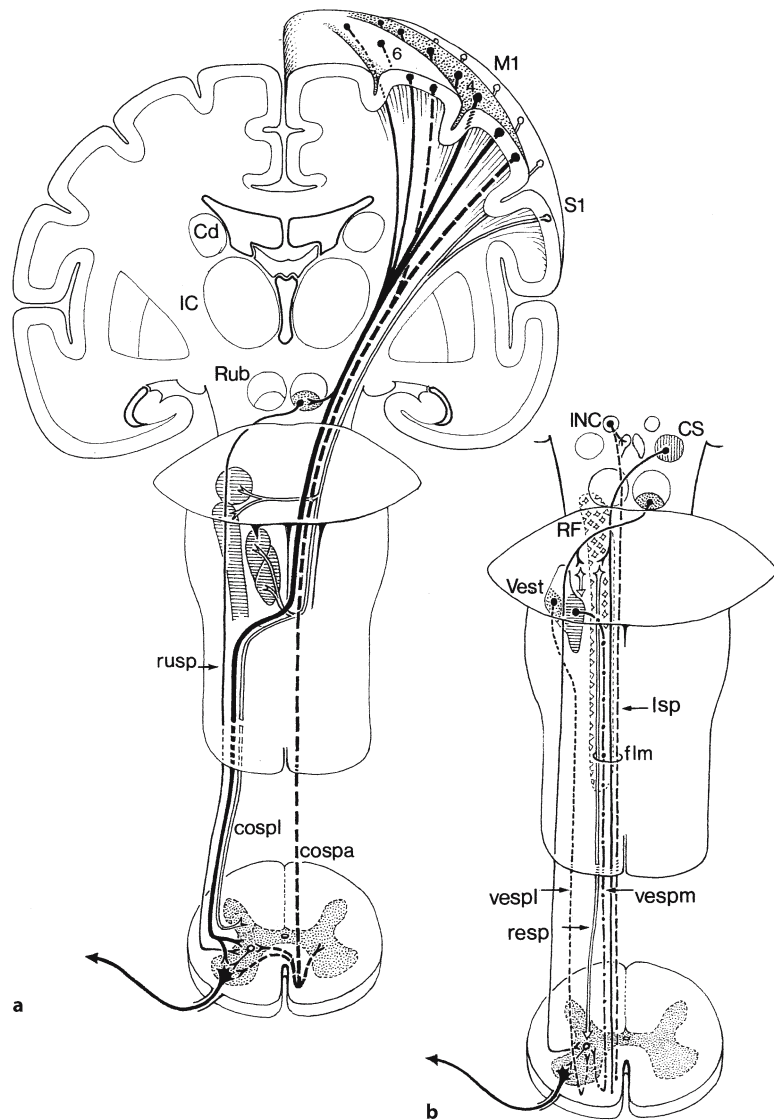
lospinal fibres and, much later, by rubrospinal and, if present, corticospinal projections. Throughout vertebrates including humans, the flm is the first descending pathway to be formed. Interstitiospinal fibres 'pioneer' this tract, and are joined by reticulospinal fibres. Vestibulospinal fibres (the medial vestibulospinal tract) follow much later. The early-arising lateral vestibulospinal tract and the late-arriving rubrospinal and corticospinal tracts take a separate course through the brain stem.

6.7.1 Descending Projections from the Brain Stem

In rats, early brain stem–spinal cord projections were studied using the carbocyanine dye DiI in fixed embryos (Auclair et al. 1993, 1999; de Boer-van Huizen

and ten Donkelaar 1999), and biotinylated dextran amine (BDA) in an isolated embryonic brain–spinal cord preparation (de Boer-van Huizen and ten Donkelaar 1999). With both techniques it was shown that in embryos at least 12 days of age (E12), i. e. at the time of closure of the posterior neuropore (Theiler stage 12), a variety of brain stem centres already innervates the spinal cord (Table 6.2). In the interstitial nucleus of the flm and various parts of the reticular formation – mesencephalic, pontine as well as medullary – mainly large immature, bipolar labelled neurons were observed. In later stages (E13, E14), the number of labelled neurons increased and more mature, multipolar cells were found. At E13 (stage 15), labelled neurons were also observed in the vestibular nuclear complex. Raphespinal neurons were not labelled before E14 (stage 17). Just below the cerebellum a conspicuous small group of neurons

Table 6.2 The development of descending supraspinal projections in rats and humans (after ten Donkelaar 2000)

Nuclei	Time of neuron origin in rats[a]	Innervation of high cervical cord in rats[b]	Innervation of lumbosacral cord in rats[c]	Estimated time of neuron origin in humans (postovulatory weeks)[d]	Estimated innervation of the cervical spinal cord in humans (Carnegie stages)
Reticular formation					
Medullary	E11–E15	E12	E17/19	4.1–7.0	~14/15[i]
Pontine	<E11–E15	E12	E18	4.1–7.0	
Mesencephalic	?	E12	E18	5.3–7.0	
Interstitial nucleus flm	?	E12	E18	4.1–5.7 (related Darkschewitsch nucleus)	14?[j,k]
Raphe nuclei	E11–E15	E14	E17	3.5–7.0	
Serotonergic projections[e]		E14	E17		?
Vestibular nuclei					
Lateral vestibular nucleus	E11–E14	E13	E17	4.1–5.7	~17/18[k]
Medial and inferior vestibular nuclei	E12–E15	?	E18–E21	4.1–7.0	Before end of embryonic period[j,k]
Locus coeruleus					
Coeruleospinal neurons	Peak E12	E12?	E20	Peak 4.1–5.2	
Noradrenergic projections[f]		<E16	E17/18		18[l]
Red nucleus	E13–E14	E17[g]	E21[g]	5.3–6.6	?
Hypothalamus					
Paraventricular nucleus	Peak E14–E15		P1	5.3–7.0	?
Corticospinal projections	Peak E15–E17	P0[h]	P7–P9[h]	(5.8)6.7–9.9	Early fetal period[m]

[a] Altman and Bayer (1980a–d, 1981)
[b] de Boer-van Huizen and ten Donkelaar (1999)
[c] Lakke (1997)
[d] Bayer et al. (1995)
[e] Rajaofetra et al. (1989)
[f] Rajaofetra et al. (1992)
[g] Lakke and Marani (1991)

[h] Gribnau et al. (1986)
[i] Windle and Fitzgerald (1937)
[j] Müller and O'Rahilly (1988a, b, 1990b)
[k] Windle (1970)
[l] Puelles and Verney (1998)
[m] Humphrey (1960)

was found labelled in a position reminiscent of the locus coeruleus. In their extensive birthdating studies in rats, Altman and Bayer (1980a–d, 1981) showed that (1) neurons in the medullary reticular formation are produced between E11 and E15 along a caudorostral gradient, (2) those in the pontine reticular formation are generated even earlier, (3) large vestibular neurons in the lateral (Deiters) nucleus are generated before the smaller neurons in other vestibular nuclei, (4) neurons in the locus coeruleus are produced mostly at E12 and (5) neurons in the nucleus of Darkschewitsch, related to the interstitial nucleus of the flm for which no data are available, are produced at E12 and E13 (Table 6.2). Comparison of the data on the time of origin with those on the ingrowth of brain stem fibres into the cord suggests that interstitiospinal and reticulospinal neurons start projecting spinalwards shortly after they are generated. Since the distance to the site of tracer application for the interstitial nucleus of the flm and the pontine reticular formation by far exceeds that of the medullary reticular formation, it is most likely that intersti-

tiospinal and pontine reticulospinal axons are the first supraspinal fibres to invade the spinal cord. Kudo et al. (1993) and Lakke (1997) studied the gradual descent of supraspinal fibres into the spinal cord. At E17, fibres from the lateral vestibular nucleus, the serotonergic raphe magnus nucleus and the gigantocellular reticular nucleus have reached lumbosacral levels, followed at E18 by fibres from many other brain stem nuclei. Last to arrive prenatally (E21) are the rubrospinal and medial vestibulospinal tracts. Hypothalamospinal fibres reach the lumbosacral cord on P1.

Assuming that the stages of neural development are similar in rats and man even though their exact chronological ages are different, Bayer et al. (1995) estimated human neurogenetic timetables by extrapolating the rat data to the longer span of human development. Most brain stem nuclei innervating the spinal cord are born between 4 and 7 weeks after fertilization (Table 6.2). The first descending brain stem projections to the spinal cord in human embryos arise in the interstitial nucleus of the flm and in the
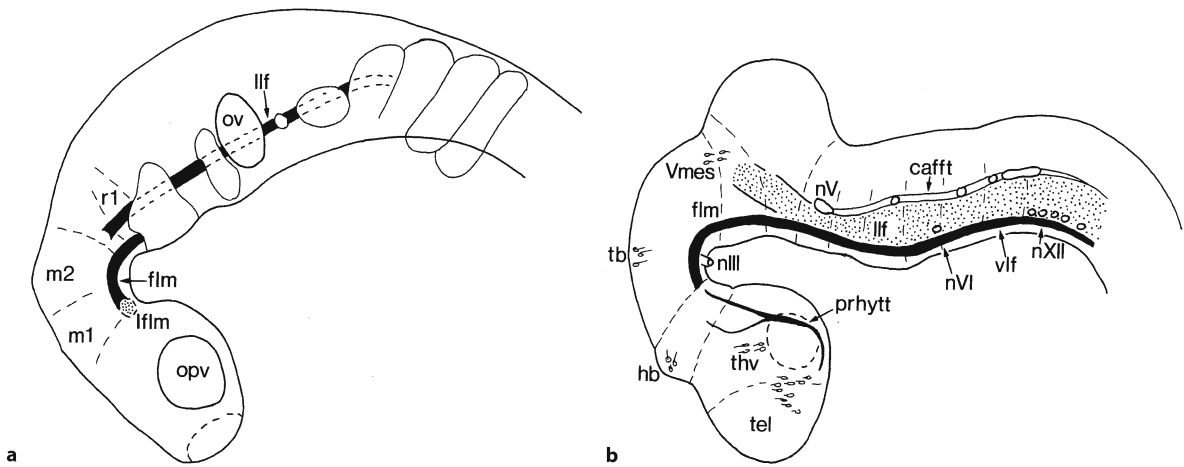
Fig. 6.19 The extent of the fasciculus longitudinalis medialis (*flm*) and other longitudinal tracts in stage 13 (**a**) and stage 14 (**b**) human embryos. *cafft* central afferent tract, *hb* habenula, *lflm* interstitial nucleus of the flm, *llf* lateral longitudinal fascicle, *m1*, *m2* mesomeres; *nIII*, *nV*, *nVI*, *nXII* cranial nerves, *opv* optic vesicle, *ov* otic vesicle, *prhytt* pretectohypothalamic tract, *r1* rhombomere 1, *tb* tectobulbar tract, *tel* telencephalon, *thv* ventral thalamus, *vlf* ventrolateral fascicle, *Vmes* mesencephalic nucleus of the trigeminal nerve. (After Müller and O'Rahilly 1988a, b)

reticular formation. Descending fibres from the medullary reticular formation reach the spinal cord in embryos of 10–12-mm crown–rump length (CRL; Windle and Fitzgerald 1937). Interstitiospinal fibres from the interstitial nucleus of the flm start to descend in the flm at stage 13 (Fig. 6.19), i.e. at E28 (Müller and O'Rahilly 1988a, b). In 12-mm-CRL embryos (about stage 17/18), vestibulospinal projections were found (Windle 1970). The red nucleus can first be recognized in stage 17 embryos (Cooper 1946; Müller and O'Rahilly 1989b), but data on the development of a rubrospinal tract are not available. At the end of the embryonic period, the flm is well-developed, and receives ascending and descending (the medial vestibulospinal tract) components from the vestibular nuclear complex (Müller and O'Rahilly 1990b). The lateral vestibular tract arises from the lateral (Deiters) vestibular nucleus.

Monoaminergic projections also appear to arise early in human development. In 8-mm-CRL embryos (about stage 14), Windle and Fitzgerald (1942) observed that descending fibres from the presumptive locus coeruleus join the lateral longitudinal fascicle. A definite locus coeruleus can be distinguished at stage 17 (Müller and O'Rahilly 1989b). Olson et al. (1973) detected neurons containing catecholamines or serotonin in embryonic brains as early as 8 weeks (21-mm CRL), and some catecholaminergic medullary neurons with spinal projections in 10-week-old fetuses (40–45-mm CRL). Using antibodies against enzymes of the catecholaminergic pathway, noradrenergic cell groups were labelled in the medulla obongata and in the locus coeruleus as early as

6 weeks of gestation (Verney et al. 1991; Zecevic and Verney 1995; Puelles and Verney 1998).

Fibre tracts that appear early in development generally undergo myelination before later-appearing tracts (Yakovlev and Lecours 1967; Gilles et al. 1983; Brody et al. 1987; Kinney et al. 1988; Altman and Bayer 2001; Table 6.3). In the brainstem, myelination starts in the flm at eight postovulatory weeks. The vestibulospinal tracts become myelinated at the end of the second trimester, whereas the pyramidal tracts begin very late (at the end of the third trimester). Early myelination of spinal pathways was extensively studied using antibodies against myelin-associated proteins, MBP in particular (Tohyama et al. 1991; Weidenheim et al. 1992, 1993, 1996; Bodhireddy et al. 1994). The temporal and spatial MBP expression in the first and early second trimester of the human spinal cord is shown in Fig. 6.20. MBP is expressed in a rostral-to-caudal and an anterolateral-to-posterior manner in most tracts of the spinal cord. In the fasciculus gracilis, however, myelination starts at the lumbar level.

6.7.2   Development of the Pyramidal Tract in Rodents

Data on the early outgrowth and guidance of corticospinal tract axons in rodents are discussed in Chap. 2. In rats and mice, corticospinal fibres do not reach upper cervical spinal segments before birth (Schreyer and Jones 1982; Terashima et al. 1983; Gribnau et al. 1986). The vast literature on the **outgrowth**
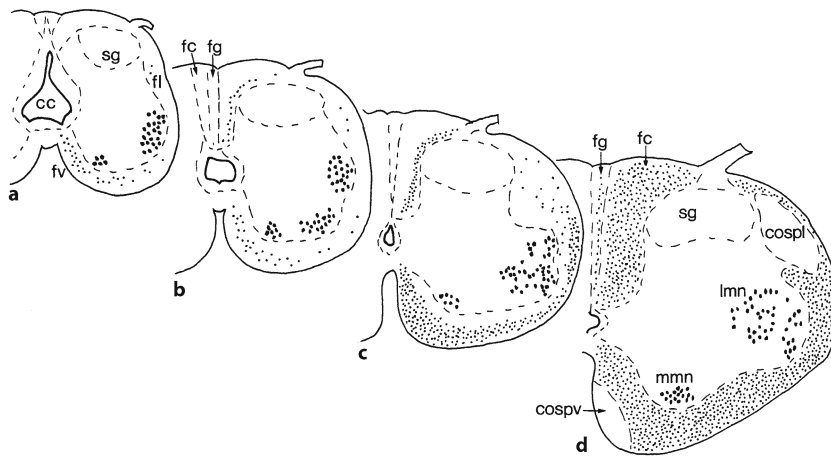
Fig. 6.20 The development of myelination in the early human spinal cord as found by the expression of myelinated basic protein. **a**–**d** Transverse sections through the cervical spinal cord of specimens of 10, 12, 16 and 23 gestational weeks of age, respectively. *cc* central canal, *cospl* lateral corticospinal tract, *cospv* vantral corticospinal tract, *fc* fasciculus cuneatus, *fg* fasciculus gracilis, *fl* lateral funiculus, *fv* ventral funiculus, *lmn* lateral motoneuron column, *mmn* medial motoneuron column, *sg* substantia gelatinosa. (Based on data by Weidenheim et al. 1993, 1996; Bodhireddy et al. 1994)

Table 6.3 Development of myelination of the main fibre tracts in the human spinal cord (after Weidenheim et al. 1993, 1996; Altman and Bayer 2001)

Fibre tract	First evidence of myelin basic protein staining	Onset of reactive gliosis	Onset of myelination
Ascending tracts			
Cuneate fascicle	14 gestational weeks	20 gestational weeks	At 33 gestational weeks, myelination well advanced throughout
Gracile fascicle	16 gestational weeks	20 gestational weeks	At 33 gestational weeks, wedge area myelinating
Dorsal spinocerebellar tract	20 gestational weeks	26 gestational weeks	33 gestational weeks
Ventral spinocerebellar tract	20 gestational weeks	Later than dorsal spino- cerebellar tract	Late 3rd trimester
Spinothalamic tract	20 gestational weeks	33 gestational weeks	Late-term neonate
Descending tracts			
Vestibulospinal tracts	9.5 gestational weeks	By 20 gestational weeks, first sign of reactive gliosis in medial vestibulospinal tract	33 gestational weeks
Reticulospinal tracts	9.5 gestational weeks	Comparable to vestibulo- spinal tracts	33 gestational weeks
Corticospinal tracts			
Lateral corticospinal tract		At birth few glia present	After birth
Anterior corticospinal tract		At birth few glia present	After birth

of the rodent **corticospinal tract** has been summarized in several reviews (Stanfield 1992, O'Leary and Koester 1993; Terashima 1995a, Joosten and Bär 1999). In rats, the postnatal development of the corticospinal tract can be divided into three periods: (1) an outgrowth phase (P1–P10); (2) a myelination phase (P10–P28); and (3) a maturation phase (P28 to adult). The outgrowth of the rat corticospinal tract is shown in Fig. 6.21. A delay of 2 days was found between the arrival of corticospinal axons at a certain level of the spinal cord and their ingrowth into the spinal grey matter. Initially, most parts of the cerebral

Fig. 6.21 The outgrowth of the corticospinal tract into the spinal cord of P1–P9 rats. The corticospinal tract was labelled with wheat germ agglutinin–horseradish peroxidase (after Gribnau et al. 1986)
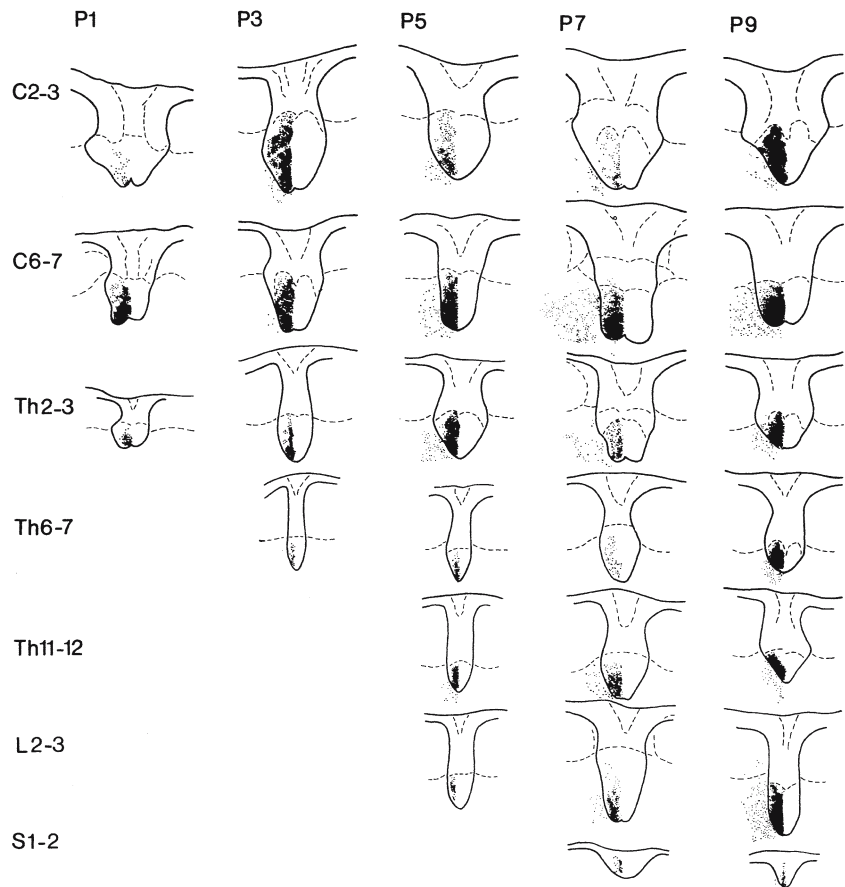
cortex including the occipital lobe innervate the spinal cord (Stanfield and O'Leary 1985; O'Leary and Stanfield 1986; Joosten et al. 1987). Axons from frontal regions arrive first and those from the occipital lobe come last. The withdrawal of collaterals probably accounts for the dramatic loss of fibres from the corticospinal tract during development (Schreyer and Jones 1988). In the development of cortical axons arising from layer V neurons three stages can be distinguished (O'Leary et al. 1990; Fig. 2.32): (1) layer V axons extend out of the cortex towards the spinal cord, bypassing their subcortical targets; (2) the subcortical targets are exclusively contacted by axon collaterals that develop by delayed interstitial branching off the flank of a spinally directed primary axon; and (3) specific branches and segments of the primary axon are selectively eliminated to yield the mature projections functionally appropriate for the area of the cortex in question. In mutant rodents with extensive perturbations in the development of the cerebral cortex such as the reeler mouse and the shaking rat Kawasaki, corticospinal tract neurons are spread throughout all layers of the mutant cortex (Terashima et al. 1983; Inoue et al. 1991; Ikeda and Terashima 1997; Fig. 10.17). The specificity of corticospinal connections is relatively unaffected (Tera-

shima 1995a, b). Myelination of the rat pyramidal tract starts in the caudal medulla at P7 (Gorgels 1990, 1991). Myelination of corticospinal axons in the spinal cord begins rostrally (C5) at about P14 and continues caudalwards during the third postnatal week (Joosten et al. 1989). A close temporal relationship exists between the appearance of the forelimb and hindlimb placing responses and the arrival of corticospinal axons in the spinal grey matter (Donatelle 1977). Forelimb placing is first seen between P4 and P7, and hindlimb placing between P9 and P13.

Several **mechanisms** control **corticospinal fibre outgrowth** into their target areas (O'Leary et al. 1990; Joosten and Bär 1999). A diffusible chemotropic signal may be one of the environmental cues involved in axonal outgrowth and guidance. The pons becomes innervated by controlling the budding and directed outgrowth of corticospinal axon collaterals through the release of a diffusible chemotropic substance (Heffner et al. 1990; O'Leary et al. 1990). Similarly, the cervical spinal grey matter becomes innervated by corticospinal axons through the release of a diffusible chemotropic factor (Joosten et al. 1991). The neuron-specific phosphoprotein B-50 (or GAP43), a major substrate of kinase C in fetal nerve growth

cones, is strongly expressed during the outgrowth of the pyramidal tract (Gorgels et al. 1987). The cell adhesion molecule L1 (L1CAM) may be involved in fascicle formation of outgrowing, later-arriving corticospinal fibres (Joosten et al. 1990; Fujimori et al. 2000). In L1 mutant mice, the L1 mutation causes a primary pathfinding deficit in the development of the corticospinal decussation (Cohen et al. 1997; Dahme et al. 1997; Castellani et al. 2000). A varying, but reduced number of corticospinal fibres were observed in the posterior columns of L1-deficient mice. These fibres did not extend beyond cervical levels. Moreover, a substantial number of corticospinal axons failed to cross the midline.

Various **mechanisms** are involved in the proper **decussation** of the pyramidal tract. During its outgrowth, Joosten and Gribnau (1989) noted a prominent vimentin-immunoreactive glial septum in the midline raphe of the hindbrain and spinal cord. Such a glial septum is absent in the decussation area of corticospinal tract fibres. This glial septum may act as a physical barrier during the outgrowth of the corticospinal tract by preventing its decussation. Oligodendrocytes and CNS myelin contain potent, membrane-bound inhibitors of neurite growth (Caroni and Schwab 1988 a, b). Oligodendrocyte-associated neurite growth inhibitors (NI-35 and NI-250) in the earlier myelinated cuneate and gracile fascicles play an important role in channelling and 'guard-rail' function to keep the corticospinal tract axons in a compact tract and to prevent the ingrowth into the neighbouring sensory tracts (Schwab and Schnell 1991). Through Eph receptors, ephrin-B3 may function as a midline-anchored repellent that prevents corticospinal fibres from crossing back into the ipsilateral side of the spinal cord (Kullander et al. 2001; Yokoyama et al. 2001). Ephrin-B3, a ligand for the receptors EphB3 and EphA4, has a restricted expression pattern along the midline of the neural tube (Bergemann et al. 1998; Imondi et al. 2000). EphA4 is expressed in postnatal corticospinal neurons as their axons find their way down the contralateral spinal cord (Dottori et al. 1998). In *ephrin-B3* mutant mice, corticospinal tract axons fail to respect the midline boundary of the spinal cord and bilaterally innervate both contralateral and ipsilateral motoneuron populations (Yokoyama et al. 2001). In EphA4-deficient mice, comparable observations were made (Coonan et al. 2001). Netrin-1 receptors also appear to be necessary for a proper decussation of the pyramidal tract (Finger et al. 2002). *Robo3* promotes crossing of pyramidal tract axons. In *Robo3*-deficient mice, axons fail to cross the midline (Sabatier et al. 2004). In the rare human disorder *horizontal gaze palsy with progressive scoliosis* (*HGPPS*) and *hindbrain dysplasia* (Chap. 7), a *ROBO3* mutation disrupts the crossing of the corticospinal tracts in the hindbrain (Jen et al. 2004).

6.7.3   Development of the Pyramidal Tract in Macaque Monkeys

In the rhesus monkey, corticospinal fibres have reached at least to the level of the lower cervical segments at birth (Kuypers 1962; Fig. 6.22). Tract-tracing experiments in fetal macaque monkeys show that the areal distribution of corticospinal neurons in the cerebral cortex is greater than in mature macaques (Galea and Darian-Smith 1995; Killackey et al. 1997). Both the areal distribution of the cortical origin and the relative number of corticospinal neurons with spinal axons regress very substantially over a period of 2 years (Galea and Darian-Smith 1995). Direct corticomotoneuronal projections do not develop until 6–8 months of age. Lawrence and Hopkins (1976) extensively studied the development of hand and finger movements in infant rhesus monkeys. The earliest signs of reaching were found at 3–4 weeks of age. Reaching was inaccurate and grasping of food was part of a rather gross whole arm and hand movement. Smooth reaching occurred in the third month and relatively independent finger movements developed between the second and eighth months. This developmental time course correlates well with the appearance of corticomotoneuronal projections (Kuypers 1962; Armand et al. 1994, 1996, 1997; Galea and Darian-Smith 1995). In monkeys pyramidotomized at birth, there was no appreciable difference in the development of general motor activity including running, walking and climbing. Reaching developed in the normal fashion, but the monkeys did not develop any relatively independent finger movements (Lawrence and Hopkins 1976; Galea and Darian-Smith 1997 a, b). Transcranial magnetic stimulation studies showed a correlation between the maturation of the corticospinal tract and the development of relatively independent finger movements (Flament et al. 1992 a, b; Olivier et al. 1997), suggesting a staggered development of corticospinal projections to forelimb and hindlimb. Cortically evoked responses in hand muscles could be recorded about 1 month earlier than those in foot muscles.
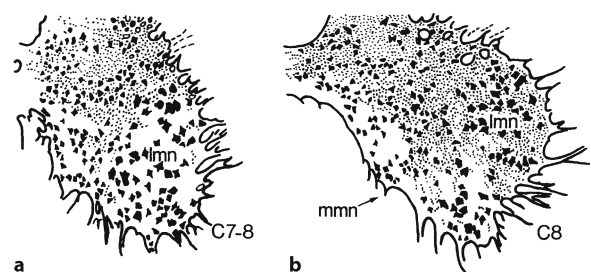
Fig. 6.22 The distribution of corticospinal terminations in the ventral horn of the rhesus monkey: **a** at 4 days of development; **b** in an adult. *lmn* lateral motoneurons, *mmn* medial motoneurons. (After Kuypers 1962)

Fig. 6.23 The outgrowth of the human corticospinal tract through the brain stem, shown for 9, 13 and 18 gestational weeks. *cb* cerebellum, *cc* corpus callosum, *Cd* caudate nucleus, *cospa* anterior corticospinal tract, *cospl* lateral corticospinal tract, *cp* cerebral peduncle, *cs* colliculus superior, *ic* internal capsule, *Put* putamen, *thal* thalamus. (After Humphrey 1960; Altman and Bayer 2001)
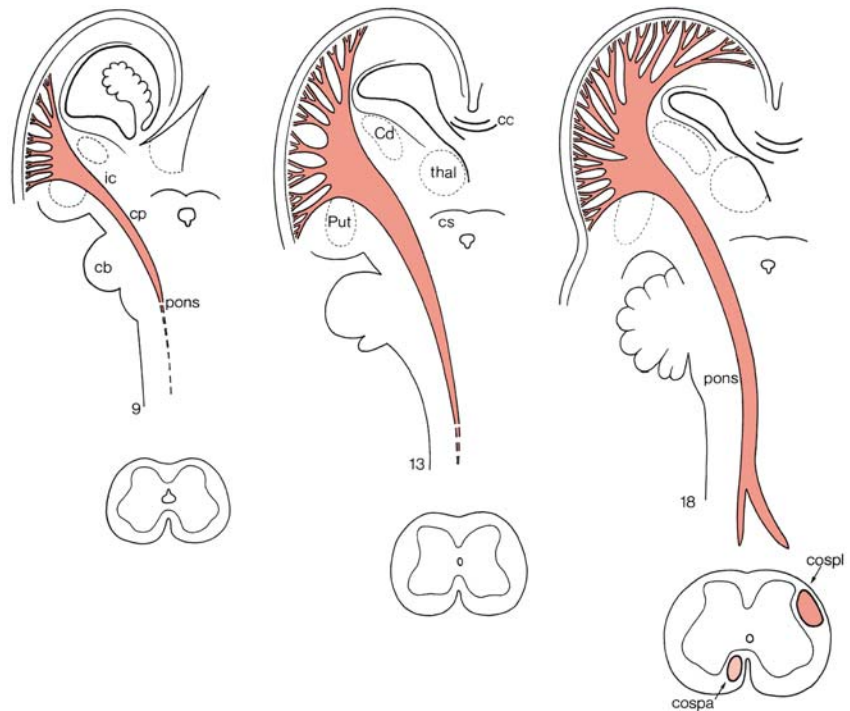
6.7.4   Development of the Human Pyramidal Tract

The development of the human corticospinal tract was studied with silver and other fibre or myelin staining techniques (Humphrey 1960; Müller and O'Rahilly 1990b; Eyre et al. 2000; Altman and Bayer 2001). The pyramidal tract reaches the level of the pyramidal decussation at the end of the embryonic period (Humphrey 1960; Müller and O'Rahilly 1990b; Fig. 6.23). After reaching the level of the pyramidal decussation at the end of the embryonic period, a rather long waiting period occurs. Pyramidal decussation is complete by 17 weeks' gestational age, and the rest of the spinal cord is invaded by 19 gestational weeks (lower thoracic cord) and 29 gestational weeks (lumbosacral cord) (Humphrey 1960; Fig. 6.24). Using GAP43 immunohistochemistry, Eyre et al. (2000) showed that by 29 gestational weeks, the corticospinal tracts are the only major tracts expressing this neuron-specific phosphoprotein in the lower cervical cord. Following a waiting period of up to several weeks, corticospinal fibres progressively innervated the grey matter. By 35 gestational weeks, GAP43 immunoreactivity was greatly increased in the grey matter, the dorsal and ventral horns in particular. At 37 gestational weeks, when the great majority of axons expressing GAP43 appeared to derive from the corticospinal tracts, Nissl-stained motoneuron cell bodies were closely opposed by GAP43-immunoreactive varicose axons, indicating the presence of direct corticomotoneuronal projections prenatally. Some caution would be appropriate, however, since at least
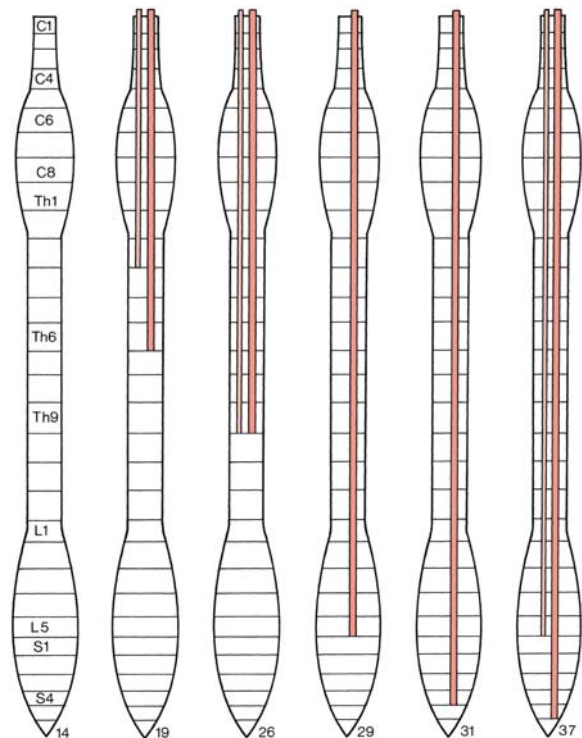
Fig. 6.24 The spinal outgrowth of the human corticospinal tracts, shown for 14, 19, 26, 30, 31 and 37 gestational weeks. The small bundles (*light red*) show the outgrowth of the anterior corticospinal tract (not found by Altman and Bayer in their fetal material of 29 and 31 weeks), whereas the larger bundles (*red*) show the outgrowth of the lateral corticospinal tract. *C1, C4, C6, C8, Th1, Th6, Th9, L1, L5, S1* and *S4* indicate spinal segments. (After Humphrey 1960; and Altman and Bayer 2001)

some of these GAP43-labelled axons may be derived from other spinal systems. At term, direct cortical projections to Ia-inhibitory interneurons were shown with electrophysiological techniques (Eyre et al. 2000).

The maturation of human skilled finger movements requires a much longer period of development than in the rhesus monkey (Forssberg et al. 1991), and is also dependent on that of the corticospinal tracts (Eyre et al. 1991; Müller et al. 1991, 1997). During the first 2 years of life, the central conduction time of responses to magnetic stimulation of the cerebral cortex rapidly declines. Adult values for central conduction times were achieved around 2–4 years of age. This extended time course is in keeping with the protracted period during which myelination of the human pyramidal tract continues. The early direct corticospinal innervation presumably permits cortical involvement in activity dependent maturation of spinal motor centres during a critical period of perinatal development. Neonates have ipsilateral corticospinal responses with shorter onsets than contralateral responses but similar thresholds and amplitudes (Eyre et al. 2000). Differential development was present from 3 months onwards so that by 18 months ipsilateral responses were smaller and had higher thresholds and longer onset latencies than contralateral responses. These data suggest that the development of the corticospinal tract may diverge between man and macaque monkeys at least in two ways: (1) the prenatal establishment of corticomotoneuronal connections in human fetuses well before the presence of relatively independent finger movements, whereas there is a close correspondence between these two events in infant monkeys; and (2) the coexistence in human neonates of fast-conducting contralateral and ipsilateral corticospinal projections which are differentially withdrawn during the postnatal period, whereas ipsilateral corticospinal projections are sparse in neonate macaques.

Myelination of the pyramidal tract is already in progress at the level of the pyramidal decussation in a 220-mm-CRL fetus at 25 weeks of gestation (Woźniak and O'Rahilly 1982). Myelination of the pyramidal tract occurs over a protracted period (Yakovlev and Lecours 1967; Altman and Bayer 2001). In the fetal and neonatal spinal cord, in MBP or Weigert stained sections the massive lateral corticospinal tracts stand out as unstained areas in the white matter (Fig. 6.34 a, b). The cranial part of the pyramidal tract is myelinated much earlier than its spinal part. Myelination of the entire corticospinal tract may be completed between 1 and 2 years of age. The MRI pattern of myelination lags several weeks behind if compared with the histological timetable, probably owing to the minimal concentration of myelin required to change the signal intensity on the magnetic resonance image (van der Knaap and Valk 1995). Apart from a clear rostral-to-caudal gradient in the progression of reactive gliosis and subsequent myelination within the lateral corticospinal tract, a medial-to-lateral gradient also seems likely (Altman and Bayer 2001). Since Foerster's (1936) studies, a rather precise segmental organization of corticospinal tract fibres is thought to be present in the cervical cord (but see Brodal 1981 for critique). According to this scheme, corticospinal fibres terminating in the upper cervical cord are located most medially, and fibres for more caudal levels of the spinal cord form shells in a medial-to-lateral sequence. Myelination starts in a medial fascicle related to the cervical and thoracic cord, followed by an intermediate fascicle for the lumbar cord, and finally a lateral fascicle for the sacral cord (Altman and Bayer 2001). Myelination spreads along the entire cervical cord by 3–4 months, reaches the thoracic cord by 5–7 months, and at 10–11 months myelination is in progress in the lumbar cord. Myelination of the corticospinal tract is correlated with motor behaviour.

6.8 Developmental Anomalies of the Spinal Cord

Developmental anomalies of the spinal cord include rare malformations such as anomalies of histogenesis, duplications, neurenteric cysts and abnormal course or even absence of fibre tracts and more common malformations such as tethered spinal cord and syringomyelia. The most common malformations involving the spinal cord (the neural tube defects) are discussed in Chap. 4.

6.8.1 Anomalies of Histogenesis

Small grey matter ectopia are found regularly in the spinal cord. Hori (1981, 1998) noted a frequency of 2% in autopsies. Neuronal heterotopia in the white matter were also found incidentally in 2% of autopsies (Hori 1981, 1998). Intramedullary heterotopic nerve cells may be more frequent in amyotrophic lateral sclerosis (Kozlowski et al. 1989; Martin et al. 1993; Sasaki and Iwata 1998). Quite often there are heterotopic nerve cells in the posterior as well as in the anterior spinal nerve roots (Hori 1988a). Heterotopic neurons in the posterior roots originate from the posterior spinal ganglion and those in the anterior roots may originate from the anterior horn as well as from the posterior spinal ganglion.
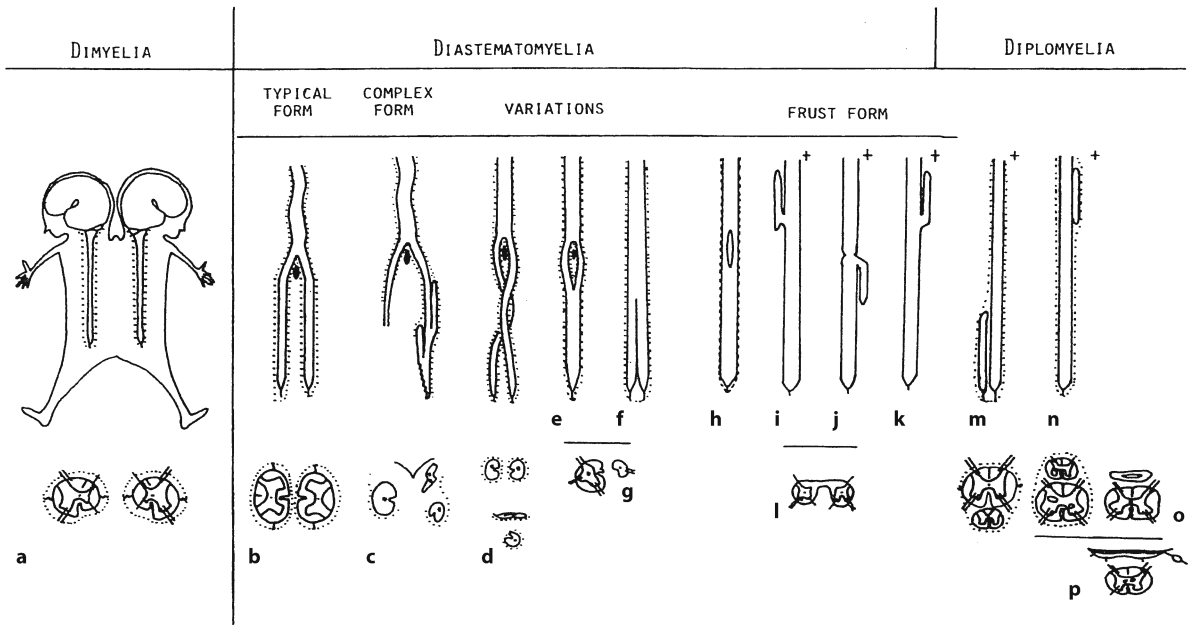
Fig. 6.25 Duplications of the spinal cord. Summary of the morphologic features of cases of dimyelia, diastematomyelia and diplomyelia: **a**–**c** (Hori et al. 1982); **d** (Rokos 1975); **e** (Benstead 1953); **f** (James and Lassman 1964); **g, l** (Emery and Lendon 1974; reverse form of **l** with four posterior and two anterior columns: Vinters and Gilbert 1981); **h** (Kersten 1954; James and Lassman 1972); **i** (Griepentrog 1953); **j** (Haas 1952); **k** (von Sántha 1930); **m** (Hori et al. 1982; Clinical Case 6.1); **n** (Dominok 1962); **o** (Környey 1925); **p** (Schneideling 1938). Apart from those indicated by *crosses* (left lateral views), anteroposterior views of the spinal cord are shown. *Broken lines* indicate the dura. (After Hori et al. 1982)

6.8.2   Duplications of the Spinal Cord

Ectopic expression of *Gcm1*, a murine homologue of the transcription factor glial cells missing (Gcm) in *Drosophila*, induces congenital spinal cord abnormalities (Nait-Oumesmar et al. 2002). Brief ectopic expression of *Gcm1* in mouse embryonic tail buds leads to spina bifida and/or multiple neural tubes. *Duplications* of the *spinal cord* are rare malformations of the human nervous system. Hori et al. (1982) described four types of total or partial duplication of the human spinal cord, using the following subdivision (Fig. 6.25): (1) dimyelia, a complete duplication of the spinal cord; (2) diplomyelia, an isolated accessory spinal cord without roots at the ventral lumbosacral level; (3) complex diastematomyelia (*diastema* is Greek for split); and (4) typical diastematomyelia. *Dimyelia* was observed in a female stillborn dicephalus dibrachius. Histologically, the two spinal cords showed symmetric medial hemihypoplasia that included the spinal roots (Fig. 6.25). The term dimyelia should be restricted to cases with a total duplication of the spinal cord. *Diplomyelia* was found in a newborn girl with a cardiovascular malformation (Clinical Case 6.1). The term diplomyelia should be limited to cases of an isolated accessory spinal cord, ventral or dorsal to the normal cord (Környey
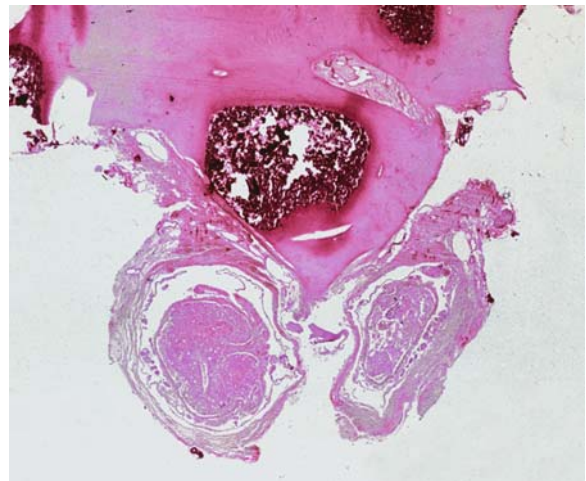
Fig. 6.26 A case of complex diastematomyelia showing a bony spur dividing the lumbar spinal cord in two parts

1925; Schneiderling 1938; Dominok 1962; Hori et al. 1982; Hori 1998). *Diastematomyelia* means a lateral bifurcation of the spinal cord, independent of whether or not the branches show completely differentiated cord structures with four columns and segmental roots. Diastematomyelia is usually associated

Clinical Case 6.1
Diplomyelia

Multiplication of the spinal cord in human embryos has occasionally been described (Fig. 6.25). Környey (1925) described an isolated dorsal accessory cervical cord associated with extensive malformations of the brain. Dominok (1962) published a case with a dorsal thoracolumbar accessory cord with rudimentary posterior roots, whereas the dorsal thoracolumbar accessory cord in Scheiderling's case (1938) was less differentiated and formed a medullary plate, but with spinal roots as well as a spinal ganglion in the subdural space. Hori et al. (1982) described a case of diplomyelia (see Case Report).

Case Report. The mother, a primigravida and primipara, had an uneventful pregnancy with labour beginning at term. The newborn girl appeared unremarkable at birth and had Apgar scores of 9 at 1 min and 10 at 5 min. The following day, however, she became cyanotic, femoral pulses could not be palpated, and an echocardiogram showed left cardiac hypoplasia. She died of acute cardiac insufficiency 4 h after her first examination on the second postnatal day. At autopsy, severe hypoplasia of the left ventricle with severe endocardial fibrosis, moderate hypoplasia of the aortic arch and the ascending aorta, an open foramen ovale and a patent ductus arteriosus were found. The macroscopically normal brain weighed 376 g after fixation. Histologically it was normal, apart from heterotopic neuronal nests in the cerebellar white matter. An *accessory spinal cord* was found between the lower lumbar segment and the cauda equina ventral to the regular spinal cord (Fig. 6.27a). The accessory cord had no roots and no denticulate ligaments. For histological examination, it was, together with the regular cord, embedded in paraffin and studied in serial sections. The grey and the white matter of the accessory cord were abundant, but the posterior columns appeared hypoplastic, although well myelinated (Fig. 6.27b). The regular and the accessory spinal cords were covered by a common dura and arachnoidea. There was no separating tissue between the two cords and no bony spine in the spinal canal. The regular cord had a proper pia, but the accessory cord had only a circumscibed rudimentary pia. There was no parenchymal continuity between the two cords. In a root of the cauda equina of the regular cord at the level of the filum terminale, there was a subdural heterotopic spinal ganglion as well as several isolated preganglionic neurons in the root itself. No other anomalies were found in the regular spinal cord. Subdural heterotopic spinal ganglia were also observed in cases of an accessory cord as well as in diastematomyelia (Schneiderling 1938).

References

Dominok GW (1962) Zur Frage der Diplomyelie. Dtsch Z Nervenheilk 183:340–350

Hori A, Fischer G, Dietrich-Schott B, Ikeda K (1982) Dimyelia, diplomyelia, and diastematomyelia. Clin Neuropathol 1:23–30

Környey S (1925) Beiträge zur Entwicklungsmechanik und Pathologie des foetalen Zentralnervensystems. Arch Psychiatr Nervenkrh 72:755–787

Schneiderling W (1938) Unvollkommene dorso-ventrale Verdoppelung des Rückenmarkes. Virchows Arch Pathol Anat Physiol 31:479–489

Fig. 6.27 Macroscopic (**a**) and microscopic (**b**) views of a case of diplomyelia (from Hori et al. 1982)

with a bony spur or a cartilaginous or fibrous septum in the spinal canal. Typical, complex and 'forme fruste' forms can be distinguished (Fig. 6.25). A complex form was found in a 9-day-old boy with a Chiari II malformation and a thoracic meningomyelocele. The left branch of the cord showed further complex anomalies. A typical form was observed in a stillborn girl, born to an adolescent mother at 34 weeks of gestation (Fig. 6.26, see page 251).

6.8.3   Neurenteric Cysts

Enterogenous or *neurogenic cysts* are rare developmental anomalies that can be seen anywhere along the gastrointestinal tract (Veeneklaas 1952; Bentley and Smith 1960; Kumar et al. 2001; ten Donkelaar et al. 2002). They may extend into the intradural compartment, especially around the spinal cord. The latter cases are frequently associated with midline fusion abnormalities of the vertebral column. Cervical and upper thoracic segments are most often affected. Enterogenous cysts are considered to be the result of a disturbance in the interrelations between the ectoderm, the notochord and the endoderm. During its development at the end of the third embryonic week, the notochord is intimately related to endodermal cells (Fig. 6.28). If the notochord fails to detach itself from the endodermal layer, endodermal cells can be dragged forwards and upwards. This may lead to the formation of a cyst. Any adhesion between the ectoderm and the endoderm in the presomite embryo in which the two layers are in close proximity may split or divert the notochord during its caudorostral development and may give rise to an enterogenous cyst (Clinical Case 6.2).

Fig. 6.28 The possible developmental history of enterogenous or neurenteric cysts and related disorders. The numbers in *italics* refer to the developmental stages shown. **a** An adhesion (*adh*) between the ectoderm (*ec*) and the endoderm (*en*) may lead to a split notochord syndrome. In this situation the notochordal process (*np*) will be split into two notochords (*nch*), resulting in hemivertebrae, a split neural tube (*nt*) giving rise to diastematomyelia, and various forms of enterogenous structures such as a posterior enteric fistula, dermoid cysts and dermal sinus tracts (Chap. 4). **b** *Top*: The development of the notochordal process into the notochord between stages 8 and 12. The neurenteric canal begins at the primitive pit (*pp*) and opens into the yolk sac (*YS*). *Bottom*: the possible mechanism of development of an enterogenous cyst. **c** Persistence of the neurenteric canal (*neurc*) results in the split notochord syndrome with hemivertebrae, a double spinal cord and a dorsal enteric cyst. *AC* amniotic cavity, *as* allantois, *cm* cloacal membrane, *cs* connecting stalk, *pchp* prechordal plate, *ps* primitive streak, *sc* spinal cord, *vb* vertebral bodies. (After Bremer 1952; Bentley and Smith 1960; Skandalakis and Gray 1994; O'Rahilly and Müller 2001; ten Donkelaar et al. 2002)

Case Report. In a newborn girl, the second child of non-consanguineous parents, a large intradural extramedullary cystic lesion was found that severely compressed the spinal cord (ten Donkelaar et al. 2002). Pregnancy was complicated by gestational diabetes. The mother noted long periods of strange, rhythmic movements of the fetus during the last months of pregnancy. Labour was induced at a gestational age of 38 weeks. Delivery was uncomplicated with Apgar scores of 7 and 8 after 1 and 5 min, respectively. The birth weight was 3,525 g. Physical examination showed severe contractures of all extremities, and a midline area of abnormal skin on the back with a maximum diameter of 2 cm. Muscle tone was elevated in both arms and legs. The biceps and triceps tendon reflexes were absent, whereas in the legs pathological hyperreflexia was found. Spontaneous micturition was absent. During the first hours of life, respiratory insufficiency gradually developed, and necessitated artificial ventilation during the first day of life. MRI of the spine showed a large solitary mass, extending from C4 to T2 (Fig. 6.29). The mass was homogeneous and hyperintense on T2-weighted images. There was severe compression and dorsal displacement of the spinal cord, and extensive hydrocephalus. An extensive spina bifida was found in the lower part of the cervical vertebral column with almost completely absent spinal arcs. The corpora of the vertebrae C7–T2 were somewhat malformed, but not split anywhere. Neurosurgical exploration revealed a tract from the atypical cutis to the muscular fascia and a large intradural, extramedullary cystic lesion, severely compressing the spinal cord. A biopsy was taken from

Fig. 6.29 Sagittal T2 MRI showing the extent of the intradural cyst with severe spinal cord depression. Note the malformed vertebral bodies from C7 to T2 (from ten Donkelaar et al. 2002)

Fig. 6.30 Macroscopical (**a**–**c**) and microscopical (**d**–**i**) neuropathological findings in a spinal intradural enterogenous cyst. **a**, **b** The in situ position of the cyst and more cranial (*arrow*) and caudal (*arrowhead*) parts of the spinal cord, in **a** after removal of the vertebral bodies and opening of the dural sac and in **b** after removal of the dural sac plus contents from the spinal canal. **c**, **d** A cross section of the intradural lesion after fixation (**c**) and in a haematoxylin–eosin-stained slice (**d**). Note the concentric architecture of the lesion with mucosa at the inner surface of the wall, and a prominent surrounding layer of smooth muscle tissue (*arrowheads*) resembling muscularis propria. On the *right*, the transition to the dural sac is seen. **e**–**g** Higher magnifications of the areas indicated in **d** by arrows (haematoxylin–eosin staining). Note that the mucosa in **e** resembles fundus-type gastric mucosa with mucus-producing columnar cells in the superficial part and parietal cells in the deeper portions of the glands. The *arrowhead* in **e** indicates a cluster of ganglion cells in the submucosa. In **f**, a transition between mucus-producing mucosa and non-keratizing squamous epithelium is seen, the latter resembling the mucosa of the esophagus; In **g**, compressed neuroglial tissue in the periphery of the dorsal part of the lesion is seen; the *arrowhead* indicates the central canal with ependymal lining. **h** An α-smooth muscle actin staining accentuates the muscularis mucosa (*arrowheads*) and the internal and external layer of the muscularis propria (*one* and *two asterisks*, respectively) in the wall of the cystic lesion. The area in the *rectangle* in **h** is shown at higher magnification in **i**, and contains a cluster of ganglion cells, consistent with a plexus myentericus. *Bars* in **b** and **c** 0.5 cm; magnification in **e**–**g** × 200, in **h** × 50. (From ten Donkelaar et al. 2002)

the cystic wall. The clinical course was characterized by a slow progression of the respiratory failure due to severe myelopathy. The child died on the 19th day of life.

At autopsy, the cervicothoracic part of the spinal canal and dural sac were found to be widened, and largely filled with an intradural mass with a smooth surface (Fig. 6.30 a, b). The adjacent parts of the spinal cord were dorsally displaced, compressed and severely atrophic. The tumour with a size of 2 cm × 1.8 cm × 1 cm had a concentric architecture, with microscopically mucosa at the inner surface of the wall, surrounded by fibrous, submucosal tissue and a prominent layer of smooth muscle tissue, the latter consistent with muscularis propria (Fig. 6.30 c–g). In both submucosa and muscularis propria dispersed clusters of ganglion cells were present. The gastrointestinal and respiratory tracts were completely normal. The large, intradural cyst appeared to be of mixed origin, and consisted of gastric, oesophageal and respiratory
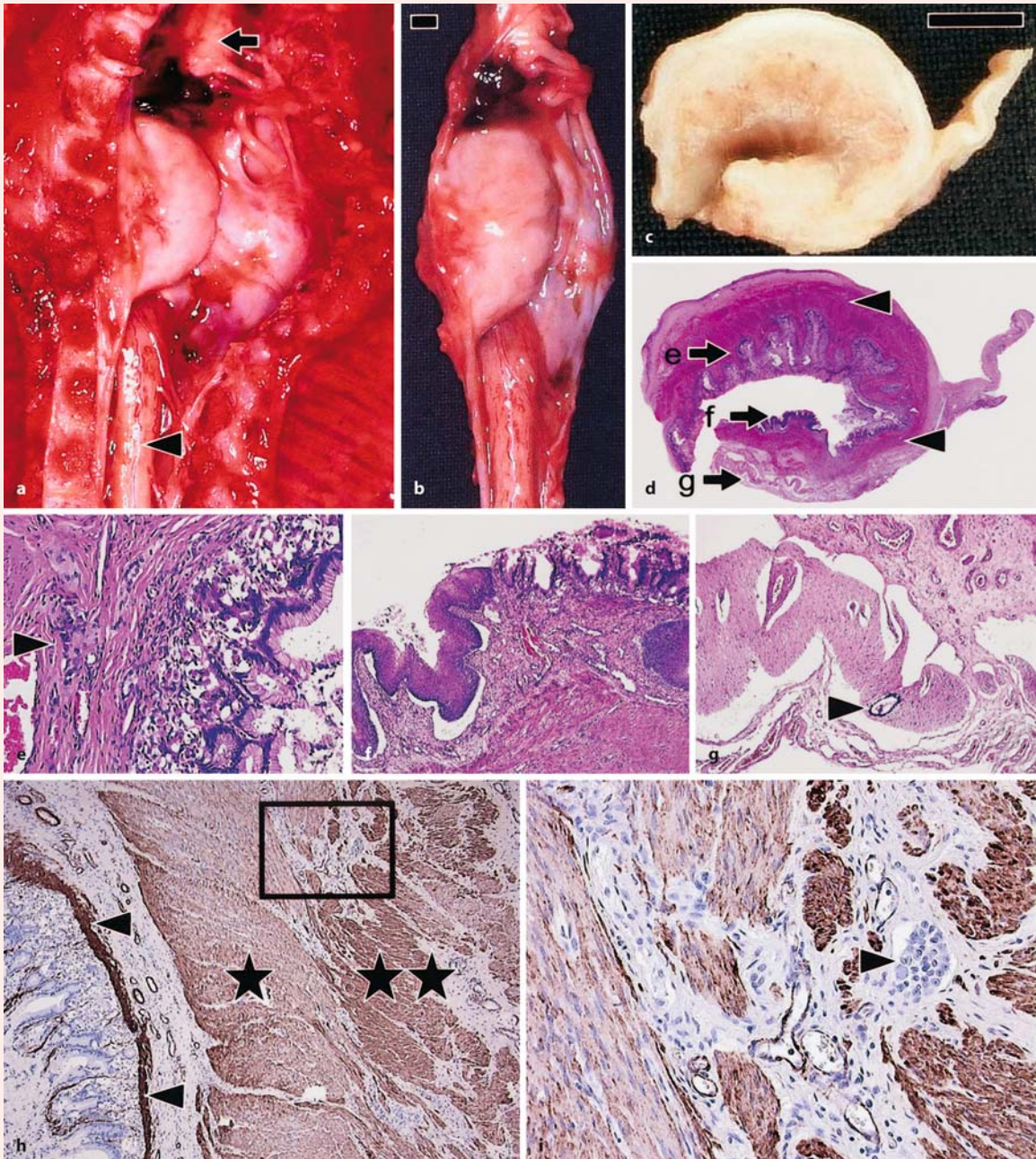
components. The presence of a bona fide muscularis propria suggests that the cyst is a duplication of the gastrointestinal tract, displaced into the spinal canal.

Hypotheses on the pathogenetic mechanism by which enterogenous cysts develop all focus on early embryogenesis (Fig. 6.28). They are formed by a disturbance in the interrelations between the notochord, ectoderm and endoderm. During the outgrowth of the notochordal process, any adhesion between the ectoderm and the endoderm may split or divert the notochord during its caudorostral development (Fig. 6.28a), resulting in malformations known as the split notochord syndrome (Feller and Sternberg 1929; Bentley and Smith 1960; Pang et al. 1992), in extreme form characterized by the presence of a double spinal cord. Such adhesions may give rise to an accessory neurenteric canal around which an endomesenchymal tract condenses that bisects the developing notochord and causes formation of two hemineural plates. It is conceivable that a less severe malformation may lead to the presence of an enterogenous cyst ventral to the spinal cord with subsequent fusion of split vertebrae. The presence of a tract from the atypical cutis to the muscular fascia may support such an explanation. Alternatively, persistence of the transient neurenteric canal may give rise to the split notochord syndrome (Bremer 1952; O'Rahilly and Müller 2001; Fig. 6.28c). Another mechanism for the formation of dorsal enterogenous cysts may lie in the early, intimate relationship of the notochordal process and the endoderm (Fig. 6.28b). Normally, the notochord separates from the endoderm, and a normal gut and vertebral column result. However, if during this process a portion of the notochord and the developing gut fail to separate, differences in growth between the two structures will put a cord of endodermal cells from the roof of the gut, leading to a diverticulum or cyst (Skandalakis and Gray 1994).

References

Bentley JFR, Smith JR (1960) Developmental posterior remnants and spinal malformations. The split notochord syndrome. Arch Dis Child 35:76–86

Bremer JL (1952) Dorsal intestinal fistula; accessory neurenteric canal; diastematomyelia. Arch Pathol 54:132–138

Feller A, Sternberg H (1920) Zur Kenntnis der Fehlbildungen der Wirbelsäule. I. Die Wirbelkörperspalte und ihre formale Genese. Virchows Arch Pathol Anat 272:613–640

O'Rahilly R, Müller F (2001) Human Embryology & Teratology, 3rd ed. Wiley-Liss, New York

Pang D, Dias MS, Ahdab-Barmada M (1992) Split notochord malformation. Part I: A unified theory of embryogenesis for double spinal cord malformations. Neurosurgery 31:451–480

Skandalakis JE, Gray SW (1994) Embryology for Surgeons, 3rd ed. Williams & Wilkins, Baltimore, MD

ten Donkelaar HJ, Willemsen MAAP, van der Heijden I, Beems T, Wesseling P (2002) A spinal intradural enterogenous cyst with well-differentiated muscularis propria. Acta Neuropathol (Berl) 104:538–542

6.8.4 Syringomyelia

The term *syringomyelia* means tubular cavitation of the spinal cord extending over several segments (Fig. 6.31). Cavities in the medulla (*syringobulbia*) are often associated with syringomyelia. Spiller (1906) described a case of syringomyelia, extending from the sacral region of the spinal cord through the medulla oblongata, the right side of the pons and the right cerebral peduncle to the upper part of the right internal capsule. About 90% of patients with idiopathic syringomyelia have a Chiari I malformation (Sherman et al. 1986; Harding and Copp 1997). Clinically, the disorder usually does not start before the second decade and is slowly progressive. The lesion interrupts the spinothalamic fibres as they cross the midline in the anterior white commissure just below the central canal (Fig. 6.31b). Usually, syringomyelia occurs in the lower cervical region and and causes a cape-like distribution of pain and temperature deficit in the cervical and upper thoracic region.

6.8.5 Abnormal Course or Absence of Fibre Tracts

An *abnormal course* of the *posterior columns* is rare (Hori 1988b; Fig. 6.32). More common is a deviated longitudinal posterior septum, resulting in a J-form deviation of the posterior septum (Hori 1983, 1998; Parkinson and del Bigio 1996). Rudimentary development of the dorsal roots and of the posterior columns are rare malformations (Op de Coul and Slooff 1975; Kirkland 1979; Friede 1989; Vogel et al. 1990). In a 12-year-old boy with a familial insensitivity to pain, absence of small DRG cells, lack of small dorsal root fibres, absence of Lissauer's tract and reduction in size of the spinal tract of the trigeminal nerve were described (Swanson et al. 1965). Friede (1989) described *aplasia* of the *posterior columns* in a 3-day-old boy, born severely hypotonic and areflexic after Caesarean section at term to a white mother. The pregnancy was complicated by first trimester bleeding. There were three normal girls, one miscarriage and one brother who had also been areflexic and floppy and died at the age of 1 week, but no au-

Fig. 6.31 a Syringomyelia observed in a 13-year-old girl with tuberous sclerosis; **b** the lesion interrupts spinothalamic fibres, leading to a cape-like distribution of pain and temperature deficit (**c**)
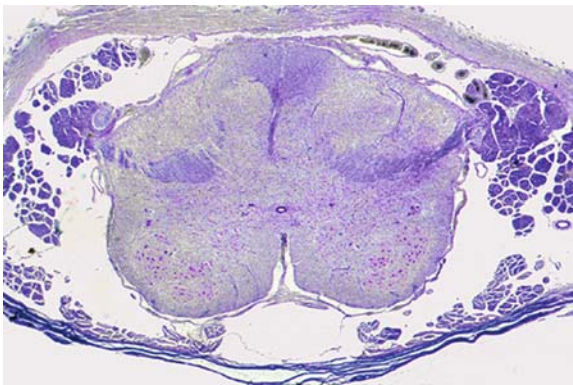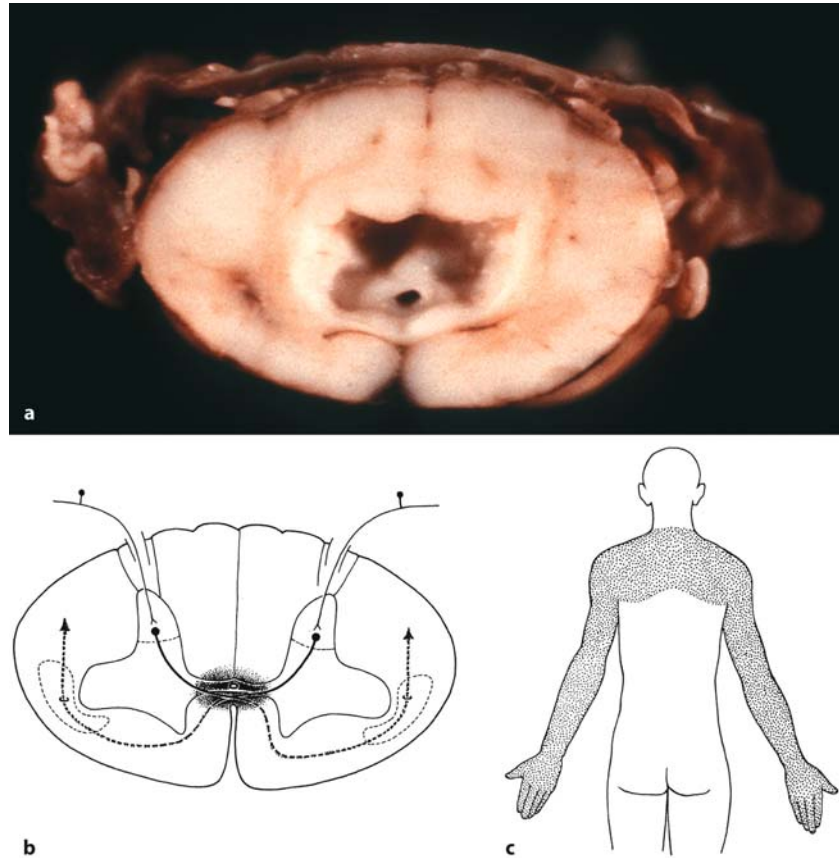
Fig. 6.32 Abnormal course of the posterior roots, entering the spinal cord lateral to the posterior horn (from Hori 1988b)

topsy was performed. In the case reported, some craniofacial anomalies (low-set ears, mandibular hypoplasia) and hepatosplenomegaly were observed. Spontaneous movements were normal. The infant died on the third day from massive pulmonary haemorrhage. No gross anomalies of the CNS were found. Microscopic examination of the spinal cord showed an extreme degree of hypoplasia of the gracile and cuneate fasciculi and lifting up of the dorsal horns so

that they nearly touched each other. Only thin vestiges of dorsal roots were seen, but the ventral roots were normal. Vogel et al. (1990) reported a case of a male infant with arthrogryposis multiplex congenita who survived for 19 weeks after birth at 36 weeks' gestational age. Severe hypoplasia of the dorsal roots and posterior columns was found.

Abnormal course or even *absence* of the *pyramidal tracts* is also rare but is more common than anomalies of the ascending systems. Several variations in the funicular trajectory of the human pyramidal tract have been described in otherwise normally developed cases (Figs. 6.33, 6.34), the most obvious being those with uncrossed pyramidal tracts (Flechsig 1876; Mestrom 1911; Kramer 1949; Verhaart and Kramer 1952; Nathan and Smith 1955; Nyberg-Hansen and Rinvik 1963; Yakovlev and Rakic 1966; Nathan et al. 1990; ten Donkelaar et al. 2004). Various *aberrant pyramidal tract bundles* have been described which are usually asymptomatic. The most common are the *pes lemnisci* bundles, two fibre bundles which descend partly within the cerebral peduncle and partly in the region of the medial lemniscus (Déjérine 1901; Kuypers 1958; Lankamp 1967, Verhaart 1935, 1970). The medial or superficial pes lemnisci leaves the medial part of the cerebral peduncle to descend through the medial lemniscus into the
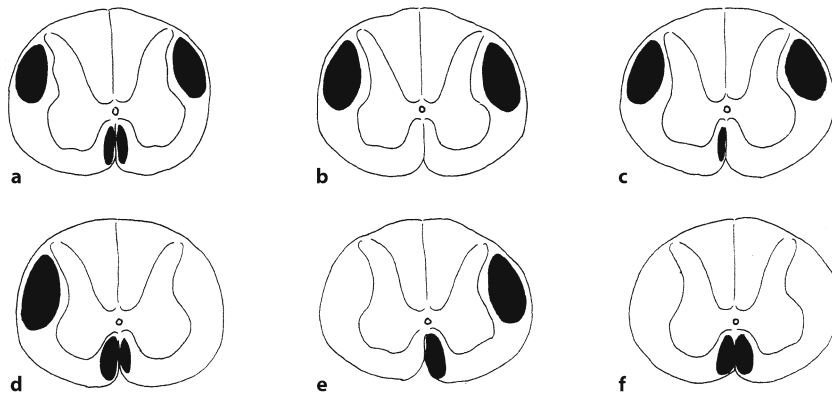
Fig. 6.33 The possible variations of the decussation of the pyramidal tracts. The following percentages refer to data by Yakovlev and Rakic (1966): **a** the common pattern of partial decussation (66.9%); **b** complete decussation (16.2%); **c** complete crossing of one pyramidal tract (13.9%); **d** complete non-decussation of one pyramid (after Norman et al. 1995); **e** unilateral absence of pyramidal tracts (one case); **f** uncrossed pyramidal tracts (2.3%). (After Mestrom 1911)

medulla, whereas a lateral or deep pes lemnisci detaches itself from the dorsal part of the cerebral peduncle, and descends in or near the medial lemniscus. Corticospinal fibres may leave the pyramidal tract at the pontine level and descend lateral to the inferior olive into the ipsilateral anterolateral funiculus (Barnes 1901; Winkler 1926). Hoche (1897a, b) described a bundle of fibres leaving the pyramidal tract at the level of the VIIth cranial nerve, crossing the midline to join the contralateral pyramidal tract. Frequently, a bundle of Pick occurs (Pick 1890; Verhaart 1934). This bundle consists of recurrent pyramidal tract fibres, which after decussating in the lower medulla ascend in the bulbar lateral tegmental field (Kuypers 1958). Moreover, a recurrent circumolivary pyramidal bundle may occur (Swank 1934), a portion of which may descend as an anterolateral pyramidal tract as far as the lumbar level. In some cases a bundle of pyramidal fibres may pass from the decussation into the posterior columns (Bumke 1907; Roessmann and Hori 1985), a trajectory similar to that found in marsupials and rodents. Another rare anomaly is the presence of a superficially placed lateral corticospinal tract (Kramer 1949; Verhaart and Kramer 1952; Friede 1989). The functional significance of such aberrant bundles remains obscure.

Yakovlev and Rakic (1966) studied the spinal cord of fetuses and neonates with the Loyez technique for staining myelin sheaths. The unmyelinated pyramidal tracts could be followed as unstained bundles in their course through the medulla and the spinal cord. In 66.9% of their cases there was partial decussation of the pyramidal tracts, leading to a larger crossed and a smaller uncrossed pyramidal tract on both sides (Figs. 6.33a, 6.34a). Complete decussation of both pyramids with absence of both anterior pyramidal tracts was found in 16.2% of cases (Fig. 6.33b). In the next most common pattern (13.9%), one pyramidal tract crossed completely (Figs. 6.33c, 6.34b). A complete decussation of the left pyramidal tract occurred six times more often than a complete decussation of the right pyramid. Complete non-decussation of one pyramid was observed by Norman et al. (1995; Fig. 6.33d). In one specimen the lateral and anterior pyramidal tracts were absent on the side of the completely crossed pyramid (Fig. 6.33e). Complete absence of decussating bundles, leading to the absence of both lateral pyramidal tracts was found in three specimens (2.3%; Fig. 6.33f). In more than two thirds of their specimens, the fibres of the left pyramid crossed to the right side of the spinal cord at higher, more cranial levels in the decussation than the fibres of the right pyramid. Moreover, more fibres of the left pyramid decussated than of the right pyramid, whereas more fibres of the right pyramid than of the left one remained uncrossed (Nathan et al. 1990). The resulting greater number of corticospinal fibres on the right side of the spinal cord appears to be unrelated to handedness (Kertesz and Geschwind 1971).

Owing to its long, protracted development, malformations of the pyramidal tract may occur over almost the entire prenatal period, the most obvious of which is complete *absence* of the *pyramidal tracts*. The corticospinal tracts are most easily accessed in a transverse section of the medulla, where they form the pyramids. *Aplasia* of the pyramidal tracts is characterized by the absence of the pyramids. Bilateral absence of the pyramidal tracts is usual in anencephaly and holoprosencephaly. It also occurs in many cases of antenatal and perinatal destructive lesions such as porencephaly and hydranencephaly, in X-linked congenital aqueduct stenosis, in micro-
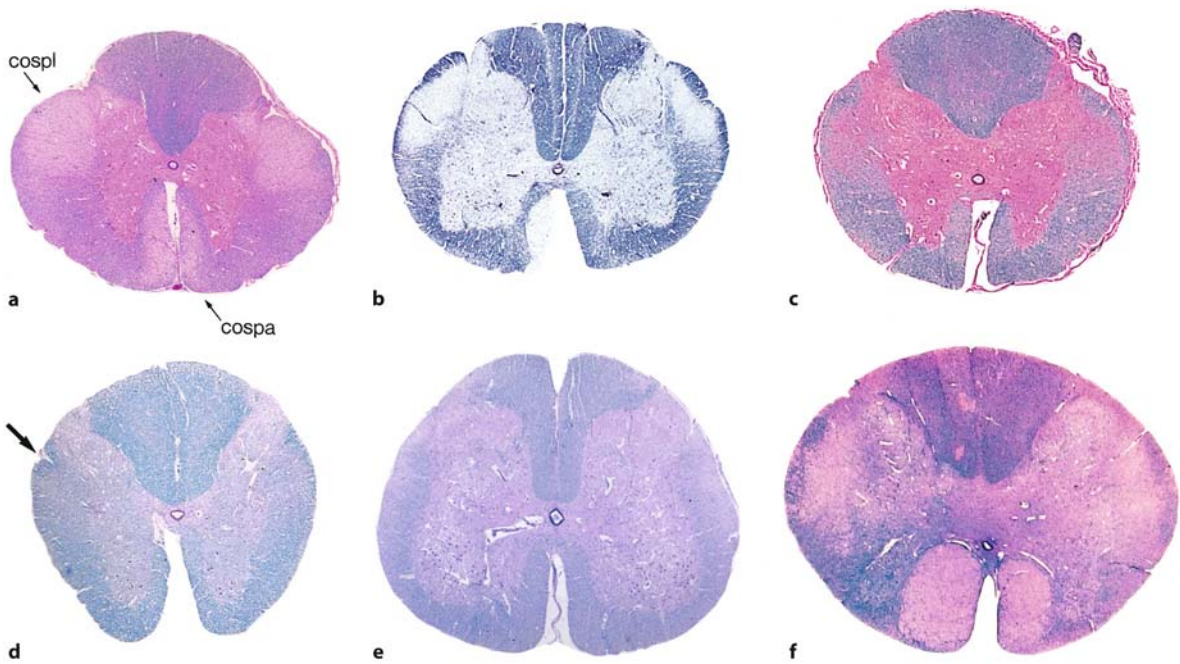
Fig. 6.34 Microscopy of the pyramidal tracts at the spinal level. In a neonatal control case (**a**), the corticospinal tracts stand out in the thoracic cord as unstained pathways. Unilateral crossing of one pyramid is shown in **b**. Absence of the corticospinal tracts is shown for **c** X-linked hydrocephalus (thoracic cord), **d** a microcephaly case (thoracic spinal cord) – note the abnormal sulcus just below the dorsal horn (*arrow*) – and **e** holoprosencephaly (lumbar cord). **f** Non-decussation of the pyramidal tracts for a severe, lethal form of Möbius syndrome (cervical cord). *cospa* anterior corticospinal tract, *cospl* lateral corticospinal tract

cephaly, and it may occur in neuronal migration disorders of the cerebral cortex (Chow et al. 1985; Friede 1989; Norman et al. 1995; ten Donkelaar et al. 1999, 2004; Clinical Case 6.3). Uncommonly large pyramids were found in three cases of cerebellar hypoplasia (Anton 1922). Bilateral *corticospinal tract hypertrophy* was found in the X-linked form of Kallmann syndrome (Krams et al. 1999). Unilateral hypertrophy of the pyramidal tract is uncommon, and is usually associated with an early destructive lesion in the contralateral hemisphere (Déjérine and Déjérine 1902; Verhaart 1950; Friede 1989). It may also occur in hemimegalencephaly with its obvious asymmetry of the pyramids (Dambska et al. 1984; Robain et al. 1988). Malformations of the pyramidal tract due to secondarily acquired injury are discussed in Chap. 10.

Anomalies of the *decussation* of the *pyramidal tract* are mostly non-specific, coincidental anomalies (Luhan 1959; Roessmann and Hori 1985; Vogel et al. 1990; Norman et al. 1995), but are frequently found in posterior fossa malformations such as occipital encephaloceles (Verhaart and Kramer 1952), the Dandy–Walker malformation (D'Agostino et al. 1963; Lagger 1979; Janzer and Friede 1982), Joubert syndrome (Friede and Boltshauser 1978; Yachnis and Rorke 1999; ten Donkelaar et al. 2000), in *ROBO3* mutations (Sect. 6.7.2) and in cases with extensive malformations of the brain stem such as in Möbius syndrome (Chap. 7).

Owing to their long, protracted development, malformations of the pyramidal tracts may occur over almost the entire prenatal period, the most obvious of which is complete *absence* of the *pyramidal tracts*. The corticospinal tracts are most easily accessed in a transverse section of the medulla, where they form the pyramids. *Aplasia* of the pyramidal tracts is characterized by the absence of the pyramids. The olivary nuclei abut the ventral surface of the medulla, covered by a thin layer of marginal glia. Examples of aplasia and secondary malformations of the pyramidal tract are shown in cases of an extreme, familiar form of microcephaly, holoprosencephaly and porencephaly in Figs. 6.34–6.36.

Bilateral absence of the pyramidal tracts is usual in anencephaly and holoprosencephaly. It also occurs in many cases of antenatal and perinatal destructive lesions such as porencephaly and hydranencephaly, in X-linked congenital aqueduct stenosis, in microcephaly, and it may occur in neuronal migration disorders (ten Donkelaar et al. 2004). Chow et al. (1985) found bilateral absence of the pyramids in 0.7 % of 2,850 autopsies carried out at the Royal Children's Hospital in Melbourne (Australia). They found a strong association with X-linked congenital aqueduct stenosis. X-linked hydrocephalus was first described by Bickers and Adams (1949) in a British family with several male siblings that died at birth from congenital hydrocephalus due to aqueduct stenosis. The discovery that *L1CAM* mutations may lead to an X-linked recessive disorder with manifestations including hydrocephalus, adducted thumbs, spastic hemiplegia, hypoplasia or agenesis of the corpus callosum and mental retardation led to a steadily increasing list of familiar and isolated cases. Since the first mutation report (Rosenthal et al. 1992), more than 100 families and isolated cases with *L1CAM* mutations have been
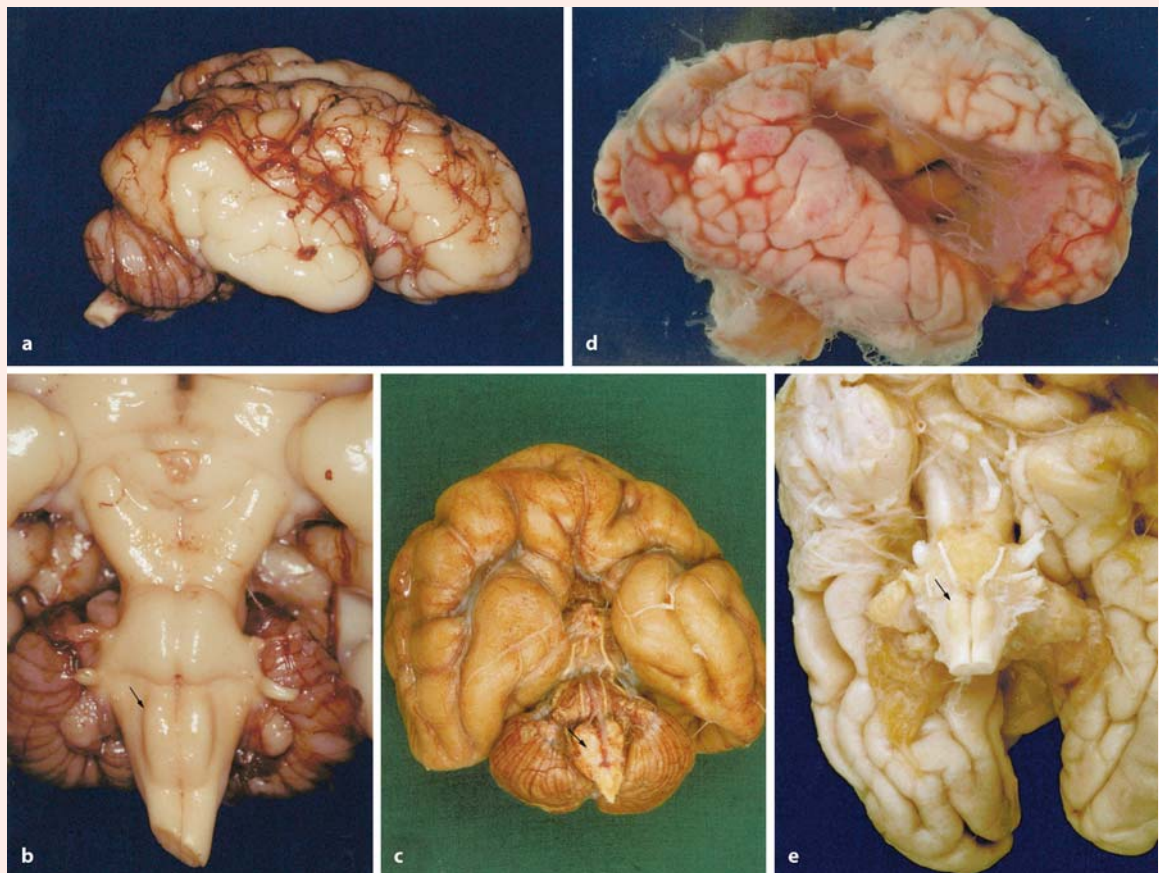
Fig. 6.35 Macroscopy of some cases with malformations involving the pyramidal tracts: **a**, **b** lateral and basal views of the brain in an extreme, familial case of microcephaly (from ten Donkelaar et al. 1999); **c** basal view of the brain of a patient with holoprosencephaly; **d**, **e** lateral and basal views of a case of porencephaly. Note the medially located inferior olives in all cases (*small arrows*)
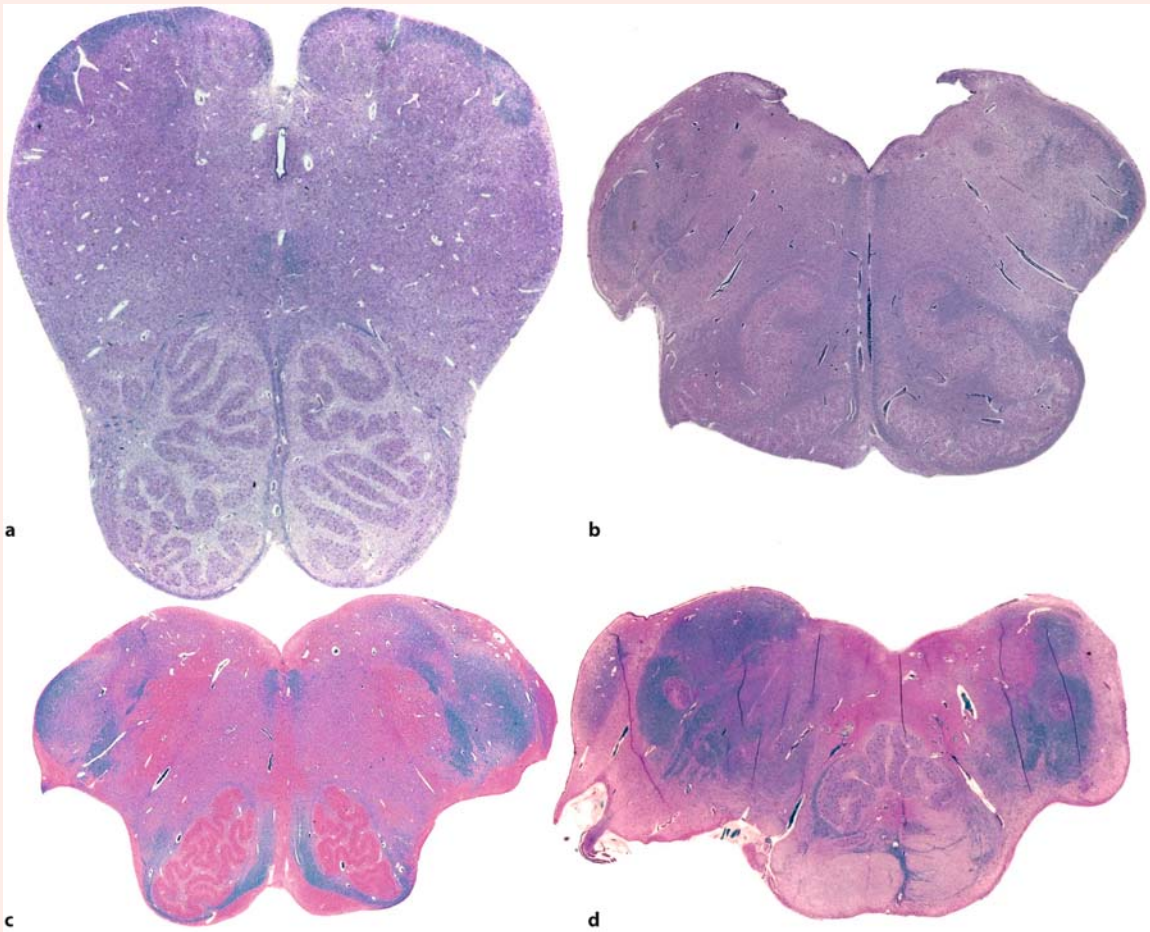
Fig. 6.36 Microscopy of the pyramidal tracts at the medullary level. Absence of the pyramids is shown for **a** an extreme, familial case of microcephaly (from ten Donkelaar et al. 1999), **b** holoprosencephaly and **c** X-linked hydrocephalus. **d** Brain stem malformations including medial inferior olives above malformed pyramids, possibly leading to non-decussation of the pyramidal tracts (Fig. 6.34 f) for a severe, lethal form of Möbius syndrome

described (Fransen et al. 1997; Finckh et al. 2000). Previously described disorders such as X-linked hydrocephalus, MASA (mental retardation, adducted thumbs, spastic paraparesis, agenesis of the corpus callosum) syndrome, X-linked agenesis of the corpus callosum and spastic paraplagia type 1 represent phenotypic variants of *L1CAM* mutations. In a screening study of 153 cases with prenatally or clinically suspected X-chromosomal hydrocephalus, Finckh et al. (2000) found a mutation detection rate of 74.2% for patients with at least two additional cases in the family, but only 16 mutations in the 102 cases with negative family history (15.7% detection rate). In a 2-week-old male neonate with an *L1CAM* mutation, Dobson et al. (2001) found normal pyramidal decussation and axonal projections to the spinal cord.

References

Bickers DS, Adams RD (1949) Hereditary stenosis of the aqueduct of Sylvius as a cause of congenital hydrocephalus. Brain 72:246–252

Chow CW, Halliday JL, Anderson RM, Danks DM, Fortune DW (1985) Congenital absence of pyramids and its significance in genetic diseases. Acta Neuropathol (Berl) 65:313–317

Dobson CB, Villagra F, Clowry GJ, Smith M, Kenwrick S, Donnai D, Miller S, Eyre JA (2001) Abnormal corticospinal function but normal axonal guidance in human L1CAM mutations. Brain 124:2393–2406

Finckh U, Schröder J, Ressler B, Veske A, Gal A (2000) Spectrum and detection rate of *L1CAM* mutations in isolated and familial cases with clinically suspected L1-disease. Am J Med Genet 92:40–46

Fransen E, van Camp G, Vits L, Willems PJ (1997) L1-associated diseases: Clinical geneticists divide, molecular geneticists unite. Hum Mol Genet 6:1625–1632

Rosenthal A, Jouet M, Kenwrick SA (1992) Aberrant splicing of neural cell adhesion molecule L1 mRNA in a family with X-linked hydrocephalus. Nat Genet 2:107–112

ten Donkelaar HJ, Lammens M, Wesseling P, Hori A, Keyser A, Rotteveel J (2004) Development and malformations of the human pyramidal tract. J Neurol 251:1429–1442

References

Altman J, Bayer SA (1980a) Development of the brain stem of the rat. I. Thymidine-radiographic study of the time of origin of neurons of the lower medulla. J Comp Neurol 194:1–35

Altman J, Bayer SA (1980b) Development of the brain stem of the rat. II. Thymidine-radiographic study of the time of origin of neurons of the upper medulla, excluding the vestibular and auditory nuclei. J Comp Neurol 194:37–56

Altman J, Bayer SA (1980c) Development of the brain stem of the rat. III. Thymidine-radiographic study of the time of origin of neurons of the vestibular and auditory nuclei. J Comp Neurol 194:877–904

Altman J, Bayer SA (1980d) Development of the brain stem of the rat. IV. Thymidine-radiographic study of the time of origin of neurons in the pontine region. J Comp Neurol 194:905–929

Altman J, Bayer SA (1981) Development of the brain stem of the rat. V. Thymidine-radiographic study of the time of origin of neurons in the midbrain tegmentum. J Comp Neurol 198:677–716

Altman J, Bayer SA (1984) The development of the rat spinal cord. Adv Anat Embryol Cell Biol 85:1–166

Altman J, Bayer SA (2001) Development of the Human Spinal Cord. An interpretation based on experimental studies in animals. Oxford University Press, New York

Anton G (1922) Ueber Ersatz der Bewegungsleistungen beim Menschen und Entwicklungsstörungen des Kleinhirns. Zbl Ges Neurol Psychiatr 30:372–374

Arber S, Han B, Mendelsohn M, Smith M, Jessell TM, Sockanathan S (1999) Requirement for the homeobox gene Hb9 in the consolidation of motor neuron identity. Neuron 23:659–674

Arber S, Ladle DR, Lin JH, Frank E, Jessell TM (2000) ETS gene *Er81* controls the formation of functional connections between group Ia sensory afferents and motor neurons. Cell 101:485–498

Armand J, Edgley SA, Lemon RN, Olivier E (1994) Protracted postnatal development of corticospinal projections from the primary motor cortex to hand motoneurones in the macaque monkey. Exp Brain Res 101:178–182

Armand J, Olivier E, Edgley SA, Lemon RN (1996) The structure and function of the developing corticospinal tract: Some key issues. In: Wing AM, Haggard P, Flanagan JR (eds) Hand and Brain. The neurophysiology and psychology of hand movements. Academic, San Diego, CA, pp 125–145

Armand J, Olivier E, Edgley SA, Lemon RN (1997) Postnatal development of corticospinal projections from motor cortex to the cervical enlargement in the macaque monkey. J Neurosci 17:251–266

Asanuma C, Ohkawa R, Stanfield BB, Cowan WM (1988) Observations on the development of certain ascending inputs to the thalamus in rats. I. Postnatal development. Dev Brain Res 41:159–170

Auclair F, Bélanger M-C, Marchand R (1993) Ontogenetic study of early brain stem projections to the spinal cord in the rat. Brain Res Bull 30:281–289

Auclair F, Marchand R, Glover JC (1999) Regional patterning of reticulospinal and vestibulospinal neurons in the hindbrain of mouse and rat embryos. J Comp Neurol 411:288–300

Barnes S (1901) Degeneration in hemiplegia: With special reference to a ventrolateral pyramidal tract, the accessory fillet and Pick's bundle. Brain 24:463–501

Bayer SA, Altman J (2002) The Spinal Cord from Gestational Week 4 to the 4th Postnatal Month. CRC, Boca Raton, FL

Bayer SA, Altman J, Russo RJ, Zhang X (1995) Embryology. In: Duckett S (ed) Pediatric Neuropathology. Williams & Wilkins, Baltimore, MD, pp 54–107

Beal JA, Bice TN (1994) Neurogenesis of spinothalamic and spinocerebellar tract neurons in the lumbar spinal cord of the rat. Brain Res 78:49–56

Benstead JG (1953) A case of diastematomyelia. J Pathol Bacteriol 66:553–557

Bentley JFR, Smith JR (1960) Developmental posterior remnants and spinal malformations. The split notochord syndrome. Arch Dis Child 35:76–86

Bergemann AD, Zhang L, Chiang MK, Brambilla R, Klein R, Flanagan JG (1998) Ephrin-B3, a ligand for the receptor EphB3, expressed in the midline of the developing neural tube. Oncogene 16:471–480

Bermingham NA, Hassan BA, Wang VY, Fernandez M, Banfi S, Bellen HJ, Fritzsch B, Zoghbi NY (2001) Proprioceptor pathway development is dependent on Math1. Neuron 30:411–422

Bodhireddy SR, Lyman WD, Rashbaum WK, Weidenheim KM (1994) Immunohistochemical detection of myelin basic protein is a sensitive marker of myelination in second trimester human fetal spinal cord. J Neuropathol Exp Neurol 53:144–149

Bremer JL (1952) Dorsal intestinal fistula; accessory neurenteric canal; diastematomyelia. Arch Pathol 54:132–138

Briscoe J, Ericson J (2001) Specification of neuronal fates in the ventral neural tube. Curr Opin Neurobiol 11:43–49

Briscoe J, Pierani A, Jessell TM, Ericson J (2000) A homeodomain protein code specifies progenitor cell identity and neuronal fate in the ventral neural tube. Cell 101:435–445

Brodal A (1981) Neurological Anatomy in Relation to Clinical Medicine, 3rd ed. Oxford University Press, Oxford

Brodal P (1992) The Central Nervous System. Structure and function. Oxford University Press, Oxford

Brody BA, Kinney HC, Kloman AS, Gilles FH (1987) Sequence of central nervous system myelination in human infancy. I. An autopsy study of myelination. J Neuropathol Exp Neurol 46:283–301

Bumke OCE (1907) Ueber Variationen im Verlauf der Pyramidenbahn. Arch Psychiatr Nervenkr 42:1–18

Burrill JD, Moran L, Goulding MD, Saueressig H (1997) PAX2 is expressed in multiple spinal cord interneurons, including a population of EN1+ interneurons that require PAX6 for their development. Development 124:4493–4503

Caroni P, Schwab ME (1988a) Two membrane protein fractions from rat central myelin with inhibitory properties for neurite growth and fibroblast spreading. J Cell Biol 106:1281–1288

Caroni P, Schwab ME (1988b) Antibody against myelin-associated inhibitors of neurite growth neutralizes nonpermissive substrate properties of CNS white matter. Neuron 1:85–96

Caspary T, Anderson KV (2003) Patterning cell types in the dorsal spinal cord: What the mouse mutants say. Nat Rev Neurosci 4:290–298

Castellani V, Chédotal A, Schachner M, Faivre-Sarrailh C, Rougon G (2000) Analysis of the L1-deficient mouse phenotype reveals cross-talk between Sem3A and L1 signaling pathways in axonal guidance. Neuron 27:237–249

Cauna N, Mannon G (1959) Development and postnatal changes of digital Pacinian corpuscles (corpuscula lamellosa) in the human hand. J Anat (Lond) 93:271–286

Cauna N, Mannon G (1961) Organization and development of the preterminal nerve pattern in the palmar digital tissues in man. J Comp Neurol 117:309–328

Chiang C, Litingtung Y, Lee E, Young KE, Corden JL, Westphal H, Beachy PA (1996) Cyclopia and defective axial patterning in mice lacking Sonic hedgehog gene function. Nature 383:407–413

Chimelli L, Scaravilli F (1987) The development of the gracile nucleus in the rat: The time of ingrowth of ascending primary sensory fibers and the effect of early deafferention. Neuroscience 22:661–670

Chow CW, Halliday JL, Anderson RM, Danks DM, Fortune DW (1985) Congenital absence of pyramids and its significance in genetic diseases. Acta Neuropathol (Berl) 65:313–317

Christ B (1990) Entwicklung der Rumpfwand. In; Hinrichsen KV (Hrsg) Humanembryologie. Springer, Berlin Heidelberg New York, pp 823–837

Cohen NR, Taylor JSH, Scott LB, Guillery RW, Soriano P, Furley AJ (1997) Errors in corticospinal axon guidance in mice lacking the neural cell adhesion molecule L1. Curr Biol 8:26–33

Coonan JR, Greferath U, Messenger J, Hartley L, Murphy M, Boyd AW, Dottori M, Galea MP, Bartlett Pf (2001) Development and reorganization of corticospinal projections in EphA4 deficient mice. J Comp Neurol 436:248–262

Cooper ERA (1946) The development of the human red nucleus and corpus striatum. Brain 69:34–44

D'Agostino AN, Kernohan JW, Brown JR (1963) The Dandy-Walker syndrome. J Neuropathol Exp Neurol 22:450–470

Dahme M, Bartsch U. Martini R, Anliker B, Schachner M, Mantei N (1997) Disruption of the mouse L1 gene leads to malformations of the nervous system. Nat Genet 17:346–349

Dambska M, Wisniewski K, Sher JH (1984) An autopsy case of hemimegalencephaly. Brain Dev 6:60–64

de Boer-van Huizen RT, ten Donkelaar HJ (1999) Early development of descending supraspinal pathways: A tracing study in fixed and isolated rat embryos. Anat Embryol (Berl) 199:539–547

Déjérine J (1901) Anatomie des centres nerveux, Tôme 2. Rueff, Paris

Déjérine J, Déjérine A (1902) Sur l'hypertrophie compensatrice des faisceaux pyramidal du côté sain, dans un cas d'hémiplégie cérébrale infantile. Rev Neurol 10:642–646

de Vries JIP, Visser GHA, Prechtl HFR (1982) The emergence of fetal behavior. I. Qualitative aspects. Early Human Devl 7:301–322

de Vries JIP, Visser GHA, Prechtl HFR (1984) Fetal motility in the first half of pregnancy. In: Prechtl HFR (ed) Continuity of Neural Functions from Prenatal to Postnatal Life. Spastics International, Oxford, pp 46–64

Diez del Corral R, Storey KG (2001) Markers in vertebrate neurogenesis. Nat Rev Neurosci 2:835–839

Dominok GW (1962) Zur Frage der Diplomyelie. Dtsch Z Nervenheilk 183:340–350

Donatelle JM (1977) Growth of the corticospinal tracts and the development of placing reactions in the postnatal rat. J Comp Neurol 175:207–232

Dottori M, Hartley L, Galea M, Paxinos G, Polizotto M, Kilpatrick T, Bartlett PF, Murphy M, Köntgen F, Boyd AW (1998) EphA4 (Sek1) receptor tyrosine kinase is required for the development of the corticospinal tract. Proc Natl Acad Sci USA 95:13248–13253

Echelard Y, Epstein DJ, St-Jacques B, Shen L, Mohler J, McMahon JA, McMahon AP (1993) Sonic hedgehog, a member of a family of putative signalling molecules, is implicated in the regulation of CNS polarity. Cell 75:1417–1430

Emery JL, Lendon RG (1974) The local cord lesion in neurospinal dysraphism (meningomyelocele). J Pathol 110:83–96

Ericson J, Morton S, Kawakami A, Roelink H, Jessell TM (1996) Two critical periods of Sonic Hedgehog signaling required for the specification of motor neuron identity. Cell 87:661–673

Ericson J, Briscoe J, Rashbass P, van Heyningen V, Jessell TM (1997) Graded sonic hedgehog signaling and the specification of cell fate in the ventral neural tube. Cold Spring Harb Symp Quant Biol 62:451–466

Eyre JA, Miller S, Romesh V (1991) Constancy of central production delays during development in man: Investigation of motor and somatosensory pathways. J Physiol (Lond) 434:441–452

Eyre JA, Miller S, Clowry GJ, Conway EA, Watts C (2000) Functional coticospinal projections are established prenatally in the human foetus permitting involvement in the development of spinal motor centres. Brain 123:51–64

Eyre JA, Taylor JP, Villagra F, Smith M, Miller S (2001) Evidence of activity-dependent withdrawal of corticospinal projections during human development. Neurology 57:1543–1554

Feller A, Sternberg H (1929) Zur Kenntnis der Fehlbildungen der Wirbelsäule. I. Die Wirbelkörperspalte und ihre formale Genese. Virchows Arch Pathol Anat 272:613–640

Finger JH, Bronson RT, Harris B, Johnson K, Przyborski SA, Ackerman SL (2002) The netrin receptors Unc5h3 and Dcc are necessary at multiple choice points for the guidance of corticospinal tract axons. J Neurosci 22:10346–10356

Flament D, Goldsmith P, Lemon RN (1992a) The development of corticospinal projections to tail and hindlimb motoneurons studied in infant macaques using magnetic brain stimulation. Exp Brain Res 90:225–228

Flament D, Hall EJ, Lemon RN (1992b) The development of corticomotoneuronal projections investigated using magnetic brain stimulation in the infant macaque. J Physiol (Lond) 447:755–768

Flechsig P (1876) Die Leitungsbahnen im Gehirn und Rückenmark des Menschen auf Grund entwicklungsgeschichtlicher Untersuchungen. Engelmann, Leipzig

Foerster O (1936) Motorische Felder und Bahne. In: Bumke O, Foerster O (Hrsg) Handbuch der Neurologie, Band 6. Springer, Berlin Heidelberg New York, pp 1–357

Forssberg H, Eliasson AC, Kinoshita H, Johansson RS, Westling G (1991) Development of human precision grip. I. Basic coordination of force. Exp Brain Res 85:451–457

Friede RL (1989) Developmental Neuropathology, 2nd ed. Springer, Berlin Heidelberg New York

Friede RL, Boltshauser E (1978) Uncommon syndromes of cerebellar vermis aplasia. I. Joubert syndrome. Dev Med Child Neurol 20:758–763

Fujimori KE, Takeuchi K, Yazaki T, Uyemura K, Nojyo Y, Tamamaki N (2000) Expression of L1 and TAG-1 in the corticospinal, callosal, and hippocampal commissural neurons in the developing rat telencephalon as revealed by retrograde and in situ hybridization double labeling. J Comp Neurol 417:275–288

Galea MP, Darian-Smith I (1995) Postnatal maturation of the direct corticospinal projections in the macaque monkey. Cereb Cortex 5:518–540

Galea MP, Darian-Smith I (1997a) Corticospinal projection patterns following unilateral section of the spinal cord in the newborn and juvenile macaque monkey. J Comp Neurol 381:282–306

Galea MP, Darian-Smith I (1997b) Manual dexterity and corticospinal connectivity following unilateral section of the cervical spinal cord in the macaque monkey. J Comp Neurol 381:307–319

Gilles FH, Shankle W, Dooling EC (1983) Myelinated tracts. In: Gilles FH, Leviton A, Dooling EC (eds) The Developing Human Brain. Wright, Bristol, pp 117–183

Gómez-Skarmeta JL, Campuzano S, Modolell J (2003) Half a century of neural prepatterning: The story of a few bristles and many genes. Nat Rev Neurosci 4:587–598

Gorgels TGMF (1990) A quantitative analysis of axon outgrowth, axon loss, and myelination in the rat pyramidal tract. Dev Brain Res 54:51–61

Gorgels TGMF (1991) Outgrowth of the pyramidal tract in the rat cervical spinal cord: Growth cone ultrastructure and guidance. J Comp Neurol 306:95–116

Gorgels TGMF, Oestreicher AB, de Kort EJM, Gispen WH (1987) Immunocytochemical distribution of the protein kinase C substrate B-50 (GAP43) in developing rat pyramidal tract. Neurosci Lett 83:59–64

Gowan K, Helms AW, Hunsaker TL, Collisson T, Ebert PJ, Odom R, Johnson JE (2001) Crossinhibitory activities of Ngn1 and Math1 allow specification of distinct dorsal interneurons. Neuron 31:219–232

Gribnau AAM, de Kort EJM, Dederen PJWC, Nieuwenhuys R (1986) On the development of the pyramidal tract in the rat. II. An anterograde tracer study of the outgrowth of the corticospinal fibers. Anat Embryol (Berl) 175:101–110

Griepentrog F (1953) Eine seltene Form von Rückenmarksmißbildung (Partielle unfreie Diplomyelie). Zentralbl Pathol 90:380–384

Grillner S (2003) The motor infrastructure: From ion channels to neuronal networks. Nat Rev Neurosci 4:573–586

Gross MK, Dottori M, Goulding M (2002) Lbx1 specifies somatosensory association interneurons in the dorsal spinal cord. Neuron 34:535–549

Haas E (1952) Eine fortsatzähnliche Mißbildung des Rückenmarkes und ihre Abgrenzung von den Diastematomyelien. Zentralbl Pathol 88:16–20

Harding B, Copp AJ (1997) Malformations. In: Graham DI, Lantos PL (eds) Greenfield's Neuropathology, 6th ed. Arnold, London, pp 397–533

Heffner CD, Lumsden AGS, O'Leary DDM (1990) Target control of collateral extension and directional growth in the mammalian brain. Science 247:217–220

His W (1886) Zur Geschichte des menschlichen Rückenmarkes und der Nervenwurzeln. Abh Kön Sächs Ges Wiss Math Phys Kl 13:313–372

Hoche A (1897a) Ueber Variationen im Verlaufe der Pyramidenbahn. Neurol Zbl 16:993–997

Hoche A (1897b) Beiträge zur Anatomie der Pyramidenbahn und der oberen Schleife, nebst Bemerkungen über die abnorme Bündel in Pons und Medulla oblongata. Arch Psychiatr Nervenkr 30:103–136

Hogg ID (1941) Sensory nerves and associated structures in the skin of human fetuses of 8 to 14 weeks of menstrual age correlated with functional capability. J Comp Neurol 75:371–410

Holstege G (1991) Descending motor pathways and the spinal motor system: Limbic and non-limbic components. Prog Brain Res 87:307–421

Hooker D (1938) The origin of grasping movement in man. Proc Philos Soc 79:597–606

Hooker D (1954) Early human fetal behavior, with a preliminary note on double simultaneous fetal stimulation. Res Public Assoc Nerv Ment Dis 33:98–113

Hori A (1981) Microdysgenesia of the human spinal cord (in Japanese). Shinkei Byori Gaku (Neuropathology) 2:147–149

Hori A (1983) Microdysplasia of human spinal cord. Part 2: A case of deviated dorsal longitudinal septum (in Japanese). Shinkei Byori Gaku (Neuropathology) 4:1–2

Hori A (1988a) Heterotopic neurons in human spinal nerve roots: What is their clinical significance? J Neurol 235:348–351

Hori A (1988b) Abnormal course of spinal posterior roots and tracts associated with brain malformations. Sensory pathway malformation. Acta Neuropathol (Berl) 75:637–639

Hori A (1998) Developmental anomalies of the spinal cord. Neuropathology 18:433–443

Hori A, Fischer G, Dietrich-Schott B, Ikeda K (1982) Dimyelia, diplomyelia, and diastematomyelia. Clin Neuropathol 1:23–30

Humphrey T (1960) The development of the pyramidal tracts in human fetuses, correlated with cortical differentiation. In: Tower DB, Schadé JP (eds) Structure and Function of the Cerebral Cortex. Elsevier, Amsterdam, pp 93–103

Humphrey T (1964) Some correlations between the appearance of human fetal reflexes and the development of the nervous system. Prog Brain Res 4:93–135

Ikeda Y, Terashima T (1997) Corticospinal tract neurons are radially malpositioned in the sensory-motor cortex of the *shaking rat Kawasaki*. J Comp Neurol 383:370–380

Imondi R, Wideman C, Kaprielian Z (2000) Complementary expression of transmembrane ephrins and their receptors in the mouse spinal cord: A possible role in constraining the orientation of longitudinally projecting axons. Development 127:1397–1410

Inoue K, Terashima T, Inoue Y (1991) The intracortical position of pyramidal tract neurons in the motor cortex of the reeler changes from postnatal day 10 to adulthood. Dev Brain Res 62:146–150

James CCM, Lassman LP (1964) Diastematomyelia. A critical survey of 24 cases submitted to laminectomy. Arch Dis Childh 39:125–130

James CCM, Lassman LP (1972) Spinal Dysraphism. Spina bifida occulta. Butterworths, London

Janzer RC, Friede RL (1982) Dandy-Walker syndrome with atresia of the fourth ventricle and multiple rhombencephalic malformations. Acta Neuropathol (Berl) 58:81–86

Jen JC, Chan W-M, Bosley TM, Wan J, Carr JR, Rüb U, Shattuck D, Salamon G, Kudo LC, Ou J, et al. (2004) Mutations in a human *ROBO* gene disrupt hindbrain axon pathway crossing and morphogenesis. Science 304:1509–1513

Jessell TM (2000) Neuronal specification in the spinal cord: Inductive signals and transcriptional codes. Nature Rev Genet 1:20–29

Joosten EAJ, Bär DPR (1999) Axon guidance of outgrowing corticospinal fibres in the rat. J Anat (Lond) 194:15–32

Joosten EAJ, Gribnau AAM (1989) Astrocytes and guidance of outgrowing corticospinal tract axons in the rat. An immunocytochemical study using anti-vimentin and anti-glial fibrillary acidic protein. Neuroscience 31:439–452

Joosten EAJ, Gribnau AAM, Dederen PJWC (1987) An anterograde tracer study of the developing corticospinal tract in the rat: Three components. Dev Brain Res 36:121–130

Joosten EAJ, Gribnau AAM, Dederen PJWC (1989) Postnatal development of the corticospinal tract in the rat. An ultrastructural anterograde HRP study. Anat Embryol 179:449–456

Joosten EAJ, Gribnau AAM, Gorgels TGMF (1990) Immunoelectron microscopic localization of cell adhesion molecule L1 in developing rat pyramidal tract. Neuroscience 38:675–686

Joosten EAJ, van der Ven PFM, Hooiveld MHW, ten Donkelaar HJ (1991) Induction of corticospinal target finding by release of a diffusible, chemotropic factor in cervical spinal grey matter. Neurosci Lett 128:25–28

Kania A, Johnston RL, Jessell TM (2000) Coordinate roles for LIM homeobox genes in directing the dorsoventral trajectory of motor axons in the vertebrate limb. Cell 102:161–173

Kersten W (1954) Rückenmarksmißbildung beim Hund und Menschen. Dtsch Tierärtzl Wochenschr 61:338–346

Kertesz A, Geschwind N (1971) Patterns of pyramidal decussation and their relationship to handedness. Arch Neurol 24:326–332

Kiehn O, Butt SJB (2003) Physiological, anatomical and genetic identification of CPG neurons in the developing mammalian spinal cord. Prog Neurobiol 70:347–361

Killackey HP, Dehay C, Giroud P, Berland M, Kennedy H (1997) Distribution of corticospinal projection neurons in the neocortex of the fetal macaque monkey. Soc Neurosci Abstr 23:902

Kinney HC, Brody BA, Kloman AS, Gilles FH (1988) Sequence of central nervous system myelination in human infancy. II. Patterns of myelination in autopsied infants. J Neuropathol Exp Neurol 47:217–234

Kirkland JA (1979) Spinal cords with no roots. Lancet 1979 (ii):740

Konstantinidou AD, Silos-Santiago I, Flaris N, Snider WD (1995) Development of the primary afferent projection in human spinal cord. J Comp Neurol 354:1–12

Környey S (1925) Beiträge zur Entwicklungsmechanik und Pathologie des foetalen Zentralnervensystems. Arch Psychiatr Nervenkrh 72:755–787

Kozlowski MA, Williams C, Hinton DR, Miller CA (1989) Heterotopic neurons in spinal cord of patients with ALS. Neurology 39:644–648

Kramer W (1949) De ongekruiste pyramidebaan. Een neuro-anatomisch onderzoek. Thesis, University of Indonesia, Batavia

Krams M, Quinton R, Ashburner J, Friston KJ, Frackowiak RSJ, Bouloux P-MG, Passingham RE (1999) Kallmann's syndrome: Mirror movements associated with bilateral corticospinal tract hypertrophy. Neurology 52:816–822

Kudo N, Yamada T (1987) Morphological and physiological studies of the development of the monosynaptic reflex pathway in the rat lumbar spinal cord. J Physiol (Lond) 389:441–459

Kudo N, Furukawa F, Okado N (1993) Development of descending fibers to the rat embryonic spinal cord. Neurosci Res 16:131–141

Kullander K, Croll SD, Zimmer M, Pan L, McClain J, Hughes V, Zabski S, DeChiara TM, Klein R, Yancopoulos GD, Gale NW (2001) Ephrin-B3 is the midline barrier that prevents corticospinal tract axons from recrossing, allowing for unilateral motor control. Genes Dev 15:877–888

Kumar R, Jain R, Rao KM, Hussain R (2001) Intraspinal neurenteric cysts – report of three paediatric cases. Child Nerv Syst 17:584–588

Kuypers HGJM (1958) Corticobulbar connexions to the pons and lower brain stem in man. An anatomical study. Brain 81:364–388

Kuypers HGJM (1962) Corticospinal connections. Postnatal development in the rhesus monkey. Science 138:678–680

Kuypers HGJM (1981) Anatomy of the descending pathways. In: Brooks VB, Brookhart JM, Mountcastle VB (eds) Handbook of Physiology – The Nervous System, Vol 2: Motor Systems. American Physiological Society, Bethesda, MD, pp 597–666

Lagger RL (1979) Failure of pyramidal tract decussation in the Dandy-Walker syndrome. J Neurosurg 50:382–387

Lakke EAJF (1997) The projections to the spinal cord of the rat during development. A time-table of descent. Adv Anat Embryol Cell Biol 135:1–143

Lakke EAJF, Marani E (1991) Prenatal descent of rubrospinal fibers through the spinal cord of the rat. J Comp Neurol 314:67–78

Lankamp DJ (1967) The fibre composition of the pedunculus cerebri (crus cerebri) in man. Thesis, University of Leiden

Lawrence DG, Hopkins DA (1976) The development of motor control in the rhesus monkey: Evidence concerning the role of corticomotoneuronal connections. Brain 99:235–254

Leber SM, Breedlove SM, Sanes JR (1989) Lineage of motoneurons in chick spinal cord studied with a retroviral marker. Ann Neurol 26:447–448

Leber SM, Breedlove SM, Sanes JR (1990) Lineage, arrangement, and death of clonally related motoneurons in chick spinal cord. J Neurosci 10:2451–2462

Lee KJ, Jessell TM (1999) The specification of dorsal cell fates in the vertebrate central nervous system. Annu Rev Neurosci 22:261–294

Litingtung Y, Chiang C (2000) Control of Shh activity and signaling in the neural tube. Dev Dyn 219:143–154

Luhan JA (1959) Long survival after unilateral stab wound of medulla with unusual pyramidal tract distribution. Arch Neurol 1:427–434

Ma Q, Fode C, Guillemot F, Anderson DJ (1999) *Neurogenin1* and *neurogenin2* control two distinct waves of neurogenesis in developing dorsal root ganglia. Genes Dev 13:1717–1728

Marti E, Bovolenta P (2002) Sonic hedgehog in CNS development: One signal, multiple outputs. Trends Neurosci 25:89–96

Marti E, Bumcrot DA, Takada R, McMahon AP (1995) Requirement of 19K form of Sonic hedgehog for induction of distinct ventral cell types in CNS explants. Nature 375:322–325

Martin JE, Mather K, Swash M (1993) Heterotopic neurons in amyotrophic lateral sclerosis. Neurology 43:1420–1422

Matise M (2002) A dorsal elaboration in the spinal cord. Neuron 34:491–493

Matise MP, Joyner AL (1997) Expression patterns of developmental control genes in normal and Engrailed-1 mutant mouse spinal cord reveal early diversity in developing interneurons. J Neurosci 17:7805–7816

Mestrom LHJ (1911) Variaties in de pyramidenkruising. Thesis, University of Amsterdam. Van Langenhuysen, Amsterdam

Mirnics K, Koerber HR (1995) Prenatal development of rat primary afferent fibers. II. Central projections. J Comp Neurol 355:601–614

Moran-Rivard L, Kagawa T, Saueressig H, Gross MK, Burrill J, Goulding M (2001) Evx1 is a postmitotic determinant of V0 interneuron identity in the spinal cord. Neuron 29:385–399

Müller F, O'Rahilly R (1988a) The development of the human brain from a closed neural tube at stage 13. Anat Embryol (Berl) 177:203–224

Müller F, O'Rahilly R (1988b) The first appearance of the future cerebral hemispheres in the human embryo at stage 14. Anat Embryol (Berl) 177:495–511

Müller F, O'Rahilly R (1989a) The human brain at stage 16, including the initial evagination of the neurohypophysis. Anat Embryol (Berl) 179:551–569

Müller F, O'Rahilly R (1989b) The human brain at stage 17, including the appearance of the future olfactory bulb and the first amygdaloid nuclei. Anat Embryol (Berl) 180:353–369

Müller F, O'Rahilly R (1990a) The human brain at stages 21-23, with particular reference to the cerebral cortical plate and to the development of the cerebellum. Anat Embryol (Berl) 182:375–400

Müller F, O'Rahilly R (1990b) The human rhombencephalon at the end of the embryonic period proper. Am J Anat 189:127–145

Müller F, O'Rahilly R, Benson DR (1986) The early origin of vertebral anomalies, as illustrated by a 'butterfly vertebra'. J Anat (Lond) 177:3–19

Müller K, Hömberg V, Lenard H-G (1991) Magnetic stimulation of motor cortex and nerve roots in children. Maturation of corti-co-motoneuronal projections. Electroencephalogr Clin Neurophysiol 81:63–70

Müller K, Kass-Illiyya F, Reitz M (1997) Ontogeny of ipsilateral corticospinal projections: A developmental study with transcranial magnetic stimulation. Ann Neurol 42:705–711

Müller T, Brohmann H, Pierani A, Heppenstall PA, Lewin GR, Jessell TM, Birchmeier C (2002) The homeodomain factor Lbx1 distinguishes two major programs of neuronal differentiation in the dorsal spinal cord. Neuron 34:551–562

Nait-Oumesmar B, Stecca B, Fatterpekkar G, Naidich T, Corbin J, Lazzarini RA (2002) Ectopic expression of *Gcm1* induces congenital spinal cord abnormalities. Development 129:3957–3964

Nandi KN, Knight DS, Beal JA (1993) Spinal neurogenesis and axon projection: A correlative study in the rat. J Comp Neurol 328:252–262

Nathan PW, Smith MC (1955) Long descending tracts in man. I. Review of present knowledge. Brain 78:248–303

Nathan PW, Smith MC (1981) The rubrospinal and central tegmental tracts in man. Brain 105:223–269

Nathan PW, Smith MC, Deacon P (1990) The corticospinal tracts in man. Course and location of fibres at different segmental levels. Brain 113:303–324

Nathan PW, Smith MC, Deacon P (1996) Vestibulospinal, reticulospinal and descending propriospinal nerve fibers in man. Brain 119:1809–1833

Natsuyama E (1991) In utero behavior of human embryos at the spinal-cord stage of development. Biol Neonate 60(Suppl 1):11–29

Norman MG, McGillivray BC, Kalousek DK, Hill A, Poskin KJ (1995) Congenital Malformations of the Brain. Pathologic, embryologic, clinical, radiologic and genetic aspects. Oxford University Press, New York

Nornes HO, Carry M (1978) Neurogenesis in the spinal cord of the mouse: An autoradiographic analysis. Brain Res 159:1–16

Nyberg-Hansen R, Rinvik E (1963) Some comments on the pyramidal tracts, with special reference to its individual variations in man. Acta Neurol Scand 39:1–30

Okado N (1980) Development of the human cervical spinal cord with reference to synapse formation in the motor nucleus. J Comp Neurol 191:495–513

Okado N (1981) Onset of synapse formation in the human spinal cord. J Comp Neurol 201:211–219

Okado N, Kojima T (1984) Ontogeny of the central nervous system, neurogenesis, fibre connections, synaptogenesis and myelination in the spinal cord. In: Prechtl HFR (ed) Continuity of Neural Functions from Prenatal to Postnatal Life. Spastics Int Med Publ, Oxford, pp 31–45

Okado N, Kakimi S, Kojima T (1979) Synaptogenesis in the cervical cord of the human embryo: Sequence of synapse formation in a spinal reflex pathway. J Comp Neurol 184:491–517

O'Leary DDM, Koester SE (1993) Development of projection neuron types, axon pathways, and patterned projections of the mammalian cortex. Neuron 10:991–1006

O'Leary DDM, Stanfield BB (1986) A transient pyramidal tract projection from the visual cortex in the hamster and its removal by selective collateral elimination. Dev Brain Res 27:89–99

O'Leary DDM, Bicknese AR, de Carlos JA, Heffner CD, Koester SE, Kutka LJ, Terashima T (1990) Target selection by cortical axons: Alternative mechanisms to establish axonal connections in the developing brain. Cold Spring Harbor Symp Quant Biol 55:453–468

Olivier E, Edgley SA, Armand J, Lemon RN (1997) An electrophysiological study of the postnatal development of the corticospinal system in the macaque monkey. J Neurosci 17:267–276

Olson L, Boreus LO, Seiger Å (1973) Histochemical demonstration and mapping of 5-hydroxytryptamine and catecholamine containing neuron systems in the human fetal brain. Z Anat Entw Gesch 139:259–282

Op de Coul AAW, Slooff JL (1975) A clinical and neuropathologic study of a patiënt with abrachia (congenital absence of both arms). Clin Neurol Neurosurg 78:139–147

O'Rahilly R, Meyer DB (1979) The timing and sequence of events in the development of the human vertebral column during the embryonic period proper. Anat Embryol (Berl) 157:167–176

O'Rahilly R, Müller F (2001) Human Embryology & Teratology, 3rd ed. Wiley-Liss, New York

O'Rahilly R, Müller F, Meyer DB (1980) The human vertebral column at the end of the embryonic period proper. 1. The column as a whole. J Anat (Lond) 131:565–575

O'Rahilly R, Müller F, Meyer DB (1983) The human vertebral column at the end of the embryonic period proper. 2. The occipitocervical region. J Anat (Lond) 136:181–195

O'Rahilly R, Müller F, Meyer DB (1990a) The human vertebral column at the end of the embryonic period proper. 3. The thoracicolumbar region. J Anat (Lond) 168:81–93

O'Rahilly R, Müller F, Meyer DB (1990b) The human vertebral column at the end of the embryonic period proper. 4. The sacrococcygeal region. J Anat (Lond) 168:95–111

Orentas DM, Hayes H, Dyer KL, Miller R (1999) Sonic hedgehog signaling is required during the appearance of spinal cord oligodendrocyte precursors. Development 126:2419–2429

Ozaki S, Snider WD (1997) Initial trajectories of sensory axons toward laminar targets in the developing mouse spinal cord. J Comp Neurol 380:215–229

Pang D, Dias MS, Ahdab-Barmada M (1992) Split notochord malformation. Part I: A unified theory of embryogenesis for double spinal cord malformations. Neurosurgery 31:451–480

Parkinson D, del Bigio MR (1996) Posterior 'septum' of the human spinal cord: Normal developmental variations, composition, and terminology. Anat Rec 244:572–578

Patten I, Kulesa P, Shen MM, Fraser S, Placzek M (2003) Distinct modes of floor plate induction in the chick embryo. Development 130:4809–4821

Pfaff S, Kintner C (1998) Neuronal diversification: Development of motor neuron subtypes. Curr Opin Neurobiol 8:27–36

Pick A (1890) Ueber ein abnormes Bündel der menschlichen Medulla oblongata. Arch Psychiatr Nervenkr 21:636–640

Pierani A, Brenner-Morton S, Chiang C, Jessell TM (1999) A Sonic Hedgehog-independent, retinoid-activated pathway of neurogenesis in the ventral spinal cord. Cell 97:903–915

Pierani A, Moran-Rivard L, Sunshine MJ, Littman DR, Goulding M, Jessell TM (2001) Control of interneuron fate in the developing spinal cord by the progenitor homeodomain protein Dbx1. Neuron 29:367–384

Placzek M, Dodd J, Jessell TM (2000) The case for floor plate induction by the notochord. Curr Opin Neurobiol 10:15–22

Price SR, Briscoe J (2004) The gene ratio- and diversification of spinal motor neurons: Signals and responses. Mech Dev 121:1103–1115

Puelles L, Verney C (1998) Early neuromeric distribution of tyrosine-hydroxylase-immunoreactive neurons in human embryos. J Comp Neurol 394:283–308

Rajaofetra N, Sandillon F, Geffard M, Privat A (1989) Pre- and postnatal ontogeny of serotonergic projections to the rat spinal cord. J Neurosci Res 22:305–321

Rajaofetra N, Poulat P, Marlier L, Geffard M, Privat A (1992) Pre- and postnatal development of noradrenergic projections to the rat spinal cord: an immunocytochemical study. Dev Brain Res 67:237–246

Rexed B (1952) The cytoarchitectonic organization of the spinal cord in the cat. J Comp Neurol 96:415–495

Rexed B (1954) A cytoarchitectonic atlas of the spinal cord in the cat. J Comp Neurol 100:297–379

Rhines R, Windle WF (1941) The early development of the fasciculus longitudinalis medialis and associated secondary neurons in the rat, cat and man. J Comp Neurol 75:165–189

Rickenbacher J, Landolt AM, Theiler K (1982) Von Lanz/Wachsmuth – Praktische Anatomie, Band II/7: Rücken. Springer, Berlin Heidelberg New York

Robain O, Floquet C, Heldt N, Rozenberg F (1988) Hemimegalencephaly: a clinicopathological study of four cases. Neuropathol Appl Neurobiol 14:125–135

Roelink H, Augsburger A, Heemskerk J, Korzh V, Norlin S, Ruiz i Altaba A, Tanabe Y, Placzek M, Edlund T, Jessell TM, Dodd J (1994) Floor plate and motor neuron induction by vhh-1, a vertebrate homolog of hedgehog expressed by the notochord. Cell 76:761–775

Roessmann U, Hori A (1985) Agyria (lissencephaly) with anomalous pyramidal crossing. Case report and review of literature. J Neurol Sci 69:357–364

Rokos J (1975) Pathogenesis of diastematomyelia and spina bifida. J Pathol 117:155–161

Ruiz i Altaba A, Nguyên V, Palma V (2003) The emergent design of the neural tube: Prepattern, SHH morphogen and GLI code. Curr Opin Genet Dev 13:513–521

Sabatier C, Plump AS, Ma L, Brose K, Tamada A, Murakami F, Lee EY-HP, Tessier-Lavigne M (2004) The divergent Robo family protein Rig-1/Robo3 is a negative regulator of Slit responsiveness required for midline crossing by commissural axons. Cell 117:157–169

Sanes JR, Yamagata M (1999) Formation of lamina-specific synaptic connections. Curr Opin Neurobiol 9:79–87

Sasaki S, Iwata M (1998) Characterizations of heterotopic neurons in the spinal cord of amyotrophic lateral sclerosis patients. Acta Neuropathol 95:367–372

Saueressig H, Burrill J, Goulding M (1999) Engrailed-1 and netrin-1 regulate axon pathfinding by association interneurons that project to motor neurons. Development 126:4201–4212

Schneiderling W (1938) Unvollkommene dorso-ventrale Verdoppelung des Rückenmarkes. Virchows Arch Pathol Anat Physiol 31:479–489

Schoenen J, Faull RLM (1990) Spinal cord: Cytoarchitectural, dendroarchitectural, and myeloarchitectural organization. In: Paxinos G (ed) The Human Nervous System. Academic, San Diego, CA, pp 19–53

Schreyer DJ, Jones EG (1982) Growth and target finding by axons of the corticospinal tract in prenatal and postnatal rats. Neuroscience 7:1837–1853

Schreyer DJ, Jones EG (1988) Axon elimination in the developing corticospinal tract of the rat. Dev Brain Res 38:103–119

Schwab ME, Schnell L (1991) Channeling of developing rat corticospinal tract axons by myelin-associated neurite growth inhibitors. J Neurosci 11:709–721

Sharma K, Frank E (1998) Sensory axons are guided by local cues in the developing dorsal spinal cord. Development 125: 635–643

Sharma K, Peng C-Y (2001) Spinal motor circuits: Merging development and function. Neuron 29:321–324

Sherman JL, Barkovich AJ, Citrin CM (1986) The MR appearances of syringomyelia: New observations. Am J Neuroradiol 7:985–995

Silos-Santiago I, Snider WD (1992) Development of commissural neurons in the embryonic rat spinal cord. J Comp Neurol 325:514–526

Silos-Santiago I, Snider WD (1994) Development of interneurons with ipsilateral projections in embryonic rat spinal cord. J Comp Neurol 342:221–231

Sims TJ, Vaughn JE (1979) The generation of neurons involved in an early reflex pathway of embryonic rat spinal cord. J Comp Neurol 183:707–720

Skandalakis JE, Gray SW (1994) Embryology for Surgeons, 3rd ed. Williams & Wilkins, Baltimore, MD

Snider WD, Zhang L, Yusoof S, Gorukanti N, Tsering C (1992) Interactions between dorsal root axons and their target motor neurons in developing mammalian spinal cord. J Neurosci 12:3494–3508

Spiller WG (1906) Syringomyelia, extending from the sacral region of the spinal cord through the medulla oblongata, right side of the pons and right cerebral peduncle to the upper part of the right internal capsule (syringobulbia). Br Med J 2:1017–1021

Stanfield BB (1992) The development of the corticospinal projection. Prog Neurobiol 38:169–202

Stanfield BB, O'Leary DDM (1985) The transient corticospinal projection from the occipital cortex during the postnatal development of the rat. J Comp Neurol 238:236–248

Streeter GF (1919) Factors involved in the formation of the filum terminale. Am J Anat 25:1–11

Swank RL (1934) The relationship between the circumolivary pyramidal fascicles and the pontobulbar body in man. J Comp Neurol 60:309–317

Swanson AG, Buchan GC, Alvord EC Jr (1965) Anatomic changes in congenital insensitivity to pain. Arch Neurol 12:12–18

ten Donkelaar HJ (2000) Development and regenerative capacity of descending supraspinal pathways in tetrapods: A comparative approach. Adv Anat Embryol Cell Biol 145:1–145

ten Donkelaar HJ, Wesseling P, Semmekrot BA, Liem KD, Tuerlings J, Cruysberg JRM, de Wit PEJ (1999) Severe, non X-linked congenital miocrocephaly with absence of the pyramidal tracts in two siblings. Acta Neuropathol (Berl) 98:203–211

ten Donkelaar HJ, Hoevenaars F, Wesseling P (2000) A case of Joubert's syndrome with extensive cerebral malformations. Clin Neuropathol 19:85–93

ten Donkelaar HJ, Willemsen MAAP, van der Heijden I, Beems T, Wesseling P (2002) A spinal intradural enterogenous cyst with well-differentiated muscularis propria. Acta Neuropathol (Berl) 104:538–542

ten Donkelaar HJ, Lammens M, Wesseling P, Hori A, Keyser A, Rotteveel J (2004) Development and malformations of the human pyramidal tract. J Neurol 251:1429–1442

Terashima T (1995a) Anatomy, development and lesion-induced plasticity of rodent corticospinal tract. Neurosci Res 22:139–161

Terashima T (1995b) Course and collaterals of corticospinal fibers arising from the sensorimotor cortex in the reeler mouse. Dev Neurosci 17:8–19

Terashima T, Inoue K, Inoue Y, Mikoshiba K, Tsukada Y (1983) Distribution and morphology of corticospinal tract neurons in reeler mouse cortex by the retrograde HRP method. J Comp Neurol 218:314–326

Theiler K (1988) Vertebral malformations. Adv Anat Embryol Cell Biol 112:1–99

Tohyama L, Lee VM-Y, Rorke LB, Trojanowski JQ (1991) Molecular milestones that signal axonal maturation and the commitment of human spinal cord precursor cells to the neuronal or glial phenotype in development. J Comp Neurol 310:285–299

Töndury G (1958) Entwicklungsgeschichte und Fehlbildungen der Wirbelsäule. Hippokrates, Stuttgart

Tsuchida T, Ensini M, Morton SB, Baldassare M, Edlund T, Jessell TM, Pfaff SL (1994) Topographic organization of embryonic motor neurons defined by expression of LIM homeobox genes. Cell 79:957–970

van der Knaap MS, Valk J (1995) Magnetic Resonance of Myelin, Myelination and Myelin Disorders, 2nd ed. Springer, Berlin Heidelberg New York

Vaughn JE, Sims T, Nakashima M (1977) A comparison of the early development of axodendritic and axosomatic synapses upon embryonic mouse spinal motor neurons. J Comp Neurol 175:79–100

Veeneklaas GMH (1952) Pathogenesis of intrathoracic gastrogenic cysts. Am J Dis Child 83:500–507

Verbout AJ (1985) The development of the vertebral column. Adv Anat Embryol Cell Biol 90:1–122

Verhaart WLC (1934) Zehn Fällen des Pickschen Bündels. Psychiatr Neurol Bl 38:85–95

Verhaart WJC (1935) Die aberrierenden Pyramidenfasern bei Menschen und Affen. Schweiz Arch Neurol 36:170–190

Verhaart WJC (1950) Hypertrophy of pes pedunculi and pyramid as result of degeneration of contralateral corticofugal fiber tracts. J Comp Neurol 92:1–15

Verhaart WJC (1970) Comparative Anatomical Aspects of the Mammalian Brain Stem and the Cord. Van Gorcum, Assen, The Netherlands

Verhaart WJC, Kramer W (1952) The uncrossed pyramidal tract. Acta Psychiatr Neurol Scand 27:181–200

Verney C, Zecevic N, Nikolic B, Alvarez C, Berger B (1991) Early evidence of catecholaminergic cell groups in 5- and 6-week-old human embryos using tyrosine hydroxylase and dopamine-,-hydroxylase immunocytochemistry. Neurosci Lett 131:121–124

Vinters HV, Gilbert JJ (1981) Neurenteric cysts of the spinal cord mimicking multiple sclerosis. Can J Neurol Sci 8:159–161

Vogel H, Halpert D, Horoupian DS (1990) Hypoplasia of posterior spinal roots and dorsal spinal tracts with arthrogryposis multiplex congenita. Acta Neuropathol (Berl) 79:692–696

von Sántha K (1930) Ueber das Verhalten des Kleinhirns in einem Falle von endogen-afamiliärer Idiotie. Zur Differentialdiagnose der Marieschen und der sonstigen endogenen Kleinhirnerkrankungen nebst Beitrag zur Lehre der Diplomyelie. Z Neurol Psychiatr 123:717–793

Weidenheim KM, Kress Y, Epshteyn I, Rashbaum WK, Lyman WD (1992) Early myelination in the human fetal lumbosacral spinal cord: Characterization by light and electron microscopy. J Neuropathol Exp Neurol 51:142–149

Weidenheim KM, Epshteyn I, Rashbaum WK, Lyman WD (1993) Neuroanatomical localization of myelin basic protein in the late first and early second trimester human foetal spinal cord and brainstem. J Neurocytol 22:507–516

Weidenheim KM, Bodhireddy SR, Rashbaum WK, Lyman WD (1996) Temporal and spatial expression of major myelin proteins in the fetal spinal cord during the second trimester. J Neuropathol Exp Neurol 55:734–745

Wenner P, O'Donovan MJ (1999) Identification of an interneuronal population that mediates recurrent inhibition of motor neurons in the developing chick spinal cord. J Neurosci 19:7557–7567

Wenner P, Matise MP, Joyner A, O'Donovan MJ (1998) Physiological and molecular characterization of interneurons in the developing spinal cord. Ann NY Acad Sci 860:425–427

Wentworth LE (1984a) The development of the cervical spinal cord of the mouse embryo. I. A Golgi analysis of ventral root neuron differentiation. J Comp Neurol 222:81–95

Wentworth LE (1984b) The development of the cervical spinal cord of the mouse embryo. II. A Golgi analysis of sensory, commissural, and association cell differentiation. J Comp Neurol 222:96–115

Wessels WJT, Feirabend HKP, Marani E (1991) Development of projections of primary afferent fibers from the hindlimb to the gracile nucleus: A WGA-HRP study in the rat. Dev Brain Res 63:265–279

Willis WD Jr, Coggeshall RE (1991) Sensory Mechanisms of the Spinal Cord, 2nd ed. Plenum, New York

Windle WF (1970) Development of neural elements in human embryos of four to seven weeks gestation. Exp Neurol Suppl 5:44–83

Windle WF, Fitzgerald JE (1937) Development of the spinal reflex mechanism in human embryos. J Comp Neurol 67:493–509

Windle WF, Fitzgerald JE (1942) Development of human mesencephalic trigeminal root and related neurons. J Comp Neurol 77:597–608

Winkler C (1926) De bouw van het zenuwstelsel, IV. Bohn, Haarlem, The Netherlands

Woźniak W, O'Rahilly R (1982) An electron microscopic study of myelination of pyramidal fibers at the level of the pyramidal decussation. J Hirnforsch 23:331–342

Yachnis AT, Rorke LB (1999) Neuropathology of Joubert's syndrome. J Child Neurol 14:655–659

Yakovlev PI, Lecours AR (1967) The myelogenetic cycles of regional maturation of the brain. In: Minkowski A (ed) Regional Development of the Brain in Early Life. Blackwell, Oxford, pp 3–70

Yakovlev PI, Rakic P (1966) Patterns of decussation of bulbar pyramids and distribution of pyramidal tracts on two sides of the spinal cord. Trans Am Neurol Assoc 91:366–367

Yokoyama N, Romero MI, Cowan CA, Galvan P, Heimbacher F, Charnay P, Parada LF, Henkemeyer M (2001) Forward signaling mediated by Ephrin-B3 prevents contralateral corticospinal axons from recrossing the spinal cord midline. Neuron 29:85–97

Zecevic N, Verney C (1995) Development of the catecholamine neurons in human embryos and fetuses, with special emphasis on the innervation of the cerebral cortex. J Comp Neurol 351:509–535

Development and Developmental Disorders of the Brain Stem

Hans J. ten Donkelaar, Martin Lammens, Johannes R.M. Cruysberg and Cor W.J.R. Cremers

7.1   Introduction

The brain stem is composed of the midbrain (the *mesencephalon*) and the hindbrain (the *rhombencephalon*), and is, at least during development, segmentally organized. The midbrain is composed of two temporarily present segments known as mesomeres, whereas the hindbrain is composed of eight, also temporarily present, rhombomeres (Fig. 7.1). The cerebellum largely arises from the first rhombomere (Chap. 8). The brain stem contains the reticular formation which is involved in the control of respiration, circulation, wakefulness and locomotion. The brain stem also contributes ten of the 12 pairs of cranial nerves, III–XII. The motor nuclei for the extraocular muscles arise from mesomere 2 (the oculomotor nucleus) and rhombomeres 1 (the trochlear nucleus) and 5 (the abducens nucleus). The motor nuclei of the cranial nerves, innervating the branchial arch musculature, arise from the second, fourth, sixth and seventh rhombomeres. The neural crest, flanking the developing rhombencephalon, makes important contributions to the branchial arches (Chap. 5). A great number of genes are involved in the proper development of the brain stem (Cordes 2001; Moens and Prince 2002). The isthmus organizer regulates the early development of the mesencephalon and of the rostral part of the rhombencephalon (Wurst and Bally-Cuif 2001; Joyner 2002). Mutations of genes involved such as *Otx2*, *En1* and *En2* result in extensive
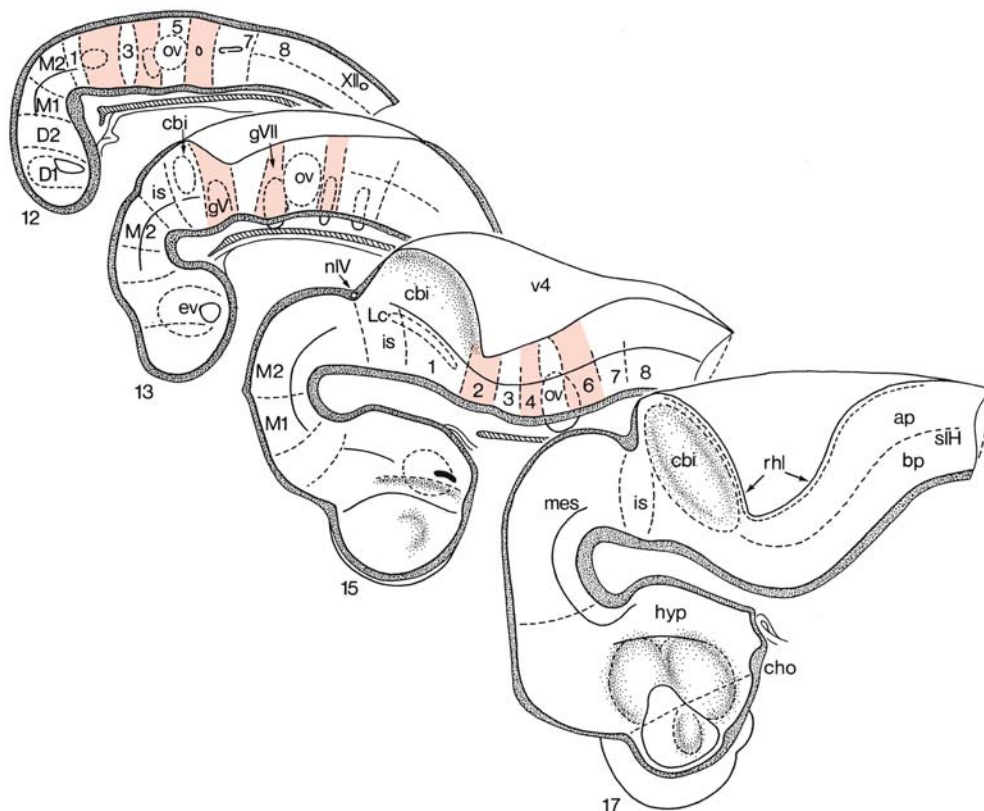
Fig. 7.1 Segmentation of the brain stem (medial views of the brain at Carnegie stages 12, 13, 15 and 17). *ap* alar plate, *bp* basal plate, *cbi* internal cerebellar bulge, *cho* chiasma opticum, *D1*, *D2* diencephalic neuromeres, *ev* eye vesicle, *gV* trigeminal ganglion, *gVII* facial ganglion, *hyp* hypothala-mus, *is* isthmus, *Lc* locus coeruleus, *mes* mesencephalon, *M1*, *M2* mesomeres, *nIV* trochlear nerve, *ov* otic vesicle, *rhl* rhombic lip, *slH* sulcus limitans of His, *v4* fourth ventricle, *XII* hypoglossal nucleus, *1–8* rhombomeres. (After O'Rahilly and Müller 1999)
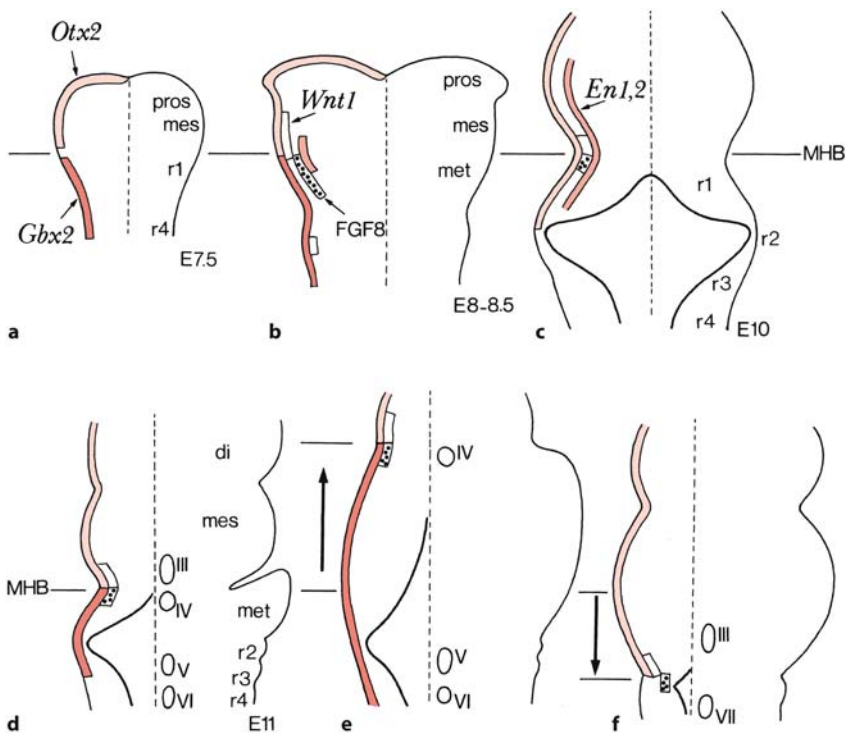
Fig. 7.2 Gene expression patterns at the midbrain–hindbrain boundary (*MEB*) shown in dorsal views of the mouse embryonic neural plate (**a**–**c**), and in *Otx2* (**e**) and *Gbx2* (**f**) knockout mice. *Otx2* expression is shown in *light red*, *En1/2* expression in *medium red* and *Gbx2* expression in *red*. Comparison with the normal pattern shown in **d** indicates the severe effects of the absence of these genes on the formation of the brain stem (see text for further explanation). *mes* mesencephalon, *met* metencephalon, *pros* prosencephalon, *r1–r4* rhombomeres, *III–VII* motor nuclei of cranial nerves. (After Wurst and Bally-Cuif 2001)

defects in the midbrain, the cerebellum and the pons. Each rhombomere is characterized by a unique combination of *Hox* genes, its *Hox* code. In mice, spontaneous and targeted (knockout) mutations in these genes result in specific, rhombomere-restricted disruptions in the development of motor nuclei of cranial nerves. Such '*rhombomeropathies*' have not been found in humans, although congenital facial paralysis and Möbius syndrome may be good candidates.

In this chapter, patterning of the brain stem, its segmentation and the development and developmental disorders of the cranial nerves and their nuclei will be discussed. Developmental anomalies of one or more cranial nerves, with primary or secondary dysinnervation, may lead to congenital, non-progressive, sporadic or familial abnormalities of cranial musculature, currently grouped as *congenital cranial dysinnervation disorders* (*CCDDs*; Gutowski et al. 2003). Congenital defects of any component of the ear may cause hearing impairment. About 1 in 1,000 children is born with hearing loss or deafness present at birth or during early childhood (Petit et al. 2001a, b). Syndromic deafness contributes to about 30% of the cases of prelingual deafness. Several hundreds of syndromes including hearing loss have been described (Toriello et al. 2004). Rapid progress has been made in identifying deafness genes in mice and men. More than 100 genes have now been identified that affect inner ear development or function (Fekete 1999; Petit et al. 2001a, b; Steel and Kros 2001; Kiernan et al. 2002; Friedman and Griffith 2003).

7.2 Pattern Formation and Segmentation of the Brain Stem

7.2.1 Pattern Formation of the Brain Stem

The **midbrain–hindbrain boundary organizer** (MHB organizer) or **isthmic organizer** is responsible for specifying the fate of the midbrain and cerebellum. It was first identified through transplantation experiments in chick embryos. When MHB tissue was transplanted into the caudal forebrain of chick embryos, the surrounding host tissue adopted an isthmic or midbrain character (Martínez et al. 1991; Marín and Puelles 1994; Wassef and Joyner 1997). A restricted dorsal domain of the isthmic organizer (the isthmic node) is necessary for the formation and positioning of the roof plate (Alexandre and Wassef 2003). Several genes, encoding transcription factors such as the *Engrailed* (*En*), *Pax*, *Otx* and *Gbx* families or secreted proteins of the Wnt and Fgf families, are expressed within the MHB at early embryonic stages (Wassef and Joyner 1997; Acampora et al. 2001; Rhinn and Brand 2001; Liu and Joyner 2001; Wurst and Bally-Cuif 2001; Joyner 2002). The isthmus organizer itself is set up by the expression of a complex array of genes, two of which are central to its development (Fig. 7.2). The first, *Otx2* (one of the mouse homologues of the *Drosophila* gene orthodenticle), is expressed in the prosencephalon and mesencephalon. Its posterior limit of expression marks the anterior
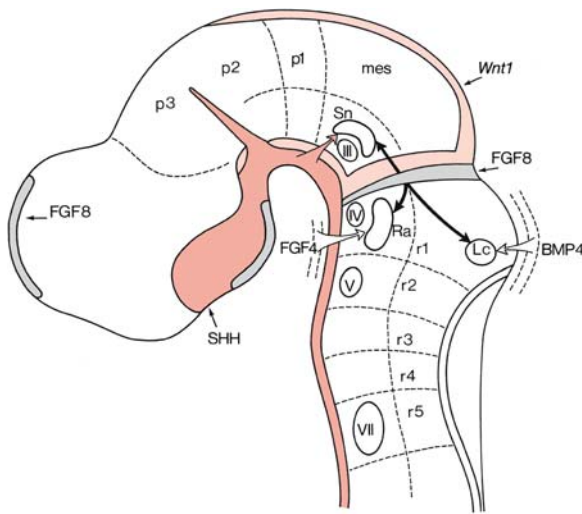
Fig. 7.3 Development of catecholaminergic (substantia nigra, *Sn*, locus coeruleus, *Lc*) and serotonergic (raphe nuclei, *Ra*) cell groups in the brain stem and the role of various signalling factors (BMP4, FGF4, FGF8, SHH and *Wnt1*; see text for further explanation). SHH expression is shown in *red*, FGF8 expression in *grey* and *Wnt1* expression in *light red*. *mes* mesencephalon, *p1–p3* prosomeres, *r1–r5* rhombomeres; *III–V, VII* motor nuclei of cranial nerves. (After Wurst and Bally-Cuif 2001)

limit of the MHB. A second gene, *Gbx2* (a homologue of the *Drosophila* gene unplugged), is expressed in the rostral part of the hindbrain. Its anterior limit marks the posterior limit of the MHB. In *Otx2* knockout mice, the rostral neuroectoderm is not formed, leading to the absence of the prosencephalon and the rostral part of the brain stem (Acampora et al. 2001; Wurst and Bally-Cuif 2001). Mice with the genotype *Otx2–/+; Otx1–/–* or *Otx2–/+; Otx1–/+* do not form a mesencephalon and show an extension of metencephalic tissue, leading to a giant cerebellum (Fig. 7.2 e). In *Gbx2* knockouts, all structures arising from the first three rhombomeres, including the cerebellum and pons, are absent (Fig. 7.2 f).

MHB cells secrete fibroblast growth factors (FGFs) and *Wnt* (mouse homologues of the *Drosophila* gene wingless) proteins which are required for the differentiation and patterning of the midbrain and hindbrain (Nakamura 2001; Rhinn and Brand 2001; Joyner 2002; Chi et al. 2003; Fig. 7.3). In *Wnt1* knockout mice, the mesencephalon is malformed and a cerebellum is hardly present (McMahon et al. 1992; Mastick et al. 1996). A number of homeobox-containing transcription factors are expressed across the isthmus, including the homeobox genes *En1* and *En2* and the paired box genes *Pax2*, *Pax5* and *Pax8*. Expression of the two *En* genes is the earliest known marker for mesencephalic polarity (Joyner 1996). They are expressed in almost similar domains in a

gradient that decreases anteriorly through the mesencephalon and posteriorly through the first rhombomere. Graded expression of the *En* genes appears to be regulated by signalling from the isthmus. Mutations in these genes cause deletions of mesencephalic and cerebellar structures (Millen et al. 1994; Wurst et al. 1994; Kuemerle et al. 1997). *En1* knockout mice have complete cerebellar aplasia, whereas *En2* deletions are less severe and only cause cerebellar hypoplasia with abnormal foliation (Millen et al. 1994; Kuemerle et al. 1997). *Pax2*, *Pax5* and *Pax8* are also required for specification of the isthmus. The isthmus is deleted in *Pax5–/–* mice (Urbanek et al. 1994). A possible human homologue of the *En2* knockout mice was recently found by Sarnat et al. (2002; Clinical Case 7.1). They described two cases of agenesis of the mesencephalon and metencephalon with cerebellar hypoplasia, possibly due to mutations in the *EN2* gene.

FGF8 is also essential for the formation of the nuclei of the oculomotor and trochlear nerves, the dopaminergic neurons in the substantia nigra and related ventral tegmental area, serotonergic neurons in the rostral raphe nuclei and noradrenergic neurons in the locus coeruleus (Wurst and Bally-Cuif 2001; Holzschuh et al. 2003; Fig. 7.3). However, a proper interplay with other signalling molecules (SHH, FGF4 and BMP4) is necessary: for the oculomotor and trochlear neurons and the substantia nigra the interplay of SHH and FGF8, for serotonergic neurons FGF4 from the rostral mesoderm and for the locus coeruleus BMP4 from the non-neural dorsal ectoderm. *Pitx3* is required for survival of the subset of midbrain dopaminergic neurons (van den Munckhof et al. 2003).

7.2.2 Segmentation of the Brain Stem

The process of segmentation is particularly evident in the hindbrain. A modular organization of its neuronal subtypes and nuclei is set up by its early transverse subdivision into eight rhombomeres (Lumsden and Keynes 1989; Lumsden 1990; Guthrie 1996; Moens and Prince 2002; Pasini and Wilkinson 2002). Rhombomere identity is controlled by *Hox* genes. Signalling by FGF8 from the isthmus patterns the anterior hindbrain and establishes the anterior limit of *Hox* gene expression (Irving and Mason 2000; Moens and Prince 2002). Rhombomere 1 is the only hindbrain segment in which no *Hox* genes are expressed. It gives rise to the entire cerebellum and lacks branchiomotor neurons. The neuronal organization of the caudal hindbrain is less overtly segmental than that of the rostral hindbrain. The segmentation and patterning of the hindbrain and the pharyngeal arches are intimately related.

In mutant mice, a number of malformations of the midbrain and rostral hindbrain have been described. Congenital absence of the midbrain and upper pons is very rare in humans. Sarnat et al. (2002) described two cases of agenesis of the mesencephalon and metencephalon with cerebellar hypoplasia, one of which came to autopsy (see Case Report).

Case Report. A 3,066-g male neonate was born at term as the first child of a 32-year-old, healthy mother after an uncomplicated pregnancy. Apgar scores were 3/7/9. He had a mildly dysmorphic face with micrognathia, a normal palate, low-set ears, and exhibited mild tachypnea. The corneal reflex was absent, ocular movements were minimal and muscle stretch reflexes were overactive. Abdominal ultrasound examination revealed hydronephrosis with ureteral obstruction. Chromosomes showed a normal 46XY karyotype. Furthermore, an ectopic lingual thyroid gland was found that was associated with hypothyroidism during life. Unusual postures and movements were noted with recurrent episodes of agitation. The postures did not correspond to decorticate or decerebrate rigidity. MRI of the brain showed absence of the midbrain and upper pons with global cerebellar hypoplasia. Supratentorial and lower brain stem structures appeared normal (Fig. 7.4a). The infant continued to have recurrent unprovoked apneic episodes with brachycardia, and died at 7 weeks of age.

At autopsy, the minor dysmorphic features were confirmed. The tracheal thyroid gland was absent but there was a small lingual thyroid. The heart showed a patent foramen ovale and two small apical ventricular septal defects. The right lung showed acute purulent bronchopneumonia, and right hydronephosis, marked pyelonephritis and ureteral dilatation were found. Brain weight was normal (485 g). After removal of the brain, the cranial base appeared normal except for two anomalous midline foramina in the clivus, through which a nerve-like cord entered and exited (Fig. 7.4b, c). The internal carotid, middle and anterior cerebral arteries were present, but the circle of Willis was poorly developed owing to anomalies of the vertebrobasilar circulation associated with brain stem dysgenesis. A large anomalous basilar artery was found which arose from the left vertebral artery and passed rostrally from the extreme left caudal end of the brain stem, across the left trigeminal root towards the midline, where it anastomosed with other abnormal unidentified arteries in the region of the circle of Willis. The posterior cerebral arteries were replaced by several small arteries. Macroscopically, the cerebral hemispheres appeared normal with present olfactory bulbs and tracts (Fig. 7.4d). The midbrain and upper pons were absent and the resulting space was filled with liquor. A thin 1–2-mm-wide midline cord passed from the diencephalon into an abnormal midline foramen in the clivus and emerged 1 cm posteriorly to enter the lower brain stem. Therefore, the diencephalon and lower hindbrain were connected only by a very thin nervous cord. Pyramids were absent and the inferior olives were inconspicuous. The vermis and the cerebellar hemispheres were hypoplastic (Fig. 7.4e). Frontal sections of the cerebral hemispheres showed normal-sized lateral and third ventricles, a thin corpus callosum, a narrow cavum septi pellucidi and normal hippocampal formations. The thin internal capsules converged and fused in the ventral midline below the third ventricle. No cerebral aqueduct could be identified. This rare malformation may result from a mutation or deletion in the *EN2* gene (Sarnat et al. 2002).

This case was kindly provided by Harvey B. Sarnat (Departments of Pediatrics and Pathology, Faculty of Medicine, University of Calgary).

Reference

Sarnat HB, Benjamin DR, Siebert JR, Kletter GB, Cheyette SR (2002) Agenesis of the mesencephalon and metencephalon with cerebellar hypoplasia: Putative mutation in the *EN2* gene – Report of 2 cases in early infancy. Ped Dev Pathol 5:54–68

Experimental data from avian and zebrafish embryos show two patterns of **metameric cellular organization** in the embryonic hindbrain. The first is a repeat pattern through every segment involving eight identified types of reticulospinal neurons (Chap. 2). The second is a two-segment repeat pattern involving the branchial motoneurons (Fig. 7.5). They first appear in the even-numbered rhombomeres, r2 (trigeminal), r4 (facial) and r6 (glossopharyngeal), the respective exit sites of these cranial nerves. Thereafter, further neurons are formed in the intervening odd-numbered rhombomeres, each in association
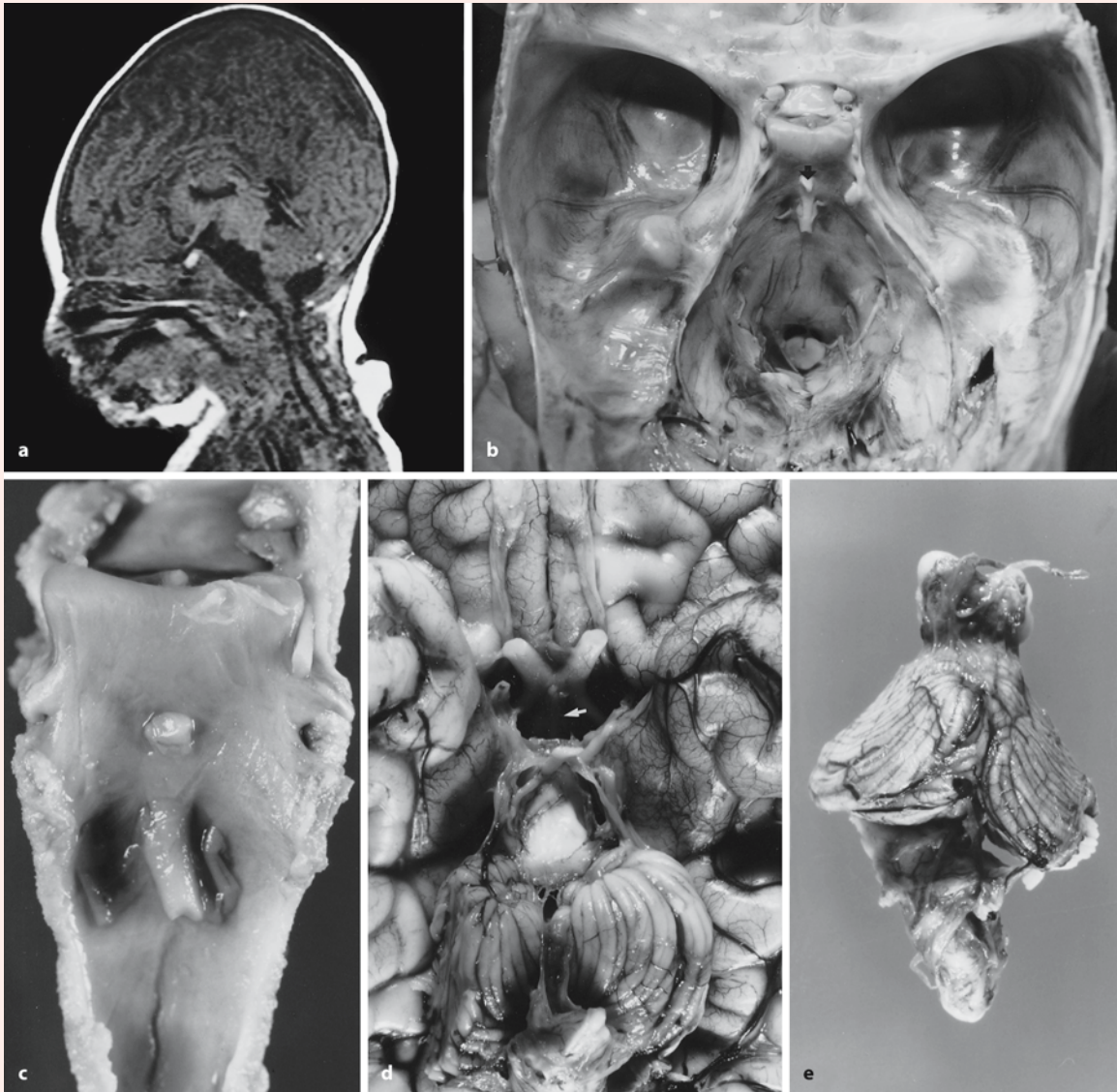
Fig. 7.4 Agenesis of the mesencephalon and metencephalon with cerebellar hypoplasia: **a** midsagittal MRI, showing absence of the midbrain and pons, cerebellar hypoplasia and rostral displacement of the cerebellum; **b** skull base: a ventral midline cord, connecting the diencephalon with the lower brain stem, was the only representation of the mesencephalon and upper pons, and passed through aberrant foramina in the midline (*arrowhead*); **c** resected block of the clivus; **d** basal view of the brain, showing normal olfactory bulbs and tracts, normal optic nerves and chiasm, absence of the midbrain (*arrow*), and a hypoplastic cerebellum; **e** dorsal view of the cerebellum and brain stem, showing cerebellar hypoplasia, particularly of the vermis (from Sarnat et al. 2002, with permission; courtesy Harvey B. Sarnat, Calgary)

with the cluster of motoneurons in the rostrally adjacent rhombomere (Lumsden and Keynes 1989; Lumsden 2004). Later in development, the segmental origins of the branchiomotor neurons become obscured as the motor nuclei condense and migrate to new positions. This two-segment periodicity of the early hindbrain is also found in the migration of neural crest cells to the branchial arches: neural crest cells migrate from r2, r4 and r6 into the first, second and third arches, respectively (Chap. 5). Vaage (1969) suggested subdividing the first rhombomere into two distinct domains, 'r0' or the so-called isthmic rhom-
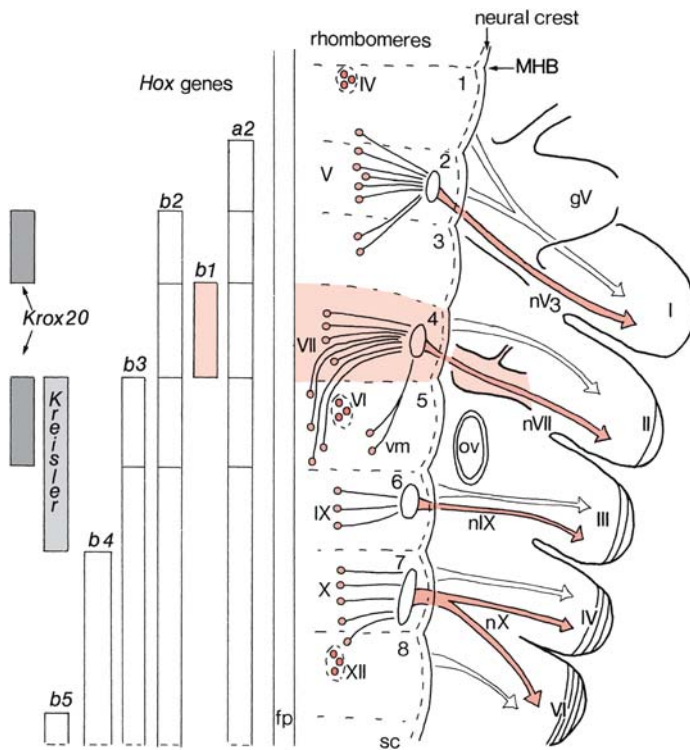
Fig. 7.5 Relations of the rhombomeres (*1–8*) with the pharyngeal arches (*I–IV*, *VI*), the innervation of head and neck muscles, the neural crest and the expression of *Hox*, *Kreisler* and *Krox20* genes. *fp* floor plate, *gV* trigeminal ganglion, *MHB* midbrain–hindbrain boundary, *nV3* mandibular nerve, *nVII* facial nerve, *nIX* glossopharyngeal nerve, *nX* vagus nerve, *ov* otic vesicle, *sc* spinal cord, *vm* visceromotor neurons of facial nerve, *IV–VII*, *IX*, *X*, *XII* motor nuclei of cranial nerves

bomere rostrally, and a narrower r1 caudally (Puelles 1995). In chick embryos, no molecular markers of this r0–r1 boundary have been identified, but data for zebrafish suggest that anterior and posterior parts of r1 are patterned independently (Moens and Prince 2002).

Rhombomeres are thought to acquire their individual identities under the influence of *Hox* genes that are expressed in overlapping, or nested, domains (Wilkinson et al. 1989; Krumlauf 1994; Lumsden and Krumlauf 1996; Moens and Prince 2002; Chap. 2). *Hox* gene expression precedes rhombomere foundation but becomes progressively sharpened such that the borders of the expression domains coincide with the emerging rhombomere boundaries. In the fully segmented hindbrain, many *Hox* genes show a two-rhombomere periodicity. Each rhombomere and pharyngeal or branchial arch is characterized by a unique combination of *Hox* genes, its *Hox* code (Fig. 7.5). Available human data suggest that the pattern of *HOX* gene expression in the rhombomeres and pharyngeal arches is comparable to that of *Hox* genes in mice (Vieille-Grosjean et al. 1997). In mice, spontaneous and targeted (knockouts) mutations in these genes result in specific, rhombomere-restricted disruptions in the development of the cranial motor nuclei (Fig. 7.6).

7.3   Development and Developmental Disorders of the Cranial Nerves

In the last 10 years, we have begun to understand the molecular mechanisms of cranial nerve development through the analysis of mouse mutants (Cordes 2001; Pasqualetti and Rijli 2001; Table 7.1). Cranial nerve identity is impaired by genes involved in anteroposterior patterning such as certain *Hox* genes, *Kreisler* and *Krox20*. Neuronal determinants, including *Lim* homeobox genes, dictate neuronal subtype along the dorsoventral axis (Cordes 2001). Subsequent neuronal differentiation, cell migration and axon outgrowth is controlled by subtype-specific gene expression. First data for rodents will be discussed.

7.3.1   Development of the Cranial Nerves and Their Nuclei in Rodents

Figure 7.5 shows the relations between rhombomeres, somatomotor and branchiomotor neurons, associated pharyngeal arches, and the expression of several *Hox* genes, *Kreisler* and *Krox20*. Many other genes play a role in the differentiation, migration, axon formation and guidance of (moto)neurons. The *Nkx* and *Phox* genes are important for the differentiation of motoneurons (Pattyn et al. 2000a, b;
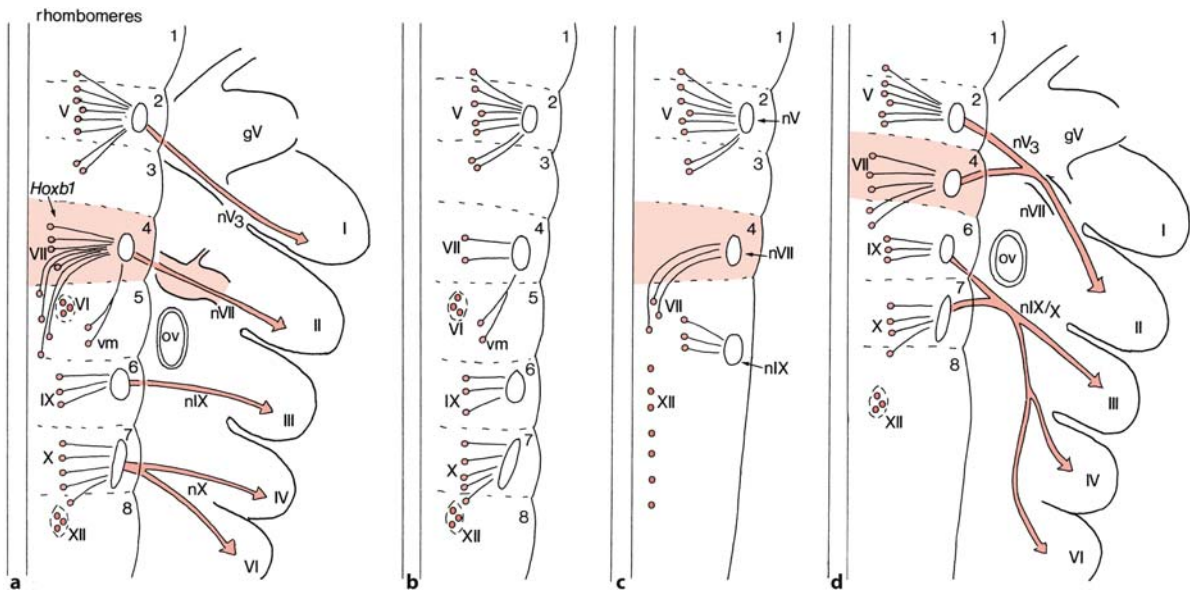
Fig. 7.6 Effects of mutations in *Hoxb1*, *Kreisler* and *Krox20* genes on rhombomeres (*1–8*) and pharyngeal arches (*I–IV*, *VI*) and their innervation: **a** wild type; **b** *Hoxb1* mutant; **c** *kreisler* mouse; **d**, *Krox20–/–* mouse (see text for explanation). *gV* trigeminal ganglion, *nV3* mandibular nerve, *nVII* facial nerve, *nIX* glossopharyngeal nerve, *nX* vagus nerve, *ov* otic vesicle, *vm* visceromotor neurons of facial nerve, *V–VII*, *IX*, *X*, *XII* motor nuclei of cranial nerves

Pasqualetti and Rijli 2001; Müller et al. 2003). In rats, cranial nerve motoneurons are mainly born on embryonic days 12 (E12) and 13 (Altman and Bayer 1982; Bayer et al. 1995). Hypoglossal and trigeminal motoneurons are born first (E11–E12), whereas facial motoneurons are generated over a longer period, between E12 and E14 (Table 7.2). *Facial branchiomotor neurons* are born in rhombomere 4 and migrate through r5 to r6 (Altman and Bayer 1982; Ashwell and Watson 1983; Auclair et al. 1996; Studer 2001), where they form the facial motor nucleus (Fig. 7.5). This pattern of migration gives rise to the internal genu of the facial nerve. Facial motoneurons do not start their migration simultaneously. In mice with a 2-days-shorter prenatal development than rats, the first neurons cross the r4–r5 boundary at embryonic day (E) 10.5, and reach their final destination in r6 at E12, whereas the last neurons leave r4 at E12.5 and complete their migration by E16. By contrast, *facial visceromotor neurons* develop exclusively in r5 (Jacobs and Guthrie 2000). *Trigeminal motoneurons* remain within their rhombomeres of origin, and move dorsolaterally to the point of exit of the Vth nerve in the dorsal half of r2/r3 (Studer et al. 1996).

Morphological analysis of *Hox* mutants and 'spontaneous' mutations such as the *kreisler* mouse has focussed largely on the facial and trigeminal branchiomotor neurons (Rijli et al. 1998; Trainor and Krumlauf 2000; Cordes 2001; Pasqualetti and Rijli 2001; Fig. 7.6). In *Hoxa2* knockouts, the border between rhombomeres 1 and 2 is absent, rhombomeres 2 and 3 are strongly reduced and the cerebellum extends more caudally than normally (Barrow et al. 2000). In *Hoxa1* knockout mice, rhombomeres 3–6 are not formed (Carpenter et al. 1993; Gavalas et al. 1998, 2003; Rossel and Capecchi 1999), whereas in the *Hoxa3* mutant derivatives of the third pharyngeal arch such as the thymus and parathyroids are not formed, and the thyroid is hypoplastic, reminiscent of the DiGeorge sequence (Chap. 5). Mice with targeted disruption of *Hoxb1* fail to form the motor nucleus of the facial nerve (Goddard et al. 1996; Studer et al. 1998). The facial motor nucleus is not only strongly reduced but, moreover, no migration of the facial motoneurons to the fifth rhombomere has taken place (Fig. 7.6b). In the *kreisler* mouse (Fig. 7.6c), rhombomeres 5 and 6 and their derivatives are absent (Deol 1964; McKay et al. 1997; Sadl et al. 2003). The nucleus of the abducens and the visceromotor, parasympathetic motoneurons of the facial nerve, normally present in the fifth rhombomere, are absent (Fig. 7.6c). In *Krox20–/–* mice (Fig. 7.6d), rhombomeres 3 and 5 are lacking (Schneider-Maunoury et al. 1997). In these rhombomeres, *Krox20* is normally expressed (Fig. 7.5). The abducens nucleus and the visceromotor component of the facial nerve

Table 7.1 Some genes required for the development of the cranial nerves in mice (after Cordes 2001)

Gene	Primary process affected	Cranial nerve malformations of mouse mutants
Patterning genes		
Rarγ/Rarβ compound	A-P patterning	No abducens nerve
Wnt1	A-P patterning	No trigeminal nerve
Gbx2	A-P patterning	No trigeminal nerve
Kreisler	A-P patterning	No abducens nerve; visceral facial motoneurons from rhombomere 5 missing; axonal projections and somata of facial motor nerve abnormally located (posterior to rhombomere 4)
Krox20	A-P patterning	Facial motoneurons migrate from rhombomere 4 to rhombomere 6, trigeminal motor nucleus reduced; fusion of nerves V and VII/VIII as well as of nerves IX and X
Hoxa1	A-P patterning	Trigeminal and facial motor nuclei in overlapping domains; defects in facial nerve
Hoxa2	A-P patterning	Disorganization and reduction of trigeminal nerve; defects in facial nerve
Hoxa3	A-P patterning	Hypoplasia of IXth cranial ganglia and sparse connection of IXth nerve with medulla
Hoxb1	A-P patterning	Loss of facial motoneurons; no facial nerve present
Hoxb2	A-P patterning	Facial motoneurons do not migrate out of rhombomere 4 to form facial nerve
Hoxb3	A-P patterning	Glossopharyngeal nerve severely reduced
Dreher (Lmx1a)	Dorsal patterning	Lateral projections of facial motoneurons more diffuse; IXth ganglion reduced; branches of accessory nerve connect abnormally to Xth ganglion
Genes for neuronal specification and determination		
COUP-TFI	Neuronal specification	Missing glossopharyngeal ganglia
GATA2	Neuronal determinant	Loss of efferent projections from contralateral vestibuloacoustic nucleus and migration of facial motoneurons
GATA3	Neuronal determinant	Loss of efferent projections from contralateral vestibuloacoustic nucleus and migration of facial motoneurons; loss of noradrenergic and serotonergic neurons
Lhx3/Lhx4 compound homozygotes	Motoneuron-subtype-specific determinant	Abducens and hypoglossal nerves missing
Phox2b	Neuronal determinant	Loss of cranial branchio- and visceromotoneurons
Phox2a	Neuronal determinant	Loss of noradrenergic neurons, parasympathetic neurons and epibranchial-placode-derived sensory neurons of cranial sensory ganglia
ErbB2, ErbB3	Sensory neuron development	Defects in proximal cranial sensory ganglia derived from trigeminal and otic placodes and from neural crest
Neurogenin 1	Neuronal determinant	Loss of proximal cranial sensory neurons derived from trigeminal and otic placodes and from neural crest
Neurogenin 2	Neuronal determinant	Loss of distal epibranchial-placode-derived sensory neurons
Mash1	Neuronal determinant	Loss of noradrenergic and parasympathetic neurons

A-P anteroposterior

are absent. Axons of trigeminal motoneurons join the facial nerve and enter the second pharyngeal arch. Since these axons do not find their proper targets (the masticatory muscles), their parent motoneurons die. Moreover, fusion of the glossopharyngeal and vagal nerves occurs.

The transcription factor *Nkx6.1* is not only required for the early specification of spinal motoneurons (Chap. 6), but also for the early specification of somatomotor, branchiomotor and visceromotor neurons in the brain stem (Müller et al. 2003; Pattyn et al. 2003). In *Nkx6.1* mutants, the abducens and hypoglossal nerves are missing (Briscoe et al. 1999; Sander et al. 2000). *Phox* genes play an important role in the differentiation of motoneurons and noradrenergic neurons of the locus coeruleus and other brainstem cell groups (Morin et al. 1997; Pattyn et al. 2000; Brunet and Pattyn 2002). *Phox2b* is required for the

Table 7.2 Time of neuron origin of cranial nerve nuclei in rats and humans (after Altman and Bayer 1982; Müller and O'Rahilly 1990; Bayer et al. 1995)

Cranial nerve nuclei	Birthday in rats	Human 'birthday' (Carnegie stages)	Migration of human neurons (Carnegie stages)	Appearance of peripheral fibres (Carnegie stages)	Settling of neurons (Carnegie stages)
Medulla					
Abducens	E12(E13)	13/14			
Trigeminal	(E11)E12	13	14	14	17
Facial	(E12)E13(E14)	13	13 to fetal	14/15	23 or later
Glossopharyngeal	E15	13	13–17	14/15	16/17
Vagal	(E12)E13	13	13–17	14/15	16/17
Accessory		13	13–17	13	16/17
Hypoglossal	(E11)E12	12		12/13	
Isthmus					
Trochlear	E12–E13	13		16	
Midbrain					
Oculomotor	E12–E13	13		15	

differentiation of branchiomotor and visceromotor neurons, whereas *Phox2a* is essential for the development of oculomotor and trochlear motoneurons and locus coeruleus neurons. In *Phox2a* knockouts, the locus coeruleus is absent. Like in the spinal cord (Chap. 6), Lim homeodomain proteins determinate the fate of brain stem motoneurons. Somatomotor, branchiomotor and visceromotor neurons express a subset of Lim proteins that define early motoneuron pool identity in the hindbrain (Tsuchida et al. 1994; Varela-Echeverria et al. 1996). In mice with mutations for both *Lhx3* and *Lhx4* Lim proteins, somatomotor neurons in the hindbrain (VI and XII) are lost (Sharma et al. 1998).

7.3.2   Development of Cranial Nerve Ganglia in Rodents

Cranial sensory ganglia can be subdivided into two distinct populations which occupy distinct anatomical locations (Chap. 5). The *proximal subset* is derived from the cranial neural crest and trigeminal and otic placodes. Neurons from the proximal subset form the dorsomedial region of the trigeminal ganglion, a small portion of the proximal facial ganglion, the acoustic ganglion and the proximal parts of the glossopharyngeal and vagal ganglia. This subset requires the basic helix–loop–helix transcription factor neurogenin 1 for its specification (Ma et al. 1998). Further development of these sensory ganglia is dependent on a family of cell-surface receptors with structural similarity to the epidermal growth factor receptor,

the ErB2 and ErB3 receptors, and their ligand neuregulin (Lee et al. 1995; Meyer and Birchmeier 1995; Erickson et al. 1997). The *distal subset* gives rise to most of the sensory neurons of the VIIth, IXth and Xth ganglia, and is specified by neurogenin 2 (Fode et al. 1998). These distal sensory neurons depend on the paired homeodomain proteins Phox2a and Phox2b for their differentiation and survival. In *Phox2a–/–* and *Phox2b–/–* mice, epibranchial placodes give rise to the normal number of neuroblasts, but after some general differentiation, these neuroblasts fail to express their more specific differentiation programme (Morin et al. 1997; Pattyn et al. 1999, 2000a).

7.3.3   Developmental and Developmental Disorders of the Human Cranial Nerves

The developmental relations of the human cranial nerve nuclei and their motor and sensory components are shown in Fig. 7.7. The developmental relations of brain stem columns of motor and sensory nuclei from the basal and alar plates, respectively, are shown in Fig. 7.8. The development of the trigeminal nerve and of the facial nerve is shown in Figs. 7.9 and 7.10. The development of the human cranial nerves and their parent nuclei has been extensively studied by Streeter (1904, 1906, 1911, 1912) and Pearson (1938, 1939, 1943, 1944, 1946). Mann (1927), Jacobs (1970) and Gasser (1967) studied the development of the oculomotor, trigeminal and facial nuclei, respectively. In human embryos, cranial nerve motoneurons arise around Carnegie stage 13 (Müller and O'Rahilly
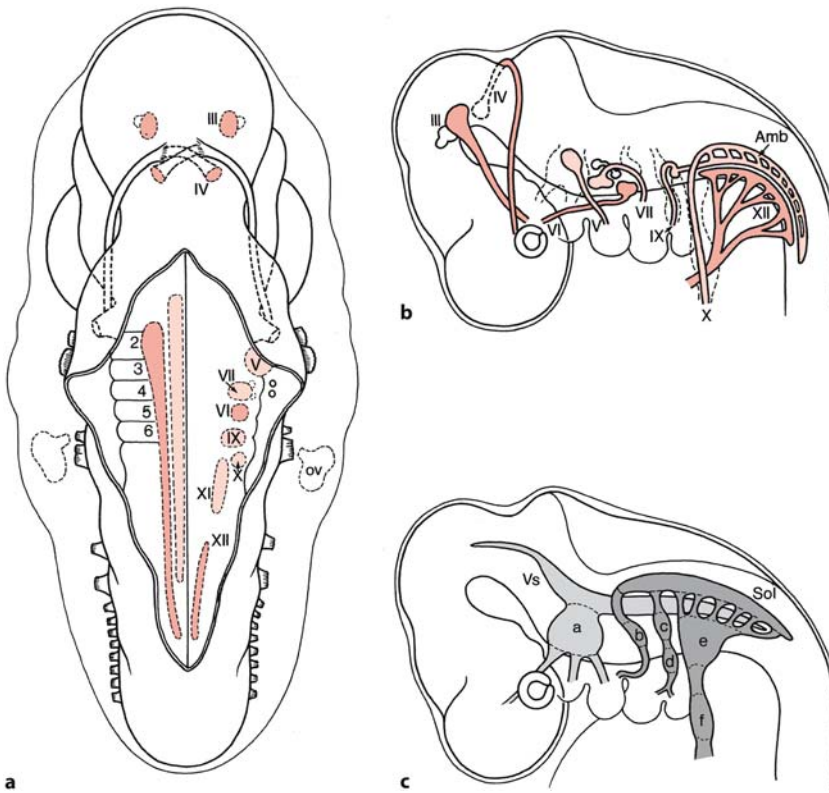
Fig. 7.7 The development (**a**) and position of motor (**b**) and sensory (**c**) components of human cranial nerve nuclei. Somatomotor nuclei are shown in *red* and branchiomotor nuclei in *light red*. *a* trigeminal ganglion, *Amb* nucleus ambiguus (motor nucleus of IXth and Xth nerves), *b* geniculate ganglion of facial nerve, *c* superior ganglion of glossopharyngeal nerve, *d* inferior ganglion of glossopharyngeal nerve, *e* superior (jugulare) ganglion of vagus nerve, *f* inferior (nodosum) ganglion of vagus nerve, *ov* otic vesicle, *Sol* nucleus of the solitary tract, *Vs* sensory trigeminal nuclei, *III–VII*, *IX–XII* cranial nerve nuclei and nerves, *2–6* rhombomeres. (After Hinrichsen 1990)
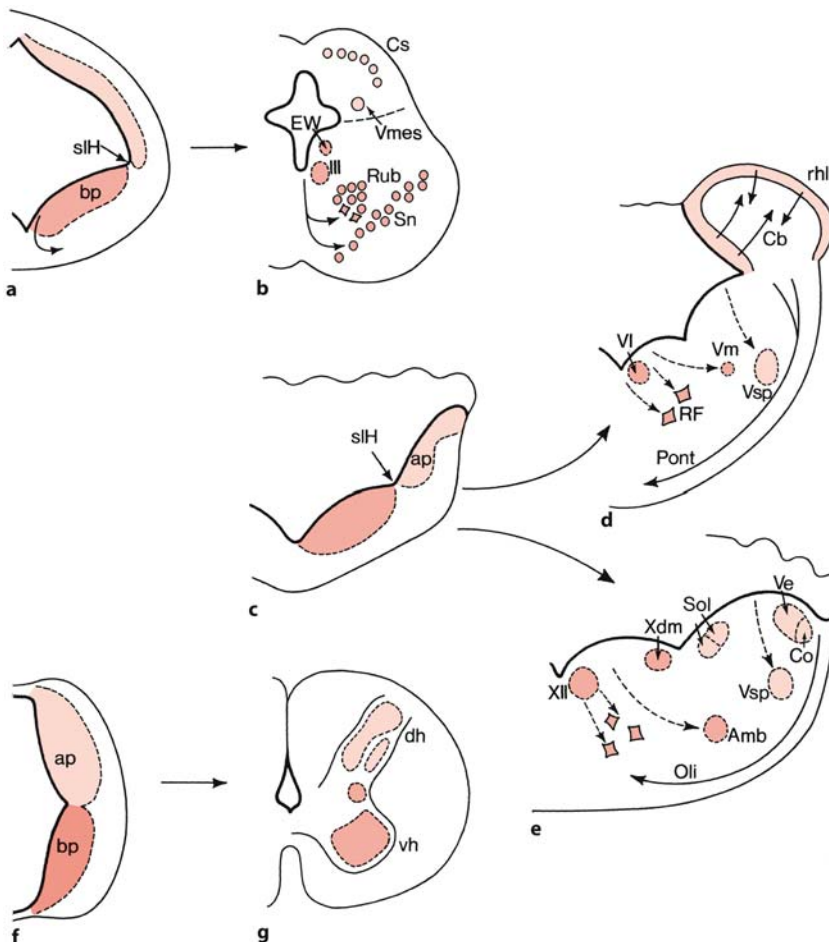
Fig. 7.8 Derivatives of the alar (*light red*) and basal (*red*) plates in the brain stem: **a**, **b** the mesencephalon; **c–e** the rhombencephalon (**d** the metencephalon; **e** the medulla oblongata); **f**, **g** the spinal cord for comparison. *Amb* nucleus ambiguus, *ap* alar plate, bp basal plate, *Cb* cerebellar anlage, *Co* cochlear nuclei, *Cs* colliculus superior, *dh* dorsal horn, *EW* nucleus of Edinger–Westphal, *Oli* oliva inferior, *Pont* pontine nuclei, *RF* reticular formation, *rhl* rhombic lip, *Rub* nucleus ruber, *slH* sulcus limitans of His, *Sn* substantia nigra, *Sol* nucleus of the solitary tract, *Ve* vestibular nuclei, *vh* ventral horn, *Vm* trigeminal motor nucleus, *Vmes* mesencephalic trigeminal nucleus, Vsp spinal trigeminal nucleus, *Xdm* dorsal motor (parasympathetic) vagus nucleus, *III*, *VI*, *XII* motor nuclei of cranial nerves
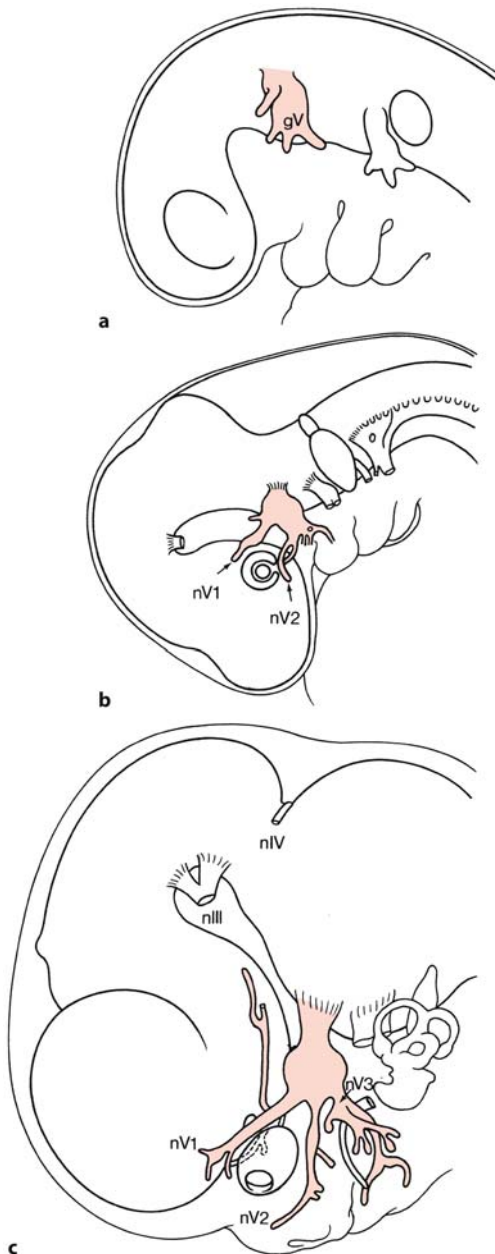
Fig. 7.9 Three stages in the development of the trigeminal nerve in man: **a** Carnegie stage 12; **b** Carnegie stage 14; **c** Carnegie stage 18. *gV* trigeminal ganglion, *nIII* oculomotor nerve, *nIV* trochlear nerve, *nV1* ophthalmic nerve, *nV2* maxillary nerve, *nV3* mandibular nerve. (After Hinrichsen 1990)

1990; Table 7.2), i.e. at about 4 weeks of development. Trigeminal motoneurons are born in the second rhombomere, facial motoneurons in the fourth rhombomere and motoneurons of the abducens nerve in the fifth rhombomere. The facial motoneurons migrate caudalwards until far in the fetal period, passing the abducens nucleus. This caudal migration

of the facial motoneurons may explain the combination of facial and abducens motoneuron loss seen in cases of the Möbius syndrome and related disorders. Any focal destructive brain stem lesion, hypoxic-ischemic, haemorrhagic or due to other reasons, in the fifth rhombomere from about the fifth week of development until far in the fetal period may result in such a combination. The extent of such destructive lesions may explain the involvement of other brain stem motor nuclei and passing long fibre systems such as the pyramidal tract. A direct link between the many *Hox* and *Nkx* gene mutations in mice with human developmental brain stem disorders has not yet been identified (Cordes 2001; Pasqualetti and Rijli 2001). Homozygous mutations in *PHOX2A* may cause congenital fibrosis of the extraocular muscles type 2 (Nakano et al. 2001).

Congenital anomalies have been described for all cranial nerves (Mellinger and Gomez 1987; Aicardi 1998). Their incidence is relatively small if the olfactory and optic nerves are excluded. Even in anencephaly, the cranial nerves are usually present (Lemire et al. 1978). Most disorders of the cranial nerves present at birth appear to be due to focal necrosis, rather than to primary malformations (Lemire et al. 1975). For the cranial nerves innervating the extraocular muscles, dysgenesis includes congenital ptosis (Walsh and Hoyt 1969), oculomotor nerve paralysis (Victor 1976), congenital trochlear nerve paralysis (Reynolds et al. 1984; Von Noorden et al. 1986) and in about 50% of cases the retraction or Duane syndrome (Duane 1905; Hotchkiss et al. 1980). Comparative anomalies of the Vth nerve are infrequent (Mellinger and Gomez 1987). Similarly, congenital trigeminal anaesthesia due to an anomaly of the Vth nerve is a rare disorder (Cruysberg et al. 1998). The first symptom is usually the presence of corneal ulcerations which typically appear between the ages of 8 and 12 months (Rosenberg 1984), although the sensory loss is present from birth. Primary abnormalities of the VIIIth cranial nerve will be discussed in Sect. 7.4.3. There are no commonly encountered syndromes in which developmental anomalies of the cranial nerves IX, X, XI and XII are involved (Mellinger and Gomez 1987; Aicardi 1998).

7.3.4 Congenital Cranial Dysinnervation Disorders

A group of congenital neuromuscular diseases, characterized by abnormal eye, eyelid and/or facial movement, are currently termed the ***congenital cranial dysinnervation disorders (CCDDs)***. They include congenital, non-progressive, sporadic or familial abnormalities of cranial musculature that result from

Fig. 7.10 Three stages in the development of the facial nerve in man: **a** Carnegie stage 13; **b** Carnegie stage 18; **c** Carnegie stage 22. *cht* chorda tympani, *nV* trigeminal nerve, *nVII* facial nerve, *nVIII* vestibulocochlear nerve, *pp* plexus parotideus. (After Gasser 1967; Hinrichsen 1990)

developmental abnormalities of, or the complete absence of, one or more cranial nerves with primary or secondary muscle dysinnervation (Gutowski et al. 2003). *Primary dysinnervation* in the CCDDs may result from absence of normal muscle innervation by the appropriate motoneurons, either because they do not develop or because they are misguided during development. *Secondary dysinnervation* may occur when a muscle lacking normal innervation becomes aberrantly innervated by branches of other nerves during development. Dysinnervation may be associated with secondary muscle pathology and/or other orbital and bony structural abnormalities. Three groups of CCDDs can be distinguished (Gutowski et al. 2003): (1) disorders involving predominantly *vertical ocular motility defects*, likely due to abnormalities in the development of oculomotor and trochlear nerves and/or nuclei (congenital fibrosis of the extraocular muscles, CFEOM, variants and congenital

ptosis); (2) disorders involving predominantly *horizontal ocular motility defects*, likely due to abnormalities in the development of the abducens nerve and/or nucleus (Duane syndrome and horizontal gaze paralysis with progressive scoliosis, HGPPS); and (3) disorders involving predominantly *facial weakness*, likely due to abnormal development of the facial nerve and/or nucleus, sometimes with associated ocular motor abnormalities (congenital facial weakness and Möbius syndrome). Examples are presented in Figs. 7.11 to 7.14.

The **oculomotor nucleus** contains five subnuclei (Büttner-Ennever and Akert 1981; Büttner-Ennever and Horn 2004). Maldevelopment of these subnuclei, in isolation or in combination, may result in various phenotypes (Engle 2002; Engle and Leigh 2002). *Congenital fibrosis of the extraocular muscles type 1 (CFEOM1)* appears to result from maldevelopment of the superior division of the oculomotor nerve and

Fig. 7.11 Retraction of the eye and narrowing of the palpebral fissure on attempted adduction in Duane syndrome

corresponding motoneurons, which innervate the levator palpebrae superioris and the superior rectus, resulting in bilateral ptosis and infraducted globes (Engle et al. 1997). In contrast, *CFEOM3* may be caused by maldevelopment of all oculomotor motoneurons (Doherty et al. 1999). These disorders have been mapped to multiple genetic loci, but the mutated genes have yet to be identified, with the exception of CFEOM2 (Engle and Leigh 2002; Gutowski et al. 2003). *CFEOM2* is an autosomal recessive disorder, described in consanguineous pedigrees, that maps to the CFEOM2 locus (Wang et al. 1998). Affected individuals are born with bilateral exotropia and ptosis, and have mutations in *PHOX2A* (Nakano et al. 2001). In mice, *Phox2a* is essential for the development of oculomotor and trochlear motoneurons (Sect. 7.3.1). Therefore, CFEOM2 results from an error in cranial nuclear development. The **abducens nucleus** lies in the pontomedullary part of the brain stem and together with the internal genu of the facial nerve forms a dorsal protrusion into the fourth ventricle, known as the facial colliculus. The abducens nucleus contains motoneurons innervating the lateral rectus,

internuclear neurons and neurons with projections to the cerebellar flocculus (Leigh and Zee 1999; Büttner-Ennever and Horn 2004). Axons of the internuclear abducens neurons ascend in the contralateral medial longitudinal fascicle (MLF) and terminate in the medial rectus subnucleus of the oculomotor nerve. Some forms of Duane syndrome appear to result from selective absence of abducens motoneurons, sparing the internuclear neurons (Hotchkiss et al. 1980; Miller et al. 1982). Therefore, patients with Duane syndrome typically lack abduction, but because the internuclear neurons are spared, the contralateral eye can adduct on attempted lateral gaze. Patients with Möbius syndrome have horizontal gaze paralysis and facial weakness and, frequently, additional lower cranial nerve abnormalities. In autosomal recessive *familial horizontal gaze paralysis with progressive scoliosis (HGPPS),* MRI examination showed pontine hypoplasia with absence of the facial colliculi, suggestive for absence of the abducens nuclei, and medullary dysplasia (Jen et al. 2002; Pieh et al. 2002). *Duane's retraction syndrome* is characterized by (1) congenital ocular abduction deficiency, (2) variable limitation of adduction and (3) retraction of the eye (with narrowing of the palpebral fissure) on attempted adduction. In unilateral cases, involvement of the left eye is more common than that of the right eye. The association with other congenital anomalies is not unusual (Cruysberg et al. 1986). The retraction phenomenon of the eyes (Fig. 7.11) is caused by aberrant IIIrd nerve innervation and co-contraction of the lateral rectus muscle. Depending on the variation of aberrant lateral rectus innervation, four types of Duane syndrome have been distinguished clinically. Duane type I has mainly limitation of abduction (Fig. 7.12a). Duane type II has mainly limitation of adduction (Fig. 7.12b). Duane type III has limitation of abduction and adduction (Fig. 7.12c). In Duane type IV there is abduction on attempted adduction (Fig. 7.12d), resulting in synergistic divergence (Cruysberg et al. 1989; Cruysberg and Huygen 1990).

Congenital bilateral facial paralysis was first described by the German ophthalmologist Albrecht von Graefe (1880) as congenital facial diplegia. It may be associated with paralysis of the lateral rectus muscle, innervated by the abducens nerve, as first described by Möbius (1888). Since then, the term 'Möbius syndrome' has come to be used for a heterogeneous group of disorders that may include paralysis of other cranial nerves, central respiratory depression, and a combination of paralysis of cranial nerves, arthrogryposis and a variety of limb and/or muscle abnormalities. Gorlin et al. (1990) introduced a broad definition of Möbius syndrome, accepting unilateral facial paresis, involvement of other cranial nerves (predominantly III, IV, IX and XII), limb defects of
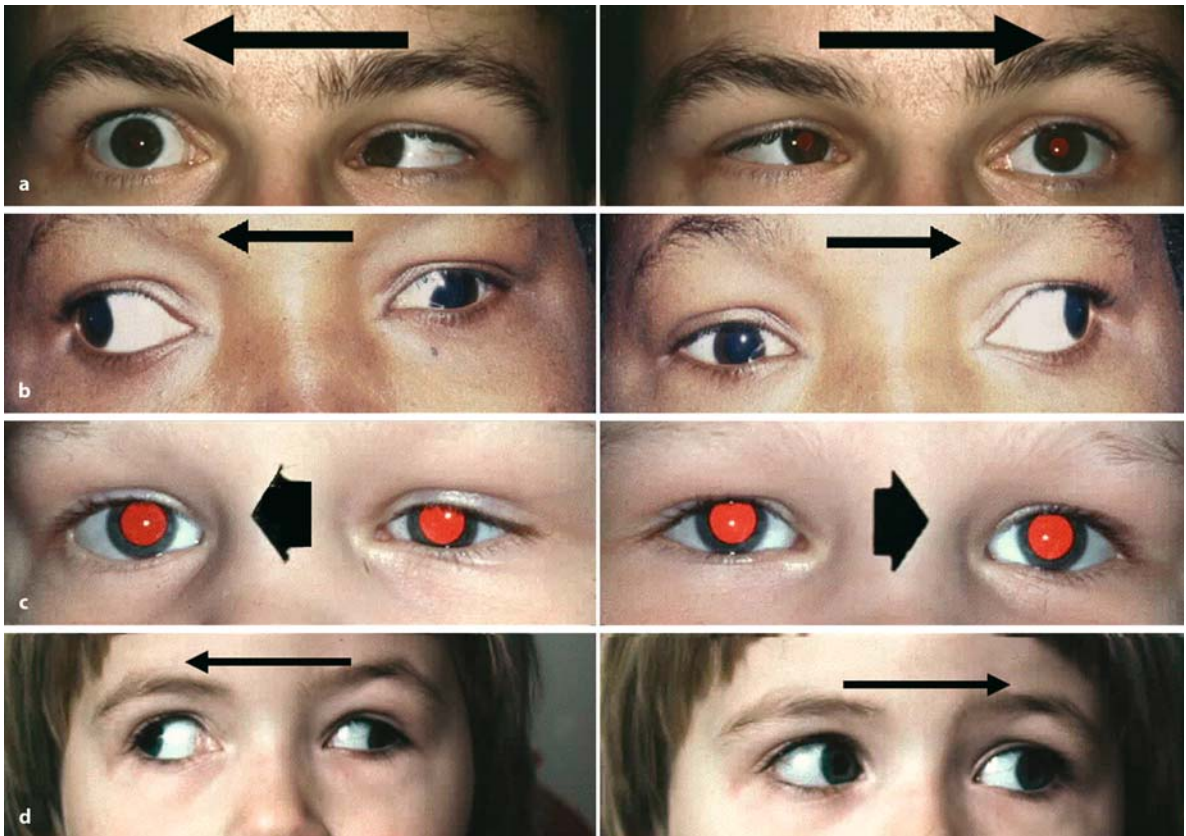
Fig. 7.12 Various types of Duane syndrome: **a** Duane type I of both eyes; **b** Duane type II of both eyes; **c** Duane type III of both eyes; **d** Duane type IV of the left eye. Note narrowing of the palpebral fissure on attempted adduction in all types of Duane syndrome. (**c** From Cruysberg et al. 1986, with permission; **d** from Cruysberg et al. 1989, with permission)

various kinds in up to 50% of cases and a variety of other defects (Kumar 1990). ***Hereditary congenital facial palsy*** is a separate entity. Whereas unilateral facial palsy may be caused by an obstetric trauma (May and Schaitkin 2000), facial palsy in the absence of trauma, either unilateral or bilateral, appears to be a genetic condition for which at least three separate loci were found (Kremer et al. 1996; Verzijl et al. 1999; Punal et al. 2001). Verzijl et al. (2005) studied the facial nucleus in three members of a family with autosomal dominant congenital, non-progressive facial palsy, either unilateral or bilateral (Clinical Case 7.2).

Norman et al. (1995) advocated restricting the use of the term ***'Möbius syndrome'*** for those patients with a bilateral VIth and VIIth nerve paralysis. The morphological basis for such a combined involvement is that the axons of the facial nerve swing around the abducens nucleus, and any destructive lesion in the vicinity of the VIth nerve nucleus destroys axons of the facial nerve in this trajectory. Very localized foci of necrosis can occur in the brain stem (Thakkar et al. 1977; Towfighi et al. 1979). Towfighi et al. (1979) distinguished four groups of pathology: (1) group I, characterized by hypoplasia of cranial nerve nuclei, probably due to rhombomeric maldevelopment; (2) group II, with neuronal loss and evidence of neuronal degeneration, possibly due to damage to the peripheral part of the facial nerve; (3) group III, with additional focal necrosis, characterized by gliosis and calcifications in the pontine/medullary tegmentum, possibly due to vascular anomalies; and (4) group IV, consisting of primary myopathic changes without lesions in cranial nerves and/or nuclei.

Verzijl et al. (2003) studied 37 patients with Möbius syndrome. In the majority of patients, a homogeneous clinical picture was found, characterized by facial diplegia of the upper and lower facial muscles, bilateral eye abduction impairment, hypoglossia, craniofacial and limb malformations, and symptoms of the long fibre tracts. Hypotonia at birth was often present and motor development and coordination did not reach normal levels at older age. The lack of fine motor skills as well as the poor coordination and balance performance may be characterized as clumsiness. This clumsiness may be the result of hypoplasia of long fibre tracts such as corticospinal

Clinical Case 7.2
Congenital Facial Palsy

Neuropathological data on *hereditary congenital facial palsy* are scarce. Verzijl et al. (2005) described a marked decrease in the number of neurons in the facial motor nucleus in three members of a family with autosomal dominant congenital facial palsy (see Case Report).

Case Report. Brain stem pathology could be studied in three affected female members of a family with autosomal dominant congenital, non-progressive facial palsy linked to chromosome 3q (Kremer et al. 1996). Two of them, sisters, died at the ages of 88 and 86 years, respectively, owing to unspecific causes. The third patient, a granddaughter of the second patient, died suddenly because of an undiagnosed acute bacterial meningitis, at the age of 41 years. Patients 1 and 2 showed bilateral congenital facial paresis. In the first patient, the left side was more affected than the right side, whereas in the second pa-

tient the right side was more affected than the left side. The third patient showed a congenital right-sided facial palsy. Data on the facial motor nuclei of one of the two sisters and of the granddaughter are shown in Fig. 7.13. The number of cells in each facial nucleus was estimated by counting the distinct nucleoli of facial motoneurons in every tenth 8-μ-thick, cresyl violet stained section and by multiplying the number obtained by 10. The number of facial motoneurons clearly corresponded with the presence of ipsilateral or bilateral facial palsy and the grade of affection. The first case showed a bilateral decrease in the number of facial motoneurons, the left side (Fig. 7.13 c) being more affected than the right side (Fig. 7.13 d). In the left facial motor nucleus 520 motoneurons were estimated and in the right nucleus 950. In the second case, the right side was more affected than the left side. The number of facial motoneurons was estimated to be 960 at the left side and 600 at the right side. In the third case, with ipsilateral, right-sided facial palsy, in the right facial motor nucleus only 280 motoneurons were present (Fig. 7.13 f), whereas in the left, apparently normally functioning
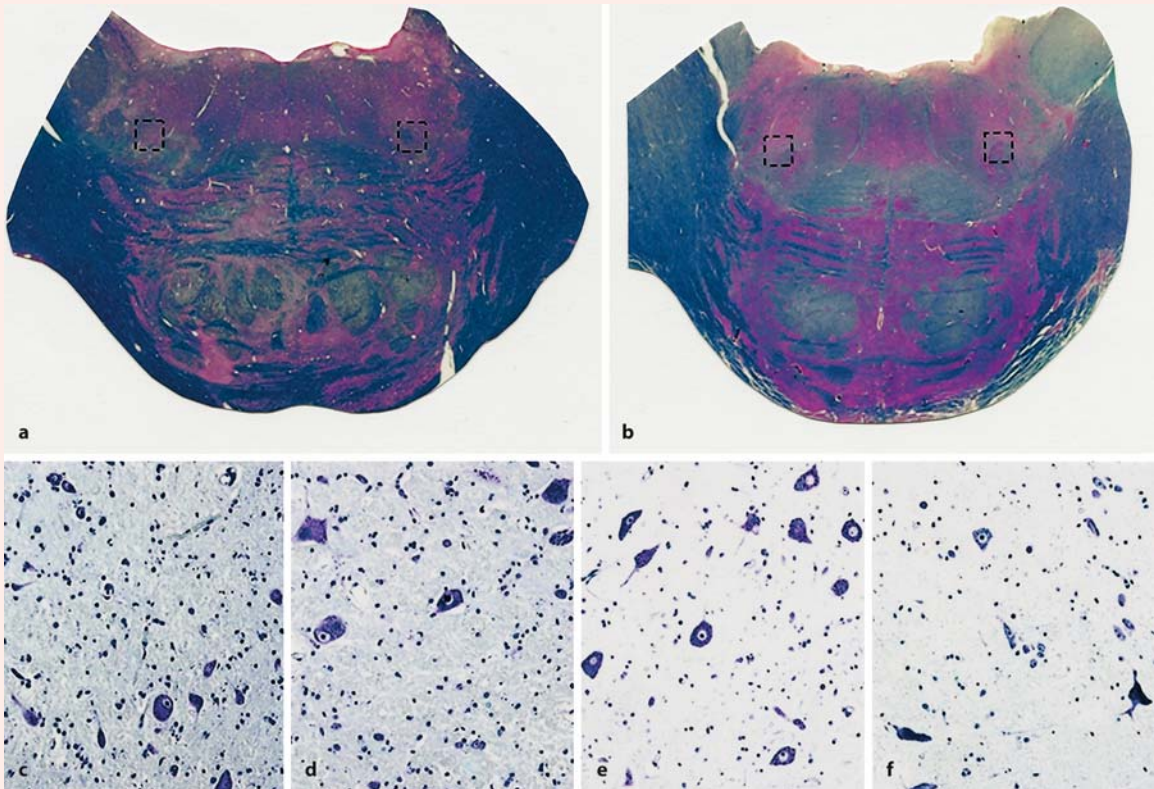
Fig. 7.13 Two related cases, an 88-year-old woman (**a**, **c**, **d**) and her 41-year-old granddaughter (**b**, **e**, **f**) with congenital facial paralysis: **a**, **b** sections through the pons with the level of the facial nuclei indicated; **c**, **d** details of the left and right facial motor nuclei in the first patient; **e**, **f** details of the left and right facial motor nuclei of her granddaughter

left facial motor nucleus (Fig. 7.13 e) 1,680 neurons were estimated. In three age-matched control cases, the number of neurons ranged between 5,030 and 8,700, comparable to van Buskirk's (1945) data obtained from 37 control cases (4,500–9,460 facial motoneurons, with a mean of 6,811).

References

Kremer H, Kuyt LP, van den Helm B, van Reen M, Leunissen JAM, Hamel BC, Jansen C, Mariman ECM, Frants RR, Padberg GW (1996) Localization of a gene for Möbius syndrome to chromosome 3q by linkage analysis in a Dutch family. Hum Mol Genet 5:1367–1371

van Buskirk C (1945) The seventh nerve complex. J Comp Neurol 82:303–333

Verzijl HTFM, van der Zwaag B, Lammens M, ten Donkelaar HJ, Padberg GW (2005) The neuropathology of hereditary congenital facial palsy versus Möbius syndrome. Neurology 64:649–653

or cortico-ponto-cerebellar tracts. In a minority of cases primary respiratory dysfunction was found, suggesting that the caudal part of the brain stem was poorly developed. These data suggest that Möbius syndrome is more than a cranial nerve or nuclear developmental disorder. It should be redefined as a syndrome of rhombencephalic maldevelopment, involving predominantly motor nuclei as well as traversing long fibre tracts. MRI findings confirmed hypoplasia of the lower brain stem in Möbius syndrome (Lengyel et al. 2000; Pedraza et al. 2000). The clinical heterogeneity of Möbius syndrome with congenital facial weakness accompanied by impairment of ocular abduction as its prime features may be due to a combination of a number of loci involved and different types of mutations at each locus. The spectrum of Möbius syndrome may be the sum of changes in a number of genes involved in patterning and specification of the lower brain stem at a specific gestational age.

Most cases of Möbius syndrome coming to autopsy are the most severe cases that show ischemic lesions of the tegmentum (Towfighi et al. 1979; Norman et al. 1995; Lammens et al. 1998; Verzijl et al. 2005; Clinical Case 7.3). The **vascular hypothesis** for Möbius syndrome supposes that ischemic events in the paramedian watershed zones of the lower brain stem are the result of hypoperfusion or occlusion of the developing primitive subclavian artery (Bouwes Bavinck and Weaver 1986; Leong and Ashwell 1997; Sarnat 2004). The ***subclavian artery supply disruption sequence (SASDS),*** suggested by Bouwes Bavinck and Weaver (1986), included Möbius syndrome and other malformations such as the Poland anomaly (absence of the pectoralis major), the Sprengel anomaly (absence of the serratus anterior) and the Klippel–Feil anomaly. Bouwes Bavinck and Weaver (1986) suggested that at 4–6 weeks of gestation premature regression, obstruction or disruption of the primitive trigeminal arteries or blood supply of the vertebral and basilar arteries, occurring prior to the maturation of blood supply of the brain stem,

results in the Möbius syndrome. St. Charles et al. (1993) presented an infant with bilateral facial nerve palsy, external ophthalmoplegia (IV and VI), paresis of cranial nerves V, IX, X, XI and XII, absence of the pectoralis major, terminal transverse limb defects and absence of the right diaphragm. Moreover, discrete foci of brain stem calcifications were found. They suggested that these anomalies would be due to vascular insufficiency prior to the sixth week of gestation, involving the proximal sixth intersegmental artery. Lammens et al. (1998) described two comparable cases with extensive brain stem lesions (Clinical Case 7.3).

During the embryological period, the basilar artery arises from two longitudinal arteries (Fig. 7.15). Initially, the basilar artery is supplied from the internal carotids through a paired series of transient communicating arteries, the primitive trigeminal, otic and hypoglossal arteries, and the blood-flow direction is rostrocaudalwards. This flow changes to the mature caudorostral direction by subsequent formation of the vertebral arteries, accompanied by the disappearance of the primitive communicating vessels, and the development of the posterior cerebral arteries by bifurcation at the top of the basilar artery. At 8–9 weeks of gestation, about 25–30 sets of 'segmentally' arranged paramedian penetrating, short circumferential and long circumferential branches arise from the basilar artery. Agenesis of the basilar artery is very rare and often is associated with haemangiomas of the head, neck and chest (Pascual-Castroviejo et al. 2002). The watershed zone in the brain stem is found between the territories supplied by the paramedian penetrating and long circumferential branches. Systemic hypotension and other conditions of reduced basilar perfusion in the fetus, either early or late in gestation, may lead to symmetrical longitudinal columns of infarction in the tegmentum of the midbrain, the pons and the medulla oblongata and to laminar necrosis of the colliculi. Within these columns the motor nuclei of cranial nerves III–VII, and IX–XII, that subserve such diverse

Clinical Case 7.3
Möbius Syndrome

Möbius syndrome is characterized by a combination of bilateral VIth and VIIth nerve paralysis (Möbius 1888). It represents a syndrome of rhombencephalic maldevelopment (Verzijl et al. 2003), of which only the most severely affected cases come to autopsy. Two cases are included as case reports.

Case Report.   The first case concerns a girl born at 37 weeks after an uneventful pregnancy who died after 11 days owing to severe primary respiratory dysfunction. She showed facial diplegia, horizontal gaze palsy, oral dysfunction, craniofacial and limb malformations and severe muscle hypotonia. At autopsy, the cerebral hemispheres and the cerebellum were normal. The brain stem was asymmetric and hypoplastic with dysplastic, medially situated inferior olives and dysplastic pyramids (Fig. 7.14 a). The pyramidal tracts failed to decussate (Fig. 6.34 f). Microscopically, neuronal loss, gliosis and calcifications were found in the brain stem tegmentum (Fig. 7.14 b), affecting the VIth, VIIth and XIIth motor nuclei.

The second case was part of an originally triplet pregnancy following in vitro fertilization of a 30-year-old woman. Embryo reduction was performed which resulted in an uneventful twin pregnancy. After induced delivery at 36 weeks and 3 days, the first-born boy (birth weight 2,520 g) suffered from respiratory distress and had multiple congenital anomalies. The second boy (birth weight 2,320 g) showed no evidence of any malformation. Physical examination of the first boy revealed hypertelorism, epicanthic folds, bilateral paralysis of the facial and abducens nuclei
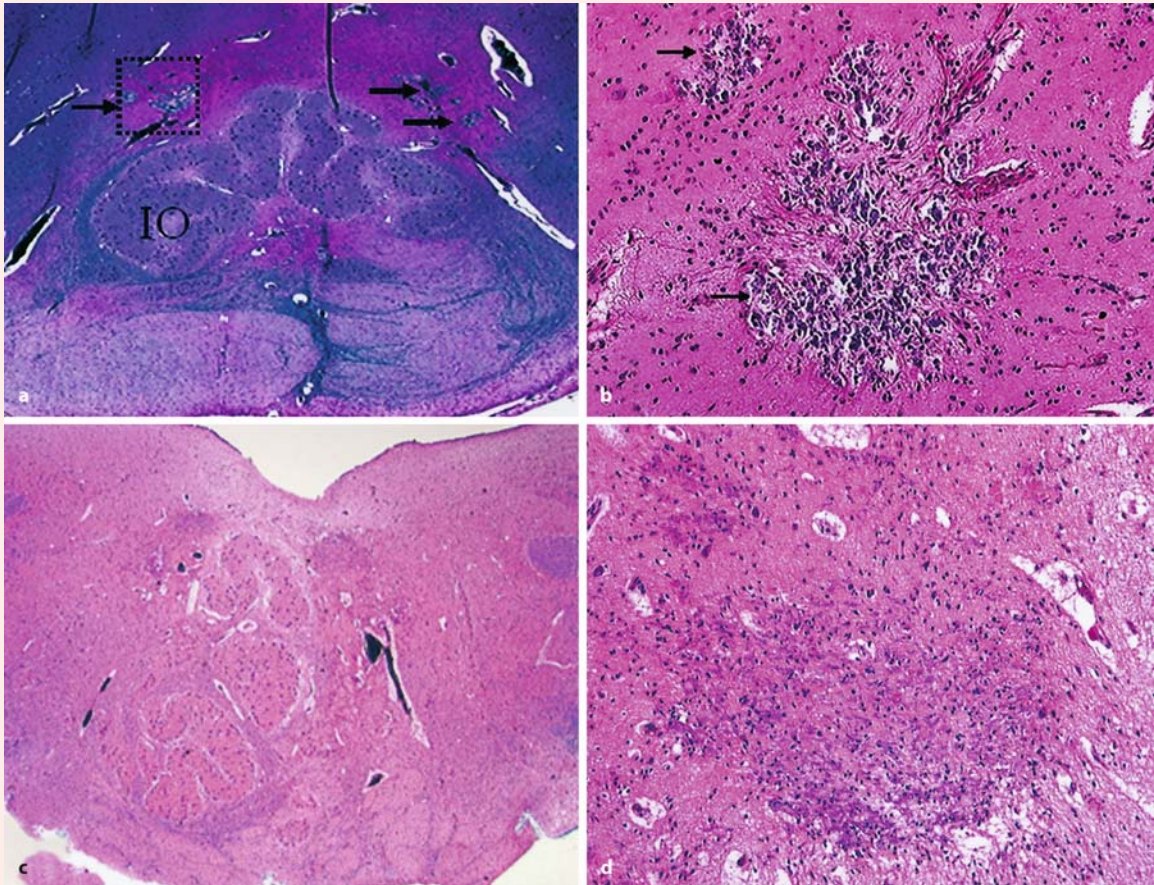
Fig. 7.14 Two cases of Möbius syndrome: **a**, **b** section through the lower brain stem in a girl born at 37 weeks of gestation, showing the malformed pyramids and medially placed inferior olives (*IO*), and calcifications in the lower brain stem, indicated by *arrows* in **a**; **c**, **d**, section through the lower brain stem of a boy born at 36 weeks of gestation, showing asymmetric inferior olives and pyramids, and dystrophic calcifications (**a**, **b** courtesy Pieter Wesseling, Nijmegen; **c**, **d** courtesy Martin Lammens, Gent/Nijmegen)

and a flattened nasal bridge. The right upper limb showed brachydactyly and aplasia of the thumb, whereas the left hand had aplasia of three beams. On a CT scan multiple calcifications were observed in the brain stem. After 1 week the child died from respiratory failure. At autopsy, the cerebral hemispheres and cerebellum were normal. The brain stem was asymmetric with shortening of the pons at the right side. The inferior olives and the pyramids were asymmetric (Fig. 7.14 c). Microscopically, severe loss of neurons, gliosis and dystrophic calcifications (Fig. 7.14 d)

were observed in the brain stem tegmentum, especially at the level of the VIth, VIIth, IXth and XIIth motor nuclei.

References

Möbius PJ (1888) Über angeborene doppelseitige Abducens-Facialis-Lähmung. Münch Med Wochenschr 35:91–94

Verzijl HFTM, van der Zwaag B, Cruysberg JRM, Padberg GW (2003) Möbius syndrome redefined. A syndrome of rhombencephalic maldevelopment. Neurology 61:327–333
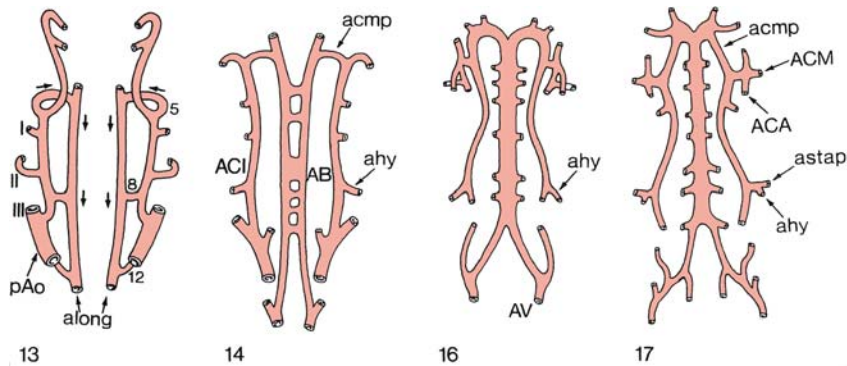
Fig. 7.15 Development of the vascularization of the brain stem between Carnegie stages 13 and 17. *AB* a. basilaris, *ACA* a. cerebri anterior, *ACI* a. carotis interna, *ACM* a. cerebri media, *acmp* a. communicans posterior, *ahy* hyoid artery, *along* a. longitudinalis, *astap* a. stapedia, *AV* a. vertebralis, *pAo* posterior aorta, *I–III* aortic branches, *5*, *8*, *12* primitive trigeminal, otic and hypoglossal arteries. (After Padget 1948)

functions as eye movements, mastication, swallowing and tongue movements, as well as the nucleus of the solitary tract, the central pneumotaxic centre, are found. Watershed infarcts in the fetal and neonatal brain stem are clinically expressed as multiple cranial neuropathies, failure of central respiratory drive and apnea, dysphagia and aspiration, Möbius syndrome and Pierre Robin sequence (Sarnat 2004).

7.3.5 The Sudden Infant Death Syndrome

The *sudden infant death syndrome* (*SIDS*) is defined as the sudden death of an infant under the age of 1 year which remains unexplained after a thorough case investigation, including a complete autopsy, examination of the death scene and review of the clinical history (Willinger et al. 1991). The pathogenetic mechanisms may include cardiac, respiratory and autonomous nervous system abnormalities, possibly due to hypoplasia of the arcuate nucleus of the lower brain stem (Filiano and Kinney 1992, 1994; Matturi et

al. 2000, 2002). The human arcuate nucleus has been implicated in central chemoreception, cardiorespiratory control and blood pressure responses (Folgering et al. 1979; Filiano et al. 1990). Using 1,1'-dioctadecyl-3,3,3',3'-tetramethylindocarbocyanine perchlorate (DiI) labelling, Zec et al. (1997) demonstrated connections between the arcuate nucleus and the caudal raphe which is also involved in cardiorespiratory control.

7.4 Development of the Auditory System

The embryonic and fetal development of the human auditory system follows a precise timetable over the period of gestation in which the vital skeletal, muscular and neural structures are formed and mature to functional status (Anson and Davies 1980; O'Rahilly 1983; Van De Water et al. 1988; O'Rahilly and Müller 2001; Counter 2002; Sulik and Cotanche 2004). From the formation of the otic placode and the otocyst in

the third week of development to the growth of mesenchymal and endodermal tissues that form the outer and middle ear structures, the embryogenesis of the ear is guided by intricate genetic inductive cues. A defect in any component of the outer, middle or inner ear may hinder the signal transmission capacity of the hearing organ and lead to deafness. Prenatal development of the ear may be disrupted by a variety of factors, such as viral infections. Congenital cytomegalovirus infection may be a frequent cause of severe sensorineural hearing loss in neonates (Pappas 1983; deSa 1997). Human fetuses exposed to rubella in the first trimester of pregnancy may develop bilateral sensorineural hearing loss (Bordley 1973; Brookhouser and Bordley 1973; Hardy 1973; Smithells et al. 1990). The characteristic pathological finding is cochleosaccular dysplasia (Nager 1952; Schuknecht 1993). The principal drugs with teratogenic effects on the ear are thalidomide, diphenyl hydantoin, retinoic acid and quinine and its derivatives (Schuknecht 1993).

About 1 in 1,000 children is born with significant hearing loss or deafness present at birth or during early childhood, that is in the prelingual period (Petit et al. 2001 a, b). Syndromic deafness contributes to about 30% of the cases of prelingual deafness. The syndromic forms of prelingual deafness may be conductive owing to external and/or middle ear defects, sensorineural, or mixed, whereas the non-syndromic forms are almost exclusively sensorineural. An additional 1 in 1,000 children becomes deaf before adulthood. These forms are usually less severe and progressive (Petit et al. 2001a, b; Toriello et al. 2004). Syndromic forms of deafness are almost exclusively hereditary in developed countries. Several hundreds of syndromes including hearing loss have been described (Petit et al. 2001a, b; Steel and Kros 2001; Toriello et al. 2004). Three classes may be distinguished: (1) the forms with external and middle ear anomalies, with or without a sensorineural component to the deafness; (2) the forms with middle ear anomalies, with or without sensorineural deafness; and (3) the sensorineural forms. The non-syndromic forms of deafness are genetically highly heterogeneous and appear to be almost exclusively monogenic diseases.

7.4.1   Development of the Ear

The ear or vestibulocochlear organ is composed of external, middle and inner parts. The external ear consists of the auricle and the external acoustic meatus with the outer layer of the tympanic membrane. The middle ear is formed by the tympanic cavity, the auditory ossicles and the inner layer of the tympanic membrane. The inner ear comprises the labyrinth, a

series of fluid-filled spaces in the temporal bone. The embryonic development of the human ear is summarized in Fig. 7.16.

The **auricle** or **pinna** arises from a series of elevations (the **auricular hillocks**) around the first pharyngeal cleft. They begin to appear in pharyngeal arches 1 and 2 at 5 weeks of development, and by the sixth week six hillocks are found, three in each pharyngeal arch, but soon they lose their identity. The first three hillocks from the mandibular arch are supposed to form the tragus and the crus of the helix (Streeter 1922; Hochstetter 1948). The hyoid hillocks probably form the helix and the antitragus. The **external acoustic meatus** develops from the first pharyngeal cleft and first forms a 'keyhole' between the auricular hillocks. Here the future cartilaginous part of the meatus is formed (Nishimura and Kumoi 1992). Early in the fetal period, a solid core of epithelial cells grows medialwards as a meatal plug in which later the osseous part of the meatus will form (O'Rahilly and Müller 2001). A lumen will form in the meatal plug and the external acoustic canal is fully patent by 20 weeks of development. At the end of the embryonic period, the **tympanic membrane** forms at the point of contact between the ectodermal meatal plug and the endodermal tubotympanic recess, and is composed of three layers: an outer ectodermal layer, continous with the outer layer of the external meatus, an intermediate mesodermal layer and an inner endodermal layer that is continuous with the mucous membrane of the middle ear cavity (Fig. 7.16).

The **tympanic cavity** develops from the tubotympanic recess of the first pharyngeal pouch (Kanagasuntheram 1967). When the tubotympanic recess and the external acoustic meatus approach each other, the auditory ossicles develop in the interposed mesenchyme (Fig. 7.16). The origin of the **auditory ossicles** is not entirely clear (Anson et al. 1948, 1960; Hanson et al. 1962; O'Rahilly and Müller 2001). Presumably, the head of the malleus and the body and short crus of the incus arise from the first pharyngeal arch, whereas the handle of the malleus, the long crus of the incus and the stapes may arise from the second pharyngeal arch. Early fetally, the handle of the malleus becomes anchored to the tympanic membrane. Around the same time, the base of the stapes appears in the lateral wall of the otic capsule and occupies the fenestra vestibuli or oval window. The auditory ossicles begin to ossify during the second trimester. The middle ear muscles (the m. tensor tympani and the m. stapedius) develop from the first and second pharyngeal arches, respectively, by the 16th week (Anson and Davies 1980). The middle ear reaches its adult size before birth (O'Rahilly and Müller 2001).

The **inner ear** consists of the organ of Corti, afferent and efferent parts of the auditory nerve and the
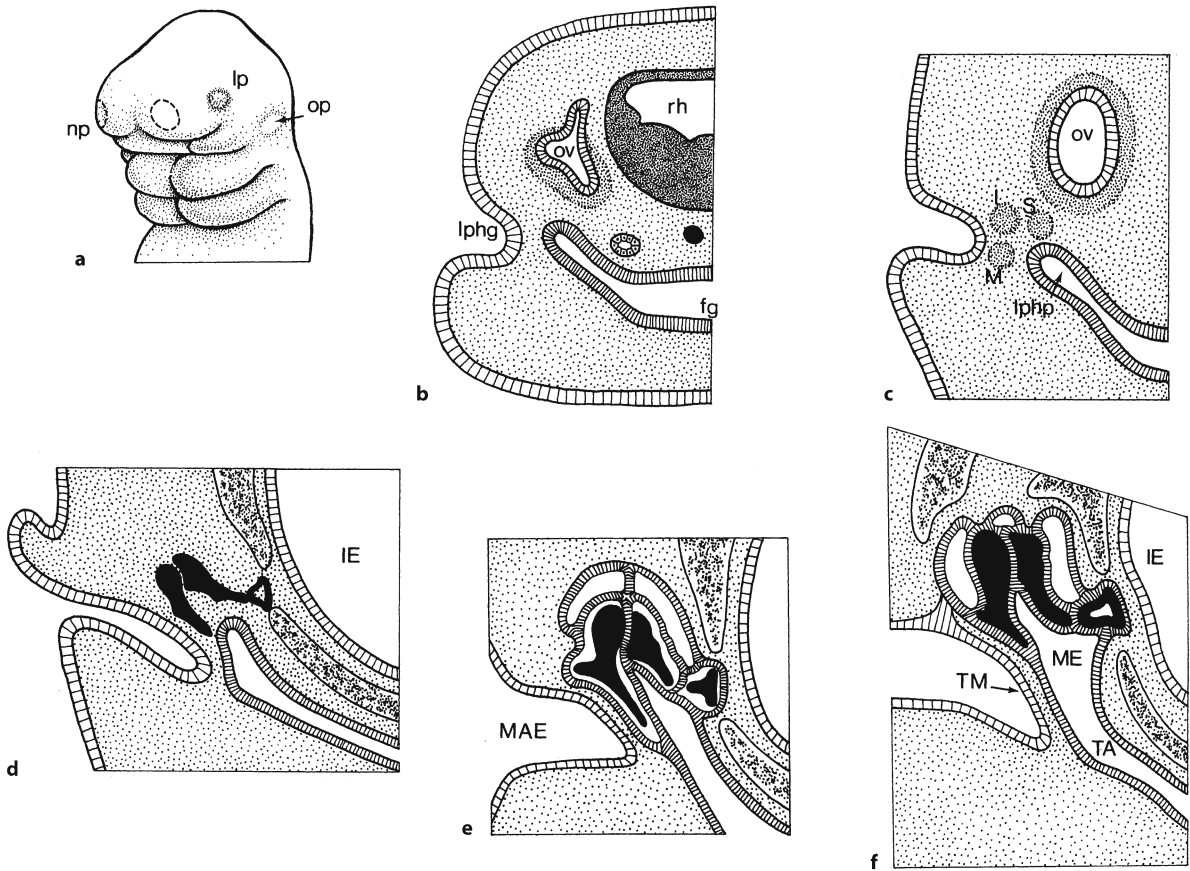
Fig. 7.16 Development of the human ear. *I* incus, *IE* internal ear, *Iphg* first pharyngeal groove, *Iphp* first pharyngeal pouch, *lp* lens placode, *M* malleus, *MAE* meatus acusticus externus, *ME* middle ear, *np* nasal placode, *op* otic placode, *ov* otic vesicle, *S* stapes, *TA* tuba auditiva, *TM* tympanic membrane. (After Hamilton and Mossman 1972)

vestibular components: the otolith organs (the utriculus and sacculus), the endolymphatic duct and sac, and the three semicircular canals. Each of these structures is contained within a membranous labyrinth, housed in a surrounding bony labyrinth. The inner ear is the first part of the ear to develop. The ectoderm of the head is 'determined' to form an **otic field** by the inductive action of chordamesoderm (Peck 1994; Fekete 1999; Groves and Bronner-Fraser 2000; Baker and Bronner-Fraser 2001; Kiernan et al. 2002). Migrating neural crest cells may then interact with this field to induce the formation of the otic disc. The **otic disc** appears at 3.5 weeks of development (Carnegie stage 9: Müller and O'Rahilly 1983) and becomes 'invaginated' so that the **otic pit** is formed (Figs. 7.16, 7.17), probably largely by elevation of the surrounding structures. The opening of the pit becomes narrowed and closes so that the **otic vesicle** or **otocyst** is formed. The otocyst divides into dorsal and ventral segments that will become the vestibular (the semicircular canals, the sacculus and the utriculus) and auditory (cochlear) parts, respectively

(Fig. 7.18). Around day 34, the endolymphatic appendage appears dorsally and the cochlear duct elongates ventrally. The mesenchyme surrounding the otocyst becomes condensed and forms the **otic capsule**. Its formation is induced by the otocyst. Then, the lateral semicircular canals appear, followed by the spiralling of the cochlear duct. Development of the utriculus, the endolymphatic duct, the sacculus, the cochlea and the semicircular canals is associated with localized apoptosis (Nishikori et al. 1999).

The **cochlea** is a fluid-filled tube that is coiled two and a half times. In cross section, it has a broad base, a pointed apex and a central pillar called the modiolus. The cochlea is composed of three chambers or scalae: the scala vestibuli, the scala media and the scala tympani (Fig. 7.19). The inner scala media is filled with endolymph, which is rich in potassium and is similar to CSF in its protein composition. The perilymph of the outer scalae vestibuli and tympani has a substantially higher sodium and protein concentration. The two perilymph compartments form one space, since they are continuous with each other

Fig. 7.17 Photomicrographs showing the development of the human ear in Carnegie stages 11 (**a**), 12 (**b**) and 14 (**c**). *gV* trigeminal ganglion, *nVII* facial nerve, *op* otic placode, *ov* otic vesicle, *r2*, *r4* rhombomeres. (From the Kyoto Collection of Human Embryos; courtesy Kohei Shiota)
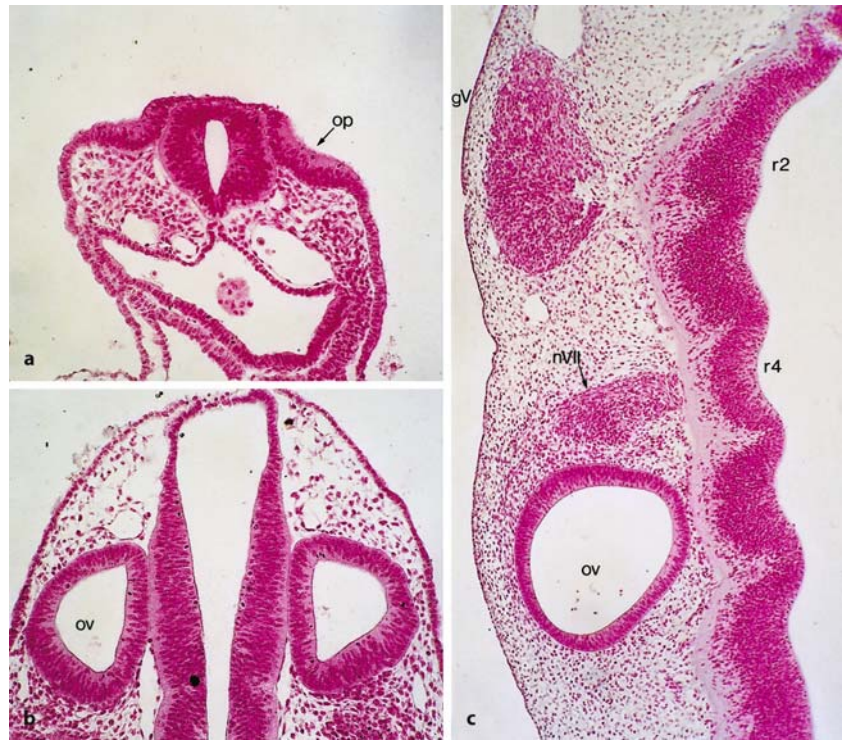
Fig. 7.18 Development of the membranous labyrinth from the otocyst: **a** anterolateral view of 4.3-mm embryo; **b** lateral view of a 6.6-mm embryo; **c** lateral view of an 11-mm embryo; **d** lateral view of a 20-mm embryo; **e**, **f** lateral and medial views of a 30-mm embryo. *asd* anterior (superior) semicircular duct, *cc* crus commune, *cd* cochlear duct, *cn* cochlear nerve, *ed* endolymphatic diverticle, *es* endolymphatic sac, *lsd* lateral semicircular duct, *psd* posterior semicircular duct, *S* sacculus, *U* utriculus, *vn* vestibular nerve. (After His 1889; Streeter 1906, 1918)
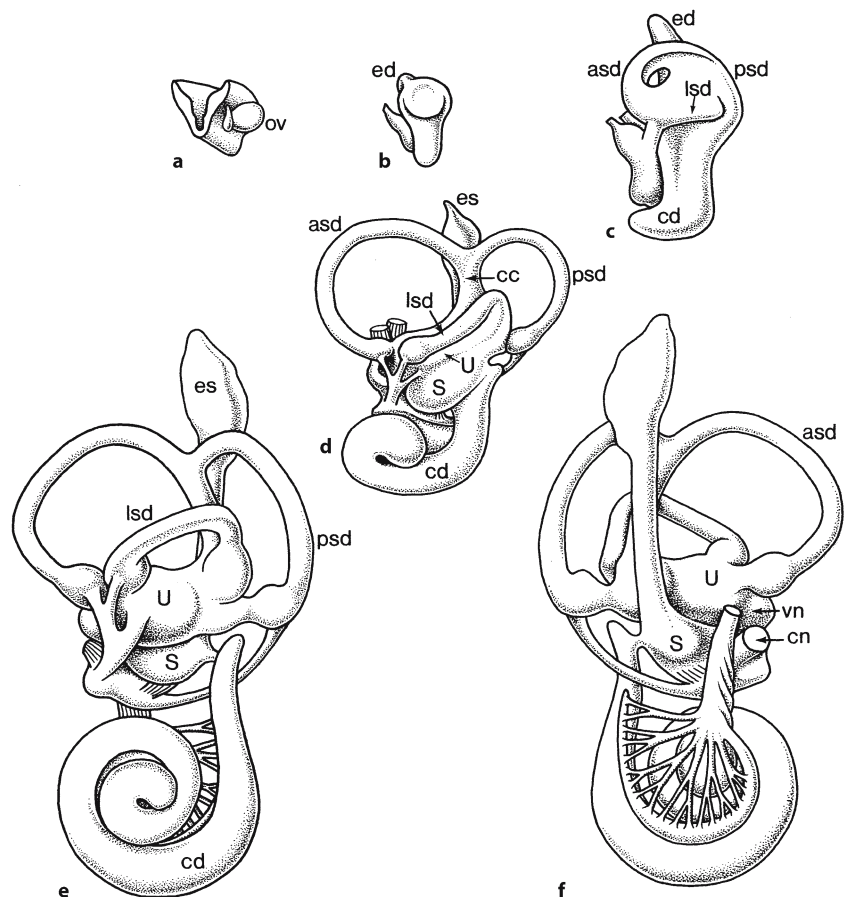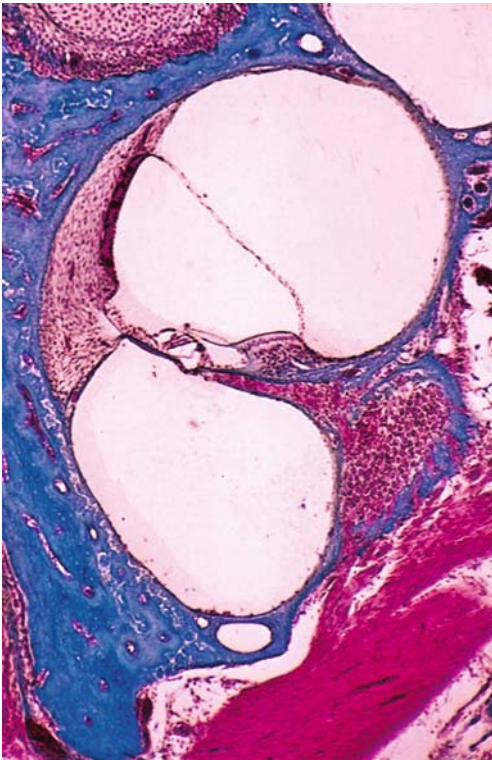
Fig. 7.19 Photomicrograph of the human cochlea (courtesy Jo Curfs, Nijmegen)

at the apex of the cochlea (the helicotrema). The **scala media** or **cochlear duct** contains the **organ** of **Corti**, which is composed of a single row of differentiated epithelial cells (the inner hair cells) and three rows of outer hair cells. The inner and outer hair cells interface with supportive cells and pillar cells which are separated by the tunnel of Corti. On their apical side, the hair cells contain contractile proteins, including an actin cuticular plate and about 100 stereocilia, graduated in length, and which extend to the overlying tectorial membrane. The stereocilia are composed of the active contractile proteins actin and myosin (Flock 1980). The inner and outer hair cells of the organ of Corti are innervated by afferent and efferent VIIIth nerve fibres. The myelinated type I afferent auditory fibres (about 90%) innervate the inner hair cells. The unmyelinated type II fibres innervate the outer hair cells. Throughout the cochlea the inner and outer hair cells are also innervated by efferent fibres from the **olivocochlear bundle** of **Rasmussen**, which originates in the peri-olivary nuclei around the superior olivary nucleus.

The mesenchyme of the **otic capsule** is remodelled by cavitation of the otic capsule to form the openings of the developing bony **labyrinth**. This cavitation leads to the formation of the scala vestibuli and the scala tympani (Fig. 7.20). The capsule becomes ossi-

fied around the 16th week of development, from the base of the cochlea to the distal parts of the semicircular canals. The sensory epithelium of the cochlear duct begins to develop in the medial wall of the duct during the seventh week, just as the duct is beginning to coil. At this stage, the sensory epithelium is composed of about six tightly packed layers of nuclei. Growth of the cells in the epithelium results in the formation of the embryonic precursor of the organ of Corti, Kölliker's organ. Kölliker's organ undergoes a rapid series of changes in the embryo so that only some of its cells end up as part of the mature organ of Corti (Sulik and Cotanche 2004). The **organ** of **Corti** develops in the basal sections first, followed by the middle and apical sections. Afferent and efferent innervation starts late in the embryonic period, and may not be complete until postnatally. From the ninth to the 20th week, the receptor cells undergo differentiation and mature. By the 26th week, the human inner ear is fully developed. The ear is functionally active by the fifth month of gestation when the fetus is capable of responding to internal and external sounds (Johansson et al. 1964). It is likely that the fetal ear is functionally capable of responding to a variety of biologically significant sounds by the 28th week of gestation (Peck 1995; Counter 2002).

At birth, humans have about 20,000 inner and outer hair cells which often do not last a lifetime as they do not regenerate when lost (Stone et al. 1998). By the age of 65–75 years, many individuals have a bilateral, high-frequency progressive hearing loss known as presbycusis associated with hair cell attrition. Hair cell loss is the most common cochlear defect causing hearing impairment in presbycusis and noise-induced hearing loss. Hearing loss due to inner hair cell absence is rare, but may occur as a congenital defect or as a result of advanced degeneration of the organ of Corti. Transduction of sound occurs in the sensory cells of the organ of Corti. The inner and outer hair cells have different roles in the transduction of energy within the cochlea. Inner hair cells provide direct input to almost all of the axons in the cochlear nerve. Their activity is modified by local amplification of the motion of the basilar membrane produced by the outer hair cells (Moore and Linthicum 2004). Several molecules have been identified as having a vital role in hair-cell transduction. They are specifically expressed in or around the stereocilia and mutations in their genes lead to deafness (Steel and Kros 2001). In mice, specific defects have been discovered for three unconventional myosins: myosins VI, VIIA and XV. Mutant myosin VI leads to progressive fusion of hair cell stereocilia, mutant myosin XV results in short stereocilia, whereas mutant myosin VIIA leads to progressive disorganization of the stereocilia bundle. Defects in myosins VIIA and XV are also involved in human deafness.

Fig. 7.20 Development of the cochlear duct: **a** section through the cochlear duct (*cd*) at 10 weeks of development, showing the adjacent scala tympani (*st*); **b** at 14 weeks the cochlear duct is situated beteen the scala tympani and the scala vestibuli (*sve*) with the spiral organ (*spo*) differentiating; **c** at 16 weeks various turns of the cochlea are present; cochlear nerve (*cn*) fibres pass through a central pillar, the modiolus (*mod*), whereas their cells of origin form the spiral ganglia (*spg*); **d** details of the spiral organ are present at 25 weeks of development. *bm* basilar membrane, *ihc* inner hair cell, *ohc* outer hair cell, *sva* stria vascularis, *tC* tunnel of Corti, *vm* vestibular (Reissner) membrane. (After O'Rahilly and Müller 2001)
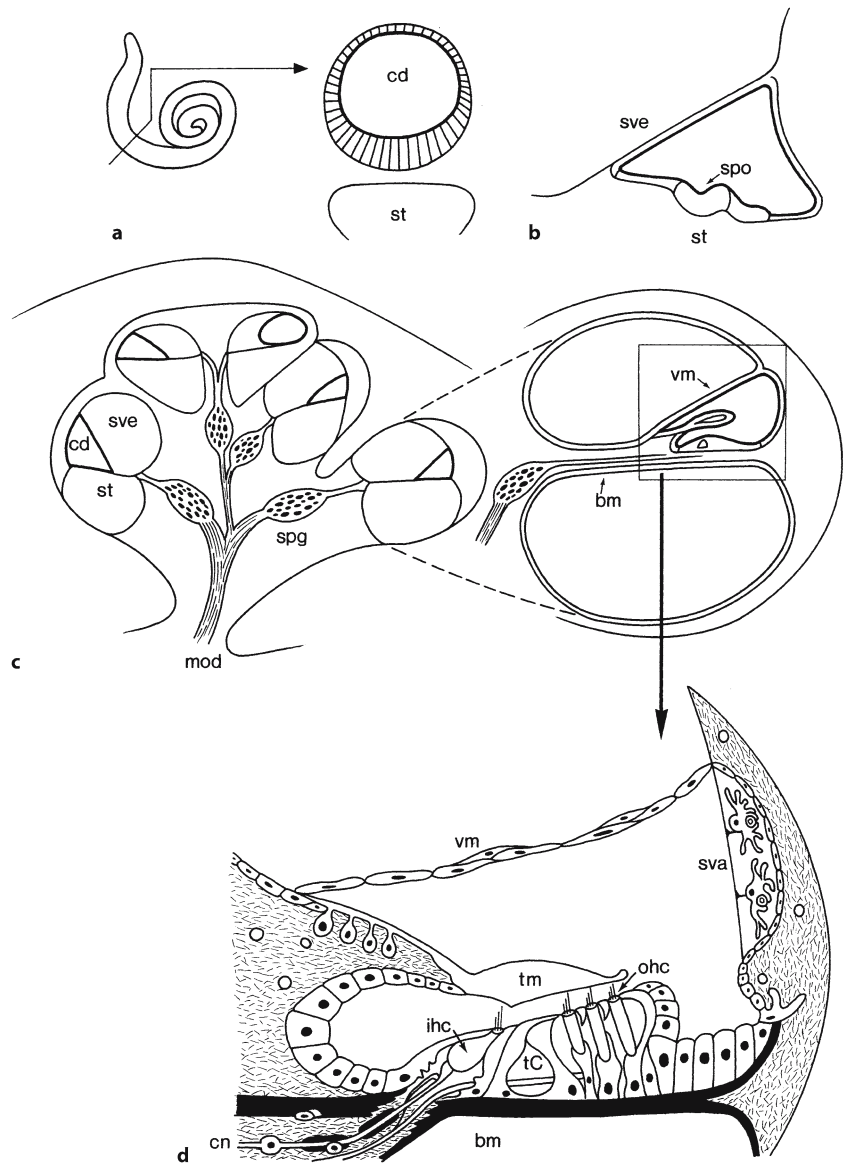
7.4.2 Development of the Auditory Projections

The principal auditory pathway (Fig. 7.21) passes from the cochlea, via the cochlear nuclei, the inferior colliculus and the medial geniculate body to the contralateral auditory cortex on the dorsal surface of the superior temporal gyrus (Nieuwenhuys 1984; Nieuwenhuys et al. 1988; Moore and Linthicum 2004). All components of this pathway are tonotopically organized. The human cochlear nuclei consist of a larger ventral nucleus and a smaller dorsal nucleus (Moore and Osen 1979). Around 16 weeks of gestation, neurons of the ventral cochlear nucleus can be distinguished, and their number increases to about 40,000 by 21 weeks, after which it remains stable throughout fetal and postnatal life. Cytoarchitectural features of the main ventral cochlear neuron types gradually develop in the second half of pregnancy (Nara et al. 1993), those in the inferior colliculus some weeks earlier (Nara et al. 1996). The human olivocochlear system has been identified with acetylcholinesterase histochemistry (Schuknecht et al. 1959) and choline acetyltransferase immunohistochemistry (Moore et al. 1999; Moore and Linthicum 2004). Neurofilament staining indicates that olivocochlear fibres grow out between 22 and 29 weeks of gestation (Moore et al. 1997), in line with data on the first appearance of efferent fibres and terminals (Igarashi and Ishii 1980) and the first appearance of mature synapses on outer hair cells (Lecanuet and Schaal 1996). Moore et al. (1997) studied the develop-
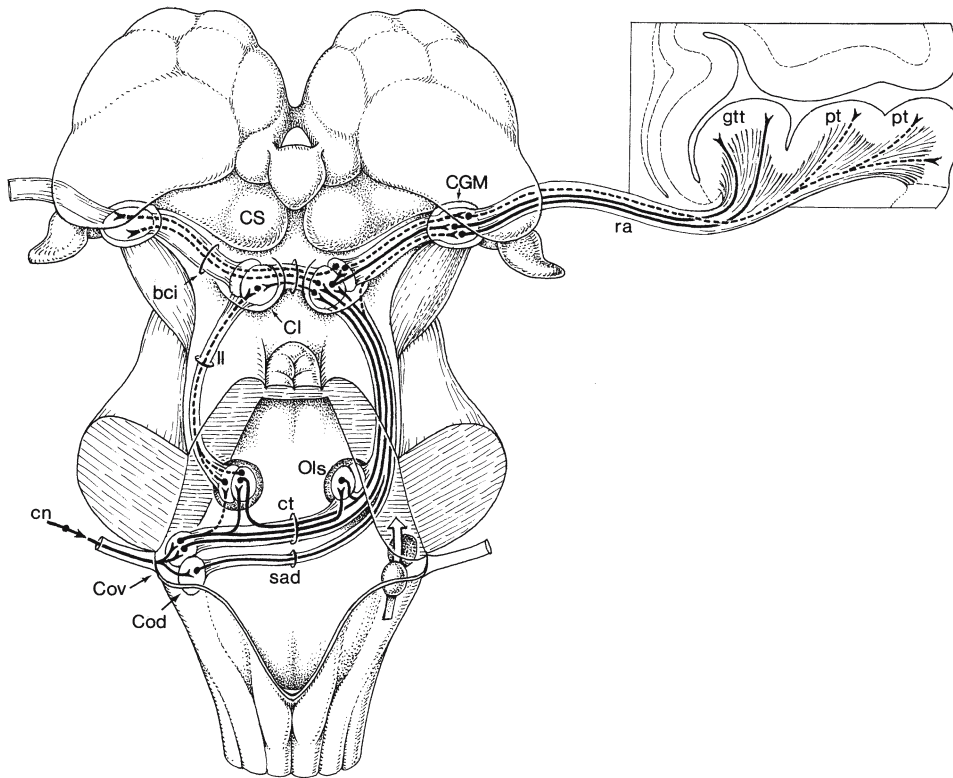
Fig. 7.21 Auditory projections. *bci* brachium of the colliculus inferior, *CGM* corpus geniculatum mediale, *CI* colliculus inferior, *cn* cochlear nerve, *Cod* dorsal cochlear nucleus, *Cov* ventral cochlear nucleus, *CS* colliculus superior, *ct* corpus trapezoid-eum, *gtt* gyrus temporalis transversus (Heschl), *ll* lemniscus lateralis, *Ols* oliva superior, *pt* planum temporale, *ra* radiatio acustica, *sad* stria acustica dorsalis. (After Nieuwenhuys et al. 1988)

ment of ascending, commissural and descending components of the auditory system with neurofilament immunohistochemistry. The first cochlear nerve fibres invade the ventral cochlear nucleus by 16 weeks of gestation. At about the same time, several trapezoid body–lateral lemniscus axons reach the superior olivary nucleus and the inferior colliculus. The ascending auditory pathway undergoes a marked expansion between 16 and 26 weeks of gestation, with collateralization of ascending axons by 26 weeks of gestation and formation of terminal plexuses in target nuclei between 26 and 29 weeks of gestation. Myelination of the auditory pathways begins at about 26 weeks of gestation when linear arrays of oligodendrocytes are located alongside axons in all segments of the auditory pathway (Moore et al. 1995). At 29 weeks of gestation, the cochlear nerve contains lightly myelinated axons and the primary axons can be seen to bifurcate and radiate within the ventral cochlear nucleus. In the lateral lemniscus and the trapezoid body, myelination is present by 26 weeks of gestation, whereas myelination in the brachium of the inferior colliculus starts from 29 weeks of gestation. Myelination continues into the first postnatal year. By 1 year of age, auditory pathway myelination appears comparable to that in the mature brain. Studies of the development of the auditory blink–startle response indicate that the first short-latency responses to sound may be present by 25–26 weeks of gestation (Birnholtz and Benecarraf 1983; Kuhlman et al. 1988). This reflex is seen in virtually all fetuses by 28 weeks of gestation, closely parallelling the development of myelination in the auditory pathways. Both prenatal and postnatal studies of auditory-evoked responses (AERs) indicate that the higher auditory tracts and nuclei develop rapidly and continue to develop during the first years of life. The development of the auditory-evoked cortical response is shown in Fig. 7.22. AERs can be subdivided into their latency in the brain stem (ABR), middle latency (MLR) and cortical (ACR) AERs.
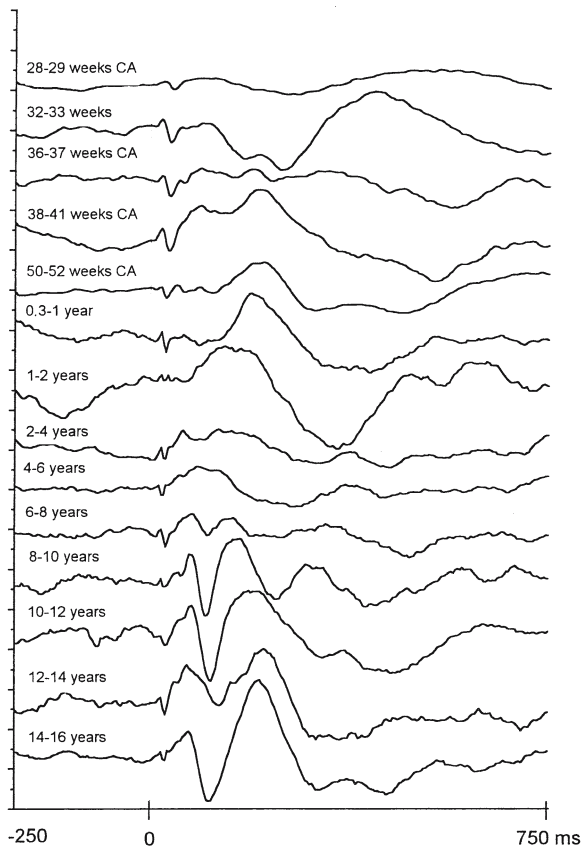
Fig. 7.22 Maturation of the auditory evoked response wave form between 28 weeks' conceptional age (*CA*) and 12 years of age (from Pasman 1997; courtesy Jacko Pasman, Nijmegen)

7.4.3   Developmental Disorders of the Auditory System

Congenital defects of any compartment of the ear may cause significant hearing loss. *Congenital anomalies* of the *external ear* include atresia of the external acoustic meatus and malformations of the auricle. Common anomalies of the outer ear are microtia and macrotia that are often associated with syndromes of the head and neck (Gorlin et al. 2001; Karmody and Annino 1995; Tewfik and Der Kaloustian 1997; Allanson 2004). Malformation of the auricle is also seen in disruptions of the first pharyngeal arch such as Treacher Collins syndrome (Chap. 5). *Congenital abnormalities* of the *external auditory meatus* are usually caused by incomplete closure of the first branchial groove or by incomplete fusion of the auricular hillocks (Altmann 1951; Nager and Levin 1980; Marquet et al. 1988; Friedmann and Arnold 1993). The most important malformation of the external meatus is *congenital aural atresia* which is frequently associated with middle ear malformations as in Treacher Collins syndrome (Schuknecht 1993).

Duplication of the external auditory meatus is rare (Franz 1959; Beck 1970; Stennert and Arold 1973).

Anomalies of the *middle ear* are frequently combined with stenosis or atresia of the external acoustic meatus, and include abnormalities of the facial nerve and the auditory ossicles (Anson et al. 1948, 1960; Sando and Wood 1971; Marquet et al. 1988; Tos 2000). *Otosclerosis*, the second common middle ear disorder in childhood (after otitis media), is an autosomal dominant disorder that results in the production of excess osseous tissue in the tympanic cavity and fixation of the footplate of the stapes in the fenestra vestibuli. The resulting interference with the conduction of sound vibrations causes progressive loss of hearing. Congenital middle ear disorders may be associated with syndromes such as Apert's acrocephalosyndactyly, Goldenhar–Gorlin syndrome and Pierre Robin sequence (Chap. 5).

Congenital ossicular fixations and *defects* are usually divided into major and minor malformations (Tos 2000). The major malformations involve both the tympanic cavity and the external ear (*congenital aural atresia*) and occur in approximately 1 in 11,000 births (Nager and Levin 1980). The minor malformations involve fixations and defects of the ossicular chain and malformations of the oval and round window regions, with a normal eardrum and external acoustic meatus. Their incidence is also very small (Tos 2000). Several classifications of minor congenital ear anomalies have been proposed; the most commonly used is that of Cremers and Teunissen (Cremers and Teunissen 1991; Teunissen 1992), and modified by Tos (2000). The Cremers–Teunissen classification is based on the analysis of 144 ears with minor congenital malformations, operated in the Nijmegen Otorhinolaryngological Clinic in the period between 1964 and 1990. The minor anomalies of the ear were subdivided into four classes: (1) isolated congenital stapes ankylosis without other deformities in the middle ear (30.6%); (2) stapes ankylosis associated with other congenital ossicular chain abnormalities (38.2%); (3) congenital anomalies of the auricular chain with a mobile stapes footplate (21.6%); and (4) congenital aplasia (6.9%) and severe dysplasia (2.8%) of the oval or round window, the dysplasias being due to a crossing (prolapsed) facial nerve or a persistent stapedial artery. This classification is mainly based on the mobility of the stapes footplate and gives more insight into the frequency of these isolated or associated congenital middle ear anomalies. A persistent stapedial artery is a very rare anomaly (House and Patterson 1964; Gerhardt and Otto 1970; Govaerts et al. 1993).

The tortuous peripheral course of the **facial nerve** from the pons to the parotid is fairly constant and, although several variations with clinical significance have been described, variation is the exception rather
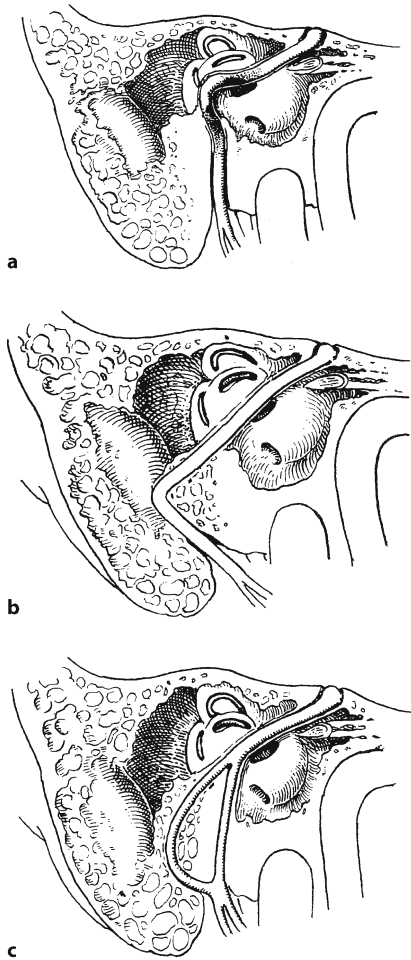
Fig. 7.23 Variations in the course of the facial nerve through the temporal bone: **a** a hump posterior and lateral to the prominence of the lateral semicircular canal; **b** a course more posterior to the prominence of the lateral semicircular canal; **c** division of the vertical portion of the facial nerve with uniting at the stylomastoid foramen. (After Fowler 1961)

than the rule (Gasser and May 2000). At birth, before the mastoid process has developed, the stylomastoid foramen and the facial nerve lie superficially. Here, the facial nerve is susceptible to damage by obstetrical forceps and by postauricular incisions. As the mastoid develops, it overlies the stylomastoid foramen and shields the nerve. *Variations* observed include (1) variations within an intact facial canal (Fowler 1961; Proctor and Nager 1982; Fig. 7.23) and (2) congenital bony dehiscences in the facial canal, mainly in the tympanic segment (Dietzel 1961; Baxter 1971).

Developmental dysgenesis of the *membranous labyrinth* has been grouped into four pathological variations (Ormerod 1960; Suehiro and Sando 1979; Friedmann and Arnold 1993): (1) the Michel type (Michel 1863); (2) the Mondini–Alexander type

(Mondini 1791; Alexander 1904); (3) the Bing–Siebenmann type (Siebenmann and Bing 1907); and (4) the Scheibe type (Scheibe 1892a, b). Schuknecht (1993), however, proposed a simpler classification into three types: Scheibe, Mondini and trisomy types. In his opinion, other types of dysplasia such as the Bing–Siebenmann type with a normal bony labyrinth and underdeveloped membranous labyrinth were inadequately documented, both clinically and histologically. Moreover, Michel dysplasia, characterized by complete failure of development of the inner ear, is very rare (Schuknecht 1980, 1993; deSa 1997). The *Scheibe type* has a normal vestibular apparatus, but the membranous cochlea and the sacculus are underdeveloped. The *Mondini type* shows the presence of a single curved tube representing the cochlea with a reduced numbers of spirals, associated with immaturity of the vestibule and canals affecting both membranous and bony components. This malformation occurs in Usher, Wildervanck, Waardenburg and Pendred syndromes (Schuknecht 1980, 1993).

7.4.4 Genes Involved in Deafness

Rapid progress has been made in identifying deafness genes in mice and men. More than 100 genes have now been identified that affect inner ear development or function, with many more loci known to be involved in deafness but not yet identified (Fekete 1999; Petit et al. 2001a, b; Steel and Kros 2001; Griffith and Friedman 2002; Kiernan et al. 2002; Steel et al. 2002; Friedman and Griffith 2003). In addition to these, many other genes have been identified that affect the middle ear or central auditory pathways (Steel et al. 2002). Studies of knockout and mutant mice in which one or more divisions of the ear are abnormal (Fekete 1999; Kiernan et al. 2002) are summarized in Figs. 7.24 and 7.25. Murine mutations can be divided into (1) mutations that affect the outer ear (in extreme cases, the entire outer ear is missing as found in the double mutant of *Hoxa1/Hoxb1*: Gavalas et al. 1998), (2) mutations that affect the middle ear (e.g. *goosecoid*, *Dlx2*, *retinoic acid receptors*, *Prx1*, *Otx2*, *Hoxa1*, *Hoxb1*, and endothelin-related molecules; Fig. 7.24), (3) mutations that affect the gross anatomy of the inner ear (e.g. *Hoxa1*, *Kreisler*, *Fgf3*, *Pax2*, *Otx1*, *Eya1*, *Prx1/Prx2* and *Rars*, affecting the entire or specific parts of the inner ear; Fig. 7.25) and (4) mutations that affect the cell types and tissues of the inner ear. Some mutations that alter specific cell types or tissues in the mammalian cochlea are shown in Fig. 7.26. A number of neurotrophins and their receptors are essential for the normal development of cochlear (and) vestibular neurons, including nerve growth factor (NGF), brain-derived neurotrophic

Fig. 7.24 Murine mutations that alter the morphology of the outer or middle ear: **a** normal situation; **b** *Otx2+/−* mutant; **c** *Dlx1* mutant; **d** *Dlx2* mutation; **e** *Prx1* and *Hoxa2* mutants; **f** *Hoxa1* mutant. *I* incus, *IE* internal ear, *M* malleus, *MAE* meatus acusticus externus, *ME* middle ear, *S* stapes, *TA* tuba auditival, *tm* tympanic membrane, *tr* tympanic ring. (After Fekete 1999)
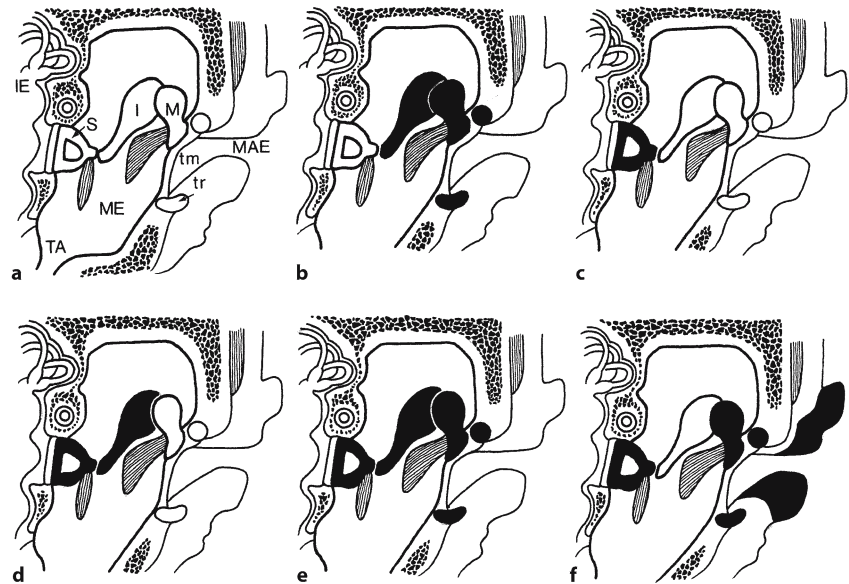
Fig. 7.25 Murine mutations that alter the morphology of the inner ear, its sensory organs or the statoacustic ganglion cells: **a** *Hoxa2*, *Hoxa1/Hoxb1*, *Kreisler* and *Fgf3* mutants; **b** *Otx1*, *Prx1/Prx2* mutants; **c** *Pax2* mutant; **d** *Pou4f3* mutant, affecting the hair cells; **e** *Ngn1* mutant; **f** *Rarα/Rarγ* mutants, in which the organ of Corti and the spiral ganglion are affected. *asd* anterior semicircular duct, *cc* crus commune, *cd* cochlear duct, *ed* endolymphatic duct, *es* endolymphatic sac, *hsd* horizontal (lateral) semicircular duct, *psd* posterior semicircular duct, *S* sacculus, *U* utriculus. (After Fekete 1999)
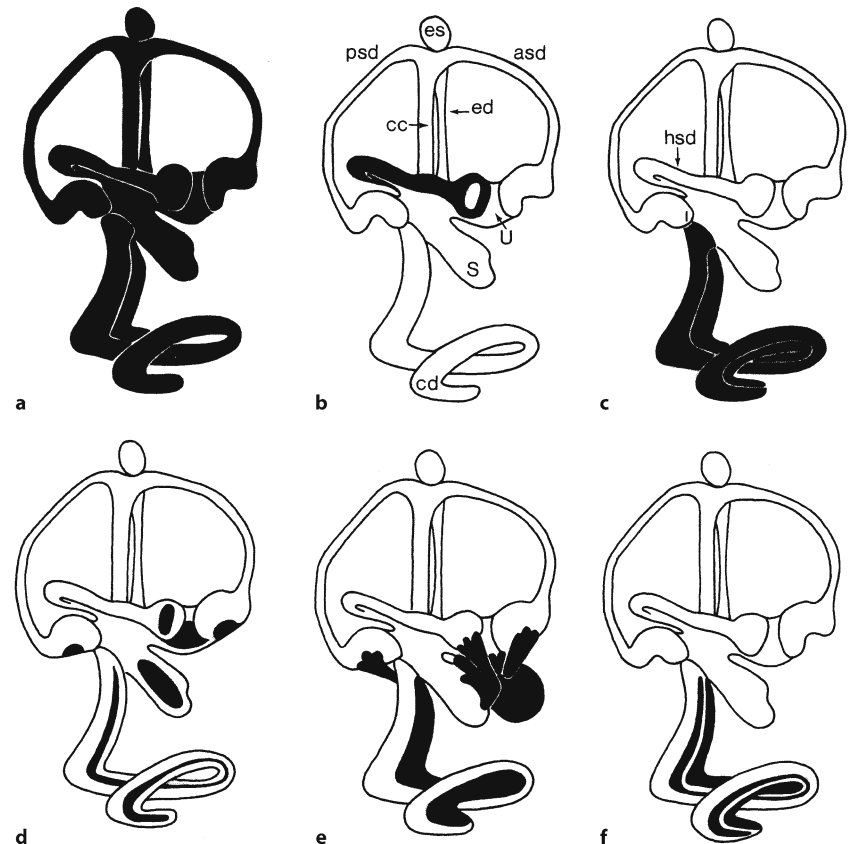
factor (BDNF), and neurotrophins 3 and 4/5 (Ensfors et al. 1995; Fritzsch et al. 1997; Phippard et al. 1999). Genes involved in deafness may be subdivided into four groups (Holme and Steel 1999; Steel and Kros 2001): (1) mutations affecting inner ear development; (2) mutations affecting sensory hair cells; (3) mutations affecting melanocyte development; and (4) mutations affecting endolymph homeostasis. The biological roles of identified genes for human non-syndromic hearing loss are summarized in Table 7.3.

Table 7.3 Biological roles of identified genes from human non-syndromic hearing loss (after Friedman and Griffith 2003)

Biological role	Gene product	Gene symbol	Locus/location	Other phenotypes	Mouse model or gene symbol
Adhesion	Cadherin 23	*CDH23*	DFNB12/10q21-q22	Usher type 1D	Waltzer
Cytoskeleton	Espin	*ESPN*	DFNB36/1p36		
Enzyme	TMPRSS3	*TMPRSS3*	DFNB8, DFNB10/21q22.3		
Extracellular matrix	Cochlin	*COCH*	DFNA9/14q12-q13	Stickler type 3	*Col11a2–/–*
	α2(XI)–collagen	*COL11A2*	DFNA13/7q22.1		
	Otoancorin	*OTOA*	DFNB22/6p12.2		
	α-Tectorin	*TECTA*	DFNA8, DFNA10, DFNA12, DFNB21/11q22-q24		*Tecta–/–*
Gap junction	Connexin 26	*GJB2*	DFNB1, DFNA3/13q12	Keratodermia	*Gjb2–/–*
	Connexin 31	*GJB3*	DFNA2/1p34		*Gjb3–/–*
	Connexin 43	*GJA1*	Not available/6q21-q23.2		
Ion channel, transporter	KCNQ4	*KCNQ4*	DFNA2/1p34	Pendred syndrome	*Pds–/–*
	Pendrin	*SLC26A4*	DFNB4/7q31		
Integral membrane protein	TMC1	*TMC1*	DFNB7, DFNB11, DFNA36/9q13-q21		Beethoven, deafness
	TMIE	*TMIE*	DFNB6/3p14-p21		Spinner
Motor	Myosin IIIA	*MYO3A*	DFNB30/10p12.1		
	Myosin VI	*MYO6*	DFNA22, DFNB37/6p13		Snell's Waltzer
	Myosin VIIA	*MYO7A*	DFNB2, DFNA11/11q12.3	Usher 1B	Shaker 1
	Myosin XVA	*MYO15A*	DFNB3/17p11.2		Shaker 2
Macromolecular organizer	Harmonin	*USH1C*	DFNB18/11p15.1	Usher 1C	
Neuron/synapse	Otoferlin	*OTOF*	DFNB9/2p22-p23		
Tight junction	Claudin 14	*CLDN14*	DFNB29/21q22		
Translation	12S rRNA		Mitochondrial gene		
	tRNA-Ser (UNC)		Mitochondrial gene	Myoclonic epilepsy, ataxia	
Transcription regulator	EYA4	*EYA4*	DFNA10/6q22-q23		
	POU3F4	*POU3F4*	DFN3/Xq21.1		*Pou3f4–/–*
	POU4F3	*POU4F3*	DFNA15/5q31		*Brn3c–/–*
Unknown	μ-crystallin	*CRYM*	Not available/16p13.11–p12.3		
	Stereocilin	*STRC*	DFNB16/15q21–q22		
	Wolframin	*WFS1*	DFNA6, DFNA14, DFNA38/4p16	Wolfram syndrome	
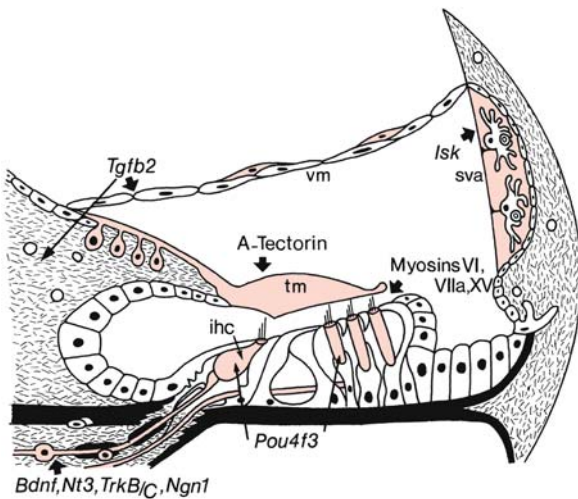
Fig. 7.26 Mutations that alter cell types or tissues in the mammalian cochlea. Structures that develop abnormally when the genes or proteins indicated are mutant or absent are depicted in *red*. *ihc* internal hair cell, *sva* stria vascularis, *tm* tectorial membrane, *vm* vestibular membrane. (After Fekete 1999)

Mutations Affecting Inner Ear Development

In mice, several genes have been identified that are expressed in the otic epithelium and are required for its patterning (Figs. 7.24, 7.25). Human homologues of these genes have not yet been associated with deafness. Two human deafness genes are expressed in the otic epithelium, and may be involved in its patterning. *SALL1* and *EYA1* encode transcription factors, mutations of which lead to Townes–Brocks (Kohlhase et al. 1998) and branchio-oto-renal (BOR; Abdelhak et al. 1997) syndromes, respectively. Total loss of expression of *Eya1* leads to one of the most severe inner ear phenotypes, since the otocyst fails to undergo all structural specializations, including formation of the otic ganglion (Kalatzis et al. 1998; Xu et al. 1999). In patients with **branchio-oto-renal syndrome** (**BOR**), the cochlea and semicircular canals are either undeveloped or completely absent (Clinical Case 7.4). BOR is an autosomal dominant disorder that in its full expression consists of preauricular pits, deformed auricles, lateral branchial (cervical) sinuses, cysts or fistulae, renal malformations and hearing loss that can be conductive, sensorineural or mixed (Gimsing and Dyrmose 1986; Kemperman et al. 2001, 2002a, b; Ceruti et al. 2002). These cardinal signs may be accompanied by stenosis of the lacrimal ducts, facial palsy and vestibular abnormalities (Fitch et al. 1976). Mondini anomalies have been described, as well as fixation of the ossicles (Fitch et al. 1976; Schuknecht 1993).

Mutations Affecting Sensory Hair Cells

An ever-increasing number of early markers of hair cell differentiation have been identified, including structural markers such as myosins VIIa and VI (Xiang et al. 1998) and calcium-binding proteins (Zheng and Gao 1997; Xiang et al. 1998). Within the inner ear, sensory regions express *Math1*, a homologue of the Drosophila gene *atonal*. *Math1–/–* mutants do not produce hair cells (Bermingham et al. 1999). Overexpression of *Math1* induces robust production of extra hair cells in postnatal rat inner ears (Zheng and Gao 2000). Mutations in at least three unconventional myosins lead to deafness in mice and/or man. Mutations in *Myo7a/MYO7A* result in deafness in *shaker 1* mice and in Usher syndrome type 1B (Gibson et al. 1995; Weil et al. 1995; Self et al. 1998), mutations in *Myo6* produce deafness in *Snell's waltzer* mice (Avraham et al. 1995), whereas mutations in *Myo15/MYO15* lead to deafness in *shaker 2*

mice and in DFNB3 (one of the at least 40 non-syndromic autosomal dominant forms of sensorineural hearing loss) patients (Probst et al. 1998; Wang et al. 1998; Pennings 2004). *Pou4f3/POU4F3* is required for the maturation and maintenance of hair cells (Erkman et al. 1996; Xiang et al. 1997). Mutations in *POU4F3* lead to DFNA15, one of the at least 50 non-syndromic autosomal recessive forms of sensorineural impairment (Toriello et al. 2004).

In 1914, the British ophthalmologist Usher (1914) described familial retinal pigment disorders associated with hearing impairment. However, as long ago as1858, Albrecht von Graefe (1958) briefly mentioned the association between deafness and retinitis pigmentosa, for which he credited his cousin, also an ophthalmologist, Alfred von Graefe. Liebreich (1861) systematically examined the deaf population of Berlin. He was struck by the high frequency of retinitis pigmentosa among deaf Jewish families. **Usher syndrome** is an autosomal recessive form of sensorineural hearing impairment with retinitis pigmentosa. Three different types may be defined based on their clinical presentation (Kimberling and Möller 1995; Keats and Corey 1999; Petit et al. 2001a, b; Kimberling 2004). In Usher type I, hearing loss is profound, vestibular function extinct and retinitis pigmentosa starts before puberty. Patients with Usher type II have a moderate, stable or slowly progressive hearing loss which may result in severe hearing impairment. Vestibular function is intact and retinitis pigmentosa is generally diagnosed around puberty. Usher type III is rare, mainly diagnosed in Finland, and characterized by mild hearing loss which is progressive over the years. Vestibular function varies and retinitis pigmentosa occurs around the same time as in Usher type II. The histopathology of the temporal bone of Usher patients was studied repeatedly since the first studies by Siebenmann and Bing (1907) and Nager (1927). Cremers and Delleman (1988) described the temporal bone pathology of a presumably Usher type II patient (Fig. 7.29), and van Aarem et al. (1995) and Wagenaar et al. (2000) described that in Usher type I patients. Temporal bone pathology of two Usher type I patients was described by Wagenaar et al. (2000; Clinical Case 7.5). The cochlear nuclei of these two patients were studied by Wagenaar et al. (1999). Only minor degenerative changes were apparent in the cochlear nuclei of Usher type I patients, who were deprived of acoustic stimuli since birth.

Clinical Case 7.4
Branchio-oto-renal Syndrome

The **branchio-oto-renal** (**BOR**) **syndrome** is an autosomal dominant inherited syndrome, in which patients show sensorineural, mixed or conductive hearing loss, preauricular pits, branchial fistulae or cysts in the second branchial arch, structural defects of the outer, middle and inner ear, and renal anomalies ranging from mild hypoplasia to complete agenesis. Kemperman et al. (2001) reported imaging data in two BOR syndrome patients, a father and a son, who had already been followed up for a long time with repeated audiometric and caloric tests (see Case Report).

Case Report. Both patients underwent imaging studies to detect inner ear anomalies. Over the previous 23 years, longitudinal audiometric analysis of the hearing threshold data and caloric tests had been performed. The father, a 55-year-old man, was seen for the first time in 1976 at the age of 33 years, because of bilateral discharging cervical fistulae and preauricular sinuses. On examination, bilateral cervical fistulae and preauricular sinuses (Fig. 7.27a) were seen. Examination of the tympanic membranes showed no anatomical abnormalities. A previous intravenous pyelogram revealed a renal malformation. Bilateral mixed hearing loss of 90 dB was present. Caloric tests, performed at ages 32 and 44 years, demonstrated vestibular areflexia on the left side. The

bilateral cervical fistulae were removed surgically, as well as the preauricular fistula, which communicated with the tympanic cavity. CT examination of the temporal bones showed a wide, plump internal acoustic canal and a hypoplastic cochlea on both sides (Fig. 7.28a). The left vestibule appeared to be hypoplastic. Increasing bilateral hearing loss from about 90 dB in 1976 to 100–105 dB in 1998 was evident in the follow-up period.

The 30-year-old son was first examined at the age of 7 years. He was found to have a 50–80-dB mixed hearing loss. Physical examination revealed bilateral cervical fistulae as well as preauricular sinuses (Fig. 7.27 b, c). There were no preauricular tags but his auricles were slightly cup-shaped. Otoscopy showed no abnormalities. In 1976, temporal bone tomography showed scarcely pneumatized mastoids, an abnormal configuration of the ossicular chain and a Mondini-type cochlear dysplasia. Renal malformations were demonstrated on a previously made intravenous pyelogram. The cervical fistulae were excised. Exploratory tympanotomy of the right ear revealed a dysplastic, plump long process of the incus and incomplete stapedial crurae. The patient suffered from recurrent otitis media and external otitis. CT examination of the temporal bones (Fig. 7.28 b) showed a widened internal meatus on both sides, widened vestibular aqueducts and hypoplastic cochleae. Caloric tests, performed at ages 10 and 16 years, revealed hyporeflexia on the left side. The audiometric follow-up over 23 years demonstrated clear progres-
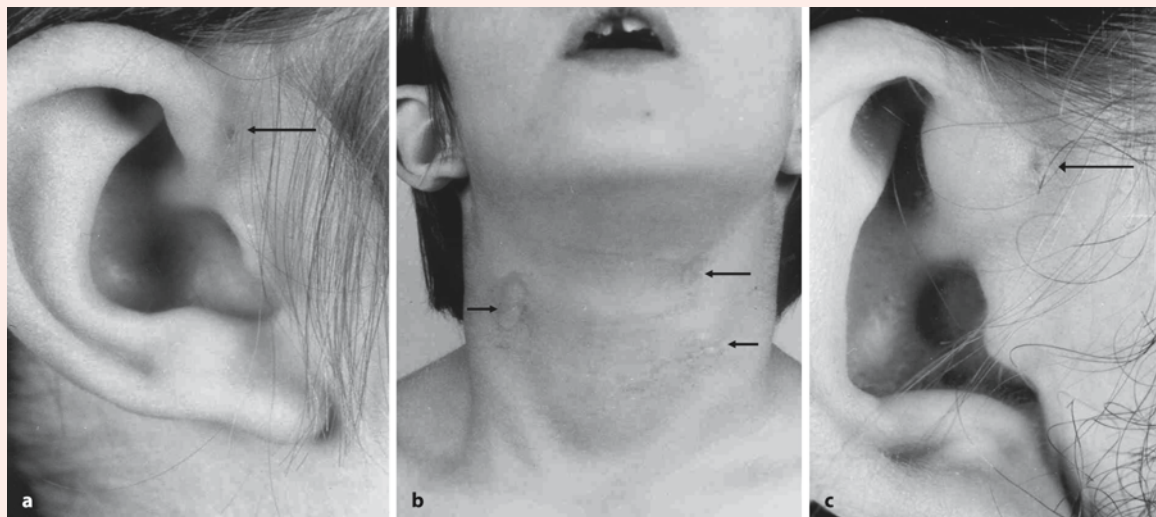
Fig. 7.27 Dysmorphology found in the branchio-oto-renal syndrome: **a** slightly malformed right auricle and preauricular sinus (*arrow*) in patient A; **b** bilateral second branchial arch fistulae (*arrows*) of patient B at 7 years of age; **c** slightly malformed right auricle and preauricular sinus (*arrowhead*) in the same patient (from Kemperman et al. 2001, with permission)
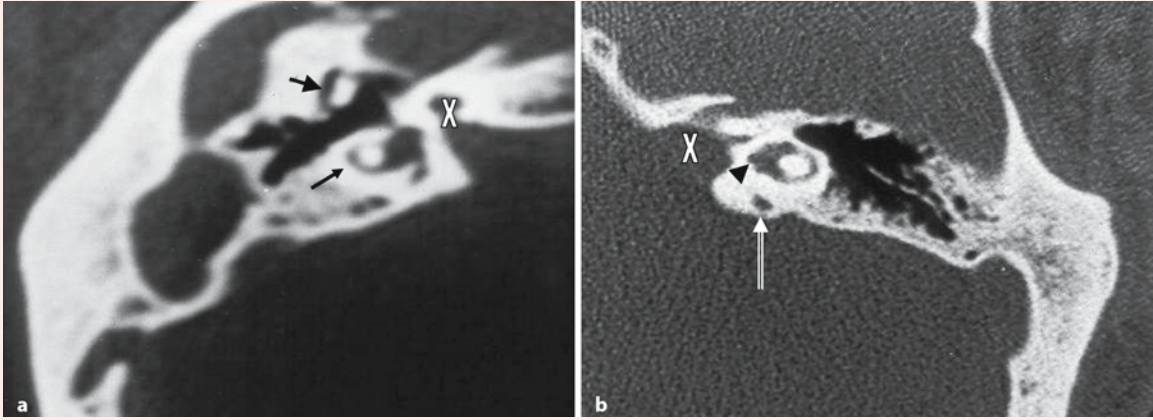
Fig. 7.28 Branchio-oto-renal syndrome: CT scans, showing a widened internal acoustic canal (*crosses*) and hypoplastic cochlea (*arrowheads*) in patients A (**a** right ear) and B (**b** left ear)

sion of hearing loss. These findings suggest a correlation between progressive, fluctuant sensorineural hearing loss with caloric hypofunction and the presence of an enlarged vestibular aqueduct in the BOR syndrome.

Reference

Kemperman MH, Stinckens C, Kumar S, Huygen PL, Joosten FB, Cremers CW (2001) Progressive fluctuant hearing loss, enlarged vestibular aqueduct, and cochlear hypoplasia in the branchio-oto-renal syndrome. Otol Neurotol 22:637–643
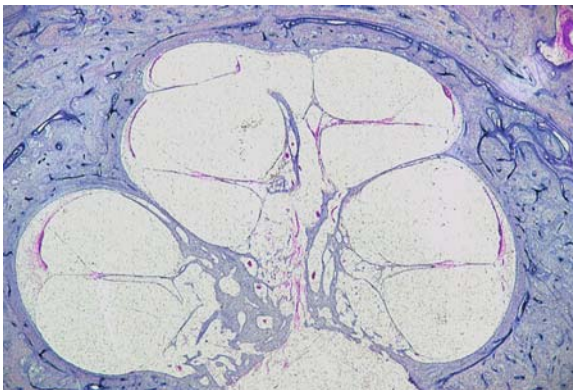
Fig. 7.29 Severely atrophic organ of Corti and severe loss of cochlear neurons of the right ear in Usher syndrome type II (from Cremers and Delleman 1988, with permission)

Mutations Affecting Melanocyte Development

The stria vascularis contains three primary cell types, marginal, basal and melanocyte-like intermediate cells (Fig. 7.20). The melanocytes are presumably of neural crest origin (Chap. 5). Mutant mice that lack melanocytes have an extremely low endocochlear potential compared with normal mice (Steel and Barkway 1989). Mutations in genes controlling melanocyte development can cause deafness. Melanocyte development is disrupted in Waardenburg syndrome. **Waardenburg syndrome** (Waardenburg 1951) forms a heterogeneous set of auditory–pigmentary syndromes, the primary cause of which is a patchy lack of melanocytes in the hair, eyes, skin and stria vasculosa. The syndrome can be classified into four subtypes (Read 2001): (1) type 1 with dystopia canthorum, caused by *PAX3* mutations (Tassabehji et al. 1992; Hoth et al. 1993); (2) the heterogeneous type 2 without dystopia, caused by changes in the *MITF* and *SLUG* genes (Tassabehji et al. 1994); (3) the rare type 3, resembling type 1 but with additional contractures or hypoplasia of the upper limb joints and muscles, also due to *PAX3* mutations (Hoth et al. 1993); and (4) the heterogeneous type 4, with Hirschsprung disease, caused by mutations in the *EDN3*, *EDNRB*, *SOX10* and other unidentified genes (Pingault et al. 1998). In *dominant megacolon* mice, *Sox10* is disrupted (Herbarth et al. 1998). Waardenburg syndrome is an example of an **auditory–pigmentary syndrome**. Related syndromes are known in many mammals and particularly in mice (see Spritz et al. 2003). The mouse mutants fall into the cochleosaccular group of Steel, which is due to the absence of melanocytes from areas of the hair, eye, skin and stria vascularis. Without melanocytes in the stria vascularis, no endocochlear potential is generated, and there is no hearing. All melanocytes except

Clinical Case 7.5
Usher Syndrome

Usher syndrome is an autosomal recessive form of sensorineural hearing impairment with retinitis pigmentosa. Wagenaar et al. (1999, 2000) studied the temporal bones and the cochlear nuclei of two Usher patients who were clinically diagnosed as Usher type I (see Case Report).

Case Report. The first patient, an 82-year-old woman, had four siblings who were also born deaf and were visually impaired at an early age. The patient attended a school for the deaf until the age of 16. She was legally blind at 35 years of age. Ophthalmoscopic examination in 1945 showed tapetoretinal degeneration, typical for Usher syndrome. Hearing thresholds could not be measured during audiometry. In 1979, the patient was admitted to the newly opened Centre for the Deaf and Blind 'Kalorama' in Beek-Ubbergen near Nijmegen, where she died in 1994 because of urosepsis and respiratory failure. The second patient, a 64-year-old man, had one sister with Usher syndrome type I. Both were said to be born deaf and attended an institute for the deaf. Tapetoretinal degeneration was confirmed by ophthalmological examination and the patient was legally blind at the age of 50 years. The first audiometric examination in 1979 showed no detectable hearing thresholds. The patient lived at 'Kalorama' from 1979 until he died in 1994 after a cerebrovascular accident. Neuropathological examination revealed recent ischemic damage in the domain of the left middle cerebral artery.

The temporal bones of both Usher type I patients were examined using light microscopy. In both patients, histopathological examination of the cochlea showed degeneration of the organ of Corti that was marked in the basal turn, atrophy of the stria vascularis and a decrease of spiral ganglion cells (Fig. 7.30). The cochlear nerves appeared diminished in number of fibres. The sensory epithelium of the saccular and utricular maculae of the female patient was normal for her age. The left temporal bone of the second patient (genotyped as *USH1D* or *USH1F*) demonstrated the typical picture of severe cochleosaccular degeneration. Only minor degenerative changes were apparent in the cochlear nuclei of these patients who were deprived of acoustic stimuli since birth. Morphometric analysis suggested a decrease in the mean cell diameter of the ventral cochlear nucleus.
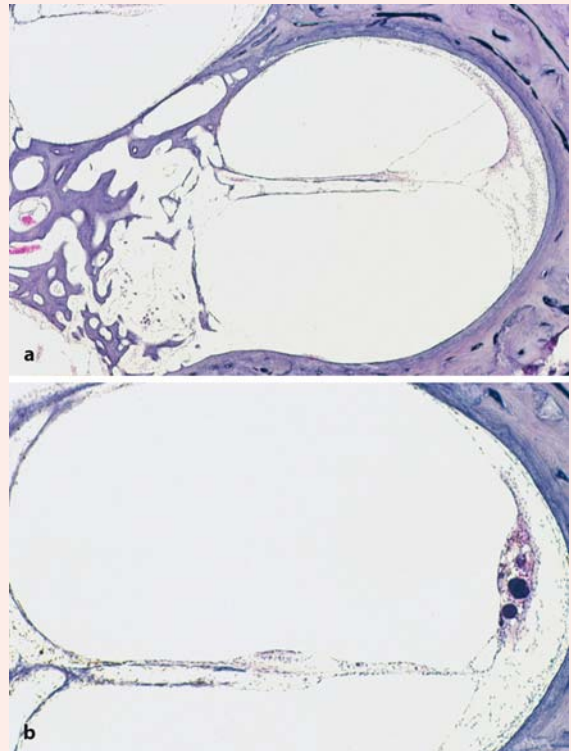
Fig. 7.30 The left cochleae of two patients with Usher syndrome type I: **a** severe degeneration of the organ of Corti and atrophy of the stria vasularis (patient A); **b** severely degenerated organ of Corti and severe disorganization of the stria vascularis (patient B) (from Wagenaar et al. 2000, with permission)

References

Wagenaar M, Draaijer P, Meek H, ten Donkelaar HJ, Wesseling P, Kimberling W, Cremers C (1999) The cochlear nuclei in two patients with Usher syndrome type I. Int J Ped Otorhinolaryngol 50:185–195

Wagenaar M, Schuknecht H, Nadol J, Benraad-van Rens MJL, Kimberling WJ, Cremers CWRJ (2000) Histopathology of the temporal bone in Usher syndrome type I. Arch Otolaryngol Head Neck Surg 126:1018–1023

those of the retinal pigment epithelium derive from the neural crest (Chap. 5). Waardenburg types 1, 3 and 4 are neurocristopathies, affecting more than one neural crest derivative (Chap. 5). Type 2 appears to be melanocyte-specific (Read 2001).

Fisch (1959) studied the temporal bones of a profoundly deaf 3-year-old girl with partial heterochromia iridis and typical eyelid deformities. On microscopic examination, atrophy of the organs of Corti, striae vasculares and cochlear ganglionic neurons was found, but no apparent abnormalities of the vestibular sense organs. Rarey and Davis (1984) studied the temporal bones of a case of Waardenburg type 4 with Hirschsprung disease. They found atrophy of the organs of Corti, striae vasculares, and vestibular organs and nerves. In another Waardenburg type 4 case, Nakashima et al. (1984) found in a 3-year-old girl bilateral cochleosaccular degeneration and absence of pigment in the inner ears. Schuknecht (1993) presented a Waardenburg mutation de novo in a male neonate of 3 days of age, born at the 34th week of gestation.

Mutations Affecting Endolymph Homeostasis

A steadily increasing number of mutations affecting endolymph homeostasis have been found to result in hearing loss (Steel and Kros 2001; Friedman and Griffith 2003). Four genes encoding gap junction proteins, that are involved in endolymph homeostasis, have been identified: *GJA1*, *GJB2*, *GJB3* and *GJB6* (Table 7.3). Gap junction proteins form intercellular channels that enable the passage of small ions and metabolites (Steel and Kros 2001). Mutations in these gap junctions cause dominant and recessive non-syndromic hearing loss, but may also cause syndromic hearing loss. Mutations in the *GJB2* gene, encoding connexin 26, seem to account for recessive non-syndromic hearing loss in almost 50% of all patients in southern Europe (Bitner-Glindzicz 2002; Wangemann 2002), against 10–20% in northern Europe (Kemperman et al. 2002c). Potassium channels are also involved in ion homeostasis of the inner ear. Mutations in the *KCNQ1*, *KCNQ4* and *KCNE1* genes, encoding potassium channel proteins, result in hearing loss. *KCNQ4* mutations lead to a progressive type of high-frequency hearing loss, classified as DFNA2 (Pennings et al. 2003). *KCNQ1* and *KCNE1* are involved in the Jervill and Lange-Nielsen syndrome, a rare autosomal recessive disorder, characterized by congenital deafness and heart conduction defects (Tyson et al. 1997). Recessive mutations in the *SLC26A4* gene cause DFNB4 and Pendred syndrome (Campbell et al. 2001). Pendred syndrome is characterized by hearing loss and goiter. On CT and MRI scans, these patients show enlarged vestibular aqueducts, endolymphatic sacs and endolymphatic ducts.

Pendrin is a transmembrane protein that functions as a sodium-independent cotransporter of chloride and anions (Scott et al. 1999). Mutations in two genes, *ATP6B1* and *BSND*, lead to disorders of inner ear homeostasis in combination with renal disorders (Karet et al. 1999; Birkenhäger et al. 2001).

References

Abdelhak S, Kalatzis V, Heilig R, Compain S, Samson D, Vincent C, Weil D, Cruaud C, Sahly I, Leibovici M, et al. (1997) A human homologue of the *Drosophila eyes absent* gene underlies branchio-oto-renal (BOR) syndrome and identifies a novel gene family. Nat Genet 15:157–164

Acampora D, Gulisano M, Broccoli V, Simeone A (2001) *Otx* genes in brain morphogenesis. Prog Neurobiol 64:69–95

Aicardi J (1998) Diseases of the Nervous System in Childhood, 2nd ed. Mac Keith, London

Alexander G (1904) Zur Pathologie und pathologischen Anatomie der kongenitalen Taubheit. Arch Ohr-Nase- Kehlkopfheilkd 61:183–219

Alexandre P, Wassef M (2003) The isthmic organizer links antero-posterior and dorsoventral patterning in the mid/hindbrain by generating roof plate structures. Development 130:5331–5338

Allanson J (2004) Genetic hearing loss associated with external ear anomalies. In: Toriello HV, Reardon W, Gorlin RJ (eds) Hereditary Hearing Loss and Its Syndromes, 2nd ed. Oxford University Press, Oxford, pp 83–125

Altman J, Bayer SA (1982) Development of the cranial nerve ganglia and related nuclei in the rat. Adv Anat Embryol Cell Biol 74:1–90

Altmann F (1951) Malformations of the auricle and the external auditory meatus. Arch Otolaryngol 54:115–139

Anson BJ, Davies J (1980) Embryology of the ear: Developmental anatomy of the ear. In: Paparella MM, Shumrick DA, Meyerhoff WL, Seid AB (eds) Otolaryngology, 2nd ed. Saunders, Philadelphia, PA, pp 3–25

Anson BJ, Bast TH, Cauldwell EW (1948) The development of the auditory ossicles, the otic capsule and the extracapsular tissues. Ann Otol Rhinol Laryngol 57:603–632

Anson BJ, Hanson JS, Richany SF (1960) Early embryology of the auditory ossicles and associated structures in relation to certain anomalies observed clinically. Ann Otol Rhinol Laryngol 69:427–447

Ashwell KW, Watson CR (1983) The development of facial motoneurones in the mouse – neuronal death and the innervation of the facial muscles. J Embryol Exp Morphol 77:117–141

Auclair F, Valdes N, Marchand R (1996) Rhombomere-specific origin of the branchial and visceral motoneurons of the facial nerve in the rat embryo. J Comp Neurol 369:451–461

Avraham KB, Hasson T, Steel KP, Kingsley DM, Russell LB, Mooseker MS, Copeland NG, Jenkins NA (1995) The mouse Snell's waltzer deafness gene encodes an unconventional myosin required for structural integrity of inner hair cells. Nat Genet 11:369–375

Baker CV, Bronner-Fraser M (2001) Vertebrate cranial placodes. I. Embryonic induction. Dev Biol 232:1–61

Barrow JR, Stadler HS, Capecchi MR (2000) Roles of *Hoxa1* and *Hoxa2* in patterning the early hindbrain of the mouse. Development 127:933–944

Baxter A (1971) Dehiscence of the Fallopian canal. J Laryngol Otol 85:587–594

Bayer SA, Altman J, Russo RJ, Zhang X (1995) Embryology. In: Duckett S (ed) Pediatric Neuropathology. Williams & Wilkins, Baltimore, MD, pp 54–107

Beck C (1970) Duplication of the external auditory ear. HNO 18:307–308

Bermingham NA, Hassan BA, Price SD, Vollrath MA, Ben-Arie N, Eatock RA, Beller HJ, Lysakowski A, Zoghbi HY (1999) Math1: An essential gene for the generation of inner ear hair cells. Science 284:1837–1841

Birkenhäger R, Otto E, Schürmann MJ, Vollmer M, Ruf E-M, Maier-Lutz I, Beckmann F, Fekete A, Omran H, Feldmann D, et al. (2001) Mutation of BSND causes Bartter syndrome with sensorineural deafness and kidney failure. Nat Genet 29:310–314

Birnholtz JC, Benacerraf BR (1983) The development of fetal hearing. Science 222:516–518

Bitner-Glindzicz M (2002) Hereditary deafness and phenotyping in humans. Br Med Bull 63:73–94

Bordley JE (1973) The effect of viral infection on hearing. A state-of-the-art report with special emphasis on congenital rubella. Arch Otolaryngol 98:217

Bouwes Bavinck JN, Weaver DD (1986) Subclavian artery supply disruption sequence: Hypothesis of a vascular etiology of Poland, Klippel-Feil, and Möbius anomalies. Am J Med Genet 23:903–918

Briscoe J, Sussel L, Serup P, Hartigan-O'Connor D, Jessell TM, Rubinstein JLR, Ericson J (1999) Homeobox gene Nkx2.2 and specification of neuronal identity by graded Sonic hedgehog signalling. Nature 398:622–627

Brookhouser PE, Bordley JE (1973) Congenital rubella deafness. Pathology and pathogenesis. Arch Otolaryngol 98:252–257

Brunet J-F, Pattyn A (2002) Phox2 genes – from patterning to connectivity. Curr Opin Genet Dev 12:435–440

Büttner-Ennever JA, Akert K (1981) Medial rectus subgroups of the oculomotor nucleus and their abducens internuclear input in monkey. J Comp Neurol 197:17–27

Büttner-Ennever JA, Horn AKE (2004) Reticular formation: Eye movements, gaze and blink. In: Paxinos G, Mai JK (eds) The Human Nervous System, 2nd ed. Elsevier, Amsterdam, pp 479–510

Campbell C, Cucci RA, Prasad S, Green GE, Edeal JB, Galer CE, Karniski LP, Sheffield VC, Smith RJH (2001) Pendred syndrome, DFNB4, and PDS/SLC26A4 identification of eight novel mutations and possible genotype-phenotype correlations. Hum Mutat 17:403–411

Carpenter EM, Goddard JM, Chisaka O, Manley NR, Capecchi MR (1993) Loss of Hox-A1 (Hox-1.6) function results in the reorganization of the murine hindbrain. Development 118:1063–1075

Ceruti S, Stinckens C, Cremers C, Casselman JW (2002) Temporal bone anomalies in the branchio-oto-renal syndrome: Detailed computer tomographic and magnetic resonance imaging findings. Otol Neurootol 23:200–207

Chi CL, Martinez S, Wurst W, Martin GR (2003) The isthmic organizer signal FGF8 is required for cell survival in the prospective midbrain and cerebellum. Development 130:2633–2644

Cordes SP (2001) Molecular genetics of cranial nerve development in mouse. Nat Rev Neurosci 2:611–623

Counter SA (2002) Fetal and neonatal development of the auditory system. In: Lagercrantz H, Hanson M, Evrard P, Rodeck C (eds) The Newborn Brain. Neuroscience and clinical applications. Cambridge University Press, Cambridge, pp 226–251

Cremers CWRJ, Delleman WJW (1988) Usher's syndrome, temporal lobe pathology. Int J Pediatr Otolaryngol 16:23–30

Cremers CWRJ, Teunissen E (1991) A classification of minor congenital ear anomalies and short- and long-term results of surgery in 104 ears. In: Charachon R, Garcia-Ibanes E (eds) Long-term Results and Indications in Otology and Otoneuro-surgery. Kugler, Amsterdam, pp 11–12

Cruysberg JRM, Huygen PLM (1990) Congenital monocular adduction palsy with synergistic divergence diagnosed in a young infant. Neuro-ophthalmol 10:253–256

Cruysberg JRM, Mtanda AT, Duinkerke-Eerola KU, Stoelinga GBA (1986) Bilateral Duane's retraction syndrome associated with congenital panhypopituitarism. Neuro-ophthalmol 6:165–168

Cruysberg JRM, Mtanda AT, Duinkerke-Eerola KU, Huygen PLM (1989) Congenital adduction palsy and synergistic divergence; a clinical and electro-oculographic study. Br J Ophthalmol 73:68–75

Cruysberg JRM, Draaijer RW, Pinckers A, Brunner HG (1998) Congenital corneal anesthesia in children with the VACTERL association. Am J Ophthalmol 125:96–98

Deol MS (1964) The abnormalities of the inner ear in Kreisler mice. J Embryol Exp Morphol 12:475–490

deSa DJ (1997) The ear. In: Gilbert-Barness E (ed) Potter's Pathology of the Fetus and Infant. Mosby, St. Louis, MI, pp 1522–1540

Dietzel K (1961) Über die Dehiszenzen des Facialiskanals. Z Laryngol Rhinol Otol 40:366–376

Doherty E, Macy M, Wang S, Dykeman C, Melanson M, Engle E (1999) CFEOM3: A new extraocular congenital fibrosis syndrome that maps to 16q24.2-q24.3. Invest Ophthalmol Vis Sci 40:1687–1694

Duane A (1905) Congenital deficiency of abduction associated with impairment of abduction, retraction movements, contractions of the palpebral fissure and oblique movements of the eye. Arch Ophthalmol 34:133–159

Engle EC (2002) Applications of molecular genetics to the understanding of congenital ocular motility disorders. Ann NY Acad Sci 956:55–63

Engle EC, Leigh RJ (2002) Genes, brainstem development, and eye movements. Neurology 59:304–305

Engle EC, Castro AE, Macy ME, Knoll JHM, Beggs AH (1997) A gene for isolated congenital ptosis maps to a 3cM region within 1p32-p34.1. Am J Hum Genet 60:1150–1157

Ensfors P, Vandewater T, Loring J, Jaenisch R (1995) Complementary roles of BDNF and NT-3 in vestibular and auditory development. Neuron 14:1153–1164

Erickson SL, O'Shea KS, Ghaboosi N, Loterro L, Frantz G, Bauer M, Liu LH, Moore MW (1997) ErbB3 is required for normal cerebellar and cardiac development: A comparison with ErbB2- and neuregulin-deficient mice. Development 124:4999–5011

Erkman L, McEvilly RJ, Luo L, Ryan AK, Hooshmand F, O'Connell SM, Keithley EM, Rapaport DH, Ryan AF, Rosenfeld MG (1996) Role of transcription factors Brn-3.1 and Brn-3.2 in auditory and visual system development. Nature 381:603–606

Fekete DM (1999) Development of the vertebrate ear: Insights from knockouts and mutants. Trends Neurosci 22:263–269

Filiano JJ, Kinney HC (1992) Arcuate nucleus hypoplasia in the sudden infant death syndrome. J Neuropathol Exp Neurol 51:394–405

Filiano JJ, Kinney HC (1994) A perspective on neuropathological findings in victims of the sudden infant death syndrome: The triple-risk model. Biol Neonate 65:194–197

Filiano JJ, Choi JC, Kinney HC (1990) Candidate cell populations for respiratory chemosensitive fields in the human infant medulla. J Comp Neurol 293:448–465

Fisch L (1959) Deafness as part of an hereditary syndrome. J Laryngol Otol 73:355–382

Fitch N, Lindsay JR, Srolovitz H (1976) The temporal bone in the preauricular pit, cervical fistula, hearing loss syndrome. Ann Otol Rhinol Laryngol 85:268–275

Flock Å (1980) Contractile proteins in hair cells. Hearing Res 2:411–412

Fode C, Gradwohl G, Morin X, Dierich A, LeMeur M, Goridis C, Guillemot F (1998) The bHLH protein NEUROGENIN 2 is determination factor for epibranchial placode-derived sensory neurons. Neuron 20:483–494

Folgering H, Kuyper F, Kille JF (1979) Primary alveolar hypoventilation (Ondine's curse syndrome) in an infant without external arcuate nucleus: Case report. Bull Eur Physiopathol Respir 15:659–665

Fowler EP (1961) Variations in the temporal bone course of the facial nerve. Laryngoscope 71:937–946

Franz H (1959) Über Gehörorgansduplikaturen. Z Laryngol Rhinol 38:16–22

Friedman TB, Griffith AJ (2003) Human nonsyndromic sensorineural deafness. Annu Rev Genomics Hum Genet 4:341–402

Friedmann I, Arnold W (1993) Pathology of the Ear. Churchill Livingstone, Edinburgh

Fritzsch B, Silos-Santiago I, Bianchi LM, Farinas I (1997) The role of neurotrophic factors in regulating the development of inner ear development. Trends Neurosci 20:159–164

Gasser RF (1967) The development of the facial nerve in man. Ann Otol Rhinol Laryngol 76:37–56

Gasser RF, May M (2000) Embryonic development. In: May M, Schaitkin BM (eds) The Facial Nerve, May's 2nd ed. Thieme, New York, pp 1–17

Gavalas A, Studer M, Lumsden A, Rijli FM, Krumlauf R, Chambon P (1998) Hoxa1 and Hoxb1 synergize in patterning the hindbrain, cranial nerves and second pharyngeal arch. Development 125:1123–1136

Gavalas A, Ruhrberg C, Livet J, Henderson CE, Krumlauf R (2003) Neuronal defects in the hindbrain of Hoxa1, Hoxb1 and Hoxb2 mutants reflect regulatory interactions among these Hox genes. Development 130:5663–5679

Gerhardt HJ, Otto HD (1970) Steigbügelmissbildungen. Acta Otolaryngol (Stockholm) 70:35–44

Gibson F, Walsh J, Mburu P, Varela A, Brown KA, Antonio M, Beisel KW, Steel KP, Brown SD (1995) A type VII myosin encoded by the mouse deafness gene shaker-1. Nature 374:62–64

Gimsing S, Dyrmose J (1986) Branchio-oto-renal dysplasia in three families. Ann Otol Rhinol Laryngol 95:421–426

Goddard JM, Rossel M, Manley NR, Capecchi MR (1996) Mice with targeted disruption of Hoxb-1 fail to form the motor nucleus of the VIIth nerve. Development 122:3217–3228

Gorlin RJ, Cohen MM Jr, Levin LS (1990) Syndromes of the Head and Neck, 3rd ed. Oxford University Press, New York, pp 666–671

Gorlin RJ, Cohen MM Jr, Hennekam RCM, eds (2001) Syndromes of the Head and Neck, 4th ed. Oxford University Press, Oxford

Govaerts PJ, Cremers CWRJ, Marquet TF, Offeciers FE (1993) The persistent stapedial artery: Does it prevent successful surgery? Ann Otol Rhinol Laryngol 102:724–728

Griffith AJ, Friedman TB (2002) Autosomal and X-linked auditory disorders. In: Keats BJB, Popper AN, Fay RR (eds) Handbook of Auditory Research, Vol 14: Genetics and Auditory Disorders. Springer, Berlin Heidelberg New York, pp 121–227

Groves AK, Bronner-Fraser M (2000) Competence, specification and commitment in otic placode induction. Development 127:3489–3499

Guthrie S (1996) Patterning the hindbrain. Curr Opin Neurobiol 6:41–48

Gutowski NJ, Bosley TM, Engle E (2003) Workshop Report 110th ENMC International Workshop: The congenital cranial dysinnervation disorders (CCDDs). Neuromusc Disord 13:573–578

Hamilton WJ, Mossman HW (1972) Hamilton, Boyd and Mossman's Human Embryology. Prenatal development of form and function, 4th ed. Heffer, Cambridge

Hanson JR, Anson BJ, Strickland EM (1962) Branchial sources of the auditory ossicles in man. Arch Otolaryngol 76:100–122, and 200–215

Hardy JB (1973) Fetal consequences of maternal viral infections in pregnancy. Arch Otolaryngol 98:218–227

Herbarth B, Pingault V, Bondurand N, Kuhlbrodt K, Hermans-Borgmeyer I, Puliti A, Lemort N, Goossens M, Wegner M (1998) Mutation of the Sry-related Sox10 gene in Dominant megacolon, a mouse model for human Hirschsprung disease. Proc Natl Acad Sci USA 95:5161–5165

Hinrichsen KV (1990) Peripheres Nervensystem. In: Hinrichsen KV (Hrsg) Humanembryologie. Springer Verlag, Berlin Heidelberg New York, pp 449–475

His W Jr (1889) Zur Entwicklungsgeschichte des Acustico-Facialisgebietes beim Menschen. Arch Anat Physiol Anat Abt Suppl:1–28

Hochstetter F (1948) Entwicklungsgeschichte der Ohrmuschel und des äusseren Gehörganges des Menschen. Denkschr Akad Wiss Wien Math-Naturwiss Kl 108:1–50

Holme RH, Steel KP (1999) Genes involved in deafness. Curr Opin Genet Dev 9:309–314

Holzschuh J, Hauptmann G, Driever W (2003) Genetic analysis of the roles of Hh, FGF8, and nodal signaling during catecholaminergic system development in the zebrafish brain. J Neurosci 23:5507–5519

Hotchkiss MG, Miller NR, Clark AW, Green WR (1980) Bilateral Duane's retraction syndrome: A clinico-pathologic case report. Arch Ophthalmol 98:870–874

Hoth CF, Milunsky A, Lipsky N, Sheffer R, Clarren SK, Baldwin CT (1993) Mutations in the paired domain of the human PAX3 gene cause Klein-Waardenburg syndrome (WS-III) as well as Waardenburg syndrome type I (WS-I). Am J Hum Genet 53:455–462

House HP, Patterson ME (1964) Persistent stapedial artery: Report of two cases. Trans Am Acad Ophthalmol Otolaryngol 68:644–646

Igarashi Y, Ishii T (1980) Embryonic development of the human organ of Corti: Electron microscopic study. Int J Paediatr Otorhinolaryngol 2:51–62

Irving C, Mason I (2000) Signalling by FGF8 from the isthmus patterns anterior hindbrain and establishes the anterior limit of Hox gene expression. Development 127:177–188

Jacob J, Guthrie S (2000) Facial visceral motor neurons display specific rhombomere origin and axon pathfinding behavior in the chick. J Neurosci 20:7664–7671

Jacobs MJ (1970) The development of the human motor trigeminal complex and accessory facial nucleus and their topographic relations with the facial and abducens nuclei. J Comp Neurol 138:161–194

Jen J, Coulin C, Bosley TM, Salih MAM, Sabatti C, Nelson SF, Baloh RW (2002) Familial horizontal gaze with progressive scoliosis (HGPS) maps to chromosome 11q23-25. Neurology 59:432–435

Johansson B, Wedenberg E, Weston B (1964) Measurement of tone response by the human fetus. Acta Otolaryngol 57:188–192

Joyner AL (1996) Engrailed, Wnt and Pax genes regulate midbrain-hindbrain development. Trends Genet 12:15–20

Joyner AL (2002) Establishment of anterior-posterior and dorsal-ventral pattern in the early central nervous system. In: Rossant J, Tam PPL (eds) Mouse Development. Patterning, morphogenesis, and organogenesis. Academic, San Diego, CA, pp 107–126

Kalatzis V, Sahly I, El-Amraoui A, Petit C (1998) Eya1 expression in the developing ear and kidney: Towards the understanding of the pathogenesis of Branchio-Oto-Renal (BOR) syndrome. Dev Dyn 213:486–499

Kanagasuntheram R (1967) A note on the development of the tubotympanic recess in the human embryo. J Anat (Lond) 101:731–741

Karet FE, Finberg KE, Nelson RD, Nayir A, Mocan H, Sanjed SA, Rodriguez-Soriano J, Santos F, Cremers CWRJ, Di Pietro A, et al. (1999) Mutations in the gene encoding B1 subunit of H$^+$-ATPase cause renal tubular acidosis with sensorineural deafness. Nat Genet 21:84–90

Karmody CS, Annino DJ Jr (1995) Embryology and anomalies of the external ear. Facial Plast Surg 11:251–256

Keats BJB, Corey DP (1999) The Usher syndromes. Am J Med Genet 89:158–166

Kemperman MH, Stinckens C, Kumar S, Huygen PLM, Joosten FBM, Cremers CWRJ (2001) Progressive, fluctuant hearing loss, an enlarged vestibular aqueduct and cochlear hypoplasia in the BOR syndrome. Otol Neurotol 22:637–643

Kemperman MH, Stinckens C, Kumar S, Joosten FBM, Huygen PLM, Cremers CWRJ (2002a) The branchio-oto-renal syndrome. Adv Oto-Rhino-Laryngol 61:192–200

Kemperman MH, Koch SMP, Joosten FBM, Kumar S, Huygen PLM, Cremers CWRJ (2002b) Inner ear anomalies are frequent but non-obligatory features of the branchio-oto-renal syndrome. Arch Otolaryngol Head Neck Surg 128:1033–1038

Kemperman MH, Hoefsloot LH, Cremers CWRJ (2002c) Hearing loss and connexin 26. J R Soc Med 95:171–177

Kiernan AE, Steel KP, Fekete DM (2002) Development of the mouse inner ear. In: Rossant J, Tam PPL (eds) Mouse Development. Patterning, morphogenesis, and organogenesis. Academic, San Diego, CA, pp 539–566

Kimberling WJ (2004) Genetic hearing loss associated with eye disorders. In: Toriello HV, Reardon W, Gorlin RJ (eds) Hereditary Hearing Loss and Its Syndromes, 2nd ed. Oxford University Press, Oxford, pp 126–165

Kimberling WJ, Möller C (1995) Clinical and molecular genetics of Usher syndrome. J Am Acad Audiol 6:63–72

Kohlhase J, Wischermann A, Reichenbach H, Froster U, Engel W (1998) Mutations in the SALL1 putative transcription factor gene cause Townes-Brocks syndrome. Nat Genet 18:81–83

Kremer H, Kuyt LP, van den Helm B, van Reen M, Leunissen JAM, Hamel BC, Jansen C, Mariman ECM, Frants RR, Padberg GW (1996) Localization of a gene for Möbius syndrome to chromosome 3q by linkage analysis in a Dutch family. Hum Mol Genet 5:1367–1371

Krumlauf R (1994) Hox genes in vertebrate development. Cell 78:191–201

Kuemerle B, Zanjani H, Joyner A, Herrup K (1997) Pattern deformities and cell loss in Engrailed-2 mutant mice suggest two separate patterning events during cerebellar development. J Neurosci 17:7881–7889

Kuhlman KA, Burns KA, Depp R, Sabbagha RE (1988) Ultrasound imaging of normal fetal response to external vibratory acoustic stimulation. Am J Obstet Gynecol 158:47–51

Kumar D (1990) Moebius syndrome. J Med Genet 27:122–126

Lammens M, Moerman P, Fryns JP, Schröder JM, Spinnewyn D, Casaer P, Dom R (1998) Neuropathological findings in Moebius syndrome. Clin Genet 54:136–141

Lecanuet J-P, Schaal B (1996) Fetal sensory competencies. Eur J Obstet Gynecol 68:1–23

Lee K-F, Simon H, Chen H, Bates B, Hung M-C, Hauser C (1995) Requirement for neuregulin receptor erbB2 in neural and cardiac development. Nature 378:394–398

Leigh R, Zee D (1999) The Neurology of Eye Movements, 3rd ed. Oxford University Press, New York

Lemire RJ, Loeser JD, Leech RW, Alvord EC Jr (1975) Normal and Abnormal Development of the Human Nervous System. Harper & Row, Hagerstown, MD

Lemire RJ, Beckwith JB, Warkany J (1978) Anencephaly. Raven, New York

Lengyel D, Zaunbauer W, Keller E, Gottlob I (2000) Möbius syndrome: MRI findings in three cases. J Pediatr Ophthalmol Strabismus 37:305–308

Leong S, Ashwell KW (1997) Is there a zone of vascular vulnerability in the fetal brainstem? Neurotoxicol Teratol 19:265–275

Liebreich R (1861) Abkunft und Ehen unter Blutsverwandten als Grund von Retinitis pigmentosa. Dtsch Klin 13:53–55

Liu A, Joyner AL (2001) Early anterior/posterior patterning of the midbrain and cerebellum. Annu Rev Neurosci 24:869–896

Lumsden A (1990) The cellular basis of segmentation in the developing hindbrain. Trends Neurosci 13:329–335

Lumsden A (2004) Segmentation and compartition in the early avian hindbrain. Mech Dev 121:1081–1088

Lumsden A, Keynes R (1989) Segmental patterns of neuronal development in the chick hindbrain. Nature 337:424–428

Lumsden A, Krumlauf R (1996) Patterning the vertebrate neuraxis. Science 274:1109–1115

Ma Q, Chen ZF, Del Braco Barrantes I, De la Pompe JL, Anderson DJ (1998) neurogenin 1 is essential for the determination of neuronal precursors for proximal cranial sensory ganglia. Neuron 20:469–482

Mann IC (1927) The developing third nerve nucleus in human embryos. J Anat (Lond) 61:424–438

Marín F, Puelles L (1994) Patterning of the embryonic avian midbrain after experimental inversions: A polarizing activity from the isthmus. Dev Biol 163:19–37

Marquet JF, Declau FR, De Cock M (1988) Congenital middle ear malformations. Acta Oto-Rhino-Laryngol Belg 42:117–302

Martínez S, Wassef M, Alvarado-Mallart RM (1991) Induction of a mesencephalic phenotype in the 2-day-old chick prosencephalon is preceded by the early expression of the homeobox gene En. Neuron 6:971–981

Mastick GS, Fan C-M, Tessier-Lavigne M, Serbedzija GN, McMahon AP, Easter SS Jr (1996) Early detection of neuromeres in Wnt-1-/- mutant mice: Evaluation by morphological and molecular markers. J Comp Neurol 374:246–258

Matturi L, Biondo B, Mercurio P, Rossi L (2000) Severe hypoplasia of medullary arcuate nucleus. Quantitative analysis in sudden infant death syndrome. Acta Neuropathol (Berl) 99:371–375

Matturi L, Biondo B, Suárez-Mier MP, Rossi L (2002) Brain stem lesions in the sudden infant death syndrome: Variability in the hypoplasia of the arcuate nucleus. Acta Neuropathol (Berl) 104:12–20

May M, Schaitkin BM, eds (2000) The Facial Nerve, May's 2nd ed. Thieme, New York, Stuttgart

McKay IJ, Lewis J, Lumsden A (1997) Organization and development of facial motor neurons in the Kreisler mutant mouse. Eur J Neurosci 9:1499–1506

McMahon AP, Joyner AL, Bradley A, McMahan JA (1992) The midbrain-hindbrain phenotype of Wnt-1-/Wnt-1- mice results from stepwise deletion of engrailed-expressing cells by 9.5 days postcoitum. Cell 69:581–595

Mellinger JF, Gomez MR (1987) Agenesis of the cranial nerves. Handb Clin Neurol 50:211–223

Meyer D, Birchmeier C (1995) Multiple essential functions of neuregulin in development. Nature 378:386–390

Michel EM (1863) Mémoire sur les anomalies congénitales de l'oreille interne. Gaz Méd Strasb 3:55–58

Millen KJ, Wurst W, Herrup K, Joyner AL (1994) Abnormal embryonic cerebellar development and patterning of postnatal foliation in two mouse Engrailed-2 mutants. Development 120: 695–706

Miller NR, Kiel SM, Green WR, Clark AW (1982) Unilateral Duane's retraction syndrome (type 1). Arch Ophthalmol 100:1468–1472

Möbius PJ (1888) Über angeborene doppelseitige Abducens-Facialis-Lähmung. Münch Med Wochenschr 35:91–94

Moens CB, Prince VE (2002) Constructing the hindbrain: Insights from the zebrafish. Dev Dyn 224:1–17

Mondini C (1791) Anatomia surdi nedi sectio. De Bononiensii Scientarum et Artium Instituto Atque Academi Commentarii. Bologna, pp 419–431

Moore JK, Osen KK (1979) The cochlear nuclei in man. Am J Anat 154:393–418

Moore JK, Linthicum FH Jr (2004) Auditory system. In: Paxinos G, Mai JK (eds) The Human Nervous System, 2nd ed. Elsevier, Amsterdam, pp 1241–1279

Moore JK, Perazzo LM, Braun A (1995) Time course of axonal myelination in the human brainstem auditory pathway. Hearing Res 87:21–31

Moore JK, Guan Y-L, Shi S-R (1997) Axogenesis in the human fetal auditory system, demonstrated by neurofilament immunohistochemistry. Anat Embryol (Berl) 195:15–30

Moore JK, Simmons DD, Guan Y-L (1999) The human olivocerebellar system: Organization and development. Audiol Neurootol 4:311–325

Morin X, Cremer H, Hirsch M-R, Kapur RP, Gotidis C, Brunet J-F (1997) Defects in sensory and autonomic ganglia and absence of locus coeruleus in mice deficient for the homeobox gene *Phox2a*. Neuron 18:411–423

Müller F, O'Rahilly R (1983) The first appearance of the major divisions of the human brain at stage 9. Anat Embryol (Berl) 168:419–432

Müller F, O'Rahilly R (1990) The human rhombencephalon at the end of the embryonic period proper. Am J Anat 189:127–145

Müller M, Jabs N, Lorke DE, Fritzsch B, Sander M (2003) Nkx6.1 controls migration and axon pathfinding of cranial branchio-motoneurons. Development 130:5815–5826

Nager FR (1927) Zur Histologie der Taubstummheit bei Retinitis pigmentosa. Beitr Pathol Anat 77:288–303

Nager FR (1952) Histologische Ohruntersuchungen bei Kindern nach mütterlicher Rubella. Pract Otorhinolaryngol 14:337–359

Nager GT, Levin LS (1980) Congenital aural atresia: Embryology, pathology, classification, genetics, and surgical management. In: Paparella MM, Shumrick DA, Meyerhoff WL, Seid AB (eds) Otolaryngology, 2nd ed. Saunders, Philadelphia, PA, pp 1303–1344

Nakamura H (2001) Regionalization of the optic tectum: Combinations of gene expression that define the tectum. Trends Neurosci 24:32–39

Nakano M, Yamada K, Fain J, Sener EC, Selleck CJ, Awad AH, Zwaan J, Mullaney PB, Bossy TM, Engle EC (2001) Homozygous mutations in ARIX (PHOX2A) result in congenital fibrosis of the extraocular muscles type 2. Nat Genet 29:315–320

Nakashima S, Sando I, Takahashi H, Hashida Y (1992) Temporal bone histopathologic findings of Waardenburg's syndrome: A case report. Laryngoscope 102:563–567

Nara T, Goto N, Nakae Y, Okada A (1993) Morphometric development of the human auditory system: Ventral cochlear nucleus. Early Hum Dev 32:93–102

Nara T, Goto N, Hamano S-I, Okada A (1996) Morphometric development of the human fetal auditory system: Inferior collicular nucleus. Brain Res 18:35–39

Nieuwenhuys R (1984) Anatomy of the auditory pathways, with emphasis on the brain stem. Adv Oto-Rhino-Laryngol 34:25–38

Nieuwenhuys R, Voogd J, van Huijzen C (1988) The Human Central Nervous System, 3rd ed. Springer, Berlin Heidelberg New York

Nishikori T, Hatta T, Kawauchi H, Otani H (1999) Apoptosis during inner ear development in human and mouse embryos: An analysis by computer-assisted three-dimensional reconstruction. Anat Embryol (Berl) 200:19–26

Nishimura Y, Kumoi T (1992) The embryonic development of the human external auditory meatus. Preliminary report. Acta Otolaryngol 112:496–503

Norman MG, McGillivray BC, Kalousek DK, Hill A, Poskitt KJ (1995) Congenital Malformations of the Brain. Pathologic, embryologic, clinical, radiologoc and genetic aspects. Oxford University Press, New York

O'Rahilly R (1983) The timing and sequence of events in the development of the human eye and ear. Anat Embryol (Berl) 168:87–99

O'Rahilly R, Müller F (1999) The Embryonic Human Brain. An atlas of developmental stages, 2nd ed. Wiley-Liss, New York

O'Rahilly R, Müller F (2001) Human Embryology & Teratology, 3rd ed. Wiley-Liss, New York

Ormerod C (1960) Pathology of congenital deafness. J Laryngol Otol 74:919–950

Padget DH (1948) The development of the cranial arteries in the human embryo. Contrib Embryol Carnegie Instn 32:205–261

Pappas DG (1983) Hearing impairments and vestibular abnormalities among children with subclinical cytomegalovirus. Ann Otol Rhinol Laryngol 92:552–557

Pascual-Castroviejo I, Pascual-Pascual SI (2002) Congenital vascular malformations in childhood. Semin Pediatr Neurol 9:254–273

Pasini A, Wilkinson DG (2002) Stabilizing the regionalisation of the developing vertebrate central nervous system. BioEssays 24:4270438

Pasman JW (1997) Auditory Evoked Responses in Preterm Infants. Thesis, University of Nijmegen

Pasqualetti M, Rijli FM (2001) Homeobox gene mutations and brain-stem developmental disorders: Learning from knockout mice. Curr Opin Neurol 14:177–184

Pattyn A, Morin X, Cremer H, Goridis C, Brunet J-F (1999) The homeobox gene Phox2b is essential for development of autonomic neural crest derivatives. Nature 399:366–370

Pattyn A, Goridis C, Brunet J-F (2000a) Specification of the central noradrenergic phenotype by the homeobox gene *Phox2b*. Mol Cell Neurosci 15:235–243

Pattyn A, Hirsch M-R, Goridis C, Brunet J-F (2000b) Control of hindbrain motor neuron differentiation by the homeobox gene *Phox2b*. Development 127:1349–1358

Pattyn A, Vallstedt A, Dias JM, Sander M, Ericson J (2003) Complementary roles for Nkx6 and Nkx2 class proteins in the establishment of motoneuron identity in the hindbrain. Development 130:4149–4159

Pearson AA (1938) The spinal accessory nerve in human embryos. J Comp Neurol 68:243–266

Pearson AA (1939) The hypoglossal nerve in human embryos. J Comp Neurol 71:21–39

Pearson AA (1943) The trochlear nerve in human fetuses. J Comp Neurol 78:29–43

Pearson AA (1944) The oculomotor nucleus in the human fetus. J Comp Neurol 80:47–63

Pearson AA (1946) The development of the motor nuclei of the facial nerve in man. J Comp Neurol 85:461–476

Peck JE (1994) Development of hearing. Part II. Embryology. J Am Acad Audiol 5:359–365

Peck JE (1995) Development of hearing. Part III. Postnatal development. J Am Acad Audiol 6:113–123

Pedraza S, Gámez J, Rovira A, Zamora A, Grive E, Raguer N, Ruscolleda J (2000) MRI findings in Möbius syndrome: Correlations with clinical features. Neurology 55:1058–1060

Pennings RJE (2004) Hereditary Deaf-Blindness. Clinical and genetic aspects. Thesis, University of Nijmegen

Pennings RJE, Huygen PLM, Van Camp G, Cremers CWRJ (2003) A review of progressive phenotypes in nonsyndromic autosomal dominant hearing impairment. Audiol Med 1:47–55

Petit C, Levilliers J, Hardelin J-P (2001a) Molecular genetics of hearing loss. Annu Rev Genet 35:589–646

Petit C, Levilliers J, Marlin S, Hardelin J-P (2001b) Hereditary hearing loss. In: Scriver CR, Beaudet AL, Sly WS, Valle D (eds) The Metabolic & Molecular Bases of Inherited Disease. McGraw-Hill, New York, pp 6281–6328

Phippard D, Lu L, Lee D, Saunders JC, Crenshaw EB (1999) Targeted mutagenesis of the POU-domain gene *Brn4/Pou3f4* causes developmental defects in the inner ear. J Neurosci 19:5980–5989

Pieh C, Lengyel D, Neff A, Fretz C, Gottlob I (2002) Brain stem hypoplasia in familial congenital horizontal gaze paralysis (FCGP) and kyphoscoliosis. Neurology 59:462–463

Pingault V, Bondurand N, Kuhlbrodt K, Goerich DE, Preho MO, Puliti A, Herbarth B, Hermans-Borgmeyer I, Legius E, Matthys G, et al. (1998) SOX10 mutations in patients with Waardenburg-Hirschsprung disease. Nat Genet 18:171–173

Probst FJ, Fridell RA, Raphael Y, Saunders TL, Wang A, Liang Y, Morell RJ, Touchman JW, Lyons RH, Noben-Trauth K, et al. (1998) Correction of deafness in shaker-2 mice by an unconventional myosin in a BAC transgene. Science 280:1444–1447

Proctor B, Nager GT (1982) The facial canal: Normal anatomy, variations and anomalies. Ann Otol Rhinol Laryngol 91:33–61

Puelles L (1995) A segmental morphological paradigm for understanding vertebrate forebrains. Brain Behav Evol 46:319–337

Punal JE, Siebert MF, Angueira FB, Lorenzo AV, Castro-Gago M (2001) Three new patterns with congenital unilateral facial nerve palsy due to chromosome 22q11 deletion. J Child Neurol 16:450–452

Rarey KE, Davis LE (1984) Inner ear anomalies in Waardenburg's syndrome associated with Hirschsprung's disease. Int J Pediatr Otolaryngol 8:181–189

Read AP (2001) Waardenburg syndrome. In: Scriver CR, Beaudet AL, Sly WS, Valle D (eds) The Metabolic & Molecular Bases of Inherited Disease. McGraw-Hill, New York, pp 6097–6116

Reynolds JD, Biglan AW, Hiles DA (1984) Congenital superior oblique palsy in infants. Arch Ophthalmol 102:1503–1505

Rhinn M, Brand M (2001) The midbrain-hindbrain organizer. Curr Opin Neurobiol 11:34–42

Rosenberg ML (1984) Congenital trigeminal anesthesia, review and classification. Brain 107:1073–1082

Rossel M, Capecchi MR (1999) Mice mutant for both *Hoxa1* and *Hoxb1* show extensive remodeling of the hindbrain and defects in craniofacial development. Development 126:5027–5040

Rijli FM, Gavalas A, Chambon P (1998) Segmentation and specification in the branchial region of the head: The role of the *Hox* selector genes. Int J Dev Biol 42:393–401

Sadl VS, Sing A, Mar L, Jin F, Cordes SP (2003) Analysis of hindbrain patterning defects caused by the *kreisler^neu* mutation reveals multiple roles of *Kreisler* in hindbrain segmentation. Dev Dyn 227:134–142

Sander M, Paydar S, Ericson J, Briscoe J, Berber E, German M, Jessell TM, Rubinstein JLR (2000) Ventral neural patterning by Nkx homeobox genes: Nkx6.1 controls somatic motor neuron and ventral interneuron fates. Genes Dev 14:2134–2139

Sando I, Wood RF (1971) Congenital middle ear anomalies. Otolaryngol Clin North Am 4:291–318

Sarnat HB (2004) Watershed infarcts in the fetal and neonatal brainstem. An aetiology of central hypoventilation, dysphagia, Möbius syndrome and micrognathia. Eur J Pediatr Neurol 8:71–87

Sarnat HB, Benjamin DR, Siebert JR, Kletter GB, Cheyette SR (2002) Agenesis of the mesencephalon and metencephalon with cerebellar hypoplasia: Putative mutation in the *EN2* gene – report of two cases in early infancy. Ped Dev Pathol 5:54–62

Scheibe A (1892a) Ein Fall von Taubstummheit mit Acusticusatrophie und Bildungsanomalien in häutigen Labyrinth beiderseits. Z Ohrenheilk 22:11–24

Scheibe A (1892b) A case of deaf-mutism, with auditory atrophy and anomalies of development in the membranous labyrinth of both ears. Arch Otol 21:12–22

Schneider-Maunoury S, Seitanidou T, Charnay P, Lumsden A (1997) Segmental and neuronal architecture of the hindbrain of *Krox-20* mouse mutants. Development 124:1215–1226

Schuknecht HF (1980) Dysmorphogenesis of the inner ear. Birth Defects 16:47–71

Schuknecht HF (1993) Pathology of the Ear. Lea & Febiger, Philadelphia, PA

Schuknecht HF, Churchill JA, Doran R (1959) The localization of acetylcholinesterase in the cochlea. Arch Otolaryngol 69:549–559

Scott DA, Wang R, Kreman TM, Sheffield VC, Karniski LP (1999) The Pendred syndrome gene encodes a chloride-iodide transport protein. Nat Genet 21:440–443

Self T, Mahony M, Fleming J, Walsh J, Brown SD, Steel KP (1998) Shaker-1 mutations reveal roles for myosin VIIA in both development and function of cochlear hair cells. Development 125:557–566

Siebenmann F, Bing R (1907) Über den Labyrinth- und Hirnbefund bei einem an Retinitis pigmentosa erblindeten angeborenen Taubstummen. Z Ohrenheilkd 54:265–280

Sharma K, Sheng HZ, Lettier K, Li H, Karavanov A, Potter S, Westphal H, Pfaff SL (1998) LIM homeodomain factors Lhx3 and Lhx4 assign subtype identities for motor neurons. Cell 95:817–828

Smithells R, Sheppard S, Holzel H, Jones G (1990) Congenital rubella in Great Britain 1971-1988. Health Trends 22:73–76

Spritz RA, Chiang P-W, Oiso N, Alkhateeb A (2003) Human and mouse disorders of pigmentation. Curr Opin Genet Dev 13:284–289

St. Charles S, DiMario FJ Jr, Grunnet ML (1993) Möbius sequence: Further in vivo support for the subclavian artery supply disruption sequence. Am J Med Genet 47:289–293

Steel KP, Barkway C (1989) Another role for melanocytes: Their importance for normal stria vascularis development in the mammalian inner ear. Development 107:453–463

Steel KP, Kros CJ (2001) A genetic approach to understanding auditory function. Nat Genet 27:143–149

Steel KP, Erven A, Kiernan AE (2002) Mice as models for human hereditary deafness. In: Keats BJB, Popper AN, Fay RR (eds) Handbook of Auditory Research, Vol 14: Genetics and Auditory Disorders. Springer, Berlin Heidelberg New York, pp 247–296

Stennert E, Arold R (1973) Der doppelte Gehörgang. Klinische Studie einer seltenen Missbildung mit besonderer Berücksichtigung der anatomischen Beziehung zum extratemporalen Facialisverlauf. HNO 21:293–296

Stone JS, Oesterle EC, Rubel EW (1998) Recent insights into regeneration of auditory and vestibular hair cells. Curr Opin Neurol 11:17–24

Streeter GL (1904) The development of the cranial and spinal nerves in the occipital region of the human embryo. Am J Anat 4:83–116

Streeter GL (1906) On the development of the membranous labyrinth and the acustic and facial nerves in the human embryo. Am J Anat 6:139–165

Streeter GL (1911) Die Entwicklung des Nervensystems. In: Keibel F, Mall FP (Hrsg) Handbuch der Entwicklungsgeschichte des Menschen, Zweiter Band. Hirzel, Leipzig, pp 1–156

Streeter GL (1912) The development of the nervous system. In: Keibel F, Mall FP (eds) Manual of Human Embryology, Vol 2. Lippincott, Philadelphia, PA, pp 1–156

Streeter GL (1918) The histogenesis and growth of the otic capsule and its contained periotic tissue-spaces in the human embryo. Contrib Embryol Carnegie Instn 7:5–54

Streeter GL (1922) Development of the auricle in the human embryo. Contrib Embryol Carnegie Instn 14:111–138

Studer M (2001) Initiation and growth of facial motoneurone migration is dependent on rhombomeres 5 and 6. Development 128:3707–3716

Studer M, Lumsden A, Ariza-McNaughton L, Bradley N, Krumlauf R (1996) Altered segmental identity and abnormal migration of motor neurons in mice lacking Hoxb-1. Nature 384:630–634

Studer M, Gavalas A, Marshall H, Ariza-McNaughton L, Rijli FM, Chambon P, Krumlauf R (1998) Genetic interactions between *Hoxa1* and *Hoxb1* reveal new roles in regulation of early hindbrain patterning. Development 125:1025–1036

Suehiro S, Sando I (1979) Congenital anomalies of the inner ear. Ann Otol 88(Suppl 59):1–24

Sulik KK, Cotanche DA (2004) Embryology of the ear. In: Toriello HV, Reardon W, Gorlin RJ (eds) Hereditary Hearing Loss and Its Syndromes, 2nd ed. Oxford University Press, Oxford pp 17–36

Tassabehji M, Read AP, Newton VE, Harris R, Balling R, Gruss P, Strachan T (1992) Waardenburg's syndrome patients have mutations in the human homologue of the Pax-3 paired box gene. Nature 355:635–636

Tassabehji M, Newton VE, Read AP (1994) Waardenburg syndrome type 2 caused by mutations in the human microphthalmia (MITF) gene. Nat Genet 8:251–255

Teunissen E (1992) Major and Minor Congenital Anomalies of the Ear. Classification and surgical results. Thesis, University of Nijmegen

Tewfik TL, Der Kaloustian VM, eds (1997) Congenital Anomalies of the Ear, Nose, and Throat. Oxford University Press, New York

Thakkar N, O'Neil W, Duvally J, Liu C, Ambler M (1977) Möbius syndrome due to brain stem tegmental necrosis. Arch Neurol 34:124–126

Toriello HV, Reardon W, Gorlin RJ, eds (2004) Hereditary Hearing Loss and Its Syndromes, 2nd ed. Oxford University Press, Oxford, New York

Tos M (2000) Surgical Solutions for Conductive Hearing Loss. Thieme, Stuttgart

Towfighi J, Marcks K, Palmer E, Vannucci R (1979) Möbius syndrome. Neuropathologic observations. Acta Neuropathol (Berl) 48:11–17

Trainor PA, Krumlauf R (2000) Patterning the cranial neural crest: Hindbrain segmentation and *Hox* gene plasticity. Nature Rev Neurosci 1:116–124

Tsuchida T, Ensini M, Morton SB, Baldassare M, Edlund T, Jessell TM, Pfaff SL (1994) Topographic organization of embryonic motor neurons defined by expression of LIM homeobox genes. Cell 79:957–970

Tyson J, Tranebjaerg L, Bellman S, Wren C, Taylor JF, Bathen J, Aslaksen B, Sorland SJ, Lund O, Malcolm S (1997) ISK and KVLQT1: Mutation in either of the two subunits of the slow component of the delayed rectifier potassium channel can cause Jervell and Lange-Nielsen syndrome. Hum Mol Genet 6:2179–2185

Urbanek P, Wang ZQ, Fetka L, Wagner EF, Busslinger M (1994) Complete block of early B cell differentiation and altered patterning of the posterior midbrain in mice lacking Pax5/BSAP. Cell 79:901–912

Usher CH (1914) On the inheritance of retinitis pigmentosa, with notes of a case. R Lond Ophthalmol Hosp Rep 19:130–236

Vaage S (1969) The segmentation of the primitive neural tube in chick embryos (Gallus domesticus). Ergebn Anat Entw Gesch 41:1–88

Vahava O, Morell R, Lynch ED, Weiss S, Kagan ME, Ahituv N, Morrow JE, Lee MK, Skvorak AB, Morton CC, et al. (1998) Mutation in transcription factor *POU4F3* associated with inherited progressive hearing loss in humans. Science 279:1950–1954

van Aarem A, Cremers CWRJ, Benraad-van Rens MJL (1995) The Usher syndrome: A temporal bone report. Arch Otolaryngol Head Neck Surg 121:916–921

van den Munckhof P, Luk KC, Ste-Marie L, Montgomery J, Blanchet PJ, Sadikot AF, Drouin J (2003) Pitx3 is required for motor activity and for survival of a subset of midbrain dopaminergic neurons. Development 130:2535–2542

Van De Water TR, Noden DM, Maderson PFA (1988) Embryology of the ear: Outer, middle and inner. Otol Med Surg 1:3–27

Varela-Echeverria A, Pfaff SL, Guthrie S (1996) Differential expression of LIM homeobox genes among motor neuron populations in the developing chick brain stem. Mol Cell Neurosci 8:242–257

Verzijl HTFM, van den Helm B, Veldman B, Hamel BCJ, Kuyt LP, Padberg GW, Kremer H (1999) A second gene for autosomal dominant Möbius syndrome is localized to chromosome 10q in a Dutch family. Am J Hum Genet 65:752–756

Verzijl HTFM, van der Zwaag B, Cruysberg JRM, Padberg GW (2003) Möbius syndrome redefined. A syndrome of rhombencephalic maldevelopment. Neurology 61:327–333

Verzijl HTFM, van der Zwaag B, Lammens M, ten Donkelaar HJ, Padberg GW (2005) The neuropathology of hereditary congenital facial palsy versus Möbius syndrome. Neurology 64:649–653

Victor DI (1976) The diagnosis of congenital third-nerve palsy. Brain 99:711–718

Vieille-Grosjean I, Hunt P, Gulisano M, Boncinelli E, Thorogood P (1997) Branchial HOX gene expression and human craniofacial development. Dev Biol 183:49–60

von Graefe A (1858) Vereinzelte Beobachtungen exceptionelles Verhalten des Gesichtsfeldes bei Pigmentartung der Netzhaut. Albrecht von Graefe's Arch Klin Ophthalmol 4:250–253

von Graefe A (1880) In: von Graefe A, Saemisch T (Hrsg) Handbuch der gesamten Augenheilkunde, Vol 6. Engelmann, Leipzig, p 60

Von Noorden GK, Murray E, Wong SY (1986) Superior oblique paralysis: A review of 270 cases. Arch Ophthalmol 104:1771–1776

Waardenburg PJ (1951) A new syndrome combining developmental anomalies of the eyelids, eyebrows and nose root with pigmentary defects of the iris and head hair and with congenital deafness. Am J Hum Genet 3:195–253

Wagenaar M, Draaijer P, Meek H, ten Donkelaar HJ, Wesseling P, Kimberling W, Cremers C (1999) The cochlear nuclei in two patients with Usher syndrome type I. Int J Pediatr Otolaryngol 50:185–195

Wagenaar M, Schuknecht H, Nadol J Jr, Benraad-van Rens MJL, Kimberling WJ, Cremers CWRJ (2000) Histopathology of the temporal bone in Usher syndrome type I. Arch Otolaryngol Head Neck Surg 126:1018–1023

Wang A, Liang Y, Fridell RA, Probst FJ, Wilcox ER, Touchman JW, Morton CC, Morell RJ, Noben-Trauth K, Camper SA, Friedman TB (1998) Association of unconventional myosin MYO15 mutations with human nonsyndromic deafness DFNB3. Science 280:1447–1451

Wang S, Zwaan J, Mullaney P, Jabok MH, Al-Awad A, Beggs AH, Engle EC (1998) Congenital fibrosis of the extraocular muscles type 2 (CFEOM2), an inherited exotropic strabismus fixus, maps to distal 11q13. Am J Hum Genet 63:517–525

Wangemann P (2002) K$^+$ cycling and its regulation in the cochlea and the vestibular labyrinth. Audiol Neurootol 7:199-205

Wassef M, Joyner AL (1997) Early mesencephalon/metencephalon patterning and development of the cerebellum. Persp Dev Neurobiol 5:3–16

Weil D, Blanchard S, Kaplan J, Guilford P, Gibson F, Walsh J, Mburu P, Varela A, Levilliers J, Weston MD, et al. (1995) Defective myosin VIIa responsible for Usher syndrome type 1B. Nature 374:60–61

Wilkinson DG, Bhatt S, Cook M, Boncinelli E, Krumlauf R (1989) Segmental expression of Hox-2 homeobox-containing genes in the developing mouse hindbrain. Nature 341:405–409

Willinger M, James LS, Catz C (1991) Defining the sudden infant death syndrome (SIDS): Deliberations of an expert panel convened by the National Institute of Child Health and Human Development. Pediatr Pathol 11:677–684

Wurst W, Bally-Cuif L (2001) Neural plate patterning: Upstream and downstream of the isthmic organizer. Nat Rev Neurosci 2:99–108

Wurst W, Auerbach AB, Joyner AL (1994) Multiple developmental defects in Engrailed-1 mutant mice: An early mid-hindbrain deletion and patterning defects in forelimbs and sternum. Development 120:2065–2075

Xiang M, Gan L, Li D, Chen ZY, Zhou L, O'Malley BW Jr, Klein W, Nathans J (1997) Essential role of POU-domain factor Brn-3c in auditory and vestibular hair cell development. Proc Natl Acad Sci USA 94:9445–9450

Xiang M, Gao WQ, Hasson T, Shin JJ (1998) Requirement for Brn-3c in maturation and survival, but not in fate determination of inner ear hair cells. Development 125:3935–3946

Xu PX, Adams J, Peters H, Brown MC, Heaney S, Maas R (1999) Eya1-deficient mice lack ears and kidneys and show abnormal apoptosis of organ primordia. Nat Genet 23:113–117

Zec N, Filiano JJ, Kinney HC (1997) Anatomic relationships of the human arcuate nucleus of the medulla: A diI-labeling study. J Neuropathol Exp Neurol 56:509–522

Zheng JL, Gao WQ (1997) Analysis of rat vestibular hair cell development and regeneration using calretinin as an early marker. J Neurosci 17:8270–8282

Zheng Jl, Gao WQ (2000) Overexpression of math1 induces robust production of extra hair cells in postnatal rat inner ears. Nat Neurosci 3:580–586

Development and Developmental Disorders of the Human Cerebellum

Hans J. ten Donkelaar, Martin Lammens, Pieter Wesseling and Akira Hori

Introduction

The cerebellum is one of the best studied parts of the brain. Its three-layered cortex and well-defined afferent and efferent fibre connections make the cerebellum a favourite field for research on development and fibre connections of the central nervous system (Voogd et al. 1996). The cerebellar cortex is composed of four main types of neurons: granule cells, Purkinje cells and two types of inhibitory interneurons, the Golgi cells and the stellate/basket cells. The cortex receives three kinds of input: the mossy fibres (most afferent systems), the climbing fibres from the inferior olive, and diffusely organized monoaminergic and cholinergic fibres. The cerebellum plays a role not only in motor control but also in motor learning and cognition (Middleton and Strick 1998; Marien et al. 2001). The cerebellum develops over a long period, extending from the early embryonic period until the first postnatal years. The main cell types of the cerebellum arise at different times of development and at different locations. The Purkinje cells and the deep cerebellar nuclei arise from the ventricular zone of the metencephalic alar plate, whereas the granule cells are added from the rostral part of the rhombic lip, known as the upper rhombic lip. The caudal part of the rhombic lip (the lower rhombic lip) gives rise to the precerebellar nuclei, which include the pontine nuclei, the inferior olivary nucleus and some smaller nuclei with projections largely aimed at the cerebellum.

Its protracted development makes the cerebellum vulnerable to a broad scala of developmental disorders, ranging from the Dandy–Walker and related malformations to medulloblastoma, a neoplasia of granule precursor cells (Friede 1989; Norman et al. 1995; Ramaeckers et al. 1997; Ramaeckers 2000; ten Donkelaar et al. 2003; Boltshauser 2004). Ultrasound and MRI allow detection of cerebellar malformations at an early stage of development (Kollias and Ball 1997; Barkovich 2000). Cerebellar anomalies, of the vermis in particular, have also been found in neurobehavioural disorders such as autism and developmental dyslexia (Chap. 10). In mice, the molecular mechanisms of cerebellar development are rapidly being unravelled (Hatten et al. 1997; Goldowitz and Hamre 1998; Oberdick et al. 1998; Millen et al. 1999; Wang and Zoghbi 2001; Wingate 2001). Similar mechanisms are likely to be involved in the development of the human cerebellum. In this chapter the morphogenesis and histogenesis of the cerebellum and the precerebellar nuclei, the mechanisms involved, and the more frequent developmental disorders of the cerebellum, such as the Dandy–Walker anomaly and pontocerebellar hypoplasias, are discussed and illustrated with MRI data and autopsy cases.

Some Notes on the Anatomy of the Cerebellum

Subdivision

Transverse fissures divide the cerebellum into lobes, lobules and folia, whereas paramedian sulci separate the median vermis from the hemispheres (Fig. 8.1). The flocculus and the nodule form the caudal floccu-
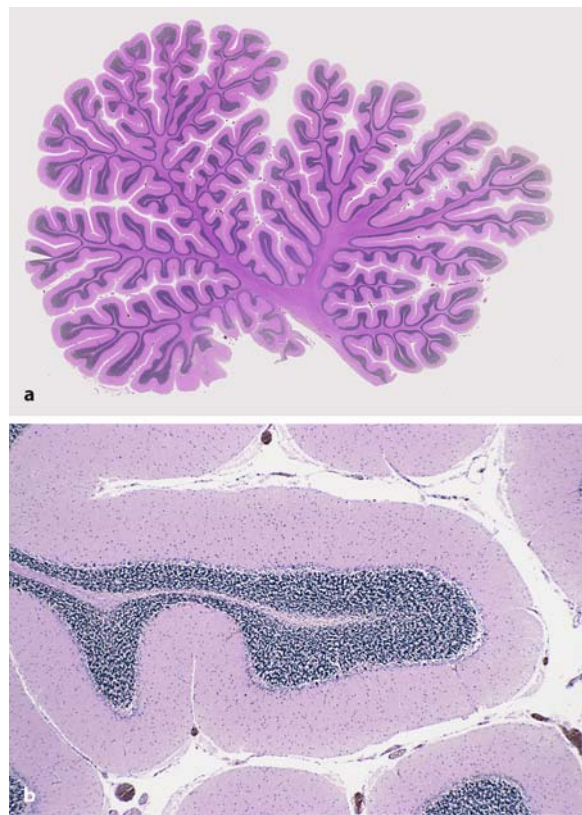
Fig. 8.1 Median section (**a**) and detail (**b**) of human cerebellum (courtesy Gerard van Noort, Enschede)
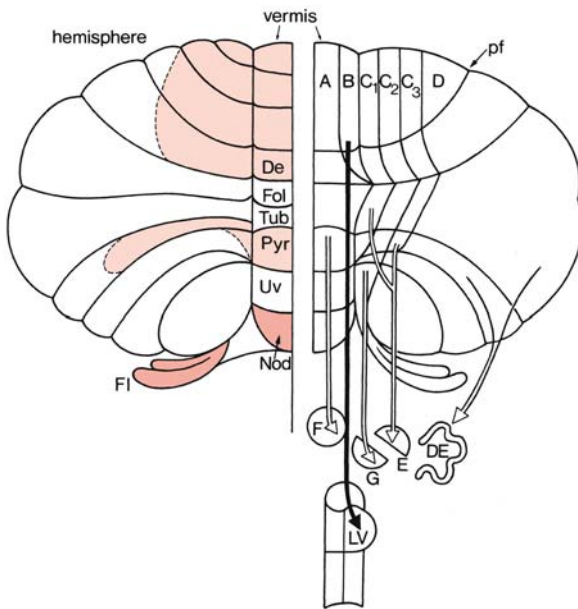
Fig. 8.2 Subdivision of the cerebellum. At the *left*, the spinocerebellum is shown in *light red* and the vestibulocerebellum in *red*. The remaining, non-coloured part forms the pontocerebellum. *A, B, C$_1$, C$_2$, C$_3$, D* longitudinal zones, *De* declive, *DE* dentate nucleus, *E* emboliform nucleus, *F* fastigial nucleus, *Fl* flocculus, *Fol* folium, *G* globose nucleus, *LV* lateral vestibular (Deiters) nucleus, *Nod* nodulus, *pf* primary fissure, *Pyr* pyramis, *Tub* tuber, *Uv* uvula. (After Voogd 1995; Voogd et al. 1996)

lonodular lobe that is also known as the *vestibulocerebellum* or *archicerebellum*. This lobe receives primary (from the vestibular organs) and secondary (from the vestibular nuclei) vestibular projections. The corpus cerebelli, i.e. the vermis and the hemispheres, consists of the *spinocerebellum* (or *paleocerebellum)* medially, and the *pontocerebellum* (or *neocerebellum*) laterally. The spinocerebellum receives projections from the spinal cord and trigeminal system, whereas the pontocerebellum is innervated by pontocerebellar fibres. The fissura prima divides the cerebellar hemispheres into anterior and posterior lobes. The cerebellum is organized as longitudinal zones of Purkinje cells (A-, B-, C- and D-zones), each projecting to its own cerebellar nucleus (Fig. 8.2) and receiving input from different parts of the inferior olive (Voogd 1967, 1995, 2003, 2004; Voogd et al. 1996; Voogd and Glickstein 1998). The central cerebellar nuclei are the medial *nucleus fastigii*, the intermediate *nucleus globosus* and the *nucleus emboliformis* (together also known as the nucleus interpositus), and the laterally situated, large *nucleus dentatus*. The vermis contains a **medial zone** (*A-zone*), projecting to the nucleus fastigii, and a small *B-zone* that innervates the lateral vestibular nucleus of Deiters. The cerebellar hemispheres can be divided into intermediate and lateral zones. The

intermediate zone consists of three *C-zones*, projecting to the nucleus emboliformis (C1 and C3) and the nucleus globosus (C2). The large **lateral zone** (*D-zone*) innervates the nucleus dentatus. The **lobus flocculonodularis** innervates the vestibular nuclear complex.

8.2.2   Compartmentalization

A **modular organization** of the cerebellar cortex is found in mammals and birds (Voogd 1967; Oscarsson 1980; Voogd and Bigaré 1980; Marani 1982; Feirabend 1983; Ito 1984; Feirabend and Voogd 1986; Voogd et al. 1990, 1996). Purkinje cells of a zone project to a particular cerebellar or vestibular target nucleus. Zones can extend across one or more lobules; some span the entire rostrocaudal length of the cerebellum (Fig. 8.2). The olivocerebellar projection is arranged in a similar way. Subnuclei of the inferior olive project to a single Purkinje-cell zone or to a pair of zones sharing the same target nucleus. These longitudinal zones are not evident on the outside of the cerebellum. However, a system of compartments in the white matter, which contains the axons of the Purkinje cells and the climbing fibres, can be visualized. Moreover, a strong heterogeneity has been found in the expression of certain proteins by subpopulations of Purkinje cells, distributed in alternating longitudinal zones. This pattern, described by Scott (1964) and Marani (1982) for the 5'-nucleotidase pattern (Fig. 8.3), and subsequently by Hawkes and Leclerc (1987) for the '**zebrin**' epitope on the rat cerebellum, is shared by the expression of several other proteins in Purkinje cells and in Bergmann glia (Voogd et al. 1996; Herrup and Kuemerle 1997). The antibodies zebrins I and II specifically stain a subset of Purkinje cells, distributed into multiple longitudinal zones and separated by zebrin-negative areas in rodents (Hawkes et al. 1985; Hawkes and Leclerc 1987), but not in macaque monkeys, where antibodies against zebrin stain all
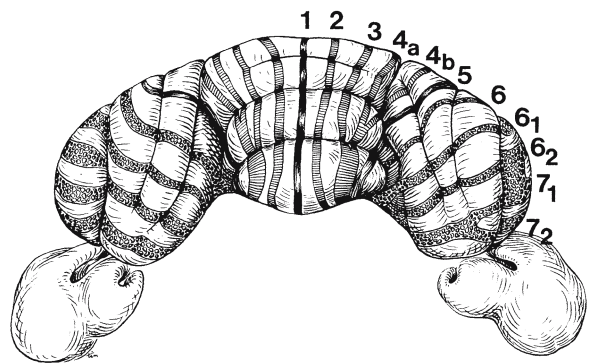
Fig. 8.3 5′-Nucleotidase pattern in the rat cerebellar cortex (from Marani 1982; courtesy Enrico Marani, Leiden)
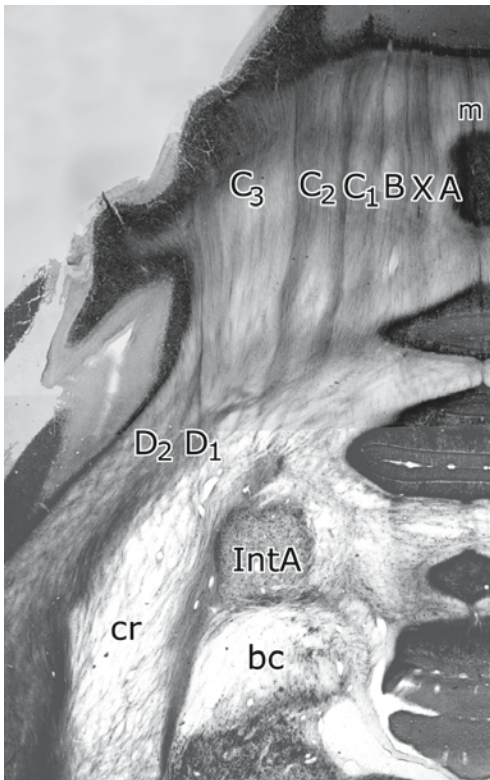
Fig. 8.4 Transverse, acetylcholinesterase-stained section of the anterior cerebellar lobe of the macaque monkey, showing the modular organization of the cerebellum. *A*, *B*, C_1, C_2, C_3, D_1, D_2, *X* longitudinal zones, *bc* brachium conjunctivum, *cr* corpus restiforme, *IntA* nucleus interpositus anterior, *m* midline. (Kindly provided by Jan Voogd, Oegstgeest)

Fig. 8.5 Connections of the dentate and interposed nuclei. *bc* brachium conjunctivum, *cosp* corticospinal tract, C_1, C_2, C_3, *D* longitudinal zones, *DE* dentate nucleus, *E* emboliform nucleus, *G* globose nucleus, *NRTP* nucleus reticularis tegmenti pontis, *Rm* magnocellular part of red nucleus, *Rp* parvocellular part of red nucleus, *rusp* rubrospinal tract, *thal* thalamus, *vm* vermis, *4* primary motor cortex, *6* premotor cortex. (After Voogd 1995)

Purkinje cells (Leclerc et al. 1990). In the human cerebellum, no clear arrangement of zebrin I-stained Purkinje cells was found (Plioplys et al. 1985). Acetylcholinesterase (AChE) histochemistry is a useful marker for the delineation of parasagittal compartments in the cerebellum of adult mammals (Marani and Voogd 1977; Hess and Voogd 1986; The borders between compartments are selectively stained with AChE and this staining is especially distinct in monkeys (Fig. 8.4).

8.2.3   Major Fibre Connections

Afferent and efferent fibre connections of the cerebellum pass through the cerebellar peduncles. The **pedunculus cerebellaris inferior** or **corpus restiforme** contains cerebellar afferents: the *tractus spinocerebellaris posterior* and the *fibrae cuneocerebellares* from the spinal cord, *trigeminocerebellar fibres* from sensory trigeminal nuclei, *olivocerebellar fibres* and *vestibulocerebellar fibres*. The **pedunculus cere-**

bellaris medius or **brachium pontis** is formed by the massive *pontocerebellar system*. The pontine nuclei are innervated by the cerebral cortex via two tracts: the *frontopontine tract* from the frontal lobe, motor and premotor areas in particular, and the *parietotemporo-occipitopontine tract*, particularly arising in the somatosensory areas and the adjacent area 5. The **pedunculus cerebellaris superior** contains the *tractus spinocerebellaris anterior* and the main efferent system of the cerebellum, i.e. the *brachium conjunctivum*. The cerebellar nuclei are the **output centres** of the cerebellum. The targets of these nuclei differ considerably. The dentate and interposed nuclei mainly innervate the thalamus and the red nucleus, and control corticospinal and rubrospinal projections (Fig. 8.5). The fastigial nucleus and the nucleus of Deiters control the reticulospinal and vestibulospinal projections (Fig. 8.6). The subdivision of descending supraspinal pathways into lateral and medial systems (Chap. 6) is therefore also found in the cerebellar control system. The dentate nucleus also has important feedback loops to the cerebellum through the
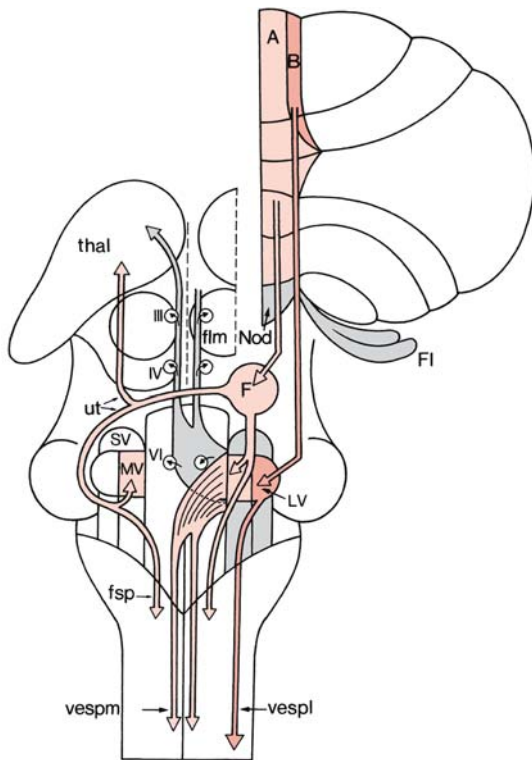
Fig. 8.6 Connections of the fastigial and vestibular nuclei. *A*, *B* longitudinal zones, *F* fastigial nucleus, *Fl* flocculus, *flm* fasciculus longitudinalis medialis, *fsp* fastigiospinal tract, *LV* lateral (Deiters) vestibular nucleus, *MV* medial vestibular nucleus, *Nod* nodulus, *SV* superior vestibular nucleus, *thal* thalamus, *ut* uncinate tract, *vespl* lateral vestibulospinal tract, *vespm* medial vestibulospinal tract, *III*, *IV*, *VI* cranial nerve nuclei. (After Voogd 1995)

Fig. 8.7 Early development of the rat cerebellum: at the *left* gross development is shown at E12, E14 and E16 and at the *right* a closer look at the cerebellum and rhombic lip. *ap* alar plate, *bp* basal plate, *lrl* lower rhombic lip, *mes* mesencephalon, *url* upper rhombic lip. (After van de Voort 1960)

nucleus reticularis tegmenti pontis (Fig. 8.5) and the dentato-rubro-olivary loop. Projections from the small-celled part of the red nucleus to the inferior olive pass via the central tegmental tract.

8.2.4   Precerebellar Nuclei

The precerebellar nuclei form a group of brain stem nuclei with efferent projections largely or exclusively to the cerebellum. They all arise from the lower rhombic lip. The pontine nuclei and the pontine reticular tegmental nucleus form the upper precerebellar nuclei, whereas the inferior olivary nucleus with its accessory olivary nuclei, the external cuneate nucleus and the lateral reticular nucleus form the lower precerebellar nuclei (Altman and Bayer 1997). Olivocerebellar fibres show a sagittal zonal organization (Groenewegen et al. 1979; Voogd et al. 1996; Voogd 2004). The terminal fields of the climbing-fibre projections from subdivisions of the inferior

olive constitute narrow, parasagittal zones which coincide with the corticonuclear projection zones: (1) the caudal halves of the accessory inferior olives innervate the A- and B-zones of the vermis; (2) olivocerebellar fibres to the C-zones of the intermediate part of the cerebellum arise from the rostral halves of the accessory inferior olives; and (3) fibres from the principal inferior olive terminate in the D-zones.

8.3   Morphogenesis of the Cerebellum

The cerebellum arises bilaterally from the alar layers of the first rhombomere (O'Rahilly and Müller 2001). An overview of the development of the rat cerebellum is shown in Fig. 8.7. The two cerebellar primordia are generally considered to unite dorsally to form the vermis (Altman and Bayer 1997), early in the fetal period. Rostrally, the paired cerebellar anlagen are not completely separated, however. Sidman and Rakic (1982), therefore, advocated Hochstetter's (1929)
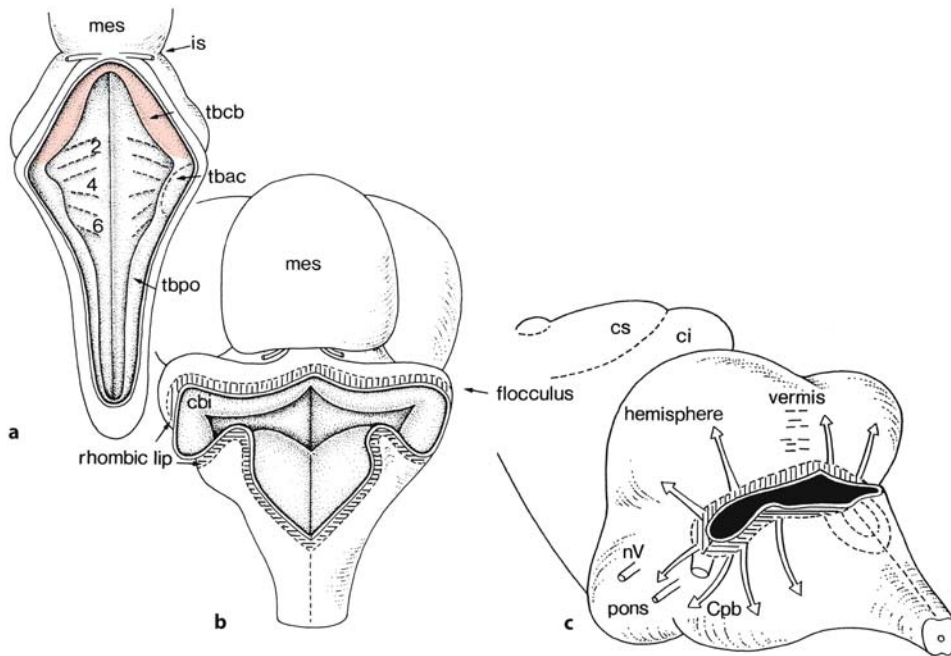
Fig. 8.8 Early development of the human cerebellum: **a** at approximately 4 weeks of development; **b** at the end of the embryonic period; **c** at 13 weeks of development. The V-shaped tuberculum cerebelli is shown in *light red*, and the upper and lower rhombic lips by *vertical* and *horizontal hatching*, respectively. In **c** *arrows* show the migration paths from the rhombic lips. *cbi* internal cerebellar bulge, *ci* colliculus inferior, *Cpb* corpus pontobulbare, *cs* colliculus superior, *is* isthmus, *mes* mesencephalon, *nV* trigeminal nerve, *tbac* tuberculum acusticum, *tbcb* tuberculum cerebelli, *tbpo* tuberculum ponto-olivare, *2, 4, 6* rhombomeres. (**a** After Jakob 1928; **b** after Hochstetter 1929; **c** after Sidman and Rakic 1982)

view that such a fusion does not take place, and suggested one cerebellar primordium. This tuberculum cerebelli consists of a band of tissue in the dorsolateral part of the alar plate that straddles the midline in the shape of an inverted V (Fig. 8.8 a). The arms of the V are directed caudally as well as laterally, and thicken enormously, accounting for most of the early growth of the cerebellum. The rostral, midline part of the V, however, remains small and relatively inconspicuous. The further morphogenesis of the cerebellum can be summarized as follows: (1) the caudally and laterally directed limbs of the tuberculum cerebelli thicken rapidly during the sixth week of development and bulge downwards into the fourth ventricle, on each side giving rise to the internal cerebellar bulge or *innerer Kleinhirnwulst* of Hochstetter which together form the corpus cerebelli (Fig. 8.8 b); (2) during the seventh week of development, the rapidly growing cerebellum bulges outwards as the external cerebellar bulges (Hochstetter's *äusserer Kleinhirnwulst*) which represent the flocculi, which are delin-

eated by the posterolateral fissures; (3) during the third month of development, i.e. in the early fetal period, growth of the midline component accelerates and begins to fill the gap between the limbs of the V, thereby forming the vermis; and (4) by the 12th to 13th weeks of development, outward, lateral and rostral growth processes have reshaped the cerebellum to a transversely oriented bar of tissue overriding the fourth ventricle (Fig. 8.8 c).

At the 12th week of development, fissures begin to form transverse to the longitudinal axis of the brain, first on the vermis and then spreading laterally into the hemispheres (Fig. 8.9). The first fissure to appear, i.e. the fissura posterolateralis, separates the main body of the cerebellum from the flocculonodular lobe.
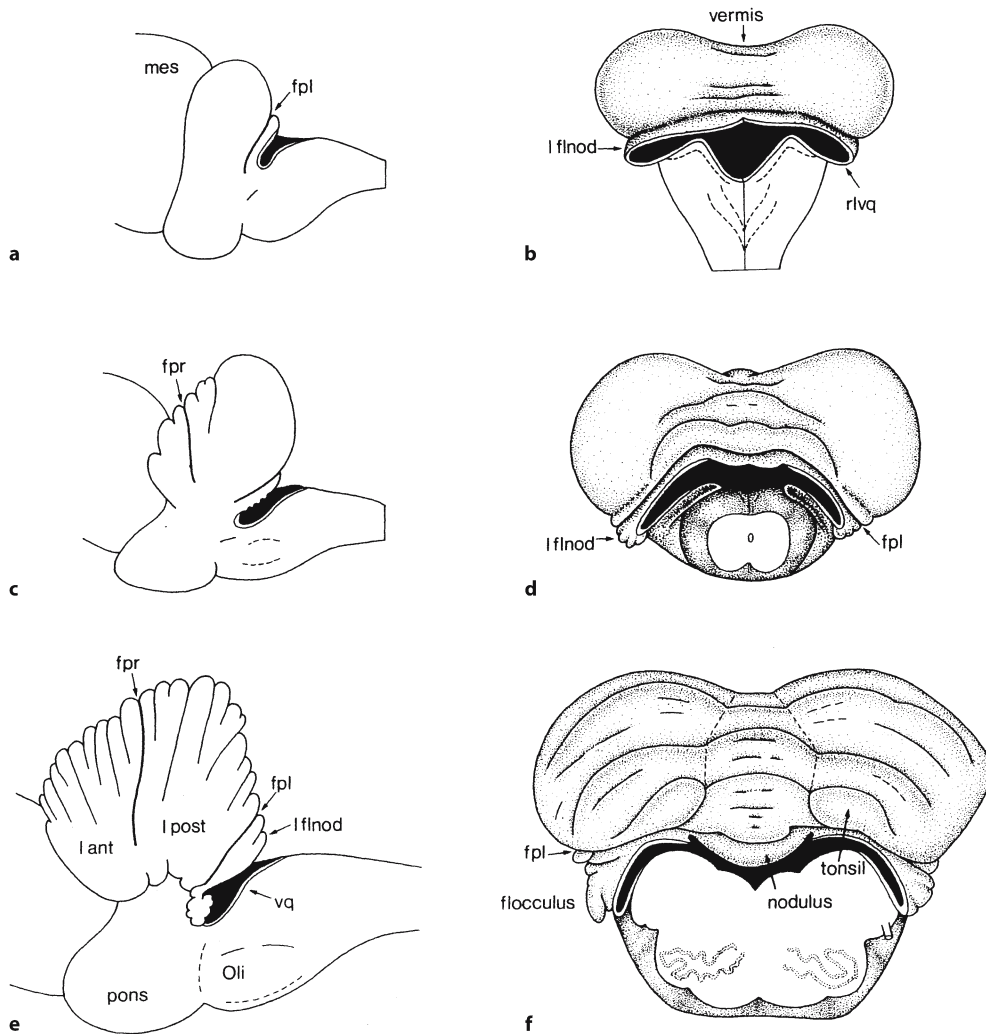
Fig. 8.9 Fetal development of the human cerebellum shown in lateral (on the *left*) and dorsal (on the *right*) views: **a**, **b** 13 weeks of development; **c**, **d** 4 months of development; **e**, **f** 5 months of development. *fpl* fissura posterolateralis, *fpr* fissura prima, *l ant* lobus anterior, *l flnod* lobus flocculonodularis, *l post* lobus posterior, *mes* mesencephalon, *Oli* oliva inferior, *rlvq* lateral recess of fourth ventricle, *vq* ventriculus quartus. (After Streeter 1912)

8.4   Four Basic Steps in the Histogenesis of the Cerebellum

The histogenesis of the cerebellum occurs in four basic steps (Hatten and Heintz 1995; Altman and Bayer 1997; Hatten et al. 1997; Goldowitz and Hamre 1998; Millen et al. 1999; Wang and Zoghbi 2001): (1) characterization of the cerebellar territory in the hindbrain; (2) formation of two compartments of cell proliferation, giving rise to the Purkinje cells and the granule cells, respectively; (3) inward migration of the granule cells; and (4) differentiation of cerebellar neurons. A large number of genes are involved in the formation of the cerebellum (Goldowitz and Hamre 1997; Hatten et al. 1997; Millen et al. 1999; Wang and Zoghbi 2001; Table 8.1). More than 20 spontaneous

mice mutations are known that affect the cerebellum (Caviness and Rakic 1978; Mullen et al. 1997; Millen et al. 1999; Sect. 8.6).

8.4.1   Characterization of the Cerebellar Territory

Transplantation and gene expression studies in chick and mice embryos have shown that the *isthmus organizer*, i.e. a transverse patterning centre at the midbrain–hindbrain boundary (MHB), regulates the early development of the mesencephalon and the rostral part of the rhombencephalon (Wassef and Joyner 1997; Rhinn and Brand 2001; Wurst and Bally-Cuif 2001). In avian embryos, Louvi et al. (2003) found that

Table 8.1 Expression of segment polarity and related genes during cerebellar development (after Oberdick et al. 1998; Wang and Zoghbi 2001)

Drosophila	Mouse, rat	Embryonic development	Postnatal development	Mouse mutants
Engrailed	En1	MHB		Complete cerebellar absence
	En2	MHB	Granule cells	Cerebellar hypoplasia, abnormal foliation
Wingless	Wnt1	Rostral to MHB		Cerebellum hardly present; mesencephalon malformed
	Wnt3	MHB	Purkinje cells	
Hedgehog	Shh	Floor plate	Purkinje cells	
Odd-paired	Zic1	Granule cell precursors	Granule cells	Smaller cerebellum; foliation defects
Patched	Patched1 (Ptc)	Granule cells	Purkinje cells, granule cells	
Atonal	Math1	Rhombic lip derivatives	Granule cell precursors	Lack of rhombic lip derivatives
Homeotic genes	Hoxa2	Rostral hindbrain		
	Hoxa5	Hindbrain	Purkinje cells	
	Lmx1a (Dreher)	MHB		Vemis absent
Orthodenticle	Otx1		External granular layer	
	Otx2	Cerebellar precursor cells	External and internal granular layers	
Unplugged	Gbx2	MHB		
Pair-rule genes	Pax2	MHB		Absence of cerebellum and posterior mesencephalon
	Pax3	Cerebellum	Cerebellum	
	Pax5	MHB	Granule cells	Mild phenotype
	Pax6	Cerebellum	Cerebellum, external granular layer	Abnormal cerebellum; foliation defects

MHB midbrain–hindbrain boundary
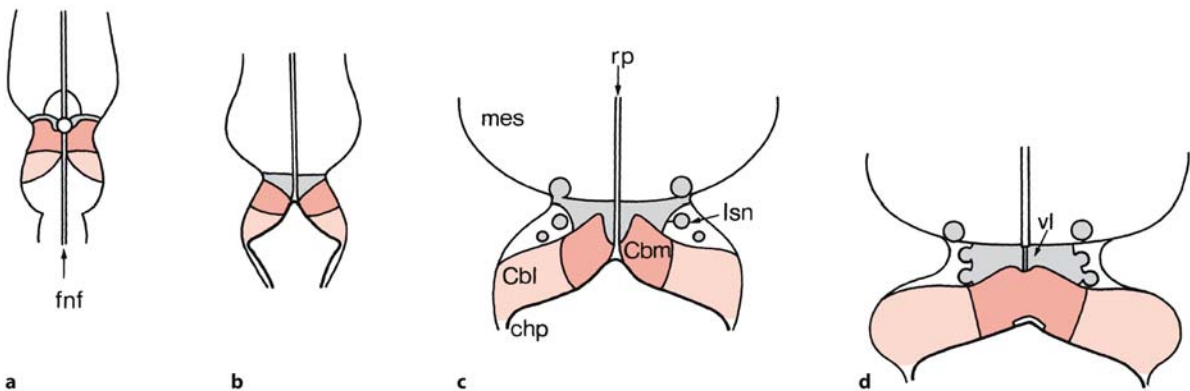
Fig. 8.10 Morphogenetic movements in the dorsal part of the neural tube at the midbrain–hindbrain boundary, based on observations in chick and mouse embryos. Dorsal views are shown, representative for chick HH10 stage (**a**), chick HH17–HH18 stage and mouse E9.5 (**b**), chick HH24 stage and mouse E13–E15 (**c**) and later (**d**). The isthmus and its contributions are indicated in *grey*, the medial cerebellum is indicated in *red* and the lateral cerebellum in *light red*. *Cbl* lateral part of the cerebellum, *Cbm* medial part of cerebellum, *chp* choroid plexus, *fnf* fused neural folds, *Isn* isthmic nuclei, *mes* mesencephalon, *rp* roof plate, *vl* velum medullare (anterius). (After Louvi et al. 2003)

divergent cell movements originating from a restricted medial domain located at the MHB produce the roof plate of the midbrain–hindbrain domain (Fig. 8.10). Cells migrating rostrally from this region populate the caudal midbrain roof plate, whereas cells migrating caudalwards populate the cerebellar roof plate. The adjacent paramedian isthmic neuroepithelium also migrates caudalwards and partici-
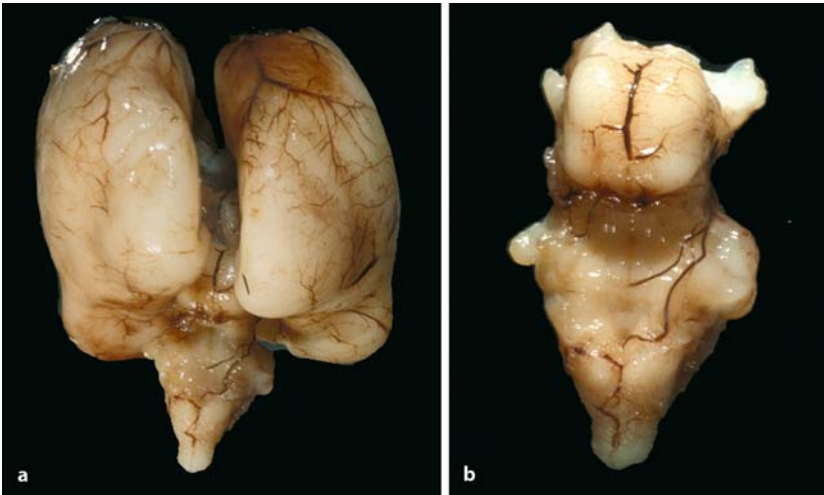
Fig. 8.11 Cerebellar agenesis before (**a**) and after (**b**) removal of the cerebrum in a male fetus born spontaneously at the 22nd gestational week (from the Department of Neuropathology, Medizinische Hochschule Hannover; courtesy Akira Hori)
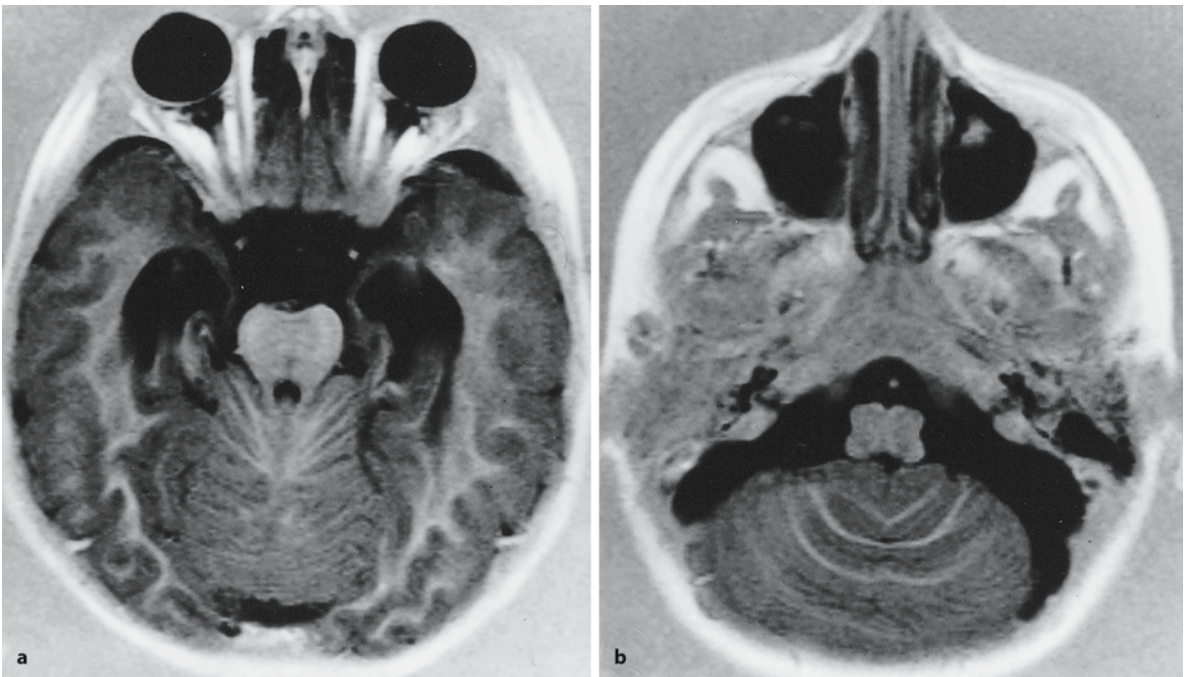
Fig. 8.12 Axial fluid attenuated inversion recovery images of a patient with rhombencephalosynapsis: **a** abnormal appearance of the vermis and enlarged temporal horns; **b** the cerebellar folia are continuous across the midline, meaning fusion of the cerebellar hemispheres without an intervening vermis (courtesy Berit Verbist, Leiden)

pates in the formation of two distinct cerebellar midline structures: (1) the late-developing velum medullare anterius that intervenes between the vermis and the midbrain; and (2) a midline domain upon which the cerebellum fuses. Elimination or overgrowth of the isthmic domain in $Wnt1^{sw/sw}$ and $En1^{+/Otx2lacZ}$ mutant mice impair cerebellar midline fusion (Louvi et al. 2003). These data suggest that isthmus-derived cells are essential for the cerebellar fusion process.

MHB cells secrete fibroblast growth factors (FGFs) and *Wnt* (mouse homologues of the *Drosophila* gene wingless) proteins which are required for the differentiation and patterning of the midbrain and hindbrain (Rhinn and Brand 2001). *Wnt* is a fusion of the name of the *Drosophila* segment polarity gene wingless with that of one of its vertebrate homologues, integrated. In *Wnt1* knockout mice, the mesencephalon is malformed and a cerebellum is hardly present (McMahon et al. 1992; Mastick et al. 1996). A number

of homeobox-containing transcription factors are expressed across the isthmus, such as the homologues of the *Drosophila* gene engrailed *En1* and *En2*. Mutations in these genes cause deletions of mesencephalic and cerebellar structures (Millen et al. 1994, 1995; Wurst et al. 1994; Kuemerle et al. 1997; Wassef and Joyner 1997; Bilovocky et al. 2003). *En1* knockout mice have complete cerebellar aplasia, whereas *En2* deletions only cause cerebellar hypoplasia with abnormal foliation (Millen et al. 1994, 1995; Kuemerle et al. 1997). Recently, Sarnat et al. (2002) described two neonates with congenital absence of the midbrain and hypoplasia of the cerebellum and rostral pons, showing striking resemblance to the phenotype of the *En2* knockout mice (Clinical Case 7.1).

Cerebellar agenesis is extremely rare. Combettes (1831) reported the first case in an 11-year-old girl in whom, at autopsy, the cerebellum was found to be virtually absent. Sternberg (1912) described a case of a 46-year-old woman who died in hospital of carcinoma of the stomach. At autopsy, the cerebellum and precerebellar nuclei were found to be completely absent. Anton and Zingerle (1914) described the brain of a 6-year-old girl with complete absence of the cerebellum. In all cases, severe motor deficits were present. A similar pattern of severe developmental motor deficits was found in all cases of total or near-total cerebellar agenesis (Baker and Graves 1931; Cohen 1942; Glickstein 1994). More recently, *near-total absence* of the *cerebellum* was proposed as a distinct entity, associated with pontine hypoplasia and relatively mild clinical affection (Gardner et al. 2001; Sect. 8.7.3). Zafeiriou et al. (2004) reported a case of a 7-year-old girl with cerebellar agenesis and diabetes insipidus. A fetal case of cerebellar agenesis is shown in Fig. 8.11. The fetus had no general gross malformations. In the brain, complete cerebellar agenesis and absence of cerebellar peduncles was found.

Less is known about the dorsoventral patterning of the cerebellar territory (Lee and Jessell 1999). *Rhombencephalosynapsis* (Fig. 8.12, Clinical Case 8.1), a rare cerebellar malformation character-

---

Clinical Case 8.1
Rhombencephalosynapsis

Rhombencephalosynapsis is a rare, mostly sporadic, cerebellar malformation characterized by agenesis or hypogenesis of the vermis, leading to 'fusion' of the hemispheres, and closely apposed or fused dentate nuclei. Most patients die early in life (see Case Report).

Case Report. At 30 weeks' gestational age, ultrasound examination of a male fetus revealed hydrocephalus. After spontaneous rupture of the membranes at 36 weeks, a boy of 3,130 g and a head circumference of 45.5 cm was born by Caesarean section. Little resuscitation was required. Elective insertion of a ventriculoperitoneal shunt was performed shortly after birth, after which the patient did well and was discharged at the age of 3 weeks with a weight of 3,125 g. No abnormalities were noted on a CT scan. Two months later, he weighed 4,140 g, had a length of 51 cm and a head circumference of 43.2 cm. His parents reported that he was slow to feed but that he appeared to be following with his eyes and reacted to sound. He was readmitted at the age of 3 months with drowsiness and anorexia, found to be the result of a blocked shunt. One month later, he had a cardiac arrest from which he was not resuscitated. At autopsy, rhombencephalosynapsis was found (Fig. 8.13).

This case was kindly provided by Jennian Geddes (Royal London Hospital, Whitechapel, London).
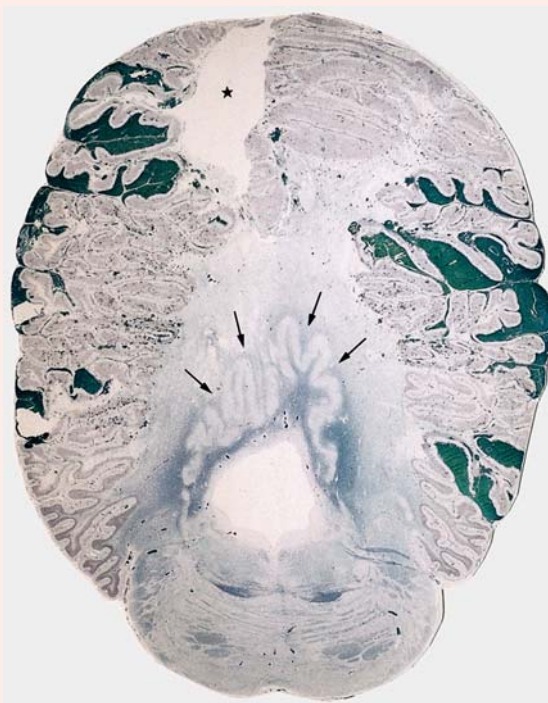
Fig. 8.13 Rhombencephalosynapsis. Note the dorsal fusion of the cerebellar hemispheres and dentate nuclei (*arrows*). The *asterisk* marks an artefact (courtesy Jennian Geddes, London)
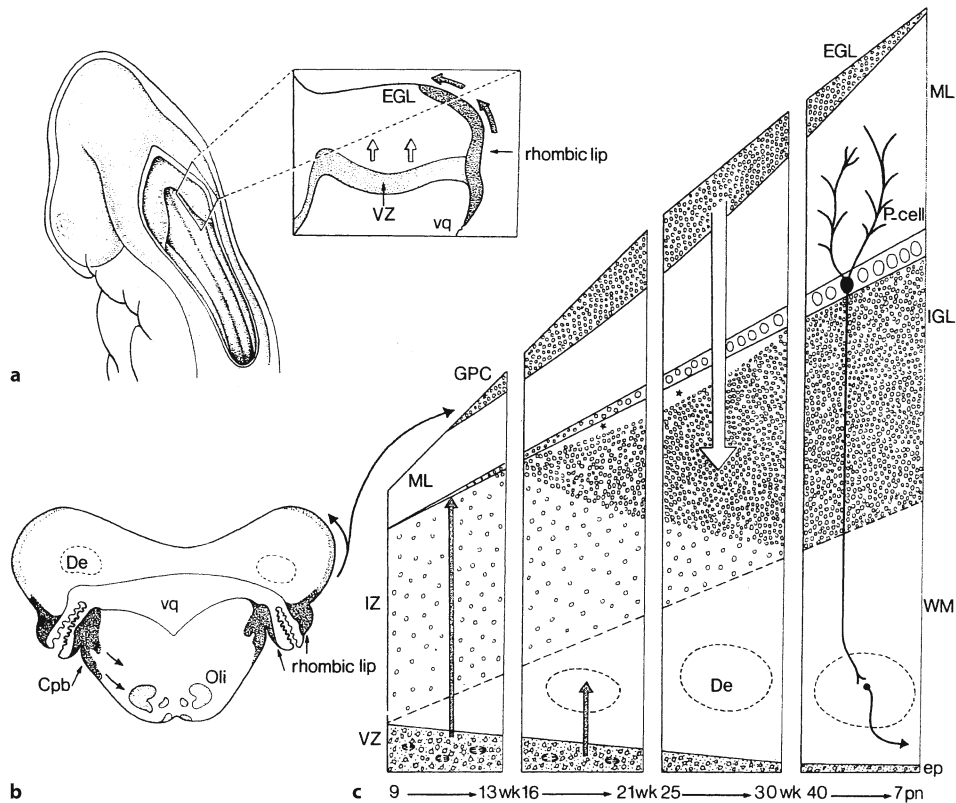
Fig. 8.14 Overview of the histogenesis of the cerebellum. **a** A dorsolateral view of a human embryo and part of the tuberculum cerebelli is enlarged, showing the two proliferative compartments: the ventricular zone (*VZ*), giving rise to the Purkinje cells and the deep cerebellar nuclei, and the external germinal or granular layer (*EGL*), giving rise to the granule cells. **b** The position of the *rhombic lip* in a transverse section at the level of the lateral recess of the fourth ventricle. The upper rhombic lip is found lateral to the lateral recess, and the lower rhombic lip medial to this recess. **c** The formation of the layers of the cerebellum is shown in four periods from the early fetal period until 7 weeks postnatally. The lamina dissecans is indicated with *asterisks*. The *arrows* in **a**–**c** show the migration paths. *Cpb* corpus pontobulbare, *De* dentate nucleus, *ep* ependyma, *GPC* granule precursor cells, *IGL* internal granular layer, *IZ* intermediate zone, *ML* molecular layer, *Oli* oliva inferior, *P-cell* Purkinje cell, *vq* ventriculus quartus; *WM* white matter. (After Sidman and Rakic 1982; Hatten et al. 1997; O'Rahilly and Müller 2001)

ized by vermian agenesis or hypogenesis, and dorsal 'fusion' of the cerebellar hemispheres and dentate nuclei (Obersteiner 1914; Gross and Hoff 1959; Schachenmayr and Friede 1982; Truwitt et al. 1991; Utsunomiya et al. 1998; Danon et al. 2000; Toelle et al. 2002; Yachnis 2002), may be explained by an embryological defect of dorsal patterning at the MHB (Yachnis 2002), possibly by underexpression of a dorsalizing gene (Sarnat 2000). A candidate molecule may be *Lmx1a*, identified in the neurological mutant mouse *dreher*. Owing to a homozygous mutation of *Lmx1a*, this mouse lacks a vermis, resulting in apparent fusion of the cerebellar hemispheres and inferior colliculi (Manzanares et al. 2000; Millonig et al. 2000). In rhombencephalosynapsis, clinical findings range from mild truncal ataxia and normal cognitive abilities to severe cerebral palsy and mental retardation

(Toelle et al. 2002). Most cases are sporadic, and most patients die early in life.

8.4.2 Formation of Two Proliferative Compartments

The histogenesis of the cerebellum comprises the three further steps of cerebellar development: formation of two proliferative compartments, inward migration of granule cells, and formation of cerebellar circuitry and further differentiation (Fig. 8.14). The main cell types of the cerebellum arise at different times of development and at different locations (Miale and Sidman 1961; Altman and Bayer 1978a, b, 1987a–c, 1997; Hatten and Heintz 1995). The Purkinje cells, the deep cerebellar nuclei and later the Golgi,

Table 8.2 Time of neuron origin data cerebellum and precerebellar nuclei (after Bayer et al. 1995)

Structure	Time of neuron data in rats	Estimated human time of neuron data
Cerebellum		
Deep nuclei	(E13)E14(E15)	Early week 5 to week 6 of gestation
Purkinje cells	(E14)E15	Early week 5 to week 6
Golgi cells	E19–P2	Beginning week 10 to week 23 of gestation
Basket cells	P4–P7	From about week 19 to birth
Stellate cells	P9, P10	From about week 19 to birth
Granule cells	P8–P15	From about week 19 to birth
Precerebellar nuclei		
Inferior olive	E13	Early week 5 to week 6 of gestation
Lateral reticular nucleus	E13–E15	Early week 5 to week 7
Nucleus reticularis tegmenti pontis	E16	Week 7 to week 8
Pontine nuclei	E17, E18	Week 7 to week 11 of gestation

stellate and basket cells arise from the ventricular zone of the metencephalic alar plates. Purkinje cells migrate along radial glial cells to their future position, making use of a Reelin-dependent pathway. Using adenoviral vectors, Hashimoto and Mikoshiba (2003) showed that Purkinje cells that shared the same birth date formed specific subsets of mediolateral clusters in the cerebellum. Each subset of clusters along the mediolateral axis displayed nested and complementary patterns. These patterns remained unchanged from late embryonic stages to adulthood, suggesting that Purkinje cell progenitors are fated to form specific subsets of mediolateral clusters after their birth between E10.5 and E12.5. Bayer et al. (1995) estimated that in man the deep cerebellar nuclei as well as the Purkinje cells are generated from the early fifth up to and including the sixth weeks of development (Table 8.2). Towards the end of the embryonic period, granule cell precursors are added from the rhombic lip. The rhombic lip, the *Rautenleiste* of His (1890), is the dorsolateral part of the alar plate, and it forms a proliferative zone along the length of the hindbrain (Fig. 8.7 c). Cells from its rostral part reach the superficial part of the cerebellum, and form the external germinal or granular layer at the end of the embryonic period. The *Math1* (mouse atonal homologue) gene is expressed in the rhombic lip (Ben-Arie et al. 1997; Jensen et al. 2004). Migratory granule cell precursors exclusively maintain expression of *Math1*, *Zic1* (Aruga et al. 1994, 1998) and *Zipro1*. *Zipro1* (formerly known as the zinc-finger-containing factor RU49) marks the expression of cerebellar granule cells. *Zipro1* expression is maintained at all stages of cerebellar granule cell differentiation (Alder et al. 1996; Yang et al. 1996). In *Math1* knockout mice, no granular layer is formed. Granule cell precursors express the netrin receptors

DCC, *Unc5H2* and *Unc5H3* (Przyborski et al. 1998; Engelkamp et al. 1999; Alcantara et al. 2000). Disruption of *Unc5H3* signalling leads to the rostral cerebellar malformation in which granule and Purkinje cells spread ectopically into the caudal mesencephalon (Ackerman et al. 1997; Eisenman and Brothers 1998; Engelkamp et al. 1999). Netrin has a general role in guiding ventral migration of rhombic lip derivatives (Yee et al. 1999; Bloch-Gallego et al. 1999; Alcantara et al. 2000), but its role in the migration of granule cell precursors to the external granular layer is not entirely clear. Cerebellar development is undisturbed in *Netrin-1* knockout mouse (Bloch-Gallego et al. 1999).

8.4.3   Inward Migration of Granule cells

Granule cells are formed in the external germinal layer. The granule cells form axons, the parallel fibres, and migrate along the processes of Bergmann glia cells to their deeper, definitive site, the internal granular layer (Fig. 8.14). In the fetal period, the internal granular layer is formed by further proliferation and migration of the external germinal cells. This layer, situated below the layer of Purkinje cells, is the definitive granular layer of the cerebellar cortex. A transient layer, the lamina dissecans, separates the internal granular layer from the Purkinje cells. Ultimately, it is filled by migrating granule cells and disappears (Rakic and Sidman 1970). During the inward migration of the postmitotic granule cells (16–25 weeks), the Purkinje cells enlarge and develop dendritic trees (Milosevic and Zecevic 1998, and Miyata et al. 1999). The external germinal layer appears at the end of the embryonic period and persists for several months to 1–2 years after birth (Lemire et al. 1975).
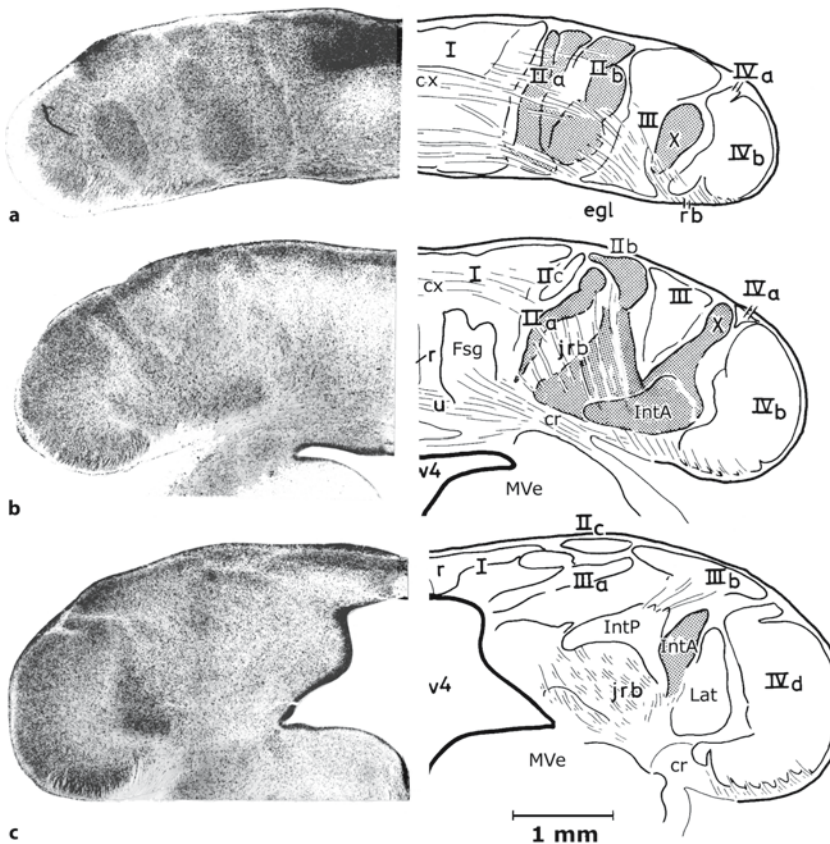
Fig. 8.15 Purkinje cell clusters in a 55-day-old rhesus monkey fetus, shown in three sections from rostral (**a**) to caudal (**c**). Purkinje cell clusters are indicated by *Roman numerals*. *cr* corpus restiforme, *cx* cerebellar commissure, *egl* external granular layer, *Fl* flocculus, *IntA* anterior interposed nucleus, *IntP* posterior interposed nucleus, *jrb* juxtaresti-form body, *Lat* lateral (dentate) nucleus, *Mve* medial vestibular nucleus, *v4* fourth ventricle. (From Kappel 1981; courtesy Rita Kappel, Nijmegen)

In monkey fetuses (Fig. 8.15), an interdigitating pattern of **Purkinje cell clusters** develops in the cortical plate between days 48 and 54 of gestation (Kappel 1981). The subsequent development of the first transverse fissures and the inward migration of the granule cells transforms the Purkinje cell clusters into longitudinal zones. Cell strands connect these zones with the borders of the cerebellar nuclei. The resulting zonal pattern is very similar to the patterns based on corticonuclear and olivocerebellar projections in adult mammals (Voogd 1992, 2004). With the transformation of the multicellular clusters into a monolayer of Purkinje cells, the borders between the zones become lost around the 70th day of gestation. The pattern that evolves from the position of the clusters in the cortical plate and their corticonuclear relations is very similar to the adult longitudinal patterns in the corticonuclear projection. Clustering of Purkinje cells in the cortical plate has also been observed in human fetuses (Hochstetter 1929; Korneliussen 1968; Maat 1981; Fig. 8.16).

Sonic hedgehog (Shh), a member of the hedgehog family of secreted signalling proteins, is expressed in migrating and settled Purkinje cells, and acts as a potent mitogenic signal to expand the granule cell progenitor population (Dahmane et al. 2001; Wechsler-Reya and Scott 2001; Ho and Scott 2002; Marti
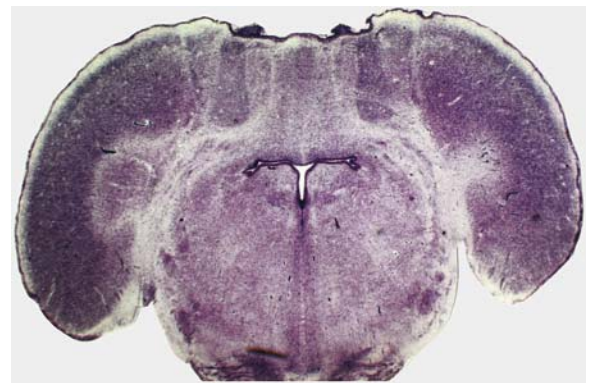
Fig. 8.16 Purkinje cell clusters in a coronal section of a 65-mm crown–rump-length human fetus. The Purkinje cells are located in five multicellular clusters on both sides of the midline. (From the Schenk Collection; courtesy Max Kros, Rotterdam)

and Bovolenta 2002). ***Medulloblastoma***, a brain stem tumour of childhood, may originate from granule cell precursor cells that become transformed and fail to undergo normal differentiation. Mutations in the *PATCHED1* (*PTCH1*) gene that is activated by SHH, may give rise to medulloblastoma (Wechsler-Reya and Scott 2001).

Fig. 8.17 Lhermitte–Duclos disease: **a** axial MRI showing a cerebellar gangliocytoma (between *arrowheads*; courtesy Guido Willems, Leuven); **b** dystrophic gangliocytoma grade I with characteristic hyperplastic cerebellar folia (*arrows*); **c** haematoxylin–eosin-stained section in which the Purkinje-cell layer is lacking and large, dispersed cells are found (*arrows*)
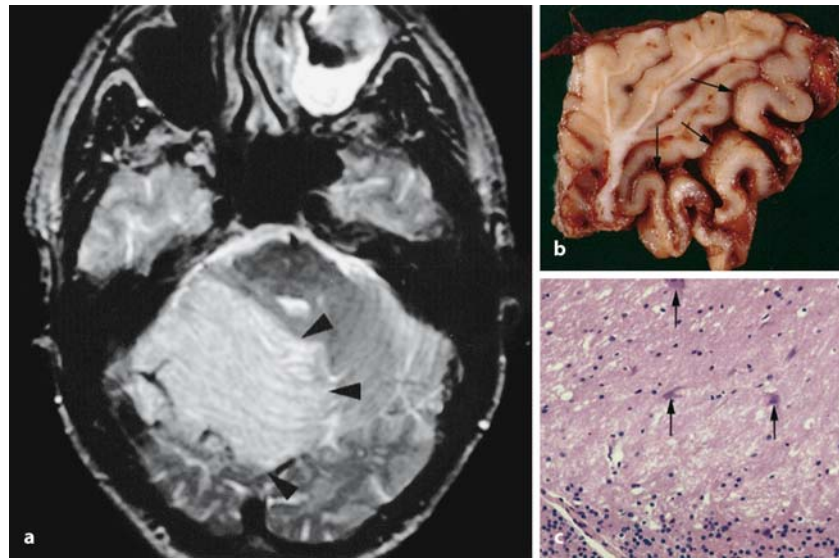
Disturbed proliferation and differentiation of granule cell precursors may give rise to *diffuse hypertrophy* of the *cerebellar cortex* (Beuche et al. 1983), known as Lhermitte–Duclos disease (Lhermitte and Duclos 1920). The gene involved, *PTEN*, is a tumour-suppressor gene playing roles in cell cycle control, apoptosis and mediation of adhesion and migration signalling. *PTEN* germline mutations have been detected in various familial tumour syndromes, including Cowden syndrome and Bannayan–Zonana syndrome. These syndromes are characterized by developmental defects, benign tumours and hamartomas, and a propensity to develop thyroid and breast cancer (Lloyd and Dennis 1963). A subset of patients with Cowden disease develop *cerebellar gangliocytoma* with abnormal and enlarged foliation caused by thickened and broadened layers of dysplastic and disorganized neurons (Fig. 8.17), also known as *Lhermitte–Duclos disease*. Microscopically, a thick layer of abnormal nerve cells underneath the molecular layer replaces the granular layer. Some of these cells are as large as Purkinje cells (Ambler et al. 1969; Friede 1989). These patients can show macrocephaly and mental retardation, and codevelop seizures (Padberg et al. 1991). *Pten*$^{-/-}$ mice show overgrowth of cells and disorganized cell layers in cephalic and caudal regions, resulting in early embryonic lethality (Di Cristofano et al. 1998; Podsypanina et al. 1999). Mice chimeric or heterozygous for *Pten* show an increased spontaneous tumour incidence, whereas inactivation of just one *Pten* allele increases proliferation and cell survival and decreases apoptosis (Di Cristofano et al. 1998; Podsypanina et al. 1998). By inactivating *Pten* at two different times of cerebellar development, Marino et al. (2002) showed that PTEN is essential for cell migration but is not required for cell differentiation

in the cerebellum. Inactivation of *Pten* later during CNS development did not result in proliferation (Backman et al. 2001; Kwon et al. 2001).

8.4.4   Differentiation of Cerebellar Neurons

The differentiation of cerebellar neurons is summarized in Fig. 8.18. Granule cell differentiation is characterized by a prolonged period of clonal expansion that occurs after progenitors have been specified. In contrast, Purkinje cells cease proliferation within the ventricular zone and rapidly express numerous differentiation markers (Hatten and Heintz 1995). *Math1* is expressed in the rhombic lip and, subsequently, in the external granular layer, but its expression is downregulated at later stages of granule cell development (Ben-Arie et al. 1997). In chick embryos, cerebellar rhombic lip derivatives demonstrate a temporal organization with respect to their morphology and response to guidance cues (Gilthorpe et al. 2002). Early-born cells, which migrate into rhombomere 1, have a single long leading process that turns at the midline and becomes an axon. Later-born granule cell precursors also migrate ventrally but halt at the lateral edge of the cerebellum, correlating with a loss of sensitivity to netrin-1 and expression of *Robo2*. The rhombic lip and ventral midline express *Slit2*. Later stages of granule cell development are characterized by changing patterns of gene expression (Kuhar et al. 1993; Hatten et al. 1997). Axon extension is characterized by the expression of the membrane proteins TAG1 and L1, and the migration of granule cells along Bergmann glia into the internal granular layer requires the formation of a cell-surface-neuronal glycoprotein, astrotactin (Zheng et al.
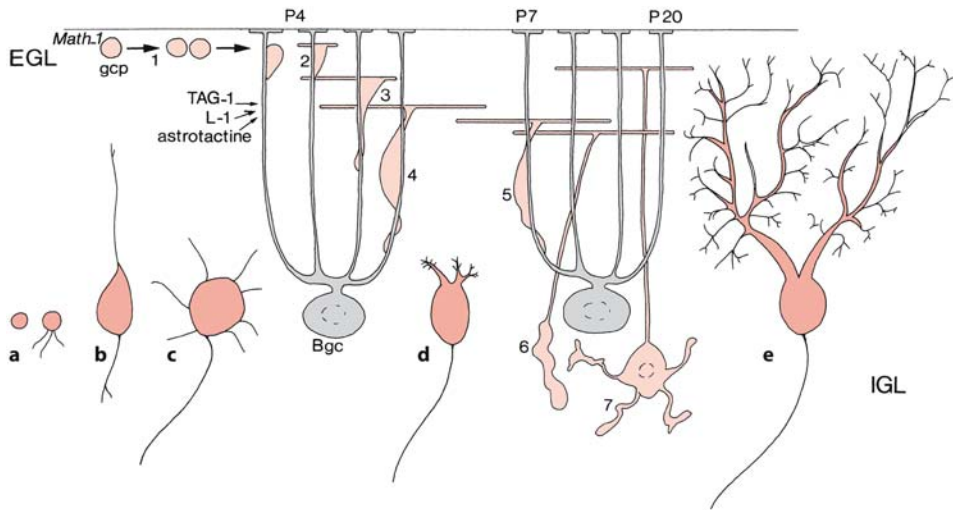
Fig. 8.18 Differentiation of cerebellar cortical neurons. Granule cells (*light red*) arise (*1*) from granule cell precursor cells (*gcp*) in the external granular layer (*EGL*), migrate in several steps (*2–7*) along the dendrites of Bergmann glia cells (*Bgc*) to the internal granular layer (*IGL*). The development of Purkinje cells (*red*) also involves several steps (**a**–**e**). (After Hatten et al. 1997)

1996). *Pax6* regulates granule cell proliferation during parallel fibre formation in the developing cerebellum (Yamasaki et al. 2001). In *Small eye* mice, a naturally occurring mutation resulting from mutations in *Pax6* (Chap. 9), granule cells in the external granular layer fail to form parallel fibre axons and do not migrate tangentially along these fibres.

Milosevic and Zecevic (1998) studied developmental changes in the human cerebellum with antibodies against calcium-binding proteins and phosphorylated and non-phosphorylated neurofilament proteins (SMI31 and SMI32). Calbindin D-28k and both forms of neurofilament proteins were already observed at four to five gestational weeks, parvalbumin appeared in the external granular layer and in a few Purkinje cells at 11 gestational weeks, and there was a diffuse immunostaining for IP$_3$R1 and synaptophysin at 13 gestational weeks. Purkinje cells expressed all examined markers of intracellular calcium signalling as well as the forms of neurofilament protein. At the same time, compartmentalization of the Purkinje cell layer was detected with calcium-signalling molecules and SMI32. Miyata et al. (1999) found that IP$_3$R1 immunoreactivity was first detectable in the somata of multilayered Purkinje cells, just below the molecular layer at 16 weeks of gestation. The IP$_3$R1 immunoreactivity gradually increased from soma to dendrites and spiny branches, and dendritic outgrowth especially progressed until 6 months after birth. Yu et al. (1996) studied the presence of GABA in the developing human cerebellum. As early as the 16th week of gestation, GABA im-

munoreactivity was observed in the cerebellar cortex and the deep nuclei. GABA-positive neurons included Purkinje cells, stellate and basket cells of the cerebellar cortex and neurons in the deep nuclei. GABA-immunoreactive mossy fibres were observed in the granular layer at 16 weeks. By 28 weeks, a robust fibre network was present in the cortex and cerebellar nuclei.

The **deep cerebellar nuclei** arise from the ventricular zone and migrate as two broad streams during the second month of gestation (Sidman and Rakic 1982; Bayer et al. 1995). Cells in the *medial stream* segregate by about the fourth month into fastigial, emboliform, globose and dentate nuclei, whereas those of the *lateral* stream contribute almost only to the dentate nucleus. Murofushi (1974) studied the fetal development of the human **dentate nucleus** (Fig. 8.19). From its early kidney-like form at the end of the embryonic period, the characteristic undulation of the dentate nucleus develops in the fifth fetal month (Jakob 1928), reaching its full gyrification by the seventh fetal month. *Dysplasias* of the dentate nucleus occur in three forms (Friede 1989): (1) a broadened cell band without, or with indistinct, undulation; (2) fragmentation of the nucleus into a string of islands of grey matter; and (3) accessory layers of grey matter. Such dysplasias may occur as isolated, incidental lesions (Murofoshi 1974) or are associated with other malformations. The fragmentation of the dentate nucleus found in histological sections is, in three-dimensional reconstructions, practically a fenestration (Tanaka et al. 1976). Hori et al. (1980)
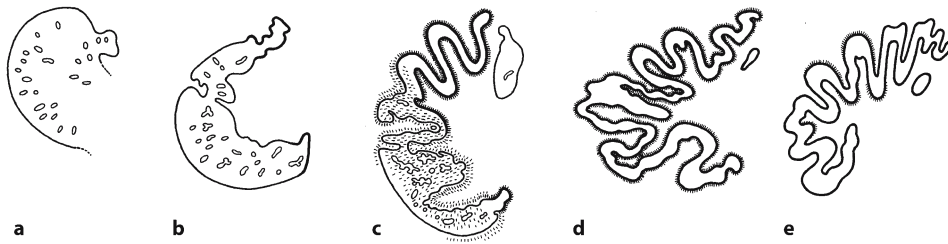
Fig. 8.19 Development of the human dentate nucleus: **a** a 130-mm embryo; **b** a 230-mm embryo; **c** a 250-mm embryo; **d** a 380-mm embryo; **e** at the first postnatal day. The islands indicated in **a** and **b** indicate cell-poor areas. Gyrification is shown in **b**–**e**. (After Murofushi 1974)

Fig. 8.20 Dentate heterotopia (**a**, **b**) and flocculonodular dysgenesis (**c**). **a** Macroscopical section through the cerebellum and brain stem of a 20-year-old man with non-Hodgkin lymphoma who died after pneumonia and toxic colitis. The only neuropathological finding was a small, round heterotopia in the cerebellar white matter. **b** Histologically, this heterotopia appeared to be a differentiated cerebellocortical structure. **c** Example of flocculonodular dysgenesis (courtesy Akira Hori, Toyohashi)
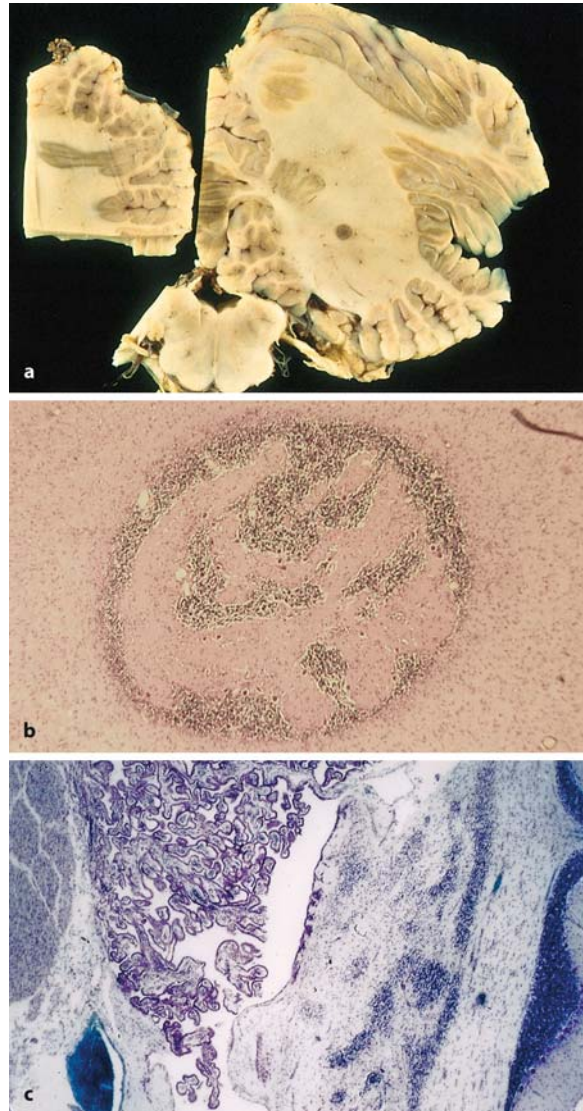
described a completely developed cerebellar cortical heterotopia in the dentate nucleus in Patau syndrome (Clinical Case 8.2). Heterotopic cortical fragments of the differentiated form may be observed in the cerebellar white matter as an incidental finding (Fig. 8.20 a, b). In trisomy cases, especially in trisomy 13 (Patau syndrome) and trisomy 18 (Edwards syndrome), such heterotopia are more frequently found in fetal structure, that is the granule cells are undifferentiated (Friede's matrix cells) and the heterotopic cortical structure is more or less disorganized. A small disorganized cortical structure such as a fragment, consisting of Purkinje cells, granule cells and possibly a molecular layer, is found in the nodulus and flocculus (Fig. 8.20 c), frequently in fetuses and infants with trisomies 13, 18 and 21, but may also be found in otherwise normal brains. A small group of neurons in the cerebellar white matter, probably originating from the dentate nucleus, may also be found incidentally. The frequency of this type of heterotopia is 27.7 % in fetuses, 20 % in infants under 1 year of age and 13.3 % in adults of serial autopsies (Hori 2002). The difference in the frequency between age groups remains unexplained.

Cerebello-cortical Heterotopia in the Dentate Nucleus

CNS malformations in *Patau syndrome* mainly belong to the wide spectrum of holoprosencephaly, combined with cerebellar dysplasias. Hori et al. (1980) described a completely developed cerebellar cortical heterotopia in the dentate nucleus (see Case Report).

Case Report. In a 14-week-old girl with Patau syndrome who died after pneumonia, the following main pathology was found in the CNS: (1) in the cerebrum, enlarged lateral ventricles, aplasia of the olfactory nerves, hyperplasia of the indusium griseum and basal gliomesenchymal dysgenesis; (2) in the cerebellum, flocculonodular dysgenesis, neuronal heterotopia in the white matter, 'heterotaxia' and spindle-shaped cell heterotopia in cerebellar nuclei; and (3) in the brain stem, hyperplasia of the cochlear nuclei and pontine gliomesenchymal dysgenesis. Heterotopic nerve cells, originating from pontine nuclei, were observed in the white matter. Disorganized cerebello-cortical structures, known as 'heterotaxia', were observed in the central white matter. Moreover, a completely differentiated and organized cerebello-cortical structure was found in the dentate nucleus

(Fig. 8.21 a, b). These heterotopic areas contained the usual cerebellar cortical elements, consisting of the internal granular layer, the Purkinje-cell layer, the molecular layer, the fetal external granular layer and vessels with possibly leptomeninges. Spindle-shaped cell nests in the cerebellar nuclei occur in high incidence in premature and full-term infants under 4 months of age (Jellinger 1972; Friede 1973). They are considered to be a variation of normal development. Those seen in cases of trisomy, however, have been viewed differently. Hori et al. (1976) found a spatial continuity of external granular cells to spindle cells in the dentate nucleus, suggesting that spindle-shaped cell nests in the cerebellar nuclei should be regarded as heterotopic external granular cells.

References

Friede RL (1973) Dating the development of human cerebellum. Acta Neuropathol (Berl) 5:243–251

Hori A, Murofushi K, Iizuka R (1976) Zentralnervöse Dysgenesien bei Dyscranio-pygo-phalangia. Acta Neuropathol 35:327–332

Hori A, Peiffer J, Pfeiffer RA, Iizuka R (1980) Cerebello-cortical heterotopia in dentate nucleus, and other microdysgeneses in trisomy D1 (Patau) syndrome. Brain Dev 2:345–352

Jellinger K (1972) Embryonal cell nests in human cerebellar nuclei. Z Anat Entwickl-Gesch 138:145–154
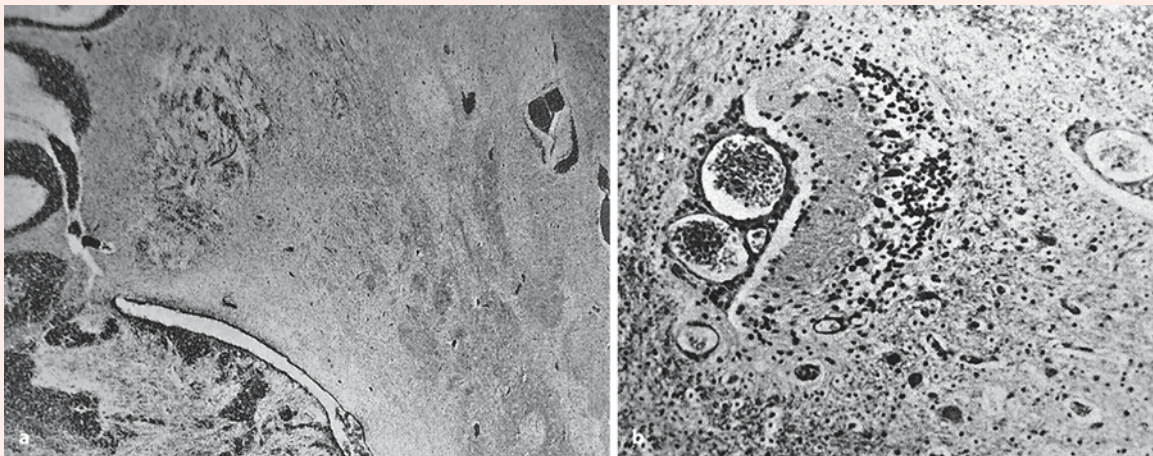
Fig. 8.21 Cortical heterotopia in the dentate nucleus: **a** disorganized cerebello-cortical structure in the cerebellar white matter; **b** completely differentiated and organized cerebello-cortical structure in the dentate nucleus (from Hori et al. 1980, with permission; courtesy Akira Hori, Toyohashi)

Fig. 8.22 Gross morphogenetic events in the rat cerebellum between E13 (**a**) and E16 (**b**). The cerebellar primordium and the precerebellar primordium are shown in *light red* and *red*, respectively. *CP* cerebellar primordium, *mes* mesencephalon, *PCN* precerebellar primordium, *v4* fourth ventricle. (After Altman and Bayer 1997)
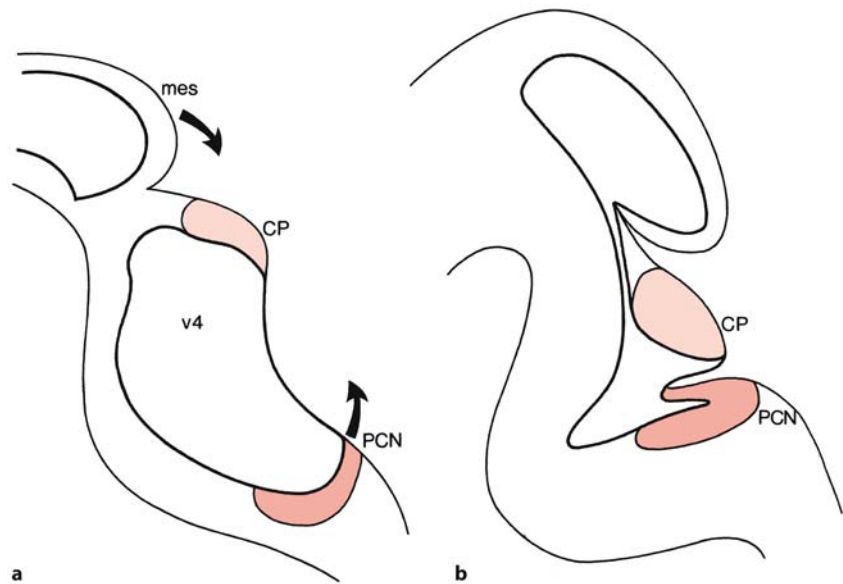
8.5   Development of the Precerebellar Nuclei

The caudal part of the rhombic lip, i.e. the lower rhombic lip, gives rise to the pontine nuclei, the pontine reticulotegmental nucleus, the inferior olivary nucleus, the external cuneate nucleus and the lateral reticular nucleus (Essick 1912; Altman and Bayer 1987a–c, 1997; Wingate 2001; Fig. 8.22). Neurons of these upper and lower precerebellar systems migrate along various pathways, the corpus pontobulbare in particular, to their ultimate position in the brain stem (Altman and Bayer 1997). In their extensive [³H]thymidine studies in rats, Altman and Bayer (1978b, 1987a–c) showed that the precerebellar nuclei arise sequentially: (1) 72 % of the neurons of the inferior olive are generated on E13; (2) the lateral reticular nucleus is generated between E13 and E15; (3) the nucleus reticularis tegmenti pontis has a neurogenetic peak on E16; and (4) neurons for the pontine nuclei are mainly produced on E17 and E18. Bayer et al. (1995) estimated that the human precerebellar nuclei are generated from the early fifth week up to and including the 11th week of development, presumably in a similar sequence (Table 8.2). Altman and Bayer (1987a–c, 1997) distinguished anterior (secondary) and posterior (primary) parts of the precerebellar neuroepithelium, giving rise to the upper and lower precerebellar nuclei, respectively (Fig. 8.23). Netrin has a general role in guiding ventral migration of precerebellar neurons (Bloch-Gallego et al. 1999; Yee et al. 1999; Alcantara et al. 2000).
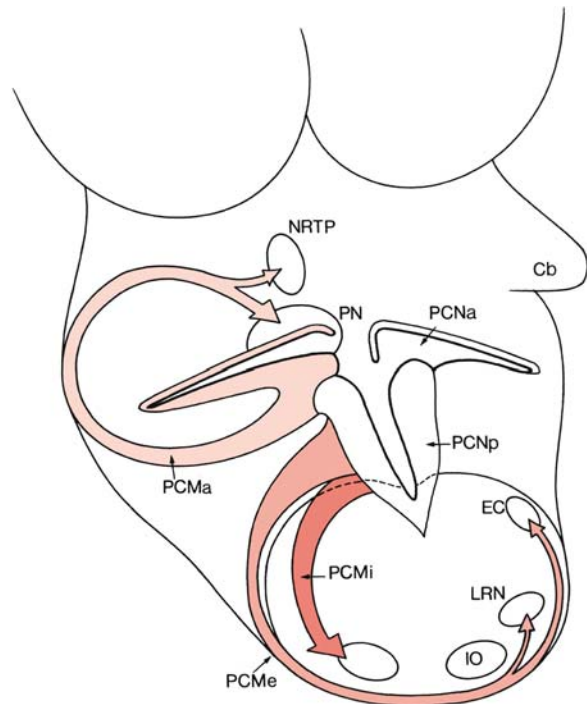
Fig. 8.23 Migratory pathways of the precerebellar nuclei. *Cb* cerebellum, *EC* external cuneate nucleus, *LRN* lateral reticular nucleus, *IO* inferior olive, *NRTP* nucleus reticularis tegmenti pontis, *PCMa* anterior (pontine) precerebellar migration, *PCMe* extramural (superficial) precerebellar migration, *PCMi* intramural (olivary) precerebellar migration, *PCNa* anterior precerebellar neuroeipthelium, *PCNp* posterior precerebellar neuroeipthelium, *PN* pontine nuclei. (After Altman and Bayer 1997)

8.5.1 Upper Precerebellar System

The pontine nuclei and the nucleus reticularis tegmenti pontis form the upper precerebellar system and arise from the anterior precerebellar neuroepithelium in the rostral part of the lower rhombic lip. Via the *anterior precerebellar migration* or *pontine stream* these neurons reach their final position in about 3 days in rats (Altman and Bayer 1987c; Fig. 8.23). Neurons migrating towards the pontine nuclei express the netrin receptor *DCC* (Engelkamp et al. 1999; Yee et al. 1999; Alcantara et al. 2000) and upregulate a second receptor, *Unc5H3*, at their target (Engelkamp et al. 1999).

8.5.2 Lower Precerebellar System

Neurons of the lower precerebellar system are the first cells to arise from the posterior precerebellar neuroepithelium of the lower rhombic lip. Via two streams they reach their final position (Fig. 8.23): (1) the *posterior precerebellar intramural migration* or *olivary stream* forms the inferior olive; and (2) the *posterior precerebellar extramural migration* or *superficial stream* forms the lateral reticular and external cuneate nuclei. In rats, inferior olivary neurons reach their final position in about 4 days, lateral reticular neurons in 4 days and external cuneate neurons in 5 days (Altman and Bayer 1987 a, b). Cells migrating to the inferior olive, like neurons for the pontine nuclei, express *DCC* and *Unc5H* homologues. Netrin signalling may play a role in the finer subdivision of this nucleus. In *Netrin-1* knockout mice, a reduced inferior olive and ectopic neurons expressing inferior olive markers were found (Bloch-Gallego et al. 1999). The cells of the superficial stream are preceded by long leading processes (Kyriakopoulou et al. 2002). The adhesion molecule TAG-1 is involved in the su-
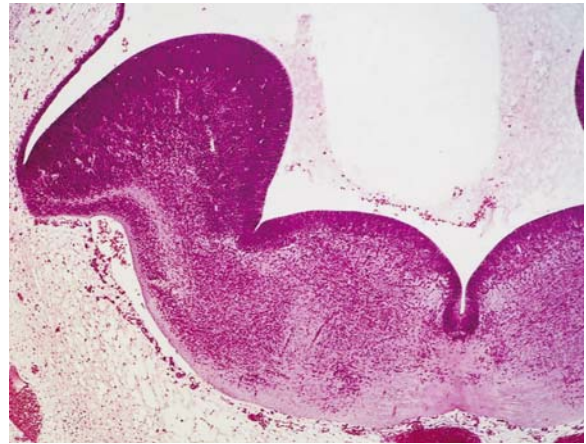
Fig. 8.24 Migration stream to inferior olive shown in a Carnegie stage 20 embryo (from the Kyoto Collection of Human Embryos; courtesy Kohei Shiota)

perficial migration. The olivary stream in a Carnegie stage 20 human embryo is shown in Fig. 8.24. Murofushi (1974) studied the development of the human inferior olive (Fig. 8.25). From its plump, U-shaped early form at the end of the embryonic period, gyrification occurs and is fully developed by the sixth fetal month. With the rapid Golgi technique, Marín-Padilla (1985) studied the development of climbing fibres in the human cerebellum. Climbing fibres arrive at the Purkinje cell plate by the 28th week of gestation and establish a transient plexus before contacting Purkinje cells. They start to form pericellular nests around Purkinje cells by the 29th week. These nests are rapidly transformed into transient supracellular 'capuchones' by the 34th week from which the climbing process starts. Climbing fibres climb the dendrites of the Purkinje cells from the 36th week of gestation until late prenatal and early postnatal life.
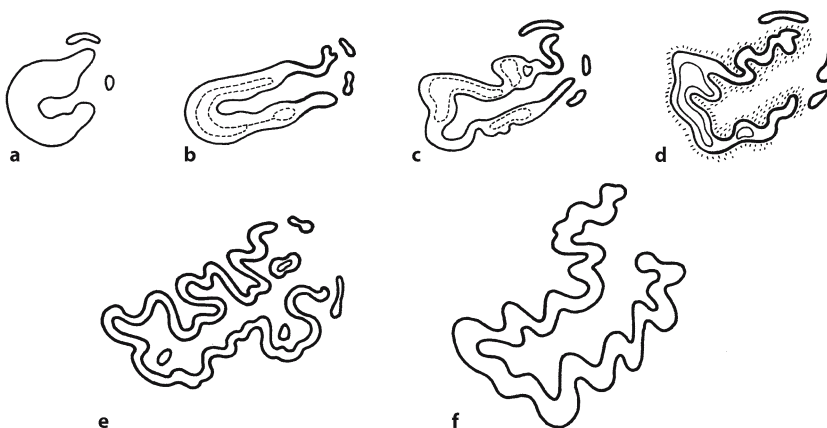
Fig. 8.25 Development of human inferior olivary nucleus: **a** a 130-mm embryo; **b** a 200-mm embryo; **c** a 250-mm embryo; **d** a 260-mm embryo; **e** a 300-mm embryo; **f** at the first postnatal day (after Murofushi 1974)

Fig. 8.27 Inferior olivary heterotopia in a case of Miller–Dieker syndrome (courtesy Martin Lammens, Nijmegen)

Fig. 8.26 Inferior olivary malformations: **a** medially situated inferior olives in a case of X-linked hydrocephalus; **b** overgyrification in a case of occipital encephalocele; **c** plump, nongyrified inferior olives in a case of X-linked hydrocephalus (courtesy Pieter Wesseling, Nijmegen)

8.5.3   Inferior Olivary Malformations

Two types of dysplasias of the inferior olivary nuclei can be distinguished (Hanaway and Netsky 1971; Friede 1989): (1) heterotopia; and (2) a dysplastic shape of the nucleus. Examples are given in Figs. 8.26 and 8.27. *Heterotopia* of the inferior olivary nuclei typically associate with lissencephalies (Friede 1989). They are also found with the Dandy–Walker malformation and other vermis malformations. They consist of single or multiple irregularly shaped islands of grey matter dispersed along a line extending from its normal position to the lateral floor of the fourth ventricle near the corpus restiforme (Friede 1989). Less frequently, heterotopic islands are found more medially. Olivary heterotopia mimic the characteristic convoluted shape of the inferior olive. *Dysplasias* of the shape of the inferior olivary nucleus occur with cerebellar malformations, trisomies 13 and 18, Zellweger syndrome and holoprosencephaly. Segments of the nucleus are thickened with obliteration of the normal undulating profile. In more severe lesions, the inferior olive has a greatly simplified C-shape.

Absence of the inferior olivary nuclei has been found in *congenital olivopontocerebellar atrophy*. Park et al. (1998) reported two siblings born at 32 and 37 gestational weeks, respectively, with microcephaly, an atrophic pons with near-total loss of pontine nuclei and transverse pontocerebellar tracts, absent inferior olivary and arcuate nuclei, and hypoplasia of the cerebellum with rudimentary dentate nuclei and profound loss of Purkinje cells. These abnormalities presumably result from antenatal degeneration or atrophy of neurons in the involved sites rather than hypoplasia or developmental arrest.

8.6   Mouse Mutants with Cerebellar Malformation

More than 20 mouse mutants are known that affect the cerebellum, the best studied of which are *reeler*, *weaver* and *staggerer* (Caviness and Rakic 1978; Mullen et al. 1997; Millen et al. 1999; Table 8.3). The *reeler* mutant mouse has generated more interest than any other mutant mouse since its discovery by Falconer (1951). *Reeler* mice show severe malformations of the CNS, of the cerebellum in particular, owing to mutations of the *Reelin* (*Reln*) gene (Mullen et al. 1997). The cerebellum is atrophic and hardly shows fissures. The majority of the Purkinje cells fail to migrate, and they reside in an ectopic position (Figs. 8.28, 8.29c). Granule cells reach the internal granular layer but are greatly reduced in number.

Table 8.3 Mouse mutants with cerebellar malformation (after Caviness and Rakic 1978; Mullen et al. 1997; Millen et al. 1999)

Mutant and gene symbol	Inheritance	Cerebellar malformations	References
Dreher (Dr)	Autosomal recessive	Most of vermis is missing	Lyon (1961); Deol (1964); Wahlsten et al. (1983); Washburn and Eicher (1986); Sekiguchi et al. (1992)
Leaner (tg^{1a})	Autosomal recessive	Degeneration of granule cells in anterior and nodular lobes	Sidman (1968); Meyer and MacPike (1971)
Lurcher (Lc)	Autosomal semidominant	Homozygotes die perinatally; the cerebellum of heterozygotes is only half normal size. Purkinje cells degenerate	Hilips (1960); Caddy and Briscoe (1975); Swisher and Wilson (1977)
Meander tail (Mea)	Autosomal recessive	Affects anterior cerebellar structure; cell patterning disrupted	Ross et al. (1989); Hamre et al. (1997); Rosario et al. (1997)
Nervous (Nr)	Autosomal recessive	90% of Purkinje cells die between 3 and 6 weeks of age	Landis (1973); Mullen and LaVail (1975)
Purkinje cell degeneration (Pcd)	Autosomal recessive	Degeneration of all Purkinje cells between the 15th day and the 3rd month of age	Mullen et al. (1976); Landis and Mullen (1978)
Reeler (Rl)	Autosomal recessive	Malposition of neuron classes in cerebellum and other structures	Falconer (1951); Rakic (1976); Mariani et al. (1977)
Rostral cerebellar malformation (Rcm)	Autosomal recessive	Cerebellar tissue extends rostrally into the midbrain	Lane et al. (1992); Ackerman et al. (1997); Eisenman and Brothers (1998); Przyborski et al. (1998)
Staggerer (Sg)	Autosomal recessive	Dysplastic dendritic trees of Purkinje cells; no Purkinje cell – parallel fibre synapses	Sidman et al. (1962); Sotelo (1975a); Landis and Reese (1977)
Swaying (Sw)	Autosomal recessive	Deletion of cerebellar anterior midline structures and of inferior colliculus	Lane (1970); Thomas et al. (1991)
Weaver (Wv)	Autosomal recessive	Most cells of external granular layer degenerate before migration	Lane (1964); Rezai and Yoon (1972); Rakic and Sidman (1973a, b); Sotelo (1975b)
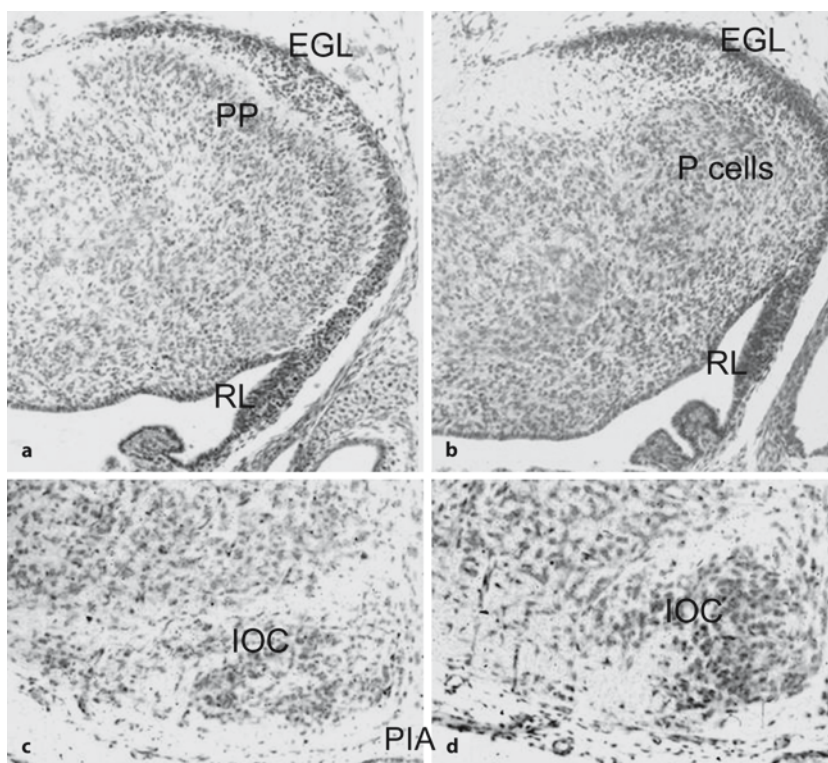
Fig. 8.28 Normal (**a**, **c**) and reeler-like (**b**, **d**) sections through the cerebellum (**a**, **b**) of E15 mice and the inferior olivary complex (*IOC*; **c**, **d**) of E17.5 mice. *EGL* external granular layer, *P cells* disorganized Purkinje-cell-layer, *PP* Purkinje cell plate, *RL* rhombic lip. (Reproduced with permission from Tissir and Goffinet 2003, *Nat. Rev. Neurosci.* 4:496–505; copyright 2003, Macmillan Magazines Ltd.)
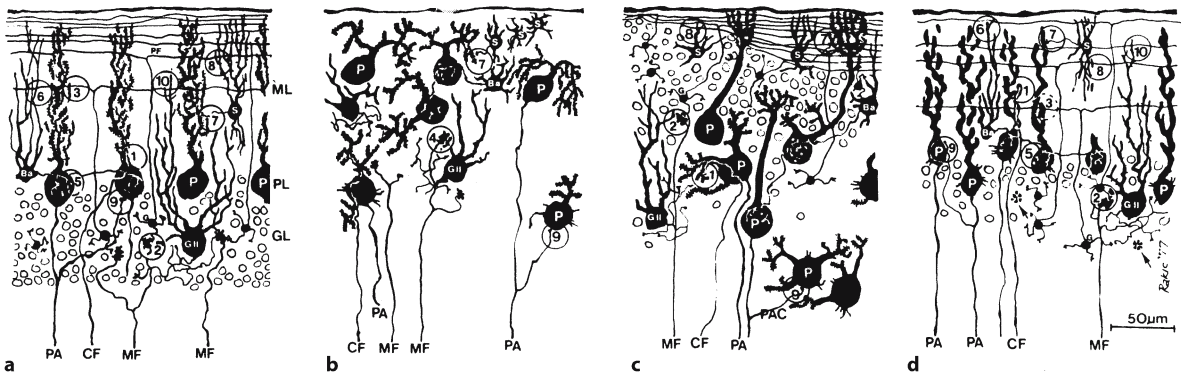
Fig. 8.29 Neuronal arrangement and synaptic circuitry of normal (**a**), homozygous *weaver* (**b**), *reeler* (**c**) and *staggerer* (**d**) mice (see text for further explanation). *Ba* basket cells, *CF* climbing fibre, *G* granule cell, *GII* Golgi type II cell, *MF* mossy fibre, *P* Purkinje cell, *PA* Purkinje cell axon, *PF* parallel fibre, *S* stellate cell. The numbers refer to major classes of synapses. (Reprinted with permission from Caviness and Rakic 1978, *Annu. Rev. Neurosci.* 1:297–326; copyright 1978, Annual Reviews)

Malformations in the inferior olivary nucleus are also present (Goffinet 1983; Goffinet et al. 1984). The human *Reelin* (*RELN*) gene is localized on chromosome 7q22. *RELN* mutations cause autosomal recessive lissencephaly with cerebellar hypoplasia (Hong et al. 2000; Chap. 10).

In the mouse mutant *weaver*, the granule cells degenerate after their first cell division (Mullen et al. 1997). *Weaver* mice have a near-total loss of granule cells in the cerebellar vermis that accounts for a diminutive cerebellum and an ataxic gait. Rakic and Sidman (1973a, b) described the developmental and mature phenotypes of the homozygous and heterozygous mutant cerebellum (Fig. 8.29b). Bergmann glia are abnormal in the *weaver* cerebellum, resulting in disruption of radial migration of postmitotic granule cells in the external granular layer and their death (Rakic and Sidman 1973c). Zebrin-labelling showed regionalization defects in *weaver* cerebellum (Eisenman et al. 1998). The most obvious defect in adult homozygous *staggerer* mice is the near-total absence of granule cells (Sidman et al. 1962). This absence is due to both a reduced proliferation (Yoon 1972) and degeneration of granule cells after they have migrated to the internal granular layer. Abnormalities in Purkinje cells include small size, ectopic location and a reduced dendritic tree (Hirano and Dembitzer 1975; Landis and Sidman 1978; Fig. 8.29d). About 60–90% of the Purkinje cells are missing in *staggerer* mice (Herrup 1983). Herrup and Mullen (1979a, b) demonstrated that in *staggerer* mice granule cell loss is secondary to the Purkinje cell defect. The *staggerer* mutation is a deletion in a gene encoding an orphan nuclear hormone receptor, RORα (Hamilton et al. 1996).

8.7 Developmental Disorders of the Cerebellum

Anatomically, cerebellar malformations may be classified into unilateral and bilateral abnormalities. Unilateral cerebellar malformations are most likely due to acquired insults, such as intracerebellar bleeding associated with prematurity (Grunnet and Shields 1976). Depending on the part of the cerebellum involved, bilateral cerebellar malformations may be further classified into midline or vermis malformations, and malformations affecting both the vermis and the cerebellar hemispheres (Kollias and Ball 1997; Ramaeckers et al. 1997; ten Donkelaar et al. 2003). The combination of pontine hypoplasia with cerebellar malformation is considered as a separate group, i.e. the pontocerebellar hypoplasias (Barth 1993; Ramaeckers et al. 1997). Cortical dysplasias are discussed separately.

8.7.1 Midline or Vermis Malformations

Agenesis or hypoplasia of the vermis may be found in a large number of malformations of the brain (Hart et al. 1972; Friede 1989; Bordarier and Aicardi 1990; Costa and Hauw 1995; Norman et al. 1995; Kollias and Ball 1997; Ramaeckers et al. 1997; Barkovich 2000), including (1) the Dandy–Walker malformation and syndromes with agenesis of the vermis as a constant feature, such as the Joubert syndrome and Walker–Warburg syndrome, (2) a large group of syndromes in which absence of the vermis may occur, such as the Meckel–Gruber and Smith–Lemli–Opitz syndromes, and (3) dysgenesis of the vermis in rare disorders,

such as rhombencephalosynapsis, tectocerebellar dysraphia and Lhermitte–Duclos disease. Major malformations of the cerebellar midline structures are also found in the Chiari malformations. The most common type, i.e. type II Chiari malformation, is almost always associated with a myelomeningocele, and is part of the neural tube defect spectrum (Chap. 4). A high percentage of diagnosed dyslexic children show behavioural evidence of abnormal cerebellar function (Habib 2000; Nicholson et al. 2001; Voeller 2004). Quantitative MRI studies showed that lobules VI–VII of the vermis are reduced in idiopathic autism, whereas increased size was noted when autism was associated with fragile X syndrome. These data suggest that lobules VI–VII are hyperplastic in a subset of boys with idiopathic autism and cerebral and hippocampal enlargements in fragile X syndrome (Kaufmann et al. (2003).

The **Dandy–Walker malformation**, named by Benda (1954) after the first descriptions of Dandy and Blackfan (1914) and Taggart and Walker (1942), is characterized by the following triad (Hart et al. 1972; Friede 1989; Bordarier and Aicardi 1990; Osborn 1994; Norman et al. 1995; Kollias and Ball 1997; Barkovich 2000): (1) cystic dilatation of the fourth ventricle and an enlarged posterior fossa with upward displacement of the lateral sinuses, confluens sinuum and tentorium cerebelli; (2) varying degrees of vermian aplasia or hypoplasia; and (3) hydrocephalus (Fig. 8.30 b, c). Hydrocephalus, associated with a bulging occiput, is unusual at birth but is present by 3 months of age in about 75 % of patients (Barkovich 2000). Early shunting of the cyst and hydrocephalus is advocated because early management may give mental development a better chance and improve prognosis (Bordarier and Aicardi 1990). Mental retardation and seizures have been reported in up to 50 % of cases with a Dandy–Walker malformation (Pascual-Castroviejo et al. 1991). Most cases are sporadic. Associated CNS malformations are present in up to 68 % of the cases, the most common of which is agenesis or hypogenesis of the corpus callosum (Fig. 8.30 b, c). Other CNS malformations include neuronal heterotopias, polymicrogyria, schizencephaly, occipital encephaloceles and lumbosacral meningoceles (Hart et al. 1972; Bordarier and Aicardi 1990). Extraneural malformations are found in about one third of the cases, particularly in familial ones, and include cleft lip and palate, cardiac malformations, urinary tract anomalies, polydactyly and syndactyly and minor facial dysmorphisms (Hart et al. 1972; Bordarier and Aicardi 1972; Clinical Case 8.3).

The aetiology of the Dandy–Walker malformation remains unknown. Probably, the malformation arises late in the embryonic period. Hypotheses include developmental arrest in the formation of the hindbrain, atresia of the fourth ventricular outlet foramina and delayed opening of the aperture of Magendie. The choroid plexus of the fourth ventricle arises in the middle of the thin roof of the hindbrain (Brodal and Hauglie-Hanssen 1959; Brocklehurst 1969). The area rostral to the plexus, i.e. the area membranacea superior of Weed, disappears during the formation of the vermis (Fig. 8.30 a). Late in the embryonic period, the median aperture or foramen of Magendie arises in the area membranacea inferior, caudal to the plexus, and forms a connection between the fourth ventricle and the subarachnoid space. The lateral apertures or foramina of Luschka are formed in the fetal period. In one fifth of a large series of normal brains examined, the apertures of Luschka were not open, mostly bilaterally (Alexander 1931); therefore, atresia of the apertures of Luschka does not play a role in the aetiology of the Dandy–Walker malformation. If the superior membranaceous area is not incorporated into the developing choroid plexus or if there is delayed opening of the aperture of Magendie, the roof of the fourth ventricle can balloon posteriorly to form a fourth ventricular cyst, identical to what is seen in the Dandy–Walker malformation (Brodal and Hauglie-Hanssen 1959; Barkovich 2000). Evidence that such a phenomenon may occur comes from a strain of mice with congenital hydrocephalus in which the superior membranaceous area remains, leading to a large cyst between the vermis and the choroid plexus (Bonnevie and Brodal 1946). The formation of a large cyst in the posterior fossa impairs normal outgrowth of the vermis and corpus callosum.

Barkovich and others (Barkovich et al. 1989; Bordarier and Aicardi 1990; Barkovich 2000) advocated the **Dandy–Walker complex** as a continuum of posterior fossa anomalies comprising the Dandy–Walker malformation, the Dandy–Walker variant and mega cisterna magna. In the Dandy–Walker variant, the posterior fossa is hardly enlarged; there is agenesis of the vermis, communication between the fourth ventricle and arachnoid space, and no hydrocephalus is present (Fig. 8.30 d). The mega cisterna magna consists of an enlarged posterior fossa, secondary to an enlarged cisterna magna, but a normal vermis and fourth ventricle are found. For malformations of the posterior fossa with prominent cyst-like CSF-containing spaces that fail to fulfil all the criteria for the diagnosis Dandy–Walker malformation, such as the absence of hydrocephalus, Kollias and Ball (1997) suggested the broad term *vermian-cerebellar hypoplasia*. Association of vermian-cerebellar hypoplasia with supratentorial abnormalities similar to those found in the Dandy–Walker malformation, such as absence or hypoplasia of the corpus callosum, indicates that these defects occur at the same time of development, presumably in the early fetal period. Although true Dandy–Walker malformation and ver-
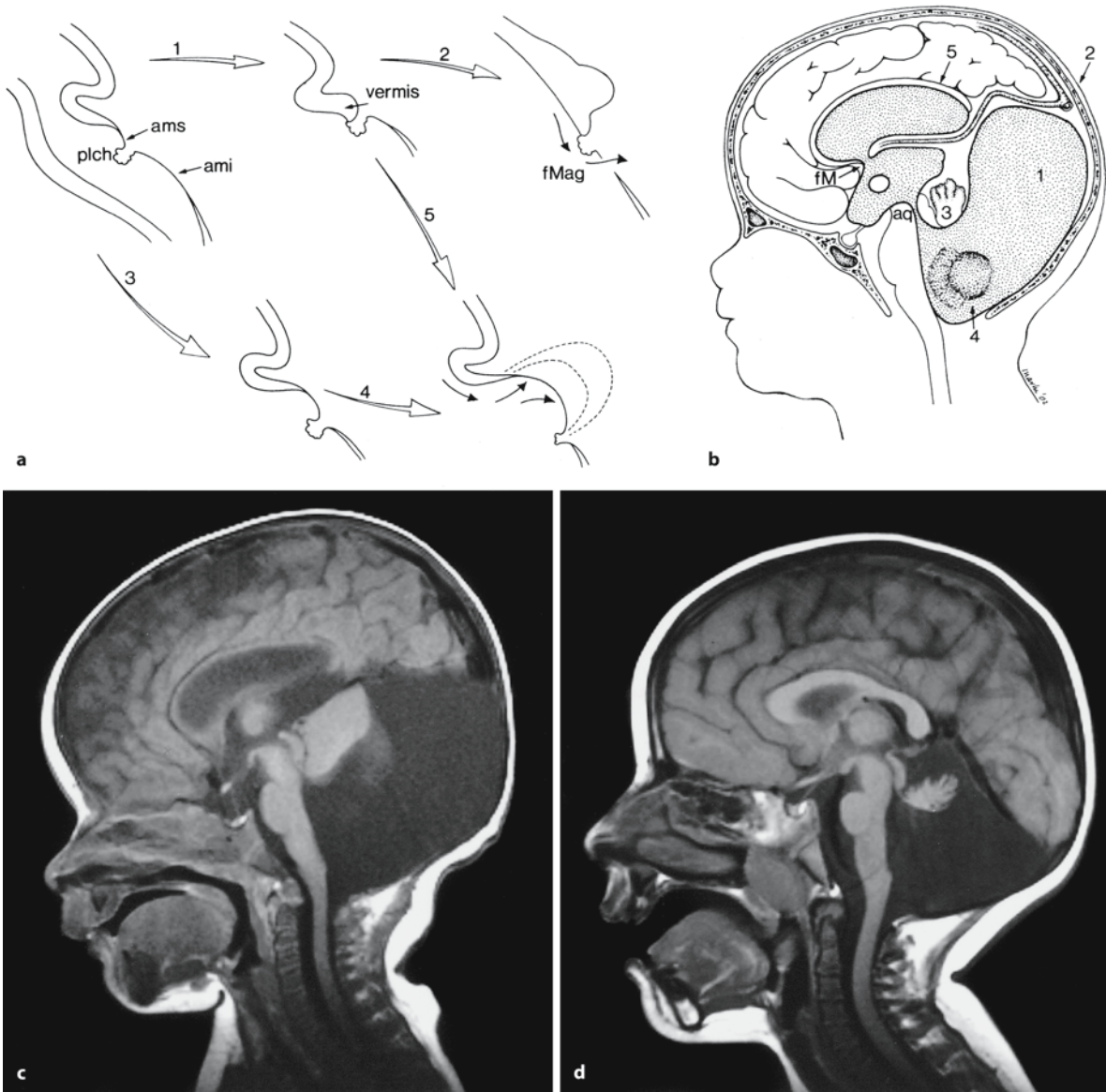
Fig. 8.30 The Dandy–Walker malformation. **a** Its possible pathogenesis. The area membranacea superior of Weed (*ams*), rostral to the plexus choroideus of the fourth ventricle (*plch*), normally disappears during the formation of the *vermis* (*1*). Late embryonically, the foramen of Magendie (*fMag*) arises in the area membranacea inferior (*ami*; *2*). A delayed development with persistence of the area membranacea superior (*3*, *4*), or late opening of the foramen of Magendie (*5*) may give rise to the Dandy–Walker malformation. **b** Its key features: *1* a large cyst in the posterior cranial fossa; *2* elevation of the confluens sinuum (torcular Herophili); *3* hypoplastic vermis; *4* hypoplastic cerebellar hemispheres; *5* hypoplasia of the corpus callosum. *aq* aqueduct, *fM* foramen of Monro. **c**, **d** MRI of a Dandy–Walker malformation (**c**), and a Dandy–Walker variant (**d**). Note in **c** the large cyst in the posterior fossa, the hydrocephalus, elevation of the structures, forming the roof of the posterior fossa, and hypoplasia of the corpus callosum. In the Dandy–Walker variant (**d**), no hydrocephalus and a normal corpus callosum can be seen. (**a** After Brocklehurst 1969; **b** after Osborn 1994; **c**, **d** courtesy Henk Thijssen, Nijmegen)

mian-cerebellar hypoplasia are often associated with supratentorial and extraneural malformations, most of these cases cannot be classified according to well-defined syndromes (Kollias and Ball 1997).

Distinguishing inheritable syndromes from isolated cases of vermian-cerebellar hypoplasia is important for genetic counselling. Bordarier and Aicardi (1990) classified the genetically heritable syndromes with complex vermian-cerebellar hypoplasia into two groups: (1) those in which vermis aplasia is a constant feature, the most common entities being Joubert syndrome, Walker–Warburg syndrome and

related cerebro-oculomuscular syndromes; and (2) those in which vermis aplasia is an occasional component, such as Meckel–Gruber syndrome, oro-facio-digital syndromes, Coffin–Siris syndrome, Smith–Lemli–Opitz syndrome and Ellis–van Creveld syndrome, all autosomal recessive traits. Vermian aplasia may also occur in X-linked disorders such as Aicardi syndrome. Most of these syndromes include severe mental retardation and have a worse prognosis than isolated vermian-cerebellar hypoplasia or the Dandy–Walker malformation. Moreover, the risk of recurrence in siblings is high (Bordarier and Aicardi 1990; Aicardi 1998).

Joubert syndrome is a relatively rare, autosomal recessive disorder defined by vermis hypoplasia (Clinical Case 8.4), hypotonia, developmental delay and at least one of two additional manifestations: abnormal breathing pattern (hyperpnea intermixed with central apnea in the neonatal period) or abnormal eye movements (De Haene 1955; Joubert et al. 1969; Kendall et al. 1990; Saraiva and Baraitser 1992; Yachnis and Rorke 1999; ten Donkelaar et al. 2000). Recent diagnostic criteria (Maria et al. 1999) include typical facial features (prominent forehead, upturned nose, open mouth). In the ophthalmological literature, Joubert syndrome is known as a condition with a variable combination of CNS defects together with a distinctive congenital retinal dystrophy and oculomotor abnormalities in early infancy (Lambert et al. 1989). So far, the underlying gene defect is unknown. In addition, no evidence for *WNT1* mutations was found (Pellegrino et al. 1997). A role for *EN1*, *EN2* and FGF8 has also been excluded (Blair et al. 2002). Ataxia, mental retardation and behavioural disorders become manifest in late infancy and childhood, at a time when the respiratory anomalies decrease and become undetectable (Aicardi 1998). The prognosis for Joubert syndrome is poor. There is severe mental and motor retardation and the 5-year survival is about 50% (Saraiva and Baraitser 1992).

8.7.2   Cerebellar Hypoplasia

In cerebellar hypoplasia, the cerebellum does not reach its normal size. Global cerebellar hypoplasia may result from a variety of exogenous or endogenous factors (Sarnat and Alcalá 1980; Friede 1989; Norman et al. 1995; Ramaeckers et al. 1997). It is found as a result of intrauterine exposure to drugs (e.g. phenytoin) or irradiation, and as an autosomal recessive trait in a variety of chromosomal disorders, such as trisomies 13, 18 and 21. Moreover, cerebellar hypoplasia may be found in various complex malformations involving the brain and other systems (Ramaeckers et al. 1997). *Primary degeneration* of the *granular layer* of the cerebellum or *granular layer*

aplasia (*GLA*) occurs as an autosomal regressive disorder (Norman 1940; Sarnat and Alcalá 1980; Pascual-Castroviejo et al. 1994). All of the pathologically documented GLA cases showed aplasia or severe hypoplasia of the cerebellar granule layer accompanied by widespread architectonic disturbances of the Purkinje cell layer, especially the presence of heterotopic Purkinje cells with dendritic abnormalities in the molecular layer (Pascual-Castroviejo et al. 1994). Pascual-Castroviejo (2002) found seven patients with features consistent with GLA to have elevated levels of serum asialotransferrin and heterozygous deficiency of phosphomannomutase type 2 (PMM2). This deficit is involved in the *congenital disorders of glycosylation* (*CDGs*). GLA and the CDG type 1 syndrome may constitute a single nosological entity (Pascual-Castroviejo 2002). Recently, Pascual-Castroviejo et al. (2003) described a case of cerebellar hypoplasia with heterotopic Purkinje cells in the molecular layer and preservation of the granule layers associated with severe encephalopathy.

8.7.3   Pontocerebellar Hypoplasias

The *pontocerebellar hypoplasias* form a large group of disorders characterized by a smaller volume of the pons and varying degrees of cerebellar hypoplasia up to near-total absence of the cerebellum (Barth 1993; Ramaeckers et al. 1997; Gardner et al. 2001). Most types of pontocerebellar hypoplasia arise in the fetal period, suggesting a rhombic lip defect and the *MATH1* gene as a candidate for this disorder. Most pontocerebellar hypoplasias are autosomal recessive disorders; for most of these the responsible gene defect has not yet been identified. Two cases of pontocerebellar hypoplasia are illustrated in Figs. 8.34 and 8.35. Pontocerebellar hypoplasias can be classified into congenital olivopontocerebellar atrophy (Young et al. 1992; Park et al. 1998), the type I and type II pontocerebellar hypoplasias with spinal atrophy (Goutières et al. 1977; Weinberg and Kirkpatrick 1995) and extrapyramidal dysfunction (Peiffer and Pfeiffer 1977; Barth et al. 1990), respectively, and the CDGs, types I and III (Stibler and Jaeken 1990; Stibler et al. 1993; Jaeken and Casaer 1997). CDGs, formerly known as carbohydrate-deficient glycoprotein syndromes, are autosomal recessive, multisystemic disorders characterized by glycosylation defects of glycoproteins which are involved in many different metabolic functions (Hagberg et al. 1993; Keir et al. 1999; Jaeken and Carchon 2000). The *type I CDG syndrome* or Jaeken syndrome is a multisystem disorder with major neurological involvement (Clinical Cases 3.5, 8.5). The major manifestations are dysmorphic features (internal strabism, large dysplastic ears, subcutaneous fat deposits at the lower part of the back as

Dandy–Walker Syndrome

The ***Dandy–Walker malformation*** is characterized by (1) cystic dilatation of the fourth ventricle and an enlarged posterior fossa with upward displacement of the tentorium and its sinuses, (2) varying degrees of vermian aplasia or hypoplasia and (3) hydrocephalus, mostly appearing a few months after birth. A fetal case is shown as the Case Report.

Case Report.   Twin girls were born immaturely after 23 weeks of gestation. At autopsy, the first infant showed no malformations, whereas the second girl had craniofacial, heart and CNS malformations. The weight of the second child was 422 g and her crown–heel length was 27.5 cm. The placenta was monochorionic and biamnionic, suggesting that the twins were monozygotic. The craniofacial malformations included lateral clefts of the upper lip, philtrum and gingiva, extending into a widely clefted palate, rudimentary eyes with focal presence of retinal pigment and a severely malformed left ear with absence of the external acoustic meatus (Fig. 8.31a, b). The heart showed a form of the tetralogy of Fallot with a strongly overriding aorta. The CNS showed a Dandy–Walker malformation with hypoplasia of the vermis, a median cyst in the posterior cranial fossa and slight hydrocephalus (Fig. 8.31 c, d), and absence of the septum pellucidum.

This case was kindly provided by Gerard van Noort (Laboratory for Pathology East-Netherlands, Enschede, The Netherlands).

Fig. 8.31 Dandy–Walker malformation in a fetus: **a**, **b** frontal and lateral views, showing craniofacial malformations including lateral clefts of the upper lip, rudimentary eyes and severely malformed left ear; **c**, **d** dorsal views of the cerebellum and brain stem, showing hypoplasia of the vermis and a wide fourth ventricle (courtesy Gerard van Noort, Enschede)
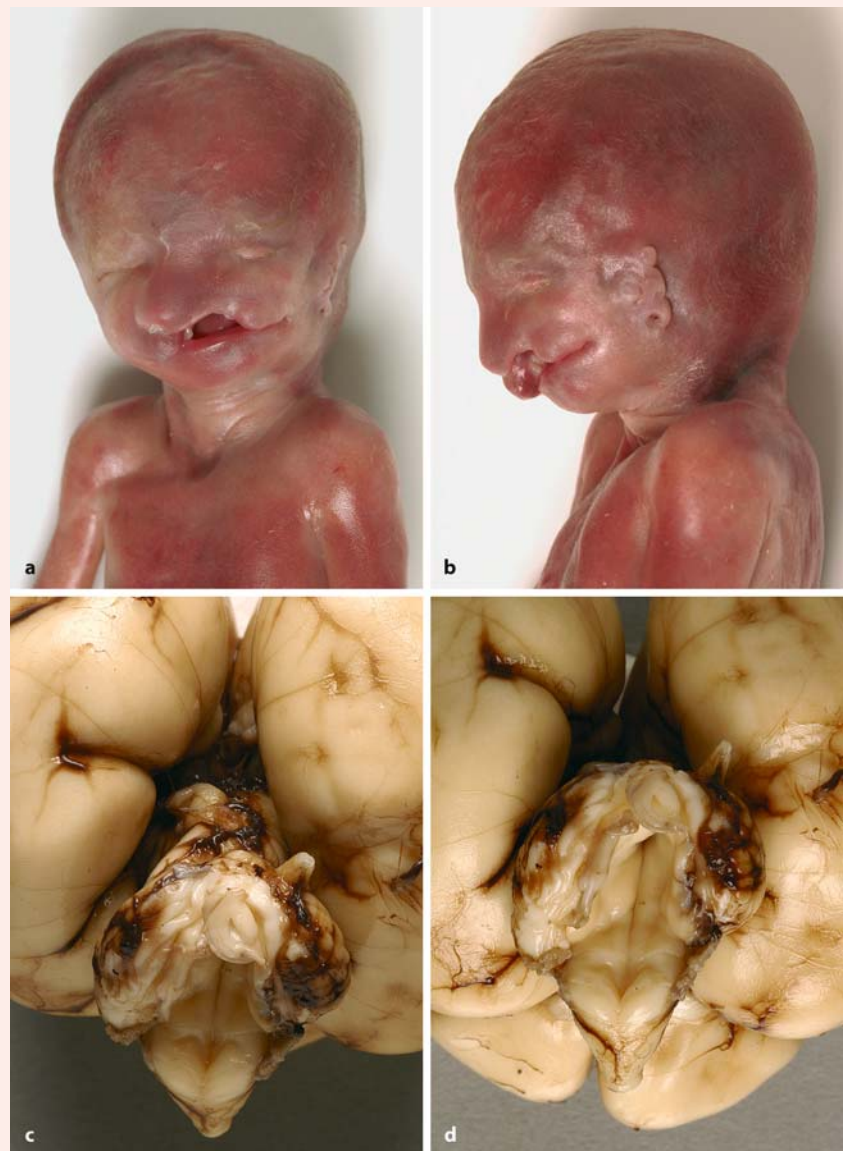
Joubert Syndrome

Joubert syndrome is a relatively rare, autosomal re-cessive disorder defined by vermis hypoplasia, hypo-tonia, developmental delay and at least one of two ad-ditional manifestations: abnormal breathing pattern (hyperpnea intermixed with central apnea in the neonatal period) or abnormal eye movements (Jou-bert et al. 1969). ten Donkelaar et al. (2000) presented imaging and neuropathological data of a case of Jou-bert syndrome in which extensive malformations of the cerebrum were also found (see Case Report).

Case Report. The patient, the second child of a 31-year-old woman, was born at home after 40 weeks of gestation. The birth weight of the girl was

3,290 g and she had a length of 48 cm. Directly after birth, a persisting, groaning respiration was noted for which she was admitted to the pediatric department of a general hospital. She presented with a groaning respiration with alternate periods of hyperpnea and apnea. Irregular, jerky eye movements were frequent-ly seen. As Joubert syndrome was suspected, MRI of the brain was made at the age of 6 days. The MRI showed vermis aplasia and various malformations of the cerebrum. The following years were characterized by a severe mental retardation, frequent epileptic in-sults, feeding problems and respiratory and urinary infections. At the age of 1 year and 4 months new MRI was made to evaluate the clinical findings, the epilep-sy in particular. On sagittal sections, the vermis and the corpus callosum were absent, with normal cere-bellar hemispheres (Fig. 8.31 a–c). The ventricles were enlarged with irregular contours of the lateral ventri-
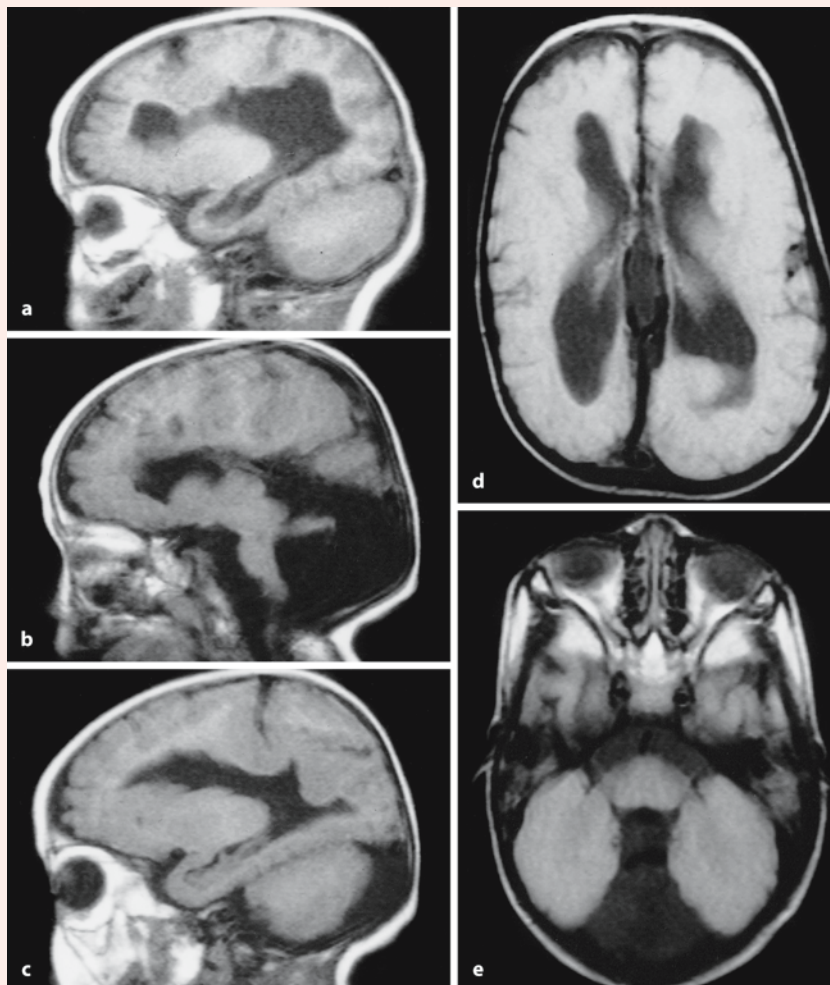
Fig. 8.32 Joubert syndrome: Sagittal (**a**–**c**) and axial (**d**, **e**) T1-weighted MRI made at the age of 1 year and 4 months, showing the large fluid-filled cyst in the posterior fossa (**b**, **e**), enlarged lateral ventri-cles (**a**–**d**) and extensive nodular heterotopia in the cerebrum (**a**–**d**) (from ten Donkelaar et al. 2000, with permission)

cles, possibly due to heterotopia. Ox axial sections, the absence of the vermis (Fig. 8.31e) and the enlarged lateral ventricles with nodular heterotopia (Fig. 8.31d) was evident.

The child died at the age of 3 years following a high fever resulting in a status epilepticus. At autopsy, the absence of the vermis, the corpus callosum and a gyrus cinguli was evident (Fig. 8.32 a). The cerebellar hemispheres did not show obvious malformations, and were separated by a large arachnoidal pseudo-cyst (Fig. 8.32 b). No posterior bulging of the roof of the fourth ventricle was observed. A relatively large fourth ventricle and a rather wide aqueduct were found (Fig. 8.32 a). The medulla oblongata showed, apart from relatively small inferior olives, no obvious changes. After cutting the brain into frontal slices, the extent of the nodular heterotopia within the cerebrum became evident (Fig. 8.32 c). Many nodular het-

erotopia were present in the cerebral cortex, the basal ganglia, the amygdala and the diencephalon. The dentate nuclei were broken into islands and showed few heterotopia within the superior cerebellar peduncles. The inferior olives were plump and dysplastic, and almost complete absence of the pyramidal decussation was found.

References

Joubert M, Eisenring J-J, Robb JP, Andermann F (1969) Familial agenesis of the cerebellar vermis. A syndrome of episodic hyperpnea, abnormal eye movements, ataxia, and retardation. Neurology 19:813–825

ten Donkelaar HJ, Hoevenaars F, Wesseling P (2000) A case of Joubert's syndrome with extensive cerebral malformations. Clin Neuropathol 19:85–93
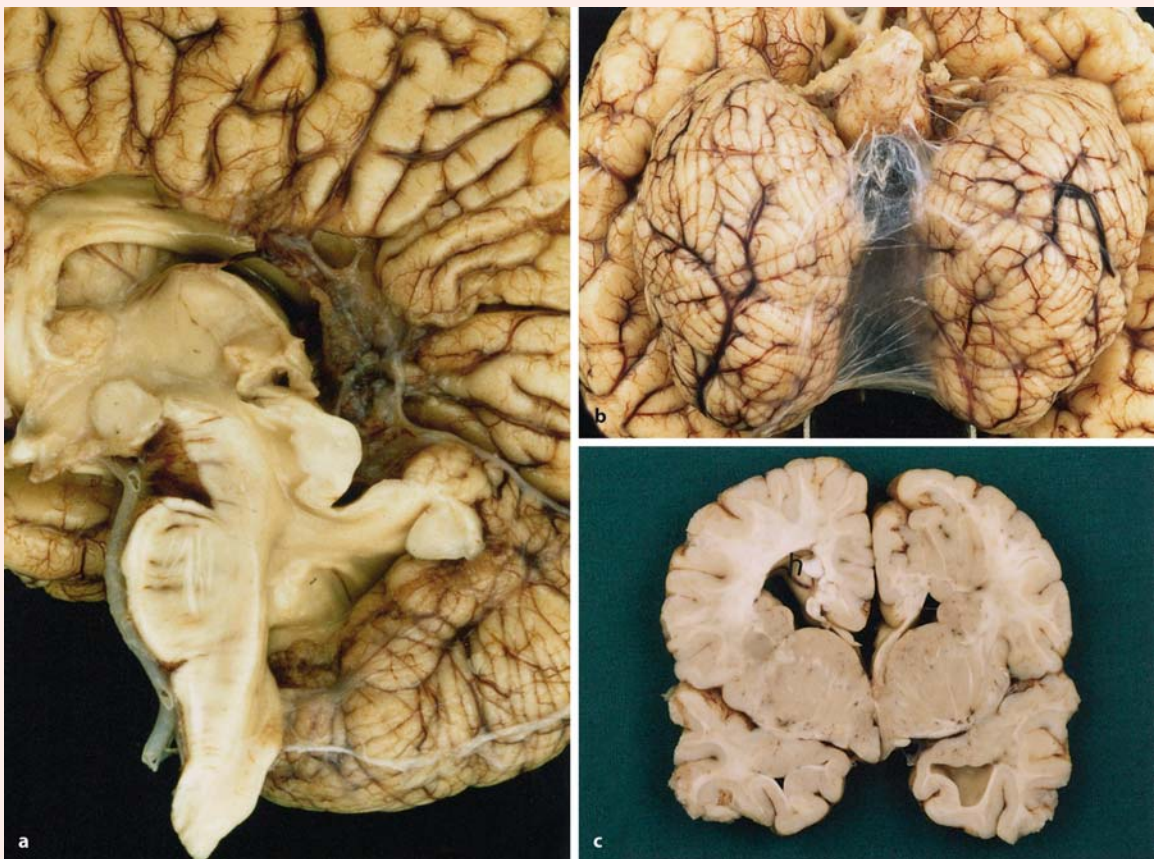
Fig. 8.33 Autopsy data in a case of Joubert syndrome showing the absence of the vermis (**a**, **b**) and associated nodular heterotopia (**c**) throughout the forebrain (from ten Donkelaar et al. 2000, with permission)
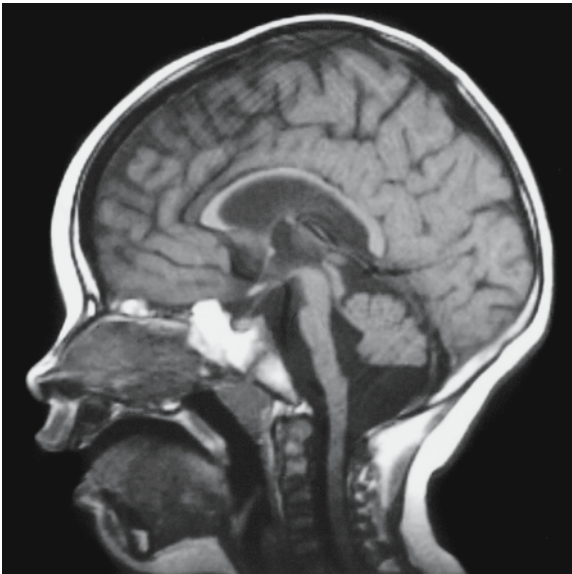
Clinical Case 8.5
Pontocerebellar Hypoplasia

Pontocerebellar hypoplasia is one of the characteristics of type 1a congenital disorders of glycosylation (see Case Report). Apart from the brain, many other organs are usually severely affected (Clinical Case 3.5). The defective gene is *PMM2*.

Case Report. A girl was born at term after an uneventful pregnancy. She was a cousin in the second degree of a girl with the same metabolic disorder. She was dystrophic, dysmature (birth weight 2,230 g) and showed peculiar fat pads over the upper outer parts of the buttocks, retrognathia, large ears, a small thorax and restricted joint movements. She presented with important feeding difficulties, failure to thrive and psychomotor retardation. There were recurrent pericardial effusions and episodes of ascites. Growth retardation persisted. CT examination of the brain showed a hypoplastic cerebellum. The diagnosis of congenital disorder of glycosylation type 1a was confirmed by immunoisoelectric focussing of transferrin. Later a mutation of the *PMM2* gene was found (G. Matthijs, Leuven). The girl died at the age of 22 months owing to haemorrhagic shock after bleeding from a bulbar ulcus as part of acute liver failure. At autopsy, liver fibrosis with diffuse microvesicular steatosis, renal cortical cysts and very small ovaries were found. The brain (Fig. 8.35) showed almost complete neuronal loss in the cerebellar hemispheres, the vermis and the inferior olives. Severe neuronal loss and gliosis was found in the nuclei pontis. The dentate nuclei were more mildly affected. Gliosis was also found in the caudate nucleus, the

Fig. 8.35 Basal view of a brain with pontocerebellar hypoplasia due to congenital disorders of glycosylation type I. Note that the width of the pons does not exceed that of the medulla (courtesy Martin Lammens, Nijmegen)

putamen, the subthalamic nucleus, the subcortical white matter and the posterior columns of the spinal cord.

well as lipodystrophy, and orange-peel skin), mental retardation, retinopathy, hyporeflexia, trunk ataxia and hypogonadism. The basic biochemical defect is deficient transformation of mannose-6-phosphate into mannose-1-phosphate owing to deficiency of the enzyme phosphomannomutase. Matthijs et al. (1997) identified 11 different missense mutations at the phosphomannomutase gene *PMM2* on chromosome 16p13 in 50 patients. Dandy–Walker malformations were found in type III CDG syndrome (Kumar et al. 1992; Stibler et al. 1993), and in a new entity, CDG type IId (Peters et al. 2002). CDGs can be demonstated by isoelectric focussing of the serum transferrin pattern.

8.7.4   Cortical Dysplasias

Microscopic *cerebellar dysplasias* are common in the cerebellar white matter, dentate nuclei, nodulus and cochlear nuclei during the neonatal period (Rorke et al. 1968; Friede 1989; Yachnis et al. 1994). They are considered normal variations and usually consists of single or mixed cell layers arranged in a disorganized manner. A *heterotopic cerebellum* occurring far away from its normal location usually shows organized, normal, cellular structures. Far-distant cerebellar heterotopia have been reported for the spine (Kudryk et al. 1991; Chung et al. 1998), the orbit (Kagotani et al. 1996) and the frontal encephalocele (Sarnat et al. 1982), and are associated with ovarian (Ferrer et al. 1986) and nasopharyngeal (Takhtani et al. 2000) teratomas. The presence of cerebellar heterotopia associated with teratomas is presumably due to their origin from pleuripotent stem cells detached during embryogenesis. *Focal* or *diffuse cortical dysplasias* can be found as incidental lesions or adjacent to a local defect (Friede 1989). Extensive cerebellar dysplasias are found in oculocerebral syndromes such as Walker–Warburg syndrome and Fukuyama dystrophy. Exceptionally severe cerebellar dysplasia may lead to atresia of the fourth ventricle (Clinical Case 8.6). Friede (1989) reported a case in which the fourth ventricle was replaced by masses of heterotopic tissue reminiscent of cerebellar cortex or cerebellar nuclei. The patient had a most unusual type of fusion of the cerebral hemispheres in the occipital lobes.

Clinical Case 8.6
Dysplasia of the Cerebellum with Extreme Hydrocephalus

Severe cerebellar dysplasia may lead to atresia of the fourth ventricle and is incompatible with life (see Case Report).

Case Report. A boy was born after 39 weeks of gestation. It was the first pregnancy of unrelated, healthy parents. The amnion was prematurely broken 4 days before delivery. The presence of a very large head (skull diameter 42 cm) urged the removal of 700 ml of liquor by transvaginal puncture before vaginal delivery was found to be possible. Birth weight was 2,997 g, crown–heel length was 59 cm and the Apgar scores were 4/7/8. Epileptic seizures were present from the first hours onwards. The boy died at day 2. At autopsy, except for the hydrocephalus and aspiration pneumonia, no deformities or visceral abnormalities were found. Brain weight was 405 g. Several epidural, subdural and subarachnoidal haemorrhages were present, probably due to the prenatal ventricular puncture. The severe hydrocephalus resulted in flattened but otherwise normal cerebral gyri. Microscopically, the cerebral cortex was normally structured. The basal ganglia and the thalamus were quite normal. The aqueduct was stenotic owing to a large tumorous mass which originated from the cerebellum, filled the whole fourth ventricle, the aqueduct and the inferior part of the third ventricle, and indent-
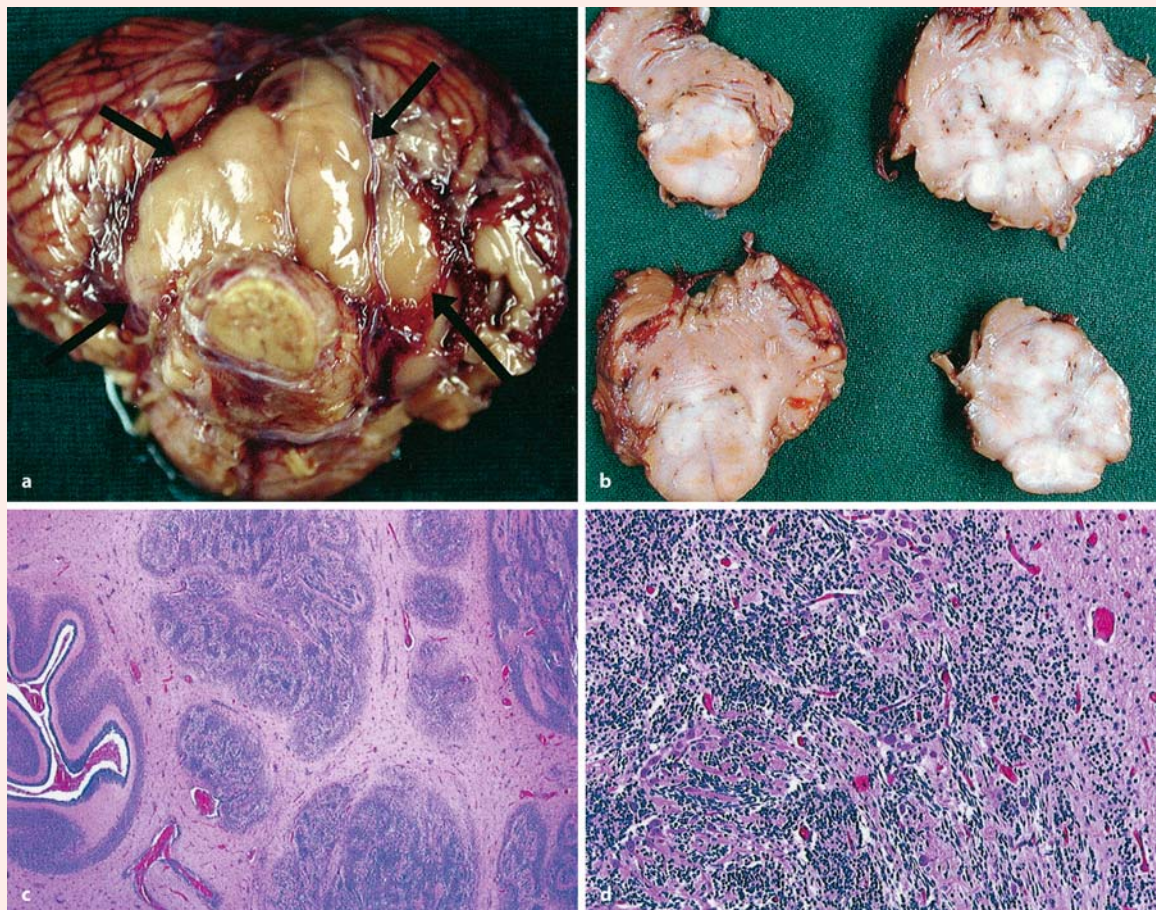
Fig. 8.36 Extreme dysplastic cerebellum: **a** tumorous mass (*between arrows*), protruding from the inferior part of the cerebellum and compressing the brain stem; **b** horizontal sections through the brain stem and cerebellum, illustrating that the tumorous process fills up the entire fourth ventricle throughout its extent; **c** haematoxylin–eosin-stained section of the cerebellum; on the left, normal cerebellar tissue is present; the rest of the section (and the tumorous mass) is composed of ill-defined undulating fields of granule cells, Purkinje cells and white matter; **d** detail, showing granule cells and the larger Purkinje cells in between (courtesy Martin Lammens, Nijmegen)

ed the pons and the medulla oblongata (Fig. 8.36). The tumour was formed by a mass of well-recognizable aberrant, dysplastic multinodular cerebellar cortex and extended from the inferior part of the cerebellar hemispheres and the vermis. In these cerebellar cortical noduli, well-formed Purkinje cells were intermingled with many small granular neurons. Mitotic acivity was very low. Reactive astrocytes were found superficially in the cerebellar cortex. Small tubuli covered with ependyma were found as remnants of the preexisting fourth ventricle. Both dentate nuclei could be identified in the tumorous mass. The pyramids were small.

References

Ackerman SL, Kozak LP, Przyborski SA, Rund LA, Boyer BB, Knowles BB (1997) The mouse rostral cerebellar malformation gene encodes an UNC-5-like protein. Nature 386:838–842

Aicardi J (1998) Diseases of the Nervous System in Childhood, 2nd ed. Cambridge University Press, Cambridge

Alcantara S, Ruiz M, De Castro F, Soriano E, Sotelo C (2000) Netrin 1 acts as an attractive or as a repulsive cue for distinct migrating neurons during the development of the cerebellar system. Development 127:1359–1372

Alder J, Cho NK, Hatten ME (1996) Embryonic precursor cells from the rhombic lip are specified to a cerebellar granule neuron identity. Neuron 17:389–399

Alexander L (1931) Die Anatomie der Seitentaschen der vierten Hirnkammer. Z Anat 95:531–707

Altman J, Bayer SA (1978a) Prenatal development of the cerebellar system in the rat. I. Cytogenesis and histogenesis of the deep cerebellar nuclei and the cortex of the cerebellum. J Comp Neurol 179:23–48

Altman J, Bayer SA (1978b) Prenatal development of the cerebellar system in the rat. II. Cytogenesis and histogenesis of the inferior olive, pontine gray, and the precerebellar reticular nuclei. J Comp Neurol 179:49–76

Altman J, Bayer SA (1987a) Development of the precerebellar nuclei in the rat. II. The intramural olivary migratory stream and the neurogenetic organization of the inferior olive. J Comp Neurol 257:490–512

Altman J, Bayer SA (1987b) Development of the precerebellar nuclei in the rat. III. The posterior precerebellar extramural migratory stream and the lateral reticular and external cuneate nuclei. J Comp Neurol 257:513–528

Altman J, Bayer SA (1987c) Development of the precerebellar nuclei in the rat. IV. The anterior precerebellar extramural migratory stream and the nucleus reticularis tegmenti pontis and the basal pontine gray. J Comp Neurol 257:529–552

Altman J, Bayer SA (1997) Development of the Cerebellar System: In relation to its evolution, structure and functions. CRC, Boca Raton, FL

Ambler M, Pogacar S, Sidman R (1969) Lhermitte-Duclos disease (granule cell hypertrophy of the cerebellum). Pathological analysis of the first familial cases. J Neuropathol Exp Neurol 28:622–647

Anton G, Zingerle H (1914) Genaue Beschreibung eines Falles von beiderseitigem Kleinhirnmangel. Arch Psychiat (Berl) 54:8–75

Aruga J, Yokota N, Hashimoto M, Furuichi T, Fukuda M, Mikoshiba K (1994) A novel zinc finger protein, zic, is involved in neurogenesis, especially in the cell lineage of cerebellar granule cells. J Neurochem 63:1880–1890

Aruga J, Minowa O, Yaginuma H, Kuno J, Nagai T, Noda T, Mikoshiba K (1998) Mouse Zic1 is involved in cerebellar development. J Neurosci 18:284–293

Baker RC, Graves GO (1931) Cerebellar agenesis. Arch Neurol Psychiatry 25:548–555

Backman SA, Stambolic V, Suzuki A, Haight J, Elia A, Pretorius J, Tsao MS, Shannon P, Bolon B, Ivy GO, et al. (2001) Deletion of Pten in mouse brain causes seizures, ataxia and defects in soma size resembling Lhermitte-Duclos disease. Nat Genet 29:396–403

Barkovich AJ (2000) Pediatric Neuroimaging, 3rd ed. Lippincott, Philadelphia, PA

Barkovich AJ, Kjos BO, Norman D, Edwards MS (1989) Revised classification of posterior fossa cysts and cyst-like malformations based on the results of multiplanar MR imaging. AJNR Am J Neuroradiol 10:977–988

Barth PG (1993) Pontocerebellar hypoplasias. An overview of a group of inherited neurodegenerative disorders with fetal onset. Brain Dev 15:411–422

Barth PG, Vrensen GFJM, Uylings HBM, Oorthuys JWE, Stam FC (1990) Inherited syndrome of microcephaly, dyskinesia and pontocerebellar hypoplasia: A systemic atrophy with early onset. J Neurol Sci 97:25–42

Bayer SA, Altman J, Russo RJ, Zhang X (1995) Embryology. In: Duckett S (ed) Pediatric Neuropathology. Williams & Wilkins, Baltimore, MD, pp 54–107

Ben-Arie N, Bellen HJ, Armstromg DL, McCall AE, Gordadze PR, Guo Q, Matzuk MM, Zoghbi HY (1997) Math1 is essential for genesis of cerebellar granule neurons. Nature 390:169–172

Benda CE (1954) The Dandy-Walker syndrome or the so-called atresia of the foramen of Magendie. J Neuropathol Exp Neurol 13:14–29

Beuche W, Wickboldt J, Friede RL (1983) Lhermitte-Duclos disease. Its minimal lesions in electron microscope data and CT findings. Clin Neuropathol 2:163–170

Bilovocky NA, Romito-DiGiacomo RR, Murcia CL, Maricich SM, Herrup K (2003) Factors in the genetic background suppress the Engrailed-1 cerebellar phenotype. J Neurosci 23:5105–5112

Blair IP, Gibson RR, Bennett CL, Chance PF (2002) Search for genes involved in Joubert syndrome: Evidence that one or more major loci are yet to be identified and exclusion of candidate genes EN1, EN2, FGF8, and BARHL1. Am J Med Genet 107:190–196

Bloch-Gallego E, Ezan F, Tessier-Lavigne M, Sotelo C (1999) Floor plate and netrin-1 are involved in the migration and survival of inferior olivary neurons. J Neurosci 19:4407–4420

Boltshauser E (2004) Cerebellum – small brain but large confusion: A review of selected cerebellar malformations and disruption. Am J Med Genet 126AS:376–385

Bonnevie K, Brodal A (1946) Hereditary hydrocephalus in the house mouse: IV. The development of the cerebellar anomalies during foetal life with notes on the normal development of the mouse cerebellum. Skr Norske Vid Akad I Math-Naturv Kl 4:1–60

Bordarier C, Aicardi J (1990) Dandy-Walker syndrome and agenesis of the cerebellar vermis: Diagnostic problems and gebetic counseling. Dev Med Child Neurol 32:285–294

Brocklehurst G (1969) The development of the human cerebrospinal fluid pathway with particular reference to the roof of the fourth ventricle. J Anat (Lond) 105:467–475

Brodal A, Hauglie-Hanssen E (1959) Congenital hydrocephalus with defective development of the cerebellar vermis (Dandy-Walker syndrome). J Neurol Neurosurg Psychiatr 22:99–106

Caddy KWT, Biscoe TJ (1975) Preliminary observations on the cerebellum in the mutant mouse Lurcher. Brain Res 91:276–280

Caviness VS Jr, Rakic P (1978) Mechanisms of cortical development: A view from mutations in mice. Annu Rev Neurosci 1:297–326

Chung J, Castillo M, Fordham L, Mukherji S, Boydston W, Hudgins R (1998) Spinal intradural cerebellar ectopia. AJNR Am J Neuroradiol 18:897–899

Cohen I (1942) Agenesis of the cerebellum (verified by operation). J Mt Sinai Hosp 8:441–446

Combettes M (1831) Absence complète du cervelet, des pédoncules postérieurs et la protubérance cérébrale chez une jeune fille mort dans sa onzième anneé. Bull Soc Anat Paris 5:148–157

Costa C, Hauw J-J (1995) Pathology of the cerebellum, brain stem, and spinal cord. In: Duckett S (ed) Pediatric Neuropathology. Williams & Wilkins, Baltimore, MD, pp 217–238

Dahmane N, Sanchez P, Gitton Y, Palma V, Sun T, Beyna M, Weiner H, Ruiz i Altaba P (2001) The Sonic hedgehog-Gli pathway regulates dorsal brain growth and tumorigenesis. Development 128:5201–5212

Dandy WE, Blackfan KD (1914) Internal hydrocephalus. An experimental, clinical, and pathological study. Am J Dis Child 8:406–482

Danon O, Elmaleh M, Boukobza B, Fohlen M, Hadjnacer K, Hasan M (2000) Rhombencephalosynapsis diagnosed in childhood: Clinical and MRI findings. Magn Reson Imaging 18:99–101

De Haene A (1955) Agénésie partielle du vermis du cervelet à caractère familial. Acta Neurol Belg 55:622–628

Deol MS (1964) The origin of the abnormalities of the inner ear in dreher mice. J Embryol Exp Morphol 12:727–733

Di Christofano A, Pesce B, Cordon-Cardo C, Pandolfi PP (1998) Pten is essential for embryonic development and tumour suppression. Nat Genet 19:348–355

Eisenman LM, Brothers R (1998) Rostral cerebellar malformation (*rcm/rcm*): A murine mutant to study regionalization of the cerebellum. J Comp Neurol 394:106–117

Eisenman LM, Gallagher E, Hawkes R (1998) Regionalization defects in the *weaver* mouse cerebellum. J Comp Neurol 394:431–444

Engelkamp D, Rashbass P, Seawright A, van Heyningen V (1999) Role of Pax6 in development of the cerebellar system. Development 126:3585–3596

Essick CR (1912) The development of the nuclei pontis and the nucleus arcuatus in man. Am J Anat 13:25–54

Falconer DS (1951) Two new mutants, 'Trembler' and 'Reeler', with neurological actions in the house mouse. J Genet 50:192–201

Feirabend HKP (1983) Anatomy and Development of Longitudinal Patterns in the Architecture of the Cerebellum of the White Leghorn (Gallus domesticus). Thesis, University of Leiden

Feirabend HKP, Voogd J (1986) Myeloarchitecture of the cerebellum of the chicken (*Gallus domesticus*): An atlas of the compartmental subdivision of the cerebellar white matter. J Comp Neurol 251:44–66

Ferrer I, Galofre E, Soler T (1986) Structure of an isolated cerebellum and related nuclei developed within the matrix of a mature ovarian teratoma. Childs Nerv Syst 2:266–269

Friede RL (1989) Developmental Neuropathology, 2nd ed. Springer, Berlin Heidelberg New York

Gardner RJM, Coleman LT, Mitchell LA, Smith LJ, Harvey AS, Scheffer IE, Storey E, Nowotny MJ, Sloane RA, Lubitz L (2001) Near-total absence of the cerebellum. Neuropediatrics 32:62–68

Gilthorpe JD, Papantoniou E-K, Chédotal A, Lumsden A, Wingate RJT (2002) The migration of cerebellar rhombic lip derivatives. Development 129:4719–4728

Glickstein M (1994) Cerebellar agenesis. Brain 117:1209–1212

Goffinet AM (1983) The embryonic development of the inferior olivary complex in normal and *reeler* mutant mice. J Comp Neurol 219:10–24

Goffinet AM, So K-F, Yamamoto M, Edwards M, Caviness VS Jr (1984) Architectonic and hodological organization of the cerebellum in *reeler* mutant mice. Dev Brain Res 16:263–276

Goldowitz D, Hamre K (1998) The cells and molecules that make the cerebellum. Trends Neurosci 21:375–382

Goutières F, Aicardi J, Farkas E (1977) Anterior horn cell disease associated with pontocerebellar hypoplasia in infants. J Neurol Neurosurg Psychiatr 40:370–378

Groenewegen HJ, Voogd J, Freedman SL (1989) The parasagittal zonation within the olivocerebellar projection. II. Climbing fiber distribution in the intermediate and hemispheric parts of cat cerebellum. J Comp Neurol 183:551–602

Gross H, Hoff H (1959) Sur les dysraphies crâniocéphaliques. In: Heuyer G, Feld M, Gruner J (eds) Malformations congénitales du cerveau. Masson, Paris, pp 287–296

Grunnet ML, Shields WD (1976) Cerebellar hemorrhage in the premature infant. J Pediatr 88:605–608

Habib M (2000) The neurological basis of developmental dyslexia: An overview and working hypothesis. Brain 123:2373–2399

Hagberg BA, Blennow G, Kristiansson B, Stibler H (1993) Carbohydrate-deficient glycoprotein syndromes: A peculiar group of new disorders. Pediatr Neurol 9:255–262

Hamilton BA, Frankel WN, Kerrebrock AW, Hawkins TL, Fitzhugh W, Kusumi K, Russell LB, Mueller KL, Van Berkel V, Birren BW, et al. (1996) Disruption of the nuclear hormone receptor RORα in *staggerer* mice. Nature 379:736–739

Hamre KM, Goldowitz D (1997) Meander tail acts intrinsic to granule cell precursors to disrupt cerebellar development: Analysis of meander tail chimeric mice. Development 124:4201–4212

Hanaway J, Netsky MG (1971) Heterotopias of the inferior olive: Relation to Dandy-Walker malformation and correlation with experimental data. J Neuropathol Exp Neurol 30:380–389

Hart HN, Malamud N, Ellis WG (1972) The Dandy-Walker syndrome. A clinicopathological study based on 28 cases. Neurology 22:771–780

Hashimoto M, Mikoshiba K (2003) Mediolateral compartmentalization of the cerebellum is determined on the "birth date" of Purkinje cells. J Neurosci 23:11342–11351

Hatten ME, Heintz N (1995) Mechanisms of neural patterning and specification in the developing cerebellum. Annu Rev Neurosci 18:385–408

Hatten ME, Alder J, Zimmerman K, Heintz N (1997) Genes involved in cerebellar cell specification and differentiation. Curr Opin Neurobiol 7:40–47

Hawkes R, Leclerc N (1987) Antigenic map of the rat cerebellar cortex: The distribution of sagittal bands as revealed by monoclonal anti-Purkinje cell antibody mabQ113. J Comp Neurol 256:29–41

Hawkes R, Colonnier M, Leclerc N (1985) Monoclonal antibodies reveal sagittal banding in the rodent cerebellar cortex. Brain Res 333:359–365

Herrup K (1983) Role of the *staggerer* gene in determining cell number in the cerebellar cortex. I. Granule cell death is an indirect consequence of *staggerer* gene action. Dev Brain Res 11:267–274

Herrup K, Kuemerle B (1997) The compartmentalization of the cerebellum. Annu Rev Neurosci 20:61–90

Herrup K, Mullen RJ (1979a) Regional variation and absence of large neurons in the cerebellum of the *staggerer* mouse. Brain Res 172:1–12

Herrup K, Mullen RJ (1979b) *Staggerer* chimeras: Intrinsic nature of Purkinje cell defects and implications for cerebellar development. Brain Res 178:443–457

Hess DT, Voogd J (1986) Chemoarchitectonic zonation of the monkey cerebellum. Brain Res 369:383–387

Hirano A, Dembitzer HB (1975) The fine structure of *staggerer* cerebellum. J Neuropathol Exp Neurol 34:1–11

His W (1890) Die Entwickelung des menschlichen Rautenhirns vom Ende des ersten bis zum Beginn des dritten Monats. I. Verlängertes Mark. Abh Kön Sächs Ges Wiss Math Phys Kl 29:1–74

Ho KS, Scott MP (2002) Sonic hedgehog in the nervous system: Functions, modifications and mechanisms. Curr Opin Neurobiol 12:57–63

Hochstetter F (1929) Beiträge zur Entwicklungsgeschichte des menschlichen Gehirns, II. Teil, 3. Lieferung: Die Entwicklung des Mittel- und Rautenhirns. Deuticke, Vienna

Hong SE, Shugari YY, Huang DT, Al Shahwan S, Grant PE, Hourihane JO, Martin NDT, Walsh CA (2000) Autosomal recessive lissencephaly with cerebellar hypoplasia is associated with human *RELN* mutations. Nat Genet 26:93–96

Hori A (2002) Normale und pathologische Entwicklung des Nervensystems. In: Peiffer J, Schröder JM, Paulus W (Hrsg) Neuropathologie. Morphologische Diagnostik der Krankheiten des Nervensystems und der Skelettmuskulatur, 3. Aufl. Springer, Berlin Heidelberg New York, pp 21–61

Hori A, Peiffer J, Pfeiffer RA, Iizuka R (1980) Cerebello-cortical heterotopia in dentate nucleus, and other microdysgeneses in trisomy D1 (Patau) syndrome. Brain Dev 2:345–352

Ito M (1984) The Cerebellum and Neural Control. Raven, New York

Jaeken J, Casaer P (1997) Carbohydrate-deficient glycoconjugate (CDG) syndromes: A new chapter of neuropediatrics. Eur J Paediatr Neurol 1:61–66

Jaeken J, Carchon H (2000) What's new in congenital disorders of glycosylation? Eur J Paediatr Neurol 4:163–167

Jakob A (1928) Das Kleinhirn. In: von Möllendorf W (ed) Handbuch der mikroskopischen Anatomie des Menschen, Vol 4, Teil 1. Springer, Berlin Heidelberg New York, pp 674–916

Jensen P, Smeyne R, Goldowitz D (2004) Analysis of cerebellar development in *math1* null embryos and chimeras. J Neurosci 24:2202–2211

Joubert M, Eisenring J-J, Robb JP, Andermann F (1969) Familial agenesis of the cerebellar vermis. A syndrome of episodic hyperpnea, abnormal eye movements, ataxia, and retardation. Neurology 19:813–825

Kagotani Y, Takao K, Nomura K, Imai Y, Hashimoto K (1996) Intraorbital cerebellar heterotopia associated with Chiari I malformation. J Pediatr Ophthalmol Strabismus 33:262–265

Kappel RM (1981) The Development of the Cerebellum in Macaca mulatta. A study of regional differences during corticogenesis. Thesis, University of Leiden

Kaufmann WE, Cooper Kl, Mostofsky SH, Capone GT, Kates WR, Newschaffer CJ, Bukelis I, Stump MH, Jann AE, Lanham DC (2003) Specificity of cerebellar vermian abnormalities in autism: A quantitative magnetic resonance imainig study. J Child Neurol 18:463–470

Keir G, Winchester BG, Clayton P (1999) Carbohydrate-deficient glycoprotein syndromes: Inborn errors of protein glycosylation. Ann Clin Biochem 36:20–36

Kendall B, Kingsley D, Lambert SR, Taylor D, Finn P (1990) Joubert syndrome: A clinico-radiological study. Neuroradiology 31:502–506

Kollias SS, Ball WS (1997) Congenital malformations of the brain. In: Ball WS (ed) Pediatric Neuroradiology. Lippincott-Raven, Philadelphia, PA, pp 91–174

Korneliussen HK (1968) Comments on the cerebellum and its division. Brain Res 8:229–236

Kudryk ET, Coleman JM, Murtagh FR, Arrington JA, Silbiger ML (1991) MR imaging of an extreme case of cerebellar ectopia in a patient with Chiari II malformation. AJNR Am J Neuroradiol 12:705–706

Kuemerle B, Zanjani H, Joyner A, Herrup K (1997) Pattern deformities and cell loss in *Engrailed-2* mutant mice suggest two separate patterning events during cerebellar development. J Neurosci 17:7881–7889

Kuhar SG, Feng L, Vidan S, Ross ME, Hatten ME, Heintz N (1993) Changing patterns of gene expression define granule neuron differentiation. Development 117:97–104

Kumar AJ, Naidich TP, Stetter G (1992) Chromosomal disorders: Background and neuroradiology. AJNR Am J Neuroradiol 13:577–593

Kwon CH, Zhu X, Zhang J, Knoop LL, Tharp R, Smeyne RJ, Eberhart CG, Burger PC, Baker SJ (2001) Pten regulates neuronal soma size: A mouse model of Lhermitte-Duclos disease. Nat Genet 29:404–411

Kyriakopoulou K, de Diego I, Wassef M, Karagogeos D (2002) A combination of chain and neurophilic migration involving the adhesion molecule TAG-1 in the caudal medulla. Development 129:287–296

Lambert SR, Kriss A, Gresty M, Benton S, Taylor D (1989) Joubert syndrome. Arch Ophthalmol 107:709–713

Lane PW (1964) Personal communication. Mouse News Lett 30:32

Lane PW (1970) [Swaying, sw, linkage]. Mouse News Lett 36:40

Lane PW, Bronson RT, Spencer CA (1992) Rostral cerebellar malformation (*rcm/rcm*): A new recessive mutation on chromosome 3 of the mouse. J Hered 83:315–318

Landis DMD, Reese TS (1977) Structure of the Purkinje cell membrane in *staggerer* and *weaver* mutant mice. J Comp Neurol 171:247–260

Landis DMD, Sidman RL (1978) Electron microscopic analysis of postnatal histogenesis in the cerebellar cortex of *staggerer* mutant mice. J Comp Neurol 179:831–864

Landis S (1973) Ultrastructural changes in the mitochondria of cerebellar Purkinje cells of nervous mutant mice. J Cell Biol 57:782–797

Landis S, Mullen RJ (1978) The development and degeneration of Purkinje cells in *pcd* mutant mice. J Comp Neurol 177:125–143

Leclerc N, Doré L, Parent A, Hawkes R (1990) The compartmentalization of the monkey and rat cerebellar cortex: Zebrin I and cytochrome oxidase. Brain Res 506:70–78

Lee KJ, Jessell TM (1999) The specification of dorsal cell fates in the vertebrate central nervous system. Annu Rev Neurosci 22:261–294

Lemire RJ, Loeser JD, Leech RW, Alvord EC (1975) Normal and Abnormal Development of the Human Nervous System. Harper & Row, Hagerstown, MD

Lhermitte J, Duclos P (1920) Sur un ganglioneurome diffuse du cortex du cervelet. Bull Assoc Franç Etude Cancer 9:99–107

Lloyd K, Dennis M (1963) Cowden's disease: A possible new symptom complex with multiple system involvement. Ann Inter Med 58:136–142

Louvi A, Alexandre P, Métin C, Wurst W, Wassef M (2003) The isthmic neuroepithelium is essential for cerebellar midline fusion. Development 130:5319–5330

Lyon MF (1961) Linkage relations and some pleiotropic effects of the dreher mutant of the house mouse. Genet Res 2:92–95

Maat GJR (1981) Histogenetic aspects of the cerebellar cortex in man. Acta Morphol Neerl-Scand 19:82–83

Manzanares M, Trainor PA, Ariza-McNaughton L, Nonchev S, Krumlauf R (2000) Dorsal patterning defects in the hindbrain, roof plate and skeleton in the dreher [dr(J)] mouse mutant. Mech Dev 94:147–156

Marani E (1982) Topographic Enzyme Histochemistry of the Mammalian Cerebellum: 5′-Nucleotidase and Acetylcholinesterase. Thesis, University of Leiden

Marani E, Voogd J (1977) An acetylcholinesterase band pattern in the molecular layer of the cat cerebellum. J Anat (Lond) 124:335–345

Maria BL, Boltshauser E, Palmer SC, Tran TX (1999) Clinical features and revised diagnostic criteria in Joubert syndrome. J Child Neurol 14:583–591

Mariani J, Crepel F, Mikoshiba K, Changeux J-P, Sotelo C (1977) Anatomical, physiological and biochemical studies of the cerebellum from reeler mutant mouse. Philos Trans R Soc Lond 281:1–28

Marien P, Engelborghs S, De Deyn PP (2001) Cerebellar neurocognition: A new avenue. Acta Neurol Belg 101:96–109

Marín-Padilla M (1985) Neurogenesis of the climbing fibers in the human cerebellum: A Golgi study. J Comp Neurol 235:82–96

Marino S, Krimperfort P, Leung C, van der Korput HAGM, Trapman J, Camenisch I, Berns A, Brandner S (2002) PTEN is essential for cell migration but not for fate determination and tumourigenesis in the cerebellum. Development 129:3513–3530

Marti E, Bovolenta P (2002) Sonic hedgehog in CNS development: One signal, multiple outputs. Trends Neurosci 25:89–96

Mastick GS, Fan C-M, Tessier-Lavigne M, Serbedzija GN, McMahon AP, Easter SS Jr (1996) Early detection of neuromeres in *Wnt-1* -/- mutant mice: evaluation by morphological and molecular markers. J Comp Neurol 374:246–258

Matthijs G, Schollen E, Pardon E, Veiga-Da Cunha M, Jaeken J, Cassiman JJ, Van Schaftingen E (1997) Mutations in PMM2, a phosphomannomutase gene on chromosome 16p13, in carbohydrate-deficient glycoprotein type I syndrome (Jaeken syndrome). Nat Genet 16:88–92

McMahon AP, Joyner AL, Bradley A, McMahon JA (1992) The midbrain-hindbrain phenotype of *Wnt-1-/Wnt-1-* mice results from stepwise deletion of *engrailed*-expressing cells by 9.5 days postcoitum. Cell 69:581–595

Meier H, MacPike AD (1971) Three syndromes produced by two mutant genes in the mouse. J Hered 62:297–302

Miale IL, Sidman RL (1961) An autoradiographic analysis of histogenesis in the mouse cerebellum. Exp Neurol 4:277–296

Middleton FA, Strick PL, eds (1998) Special issue: Cerebellum. Trends Neurosci 21:367–419; Trends Cogn Sci 2:313–371

Millen KJ, Wurst W, Herrup K, Joyner AL (1994) Abnormal embryonic cerebellar development and patterning of postnatal foliation in two mouse Engrailed-2 mutants. Development 120:695–706

Millen KJ, Hui CC, Joyner AL (1995) A role for En-2 and other murine homologues of *Drosophila* segment polarity genes in regulating positional information in the developing cerebellum. Development 121:3935–3945

Millen KJ, Millonig JH, Wingate RJT, Alder J, Hatten ME (1999) Neurogenetics of the cerebellar system. J Child Neurol 14:574–582

Millonig JH, Millen KJ, Hatten ME (2000) The mouse Dreher gene Lmx1a controls formation of the roof plate in the vertebrate CNS. Nature 403:764–769

Milosevic A, Zecevic N (1998) Developmental changes in human cerebellum: Expression of intracellular calcium receptors, calcium-binding proteins, and phosphorylated and nonphosphorylated neurofilament protein. J Comp Neurol 396:442–460

Miyata M, Miyata H, Mikoshiba K, Ohama E (1999) Development of Purkinje cells in humans: An immunohistochemical study using a monoclonal antibody against the inositol 1,4,5-triphosphate type 1 receptor (IP$_3$R1). Acta Neuropathol (Berl) 98:226–232

Mullen RJ, LaVail MM (1975) Two new types of retinal degeneration in cerebellar mutant mice. Nature 258:528–530

Mullen RJ, Eicher EM, Sidman RL (1976) Purkinje cell degeneration, a new neurological mutation in the mouse. Proc Natl Acad Sci USA 73:208–212

Mullen RJ, Hamre KM, Goldowitz D (1997) Cerebellar mutant mice and chimeras revisited. Persp Dev Neurobiol 5:43–55

Murofushi K (1974) Normalentwicklung und Dysgenesien von Dentatum und Oliva Inferior. Acta Neuropathol (Berl) 27:317–328

Nicolson RI, Fawcett AJ, Dean P (2001) A TINS debate – Hindbrain versus forebrain: A case for cerebellar deficit in developmental dyslexia. Trends Neurosci 24:508–516

Norman MG, McGillivray BC, Kalousek DK, Hill A, Poskitt KJ (1995) Congenital Malformations of the Brain. Pathological, embryological, clinical, radiological and genetic aspects. Oxford University Press, New York

Norman RM (1940) Primary degeneration of the granular layer of the cerebellum: An unusual form of familial cerebellar atrophy occurring in early life. Brain 63:365–379

Oberdick J, Baader SL, Schilling K (1998) From zebra stripes to postal zones: Deciphering patterns of gene expression in the cerebellum. Trends Neurosci 21:383–390

Obersteiner H (1914) Ein Kleinhirn ohne Wurm. Arb Neurol Inst (Wien) 21:124–136

O'Rahilly R, Müller F (2001) Human Embryology and Teratology, 3rd ed. Wiley–Liss, New York

Osborn AG (1994) Diagnostic Neuroradiology. Mosby, St. Louis, MI

Oscarsson O (1980) Functional organization of olivary projections to the cerebellar anterior lobe. In: Courville J (ed) The Inferior Olivary Nucleus, Anatomy and Physiology. Raven, New York, pp 279–289

Padberg GW, Schot JD, Vielvoye GJ, Bots GT, de Beer FC (1991) Lhermitte-Duclos disease and Cowden's disease: A single phakomatosis. Ann Neurol 29:517–523

Park S-H, Becker-Catania S, Gatti RA, Crandall BF, Emelin JK, Vinters HV (1998) Congenital olivopontocerebellar atrophy: Report of two siblings with paleo- and neocerebellar atrophy. Acta Neuropathol (Berl) 96:315–321

Pascual-Castroviejo I (2002) Congenital disorders of glycosylation syndromes. Dev Med Child Neurol 44:357–358

Pascual-Castroviejo I, Velez A, Pascual-Pascual S-I, Roche MC, Villarejo F (1991) Dandy-Walker malformation: An analysis of 38 cases. Child Nerv Syst 7:88–97

Pascual-Castroviejo I, Gutierrez M, Morales C, Gonzalez-Mediero I, Martínez-Bermejo A, Pascual-Pascual S-I (1994) Primary degeneration of the granular layer of the cerebellum. A study of 14 patients and review of the literature. Neuropediatrics 25:183–190

Pascual-Castroviejo I, Pascual-Pascual SI, Gutierrez-Molina M, Urich H, Katsetos CD (2003) Cerebellar hypoplasia with heterotopic Purkinje cells in the molecular layer and preservation of the granule layers associated with severe encephalopathy. A new entity? Neuropediatrics 34:160–164

Peiffer J, Pfeiffer RA (1977) Hypoplasia ponto-neocerebellaris. J Neurol 215:241–251

Pellegrino JE, Lensch MW, Muenke M, Chance PF (1997) Clinical and molecular analysis in Joubert syndrome. Am J Med Genet 72:59–62

Peters V, Penzien JM, Reiter G, Körner C, Hackler R, Assmann B, Fang J, Schaefer JR, Hoffmann GF, Heidemann PH (2002) Congenital disorder of glycosylation IId (CDG-IId) – a new entity: Clinical presentation with Dandy-Walker malformation and myopathy. Neuropediatrics 33:27–32

Phillips RJS (1960) "Lurcher". A new gene in linkage group XI of the house mouse. J Genet 57:35–42

Plioplys AV, Thibault J, Hawkes R (1985) Selective staining of a subset of Purkinje cells in the human cerebellum with monoclonal antibody mabQ113. J Neurol Sci 70:245–256

Podsypanina K, Ellenson LH, Nemes A, Gu J, Tamura M, Yamada KM, Cordon-Cardo C, Catoretti G, Fisher PE, Parsons R (1999) Mutation of Pten/Mmac1 in mice causes neoplasia in multiple organ systems. Proc Natl Acad Sci USA 96:1563–1568

Przyborski SA, Knowles BB, Ackerman SL (1998) Embryonic phenotype of Unc5h3 mutant mice suggests chemorepulsion during the formation of the rostral cerebellar boundary. Development 125:41–50

Rakic P (1976) Synaptic specificity in the cerebellar cortex: Study of anomalous circuits induced by single gene mutations in mice. Cold Spring Harbor Symp Quant Biol 40:333–346

Rakic P, Sidman RL (1970) Histogenesis of cortical layers in human cerebellum, particularly the lamina dissecans. J Comp Neurol 139:473–500

Rakic P, Sidman RL (1973a) Sequence of developmental abnormalities leading to granule cell deficits in cerebellar cortex of *weaver* mutant mice. J Comp Neurol 152:103–132

Rakic P, Sidman RL (1973b) Organization of cerebellar cortex secondary to deficits of granule cells in *weaver* mutant mice. J Comp Neurol 152:133–162

Rakic P, Sidman RL (1973c) Weaver mutant mouse cerebellum: Defective neuronal migration secondary to abnormality of Bergmann glia. Proc Natl Acad Sci USA 70:240–244

Ramaeckers VT (2000) Cerebellar malformations. In: Klockgether T (ed) Handbook of Ataxia Disorders. Dekker, New York, pp 115–150

Ramaeckers VT, Heimann G, Reul J, Thron A, Jaeken J (1997) Genetic disorders and cerebellar structural abnormalities in childhood. Brain 120:1739–1751

Rezai Z, Yoon CH (1972) Abnormal rate of granule cell migration in the cerebellum of "weaver" mutant mice. Dev Biol 29:17–26

Rhinn M, Brand M (2001) The midbrain-hindbrain boundary organizer. Curr Opin Neurobiol 11:34–42

Rorke LB, Fogelson MH, Riggs HE (1968) Cerebellar heterotopia in infancy. Dev Med Child Neurol 10:644–650

Rosario CM, Yandava BD, Kosara B, et al. (1997) Differentiation of engrafted multipotent neural progenitors towards replacement of missing granule neurons in meander tail cerebellum may help determine the locus of mutant gene action. Development 124:4213–4224

Ross ME, Fletcher C, Mason CA, Hatten ME, Heintz N (1989) Meander tail reveals a discrete developmental unit in the mouse cerebellum. Proc Natl Acad Sci USA 87:4189–4192

Saraiva JM, Baraitser M (1992) Joubert syndrome: A review. Am J Med Genet 43:726–731

Sarnat HB (2000) Molecular genetic classification of central nervous system malformations. J Child Neurol 15:675–687

Sarnat HB, Alcalá H (1980) Human cerebellar hypoplasia – a syndrome of diverse causes. Arch Neurol 37:300–305

Sarnat HB, de Mello DE, Blair JD, Siddiqui SY (1982) Heterotopic growth of dysplastic cerebellum in frontal encephalocele in an infant of a diabetic mother. Can J Neurol Sci 9:31–35

Sarnat HB, Benjamin DR, Siebert JR, Kletter GB, Cheyette SR (2002) Agenesis of the mesencephalon and metencephalon with cerebellar hypoplasia: Putative mutation in the *EN2* gene – report of two cases in early infancy. Ped Dev Pathol 5:54–68

Schachenmayr W, Friede RL (1982) Rhombencephalosynapsis: A Viennese malformation? Dev Med Child Neurol 24:178–182

Scott TG (1964) A unique pattern of localization within the cerebellum of the mouse. J Comp Neurol 122:1–8

Sekiguchi M, Shimai K, Guo H, Nowakowski RS (1992) Cytoarchitectonic abnormalities in hippocampal formation and cerebellum of dreher mutant mouse. Dev Brain Res 67:105–112

Sidman RL (1968) Development of interneuronal connections in brains of mutant mice. In: Carlson FD (ed) Physiological and Biochemical Aspects of Nervous Integration. Prentice-Hall, Englewood-Cliffs, NJ, pp 163–193

Sidman RL, Rakic P (1982) Development of the human central nervous system. In: Haymaker W, Adams RD (eds) Histology and Histopathology of the Nervous System. Thomas, Springfield, IL, pp 3–145

Sidman RL, Lane PW, Dickie MM (1962) *Staggerer*, a new mutation in the mouse affecting the cerebellum. Science 137:610–612

Sotelo C (1975a) Dendritic abnormalities of Purkinje cells in cerebellum of neurological mutant mice (weaver and staggerer). Adv Neurol 12:335–351

Sotelo C (1975b) Anatomical, physiological and biochemical studies of the cerebellum from mutant mice. II. Morphological study of cerebellar cortical neurons and circuits in the weaver mouse. Brain Res 94:19–44

Sternberg L (1912) Ueber vollständigen Defekt des Kleinhirnes. Verhandl Dtsch Path Gesellsch 15:353–359

Stibler H, Jaeken J (1990) Carbohydrate-deficient serum transferrin in a new systemic hereditary syndrome. Arch Dis Child 65:107–111

Stibler H, Westerberg B, Hanefeld F, Hagberg B (1993) Carbohydrate-deficient glycoprotein (CDG) syndrome – a new variant, type III. Neuropediatrics 24:51–52

Streeter GL (1912) The development of the nervous system. In: Keibel F, Mall FP (eds) Manual of Human Embryology, Vol 2. Lippincott, Philadelphia, PA, pp 1–156

Swisher DA, Wilson DB (1977) Cerebellar histogenesis in the Lurcher (*Lc*) mutant mouse. J Comp Neurol 173:205–218

Taggart JK, Walker AE (1942) Congenital atresia of the foramens of Luschka and Magendie. Arch Neurol Psychiatr 48:583–612

Takhtani D, Melhem ER, Carson BS (2000) A heterotopic cerebellum presenting as a suprasellar mass with associated nasopharyngeal teratoma. AJNR Am J Neuroradiol 21:1119–1121

Tanaka Y, Ogasawara Y, Miyakawa K, Murofushi K (1976) A neuropathological study on two autopsy cases of congenital hydrocephalus, with special reference to morphogenesis concerning micropolygyria of the dentate nucleus. No to Hattatsu 8:137–144 (in Japanese)

ten Donkelaar HJ, Hoevenaars F, Wesseling P (2000) A case of Joubert's syndrome with extensive cerebral malformations. Clin Neuropathol 19:85–93

ten Donkelaar HJ, Lammens M, Wesseling P, Thijssen HOM, Renier WO (2003) Development and developmental disorders of the human cerebellum. J Neurol 250:1025–1036

Tissir F, Goffinet A (2003) Reelin and brain development. Nat Rev Neurosci 4:496–505

Toelle SP, Yalcinkaya C, Kocer N, Deonna T, Overweg-Plandsoen WCG, Bast T, Kalmanchey R, Barsi P, Schneider JFL, Capone Mori A, Boltshauser E (2002) Rhombencephalosynapsis: Clinical findings and neuroimaging in 9 children. Neuropediatrics 33:209–214

Truwitt CL, Barkovich AJ, Shanahan R, Maroldo TV (1991) MR imaging of rhombencephalosynapsis. J Comput Assist Tomogr 17:211–214

Utsunomiya H, Takano K, Ogasawara T, Hashimoto T, Fukushoma T, Okazaki M (1998) Rhombencephalosynapsis: Cerebellar embryogenesis. AJNR Am J Neuroradiol 19:547–549

van de Voort MRMJ (1960) De ontwikkeling van de ruitlijst bij de witte rat. Thesis, University of Nijmegen

Voeller KKS (2004) Dyslexia. J Child Neurol 19:740–744

Voogd J (1967) Comparative aspects of the structure and fibre connexions of the mammalian cerebellum. Prog Brain Res 25:94–134

Voogd J (1992) The morphology of the cerebellum the last 25 years. Eur J Morphol 30:81–96

Voogd J (1995) The cerebellum. In: Williams PL et al. (eds) Gray's Anatomy, 38th ed. Churchill Livingstone, New York, pp 1027–1064

Voogd J (2003) The human cerebellum. J Chem Neuroanat 26:243–252

Voogd J (2004) Cerebellum and precerebellar nuclei. In: Paxinos G, Mai JK (eds) The Human Nervous System, 2nd ed. Elsevier, Amsterdam, pp 321–392

Voogd J, Bigaré F (1980) Topographical distribution of olivary and cortico nuclear fibers in the cerebellum: A review. In: Courville J et al. (eds) The Inferior Olivary Nucleus: Anatomy and Physiology. Raven, New York, pp 207–234

Voogd J, Glickstein M (1998) The anatomy of the cerebellum. Trends Neurosci 21:370–375

Voogd J, Feirabend HKP, Schoen JHR (1990) Cerebellum and precerebellar nuclei. In: Paxinos G (ed) The Human Nervous System. Academic, San Diego, CA, pp 321–386

Voogd J, Jaarsma D, Marani E (1996) The cerebellum: Chemoarchitecture and anatomy. In: Swanson LW, Björklund A, Hökfelt T (eds) Handbook of Chemical Neuroanatomy, Vol 12: Integrated systems of the CNS, Part III. Elsevier, Amsterdam, pp 1–369

Wahlsten D, Lyons JP, Zagaja W (1983) Four dominant autosomal mutations affecting skin and hair development in the mouse. J Hered 74:421–425

Wang VY, Zoghbi HY (2001) Genetic regulation of cerebellar development. Nat Rev Neurosci 2:484–491

Washburn LL, Eicher EM (1986) A new mutation at the dreher locus (drzJ). Mouse News Lett 75:28–29

Wassef M, Joyner AL (1997) Early mesencephalon/metencephalon patterning and development of the cerebellum. Persp Dev Neurobiol 5:3–16

Wechsler-Reya R, Scott MP (2001) The developmental biology of brain tumors. Annu Rev Neurosci 24:385–428

Weinberg AG, Kirkpatrick JB (1995) Cerebellar hypoplasia in Werdnig-Hoffmann disease. Dev Med Child Neurol 17:511–516

Wingate RJT (2001) The rhombic lip and early cerebellar development. Curr Opin Neurobiol 11:82–88

Wurst W, Bally-Cuif L (2001) Neural plate patterning: Upstream and downstream of the isthmic organizer. Nat Rev Neurosci 2:99–108

Wurst W, Auerbach AB, Joyner AL (1994) Multiple developmental defects in Engrailed-1 mutant mice: An early mid-hindbrain deletion and patterning defects in forelimbs and sternum. Development 120:2065–2075

Yachnis AT (2002) Rhombencephalosynapsis with massive hydrocephalus: Case report and pathogenetic considerations. Acta Neuropathol (Berl) 103:301–304

Yachnis AT, Rorke LB (1999) Neuropathology of Joubert syndrome. J Child Neurol 14:655–659

Yachnis AT, Rorke LB, Trojanowski JQ (1994) Cerebellar dysplasia in humans: Development and possible relationship to glial and primitive neuroectodermal tumors of the cerebellar vermis. J Neuropathol Exp Neurol 53:61–71

Yamasaki T, Kawaji K, Ono K, Bito H, Hirano T, Osumi N, Kengaku M (2001) *Pax6* regulates granule cell polarization during parallel fiber formation in the developing cerebellum. Development 128:3133–3144

Yang XW, Zhong R, Heintz N (1996) Granule cell specification in the developing mouse brain as defined by expression of the zinc finger transcription factor *RU49*. Development 122:555–566

Yee KT, Simon HH, Tessier-Lavigne M, O'Leary DDM (1999) Extension of long leading processes and neuronal migration in the mammalian brain directed by the chemoattractant netrin-1. Neuron 24:607–622

Yoon CH (1972) Developmental mechanisms for changes in cerebellum of staggerer mouse, a neurological mutant of genetic origin. Neurology 22:743–754

Young ID, McKeever PA, Squier MV, Grant J (1992) Lethal olivopontoneocerebellar hypoplasia with dysmorphic features in sibs. J Med Genet 29:733–735

Yu MC, Cho E, Luo CB, Li WWY, Shen WZ, Yew DT (1996) Immunohistochemical studies of GABA and parvalbumin in the developing human cerebellum. Neuroscience 70:267–276

Zafeiriou DI, Vargiami E, Boltshauser E (2004) Cerebellar agenesis and diabetes insipidus. Neuropediatrics 35:364–367

Zheng C, Heintz N, Hatten ME (1996) CNS gene encoding astrotactin, which supports neuronal differentiation along glial fibers. Science 272:417–419

Development and Developmental Disorders of the Forebrain

Hans J. ten Donkelaar, Martin Lammens, Johannes R.M. Cruysberg, Akira Hori, Kohei Shiota and Berit Verbist

9.1 Introduction

The forebrain comprises those structures that are derived from the most rostral part of the neural plate, i.e. the **primary prosencephalon**. The primary prosencephalon divides into two major components, the (epichordal) caudal diencephalon and the rostral secondary prosencephalon. The **secondary prosencephalon** is the entire prechordal part of the neural tube, and includes the rostral diencephalon or hypothalamus, the optic vesicles, the preoptic region and the telencephalon. The two major telencephalic subdivisions are the pallium (the roof) and the subpallium (the base). The pallium gives rise to the cerebral cortex, whereas the basal ganglia and most cortical interneurons derive from the subpallium. The amygdala has pallial as well as subpallial origins. Like the rest of the neural tube, the embryonic forebrain appears to be organized into transverse (prosomeres) and longitudinal subdivisions (alar and basal plates; Fig. 9.1). The caudal diencephalon arises from prosomeres 1–3, whereas the rostral diencephalon was suggested to arise from prosomeres 4–6 (Bergquist and Källén 1954; Puelles 1995; Rubinstein et al. 1998; Puelles et al. 2000). The relationship of these postulated segments to telencephalic subdivisions, however, remained controversial. Recently, Puelles and Rubinstein (2003) revised their prosomeric subdivision of the forebrain by advocating a single, complex protosegment for the secondary prosencephalon, not further subdividable into prosomeres 4–6.

Patterning of the forebrain involves the two general sets of mechanisms common to the neural plate, one along the anteroposterior axis and the other along the mediolateral axis (Chap. 2). An additional dorsal–ventral patterning mechanism is important for subdividing the telencephalon into dorsal, pallial and ventral, subpallial structures (Marín and Rubinstein 2002; Campbell 2003; Zaki et al. 2003). Genetic engineering has produced a great variety of knockout mice and zebrafish, the study of which has greatly improved our knowledge of these patterning mechanisms (Schier 2001; Marín and Rubinstein 2002; Rallu et al. 2002b; Zaki et al. 2003). Defects in
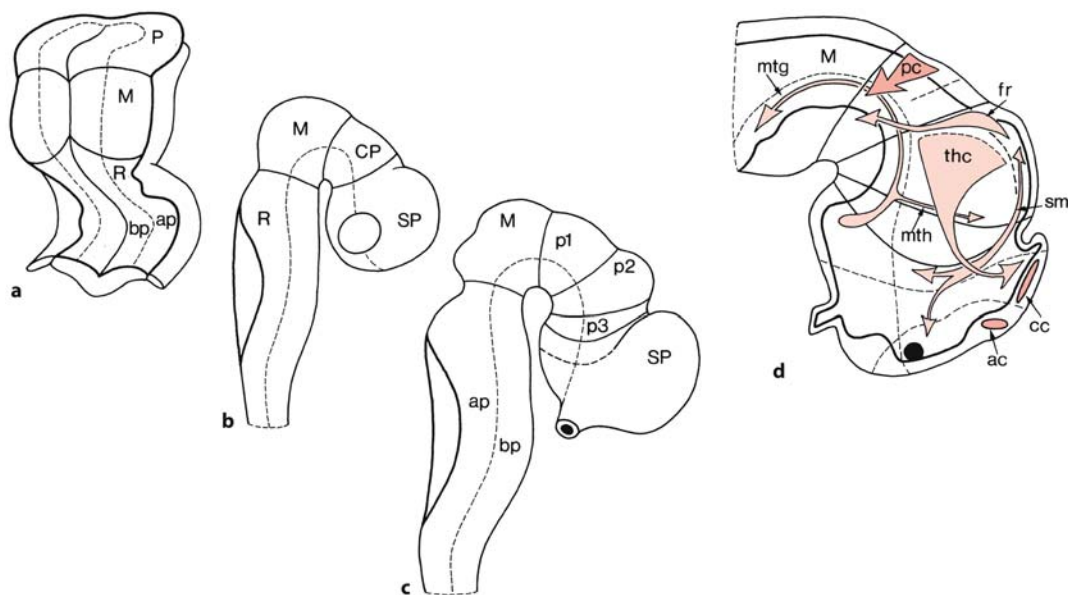
Fig. 9.1 a–c Prosomeric segmentation of the murine brain at E8.5 (**a**), E9.5 (**b**) and E10.5 (**c**) and **d** segmental organization of the murine diencephalon. *ac* anterior commissure, *ap* alar plate, *bp* basal plate, *cc* corpus callosum, *CP* caudal prosencephalon, *fr* fasciculus retroflexus, *M* mesencephalon, *mtg* mamillotegmental tract, *mth* mamillothalamic tract, *P* prosencephalon, *pc* posterior commissure, *p1–p3* prosomeres, *R* rhombencephalon, *sm* stria medullaris, *SP* secondary prosencephalon, *thc* thalamocortical projection. (After Martínez and Puelles 2000)

mediolateral patterning lead to the *prosencephalies*, a group of complex malformations of the forebrain, involving the hypothalamus, the eyes and the basal telencephalon. *Holoprosencephaly* (*HPE*) is the most common developmental malformation of the forebrain, ranging from 1 in 16,000 in live births to 1 in 250 in spontaneous abortions (Matsunaga and Shiota 1977; Shiota 1993; Muenke and Beachy 2001; Cohen and Shiota 2002). Several developmental pathways such as those operating the Sonic hedgehog (SHH) and Nodal signalling factors are involved in the pathogenesis of HPE and laterality defects (Roessler and Muenke 2001). In this chapter the development of the various derivatives of the embryonic forebrain and disorders that may appear during this development, HPE in particular, will be discussed. The further development of the cerebral cortex and its disorders will be discussed in Chap. 10.

9.2   Prosomeres and Pattern Formation of the Forebrain

Already during neurulation, the prosencephalon becomes subdivided into two transverse **proneuromeric regions**, known as the caudal, epichordal, proneuromere, giving rise to the caudal diencephalon, and the rostral, prechordal, proneuromere forming the secondary prosencephalon (Fig. 9.1). The secondary prosencephalon gives rise to the telencephalon, the eye vesicles and the hypothalamus or rostral diencephalon (Puelles 1995; Shimamura et al. 1995; Rubinstein et al. 1998; Puelles and Rubinstein 2003). The prosencephalic proneuromeres were subsequently subdivided into smaller transverse domains known as **prosomeres** (Puelles et al. 1987; Bulfone et al. 1993; Puelles 1995; Rubinstein et al. 1998; Puelles et al. 2000), which are composed of alar and basal components. Prosomeres P1–P3 form the diencephalon proper or **caudal diencephalon**: P1 is known as the synencephalon, P2 as the caudal parencephalon and P3 as the rostral parencephalon. The alar component of the synencephalon forms the pretectum, that of the caudal parencephalon the epithalamus and dorsal thalamus, and that of the rostral parencephalon the ventral thalamus or prethalamus. The basal components form the dopaminergic substantia nigra–ventral tegmental area of Tsai (VTA) complex and the prerubral tegmentum, including the interstitial nucleus of Cajal, some related nuclei and the fields of Forel. Figdor and Stern (1993) further subdivided the synencephalon into posterior and anterior regions. An overt segmental pattern was not found in the avian diencephalon (Larsen et al. 2001; Zeltser et al. 2001). Molecular marker expression data and the dispersal of labelled cell clones in chicken embryos are not in agreement with the prosomeric model. In-

stead, these data suggest the zona limitans intrathalamica as a bona fide compartment with local signalling function. The **protosegment**, previously described as prosomeres P4–P6 gives rise to the secondary prosencephalon. From this prechordal part of the prosencephalon the hypothalamus or **rostral diencephalon**, the optic vesicles and the telencephalon arise (Puelles and Rubinstein 2003). The basal and floor plates of the secondary prosencephalon give rise to various subdivisions of the hypothalamus, as originally defined for human embryos by His (1893; Keyser 1972, 1979), and the subthalamic nucleus, whereas from the alar part the anterior hypothalamus, the supraoptic nucleus (SON) and the paraventricular nucleus (PVN) and the entire telencephalon arise.

Fate mapping experiments suggest that the telencephalon derives from the anterolateral neural plate and the anterior neural ridge (Chap. 2). Ventral parts of the forebrain such as the hypothalamus and the eye vesicles arise from the medial part of the prosencephalic part of the neural plate. Pallial and subpallial parts of the telencephalon arise from the lateral parts of the prosencephalic neural plate. The lateral border of this part of the neural plate forms the dorsal, median part of the telencephalon and the commissural plate from which the anterior commissure, the corpus callosum and the hippocampal commissure arise. During the formation of the neural plate, **anteroposterior patterning** within the forebrain appears to be controlled by the **anterior neural ridge** at the rostral end of the neural plate (Shimamura and Rubinstein 1997; Houart et al. 1998, 2002; Marín and Rubinstein 2002; Rallu et al. 2002b). Its patterning properties may be mediated by FGF8. FGF8 signalling regulates the expression of *Foxg1* (earlier known as *brain factor 1* or *BF1*), a transcription factor that is required for normal telencephalic and cortical morphogenesis (Shimamura et al. 1995; Shimamura and Rubinstein 1997; Monuki and Walsh 2001). Coordinate regulation and synergistic actions of BMP4, SHH and FGF8 in the rostral prosencephalon regulate morphogenesis of the telencephalic and optic vesicles (Ohkubo et al. 2002). In mice, reduction in FGF8 expression in the anterior neural ridge leads to rostral midline defects in the forebrain (Shanmugalingam et al. 2000), similar to that described in mice lacking the *Foxg1* gene (Xuan et al. 1995; Dou et al. 1999). Fibroblast growth factor (FGF) signalling is also required for olfactory bulb morphogenesis (Hébert et al. 2003). The olfactory bulb may be particularly susceptible to FGF signalling as observed in mouse embryos carrying a hypomorphic allele of *Fgf8* (Meyers et al. 1998): they lack olfactory bulbs. Hébert et al. (2003) showed that the FGF receptor gene *Fgfr1* is essential for the formation of the olfactory bulb. In *Fgfr1* mutant mice, only small bulb-like
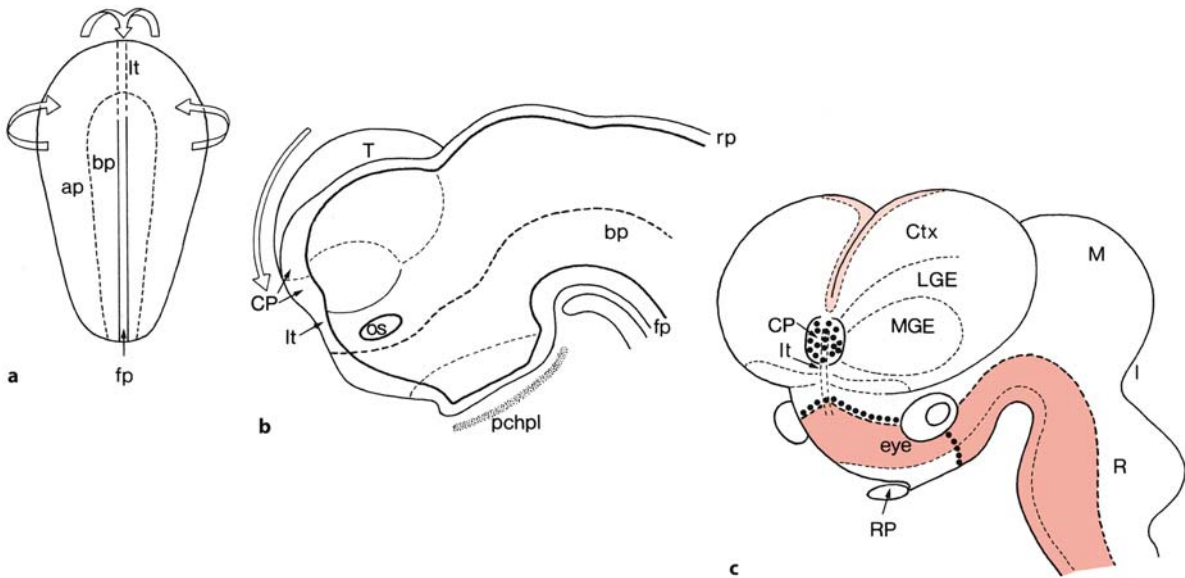
Fig. 9.2 The longitudinal organization and signalling centres of the developing murine prosencephalon: **a** model of the longitudinal domains of the neural plate; **b** medial view of the neural tube; **c** signalling centres in the prosencephalon. The expression of FGF8 is indicated by *dots*, that of BMP4 and WNT3a in *light red* and that of SHH in *red*. *ap* alar plate, *bp* basal plate, *CP* commissural plate, *Ctx* cortex, *fp* floor plate, *I* isthmus, *LGE* lateral ganglionic eminence, *lt* lamina terminalis, *M* mesencephalon, *MGE* medial ganglionic eminence, *os* optic stalk, *pchpl* prechordal plate, *R* rhombencephalon, *RP* Rathke's pouch, *rp* roof plate, *T* telencephalon. (After Shimamura et al. 1995; Marín and Rubinstein 2002)

protrusions are formed. Anteroposterior patterning of the rest of the telencephalon appears to be largely normal in *Fgfr1* mutants.

Whereas anteroposterior patterning of the forebrain generates transverse subdivisions, i.e. the prosomeres, mediolateral patterning generates longitudinal subdivision of the neural plate into alar and basal plates (Fig. 9.2). **Mediolateral patterning** of the forebrain involves signals from the axial mesendoderm (the prechordal plate) and non-neural ectoderm (Rubinstein and Beachy 1998; Lee and Jessell 1999). **Medial** or **ventral patterning** of the prosencephalic part of the neural plate is primarily regulated by the prechordal plate through SHH signalling, whereas its **lateral** or **dorsal patterning** is mediated by members of the transforming growth factor β (TGFβ) superfamily such as bone morphogenetic proteins (BMPs) and growth differentiating factors, largely derived from the neural ridge and non-neural ectoderm flanking the anterior neural plate. Mouse embryos that lack SHH fail to form normal ventral brain structures and show markedly reduced expression of ventral markers (Chiang et al. 1996; Litingtung and Chiang 2000; Rallu et al. 2002a, b). In *Drosophila*, all hedgehog signalling is mediated through the *cubitus interruptus* (*ci*) gene (Aza-Blanc and Kornberg 1999). The mammalian homologues of *ci*, the *Gli* genes, have a similar function. *Gli1* and *Gli2*

act as activators, and *Gli3* mainly as a repressor (Matise and Joyner 1999). In *Gli3* mutant mice, ventral telencephalic markers expand dorsally into the cortex (Grove et al. 1998; Theil et al. 1999; Rallu et al. 2002a, b). The balance between *Shh* and *Gli3* gene function appears to be crucial for the establishment of dorsoventral patterning within the telencephalon (Rallu et al. 2002b). The SHH–Gli pathway may be deregulated in brain tumours (Dahmane et al. 2001; Chap. 8).

9.3   Development of the Diencephalon

The diencephalon in its classic, columnar view (Herrick 1910; Droogleever Fortuyn 1912) was divided into four dorsoventrally arranged columns separated by ventricular sulci, i.e. the epithalamus, the dorsal thalamus, the ventral thalamus or subthalamus, and the hypothalamus (Fig. 9.3). Extensive embryological studies by the Swedish school of neuroembryologists (Bergquist and Källén 1954; Chap. 2) and a more recent Spanish school initiated by Luis Puelles made it clear that the thalamic 'columns' are derived from transversely oriented zones, the prosomeres. Currently, the diencephalon is subdivided into three segmental units (Fig. 9.1) which, from caudal to rostral,
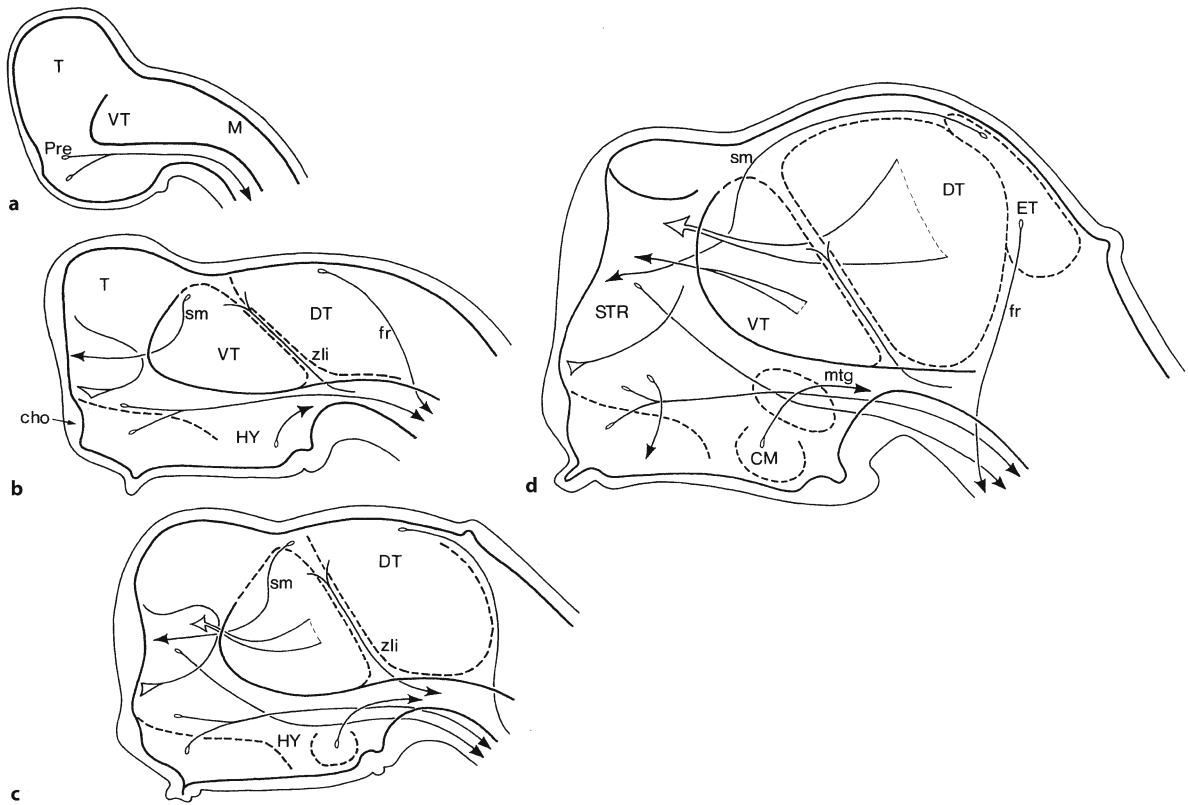
Fig. 9.3 Classic subdivision of the human diencephalon and early phases in the development of fibre connections of the forebrain. **a** 6-mm crown–rump length (*CRL*); **b** 9.5-mm CRL; **c** 11-mm CRL; **d** 18-mm CRL. Note that this figure precludes the prosomeric subdivision of the prosencephalon. Dorsal thalamic, ventral thalamic and hypothalamic domains are found in a caudorostral position to each other, not dorsoventral. *cho* chiasma opticum, *CM* corpus mamillare, *DT* dorsal thalamus, *ET* epithalamus, *fr* fasciculus retroflexus, *HY* hypothalamus, *M* mesencephalon, *mtg* mamillotegmental tract, *Pre* preoptic area, *sm* stria medullaris, *STR* striatum, *T* telencephalon, *VT* ventral thalamus, *zli* zona limitans intrathalamica. (After Gilbert 1935)

contain in their alar domains the pretectum (prosomere 1 or P1), the epithalamus and the dorsal thalamus (P2), and the ventral thalamus and the eminentia thalami (P3). The diencephalic basal plate contains the substantia nigra–VTA complex, the interstitial nucleus of Cajal and related nuclei, the prerubral tegmentum and the fields of Forel. The entire hypothalamus arises from the alar and basal components of the secondary prosencephalic protomere. The neurohypophysis appears to arise very rostrally (previously known as P6). Several genes show a diencephalic prosomere-related pattern, including *Gbx2* (Bulfone et al. 1993; Miyashita-Lin et al. 1999), *Otx1/Otx2* (Simeone et al. 1992, 1993; Larsen et al. 2001; Zeltser et al. 2001), *Pax6* (Stoykova et al. 1996; Grindley et al. 1997), *Dlx2* (Larsen et al. 2001; Zeltser et al. 2001), and *Dlx5* and *Math4a* (González et al. 2002; Figs. 2.13, 9.26). *Emx2* cooperates with *Otx2* at the onset of its expression to generate the territory of the future diencephalon (Suda et al. 2001).

9.3.1   Development of the Thalamus

The development of the human thalamus has been rather extensively studied with classical staining techniques (Schwalbe 1880; Gilbert 1935; Cooper 1950; Dekaban 1954; Kuhlenbeck 1954; Yamadori 1965; Richter 1966; Yakovlev 1969; Mojsilović and Zečević 1991). The thalamus is involved in central processing of sensory, motor and limbic functions. Early in development, the human diencephalon is thin-walled, but later the anlage of the thalamus expands enormously (Fig. 9.3). Owing to this expansion, the telencephalic–diencephalic boundary plane enlarges and changes its orientation from more or less transverse to almost rostrocaudal. Moreover, the lateral geniculate body becomes laterocaudally displaced.

The **dorsal thalamus** is largely composed of nuclei, relaying sensory, motor and limbic information to the cerebral cortex and subpallial structures. The
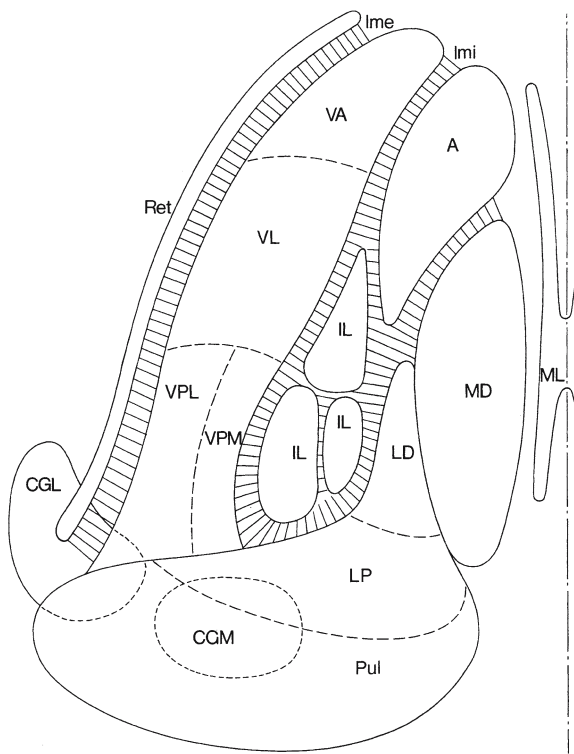
Fig. 9.4 Principal cell masses in the human thalamus shown in a horizontal section. *A* anterior thalamic nucleus, *CGL* corpus geniculatum laterale, *CGM* corpus geniculatum mediale, *IL* intralaminar nuclei, *LD* laterodorsal nucleus, *Ime* external medullary lamina, *Imi* internal medullary lamina, *LP* nucleus lateralis posterior, *MD* mediodorsal nucleus, *ML* midline nuclei, *Pul* pulvinar, *Ret* nucleus reticularis thalami, *VA* nucleus ventralis anterior, *VL* nucleus ventralis lateralis, *VPL* nucleus ventralis posterolateralis, *VPM* nucleus ventralis posteromedialis

following groups are usually distinguished (Jones 1985; Hirai and Jones 1989; Armstrong 1990; Onye 1990; Morel et al. 1997; Voogd et al. 1998; Percheron 2004), partly separated by the internal medullary lamina (Fig. 9.4):

1) A **lateral group**, involved in somatosensory relay (*nucleus ventralis posterior complex*) and motor control (*nuclei ventralis lateralis* and *ventralis anterior*).
2) A **medial group**, formed by the *mediodorsal nucleus* with extensive projections to the prefrontal cortex, and *midline* and *intralaminar nuclei* with projections to the striatum and to that part of the cerebral cortex that innervates the same part of the striatum.
3) An **anterior group**, relaying information from the mamillary nuclei to the limbic cortex, the cingulate cortex in particular. The more posteriorly

situated *laterodorsal nucleus* is often associated with the anterior group for its connections with the cingulate gyrus.
4) A large **posterior group** is composed of the *posterior complex*, involved in pain transmission, the *nucleus lateralis posterior* and the *pulvinar*, involved in visual orientation, eye movements and accommodation, and the *medial* and *lateral geniculate nuclei* which relay auditory and visual information, respectively.

The cortical projection areas of the main thalamic nuclei in the adult human brain are shown in Fig. 9.5.

The **ventral thalamus** is usually said to be composed of the ventral lateral geniculate or pregeniculate nucleus, the thalamic reticular nucleus and the zona incerta. Recently, Puelles and Rubinstein (2003) advocated the term prethalamus as an alternative. The subthalamic nucleus is usually included in the basal ganglia (Sect. 9.8.1). The **thalamic reticular nucleus** is a shell-like structure along the lateral border of the dorsal thalamus, and is situated between the external medullary lamina and the internal capsule (Fig. 9.4). The human fetal reticular nucleus consists of four subdivisions, clearly visible in the sixth/seventh gestational month (Ulfig et al. 1998; Ulfig 2002b). The main portion and the perireticular nucleus are prominent structures. Both parts are dramatically reduced in size during further development. The *perireticular nucleus* is not even visible in the adult brain (Ulfig et al. 1998). In rats, the perireticular nucleus also disappears almost completely (Mitrofanis and Baker 1993; Earle and Mitrofanis 1996). These transient features can be correlated with the role of the reticular nucleus in guiding outgrowing thalamocortical axons and as an intermediate target for corticofugal fibres (Mitrofanis 1992; Mitrofanis and Baker 1993; Earle and Mitrofanis 1996).

In rodents, the **birthdays** of the thalamic nuclei have been extensively analysed in [³H]thymidine studies (Angevine 1970, 1978; Keyser 1972; McAllister and Das 1977; Altman and Bayer 1979a–c; Bayer and Altman 1995a, b). Most thalamic nuclei are born between E13 and E19 (Table 9.1). Spatiotemporal gradients were found in the time of origin of thalamic nuclei (Fig. 9.6), in general, caudorostrally, ventrodorsally and outside-in oriented. Cells of posterior thalamic nuclei are born before those of anterior nuclei. Ventral thalamic nuclei such as the reticular nucleus are generated slightly earlier than dorsal thalamic nuclei. Lateral nuclei are born before medial nuclei such as the mediodorsal nucleus. Bayer et al. (1995) estimated that in human embryos the reticular nucleus and the medial and lateral geniculate nuclei are generated from late in week 5 to week 6 of development, ventrobasal complex neurons from late in
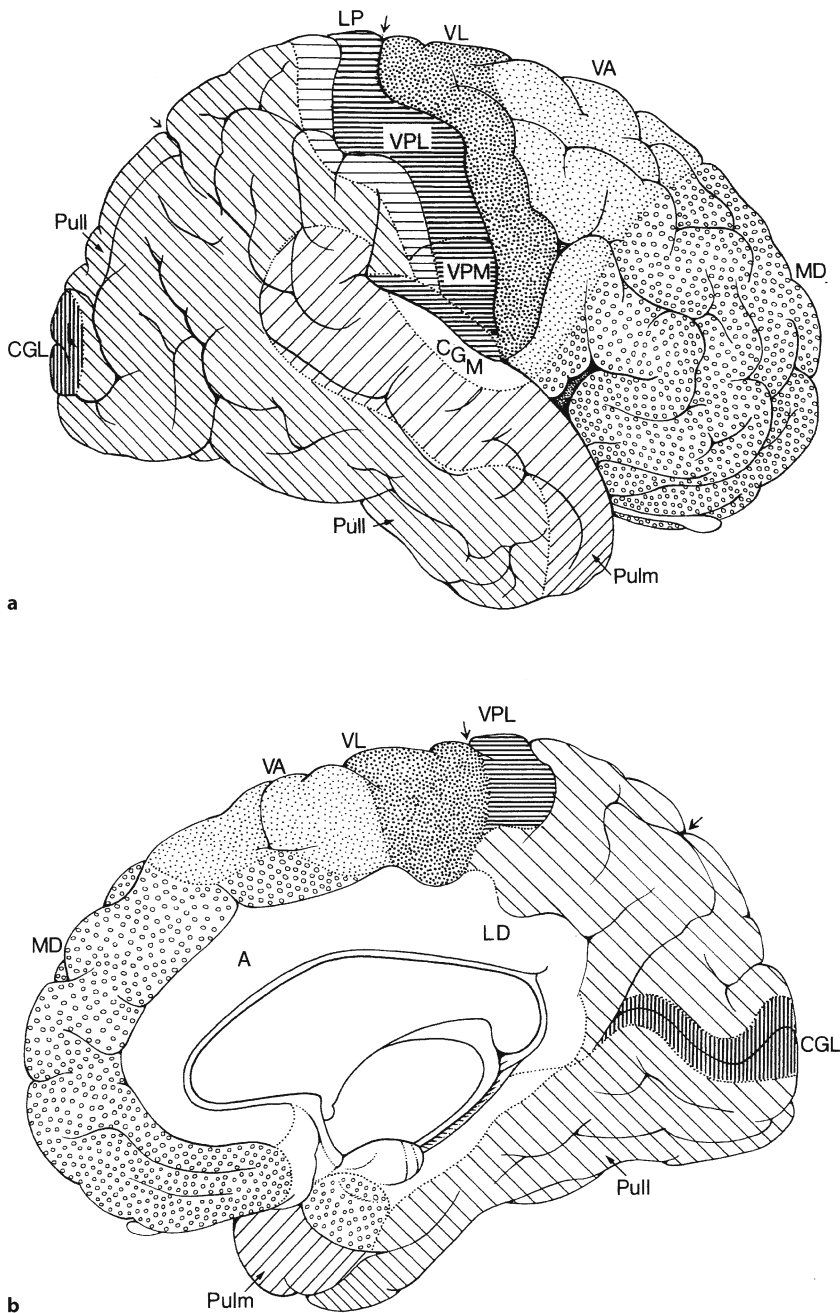
Fig. 9.5 Thalamocortical projection areas shown in lateral (**a**) and medial views (**b**) of the human cerebrum. *Arrows* indicate the central and parieto-occipital sulci. *A* anterior nucleus, *CGL* corpora geniculata laterale, *CGM* corpora geniculata mediale, *LD* laterodorsal nucleus, *LP* nucleus lateralis posterior, *MD* mediodorsal nucleus, *Pull* lateral part of pulvinar, *Pulm* medial part of pulvinar, *VA* nucleus ventralis anterior, *VL* nucleus ventralis lateralis, *VPL* nucleus ventrales posterolateralis, *VPM* nucleus ventrales posteromedialis

week 5 up to the middle of week 7 of development, and the anterior complex from weeks 7–11 (Table 9.1). Two thalamic nuclei in particular received much attention, the **lateral geniculate nucleus** (**LGN**) and the pulvinar.

The development of the LGN or **corpus geniculatum laterale** (**CGL**) has been extensively studied in rat (Brückner et al. 1976; Lund and Mustari 1977), cat (Shatz et al. 1990), ferret (Sur and Leamey 2001), rhesus monkey (Rakic 1977 a, b) and human (Gilbert 1935; Cooper 1945, Dekaban 1954; Hitchcock and

Hickey 1980; Hevner 2000) embryonic and fetal material. In the rhesus monkey, LGN neurons are generated during 8–9 days at the end of the first quarter of the 165-day gestational period. The first neurons are generated at E36, approximately 6 days after the first retinal ganglion cells are being born (Rakic 1977 a, b). Several generations of neurons produced in a restricted area of the ventricular zone appear to migrate along a single cellular fascicle and accumulate in a column-shaped aggregate. Neurons are generated along an outside-in gradient (Fig. 9.7). Initially, the

Table 9.1 Time of neuron origin data of diencephalic nuclei in Chinese hamsters (after Keyser 1972) and rats (after Altman and Bayer 1978a, b, 1979a–c), and estimated data for the human brain (after Bayer et al. 1995)

Diencephalic nuclei	Time of neuron origin data in Chinese hamsters in embryonic days (gestation time 20–21 days)	Time of neuron origin data in rats in embryonic days (gestation time 21–22 days)	Estimated data human brain (developmental weeks)	
			Time of neuron origin	Migration and settling
Dorsal thalamus				
Anterior nuclei	?	E15–E16(17)	6–8	7–11
Ventrobasal complex	?	E(14)15–E16	Late 5 to middle 7	7–9
Lateral geniculate nucleus	E14	E14–E15	Late 5 to 6	7–9
Medial geniculate nucleus	E13	E14(15)	Late 5 to late in 6	End of 6 to 8
Ventral thalamus				
Reticular nucleus	E14	E(13)14–E15	Late 5 to 7	Late 7 to 11
Hypothalamus				
Supraoptic and paraventricular nuclei	E13	E13–E15	Early 5 to beginning of 7	Middle 7
Suprachiasmatic nucleus	E14–E16	E14–E17	5-6	Late 5 to 7
Lateral hypothalamus	?	E(12)13–E14(15)	Early 5 to beginning of 7	Late 5 to 7
Mamillary body				
Lateral	E13	E13–E14(15)	4–6	5–7
Medial	E14	E(14)15–E16	5–8	7–14
Preoptic regions				
Median	E15?	E13–E15(17)	4–10	5–7
Medial	E13	E(14)15–E17(19)	4–8	5–7
Lateral	E12	E12–E14(15)	4–7	5–7
Sexually dimorphic nucleus	?	E(15)16–E19(20)	End of 6 to 11	?
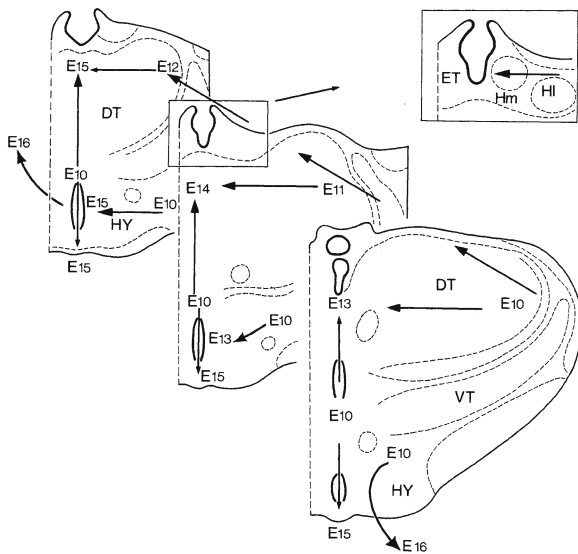
Fig. 9.6 Summary of rodent [³H]thymidine data for the diencephalon. The various caudorostral, ventrodorsal, dorsoventral and lateromedial gradients are indicated with *arrows*. *DT* dorsal thalamus, *ET* epithalamus, *Hl* lateral habenular nuclei, *Hm* medial habenular nucleus, *HY* hypothalamus, *VT* ventral thalamus. (After Angevine 1970)
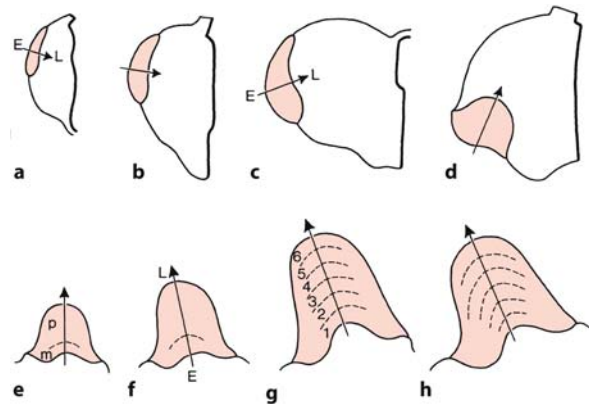
Fig. 9.7 Development of the monkey lateral geniculate nucleus in coronal sections of the diencephalon at E48 (**a**), E58 (**b**), E77 (**c**), E84 (**d**), E91 (**e**), E97 (**f**), E112 (**g**) and P60 (**h**). The *E–L* axis indicates the early-to-late gradient of generated neurons. *m* magnocellular part, *p* parvocellular part, *1–6* layers emerging between E90 and E105. (After Rakic 1977b)
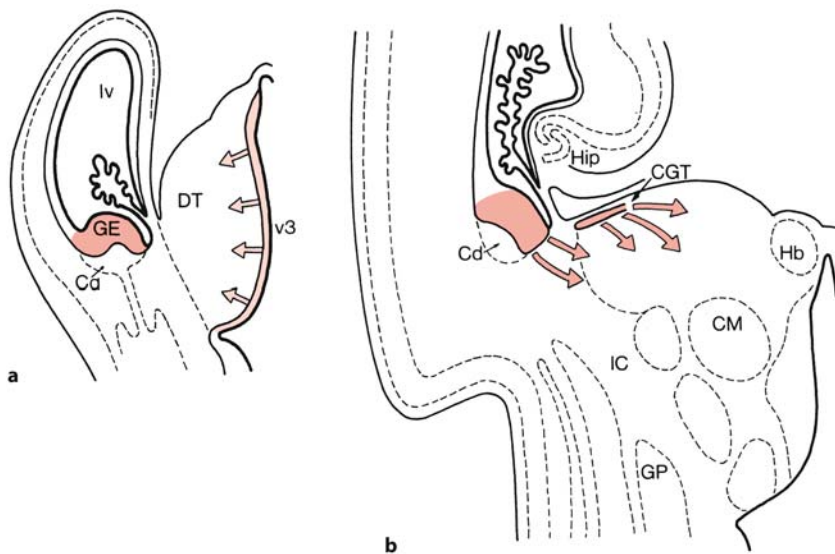
axis of this gradient is oriented lateromedially but later becomes oriented ventrodorsally, so that in the mature monkey, early generated neurons lie in the ventral magnocellular layers, whereas neurons generated later become part of the dorsal parvocellular layers. In the human brain, the CGL develops its characteristic six-layered structure from the 22nd until the 25th gestational week (Cooper 1945; Dekaban 1954; Hitchcock and Hickey 1980). Its cell layers are initially oriented parallel to the dorsoventral axis but, owing to rotation and differential growth of the thalamus, become oriented almost parallel to the mediolateral axis by the time of birth (Hevner 2000).

The **pulvinar**, the most prominent thalamic nucleus in the human brain, is not only generated in the diencephalic ventricular zone but, moreover, receives neurons from the ganglionic eminence of the telencephalon (Fig. 9.8). Rakić and Sidman (1969) showed that between the 16th and 34th week of gestation, cells pass from the medial ganglionic eminence into the lateral and posterior parts of the thalamus. Most of these neurons appear to migrate along a transient fetal structure, the **gangliothalamic body**. In a subsequent study of the fetal monkey brain, Ogren and Rakic (1981) were unable to demonstrate the presence of a gangliothalamic body, and suggested that this migration pathway is a unique feature of the developing human brain. Letinić and Kostović (1997) found the gangliothalamic body between 15 and 34 gestational weeks along the entire rostrocaudal thalamus, particularly at the level of the anterior nuclear complex, the mediodorsal nucleus, the pulvinar and the CGL, and suggested that, apart from the pulvinar, also the mediodorsal and anterior nuclei and the CGL are recipients of telencephalic neurons. Letinić and Rakic (2001) showed that these neurons are GABAer-

gic and express *Dlx1/Dlx2*. A similar migratory pathway has not been found in non-human primates and rodents (Anderson et al. 1997a, 1999; Lavdas et al. 1999; Wichterle et al. 1999, 2001), supporting the idea that it may be a special feature of human thalamic development. GABAergic neurons are absent in many thalamic nuclei, except for the CGL (Harris and Hendrickson 1978; Ottersen and Storm-Mathisen 1984), but in the primate brain GABAergic cells form approximately 30 % of the neurons in every thalamic nucleus (Montero and Zempel 1986).

Thalamocortical projections arise rather early in development. Yamadori (1965) studied the development of thalamocortical projections in 5–130-mm-long human embryos. The first fibres were already recognized in the thalamus of a 5-mm embryo (approximately 3 weeks of development). Developing thalamocortical axons leave the dorsal thalamus ventrally and turn dorsolaterally at the telencephalic–diencephalic boundary (Fig. 9.3). They advance below the ganglionic eminences and pause at the corticostriatal junction before entering the developing cerebral cortex. The earliest corticofugal projections, most of which originate from preplate neurons as shown in rodents, pause within the corticostriatal junction. In rodents, the **corticostriatal junction** has been characterized by lack of both *Emx1* and *Dlx1* gene expression and the presence of *Pax6* expression (Smith-Fernández et al. 1998; Puelles et al. 2000; Zaki et al. 2003; Fig. 9.26, Table 9.2). Experiments in rodents indicate that the ganglionic eminence may be an intermediate target for corticofugal and thalamocortical axons (Métin and Godement 1996; Garel et al. 2002), and that the corticostriatal junction plays an active role in the further development of these connections (Molnár et al. 1998; Auladell et al. 2000;

Table 9.2 Summary of mutant mice with altered early thalamocortical development (after Molnár and Hannan 2000; López-Bendito and Molnár 2003)

Gene mutated	Type of mutation	Phenotype	Molecular mechanism	References
Emx2	Targeted KO	Primary defect in cortical development; disturbed thalamocortical growth at diencephalotelencephalic boundary	Not known	Mallamaci et al. (2000)
Tbr1	Targeted KO	Thalamocortical and corticothalamic axon elongation defect	Not known	Hevner et al. (2001)
Gbx2	Targeted KO	Thalamocortical and corticothalamic axon elongation disrupted at IC	Not known	Hevner et al. (2002)
Mash1	Targeted KO	No thalamic fibre outgrowth beyond IC	Not known; IC cells with thalamic projections missing	Tuttle et al. (1999)
Pax6$^{Sey/Sey}$	Spontaneous mutation (Small eye)	Thalamocortical and corticofugal axon elongation disrupted at IC	Not known	Kawano et al. (1999); Hevner et al. (2002)
Pax6/LacZ	Targeted KO	Disturbed thalamocortical and corticothalamic axon elongation at the corticostriatal junction	Not known	Stoykova et al. (2000); Jones et al. (2002)
L1	Targeted KO	Thalamocortical axon fasciculation defects in IC and at the corticostriatal junction	Selective fasciculation defect mediated by L1	Cohen et al. (1997); Dahme et al. (1997)

IC internal capsule, *KO* knockout

Molnár and Hannan 2000; Molnár and Butler 2002). Subsequent to their interaction with cells at the corticostriatal junction, thalamocortical and corticofugal fibres proceed, intimately associated with each other, to their targets. They become 'captured' for a **waiting period** in the subplate before entering the cortical plate (Shatz et al. 1990).

Thalamocortical projections display **two levels** of **topographic organization** (Molnár 1998; López-Bendito and Molnár 2003; Marín 2003). First, specific dorsal thalamic nuclei, relaying distinct modalities of sensory (visual, somatosensory, auditory) or motor information, project to specific neocortical areas (**interareal topography**). In rodents, these thalamic nuclei are arranged following a more or less caudolateral to rostromedial gradient, whereas their corresponding cortical targets are found in caudorostral progression in the cortex. This interareal topography arises early in development and appears to be largely independent of functional activity within the thalamocortical radiation. The second level of topographic organization concerns the **topic representation** of different parts of the body, retina or inner ear in projections of thalamic nuclei to their cortical targets, resulting in somatotopic, retinotopic and tonotopic maps, respectively. This second level of topographic mapping appears later in development than interareal topography. It is redefined during the first postnatal weeks, partly through activity-dependent mechanisms (López-Bendito and Molnár 2003). Interareal topography may be explained by the expression of localized cues within the cortex, controlling the targeting of thalamic axons, or by the '**handshake hypothesis**' (Blakemore and Molnár 1990; Molnár and Blakemore 1995; Molnár 1998; Fig. 9.9). In this hypothesis it has been proposed that axons from the thalamus and from the early-born cortical preplate cells meet and intermingle in the basal telencephalon, so that thalamic axons grow over the scaffold of preplate axons. In mouse mutants (Table 9.2), often the disruption of thalamocortical and corticothalamic fibres is correlated (Cohen et al. 1997; Dahme et al. 1997; Kawano et al. 1999; Tuttle et al. 1999; Braisted et al. 2000; Mallamacci et al. 2000; Stoykova et al. 2000; Hevner et al. 2001, 2002; Jones et al. 2002; Molnár and Butler 2002). More recently, Garel et al. (2002) showed that the establishment of topographic thalamocortical projections is not strictly determined by cortical cues, but instead is influenced by the relative position of thalamic axons inside the ventral telencephalon (Vanderhaeghen and Polleux 2004). It seems likely that the topographic organization that thalamic axons adopt in the cortex is already set upon their entry into the telencephalon, and that any alteration of their topography in this intermediate target results in a parallel perturbation of their topography in the cortex. Therefore, the development of interareal topography within the thalamocortical system occurs through the sorting out of thalamocortical axons in the ventral telencephalon. This sorting out is controlled by ephrins (Dufour et al. 2003; Seibt et al. 2003; Vanderhaeghen and Polleux 2004).
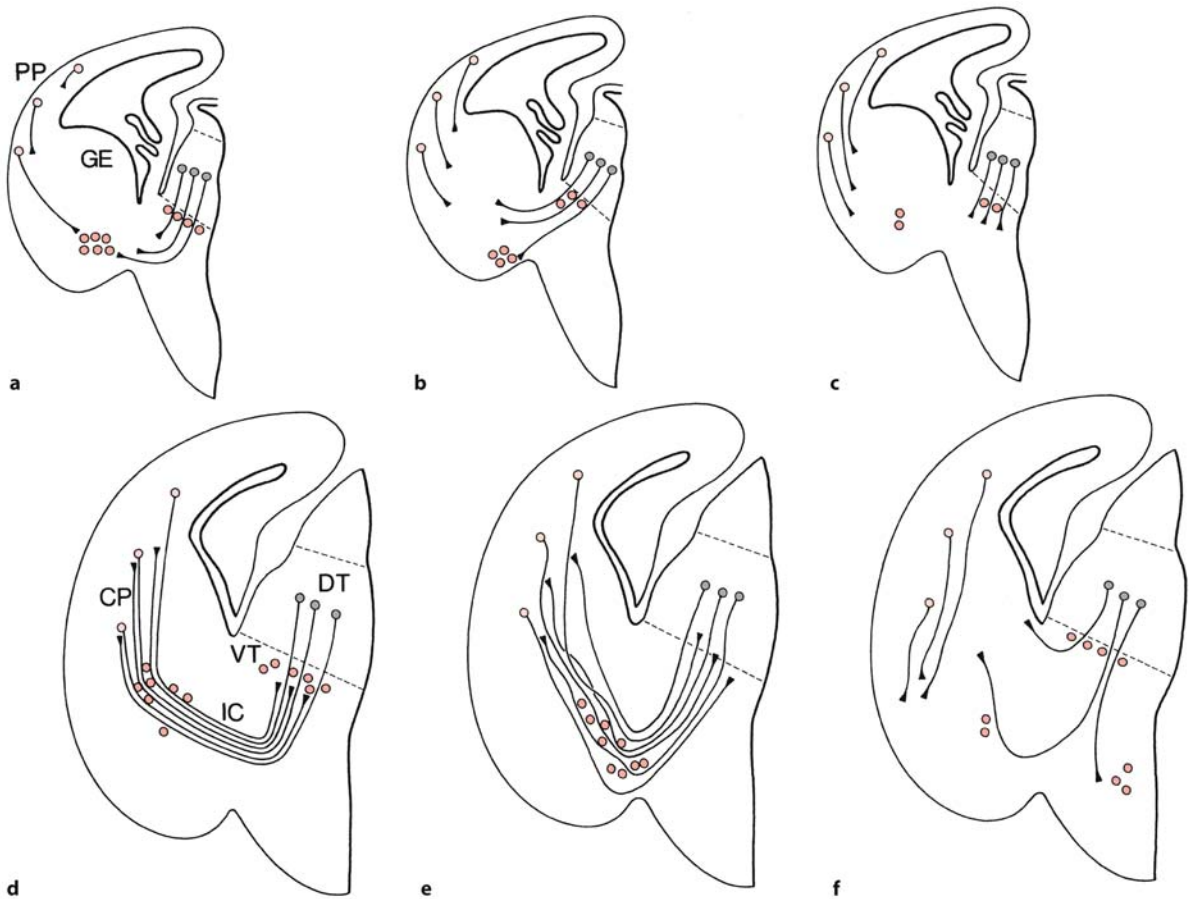
Fig. 9.9 Thalamocortical projections: data in the developing rat brain/mouse mutants. **a**, **b** Normal rat E13.5 and E18.5 embryos, illustrating the 'handshake' hypothesis (Fig. 2.30). **c**, **d** Comparable data in an *Emx2–/–* mutant. **e**, **f** Comparable data in a *Pax6/LacZ–/–* mutant (see text for explanation). 'Guidepost' cells in the ventral thalamus (*VT*), the basal fore- brain and the internal capsule (*IC*) are indicated in *red*, thalam- ocortical projection neurons in *grey* and corticofugal neurons in *light red*. *CP* cortical plate, *DT* dorsal thalamus, *GE* ganglion- ic eminence, *PP* preplate. (After López-Bendito and Molnár 2003)

9.3.2   Development of the Hypothalamus

The hypothalamus is involved in a wide variety of functions in the brain. Alterations in hypothalamic nuclei are found in various endocrine diseases such as diabetes insipidus, Wolfram and Prader–Willi syndromes, and in various neurodegenerative diseases such as Alzheimer, Parkinson and Huntington diseases (reviewed in Swaab 1997, 2004). The hypothalamus is usually subdivided into four regions (Fig. 9.10), from caudal to rostral: (1) the mamillary region; (2) the tuberal region; (3) the anterior complex; and (4) the preoptic region (Braak and Braak 1987, 1992; Swaab et al. 1993; Swaab 1997, 2003; Voogd et al. 1998; Saper 2004). From a developmental point of view, however, three longitudinal subdivisions of the hypothalamus can be distinguished (Angevine 1970; Altman and Bayer 1986; Mai and Ashwell 2004)

as originally proposed by Crosby and Woodburne (1940; Nauta and Haymaker 1969): a periventricular zone, an intermediate zone and a lateral zone. The entire hypothalamus is now thought to arise from that part of the secondary prosencephalon that is known as the rostral diencephalon (Puelles and Rubinstein 2003).

Early steps in the development of the hypothalamus include the induction of hypothalamic identity and the migration of hypothalamic precursors. The prechordal plate provides the SHH protein necessary for the formation of the hypothalamus. In mice lacking the *Shh* gene, hypothalamic tissue is absent, whereas overexpression of SHH leads to ectopic expression of hypothalamic markers (Mathieu et al. 2002). Disturbance of the development of hypothalamic nuclei may be due to disruption of genes involved in neurogenesis (*Otp*), cell migration (*Otp*,
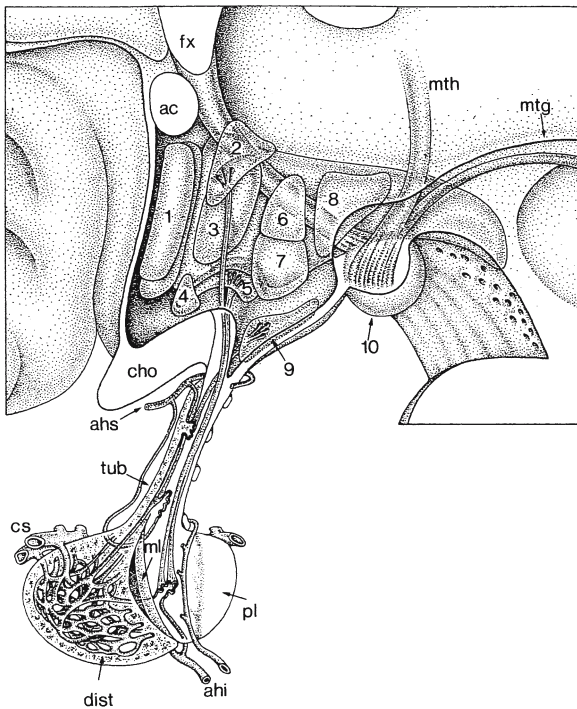
Fig. 9.10 Organization of the human hypothalamus and hypothalamohypophysial relations. *ac* anterior commissure, *ahi* inferior hypophysial artery, *ahs* superior hypophysial artery, *cho* chiasma opticum, *cs* sinus cavernosus, *dist* distal part of anterior pituitary lobe, *fx* fornix, *ml* middle pituitary lobe, *mtg* mamillotegmental tract, *mth* mamillothalamic tract, *pl* posterior pituitary lobe, *tub* tuberal part of anterior pituitary lobe, *1* preoptic nucleus, *2* paraventricular nucleus, *3* anterior nucleus, *4* suprachiasmatic nucleus, *5* supraoptic nucleus, *6* dorsomedial nucleus, *7* ventromedial nucleus, *8* posterior nucleus, *9* arcuate nucleus, *10* corpus mamillare. (After Nauta and Haymaker 1969)

SF-1), cell death (*Brn2*, *Sim1*, *Arnt2*) and differentiation (*Nkx2.1*). *Brn4* knockout mice show a loss of the SON and the PVN, and in mice with mutations in the gene encoding for the nuclear receptor SF-1 the ventromedial hypothalamic nucleus is absent (Martin and Camper 2001). These data suggest that similar defects may exist in human disease (Swaab 2003).

In rodents, in autoradiographic studies the hypothalamic nuclei were found to be generated mainly from E13 until E16, and preoptic nuclei over an even more protracted period, extending from E12 until E19 (Angevine 1970, 1978; Keyser 1972; Altman and Bayer 1978a, b; 1986; Bayer and Altman 1987a; Fig. 9.6, Table 9.1). The sexually dimorphic nucleus (SDN; Gorski et al. 1978) originates exceptionally late (E15–E19). Extrapolated to the human brain, hypothalamic nuclei would be generated between the fifth and the eighth week of development, and those from

the preoptic region from weeks 4 to 11 of development (Bayer et al. 1995; Table 9.1). In the fetal human hypothalamus, Koutcherov et al. (2002; Mai and Ashwell 2004) found three waves of neurogenesis and migration as in the rodent brain (Altman and Bayer 1986). The first neurons generated migrate into the future lateral longitudinal zone of the hypothalamus where they form the lateral hypothalamic area, the posterior hypothalamus, the lateral tuberal nucleus and the perifornical nucleus. The second wave of postmitotic neurons form the nuclei of an intermediate longitudinal zone, including the medial preoptic nucleus, the anterior hypothalamic nucleus, the ventromedial and the dorsomedial nuclei, and the mamillary body. The last neurons to be generated differentiate in close proximity to the periventricular zone, and form the suprachiasmatic nucleus, the arcuate nucleus, the PVN and the SON. All nuclei are apparent early fetally.

In humans, the **sexually dimorphic nucleus (SDN)** is located between the SON and the PVN. In young adult males, this nucleus is twice as large as in adult women (Swaab and Fliers 1985; Swaab et al. 1993; Swaab 1997, 2003). At birth, only about 20% of the SDN neurons are present and sexual dimorphism is not found in the human brain. From birth up to the age of 4 years, cell numbers increase equally rapidly in both sexes. About the fourth year postnatally, the number of cells starts to decrease in girls (Swaab and Hofman 1988). The large neurosecretory cells of the **supraoptic nucleus (SON)** and **paraventricular (PVN) nucleus** produce the neuropeptides vasopressin and oxytocin, and innervate the neurohypophysis (Dierickx and Vandesande 1977). Vasopressin acts as an antidiuretic hormone in the kidney and, in women, oxytocin is involved in labour and lactation. The **infundibular nucleus** contains, among many other neuropeptides and transmitters, gonadotropin-releasing hormone (GnRH) neurons, earlier known as luteinizing hormone-releasing hormone (LHRH) neurons (Muske 1993; Swaab 1997, 2003). GnRH neurons are found in the human fetal hypothalamus from the 9th week of development. The GnRH neurons are generated in the epithelium of the medial olfactory pit and migrate from the nose into the forebrain along branches of the terminal and vomeronasal nerves rich in the neural cell adhesion molecule NCAM (Schwanzel-Fukuda and Pfaff 1989; Schwanzel-Fukuda et al. 1989). No GnRH neurons were seen in the brain until a bridge of the terminal and vomeronasal nerves was formed between the nose and the forebrain. Observations in Kallmann syndrome (Sect. 9.7.4) suggested that GnRH neurons fail to migrate from the olfactory placode into the developing brain (Schwanzel-Fukuda et al. 1989). In human embryos, GnRH immunoreactivity was first detected in the olfactory epithelium and in cells associ-
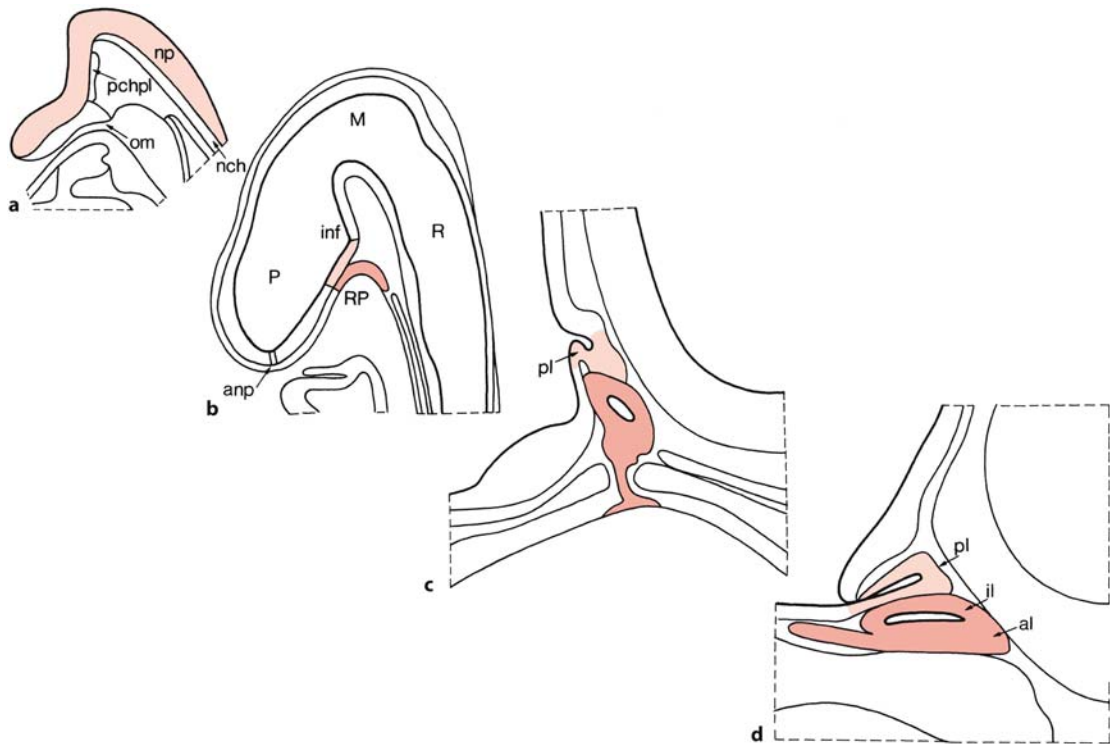
Fig. 9.11 Rodent pituitary development: **a** growth of the pre-infundibular part of the neural plate and establishment of the presumptive Rathke's pouch area (rat E8.5; mouse E8.0–E8.5) **b** formation of a rudimentary pouch (rat E11; mouse E9.5); **c** formation of the definitive pouch (rat E14.5; mouse E12); **d** developing pituitary gland (rat E19.5; mouse E17). The neural plate (*np*) and the neurohypophysis are indicated in *light red*

and the developing adenohypophysis in *red*. *al* anterior lobe, *anp* anterior neuropore, *il* intermediate lobe, *inf* infundibulum, *M* mesencephalon, *nch* notochord, *om* oral membrane, *P* prosencephalon, *pchpl* prechordal plate, *pl* posterior lobe, *R* rhombencephalon, *RP* Rathke's pouch. (After Schwind 1928; Sheng and Westphal 1999)

ated with the terminal and vomeronasal nerves at 42 days of gestation (Schwanzel-Fukuda et al. 1996). GnRH neurons appear to have multiple embryonic origins (Muske 1993; Northcutt and Muske 1994), however: the olfactory placode giving rise to the septo-preoptic system, and a second, non-placodal structure giving rise to the posterior GnRH neurons.

9.3.3   Development of the Pituitary Gland

The development of the human **hypophysis cerebri** or **pituitary gland** has been extensively studied (Atwell 1926; Conklin 1968; Andersen et al. 1971; Ikeda et al. 1988; O'Rahilly and Müller 2001). It consists of two main parts, the adenohypophysis and the neurohypophysis that form the sellar pituitary. The two components are in close contact from the beginning (Figs. 9.11–9.13). The area of contact between Rathke's pouch (Rathke 1838) and the forebrain gradually moves from rostral to caudal and, after 13 weeks of development, has a position similar to that found in the newborn (Ikeda et al. 1988).

The **adenohypophysial primordium** is induced by the adjacent floor of the rostral forebrain, from which the neurohypophysis develops (Sheng and Westphal 1999). In amphibian and avian embryos, the adenohypophysis originates from the anterior neural ridge (Eagleson et al. 1986; Couly and Le Douarin 1987; Fig. 2.8). In rats, it arises from a small area just anterior to the rostral end of the neural plate (Kouki et al. 2001). The neurohypophysis arises from the most rostral part of the secondary prosencephalon (Puelles and Rubinstein 2003). At the time Rathke's pouch forms, the oral ectoderm is in direct contact with the neuroectoderm of the ventral forebrain (Fig. 9.11), without intervening mesoderm (Schwind 1928). In in vitro tissue recombination assays a dramatic effect of neuroectoderm on the growth and differentiation of Rathke's pouch has been demonstrated (Daikoku et al. 1982; Watanabe 1982). The homeobox gene *Nkx2.1*, expressed in the ventral forebrain but not in the oral ectoderm or Rathke's pouch (Lazzaro et al. 1991), may provide the inductive signal. In *Nkx2.1* mutants, apart from severe defects in the development of the forebrain, the pituitary gland is

Fig. 9.12 Development of the human pituitary gland: **a** median section at 4.5 weeks of development (Carnegie stage 11); **b** embryo of 4.5 weeks of development (stage 14), showing Rathke's pouch; **c** at 6 weeks (stage 17); **d** at stage 19; **e** at the end of the embryonic period (stage 23); **f** fetal pituitary. The developing neurohypophysis (*nh*) is indicated in *light red* and the adenohypophysis in *red*. *D* diencephalon, *dist* distal part, *inf* infundibulum, *int* intermediate part, *M* mesencephalon, *nch* notochord, *om* oral membrane, *ot* otocyst, *php* pharyngeal pituitary, *pl* posterior lobe, *R* rhombencephalon, *RP* Rathke's pouch, *tub* tuberal part. (After O'Rahilly and Müller 2001)
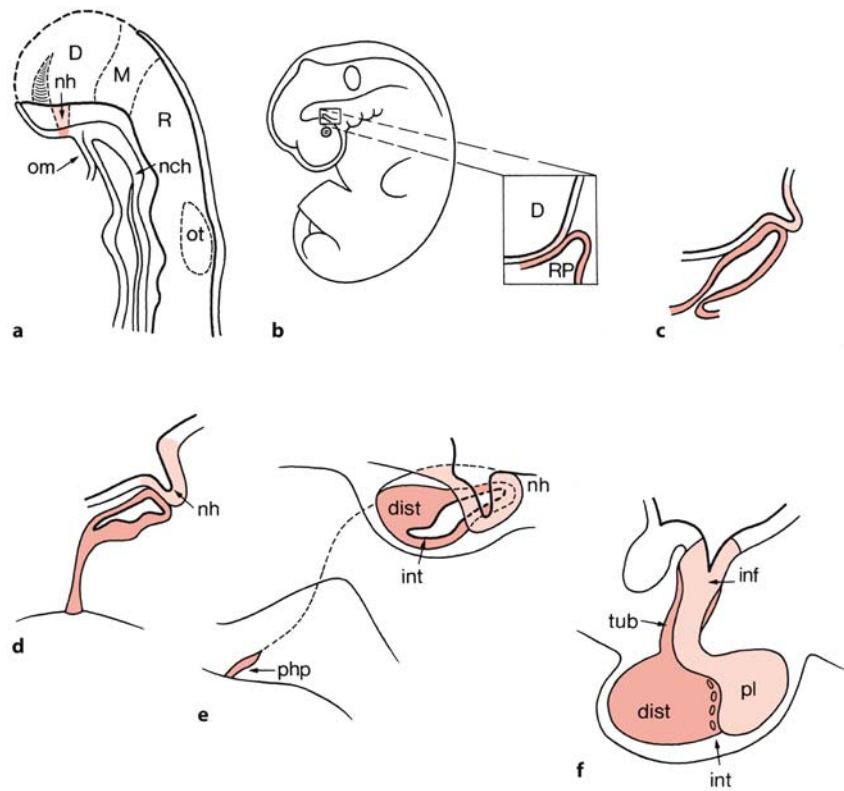
ablated (Kimura et al. 1996). A **two-step induction** of Rathke's pouch is required (Watkins-Chow and Camper 1998; Sheng and Westphal 1999; Dattani and Robinson 2000; Zhu and Rosenfeld 2004). Both a BMP4 signal and FGF8 activity from the ventral forebrain are required for the development of a definitive pouch. Initially, at E8.5, BMP4 induces the oral ectoderm to form a pouch placode. Formation of the definitive pouch requires the activation of two LIM homeobox factors (*Lhx3* and *Lhx4*) in the rudiment. FGF8, expressed in the ventral forebrain at E9.25, provides the signal that initiates and maintains *Lhx* gene expression in the pouch (Sheng et al. 1997; Sheng and Westphal 1999; Zhu and Rosenfeld 2004). Hedgehog signalling is also required for pituitary gland development (Treier et al. 2001). In rats, by E12.5 pituitary-specific cell types are formed (Camper et al. 2002). *Pitx1* and *Pitx2* regulate precursor and cell-type specific proliferation (Szeto et al. 1999; Suh et al. 2002). Targeted disruption of the *Pitx1* gene results in minor defects in later phases of pituitary development and defects in hindlimb and craniofacial morphogenesis (Kioussi et al. 2002), whereas *Pitx–/–* mice display multiple developmental defects, including failure of body-wall closure, cardiac outflow tract abnormalities and defects in pituitary, eye and tooth development (Gage et al. 1999; Kitamura et al. 1999; Lin et al. 1999). Invagination of Rathke's pouch and direct con-

tact with the neuroepithelium occur normally, but the pituitary is developmentally arrested by E10.5. *Hesx1* regulates pituitary proliferation indirectly through the interaction with *Tle* genes (Dasen et al. 2001). Deletion of *Hesx1* results in either a complete lack of the pituitary gland (5%) or multiple oral ectoderm invagination and/or cellular overproliferation of all pituitary cell types (Dattani et al. 1998; Martinez-Barbera et al. 2000; Dasen et al. 2001). Members of the *Six* homeodomain gene family (*Six1*, *Six3*, *Six6*) are required for tissue-specific precursor proliferation (Zhu and Rosenfeld 2004). *Six1* and *Eya* modulate precursor cell proliferation in many organs, including the eyes, the pituitary, the auditory system, the kidneys and somites (Li et al. 2003).

In human embryos, the primordium of the adenohypophysis is situated immediately rostral to the oropharyngeal membrane at stage 11, and forms the **adenohypophysial pouch**. Between stages 14 and 17, the floor of the forebrain forms the **neurohypophysial evagination**, and by stages 20 and 21, the pouch loses its contact with the roof of the mouth (Figs. 9.12, 9.13). The portion of the pouch that is in contact with the neurohypophysial evagination forms the **pars intermedia** of the hypophysis. Other parts of the adenohypophysis that surround the stalk of the neurohypophysis form the **pars tuberalis**, and the remaining part forms the the **pars distalis**. The
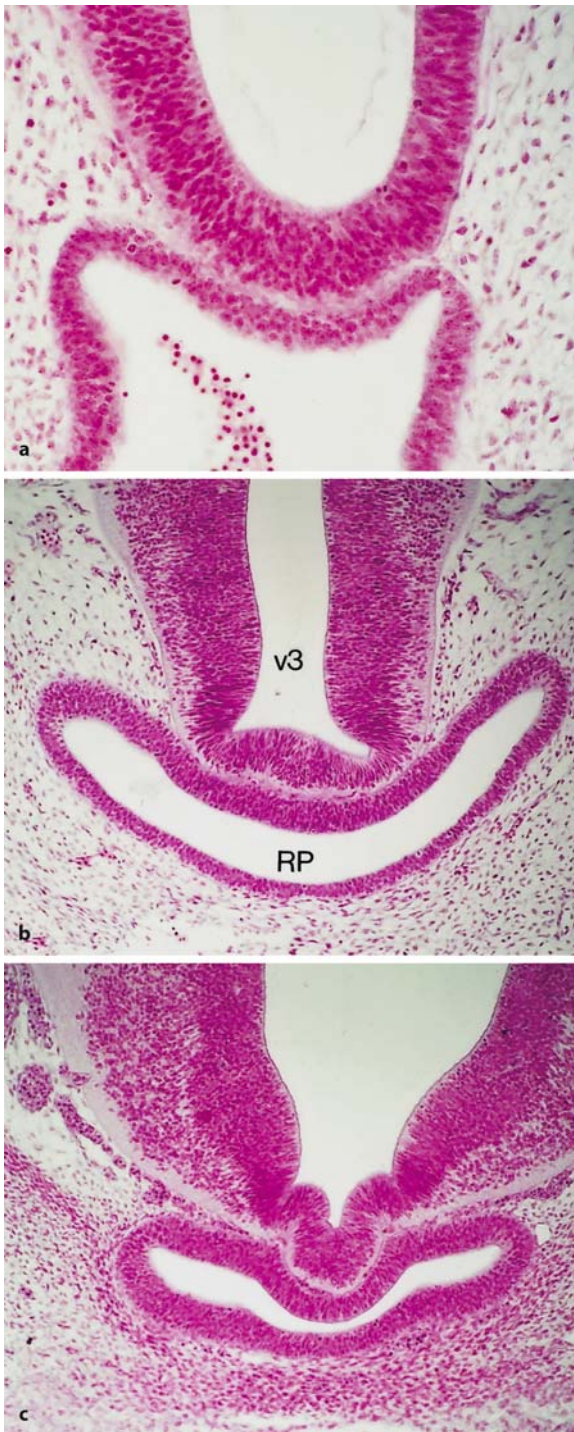
Fig. 9.13 Series of photomicrographs showing the development of the human pituitary gland at Carnegie stages 14 (**a**), 16 (**b**), and 18 (**c**); haematoxylin–eosin staining. *RP* Rathke's pouch, *v3* third ventricle. (From the Kyoto Collection of Human Embryos)

oropharyngeal part remains as the **pharyngeal hypophysis** throughout life (Boyd 1956). Rathke's pouch migrates together with the pituitary cells, and remnants may be found in the sellar pituitary (Kjaer and Fischer-Hansen 1995; Hori et al. 1999b). Pituitary hormones are produced at the end of the embryonic period. In immunohistochemical studies of human embryonic and fetal pituitaries, adrenocorticotropic hormone and somatotropic hormone were demonstrated at gestational week 8, whereas thyrotropic hormone, follicle-stimulating hormone, luteinizing hormone and prolactin-releasing hormone were found at week 12 (Asa et al. 1986, 1988; Ikeda et al. 1988).

9.3.4 Developmental Disorders of the Hypothalamus and the Pituitary Gland

Developmental disorders of the *hypothalamus* are common in anencephaly and in HPE and related disorders. In *anencephaly* and in fetuses with HPE, adenohypophysial tissue was found not only in the sella turcica but also in the open craniopharyngeal canal (Nakano 1973; Kjaer and Fischer-Hansen 1995; Hori et al. 1999 a, b). The intermediate part of the pituitary and the neurohypohysis are absent in most of the anencephalic cases studied (Nakano 1973; Visser and Swaab 1979). The adrenocorticotropic deficiency of the distal part of the pituitary is evident from the fact that the adrenal glands in anencephalics are invariably hypoplastic (Nakano 1973; Visser and Swaab 1979; Mazzitelli et al. 2002). At 17–18 weeks of gestation, the number and size of adrenocorticotropic hormone cells in the anencephalic pituitary gland are normal, but after 32 weeks their number and size are reduced (Pilavdzic et al. 1997). The involvement of the hypothalamus in HPE is discussed in Sect. 9.7.2.

Panhypopituitarism may also occur in *transsphenoidal encephaloceles* (Chong and Newton 1973; Brodsky et al. 1995; Morioka et al. 1995). These sporadic and rare anomalies are often associated with other midline anomalies such as cleft palate, hypertelorism, colobomata and agenesis of the corpus callosum. A 50% reduction in the number of oxytocinergic PVN neurons was found in patients with *Prader–Willi syndrome* (Gabreëls et al. 1994, 1998; Gabreëls 1998), which is characterized by gross obesity and insatiable hunger. This syndrome is further characterized by diminished fetal motility, severe infantile hypotonia, mental retardation, hypogonadism and hypogenitalism (Prader et al. 1956). *Diabetes insipidus* may have different hypothalamic causes. Apart from trauma, haemorrhage, inflammation and surgical manipulations, familial hypothalamic dia-

betes insipidus is found, owing to point mutations in the vasopressin–neurophysin–glycopeptide gene (Ito et al. 1991; Bahnsen et al. 1992; Nagasaki et al. 1995; Rittig et al. 1996). Available postmortem data suggest severe neuronal death in the SON and PVN in cases of familial hypothalamic diabetes insipidus associated with a loss of innervation of the posterior pituitary (Braverman et al. 1965; Nagai et al. 1984; Bergeron et al. 1991). Diabetes insipidus is also observed as part of midline developmental anomalies such as HPE and septo-optic dysplasia. The SON and PVN are also affected in **Wolfram syndrome**, an autosomal recessive disorder involving diabetes insipidus, diabetes mellitus, slowly progressive atrophy of the optic nerve and deafness (Wolfram 1938; Carson et al. 1977; Cremers et al. 1977). Vasopressin neurons are present in the PVN but apparently do not produce vasopressin, probably by a deficiency in processing of the precursor.

Pituitary malformations include agenesis of the anterior pituitary gland (Brewer 1957; Larroche 1981), partial agenesis of anterior pituitary components (Miyai et al. 1971; Sato et al. 1975), duplication of the entire pituitary (Hori 1983; Hori et al. 1999b; Clinical Case 9.1) and ectopias (Decker 1985; Colohan et al. 1987; Ikeda et al. 1987). *Developmental anomalies* of the *anterior pituitary* include non-separation of the primary pituitary gland into sellar and pharyngeal components, a *pharyngosellar pituitary* (Hori et al. 1995; Clinical Case 9.2) and ectopic migration into the subarachnoid space. Invasion of basophil cells into the posterior lobe, the frequency and intensity of which increase in accordance with aging, is rather a physiological phenomenon (Hori et al. 1999a, b; Swaab 2004). Novel mutations in the homeobox gene *Hesx1/HESX1* may play a role in *undescended* or *ectopic posterior pituitary* (Brickman et al. 2001).

Clinical Case 9.1
Duplication of the Pituitary Gland

Duplication of parts of the CNS has been observed occasionally. In a 26-day-old female baby, Hori (1983) described a brain with two complete pituitary glands, associated with malformations of ventral midline structures of the CNS and cranium (see Case Report). This rare condition of double hypophysis should be classified among the median cleft face syndrome (DeMyer 1967; Gorlin et al. 1977) in contrast to reported cases of double hypophysis in partial twinning (Ahlfeld 1880; Morton 1957; Warkany 1971). In the present case, the pituitary anlage, both of neurohypophysis and of adenohypophysis, may have been divided during early development owing to a median cleft. Subsequent histogenesis of each separate anlage may have caused duplication of the hypophysis.

Case Report. The child was born at term after an uncomplicated pregnancy and delivery, apart from an umbilical hernia operation on the 23-year-old mother early in her pregnancy. Apgar scores were 6/7/9 and asphyxia was evident, so the baby received assisted respiration for several days until her discharge. She was readmitted at the age of 26 days because of feeding difficulties. General examination revealed a V-shaped frontal hair line, hypertelorism, cleft palate, low-set ears, retrognathia, a wide prominent nasal root and a split on the top of the nose. Neurological and laboratory (chromosomal, amino acid and blood analyses) findings were normal. On X-ray examination no clear contour of the sella turcica was seen.

The baby was in no distress at the time of admission. Shortly after feeding, she was found dead in bed the same evening. Hereditary diseases or malformations were not apparent in the family.

At autopsy, body weight was 2,750 g and length 54 cm. The head was not enlarged and the fontanelles were of normal size. After removal of the brain, the 'sella' appeared shallow and empty. Instead, two sellae were found situated on either side of the regular one, posterior to both optic canals (Fig. 9.14a). Both sellae contained a pituitary gland beneath the sellar diaphragm. Histologically, both hypophyses were completely normal. The distance between the optic canals was 2.3 cm (normal about 1.1 cm), and that between the cribriform plates 2 cm (normal about 0.8 cm). The very short clivus had a round midline defect, through which a stalk of connective tissue, extending from the leptomeninx of the pontine base, protruded into the nasal cavity. Histologically, the connective tissue consisted of collagen fibres and striated tissue with a small penetrating artery. The posterior fossa was of normal size. At the base of the brain (Fig. 9.14b), the olfactory bulbs and tracts were set widely apart, and the optic chiasm had a wide angle. A mass of hyperplastic tissue displaced the mamillary bodies laterally. The circle of Willis was abnormal with a very short basilar artery and elongated posterior communicating arteries. Between these communicating arteries and the vertebral arteries, two ectopic masses were found, measuring 2.5 mm × 4 mm and 3 mm × 5 mm, respectively. These contained neurons and myelinated fibres. In the forebrain, the corpus callosum, the anterior commissure and the posterior cingulate gyri were absent. The pineal gland had its normal position.
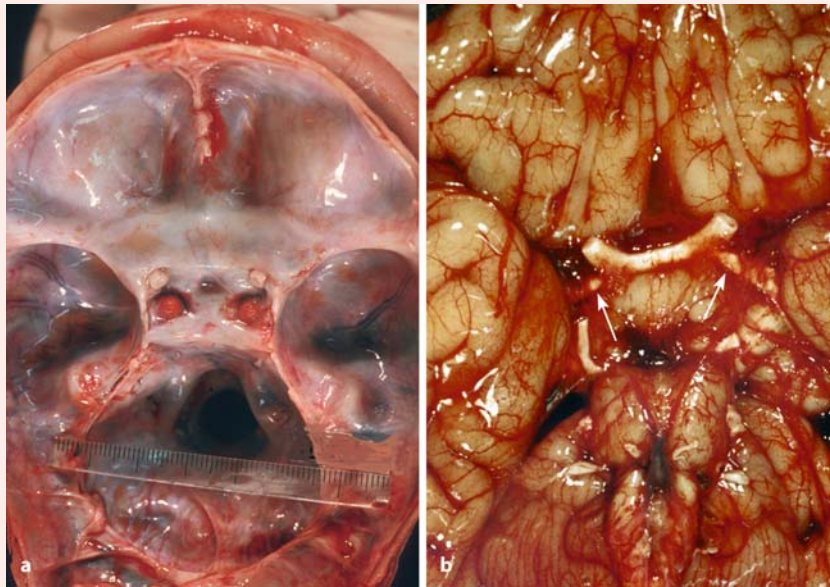
Fig. 9.14 Duplication of the pituitary gland: **a** skull base with two hypophyses, in between is an empty sella; note the wide distance between the cribriform laminae and optic canals; **b** basal view of the brain showing duplicated pituitary glands (*arrows*) behind the optic nerves (from Hori 1983, with permission)

Between the laterally displaced mamillary bodies, a mass of hypothalamic tissue formed the base of the third ventricle. This tissue contained magnocellular and medium-sized neurons without glial proliferation of any importance. Posterior to the chiasm, two hypophyseal stalks were present. Heterotopia were found in the tegmental raphe ventral to the aqueduct, in a slit-like deep floor of the rhomboid fossa of the medulla oblongata and in the dentate nuclei. The spinal cord showed a duplicated anterior median fissure at the cervico-thoracic level. In between, hyperplastic grey matter with myelinated fibres protruded from the central spinal grey matter. Posterior roots entered the cord not only medial but also lateral to the posterior horn. Immunohistochemical staining for anterior pituitary hormones, performed recently, revealed no abnormalities in the distribution of the hormone-producing cells in both of the pituitary glands.

References

Ahlfeld F (1880) Die Mißbildungen des Menschen. Grunow, Leipzig

DeMyer W (1967) The median cleft face syndrome. Differential diagnosis of cranium bifidum occultum, hypertelorism, and median cleft nose, lip and palate. Neurology 17:961–971

Gorlin RJ, Červenka J, Cohen MM Jr (1977) "Newer" facial clefting syndromes. Birth Defects Orig Artic Ser 13:1–9

Hori A (1983) A brain with two hypophyses in median cleft face syndrome. Acta Neuropathol (Berl) 59:150–154

Morton WRM (1957) Duplication of the pituitary and stomatodaeal structures in a 38-week male infant. Arch Dis Child 32:135–141

Warkany J (1971) Congenital Malformations. Year Book, Chicago, IL p 419

■ **Clinical Case 9.2**
Pharyngosellar Pituitary

In ***pharyngosellar pituitary***, the anterior part of the gland is continuous from the pharyngeal roof to the sella turcica. Hori et al. (1995) described this rare malformation in a 17-gestational-week-old male fetus with an encephalocele and amnion rupture sequence (see Case Report). The first description of this anomaly was made by Müller (1958), in whose case the pituitary could not be observed from the side of the cranial cavity, since the diaphragma sellae showed no perforation. Later, this anomaly was found in several cases of trisomy 18 (Kjaer et al. 1998).

■ **Case Report.** The pregnancy of a 27-year-old mother was unremarkable until at gestational week 17 the amnion was ruptured and the fetus was aborted spontaneously. The male fetus had a crown–heel length of 19 cm, a head circumference of 10 cm and weighed 190 g. Morphological examina-
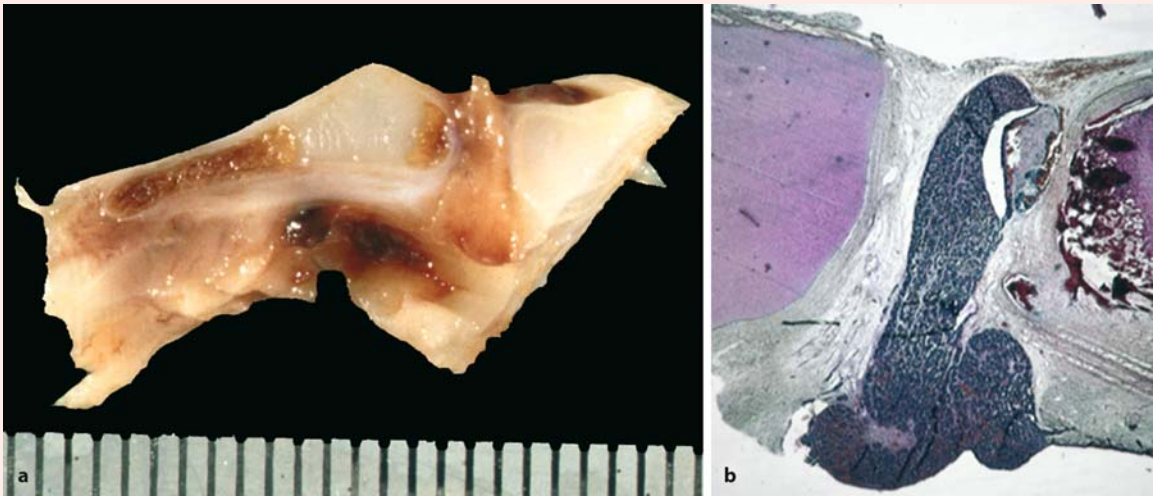
Fig. 9.15 Pharyngosellar pituitary: **a** gross appearance of the pituitary gland in the craniopharyngeal canal; **b** Gomori-stained section, showing the pharyngeal pituitary attached to the posterior lobe. (from Hori et al. 1995; with permission)

tion of the fetus revealed a slight double cleft lip, left cleft palate, adhesive strangs at the nose, forehead and right hand, and short eye fissures with slight hypertelorism. A large encephalocele covered with skin was observed in the vertex of the microcephalic head, and an additional smaller encephalocele was found on the left forehead. After removing the covering of the head, a large round skull defect was found through which the larger encephalocele herniated. The skull base was hypoplastic: the anterior cranial fossa was narrow in transverse diameter, the middle fossa was shallow and the posterior fossa was normal in size. Anterior and posterior protuberances of the sella were absent. The pituitary gland was found in the ordinary position when observed from the cranial base. The encephalocele consisted of telencephalic tissue with molecular and neuronal cortical cell layers, white matter as well as basal ganglia-like structures. Part of the skull base, including the sella turcica, clivus and pharyngeal roof, was removed and divided through the midline (Fig. 9.15 a); both blocks were embedded in paraffin without decalcification and sliced serially. Sections were stained by haematoxylin and eosin, periodic acid–Schiff (PAS) stain and Gomori's reticulin staining. Immunostaining for pituitary hormones was also performed.

The pituitary gland was found in the persistent craniopharyngeal canal as an elongated structure expanding from the pharyngeal roof to the sella turcica (Fig. 9.15 b), forming a pharyngosellar pituitary. Reconstruction of the pharyngosellar pituitary from the histological sections revealed that the pituitary was composed of sellar and pharyngeal parts. The pituitary tissue was covered with a poorly ciliated epithe-

lial layer at its pharyngeal end. The majority of the cell constituents of the pituitary gland were histologically chromophobic. The pituitary stalk and the posterior lobe were histologically normal. Immunohistochemical examination for anterior pituitary hormones showed that the distribution of hormone-producing cells in the malformed pituitary tissue was irregular: thyrotropic hormone (TSH) producing, follicle stimulating hormone (FSH) producing and luteinizing hormone (LH) producing cells were nearly absent in the sellar and middle sections of the pituitary but were found in small numbers mainly in the pharyngeal part of the pituitary. Somatotropic hormone (STH) producing, prolactin releasing hormone (PRL) producing and adrenocorticotropic hormone (ACTH) producing cells were distributed diffusely. ACTH-producing cells were abundant in the pharyngeal part. Only few TSH-, FSH- and LH-producing cells were found in the sellar and middle sections. They were mostly found in the pharyngeal section.

References

Hori A, Schmidt D, Feyerabend B (1995) Pharyngosellar pituitary: A rare developmental anomaly of the pituitary gland. Acta Neuropathol (Berl) 89:459–463

Kjaer I, Kreeling JW, Reintoft I, Hjalgrim H, Nolting D, Hansen BF (1998) Pituitary gland and sella turcica in human trisomy 18 fetuses. Am J Med Genet 76:87–92

Müller W (1958) On the pharyngeal hypophysis. In: Currie AR (ed) Endocrine Aspects of Breast Cancer. Proceedings of a Conference held at the University of Glasgow, 8–10 July 1957. Livingstone, Edinburgh, pp 106–110
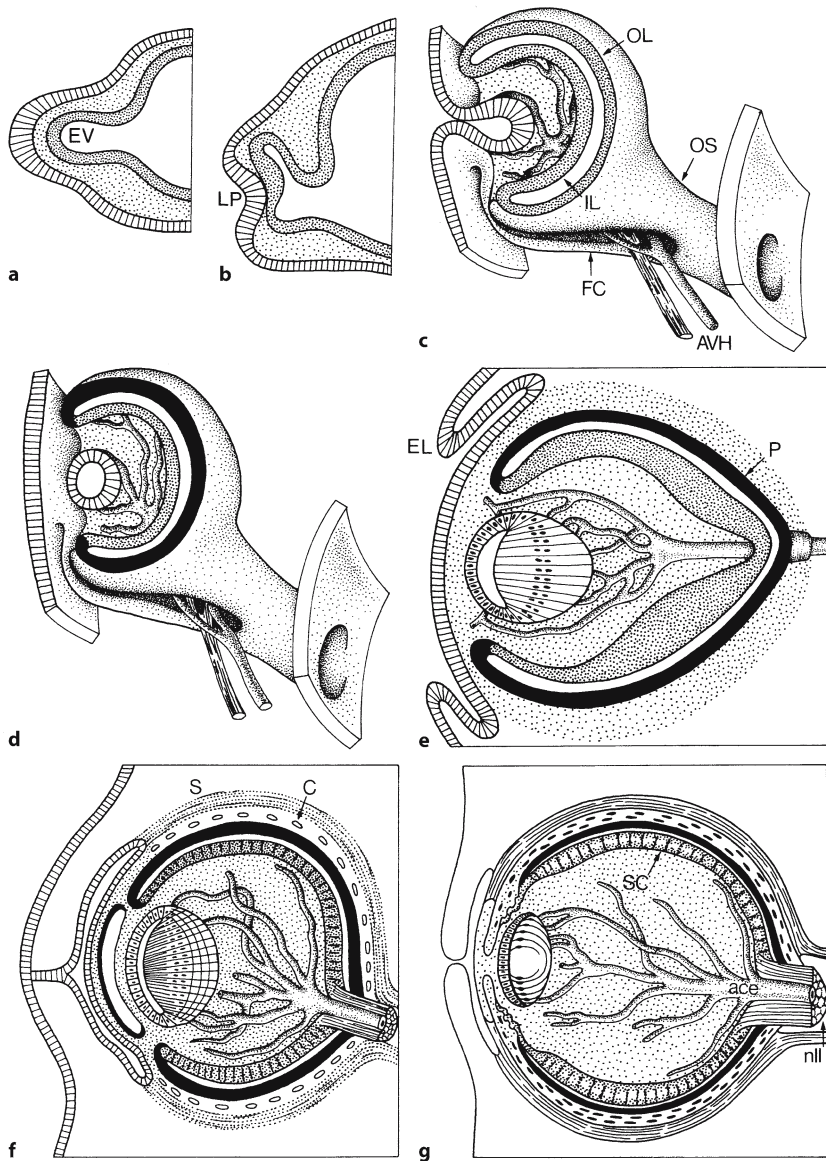
Fig. 9.16 Development of the human eye in the fourth (**a**), fifth (**b**), sixth (**c**), seventh (**d**), eighth (**e**) and ninth (**f**) week and in the seventh month (**g**) of development. *ace* a. centralis retinae, *AVH* hyaloid artery and vein, *C* choroid, *EL* eyelid, *EV* eye vesicle, *FC* fissura choroidea, *IL* inner layer of eye cup, *LP* lens placode, *nII* optic nerve, *OL* outer layer of eye cup, *OS* optic stalk, *P* pigment layer of retina, *S* sclera, *SC* stratum cerebrale of retina. (After Hamilton and Mossman 1972, based on reconstructions by Mann 1928)

9.4   Development of the Visual System

9.4.1   Development of the Eye

The optic primordia are present very early in development (Mann 1928; O'Rahilly 1966; Hinrichsen 1990; Barishak 2001; O'Rahilly and Müller 2001). Presumably, a single eye field exists at the rostral end of the neural plate, the median part of which is suppressed under the influence of the prechordal plate, resulting in bilateral optic primordia (Li et al. 1997). In pioneering studies in *Ambystoma*, Adelmann (1929a, b, 1930, 1936a, b) showed that the vertebrate eye first develops as a single developmental field. Factors supplied by the prechordal plate are then required for its separation into two distinct eye structures. The lens arises from the surface ectoderm. In

human embryos, the **optic primordium** becomes first visible as the **optic sulcus** appears in each neural fold at stage 10, i.e. at about 4 weeks of development. The right and left primordia are connected by a ridge that will become the optic chiasm. The optic sulcus deepens and forms an evagination at stage 11, leading to the formation of the **optic vesicle** at stage 12 (Figs. 9.16, 9.17). By 4.5 weeks, the optic vesicle and the adjacent surface ectoderm thicken and form at stage 13 the **retinal disc** and the **lens disc**, respectively. The retinal disc becomes invaginated, resulting in a double-layered **optic cup**. This invagination extends partly onto the stalk of the optic cup to form the transient **retinal fissure**. A disturbance in the closure of the retinal fissure may lead to a *coloboma* (Fig. 9.18). The inverted layer of the optic cup is readily comparable to the wall of the developing fore-
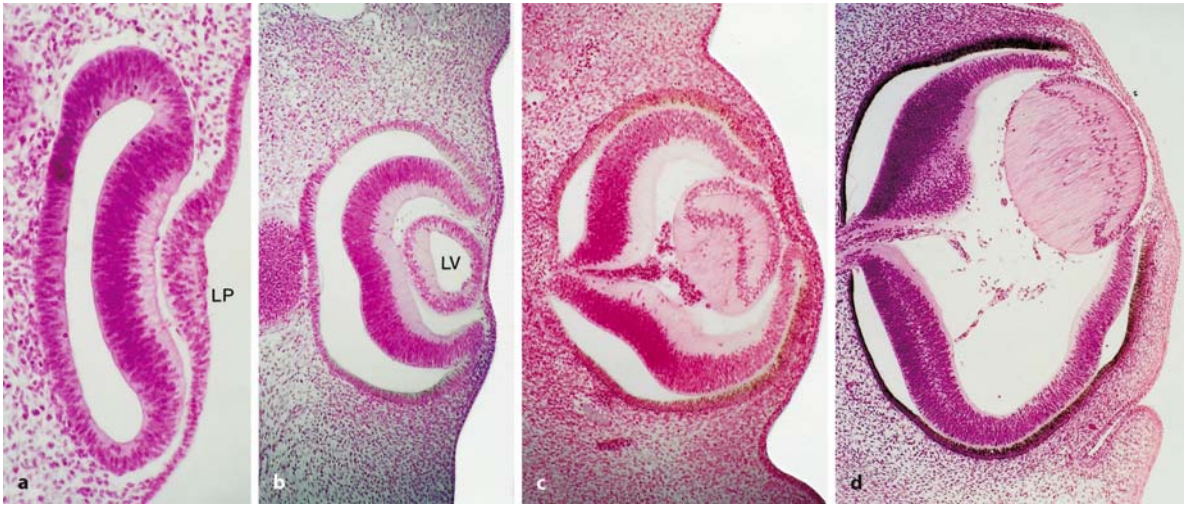
Fig. 9.17 Series of photomicrographs showing the development of the human eye at Carnegie stages 14 (**a**), 16 (**b**), 18 (**c**) and 20 (**d**); haematoxylin–eosin staining. *LP* lens placode, *LV* lens vesicle. (From the Kyoto Collection of Human embryos)
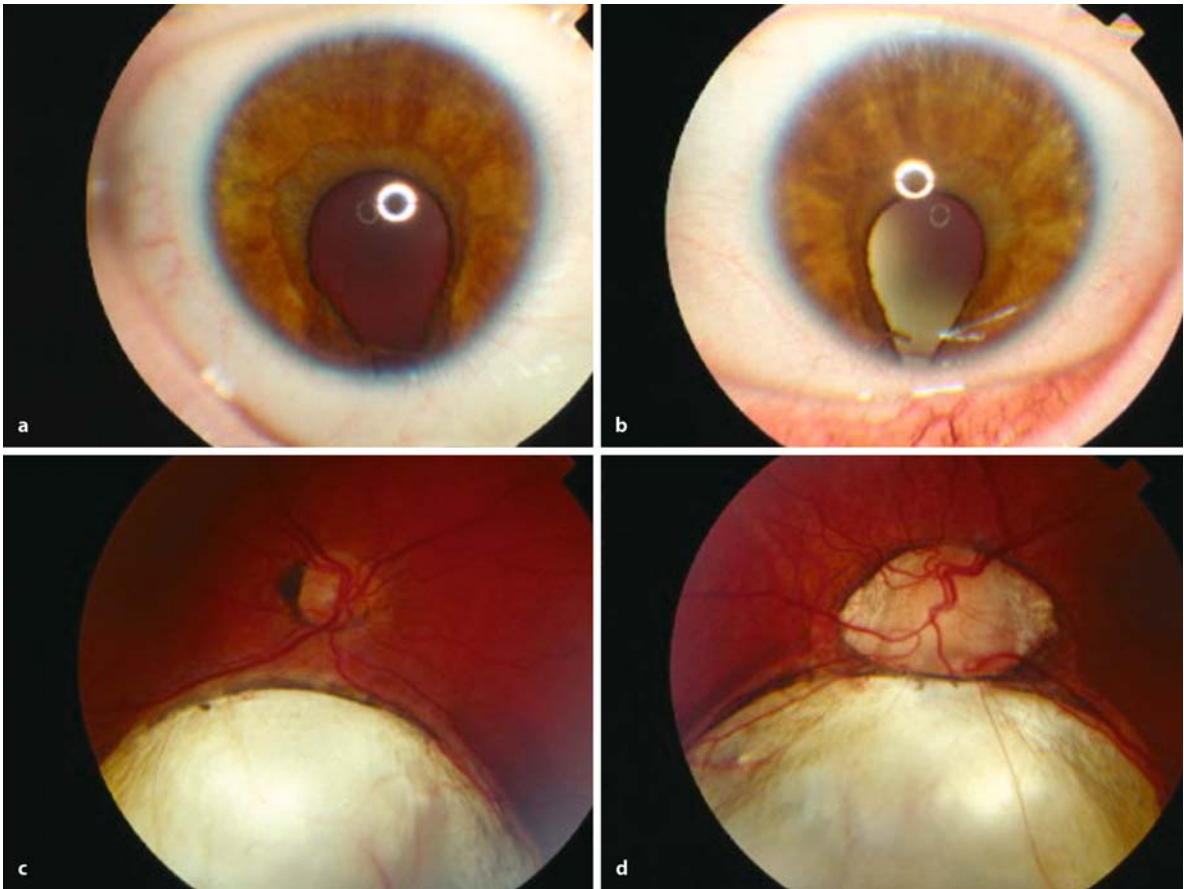
Fig. 9.18 Colobomas present in one patient: **a**, **b** iris colobomas of right and left eye, respectively; **c**, **d** retinal colobomas of both eyes and optic disk coloboma of the left eye (**d** courtesy Hans Cruysberg, Nijmegen)
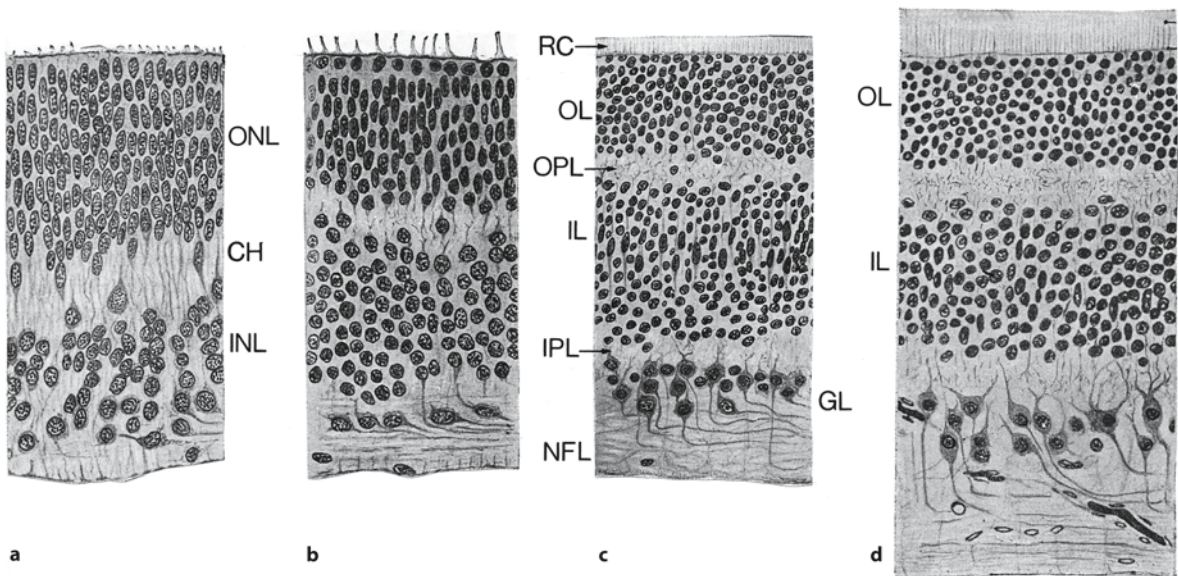
Fig. 9.19 Development of the human retina in an embryo of 7 weeks (**a**), and fetuses of about 11 (**b**), 19 (**c**) and 27 (**d**) weeks of development. *CH* transient fibre layer of Chievitz, *ELM* external limiting membrane, *GL* ganglion cell layer, *IL* inner nuclear layer (bipolar cells), *INL* inner neuroblast layer, *IPL* inner plexiform layer, *NFL* nerve fibre layer, *OL* outer nuclear layer (nuclei of rods and cones), *ONL* outer neuroblast layer, *OPL* outer plexiform layer, *RC* layer of rods and cones. (After Mann 1928)

brain. The walls of the optic cup form the optic part of the retina and the epithelium of the ciliary body and the iris. The lens disc becomes indented to form the **lens pit** at stage 14 which closes at stage 15 to form the **lens vesicle**. At the same time, retinal pigment appears in the external layer of the optic cup. The cells of the deep wall of the lens vesicle become elongated and form the primary lens fibres. Anterior cells of the lens form a simple epithelium from which the secondary lens fibres arise that form the bulk of the mature lens. Moreover, the **primary vitreous body** and the **hyaloid artery** develop. The hyaloid artery enters the vitreous cavity through the retinal fissure and supplies the thickened inner layer, the lens vesicle and the intervening mesenchyme. Later, the hyaloid artery disappears within the eye. Its stem forms the central retinal artery. The optic cup is anchored to the forebrain by the **optic stalk** that will form the optic nerve. Axons of retinal ganglion cells grow via the optic stalk to the brain. The lumen of the optic stalk is gradually obliterated as axons of ganglion cells accumulate in the inner layer of the optic stalk, resulting in the formation of the optic nerve between the sixth and eighth weeks of development. The optic vesicle becomes enveloped by a sheath of neural-crest-derived mesenchyme. This sheath forms the two coverings of the eye: the thin inner **choroid** and the fibrous outer **sclera**.

The development of the **retina** is shown in Fig. 9.19. The thinner outer layer of the optic cup becomes the **pigmented layer** of the retina. The inner layer can soon be divided into a thicker nine-layered posterior part, the **pars optica retinae**, which develops into the visual receptive part of the retina, and a thinner, one-layered part, the **pars caeca retinae**. The pars caeca does not develop photoreceptive cells and becomes subdivided into a posterior part, the **pars ciliaris retinae**, and an anterior part firmly fused with the outer pigmented layer to form the **pars iridis retinae**. The cavity of the optic vesicle is soon occluded by the apposition of its inner layer to the pigmented layer. The **intraretinal space**, separating the two layers, is obliterated as the retina develops, but the two layers never fuse firmly. The differentiation of the neural retina takes place between the sixth week and the eighth month (Mann 1928; Hinrichsen 1990; O'Rahilly and Müller 2001). By the fifth week the first of a series of shifts in nuclear arrangement occurs, resulting in the formation of an inner layer devoid of cells and an outer nuclear layer. About the middle of the sixth week cells of the outer nuclear layer migrate centrally and form an inner cellular zone. Between the two layers the transient layer of Chievitz appears. In the third month the ganglion cells arise from the inner neuroblastic layer. As additional cells migrate from the outer neuroblastic layer to the inner zone,

the layer of Chievitz disappears. Now, three nuclear zones can be distinguished separated by fibrous layers. From within outwards, these nuclear zones are the ganglion cell layer, the inner nuclear layer and the outer nuclear layer. The majority of the cells of the inner nuclear layer give rise to the bipolar neurons which relay impulses from the rods and cones to the ganglion cells. The cells in the outer layer form the rods and cones. **Vascularization** of the retina begins at about 15 weeks of development (Ashton 1970). **Retinal cell diversity** is achieved by the sequential production of cell types in a defined histogenetic order (Provis et al. 1985a; Young 1985; Dowling 1987; Fuhrmann et al. 2000; Marquardt and Gruss 2002). Retinal ganglion cells and horizontal cells differentiate first, followed in overlapping phases by cone photoreceptors, amacrine cells, rod photoreceptors, bipolar cells and, finally, Müller glia cells.

9.4.2 Congenital Malformations of the Eye

Genetic control of **eye development** has been extensively studied in the embryonic mouse brain (Macdonald and Wilson 1996; Graw 2000, 2003; Hirsch and Grainger 2000; Wawersik et al. 2000; Horsford et al. 2001; Pichaud and Desplan 2002). Mutations in at least ten human transcription factor genes have been shown to disrupt eye development. A large number of additional mouse transcription factor genes are also associated with developmental abnormalities of the eye (Hirsch and Grainger 2000; Graw 2000, 2003). Human eye phenotypes can involve one or more ocular structures. Developmental anomalies that affect many parts of the eye are known as panocular defects, whereas other abnormalities may be restricted to the anterior segment, the posterior segment or the differentiation or maintenance of photoreceptors. Examples of such anomalies are shown in Clinical Cases 9.3 and 9.4.

Clinical Case 9.3
Aniridia

Aniridia is a bilateral congenital ocular disorder with absent or rudimentary iris. The disorder can be autosomal dominant or sporadic, and is caused by a defect in the *PAX6* gene. Sporadic aniridia is associated with Wilms tumour (nephroblastoma in one third of the cases).

Case Report. A newborn female was referred to the Ophthalmology Clinic because of congenital absence of the iris in both eyes. Ocular examination showed bilateral aniridia, microcornea (7–8 mm; normal 9–10 mm), mild posterior polar cataract and small grey optic discs (Fig. 9.20). Systemic examination disclosed microcephaly (less than P3) and multiple ventricular septal defects with pulmonary hypertension. The patient was suspected to suffer from 11p-syndrome WAGR (Wilms tumour, aniridia, genitourinary malformations). The child died from pulmonary oedema and respiratory insufficiency at the age of 3 months. Postmortem examination confirmed the congenital heart defect, but no renal tumour or genitourinary abnormalities were found. Rao et al. (1992) described a 2-year-old female child with bilateral Wilms tumour along with multiple congenital anomalies like bilateral aniridia with congenital cataracts and nystagmus, microcephaly, mental retardation and ventricular septal defect. Karyotype
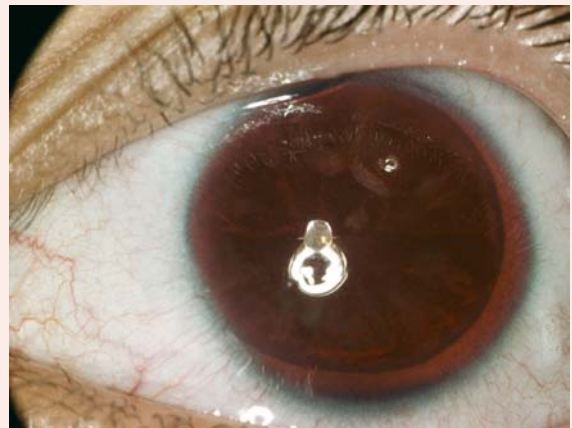
Fig. 9.20 Aniridia in a female newborn (courtesy Hans Cruysberg, Nijmegen)

analysis revealed 46XX, del 11p13-14.1. Association of ventricular septal defect with the classical features of 'Aniridia–Wilms tumour association' is an unusual feature.

Reference

Rao SR, Athale UH, Kadam PR, Gladstone B, Nair CN, Pai SK, Kurkure PA, Advani SH (1992) Aniridia-Wilms' tumour association: A case with 11p 13-14.1 deletion and ventricular septal defect. Indian J Cancer 29:117–121

Clinical Case 9.4
Retinitis Pigmentosa with CNS Malformations

Congenital disorders of glycosylation (CDGs) form a new group of autosomal recessive multisystem disorders characterized by defective glycoprotein biosynthesis. Disorders of nearly all organs and systems have been described (Jaeken and Carchon 2004; Chap. 3). Cerebral and ocular manifestations are common in the various biochemical CDG subtypes.

Case Report. A 12-year-old girl was referred to the Ophthalmology Clinic with a history of early childhood strabismus and encephalopathy of unknown aetiology. Signs of general hypotonia and psychomotor retardation were established in the first year of life. Microcephaly, short stature and inverted nipples were apparent in infancy, followed by ataxia, dyspraxia, dysmetria and progressive polyneuropathy in the first decade. Neuroimaging showed severe cerebellar vermis hypoplasia. The eyes showed convergent strabismus with slight limitation of abduction. The ocular media were clear. Ophthalmoscopy showed retinitis pigmentosa of both eyes, with typical bony spicules in the retinal periphery and an indication of bull's eye pattern maculopathy (Fig. 9.21). The electroretinogram was extinguished. At that time (1984) no systemic diagnosis could be made. At 18 years of age, the patient showed general signs of glycoprotein dysfunction, such as gonadal dysfunction and hypothyroidism. The diagnosis CDG syn-

Fig. 9.21 Retinitis pigmentosa in a 12-year-old girl (courtesy Hans Cruysberg, Nijmegen)

drome type 1a was established by finding abnormal transferrin fractions with isoelectric focussing of serum. This type is the most common form in the group of CDGs. In the third decade, the retinitis pigmentosa was progressive and posterior subcapsular cataracts developed in both eyes.

Reference

Jaeken J, Carchon H (2004) Congenital disorders of glycosylation: A booming chapter of pediatrics. Curr Opin Pediatr 16:434–439

Panocular defects are broad phenotypes (Table 9.3) that arise by at least two different general mechanisms (Horsford et al. 2001; Graw 2003). The first mechanism, shown for heterozygous mutations in the paired box gene *PAX6*, reflects the fact that the gene is expressed in and is required for the normal development of all regions of the developing eye. The second mechanism by which panocular defects arise is due to mutations in genes such as *CHX10* that are expressed in one region of the developing eye but, via secondary physiological processes, are essential for the normal development of other ocular structures. *Pax6* is one of the nine members of the *Pax* gene family unified by the presence of a paired domain. The paired domain is a 128 amino acid DNA-binding domain named after the prototypical *Drosophila* segment polarity gene *paired*. Haploinsufficiency for *PAX6* function in humans leads to **aniridia**, a heritable panocular disorder characterized by iris and foveal hypoplasia which can be accompanied by cataracts, corneal opacification and progressive glaucoma (Glaser et al. 1995; Horsford et al. 2001). Mutations in *PAX6* have also been found in patients with Peters anomaly, congenital cataract, autosomal dominant keratopathy and isolated foveal hypoplasia (Prosser and van Heyningen 1998).

In mice, a naturally occurring mutation, *Small eye* (*Sey*), results from mutations in the *Pax6* gene (Hill et al. 1991). Like human aniridia, *Sey* is inherited in a semidominant fashion, with *Sey/+* heterozygotes showing corneal and lenticular abnormalities and *Sey/Sey* homozygotes lacking eyes entirely (Hogan et al. 1986). In *Sey/Sey* embryos, the lens and nasal placodes fail to develop, the optic vesicle fails to constrict and subsequently degenerates, and mesenchymal cells become interposed between the surface ectoderm and the optic vesicle (Hogan et al. 1988). Moreover, in *Sey* homozygotes, the anterior commis-

Table 9.3 Inherited eye diseases in man and mice due to mutations in transcription factor genes: panocular defects (after Macdonald and Wilson 1996; Graw 2000, 2003; Horsford et al. 2001)

Gene	Function or required for	Disease	Inheritance and genetic mechanisms	Phenotypes
PAX6	Lens induction and all subsequent development of retina, iris, and cornea; development of forebrain, cerebellum, nasal structures and pancreas	Aniridia	AD; haploinsufficiency in most cases	Human: aniridia, accompanied by foveal or optic nerve hypoplasia, cataract, glaucoma and corneal dystrophy Mouse (heterozygotes): small eye, cataract and iris hypoplasia Mouse (homozygotes): neonatally lethal with anophthalmia, rudimentary nasal structures and forebrain and cerebellar anomalies; pancreas anomalies
CHX10	Involved in the retina and in optic nerve development	Micro-phthalmia	AR; loss of function alleles	Human: microphthalmia, cataracts, iris coloboma and blindness Mouse (homozygotes): microphthalmia, optic nerve aplasia and cataracts

AD autosomal dominant, *AR* autosomal recessive

sure, the corpus callosum and the olfactory bulbs are absent (Schmahl et al. 1993; Stoykova et al. 1996). In mice, the optic vesicle forms at E8.5 and comes into contact with the head and ectoderm at E9.0. Signals from the optic vesicle induce the lens placode to form by E9.5. At E10.0, the lens placode invaginates to form a lens pit, while the optic vesicle infolds and becomes the optic cup. The invagination of the lens pit is complete at E10.5, at which time the vesicle begins to separate from the overlying ectoderm. Normally, *Pax6* is expressed in both the head ectoderm and the optic vesicle at E8.5, prior to lens induction (Walther and Gruss 1991; Grindley et al. 1995). At E9.5, prior to thickening of the head ectoderm to form the lens placode, the expression of *Pax6* becomes restricted to the presumptive placodal region. In later stages, *Pax6* is expressed in the optic cup as well as in the invaginated lens placode. The close similarities in phenotype and mode of inheritance between aniridia and *Sey* suggest that *Pax6* functions in a similar way in human and mouse eye development (van Heyningen and Williamson 2002). Mild extraocular phenotypes are found in *Sey*, including olfactory bulb hypoplasia, axon guidance defects, cortical plate hypocellularity and decreased basal ganglia volume (Schmahl et al. 1993; Stoykova et al. 1996; Mastick et al. 1997). Using MRI and smell testing, Sisodiya et al. (2001) showed absence or hypoplasia of the anterior commissure and reduced olfaction in a large proportion of aniridia cases. Moreover, Ellison-Wright et al. (2004) found that individuals with aniridia have structural abnormalities of grey matter in the anterior cingulate cortex, the cerebellum and the medial temporal lobe as well as white matter deficits in the corpus callosum. Functional MRI demonstrated reduced activation of fronto-striato-thalamic systems during performance of, for instance, overt verbal fluency (El-

lison-Wright et al. 2004). Therefore, *PAX6* haploinsufficiency appears to cause more widespread malformations than previously thought.

CHX10, a paired-like homeodomain protein, regulates neuronal development, particularly the proliferation of interneurons. Homozygous putative null mutations of the *CHX10* homeobox gene affect only the eye, resulting in blindness with microphthalmia and cataracts (Horsford et al. 2001). Its mouse equivalent, known as *ocular retardation* (*or*), is a recessive mutant with abnormal eye development. Homozygous *or* mice are blind with obvious microphthalmia, cataract, a poorly differentiated, thin retina, and no optic nerve (Truslove 1962; Theiler et al. 1976; Silver and Robb 1979). Burmeister et al. (1996) showed that the allele *or¹* has a premature stop codon in the homeobox of the *Chx10* gene.

Anterior segment defects primarily affect the anterior chamber, iris, lens, cornea and trabecular network, and are phenotypically varied (Table 9.4). They result from mutations in a number of different transcription factor genes: the forkhead-like gene *FKHL7*, the paired-like/bicoid-like homeodomain genes *PITX2* and *PITX3*, and the leucine zipper transcription factor *MITF* (Table 9.3). Similar phenotypes result from mutations at different loci, and there is a phenotypic overlap with some *PAX6* missense mutations (Horsford et al. 2001). Genetic manipulations in murine embryos suggest that *Pax6* regulates responsiveness of the head ectoderm to the inductive effect of the optic vesicle and *Prox1* probably regulates signal reception from the retina in promoting lens fibre development. *Sox2/Sox3* and *Maf* encoded proteins are probably the key factors of lens cell differentiation. *Pax6* inhibits expression of genes for fibre characteristics in the epithelial cells, whereas *Sox1* and *c-Maf/L-Maf* support fibre differentiation (Kon-

Table 9.4 Inherited eye diseases in man and mice due to mutations in transcription factor genes: anterior segment defects (after Macdonald and Wilson 1996; Graw 2000, 2003; Horsford et al. 2001)

Gene	Function or required for	Disease	Inheritance and genetic mechanisms	Phenotypes
MITF	Regulates genes in melanin synthesis pathway; in mice, required for normal eye growth and prevention of overproliferation of the retinal pigment epithelium	Waardenburg syndrome type 2	AD; haplo-insufficiency	Human: iris pigment defects, hearing loss and white forelock Mouse (heterozygotes): minor eye and skin pigment defects Mouse (homozygotes): small eye, with hyperproliferation of RPE, defects in various other pigment cell types
FKHL7 (FOXC1)	Development of cornea and iris; murine homozygotes die perinatally with haemorrhagic hydrocephalus and skeletal defects	Axenfeld–Rieger anomaly	AD; haplo-insufficiency	Human: minor: glaucoma, iris hypoplasia; major: iridogoniodysgenesis, posterior embryotoxon Mouse (heterozygotes): anterior segment defects Mouse (homozygotes): iris hypoplasia, corneal defects, unfused eyelids
PITX2	Development of ocular mesenchyme, maxillary and mandibular epithelia, umbilicus, pituitary and laterality	Rieger syndrome, iridogonial dysgenesis syndrome	AD; haplo-insufficiency	Human: Rieger anomaly and dental hypoplasia, facial dysmorphism and umbilical abnormalities Mouse (heterozygotes): corectopia and iris abnormalities Mouse (homozygotes): optic nerve coloboma and absence of ocular muscles
PITX3	Developing lens placode and maturing lens	Anterior segment mesenchymal dysgenesis; congenital cataract	AD; haplo-insufficiency	Human: defects in all tissues of anterior eye chamber Mouse: aphakia in homozygotes

doh 1999; Hirsch and Grainger 2000). Autosomal dominant Waardenburg syndrome type 2A is associated with mutations in *MITF* (Tassabehji et al. 1994). *MITF* is expressed predominantly in developing pigment cells and neural crest cells. The mouse *microphthalmia* (*mi*) mutation, first described by Hertwig (1942), includes at least 17 mutant alleles at chromosome 6 (Steingrimsson et al. 1994). The affected gene encodes *Mitf* (microphthalmia-associated transcription factors).

Congenital aphakia (absence of the lens) in man occurs in primary and secondary forms (Vermeij-Keers 1975). Primary absence of the lens is characterized by the total absence of the lens or lens primordium, the iris and the anterior chamber, whereas secondary forms result from disturbances during lens development at a later stage by rubella infection and other factors affecting normal lens development. Several mouse mutants are known (Graw 2000).

Posterior segment defects, affecting only the retina and the optic nerve, include optic nerve defects due to mutations in *PAX2* and *HESX1* (Table 9.5). In mouse embryos, *Pax2* is expressed during the morphogenesis of the optic cup and stalk, and in the period of axogenesis (Nornes et al. 1990). In *Pax2* null mutants (Torres et al. 1996) and in the *Pax2Neu* mutation (Favor et al. 1996), the pigmented retina extends into the optic stalk, the optic fissure fails to close, leading to coloboma, no optic chiasm is formed, and some malformations of the inner ear are found. The mouse *Pax2Neu* mutation is identical to a human *PAX2* mutation in a family with renal-coloboma syndrome and results in developing defects of the brain, eye, ear and kidney (Favor et al. 1996). 'Renal coloboma syndrome' is more appropriately called **papillorenal syndrome**, because the dysplastic disks in papillorenal syndrome show no absence of ocular tissue owing to incomplete closure of the embryonic optic fissure, and consequently no characteristics of coloboma (Parsa et al. 2002). The paired-like homeobox gene *HESX1* is mutated in cases of septo-optic dysplasia (Dattani et al. 1998, 1999; Brickman et al. 2001).

Mutations in two genes, *CRX* and *NRL*, result in **abnormalities** of **photoreceptor differentiation** or **maintenance** (Table 9.6). **Leber congenital amaurosis** is characterized by generalized rod and cone dystrophy and presents at birth or early in infancy (Aicardi 1998; Graw 2003). It is responsible for 10–18% of cases of congenital blindness. The disease may present only with ophthalmological features, but in some cases it is associated with mental retardation, encephaloceles (Vaizey et al. 1977) and, especially, anomalies of the cerebellar vermis. Apart from *CRX*, at least six other genes contribute to this disorder (Fazzi et al.

Table 9.5 Inherited eye diseases in man and mice due to mutations in transcription factor genes: posterior segment defects (after Macdonald and Wilson 1996; Graw 2000, 2003; Horsford et al. 2001)

Gene	Function or required for	Disease	Inheritance and genetic mechanisms	Phenotypes
PAX2	Developing optic cup narrowed to just optic stalk, particularly retinal fissure; also expressed in kidney and otic vesicle	Papillorenal syndrome	AD; haploinsufficiency	Human: optic disc dysplasia, renal hypoplasia, vesicoureteral reflux and occasional deafness Mouse (heterozygotes): optic nerve coloboma Mouse (homozygotes): globe colobomata, optic nerve defects and absence of optic chiasm
HESX1	Forebrain, optic vesicle, nasal placode and pituitary development	Septo-optic dysplasia	AR; one allele known, with a severe loss of function	Human: optic disc hypoplasia, midline brain abnormalities, pituitary hormone defects and septum pellucidum absence Mouse: Dattani et al. (1998)

Table 9.6 Inherited eye diseases in man and mice due to mutations in transcription factor genes: abnormal photoreceptor differentiation/maintenance (after Macdonald and Wilson 1996; Graw 2000, 2003; Horsford et al. 2001)

Gene	Function or required for	Disease	Inheritance and genetic mechanisms	Phenotypes
CRX	Morphogenesis and maintenance of photoreceptor outer segment; transactivation of expression of rhodopsin and other outer-segment proteins	Cone–rod dystrophy	AD; haploinsufficiency	Human: degeneration of cone, then rod, photoreceptors Mouse (homozygotes): lack of photoreceptor outer segments and circadian rhythm abnormalities
		Leber congenital amaurosis	AD; haploinsufficiency or dominant negative alleles; AR; loss-of-function alleles	Human: congenital absence of functional photoreceptors, or early photoreceptor degeneration; mutations in at least 6 other genes known
NRL	Cotransactivator, with *CRX*, of rhodopsin expression	Retinitis pigmentosa	AD; one mutant allele known: gain-of-function allele, increasing transactivation of rhodopsin	Human: rod photoreceptor degeneration

2003; Graw 2003). At least one mutation in the *NRL* gene leads to autosomal dominant retinitis pigmentosa (Dryja 2001). **Retinitis pigmentosa** is characterized by progressive visual field loss, night blindness and pigmentary deposition in the retina. It is aetiologically very heterogeneous, in that at least 26 different genes/loci have been described (Wang et al. 2001). Retinitis pigmentosa is inherited through any of the known monogenic inheritance patterns (autosomal dominant, autosomal recessive and X-linked). A syndromic form of retinitis pigmentosa, **Kearns–Sayre syndrome**, is transmitted via a maternal or mitochondrial inheritance pattern (Dryja 2001). Most forms of retinitis pigmentosa and related retinal degenerations affect only the eye, but in a minority of cases the retinal degeneration belongs to a syndrome that includes other systemic abnormalities such as retinitis pigmentosa and deafness in Usher syndrome. Usher syndrome is discussed in Chap. 7.

In summary, mutations that lead to clinically relevant phenotypes highlight important steps in eye development (Graw 2003). Some affect genes that function at the top of the regulatory hierarchy and therefore at the initial stages of eye development. Mutations in such genes (*PAX6*, *SOX2*) lead to anophthalmia, microphthalmia and aniridia. Other genes (*FKHL7*, *PITX3* and *MAF*) function downstream or later during development. Some mutants define

genes that are important for only one particular tissue, such as the crystalline-encoding genes in the development of the lens and *PAX2* in the optic nerve.

9.4.3   Development of the Visual Projections

The optic nerves of the two eyes converge to form the optic chiasm. Here the fibres from the nasal half of each retina cross to the opposite side and pass via the optic tract to the LGN (Fig. 9.22). Fibres from the temporal half of each retina pass to the LGN without crossing. LGN neurons relay the visual input via the optic radiation to the primary visual cortex. Each optic tract as well as the LGN and geniculocalcarine tract contain information from the contralateral visual hemifield. Axons from the two eyes terminate in different layers of the six-layered LGN (Hubel and Wiesel 1977; Hubel et al. 1977). Moreover, axons of M-type ganglion cells terminate in the two ventrally located magnocellular layers of the LGN, whereas axons of the smaller P cells terminate in the four dorsal parvocellular layers. This segregation continues in the optic radiation into the striate cortex and even beyond in the extrastriate visual areas (Livingstone and Hubel 1988; Gulyas et al. 1993; Zeki 1993). *Developmental dyslexia* may be due to abnormalities of the magnocellular component of the visual system (Stein and Walsh 1997; Demb et al. 1998).

The development of visual projections has been extensively studied in rat (Brückner et al. 1976; Lund and Mustari 1977; Blakemore and Molnár 1990), ferret (Sur and Leamey 2001), cat (Shatz 1983; Shatz and Luskin 1986; Shatz et al. 1990) and rhesus monkey (Rakic 1974, 1975, 1977a, b) embryonic and fetal brains, and recently also in human fetuses (Hevner 2000). In the developing rat brain, neurons of the LGN are born between E12 and E14 (Brückner et al. 1976; Lund and Mustari 1977). Outgrowth of geniculocortical axons begins around E14–E15. By E16–E17, geniculocortical axons have reached the internal capsule and some have already accumulated in the subplate below the primary visual cortex (Lund and Mustari 1977; Blakemore and Molnár 1990). In cats, Shatz and co-workers studied the development of retinogeniculate (Shatz 1983) and geniculocortical (Shatz and Luskin 1986; McConnell et al. 1989; Shatz et al. 1990; Ghosh and Shatz 1992) projections. Axons from the LGN have entered the internal capsule by E30 (duration of gestation in cats 65 days). Axons reach the developing visual cortex by E36, and accumulate in the subplate over the following 3 weeks. Between E46 and E55, geniculocortical axons invade the marginal zone (layer 1), but an appreciable number of terminals in the cortical plate do not appear before E55. By birth, most axons have left the subplate and
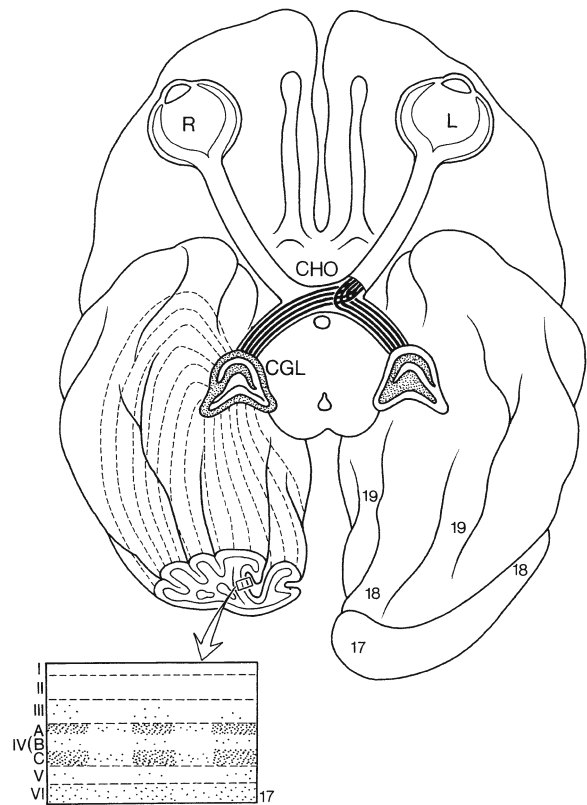
Fig. 9.22 Major visual pathways in the rhesus monkey. *CHO* chiasma opticum, *CGL* corpus geniculatum laterale, *L* left eye, *R* right eye, *I–VI* cortical layers (area *17*), *17–19* visual cortical areas. (After Rakic 1977a)

have established branches within layer 4 (Shatz and Luskin 1986; Shatz et al. 1990).

In rhesus monkeys, for which the gestation period lasts about 165 days, Rakic (1977a) showed with the [³H]thymidine birthday labelling technique that the first retinal ganglion cells are generated about the 30th day of gestation (E30), whereas those for the LGN start to be born around E36 (Rakic 1977b). Neurogenesis of neurons of the primary visual cortex takes place between about E43 and E102 (Rakic 1974, 1975). Geniculocortical axons fan up towards the cortex in the optic radiation as early as midgestation (Rakic 1976, 1977a). They gather in the subplate below the occipital cortical plate and only penetrate the plate itself after a long waiting period (Smart et al. 2002). LGN axons are visible throughout the lower layers of the primary visual cortex 3 weeks before birth, and terminals are beginning to concentrate in the lower part of layer 4. Efferent connections from the visual cortex to the LGN, the pulvinar and the superior colliculus are established in a 1-month period, E63–E97 (Shatz and Rakic 1981), roughly in synchrony with the genesis of geniculocortical pro-

jections. Geniculocalcarine fibres segregate into columns postnatally according to ocular dominance (Hubel and Wiesel 1977; Hubel et al. 1977).

In the developing human brain, optic tract fibres reach the CGL by about seven gestational weeks (Gilbert 1935; Cooper 1945), and synapses between optic fibres and CGL neurons are formed by about 13–14 gestational weeks (Khan et al. 1993, 1994). The homogeneous CGL anlage becomes separated into its characteristic six layers at about 22 weeks of gestation (Cooper 1945; Dekaban 1954; Hitchcock and Hickey 1980). Each cellular layer receives retinal fibres from only one eye. Geniculocortical axons have reached the subplate below the visual cortex as early as 8.5 weeks of gestation (Kostović and Rakic 1990). After a long waiting period, geniculocortical synapses in the cortical plate are formed around 23–25 weeks of gestation (Kostović and Rakic 1990). In a 1,1'-dioctadecyl-3,3,3',3'-tetramethylindocarbocyanine perchlorate (DiI) tracing study in fixed brains of human fetuses of 20–22 gestational weeks, Hevner (2000) showed that retinogeniculate projections were already segregated into eye-specific layers by 20 gestational weeks, preceding the cellular lamination of the CGL. Thalamocortical axons densely innervated the subplate, but hardly the cortical plate, consistent with observations on a waiting period in the human brain (Kostović and Rakic 1990). The human visual cortex attains its six-layered organization early during the third trimester (for data on the human visual cortices see Clarke and Miklossy 1990). The fetal human optic nerve shows **overproduction** and subsequent elimination of retinal ganglion cell axons. Provis et al. (1985b) found 1.9 million axons by about 10 weeks of development, 3.7 million at about 16 weeks, but only 1.1 million axons at about 27 weeks. The period of cell loss from the retinal ganglionic cell layer occurs after 30 weeks (Provis et al. 1985a), suggesting that many cells of the fetal ganglionic cell layer do not contribute axons to the optic nerve during the process between 20 and 30 weeks of development. **Myelination** of the optic nerve does not begin until about 32 weeks, and is largely complete by 7 months after birth (Magoon and Robb 1981). Myelination of the optic radiation begins at the CGL.

In *albinism*, retinofugal axons are misrouted in the optic chiasm so that some of the axons from the temporal retina, which normally stay ipsilaterally, cross to the other side. Abnormalities in the CGL of a human albino have been noted (Guillery et al. 1975). The opposite is found in *isolated absence* of the *optic chiasm* or *non-decussating retinofugal fibre syndrome* as first described by Apkarian et al. (1993, 1995) in two unrelated children, presenting with oculomotor instabilities. Comparable cases were described by Jansonius et al. (2001; Clinical Case 9.5) and Korff et al. (2003). In such cases, nasal retinal fibres project

ipsilaterally, resulting in retinothalamic and thalamocortical misprojections and aberrant retinotopic cortical mapping. *Optic nerve hypoplasia*, a developmental defect in the number of optic nerve fibres, may be unilateral or bilateral (Aicardi 1998). It may occur as an isolated defect or may be associated with other CNS defects such as absence of the septum pellucidum in *septo-optic dysplasia* (Sect. 9.7.3). Zeki et al. (1992) found that optic nerve hypoplasia can be associated with partial or complete absence of the septum pellucidum (in 52% of their cases), hydrocephalus (in 38%), porencephaly (in 24%), dilatation of the suprasellar and chiasmatic cisterns (in 19%), partial or complete absence of the corpus callosum (in 14%), or an intracranial cyst. *Colobomas* of the *optic nerve* may extend to involve the retina, the iris, the ciliary body and the choroid. Colobomas of the optic disc may be isolated, appearing as deep excavations with abnormal emergence of retinal vessels. They may be unilateral or bilateral and are often associated with agenesis of the corpus callosum, in isolation or as a component of the Aicardi syndrome (Chevrie and Aicardi 1986; Aicardi et al. 1987).

9.5 Overview of the Development of the Telencephalon

Each developing cerebral hemisphere consists of a thick basal part, the subpallium, giving rise to the basal ganglia, and a thin part, the pallium, which becomes the future cerebral cortex. The **telencephalon medium** or **impar** forms the non-evaginated part of the telencephalon. It surrounds the rostral part of the third ventricle and consists of the lamina terminalis and the preoptic region. The dorsal part of the lamina terminalis transforms into the commissural plate, from which the anterior commissure, the corpus callosum and the hippocampal commissure arise (Chap. 10). The preoptic region is usually included in the hypothalamus. Dorsal and ventral domains of the developing telencephalon are distinguished by different patterns of gene expression, reflecting the initial acquisition of regional identity by progenitor populations (Puelles et al. 2000; Schuurmans and Guillemot 2002; Campbell 2003; Zaki et al. 2003). The **subpallium** appears as medial and lateral elevations, known as the **ganglionic** (*Ganglionhügel* of His 1889) or **ventricular eminences** (Figs. 9.24, 9.25). The derivatives of the ganglionic eminences are summarized in Table 9.7. The caudal part of the ventricular eminences or **caudal ganglionic eminence (CGE)** primarily gives rise to the subpallial parts of the amygdala. The **medial ganglionic eminence (MGE)** is involved in the formation of the globus pallidus and the basal nucleus of Meynert, the source of cholinergic input to the cerebral cortex. The **lateral ganglionic**

Isolated absence of the optic chiasm or non-decussating retinofugal syndrome is very rare (Apkarian et al. 1993, 1995; Jansonius et al. 2001; Korff et al. 2003). The four patients described so far presented with oculomotor instabilities (see Case Report). In this condition, nasal retinal fibres erroneously project ipsilaterally, resulting in aberrant retinothalamocortical mapping.

■ **Case Report.** An otherwise healthy 15-year-old girl with a congenital nystagmus was evaluated at a University Department of Ophthalmology using visual evoked potential recording and subsequent MRI examination. She appeared to have the unique inborn absence of the optic chiasm (Fig. 9.23). Unlike the cases described by Apkarian et al. (1993, 1995) she did not seem to display a seesaw nystagmus (Jansonius et al. 2001).

References

Apkarian P, Bour L, Barth PG (1993) A unique achiasmatic anomaly detected in non-albinos with misrouted retinal-fugal projections. Eur J Neurosci 6:501–507

Apkarian P, Bour L, Barth PG, Wenniger-Prick L, Verbeeten B Jr (1995) Non-decussating retinal-fugal fibre syndrome: An inborn achiasmatic malformation associated with visuotopic misrouting, visual evoked potential ipsilateral asymmetry and nystagmus. Brain 118:1195–1216

Jansonius NM, van der Vliet AM, Cornelissen FW, Pott JWR, Kooijman AC (2001) A girl without a chiasm: Electrophysiologic and MRI evidence for the absence of crossing optic nerve fibers in a girl with a congenital nystagmus. J Neuro-Ophthalmol 21:26–29
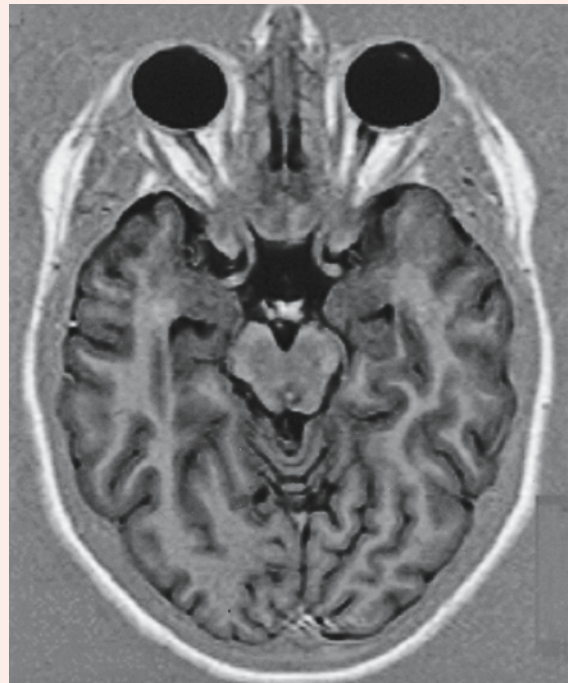
Fig. 9.23 Axial MRI, showing that both optic nerves curve to the lateral side of the suprasellar cistern without crossing over as would have been the case in the presence of a chiasm (courtesy Ton van der Vliet, Nijmegen)

Korff CM, Apkarian P, Bour LJ, Meuli R, Verrey J-D, Roulet Perez E (2003) Isolated absence of optic chiasm revealed by congenital nystagmus, MRI and VEPs. Neuropediatrics 34:219–221

This case was kindly provided by Nomdo M. Jansonius (Department of Ophthalmology, Groningen University Medical Centre) and Ton van der Vliet (Nijmegen).

eminence (LGE) gives rise to the caudate nucleus and the putamen. Both the LGE and the MGE are also involved in the formation of the cerebral cortex. The pyramidal cells of the cerebral cortex arise from the pallial ventricular zone, but its GABAergic interneurons arise from both ganglionic eminences, the medial eminence in particular (Anderson et al. 1997a, 2001; Parnavelas 2000; Marín and Rubinstein 2001, 2002). The caudal part of the human ganglionic eminence also gives rise to a contingent of GABAergic neurons for dorsal thalamic association nuclei such as the pulvinar through a transient fetal structure, the gangliothalamic body (Rakić and Sidman 1969; Letinić and Kostović 1997; Letinić and Rakic 2001). The ganglionic eminence of the human fetal brain plays an important role in prematurely born infants (Ulfig 2002a). The ganglionic eminence is the most common site of intracranial haemorrhage and this is a frequent CNS complication in prematurely born infants (Chap. 3).

The **pallium** is usually divided into a medial pallium or archipallium, a dorsal pallium or neopallium, and a lateral pallium or paleopallium (Fig. 9.26). In mice, gene-expression studies led to redefining of the pallial–subpallial boundary and to a fourth component of the pallium, the ventral pallium (Puelles et al. 2000; Marín and Rubinstein 2002; Molnár and Butler 2002; Schuurmans and Guillemot 2002; Campbell 2003; Stenman et al. 2003). The **medial pallium** or **archipallium** forms the hippocampal cortex, the
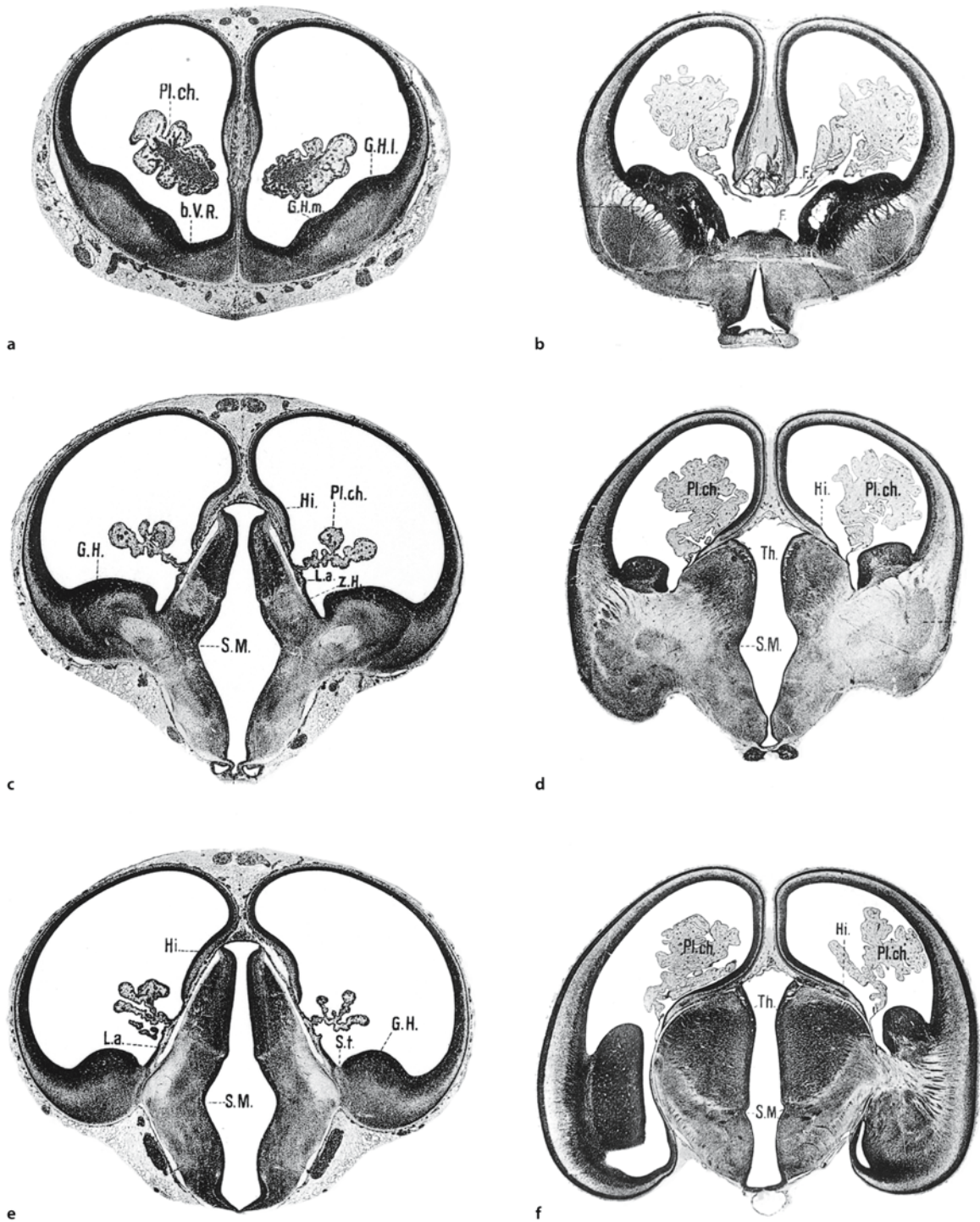
Fig. 9.24 Series of photomicrographs of the developing human forebrain: **a**–**c** a 25-mm embryo (late embryonic period); **d**–**f** early fetal period (46.5-mm CRL). *F.* fornix, *G.H.* ganglionic eminence, *G.H.l.* lateral ganglionic eminence, *G.H.m.* medial ganglionic eminence, *Hi.* hippocampus, *Pl.ch.* choroid plexus, *S.M.* medial sulcus, *Th.* thalamus. (From Hochstetter 1919)
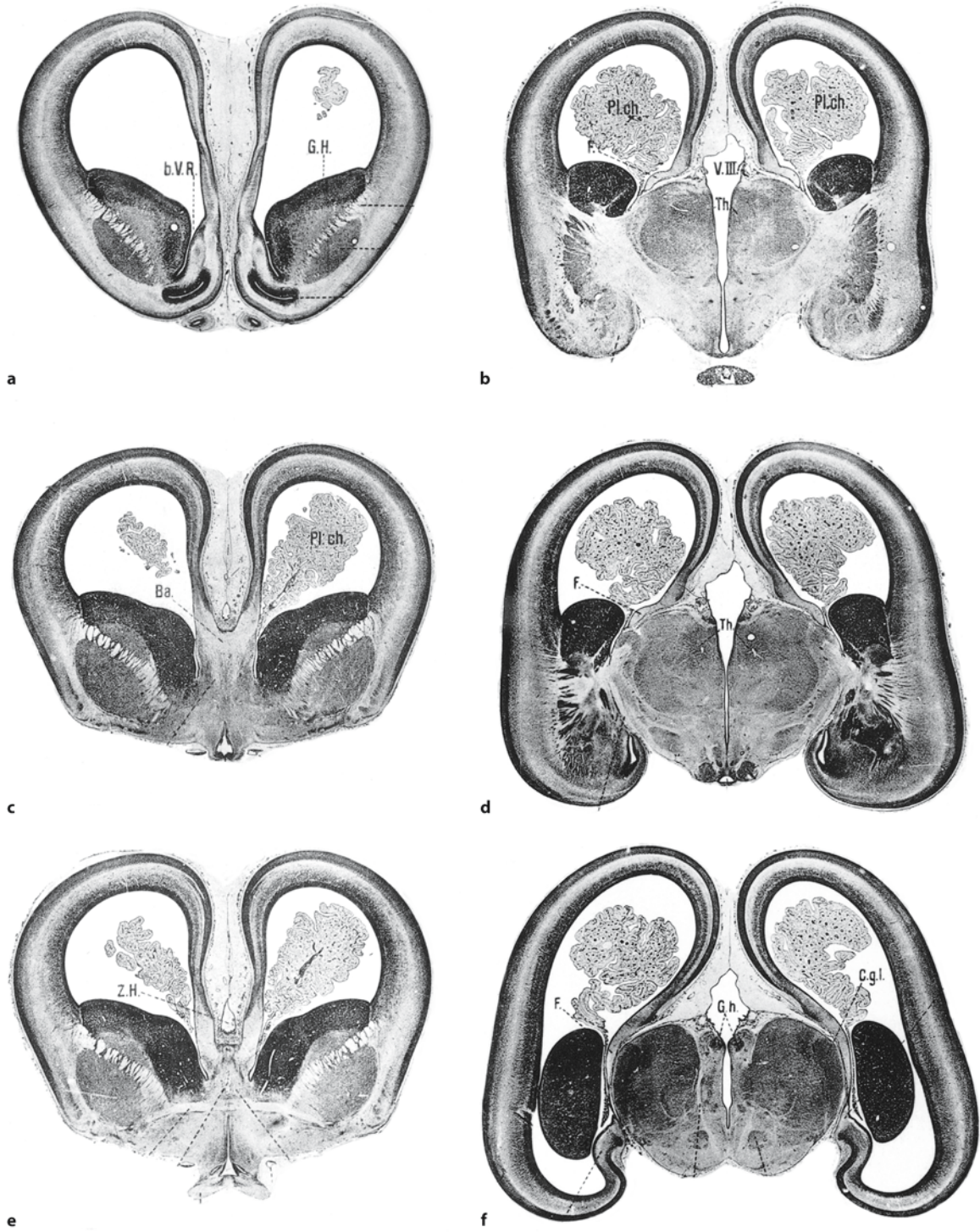
Fig. 9.25 Series of photomicrographs of the developing human forebrain in an 87-mm-CRL fetus. *C.g.l.* corpus geniculatum laterale, *F.* fornix; *G.H.* ganglionic eminence, *G.h.* ganglion habenulae (epithalamus), *Pl.ch.* choroid plexus, *Th.* thalamus, *V.III.* third ventricle. (From Hochstetter 1919)

Table 9.7 Derivatives of the ganglionic eminences (after Marín and Rubinstein 2002; Nery et al. 2002; Brazel et al. 2003)

Ganglionic eminence	'Specific' gene expression	Derivatives
Lateral ganglionic eminence	Dlx1, Dlx2, Dlx5, Dlx6	Projection neurons for caudate, putamen, accumbens and olfactory tubercle Late component neocortical interneurons Granule and periglomerular cells of olfactory bulb (SVZ) Glial cells (SVZ)
Medial ganglionic eminence	Dlx1, Dlx2, Dlx5, Dlx6; Lhx6	Projection neurons for globus pallidus and ventral pallidum Basal nucleus of Meynert Most striatal interneurons Most neocortical and hippocampal interneurons GABAergic neurons for some thalamic nuclei Glial cells (SVZ)
Caudal ganglionic eminence	Dlx2; cellular retinol binding protein 1	Amygdaloid nuclei Contribution to interneuron population cortex and hippocampus

SVZ subventricular zone
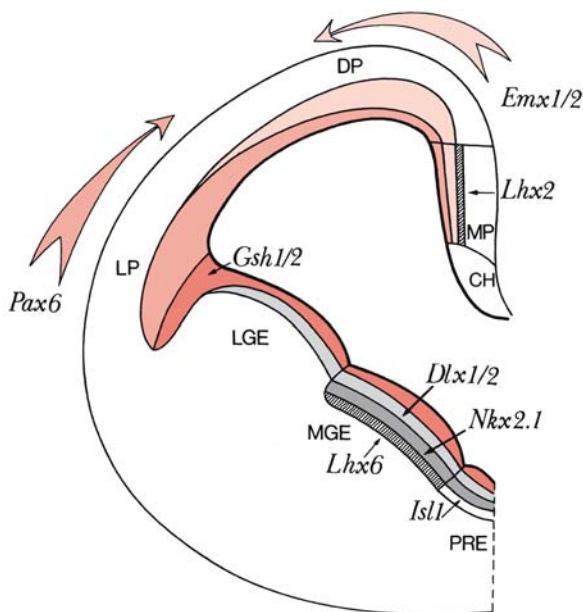
Fig. 9.26 Subdivision of the mouse forebrain and the expression of genes regulating its regionalization (see text for explanation). *DP* dorsal pallium, *LP* lateral pallium, *MP* medial pallium, *LGE* lateral ganglionic eminence, *MGE* medial ganglionic eminence, *PRE* anterior preoptic region. (After Zaki et al. 2003)

three-layered allocortex. Parts of the surrounding transitional cingulate and entorhinal cortex, the four-to-five-layered mesocortex, may have the same origin. The **dorsal pallium** or **neopallium** forms the six-layered isocortex or neocortex. The **lateral pallium** forms the olfactory cortex and the **ventral pallium** the claustro-amygdaloid complex. The development of the medial pallium and the dorsal pallium and their malformations will be discussed in Chap. 10.

The midline and paramedian areas of the telencephalon (the '**cortical hem**') form specialized structures, and give rise to the commissural plate and the choroid plexus.

The **subpallium** consists of three primary regions, the LGE, the MGE, and the telencephalic stalk. Among other structures, including cortical contributions, the LGE gives rise to the striatum and the MGE to pallidal structures. The **subpallial telencephalic stalk** is located close to the pallidal domain, and contains the anterior entopeduncular nucleus (the rodent equivalent of the internal part of the globus pallidus), the preoptic area and the major fibre bundles entering and leaving the telencephalon.

After induction of anterior neural character and specification of telencephalic character (Chap. 2), **dorsoventral regionalization** of the telencephalon occurs. **Genetic analyses** in mice have revealed that regionally restricted genes participate in the specification of the identity of the telencephalic territory in which they are expressed (Rubinstein et al. 1998; Smith-Fernández et al. 1998; Puelles et al. 2000; Marín and Rubinstein 2002; Zaki et al. 2003; Table 9.8). *Emx1* and *Emx2*, and *Dlx1* and *Dlx2* are among the earliest-expressed pallial and subpallial markers, respectively. Their expression delineates three main telencephalic subdivisions in vertebrates (Figs. 2.13, 9.26, 9.27): the pallial, intermediate or ventral pallial, and subpallial neuroepithelial domains. The **ventral pallium** uniquely expresses the homeobox gene *Dbx1* (Yun et al. 2001) and is *Emx1*-negative (Puelles et al. 2000). The specific **boundaries** of the other **pallial domains** are less easily marked by discrete gene expression. Here, graded gene expression is more common. *Emx1, Emx2* and *Lhx2* all show high expression in the medial pallium with a progressive reduction in expression in more lateral regions (Gulisano et al. 1996; Pellegrini et al. 1996; Yoshida et al. 1997;

Table 9.8 Some gene expression patterns during the development of the murine forebrain (after Rubinstein et al. 1998; Marín and Rubinstein 2002; Zaki et al. 2003)

Transcription factor gene or extracellular signalling molecule	Beginning of expression	Site of expression	Mouse mutant	Phenotype of mouse mutant	Human homologue and phenotype
Induction of anterior neural character					
Otx2	E6.5	Prosencephalon, mesencephalon	Otx2–/–	Absence of forebrain and large part of brain stem; lethal in embryonic period	
Otx1	E8	Dorsal part telencephalon, mesencephalon	Otx1–/–	Cell reduction in cerebral cortex, epilepsy	
Specification of telencephalic character					
Foxg1 (BF1)	E8	Dorsal telencephalon	Foxg1–/–	Early postnatal lethality; severe hypoplasia telencephalon with absence of subpallium	
Dorsoventral patterning telencephalon					
Gli3			Gli3–/– Extra toes	Early postnatal lethality; ventral markers expand into the cortex	GLI3 mutations lead to Greig syndrome
Shh	E8	Medial part neural plate	Shh–/–	Malformations basal telencephalon, cyclopia	SHH mutations lead to holoprosencephaly
Proneural genes					
Ngn1			Ngn1–/–	Neonatal lethal; decrease in number of neurons in preplate	
Ngn2			Ngn2–/–	Perinatal lethal; ventral markers upregulated; cortical ectopia	
Regionalization					
Pallium					
Emx2	E8	Pallium	Emx2–/–	Loss of dentate gyrus	EMX2 mutations may lead to schizencephaly
Pax6	E8	Pallium and eye primordia	Pax6^Sey/Sey	Heterozygotes: small eye, iris hypoplasia Homozygotes: absence of eyes	PAX6 mutations result in aniridia
Emx1	E9.5	Pallium	Emx1–/–	Absence of corpus callosum	
Tbr1	E10	Pallium	Tbr1–/–	Loss of certain neuron types in cortex	
Lhx2		Medial pallium	Lhx2–/–	Agenesis of hippocampal anlage; hypoplasia cortical plate and basal ganglia	
Subpallium					
Nkx2.1	E8	Medial ganglionic eminence, preoptic area	Nkx2.1–/–	Absence of pallidum and severe loss of cortical interneurons	
Ascl1 (Mash1)		Subpallium, olfactory bulb and epithelium	Mash1–/–	Widespread defects in primary olfactory pathway	
Dlx1/Dlx2	E9.5	Subpallium		Single mutants only mild phenotype	
Dlx5		Subpallium, olfactory bulb and epithelium	Dlx5–/–	Lack of innervation of olfactory bulb with other secondary defects	

Table 9.8 *(Continued)*

Transcription factor gene or extracellular signalling molecule	Beginning of expression	Site of expression	Mouse mutant	Phenotype of mouse mutant	Human homo-logue and phenotype
Lhx6		Medial ganglio-nic eminence			
Gsh1/Gsh2		Lateral ganglio-nic eminence	*Gsh2–/–*	Lateral ganglionic eminence reduced in size; medial ganglionic eminence relatively normal	
			Gsh1/Gsh2–/–	Lateral ganglionic eminence more affected than in *Gsh2–/–*; medial ganglionic eminence relatively normal	
Isl1		Preoptic area			
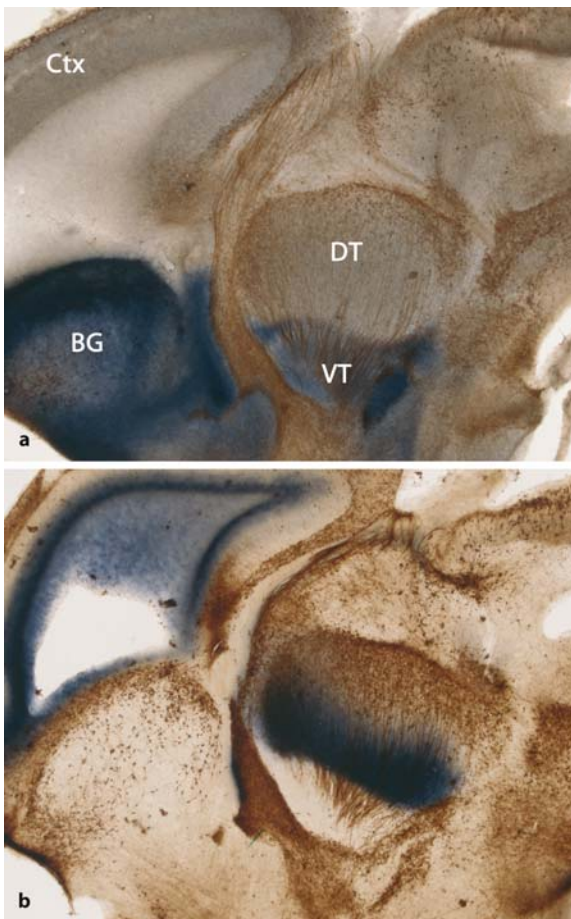
Fig. 9.27 Photomicrographs of *Dlx5* (**a**) and *Math4a* (**b**) labelling in the E14.5 mouse forebrain. *BG* basal ganglia, *Ctx* cortex, *DT* dorsal thalamus, *VT* ventral thalamus. (Courtesy Loreta Medina, Murcia)

Tole et al. 2000a; Mallamaci et al. 2000; Yun et al. 2001), whereas *Pax6* and *Tbr1* show the opposite profile, with highest expression in the lateral and ventral pallium (Puelles et al. 2000; Toresson et al. 2000; Yun et al. 2001). *Emx2* and *Pax6* are involved in many aspects of cortical morphogenesis (Chap. 10). Nevertheless, in the absence of either *Emx2* or *Pax6*, cerebral cortex does form. In *Emx2–/–; Pax6^{Sey/Sey}* double-mutant mice, however, conversion of the cerebral cortex into basal ganglia occurs (Muzio et al. 2002). It seems likely that at least one fully functional allele of either *Emx2* or *Pax6* is necessary and sufficient for activating corticogenesis and to suppress competing subpallial morphogenetic programmes.

In the **subpallium**, many genes are expressed, in particular the *Dlx1*, *Dlx2*, *Dlx5* and *Dlx6* genes (Eisenstat et al. 1999) as well as *Gsh1* and *Gsh2* (Toresson et al. 2000; Toresson and Campbell 2001; Yun et al. 2001). The ventromedial telencephalon, including the MGE and the preoptic area, expresses *Nkx2.1* (Shimamura et al. 1995; Sussel et al. 1999). The preoptic area also expresses *Isl1* (Marín and Rubinstein 2001). The CGE shares some molecular markers with both the LGE and the MGE. The CGE expresses *Dlx2* and *Ascl1* (formerly known as *Mash1*) at levels equivalent to those in the other ganglionic eminences. In contrast, *Lhx6* is highly expressed in the MGE (Lavdas et al. 1999), hardly in the LGE and in only low levels in the CGE. The CGE is further characterized by a high level of cellular retinol binding protein 1 (Nery et al. 2002).

The **pallial–subpallial** or **corticostriatal boundary** does not lie at the boundary between the ventral pallial and LGE progenitor zones but is slightly more ventral in the dorsalmost part of the LGE. The early expression of the *Pax6* and *Gsh2* homeobox transcription factors overlaps in the dorsal part of the LGE. In *Gsh2* mutants, the dorsal part of the LGE is re-specified into a ventral pallium-like structure, where-
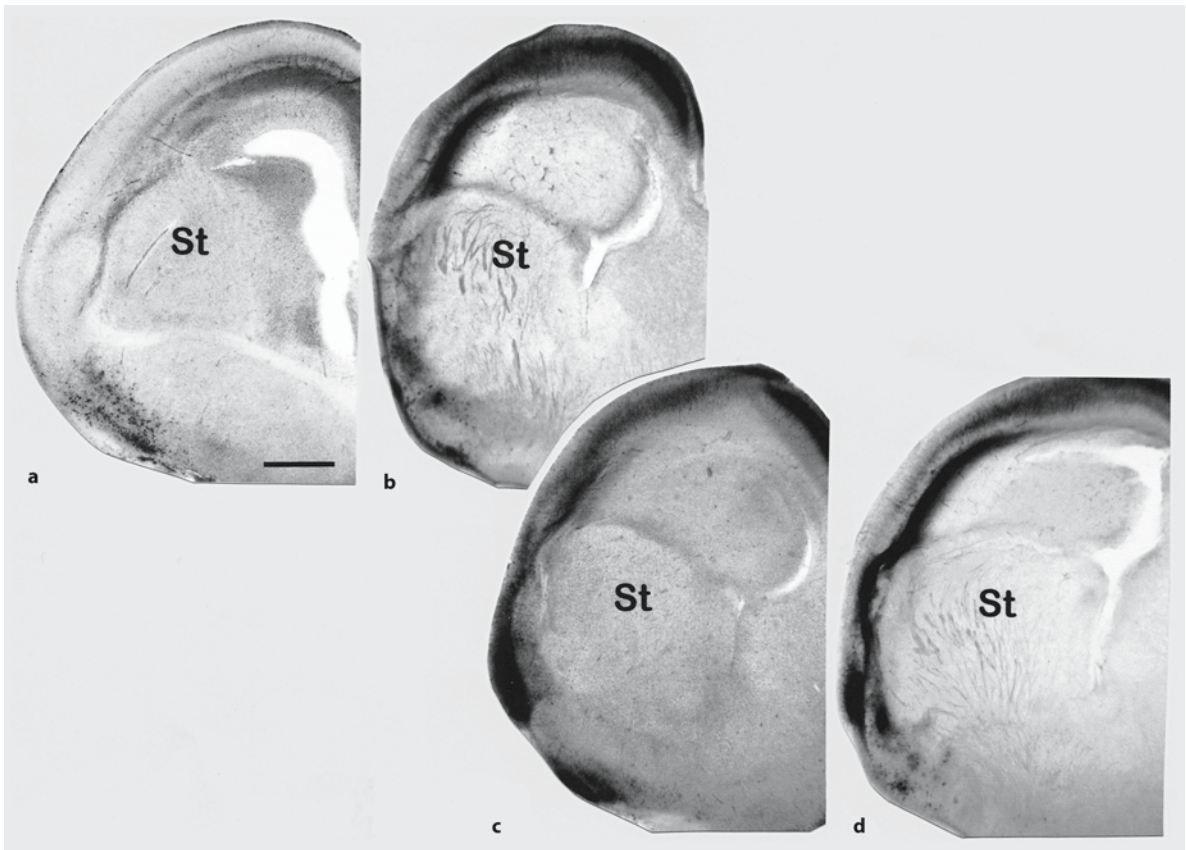
Fig. 9.28 Transverse sections through the left telencephalon of an E18.5 *Pax6/LacZ+/–* mouse (**a**) and E18.5 *Pax6/LacZ–/–* mice (**b–d**). The *Pax6/LacZ–/–* mice show a large, abnormal pallial mound dorsal to the striatum (*St*) and underneath the neocortex. *Darker areas* in the neocortex represent β-galac-tosidase staining (**a–d**), which reveals the *LacZ* gene expression driven by the *Pax6* promoter. The *dark fibres* (**b**, **d**) are L1-stained thalamocortical axons. (Courtesy Zoltán Molnár, Oxford)

as in *Pax6* mutants the ventral pallium is respecified into a dorsal LGE-like structure (Stoykova et al. 1996, 2000; Toresson et al. 2000; Yun et al. 2001). The development of a pallial mound in a *Pax6/LacZ–/–* mouse (Butler and Molnár 2002) is shown in Fig. 9.28. Patterning defects caused by loss of Pax6 function result in multiple morphological abnormalities in the brain of *Sey* mutants such as dysgenesis of the piriform, insular and lateral cortices, and of the claustrum, failure in the differentiation of a subpopulation of cortical precursors, and absence of the olfactory bulbs. *Tlx* and *Pax6* cooperate in the establishment of the pallial–subpallial boundary in the embryonic mouse telencephalon (Stenman et al. 2003). *Tlx* homozygous mutants show alterations in the development of this boundary similar, but these are less severe than those seen in *Sey/Pax6* mutants. Malformations occur in the lateral and basolateral amygdala, both of which are derived from the ventral pallium. In human embryos, *PAX6* is expressed early in the neural tube, just after its closure (Gérard et al. 1995).

Like in the spinal cord, the roof plate (Fig. 9.2) may play an essential role in **dorsal telencephalic** or **pallial patterning** through BMP signalling. Explant studies support a role for BMPs in dorsal telencephalic development (Furuta et al. 1997) and in the expression of *Lhx2* (Monuki et al. 2001). Receptor blocking studies, however, suggest that loss of BMP signalling in the dorsal telencephalon leads to a normal dorsal–ventral pattern but maldevelopment of the choroid plexus, suggesting only a local role for BMPs in the dorsal telencephalic midline (Hébert et al. 2002). Genetic ablation of the telencephalic roof plate leads to a severely reduced expression of *Lhx2* and a severe reduction in cortical size (Monuki et al. 2001). Another transcription factor that is crucial in dorsal patterning is the zinc-finger gene *Gli3* (Rallu et al. 2002b; Campbell 2003). *Gli3* is required to antagonize the ventralizing signal SHH in the dorsal telencephalon (Rallu et al. 2002a). Loss of *Gli3* function in *Extra-toes* mutants results in the loss of *Emx* gene expression as well as in the ectopic expression of cer-

tain genes characteristic of ventral telencephalic progenitors such as *Gsh2* (Theil et al. 1999; Tole et al. 2000b; Rallu et al. 2002a). *Extra-toes* mutant mice also lack the telencephalic choroid plexus and olfactory bulbs (Franz 1994). *Gli3* mutations are also reponsible for the abnormalities in the arhinencephalic *Pdn/Pdn* (homozygote of *Polydactyly Nagoya* mouse, *Pdn*) mice (Naruse and Keino 1995). In man, *GLI3* mutations lead to Greig's (Greig 1926) cephalopolysyndactyly syndrome (Vortkamp et al. 1992), characterized by the presence of hypertelorism and polysyndactyly.

The secreted glycoprotein SHH is required for **ventral telencephalic** or **subpallial patterning** as shown in *Shh*-null mice (Chiang et al. 1996; Litingtung and Chiang 2000). Although these mutants lack any sign of MGE development such as expression of the *Nkx2.1* homeodomain protein, many of them express genes normally found in both the MGE and the LGE such as *Gsh2* and *Dlx2* (Rallu et al. 2002a, b); therefore, SHH is required for ventromedial telencephalic development. A mutation in *Nkx2.1* results in the acquisition of striatal-like properties by the presumptive pallidum, suggesting that *Nkx2.1* both specifies an MGE fate and inhibits LGE phenotypes (Sussel et al. 1999). Nodal signalling is also required for induction of *Nkx2.1* expression as shown in zebrafish (Rohr et al. 2001). In *Pax6* (*Sey*) mutants, MGE markers expand into the LGE, leading to an overall reduction in the size of the striatum and expression of MGE-derived structures (Stoykova et al. 2000); therefore, *Pax6* and *Nkx2.1* both operate at the LGE–MGE border, maintaining LGE and MGE identity, respectively. *Gsh1* and *Gsh2* also encode homeodomain proteins and are important for ventral telencephalic specification. In *Gsh2* single mutants and *Gsh1/Gsh2* double mutants, dorsal markers cross the LGE–pallial boundary into the LGE, and ventral markers are suppressed (Corbin et al. 2000; Toresson et al. 2000; Toresson and Campbell 2001). Probably, *Gsh2* maintains dorsal LGE identity without directly regulating ventral marker expression (Toresson et al. 2000), whereas expression of ventral genes in the ventral part of the LGE involves a more direct role of *Gsh1* and/or *Gsh2* (Toresson and Campbell 2001; Yun et al. 2001).

Dlx1, *Dlx2*, *Dlx5* and *Dlx6* are expressed in overlapping sets of cells in the developing forebrain and single mutants have mild phenotypes, suggesting redundancy of function (Bulfone et al. 1993; Anderson et al. 1997b; Liu et al. 1997; Eisenstat et al. 1999; Panganiban and Rubinstein 2002). *Dlx2* is expressed before *Dlx1*, which is expressed before *Dlx5* and *Dlx6*. In the basal forebrain, the *Dlx*-positive cells differentiate into striatal and pallidal projection neurons as well as into interneurons for the cerebral cortex and olfactory bulb. *Dlx2* mutants have reduced numbers of
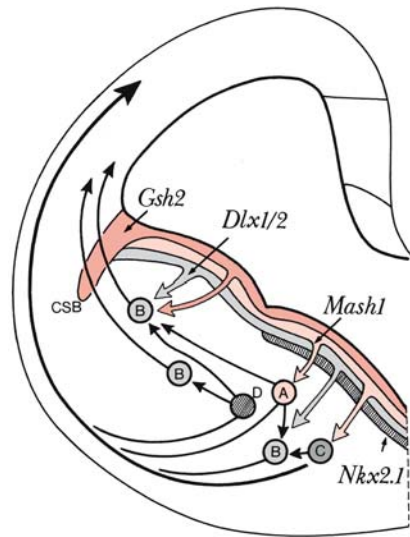
Fig. 9.29 Genes involved in specification and/or migration of tangentially migrating interneuron populations in the ventral forebrain (see text for explanation). Neurons indicated *A–D* express the following genes: A, *Mash1*; B, *Dlx1/2*; C, *Lhx6* and D, *Nkx2.1*. *CSB* corticostriatal boundary. (After Zaki et al. 2003)

dopaminergic neurons in the olfactory bulb (Acampora et al. 1999; Eisenstat et al. 1999). In *Dlx1/Dlx2* double mutants, neurogenesis in the subpallium is disturbed, in particular the subventricular zone fails to mature (Anderson et al. 1997b; Marín et al. 2000). *Dlx* function is tightly labelled to the development of neurons derived from the basal telencephalon that produce GABA, acetylcholine and dopamine (Marín and Rubinstein 2002; Panganiban and Rubinstein 2002). Ectopic expression of *Dlx2* and *Dlx5* genes induces the expression of glutamic decarboxylase (GAD), the enzyme that synthesizes GABA (Stühmer et al. 2002). Moreover, *Dlx5* regulates the development of peripheral and central components of the olfactory system (Long et al. 2003). *Ascl1*, formerly known as *Mash1*, a basic helix–loop–helix transcription factor, regulates neurogenesis in the ventral telencephalon (Casarosa et al. 1999). *Mash1* mutant mice show severe loss of progenitors, particularly of neuronal precursors in the subventricular zone of the MGE. Discrete neuronal populations of the basal ganglia and cerebral cortex are subsequently missing. Loss of *Mash1* function also causes widespread defects in the primary olfactory pathway (Murray et al. 2003).

In the forebrain two main modes of **migration** can be recognized: radial and tangential (Fig. 9.29). The coexistence of these two different methods of cell migration has been well established for the developing cerebral cortex (Chap. 10). Lineage analysis studies showed that radially and tangentially migrating cells
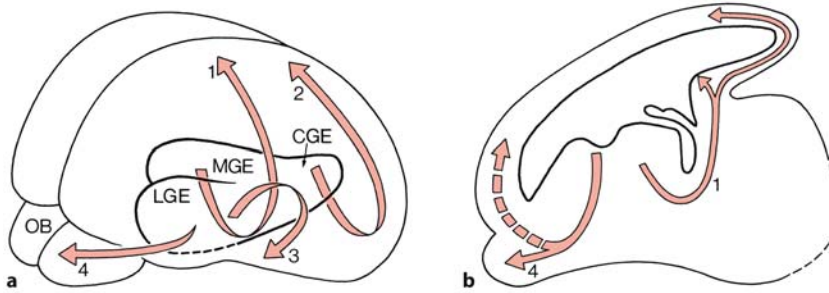
in the developing cortex arise from different progenitors (Mione et al. 1997; Tan et al. 1998). Moreover, the presence of *Dlx2*-positive neurons in the developing cortex suggested that cells of subpallial origin might have migrated tangentially into the pallium (Porteus et al. 1994). It is now clear that most cortical GABAergic neurons are born in the subpallium as already suggested by van Eden et al. (1989), and they reach the developing cortex in several tangentially migrating streams (de Carlos et al. 1996; Anderson et al. 1997a; Tamamaki et al. 1997).

After these first studies on the origin of GABAergic neurons from the subpallium, a variety of experimental studies showed that GABAergic neurons for the entire cerebral cortex, including the neocortex, the piriform cortex and the hippocampus, arise subpallially (Lavdas et al. 1999; Wichterle et al. 1999, 2001; Corbin et al. 2001; Marín and Rubinstein 2001; Nery et al. 2002; Brazel et al. 2003; Kriegstein and Noctor 2004). The three ganglionic eminences contribute different types of cells to different brain structures, and a similar pattern is likely to be present in man. The MGE appeared to be the main source of cortical interneurons (Lavdas et al. 1999; Wichterle et al. 1999, 2001). These cells express the LIM homeobox gene *Lhx6* and reach to the cerebral cortex via **dorsal** and **lateral cortical streams** (Fig. 9.30). The MGE also contributes cells to the globus pallidus and the cholinergic basal nucleus of Meynert. LGE cells migrate ventrally and anteriorly, and give rise to the GABAergic medium spiny neurons in the striatum, nucleus accumbens, and olfactory tubercle, and to granule and periglomerular cells of the olfactory bulb. The striatal and olfactory bulb cells arise from two distinct progenitor populations in the LGE (Stenman et al. 2003). Progenitor cells in the subventricular zone of the LGE generate granule and periglomerular cells for the olfactory bulb (Hinds 1968a, b; Altman 1969; Bayer 1983; Kishi 1987). In neonatal and adult rodents and primates, these cells reach their final position via a **rostral migratory stream** (Luskin 1993; Lois and Alvarez-Buylla 1994; Kornack and Rakic 2001). The CGE contributes to the posterior neocortex, the hippocampus, the amygdala and posterior parts of the striatum and globus pallidus (Nery et al. 2002).

9.6   Development of the Rhinencephalon

The mammalian **rhinencephalon**, i.e. the part of the telencephalon involved in the processing of chemosensory information, is composed of the main olfactory system, the accessory olfactory or vomeronasal system and the terminal nerve (Stephan 1975; Voogd et al. 1998). Olfactory fibres originate in the olfactory epithelium and pass as **fila olfactoria** through the cribriform plate of the ethmoid to contact the olfactory bulb. The central part of the **main olfactory system** comprises the olfactory bulb and the targets of its projections within the telencephalon, i.e. the retrobulbar region or anterior olfactory nucleus, the olfactory tubercle, the prepiriform, periamygdaloid and entorhinal cortices, and the cortical and medial nuclei of the amygdaloid complex (Lohman and Lammers 1967; Price 1990; Shipley et al. 1995; Fig. 9.31). The **accessory olfactory system**, also known as the **vomeronasal system**, comprises the vomeronasal organ of Jacobson, the accessory olfactory bulb and some nuclei of the amygdaloid complex (Halpern 1987; Shipley et al. 1995). The accessory olfactory system is primarily involved in the regulation of reproductive behaviour, elicited by pheromones, chemical messengers from other members of the same species (Dulac and Torello 2003). In humans, the vomeronasal system is established during embryonic development and regresses in the fetal period (Ortmann 1989; Kjaer and Fischer-Hansen 1996), although as many as 850 cells may be present by 4 months after birth (Oelschläger et al. 1987). The human **vomeronasal organ** of **Jacobson**, a pocket lying in the nasal septum, opens into the vomeronasal pit, about 1 cm dorsal to the columella and 1–2 mm above the floor of the nose. In some 40% of adults, this opening can be seen macroscopically (Moran et al. 1991), and even in 73% of the population using endoscopy (Trottier et al. 2000).

Fig. 9.31 Overview of the human rhinencephalon. *A* anterior nucleus, *AC* anterior commissure, *BL* basolateral amygdala, *C* cortical amygdala, *CA* cornu Ammonis, *CC* corpus callosum, *CM* corpus mamillare, *EN* entorhinal cortex, *F* fornix, *GC* gyrus cinguli, *GD* gyrus dentatus, *GPH* gyrus parahippocampalis, *IN* indudium griseum, *L* lateral olfactory stria, *M* medial olfactory stria, *MD* mediodorsal nucleus, *OB* olfactory bulb, *OT* olfactory tract, *RH* rhinal cortex, *ST* stria terminalis, *SUB* subiculum (after Nieuwenhuys et al. 1988)
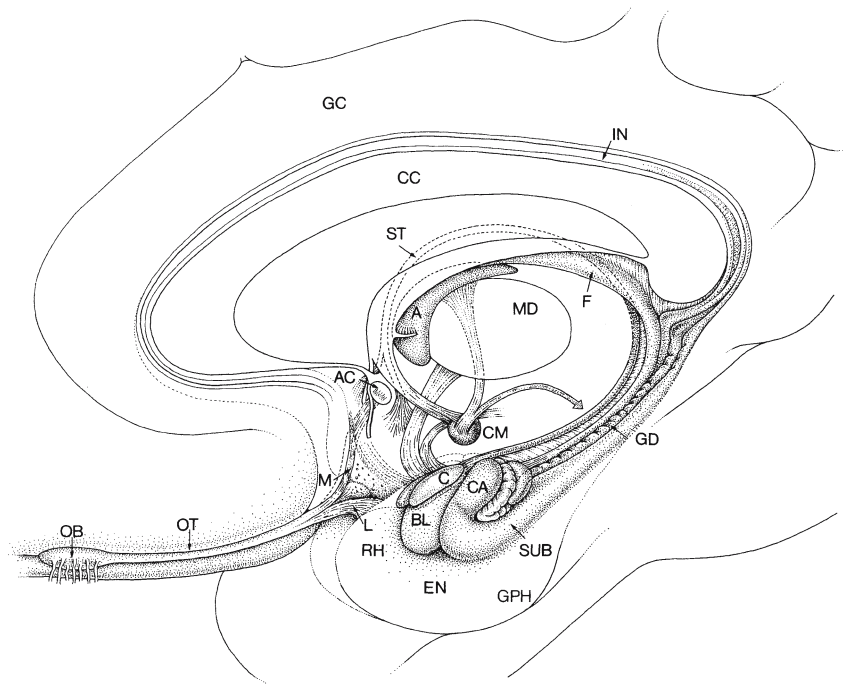
The **olfactory bulb** arises as an evagination of the rostral telencephalon (Fig. 9.32) and receives primary olfactory afferent fibres from neurons in the olfactory epithelium. The primary olfactory fibres synapse on the dendrites of glutaminergic projection neurons (the *mitral* and *tufted cells*) found in specialized structures called **glomeruli**, forming the glomerular layer. Many thousands of olfactory receptor cells synapse with the dendritic branches of one or only a few mitral cells within a glomerulus, resulting in a high degree of convergence of olfactory receptors onto mitral cells (Shepherd and Greer 1990). A large number of inhibitory, GABAergic interneurons are present in the olfactory bulb, the most common of which are the *granule* and *periglomerular cells*. Most of the periglomerular cells are GABAergic as well as dopaminergic. The following layers can be recognized in the olfactory bulb: (1) the *outer fibre layer*, consisting of the incoming olfactory fibres; (2) the *glomerular layer*, consisting of several rows of glomeruli surrounded by periglomerular cells; (3) the *external plexiform layer*, containing the dendritic branches of mitral cells and granule cells; (4) the *mitral cell layer*, not well-defined in man; (5) an ill-defined *internal plexiform layer*, largely composed of axons of mitral and tufted cells; (6) the *granular layer*, with the granule cells; and (7) a *periventricular layer*, composed of the *subventricular zone*, a reservoir of progenitor cells that produces new granule and periglomerular cells in the adult brain, and *ependymal cells*, remnants of the epithelial layer of the olfactory ventricle.

Development of the **olfactory bulb** begins with its induction and evagination from the rostral telencephalon. FGF signalling through FGFR1 is required for olfactory bulb morphogenesis (Hébert et al. 2003). Signalling from the olfactory placode may contribute to patterning the anlage of the olfactory bulb (Graziadei and Monte-Graziadei 1992; de Carlos et al. 1995; LaMantia et al. 2000). The mitral and tufted neurons have a pallial origin and are regulated by cortical transcription factors such as *Tbr1* (Bulfone et al. 1998), whereas the granule and periglomerular cells have a subpallial origin and are regulated by subpallial transcription factors such as *Dlx1* and *Dlx2* (Qiu et al. 1995; Bulfone et al. 1998). The *Dlx* family of homeobox genes is expressed in the olfactory bulb as well as in the olfactory epithelium (Acampora et al. 1999; Depew et al. 1999; Long et al. 2003). In particular, *Dlx5* is expressed in the olfactory placode, the olfactory epithelium and local circuit neurons of the olfactory bulb. In *Dlx5–/–* mutants, the size of the olfactory epithelium is reduced and the few olfactory neurons formed fail to generate axons that innervate the olfactory bulb (Long et al. 2003). Despite this lack of innervation, the olfactory bulb forms, and neurogenesis of projection and local circuit neurons proceeds. Widespread defects in the primary olfactory pathway are caused by loss of *Ascl1* (formerly *Mash1*) function (Murray et al. 2003). This homologue of the *Drosophila* proneural genes *achaete* and *scute* is normally expressed by neuronal progenitors in the developing peripheral nervous system and CNS, including the olfactory epithelium and the olfactory bulb
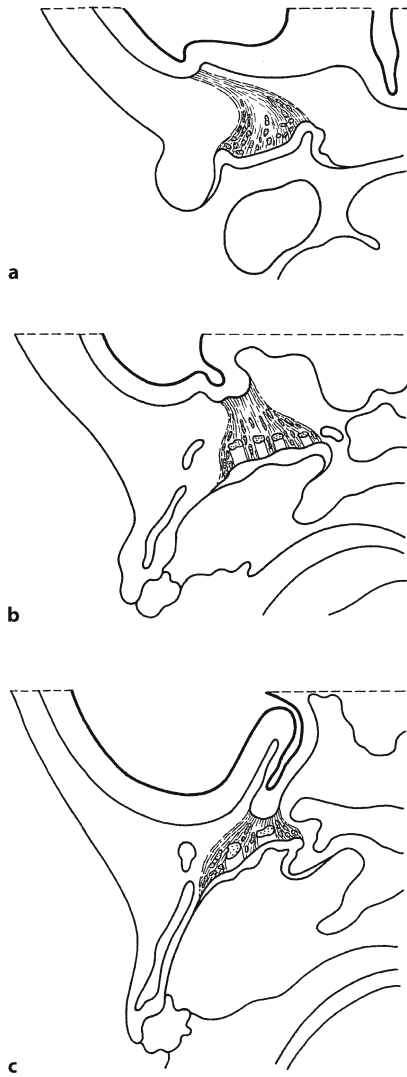
Fig. 9.32 Development of the human olfactory bulb: **a** a stage 18 embryo (about 42 days of development); **b** a 3.2-mm fetus; **c** a 4.9-mm fetus (after Pearson 1941b; Hinrichsen 1990)

and ganglionic eminences (Guillemot et al. 1993; Cau et al. 2002). *Neurogenin 1*, related to the *Drosophila* proneural gene *atonal*, is necessary for the differentiation of olfactory sensory neuron progenitors (Cau et al. 2002). In human cases of arhinencephaly as found in HPE and in Kallmann syndrome, both olfactory receptor cells and olfactory nerves are present (Braddock et al. 1995), also suggesting that the initial development of the olfactory nerves is independent of the formation of the olfactory bulb. Bilaterally enlarged olfactory bulbs with abnormal laminar structures were described as **olfactory bulb dysplasia** in a case of Pena–Shokeir phenotype (Yamanouchi et al. 1999).

Pearson (1941b, 1942) described the **development** of the **human olfactory bulb** (Fig. 9.32). At the end of the first gestational month (stage 13), the olfactory placodes can be distinguished as epithelial thickenings on either side of the head. Subsequently, the olfactory placodes are overgrown by the nasal folds, resulting in the formation of the olfactory pits (Chap. 5). The first bipolar cells appear in the olfactory placode at stage 14. At stage 16, olfactory fibres enter the wall of the telencephalon when still no olfactory bulb can be identified (Lemire et al. 1975; Bossy 1980; Pyatkina 1982; Müller and O'Rahilly 1989a). Soon afterwards, the olfactory bulb begins as a slight bulge (stage 17), and by stage 20 it consists of a slight protrusion. By stage 22 all layers of the olfactory bulb are represented (Humphrey 1967; Lemire et al. 1975; Bossy 1980; Müller and O'Rahilly 1989b).

The **vomeronasal organ** of **Jacobson** first appears as a groove in the nasal septum at stage 18 (Humphrey 1940). Nerve fibres from this region may be traced into the vomeronasal and terminal nerves. The **vomeronasal nerve** arises from cells found in the medial border of the olfactory placode and is difficult to separate from the terminal nerve which arises in the same area at the same time (Pearson 1941a, 1942; Fig. 9.33). Vomeronasal fibres pass dorsomedially
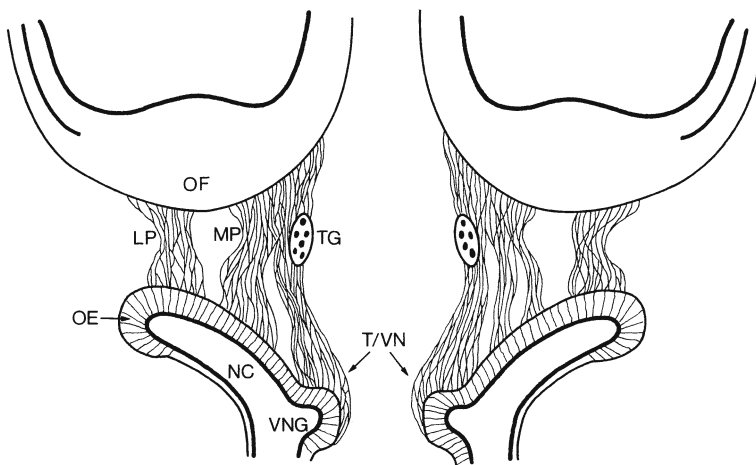
Fig. 9.33 Development of the human vomeronasal and terminal nerves at stage 18. *LP* lateral olfactory plexus, *MP* medial olfactory plexus, *NC* nasal cavity, *OE* olfactory epithelium, *OF* olfactory field, *TG* terminal ganglion, *T/VN* terminal and vomeronasal nerves, *VNG* vomeronasal groove. (After Ashwell and Waite 2004)

Fig. 9.34 Basal views of the human brain in the second (**a**), third (**b**), fourth (**c**) and sixth (**d**) months of development. *DB* diagonal band of Broca, *EN* entorhinal cortex, *OB* olfactory bulb *OT* olfactory tubercle, *PC* paleocortex, *PPF* prepiriform cortex, *PRA* perirhinal cortex, *S* septum. (After Macchi 1951; Gastaut and Lammers 1961; Kahle 1969; Stephan and Andy 1975)
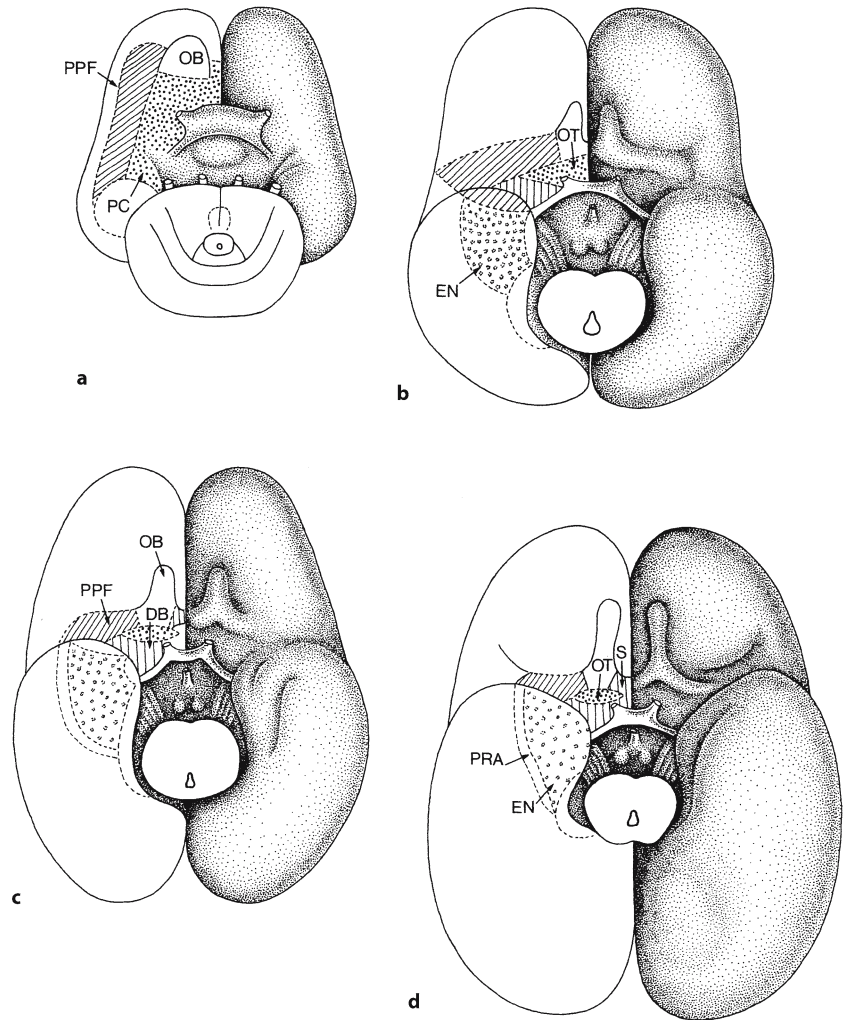
along the developing olfactory bulb to enter the accessory olfactory bulb around stage 18 (Humphrey 1940). The **accessory olfactory bulb** moves from its original dorsomedial position to a dorsolateral position. It begins to regress at the beginning of the third gestational month and is vestigial by the end of the third gestational month (Humphrey 1940; Lemire et al. 1975; Meisami and Bhatnagar 1998; Meredith 2001; Savic et al. 2001). The development of the vomeronasal nerve and accessory olfactory bulb parallels the development and regression of the vomeronasal organ in the human embryo. The **terminal nerve** is characterized by ganglion cells along its course and has been described in adults (Crosby and Humphrey 1941). At stages 16 and 17, the terminal nerve arises from cells in the medial part of the olfactory placode and is closely associated with the vomeronasal nerve (Pearson 1941a). GnRH neurons migrate along the vomeronasal and terminal nerves to the forebrain (Schwanzel-Fukuda and Pfaff 1989; Schwanzel-Fukuda et al. 1989; Boehm et al. 1994;

Berliner et al. 1996). GnRH neurons can be detected in the olfactory epithelium as early as 5.5 weeks of development (Fig. 9.47 a, b). These cells migrate along the developing vomeronasal and terminal nerves shortly afterwards (Verney et al. 1996).

The development of human primary and secondary olfactory areas is shown in basal views of the brain (Fig. 9.34). At first, olfactory regions of the brain occupy a large part of the basal aspect of the brain. Later in development, the olfactory regions become restricted to a small part of the basal frontal lobe and the rostromedial part of the temporal lobe (Macchi 1951; Gastaut and Lammers 1961; Kahle 1969; Stephan 1975).

Extensive **birthdating studies** on the **olfactory system** have been carried out in rodents. Data are available for the olfactory bulb (Hinds 1968a, b; Bayer 1983, 1986a, b), the olfactory tubercle (ten Donkelaar and Dederen 1979; Bayer 1985a; Bayer and Altman 1987b) and the primary olfactory cortex (Bayer 1985b; Bayer and Altman 1987b). In rats, mi-

Table 9.9 Subdivision of the prosencephalies (after Probst 1979; Sergi and Schmitt 2000)

Subdivision	Further subdivision	Remarks
Aprosencephaly		
Atelencephaly		
Prosencephaly		
	Complete sac category (pseudo-aprosencephaly)	
	Dorsal sac category (holosphere with dorsal sac)	Phenotypes: a) Cyclopia b) Ethmocephaly c) Cebocephaly d) Median (or bilateral cleft) lip/palate e) Minor dysplasias or without facial defects
	Intermediate category	
	Pseudohemispheric category (holosphere without sac)	
	Partial prosencephaly (anterior part of holosphere divided, posterior part continuous)	
	Middle interhemispheric variant	

tral cells in the olfactory bulb are born at E14–E16, and granule cells from E20 onwards, continuing in the adult brain. Several neurogenetic gradients in all structures receiving olfactory input were found. Bayer (1986b) suggested a relationship between these gradients in the olfactory target structures and their connections with the olfactory bulb. Bayer et al. (1995) estimated the time of neuron origin of human mitral cells between 5 and 8 weeks of development. Human granule cells are formed from the 19th week of development onwards.

The **development** of **olfactory bulb projections** has been studied in rats (Schwob and Price 1984; López-Mascaraque et al. 1996; Hongo et al. 2000). Using the fluorescent carbocyanine tracer DiI, the first olfactory projections can be detected as early as E13 (López-Mascaraque et al. 1996). Pioneering fibres begin to grow through the ventral part of the telencephalon. At E14 and E15, these fibres have reached distant parts in the basal and lateral parts of the telencephalic vesicle, and establish the first contacts with the future amygdaloid area and the primary olfactory cortex. At E16, fibres from the olfactory bulb run caudally in a fan-like fashion, the lateral olfactory tract increases considerably and some fibres course along the anterior commissure. At E17, the major fibre systems appear already established, providing the substrate of the adult pattern. The further development of axonal connections in the central olfactory system has been studied by Schwob and Price (1984). In genetic arhinencephaly mouse embryos (*Pdn/Pdn*), the olfactory bulb is not formed, and olfactory fibres do not enter the CNS. They form a tangled mass under the cerebral hemisphere at E16 (Hongo et al. 2000). *Pdn/Pdn* mice exhibit preaxial

polydactyly in both the forelimbs and hindlimbs (Naruse and Keino 1995). Newborns do not suckle milk and they die within 1 day after birth. They also exhibit various brain malformations, including absence of the olfactory bulbs and corpus callosum. Apoptosis of precursor mitral cells in the anlage of the olfactory bulb may be induced by non-innervation of olfactory neurons, and sequential apoptosis of precursor neurons in the pyriform cortex may be induced by non-innervation due to death of mitral cells (Naruse and Keino 1995).

9.7   The Prosencephalies

Prosencephalic malformations may be the result of defects in mediolateral patterning of the rostral part of the embryonic neural plate. Since this anlage gives rise to the forebrain with the eye vesicles and the hypothalamus/neurohypophysis, prosencephalic defects are usually accompanied by anomalies of the eyes and the pituitary gland. These disorders are sometimes described as *midline field defects* (Opitz 1993; Opitz et al. 1997; Roessler and Muenke 2001) but from an embryological point of view they are quite heterogeneous and a real midline field does not exist (O'Rahilly and Müller 2001). The general term *prosencephalies* (Probst 1979) includes a scala of malformations, ranging from aprosencephaly to partial or lobar HPE (Sergi and Schmitt 2000; Kakita et al. 2001; Table 9.9). The most severe forms of developmental malformations of the forebrain are complete absence of the forebrain (aprosencephaly) or of the telencephalon (atelencephaly). The most frequent prosencephalies are the various forms of HPE. Relat-

Aprosencephaly

Aprosencephaly is an extremely rare fetal CNS defect in which the forebrain structures derived from both the telencephalon and the diencephalon are absent or rudimentary (Kakita et al. 2001; see Case Report). Sergi and Schmitt (2000) reported a case in which the forebrain was missing but remnants of a forebrain bleb were observed (***pseudo-aprosencephaly***).

Case Report. On ultrasound examination of the fourth pregnancy of a 32-year-old mother with severe diabetes mellitus type 1, the fetus was suspected for anencephaly; therefore, delivery was induced at 20 gestational weeks. The immature female fetus showed multiple congenital malformations (Fig. 9.35 a–c), including the following: (1) ***aprosencephaly***, characterized by the absence of the diencephalon and the telencephalon with absence of the olfactory bulbs and a malformed optic chiasm; (2) low brain weight (6.8 g instead of the 40 g normal for 20 gestational weeks); (3) skull malformations with a strongly flattened skull cap, a malformed skull base

with absence of the crista galli and one frontal bone, and absence of fonticuli; (4) lateral cheilognatho-palataschizis on the right; (5) low-positioned, malformed ears; (6) short neck with slight webbing; and (7) skeletal malformations (immature skeleton, fusion of some ribs, open spine at the T11 level. Chromosomal analysis showed a normal 46XX karyotype. The rostral end of the mesencephalon was nodular and rounded (Fig. 9.35d). Microscopically, disorganized neuronal tissue was present without recognizable structures.

This case was kindly provided by Gerard van Noort (Laboratory for Pathology East-Netherlands, Enschede, The Netherlands).

References

Kakita A, Hayashi S, Arakawa M, Takahashi H (2001) Aprosencephaly: Histopathologic features of the rudimentary forebrain and retina. Acta Neuropathol (Berl) 102:110–116

Sergi C, Schmitt HP (2000) The vesicular forebrain (pseudo-aprosencephaly): A missing link in the teratogenic spectrum of the defective brain anlage and its discrimination from aprosencephaly. Acta Neuropathol (Berl) 99:277–284

Fig. 9.35 Aprosencephaly found in a 20-week-old fetus: **a** overview of fetus; **b** craniofacial malformations; **c** malformed skull base with absent crista galli and only one frontal bone; **d** dorsal view of the CNS. The rostral end of the mesencephalon is nodular and rounded. (Courtesy Gerard van Noort, Enschede)

ed disorders are septo-optic dysplasia (de Morsier syndrome) and isolated arhinencephaly as found in disorders such as Kallmann syndrome.

9.7.1   Aprosencephaly

Aprosencephaly and *atelencephaly* are extremely rare CNS defects. Several cases were studied neuropathologically (Garcia and Duncan 1977; Siebert et al. 1986, 1987; Lurie et al. 1979, 1980; Towfighi et al. 1987; Kim et al. 1990; Harris et al. 1994; Ippel et al. 1998; Sergi and Schmitt 2000; Kakita et al. 2001; Clinical Case 9.6). In *aprosencephaly*, the forebrain structures derived from the telencephalon (the cerebral cortex, the basal ganglia and the hypothalamus) and the diencephalon (the eyes and the thalamus) are absent or rudimentary. In *atelencephaly*, the thalami are developed and some residual hemispheres may be found. The aetiology of aprosencephaly and atelencephaly remains controversial. Some cases may be due to a destructive, encephaloclastic process (Norman et al. 1995), but could also be primary malformations (Leech and Shuman 1986; Sergi and Schmitt 2000). Sergi and Schmitt (2000) described two cases of a vesicular forebrain (*pseudo-aprosencephaly*), a possible missing link in the teratogenic spectrum of defective forebrain anlage (Table 9.9). Which genes are involved is unknown, but *OTX2* is apparently not involved (Florell et al. 1996). The case of aprosencephaly described by Kakita et al. (2001) did not show evidence of destruction. In their case, a male fetus of 20 weeks of gestation, the prosencephalon was extremely small and was replaced by a solid, cylindrical mass without hemispheric cleavage or a ventricle. The most rostral part of the CNS penetrated through a midsagittal ectopic canal in the sphenoid bone, comparable to a case of cyclopia (Kakita et al. 1997).

9.7.2   Holoprosencephaly

Holoprosencephaly (*HPE*) is usually described as a developmental field defect of impaired midline cleavage of the embryonic forebrain (DeMyer and Zeman 1963; Probst 1979; DeMyer 1987; Cohen 1989a, b; Siebert et al. 1990; Cohen and Sulik 1992; Norman et al. 1995; Golden 1998; Muenke and Beachy 2000, 2001; Roessler and Muenke 2001; Sarnat and Flores-Sarnat 2001; Cohen and Shiota 2002). HPE is frequently associated with specific craniofacial anomalies, including midline facial defects, cyclopia and nasal malformations (Chap. 5). Its incidence in live-born children with normal chromosomes has been estimated to be 0.48–0.88 per 10,000. In contrast, the rate among human abortuses was estimated at 40 per 10,000, indicating a very high rate of embryonic and fetal loss

(Matsunaga and Shiota 1977; Shiota 1993). In a large epidemiologic study in a Californian population, Croen et al. (1996) observed an overall prevalence of 1.2 per 10,000 live births and fetal deaths, whereas the prevalence for live births was 0.88 per 10,000.

HPE is aetiologically very heterogeneous. It can be associated with chromosomal abnormalities, single gene mutations, polygenic mechanisms and environmental factors such as diabetes mellitus and alcohol (Warkany 1971; Cohen 1989a; Cohen and Sulik 1992; Norman et al. 1995; Muenke and Beachy 2001; Cohen and Shiota 2002; Edison and Muenke 2003; Table 5.4). Cytogenetic studies of HPE patients suggest at least 12 putative loci (HPE1–HPE12) on 11 different chromosomes (Roessler and Muenke 1998; Nanni et al. 2000; Table 9.10), giving rise to about 15–20% of all cases of HPE (Cohen and Shiota 2002). Several HPE genes have been identified: *SHH* (also known as HPE3: Belloni et al. 1996; Roessler et al. 1996; Nanni et al. 1999), *SIX3* (HPE2: Wallis et al. 1999), *ZIC2* (HPE5: Brown et al. 1998), *TGIF* (HPE4: Gripp et al. 1998), *Patched/PTCH* (Ming and Muenke 1998; Ming et al. 2002), *GLI2* (Roessler et al. 2003) and *DHCR7* (Kelley et al. 1996). Their possible interactions with normal signalling pathways and cholesterol biosynthesis is shown in Fig. 9.36. *SHH* mutations account for about 17% of familial cases, and 3.7% of all HPE cases (Cohen and Shiota 2002). Clinical manifestations of HPE are quite variable among patients and even among family members who carry a defined type of gene mutation (Ming and Muenke 2002; Edison and Muenke 2003).

HPE is a developmental malformation sequence in which impaired midline cleavage of the forebrain up to no cleavage (a *holosphere*) is the basic feature. The more severe forms can be diagnosed prenatally by ultrasound (Blaas et al. 2002). In a majority of cases, this non-cleavage involves the basal ganglia, thalamus and hypothalamus. *Diabetes insipidus* occurs in about 67% of children with HPE (Sarnat and Flores-Sarnat 2001), but other endocrine disorders involving the anterior pituitary occur less commonly and usually in addition to diabetes insipidus. The hypothalamus shows the highest incidence of non-cleavage of subcortical structures in HPE (Simon et al. 2000). The involvement of the basal ganglia may lead to generalized chorea (Louis et al. 1995). The most severe, complete or alobar type, and the incomplete forms, including the semilobar type and the least severe lobar type, represent degrees of severity rather than clearly distinguishable forms of this disorder. Together with the associated craniofacial malformations they constitute the HPE sequence (Cohen and Sulik 1992). The craniofacial malformations also vary in extent from the most severe being cyclopia with a single proboscis located above the midline eye to mild facial abnormalities. In general, the "face pre-
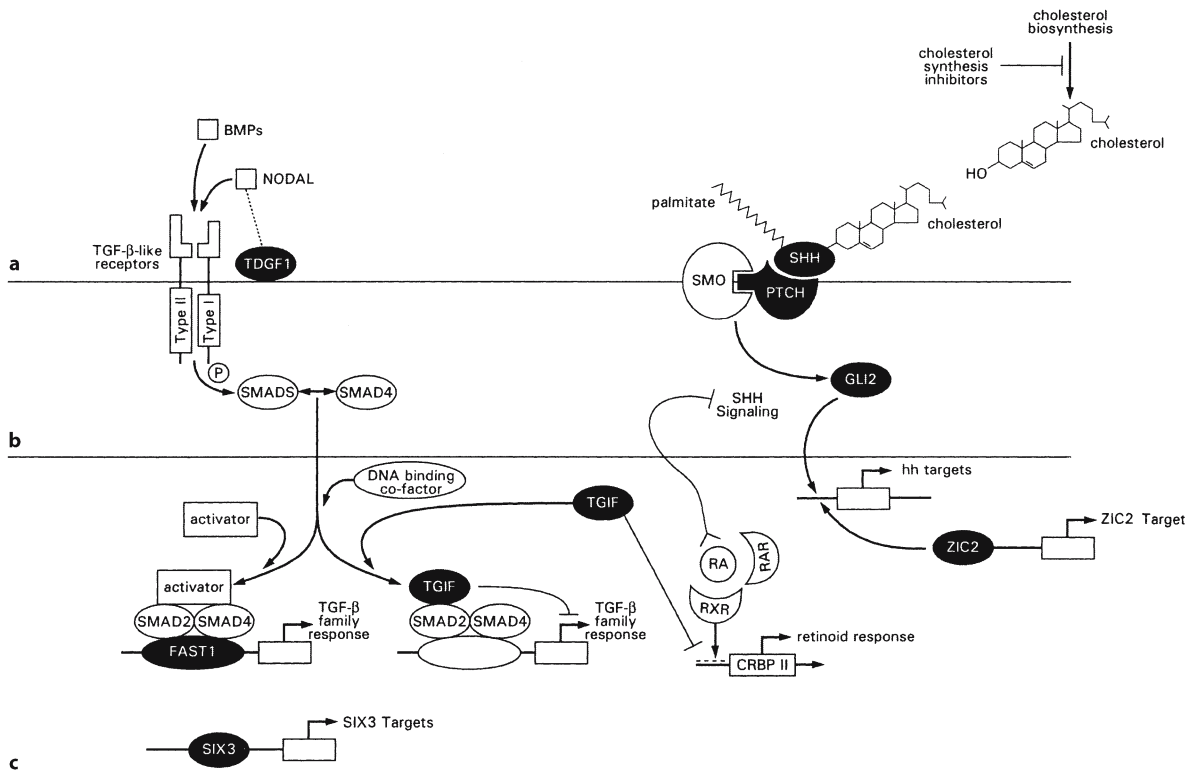
Fig. 9.36 Association of holoprosencephaly with abnormal function of signalling pathways, cholesterol biosynthesis and various transcription factors in **a** extracellular space, **b** cytoplasm and **c** nucleus (after Edison and Muenke 2003)

Table 9.10 Causative genes of human holoprosencephaly (after Roessler and Muenke 1998; Muenke and Beachy 2001)

Disorders	Loci	Genes	Functions
HPE1	21q22.3	?	
HPE2	2p21	*SIX3*	Homeoprotein important for development of eye and forebrain
HPE3	7q36	*SHH*	Secretory signalling molecule critical for embryonic development
HPE4	18pter-q11	*TGIF*	Homeoprotein interacting with Smad2
HPE5	13q32	*ZIC2*	Zinc-finger transcription factor important for neurulation
HPE6	3p24-pter	*ZIC1-ZIC4?*	
HPE7	13q12-14	*Forkhead homologue?*	
HPE8	14q13	*Thyroid transcription factor-1?*	
HPE9	20q13	*Homologue to mouse coloboma?*	
HPE10	1q42-qter	?	
HPE11	5p	?	
HPE12	6q26-qter	?	
	9q22.3	*PTCH*	Receptor for SHH
Smith–Lemli–Opitz syndrome	11q13	*DHCR7*	Defect in 7-dehydrocholesterol, an enzyme for cholesterol biosynthesis

dicts the brain" (DeMyer et al. 1964). It should be emphasized, however, that in 10–20 % of the holoprosencephalies no or only minor craniofacial abnormalities are present (Chap. 5), and that severe HPE may be present in the absence of obvious facial anomalies. Some imaging and neuropathological data on HPE patients are shown in Figs. 9.37–9.41. Embryonic data from the Kyoto Embryological Collection are
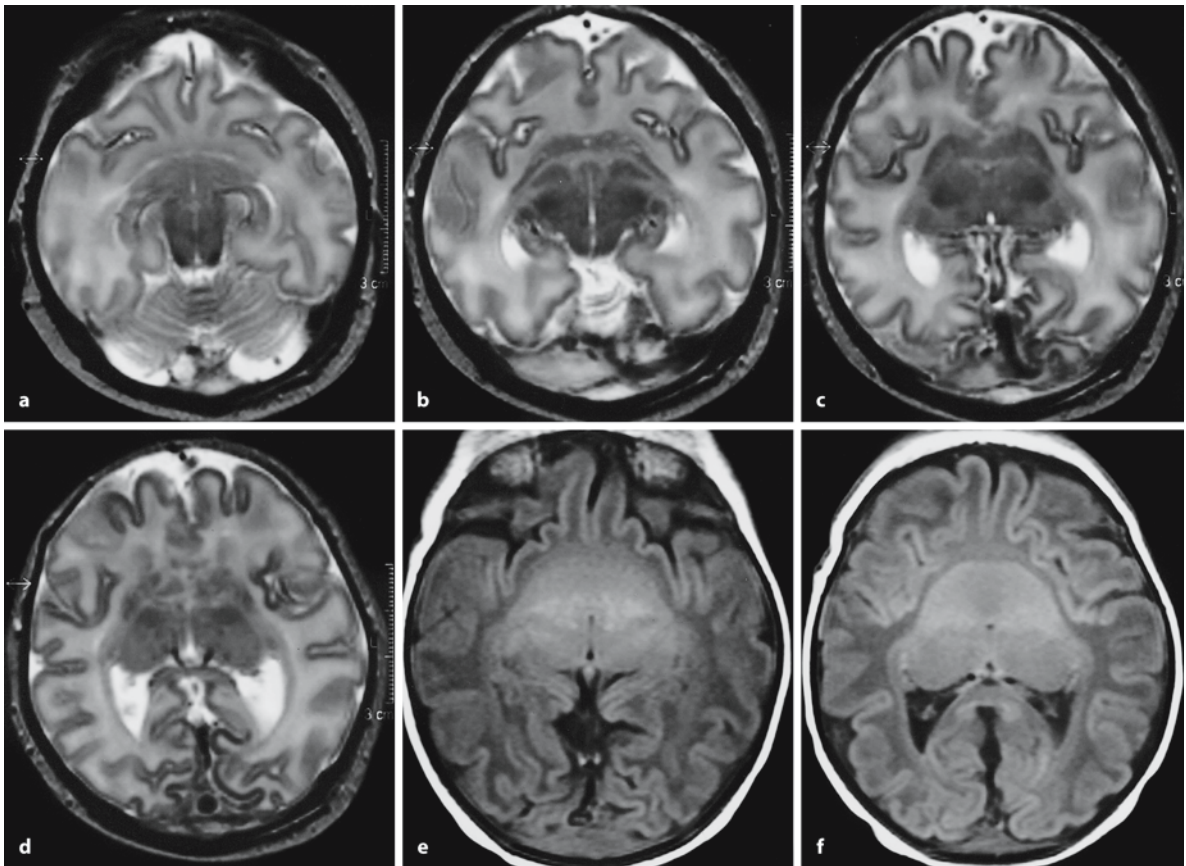
Fig. 9.37 Axial T2-weighted images of microcephalic new-borns with holoprosencephaly. **a**–**c** Lobar holoprosencephaly; note incomplete formation of interhemispheric fissure and cerebral falx and lack of sulci in the frontal lobes; the thalami are separated by a normal third ventricle; in **a**, at the *top* an un-paired anterior cerebral artery can be seen. **d**–**f** Fluid attenuat-ed inversion recovery images of a semilobar holoprosen-cephaly case, in which the incomplete separation of the cere-bral hemispheres is more severe. Rostrally, midline structures are absent, and basal ganglia and thalami are not separated. Posteriorly, the callosal splenium is present (**f**). (Courtesy Berit Verbist, Leiden)
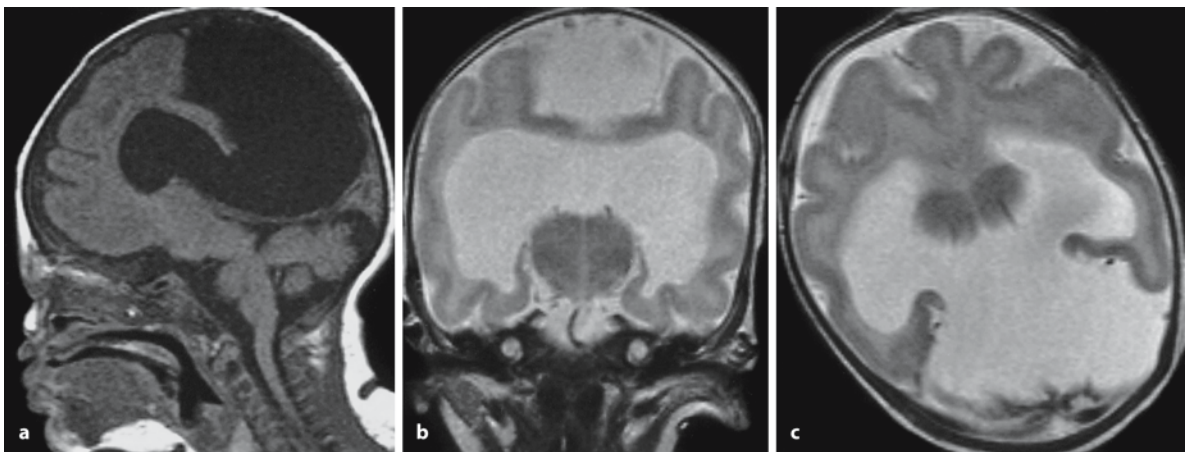
Fig. 9.38 Sagittal T1 (**a**) and coronal (**b**) and axial (**c**) T2-weighted images of a semilobar holoprosencephaly with a dorsal sac in a neonate. The thalami are separated. (Courtesy Ton van der Vliet, Nijmegen)

Fig. 9.39 Craniofacial malformations in cases of holoprosencephaly: **a** a female fetus of 26 weeks of gestation; **b** a female born at 34 weeks of gestation, showing a single nasal opening and choanal atresia; **c** a male fetus of 24 weeks of gestation with cyclopia and a proboscis; **d** a fetus with cyclopia and a proboscis; **e** a female fetus, 39 weeks of gestation, showing a single nasal opening; **f** a fetus of approximately 30 weeks of gestation. Examples of their brain malformations are shown in Fig. 9.40. (From the Department of Neuropathology, Medizinische Hochschule Hannover; courtesy Akira Hori)

shown in Figs. 9.42 and 9.43 (Yamada et al. 2004). The severity of the malformations has an anterior-to-posterior gradient, with the anterior portions being the least well formed (Cohen 1989b; Norman et al. 1995; Golden 1998; Simon et al. 2000). The **gyral pattern** of the posterior cerebrum more closely resembles the normal gyral pattern than that of the anterior cerebrum (Barkovich et al. 2002). Most HPE patients have normal cortical thickness (Barkovich et al. 2002). Syl-

vian fissures were displaced further rostrally and medially as HPE became more severe, until in the most severe cases, no Sylvian fissures could be identified at all. These data corroborate Yakovlev's (1959) cytoarchitectonic analysis of the cerebral cortex of alobar and semilobar cases of HPE. The typical motor cortex was found in the cortex of the anterior midline. The **arterial pattern** in HPE brains varies (van Overbeeke 1991; van Overbeeke et al. 1994). The rostral part of
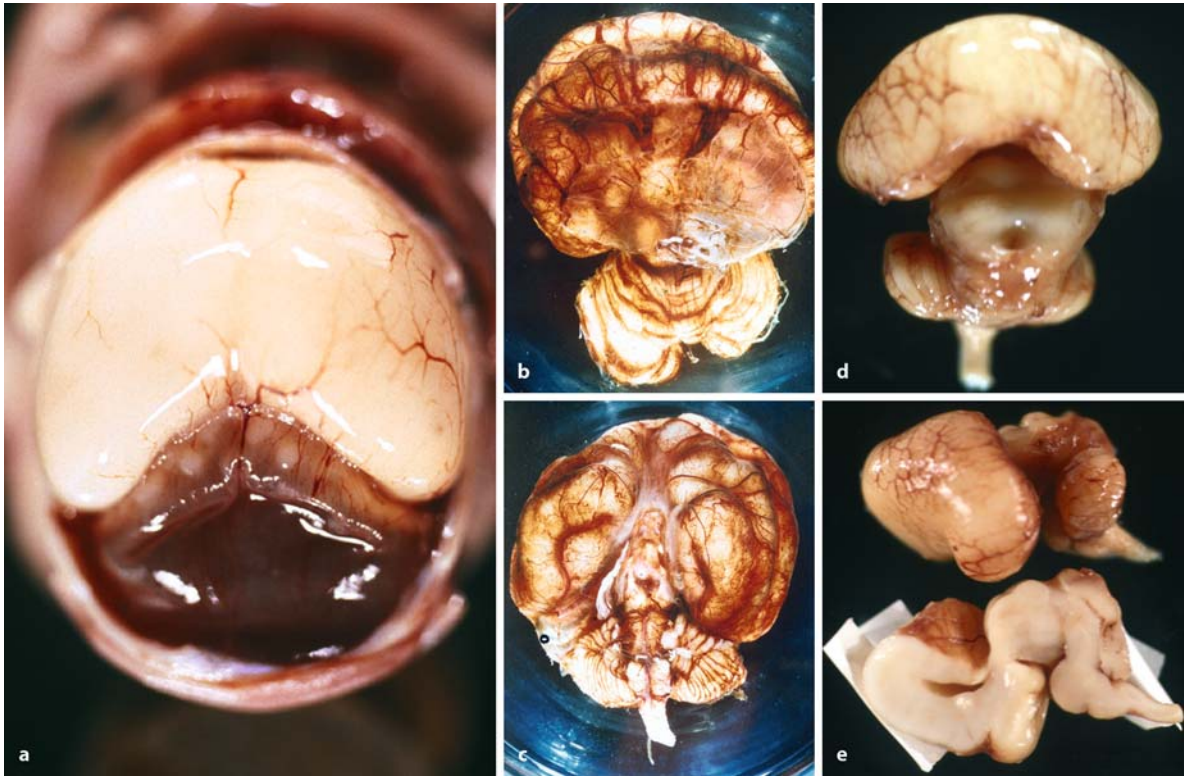
Fig. 9.40 Selection of neuropathological data in fetuses with holoprosencephaly: **a** large dorsal sac in situ, which is collapsed artificially at autopsy; **b**, **c** dorsal and basal views of the brain in the case shown in Fig. 9.39b; **d**, **e** dorsal (**d**) and lateral (**e**; *top*) views, and a median section (**e**; *bottom*) of the case shown in Fig. 9.39c. (From the Department of Neuropathology, Medizinische Hochschule Hannover; courtesy Akira Hori)

the circle of Willis is usually absent. In two cases with incomplete HPE, both internal carotid arteries contributed to the vascularization of the cerebral cortex. In six other specimens with incomplete and complete forms of HPE, one of the internal carotids supplied the largest part of the brain.

Cyclopia has been known since ancient times through the figure of the cyclopean shepherd Polyphemos in Homer's *Odyssey* (around 800 BC). Modern knowledge of cyclopia and prosencephalies originates from the three-volume treatise on teratology by Geoffroy Saint-Hilaire (1832–1837), who introduced the terms ethmocephaly and cebocephaly. In 1882, Kundrat extended these observations and distinguished six types of forebrain malformations as arhinencephaly. Much of our present knowledge on HPE dates back to the work of DeMyer and Zeman (DeMyer and Zeman 1963; DeMyer et al. 1964; DeMyer 1987), whose practical subdivision into alobar, semilobar and lobar types is commonly used. In the *alobar form*, only one single ventricle (a holosphere) of variable size is present without interhemispheric diversion. Posteriorly, a membrane usually closes the

holosphere. This membrane is actually the posterior roof of the single ventricle (Golden 1998) and may bulge dorsally to form a fluid-filled 'dorsal sac' or cyst (Fig. 9.38). The dorsal cyst may originate as a dilated suprapineal recess of the third ventricle (Sarnat and Flores-Sarnat 2001; Simon et al. 2001). Probst (1979) based his subdivision of prosencephalies on the presence and extent of the dorsal sac (Table 9.9). Siebert et al. (1990) proposed a simpler subdivision of the holoprosencephalies into *complete* and *incomplete forms*. The thalami and corpora striata are undivided. The olfactory bulbs and tracts and the corpus callosum are always absent. In the *semilobar type*, rudimentary cerebral lobes with an interhemispheric posterior fissure and a rudimentary corpus callosum may be present. The olfactory bulbs and tracts are absent or hypoplastic. In the least severe, *lobar type*, a distinct interhemispheric fissure is present with some midline continuity. The olfactory bulbs and tracts may vary from normal to absent. Midline separation of the thalami and corpora striata may be incomplete. An additional form is known as the *middle interhemispheric variant* or syntelen-

Clinical Case 9.7
Middle Interhemispheric Variant of Holoprosencephaly

The middle interhemispheric variant of holoprosencephaly (MIH) is a rare malformation in which the cerebral hemispheres fail to divide in the posterior frontal and parietal regions (Barkovich and Quint 1993; Simon et al. 2002). Autopsy was done in only a few cases (Pulitzer et al. 2004; see Case Report).

Case Report. The patient was born at 42 weeks of gestation as the fourth child of a 36-year-old healthy mother, who had already had three healthy children. There were no previous obstetrical problems. Some intrauterine growth retardation was apparent. Birth was normal with Apgar scores of 9/10. Birth weight was 3,345 g and crown–heel length was 49 cm. There were microcephaly, a midface hypoplasia, bilateral cheilognathopalatoschisis (Fig. 9.41a) and panhypopituitarism. Colobomas were found in both eyes. Ultrasound examination of the head suggested holoprosencephaly. A falx was only apparent in the frontal part of the head. MRI could not be performed anymore owing to the rapid deterioration of the child. The child died at day 8 owing to necrotizing enterocolitis with sepsis.

At autopsy, the necrotizing enterocolitis and a complicating acute respiratory distress syndrome were found. Brain weight was 300 g (normal range 420±33 g). The brain showed a gyral pattern that was somewhat less developed than normal with underdeveloped frontal lobes. From above, the presence of two hemispheres separated over their whole length was suggested (Fig. 9.41b). The olfactory bulbs and the pituitary gland were absent. The optic nerves were smaller than normal. In frontal sections (Fig. 9.41c–e), there was no subdivision of the cerebrum into two hemispheres in the rostral half of the brain. A gyrus in the depth of a midsagittal sulcus crossing from left to right gave the false impression of two hemispheres rostrally. Two hemispheres were evident from the level of the globus pallidus caudalwards. At that level a corpus callosum could be seen as well as a small third ventricle. In the posterior half of the brain the two hemispheres looked quite normal. There were no structural abnormalities in the brain stem and cerebellum, except for some hypoplasia of the pyramids.

References

Barkovich AJ, Quint DJ (1993) Middle interhemispheric fusion: an unusual variant of holoprosencephaly. AJNR Am J Neuroradiol 14:431–440

Pulitzer SB, Simon EM, Crombleholme TM, Golden JA (2004) Prenatal MR findings of the middle interhemispheric variant of holoprosencephaly. AJNR Am J Neuroradiol 25:1034–1036

Simon EM, Hevner RF, Pinter JD, Clegg NJ, Delgado M, Kinsman SL, Hahn JS, Barkovich AJ (2002) The middle interhemispheriv variant of holoprosencephaly. AJNR Am J Neuroradiol 23:151–155
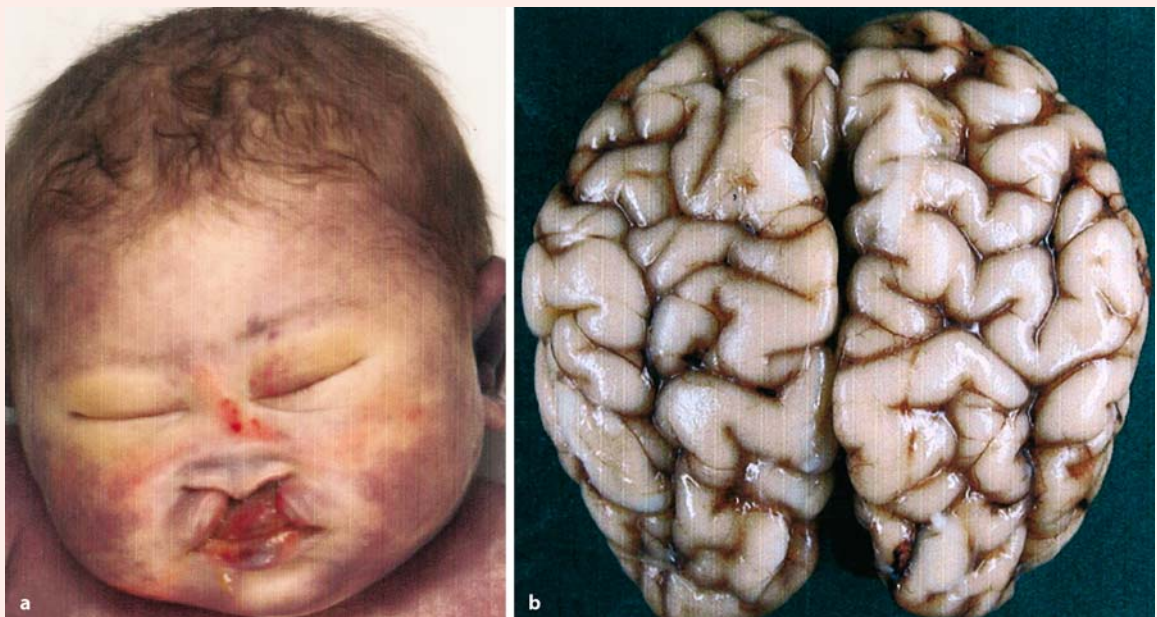
Fig. 9.41 Midline, interhemispheric variant of holoprosencephaly: **a** craniofacial malformations; **b** dorsal view of the brain
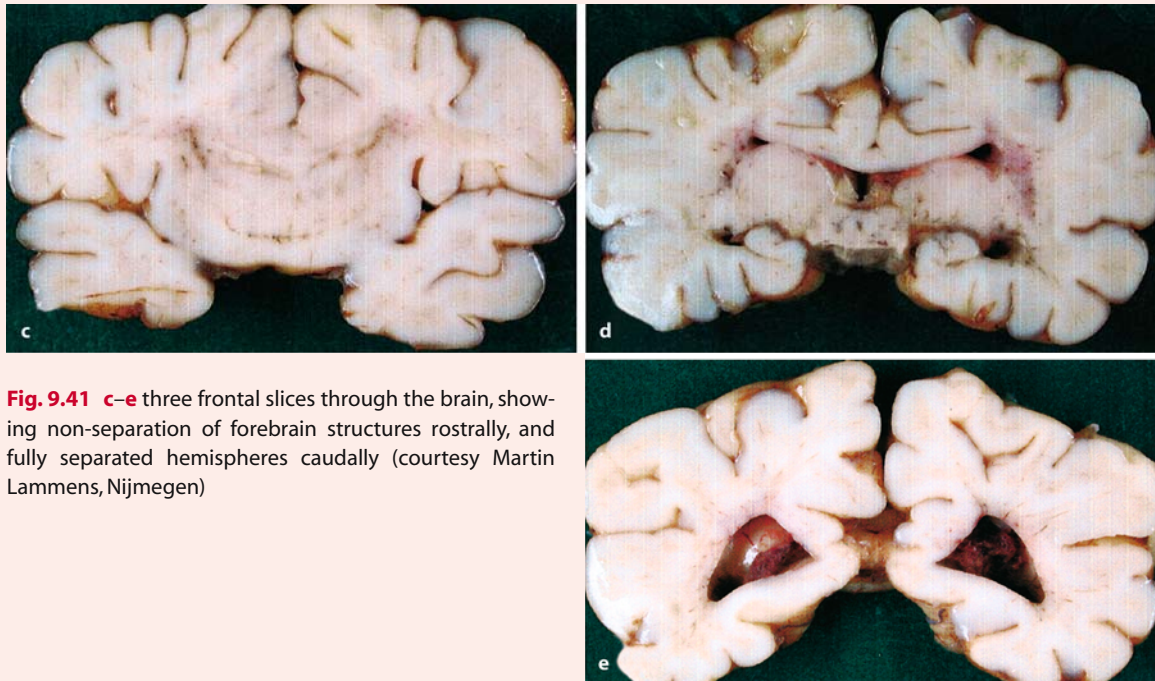
Fig. 9.41 c–e three frontal slices through the brain, showing non-separation of forebrain structures rostrally, and fully separated hemispheres caudally (courtesy Martin Lammens, Nijmegen)

cephaly (Barkovich and Quint 1993; Lewis et al. 2002; Simon et al. 2002; Pulitzer et al. 2004; Clinical Case 9.7). In this variant, the posterior and anterior portions of the falx cerebri are present, but its midportion is absent near the frontoparietal convexity. Here, the cerebral hemispheres 'fuse' in the midline, mainly in the posterior frontal lobes. The middle part of the corpus callosum may be misformed, the septum pellucidum is absent and the olfactory bulbs and tracts may show variable deficiency. This anomaly may best be explained by a focal paucity of the primitive dorsal meninx leading to failure of induction within this small area (Barkovich 2000).

Part of the phenotypic variability in human HPE as found in the Kyoto Embryological Collection is illustrated in Fig. 9.42 (Yamada et al. 2004). Other embryological cases were described by Mall (1917), Vermeij-Keers (1987; Fig. 5.17) and Müller and O'Rahilly (1989c). Embryos after Carnegie stage 18 were classified into complete (true) cyclopia (Fig. 9.43), synophthalmia (partially fused eyes in a single eye fissure), closely apposed eyes (possible forerunners of ethmocephaly and cebocephaly) and milder forms of HPE with median cleft lip (premaxillary agenesis). At Carnegie stages 13–17, when facial morphogenesis is not completed, HPE embryos showed some facial characteristics which are specific to these stages and which are different from those in older HPE embryos. The midline structures of the brain, including the pituitary gland, were lacking or seriously hypoplastic. Complete cyclopia was found in two cases after CS18 but none was found at earlier stages.
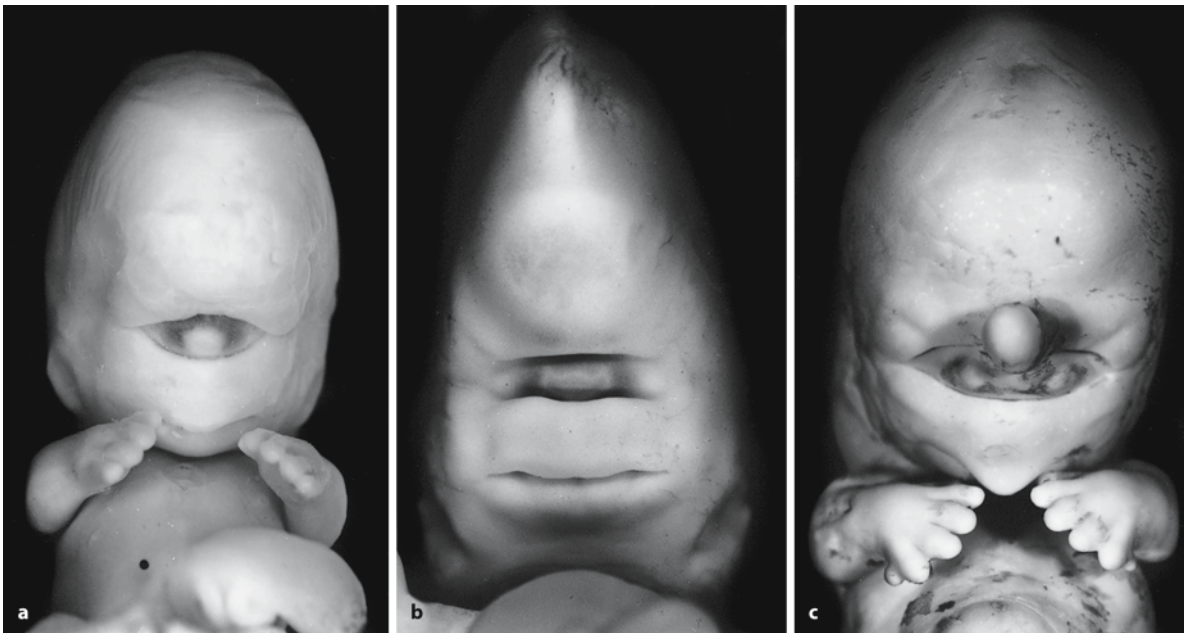
Fig. 9.42 Holoprosencephaly in human embryos: **a**, **b** complete, true cyclopia in 7-week-old (**a**) and 6-week-old (**b**) embryos; **c** synophthalmia (partially fused eyes in a single eye fissure) in a 7-week-old embryo (from Yamada et al. 2004, with permission; courtesy Shigehito Yamada, Kyoto)
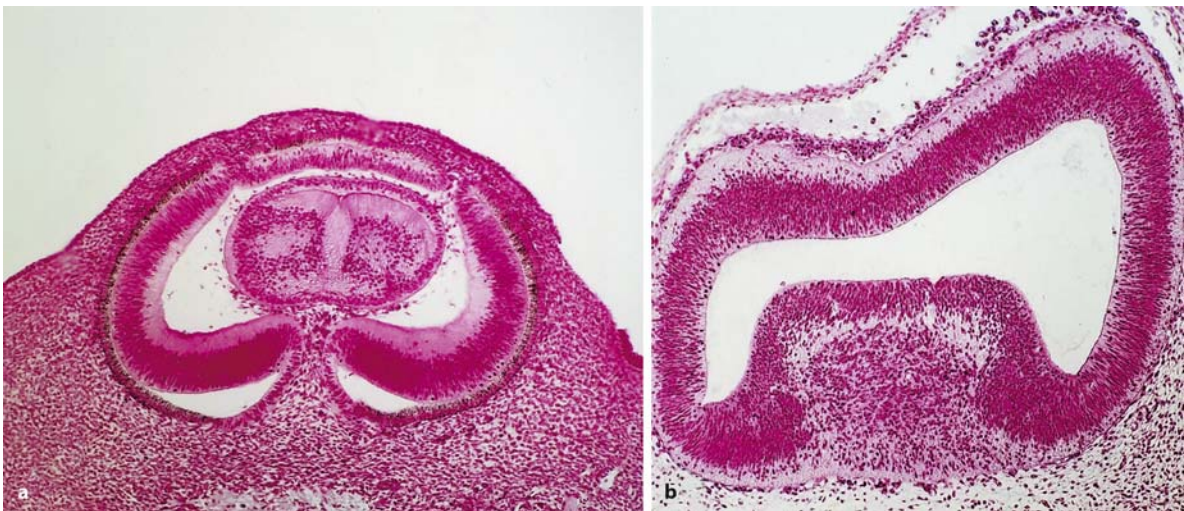
Fig. 9.43 Cyclopia (**a**) and non-separated thalami (**b**) in the embryo with holoprosencephaly shown in Fig. 9.42a (from Yamada et al. 2004, with permission; courtesy Shigehito Yamada, Kyoto)

9.7.3   Septo-optic Dysplasia

Primary absence of the *septum pellucidum* is rarely an isolated finding (Fig. 9.44) and is frequently associated with other malformations such as HPE, agenesis of the corpus callosum and septo-optic dysplasia (Bruyn 1977; Friede 1989). It may be secondary to head trauma (Corsellis et al. 1973). De Morsier (1956) emphasized the combination of optic atrophy and defects of the septum pellucidum. The cases described as *septo-optic dysplasia* (*de Morsier syndrome*) form a rather heterogeneous group of disorders (Roessmann et al. 1987; Barkovich and Norman 1989; Barkovich et al. 1989; Friede 1989; Norman et al. 1995; Clinical Case 9.8). The clinical manifestations include a characteristic triad (Morishima and Aranoff 1986; Willnow et al. 1996; Hellström et al. 2000; Miller et al. 2000): (1) hypopituitarism, ranging from panhypopituitarism to insufficiency of isolated hormones; (2) aplasia of the optic disks that present with amblyopia or hemianopia; and (3) absence of the septum pellucidum. Aetiological factors may be viral infections, gestational diabetes, vascular disruption, drug toxicity and fetal alcohol syndrome (Hellström et al. 2000; Miller et al. 2000). The homeobox gene *HESX1* is implicated in a familial form of septo-optic dysplasia (Dattani et al. 1998, 1999; Brickman et al. 2001; Thomas et al. 2001).

9.7.4   Isolated Arhinencephaly

Olfactory hypoplasia and *isolated absence* of the *olfactory bulbs* may occur without other cerebral malformations as an accidental finding at autopsy (Norman et al. 1995; Fig. 9.46). In 1856, Maestre de San Juan first observed the association of hypogonadism with olfactory system abnormalities. Isolated absence of the olfactory bulb and tract can be transmitted as a single gene defect, especially in Kallmann syndrome. *Kallmann syndrome* (hypogonadotropic hypogonadism; Kallmann et al. 1944) is inherited in various ways, as an autosomal dominant trait (KAL2) with variable penetrance, and less commonly as an autosomal recessive (KAL3) or X-linked (KAL1) disorder (Cohen 1989a; Ballabio and Rugarli 2001; Oliveira et al. 2001). It is the most common form of isolated gonadotropin deficiency due to a migration disorder. Olfactory cells (Fig. 9.47) and GnRH-producing cells in the hypothalamus fail to migrate along their normal pathway from the developing olfactory placode (Schwanzel-Fukuda and Pfaff 1989; Schwanzel-Fukuda et al. 1989, 1996; Wray et al. 1989 a, b). The gene responsible for the X-linked form (*KAL1*) encodes an extracellular matrix protein (anosmin-1) that is expressed in the olfactory bulb (Franco et al. 1991; Legouis et al. 1991; Rugarli et al. 1993; Izumi et al. 1999, 2001). It has been suggested that anosmin-1 is involved in terminal stages of olfactory axon guidance to the bulb and that olfactory bulb hypoplasia or aplasia in Kallmann syndrome is secondary to lack of innervation (Hardelin et al. 1999; Rugarli 1999; Ballabio and Rugarli 2001; Hardelin 2001). The most pertinent findings in Kallmann syndrome are abnormalities of the olfactory system such as hypoplasia or aplasia of the olfactory bulbs, and hypoplasia of the anterior aspect of the olfactory sulci (Truwit et al. 1993; Quinton et al. 1996). Recently, the *KAL2* gene was identified (Dode et al. 2003). Mutations in the *FGFR1* gene appear to be responsible for the autosomal dominant trait of Kallmann syndrome.
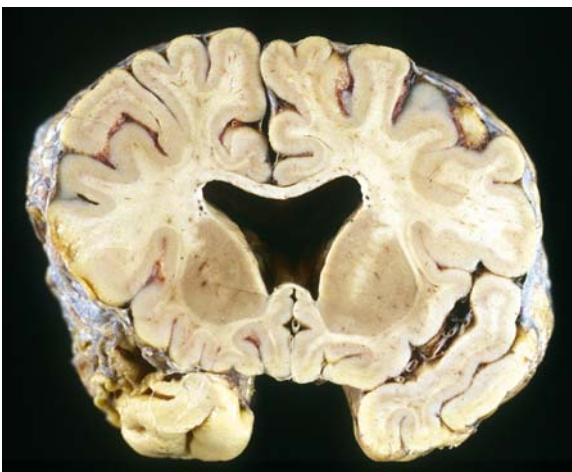
Fig. 9.44 Isolated absence of the septum pellucidum in a 42-year-old man with brain contusion and internal hydrocephalus. Note the fornices on the ventricular floor. (From the Department of Neuropathology, Medizinische Hochschule Hannover; courtesy Akira Hori)

Clinical Case 9.8
Septo-optic Dysplasia

Septo-optic dysplasia is a developmental disorder of midline structures characterized by unilateral or bilateral hypoplasia of the optic nerves, tracts and chiasm, and by the absence of the septum pellucidum, first described by de Morsier (1956). The syndrome is not rare and is highly variable (Morishima and Aranoff 1986; Roessmann et al. 1987; Miller et al. 2000; see Case Report).

Case Report. The infant was born after an uncomplicated pregnancy of her 33-year-old mother. Multiple malformations were noted at birth, including bilateral cleft lips and palate, ulnar deviation of the hands, polydactyly and frontal synostosis. The infant was septic from the second day of life. She died at the age of 1 week. The cause of death appeared to be peritonitis due to perforated colonic ulcers and bilateral bronchopneumonia. The fixed brain weighed 287 g. The olfactory nerves were absent. The right eye and optic nerve were smaller than the left eye and optic nerve, and both optic tracts were hypoplastic. The cerebellum was small. Coronal sections revealed an abnormal mass in the region of the genu of the corpus callosum that extended down to the third ventricle (Fig. 9.45). The walls of the third ventricle were fused at the base. Microscopic examination revealed marked retinal dysplasia. The lateral geniculate nuclei were reduced in size and showed no lamination. The tumour-like mass in the place of the corpus callosum consisted of a mixture of immature grey and white matter. Bundles of fibres, likely fornix fibres, were seen dorsal and ventral to the corpus callosum. Pronounced glial heterotopia were present at the base of
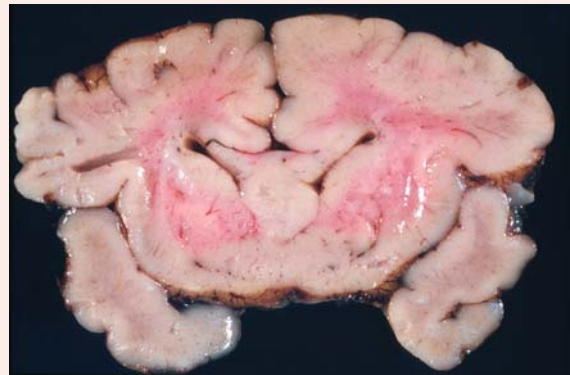
Fig. 9.45 Septo-optic dysplasia (from Roessmann et al. 1987, with permission; courtesy Akira Hori, Toyohashi)

the brain. The medullary pyramids were small, the pyramidal crossing was incomplete and corticospinal fibres in the spinal cord were found predominantly in the anterior column.

References

de Morsier G (1956) Etudes sur les dysraphies crânio-encéphaliques. III. Agénésie du septum pellucidum avec malformation du tractus optique. La dysplasie septo-optique. Schweiz Arch Neurol Psychiatr 77:267–292

Miller SP, Shevell MI, Patenaude Y, Poulin C, O'Gorman AM (2000) Septo-optic dysplasia plus: A spectrum of malformations of cortical development. Neurology 54:1701–1703

Morishima A, Aranoff GS (1986) Syndrome of septo-optic dysplasia: The clinical spectrum. Brain Dev 8:233–239

Roesmann U, Velasco ME, Small EJ, Hori A (1987) Neuropathology of "septo-optic dysplasia" (de Morsier syndrome) with immunohistochemical studies of the hypothalamus and pituitary gland. J Neuropathol Exp Neurol 46:597–608

Fig. 9.46 Isolated olfactory bulb absence found as an incidental finding at autopsy in a 9-day-old infant who died after cardiac arrest. Tegmental necrosis of the brain stem and multicystic encephalopathy were found. On the right frontal base, a rudimentary olfactory structure is present. (From the Department of Neuropathology, Medizinische Hochschule Hannover; courtesy Akira Hori)
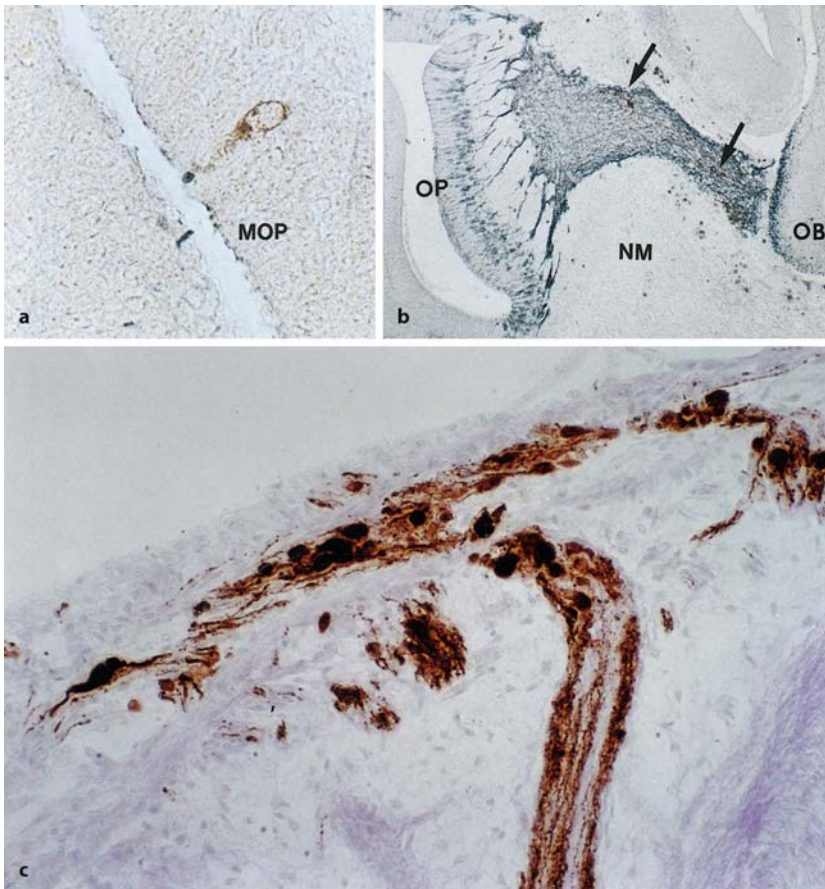
Fig. 9.47 Migration of human gonadotropin-releasing hormone (*GnRH*) expressing neurons: **a** a GnRH-immunoreactive cell in the epithelium of the medial olfactory pit (*MOP*); **b** a few GnRH-immuno-reactive cells (*arrows*) along the broad path of NCAM-immuno-reactive cell bodies and neurites, extending from the epithelium of the olfactory pit (*OP*) and forming an aggregate in the nasal mes-enchyme (*NM*) below the fore-brain and the developing olfacto-ry bulb (*OB*); **c** 19-week-old fetus with Kallmann syndrome. A large GnRH-immunoreactive branch of the terminal nerve is seen cours-ing upwards through a perforation of the cribiform plate. Clusters of GnRH-expressing neurons can be seen on the dorsal surface of the cribiform plate, where they remain. (**a**, **b** Reproduced with permission from Schwanzel-Fukuda et al. 1996, *J. Comp. Neurol.* 366:547–557; copyright 1996, Wiley-Liss Inc., a subsidiary of John Wiley & Sons, Inc.; **c** courtesy Marlene Schwanzel-Fukuda, New York)

9.8 Development and Developmental Disorders of the Basal Ganglia and the Amygdala

9.8.1 Development of the Basal Ganglia

The **basal ganglia** are a group of closely connected cell masses, forming a continuum, extending from the telencephalon to the midbrain tegmentum. This complex comprises the striatum (the nucleus cauda-tus and the putamen, largely separated by the inter-nal capsule), the globus pallidus, the subthalamic nu-cleus and the substantia nigra. In most non-primate mammals, the nucleus caudatus and the putamen are not clearly separated by an internal capsule and are known as the caudate–putamen complex. In pri-mates, the globus pallidus consists of external or lat-eral and internal or medial parts. In other mammals, the homologue of the internal segment is formed by the entopeduncular nucleus. The caudate nucleus, the putamen and the globus pallidus form the **dorsal part** of the **striatal complex**. Heimer and co-workers

(Heimer 1976; Heimer et al. 1982, 1991, 1997; Alheid et al. 1990) introduced the terms **ventral striatum** and **ventral pallidum** to include the limbic system into the basal ganglia. The nucleus accumbens, both cytoarchitectonically and histochemically closely resembling the caudate nucleus and the putamen, and the greater part of the olfactory tubercle form the ventral striatum (Fig. 9.48). The rostral part of the substantia innominata forms a ventral extension of the globus pallidus. The substantia innominata also contains the widely spread cholinergic basal nucleus of Meynert, the main source of cholinergic input to the cerebral cortex. The globus pallidus, the ventral pallidum and the substantia nigra are iron-rich areas of the brain as shown with Perl's di-aminobenzidine method (Switzer et al. 1982; Hill and Switzer 1984) and high-resolution MRI (Drayer et al. 1986).

The cerebral cortex, including its sensory and mo-tor fields, has extensive connections with the stria-tum that, via the globus pallidus and ventral thalam-ic nuclei, projects to the motor, premotor and pre-

Fig. 9.48 a–d Human basal forebrain showing the current subdivision of the basal ganglia and amygdala. Comparable structures are indicated in various colours. Transition areas are indicated as parts of the striatum, but do show some amygdaloid features. The *large dots* indicate the large, cholinergic cells of the basal nucleus of Meynert (*BM*). *ac* anterior commissure, *BL* basolateral amygdala, *BST* bed nucleus of the stria terminalis, *Cd* caudate nucleus, *Ce* central amygdala, *cho* chiasma opticum, *Cl* claustrum, *Db* diagonal band of Broca, *f* fornix, *GP* globus pallidus, *GPe* external part of globus pallidus, *GPi* internal part of globus pallidus, *Hip* hippocampus, *In* insula, *M* medial amygdala, *ot* optic tract, *Put* putamen, *S* septum, *Th* thalamus, *VP* ventral pallidum, *VS* ventral striatum. (After Heimer et al. 1991)
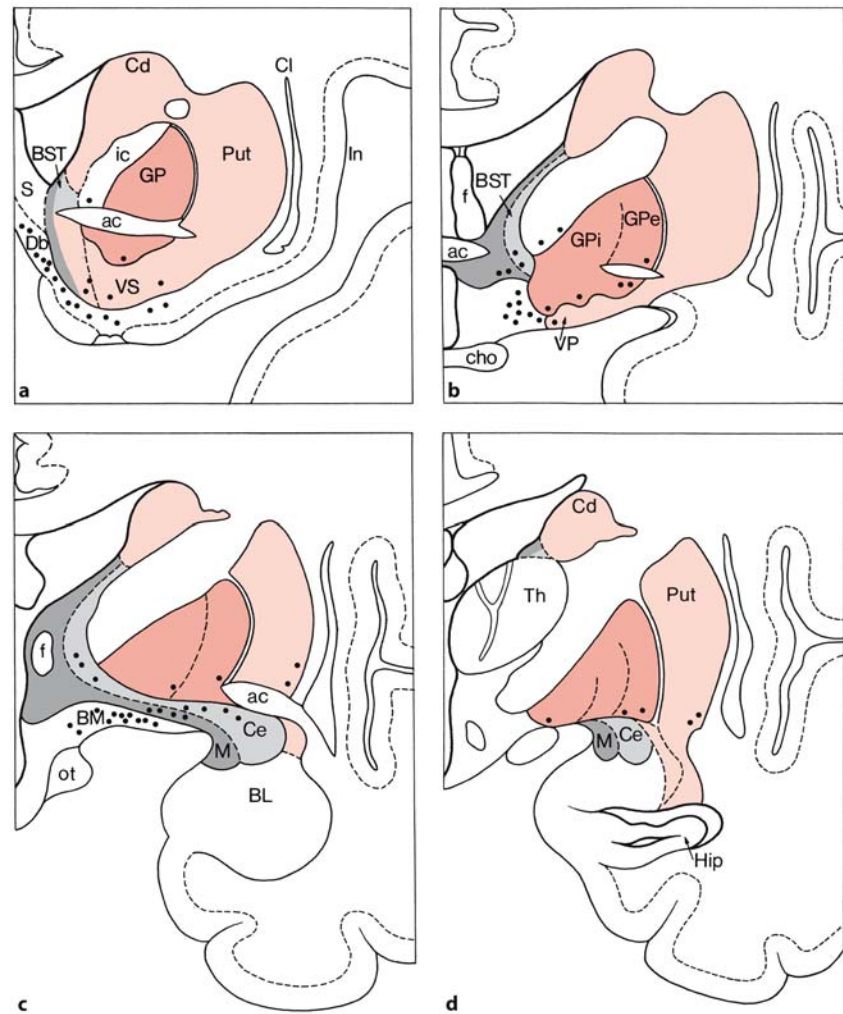
frontal areas of the cortex. This **cortico-striato-pallido-thalamocortical circuit** is known as the principal striatal circuit or loop and is involved in initiating motor activities stemming from cognitive activities (Figs. 9.49, 9.57 a). The ventral striatum and pallidum are included in a limbic striatal loop, involving the allocortex, the nucleus accumbens, the ventral pallidum, the mediodorsal thalamic nucleus, and prefrontal and limbic cortices. The ventral striatopallidum is involved in initiating movements in response to emotionally or motivationally powerful stimuli (Heimer et al. 1991, 1997; Nieuwenhuys 1996). Nearly all cortical areas in primates participate in a strip-like patterned corticostriatal projection (Kemp and Powell 1970). Input from the somatosensory and motor cortices is extensive, whereas that from the visual cortex is minimal. In the rhesus monkey, Künzle (1975) showed that the motor cortex projects almost exclusively, organized in patches and in a somatotopical pattern, to the putamen. A comparable pattern of termination was found for the primate somatosensory cortex (Künzle 1977). In contrast, associative areas of the prefrontal, temporal, parietal and anterior cingulate cortices appear to project almost exclusively to the monkey caudate nucleus (Kemp and Powell 1970; Goldman and Nauta 1977; Künzle 1978; Van Hoesen et al. 1981). The various areas of the association cortex in monkeys project to longitudinal territories that occupy restricted mediolateral domains of the striatum (Selemon and Goldman-Rakic 1985). Limbic regions, particularly the basolateral part of the amygdala, and allocortical (entorhinal, piriform and hippocampal) structures, project to the striosomes of the ventromedial part of the caudate nucleus and to the ventral striatum (Graybiel 1986; McGeorge and Faull 1989). These findings suggest that the caudate nucleus in primates is more closely related to complex and associative types of behaviour, whereas the putamen appears more directly involved in sensorimotor control. The segregation of influences from the association and sensorimotor cortices that exist in the caudate nucleus and the putamen, respectively, is not only preserved at pallidal levels, but is also maintained at nigral and thala-
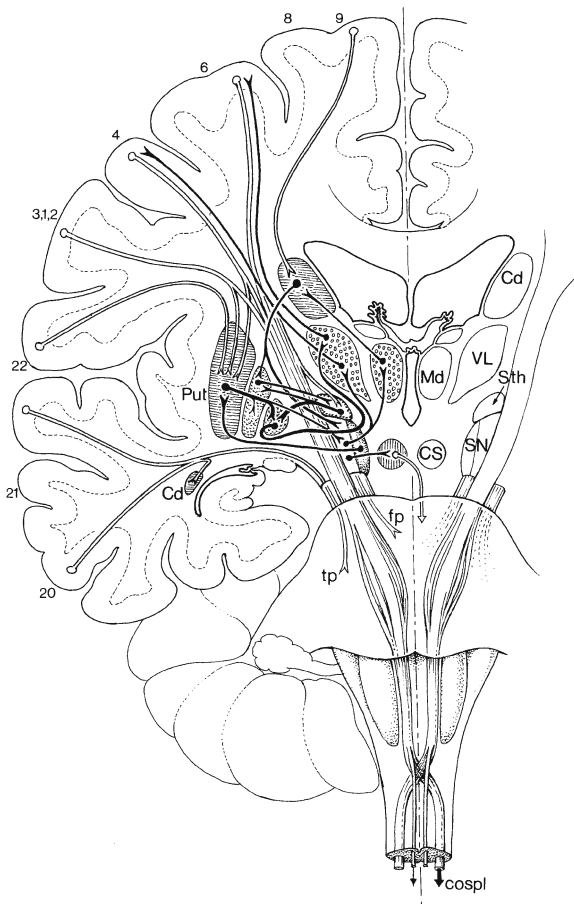
Fig. 9.49 Connectivity of the human basal ganglia. *Cd* caudate nucleus, *cospl* lateral corticospinal tract, *CS* colliculus superior, *fp* frontopontine tract, *Md* mediodorsal nucleus, *Put* putamen, *SN* substantia nigra, *Sth* subthalamic nucleus, *tp* temporopontine tract, *VL* ventrolateral nucleus

Fig. 9.50 Striosomes. Three adjacent sections through the brain of an E50–E52 kitten showing the precise match between tyrosine hydroxylase positive patches (**a**), clusters of [³H]thymidine-labelled neurons (**b**) and acetylcholinesterase-positive patches (**c**) in the caudate nucleus. *Cla* claustrum, *CN* caudate nucleus, *GE* ganglionic eminence, *NA* nucleus accumbens, *Olf T* olfactory tubercle, *P* putamen, *S* septum. (Reproduced with permission from Graybiel 1984, *Neuroscience* 13:1157–1187; copyright 1984, Elsevier)

mic levels (DeLong and Georgopoulos 1981; Alexander et al. 1986; Gerfen and Wilson 1996).

Compartmental organization of the mammalian striatum has been demonstrated with histochemistry (acetylcholinesterase staining) and immunohistochemistry (staining for tyrosine hydroxylase (TH), an enzyme necessary for dopamine biosynthesis, dopamine, enkephalins and other neuropeptides). Clustering of striatal neurons is obvious particularly in the developing mammalian striatum (Goldman-Rakic 1981, 1982; Graybiel 1984). The dopaminergic innervation of the striatum of young animals is organized in patches ('dopamine islands') as first shown with formaldehyde-induced catecholamine fluorescence (Olson et al. 1972; Tennyson et al. 1972), spatially corresponding with acetylcholinesterase-rich

patches (Graybiel et al. 1981). In adult animals, the distribution of TH or dopamine immunoreactivity does not show such prominent local inhomogeneities except in the ventral striatum–accumbens region (Graybiel et al. 1981; Graybiel 1984). With acetylcholinesterase staining, Graybiel and Ragsdale (1978) showed that within the otherwise acetylcholinesterase-rich striatal tissue (the **striatal matrix**) a mosaic of small zones of low acetylcholinesterase activity was present and called them '**striosomes**' (Fig. 9.50). In cats, during development the dopamine islands first correspond to acetylcholinesterase-rich patches of the immature striatum, but later in development to the acetylcholinesterase-poor striosomes (Graybiel 1984). A similar patchy arrangement of the striatum was shown in the developing human brain
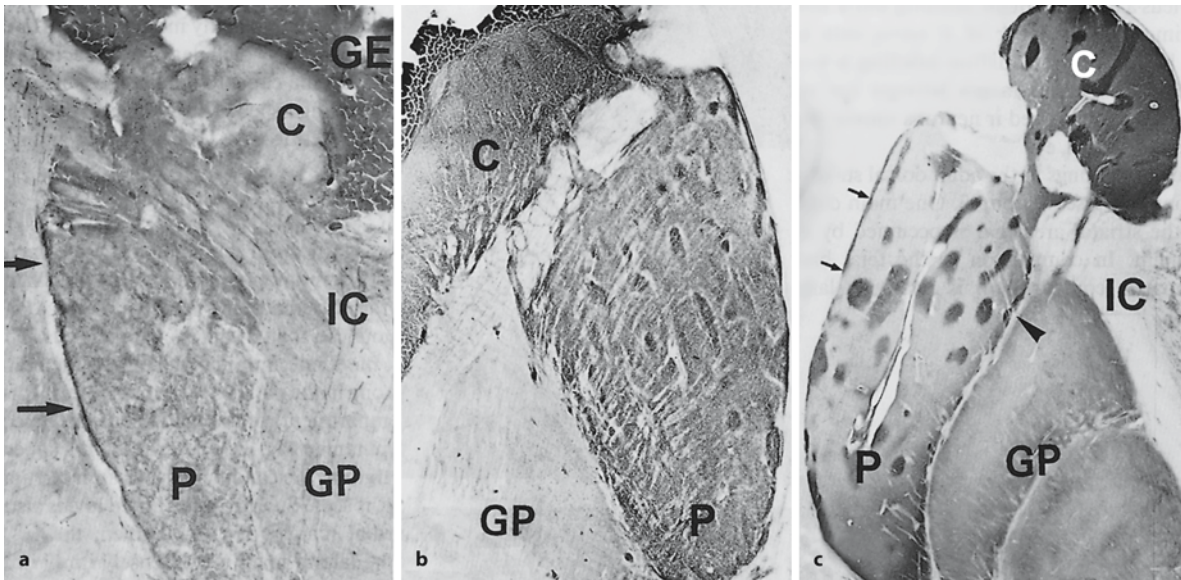
Fig. 9.51 Striosome labelling in the human basal ganglia in 16-week-old (**a**) and 22-week-old (**b**) fetuses, and in the first postnatal week (**c**); AKAP79-staining. *C* caudate nucleus, *GE* ganglionic eminence, *GP* globus pallidus, *IC* internal cap-sule, *P* putamen. (Reproduced with permission from Ulfig et al. 2001, *Cells Tissues Organs* 168:319–329; copyright 2001, S. Karger AG)

(Kostović 1986; Holt et al. 1997). Letinić and Kostović (1996) showed that patches rich in calbindin-immunoreactive neuropil correspond to acetyl-cholinesterase-rich patches of prenatal brains. Ulfig et al. (2001) showed that the expression of AKAP79, a kinase-anchoring protein enriched in postsynaptic densities, in the striatal compartments of the fetal human brain correlates with the dopaminergic innervation of the striatum (Fig. 9.51). These data provided the basis for heterogeneity in the arrangement of striatal fibre connections (Graybiel 1990; Parent and Hazrati 1995; Parent et al. 1995; Gerfen and Wilson 1996; Haber and Gdowski 2004).

The basal ganglia and the amygdala arise from the **ganglionic eminences** (Fig. 9.52) as already suggested in early studies on the developing human forebrain (His 1889; Hochstetter 1919; Macchi 1951; Hewitt 1958, 1961; Humphrey 1968, 1972; for data for rhesus monkey see Gribnau and Geysberts 1985). The olfactory tubercle and the nucleus accumbens arise from the rostral part of the LGE, the nucleus caudatus and putamen from its intermediate part, and the sub-pallial part of the amygdala from the caudal eminence (Table 9.7). The MGE gives rise to the globus pallidus, the basal nucleus of Meynert and the bed nucleus of the stria terminalis. The **nucleus basalis complex** develops the earliest acetylcholinesterase activity in the human telencephalon (Kostović 1986) and sends widely distributed fibres to the anlage of the neocortex and limbic cortex by the end of the sec-

ond trimester of gestation (Fig. 9.53). The development of the cortical layer innervation coincides with the appearance of an 'adult' pattern of topographic relationships. The LIM homeobox gene *L3/Lhx8* is necessary for proper development of basal forebrain cholinergic neurons (Mori et al. 2004). According to Richter (1965, 1966) the anlagen of both the external and internal parts of the **globus pallidus** as well as the **subthalamic nucleus** arise from the subthalamic longitudinal zone of Kahle (1956), a separate zone of the diencephalon on the basis of its early and hete-rochroneous development, and migrate simultane-ously rostralwards to their definitive site. [3H]Thymi-dine data for rodents only partly corroborate these findings (Keyser 1972; Marchand et al. 1986). It seems more likely that only the subthalamic nucleus arises from this zone.

In rodents, the **time** of **neuron origin** has been de-termined in the **basal ganglia** and related basal fore-brain (ten Donkelaar and Dederen 1979; Fentress et al. 1981; Bayer 1984; Marchand and Lajoie 1986; Marchand et al. 1986; Bayer and Altman 1987b; Van der Kooy et al. 1987). Large-celled structures such as the globus pallidus, the nucleus of the horizontal limb of the diagonal band of Broca as well as large cells in the rostral part of the substantia innominata, the caudate–putamen complex and the olfactory tu-bercle arise early (in Chinese hamsters between E11.5 and E15), whereas medium-sized and small cells in the basal forebrain have a persistent origin over a
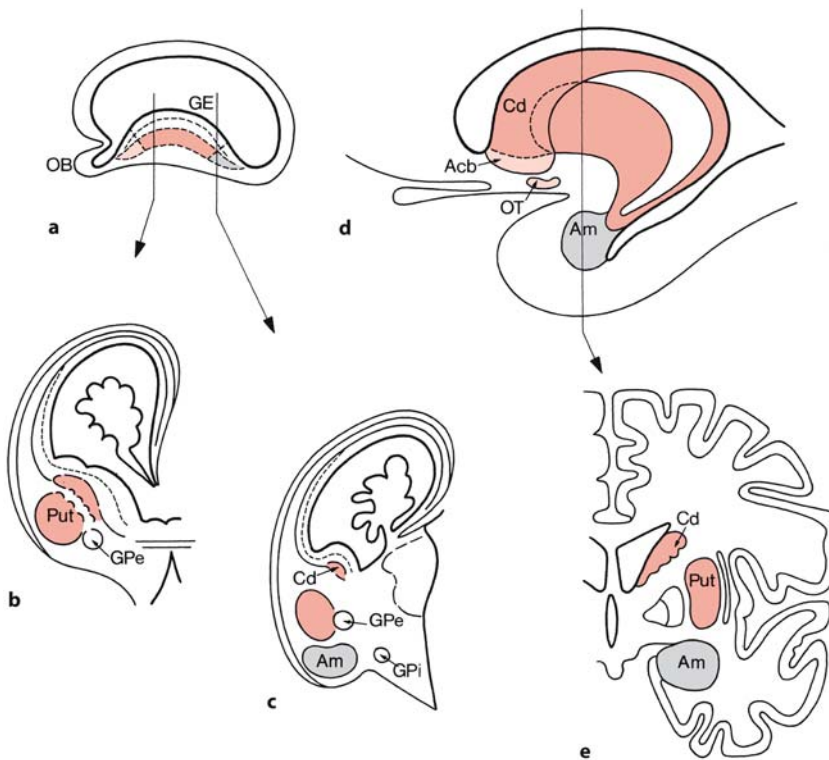
Fig. 9.52 Overview of the development of the human basal ganglia and amygdala: **a**–**c** sagittal and frontal sections of a 9-week-old fetus; **d**–**e** adult situation. The rostral part (*light red*) of the ganglionic eminence (*GE*) gives rise to the nucleus accumbens and the olfactory tubercle, the large intermediate part (*red*) to the caudate nucleus (*Cd*) and the putamen (*Put*), and the caudal part (*grey*) to the amygdala (*Am*). *Acb* nucleus accumbens, *GPe* external part of globus pallidus, *GPi* internal part of globus pallidus, *OB* olfactory bulb, *OT* olfactory tract. (Based on Nieuwenhuys 1977)
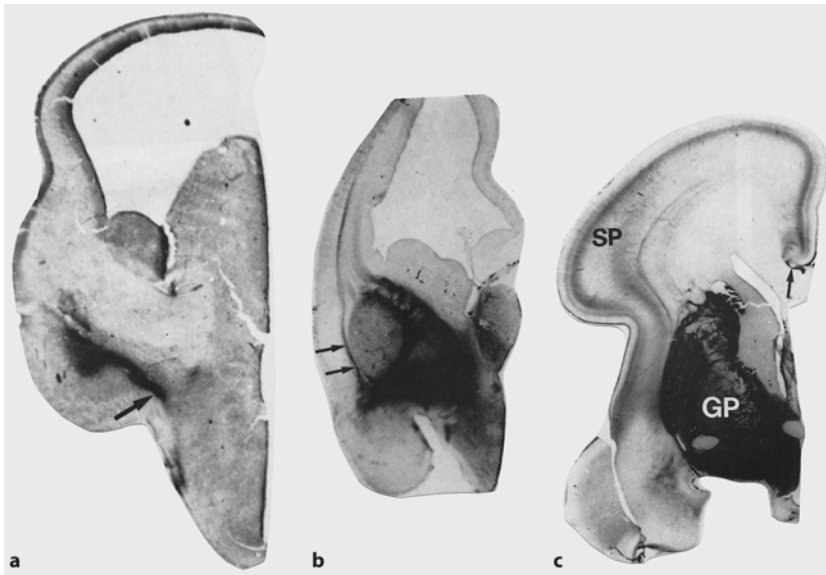
Fig. 9.53 Photomicrographs of acetylcholinesterase-stained sections of the developing forebrain in human fetuses of 9.5 (**a**), 10.5 (**b**) and 24 (**c**) weeks of age. The *arrows* in **b** indicate cholinergic fibres to the cerebral cortex. *GP* globus pallidus, *SP* subplate. (Reproduced with permission from Kostović 1986, *Neuroscience* 17:1047–1077; copyright 1986, Elsevier)

much longer period. Neuron formation in the basal forebrain persists decrementally until P4. A clear caudorostral spatiotemporal gradient as well as a distinct 'outside-in' gradient have been found in the caudate–putamen complex. The time span for neurogenesis in the nucleus accumbens is essentially the same as for the medial part of the caudate–putamen complex. Medium-sized neurons in the neostriatum and the nucleus accumbens, generated simultaneously, are usually arranged in scattered clusters. The neurons of the two striatal compartments are generated during largely non-overlapping developmental periods (Marchand et al. 1986; Van der Kooy et al. 1987). Most of the earliest-born neurons form the patch compartment, and later-born cells make up the matrix compartment. Cell counts indicate that in rats there may be as many as 2,000,000 neurons in the striatum on each side at P4, but that that number is

reduced by apoptosis to the adult figure of approximately 690,000 at P8 (Fentress et al. 1981), suggesting extensive programmed cell death in the striatum. About 97 % are medium-sized neurons and about 3 % are large cells. Itoh et al. (2001) studied the presence of programmed cell death in the human striatum and globus pallidus of fetuses and newborns (gestational age ranging from 12 to 40 weeks) with the transferase-mediated dUTP-biotin nick end-labelling (TUNEL) technique. In the caudate and putamen, TUNEL-labelled cells were observed from the 12th week of gestation onwards. The numerical density of the total number of neurons was significantly decreased, whereas the labelling index of apoptotic cells was significantly increased with advancing gestational age. In the globus pallidus, the numerical density of neurons decreased with advancing gestational age and the labelling index of apoptotic cells increased between the 24th and the 28th week, followed by a decrease until birth.

The GABAergic **striatal projection neurons** are derived from the LGE (Deacon et al. 1994; Olsson et al. 1995, 1998; Anderson et al. 1997b) and *Dlx1*, *Dlx2*, *Dlx5*, *Dlx6*, *Gsh2* and *Mash1* are involved in their specification and differentiation (Porteus et al. 1994; Anderson et al. 1997b; Casarosa et al. 1999; Eisenstat et al. 1999; Toresson and Campbell 2001). Most **striatal interneurons** appear to migrate tangentially from the MGE or the adjacent preoptic/anterior entopeduncular area, and express the NKX2.1 homeodomain protein (Marín et al. 2000). *Nkx2.1* mutants are defective in striatal interneurons (Sussel et al. 1999), whereas the number of striatal interneurons is reduced in *Mash1* and *Dlx1/Dlx2* mutants (Casarosa et al. 1999; Eisenstat et al. 1999). *Mash1* mutants primarily have a reduction of early-born striatal interneurons, whereas *Dlx1/Dlx2* mutants primarily have reduced numbers of late-born striatal interneurons.

SHH and FGF8 are essential for the formation of the **dopaminergic neurons** of the **substantia nigra** and the **ventral tegmental area** (VTA; Ye et al. 1998; Wurst and Bally-Cuif 2001; Holzschuh et al. 2003; Fig. 7.3). Several early ventral midbrain markers contribute to their specification, including *En1/En2*, *Lmx1b*, *Pax2/Pax5*, and *Wnt1* (Hynes and Rosenthal 1999; Smidt et al. 2000), before expression of dopamine-specific markers. In mice, TH is present at E11.5, shortly after expression of the orphan nuclear receptor Nurr1 (Zetterstrom et al. 1996, 1997) and the homeobox gene *Pitx3* (Smidt et al. 1997; van den Munckhof et al. 2003). *Nurr1* mutants fail to induce TH in the mesencephalic dopaminergic progenitor neurons and die soon after birth (Zetterstrom et al. 1997). *Pitx3* expression is maintained throughout life in both mice and men (Smidt et al. 1997). *Pitx3* is also expressed in the developing lens (Semina et al. 1997). *PITX3* mutations were found in two families with inherited forms of cataract and anterior segment dysgenesis (Semina et al. 1998). Abnormal lens development is also found in a naturally occurring mouse mutant, the *aphakia* mouse, which has two deletions in the *Pitx3* gene (Rieger et al. 2001). Van den Munckhof et al. (2003) showed that *Pitx3* is expressed only in the ventral tier of the substantia nigra pars compacta and in about half of the VTA neurons. In *aphakia* mice, *Pitx3* was not detectable, and selective degeneration of substantia nigra and VTA dopaminergic neurons was found, leading to a more than 90 % decrease in striatal dopamine levels and marked reduction in spontaneous locomotor activity.

Most of the neurons of the substantia nigra (pars compacta and pars reticulata) are generated between E13 and E15, according to a gradient from rostral/orsolateral to caudal/ventromedial (Hanaway et al. 1971; Altman and Bayer 1981; Marchand and Poirier 1983; Fig. 9.54 a). This gradient extends to the VTA: neurons of the VTA are born later (E14–E16) than those of the substantia nigra (Altman and Bayer 1981; Marchand and Poirier 1983). The neurons of the substantia nigra are generated at two different points of the basal plate at the level of the isthmus and migrate in a radial pattern as two definite streams towards the ventral mesencephalon (Hanaway et al. 1971; Keyser 1972; Marchand and Poirier 1983). Possibly, the pars reticulata is derived from the ventrolateral stream, and the pars compacta and the VTA from the medial cell stream (Marchand and Poirier 1983). The neurogenetic gradients in both the substantia nigra (Altman and Bayer 1981) and the caudate–putamen complex (ten Donkelaar and Dederen 1979; Fentress et al. 1981; Bayer 1984) in rodents can be correlated with the topographic principles in the nigrostriatal projections (Fig. 9.54 b). The axonal projections are arranged so that the oldest nigral neurons are located in the dorsolateral part (generated before E15), whereas the younger neurons (born after E15) are located in the ventromedial part. In the rhesus monkey, substantia nigra neurons are generated between E36 and E43 with a peak around E38–E40 and without an appreciable spatiotemporal gradient (Levitt and Rakic 1982). All neurons in the caudate nucleus and putamen are generated within the first half of gestation (Brand and Rakic 1979). Dopaminergic axons are present in the putamen around E60 (Brand and Rakic 1984). The first morphologically defined synapses appear in the putamen at E60 and in the head of the caudate at E65 (Brand and Rakic 1984). During this period the neostriatum receives its first corticostriatal input (Goldman-Rakic 1981), preceding its cytoarchitectonic differentiation into separate island and matrix cellular components (Goldman-Rakic 1982). A similar putamen-
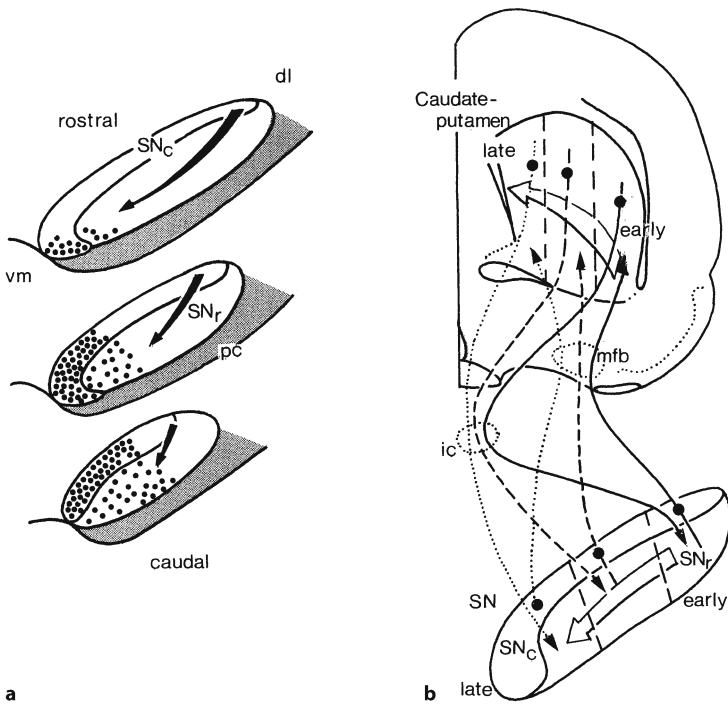
Fig. 9.54 a Pattern of cell labelling in the rat substantia nigra after [³H]thymidine injections at E15 and E16; **b** correlation between neurogenetic gradients and anatomical connections in the rat nigro-striatal system. *dl* dorsolateral, *ic* internal capsule, *mfb* medial forebrain bundle, *SNc* substantia nigra pars compacta, *SNr* substantia nigra pars reticulata, *vm* ventromedial. (**a** After Altman and Bayer 1981; **b** after Bayer 1984)
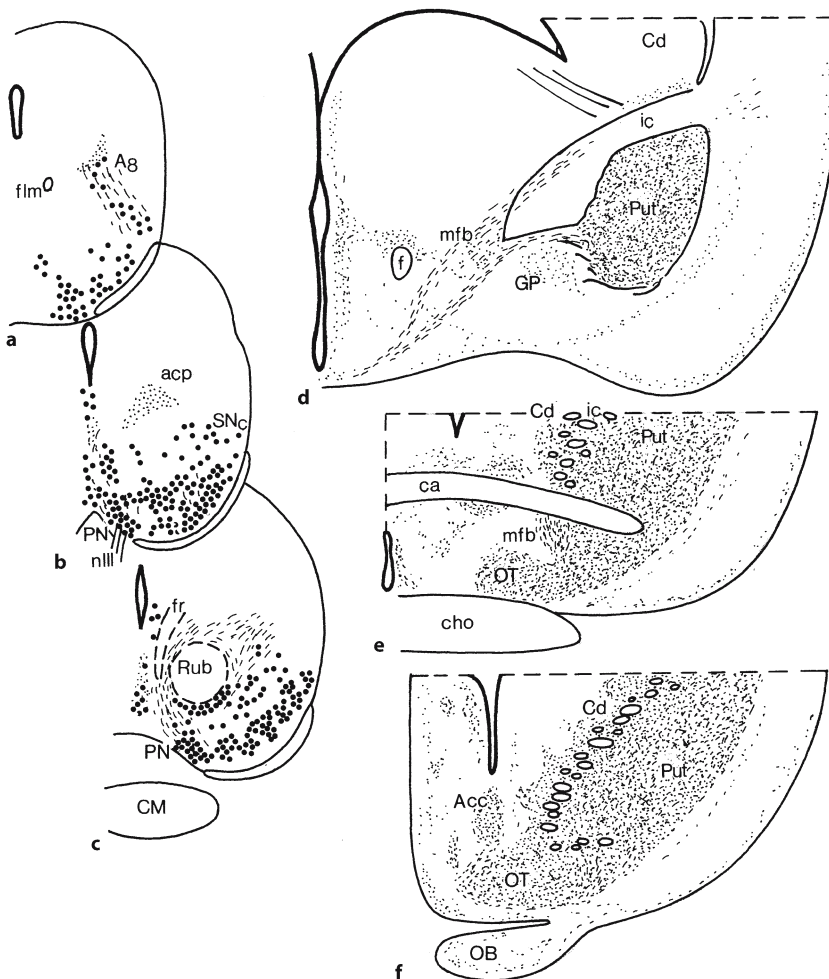
Fig. 9.55 Development of the striatal dopaminergic innervation in 3–4-month-old human fetuses. *Acc* nucleus accumbens, *acp* ascending catecholaminergic pathway, *A8* medullary catecholaminergic cell group, *C* caudate nucleus, ca commissura anterior, *cho* chiasma opticum, *CM* corpus mamillare, *flm* fasciculus longitudinalis medialis, *GP* globus pallidus, *ic* internal capsule, *mfb* medial forebrain bundle, *nIII* oculomotor nerve, *OB* olfactory bulb, *OT* olfactory tubercle, *PN* nucleus paranigralis, *Put* putamen, *Rub* nucleus ruber, *SNc* substantia nigra pars compacta. (After Nobin and Björklund 1973)

to-caudate gradient of synaptogenesis has been observed in the developing human neostriatum (Zečević and Kostović 1980).

Data on the **development** of the **human substantia nigra** are limited. Cooper (1946) first delineated the substantia nigra at the end of the embryonic period (stages 20–21), but (by extrapolating rhesus monkey data) its cells are presumably generated between stages 18 and 21. Ontogeny of human mesencephalic dopaminergic cells was studied with histofluorescence (Nobin and Björklund 1973; Olson et al. 1973) and TH immunohistochemistry (Pearson et al. 1980; Pickel et al. 1980; Freeman et al. 1991; Verney et al. 1991; Zecevic and Verney 1995; Almqvist et al. 1996; Puelles and Verney 1998). Evidence of TH-immunoreactive substantia nigra neurons is found as early as stages 15–16, i.e. at 4.5 weeks of development (Puelles and Verney 1998). DiI labelling suggests that dopaminergic neurons innervate the striatum as early as week 10 of fetal life (Sailaja and Gopinath 1994). Binding studies for dopaminergic markers suggest that dopaminoceptive neurons in the striatum expressing the dopamine receptors D1R or D2R are present in the human fetal striatum at least from week 16 of life (Brana et al. 1995, 1996) and from week 12 in the substantia nigra and the VTA (Aubert et al. 1997).

The **development** of the **striatal dopaminergic innervation** in rats has been studied with histofluorescence techniques (Olson and Seiger 1972; Seiger and Olson 1973) and immunohistochemical techniques using antibodies against TH (Specht et al. 1981 a, b) and dopamine (Voorn et al. 1988). At E14, the first dopaminergic, nigrostriatal fibres reach the striatal anlage. This projection rapidly increases in size. The developmental pattern of the dopaminergic innervation of the striatum and the nucleus accumbens and the pattern of their neurogenesis are closely related. The first dopaminergic fibres arrive in the two striatal subdivisions well before their peaks in neurogenesis. In the immature caudate–putamen complex the dopaminergic innervation is organized as a system of patches called 'dopamine islands' (Olson et al. 1972). These islands express high TH-like immunoreactivity and are also rich in acetylcholinesterase activity. In rats, at E19 the first signs of this inhomogeneous distribution of dopaminergic fibres can be observed in the dorsolateral part of the striatum. In the following prenatal and postnatal days these dopaminergic patches, i.e. the first sign of structural compartments in the developing striatum, also appear more medially. By the third postnatal week, however, most of the patches are no longer detectable and only the most dorsolaterally located (the first arising) remain visible through the adult stage (Voorn et al. 1988). Data on the development of the human nigrostriatal projection indicate that as early

as in the early fetal period the neostriatum receives dopaminergic terminals. The putamen becomes innervated somewhat earlier than the caudate nucleus (Olson et al. 1973). Nobin and Björklund (1973) studied 3–4-month-old fetuses (10–15-cm crown–rump length). At this stage of development, catecholaminergic cell groups and nigrostriatal pathways are already richly developed and innervate abundantly the basal ganglia and olfactory region (Fig. 9.55). TH studies in 9–10-week-old fetuses (about 50-mm crown–rump length) show that loose clusters of TH-immunoreactive neurons are present in the pars compacta of the substantia nigra and the VTA. In these early fetal stages, the TH-immunoreactive neurons in the substantia nigra already have well-established processes which are richly distributed in the pars reticulata and in the basal ganglia. These data strongly suggest that also in primates including man the generation of neurons in the substantia nigra and the VTA as well as the ingrowth of nigrostriatal fibres takes place in the last part of the embryonic period, i.e. between stages 17 and 23, comparable to E14–E17 in rat (Table 9.11). In rat and human embryos, the penetration of dopaminergic fibres in the cerebral cortex occurs at similar developmental stages in each species (Verney et al. 1982; Kalsbeek et al. 1988; Verney et al. 1993; Zecevic and Verney 1995).

9.8.2 Congenital and Acquired Disorders of the Basal Ganglia

Developmental malformations of the *basal ganglia* are rare, and are usually associated with malformations of other areas of the CNS (Lemire et al. 1975; Friede 1989). Sarnat (2000) reported a case of congenital absence of the basal ganglia (Fig. 9.56). *Acquired disorders* of the *basal ganglia* are much more common, especially in the perinatal period. From a clinical point of view disorders of movement due to abnormal functioning of the basal ganglia can be divided into two broad groups (Fig. 9.57): (1) the hypokinetic-rigid syndromes, the fundamental disturbances of which consist of hypokinesia and/or bradykinesia, i.e. difficulty and/or slowness in initiating and completing movements, generally associated with rigidity; and (2) the dyskinesias, including tremor, chorea and ballismus, dystonia and athetosis, tics and myoclonus (Fernández-Alvarez and Aicardi 2001; Hoon et al. 2003; Sanger 2003). Disorders with a **hypokinetic-rigid syndrome** in childhood include early-onset Parkinson disease, juvenile Huntington disease, Wilson disease, juvenile GM2 gangliosidosis, multiple-system atrophies, Hallervorden–Spatz disease and many other rare disorders (Fernández-Alvarez and Aicardi 2001; Table 9.12). Many patients with Hallervorden–Spatz disease have mutations in

Table 9.11 Development of dopaminergic cell groups in the mesencephalon and their innervation of the basal ganglia and prefrontal cortex in rats, rhesus monkeys and man (after van Domburg and ten Donkelaar 1990; Zecevic and Verney 1995; Puelles and Verney 1998)

Species	Time of neuron origin SN/VTA	First appearance of dopamine immunoreactivity	First ingrowth dopaminergic fibres	Neurogenesis neostriatum and prefrontal cortex	Start of fetal period	Gestation time (days)
Rat	SN: E13–15[a,h,k] VTA: E14–E16[a,k]	SN: E13[m,s,t,v]	Neostriatum: E14[m,s,t,v] Prefrontal cortex: E17[i]	Neostriatum: E13–P2[b] Prefrontal cortex: E13–E18[i]	E17[u]	21–22[u]
Rhesus monkey	SN: E36–E43[j] (stages 18–21) VTA: E38–E43[j] (stages 19–21)	? ?	Neostriatum: before E60[e]	Neostriatum: E36–80[d] (peak E43–E50, i.e. stages 21–23 Prefrontal cortex: E40–E90[j]	E46-50[g]	160–170[g]
Man	SN: stages 19 and 20[c,f,o] (early 5th to middle of 7th week VTA: Late 5th to 7th week[c]	SN: between weeks 5.5 and 9[l,p,q,r] ?	Neostriatum: before 9th week[n,p,q,r,w] Prefrontal cortex: by about 12weeks[l,n,x]	Early week 7 to week 18[c] Prefrontal cortex?	E56–E60[o]	260–280[o]

SN substantia nigra, *VTA* ventral tegmental area of Tsai

[a] Altman and Bayer (1981)
[b] Bayer (1984)
[c] Bayer et al. (1995)
[d] Brand and Rakic (1979)
[e] Brand and Rakic (1984)
[f] Cooper (1946)
[g] Gribnau and Geysberts (1981)
[h] Hanaway et al. (1971)
[i] Kalsbeek et al. (1988)
[j] Levitt and Rakic (1982)
[k] Marchand and Poirier (1983)
[l] Nobin and Björklund (1973)
[m] Olson and Seiger (1972)
[n] Olson et al. (1973)
[o] O'Rahilly et al. (1988)
[p] Pearson et al. (1980)
[q] Pickel et al. (1980)
[r] Puelles and Verney (1998)
[s] Seiger and Olson (1973)
[t] Specht et al. (1981a)
[u] Theiler (1972)
[v] Voorn et al. (1988)
[w] Zečević and Kostović (1980)
[x] Zecevic and Verney (1995)

the gene encoding pantothenate kinase 2 (PANK2), resulting in pantothenate kinase associated neurodegeneration (Hayflick et al. 2003). The 'eye-of-the-tiger sign' is typical on MRI examination. The medial part of the globus pallidus appears to be especially sensitive to deficiency of PANK2. *Chorea* is a relatively infrequent movement disorder in children but at least 150 causes of chorea have been described (Padberg and Bruyn 1986). Primary (idiopathic) and secondary forms of dystonia are found. *Secondary dystonias* can be classified into structural, metabolic, degenerative and miscellaneous disorders. Dystonia is a frequent symptom in the course of many inborn errors of metabolism such as *glutaric aciduria type 1*, an autosomal recessive metabolic disorder, which is characterized by severe reduction or total absence of glutarylcoenzyme A dehydrogenase (GCDH) activity (Goodman et al. 1977; Goodman and Frerman 2001). Its prevalence has been estimated to be 1 in 30,000 (Kyllerman and Steen 1980). At least 100 disease-causing mutations have been described (Goodman et al. 1998; Zschocke et al. 2000). GCDH deficiency leads to an accumulation of the marker metabolites 3-hydroxyglutaric acid, glutaric acid and glutaryl carnitine. If untreated, the disease is complicated by acute encephalopathic crises, resulting in neurodegeneration of vulnerable brain regions, especially the putamen. 3-Hydroxyglutaric acid is the major neurotoxin in this disease (Kölker et al. 2003). Clinical manifestations generally appear between 5 and 14 months of age, but mild symptoms such as slight motor delay and hypotonia can be observed earlier (Hoffmann et al. 1996; Fernández-Alvarez and Aicardi 2001). Macrocephaly at birth or somewhat later in infancy is present in about 70% of cases (Hoffmann et al. 1996). In about two thirds of cases, the disease starts abruptly, on average at 12 months of age, with focal seizures or generalized convulsions and vomiting, usually following an infectious disease. Psychomotor regression and dystonic or choreoathetotic movements then appear (Fernández-Alvarez and Aicardi 2001). Autopsy studies have shown rather minimal changes in severely affected patients who died at 1 year of age but changes much more marked in patients who died at more than 2 years of age (Goodman et al. 1977; Leibel et al. 1980; Chow et al. 1988; Soffer et al. 1992; Kimura et al. 1994; Clinical Case 9.9). These findings are remarkably similar to those in 'familial holotopistic striatal necrosis' (Miyoshi et al. 1969) or 'familial striatal degeneration' (Roessmann and Schwarz 1973).
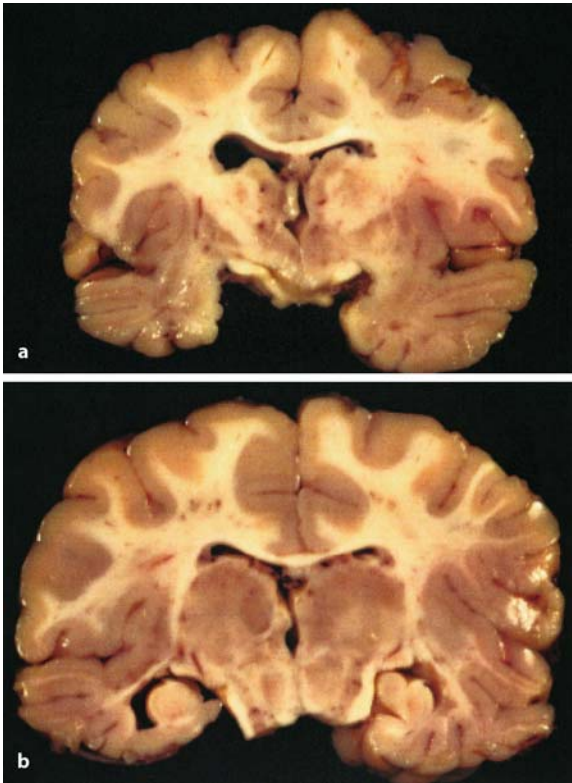
Fig. 9.56 a, b Bilateral congenital absence of the deep cerebral nuclei in a 14-month-old male infant (kindly provided by Ellsworth Alvord, Seattle)

These cases may have been unrecognized forms of glutaric aciduria.

In *subacute necrotizing encephalopathy* or *Leigh syndrome* (Leigh 1951), movement disorders of any type, including hypokinetic-rigid syndrome, chorea, myoclonus or dystonia, may be the most obvious clinical features. Leigh syndrome is characterized by multifocal, bilateral areas of subtotal necrosis in the basal ganglia, the brain stem tegmentum, the cerebellum and to some extent the spinal cord. The lesions may involve the white matter, especially the posterior columns, the corticospinal tracts, the optic nerves and the superior cerebellar peduncles (Lemire et al. 1975). This syndrome usually presents in infancy with feeding difficulties, psychomotor retardation, ophthalmoplegia, ataxia and weakness. Leigh syndrome is a heterogeneous mitochondrial disorder among children that may be associated with deficiency of pyruvate dehydrogenase and of enzymes of the respiratory chain, especially complex I and complex IV (Zeviani et al. 1996; Darin et al. 2001; Tulinius et al. 2003; Clinical Case 9.10).

A **selective vulnerability** of the basal ganglia is found in many acquired lesions such as subependymal haemorrhages affecting the ganglionic eminence, status marmoratus, subacute necrotizing encephalopathy (Leigh syndrome) and kernicterus. The basal ganglia are susceptible to injury because they are metabolically very active in the immature brain (Chugani and Phelps 1986) and possess a high concentration of excitatory receptors (Mitchell et al.
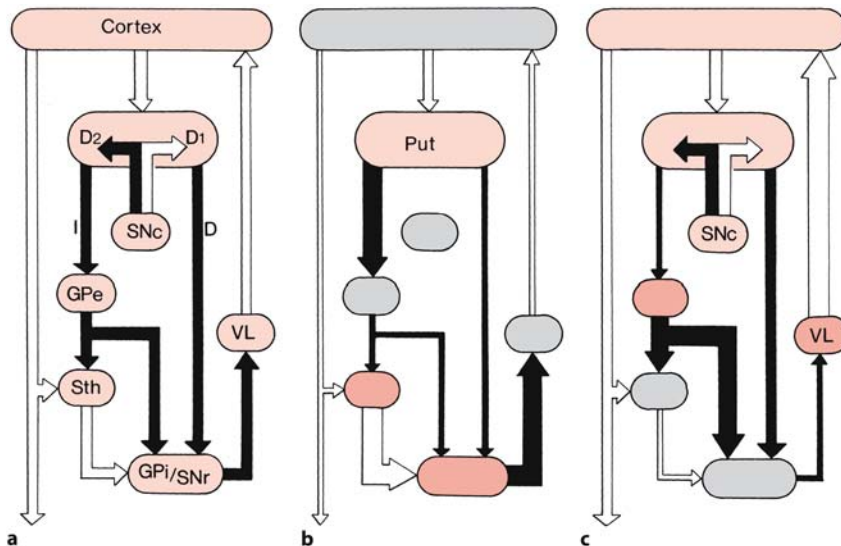
Fig. 9.57 Basal ganglia-thalamocortical circuits in the normal situation (**a**), in Parkinson disease (**b**) and in Huntington disease (**c**). Normal cell activity is indicated in *light red*, upregulation in *red* and downregulation in *grey*. Inhibitory pathways are shown as *black arrows* and excitatory pathways as *open arrows*. The size of the arrows indicates the changes occurring.

D direct pathway, *D1*, *D2* dopamine receptors, *GPe* external part of globus pallidus, *GPi* internal part of globus pallidus, *I* indirect pathway, *SNc* compact part of substantia nigra, *SNr* reticular part of substantia nigra, *Sth* subthalamic nucleus, *VL* ventrolateral thalamic nucleus. (After Alexander et al. 1986)

Table 9.12 Involvement of the basal ganglia in some childhood motor impairment syndromes (after Fernández-Alvarez and Aicardi 2001; Hoon et al. 2003)

Disorder	Inheritance/gene defect	Involvement of basal ganglia	Selected references
Bilateral striatal necrosis	Autosomal recessive; maps to chromosome 19q	Caudate, putamen, globus pallidus	Friede (1989); Basel-Vanagaite et al. (2004)
Dentatorubro-pallidoluysian atrophy	Autosomal dominant	External globus pallidus, subthalamic nucleus; (dentate and red nuclei)	Takahashi et al. (1988); Warner et al. (1994, 1995)
Glutaric aciduria type I	Autosomal recessive; deficiency in glutaryl-coenzyme A dehydrogenase	Caudate, putamen; see Clinical Case 9.9	Chow et al. (1988); Kimura et al. (1994); Goodman and Frerman (2001)
Hypoxic-ischemic encephalopathy: bilateral lesions thalamus/basal ganglia		Putamen, thalamus, perirolandic areas	Krägeloh-Mann et al. (1995, 2002); Rutherford (2002)
Juvenile Huntington disease		Caudate, putamen	Ho et al. (1995)
Kernicterus		Globus pallidus	Johnston and Hoon (2000); Yilmaz et al. (2001)
Leigh syndrome	Mitochondrial disorder; deficiency complexes I or IV	Caudate, putamen, brain stem, white matter; see Clinical Case 9.10	Leigh (1951)
Pantothenate kinase-associated neurode-generation (Haller-vorden–Spatz disease)	Autosomal recessive disorder; many patients with *PANK2* mutations	Globus pallidus, subthalamic nucleus	Hayflick et al. (2003)
Pyruvate dehydro-genase deficiency		Globus pallidus, caudate, putamen	Brown et al. (1989); Robinson (2001)
Wilson disease	Autosomal recessive disorder with abnormal deposition of copper in liver, brain, cornea, and other tissues	Putamen, globus pallidus, caudate	Brewer et al. (1999)

Clinical Case 9.9
Familial Striatal Degeneration (Glutaric Aciduria Type 1)

Glutaric aciduria type 1 (*GA-1*) is an autosomal recessive metabolic disorder which is characterized by severe reduction or total absence of glutarylcoenzyme A dehydrogenase (GCDH) activity (Goodman et al. 1977; Kimura et al. 1994; Hoffmann et al. 1996). The neuropathological findings in a 15-year-old Turkish male adolescent will be discussed as the Case Report.

Case Report. Rapidly progressive neurological symptoms were evident from birth in this 15-year old male adolescent whose parents were consanguineous to the third degree. Hypertonia began at the left side, became generalized later and ended with episodes of generalized epilepsy. His monozygous twin brother and two sisters were neurologically and developmentally normal, but a younger brother also had GA-1. They both displayed the so-far unreported mutation M801 (240 G → C) in exon 3 of the GCDH gene.

His first episode occurred at 7 months of age when, 2 weeks after gastroenteric dehydration, he had paroxysmal hypertonia of the left arm which progressed to status epilepticus with subcoma. The idiopathic relapsing fever was labelled as acute encephalopathy without any obvious metabolic cause. The second episode occurred 11 months later, again in the form of gastroenteric dehydration and encephalopathy. A peak of urinary glutaric acid (GA) and the presence of 3-OH-GA suggested the diagnosis of glutaric aciduria type 1. Blood tests were normal, but the patient's CSF revealed a raised acetic acid level. The finding of normal GCDH activity in hepatocytes and fibroblasts, however, led to the erroneous dismissal of the GA-1 diagnosis. Constant episodes of laryngeal dyspnoea when he was 4 years old led to retesting of organic acid levels. They were found to be normal and so GA-1 was completely dismissed. The patient had now severe psychomotor retardation. He suffered from dyskinetic dystonia with compulsive

nuchal torsion dystonia to the right side. Additional manifestations included hip adduction hypertonia, hyperextension and torsion of the spine. Although no fixed contractures were found, there was total loss of voluntary movements, except for visual expression and eye motility. The patient had hypotonia alternating with periods of opisthotonus and an overall dystrophic expression of the body until he died at the age of 15 years from bronchopneumonia. The diagnosis of GA-1 could only be confirmed after postmortem gene analysis.

At autopsy, the spleen and liver were found to be normal, making the diagnosis of a storage disease unlikely. The brain weighed 1,275 g. Macroscopically, there were widened lateral ventricles and loss of gyral convolutions. Frontal atrophy and a small caudate nucleus and putamen were also evident (Fig. 9.58a). The white matter appeared grossly normal. Microscopically, the striatum showed obvious neuron loss, with small neurons being more affected than large cells (Fig. 9.58b). This was marked in the putamen, moder-ate in the caudate nucleus and only mild in the globus pallidus. This neuronal loss was associated with marked astrocytic gliosis. Interestingly, on close examination of the striatum we noted that the neuronal loss and astrogliosis were non-continuous in nature. In fact, such changes were confined to areas within the sections which bore great resemblance to the patch-matrix compartments of the striatum.

References

Goodman SI, Norenberg MD, Shikes RH, Brelick DJ, Moe PG (1977) Glutaric aciduria: Biochemical and morphological considerations. J Pediatr 90:746–750

Hoffmann GF, Athanassopoulos S, Burlina AB, Duran M, de Klerck JBC, Lehnert W, Leonard JV, Monavari AA, Müller E, Muntau AC (1996) Clinical course, early diagnosis, treatment and prevention of disease in glutaryl-CoA dehydrogenase deficiency. Neuropediatrics 27:115–123

Kimura S, Hara M, Nezu A, Osaka H. Yamazaki S (1994) Two cases of glutaric aciduria type 1: Clinical and neuropathological findings. J Neurol Sci 123:38–43
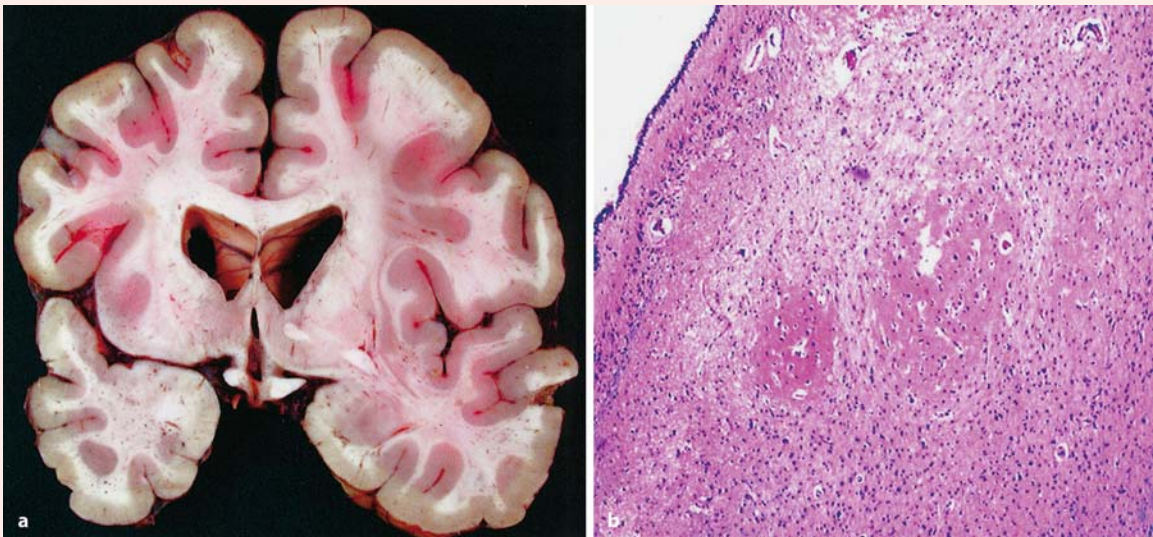
Fig. 9.58 Familial striatal degeneration: **a** frontal section through the brain demonstating very atrophic caudate nuclei; **b** histological section through the caudate nucleus with severe gliosis (*lower* and *right* parts of the picture); centrally, two round structures (striosomes) are somewhat spared from the gliosis (courtesy Martin Lammens, Nijmegen)

1999). **Subependymal** or **germinal matrix haemor-rhages** are very common in premature infants (Norman et al. 1995; Squier 2002). **Status marmoratus** (marbled state or *état marbré*) is characterized by the presence of myelinated fibres in aggregations of a density abnormal for a given site (Norman 1947). Typically, such aggregations are associated with ab-normal collections of glial fibres. Status marmoratus is usually restricted to the striatum, but may involve the globus pallidus, red nucleus and cerebral cortex (Fig. 9.61). It is usually associated with the athetoid form of cerebral palsy (Malamud 1950). Severe mental retardation, spasticity and epileptic seizures are common. **Kernicterus** may result as a complication of

Clinical Case 9.10
Leigh Syndrome

Leigh syndrome (Leigh 1951) or *subacute necrotizing encephalomyopathy* is a progressive subcortical disorder, characterized by multifocal, bilateral areas of subtotal necrosis in the basal ganglia, the brain stem tegmentum, the cerebellum and to some extent the spinal cord (see Case Report). It is the prototype of a large group of mitochondrial encephalomyopathies, currently known as defects of oxidative phosphorylation (OXPHOS defects; Chap. 3).

Case Report. A boy was born after an uncomplicated pregnancy as the second child of nonconsanguineous parents. His mother and grandmother were known to have retinitis pigmentosa. As a baby, head balance was poor and the boy was very quiet. Marked developmental delay and subsequently progressive loss of motor and social skills became evident at the age of 8 months. Cerebral MRI showed marked cerebral atrophy and abnormal signs in the basal ganglia (Fig. 9.59), suggesting Leigh syndrome. Blood lactate levels were between 1.8 and 9.4 mmol/l (normally below 2.0 mmol/l), and CSF lactate was also elevated to 4.8 mmol/l (normally 1.2–2.0 mmol/l). At the age of 11 months, respiratory failure due to pneumonia necessitated artificial ventilation. At that time a muscle biopsy was taken. Histological examination of the tissue showed no structural abnormalities of the muscle fibres. Biochemical analysis demonstrated defective respiratory chain functions. Mutation analysis finally confirmed the diagnosis Leigh syndrome by demonstration of the 8993T>G mutation in mitochondrial DNA. Although he initially recovered, the boy died at the age of 14 months owing to aspiration and subsequent respiratory failure.

At autopsy, brain weight was 830 g. Macroscopical inspection revealed bilateral slightly asymmetric, dark grey to light brown lesions in the thalamus, hypothalamus, mesencephalic tegmentum, periaqueductal grey matter and hindbrain nuclei (Fig. 9.60 a–c). The putamen and the pulvinar were bilaterally pseudocystically degenerated. All these lesions were characterized by spongiosis of the neuropil, reactive astrocytes and important capillary proliferation and endothelial swelling (Fig. 9.60 d). In the less severe lesions such as in the periaqueductal grey matter, neurons were still well recognizable. In the more severely affected regions such as the putamen, almost all neurons had disappeared, leading to pseudocystic lesions. These are the classic signs found in Leigh syndrome. Large parts of the cerebral cortex, including frontal, insular and temporobasal cortex, were atroph-
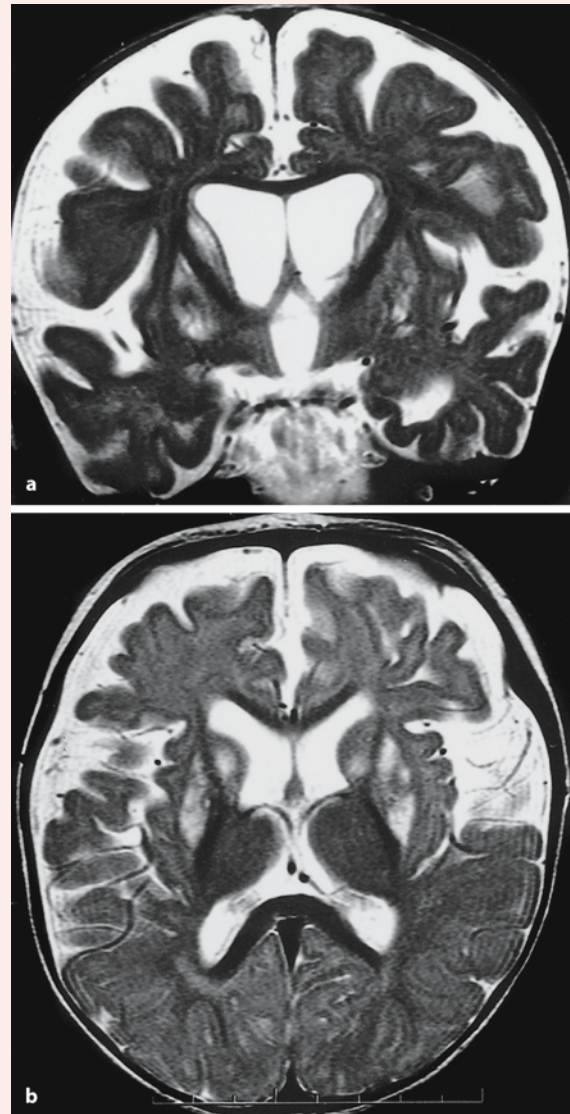
Fig. 9.59 Coronal (**a**) and axial (**b**) MRI of Leigh syndrome. Note the zones of hyperintensity in the caudate nucleus and the putamen bilaterally. (Courtesy Michèl Willemsen, Nijmegen)

ic, and showed gliosis in the molecular layer and spongiosis and neuronal loss in layer II. Such lesions are reminiscent of Alpers disease. Moreover, in the occipital cortex an ischemic lesion at the borderzone between the territories of the anterior and middle cerebral arteries was found with pseudolaminar necrosis of the complete cortex. There was also important cell loss and spongiosis in areas CA1 and CA3 of the hippocampus. Probably, these lesions resulted from generalized circulatory failure.
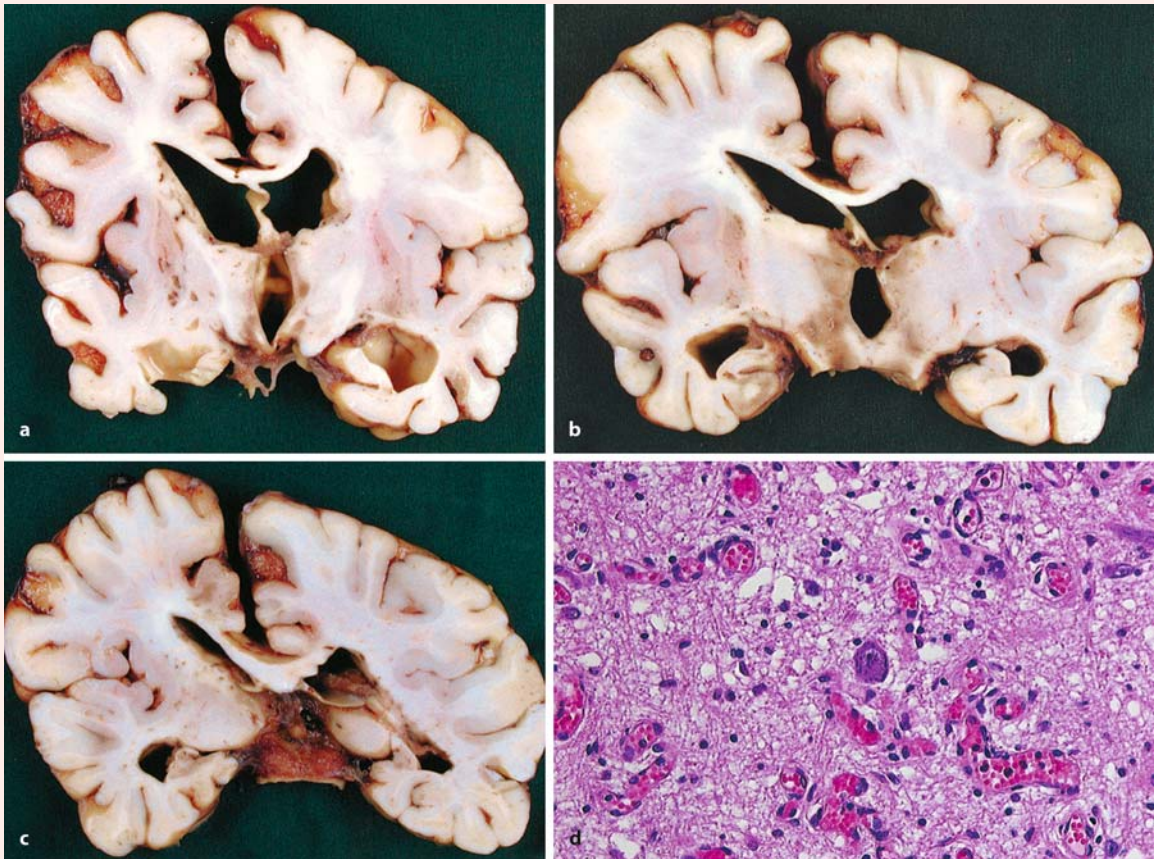
Fig. 9.60 Leigh syndrome: **a** frontal section at the level of the mamillary bodies showing atrophy of the basal ganglia and thalamus, dilatated lateral ventricles, brown discolorated regions in the right thalamus and atrophic cerebral cortex; **b** frontal section at the level of the substantia nigra; especially the regions around the left substantia nigra and both subthalamic nuclei are damaged with brown discoloration; **c** frontal section showing a cyst in the left pulvinar; **d** haematoxylin–eosin-stained section of a lesion in the left subthalamic nucleus: spongiosis, slight gliosis and capillary proliferation are present, and centrally the cell body of an intact large neuron is visible (courtesy Martin Lammens, Nijmegen)

Reference

Leigh D (1951) Subacute necrotizing encephalomyopathy in an infant. J Neurol Neurosurg Psychiatr 14:216–221

Fig. 9.61 Status marmoratus (Weigert stain). Note the gliotic regions, especially in the lateral thalamus, and zones of hypomyelination in the right internal capsule (courtesy Akira Hori, Toyohashi)
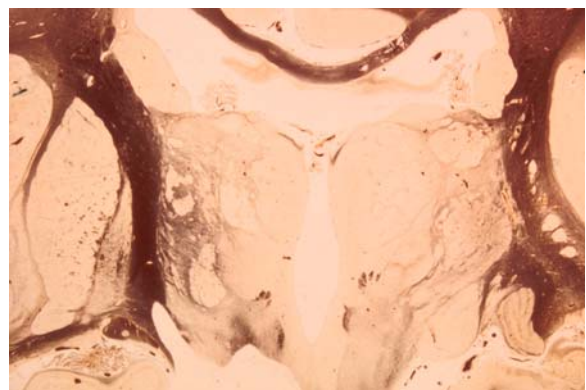
infantile hyperbilirubinaemia from any cause, and may lead to necrosis of delected brain stem, basal ganglia and cerebellar neurons (Kinney and Armstong 1997). In the term infant, the common sites of the gross lesions with a bright yellow colour are the globus pallidus, subthalamus and Ammon's horn. Kernicterus is now rare in regions where hyperbilirubinaemia can be anticipated, treated or prevented.

MRI studies have shown **bilateral lesions** of the **thalamus** and the **basal ganglia** in children with severe birth asphyxia, leading to dyskinetic and spastic types of cerebral palsy (Yokochi et al. 1991; Rutherford et al. 1992; Krägeloh-Mann et al. 1995; Rademakers et al. 1995; Rutherford 2002). In addition to hyperintensity (T2-weighed images) in the ventrolateral thalamus and the posterior part of the nucleus lentiformis, lesions of the perirolandic region and of the hippocampus were found in some patients. Bilateral lesions of the thalamus and the basal ganglia have also been found in term neonates as a consequence of severe birth asphyxia (Voit et al. 1987; Pasternak et al. 1991; Baenziger et al. 1993; Rutherford et al. 1995; Sie et al. 2000; Rutherford 2002). Krägeloh-Mann et al. (2002) defined three different patterns of MRI lesions in children with bilateral lesions of the thalamus and basal ganglia due to birth asphyxia, neonatal shock or late prenatal compromise: (1) a mild pattern with involvement of the lentiform nucleus and ventrolateral thalamus only; (2) an intermediate pattern with involvement of the lentiform nucleus, the ventrolateral thalamus and pericentral regions; and (3) a severe pattern with additional involvement of the entire thalamus and of the hippocampus. This grading of MRI findings corresponded rather well with the severity of cognitive and motor impairment and the type of cerebral palsy. Normal cognitive development and mild motor delay was only seen with the mild pattern. All children developed cerebral palsy: purely dyskinetic cerebral palsy was only found with the mild pattern, the dyskinetic-spastic or spastic forms were found in all three groups, with dyskinetic-spastic cerebral palsy more related to the moderate pattern, and purely spastic cerebral palsy more related to the severe pattern.

9.8.3   Development of the Amygdala

The **amygdala** is composed of pallial and subpallial parts (Lammers 1972; Stephan and Andy 1977; Amaral 1987; de Olmos 1990, 2004; Heimer et al. 1991). The basolateral parts and the associated cortical amygdala form the pallial part, whereas the central and medial amygdaloid nuclei form the subpallial part (Fig. 9.62). The centromedial amygdala forms a continuum with the bed nucleus of the stria termi-
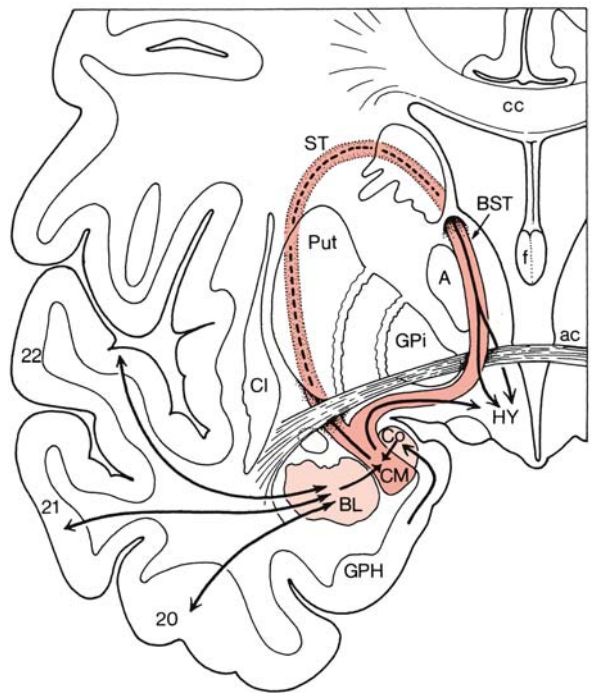
Fig. 9.62 Overview of the amygdala and extended amygdala. The centromedial nuclei and the extended amygdala is indicated in *red*, and the basolateral amygdala (*BL*) and cortical amygdala (*Co*) in *light red*. *A* anterior nucleus, *ac* anterior commissure, *BST* bed nucleus of stria terminalis, *cc* corpus callosum, *Cl* claustrum, *CM* centromedial amygdala, *f* fornix, *GPH* gyrus parahippocampalis, *GPi* internal globus pallidus, *HY* hypothalamus, *Put* putamen, *ST* stria terminalis, *20–22* temporal cortical areas

nalis, known as the extended amygdala (Alheid and Heimer 1988; Alheid et al. 1995; Heimer et al. 1997; de Olmos 2004). **Time** of **neuron origin** data in rodents indicate a rostrocaudal gradient within the amygdaloid complex (ten Donkelaar et al. 1979; Bayer 1980; McConnell and Angevine 1983) and strongly support a subdivision of the amygdala into two groups: a group of early-arising (E13–E15/E17) structures (central, medial and anterior cortical nuclei) and a group of later-born (E14/E15–E16/E17) nuclei (lateral, basolateral, basomedial and posterior cortical nuclei). This distinction between two groups of nuclei in the amygdaloid complex is comparable with the subdivision of Stephan and Andy (1977). In rhesus monkeys, neurogenesis in the amygdaloid nuclear complex starts at E33, peaks between E38 and E48, and ceases between E50 and E56 (Kordower et al. 1992).

Developmental studies on the **human amygdala** are few (Macchi 1951; Humphrey 1968, 1972; Kahle 1969; Ulfig 2002b; Ulfig et al. 2003a, b). The primor-
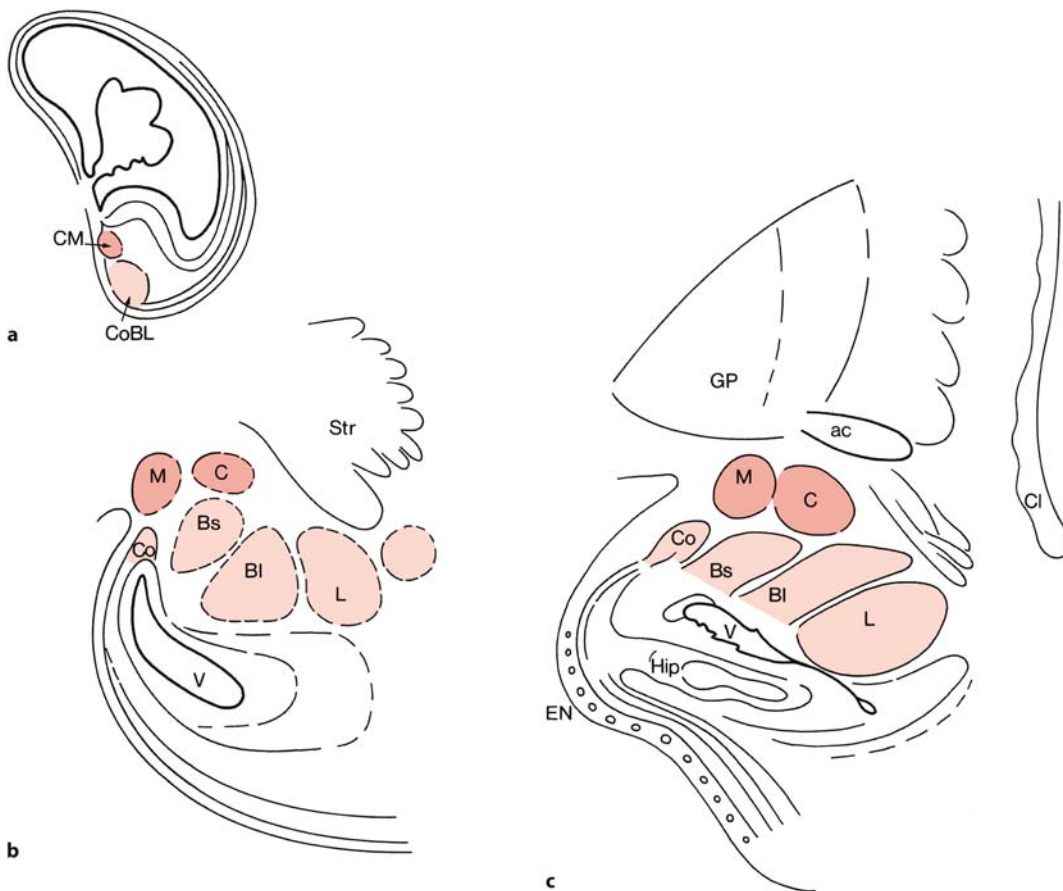
Fig. 9.63 Development of the human amygdala: **a** frontal section through the forebrain of a 35-mm-CRL embryo; **b**, **c** the amygdalar complex in a 4-month-old embryo and an 8-month-old fetus, respectively. The centromedial cell group (*CM*) and its derivatives are indicated in *red*, and the corticobasolateral cell group (*CoBL*) and its derivatives in *light red*. *ac* anterior commissure, *Bl* large-celled part of basal nucleus, *Bs* small-celled part of basal nucleus, *C* central nucleus, *Cl* claustrum, *Co* cortical nucleus, *EN* entorhinal cortex (with cell nests), *GP* globus pallidus, *Hip* hippocampus, *L* lateral nucleus, *M* medial nucleus, *Str* striatum. (**a** After Stephan 1975; **b**, **c** after Kahle 1969)

dial amygdala is recognized as a thickening in the ventrocaudal wall of the interventricular foramen as soon as the cerebral hemisphere has evaginated (stages 14–16). Apparently, slightly later, the medial nucleus develops first, followed by the basolateral complex later at stage 20. All amygdaloid nuclei are present by stages 21–22. Kahle (1969) and Ulfig and co-workers (Ulfig 2002b; Ulfig et al. 2003a, b) studied the fetal development of the human amygdala (Fig. 9.63). In the fifth and six gestational month, the inferior part of the amygdala reveals cell-dense columns merging with the caudal part of the ganglionic eminence. These columns contain vimentin-positive glial fibres which provide a scaffold for migrating neurons. In the seventh and eighth months, distinct reorganization of the cytoarchitecture of the amygdala occurs, accompanied by a rearrangement and disappearance of vimentin-positive fibres. On the whole, the amygdala has reached a high degree of maturity in the eighth month. The amygdala may be involved in Ammon's horn sclerosis and in schizophrenia and other neurobehavioural disorders (Chap. 10).

References

Acampora D, Merlo GR, Paleari L, Zerega B, Postiglione MP, Mantero S, Bober E, Barbieri O, Simeone A, Levi S (1999) Craniofacial, vestibular and bone defects in mice lacking the *Distal-less*-related gene *Dlx5*. Development 126:3795–3809

Adelmann HB (1929a) Experimental studies on the development of the eye. I. The effect of the removal of median and lateral areas of the anterior end of the urodelan neural plate on the development of the eyes (*Triton teniatus* and *Amblystoma punctatum*). J Exp Zool 54:249–290

Adelmann HB (1929b) Experimental studies on the development of the eye. II. The eye-forming potencies of the median portions of the urodelan neural plate (*Triton teniatus* and *Amblystoma punctatum*). J Exp Zool 54:291–317

Adelmann HB (1930) Experimental studies on the development of the eye. III. The effect of the substrate ('Unterlagerung') on the heterotopic development of median and lateral strips of the anterior end of the neural plate of *Amblystoma*. J Exp Zool 57:223–281

Adelmann HB (1936a) The problem of cyclopia, Part I. Quart Rev Biol 11:116–182

Adelmann HB (1936b) The problem of cyclopia, Part II. Quart Rev Biol 11:284–364

Aicardi J (1998) Disorders of visual perception. In: Aicardi J Diseases of the Nervous System in Childhood, 2nd ed. Mac Keith, London, pp 675–688

Aicardi J, Chevrie JJ, Baraton J (1987) Agenesis of the corpus callosum. Handb Clin Neurol 50:149–173

Alexander GE, DeLong MR, Strick PL (1986) Parallel organization of functionally segregated circuits linking basal ganglia and cortex. Annu Rev Neurosci 9:357–381

Alheid GF, Heimer L (1988) New perspectives in basal forebrain organization of special relevance for neuropsychiatric disorders: The striatopallidal, amygdaloid, and corticopetal components of substantia innominata. Neuroscience 27:1–39

Alheid GF, Heimer L, Switzer RC (1990) Basal ganglia. In: Paxinos G (ed) The Human Nervous System. Academic Press, San Diego, CA, pp 483–582

Alheid GF, de Olmos JS, Beltramino CA (1995) Amygdala and extended amygdala. In: Paxinos G (ed) The Rat Nervous System, 2nd ed. Academic, San Diego, CA, pp 495–578

Almqvist PM, Akesson E, Wahlberg LU, Pschera H, Seiger Å, Sundström E (1996) First trimester development of the human nigrostriatal dopamine system. Exp Neurol 139:227–237

Altman J (1969) Autoradiographic and histological studies of postnatal neurogenesis. IV. Cell proliferation and migration in the anterior forebrain, with special reference to persisting neurogenesis in the olfactory bulb. J Comp Neurol 137:433–457

Altman J, Bayer SA (1978a) Development of the diencephalon in the rat. I. Autoradiographic study of the time of origin and settling patterns of neurons of the hypothalamus. J Comp Neurol 182:945–972

Altman J, Bayer SA (1978b) Development of the diencephalon in the rat. II. Correlation of the embryonic development of the hypothalamus with the time of origin of its neurons. J Comp Neurol 192:973–994

Altman J, Bayer SA (1979a) Development of the diencephalon in the rat. IV. Quantitative study of the time of origin of neurons and the internuclear chronological gradients in the thalamus. J Comp Neurol 188:455–472

Altman J, Bayer SA (1979b) Development of the diencephalon in the rat. V. Thymidine-radiographic observations on internuclear and intranuclear gradients in the thalamus. J Comp Neurol 188:473–500

Altman J, Bayer SA (1979c) Development of the diencephalon in the rat. VI. Re-evaluation of the embryonic development of the thalamus on the basis of thymidine-radiographic datings. J Comp Neurol 188:501–524

Altman J, Bayer SA (1981) Development of the brain stem in the rat. V. Thymidine-radiographic study of the time of origin of neurons in the midbrain tegmentum. J Comp Neurol 198:677–716

Altman J, Bayer SA (1986) The development of the rat hypothalamus. Adv Anat Embryol Cell Biol 100:1–178

Amaral DG (1987) Memory: Anatomical organization of candidate brain regions. In: Handbook of Physiology, Section I: The Nervous System, Vol 5, Part 1 (Mountcastle VB, Plum F, Geiger SR, eds). Am Physiol Soc, Bethesda, MD, pp 211–294

Andersen H, von Bülow FA, Mollgård K (1971) The early development of the pars distalis of the human foetal pituitary gland. Z Anat Entw Gesch 135:117–138

Anderson SA, Eisenstat DD, Shi L, Rubinstein JLR (1997a) Interneuron migration from basal forebrain to neocortex: Dependence on Dlx genes. Science 278:474–476

Anderson SA, Qiu M, Bulfone A, Eisenstat DD, Meneses JJ, Pedersen RA, Rubinstein JLR (1997b) Mutations of the homeobox genes *Dlx-1* and *Dlx-2* disrupt the striatal subventricular zone and differentiation of late born striatal neurons. Neuron 19:27–37

Anderson SA, Mione M, Yun K, Rubinstein JLR (1999) Differential origins of neocortical projection and local circuit neurons: Role of Dlx genes in neocortical interneurogenesis. Cereb Cortex 9:646–654

Anderson SA, Marín O, Horn C, Jennings K, Rubinstein JLR (2001) Distinct cortical migrations from the medial and lateral ganglionic eminences. Development 128:353–363

Angevine JB Jr (1970) Time of neuron origin in the diencephalon of the mouse. An autoradiographic study. J Comp Neurol 139:129–188

Angevine JB Jr (1978) Embryogenesis and phylogenesis in the limbic system. In: Livingston KE, Hornykiewicz O (eds) Limbic Mechanisms. The Continuing Evolution of the Limbic System Concept. Plenum, New York, pp 23–46

Apkarian P, Bour L, Barth PG (1993) A unique achiasmatic anomaly detected in non-albinos with misrouted retinal-fugal projections. Eur J Neurosci 6:501–507

Apkarian P, Bour L, Barth PG, Wenniger-Prick L, Verbeeten B (1995) Non-decussating retinal-fugal fibre syndrome. An inborn achiasmatic malformation with visuotopic misrouting, visual evoked potential ipsilateral asymmetry and nystagmus. Brain 118:1195–1216

Armstrong E (1990) Limbic thalamus: Anterior and mediodorsal nuclei. In: Paxinos G (ed) The Human Nervous System. Academic, San Diego, CA, pp 469–481

Asa SL, Kovacs K, Laszlo FA, Domokos I, Ezrin C (1986) Human fetal adenohypophysis. Histologic and immunocytochemical analysis. Neuroendocrinology 43:308–316

Asa SL, Kovacs K, Horvath E, Losinski NE, Laszlo FA, Domokos I, Halliday WC (1988) Human fetal adenohypophysis. Electron microscopic and ultrastructural immunocytochemical analysis. Neuroendocrinology 48:423–431

Ashton W (1970) Retinal angiogenesis in the human embryo. Br Med Bull 26:103–106

Ashwell KWS, Waite PME (2004) Development of the peripheral nervous system. In: Paxinos G, Mai JK (eds) The Human Nervous System, 2nd ed. Elsevier, Amsterdam, pp 95–110

Atwell WJ (1926) The development of the hypophysis cerebri in man, with special reference to the pars tuberalis. Am J Anat 37:159–193

Aubert I, Brana C, Pellevoisin C, Giros B, Caillé I, Carles D, Vital C, Bloch B (1997) Molecular anatomy of the development of the human substantia nigra. J Comp Neurol 379:72–87

Auladell C, Pérez-Sust P, Supèr H, Soriano E (2000) The early development of thalamocortical and corticothalamic projections in the mouse. Anat Embryol (Berl) 201:169–179

Aza-Blanc P, Kornberg TB (1999) *Ci*: A complex transducer of the hedgehog signal. Trends Genet 15:458–462

Baenziger O, Martin E, Steinlin M, Good M, Largo R, Burger R, Fanconi S, Duc G, Buchli R, Rumpel H, Boltshauser E (1993) Early pattern recognition in severe perinatal asphyxia: A prospective MRI study. Neuroradiology 35:437–442

Bahnsen U, Oosting P, Swaab DF, Nahke P, Richter D, Schmale H (1992) A missense mutation in the vasopressin-neurophysin precursor gene cosegregates with human autosomal dominant neurohypophyseal diabetes insipidus. EMBO J 11:19–23

Ballabio A, Rugarli EI (2001) Kallmann syndrome. In: Scriver CR, Beaudet AL, Sly WS, Valle D (eds) The Metabolic & Molecular Bases of Inherited Disease, 8th ed. McGraw-Hill, New York, pp 5729–5740

Barishak YR (2001) Embryology of the Eye and Its Adnexa, 2nd ed. Karger, Basel

Barkovich AJ (2000) Pediatric Neuroimaging, 3rd ed. Lippincott Williams & Wilkins, Philadelphia, PA

Barkovich AJ, Norman D (1989) Absence of the septum pellucidum: A useful sign in the diagnosis of congenital brain malformations. Am J Radiol 152:353–360

Barkovich AJ, Quint DJ (1993) Middle interhemispheric fusion: An unusual variant of holoprosencephaly. AJNR Am J Neuroradiol 14:431–440

Barkovich AJ, Fram EK, Norman D (1989) Septo-optic dysplasia: MR imaging. Radiology 171:189–192

Barkovich AJ, Simon EM, Clegg NJ, Kinsman SL, Hahn JS (2002) Analysis of the cerebral cortex in holoprosencephaly with attention to the sylvian fissures. AJNR Am J Neuroradiol 23:143–150

Basel-Vanagaite L, Straussberg R, Ovadia H, Kaplan A, Magal N, Shorer Z, Shalev H, Walsh C, Shohat M (2004) Infantile bilateral striatal necrosis maps to chromosome 19q. Neurology 62: 87–90

Bayer SA (1980) Quantitative radiographic analysis of neurogenesis in the rat amygdala. J Comp Neurol 194:845–875

Bayer SA (1983) [³H]Thymidine-radiographic studies of neurogenesis in the rat olfactory bulb. Exp Brain Res 50:329–340

Bayer SA (1984) Neurogenesis in the rat neostriatum. Int J Dev Neurosci 2:163–175

Bayer SA (1985a) Neurogenesis in the olfactory tubercle and islands of Calleja in the rat. Int J Dev Neurosci 3:135–147

Bayer SA (1985b) Neurogenesis in the magnocellular basal telencephalic nuclei in the rat. Int J Dev Neurosci 3:229–243

Bayer SA (1986a) Neurogenesis in the anterior olfactory nucleus and its associated transition areas in the rat brain. Int J Dev Neurosci 4:225–249

Bayer SA (1986b) Neurogenesis in the rat primary olfactory cortex. Int J Dev Neurosci 4:251–271

Bayer SA, Altman J (1987a) Development of the preoptic area: Time and site of origin, migratory routes, and settling of its neurons. J Comp Neurol 265:65–95

Bayer SA, Altman J (1987b) Directions in neurogenetic gradients and patterns of anatomical connections in the telencephalon. Prog Neurobiol 29:57–106

Bayer SA, Altman J (1995a) Neurogenesis and migration. In: Paxinos G (ed) The Rat Nervous System, 2nd ed. Academic, San Diego, CA, pp 1041–1078

Bayer SA, Altman J (1995b) Principles of neurogenesis, neuronal migration, and neural circuit formation. In: Paxinos G (ed) The Rat Nervous System, 2nd ed. Academic, San Diego, CA, pp 1079–1098

Bayer SA, Altman J, Russo RJ, Zhang X (1995) Embryology. In: Duckett S (ed) Pediatric Neuropathology. Williams & Wilkins, Baltimore, MD, pp 54–107

Belloni E, Muenke M, Roessler E, Traverso G, Siegel-Bartelt J, Frumkin A, Mitchell HF, Donis-Keller H, Helms C, Hing AV, et al. (1996) Identification of Sonic hedgehog as a candidate gene responsible for holoprosencephaly. Nat Genet 14:353–356

Bergeron C, Kovacs K, Ezrin C, Mizzen C (1991) Hereditary diabetes insipidus: An immunohistochemical study of the hypothalamus and pituitary gland. Acta Neuropathol (Berl) 81:345–348

Bergquist H, Källén B (1954) Notes on the early histogenesis and morphogenesis of the central nervous system in vertebrates. J Comp Neurol 100:627–659

Berliner DL, Monti-Bloch L, Jennings-White C, Diaz-Sanchez V (1996) The functionality of the human vomeronasal organ (VNO): Evidence for steroid receptors. J Steroid Biochem Mol Biol 58:259–265

Blaas H-GK, Eriksson AG, Salvesen KÅ, Isaksen CV, Christensen B, Møllerløkken G, Eik-Nes SH (2002) Brains and faces in holoprosencephaly: Pre- and postnatal description of 30 cases. Ultrasound Obstet Gynecol 19:24–38

Blakemore C, Molnár Z (1990) Factors involved in the establishment of specific interconnections between thalamus and cerebral cortex. Cold Spring Harbor Symp Quant Biol 55: 491–504

Boehm N, Roos J, Gasser B (1994) Luteinizing hormone-releasing hormone (LHRH)-expressing cells in the nasal septum of human fetuses. Dev Brain Res 82:175–180

Bossy J (1980) Development of olfactory and related structures in staged human embryos. Anat Embryol (Berl) 161:225–236

Boyd JD (1956) Observations on the human pharyngeal hypophysis. J Endocrinol 14:66–77

Braak H, Braak E (1987) The hypothalamus of the human adult: Chiasmatic region. Anat Embryol (Berl) 176:315–330

Braak H, Braak E (1992) Anatomy of the human hypothalamus (chiasmatic and tuberal regions). Prog Brain Res 93:3–16

Braddock SR, Grafe MR, Jones KL (1995) Development of the olfactory nerve: Its relationship to the craniofacies. Teratology 51:252–256

Braisted JE, Catalano SM, Stimac R, Kennedy TE, Tessier-Lavigne M, Shatz CJ, O'Leary DDM (2000) Netrin-1 promotes thalamic axon growth and is required for proper development of the thalamocortical projection. J Neurosci 20:5792–5801

Brana C, Charron G, Aubert I, Carles D, Martin-Negrier ML, Trouette H, Fournier MC, Vital C, Bloch B (1995) Ontogeny of the striatal neurons expressing neuropeptide genes in the human fetus and neonate. J Comp Neurol 360:488–505

Brana C, Caillé I, Pellevoisin C, Charron G, Aubert I, Caron MG, Carles D, Vital C, Bloch B (1996) Ontogeny of the striatal neurons expressing the D_1 dopamine receptors in humans. J Comp Neurol 370:23–34

Brand S, Rakic P (1979) Genesis of the primate neostriatum: [³H]Thymidine autoradiographic analysis of the time of neuron origin in the rhesus monkey. Neuroscience 4:767–778

Brand S, Rakic P (1984) Cytodifferentiation and synaptogenesis in the neostriatum of fetal and neonatal rhesus monkeys. Anat Embryol (Berl) 169:21–34

Braverman LE, Mancini JP, McGoldrick DM (1965) Hereditary idiopathic diabetes insipidus. Ann Int Med 63:563–568

Brazel CY, Romanko MJ, Rothstein RP, Levison SW (2003) Roles of the mammalian subventricular zone in brain development. Prog Neurobiol 69:49–69

Brewer DB (1957) Congenital absence of the pituitary gland and its consequences. J Pathol Bacteriol 73:59–67

Brewer GJ, Fink JK, Hedera P (1999) Diagnosis and treatment of Wilson's disease. Semin Neurol 19:261–270

Brickman JM, Clements M, Tyrell R, McNay D, Woods K, Warner J, Stewart A, Beddington RSP, Dattani M (2001) Molecular effects of novel mutations in *Hesx1/HESX1* associated with human pituitary disorders. Development 128:5189–5199

Brodsky MC, Hoyt WF, Hoyt CS, Miller NR, Lam BL (1995) Atypical retinochoroidal coloboma in patients with dysplastic optic discs and transsphenoidal encephaloceles. Arch Ophthalmol 113:624–628

Brown GK, Brown RM, Scholem RD, Kirby DM, Dahl H-HM (1989) The clinical and biochemical spectrum of human pyruvate dehydrogenase complex deficiency. Ann NY Acad Sci 573: 360–368

Brown SA, Warburton D, Brown LY, Yu C, Roeder ER, Stengel-Rutkowski S, Hennekam RCM, Muenke M (1998) Holoprosencephaly due to mutations in *ZIC2*, a homologue of *Drosophila odd-paired*. Nat Genet 20:180–183

Brückner G, Mares V, Biesold D (1976) Neurogenesis in the visual system of the rat: An autoradiographic investigation. J Comp Neurol 166:245–256

Bruyn GW (1977) Agenesis septi pellucidi, cavum septi pellucidi, cavum Vergae, and cavum veli interpositi. Handb Clin Neurol 30:299–316

Bulfone A, Puelles L, Porteus MH, Frohman MA, Martin GR, Rubinstein JLR (1993) Spatially restricted expression of *Dlx-1, Dlx-2, (Tes-1), Gbx-2,* and *Wnt-3* in the embryonic day 12.5 mouse forebrain defines potential transverse and longitudinal boundaries. J Neurosci 13:3155–3172

Bulfone A, Wang F, Hevner RF, Anderson SA, Cutforth T, Chen S, Meneses JJ, Pedersen RA, Axel R, Rubinstein JLR (1998) An olfactory sensory map develops in the absence of normal projection neurons or GABAergic interneurons. Neuron 21:1273–1282

Burmeister M, Novak J, Liang MY, Basu S, Ploder L, Hawes NL, Vidgen D, Hoover F, Goldman D, Kalnins VI, et al. (1996) Ocular retardation mouse caused by *Chx10* homeobox null allele: Impaired retinal progenitor proliferation and bipolar cell differentiation. Nat Genet 12:376–384

Butler AB, Molnár Z (2002) Development and evolution of the collopallium in amniotes: A new hypothesis of field homology. Brain Res Bull 57:475–479

Camper S, Suh H, Raetzman L, Douglas K, Cushman L, Nasonkin I, Burrows H, Gage P, Martin D (2002) Pituitary gland development. In: Rossant J, Tam PPL (eds) Mouse Development – Patterning, Morphogenesis, and Organogenesis. Academic, San Diego, CA, pp 499–518

Campbell K (2003) Dorsal-ventral patterning in the mammalian telencephalon. Curr Opin Neurobiol 13:50–56

Carson MJ, Slager UT, Steinberg RM (1977) Simultaneous occurrence of diabetes mellitus, diabetes insipidus, and optic atrophy in a brother and sister. Am J Dis Child 131:1382

Casarosa S, Fode C, Guillemot F (1999) *Mash1* regulates neurogenesis in the ventral telencephalon. Development 126:525–534

Cau E, Casarosa S, Guillemot F (2002) *Mash1* and *Ngn1* control distinct steps of determination and differentiation in the olfactory sensory neuron lineage. Development 129:1871–1880

Chevrie JJ, Aicardi J (1986) Aicardi syndrome. In: Pedley TA, Meldrum BS (eds) Recent Advances in Epilepsy, Vol 3. Churchill Livingstone, Edinburgh, pp 189–210

Chiang C, Litingtung Y, Lee E, Young KE, Corden JL, Westphal H, Beachy PA (1996) Cyclopia and defective axial patterning in mice lacking *Sonic hedgehog* gene function. Nature 383:407–413

Chong BW, Newton TH (1993) Hypothalamic and pituitary pathology. Radiol Clin North Am 31:1147–1183

Chow CW, Haan EA, Goodman SI, Anderson RMcD, Evans WA, Kleinschmidt-DeMasters BK, Wise G, McGill JJ, Danks DM (1988) Neuropathology in glutaric acidaemia type 1. Acta Neuropathol (Berl) 76:590–594

Chugani HT, Phelps ME (1986) Maturational changes in cerebral function in infants determined by 18 FDG positron emission tomography. Science 231:840–843

Clarke S, Miklossy J (1990) Occipital cortex in man: Organization of callosal connections, related myelo- and cytoarchitecture, and putative boundaries of functional visual areas. J Comp Neurol 298:188–214

Cohen MM Jr (1989a) Perspectives on holoprosencephaly: Part I. Epidemiology, genetics, and syndromology. Teratology 40:211–235

Cohen MM Jr (1989b) Perspectives on holoprosencephaly: Part III. Spectra, distinctions, continuities, and discontinuities. Am J Med Genet 34:271–288

Cohen MM Jr, Shiota K (2002) Teratogenesis of holoprosencephaly. Am J Med Genet 109:1–15

Cohen MM Jr, Sulik KK (1992) Perspectives on holoprosencephaly: Part II. Central nervous system, craniofacial anatomy, syndrome commentary, diagnostic approach, and experimental studies. J Craniofac Genet Dev Biol 12:196–244

Cohen NR, Taylor CJSH, Scott LB, Guillery RW, Soriano P, Furley AJW (1997) Errors in corticospinal axon guidance in mice lacking the neural cell adhesion molecule L1. Curr Biol 8:26–33

Colohan ART, Grady MS, Bonnin JM, Thorner MO, Kovacs K, Jane JA (1987) Ectopic pituitary gland simulating a suprasellar tumor. Neurosurgery 20:43–48

Conklin JL (1968) The development of the human fetal adenohypophysis. Anat Rec 160:79–91

Cooper ERA (1945) The development of the human lateral geniculate body. Brain 68:222–239

Cooper ERA (1946) The development of the human substantia nigra. Brain 69:22–33

Cooper ERA (1950) The development of the thalamus. Acta Anat (Basel) 9:201–226

Corbin JG, Gaiano N, Machold RP, Langston A, Fishell G (2000) The *Gsh2* homeodomain gene controls multiple aspects of telencephalic development. Development 127:5007–5020

Corbin JG, Nery S, Fishell G (2001) Telencephalic cells take a tangent: Non-radial migration in the mammalian forebrain. Nat Neurosci 4(Suppl):1177–1182

Corsellis JAN, Bruton CJ, Freeman-Browne D (1973) The aftermath of boxing. Psychol Med 3:270–303

Couly GF, Le Douarin NM (1987) Mapping of the early neural primordium in quail-chick chimeras. II. The prosencephalic neural plate and neural folds: Implications for the genesis of cephalic congenital abnormalities. Dev Biol 120:198–214

Cremers CWRJ, Wijdeveld PGAB, Pinckers AJLG (1977) Juvenile diabetes mellitus, optic atrophy, hearing loss, diabetes insipidus, atonia of the urinary tract and bladder, and other abnormalities (Wolfram's syndrome): A review of 88 cases from the literature with personal observations on 3 new patients. Adv Paed Scand (Suppl) 264:3–16

Croen LA, Shaw GM, Lammer EJ (1996) Holoprosencephaly: Epidemiologic and clinical characteristics of a California population. Am J Med Genet 64:465–472

Crosby EC, Humphrey T (1941) Studies of the vertebrate telencephalon. II. The nuclear pattern of the anterior olfactory nucleus, tuberculum olfactorium and the amygdaloid complex in adult man. J Comp Neurol 74:309–352

Crosby EC, Woodburne RT (1940) The comparative anatomy of the preoptic area and the hypothalamus. Proc Assoc Res Nerv Ment Dis 20:52–169

Dahmane N, Sánchez P, Gitton Y, Palma V, Sun T, Beyna M, Weiner H, Ruiz i Altaba A (2001) The sonic hedgehog-Gli pathway regulates dorsal brain growth and tumorigenesis. Development 128:5201–5212

Dahme M, Bartsch U, Martini R, Anliker B, Schachner M, Mantei N (1997) Disruption of the mouse L1 gene leads to malformations of the nervous system. Nat Genet 17:346–349

Daikoku S, Chikamori M, Adachi T, Maki Y (1982) Effect of basal diencephalon on the development of Rathke's pouch in rats: A study in combined organ culture. Dev Biol 90:198–202

Darin N, Oldfors A, Moslemi A-R, Tulinius M (2001) The incidence of mitochondrial encephalomyopathies in childhood: Clinical features and morphological, biochemical, and DNA abnormalities. Ann Neurol 49:377–383

Dasen JS, Barbera JP, Herman TS, Connell SO, Olsen L, Ju B, Tollkuhn J, Baek SH, Rose DW, Rosenfeld MG (2001) Temporal regulation of a paired-like homeodomain repressor/TLE corepressor complex and a related activator is required for pituitary organogenesis. Genes Dev 15:3193–3207

Dattani MT, Robinson JC (2000) The molecular basis for developmental disorders of the pituitary gland in man. Clin Genet 57:337–346

Dattani MT, Martinez-Barbera JP, Thomas PQ, Brickman JM, Gupta R, Mårtensson IL, Toresson H, Fox M, Walsh JKH, Hindmarsh PC, et al. (1998) Mutations in the homeobox gene *HESX1/Hesx1* associated with septo-optic dysplasia in human and mouse. Nat Genet 19:125–133

Dattani MT, Martinez-Barbera JP, Thomas PQ, Brickman JM, Gupta R, Wales JKH, Hindmarsh PC, Beddington RSP, Robinson ICAF (1999) HESX1: A novel gene implicated in a familial form of septo-optic dysplasia. Acta Paediatr Suppl 88:49–54

Deacon TW, Pakzaban P, Isacson O (1994) The lateral ganglionic eminence is the origin of cells committed to striatal phenotypes: Neural transplantation and developmental evidence. Brain Res 668:211–219

de Carlos JA, López-Mascaraque L, Valverde F (1995) The telencephalic vesicles are innervated by olfactory placode-derived cells: A possible mechanism to induce neocortical development. Neuroscience 68:1167–1178

de Carlos JA, López-Mascaraque L, Valverde F (1996) Dynamics of cell migration from the lateral ganglionic eminence in the rat. J Neurosci 16:6146–6156

Decker RE (1985) The ectopic pituitary gland in cases of craniopharyngiomas. Report of two cases. J Neurosurg 62:291–292

Dekaban A (1954) Human thalamus: An anatomical, developmental, and pathological study. II. Development of the human thalamic nuclei. J Comp Neurol 100:63–97

DeLong MR, Georgopoulos AP (1981) Motor functions of the basal ganglia. In: Brooks VB (ed) Handbook of Physiology, Sect 1: The Nervous System, Vol 2: Motor Control. American Physiological Society, Bethesda, MD, pp 1017–1061

Demb JB, Boynton GM, Heeger DJ (1998) Functional magnetic resonance imaging of early visual pathways in dyslexia. J Neurosci 18:6939–6951

de Morsier G (1956) Etudes sur les dysraphies crânio-encéphaliques. III. Agénésie du septum lucidum avec malformation du tractus optique. La dysplasie septo-optique. Schweiz Arch Neurol Psychiatr 77:267–292

DeMyer WE (1987) Holoprosencephaly (cyclopia-arhinencephaly). Handb Clin Neurol 50:225–244

DeMyer WE, Zeman W (1963) Alobar holoprosencephaly (arhinencephaly) with median cleft lip and palate: Clinical, nosologic and electroencephalographic considerations. Confin Neurol 23:1–36

DeMyer WE, Zeman W, Palmer C (1964) The face predicts the brain: Diagnostic significance of median anomalies for holoprosencephaly (arhinencephaly). Pediatrics 34:256–263

de Olmos J (1990) Amygdaloid nuclear gray complex. In: Paxinos G (ed) The Human Nervous System. Academic, San Diego, CA, pp 583–710

de Olmos J (2004) Amygdala. In: Paxinos G, Mai JK (eds) The Human Nervous System, 2nd ed. Elsevier, Amsterdam, pp 739–868

Depew MJ. Liu JK, Long JE, Presley R, Meneses JJ, Pedersen RA, Rubinstein JLR (1999) Dlx5 regulates regional development of the branchial arches and sensory capsules. Development 126:3831–3846

Dierickx K, Vandesande F (1977) Immunocytochemical localization of the vasopressinergic and ocytocinergic neurons in the human hypothalamus. Cell Tissue Res 184:15–27

Dode C, Levilliers J, Dupont JM, de Paepe A, le Du N, Soussi-Yanicostas N, et al. (2003) Loss-of-function mutations in FGFR1 cause autosomal dominant Kallmann syndrome. Nat Genet 33:463–465

Dou CL, Li S, Lai E (1999) Dual role of brain factor-1 in regulating growth and patterning of the cerebral hemispheres. Cereb Cortex 9:543–550

Dowling JE (1987) The Retina: An approachable part of the brain. Belknap, Cambridge, MA

Drayer B, Burger P, Darwin R, Riederer S, Herfkens R, Johnson GA (1986) Magnetic resonance imaging of brain iron. Am J Neuroradiol 7:373–380

Droogleever Fortuyn AB (1912) Die Ontogenie der Kerne des Zwischenhirns beim Kaninchen. Arch Anat Physiol, Anat Abt 36:303–352

Dryja TP (2001) Retinitis pigmentosa and stationary night blindness. In: Scriver CR, Beaudet AL, Sly WS, Valle D (eds) The Metabolic and Molecular Bases of Inherited Disease, 8th ed. McGraw-Hill, New York, pp 5903–5933

Dufour A, Seibt J, Passante L, Depaepe V, Ciossek T, Frisén J, Kullander K, Flanagan JG, Polleux F, Vanderhaeghen P (2003) Area specificity and topography of thalamocortical projections are controlled by ephrin/Eph genes. Neuron 391:453–465

Dulac C, Torello AT (2003) Molecular detection of pheromone signals in mammals: From genes to behaviour. Nat Rev Neurosci 4:551–562

Eagleson GW, Jenks BL, van Overbeeke AP (1986) The pituitary adrenocorticotropes originates from neural ridge tissue in *Xenopus laevis*. J Embryol Exp Morphol 95:1–14

Earle KL, Mitrofanis J (1996) Genesis and fate of the perireticular thalamic nucleus during early development. J Comp Neurol 367:246–263

Edison R, Muenke M (2003) The interplay of genetic and environmental factors in craniofacial morphogenesis: Holoprosencephaly and the role of cholesterol. Cong Anom 43:1–21

Eisenstat DD, Liu JK, Mione M, Zhong W, Yu G, Anderson SA, Ghattas I, Puelles L, Rubinstein JLR (1999) DLX-1, DLX-2, and DLX-5 expression define distinct stages of basal forebrain differentiation. J Comp Neurol 414:217–237

Ellison-Wright Z, Heyman I, Frampton I, Rubia K, Chitnis X, Ellison-Wright I, Williams SCR, Suckling J, Simmons A, Bullmore E (2004) Heterozygous PAX6 mutation, adult brain structure and fronto-striato-thalamic function in a human family. Eur J Neurosci 19:1505–1512

Favor J, Sandulache R, Neuhäuser-Klaus A, Pretsch W, Chatterjee B, Senft E, Wurst W, Blanquet V, Grimes P, Spörle R, Schughart K (1996) The mouse *Pax2[1Neu]* mutation is identical to a human *PAX2* mutation in a family with renal-coloboma syndrome and results in developmental defects of the brain, ear, eye, and kidney. Proc Natl Acad Sci USA 93:13870–13875

Fazzi E, Signonni SG, Scelsa B, Bova SM, Lanzi G (2003) Leber's congenital amaurosis: An update. Eur J Pediatr Neurol 7:13–22

Fentress JC, Stanfield BB, Cowan WM (1981) Observations on the development of the striatum in mice and rats. Anat Embryol (Berl) 163:275–298

Fernández-Alvarez E, Aicardi J (2001) Movement Disorders in Children. Mac Keith London

Figdor MC, Stern CD (1993) Segmental organization of embryonic diencephalon. Nature 363:630–634

Florell SR, Townsend JJ, Klatt EC, Pysher TJ, Coffin CM, Wittwer CT, Viskochil DH (1996) Aprosencephaly and cerebellar dysgenesis in sibs. Am J Med Genet 63:542–548

Franco B, Guiolo S, Pragliola A, Incerti B, Bardoni B, Tonlorenzi R, Carrozzo R, Maestrini E, Pieretti M, Taillon-Milar P, et al. (1991) A gene deleted in Kallmann's syndrome shares homology with neural cell adhesion and axonal pathfinding molecules. Nature 353:529–536

Franz T (1994) Extra-toes (Xt) homozygous mutant mice demonstrate a role for the Gli-3 gene in the development of the forebrain. Acta Anat (Basel) 150:38–44

Freeman TB, Spence MS, Boss BD, Spector DH, Strecker RE, Ola CW, Kordower JH (1991) Development of dopaminergic neurons in the human substantia nigra. Exp Neurol 113:344–353

Friede R (1989) Developmental Neuropathology, 2nd ed. Springer, Berlin Heidelberg New York

Fuhrmann S, Chow L, Reh TA (2000) Molecular control of cell diversification in the vertebrate retina. In: Fini ME (ed) Vertebrate Eye Development. Springer, Berlin Heidelberg New York, pp 69–91

Furuta Y, Piston DW, Hogan BLM (1997) Bone morphogenetic proteins (BMPs) as regulators of dorsal forebrain development. Development 124:2203–2212

Gabreëls BATF (1998) Vasopressin Secretion Disorders in Diabetes Insipidus, Prader-Willi Syndrome and Wolfram Syndrome. Thesis, University of Amsterdam

Gabreëls BATF, Swaab DF, Seidah NG, van Duijnhoven HLP, Martens GJM, van Leeuwen FW (1994) Differential expression of the neuroendocrine polypeptide 7B2 in hypothalami of Prader-(Labhart)-Willi syndrome patients. Brain Res 657:281–293

Gabreëls BATF, Swaab DF, de Kleijn DPV, Seidah NG, van de Loo J-W, van de Ven WJM, Martens GJM, van Leeuwen FW (1998) Attenuation of the polypeptide 7B2, prohormone convertase PC2 and vasopressin in the hypothalamus of some Prader-Willi patients: Indications for a processing defect. J Clin Endocrinol Metab 83:591–599

Gage PJ, Suh H, Camper SA (1999) Dosage requirement of Pitx2 for development of multiple organs. Development 126:4643–4651

Garcia CA, Duncan C (1997) Atelencephalic microcephaly. Dev Med Child Neurol 19:227–232

Garel S, Yun K, Grosschedl R, Rubinstein JLR (2002) The early topography of thalamocortical projections shifted in *Ebf1* and *Dlx1/2* mutant mice. Development 129:5621–5634

Gastaut H, Lammers HJ (1961) Anatomie du rhinencéphale. Masson, Paris

Geoffroy Saint-Hilaire I (1832–1837) Histoire générale et particulière des anomalies de l'organisation chez l'homme et les animaux (Traité de Tératologie). Baillière, Paris

Gérard M, Abitbol M, Delezoide A-L, Dufier J-L, Mallet J, Vekemans M (1995) PAX-genes expression during human embryonic development, a preliminary report. C R Acad Sci Paris 318:57–66

Gerfen CR, Wilson CJ (1996) The basal ganglia. In: Swanson LW, Björklund A, Hökfelt T (eds) Handbook of Chemical Neuroanatomy, Vol 12: Integrated Systems of the CNS, Part III. Elsevier, Amsterdam, pp 371–468

Ghosh A, Shatz CJ (1992) Pathfinding and target selection by developing geniculocortical axons. J Neurosci 12:39–55

Gilbert M (1935) The early development of the human diencephalon. J Comp Neurol 62:81–115

Glaser T, Cai J, Epstein J, Walton DS, Jepeal L, Maas RL (1995) *PAX6* mutations in aniridia. In: Wiggs JR (ed) Molecular Genetics of Eye Diseases. Wiley, New York, pp 51–82

Golden JA (1998) Holoprosencephaly: A defect in brain patterning. J Neuropathol Exp Neurol 57:991–999

Goldman PS, Nauta WJH (1977) An intricately patterned prefrontocaudate projection in the rhesus monkey. J Comp Neurol 171:369–386

Goldman-Rakic PS (1981) Prenatal formation of cortical input and development of cytoarchitectonic compartments in the neostriatum of the rhesus monkey. J Neurosci 1:721–735

Goldman-Rakic PS (1982) Cytoarchitectonic heterogeneity of the primate neostriatum: Subdivision into *island* and *matrix* cellular compartments. J Comp Neurol 205:398–413

González G, Puelles L, Medina L (2002) Organization of the mouse dorsal thalamus based on topology, calretinin immunostaining, and gene expression. Brain Res Bull 57:439–442

Goodman SI, Frerman FE (2001) Organic acidemia due to defects in lysine oxidation: 2-Ketoadipic acidemia and glutaric acidemia. In: Scriver CR, Beaudet AL, Sly WS, Valle D (eds) The Metabolic & Molecular Bases of Inherited Disease, 8th ed. McGraw-Hill, New York, pp 2195–2206

Goodman SI, Norenberg MD, Shikes RH, Breslick DJ, Moe PG (1977) Glutaric aciduria: Biochemical and morphological considerations. J Pediatr 90:746–750

Goodman SI, Stein DE, Schlesinger S, Christensen E, Schwartz M, Greenberg CR, Elpeleg ON (1998) Glutaryl-CoA dehydrogenase mutations in glutaric acidemia (type 1): Review and report of thirty novel mutations. Hum Mutat 12:141–144

Gorski RA, Gordon JH, Shryne JE, Southam AM (1978) Evidence for a morphological sex difference within the medial preoptic area of the rat brain. Brain Res 148:333–346

Graw J (2000) Mouse mutants for eye development. In: Fini ME (ed) Vertebrate Eye Development. Springer, Berlin Heidelberg New York, pp 219–256

Graw J (2003) The genetic and molecular basis of congenital eye defects. Nat Rev Genet 4:876–888

Graybiel AM (1984) Correspondence between the dopamine islands and striosomes of the mammalian striatum. Neuroscience 13:1157–1187

Graybiel AM (1986) Neuropeptides in the basal ganglia. In: Martin JD, Barchas JD (eds) Neuropeptides in Neurologic and Psychiatric Disease. Raven, New York, pp 135–161

Graybiel AM (1990) Neurotransmitters and neuromodulators in the basal ganglia. Trends Neurosci 13:244–254

Graybiel AM, Ragsdale CW Jr (1978) Histochemically distinct compartments in the striatum of human, monkey and cat demonstrated by acetylcholinesterase staining. Proc Natl Acad Sci USA 75:5723–5726

Graybiel AM, Pickel VM, Joh TH, Reis DJ, Ragsdale CW Jr (1981) Direct demonstration of correspondence between the dopamine islands and acetylcholinesterase patches in the developing striatum. Proc Natl Acad Sci USA 78:5871–5875

Graziadei PP, Monti-Graziadei AG (1992) The influence of the olfactory placode on the development of the telencephalon in *Xenopus laevis*. Neuroscience 46:617–629

Greig DM (1926) Oxycephaly. Edinburgh Med J 33:189–218

Gribnau AAM, Geysberts LGM (1981) Developmental stages in the rhesus monkey (Macaca mulatta). Adv Anat Embryol Cell Biol 68:1–84

Gribnau AAM, Geysberts LGM (1985) Morphogenesis of the brain in staged rhesus monkey embryos. Adv Anat Embryol Cell Biol 91:1–69

Grindley JC, Davidson DR, Hill RE (1995) The role of *Pax-6* in eye and nasal development. Development 121:1433–1442

Grindley JC, Hargett LK, Hill RE, Ross A, Hogan BL (1997) Disruption of PAX6 function in mice homozygous for the *Pax6/Sey-1/Neu* mutation produces abnormalities in the early development and regionalization of the diencephalon. Mech Dev 64:111–126

Gripp KW, Edwards MC, Mowat D, Meinecke P, Richieri-Costa A, Zackai EH, Elledge S, Muenke M (1998) Mutations in the transcription factor TGIF in holoprosencephaly. Am J Hum Genet 63:A32

Grove EA, Tole S, Limon J, Yip L, Ragsdale CW (1998) The hem of the embryonic cerebral cortex is defined by the expression of multiple *Wnt* genes and is compromised in *Gli3*-deficient mice. Development 125:2315–2325

Guillemot F, Lo LC, Johnson JE, Auerbach A, Anderson DJ, Joyner AL (1993) Mammalian achaete-scute homolog 1 is required for the early development of olfactory and autonomic neurons. Cell 75:463–476

Guillery RW, Okoro AN, Witkop CJ (1975) Abnormal visual pathways in the brain of the human albino. Brain Res 96:373–377

Gulisano M, Broccoli V, Pardini C, Boncinelli E (1996) Emx1 and Emx2 show different patterns of expression during proliferation and differentiation of the developing cerebral cortex in the mouse. Eur J Neurosci 8:1037–1050

Gulyas B, Ottoson D, Roland PE (1993) Functional Organization of the Human Visual Cortex. Pergamon, Oxford

Haber SN, Gdowski MJ (2004) The basal ganglia. In: Paxinos G, Mai JK (eds) The Human Nervous System, 2nd ed. Elsevier, Amsterdam, pp 676–738

Halpern M (1987) The organization and function of the vomeronasal system. Annu Rev Neurosci 10:325–362

Hamilton WJ, Mossman HW (1972) Hamilton, Boyd and Mossman's Human Embryology, 4th ed. Heffer, Cambridge

Hanaway J, McConnell JA, Netsky MG (1971) Histogenesis of the substantia nigra, ventral tegmental area of Tsai and interpeduncular nucleus: An autoradiographic study of the mesencephalon in the rat. J Comp Neurol 142:59–74

Hardelin J-P (2001) Kallmann syndrome: Towards molecular pathogenesis. Mol Cell Endocrinol 179:75–81

Hardelin J-P, Julliard AK, Moniot B, Soussi-Yanicostas N, Verney C, Schwanzel-Fukuda M, Ayer-Le Lièvre C, Petit C (1999) Anosmin-1 is a regionally restricted component of basement membranes and interstitial matrices during organogenesis: Implications for the developmental anomalies of X chromosome-linked Kallmann syndrome. Dev Dyn 215:26–44

Harris CP, Townsend JJ, Norman MG, White VA, Viskochil DH, Pysher TJ, Klatt EC (1994) Atelencephalic aprosencephaly. J Child Neurol 9:412–416

Harris RM, Hendrickson AE (1978) Local circuit neurons in the rat ventrobasal complex – a GABA immunocytochemical study. Neuroscience 21:229–236

Hayflick SJ, Westaway SK, Levinson B, Zhou B, Johnson MA, Ching KHL, Gitschier J (2003) Genetic, clinical, and radiographic delineation of Hallervorden-Spatz syndrome. N Engl J Med 348:33–40

Hébert JM, Mishina Y, McConnell SK (2002) BMP signaling is required locally to pattern the dorsal telencephalic midline. Neuron 35:1029

Hébert JM, Lin M, Partanen J, Rossant J, McConnell SK (2003) FGF signaling through FGFR1 is required for olfactory bulb morphogenesis. Development 130:1101–1111

Heimer L (1976) The olfactory cortex and the ventral striatum. In: Livingston KE, Hornykiewicz O (eds) Limbic Mechanisms: The Continuing Evolution of the Limbic System Concept. Plenum, New York, pp 95–187

Heimer L, Switzer RD, Van Hoesen GW (1982) Ventral striatum and ventral pallidum. Components of the motor system? Trends Neurosci 5:83–87

Heimer L, de Olmos J, Alheid GF, Záborsky L (1991) "Perestroika" in the basal forebrain: Opening the border between neurology and psychiatry. Prog Brain Res 87:109–165

Heimer L, Harlan RE, Alheid GF, Garcia MM, de Olmos J (1997) Substantia innominata: A notion which impedes clinical-anatomical correlations in neuropsychiatric disorders. Neuroscience 76:957–1006

Hellström A, Aronsson M, Axelson C, Kyllerman M, Kopp S, Steffenberg S, Strömland K, Westphal O, Wiklund L-M, Albertsson-Wikland K (2000) Children with septo-optic dysplasia – how to improve and sharpen the diagnosis. Horm Res 53(Suppl 1):19-25

Herrick CJ (1910) The morphology of the forebrain in Amphibia and Reptilia. J Comp Neurol 20:413–545

Hertwig P (1942) Neue Mutationen und Koppelungsgruppen bei der Hausmaus. Z Indukt Abstammungs-Vererbungsl 80:220–246

Hevner RF (2000) Development of connections in the human visual system during fetal midgestation: A DiI-tracing study. J Neuropathol Exp Neurol 59:385–392

Hevner RF, Shi L, Justice N, Hsueh Y, Sheng M, Smiga S, Bulfone A, Goffinet AM, Campagnoni AT, Rubinstein JLR (2001) *Tbr1* regulates differentiation of the preplate and layer 6. Neuron 29:353–366

Hevner RF, Miyashita E, Rubinstein JLR (2002) Cortical and thalamic axon pathfinding defects in Tbr1, Gbx2, and Pax6 mutant mice: Evidence that cortical and thalamic axons interact and guide each other. J Comp Neurol 447:8–17

Hewitt W (1958) The development of the human caudate and amygdaloid nucleus. J Anat (Lond) 92:377–382

Hewitt W (1961) The development of the human internal capsule and lenticular nucleus. J Anat (Lond) 55:191–199

Hill JM, Switzer RC (1984) The regional distribution and cellular localization of iron in the rat brain. Neuroscience 11:595–603

Hill RE, Favor J, Hogan BLM, Ton CCT, Saunders GF, Hanson IM, Prosser J, Jordan T, Hastie ND, van Heyningen V (1991) Mouse *Small eye* results from mutations in a paired-like homeobox-containing gene. Nature 354:522–525

Hinds JW (1968a) Autoradiographic study of histogenesis in the mouse olfactory bulb. I. Time of origin of neurons and neuroglia. J Comp Neurol 134:287–304

Hinds JW (1968b) Autoradiographic study of histogenesis in the mouse olfactory bulb. II. Cell proliferation and migration. J Comp Neurol 134:305–322

Hinrichsen KV (1990) Augenentwicklung. In: Hinrichsen KV (Hrsg) Humanembryologie. Lehrbuch und Atlas der vorgeburtlichen Entwicklung des Menschen. Springer, Berlin Heidelberg New York, pp 477–500

Hirai T, Jones EG (1989) A new parcellation of the human thalamus on the basis of histochemical staining. Brain Res Rev 14:1–34

Hirsch N, Grainger RM (2000) Induction of the lens. In: Fini ME (ed) Vertebrate Eye Development, Springer, Berlin Heidelberg New York, pp 51–68

His W (1889) Die Formentwickelung des menschlichen Vorderhirns vom Ende des ersten bis zum Beginn des dritten Monats. Abh Kön Sächs Ges Wiss Math Phys Kl 15:675–735

His W (1893) Vorschläge zur Eintheilung des Gehirns. Arch Anat Physiol Anat Abt 17:172–179

Hitchcock PF, Hickey TL (1980) Prenatal development of the human lateral geniculate nucleus. J Comp Neurol 194:395–411

Ho VB, Chuang HS, Rovira MJ, Koo B (1995) Juvenile Huntington disease: CT and MR features. AJNR Am J Neuroradiol 16:1405–1412

Hochstetter F (1919) Beiträge zur Entwicklungsgeschichte des menschlichen Gehirns, I. Teil. Deuticke, Vienna

Hoffmann GF, Athanassopoulos S, Burlina AB, Duran M, de Klerck JBC, Lehnert W, Leonard JV, Monavari AA, Müller E, Muntau AC (1996) Clinical course, early diagnosis, treatment and prevention of disease in glutaryl-CoA dehydrogenase deficiency. Neuropediatrics 27:115–123

Hogan BL, Horsburgh G, Cohen J, Hetherington CM, Fisher G, Lyon MF (1986) *Small eye* (*Sey*): A homozygous lethal mutation on chromosome 2 which affects the differentiation of both lens and nasal placodes in the mouse. J Embryol Exp Neurol 97:95–110

Hogan BL, Hirst EM, Horsburgh G, Hetherington CM (1988) *Small eye* (*Sey*): A mouse model for the genetic analysis of craniofacial abnormalities. Development 103:115–119

Holt DJ, Graybiel AM, Saper CB (1997) Neurochemical architecture of the human striatum. J Comp Neurol 384:1–25

Holzschuh J, Hauptmann G, Driever W (2003) Genetic analysis of the roles of Hh, FGF8, and nodal signaling during catecholaminergic system development in the zebrafish brain. J Neurosci 23:5507–5519

Hongo T, Hakuba A, Shiota K, Naruse I (2000) Suckling dysfunction caused by defects in the olfactory system in genetic arhinencephalic mice. Biol Neonate 78:293–299

Hoon AH Jr, Belcito KM, Nagae-Poetscher LM (2003) Neuroimaging in spasticity and movement disorders. J Child Neurol 18:S25–S39

Hori A (1983) A brain with two hypophyses in median cleft face syndrome. Acta Neuropathol (Berl) 59:150–154

Hori A, Schmidt D, Feyerabend B (1995) Pharyngosellar pituitary: A rare developmental anomaly of the pituitary gland. Acta Neuropathol (Berl) 89:459–463

Hori A, Schmidt D, Rickels E (1999a) Pharyngeal pituitary: Development, malformation, and tumorigenesis. Acta Neuropathol (Berl) 98:262–272

Hori A, Schmidt D, Kuebber S (1999b) Immunohistochemical survey of migration of human anterior pituitary cells in developmental, pathological, and clinical aspects: A review. Micr Res Techn 46:59–68

Horsford DJ, Hanson I, Freund C, McInnes RR, van Heyningen V (2001) Transcription factors in eye disease and ocular development. In: Scriver CR, Beaudet AL, Sly WS, Valle D (eds) The Metabolic & Molecular Bases of Inherited Disease. McGraw-Hill, New York, pp 5987–6032

Houart C, Westerfield M, Wilson SW (1998) A small population of anterior cells patterns the forebrain during zebrafish gastrulation. Nature 391:788–792

Houart C, Caneparo L, Heisenberg C-P, Take-Uchi M, Wilson SW (2002) Establishment of the telencephalon during gastrulation by local antagonism of Wnt signaling. Neuron 35:255–265

Hubel DH, Wiesel TN (1977) Functional architecture of macaque monkey visual cortex. Proc R Soc Lond B 198:1–59

Hubel DH, Wiesel TN, LeVay S (1977) Plasticity of ocular dominance columns in monkey striate cortex. Philos Trans R Soc Lond B 278:377–409

Humphrey T (1940) The development of the olfactory and the accessory olfactory formations in human embryos and fetuses. J Comp Neurol 73:431–468

Humphrey T (1967) The development of the human tuberculum olfactorium during the first three months of life. J Hirnforsch 9:437–469

Humphrey T (1968) The development of the human amygdala during early embryonic life. J Comp Neurol 132:135–166

Humphrey T (1972) The development of the amygdaloid complex. In: Eleftheriou BE (ed) The Neurobiology of the Amygdala. Plenum, New York, pp 21–77

Hynes M, Rosenthal A (1999) Specification of dopaminergic and serotonergic neurons in the vertebrate CNS. Curr Opin Neurol 9:26–36

Ikeda H, Niizuma H, Suzuki J, Takabayashi T, Ozawa N (1987) A case of cebocephaly-holoprosencephaly with aberrant adenohypophysis. Childs Nerv Syst 3:251–254

Ikeda H, Suzuki J, Sasano N, Niizumi H (1988) The development of morphogenesis of the human pituitary gland. Anat Embryol (Berl) 178:327–336

Ippel PF, Breslau-Siderius EJ, Hack WWM, van der Blij HF, Bouve S, Bijlsma JB (1998) Atelencephalic microcephaly: A case report and review of the literature. Eur J Pediatr 157:493–497

Ito M, Mori Y, Oiso Y, Saito H (1991) A single base substitution in the coding region for neurophysin II associated with familial central diabetes insipidus. J Clin Invest 87:725–728

Itoh K, Suzuki K, Bise K, Itoh H, Mehraein P, Weis S (2001) Apoptosis in the basal ganglia of the developing human nervous system. Acta Neuropathol (Berl) 101:92–100

Izumi Y, Tatsumi K, Okamoto S, Hosokawa A, Ueno S, Fukui H, Amino N (1999) A novel mutation of the *KAL1* gene in Kallmann syndrome. Endocrinol J 46:651–658

Izumi Y, Tatsumi K, Okamoto S, Ogawa T, Hosokawa A, Matsuo T, Kato Y, Fukui H, Amino N (2001) Analysis of the *KAL1* gene in 19 Japanese patients with Kallmann syndrome. Endocrinol J 48:143–149

Jansonius NM, van der Vliet AM, Cornelissen FW, Pott JWR, Kooijman AC (2001) A girl without a chiasm: Electrophysiologic and MRI evidence for the absence of crossing optic nerve fibers in a girl with a congenital nystagmus. J Neuro-Ophthalmol 21:26–29

Johnston MV, Hoon AH (2000) Possible mechanisms in infants for selective basal ganglia damage from asphyxia, kernicterus, or mitochondrial encephalopathies. J Child Neurol 15:588–591

Jones EG (1985) The Thalamus. Plenum, New York

Jones L, López-Bendito G, Gruss P, Stoykova A, Molnár Z (2002) *Pax6* is required for the normal development of the forebrain axonal connections. Development 129:5041–5052

Kahle W (1956) Zur Entwicklung des menschlichen Zwischenhirnes. Studien über die Matrixphasen und die örtlichen Reifungsunterschiede im embryonalen menschlichen Gehirn. II. Mitteilung. Dtsch Z Nervenheilk 175:259–318

Kahle W (1969) Die Entwicklung der menschlichen Großhirnhemisphäre. Springer, Berlin Heidelberg New York

Kakita A, Wakabayashi K, Sekizuka N, Takahashi H (1997) Cyclopia: Histogenesis of the single optic nerve. Acta Neuropathol (Berl) 94:509–513

Kakita A, Hayashi S, Arakawa M, Takahashi H (2001) Aprosencephaly: Histopathological features of the rudimentary forebrain and retina. Acta Neuropathol (Berl) 102:110–116

Kallmann FJ, Schoenfeld WA, Barrera SE (1944) The genetic aspects of primary eunuchoidism. Am J Ment Defic 48:203–236

Kalsbeek A, Voorn P, Buys RM, Pool CW, Uylings HBM (1988) Development of the dopaminergic innervation in the prefrontal cortex of the rat. J Comp Neurol 269:58–72

Kawano H, Fukuda T, Kubo K, Horie M, Uyemura K, Takeuchi K, Osumi N, Eto K, Kawamura K (1999) Pax-6 is required for thalamocortical pathway formation in fetal rats. J Comp Neurol 408:147–160

Kelley RI, Roessler E, Hennekam RCM, Feldman GL, Kosaki K, Jones MC, Palumbos JC, Muenke M (1996) Holoprosencephaly in RSH/Smith-Lemli-Opitz syndrome: Does abnormal cholesterol metabolism affect the function of *Sonic Hedgehog*? Am J Med Genet 66:478–484

Kemp JM, Powell TPS (1970) The cortico-striate projection in the monkey. Brain 93:525–546

Keyser AJM (1972) The development of the diencephalon of the Chinese hamster. Acta Anat (Basel) 83(Suppl 59):1–178

Keyser AJM (1979) Development of the hypothalamus in mammals. An investigation into its morphological position during ontogenesis. In: Morgane PJ, Panksepp J (eds) Handbook of the Hypothalamus, Vol 1: Anatomy of the Hypothalamus. Dekker, New York, pp 65–136

Khan AA, Wadhwa S, Pandey RM, Bijlani V (1993) Prenatal human lateral geniculate nucleus: A quantitative light microscopic study. Dev Neurosci 15:403–409

Khan AA, Wadhwa S, Bijlani V (1994) Development of the human lateral geniculate nucleus: An electron microscopic study. Int J Dev Neurosci 7:661–672

Kim TS, Cho S, Dickson DW (1990) Aprosencephaly: Review of the literature and report of a case with cerebellar hypoplasia, pigmented epithelial cyst and Rathke's cleft cyst. Acta Neuropathol (Berl) 79:424–431

Kimura S, Hara M, Nezu A, Osaka H, Yamazaki S, Saitoh U (1994) Two cases of glutaric aciduria type 1: Clinical and neuropathological findings. J Neurol Sci 123:38–43

Kimura S, Hara Y, Pineau T, Fernandez-Salguero P, Fox CH, Ward JM, Gonzalez FJ (1996) The *T/ebp* null mouse: Thyroid-specific enhancer-binding protein is essential for the organogenesis of the thyroid, lung, ventral forebrain, and pituitary. Genes Dev 10:60–69

Kinney HC, Armstrong DD (1997) Perinatal neuropathology. In: Graham DI, Lantos PL (eds) Greenfield's Neuropathology, 6th ed. Arnold, London, pp 536–599

Kioussi C, Briata P, Baek SH, Rose DW, Hamblet NS, Herman T, Ohgi KA, Lin C, Gleiberman A, Wang J, et al. (2002) Identification of a Wnt/Dvl/beta-Catenin–Pitx2 pathway mediating cell-type-specific proliferation during development. Cell 111:673–685

Kishi K (1987) Golgi studies on the development of granule cells of the rat olfactory bulb with reference to migration in the subependymal layer. J Comp Neurol 258:112–124

Kitamura K, Miura H, Miyagawa-Tomita S, Yanazawa M, Katoh-Fukui Y, Suzuki R, Ohuchi H, Suehiro A, Motegi Y, Nakahara Y, et al. (1999) Mouse Pitx2 deficiency leads to anomalies of the ventral body wall, heart, extra- and periocular mesoderm and right pulmonary isomerism. Development 126:5749–5758

Kjaer I, Fischer-Hansen B (1995) Human fetal pituitary gland in holoprosencephaly and anencephaly. J Craniofac Genet Dev Biol 15:222–229

Kjaer I, Fischer-Hansen B (1996) The human vomeronasal organ: Prenatal developmental stage, and distribution of luteinizing hormone-releasing hormone. Eur J Oral Sci 104:34–40

Kölker S, Hoffmann GF, Schor DSM, Feyh P, Wagner L, Jeffrey I, Pourfarzam M, Okun JG, Zschocke J, Baric I, et al. (2003) Glutaryl-CoA dehydrogenase deficiency: Region-specific analysis of organic acids and acylcarnitines in postmortem brain predicts vulnerability of the putamen. Neuropediatrics 34:253–260

Kondoh H (1999) Transcription factors for lens development assessed *in vivo*. Curr Opin Genet Dev 9:301–318

Kordower JH, Piecinski P, Rakic P (1992) Neurogenesis of the amygdaloid nuclear complex in the rhesus monkey. Dev Brain Res 68:9–15

Korff CM, Apkarian P, Bour LJ, Meuli R, Verrey J-D, Roulet-Perez E (2003) Isolated absence of optic chiasm revealed by congenital nystagmus, MRI and VEPs. Neuropediatrics 34:219–223

Kornack DR, Rakic P (2001) The generation, migration, and differentiation of olfactory neurons in the adult primate brain. Proc Natl Acad Sci USA 98:4752–4757

Kostović I (1986) Prenatal development of the nucleus basalis complex and related fiber systems in man: A histochemical study. Neuroscience 17:1047–1077

Kostović I (1990) Zentralnervensystem. In: Hinrichsen KV (Hrsg) Humanembryologie. Lehrbuch und Atlas der vorgeburtlichen Entwicklung des Menschen. Springer, Berlin Heidelberg New York, pp 381–448

Kostović I, Rakic P (1990) Developmental history of the transient subplate zone in the visual and somatosensory cortex of the macaque monkey and human brain. J Comp Neurol 297:441–470

Kouki T, Imai H, Aoto K, Eto K, Shioda S, Kawamura K, Kikuyama S (2001) Developmental origin of the rat adenohypophysis prior to the formation of Rathke's pouch. Development 128:959–963

Koutcherov Y, Mai JK, Ashwell KWS, Paxinos G (2002) Organization of human hypothalamus in fetal development. J Comp Neurol 446:301–324

Krägeloh-Mann I, Petersen D, Hagberg G, Vollmer B, Hagberg B, Michaelis R (1995) Bilateral spastic cerebral palsy – MRI pathology and origin. Analysis from a representative series of 56 cases. Dev Med Child Neurol 38:379–397

Krägeloh-Mann I, Helber A, Mader I, Staudt M, Wolff M, Groenedaal F, de Vries L (2002) Bilateral lesions of thalamus and basal ganglia: Origin and outcome. Dev Med Child Neurol 44:477–484

Kriegstein AR, Noctor SC (2004) Patterns of neuronal migration in the embryonic cortex. Trends Neurosci 27:392–399

Kuhlenbeck H (1954) The human diencephalon. A summary of development, structure, function and pathology. Confin Neurol 14(Suppl):1–230

Kundrat H (1882) Arhinencephalie als typische Art von Missbildung. Von Leuschner und Lubensky, Graz

Künzle H (1975) Bilateral projections from precentral motor cortex to the putamen and other parts of the basal ganglia. An autoradiographic study in *Macaca fascicularis*. Brain Res 88:195–209

Künzle H (1977) Projections from the primary somatosensory cortex to the basal ganglia and thalamus in the monkey. Exp Brain Res 30:481–492

Künzle H (1978) An autoradiographic analysis of the efferent connections from premotor and adjacent prefrontal regions (areas 6 and 9) in *Macaca fascicularis*. Brain Behav Evol 15:185–234

Kyllerman M, Steen G (1980) Glutaric aciduria: A "common" metabolic disorder? Arch Fr Pediatr 37:279

LaMantia AS, Bhasin N, Rhodes K, Heemskerk J (2000) Mesenchymal-epithelial induction mediates olfactory pathway formation. Neuron 28:411–425

Lammers HJ (1972) The neural connections of the amygdaloid complex in mammals. In: Eleftheriou BE (ed) The Neurobiology of the Amygdala. Plenum, New York, pp 123–144

Larroche JC (1981) Agenesis of the pituitary gland. Handb Clin Neurol 42:11

Larsen CW, Zeltser LM, Lumsden A (2001) Boundary formation and compartition in the avian diencephalon. J Neurosci 21:4699–4711

Lavdas AA, Grigoriou M, Pachnis V, Parnavelas JG (1999) The medial ganglionic eminence gives rise to a population of early neurons in the developing cerebral cortex. J Neurosci 19:7881–7888

Lazzaro D, Price M, De Felice M, Di Lauro R (1991) The transcription factor TTF1 is expressed at the onset of thyroid and lung morphogenesis and in restricted regions of the foetal brain. Development 113:1093–1104

Lee KJ, Jessell TM (1999) The specification of dorsal fates in the vertebrate central nervous system. Annu Rev Neurosci 22:261–294

Leech RW, Shuman RM (1986) Holoprosencephaly and related midline cerebral anomalies: A review. J Child Neurol 1:3–18

Legouis R, Hardelin J-P, Levilliers J, Claverie J-M, Compain S, Wunderle V, Millasseau P, Le Paslier D, Cohen D, Caterina D, et al. (1991) The candidate gene for X-linked Kallmann syndrome encodes a protein related to adhesion molecules. Cell 67:423–435

Leibel RL, Shih VE, Goodman SI, Bauman ML, McCabe ERB, Zwerdling RG, Bergman I, Costello C (1980) Glutaric acidemia: A metabolic disorder causing progressive choreoathetosis. Neurology 30:1163–1168

Leigh D (1951) Subacute necrotizing encephalomyelopathy in an infant. J Neurol Neurosurg Psychiatr 14:216–221

Lemire RJ, Loeser JD, Leech RW, Alvord EC Jr (1975) Normal and Abnormal Development of the Human Nervous System. Harper & Row, Hagerstown, MD

Letinić K, Kostović I (1996) Transient patterns of calbindin-D28K expression in the developing striatum of man. Neurosci Lett 220:211–214

Letinić K, Kostović I (1997) Transient fetal structure, the ganglio-thalamic body, connects telencephalic germinal zone with all thalamic regions in the developing human brain. J Comp Neurol 384:373–395

Letinić K, Rakic P (2001) Telencephalic origin of human thalamic GABAergic neurons. Nat Neurosci 9:931–936

Levitt P, Rakic P (1982) The time of genesis, embryonic origin and differentiation of the brainstem monoamine neurons in the rgesus monkey. Dev Brain Res 4:35–57

Lewis AJ, Simon EM, Barkovich AJ, Clegg NJ, Delgado MR, Levey E, Hahn JS (2002) Middle interhemispheric variant of holoprosencephaly. A distinct cliniconeuroradiologic subtype. Neurology 59:1860–1865

Li H, Tierney C, Wen L, et al. (1997) A single morphogenetic field gives rise to two retina primordia under the influence of the prechordal plate. Development 124:603–615

Li X, Oghi KA, Zhang J, Krones A, Bush KT, Glass CK, Nigam SK, Aggarwal AK, Maas R, Rose DW, et al. (2003) Eya protein phosphatase activity regulates Six1-Dach-Eya transcriptional effects in mammalian organogenesis. Nature 426:247–254

Lin CR, Kioussi C, O'Connell S, Briata P, Szeto D, Liu F, Izpisua-Belmonte JC, Rosenfeld MG (1999) Pitx2 regulates lung asymmetry, cardiac positioning and pituitary and tooth morhogenesis. Nature 401:279–282

Litingtung Y, Chiang C (2000) Control of Shh activity and signaling in the neural tube. Dev Dyn 219:143–154

Liu JK, Ghattas I, Liu S, Chen S, Rubinstein JLR (1997) Dlx genes encode DNA-binding proteins that are expressed in an overlapping and sequential pattern during basal ganglia differentiation. Dev Dyn 210:498–512

Livingstone M, Hubel D (1988) Segregation of form, color, movement, and depth: Anatomy, physiology, and perception. Science 240:740–749

Lohman AJM, Lammers HJ (1967) On the structure and fibre connections of the olfactory system in mammals. Prog Brain Res 23:65–82

Lois C, Alvarez-Buylla A (1994) Long-distance neuronal migration in the adult mammalian brain. Science 264:1145–1148

Long JE, Garel S, Depew MJ, Tobet S, Rubinstein JLR (2003) DLX5 regulates development of peripheral and central components in the olfactory system. J Neurosci 23:568–578

López-Bendito G, Molnár Z (2003) Thalamocortical development: How are we going to get there? Nat Rev Neurosci 4:276–289

López-Mascaraque L, de Carlos JA, Valverde F (1996) Early onset of the rat olfactory bulb projections. Neuroscience 70:255–266

Louis ED, Lynch T, Cargan AL, Fahn S (1995) Generalized chorea in an infant with semilobar holoprosencephaly. Pediatr Neurol 13:355–357

Lund RD, Mustari MJ (1977) Development of the geniculocortical pathway in rats. J Comp Neurol 173:289–305

Lurie IW, Nedzved MK, Lazjuk GI, Kirillova IA, Cherstvoy ED (1979) Aprosencephaly-atelencephaly and the aprosencephaly (XK) syndrome. Am J Med Genet 3:303–309

Lurie IW, Nedzved MK, Lazjuk GI, Kirillova IA, Cherstvoy ED, Ostrovskaja TI, Shved IA (1980) The XK-aprosencephaly syndrome. Am J Med Genet 7:231–234

Luskin MB (1993) Restricted proliferation and migration of postnatally generated neurons derived from the forebrain subventricular zone. Neuron 11:173–189

Macchi G (1951) The ontogenetic development of the olfactory telencephalon in man. J Comp Neurol 95:245–305

Macdonald R, Wilson SW (1996) Pax proteins and eye development. Curr Opin Neurobiol 6:49–56

Maestre de San Juan A (1856) Teratologia: Falta total de los nervios olfactorios con anosmian en un individuo en quien existia un atrofia congenita de los testiculos y membro viril. El Siglo Med 3:211 (Quoted from Ballabio and Rugarli 2001)

Magoon EH, Robb RM (1981) Development of myelin in human optic nerve and tract. A light and electron microscopic study. Arch Ophthalmol 99:655–670

Mai JK, Ashwell KWS (2004) Fetal development of the central nervous system. In: Paxinos G, Mai JK (eds) The Human Nervous System, 2nd ed. Elsevier, Amsterdam, pp 49–94

Malamud N (1950) Status marmoratus: A form of cerebral palsy following either birth injury or inflammation of the central nervous system. J Pediatr 37:610–619

Mall FP (1917) Cyclopia in the human embryo. Contrib Embryol Carnegie Instn 6:5–33

Mallamacci A, Muzio L, Chan CH, Parnavelas J, Boncinelli E (2000) Area identity shifts in the early cerebral cortex of *Emx2-/-* mutant mice. Nat Neurosci 3:679–686

Mann IC (1928) The Development of the Human Eye. Cambridge University Press, London

Marchand R, Lajoie L (1986) Histogenesis of the striatopallidal system in the rat. Neurogenesis of its neurons. Neuroscience 17:573–590

Marchand R, Poirier LJ (1983) Isthmic origin of neurons of the rat substantia nigra. Neuroscience 9:373–381

Marchand R, Lajoie L, Blanchet C (1986) Histogenesis at the level of the basal forebrain: The entopeduncular nucleus. Neuroscience 17:591–607

Marín O (2003) Thalamocortical topography reloaded: It's not where you go, but how you get there. Neuron 39:388–391

Marín O, Rubinstein JLR (2001) A long, remarkable journey: Tangential migration in the telencephalon. Nat Rev Neurosci 2:780–790

Marín O, Rubinstein JLR (2002) Patterning, regionalization, and cell differentiation in the forebrain. In: Rossant J, Tam PPL (eds) Mouse Development – Patterning, Morphogenesis, and Organogenesis. Academic Press, San Diego, CA, pp 75–106

Marín O, Anderson SA, Rubinstein JLR (2000) Origin and molecular specification of striatal interneurons. J Neurosci 20:6063–6076

Marquardt T, Gruss P (2002) Generating neuronal diversity in the retina: One for nearly all. Trends Neurosci 25:32–38

Martin D, Camper SA (2001) Genetic regulation of forebrain and pituitary development. In: Rappaport R, Anselem S (eds) Hypothalamic-Pituitary Development. Genetic and clinical aspects. Karger, Basel, pp 1–12

Martínez S, Puelles L (2000) Neurogenetic compartments of the mouse diencephalon and some characteristic gene expression patterns. In: Goffinet AM, Rakic P (eds) Mouse Brain Development. Springer, Berlin Heidelberg New York, pp 91–104

Martinez-Barbera JP, Rodriguez TA, Beddington RS (2000) The homeobox gene Hesx1 is required in the anterior neural ectoderm for normal forebrain formation. Dev Biol 223:422–430

Mastick GS, Davis NM, Andrew GL, Easter SS Jr (1997) *Pax-6* functions in boundary formation and axon guidance in the embryonic mouse forebrain. Development 124:1985–1997

Mathieu J, Barth A, Rosa FM, Wilson SW, Peyriéras N (2002) Distinct and cooperative roles for Nodal and Hedgehog signals during hypothalamic development. Development 129:3055–3065

Matise MP, Joyner AL (1999) Gli genes in development and cancer. Oncogene 18:7852-7859

Matsunaga E, Shiota K (1977) Holoprosencephaly in human embryos: epidemiologic studies of 150 cases. Teratologia 16:261–272

Mazzitelli N, Vauthay L, Grandi C, Fuksman R, Rittler M (2002) Reviewing old concepts at the scent of a new milennium: Growth restriction, adrenal hypoplasia, and thymomegaly in human anencephaly. Teratology 66:105–114

McAllister JP, Das GD (1977) Neurogenesis in the epithalamus, dorsal thalamus and ventral thalamus of the rat: An autoradiographic and cytological study. J Comp Neurol 172:647–686

McConnell J, Angevine JB Jr (1983) Time of origin in the amygdaloid complex of the mouse. Brain Res 272:150–156

McGeorge AJ, Faull RLM (1989) The organization of the projection from the cerebral cortex to the striatum in the rat. Neuroscience 29:503–537

Meisami E, Bhatnagar KP (1998) Structure and diversity in mammalian accessory olfactory bulb. Micr Res Tech 43:476–499

Meredith M (2001) Human vomeronasal organ function: a critical review of best and worse cases. Chem Senses 26:433–445

Métin C, Godement P (1996) The ganglionic eminence may be an intermediate target for corticofugal and thalamocortical axons. J Neurosci 16:3219–3235

Meyers EN, Lewandoski M, Martin GR (1998) An Fgf8 mutant allelic series generated by Cre- and Flp-mediated recombination. Nat Genet 18:136–141

Miller SP, Shevell MI, Patenaude Y, Poulin C, O'Gorman AM (2000) Septo-optic dysplasia plus: A spectrum of malformations of cortical development. Neurology 54:1701–1703

Ming JE, Muenke M (1998) Holoprosencephaly: From Homer to hedgehog. Clin Genet 53:155–163

Ming JE, Muenke M (2002) Multiple hits during early embryonic development: Digenic diseases and holoprosencephaly. Am J Hum Genet 71:1017–1032

Ming JE, Kaupas ME, Roessler E, Brunner HG, Golabi M, Tekin M, Stratton RF, Sujanski E, Bale SJ, Muenke M (2002) Mutations in PATCHED-1, the receptor for SONIC HEDGEHOG, are associated with holoprosencephaly. Hum Genet 110:297–301

Mione MC, Cavanagh JFR, Harris B, Parnavelas JG (1997) Cell fate specification and symmetrical/asymmetrical divisions in the developing cerebral cortex. J Neurosci 17:2018–2029

Mitchell IJ, Cooper AJ, Griffiths MR (1999) The selective vulnerability of striatopallidal neurons. Prog Neurobiol 59:691–719

Mitrofanis J (1992) Patterns of antigenic expression in the thalamic reticular nucleus of developing rats. J Comp Neurol 320:161–181

Mitrofanis J, Baker GE (1993) Development of the thalamic reticular and perireticular nuclei in rats and their relationship to the course of growing corticofugal and corticopetal axons. J Comp Neurol 338:575–587

Miyai K, Azukizawa M, Kumahara Y (1971) Familial isolated thyrotrophin deficiency with cretinism. N Engl J Med 285:1043–1048

Miyashita-Lin EM, Hevner R, Wassarman KM, Martínez S, Martin GR, Rubinstein JLR (1999) Neocortical regionalization is preserved in the absence of thalamic innervation in newborn Gbx-2 mutant mice. Science 285:906–909

Miyoshi K, Matsuoka T, Mizushima S (1969) Familial holotopistic striatal necrosis. Acta Neuropathol (Berl) 13:240–249

Mojsilović J, Zečević N (1991) Early development of the human thalamus: Golgi and Nissl study. Early Hum Dev 27:119–144

Molnár Z (1998) Development of Thalamocortical Connections. Springer, Berlin Heidelberg New York, and Landes, Georgetown, TX

Molnár Z, Blakemore C (1995) How do thalamic axons find their way to the cortex? Trends Neurosci 18:389–397

Molnár Z, Butler AB (2002) The corticostriatal junction: A crucial region for forebrain development and evolution. BioEssays 24:530–541

Molnár Z, Hannan AJ (2000) Development of thalamocortical projections in normal and mutant mice. In: Goffinet AM, Rakic P (eds) Mouse Brain Development. Springer, Berlin Heidelberg New York, pp 293–332

Molnár Z, Adams R, Blakemore C (1998) Mechanisms underlying the early establishment of thalamocortical connections in the rat. J Neurosci 18:5723–5745

Montero VM, Zempel J (1986) The proportion and size of GABA-immunoreactive neurons in the magnocellular and parvocellular layers of the lateral geniculate nucleus of the rhesus monkey. Exp Brain Res 62:215–223

Monuki ES, Walsh CA (2001) Mechanisms of cerebral cortical patterning in mice and human. Nat Neurosci 4:1199–1206

Monuki ES, Porter FD, Walsh CA (2001) Patterning of the dorsal telencephalon and cerebral cortex by a roof plate-Lhx2 pathway. Neuron 32:591–604

Moran DT, Jafek BW, Carter Rowley J (1991) The vomeronasal (Jacobson's) organ in man: Ultrastructure and frequency of occurrence. J Steroid Biochem Mol Biol 39:545–552

Morel A, Magnin M, Jeanmonod D (1997) Multiarchitectonic and stereotactic atlas of the human thalamus. J Comp Neurol 387:588–630

Mori T, Yuxing Z, Takaki H, Takeuchi M, Iseki K, Hagino S, Kitanaka J, Takemura M, Misawa H, Ikawa M, et al. (2004) The LIM homeobox gene, L3/Lhx8, is necessary for proper development of basal forebrain cholinergic neurons. Eur J Neurosci 19:3129–3141

Morioka M, Marubayashi T, Matsumitsu T, Miura M, Ushio Y (1995) Basal encephaloceles with morning glory syndrome, and progressive hormonal and visual disturbances: A case report and review of the literature. Brain Dev 17:196–201

Morishima A, Aranoff GS (1986) Syndrome of septo-optic dysplasia: The clinical spectrum. Brain Dev 8:233–239

Muenke M, Beachy PA (2000) Genetics of ventral forebrain development and holoprosencephaly. Curr Opin Genet Dev 10:262–269

Muenke M, Beachy PA (2001) Holoprosencephaly. In: Scriver CR, Beaudet AL, Sly WS, Valle D (eds) The Metabolic & Molecular Bases of Inherited Disease, 8th ed. McGraw-Hill, New York, pp 6203–6230

Müller F, O'Rahilly R (1989a) The human brain at stage 16, including the initial development of the neurohypophysis. Anat Embryol (Berl) 179:551–569

Müller F, O'Rahilly R (1989b) The human brain at stage 17, including the appearance of the future olfactory bulb and the first amygdaloid nuclei. Anat Embryol (Berl) 180:353–369

Müller F, O'Rahilly R (1989c) Mediobasal prosencephalic defects, including holoprosencephaly and cyclopia, in relation to the development of the human forebrain. Am J Anat 185:391–414

Murray RC, Navi D, Fesenko J, Lander AD, Calof AL (2003) Widespread defects in the primary olfactory pathway caused by loss of Mash1 function. J Neurosci 23:1769–1780

Muske LE (1993) Evolution of gonadotropin-releasing hormone (GnRH) neuronal systems. Brain Behav Evol 42:215–230

Muzio L, DiBenedetto B, Stoykova A, Boncinelli E, Gruss P, Mallamaci A (2002) Conversion of cerebral cortex into basal ganglia in Emx2–/– Pax6$^{Sey/Sey}$ double-mutant mice. Nat Neurosci 5:737–745

Nagai L, Li CH, Hsieh SM, Kizaki T, Urano Y (1984) Two cases of hereditary diabetes insipidus, with an autopsy finding in one. Acta Endocrinol 105:318–323

Nagasaki H, Ito M, Yuasa H, Saito H, Fukase M, Hamada K, Ishikawa E, Katakami H, Oiso Y (1995) Two novel mutations in the coding region for neurophysin-II associated with familial central diabetes insipidus. J Clin Endocrinol Metab 80:1352–1356

Nakano KK (1973) Anencephaly: A review. Dev Med Child Neurol 15:383–400

Nanni L, Ming JE, Bocian M, Steinhaus K, Bianchi DW, de Die-Smulders C, Giannotti A, Imaizumi K, Jones KL, Del Campo M, et al. (1999) The mutational spectrum of the *Sonic hedgehog* gene in holoprosencephaly: SHH mutations cause a significant proportion of autosomal dominant holoprosencephaly. Hum Mol Genet 8:2479–2488

Nanni L, Croen LA, Lammer EJ, Muenke M (2000) Holoprosencephaly: Molecular study of a California population. Am J Med Genet 90:315–319

Naruse I, Keino H (1995) Apoptosis in the developing CNS. Prog Neurobiol 47:135–155

Nauta WJH, Haymaker W (1969) Hypothalamic nuclei and fiber connections. In: Haymaker W, Anderson E, Nauta WJH (eds) The Hypothalamus. Thomas, Springfield, IL, pp 136–209

Nery S, Fishell G, Corbin JG (2002) The caudal ganglionic eminence is a source of distinct cortical and subcortical populations. Nat Neurosci 5:1279–1287

Nieuwenhuys R (1977) Aspects of the morphology of the striatum. In: Cools AR, Lohman AHM, van den Bercken JHL (eds) Psychobiology of the Striatum. Elsevier/North-Holland, Amsterdam, pp 1–19

Nieuwenhuys R (1996) The greater limbic system, the emotional motor system and the brain. Prog Brain Res 107:551–580

Nobin A, Björklund A (1973) Topography of the monoamine neuron systems in the human brain as revealed in fetuses. Acta Physiol Scand Suppl 388:1–40

Norman MG, McGillivray BC, Kalousek DK, Hill A, Poskitt PJ (1995) Congenital Malformations of the Brain. Pathologic, embryologic, clinical, radiologic and genetic aspects. Oxford University Press, New York

Norman RM (1947) État marbré of the corpus striatum following birth injury. J Neurol Psychiatr 10:12–25

Nornes HO, Dressler GR, Knapik EW, Deutsch U, Gruss P (1990) Spatially and temporally restricted expression of Pax2 during murine neurogenesis. Development 109:797–809

Northcutt RG, Muske LE (1994) Multiple embryonic origins of gonadotropin-releasing hormone (GnRH) immunoreactive neurons. Dev Brain Res 78:279–290

Oelschläger HA, Buhl EH, Dann JF (1987) Development of the nervus terminalis in mammals including toothed whales and humans. Ann NY Acad Sci 519:447–464

Ogren MP, Rakic P (1981) The prenatal development of the pulvinar in the monkey: ^{3}H-thymidine autoradiographic and morphometric analyses. Anat Embryol (Berl) 162:1–20

Ohkubo Y, Chiang C, Rubinstein JLR (2002) Coordinate regulation and synergistic actions of BMP4, SHH and FGF8 in the rostral prosencephalon regulate morphogenesis of the telencephalic and optic vesicles. Neuroscience 111:1–17

Oliveira LM, Semimara SB, Beranova M, Hayes FJ, Valkenburgh SB, Schipani E, Costa EMF, Latronico C, Crowley WF, Vallejo M (2001) The importance of autosomal genes in Kallmann syndrome: Genotype-phenotype correlations and neuro-endocrine characteristics. J Clin Endocrinol Metab 86:1532–1538

Olson L, Seiger Å (1972) Early prenatal ontogeny of central monoamine neurons in the rat: Fluorescence histochemical observations. Z Anat Entw Gesch 137:301–316

Olson L, Seiger Å, Fuxe K (1972) Heterogeneity of striatal and limbic dopamine innervation: Highly fluorescent islands in developing and adult rats. Brain Res 44:283–288

Olson L, Boreus LO, Seiger Å (1973) Histochemical demonstration and mapping of 5-hydroxytryptamine and catecholamine-containing neuron systems in the human fetal brain. Z Anat Entw Gesch 139:259–282

Olsson M, Campbell K, Wictorin K, Björklund A (1995) Projection neurons in fetal striatal transplants are predominantly derived from the lateral ganglionic eminence. Neuroscience 69:1169–1182

Olsson M, Björklund A, Campbell K (1998) Early specification of striatal projection neurons and interneuronal subtypes in the lateral and medial ganglionic eminence. Neuroscience 84:867–876

Onye C (1990) Thalamus. In: Paxinos G (ed) The Human Nervous System. Academic, San Diego, CA, pp 439–468

Opitz JM (1993) Blastogenesis and the "primary field" in human development. Birth Defects 29:3–37

Opitz JM, Wilson GN, Gilbert-Barness E (1997) Abnormalities of blastogenesis, organogenesis, and phenogenesis. In: Gilbert-Barness E (ed) Potter's Pathology of the Fetus and Infant. Mosby, St. Louis, MI, pp 65–105

O'Rahilly R (1966) The early development of the eye in staged human embryos. Contrib Embryol Carnegie Instn 38:1–42

O'Rahilly R, Müller F (2001) Human Embryology & Teratology, 3rd ed. Wiley-Liss, New York

O'Rahilly R, Müller F, Hutchins GM, Moore GW (1988) Computer ranking of the sequence of appearance of 40 features of the brain and related structures in staged human embryos during the seventh week of development. Am J Anat 182:295–317

Ortmann R (1989) Über Sinneszellen am fetalen vomeronasalen Organ des Menschen. HNO 37:191–197

Ottersen OP, Storm-Mathisen J (1984) GABA-containing neurons in the thalamus and pretectum of the rodent. An immunocytochemical study. Anat Embryol (Berl) 170:197–207

Padberg G, Bruyn GW (1986) Chorea: Differential diagnosis. Handb Clin Neurol 5:549–564

Panganiban G, Rubinstein JLR (2002) Developmental functions of the *Distal-less/Dlx* homeobox genes. Development 129:4371–4386

Parent A, Hazrati L-N (1995) Functional anatomy of the basal ganglia. I. The cortico-basal ganglia-thalamo-cortical loop. Brain Res Rev 20:91–127

Parent A, Côté P-Y, Lavoie B (1995) Chemical anatomy of primate basal ganglia. Prog Neurobiol 46:131–197

Parnavelas JG (2000) The origin and migration of cortical neurones: New vistas. Trends Neurosci 23:126–131

Parsa CF, Goldberg MF, Hunter DG (2002) Papillorenal ("renal coloboma") syndrome. Am J Ophthalmol 134:300–301

Pasternak JF, Predey TA, Mikhael ME (1991) Neonatal asphyxia: Vulnerability of basal ganglia, thalamus and brainstem. Pediatr Neurol 7:147–149

Pearson AA (1941a) The development of the nervus terminalis in man. J Comp Neurol 75:39–66

Pearson AA (1941b) The development of the olfactory nerve in man. J Comp Neurol 75:199–217

Pearson AA (1942) The development of the olfactory nerve, the nervus terminalis, and the vomeronasal nerve in man. Ann Otol Rhinol Laryngol 51:317–333

Pearson J, Brandeis L, Goldstein M (1980) Appearance of tyrosine hydroxylase immunoreactivity in the human embryo. Dev Neurosci 3:140–150

Pellegrini M, Monsouri A, Simeone A, Boncinelli E, Gruss P (1996) Dentate gyrus formation requires *Emx2*. Development 122:3893–3898

Percheron G (2004) Thalamus. In: Paxinos G, Mai JK (eds) The Human Nervous System, 2nd ed. Elsevier, Amsterdam, pp 592–675

Pichaud F, Desplan C (2002) Pax genes and eye organogenesis. Curr Opin Genet Dev 12:430–434

Pickel VM, Specht LA, Sumal KK, Joh TH, Reis DJ, Hervonen A (1980) Immunocytochemical localization of tyrosine hydroxylase in the human fetal nervous system. J Comp Neurol 194:465–474

Pilavdzic D, Kovacs K, Asa SL (1997) Pituitary morphology in anencephalic human fetuses. Neuroendocrinology 65:164–172

Porteus MH, Bulfone A, Liu JK, Puelles L, Lo LC, Rubinstein JLR (1994) DLX-2, MASH-1, and MAP-2 expression and bromodeoxyuridine incorporation define molecularly distinct cell populations in the embryonic mouse forebrain. J Neurosci 14:6370–6383

Prader A, Labhart A, Willi H (1956) Ein Syndrom von Adipositas, Kleinwuchs, Kryptorchismus und Oligophrenie nach myotonieartigem Zustand im Neugeborenenalter. Schweiz Med Wochenschr 86:1260–1261

Price JL (1990) Olfactory system. In: Paxinos G (ed) The Human Nervous System. Academic, San Diego, CA, pp 979–990

Probst FP (1979) The Prosencephalies. Morphology, neuroradiological appearances and differential diagnosis. Springer, Berlin Heidelberg New York

Prosser J, van Heyningen V (1998) PAX6 mutation review. Hum Mut 11:93–108

Provis JM, van Driel D, Billson FA, Russell P (1985a) Development of the human retina: Patterns and mechanisms of cell distribution and redistribution in the ganglion cell layer. J Comp Neurol 233:429–451

Provis JM, van Driel D, Billson FA, Russell P (1985b) Human fetal optic nerve: Overproduction and elimination of retinal axons during development. J Comp Neurol 238:92–100

Puelles L (1995) A segmental morphological paradigm for understanding vertebrate forebrains. Brain Behav Evol 46:319–337

Puelles L, Rubinstein JLR (2003) Forebrain gene expression domains and the evolving prosomeric model. Trends Neurosci 26:469–476

Puelles L, Verney C (1998) Early neuromeric distribution of tyrosine-hydroxylase-immunoreactive neurons in human embryos. J Comp Neurol 394:283–308

Puelles L, Amat JA, Martínez de la Torre M (1987) Segment-related, mosaic neurogenetic pattern in the forebrain and mesencephalon of early chick embryos. I. Topography of AChE-positive neuroblasts up to stage HH18. J Comp Neurol 266:247–268

Puelles L, Kuwana E, Puelles E, Bulfone A, Shimamura K, Keleher J, Smiga S, Rubinstein JLR (2000) Pallial and subpallial derivatives in the embryonic chick and mouse telencephalon, traced by the expression of the genes Dlx-2, Emx-1, Nkx-2.1, Pax-6, and Tbr-1. J Comp Neurol 424:409–438

Pulitzer SB, Simon EM, Crombleholme TM, Golden JA (2004) Prenatal MR findings of the middle interhemispheric variant of holoprosencephaly. AJNR Am J Neuroradiol 25:1034–1036

Pyatkina GA (1982) Development of the olfactory epithelium in man. Z Mikrosk Anat Forsch 96:361–372

Qiu M, Bulfone A, Martinez S, Meneses JJ, Shimamura K, Pedersen RA, Rubinstein JLR (1995) Null mutations of Dlx-2 results in abnormal morphogenesis of proximal first and second branchial arch derivatives and abnormal differentiation in the forebrain. Genes Dev 9:2523–2538

Quinton R, Duke VM, de Zoysa PA, Platts AD, Valentine A, Kendall B, Pickman S, Kirk JMW, Besser GM, Jacobs HS, Bouloux PMG (1996) The neuroradiology of Kallmann's syndrome: A genotypic and phenotypic analysis. J Clin Endocrinol Metab 81:3010–3017

Rademakers RP, van der Knaap MS, Verbeeten B, Barth P, Valk J (1995) Central cortico-subcortical involvement: A distinct pattern of brain damage caused by perinatal and postnatal asphyxia in term infants. J Comp Assist Tomogr 19:256–263

Rakic P (1974) Neurons in rhesus monkey visual cortex: Systematic relation between time of origin and eventual disposition. Science 183:425–427

Rakic P (1975) Timing of major ontogenetic events in the visual cortex of the rhesus monkey. In: Buchwald NA, Brazier MAB (eds) Brain Mechanisms of Mental Retardation. Academic, New York, pp 3–40

Rakic P (1976) Prenatal genesis of connections subserving ocular dominance in the rhesus monkey. Nature 261:467–471

Rakic P (1977a) Prenatal development of the visual system in rhesus monkey. Philos Trans R Soc Lond B 278:245–260

Rakic P (1977b) Genesis of the dorsal lateral geniculate nucleus in the rhesus monkey: Site and time of origin, kinetics of proliferation, routes of migration and pattern of distribution of neurons. J Comp Neurol 176:23–52

Rakić P, Sidman RL (1969) Telencephalic origin of pulvinar neurons in the fetal human brain. Z Anat Entw Gesch 129:53–82

Rallu M, Machold R, Gaiano N, Corbin JG, McMahon AP, Fishell (2002a) Dorso-ventral patterning is established in the telencephalon of mutants lacking both Gli3 and Hedgehog signaling. Development 129:4963–4974

Rallu M, Corbin JG, Fishell G (2002b) Parsing the prosencephalon. Nat Rev Neurosci 3:943–951

Rathke H (1838) Über die Entstehung der Glandula pituitaria. Arch Anat Physiol Wiss Med 1838:482–485

Richter E (1965) Die Entwicklung des Globus Pallidus und des Corpus Subthalamicum. Monographien aus dem Gesamtgebiete der Neurologie und Psychiatrie, Heft 108. Springer, Berlin Heidelberg New York, pp 1–131

Richter E (1966) Über die Entwicklung des Globus Pallidus und des Corpus Subthalamicum beim Menschen. In: Hassler R, Stephan H (eds) Evolution of the Forebrain. Thieme, Stuttgart, pp 285–295

Rieger DK, Reichenberger E, MacLean W, Sidow A, Olsen BR (2001) A double-deletion mutation in the Pitx3 gene causes arrested lens development in aphakia mice. Genomics 72:61–72

Rittig S, Robertson GL, Siggaard C, Kovács L, Gregersen N, Nyborg J, Pedersen EB (1996) Identification of 13 new mutations in the vasopressin-neurophysin II gene in 17 kindreds with familial autosomal dominant neurohypophyseal diabetes insipidus. Am J Hum Genet 58:107–117

Robinson BH (2001) Lactic acidemia: Disorders of pyruvate carboxylase and pyruvate dehydrogenase. In: Scriver CR, Beaudet AL, Sly WS, Valle D (eds) The Metabolic & Molecular Bases of Inherited Disease, 8th ed. McGraw-Hill, New York, pp 2275-2295

Roessler E, Muenke M (1998) Holoprosencephaly: A paradigm for the complex genetics of brain development. J Inherit Metab Dis 21:481–497

Roessler E, Muenke M (2001) Midline and laterality defects: Left and right meet in the midline. BioEssays 23:888–900

Roessler E, Belloni E, Gaudenz K, Jay P, Berta P, Scherer SW, Tsui L-C, Muenke M (1996) Mutations in the human Sonic hedgehog gene cause holoprosencephaly. Nat Genet 14:357–360

Roessler E, Du, Y-Z, Mullor JL, Casas E, Allen WP, Gillessen-Kaesbach G, Raeder ER, Ming JE, Ruiz i Altaba A, Muenke M (2003) Loss-of-function mutations in the human GLI2 gene are associated with pituitary anomalies and holoprosencephaly-like features. Proc Nat Acad Sci USA 100:13424–13429

Roessmann U, Schwarz JF (1973) Familial striatal degeneration. Arch Neurol 29:314–317

Roessmann U, Velasco ME, Small EJ, Hori A (1987) Neuropathology of "septo-optic dysplasia" (de Morsier syndrome) with immunohistochemical studies of the hypothalamus and pituitary gland. J Neuropathol Exp Neurol 46:597–608

Rohr KB, Barth KA, Varga ZM, Wilson SW (2001) The nodal pathway acts upstream of hedgehog signaling to specify ventral telencephalic identity. Neuron 29:341–351

Rubinstein JLR, Beachy PA (1998) Patterning of the embryonic forebrain. Curr Opin Neurobiol 8:18–26

Rubinstein JLR, Shimamura K, Martínez S, Puelles L (1998) Regionalization of the prosencephalic neural plate. Annu Rev Neurosci 21:445–477

Rugarli EI (1999) Kallmann syndrome and the link between olfactory and reproductive development. Am J Hum Genet 65:943–948

Rugarli EI, Lutz B, Kuratani SC, Wawersik S, Borsani G, Ballabio A, Eichele G (1993) Expression pattern of the Kallmann syndrome gene in the olfactory system suggests a role in neuronal targeting. Nat Genet 4:19–26

Rutherford MA (2002) Magnetic resonance imaging of injury in the immature brain. In: Squier W (ed) Acquired Damage to the Developing Brain: Timing and causation. Arnold, London, pp 166–192

Rutherford MA, Pennock JM, Murdoch-Eaton DM, Cowan FM, Dubowitz LM (1992) Athetoid cerebral palsy with cysts in the putamen after hypoxic-ischemic encephalopathy. Arch Dis Childh 67:846–850

Rutherford MA, Pennock JM, Schwieso JE, Cowan FM, Dubowitz LM (1995) Hypoxic ischemic encephalopathy: Early magnetic resonance imaging findings and their evolution. Neuropediatrics 26:183–191

Sailaja K, Gopinath G (1994) Developing substantia nigra in human: A qualitative study. Dev Neurosci 16:44-52

Sanger TD (2003) Pathophysiology of pediatric movement disorders. J Child Neurol 18:S9–S24

Saper CB (2004) Hypothalamus. In: Paxinos G, Mai JK (eds) The Human Nervous System, 2nd ed. Elsevier Academic, San Diego, CA, pp 514–550

Sarnat HB (2000) Molecular genetic classification of central nervous system malformations. J Child Neurol 15:675–687

Sarnat HB, Flores-Sarnat L (2001) Neuropathologic research strategies in holoprosencephaly. J Child Neurol 16:918–931

Sato K, Mano T, Sakurai M, Furukawa T (1975) Isolated thyrotropin deficiency: A case with abnormal leukocytes function. Clin Endocrinol 23:525–529

Savic I, Berglund H, Gulyas B, Roland P (2001) Smelling of odorous sex hormone-like compounds causes sex-differentiated hypothalamic activations in humans. Neuron 30:661–668

Schier AF (2001) Axis formation and patterning in zebrafish. Curr Opin Genet Dev 11:393–404

Schmahl W, Knoedlseder M, Favor J, Davidson D (1993) Defects of neuronal migration and the pathogenesis of cortical malformations are associated with Small eye (Sey) in the mouse, a point mutation at the Pax-6-locus. Acta Neuropathol (Berl) 86:126–135

Schuurmans C, Guillemot F (2002) Molecular mechanisms underlying cell fate specification in the developing telencephalon. Curr Opin Neurobiol 12:26–34

Schwalbe G (1880) Beiträge zur Entwicklungsgeschichte des Zwischenhirns. Sitz Ber Jen Ges Med Naturwiss 20:2–7

Schwanzel-Fukuda M, Pfaff DW (1989) Origin of luteinizing hormone releasing hormone neurons. Nature 338:161–164

Schwanzel-Fukuda M, Bick D, Pfaff DW (1989) Luteinizing hormone releasing hormone (LHRH)-expressing cells do not migrate in an inherited hypogonadal (Kallmann) syndrome. Mol Brain Res 6:311–326

Schwanzel-Fukuda M, Crossin KL, Pfaff DW, Bouloux PMG, Hardelin J-P, Petit C (1996) Migration of luteinizing hormone-releasing hormone (LHRH) neurons in early human embryos. J Comp Neurol 366:547–557

Schwind JL (1928) The development of the hypophysis cerebri of the albino rat. Am J Anat 41:295–315

Schwob JE, Price JL (1984) The development of axonal connections in the central olfactory system of rats. J Comp Neurol 223:177–202

Seibt J, Schuurmans C, Gradwhol G, Dehay C, Vanderhaeghen P, Guillemot F, Polleux F (2003) Neurogenin2 specifies the connectivity of thalamic neurons by controlling axon responsiveness to intermediate target clues. Neuron 39:439–452

Seiger Å, Olson L (1973) Late prenatal ontogeny of central monoamine neurons in the rat: Fluorescence histochemical observations. Z Anat Entw Gesch 140:281–318

Selemon LD, Goldman-Rakic PS (1985) Longitudinal topography and interdigitation of corticostriatal projections of the rhesus monkey. J Neurosci 5:776–794

Semina EV, Reiter RS, Murray J (1997) Isolation of a new homeobox gene belonging to the Pitx/Rieg family: Expression during lens development and mapping to the aphakia region on mouse chromosome 19. Hum Mol Genet 6:2109–2116

Semina EV, Ferrell RE, Mintz-Hittner HA, Bitoun P, Alward WLM, Reiter RS, Funkhauser C, Daack-Hirsch S, Murray JC (1998) A novel homeobox gene PITX3 is mutated in families with autosomal-dominant cataracts and ASMB. Nat Genet 19:167–170

Sergi C, Schmitt HP (2000) The vesicular forebrain (pseudo-aprosencephaly): A missing link in the teratogenic spectrum of defective brain anlage and its discrimination from aprosencephaly. Acta Neuropathol (Berl) 99:277–284

Shanmugalingam S, Houart C, Picker A, Reifers F, Macdonald R, Barth A, Griffin K, Brand M, Wilson SW (2000) Ace/Fgf8 is required for forebrain commissure formation and patterning of the telencephalon. Development 127:2549–2561

Shatz CJ (1983) The prenatal development of the cat's retinogeniculate pathway. J Neurosci 3:482–499

Shatz CJ, Luskin MB (1986) Relationship between the geniculocortical afferents and their cortical target cells during development of the cat's primary visual cortex. J Neurosci 6:3655–3668

Shatz CJ, Rakic P (1981) The genesis of efferent connections from the visual cortex of the fetal rhesus monkey. J Comp Neurol 196:287–307

Shatz CJ, Ghosh A, McConnell SK, Allendoerfer KL, Friauf E, Antonini A (1990) Pioneer neurons and target selection in cerebral cortical development. Cold Spring Harbor Symp Quant Biol 55:469–480

Sheng HZ, Westphal H (1999) Early steps in pituitary organogenesis. Trends Genet 15:236–240

Sheng HZ, Moriyama K, Yamashita T, Li H, Potter SS, Mahon KA, Westphal H (1997) Multistep control of pituitary organogenesis. Science 278:1809–1812

Shepherd GM, Greer CA (1990) Olfactory bulb. In: Shepherd GM (ed) The Synaptic Organization of the Brain, 3rd ed. Oxford University Press, New York, pp 133–169

Shimamura K, Rubinstein JLR (1997) Inductive interactions direct early regionalization of the mouse forebrain. Development 124:2709–2718

Shimamura K, Hartigan DJ, Martínez S, Puelles L, Rubinstein JLR (1995) Longitudinal organization of the anterior neural plate and neural tube. Development 121:3923–3933

Shiota K (1993) Teratothanasia: Prenatal loss of abnormal conceptuses and the prevalence of various malformations during human gestation. Birth Defects 29:189–199

Shipley MI, McLean JH, Ennis M (1995) Olfactory system. In: Paxinos G (ed) The Rat Nervous System, 2nd ed. Academic, San Diego, CA, pp 899–926

Sie LTL, van der Knaap MS, Oostings J, de Vries L, Lafeber HN, Valk J (2000) MR pattern of hypoxic-ischemic brain damage after prenatal, perinatal or postnatal asphyxia. Neuropediatrics 31:128–136

Siebert JR, Warkany J, Lemire RJ (1986) Atelencephalic microcephaly in a 21 week human fetus. Teratology 34:9–19

Siebert JR, Kokich VG, Warkany J, Lemire RJ (1987) Atelencephalic microcephaly: Craniofacial anatomy and morphologic comparisons with holoprosencephaly and anencephaly. Teratology 36:279–285

Siebert JR, Cohen MM Jr, Sulik KK, Shaw C-M, Lemire RJ (1990) Holoprosencephaly: An overview and atlas. Wiley–Liss, New York

Silver J, Robb RM (1979) Studies on the development of the eye cup and optic nerve in normal mice and in mutants with congenital optic nerve aplasia. Dev Biol 68:175–190

Simeone A, Acampora D, Gulisano M, Stornaiuolo A, Boncinelli E (1992) Nested expression domains of four homeobox genes in developing rostral brain. Nature 358:687–690

Simeone A, Acampora D, Mallaci A, Stornaiuolo A, D'Apice MR, Nigro V, Boncinelli E (1993) A vertebrate gene related to orthodenticle contains a homeodomain of the bicoid class and demarcates anterior neuroectoderm in the gastrulating mouse embryo. EMBO J 12:2735–2747

Simon EM, Hevner RF, Pinter JD, Kinsman SL, Hahn J, Barkovich AJ (2000) Assessment of the deep gray nuclei in holoprosencephaly. AJNR Am J Neuroradiol 21:1955–1961

Simon EM, Hevner RF, Pinter JD, et al. (2001) The dorsal cyst in holoprosencephaly and the role of the thalami in its formation. Neuroradiology 43:787–791

Simon EM, Hevner RF, Pinter JD, Clegg NJ, Delgado M, Kinsman SL, Hahn JS, Barkovich AJ (2002) The middle interhemispheric variant of holoprosencephaly. AJNR Am J Neuroradiol 23:151–155

Sisodiya SM, Free SL, Williamson KA, Mitchell TN, Willis C, Stevens JM, Kendall BE, Shorvon SD, Hanson IM, Moore AT, van Heyningen V (2001) PAX6 haplo-insufficiency causes cerebral malformations and olfactory dysfunction in humans. Nat Genet 28:214–216

Smart IH, Dehay C, Giroud P, Berland M, Kennedy H (2002) Unique morphological features of the proliferative zones and postmitotic compartments of the neural epithelium giving rise to striate and extrastriate cortex in the monkey. Cereb Cortex 12:37–53

Smidt MP, van Schaick HSA, Lanctôt C, Tremblay JJ, Cox JJ, van der Kleij AAM, Wolterink G, Drouin J, Burbach PH (1997) A homeodomain gene PITX3 has highly restricted brain expression in mesencephalic dopaminergic neurons. Proc Nat Acad Sci USA 94:13305–13310

Smidt MP, Asbreuk CH, Cox JJ, Chen H, Johnson RL (2000) A second independent pathway for development of mesencephalic dopaminergic neurons requires Lmxb1. Nat Neurosci 3:337–341

Smith-Fernández A, Pieau C, Repérant J, Boncinelli E, Wassef M (1998) Expression of the Emx-1 and Dlx-1 homeobox genes define three molecularly distinct domains in the telencephalon of mouse, chick, turtle and frog embryos: Implications for the evolution of telencephalic subdivisions in amniotes. Development 125:2099–2111

Soffer D, Amir N, Elpeleg ON, Gomori JM, Shalev RS, Gottschalk-Sabeg S (1992) Striatal degeneration and spongy myelinopathy in glutaric aciduria. J Neurol Sci 107:199–204

Specht LA, Pickel VM, Joh TH, Reis DJ (1981a) Light-microscopic immunocytochemical localization of tyrosine hydroxylase in prenatal rat brain. I. Early ontogeny. J Comp Neurol 199:233–253

Specht LA, Pickel VM, Joh TH, Reis DJ (1981b) Light-microscopic immunocytochemical localization of tyrosine hydroxylase in prenatal rat brain. II. Late ontogeny. J Comp Neurol 199:255–276

Squier W (2002) Pathology of fetal and neonatal brain damage: Identifying the timing. In: Squier W (ed) Acquired Damage to the Developing Brain: Timing and Causation. Arnold. London, pp 110–127

Stein J, Walsh V (1997) To see but not to read; the magnocellular theory of dyslexia. Trends Neurosci 20:147–152

Steingrimsson E, Moore KJ, Lamoreux ML, Ferré-D'Amaré A, Burley SK, Zimring DCS, Skow LC, Hodgkinson CA, Arnheiter H, Copeland NG, Jenkins NA (1994) Molecular basis of mouse microphthalmia (mi) mutations helps explain their developmental and phenotypic consequences. Nat Genet 8:256–263

Stenman J, Yu RT, Evans RM, Campbell K (2003) Tlx and Pax6 cooperate genetically to establish the pallio-subpallial boundary in the embryonic mouse telencephalon. Development 130:1113–1122

Stephan H (1975) Allocortex. Handbuch der mikroskopischen Anatomie des Menschen, Vol 4, Teil 9. Springer, Berlin Heidelberg New York

Stephan H, Andy OJ (1977) Quantitative comparison of the amygdala in insectivores and primates. Acta Anat (Basel) 98:130–153

Stoykova A, Fritsch R, Walther C, Gruss P (1996) Roles of Pax-genes in developing and adult brain as suggested by expression patterns. J Neurosci 14:1395–1412

Stoykova A, Treichel D, Hallonot M, Gruss P (2000) Pax6 modulates the dorsoventral patterning of the mammalian telencephalon. J Neurosci 20:8042–8050

Stühmer T, Anderson SA, Ekker M, Rubinstein JLR (2002) Ectopic expression of the Dlx genes induces glutamic acid decarboxylase and Dlx expression. Development 129:245–252

Suda Y, Hossain ZM, Kobayashi C, Hatano O, Yoshida M, Matsuo I, Aizawa S (2001) Emx2 directs the development of diencephalon in cooperation with Otx2. Development 128:2433–2450

Suh H, Gage PJ, Drouin J, Camper SA (2002) Pitx2 is required at multiple stages of pituitary organogenesis: Pituitary primordium formation and cell specification. Development 129:329–337

Sur M, Leamey CA (2001) Development and plasticity of cortical areas and networks. Nat Rev Neurosci 2:251–262

Sussel L, Marín O, Kimura S, Rubinstein JLR (1999) Loss of Nkx2.1 homeobox gene function results in a ventral to dorsal molecular respecification within the basal telencephalon: Evidence for a transformation of the pallidum into the striatum. Development 126:3359–3370

Swaab DF (1997) Neurobiology and neuropathology of the human hypothalamus. In: Bloom FE, Björklund A, Hökfelt T (eds) Handbook of Chemical Neuroanatomy, Vol 13: The Primate Nervous System, Part I. Elsevier, Amsterdam, pp 39–137

Swaab DF (2003) The Human Hypothalamus: Basic and clinical aspects, Part 1: Nuclei of the human hypothalamus. Handb Clin Neurol, Vol 79

Swaab DF (2004) The Human Hypothalamus: Basic and clinical aspects, Part 2: Neuropathology of the human hypothalamus and adjacent structures. Handb Clin Neurol, Vol 80

Swaab DF, Fliers E (1985) A sexually dimorphic nucleus in the human brain. Science 228:1112–1115

Swaab DF, Hofman MA (1988) Sexual differentiation of the human hypothalamus: Ontogeny of the sexually dimorphic nucleus of the preoptic area. Dev Brain Res 44:314–318

Swaab DF, Hofman MA, Lucassen PJ, Purba JS, Raadsheer FC, van de Nes JAP (1993) Functional neuroanatomy and neuropathology of the human hypothalamus. Anat Embryol (Berl) 187:317–330

Switzer RC, Hill J, Heimer L (1982) The globus pallidus and its rostroventral extension into the olfactory tubercle in the rat: A cyto- and chemoarchitectural study. Neuroscience 7:1891–1904

Szeto DP, Rodriguez-Esteban C, Ryan AK, O'Connell SM. Liu F, Kioussi C, Gleiberman AS, Izpisua-Belmonte JC, Rosenfeld MG (1999) Role of the bicoid-related homeodomain factor Pitx1 in specifying hindlimb morohogenesis and pituitary development. Genes Dev 13:484–494

Takahashi H, Ohama E, Naito H, et al. (1988) Hereditary dentatorubro-pallido-luysian atrophy: Clinical and pathologic variants in a family. Neurology 38:1065–1070

Tamamaki N, Fujimori KE, Takauji R (1997) Origin and route of tangentially migrating neurons in the developing neocortical intermediate zone. J Neurosci 17:8313–8323

Tan SS, Kalloniatis M, Sturm K, Tam PP, Reese BE, Faulkner-Jones B (1998) Separate progenitors for radial and tangential cell dispersion during development of the cerebral cortex. Neuron 21:295–304

Tassabehji M, Newton VE, Read AP (1994) Waardenburg syndrome type 2 caused by mutations in the human microphthalmia (*MITF*) gene. Nat Genet 8:251–255

ten Donkelaar HJ, Dederen PJW (1979) Neurogenesis in the basal forebrain of the Chinese hamster (*Cricetulus griseus*). I. Time of neuron origin. Anat Embryol (Berl) 156:331–348

ten Donkelaar HJ, Lammers GJ, Gribnau AAM (1979) Neurogenesis in the amygdaloid nuclear complex in a rodent (the Chinese hamster). Brain Res 165:348–353

Tennyson VM, Barrett RE, Cohen G, Côté L, Heikkila R, Mytilineou C (1972) The developing neostriatum of the rabbit: Correlation of fluorescence histochemistry, electron microscopy, endogenous dopamine levels, and [³H] dopamine uptake. Brain Res 46:251–285

Theil T, Alvarez-Bolado G, Walter A, Ruther U (1999) *Gli3* is required for *Emx* gene expression during dorsal telencephalic development. Development 126:3561–3571

Theiler K (1972) The House Mouse – Development and normal stages from fertilization to 4 weeks of age. Springer, Berlin Heidelberg New York

Theiler K, Varnum DS, Nadeau JH, Stevens LC, Cagianut B (1976) A new allele of *ocular retardation*: Early development and morphogenetic cell death. Anat Embryol (Berl) 150:85–97

Thomas PQ, Dattani MT, Brickman JM, McNay D, Warne G, Zacharin M, Cameron F, Hurst J, Woods K, Dunger D, et al. (2001) Heterozygous *HESX1* mutations associated with isolated congenital pituitary hypoplasia and septo-optic dysplasia. Hum Mol Genet 10:39–45

Tole S, Goudreau G, Assimacopoulos S, Grove E (2000a) *Emx2* is required for growth of the hippocampus but not for hippocampal field specification. J Neurosci 20:2618–2625

Tole S, Ragsdale CW, Grove EA (2000b) Dorsoventral patterning of the telencephalon is disrupted in the mouse mutant *extratoes* (*J*). Dev Biol 217:254–265

Toresson H, Campbell K (2001) A role for *Gsh1* in the developing striatum and olfactory bulb of *Gsh* mutant mice. Development 128:4679–4689

Toresson H, Potter S, Campbell K (2000) Genetic control of dorsalventral identity in the telencephalon: Opposing roles for *Pax6* and *Gsh2*. Development 127:4361–4371

Torres M, Gomez-Pardo E, Gruss P (1996) *Pax2* contributes to inner ear patterning and optic nerve trajectory. Development 122:3381–3391

Towfighi J, Ladda RL, Sharkey FE (1987) Purkinje cell inclusions and 'atelencephaly' in 13q-chromosomal syndrome. Arch Pathol Lab Med 111:146–150

Treier M, O'Connell S, Gleiberman A, Price J, Szeto DP, Burgess R, Chuang P-T, McMahon AP, Rosenfeld MG (2001) Hedgehog signaling is required for pituitary glandular development. Development 128:377–386

Trottier D, Eloit C, Wassef M, Talmain G, Bensimon JL, Døving KB, Ferrard J (2000) The vomeronasal cavity in adult humans. Chem Senses 25:369–380

Truslove GM (1962) A gene causing ocular retardation in the mouse. J Embryol Exp Morphol 10:652–660

Truwit CL, Barkovich AJ, Grumbach MM, Martini JJ (1993) MR imaging of Kallmann syndrome, a genetic disorder of neuronal migration affecting the olfactory and genital sytems. AJNR Am J Neuroradiol 14:827–838

Tulinius M, Moslemi A-R, Darin N, Westerberg B, Wiklund L-M, Holme E, Oldfors A (2003) Leigh syndrome with cytochrome-c oxidase deficiency and a single T insertion nt 5537 in the mitochondrial tRNA^Trp gene. Neuropediatrics 34:87–91

Tuttle R, Nakagawa Y, Johnson JE, O'Leary DDM (1999) Defects in thalamocortical axon pathfinding correlate with altered cell domains in *Mash-1*-deficient mice. Development 1256:1903–1916

Ulfig N (2002a) Ganglionic eminence of the human fetal brain – new vistas. Anat Rec 267:191–195

Ulfig N (2002b) Calcium-binding proteins in the human developing brain. Adv Anat Embryol Cell Biol 165:1–95

Ulfig N, Nickel J, Bohl J (1998) Transient features of the thalamic reticular nucleus in the human foetal brain. Eur J Neurosci 10:3773–3784

Ulfig N, Neudörfer F, Bohl J (2001) Development-related expression of AKAP79 in the striatal compartments of the human brain. Cells Tissues Organs 168:319–329

Ulfig N, Setzer M, Bohl J (2003a) Ontogeny of the human amygdala. Ann NY Acad Sci 985:22–33

Ulfig N, Bohl J, Setzer M (2003b) Expression of NMDAR1 in the human fetal amygdala and the adjacent ganglionic eminence. Neuroendocrinology 2:40–42

Vaizey MJ, Sanders MD, Wybar KC, Wilson J (1977) Neurological abnormalities in congenital amaurosis of Leber. Review of 30 cases. Arch Dis Childh 52:399–402

van den Munckhof P, Luk KC, Ste-Marie L, Montgomery J, Blanchet PJ, Sadikot AF, Drouin J (2003) Pitx3 is required for motor activity and for survival of a subset of midbrain dopaminergic neurons. Development 130:2535–2542

Vanderhaeghen P, Polleux F (2004) Developmental mechanisms patterning thalamocortical projections: Intrinsic, extrinsic and in between. Trends Neurosci 27:384–391

Van der Kooy D, Fishell G, Krushel LA, Johnston JG (1987) The development of striatal compartments: From proliferation to patches. In: Carpenter MB, Jarayaman A (eds) The Basal Ganglia, Structures and Concepts – Current concepts. Plenum, New York, pp 81–98

van Domburg PHMF, ten Donkelaar HJ (1990) The human substantia nigra and ventral tegmental area. A neuroanatomical study with notes on aging and aging diseases. Adv Anat Embryol Cell Biol 121:1–132

van Eden CG, Mrzljak L, Voorn P, Uylings HBM (1989) Prenatal development of GABAergic neurons in the neocortex of the rat. J Comp Neurol 289:213–227

van Heyningen V, Williamson KA (2002) *PAX6* in sensory development. Hum Mol Genet 11:1161–1167

Van Hoesen GW, Yeterian EH, Lavizzo-Mourney R (1981) Widespread corticostriate projections from temporal cortes of the rhesus monkey. J Comp Neurol 199:205–219

van Overbeeke JJ (1991) The Development of the Variations of the Human Basal Cerebral Arteries. Thesis, University of Utrecht

van Overbeeke JJ, Hillen B, Vermeij-Keers C (1994) The arterial pattern at the base of arhinencephalic and holoprosencephalic brains. J Anat (Lond) 185(Pt 1):51 – 63

Vermeij-Keers C (1975) Primary congenital aphakia and the rubella syndrome. Teratology 11:257–266

Vermeij-Keers C (1987) 6.5-mm Human embryo with a single nasal placode: Cyclopia or hypotelorism? Teratology 36:1–6

Verney C, Berger B, Adrien J, Vigny A, Gay MC (1982) Development of the dopaminergic innervation of the rat cerebral cortex. A light microscopic immunocytochemical study using anti-tyrosine hydroxylase antibodies. Dev Brain Res 5:41–52

Verney C, Zecevic N, Nikolic B, Alvarez C, Berger B (1991) Early evidence of catecholaminergic cell groups in 5- and 6-week-old human embryos using tyrosine hydroxylase and dopamine-β-hydroxylase immunocytochemistry. Neurosci Lett 131:121–124

Verney C, Milosevic A, Alvarez C, Berger B (1993) Immunocytochemical evidence of well-developed dopaminergic and noadrenergic innervations in the frontal cerebral cortex of human fetuses at midgestation. J Comp Neurol 336:331–344

Verney C, El Amraoui A, Zecevic N (1996) Comigration of tyrosine hydroxylase- and gonadotrophin-releasing hormone-immunoreactive neurons in the nasal area of human embryos. Dev Brain Res 97:251–259

Visser M, Swaab DF (1979) Life span changes in the presence of α-melanocyte-stimulating-hormone-containing cells in the human pituitary. J Dev Physiol 1:161–178

Voit T, Lemburg P, Neuen E, Lumenta C, Strork W (1987) Damage of thalamus and basal ganglia in asphyxiated fullterm neonates. Neuropediatrics 18:176–181

Voogd J, Nieuwenhuys R, van Dongen PAM, ten Donkelaar HJ (1998) Mammals. In: Nieuwenhuys R, ten Donkelaar HJ, Nicholson C The Central Nervous System of Vertebrates. Springer, Berlin Heidelberg New York, pp 1637–2097

Voorn P, Kalsbeek A, Jorritsma-Byham B, Groenewegen HJ (1988) The pre- and postnatal development of the dopaminergic cell groups in the ventral mesencephalon and the dopaminergic innervation of the striatum of the rat. Neuroscience 25: 857–887

Vortkamp A, Franz T, Gessler M, Grzeschik K-H (1992) Deletion of *GLI3* supports the homology of the human Greig cephalopolysyndactyly syndrome (GCPS) and the mouse mutant extra toes (*Xt*). Mammalian Genome 3:461–463

Wallis DE, Roessler E, Hehr U, Nanni L, Wiltshire T, Richieri-Costa A, Gillessen-Kaesbach G, Zackai EH, Romeni J, Muenke M (1999) Mutations in the homeodomain of the human *SIX3* gene cause holoprosencephaly. Nat Genet 22:196–198

Walther C, Gruss P (1991) *Pax-6*, a murine paired box gene, is expressed in the developing CNS. Development 113:1435–1449

Wang Q, Chen Q, Zhao K, Wang L, Trabouli EI (2001) Update on the molecular genetics of retinitis pigmentosa. Ophthalmic Genet 22:133–154

Warkany J (1971) Congenital Malformations. Year Book, Chicago, IL

Warner TT, Lennox GG, Janota I, Harding AE (1994) Autosomal-dominant dentato-rubro-pallido-luysian atrophy in the United Kingdom. Mov Disord 9:289–296

Warner TT, Lennox GG, Walker RWH, et al. (1995) A clinical and molecular genetic study of dentatorubropallidoluysian atrophy in four European families. Ann Neurol 37:452–459

Watanabe YG (1982) Effects of brain and mesenchyme upon the cytogenesis of rat adenohypophysis *in vitro*. I. Differentiation of adrenocorticotropes. Cell Tissue Res 227:257–266

Watkins-Chow DE, Camper SA (1998) How many homeobox genes does it take to make a pituitary gland? Trends Genet 14:284–290

Wawersik S, Purcell P, Maas RL (2000) *Pax6* and the genetic control of early eye development. In: Fini ME (ed) Vertebrate Eye Development. Springer, Berlin Heidelberg New York, pp 15–36

Wichterle H, Garcia-Verdugo JM, Herrera DG, Alvarez-Buylla A (1999) Young neurons from medial ganglionic eminence disperse in adult and embryonic brain. Nat Neurosci 2:461–466

Wichterle H, Turnbull DH, Nery S, Fishell G, Alvarez-Buylla A (2001) In utero fate mapping reveals distinct migratory pathways and fates of neurons born in the mammalian forebrain. Development 128:3759–3771

Willnow S, Kiess W, Butenandt O, Dörr HG, Enders A, Strasser-Vogel B, Egger J, Schwartz HP (1996) Endocrinbe disorders in septo-optic dysplasia (De Morsier syndrome) – evaluation and follow-up of 18 paients. Eur J Pediatr 155:179–184

Wolfram DJ (1938) Diabetes mellitus and simple optic atrophy among siblings: Report of four cases. Proc Staff Meet Mayo Clin 13:715–718

Wray S, Nieburgs A, Elkabes S (1989a) Spatiotemporal cell expression of luteinizing hormone releasing hormone in the prenatal mouse: Evidence for an embryonic origin in the olfactory pit. Dev Brain Res 46:309–318

Wray S, Grant P, Gainer H (1989b) Evidence that cells expressing luteinizing hormone releasing hormone mRNA in the mouse are derived from progenitor cells in the olfactory placode. Proc Natl Acad Sci USA 86:8132–8136

Wurst W, Bally-Cuif L (2001) Neural plate patterning: Upstream and downstream of the isthmic organizer. Nat Rev Neurosci 2:99–108

Xuan S, Baptista CA, Balas G, Tao W, Soares VC, Lai E (1995) Winged helix transcription factor BF-1 is essential for the development of the cerebral hemispheres. Neuron 14:1141–1152

Yakovlev PI (1959) Pathoarchitectonic studies of cerebral malformations. III. Arrhinencephalies (holotelencephalies). J Neuropathol Exp Neurol 18:22–55

Yakovlev PI (1969) The development of the nuclei of the dorsal thalamus and the cerebral cortex. In: Locke S (ed) Modern Neurology (Papers in Tribute to Professor Denny Derek-Brown). Little, Brown, Boston, MA, pp 1–15

Yamada S, Uwabe C, Fujii S, Shiota K (2004) Phenotypic variability in human embryonic holoprosencephaly in the Kyoto Collection. Birth Defects Res Part A Clin Mol Teratol 70:495–508

Yamadori T (1965) Die Entwicklung des Thalamuskerns mit ihren ersten Fasersystemen bei menschlichen Embryonen. J Hirnforsch 7:393–413

Yamanouchi H, Hirato J, Yokoo H, Nako Y, Morikawa A, Nakazato Y (1999) Olfactory bulb dysplasia: A novel subtype of neuronal migration disorder. Ann Neurol 46:783–786

Ye W, Shimamura K, Rubinstein JLR, Hynes MA, Rosenthal A (1998) FGF and Shh signals control dopaminergic and serotonergic cell fatwe in the anterior neural plate. Cell 93:755–766

Yilmaz Y, Alper G, Kilicoglu G, Celik L, Karadeniz L, Yilmaz-Degirmenci S (2001) Magnetic resonance imaging findings in patients with severe neonatal indirect hyperbilirubinemia. J Child Neurol 16:452–455

Yokochi K, Aiba K, Kodama M, Fujimoto S (1991) Magnetic resonance imaging in athetotic cerebral palsied children. Acta Paediatr Scand 80:818–823

Yoshida M, Suda Y, Matsuo I, Miyamoto N, Takeda N, Kuratani S, Aizawa S (1997) *Emx1* and *Emx2* functions in development of dorsal telencephalon. Development 124:101–111

Young RW (1985) Cell differentiation in the retina of the mouse. Anat Rec 212:199–205

Yun K, Potter S, Rubinstein JLR (2001) *Gsh2* and *Pax6* play complementary roles in dorsoventral paaterning of the mammalian telencephalon. Development 128:193–205

Zaki PA, Quinn JC, Price DJ (2003) Mouse models of telencephalic development. Curr Opin Genet Dev 13:423–437

Zečević N, Kostoviç I (1980) Synaptogenesis in developing neostriatum of the human fetus. Neurosci Lett Suppl 5:S311

Zecevic N, Verney C (1995) Development of the catecholamine neurons in human embryos and fetuses, with special emphasis on the innervation of the cerebral cortex. J Comp Neurol 351:509–535

Zeki S (1993) A Vision of the Brain. Blackwell, Oxford

Zeki SM, Hollman AS, Dutton GN (1992) Neuroradiological features of patients with optic nerve hypoplasia. J Pediatr Ophthalmol Strabismus 29:107–112

Zeltser L. Larsen C, Lumsden A (2001) A novel developmental compartment in the forebrain regulated by Lunatic fringe. Nat Neurosci 4:683–685

Zetterstrom RM, Williams R, Perlmann T, Olson L (1996) Cellular expression of the intermediate early transcription factors Nurr1 and NGFI-B suggest a gene regulatory role in several brain regions including the nigrostriatal dopamine system. Mol Brain Res 41:111–120

Zetterstrom RH, Solomin L, Jansson L, Hoffer BJ, Olson L, Perlmann T (1997) Dopamine neuron agenesis in Nurr1-deficient mice. Science 276:248–250

Zeviani M, Bertagnolio B, Uziel G (1996) Neurological presentations of mitochondrial diseases. J Inher Metab Dis 19:504–520

Zhu X, Rosenfeld MG (2004) Transcriptional control of precursor proliferation in the early phases of pituitary development. Curr Opin Genet Dev 14:567–574

Zschocke J, Quak E, Guldberg P, HoffmannGF (2000) Mutation analysis in glutaric aciduria type 1. J Med Genet 37:177–181

Development and Developmental Disorders of the Cerebral Cortex

Hans J. ten Donkelaar, Martin Lammens, Willy Renier, Ben Hamel, Akira Hori and Berit Verbist

10.1 Introduction

The cerebral cortex can be divided into a large isocortex or neocortex, a much smaller allocortex (the hippocampal formation and the olfactory cortex) and a transition zone (the mesocortex) in between. The allocortex consists of three layers, the mesocortex (the gyrus cinguli and large part of the gyrus parahippocampalis) of four to five layers, and the neocortex typically of six layers. On the basis of cytoarchitectonic criteria, Brodmann (1909) subdivided the human cerebral cortex into 52 areas. Although many individual variations exist in the sulcal pattern (Ono et al. 1990; Duvernoy 1992) and in the extent of various cortical areas (Zilles 1990; Rademacher et al. 1993, 2001; Vogt et al. 1995; Amunts et al. 1999), the remarkable conservation of the pattern of areal divisions within the human brain suggests the existence of a highly conserved and rather rigidly regulated regional specification programme that controls their development (Rakic 1988, 1995). Histogenesis of the cerebral cortex progresses through three major phases: cell production, cell migration, and cortical differentiation and maturation. Migrating cells from the ventricular zone to the cortical plate form ontogenetic radial cell columns. These ontogenetic cell columns most likely develop into adult minicolumns which form the basic units of the neocortex (Mountcastle 1997). These aspects have been extensively studied in rodents, but also for the human cerebral cortex a large amount of data is available (Kostović 1990a, b; Mrzljak et al. 1990; Meyer et al. 2000b; Uylings 2001; Chan et al. 2002; Ulfig and Chan 2002). During the last decade, analysis of the genetic control of cortical development became possible (Rubinstein et al. 1999; Ragsdale and Grove 2001; O'Leary and Nakagawa 2002). Mechanisms for induction and regionalization of the cerebral cortex are being unravelled and genes that are implicated in controlling regionalization, arealization and differentiation have been discovered in the developing mouse brain. This neurogenetic approach has given a great impetus to the study of neuronal migration disorders (NMDs), previously particularly the field of a group of dedicated neuropathologists (Jellinger and Rett 1976; Barth 1987; Friede 1989; Norman et al. 1995). Advances in neurogenetics and the increasing application of MRI resulted in the distinction of a growing number of NMDs, of many of which the gene involved has been discovered (Walsh 1999; Gleeson and Walsh 2000; Barkovich et al. 2001; Pilz et al. 2002).

In this chapter, after a brief overview of the organization of the cerebral cortex and its main connections, the development of the neocortex, the hippocampus and their main fibre systems will be discussed, followed by an overview of developmental disorders of the cerebral cortex. Developmental disorders of the cerebral cortex include malformations due to abnormal cell production (Sect. 10.7.1), abnormal migration (Sect. 10.7.2), abnormal cortical organization (Sect. 10.7.3) and vascular disorders (Sect. 10.7.5). Many of these result in epilepsy (Sect. 10.7.4) and/or mental retardation (Sect. 10.7.7). Dendritic abnormalities are the most consistent findings associated with mental retardation (Kaufmann and Moser 2000). Recent studies revealed potential differences in the columnar organization of the cerebral cortex in neurobehavioural disorders (Sect. 10.7.8), such as autism and schizophrenia, and also in Down syndrome (Buxhoeveden and Casanova 2002).

10.2 Overview of the Cerebral Cortex

The Vogts (Vogt and Vogt 1919) divided the human cerebral cortex into isocortical and allocortical territories to replace Brodmann's homotypical and heterotypical cortices. The **isocortex** is the major part of the telencephalon. Ontogenetically, the isocortical areas show an almost similar development and share the characteristic six layers, at least during some stage of development. In contrast, the **allocortex** (the 'other' cortex) is quite heterogeneous (Stephan 1975; Braak 1980). The periallocortex, surrounding the allocortex, and the proisocortex along the borders of the isocortex form transitional zones, often referred to as **mesocortex** (Rose 1927 a, b). Mesocortical areas will be briefly discussed in the section on the allocortex.

10.2.1 The Neocortex

The **isocortex** or **neocortex** is composed of several types of neurons, of which the pyramidal cells and the granule cells are the most common (for a discussion of cortical cell types and their circuitry, see Nieuwenhuys 1994). The **pyramidal cells** have a pyra-

Fig. 10.1 Cortical layers. The *left column* shows Golgi-stained neurons, the *middle column* Nissl-stained cells and the *right column* myelinated fibres, such as the external (in layer IV) and internal (in layer V) stripes of Baillarger. (After Brodmann 1909; Ranson and Clark 1959)

pyramidal and fusiform cells, many of which give rise to corticothalamic projections.

The different parts of the neocortex show large variations in the development of various layers. The cortical areas that receive the primary sensory pathways via the thalamus form the **granular cortex**, in which layers II and IV are especially well developed, whereas it is difficult to distinguish pyramidal layers III and V. In the motor cortex (the precentral gyrus), layers II and IV are poorly developed (**agranular cortex**), whereas the pyramidal layers are well developed. On the basis of such regional variations in cytoarchitecture, the cerebral cortex can be divided into different areas. Brodmann (1909) identified 52 areas, which he numbered from 1 to 52 in the order in which he studied them (Fig. 10.2). Areas 3, 1 and 2 represent the primary somatosensory cortex (the postcentral gyrus), areas 4, 6 and 8 the motor cortices, areas 17, 18 and 19 the visual cortex, areas 41 and 42 the auditory cortex and areas 44 and 45 Broca's speech region. Other **brain maps** of the human cerebral cortex were made by Vogt and Vogt (1919), von Economo and Koskinas (1925), Bailey and von Bonin (1951) and Sarkissov et al. (1955). The atlas of the cerebral cortex by Sarkissov and co-workers contains photomicrographs of all cortical areas distinguished. Their brain maps integrate the findings of Brodmann and the Vogts.

The human cerebral cortex can also be subdivided into several **functional cortical fields** (Mesulam 1985; Fig. 10.3): (1) **unimodal sensory fields**, primary sensory fields receiving projections from sensory relay nuclei in the thalamus (Chap. 9), defined as S1 (area 3,1,2), A1 (area 41) and V1 (area 17), and secondary sensory fields (S2 and area 42 or A2); (2) **higher-order sensory cortical fields** such as areas 5 and 7 for further processing somatosensory information, area 22 for auditory information and areas 18 and 19 (V2–V5 fields; Zeki 1993) for visual information; (3) **multimodal** or **heteromodal association areas**, receiving information from several sensory modalities, including the parietotemporo-occipital, limbic and prefrontal association areas; (4) **higher-order motor cortex**, including the lateral premotor cortex (lateral part of area 6), the medial premotor cortex (supplementary motor area or SMA, i.e. the part of area 6 on the medial aspect of the hemisphere) and the frontal eye field (area 8); and (5) the **primary motor cortex** (area 4 or M1; Roland and Zilles 1996; Rademacher et al. 2001; Zilles 2004). The unimodal sensory fields and the primary motor cortex form only a relatively small part of the cerebral cortex as a whole.

Neuroanatomical and neurophysiological studies have identified the presence of a vertical organization of the neocortex in the form of cell columns (reviewed in Mountcastle 1997). The basic unit of the

mid-shaped cell body with an apical dendrite directed outwards and a group of basal dendrites on the side of the white matter. The **granule** or **stellate cells** are the largest group of cortical interneurons. The six layers of the neocortex are from the outside to the inside (Fig. 10.1) as follows: (1) layer I, the **molecular layer**, largely composed of axons and apical dendrites of pyramidal cells; (2) layer II, the **external granular layer**, containing mainly small pyramidal cells; (3) layer III, the **external pyramidal layer**, containing small and medium-sized pyramidal cells which, together with those in layer II, give rise to the association and commissural fibres; (4) layer IV, the **internal granular layer**, composed of small, densely packed pyramidal cells and spiny stellate cells, characteristic for layer IV; layer IV is the main recipient of thalamocortical projections; (5) layer V, the **internal pyramidal layer**, composed of medium-sized and large pyramidal cells, projecting to the striatum, the brain stem and the spinal cord; and (6) layer VI, the **multiform layer**, containing a variety of stellate,

Fig. 10.2 Brodmann's subdivision of the human cerebral cortex into 52 areas: **a** lateral surface; **b** medial surface; the *insert* shows the insular cortex (*J.ant* and *J.post*). In Brodmann's map, areas 13–16 are missing, but form the insular cortex (Gorman and Unützer 1993). (After Brodmann 1909; Braak 1980)

mature neocortex is the **minicolumn**, a narrow chain of neurons extending vertically across layers II–VI, perpendicular to the pial surface. In primates, each minicolumn contains all of the major cortical cell types, interconnected vertically. The minicolumns are produced by the iterative division of small clusters of progenitor cells in the neuroepithelium (Fig. 10.12). Minicolumns display considerable heterogeneity between areas and species (Buxhoeveden and Casanova 2002). Anomalies of minicolumn organization are discussed in Sect. 10.7.8. **Cortical columns** or **modules** are formed by many minicolumns bound together by short-range horizontal connections. They vary from about 300 to 600 μ in
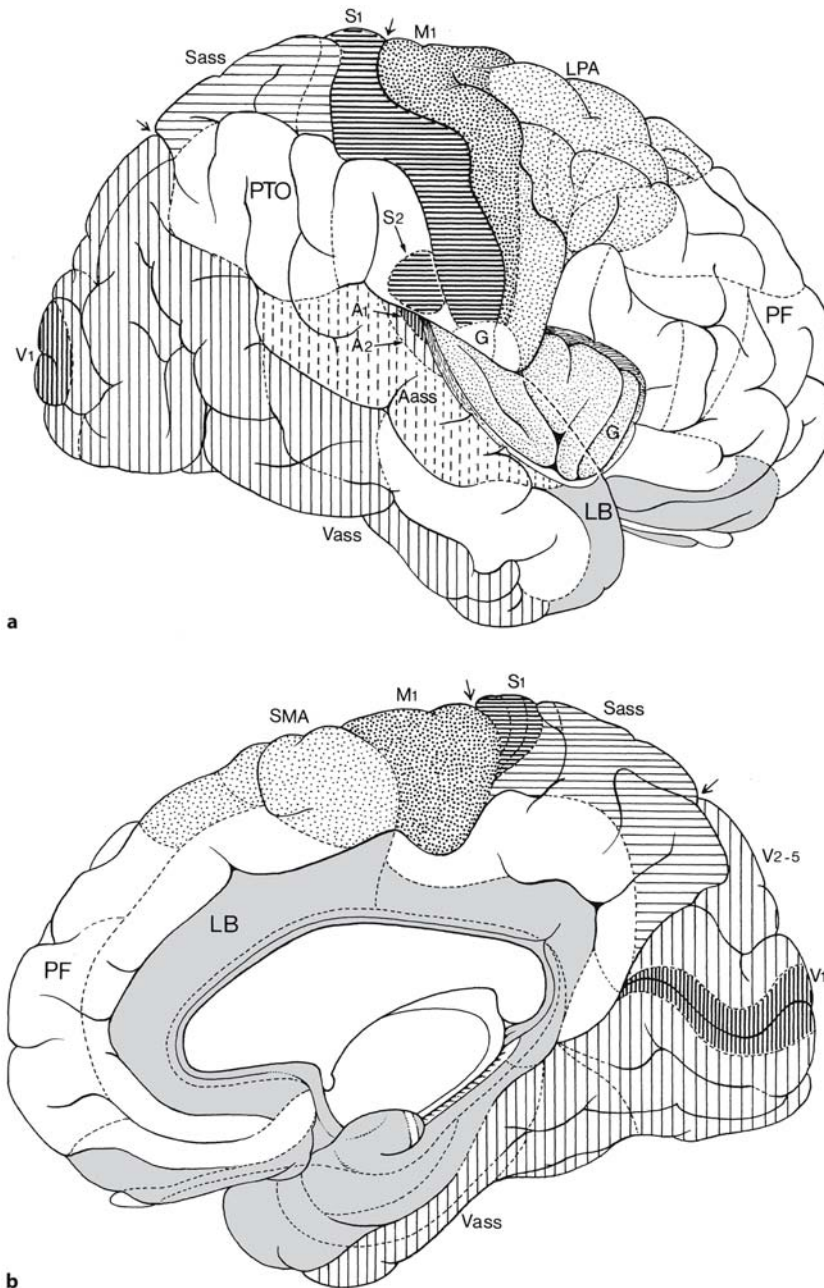
Fig. 10.3 a, b Localization of functions on the human cerebral cortex. The insular cortex is *stippled*. *Arrows* indicate the central and parieto-occipital sulci. *Aass* auditory association cortex (*broken line vertical hatching*), *A1* primary (*bold vertical hatching*) auditory cortex, *A2* secondary (*light vertical hatching*) auditory cortex, *G* gustatory cortex, *LB* limbic association cortex (*grey*), *LPA* lateral premotor area (*light stippling*), *M1* primary motor cortex (*heavy stippling*), *PF* prefrontal association cortex, *PTO* parietotemporo-occipital association cortex, *Sass* somatosensory association cortex (*light horizontal hatching*), SMA supplementary motor area (*light stippling*), *S1* primary somatosensory cortex (*bold horizontal hatching*), *S2* secondary somatosensory cortex (*bold horizontal hatching*), *Vass* visual association cortex in temporal lobe (*vertical hatching*), *V1* primary visual cortex (*bold vertical hatching*), *V2-5* visual association cortex in occipital lobe (*vertical hatching*). (After Mesulam 1985 and other sources)

diameter and function as integrated units. They were first described in the somatosensory cortex (Mountcastle 1957), but are best known in the visual cortex (Hubel and Wiesel 1962, 1977; Hubel et al. 1978; Lund et al. 2003). The 'ice-cube' model of the visual cortex in the macaque monkey is shown in Fig. 10.4. *Orientation columns*, in which neurons react on a light stimulus into a particular direction, and *ocular dominance columns* with cells preferentially involved with one of both eyes can be distinguished.

10.2.2 The Allocortex

The three-layered **allocortex** includes the olfactory cortex (the paleocortex) and the hippocampal formation (the archicortex), and is composed of an outer, plexiform layer, a central, compact layer and an inner, polymorph layer. The hippocampus belongs to the **limbic lobe**, situated on the inferomedial part of the medial surface of the hemisphere (Nieuwenhuys 1996; Duvernoy 1998; Fig. 10.5). Broca (1878) introduced the terms limbic and intralimbic gyri, or outer and inner rings, for the cortical structures surround-

ing the corpus callosum. The **limbic gyrus** (Broca's *grand lobe limbique*) consists of the subcallosal, cingulate and parahippocampal gyri. The retrosplenial cortex and a narrowed lobule, the isthmus, join the cingulate and parahippocampal gyri behind and below the splenium of the corpus callosum. The **parahippocampal gyrus** consists of two parts: (1) a narrow posterior segment, the flat superior surface of which, the **subiculum**, is separated from the hippocampus by the hippocampal sulcus; and (2) a more voluminous anterior part, the piriform lobe, comprising the **uncus** and the **entorhinal area.** The **intralimbic gyrus** or inner ring includes an anterior or *precommissural segment* in the subcallosal region (the prehippocampal rudiment of Elliot Smith 1897), a superior, *supracommissural segment* (the indusium griseum), situated on top of the corpus callosum, and a large inferior segment (the *retrocommissural part* of the hippocampus or hippocampus proper).

The **hippocampal formation** or **formatio hippocampi** develops from the medial pallium. During the outgrowth of the cerebral hemispheres, first caudalwards and subsequently ventralwards and rostralwards (Fig. 10.25), the *retrocommissural part* of the hippocampal formation becomes situated in the temporal lobe (Fig. 10.5). Rudiments of the *supracommissural hippocampus* can be found on the medial side of the hemisphere on top of the corpus callosum: the *indusium griseum*, a thin cell layer, flanked by the *stria longitudinalis medialis* and *lateralis* of Lancisi (Fig. 10.34). The hippocampal formation is composed of three, originally adjacent, cortical areas

Fig. 10.5 Overview of the limbic system. *A* anterior thalamic nucleus, *AC* anterior commissure, *BL* basolateral amygdala, *C* cortical amygdala, *CA* cornu Ammonis, *CC* corpus callosum, *CM* corpus mamillare, *EN* entorhinal cortex, *F* fornix, *GC* gyrus cinguli, *GD* gyrus dentatus, *GPH* gyrus parahippocampalis, *IN* indisium griseum, *L* lateral olfactory stria, *M* medial olfactory stria, *MD* mediodorsal thalamic nucleus, *OB* olfactory bulb, *OT* olfactory tract, *RH* rhinal cortex, *ST* stria terminalis, *SUB* subiculum. (After Nieuwenhuys et al. 1988)
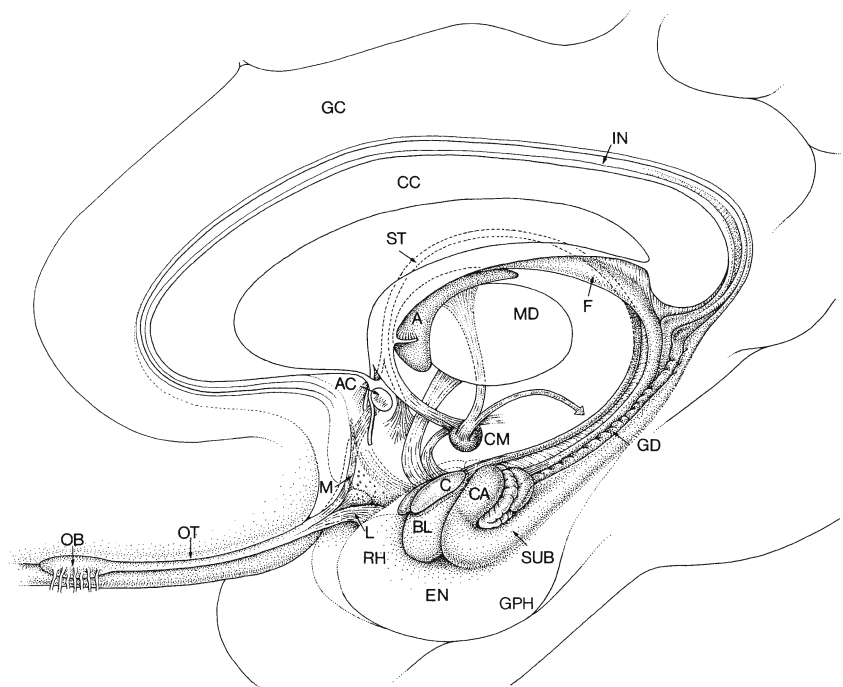
(Fig. 10.6): the dentate gyrus, the cornu Ammonis and the subiculum (Stephan 1975; Braak 1980; Amaral and Insausti 1990; Braak et al. 1996; Duvernoy 1998). The U-shaped **cornu Ammonis** consists of three fields (CA1–CA3). Within the hilus of the dentate gyrus sometimes a CA4 field is distinguished. The CA1 field and the adjacent subiculum are also known as Sommer's sector (Sommer 1880). The pyramidal cells in Sommer's sector are especially sensitive to anoxia and other metabolic disturbances, and they are often affected in temporal lobe epilepsy. Severe depletion of neurons with pronounced shrinkage of tissue, especially in Sommer's sector, is known as *hippocampal* or *Ammon's horn sclerosis* (Sect. 10.7.4). The C-shaped **dentate gyrus** is adjacent to the CA1 field, and is separated from the subiculum by the *sulcus hippocampi*. The **subiculum** borders on the entorhinal cortex (area 28) of the mesocortical parahippocampal gyrus. The **hippocampus proper** (CA1–CA3) is composed of three layers (Fig. 10.6): a polymorph layer (the *stratum oriens*), a pyramidal layer (the *stratum pyramidale*) and a molecular layer, composed of the *stratum radiatum*, the *stratum lacunosum* and the *stratum moleculare*. The dentate gyrus is also composed of three layers: a polymorph *hilus*, a granular layer (the *stratum granulosum*) and a molecular layer (the *stratum moleculare*), continuous with the molecular layer of the hippocampus.

The hippocampus receives most of its input from the entorhinal cortex. The **entorhinal cortex** is composed of entorhinal and transentorhinal (German terminology) or perirhinal (Anglo-Saxon terminology) cortical areas in the rostral part of the parahippocampal gyrus (Braak and Braak 1992; Insausti et al. 1995; Solodkin and Van Hoesen 1996; Suzuki and Amaral 2003). Its surface exhibits small, macroscopically visible wart-like elevations, the *verrucae hippocampi* (Klingler 1948; Duvernoy 1998), that are produced by clusters of neurons in layer II (or layer Pre-α). Through the adjacent perirhinal cortex much cortical information reaches the entorhinal cortex. The entorhinal cortex projects topographically to the hippocampus, its medial parts innervate the rostral hippocampus, whereas its lateral parts project to the caudal hippocampus (Insausti et al. 1987; Witter et al. 1989; Witter and Amaral 1991).

The **basic circuitry** of the hippocampus is formed by a trisynaptic circuit composed of three types of excitatory, glutaminergic synapses (Fig. 10.6): (1) fibres from the perforant path, originating in the superficial cell clusters of the entorhinal cortex, innervate the granule cells of the dentate gyrus; (2) mossy fibres from these granule cells excite the pyramidal cells in the CA3 field; and (3) the Schaffer collaterals of the pyramidal cells in CA3 innervate the pyramidal cells in CA1. A direct projection from CA1 to the entorhinal cortex closes this circuit. Numerous
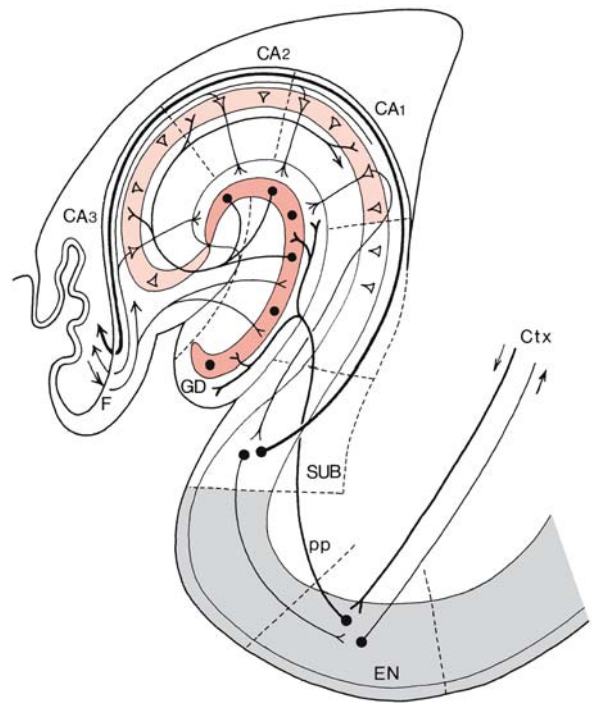
Fig. 10.6 Organization and circuitry of the human hippocampal formation. *CA1*, *CA2*, *CA3* cornu Ammonis fields (*light red*), *Ctx* input and output to associations areas of cerebral cortex, *EN* entorhinal cortex (*grey*), *F* fornix, *GD* gyrus dentatus (*red*), *pp* perforant path from the entorhinal cortex, *SUB* subiculum

types of GABAergic local circuit neurons can be found in the various parts of the hippocampal formation. The **main output centre** of the hippocampus is, however, the **subiculum**. Axons pass via the **alveus**, the superficial fibre layer of the hippocampus, via the **fimbria** into the fornix. At the level of the septum, the **fornix** divides into a *precommissural fornix* to the septum and the nucleus accumbens, and a *postcommissural fornix* to the anterior thalamic nucleus and the corpus mamillare (Fig. 10.5). From the mamillary body the large mamillothalamic tract of Vicq d'Azyr projects to the anterior thalamic nucleus which innervates the posterior cingulate cortex (area 23) and the retrosplenial cortex (areas 29 and 30).

Brodmann's (1909) brain map does not have the same level of detail for the **cingulate gyrus** as for other parts of the cerebral cortex. Braak (1976, 1979) identified an anterogenual magnocellular area rostral to the genu of the corpus callosum and a primitive gigantopyramidal area in the depth of the cingulate gyrus. Vogt et al. (1995) also showed that the human cingulate gyrus is quite heterogeneous. The *anterior cingulate cortex* is agranular and has a prominent layer V. It gives rise to part of the pyramidal tract (Sect. 10.3.2).

10.3 Overview of Main Cortical Connections

The neocortex is the end station of all sensory projections, except for olfactory information, which ends in the allocortex. The various cortical areas are interconnected by an extensive network of *corticocortical projections*. The ipsilateral corticocortical connections are known as *association fibres*, and those connecting both hemispheres as *commissural fibres*, largely passing via the corpus callosum. Commissural fibres from the temporal lobe pass largely via the commissura anterior. The long association fibres form fasciculi. The *fasciculus longitudinalis superior* or *fasciculus arcuatus* connects the sensory and motor speech areas. The *fasciculus occipitofrontalis superior* connects prefrontal and parietotemporo-occipital association areas. The *fasciculus occipitofrontalis inferior* connects the lower part of the occipital lobe and parts of the temporal lobe (the *fasciculus uncinatus*) with the prefrontal association area. The neocortex has extensive projections via the capsula interna to the basal ganglia, the thalamus, the brain stem and the spinal cord. The frontopontine and parietotemporo-occipitopontine tracts influence the cerebellum through the pontine nuclei, whereas corticobulbar and corticospinal fibres innervate sensory and motor parts of the brain stem and spinal cord, respectively.

10.3.1 Thalamocortical Projections

The (dorsal) thalamic nuclei extensively innervate the cerebral cortex (Fig. 9.5), and are reciprocally innervated by corticothalamic projections. The thalamocortical and corticothalamic projections pass with the other corticofugal fibre tracts through the various parts of the capsula interna. The **capsula interna** can be subdivided into the following components (Fig. 10.7): (1) the *crus anterius* between the head of the caudate nucleus and the lentiform nucleus, containing the frontopontine tract and thalamocortical fibres from the anterior and mediodorsal thalamic nuclei to the cingulate gyrus and the prefrontal cortex, respectively; (2) the *genu*, previously thought to contain the corticobulbar fibres; (3) the *crus posterius* between the lentiform nucleus and the thalamus, containing the parietotemporo-occipitopontine tract, all corticobulbar and corticospinal projections and thalamocortical projections arising in the motor ventral anterior/ventral lateral complex and the somatosensory ventroposterolateral/ventroposteromedial complex; (4) a *retrolenticular part* behind the lenticular nucleus, through which the optic radiation passes; and (5) a *sublenticular part* for auditory projections to the temporal lobe.
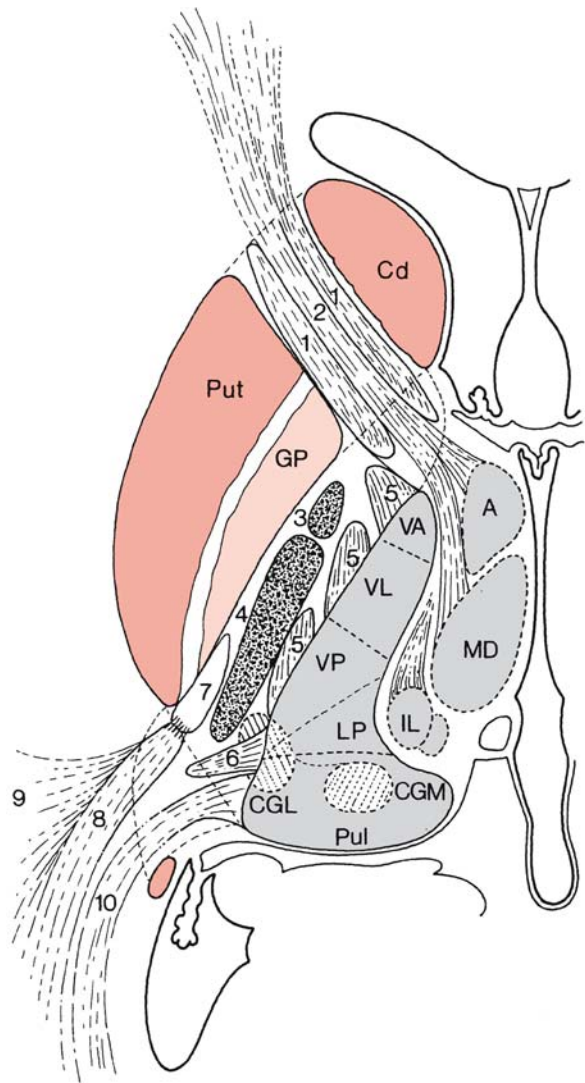
Fig. 10.7 Organization of the human capsula interna. The human internal capsule consists of an anterior limb, a genu, a posterior limb, a retrolenticular part and a sublenticular part (not visible in this section). The anterior limb contains the frontopontine tract (*1*) and the anterior thalamic radiation (*2*) from the anterior (*A*) and mediodorsal (*MD*) thalamic nuclei. The posterior limb contains corticobulbar (*3*) and corticospinal (*4*) fibres, the superior thalamic radiation (*5*) from the ventral thalamic nuclei (*VA*, *VL*, *VP*), the posterior thalamic radiation (*6*) from the pulvinar (*Pul*) and lateroposterior nucleus (*LP*) and the parietopontine tract (*7*). The retrolenticular part contains the occipitopontine tract (*8*), the temporopontine tract (*9*) and the optic radiation (*10*) from the corpus geniculatum laterale (*CGL*). The sublenticular part contains the auditory radiation from the corpus geniculatum mediale (*CGM*)
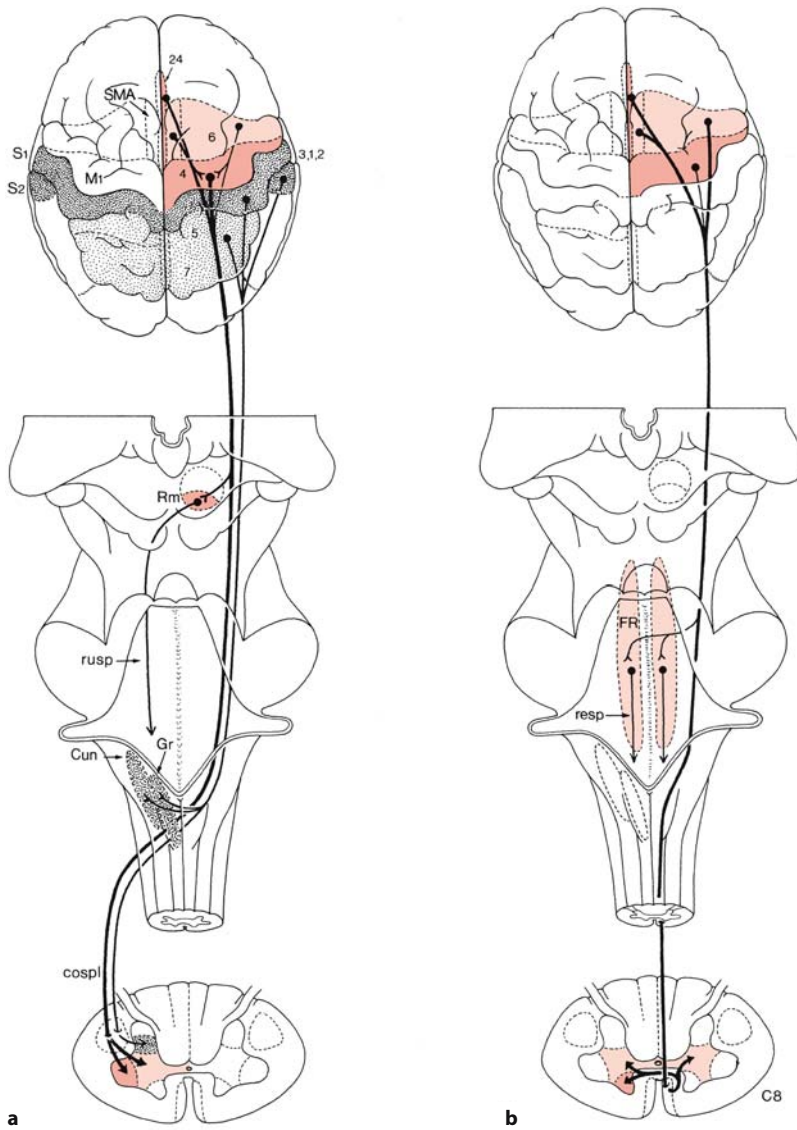
Fig. 10.8 Origin, course and site of termination of the human corticospinal tracts: **a** the lateral corticospinal tract; **b** the ventral corticospinal tract. Numbers indicate Brodmann areas. *cospl* lateral corticospinal tract, *Cun* cuneate nucleus, *FR* formatio reticularis, *Gr* gracile nucleus, *M1* primary motor cortex, *resp* reticulospinal fibres, *Rm* magnocellular part of red nucleus, *rusp* rubrospinal tract, *SMA* supplementary motor area, *S1* primary somatosensory cortex, *S2* secondary somatosensory cortex. (After Kandel et al. 1991; Porter and Lemon 1993)

10.3.2   The Pyramidal Tract

The **corticospinal** or **pyramidal tract**, i.e. the main central motor pathway (Chap. 6), arises invariably from layer V pyramidal cells, not only from motor cortices in the frontal lobe but also from the somatosensory cortices (Kuypers 1981; Armand 1982; Nudo and Masterton 1990; He et al. 1993, 1995). Several motor areas on the medial aspect of the macaque cerebral hemisphere give rise to corticospinal projections, including the SMA and various parts of the cingulate cortex (He et al. 1995). With functional brain imaging comparable non-primary motor fields have been found in the human cerebral cortex (Roland and Zilles 1996; Fink et al. 1997; Geyer et al. 2000). Spinal cord terminations of the medial wall motor areas in macaque monkeys are in many respects similar to those of efferents of the primary motor cortex

(Dum and Strick 1996). Various components of the human pyramidal tract are shown in Fig. 10.8. More than 60% of the pyramidal tract arises from the primary motor cortex (area 4 or M1) and the premotor areas in the frontal lobe (Porter and Lemon 1993; Roland and Zilles 1996). The premotor cortex in man includes the lateral premotor cortex, the medial premotor cortex (SMA) and the rostral part of the gyrus cinguli (area 24). The remaining 40% of pyramidal tract fibres originate from the primary somatosensory cortex (area 3,1,2 or S1), S2 and areas 5 and 7. The majority of corticospinal fibres decussate in the pyramidal decussation and continue as the lateral corticospinal tract. About 10–30% pass uncrossed into the anterior funiculus. Nathan et al. (1990) studied the course and site of termination of the human corticospinal tracts (Chap. 6).
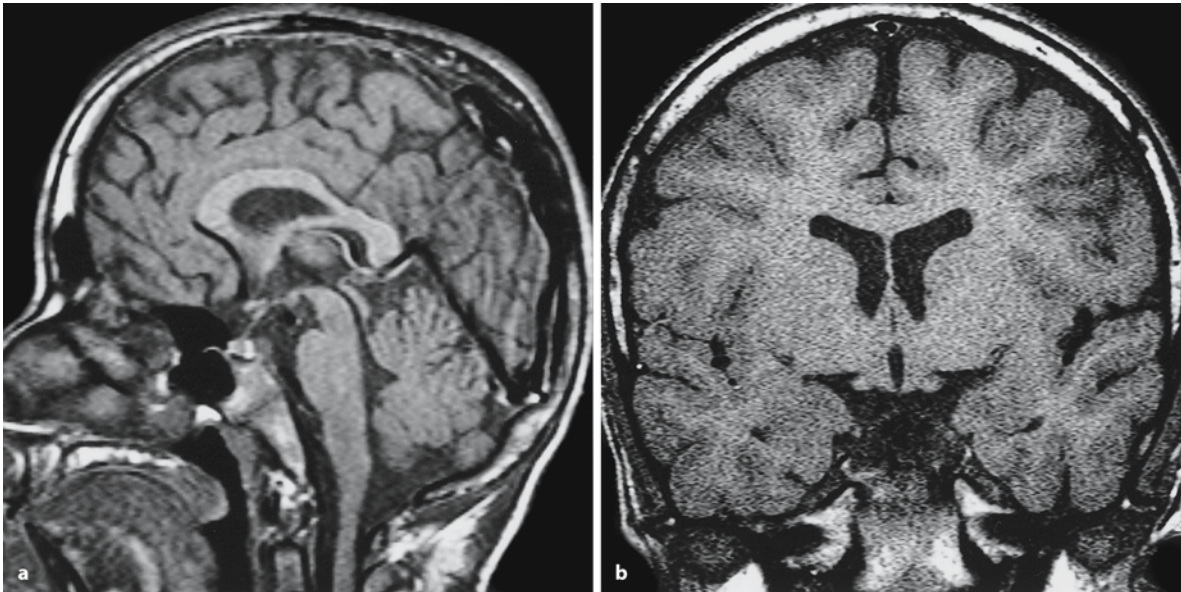
Fig. 10.9 Sagittal (**a**) and coronal (**b**) T1-weighted MRI of a normal corpus callosum in a 15-month-old boy (courtesy Berit Verbist, Leiden)

10.3.3   The Corpus Callosum

The **corpus callosum** connects the cerebral cortices of both hemispheres and is usually subdivided into four sections: (1) the rostrum; (2) the genu; (3) the body or middle part; and (4) the splenium (Fig. 10.9). The hippocampal commissure (the psalterium) comprises a variable portion of the splenium (Lamantia and Rakic 1990b; Raybaud and Girard 1998). The corpus callosum is topographically organized in relation to the cortical regions connected (Sunderland 1940; Pandya et al. 1971; de Lacoste et al. 1985; Lamantia and Rakic 1990b; Innocenti 1994). The rostrum and the genu connect the prefrontal cortices, its middle part connects motor, somatosensory and auditory cortices, and through the splenium temporal, parietal and occipital cortices are connected. The cortical map at the level of the corpus callosum is not very sharply defined. In an anterograde tracing study in the human brain, Di Virgilio and Clarke (1997) showed that heterotopic connections between non-equivalent cortical areas in each hemisphere are numerous and widespread, even in the genu and the splenium where callosal fibres are most highly segregated. Tracing studies in rhesus monkeys (Lamantia and Rakic 1990b) showed that the anterior commissure connects neocortical structures in the temporal lobes, whereas a basal telencephalic commissure, adjacent to the anterior commissure, connects paleocortical structures.

10.4   Development of the Neocortex

The development of the neocortex includes three major phases: cell production, cell migration and cortical differentiation and growth. The two principal neuronal types of the cerebral cortex, the excitatory, glutaminergic pyramidal cells and the inhibitory, GABAergic non-pyramidal interneurons, are generated in the ventricular zones of the cortical walls and ganglionic eminences, and reach their destination by radial and tangential migration, respectively. Cortical neurons, generated in the pallial ventricular zone, are formed by two distinct waves of cellular proliferation and subsequent migration (Fig. 10.10). During the first wave, postmitotic cells in the ventricular zone migrate a short distance towards the pial surface and form the preplate or primordial plexiform layer, containing the Cajal–Retzius cells (Marín-Padilla 1971, 1978, 1998; Rickmann et al. 1977; Raedler and Raedler 1978; Supèr et al. 1998b; Supèr and Uylings 2001). During the second wave, neurons from the ventricular zone migrate along radial glia into the preplate and form the cortical plate, splitting the preplate into a superficial marginal zone and an inner zone, the subplate (Fig. 10.11). The cortical plate gives rise to cortical layers II–VI. Neurogenesis within the neocortical ventricular zone lasts about 6 days in mice (Caviness 1982; Takahashi et al. 1995a), about 60 days in rhesus monkeys (Rakic 1974) and over 100 days in man (Sidman and Rakic 1982). A subpial granular layer participates in the production of Cajal–Retzius cells (Gadisseux et al. 1992; Meyer and Wahle 1999).
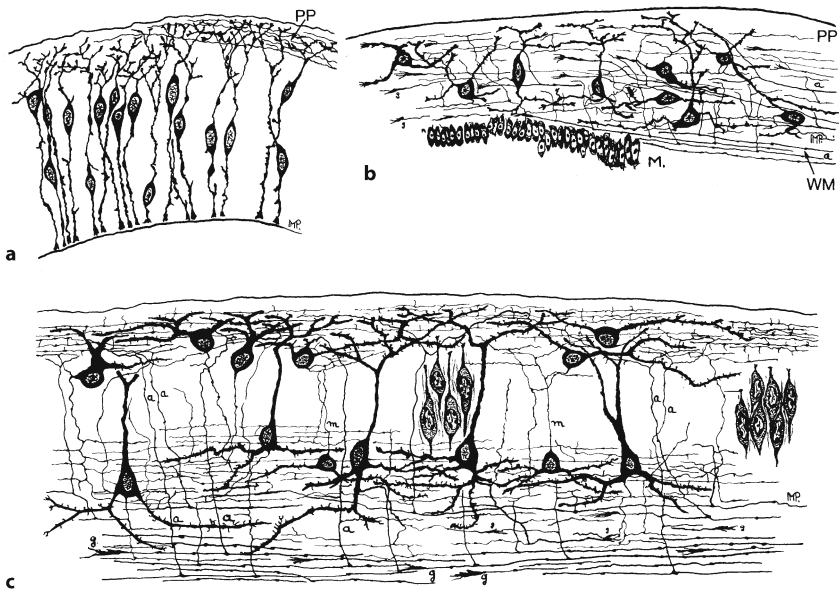
Fig. 10.10 Two waves of cellular proliferation and migration as shown by Golgi studies on the cat cerebral cortex: **a** 20th day of gestation in which corticopetal fibres can be detected in the superficial 'primordial plexiform layer' (*PP*); **b** by the 22nd day of gestation many primitive-looking neurons can be recognized in this layer; **c** 25th day of gestation in which the cortical plate is composed of only two to three layers of neurons. *WM* white matter. (From Marín-Padilla 1978, with permission)
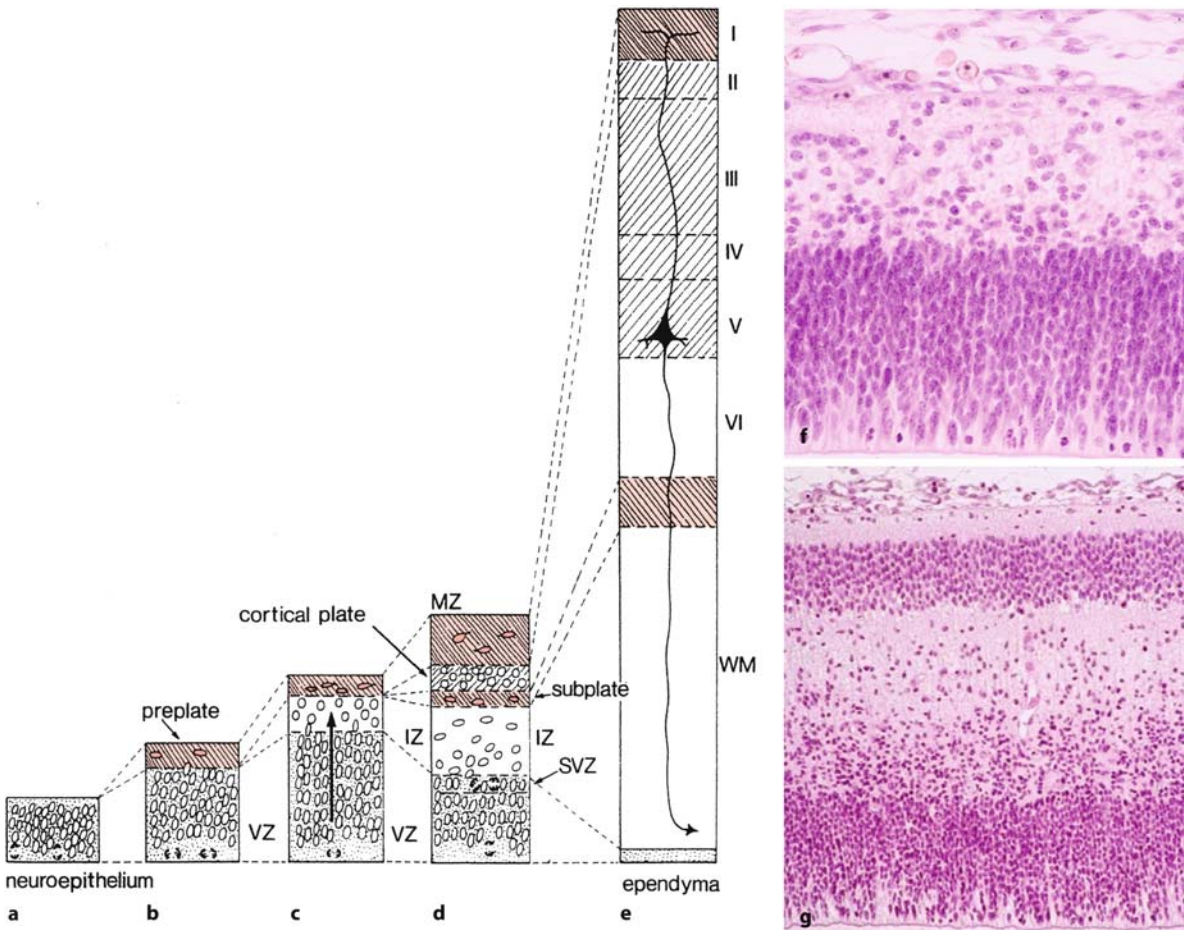
Fig. 10.11 Development of the human cerebral cortex. **a–c** The neuroepithelium forms three zones, the ventricular zone (*VZ*), the intermediate zone (*IZ*) and the preplate. During the eighth to 18th weeks of development, neurons migrate from the ventricular zone and form the cortical plate (**d**). The preplate becomes divided into the marginal zone (*MZ*) and the subplate. A second compartment for cell division, the sub- ventricular zone (*SVZ*), is mainly involved in the production of glial cells. Finally (**e**), the marginal zone forms the molecular layer (layer *I*) and the cortical plate layers *II–VI*. The intermediate zone forms the subcortical white matter (*WM*). **f**, **g** Haematoxylin–eosin-stained sections of the cerebral cortex at 7 and 11 weeks of gestation (courtesy Kohei Shiota, Kyoto)

Programmed cell death shapes the development of the cerebral cortex. It refines cell numbers and connections, and it leads not only to the disappearance of the subplate (Allendoerfer and Shatz 1994; Price et al. 1997), but also plays an important role in cell production and early morphogenesis (Spreafico et al. 1995; Blaschke et al. 1996, 1998; Thomaidou et al. 1997; Haydar et al. 1999). The glial populations of the neocortex arise from progenitor cells in the subventricular zone (Takahashi et al. 1995b; Brazel et al. 2003; Chap. 2). First, aspects of the development of the neocortex in rodents will be discussed with emphasis on the mechanisms involved, followed by an overview of the development of the human cerebral cortex.

10.4.1   Development of the Neocortex in Rodents

The histogenesis of the cerebral cortex has been extensively studied in rodents (reviewed in Bayer and Altman 1991; Caviness et al. 1995, 2000, 2003; Chenn et al. 1997; Price and Willshaw 2000). In mice, moreover, mechanisms for induction and regionalization of the cerebral cortex are rapidly being unravelled.

Patterning and Arealization of the Neocortex

Patterns of early gene expression reveal that the embryonic cortex is not homogeneous as proposed in the 'protocortex' model (O'Leary 1989). In this model, an initially homogeneous sheet of cortical neurons is patterned into areas relatively late in corticogenesis by cues from thalamocortical axons. Later studies, however, clearly showed that early cortical regionalization does not depend on thalamic innervation (Ragsdale and Grove 2001; O'Leary and Nakagawa 2002; López-Bendito and Molnár 2003). More likely, area-specific differences exist early within the ventricular zone and serve as a **protomap** (Fig. 10.12) of the future organization of the cerebral cortex (Rakic 1988; Smart and McSherry 1982), suggesting that the regional pattern of the mammalian cerebral cortex may emerge early in neurogenesis. Studies in mutant mice indicate a role for embryonic signalling centres and for specific transcription factors in regionalizing the cerebral cortex (Rubinstein et al. 1999; Ragsdale and Grove 2001; O'Leary and Nakagawa 2002). The transcription factor genes *Emx2* and *Pax6* are involved in the direct control of area identities (Fig. 10.13), possibly regulated by the fibroblast growth factor 8 (FGF8). *Emx2* is expressed in proliferating neuroblasts and in the postmitotic Cajal–Retzius cells, known to control migration of cortical neurons (Cecchi and Boncinelli 2000). In mice, ectopic expression of FGF8 in the caudal part of the neocor-
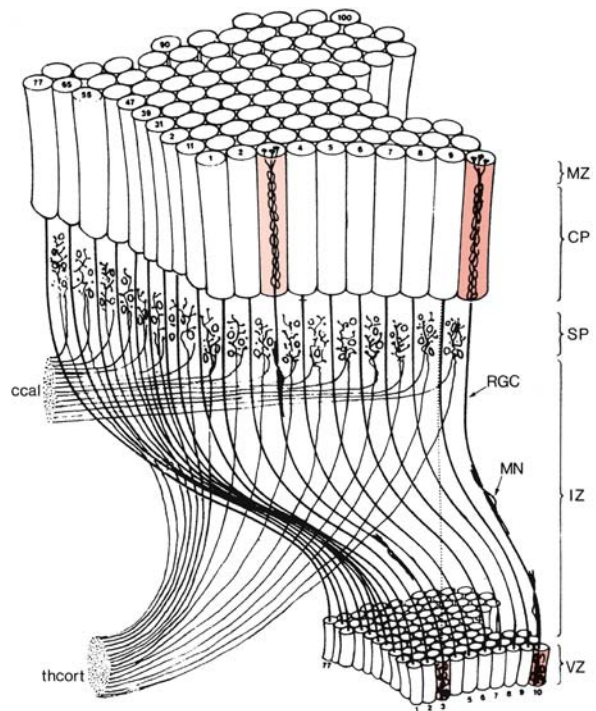
Fig. 10.12 The protomap of the cerebral cortex. Radial migration underlies the columnar organization of the neocortex. After their last division, cohorts of migrating neurons (*MN*) pass along radial glial cells (*RGC*) through the intermediate zone (*IZ*) to the subplate (*SP*) where they may interact with 'waiting' thalamocortical (*thcort*), callosal (*ccal*) and other afferents. Newly formed neurons bypass the earlier-generated ones and settle in the superficial part of the cortical plate (*CP*) just below the marginal zone (*MZ*). They form radial stacks of cells (for example, radial units *3* and *10*) that share a common site of origin but are generated at different times (between E40 and E100 in rhesus monkeys). (After Rakic 1988)

tical primordium leads to a partial duplication of the S1 barrel field (Chap. 2).

Neurogenesis and Migration

The developing cerebral wall contains several transient embryonic zones (Fig. 10.11): (1) the ventricular zone, which is composed of pseudostratified epithelium of progenitor cells that lines the lateral ventricles; (2) the subventricular zone, which acts early in development as a secondary progenitor compartment (Chap. 9) and later in development as the major source of glial cells; (3) the intermediate zone, through which migrating neurons pass along radial glial processes; (4) the subplate, thought to be essential in directing thalamocortical connectivity and pioneering corticofugal projections (Chap. 2); (5) the cortical plate, the initial condensation of postmitotic neurons that will become layers II–VI; and (6) the
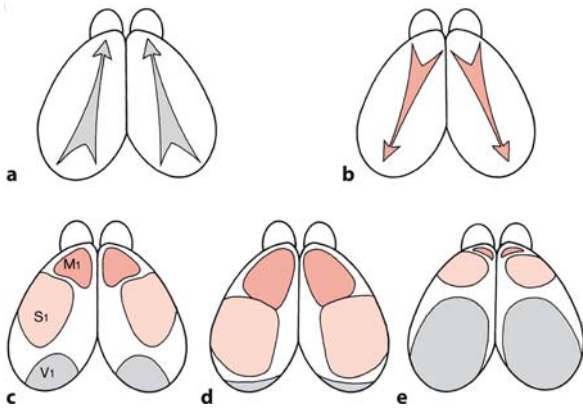
Fig. 10.13 Arealization of the neocortex depends on the graded expression of patterns of *Emx2* and *Pax6* in the neocortical ventricular zone. *Emx2* is expressed in a high caudomedial to low rostrolateral manner (**a**), whereas *Pax6* expression shows the opposite gradient (**b**). In wild-type mice (**c**), the motor area (*M1*) is medium-sized and the somatosensory (*S1*) and primary visual (*V1*) areas are relatively large. In *Emx2* mutants (**d**), rostral areas such as M1 expand, whereas in *Pax6* mutants (**e**) the opposite effect occurs, resulting in an expanded visual cortex. (After O'Leary and Nakagawa 2002)

marginal zone, the superficial, cell-sparse layer that contains the Cajal–Retzius cells. During the first wave of neurogenesis, the cells of the **preplate** or primordial plexiform layer are formed (Marín-Padilla 1971, 1978; Rickmann et al. 1977; Raedler and Raedler 1978; Bayer and Altman 1990). During the second wave of cell production, in which the **cortical plate** is generated, the cells of the neocortical pseudostratified ventricular epithelium execute a finite series of cycles in the course of which postmitotic neurons exit the epithelium (Takahashi et al. 1995a) and migrate across the embryonic cerebral wall to become assembled into neocortical layers in an inside-to-outside order with respect to their sequence of origin (Fig. 10.14). Within each cycle the fraction of postmitotic cells that exits the proliferative process (Q) increases, whereas the fraction that re-enters the S phase (P) decreases. As neurogenesis proceeds, more and more divisions give rise to neurons, until the rate of neuronal production peaks during the last third of neurogenesis (Takahashi et al. 1995a). When neurogenesis stops, the progenitor cells divide in a terminal fashion, giving rise to neurons, but no progenitors, and the precursor pool is depleted. Postmitotic neu-
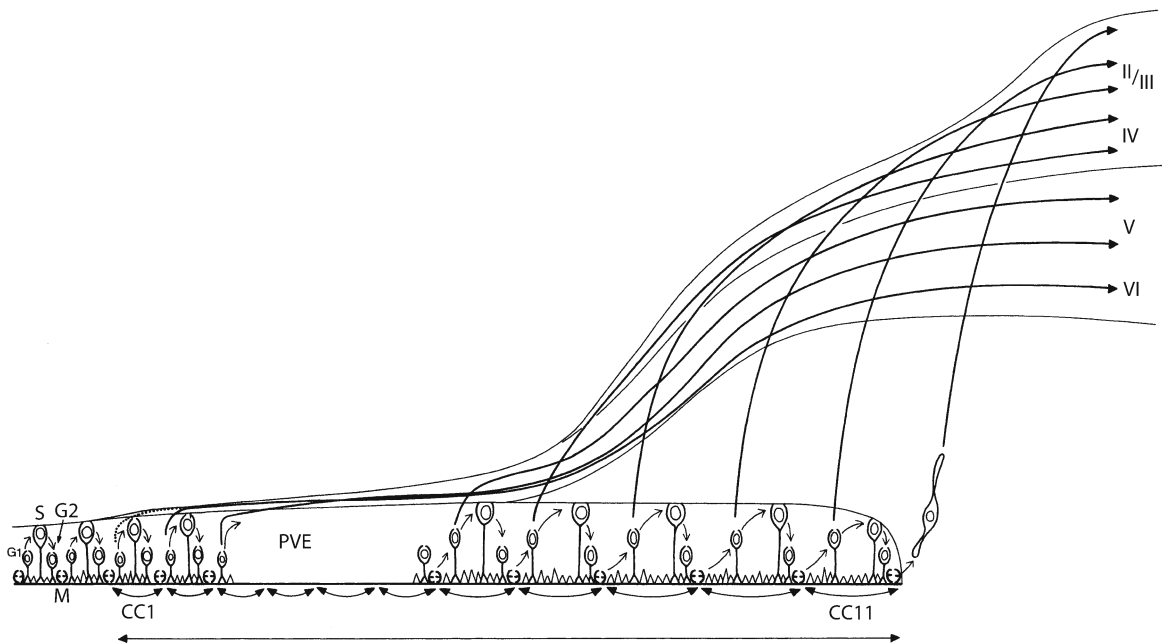
Fig. 10.14 The neocortical histogenetic sequence found in the rat brain. Cell proliferation starts in the pseudostratified ventricular epithelium (*PVE*) or ventricular zone. The founder population proliferates exponentially through an extended series of cycles of the preneuronogenetic phase during which no cells leave the cycle. Proliferative cells are attached at the ventricular margin. Their shape correlates with the phase of the cell cycle (see also Fig. 2.18). Mitosis (*M*) takes place at the ventricular surface, after which postmitotic cells in the *G1* phase elongate as the nucleus ascends to initiate the *S* phase in the outer half of the pseudostratified ventricular epitheli-um. As cells move through the *S* and *G2* phases, they shorten and the nucleus descends to undergo mitosis again. The onset of the neuronogenetic phase corresponds to the initial cell cycle (*CC1*) in which postmitotic cells exit the cycle as young neurons. The cells of the pseudostratified ventricular epithelium then execute a series of cycles (*CC1–CC11* in mice), after which the pseudostratified ventricular epithelium becomes the ependyma. The earliest-formed neurons are destined for the deepest layers of the cortex, whereas later-formed neurons will find positions at progressively more superficial levels. (After Caviness et al. 2000)

Fig. 10.15 Photomicrographs of the normal (**a**) and *reeler* (**b**) telencephalon at E14.5. *CP* cortical plate, *IZ* intermediate zone, *MZ* marginal zone, *PIA* pia mater, *SP* subplate, *VZ* ventricular zone. (Reproduced with permission from Tissir and Goffinet 2003, *Nat. Rev. Neurosci.* 4:496–505; copyright 2003, Macmillan Magazines Ltd.)
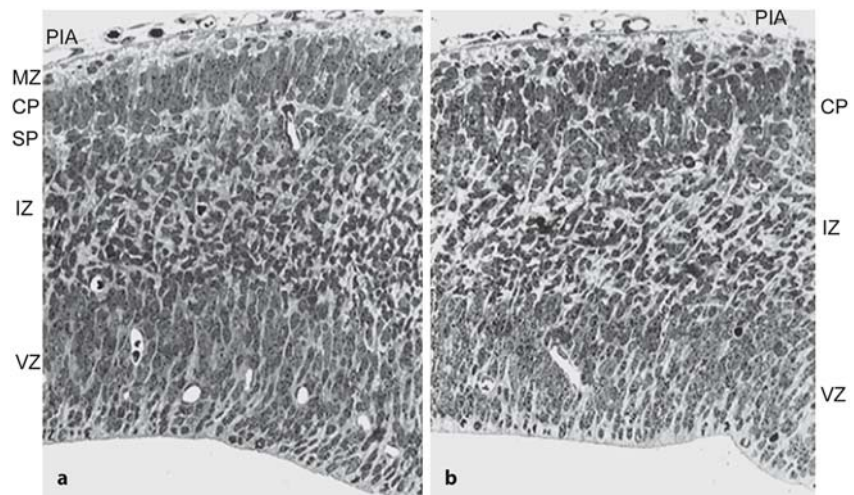
rons are generated by asymmetric division of progenitors (Chenn and McConnell 1995; Mione et al 1997). Symmetric divisions expand the precursor pool. Glial cell production is discussed in Chap. 2.

Thymidine birthdating studies have shown that the cortical cells that differentiate and leave the cell cycle earliest in development give rise to the deepest layers of the cortex, whereas the cells that exit the cell cycle later in development migrate past the early-born cells to finally reside in the more superficial layers of the cerebral cortex (Angevine and Sidman 1961; Berry and Rogers 1965; Rakic 1974; Richter and Kranz 1978, 1979a–c, 1980; Bayer and Altman 1991). In such studies, the early-generated Cajal–Retzius cells are mostly not included. Progenitor cells marked with a **retroviral lineage tracer** were found to give rise to clones of progeny that spanned multiple layers of the cortex (Luskin et al. 1988; Price and Thurlow 1988; Walsh and Cepko 1988, 1992; Kornack and Rakic 1995; Reid et al. 1995; O'Rourke et al. 1997; Tan et al. 1998). Many clones are very widely dispersed throughout the cortex and span both neocortical and allocortical areas such as the hippocampus and piriform cortex. The majority of cortical neurons are pyramidal projection neurons that use glutamate as a neurotransmitter. The non-pyramidal interneurons primarily express GABA (Götz and Bolz 1994). Retroviral lineage-tracing experiments showed that glutaminergic pyramidal neurons and GABAergic non-pyramidal cells arise from distinct progenitors (Parnavelas et al. 1991; Tan et al. 1998), confirming earlier immunohistochemical data (van Eden et al. 1989).

Neuronal migration in the cerebral cortex includes two main types, radial and tangential (Fig. 9.29). The migration of young cortical neurons to their final positions is largely dependent on radial glia. Throughout neurogenesis, radial glia extend long processes from the ventricular to the pial surface that serve as substrates for neuronal migration. Migrating neurons can also use non-radial migratory pathways (Chenn et al. 1997). Real-time imaging of migrating neurons has shown that the migratory routes and modes of migration are more diverse and complex than previously thought (Kriegstein and Noctor 2004). Moreover, radial migration of pyramidal neurons does not progress smoothly from the ventricular zone to the cortical plate, but is instead characterized by distinct migratory phases in which neurons change shape and direction of movement (Nadarajah et al. 2001; Kriegstein and Noctor 2004). Tangential migration of interneurons appears to occur in different phases (Ang et al. 2003; Tanaka et al. 2003; Xu et al. 2004). GABAergic cortical interneurons arise in the ganglionic eminences, the medial ganglionic eminence in particular, and reach the cortex via tangential migration (Anderson et al. 1999, 2001; Lavdas et al. 1999; Parnavelas 2000; Marín and Rubinstein 2001; Letinic et al. 2002; Chapt. 9).

Reeler, an autosomal recessive mutation of mice with disorganized cerebral lamination (Fig. 10.15), first described by Falconer (1951), proved to be an excellent model for studies on neuronal migration (Caviness and Sidman 1973; Caviness 1982; Goffinet 1979, 1984; Caviness et al. 1988; Frotscher 1998; Lambert de Rouvroit and Goffinet 1998; Tissir and Goffinet 2003). The characteristic inside-out layering of the cerebral cortex is perturbed and there are other characteristic disturbances in the lamination of cells in the cerebellum (Chap. 8) and the hippocampus. The molecular basis of the *reeler* trait has been unravelled (Bar et al. 1995; D'Arcangelo et al. 1995; Hirotsune et al. 1995; Ogawa et al. 1995; Rice and Curran 2001; Tissir and Goffinet 2003). The gene deleted in *reeler* mice was cloned and called *reelin* (D'Arcangelo et al. 1995; Hirotsune et al. 1995). *Reelin* and its secreted glycoprotein Reelin (D'Arcangelo et al. 1995, 1997) and an antibody (CR-50), raised by immunizing *reeler* mice with wild-type homogenates (Ogawa
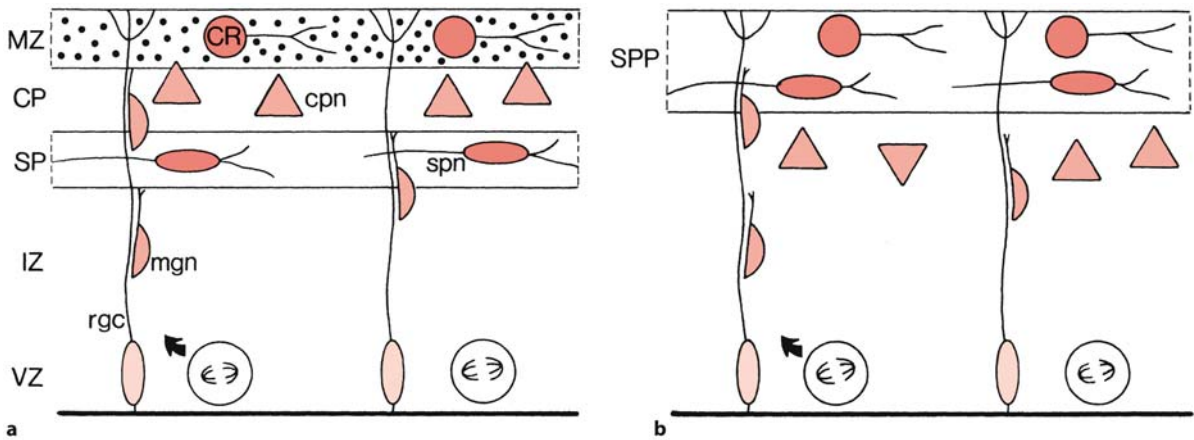
Fig. 10.16 Normal (**a**) and abnormal (**b**) formation of the mouse cortical plate. Normally, the earliest-generated cortical plate neurons (*cpn*) will divide the preplate into the marginal zone (*MZ*) with Cajal–Retzius cells (*CR*, *red*) and the subplate (*SP*) with subplate neurons (*spn*, *red*). Subsequent cohorts of cortical plate neurons, generated in the ventricular zone (*VZ*), will migrate (*mgn*, *medium red*) through the intermediate zone (*IZ*) along radial glial cells (*rgc*, *light red*). During normal development, Reelin is only expressed in the marginal zone (*dots*). In *reeler* mice, the cortical plate (*CP*) does not form within the preplate. Instead, cortical neurons accumulate beneath the undivided marginal zone and subplate neurons which remain together as the superplate (*SPP*). (After Pearlman et al. 1998)

Table 10.1 Mouse mutants with neuronal migration disorders

Mutant	Gene/protein	Cortical malformations	References
Reeler	*Reln*[rl]/Reelin	Loss of normal 'inside-out' sequence of neurogenesis, accompanied by altered cortical connections (corticospinal and thalamocortical)	Caviness (1982); Terashima (1995); Lambert de Rouvroit and Goffinet (1998); Tissir and Goffinet (2003)
Scrambler	*Dab1*/Dab1	Reeler-like	Sweet et al. (1996); González et al. (1997)
Yotari	*Dab1*/Dab1	Reeler-like	Sheldon et al. (1997)
Dab1–/–	*Dab1*/Dab1	Reeler-like	Howell et al. (1997a, b)
Cdk5–/–	Cdk5	Reeler-like	Ohshima et al. (1996)
p35–/–	p35	Reeler-like	Chae et al. (1997); Kwon and Tsai (1998)
VLDLR/ApoER2-deficient		Reeler-like	Trommsdorff et al. (1999)
Emx2–/–	*Emx2*	Leptomeningeal glioneuronal heterotopia	Ligon et al. (2003)
Presenilin-1 deficient	*PS1*/Presenilin-1	Leptomeningeal glioneuronal heterotopia	Hartmann et al. (1999); Kilb et al. (2004)
Fukutin–/–	*FCMD*/Fukutin	Targeted homozygous mutation of *FCMD* is lethal at E6.5–E7.5, prior to development of skeletal muscle or mature neurons; chimeric mice develop severe muscular dystrophy, laminar disorganization of cerebral cortex and altered cortical connections	Toda et al. (2003)

et al. 1995), were localized in the Cajal–Retzius cells in the marginal zone. In *reeler* mice, the preplate initially forms apparently normally, but neurons of the cortical plate fail to divide the preplate into a marginal zone and a subplate (Fig. 10.16). Instead, they gather in a somewhat irregular, outside-in sequence, entirely below the early-born cells, in a 'superplate'

(Caviness 1982). Normally, cortical plate neurons respond to the presence of Reelin by stopping migration. Reception of the Reelin signal requires the presence of at least one of two lipoprotein receptors, very low density lipoprotein receptor (VLDLR) and apolipoprotein E receptor type 2 (ApoER2), on the surface of the target cells (Fig. 10.17). Reelin activates
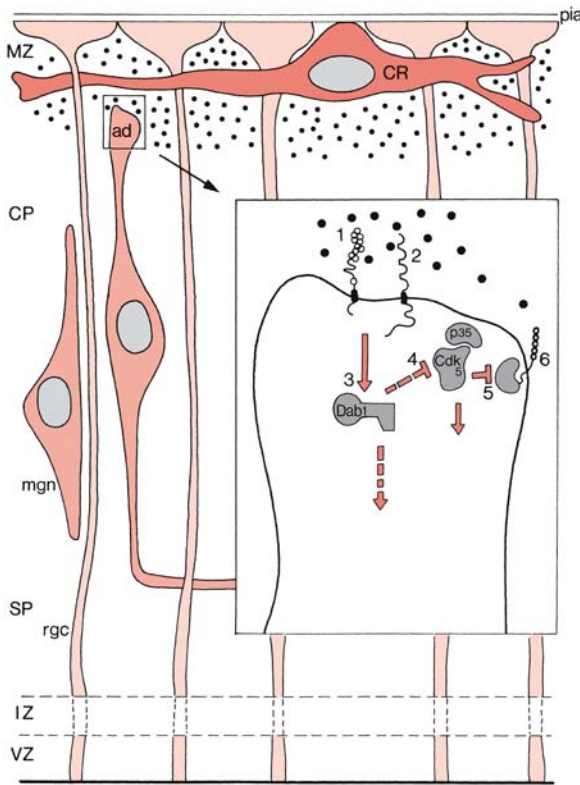
Fig. 10.17 Possible mechanism of Reelin signalling. From the ventricular zone (*VZ*) postmitotic migrating neurons (*mgn*) migrate along radial glial cells (*rgc*) through the intermediate zone (*IZ*) and the subplate (*SP*) to the cortical plate (*CP*). Reelin (*dots*) is secreted by Cajal–Retzius (*CR*) cells in the marginal zone (*MZ*). As soon as an apical dendrite (*ad*) signals the presence of Reelin, the following mechanism may result in stopping migration of the neuron (*insert*). Reelin binds to lipoprotein receptors (*1*) and to cadherin-related neuronal receptors (*2*). Through the tyrosine kinase pathway (*3*), Reelin activates the phosphorylation of Dab1 in neurons. Probably, via this Dab1 route (*4*) Reelin inhibits p35/Cdk5-kinase in migrating neurons. This enzyme inhibits N-cadherin (*6*), an adhesion molecule. Therefore, inhibition (*5*) of p35/Cdk5-kinase may lead to activation of N-cadherin which stimulates adhesion of neurons, thereby terminating migration. (After Lambert de Rouvroit and Goffinet; Homayouni and Curran 2000)

a signalling cascade, resulting in the tyrosine phosphorylation of Dab1. This intracellular adaptor is expressed in neurons that respond to Reelin such as cortical plate and Purkinje cells. Cortical malformations comparable to those in *reeler* mice were found in mutants affecting this cascade (Table 10.1). Targeted inactivation (Howell et al. 1997 a, b) and spontaneous mutations of the *Dab1* gene, such as in *scrambler* and *yotari* mice (Sweet et al. 1996; González et al. 1997; Goldowitz et al. 1997; Sheldon et al. 1997; Ware

et al. 1997), generate reeler-like phenotypes. Double mutations for the lipoprotein receptors VLDLR and ApoER2 also generate reeler-like phenotypes (Trommsdorff et al. 1999). Mice lacking either VLDLR or ApoER2 do not show an abnormal phenotype. The significance of other Reelin receptors such as cadherin-related neuronal receptors remains unclear. Reelin signalling inhibits p35/cyclin-dependent kinase 5 (Cdk5; Homayouni and Curran 2000; Tissir and Goffinet 2003; Fig. 10.17). Mice lacking Cdk5 show defective migration in the cerebral and cerebellar cortices (Ohshima et al. 1996). Cdk5 requires p35 (Nikolic et al. 1996) and *p35–/–* mice also show disruption of cortical development (Chae et al. 1997; Kwon and Tsai 1998). Recently, a possible role for Reelin in neurobehavioural disorders such as schizophrenia and autism has been suggested (Andres 2002; Costa et al. 2002; Fatemi 2002).

Leptomeningeal glioneuronal heterotopia form in *Emx2–/–* mice that are equivalent to human lesions of type 2 lissencephaly (Ligon et al. 2003). Similar malformations were found in presenilin-1 deficient mice (Hartmann et al. 1999; Kilb et al. 2004). Heterotopia were also detected in transgenic *Wnt1* mice as early as E13.5, consistent with a defect of preplate development during early phases of radial migration. Furthermore, diffuse abnormalities of reelin- and calretinin-positive cell populations in the marginal zone and subplate were observed, similar to those observed in *Emx2*-null mice (Mallamaci et al. 2000; Shinozaki et al. 2002). Another rodent model for cortical malformations is the *tish* mutant rat (Lee et al. 1997, 1998; Schottler et al. 1998), which shows bilateral heterotopia similar to those observed in humans with subcortical band heterotopia (SBH; Fig. 10.54).

Neuronal Specification and Differentiation

The layers of the cerebral cortex are different in neuronal density, morphology, connectivity and physiological properties. Retroviral lineage studies have shown that early cortical progenitor cells are multifated in that they produce clones of progeny that span the cortical layers (Reid et al. 1995). Transplant studies have shown that progenitor cells are multipotent, and that laminar identities are determined early in the cell cycle prior to a progenitor's terminal division (McConnell and Kaznowski 1991). The pyramidal neurons of the mammalian cerebral cortex project both within and outside the cortex in highly organized circuits. This precise ordering of connections between neurons in different layers and neurons within layers is essential for the development of functionally useful circuits. A striking feature of adult connectivity is the highly stereotyped, lamina-specific pattern of axonal projections that is disturbed in several mouse mutants. Many aspects of layer-specif-
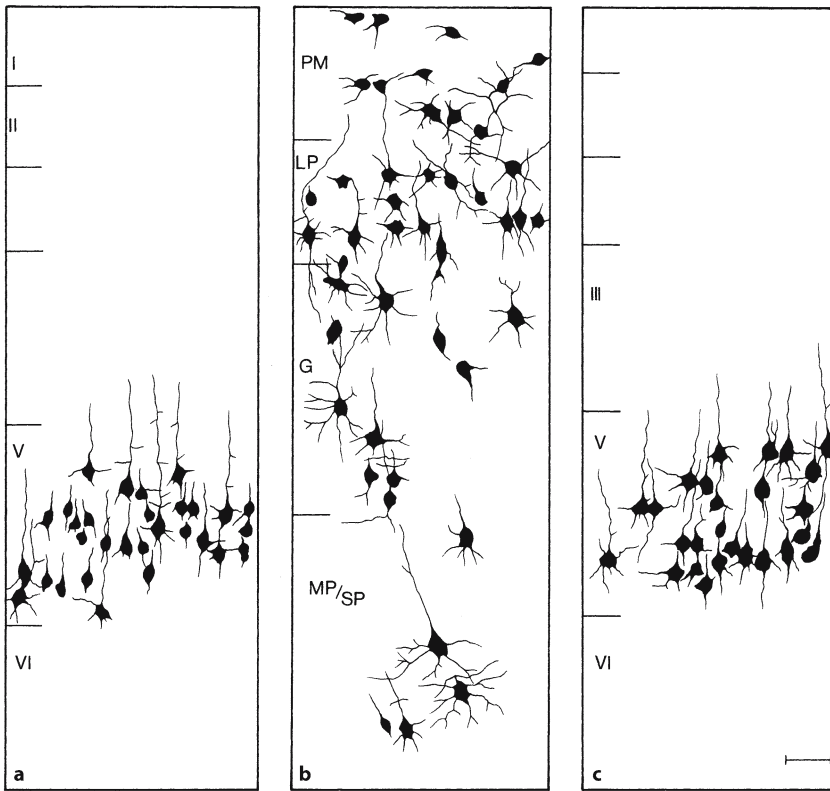
Fig. 10.18 Corticospinal neurons labelled following injection of horseradish peroxidase into the lumbar enlargement of normal (**a**), *reeler* (**b**) and normal–*reeler* chimera (**c**) mice. *G* granular cell layer (normally layer *IV*), *LP* large pyramidal cell layer (normally layer *V*), *MP/SP*, medium and small pyramidal cell layer (normally layers *II* and *III*), *PM* polymorphic cell layer (normally layer *VI*). (After Terashima 1995)
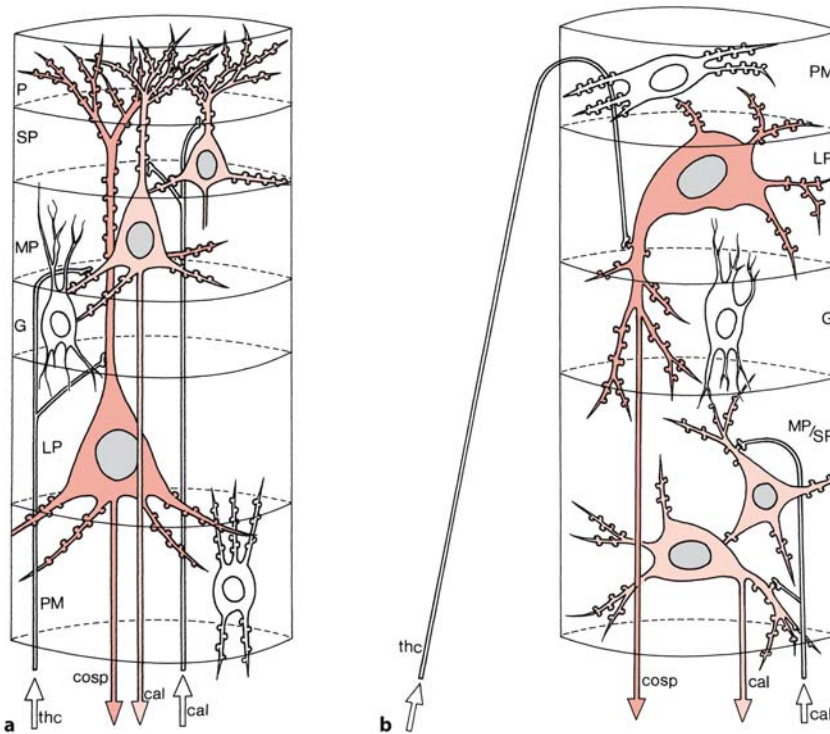
Fig. 10.19 Columnar organization in normal (**a**) and *reeler* (**b**) mice. The normal neocortex consists of the following six layers from the pial surface to the white matter: layer I (plexiform layer, *P*), layer II (small pyramidal cell layer, *SP*), layer III (medium pyramidal cell layer, *MP*), layer IV (granular cell layer, *G*), layer V (large pyramidal cell layer, *LP*) and layer VI (polymorphic cell layer, *PM*). In *reeler* mice, layer I is absent and the other cortical layers are roughly reversed. The *reeler* neocortex consists of four layers: PM, LP, G and MP+SP. Incoming thalamocortical fibres (*thc*) and outgoing callosal (*cal*) and corticospinal (*cosp*) fibres are arranged accordingly. (After Terashima 1995)

Fig. 10.20 Differentiation of pyramidal neurons in layer V of the rat cingular cortex: **a** E17–E18; **b** E19–E20; **c** E21; **d** E22; **e** P0; **f** P1–P2; **g** P5; **h** P20. (After Richter 1980)

a   b   c   d   e   f   g   h
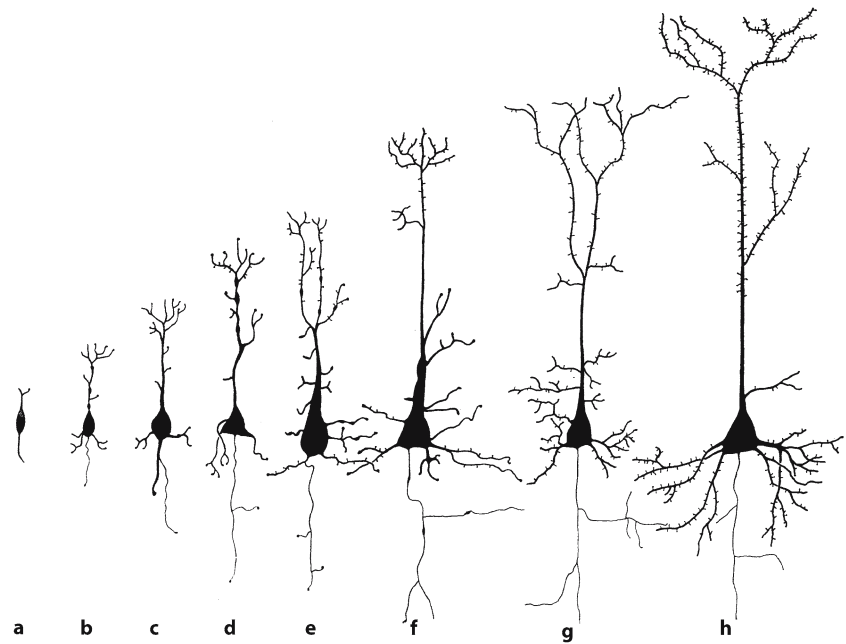
Fig. 10.21 Differentiation of granule cells in the rat cingular cortex: **a** E19; **b** E20; **c** E21; **d** E22; **e** P0; **f** P8; **g** P15. (After Richter 1980)

a   b   c   d   e   f   g
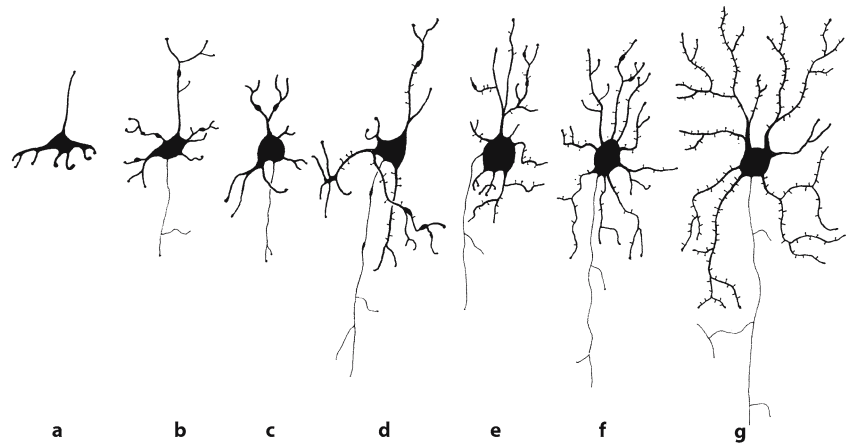
ic axon outgrowth are apparent early during the development of the cortex (O'Leary and Koester 1993; Sanes and Yamagata 1999; López-Bendito and Molnár 2003). The specification of the major classes of long-distance projections from layer V neurons, callosal and subcortical, seems to be established early in development (O'Leary and Koester 1993; McConnell et al. 1989, 1994). In *reeler* mice, corticospinal tract neurons were found scattered throughout the cortical layers (Terashima 1995; Fig. 10.18). A similar radial malpositioning was found in the *shaking rat Kawasaki* (Ikeda and Terashima 1997). The thalamocortical innervation in *reeler* mice is also disturbed and leads to the curious 'looping' pattern seen in adult *reeler* mice (Terashima 1995; Molnár et al. 1998; Fig. 10.19). Thalamic axons first pass through the cortical plate and accumulate in the 'superplate' layer for 2–3 days,

before they plung down to terminate deep in the cortical plate.

Richter (1980) and Marín-Padilla (1992) studied the maturation of mammalian pyramidal cells (Fig. 10.20), stellate cells and Cajal–Retzius cells (Fig. 10.21) in Golgi-stained preparations. In the rat cerebral cortex, calbindin-immunoreactive neurons were found from 14 days of gestation onwards, whereas parvalbumin-immunoreactive neurons were not detectable before the sixth postnatal day (Alcantara et al. 1988; Sanchez et al. 1992). The differential onset of calbindin and parvalbumin immunoreactive neurons has also been observed in the cerebral cortex of rhesus monkeys (Condé et al. 1996) and man (Sect. 10.4.2.5). The genesis of dendritic spines has been reviewed by Whitford et al. (2002) and Yuste and Bonhoeffer (2004).
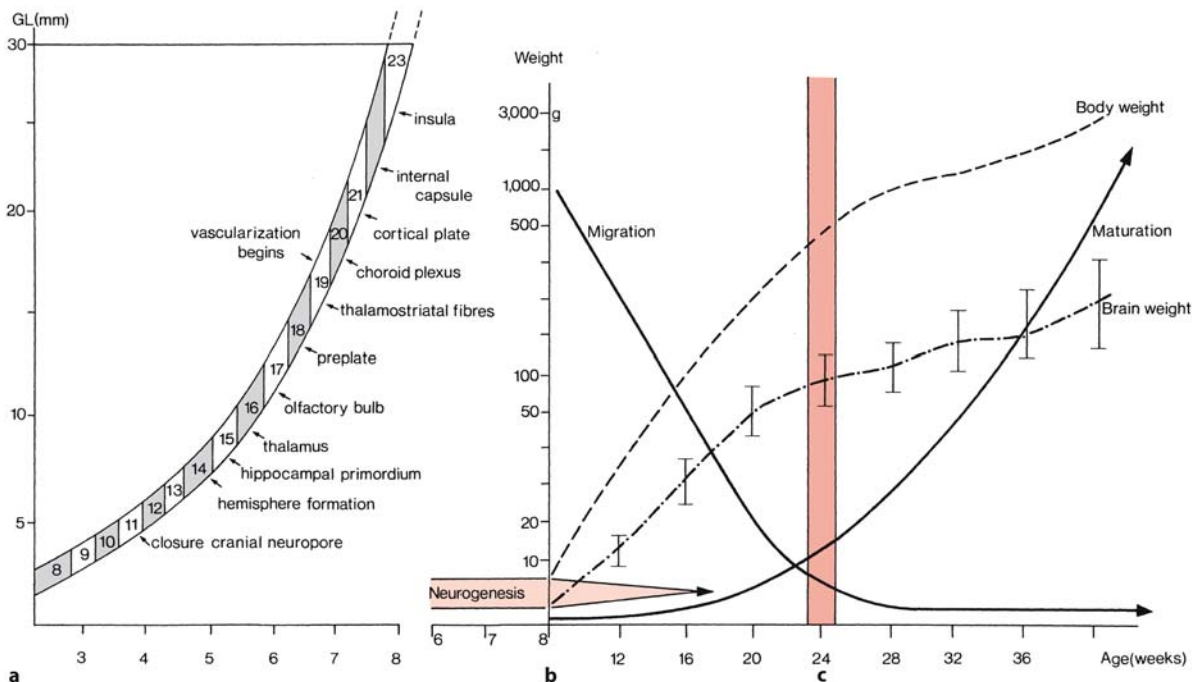
Fig. 10.22 Main events in the formation of the cerebral cortex: **a** an early, embryonic period subdivided into Carnegie stages; **b** an intermediate, fetal period; **c** a late, perinatal period. In the embryonic period, the preplate is formed, followed by the development of the cortical plate. In the fetal period, neuronal migration dominates and undifferentiated neurons gradually transfer into differentiated cortical neurons. The perinatal period is characterized by phenotypic differentiation and maturation of cortical plate neurons. The *red area* at the 24th week of gestation marks the lower limit for survival for prematurely born infants. (After Marín-Padilla 1990)

10.4.2   Development of the Human Neocortex

The development of the human cerebral cortex may be divided into three, partly overlapping periods (Marín-Padilla 1990; Fig. 10.22): (1) an **early, embryonic period** characterized by the establishment of the preplate or primordial plexiform layer, which starts around stage 17 (about 40-day-old embryos); (2) an **intermediate**, **fetal** or **migration period** characterized by the formation of the cortical plate, first visible at the end of the embryonic period around stage 21 (about 52-day-old embryos); and (3) a **late, perinatal period** characterized by specific phenotypic differentiation and functional maturation of cortical plate neurons, which starts about the 24th week of gestation. The separation between fetal and perinatal periods is somewhat arbitrary but may be clinically relevant (Marín-Padilla 1990). At that age prematures become viable. Moreover, in the fetal period so defined, disorders of neuronal migration are likely to occur, and congenital or acquired abnormalities of the structural organization of the cerebral cortex are common in the perinatal period.

Gross Development of the Cerebral Cortex

Lateral and medial views of the developing fetal human brain are shown in Figs. 10.23–10.25. In the medial views of the fetal brain the development of allocortical structures is also shown. The Sylvian fissure and insula are recognizable as early as the 14th gestational week as a shallow indentation on the lateral surface of the cerebrum. Normal cerebral sulcus formation begins around the 16th gestational week with the appearance of the parieto-occipital and cingulate sulci (Chi et al. 1977; Dooling et al. 1983; Feess-Higgins and Larroche 1987; E. Armstrong et al. 1995). On the cerebral convexity, primary sulcus formation is seen in the 20th to the 21st week (central sulcus). The arrangement of the primary sulci is perpendicular to the neuraxis, whereas secondary sulcus formation is parallel to the neuraxis, beginning in the 24th week (Hori 1996). The tertiary sulci bind the primary and secondary sulci. The normal gyration and sulcal pattern can be studied prenatally (Levine and Barnes 1999; Garel 2004) and in preterm and term neonates with MRI (van der Knaap et al. 1996; Ruoss et al. 2001). In 51 preterm and term newborn infants, their age ranging between 24 and 44 postmenstrual
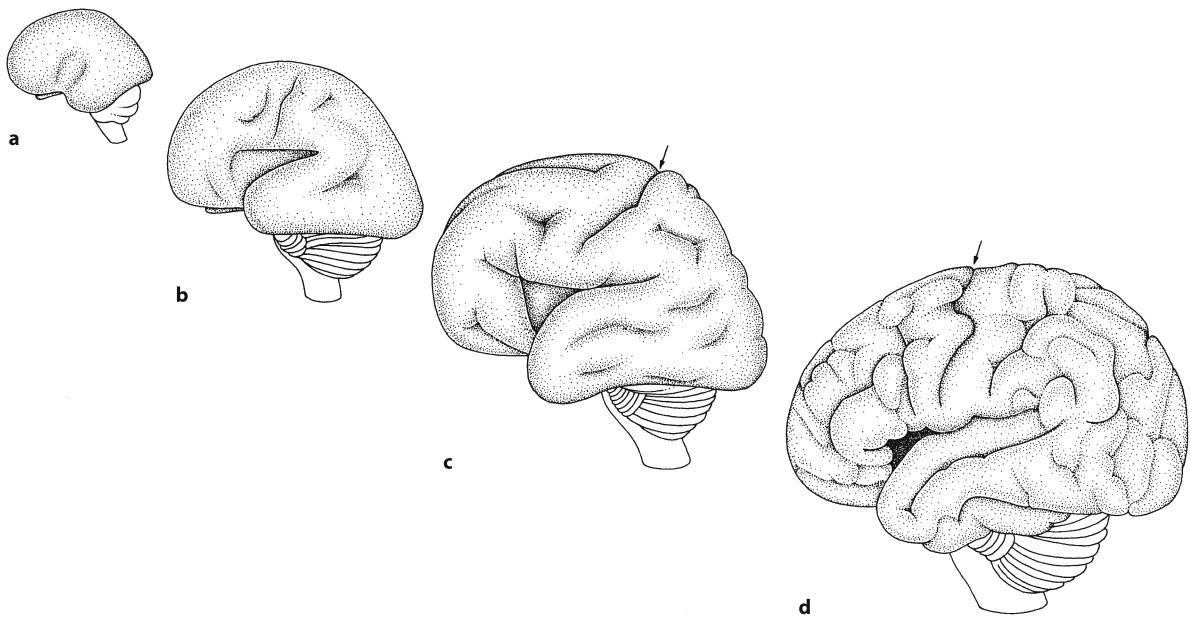
Fig. 10.23 Lateral views of the developing human brain in the fourth (**a**), sixth (**b**) and eighth (**c**) gestational months, and in a neonate (**d**). The *arrows* indicate the central sulcus (after Kahle 1969; O'Rahilly and Müller 1999)
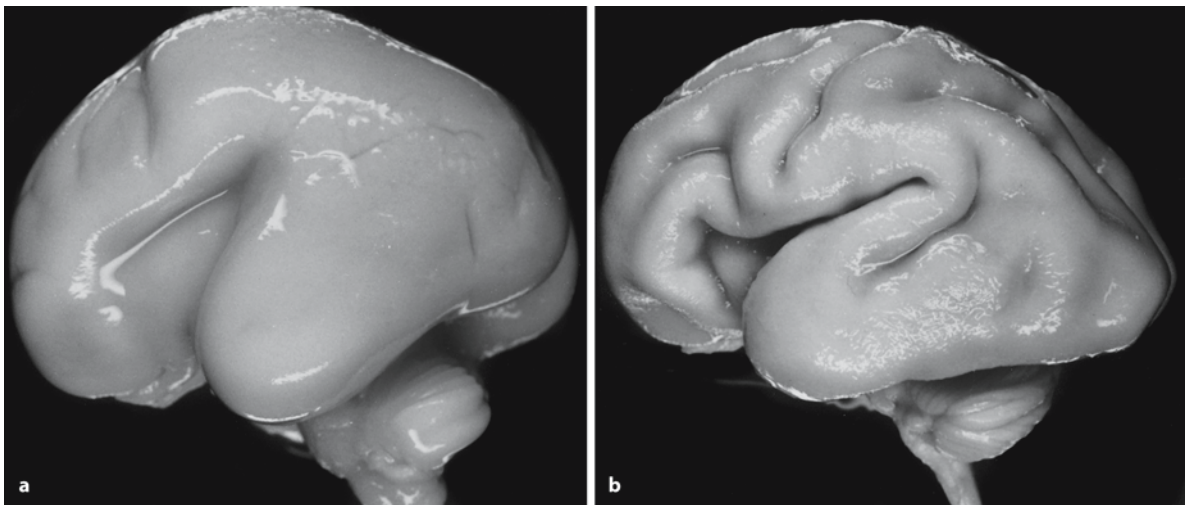
Fig. 10.24 Lateral views of fetal human brains at 20 (**a**) and 25 (**b**) weeks of gestation (courtesy Kohei Shiota, Kyoto)

weeks, brain maturation was found to start in the central area and to proceed towards the parieto-occipital cortex (Ruoss et al. 2001). The frontal cortex develops last. Known *gyral anomalies* include agyria/pachygyria (lissencephaly type 1), pachygyric polymicrogyria (lissencephaly type 2) and polymicrogyria. Anomalies of the sulci are found in a variety of hemispheric disorders, some of which appear to be an adaptation to a defect such as the radial sulci in agenesis of the corpus callosum. Hori

(1996) presented four cases of precocious cerebral development (Clinical Case 10.1).

Formation of the Preplate and the Cortical Plate

During development, the marginal zone contains several populations of transient neurons. The best characterized cell type is the **Cajal–Retzius cell**, originally described by Retzius (1893, 1894) as *Cajal'schen Zellen* in the human cerebral cortex (Fig. 10.27), com-
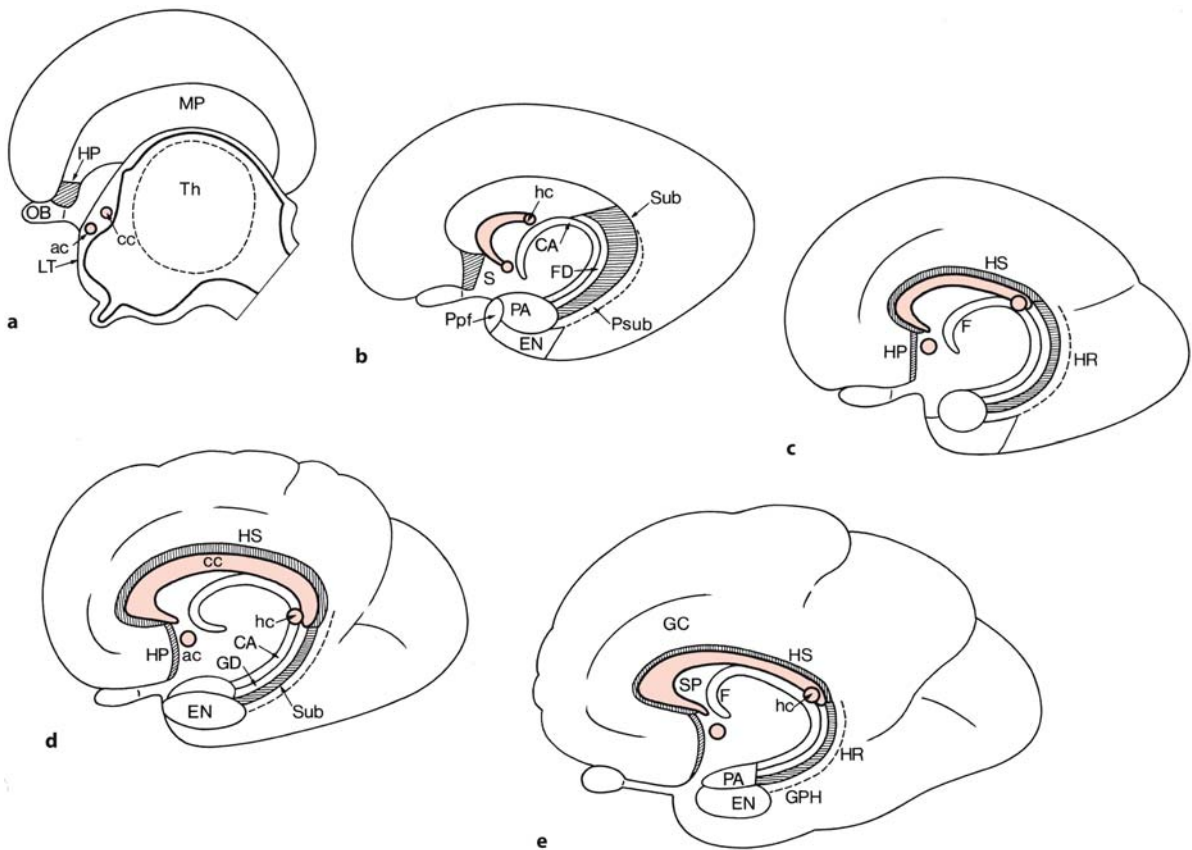
Fig. 10.25 Medial views of the developing human brain at the end of the second month (**a**), the end of the third month (**b**), the end of the fourth month (**c**), the end of the sixth month (**d**), and in a neonate (**e**). Precommissural, supracommissural and retrocommissural parts of the hippocampal formation are indicated by *obique*, *vertical* and *horizontal hatching*, respectively. *ac* anterior commissure, *CA* cornu Ammonis, *cc* corpus callosum, *EN* entorhinal cortex, *F* fornix, *FD* fascia dentata, *GC* gyrus cinguli, *GD* gyrus dentatus, *GPH* gyrus parahippocampalis, *hc* hippocampal commissure, *HP* precommissural hippocampal formation, *HR* retrocommissural hippocampal formation, *HS* supracommissural hippocampal formation, *LT* lamina terminalis, *MP* medial pallium, *OB* olfactory bulb, *PA* periamygdaloid area, *Ppf* prepiriform cortex, *Psub* parasubiculum, *S* septum, *SP* septum pellucidum, *Sub* subiculum, *Th* thalamus. (After Kahle 1969; Stephan 1975)

■ **Clinical Case 10.1**
Precocious Cerebral Development

The Sylvian fissure and the insula are recognizable as early as the 14th gestational week as a shallow indentation on the lateral surface of the cerebrum (Fig. 10.23). Normal cerebral sulcus formation starts around the 16th week of gestation, forming the parieto-occipital and cingulate gyri (Chi et al. 1977; Fig. 10.25). On the cerebral convexity, primary sulcus formation (the central sulcus) is seen in the 20th to the 21st week, whereas secondary sulcus formation starts in the 24th week. Precocious and supernumerary sulcus formation in fetal brains is rare. Hori (1996) described four brains in which the cerebrum showed precocious sulcus formation (see Case Report).

■ **Case Report.** The fetuses studied were of 14, 17, 18 and 19 weeks of gestation. Associated lesions were characterized by insufficient insular formation and agenesis of the corpus callosum. Two cases are shown in Fig. 10.26. The first fetus was born of a 30-year-old mother in the 14th gestational week by spontaneous abortion. The parents were non-consanguineous. The aborted male fetus weighed 36 g and had a crown–heel length of 110 mm. Gross inspection revealed no anomalies. Neuropathological examination of the brain showed formation of three sulci of vertical course on the dorsolateral surface of the left hemisphere, including the central sulcus (Fig. 10.26 a). There was no recognizable central sulcus on the right hemisphere. The Sylvian fissure and the insular indentation were not evident. The corpus callosum was ab-

sent and several radially arranged sulci were present on the medial surface of the cerebrum (Fig. 10.26 b). A rudimentary parieto-occipital sulcus was observed. Histological study of the telencephalon confirmed the absence of the corpus callosum and, moreover, revealed immature hippocampal gyri and an existing anterior commissure. The second case shown concerns a case of Turner syndrome revealed by amniocentesis in a fetus of 18 gestational weeks of a 26-year-old mother. Moreover, ultrasound examination showed fetal hydrops, after which abortion was induced at the 18th gestational week. The female fetus weighed 150 g with a crown–heel length of 205 mm. The developmental parameters corresponded to those of the 15th gestational week. On the lateral surface of the hemispheres supernumerary and abnormal sulci were found (Fig. 10.26 c). The Sylvian fissure was present, but it was deep with an unusual arrangement. There was no insular formation. An abnormal sulcal pattern was also found on the medial side of the hemispheres. The corpus callosum was absent, and gyri showed a radial arrangement. This radial arrangement is always seen in cases of agenesis of the corpus callosum (Sect. 10.7.6). The precociously formed sulci may be covered during further development of the brain so that these cases may well be part of a transient syndrome that occurs in mid-fetal life (Hori 1996).

References

Chi JG, Dooling EC, Gilles FH (1977) Gyral development of the human brain. Ann Neurol 1:86–93

Hori A (1996) Precocious cerebral development associated with agenesis of the corpus callosum in mid-fetal life: A transient syndrome? Acta Neuropathol (Berl) 91:120–125
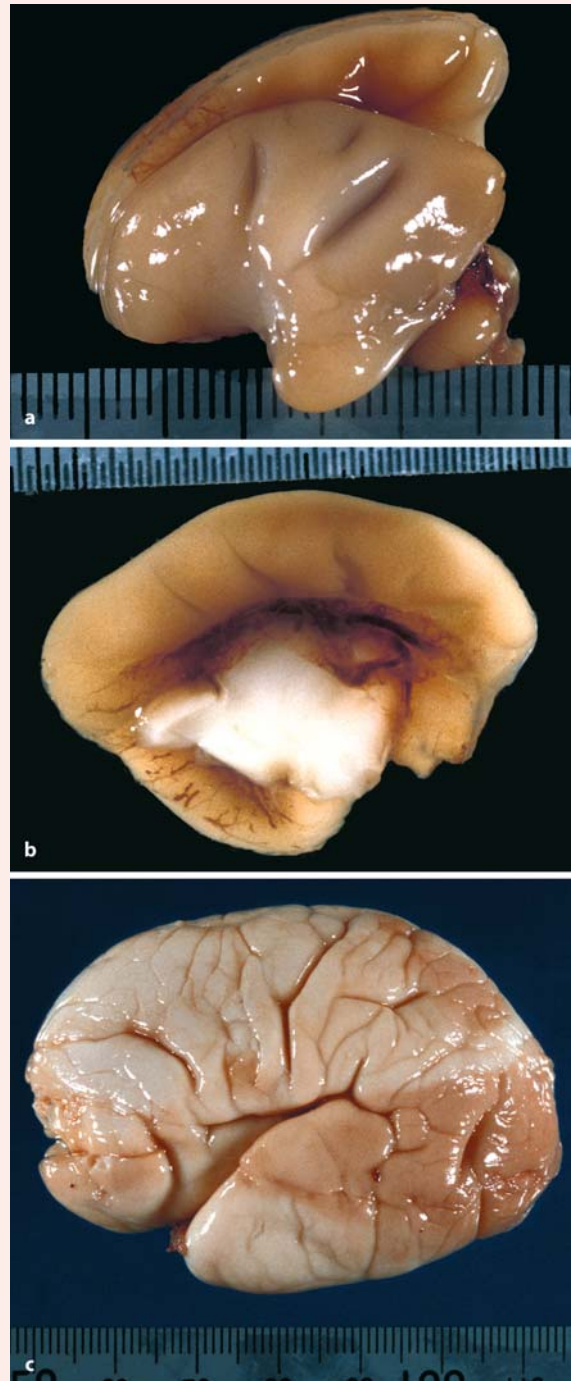
Fig. 10.26 Precocious development of cerebral sulci: **a** dorsolateral view of the cerebral hemispheres at the 14th gestational week, showing premature sulcus formation on the left lateral surface: the central sulcus and two other sulci are clearly recognizable; **b** medial view of the same brain: a rudimentary parieto-occipital sulcus can be observed, the corpus callosum is absent and several radially arranged sulci can be seen; **c** precocious tertiary sulcus formation in an 18-week-old fetus (from Hori 1996, with permission)
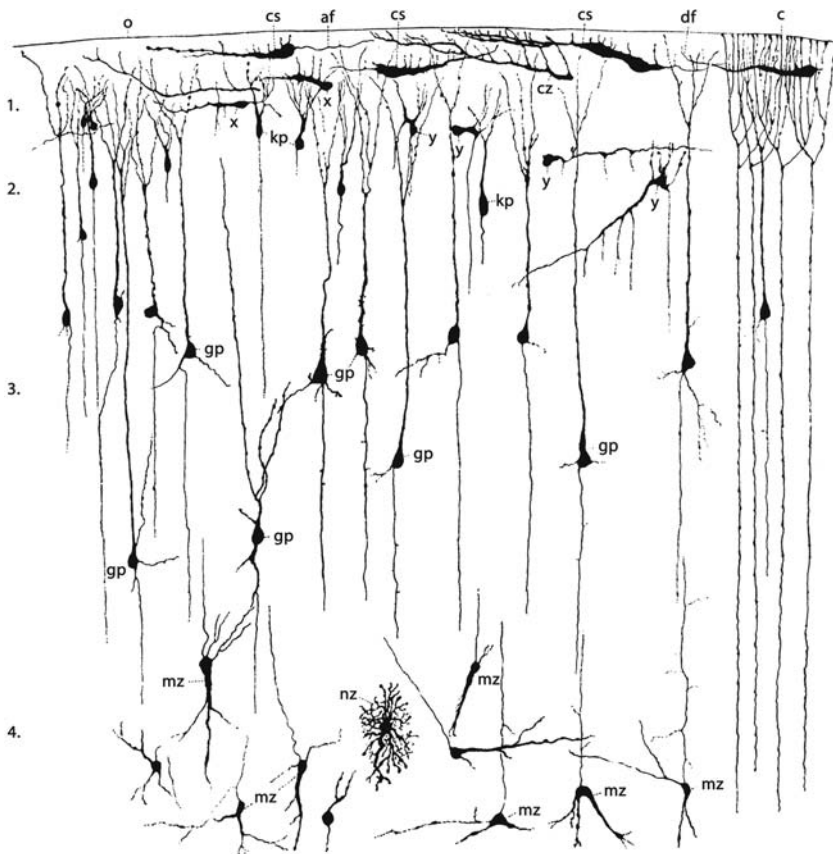
parable to cells described earlier by Ramón y Cajal (1891; for data on the history of Cajal–Retzius cells see Frotscher 1997 and Meyer et al. 1999). A second large cell population forms the **subpial granular layer** of Ranke (1910). This transient cell layer originates from the basal periolfactory subventricular zone (Sect. 10.4.2.3).

The neuronal composition of the human neocortical **preplate** appears to be more complex than generally described. Several groups of neurons participate in a sequence of events that precedes the emergence of the cortical plate (Meyer and Goffinet 1998; Spreafico et al. 1999; Zecevic et al. 1999; Meyer et al. 1999, 2000 a, b). Meyer and co-workers (Meyer and Goffinet 1998; Meyer et al. 2000b) studied early corticogenesis immunohistochemically (Reelin, calretinin, glutamic acid decarboxylase, GAD) in human embryos of Carnegie stages 16–22. The first population of Reelin-positive cells appears in the neocortical anlage at stage 16 (Fig. 10.28). At stages 19–20, a monolayer of calretinin-positive and GAD-positive, Reelin-negative neurons forms in the preplate, whereas the Reelin-positive cells shift to a subpial position. A third cell class, the pioneer projection neurons, contributes early corticofugal axons. These

cells are calretinin-positive but do not stain for Reelin or GAD. Pioneer cells first appear below the monolayer at stage 20 and form a pioneer plate at stage 21. A subset of Cajal–Retzius cells colocalizes Disabled-1 and Reelin (Deguchi et al. 2003; Meyer et al. 2003).

The **cortical plate** emerges at stage 21 and inserts itself within the preplate, which is split into a small superficial component and a larger deep component that will form the subplate. The further fetal development of the neocortical cortical plate has been subdivided into five developmental stages (Poliakov 1949; Sidman and Rakic 1982): (1) stage I, the initial formation of the cortical plate, approximately from the seventh to the tenth fetal week; (2) stage II, primary condensation of the cortical plate, approximately in the tenth and 11th fetal weeks; (3) stage III, bilateral cortical plate, most pronounced during the 11th to the 13th fetal weeks; (4) stage IV, secondary condensation, from the 13th to the 15th week; and (5) stage V, the stage of prolonged neuronal maturation, from the 16th week onwards. During these stages the cortical plate undergoes a series of dynamic transformations. The cortical plate does not contain synapses until 22–24 weeks of gestation. During the early fetal period and midgestation, the individual cortical layers
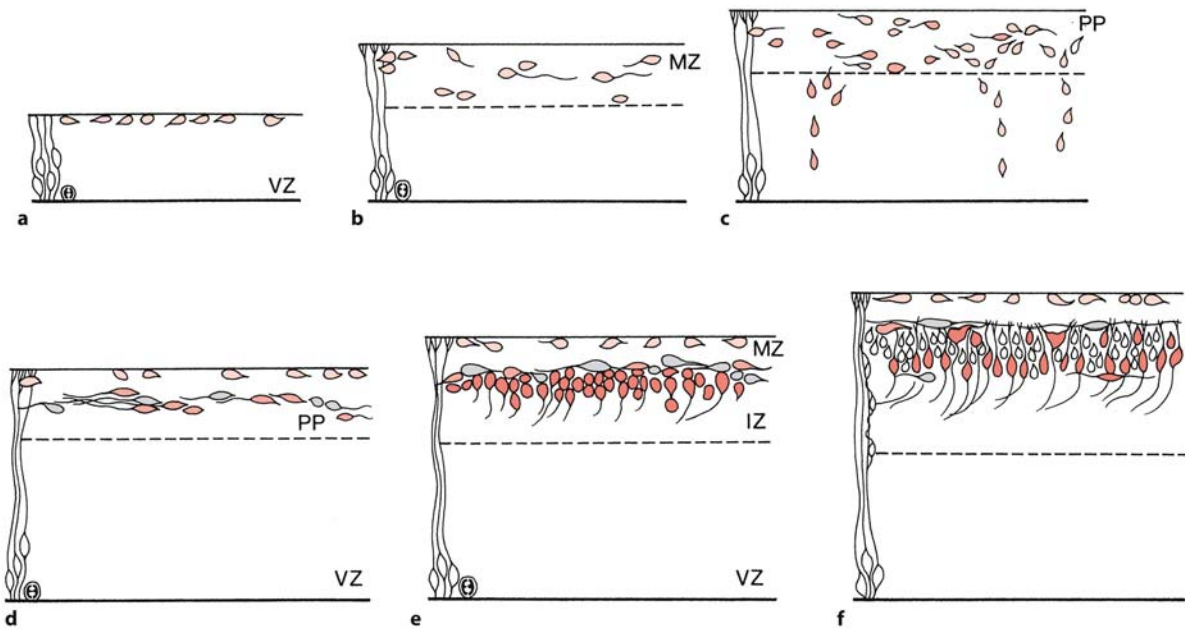
Fig. 10.28 Summary of developmental events found at Carnegie stages 16 (**a**), 18 (**b**), 19 (**c**), 20 (**d**), 21 (**e**) and 21/22 (**f**). The first Reelin-immunoreactive neurons (*light red*) appear at stage 16 in a narrow marginal zone and increase in number from stages 17 to 19. The first calretinin-immunoreactive neurons (*medium red*) appear at stage 19 in what is now recognizable as the preplate (*PP*). Together with glutamic acid decarboxylase immunoreactive neurons (*grey*), which appear at stage 20, they form a monolayer within the preplate. At the same time, Reelin-immunoreactive neurons settle in the subpial compartment. At stage 21, pioneer cells (*red*) below the monolayer give off the first corticofugal fibres. The first cohorts of cortical plate neurons (not coloured) divide the 'pioneer plate' into a minor superficial component and a large deep component (the subplate). *IZ* intermediate zone, *MZ* marginal zone, *VZ* ventricular zone. (After Meyer et al. 2000b)

are not easily identifiable since there is a continuous influx of new neurons into the superficial part of the cortical plate. Between 28 and 34 weeks of gestation, layers III and V of the cortical plate become differentiated, and counterparts of the adult cortical layers can be found in Nissl-stained sections (Mrzljak et al. 1988, 1990).

Kostović and co-workers (Kostović 1990a, b; Mrzljak et al. 1990) distinguished six periods in the development of the prefrontal cortex, spanning prenatal and postnatal development: (1) period 1 (10–25 weeks of gestation), characterized by onset of dendritic differentiation of pyramidal neurons in the cortical plate, formation of the subplate zone and maturation of subplate neurons; (2) period 2 (26–36 weeks of gestation), the late fetal or preterm infant period, characterized by the appearance of a six-layered pattern in the cortical plate, a peak in the development of the subplate followed by a reduction in its thickness, and rapid dendritic differentiation of pyramidal and non-pyramidal cortical plate neurons; (3) period 3 (first postnatal year), with persistence and gradual transformation of the subplate zone, extensive dendritic and spine growth of pyramidal neurons and differentiation of interneurons in the supragranular layers; (4) period 4 (second postnatal year), with the appearance of magnopyramidal cells in layer III of the prefrontal cortex; (5) period 5 (period of childhood and adolescence), with gradual and prolonged elaboration of adult-like Golgi architecture; and (6) period 6 (period of adult morphology), found in late adolescence and adulthood.

The Subpial Granular Layer

The transient **subpial granular layer** of Ranke (1910) develops from the basal periolfactory subventricular zone (Brun 1965; Gadisseux et al. 1992; Meyer and Wahle 1999). From here it migrates tangentially beneath the pia to cover the neocortical marginal zone from the 14th gestational week onwards (Fig. 10.29). The subpial granular layer is closely associated with a subset of Cajal–Retzius cells and disappears during the last trimester of gestation (Meyer and Gonzalez-Hernandez 1993). Subpial granular cells form a distinct cell population in the molecular layer, and are characterized by a small dark nucleus with abundant chromatin clumps and prominent nucleoli (Gadisseux et al. 1992). A subpial granular layer is not unique for the human brain as originally thought. It is also present in the developing rat brain (Meyer et
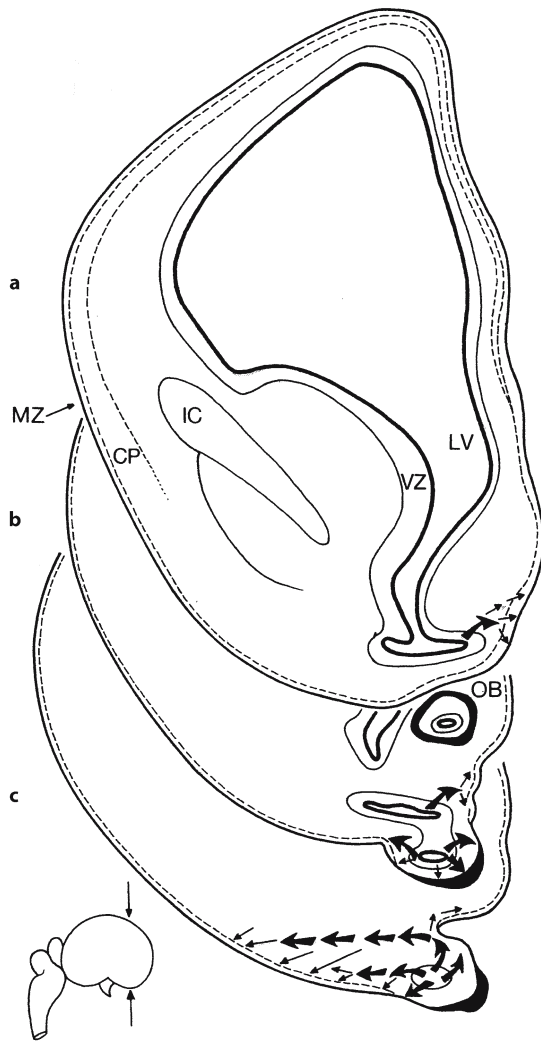
Fig. 10.29 Development of the subpial granular layer in the basal forebrain of a human fetus of 11 gestational weeks. The lateral ventricle (*LV*) is continuous with a ventral dilatation at the level of the paleocortex (**a**). The *arrow* indicates the proposed migration pathway from the medial wall of the paleocortical ventricle towards the pial surface. From here, the cells presumably continue their migration into the marginal zone (*MZ*) of the rostral cortex. The paleocortical ventricle is continuous with the olfactory ventricle inside the olfactory bulb (*OB*; **b**). At this level, cell migrations from the paleocortical ventricle are mainly directed medially. More caudally (**c**), cells migrate laterally in multiple streams towards the marginal zone of the paleocortex. *CP* cortical plate, *IC* internal capsule, *VZ* ventricular zone. (After Meyer and Wahle 1999)

al. 1998, 1999, 2000a, b; Takiguchi-Hayashi et al. 2004). Some of the subpial granular layer granule cells differentiate into Reelin-producing Cajal–Retzius-like cells of the neocortical marginal zone (Meyer and Goffinet 1998). This transient cell layer may play a significant role in the establishment of the complex cytoarchitecture of the cerebral cortex. Naturally occurring cell death is an active mechanism contributing to the disappearance of the subpial granular layer (Spreafico et al. 1999).

Formation of the Subplate

Kostović and Rakic (1990) studied the development of the transient subplate in the visual and somatosensory cortex of the macaque monkey and human brain. In both species, the subplate becomes visible at the beginning of the mid-third of gestation as a cell-poor/fibre-rich layer situated between the intermediate zone and the developing cortical plate. The subplate appears earlier in the somatosensory cortex than in the visual cortex and reaches maximal width at the beginning of the last third of gestation in both regions. At the peak of its size the ratio between the width of the subplate and the cortical plate in the somatosensory cortex is 2:1 in monkey and 4:1 in man, whereas in the visual cortex these structures have about equal width in both species. Subplate neurons provide sites for transient synaptic contacts for axons ascending from the thalamus and other cortical regions (Kostović and Rakic 1990). The dissolution of the subplate zone begins during the last trimester of gestation with degeneration of some subplate cells and the relocation of the waiting thalamocortical fibres into the cortex at about 26 weeks of gestation (Kostović and Goldman-Rakic 1983). The subplate leaves only a vestige of cells scattered throughout the subcortical white matter. Subplate neurons may also be involved in different types of periventricular lesions (Mrzljak et al. 1988; Kostović et al. 1989; Kostović and Rakic 1990; Chan et al. 2002; Kostović and Judáš 2002). The period of peak development of the subplate corresponds to the time period in which severe germinal matrix-interventricular haemorrhage, periventricular infarction and periventricular leukomalacia frequently occur (Sect. 10.7.5). With SMI-312 immunohistochemistry, the subplate can clearly be delineated (Ulfig and Chan 2002).

Cortical Differentiation and Maturation

Neocortical differentiation as seen in Golgi preparations of human fetuses has been studied by Poliakov (1949, 1959, 1965), Mrzljak et al. (1988, 1990) and Marín-Padilla (1992). The prenatal development of the main cortical neurons is shown in Fig. 10.30. The period from 22 weeks of gestation to term is the most significant period for areal, laminar and cytological differentiation of the cortical plate (Chan et al. 2002). During this period, the first thalamocortical synapses are formed within the cortical plate, with concomitant differentiation of dendritic arborizations of layers III and V pyramidal neurons and cortical
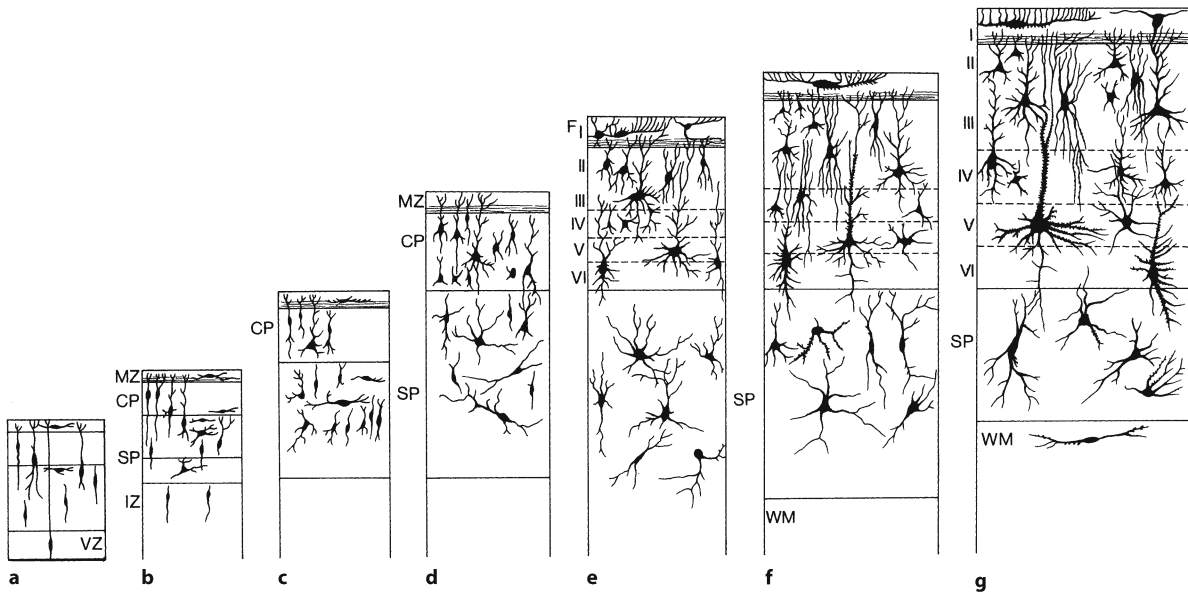
Fig. 10.30 Prenatal development of neurons in the prefrontal cortex as found in Golgi-stained sections at 10.5 (**a**), 13.5 (**b**), 17 (**c**), 19–25 (**d**), 26–29 (**e**) and 32–34 (**f**) weeks of gestation, and in a neonate (**g**). *CP* cortical plate *FI–VI* fetal cortical layers, *IZ* intermediate zone, *MZ* marginal zone, *SP* subplate, *VZ* ventricular zone, *WM* white matter. (After Mrzljak et al. 1988)

interneurons (Kostović 1990b). In the period of 22–26 weeks of gestation, the cortical plate in all neocortical areas displays dense granularity in a position corresponding to the future layer VI (Chan et al. 2002). After 28 weeks of gestation, the six-layered adult laminar pattern gradually appears owing to the progressive differentiation of the cortical plate. In Golgi-stained sections, the first acceleration in dendritic growth occurs after the arrival of thalamocortical fibres (Mrzljak et al. 1988, 1990). The major outgrowth of dendrites occurs in the first and second postnatal years, both for pyramidal and for nonpyramidal neurons. At 2–4 years of age, the mature dendritic extension has been reached (Koenderink et al. 1994; Koenderink and Uylings 1995). The mature level of outgrowth is reached at about 3–4 years (Uylings 2001). Certain cortical areas such as the frontal and parietal cortices keep increasing until the age of 12–13 years as observed in a longitudinal MRI study (Giedd et al. 1999). The postnatal development of Golgi-stained human cortical neurons was extensively studied by Conel (1939, 1941, 1947, 1951, 1955, 1959, 1963, 1967). The progressive growth of the dendritic and axonal plexus was studied in various parts of the cerebral cortex. The allocortex reaches its final structure at an earlier stage than the neocortex.

With immunohistochemical techniques, Uylings and co-workers (Koenderink et al. 1994; Koenderink and Uylings 1995; Uylings et al. 2002) studied the development of calcium binding protein immunoreactive neurons in the frontal cortex. A late postnatal onset of parvalbumin-immunoreactive neurons was found in the prefrontal cortex in contrast to the much earlier onset of calbindin-immunoreactive neurons. In the occipital cortex parvalbumin staining was observed earlier (Cao et al. 1996; Honig et al. 1996; Ulfig et al. 2001). Mature distribution of neuropeptide Y, calbindin and parvalbumin immunoreactive nonpyramidal neurons was observed in early puberty.

10.5   Development of the Hippocampal Formation

Autoradiographic data on the time of neuron origin in the rat hippocampal formation (Angevine 1965; Caviness 1973; Bayer 1980a, b; Bayer and Altman 1991) are summarized in Fig. 10.31. In the hippocampus, the first neurons to be born reside in the marginal zone (Bayer and Altman 1991; Supèr et al. 1998a). Most of these early-generated neurons disappear at late postnatal stages (Supèr et al. 1998a). The subsequently produced hippocampal neurons form a cortical plate between the marginal zone and the subplate, following an inside-out sequence. The granule cells of the dentate gyrus, however, follow an outside-in pattern of histogenesis (Bayer 1980a, b). New granule cells are produced throughout adulthood in the dentate gyrus of mammals from rodents to men (Eriksson et al. 1998; Gould et al. 1999; Cameron and McKay 2001). Cameron and McKay (2001) estimated that the number of granule cells generated each
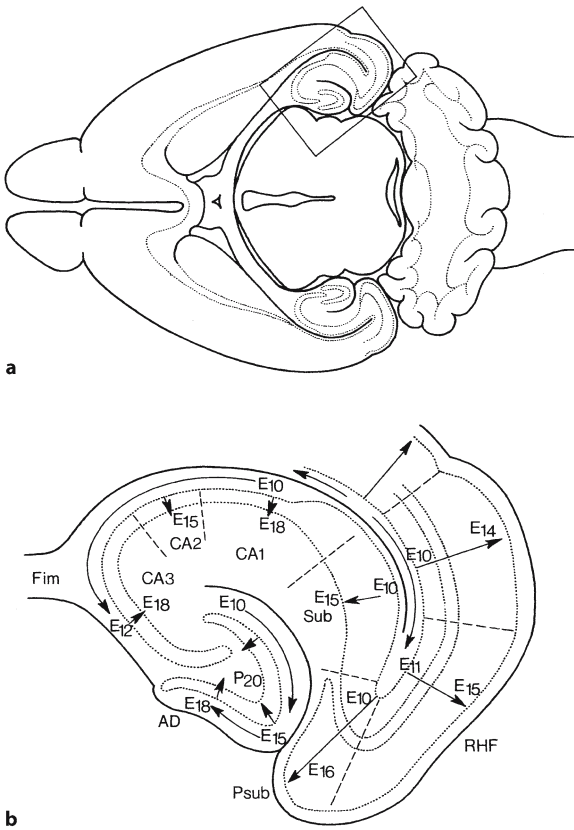
Fig. 10.31 Horizontal section (**a**) of the mouse brain and magnification of the hippocampal formation (**b**), showing the time of neuron origin and inside-out neurogenetic gradient for each part of the hippocampal formation. *AD* area dentata, *CA1, CA2, CA3* cornu Ammonis fields, *Fim* fimbriae, *Psub* presubiculum, *RHF* retrohippocampal formation, *Sub* subiculum. (After Angevine 1965)

month is 6% of the total number of the granule cell population. The large number of adult-generated granule cells supports the idea that these new neurons play an important role in hippocampal function. Adult hippocampal neurogenesis originates from precursor cells in the adult dentate gyrus (Kemperman et al. 2004). Calretinin expression marks a transient postmitotic stage in early neuronal development, whereas mature new granule cells express calbindin (Berger et al. 1993; Soriano et al. 1994; Berger and Alvarez 1996; Kemperman et al. 2004).

Many molecules appear to be involved in the proper development of the hippocampal formation (Grove and Tole 1999; Hatanaka and Jones 1999; Skutella and Nitsch 2001). Although the hippocampal cornu Ammonis fields can be distinguished by cytoarchitecture only after birth, molecular differences between fields appear by late gestation (Grove and Tole 1999). The embryonic cornu Ammonis fields are specified to develop complex, mature cornu Ammonis field identities. By E10.5–E12.5, the medial pallium can autonomously generate a patterned hippocampal primordium. Signals from the cortical hem regulate hippocampal development (Grove and Tole 1999; Zaki et al. 2003). Like in the cerebral cortex, hippocampal fields are not defined by cell lineage restriction boundaries.

Supèr and co-workers (Supèr and Soriano 1994; Supèr et al. 1998a, b) studied the **circuitry** of the embryonic and early postnatal murine hippocampus with the lipophilic tracer 1,1'-dioctadecyl-3,3,3',3'-tetramethylindocarbocyanine perchlorate (DiI; Fig. 10.32). Pyramidal neurons of the hippocampus have their somata in the basal *stratum pyramidale*, and extend dendrites towards the pial surface. Affer-
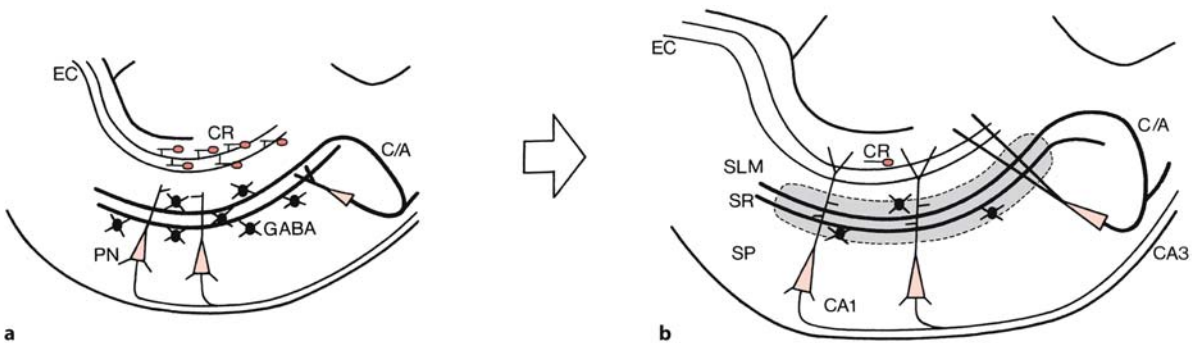
Fig. 10.32 The role of transient guidepost cells in the formation of laminar specificity in the rat hippocampus. In the embryo (**a**), Reelin-expressing Cajal–Retzius cells (*CR*) are present in the distal lamina and serve as transient synaptic targets for entorhinal axons from the cortex (*EC*) before pyramidal dendrites have arrived. GABAergic interneurons are concentrated in proximal laminae, and serve as transient synaptic targets for commissural and associational axons (*C/A*). Postnatally (**b**),

many Cajal–Retzius and GABAergic cells are lost. EC and C/A axons are confined to the stratum lacunosum-moleculare (*SLM*) and stratum radiatum (*SR*), respectively, and synapse onto distinct domains of pyramidal cell dendrites. *CA1, CA3* cornu Ammonis fields, *PN* pyramidal neurons, *SP* stratum pyramidale. (Based on data by Supèr and Soriano 1994; Supèr et al. 1998a, b; after Sanes and Yamagata 1999)

ent fibres from the ipsilateral entorhinal cortex synapse on the distal parts of these dendrites in the superficial *stratum lacunosum-moleculare*. Commissural fibres synapse on proximal parts of these dendrites in the *stratum radiatum*. Entorhinal axons were observed for the first time in the white matter of the hippocampus at E15. At E17, entorhinal fibres arborized within the stratum lacunosum-moleculare and subsequently formed dense networks. Commissural axons first entered the contralateral hippocampus at E18. They arborized within the stratum oriens and radiatum of the hippocampus. Two groups of pioneer neurons, Cajal–Retzius cells and GABAergic neurons, form layer-specific scaffolds that overlap with distinct hippocampal afferents at embryonic and early postnatal stages. At postnatal day 0 (P0)–P5, before the dendrites of pyramidal neurons develop, these pioneer neurons form preferential synaptic targets for entorhinal fibres. Therefore, distinct pioneer neurons appear to be involved in the guidance and targeting of various hippocampal afferents. A complex network of guidance signals regulates the formation of hippocampal connections during development (Skutella and Nitsch 2001; Heimrich et al. 2002; Brinks et al. 2004). Outgrowing axons are routed towards the hippocampal formation by specific expression of long-range cues such as semaphorins, netrin-1 and Slit proteins. Local membrane-anchored or substrate-anchored molecules such as ligands of the ephrin A subclass, provide layer-specific positional information. Semaphorins act as repellent guidance cues for routing afferent fibres towards and inside the hippocampus (Chédotal et al. 1998; Chen et al. 2000). Netrin-1 attracts commissural fibres (Steup et al. 1999). Slit and Robo proteins restrict outgrowth of dentate fibre systems towards the entorhinal cortex (Chédotal et al. 1998; Nguyen Ba-Charvet et al. 1999). Ephrin A3 is involved in the lamina-specific ingrowth of entorhinal fibres (Stein et al. 1999). The repulsive guidance molecule RGMa is involved in the formation of afferent connections in the dentate gyrus (Brinks et al. 2004).

The development of **GABAergic neurons** in the mammalian hippocampus has received much attention (reviewed in Ben-Ari 2001, 2002; Owens and Kriegstein 2002). In rats, at birth, 80% of CA1 pyramidal neurons have an axon but no dendrites, 10% have in addition a small apical dendrite with GABAergic synapses only, and another 10% with extended apical dendrites and basal dendrites as well have GABAergic and glutamate synapses (Soriano et al. 1989; Tyzio et al. 1999; Hennou et al. 2002). Similar observations were made in cynomolgus monkeys (Khazipov et al. 2001). Therefore, GABAergic synapses are established before glutaminergic ones and the formation of glutaminergic synapses requires that the target neuron has an apical dendrite that

reaches the distal superficial regions. Nearly all the genetic experiments completed so far have shown few, if any, developmental defects when perturbing the GABA system (Owens and Kriegstein 2002). Many GABA-deficient mouse mutants have a lower seizure threshold or show spontaneous seizures (Sect. 10.7.4).

At the beginning of the fetal period, the **human hippocampal formation** contains four layers: a ventricular zone, an intermediate layer, a hippocampal plate comprised of bipolar-shaped neurons and a marginal zone (Humphrey 1966a, b; Kahle 1969; Arnold and Trojanowski 1996 a, b). At 15–19 weeks of gestation, individual subfields can be distinguished (Fig. 10.33). A distal-to-proximal gradient of cytoarchitectonic and neuronal maturity is found, with the subiculum appearing more developed than the ammonic subfields CA1 to CA3. The dentate gyrus is the latest to develop. Most pyramidal cells in the cornu Ammonis fields are generated in the first half of pregnancy and no pyramidal neurons are formed after the 24th gestational week (Seress et al. 2001). Granule cells of the dentate gyrus proliferate at a decreasing rate during the second half of pregnancy and after birth but still occur in a low percentage during the first postnatal year (Seress et al. 2001). The cross-sectional area of the dentate gyrus is specifically reduced in autism (Saitoh et al. 2001). Reciprocal entorhinal–hippocampal connections are established by fetal midgestation (Hevner and Kinney 1996). Fibres connecting the entorhinal cortex, hippocampus and subiculum are present by about 19 weeks of gestation. The perforant path, connecting the entorhinal cortex with the dentate gyrus, and all connections with the neocortex are only beginning at 22 weeks of gestation. These data suggest that hippocampal connections develop prior to neocortical pathways, and that reciprocal entorhinal–hippocampal projections may be among the first cortico-cortical connections to be established in the human brain. Myelination is first evident near term, with strong myelin basic protein immunoreactivity present in the alveus and fimbria, and relatively scant immunoreactivity in the perforant path (Arnold and Trojanowski 1996a). Myelination in the hippocampus increases in childhood until adolescence, after which the pattern remains unchanged. The confused spatial relationship of the fornix to the corpus callosum and the anterior commissure was noted by Hori (1997). Examples of hippocampal rudiments are found occasionally (Lammens et al. 2003; Hori and Stan 2004; Fig. 10.34). In *temporal lobe dysgenesis*, a prominent feature of thanatophoric dysplasia, the hippocampal region is severely dysgenetic (Hori et al. 1983; Clinical Case 10.2).
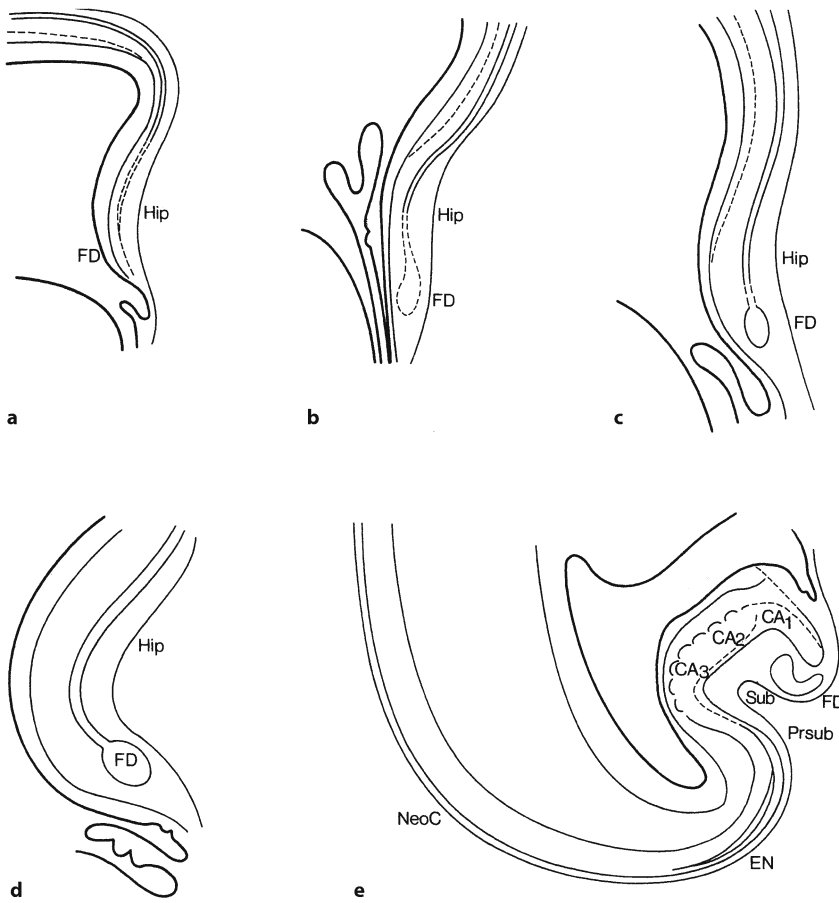
Fig. 10.33 The development of the human hippocampus at the end of the third month, shown for fetuses of 50-mm (**a**), 58-mm (**b**), 64-mm (**c**), 83-mm (**d**) and 120-mm (**e**) crown–rump length. The inrolling of the hippocampal components occurs in this period. *CA1*, *CA2*, *CA3* cornu Ammonis fields, *EN* entorhinal cortex, *FD* fascia dentata, *Hip* hippocampus anlage, *NeoC* neocortex, *Prsub* presubiculum, *Sub* subiculum. (After Kahle 1969)
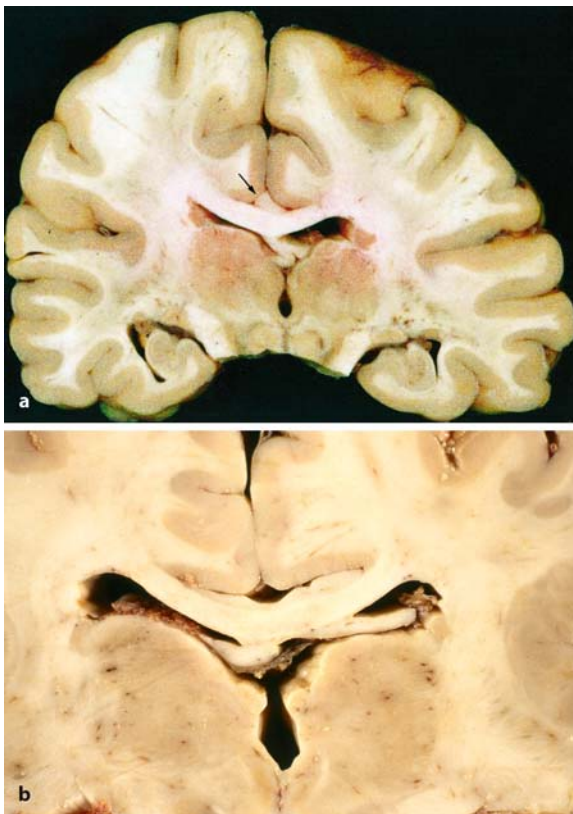
Fig. 10.34 a, **b** Supracallosal longitudinal fibre bundles in a case of Nijmegen breakage syndrome (**a**) and in a 30-year-old mentally retarded woman with microcephaly and spastic tetraparesis since childhood (**b**). Histologically, no indusium griseum was recognized. **c** Heterotopic or hyperplastic grey matter was present in the supracallosal region, possibly an incomplete form of holoprosencephaly. (**a** From Lammens et al. 2003, with permission; **b**, **c** from Hori and Stan 2004, with permission)

10.6   Development of the Main Cortical Connections

Shortly after the formation of the cortical plate, the afferent and efferent fibre connections of the cerebral cortex arise (Fig. 10.36). Axons from the first preplate neurons form a kind of scaffold along which corticofugal axons from the cortical plate and thalamocortical fibres to the cerebral cortex find their way to the targets. Important roles in the guidance of corticofugal and thalamocortical fibres are played by the subplate and, also mostly transient, cell populations in the internal capsule and ventral thalamus (Chap. 9). The human capsula interna can be distinguished late in the embryonic period (Hewitt 1961; O'Rahilly and Müller 1999). The development of the pyramidal tract also starts late in the embryonic period (Humphrey 1960; ten Donkelaar 2000; Chap. 6), whereas the development of the corpus callosum starts around the 11th week of gestation (Rakic and Yakovlev 1968).

10.6.1   Development of Thalamocortical Projections

Thalamocortical fibres arise rather early in development. Yamadori (1965) studied their development in 5–130-mm-long human embryos. The first fibres were already recognized in the thalamus of a 5-mm embryo (approximately 3 weeks of development). Developing thalamocortical axons leave the dorsal thalamus ventrally and turn dorsolaterally at the telencephalic–diencephalic boundary (Fig. 10.36). Thalamocortical fibres reach the internal capsule late in the embryonic period, and early fetally reach the subplate. Mechanisms controlling the proper outgrowth and target finding of thalamocortical projections are discussed in Chap. 9.

10.6.2   Development of the Pyramidal Tract

The first corticofugal fibres find their way to the internal capsule guided by subplate neurons. In rodents, experimental studies showed that axons from layer V pyramidal cells in the motor as well as in the visual cortex grew out to the spinal cord (Fig. 2.32), subsequently gave off collaterals to subcortical areas, and finally lost transient branches such as the spinal projections from the visual cortex (O'Leary and Koester 1993). Genes involved in pathfinding of corticospinal axons are discussed in Chaps. 2 and 6. The human pyramidal tract reaches the level of the pyramidal decussation at the end of the embryonic period (O'Rahilly and Müller 1999; Fig. 6.33). Pyramidal decussation is complete by 17 weeks' gestational age, and the rest of the spinal cord is invaded by 19 weeks' gestational age (lower thoracic cord) and 29 weeks' gestational age (lumbosacral cord) (Humphrey 1960). Functional corticospinal projections may be established prenatally in the human fetus (Eyre et al. 2000; Chap. 6). Myelination of the pyramidal tract is already in progress at the pyramidal decussation as early as 25 weeks of gestation (Yakovlev and Lecours 1967). Malformations of the pyramidal tracts may occur at various stages of development and are discussed in Chap. 6.

10.6.3   Development of the Corpus Callosum

The human corpus callosum can be distinguished at 11–12 weeks' gestational age (Rakic and Yakovlev 1968), when it develops in the commissural plate (Fig. 10.37). Fusion of the medial walls of the cerebral hemispheres does not occur in the embryonic period, but the events during the fetal period are not entirely clear (O'Rahilly and Müller 1999). Hochstetter (1919) denied fusion, whereas His (1904), Loeser and Alvord (1968) and Rakic and Yakovlev (1968), among others, suggested infolding of the dorsal part of the **lamina reuniens** (*Schlussplatte*) of His (the embryonic lamina terminalis) in the region of the medial pallium into a median groove at the end of the embryonic period. This is followed by early fetal fusion of its banks into a massa commissuralis or commissural plate which becomes the bed for the corpus callosum, as described in mice by Zuckerkandl (1901). The ventral part of the lamina reuniens becomes the *Endplatte* (**lamina terminalis** *sensu stricto*), which remains thin and forms the rostral wall of the telencephalon medium. Its dorsal part forms the *Trapezplatte* or **massa commissuralis** (O'Rahilly and Müller 1999). A definitive massa commissuralis and the anterior commissure are formed at the ninth and tenth weeks of development. The anterior commissure defines the area precommissuralis. During the tenth and 11th weeks the fornix appears and defines the primordium hippocampi. The hippocampal commissure or psalterium is formed at the 11th to 12th weeks of development. Owing to the rostrocaudal expansion of the cerebral hemispheres, the corpus callosum expands from the vicinity of the lamina reuniens, rostrally and caudally.

Temporal Lobe Dysgenesis

Cloverleaf (*Kleeblattschädel*) skull anomaly occurs in thanatophoric chondrodystrophy and in Crouzon, Pfeiffer and Apert syndromes (Chap. 5). In thanatophoric chondrodysplasia, ***temporal lobe dysgenesis*** is a prominent feature (Hori et al. 1983; Wongmongkolrit et al. 1983; see Case Report). One of the youngest fetal cases of thanatophoric chondrodystrophy is shown in Fig. 10.35.

Case Report. The second pregnancy of a 22-year-old mother was uneventful until the 27th gestational week, when an enlarged fetal head with normal configuration was observed on ultrasound exam-

ination. Further bitemporal increase in size was found at the end of the 28th week and chondrodystrophy was diagnosed, resulting in the interruption of the pregnancy in week 29. The stillborn male neonate had a body weight of 1,200 g and a length of 30 cm. Its head showed a characteristic trilobar configuration with bilateral exophthalmos, macrostomia and low displacement of the ears (Fig. 10.35 a). The extremities were very short and all joints were immobile. After autopsy, chondrodystrophy of the skeleton was confirmed. The skull had a typical cloverleaf shape. The fontanelles were not enlarged. The base of the skull showed remarkable shortening of the longitudinal axis with an extremely small posterior cranial fossa. The brain weighed 239 g and the infratentorial structures only 9 g (about half of normal). The cerebrum showed a prominent bitemporal bulging with very

Fig. 10.35 Temporal lobe dysgenesis found in an early fetal case of cloverleaf skull anomaly with thanatophoric chondrodystrophy: **a** cloverleaf skull and chondrodystrophy with facial anomalies, thorax deformity and short extremities at 29 weeks of gestation; **b** basal view of the brain; **c** aplasia of Ammon's horn, dysgenetic parahippocampal area and periventricular heterotopia in the temporal lobe. (From Hori et al. 1983, with permission)

deep secondary sulci in the temporal lobes, parallel to the sagittal plane (Fig. 10.35 b). The lateral surfaces of the brain showed a gyral pattern normal for age. No parahippocampal gyri were identified. The inferior horns of the lateral ventricles showed peculiar diverticles, protruding into the subcortical regions. These diverticles corresponded to abnormal massive gyri separated by deep sulci. The brain stem and cerebellum were grossly normal except for their small size. Histologically, the hippocampal regions were severely dysgenetic (Fig. 10.35 c). Prominent subependymal neu-

ronal heterotopia were found along the inferior horns. The amygdala was present but was not well differentiated.

References

Hori A, Friede RL, Fischer G (1983) Ventricular diverticles with localized dysgenesis of the temporal lobe in cloverleaf skull anomaly. Acta Neuropathol (Berl) 60:132–136

Wongmongkolrit T, Bush M, Roessmann U (1983) Neuropathological findings in thanatophoric dysplasia. Arch Pathol Lab Med 107:132–135
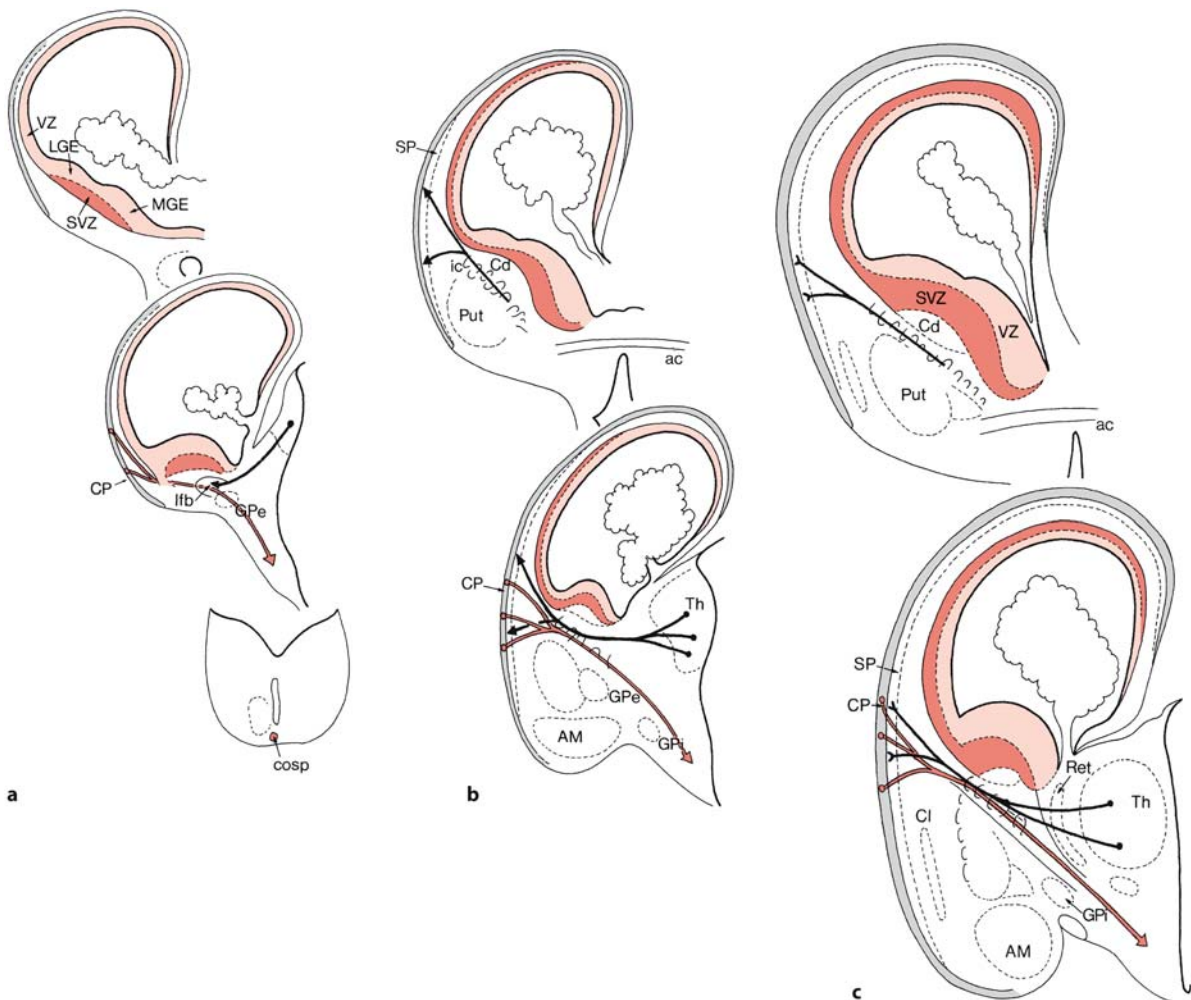
Fig. 10.36 Early development of cortical connectivity in the human brain at the end of the embryonic period (**a**), and at 9 weeks (**b**) and 13 weeks (**c**) of development. At the end of the embryonic period, the first corticofugal fibres have already reached the caudal hindbrain (**a**). Thalamocortical fibres reach the subplate by about 9 weeks of development (**b**) but have not invaded the cortical plate (*CP*) by 13 weeks of development (**c**), and are still waiting in the subplate (*SP*). The ventric-ular zone (*VZ*) is indicated in *light red*, the subventricular zone (*SVZ*) in *red* and the cortical plate in *grey*. *ac* anterior commissure, *AM* amygdala, *Cd* caudate nucleus, *Cl* claustrum, *cosp* corticospinal tract, *GPe* external part of globus pallidus, *GPi* internal part of globus pallidus, *ic* internal capsule, *lfb* lateral forebrain bundle, *LGE* lateral ganglionic eminence, *MGE* medial ganglionic eminence, *Put* putamen, *Ret* reticular thalamic nucleus, *Th* thalamus
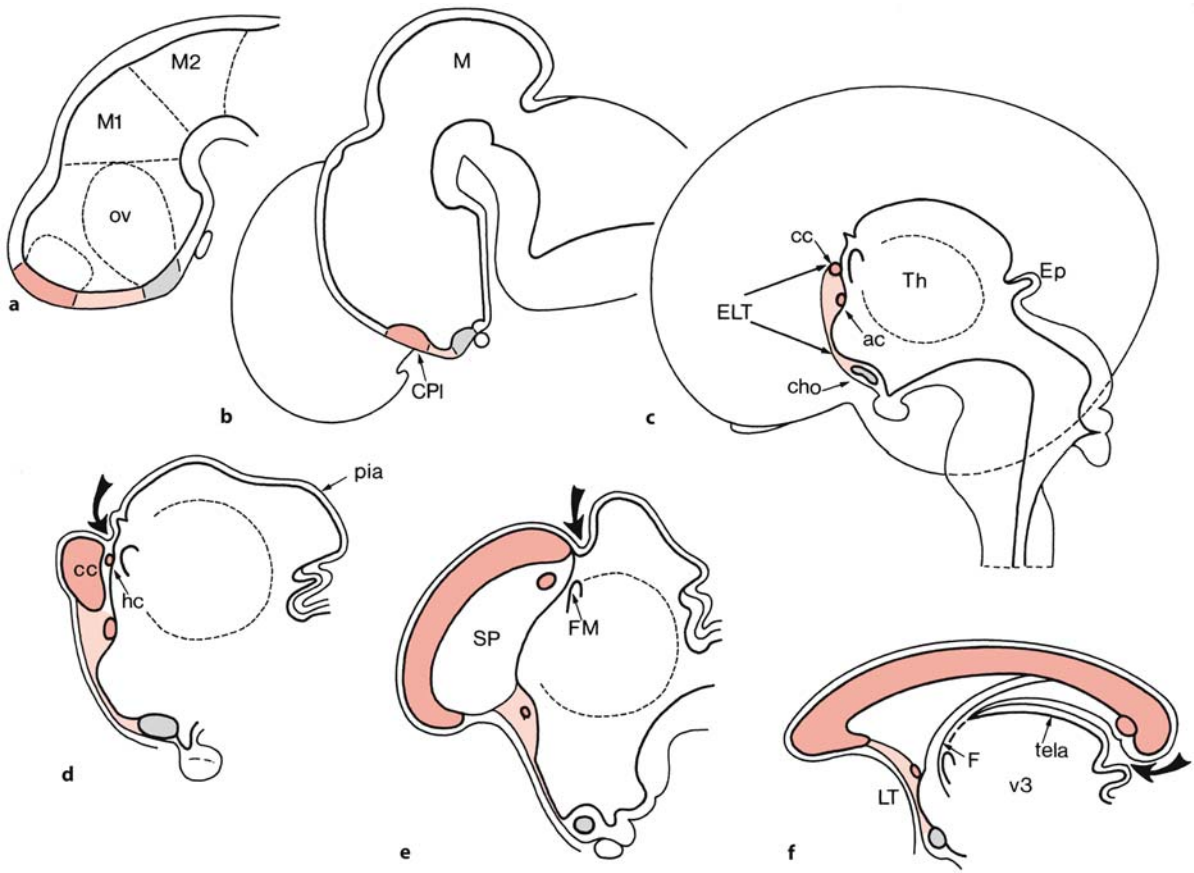
Fig. 10.37 Development of the human corpus callosum at Carnegie stages 13 (**a**) and 22 (**b**) and at 11 (**c**), 13 (**d**) and 15 (**e**) weeks of development, and in a neonate (**f**). The chiasmatic plate and the optic chiasm are indicated in *grey*, the embryonic lamina terminalis (*ELT*) and the 'adult' lamina terminalis (LT) in *light red*, and the commissural plate (*CPl*) and its derivatives in *red*. The posterior growth of the corpus callosum leads to the formation of the velum interpositum, a double fold of pia mater (*arrows* in **d**–**f**). Between these two layers, blood vessels pass forwards beneath the corpus callosum and contribute to the tela choroidea of the third ventricle. *ac* anterior commissure, *cc* corpus callosum, *cho* chiasma opticum, *Ep* epiphysis, *F* fornix, *FM* foramen of Monro, *hc* hippocampal commissure, *M* mesencephalon, *M1*, *M2* mesomeres, *ov* optic vesicle, *SP* septum pellucidum, *Th* thalamus, *v3* third ventricle. (After Keibel and Mall 1911, 1912; Hochstetter 1919; O'Rahilly and Müller 1999)

The development of the **septum pellucidum** is intimately related to the formation of the massa commissuralis and the commissures of the hemispheres (Fig. 10.38). The septum pellucidum is made up of two layers of white matter (termed *medial medullary vela* by Raybaud and Girard 1999). It is bordered by the anterior commissure, the rostral half of the corpus callosum, and by the body of the fornix. Posteriorly, the medial medullary velum is continuous with the fimbriae of the fornix. The medial medullary velum may represent the substitute for the corpus callosum, the septum pellucidum, the fornix and the psalterium (Raybaud and Girard 1999). The **cavum septi pellucidi** has been described as arising as a pocket between the walls of the infolded primordium hippocampi, bridged by the corpus callosum (Rakic and Yakovlev 1968). It was suggested that this pocket is rostrally open at first, but later becomes closed by the development of the rostrum of the corpus callosum. Alvord and co-workers (Loeser and Alvord 1968; Shaw and Alvord 1969; Lemire et al. 1975), however, concluded that the cavum is formed by necrosis within the massa commissuralis and was never open to the subarachnoid space. The two leaves of the septum pellucidum become attenuated by the rapid growth of the hippocampi and corpus callosum. A cavum septi pellucidi is present in every normal fetus up to 6 months of gestation, but it gradually narrows from the splenium towards the genu so that the posterior part is usually obliterated by the time of birth and the rostral part by about 3 months after birth (Shaw and Alvord 1969; Lemire et al. 1975). A cavum
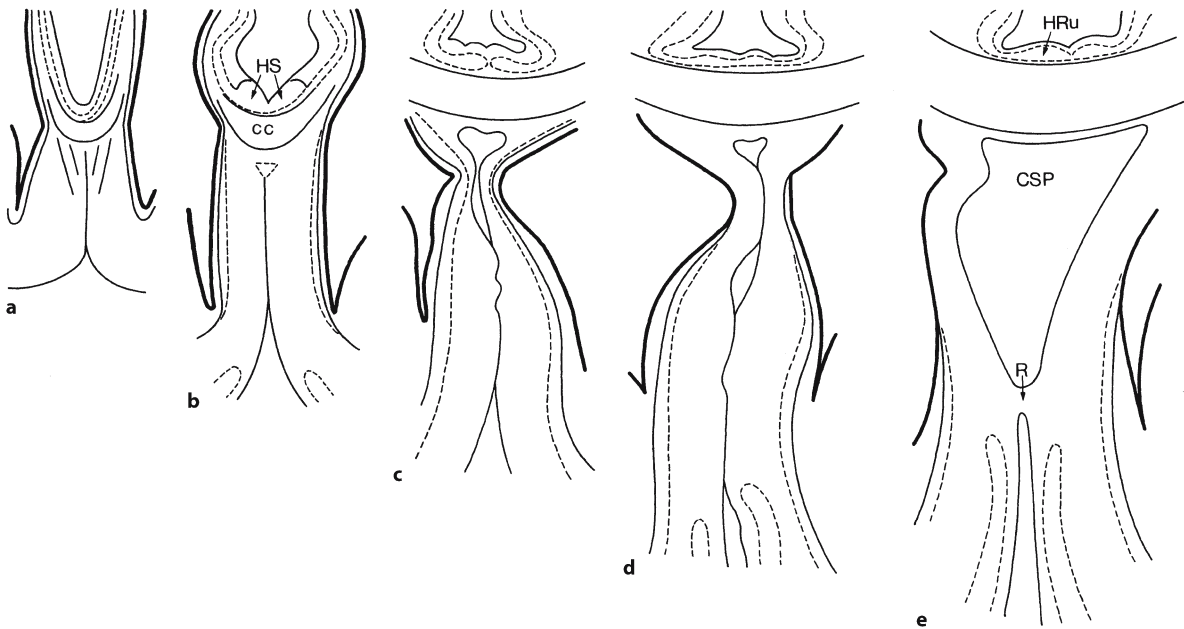
Fig. 10.38 Development of the septum pellucidum and the cavum septi pellucidi at 13 (**a**), 15 (**b**), 18 (**c**), 20 (**d**) and 22 (**e**) weeks of gestation. *cc* corpus callosum, *CSP* cavum septi pellu-cidi, *HRu* hippocampal rudiment, *HS* supracommissural hippocampal formation, *R* rostrum of corpus callosum. (After Rakic and Yakovlev 1968)

Fig. 10.39 Cavum septi pellucidi (**a**) and cavum Vergae (**b**) found as incidental findings in a 54-year-old patient (from the Department of Neuropathology, Medizinische Hochschule Hannover; courtesy Akira Hori)
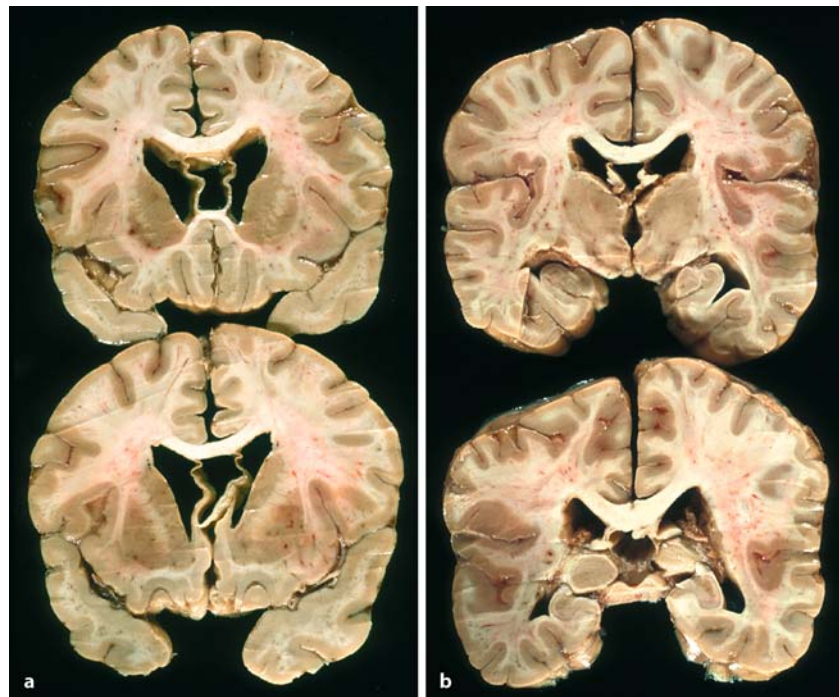
septi pellucidi remains in about 20 % of children and in 12–20 % of autopsies in adults (Shaw and Alvord 1969; Bruyn 1977; Sarwar 1989). If the rostral part persists, the cavity is known as cavum septi pellucidi (Fig. 10.39 a). If the caudal part remains open, the cavity is called cavum Vergae (Verga 1851; Fig. 10.39 b). The dividing line was arbitrarily taken as the frontal plane of the foramen of Monro. The cavum septi pellucidi and the cavum Vergae may form separate cavities, but often they communicate,

forming a single space throughout the length of the septum pellucidum. A wide cavum septi pellucidi in which the leaves are separated by more than 1 cm is frequently associated with abnormalities of neuro-behavioural function (Bruyn 1977; Sarwar 1989; Schaefer et al. 1994; Bodensteiner et al. 1998; Kwon et al. 1998; Sect. 10.7.8).

Glial cells seemed to form the first connection ('glial slings') between both hemispheres (Silver et al. 1982). Shu et al. (2003b), however, showed that the glial population is in fact a migratory population of developing neurons. Both axons from subplate and cortical plate (mainly from the future layer III) neurons form the corpus callosum (Koester and O'Leary 1994; Deng and Elberger 2001). Similar data were obtained in fetal rhesus monkeys (Lamantia and Rakic 1990a) and human fetuses (deAzevedo et al. 1997). Using DiI-tracing, deAzevedo and co-workers showed that at 25–32 postovulatory weeks the human cingulate cortex contains callosally projecting neurons in the cortical plate as well as in the subplate. Several genes are involved in the formation of the corpus callosum (Rubinstein et al. 1999). Agenesis of the corpus callosum is found in mouse mutants of the
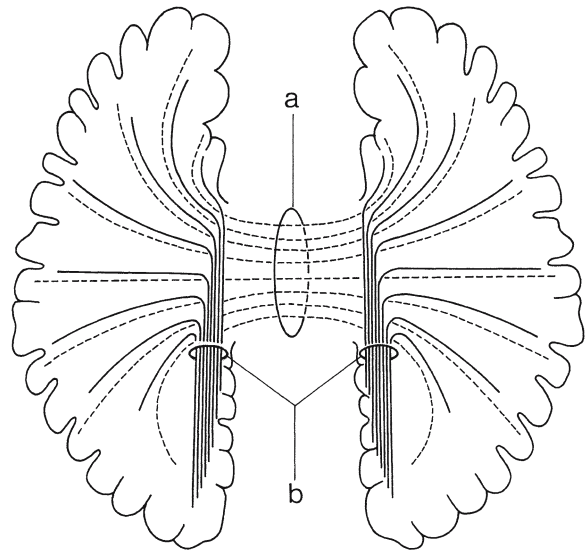
Fig. 10.40 Development of the bundles of Probst. The commissural fibres of the corpus callosum in a normal brain (*a*) are shown by *broken lines*; the abnormal longitudinal bundles of Probst (*b*) which fail to cross are shown in *solid lines*. (After Rakic and Yakovlev 1968)
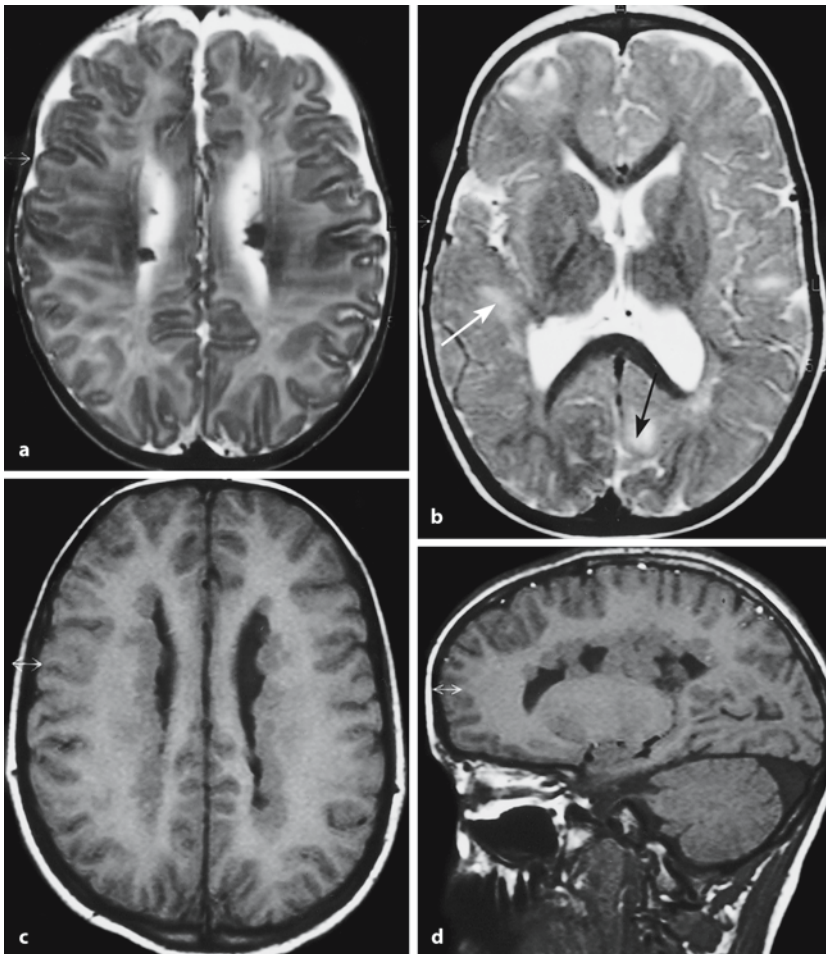
Fig. 10.41 Series of magnetic resonance images illustrating various kinds of developmental disorders of the cerebral cortex: **a**, **b** tuberous sclerosis: axial T2-weighted images in a 4-month-old girl (**a**), showing subependymal hamartomas, and in a 2-year-old boy (**b**), showing subcortical foci of high intensity (tubers; arrows); **c, d** axial and sagittal T2-weighted images of X-linked periventricular nodular heterotopia in an 8-year-old girl presenting with seizures;

Emx1, *Hesx1*, *Nfia* (Shu et al. 2003a) and *Tbr1* genes as well as in the absence of the guidance factor netrin-1. Partial or complete absence of the human corpus callosum is much more common than absence of the pyramidal tracts (Norman et al. 1995; Aicardi 1998; Barkovich 2000, 2003). Every disorder interfering with the development of the commissural plate leads to dysgenesis of the corpus callosum (Sect. 10.7.6). In failure of commissuration, callosal fibres may form abnormal longitudinal bundles, the **bundles of Probst** (the *Balkenlängsbündel* of Probst 1901), which failed to cross in the absence of the corpus callosum (Fig. 10.40).

10.7 Developmental Disorders of the Cerebral Cortex

The introduction of modern imaging techniques (CT, MRI) and recent discoveries concerning the molecular biology of malformations of cortical development have greatly increased our ability to identify and categorize patients with developmental disorders of the cerebral cortex. The revised classification of mal-

formations of cortical development proposed by Barkovich et al. (2001) is used in this chapter. This classification (Table 10.2) follows the stage of development (cell proliferation, neuronal migration, cortical organization) at which cortical development is first affected, and is based on known developmental steps, pathological features, genetics and neuroimaging data (Fig. 10.41). Identified genes for disorders of cortical development are shown in Table 10.3. In many cases, however, the precise developmental and genetic features of cortical developmental disorders are still uncertain. Many disorders of cortical development are associated with severe and often intractable epilepsy (Sect. 10.7.4). The large group of cortical malformations due to vascular disorders such as hypoxic and ischemic lesions is briefly discussed in Sect. 10.7.5. Cortical malformations may lead to disorders of cortical connectivity, of the corpus callosum and the pyramidal tract in particular (Sect. 10.7.6). Aspects of cortical malformation leading to mental retardation are dealt with in Sect. 10.7.7, whereas certain neurobehavioural disorders are discussed in Sect. 10.7.8.

Fig. 10.41 e axial MRI of a subcortical band heterotopia in a 4-month-old girl; **f** axial MRI of a non-specific case of lissencephaly in a 9-month-old boy with frontal pachygyria and occipital polymicrogyria; **g**, **h** axial and sagittal MRI of a large focal heterotopia in the internal capsule and surroundings in a 6-month-old girl (courtesy Berit Verbist, Leiden, and Henk Thijssen, Nijmegen)
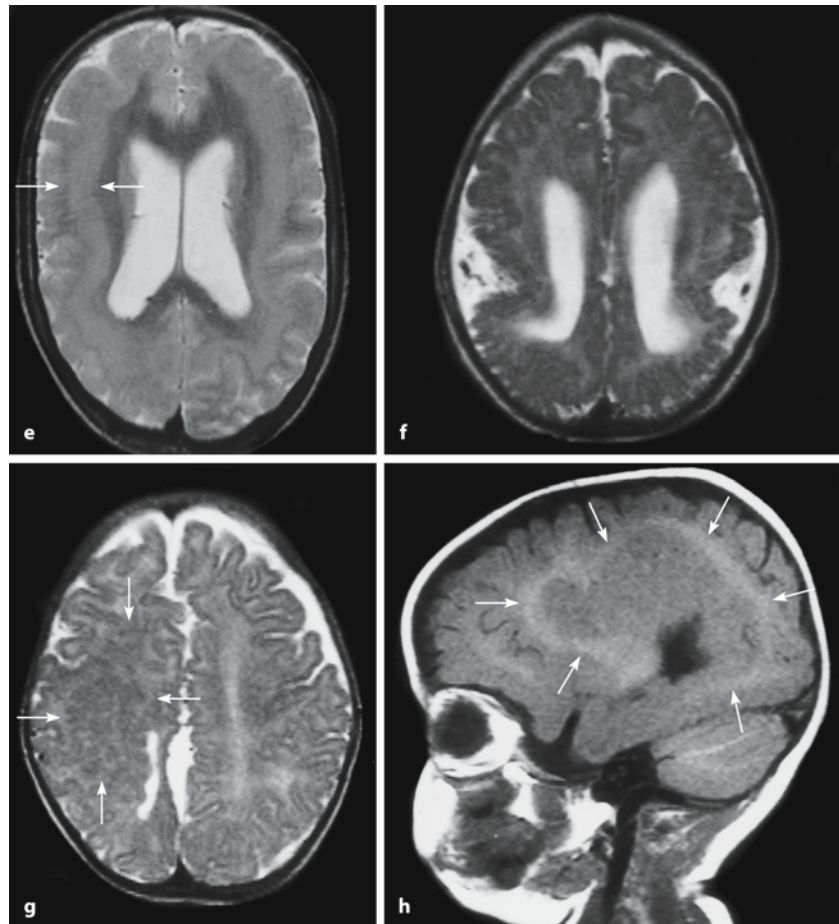
Table 10.2 Classification scheme for cortical malformations (after Barkovich et al. 2001)

I. Malformations due to abnormal neuronal and glial proliferation or apoptosis	A. Decreased proliferation or increased apoptosis: microcephalies	1. Microcephaly with normal to thin cortex 2. Microlissencephaly (extreme microcephaly with thick cortex) 3. Microcephaly with polymicrogyria/cortical dysplasias
	B. Increased proliferation or decreased apoptosis: megalencephalies	
	C. Abnormal proliferation	1. Non-neoplastic: – Cortical hamartomas of tuberous sclerosis – Cortical dysplasias with balloon cells – Hemimegalencephaly 2. Neoplastic: – Dysembryoplastic neuroepithelial tumour – Ganglioglioma – Gangliocytoma
II. Malformations due to abnormal neuronal migration	A. Lissencephaly and sub-cortical band heterotopia spectrum	
	B. Cobblestone complex	1. Congenital muscular dystrophy syndromes 2. Syndromes without muscular involvement
	C. Heterotopia	1. Subependymal (periventricular) 2. Subcortical (other than band heterotopia) 3. Marginal glioneuronal
III. Malformations due to abnormal cortical organization (including late neuronal migration)	A. Polymicrogyria and schizencephaly	1. Bilateral polymicrogyria syndromes 2. Schizencephaly (polymicrogyria with clefts) 3. Polymicrogyria with other brain malformations or abnormalities 4. Polymicrogyria or schizencephaly as part of multiple congenital anomaly/mental retardation syndromes
	B. Cortical dysplasia without balloon cells	
	C. Microdysgenesis	
IV. Malformations of cortical development, not otherwise classified	A. Malformations secondary to inborn errors of metabolism	1. Mitochondrial and pyruvate metabolic disorders 2. Peroxisomal disorders
	B. Other unclassified malformations	1. Sublobar dysplasia 2. Others

10.7.1 Malformations due to Abnormal Neuronal/Glial Proliferation/Apoptosis

The mechanisms by which this group of malformations arise are complex and poorly understood. The congenital microcephalies, megalencephaly and malformations with abnormal cell types such as tuberous sclerosis, hemimegalencephaly and neoplastic forms such as dysembryoplastic neuroepithelial tumours form this group of malformations. Human *microcephaly* comprises a heterogeneous group of conditions that are characterized by a failure of normal brain growth. Microcephaly is usually defined as a condition in which the size of the head, measured by the occipitofrontal circumference (OFC), is signif-

icantly smaller than normal for age and gender. Because an abnormally small head almost invariably reflects a small cerebrum, head size is routinely recorded by paediatricians as an indicator of brain development. Usually, an OFC of greater than two standard deviations below the mean is used to define microcephaly in clinical practice. The aetiology of microcephaly can be broadly divided into environmental and genetic causes (Haslam 1987; Mochida and Walsh 2001). Common environmental causes are congenital infections such as cytomegalovirus, intrauterine exposure to teratogenic agents, and hypoxic/ischemic injury in the fetal and perinatal periods. The genetic causes of congenital microcephaly can be further subdivided, based on (1) the presence of normal versus abnormal brain architecture as found on

Table 10.3 Identified genes for disorders of cortical development (after Lammens 2000; Barkovich et al. 2001; Ross and Walsh 2001; Guerrini et al. 2003)

Cortical malformation	Trait	Locus	Gene/protein	Clinical manifestations
Neuronal heterotopia in white matter				
Bilateral periventricular nodular heterotopia (lethal in boys)	XL	Xq28	*FLM1*/Filamin 1	Epilepsy
Classic lissencephalies				
Miller–Dieker syndrome	AD	17p13.3	Several contiguous genes/ PAFAH1B1 (LIS1)	Severe mental retardation, epilepsy, spasticity
Isolated lissencephaly	AD	17p13.3	*LIS1*/PAFAH1B1 (LIS1)	Mental retardation, epilepsy
X-linked lissencephaly (SBH in girls)	XL	Xq22.3-q23	*XLIS (DCX)*/Doublecortin	Mental retardation (less severe in girls), epilepsy
Lissencephaly with cerebellar hypoplasia				
Lissencephaly with cerebellar hypoplasia	AR	7q22	*RELN*/Reelin	Severe mental retardation, epilepsy, hypotonia
Cobblestone lissencephalies				
Walker–Warburg syndrome	AR		*POMT1*/*O*-mannosyl-transferase	Severe mental retardation, hypotonia, hydrocephalus, eye malformations, cerebellar malformations
Muscle–eye–brain disease	AR	1p32-34	*POMGnT1*	Usually severe mental retardation, epilepsy, hypotonia and glaucoma
Fukuyama congenital muscular dystrophy	AR	9q31-33	*FCMD*/Fukutin	Severe mental retardation, epilepsy (in 20%), hypotonia, mild spasticity
Polymicrogyrias				
Aicardi syndrome	XL	Xp22		Severe mental retardation, chorioretinopathy, agenesis of corpus callosum, infantile spasms
Zellweger syndrome	AR	At least 10 different genes	Peroxisomal enzymes	Cerebrohepatorenal syndrome: mental retardation, epilepsy, hypotonia, hepatomegaly, cardiac malformations, polycystic kidneys

AD autosomal dominant, *AR* autosomal recessive, *SBH* subcortical band heterotopia, *XL* X-linked

MRI examination, and (2) its combination with non-CNS abnormalities. Microcephaly is a characteristic feature in holoprosencephaly (Chap. 9) and lissencephalies, but it is usually not severe in such malformations. Extreme microcephaly has been described in early, severe Cockayne syndrome (Nance and Berry 1992), the cerebro-oculo-facio-skeletal (COFS) syndrome (Pena and Shokeir 1974) and the Neu–Laxova syndrome (Neu et al. 1971; Laxova et al. 1972), all syndromes characterized by severe microcephaly associated with ocular, facial and skeletal malformations. **Decreased proliferation** may lead to microcephaly with a normal to thin cortex (primary microcephaly or microcephaly vera, and extreme forms of microcephaly with a simplified gyral pattern), microlissencephaly (extreme microcephaly with thick

neocortex; Barkovich et al. 1998) and microcephaly with polymicrogyria or other cortical dysplasias. Examples of extreme microcephaly and microlissencephaly are shown in Clinical Cases 10.3 and 10.4.

Increased proliferation may lead to megalencephaly. Barkovich et al. (2001) mentioned a case of congenital megalencephaly, polymicrogyria and hydrocephalus. **Non-neoplastic malformations secondary to abnormal proliferation** are characterized by the presence of large cells, containing large volumes of cytoplasm (balloon cells). This subgroup includes the cortical hamartomas of the tuberous sclerosis complex, cortical dysplasias with balloon cells (Fig. 10.44a, b) and cases of hemimegalencephaly (Fig. 10.44c). Several **neoplastic malformations** may be associated with a disordered cortex.

Infants presenting with microcephaly, microphthalmia, cataract and joint contractures with associated anomalies may fall into three groups (Winter et al. 1981): (1) those with a relatively normal birth weight and progressive postnatal growth deficiency and CNS pathology such as in cerebro-oculo-facio-skeletal (COFS) syndrome; (2) cases of COFS syndrome with a low birth weight who died within the first weeks of life, and more recently described microcephaly cases by Chow et al. (1985, 1987) and Coad et al. (1997); and (3) the highly lethal Neu–Laxova syndrome (Neu et al. 1971; Laxova et al. 1972; Ostrovskaya and Lazjuk 1988). In two siblings (a female and a male neonate), severe microcephaly, bilateral absence of the pyramids, severe hypoplasia of the cerebral peduncles and dysplasia of the inferior olives were found together with microphthalmia, facial malformations and multiple contractures of the extremities (ten Donkelaar et al. 1999; see Case Report). In both cases, the cerebral hemispheres showed a more or less normal, although simplified gyral pattern with the insula incompletely covered by the opercula.

Case Report. Patient 1, a girl, was the second child of a 32-year-old woman, who had presented at 35 weeks of gestation because of intrauterine growth retardation. Her first pregnancy resulted in the term birth, in breech position, of a normal girl, with normal biometry. In the second pregnancy, echo-Doppler flow profiles of the placenta were normal, suggesting a fetal cause of the growth retardation. Only two blood vessels were present in the umbilical cord. Subsequently, hydrops fetalis and polyhydramnios developed, and there seemed to be an abnormal position of the hands and feet. Also, the face appeared to be abnormal with micrognathia and a flat forehead. Amniotic fluid karyotyping revealed a normal 46,XX karyotype. Labour was induced at 39 weeks and 5 days. The child was a girl with a birth weight of 1,965 g (400 g less than the 2.3rd percentile, P2.3), a crown–heel length of 42 cm (4 cm<P2.3) and a head circumference of 27 cm (5 cm<P2.3). Besides severe microcephaly, several dysmorphic features could be observed. The face (Fig. 10.42 a) showed micrognathia, a small tongue and median palatoschisis (compatible with Pierre Robin sequence), low implantation of anteriorly rotated ears, and a broad and prominent nasal bridge with a flat nose. There was microphthalmia and blepharophimosis with antimongoloid scants. The child died 52 min after birth. Additional investigations revealed a negative screening for

congenital infections (toxoplasmosis, rubella, cytomegalovirus, herpes and syphilis), and normal lysosomal enzymes in skin fibroblasts.

During the following year the mother had her third pregnancy. The fetus developed the same abnormalities as the preceding one: growth retardation, polyhydramnios and abnormal position of the hands and feet. Only two blood vessels were present in the umbilical cord. Amniotic fluid karyotyping revealed a normal 46,XY karyotype. Labour was induced at 39 weeks, after which a boy was born, in breech position. Birth weight was 1,915 g (500 g < P2.3), crown–heel length 38 cm (8 cm < P2.3) and head circumference 26 cm (6.5 cm < P2.3). The child had severe microcephaly, microphthalmia, normal slants with telecanthus, a broad and prominent nasal bridge, and blepharophimosis. There was severe micrognathia, with a small tongue and median palatoschisis, and microstomia (Fig. 10.42 b). There was a normal male genital, with both testes in a high scrotal position. Both hands showed Simian creases and ulnar deviation, with flexion of the wrists, extension of the metacarpophalangeal joints and flexion of the proximal and distal interphalangeal joints (Fig. 10.42 c). The joints of the extremities showed multiple contractures. The child died 42 min after birth. As for the girl, additional investigations revealed no evidence for congenital infections and normal lysosomal enzymes in skin fibroblasts.

At autopsy, the brains were severely microcephalic (64 and 58.5 g, respectively; normal for body weight 250±60 g). The spinal cord, brain stem and cerebellum were relatively spared. In both cases, the cerebral hemispheres showed a more or less normal gyral pattern with the insula incompletely covered by the opercula (Fig. 10.42 d), and a during autopsy artificially torn but otherwise intact corpus callosum. Macroscopically, the cerebral peduncles showed severe hypoplasia and the pyramids were completely absent, with relatively large olives reaching the midline (Fig. 10.42 e). Microscopically, the corticospinal tracts in the brain stem and spinal cord were severely hypoplastic or absent. In the midbrain, the cerebral peduncles were reduced to a small strip ventral to the well-developed substantia nigra. In the pons, 'crowding' of the pontine islands of grey matter was found. In the medulla, the inferior olivary nuclei abutted the ventral paramedian surface of the brain stem, covered only by a small fibre layer and the arcuate nuclei (Fig. 6.36 a). The cerebellum showed a normal neonatal structure with a still prominent external granular layer and a normal vermis. In case 2, the dentate nucleus was dysplastic and on one side contained an additional, lateral nucleus. In the spinal cord, the lateral and anterior corticospinal tracts could not be found, whereas the dorsal columns were well developed and
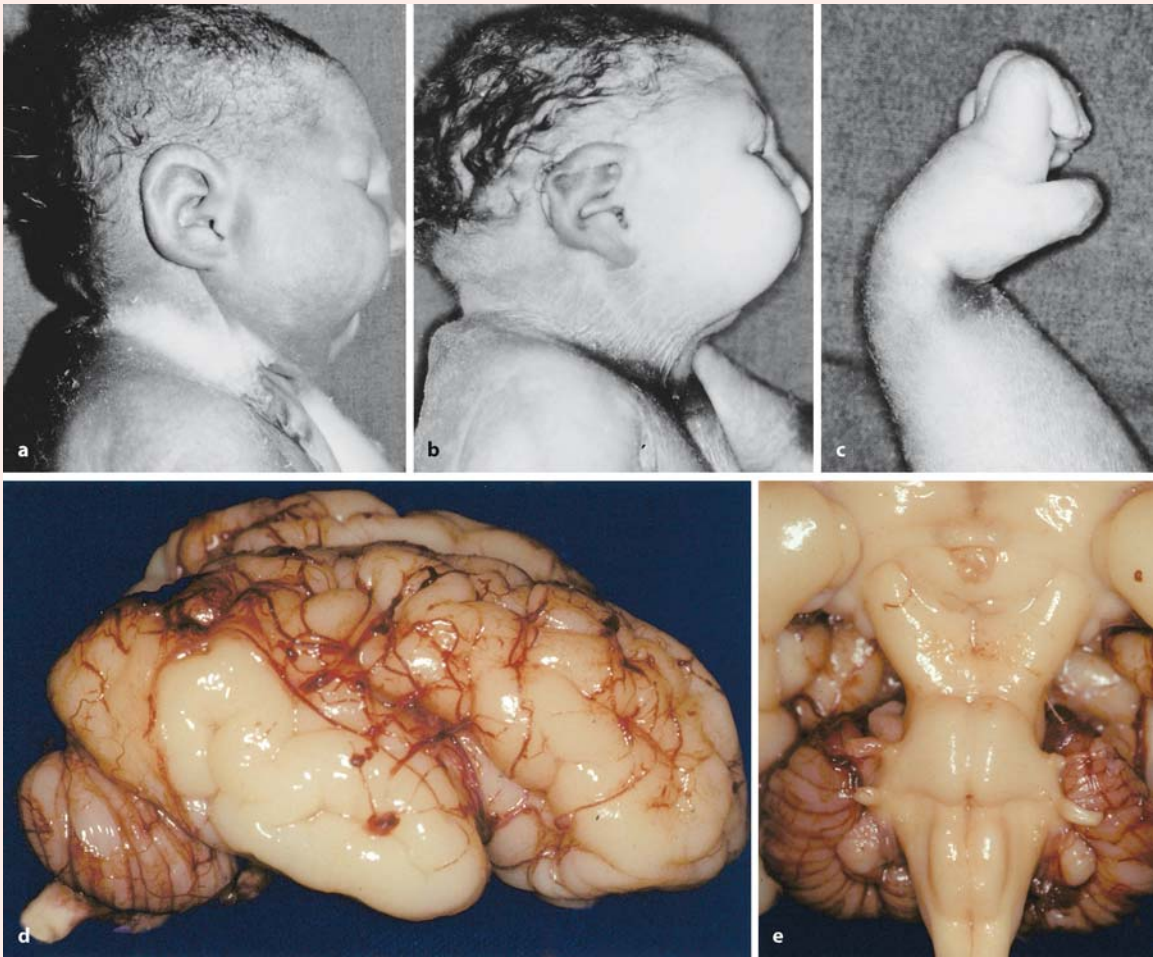
Fig. 10.42 Extreme microcephaly in a case of severe, non-X-linked congenital microcephaly with absence of the pyramidal tracts in two siblings.: **a**, **b** Lateral facial appearance of cases 1 and 2. Note the sloping forehead and micrognathia. **c** Congenital contracture of the hand and ichthyosis-like skin in case 2, with extension of the metacarpal, and flexion of the proximal and distal interphalangeal joints. **d**, **e** Lateral and ventral views of the brain in case 2. Note the absence of the pyramids, the medial position of the inferior olives, the small pons and the hypoplastic cerebral peduncles. (From ten Donkelaar et al. 1999, with permission)

the dorsal horns were displaced to a more lateral position (Fig. 6.34d). In the forebrain, no gross malformations were observed in the diencephalon. The basal ganglia were small but present, although the globus pallidus was difficult to localize. The hippocampal formation was present, but not completely folded inwards. In case 1, oedematous changes were found in the normally structured cerebral cortex. In case 2, some cortical dysgenesis was observed. The parieto-occipital cortex focally showed polymicrogyria with fused molecular zones. Ophthalmological examination of the eyes of the youngest of the two siblings showed clear microcornea, normal anterior chambers, miosis of pupils and mature congenital cataracts of both eyes. Microscopically, the lens contained focal calcium deposits, but the rest of the eye (including the retina) showed a normal architecture. These two cases can be characterized as a rapidly fatal, familial syndrome, probably transmitted as an autosomal recessive trait.

References

Chow CW, Halliday JL, Anderson RM, Danks DM, Fortune DW (1985) Congenital absence of the pyramids and its significance in genetic diseases. Acta Neuropathol (Berl) 65:313–317

Chow CW, Anderson RM, Kenny GT (1987) Neuropathology in cerebral lactic acidosis. Acta Neuropathol (Berl) 74:393–396

Coad JE, Angel C, Pierpont MEM, Gorlin RJ, Anderson ML (1997) Microcephaly with agenesis of corticospinal tracts and arthrogryposis, hypospadias, single umbilical artery, hypertelorism, and renal and adrenal hypoplasia – previously undescribed syndrome. Am J Med Genet 71:458–462

Laxova R, Ohara PT, Timothy JAD (1972) A further example of a lethal autosomal recessive condition in sibs. J Ment Defic Res 16:139–143

Neu RL, Kajii T, Gardner LI, Nagyfy SF, King S (1971) A lethal syndrome of microcephaly with multiple congenital anomalies in three siblings. Pediatrics 47:610–612

Ostrovskaya TI, Lazjuk GI (1988) Cerebral abnormalities in the Neu-Laxova syndrome. Am J Med Genet 30:747–756

ten Donkelaar HJ, Wesseling P, Semmekrot BA, Liem KD, Tuerlings J, Cruysberg JRM, de Wit PEJ (1999) Severe, non X-linked congenital microcephaly with absence of the pyramidal tracts in two siblings. Acta Neuropathol (Berl) 98:203–211

Winter RM, Donnai D, d'A Crawfurd M (1981) Syndromes of microcephaly, microphthalmia, cataracts, and joint contractures. J Med Genet 18:129–133

Clinical Case 10.4
Microlissencephaly

Case Report. The first child of unrelated parents was born spontaneously after terminal intrauterine death at 39 weeks of gestation. The boy was small with a birth weight of 765 g (less than P2.3), a crown–heel length of 34 cm, and presented with a small flat head, many flexion contractures of all limbs, severe scoliosis and palatoschisis. The lungs were hypoplastic (6.7 g; normal 50 g), the bowels were malrotated and the kidneys and renal arteries were completely absent. The brain was extremely small (11.5 g) and its length was only 2.8 cm. Especially the frontal lobes were extremely underdeveloped (Fig. 10.43 a). Both cerebral hemispheres had a smooth surface. The corpus callosum was absent, but a bundle of Probst was not found. There was some layering of the cortex on the convexity of the brain, although the normal six layers could not be observed (Fig. 10.43 b). In the temporobasal and occipitobasal cortex, no layering of the cortex whatsoever was present, and the cortex and leptomeninges were not clearly separated. Instead, pseudoglomerular vascular formations were intermingled with noduli of neurons, some of which were binuclear, and glial proliferations (Fig. 10.43 c, d). The normal layering of the hippocampus was absent. The cerebellum was small, but proportionate to the rest of the brain. The cerebellar cortex was rather prematurely formed with relatively many Purkinje cells. The inferior olivary nucleus had an abnormal, plump C-form instead of its normal gyrification.

The second child of this family was a girl. Ultrasound examination revealed oligohydramnios and microcephaly. Abortion was induced at 17 weeks of gestation. The child had a normal weight (100 g), normal extremities, a short and flat forehead, hypertelorism, a wide mouth and a closed palate. There was hygroma colli. Small dysplastic kidneys with absent ureters and bladder were found. Brain weight was only 7 g. Like in the first child, the frontal part of the hemispheres was underdeveloped. No olfactory bulbs were present. The brain was smooth, which is normal at this stage of development. The corpus callosum was absent. The cortex showed a normal layering without pseudoglomerular formations. Binuclear neurons were found in the basal ganglia and the thalamus. Both children showed a comparable disorder with severe cerebral and renal malformation, suggesting the presence of an autosomal recessive mutation.

Fig. 10.43 Microlissence-phaly: **a** ventral view of the brain with a smooth cerebral cortex; **b** haematoxylin–eosin-stained section of the occipital cortex with irregular layering; **c**, **d** ectopic glial cells in the meninges of the occipital cortex. There is no layering of the cortex. Small and large neurons are intermingled with capillaries. (Courtesy Martin Lammens, Nijmegen)
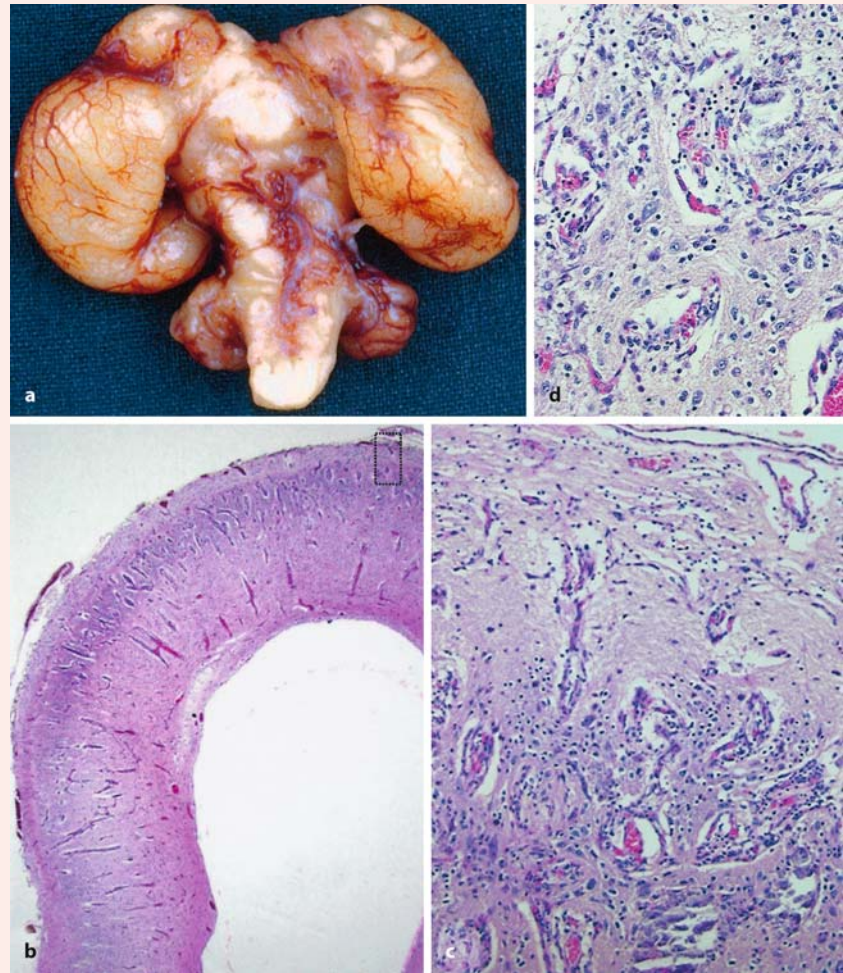
The *tuberous sclerosis complex (TSC)* is a multisystem, autosomal dominant syndrome that most commonly affects the brain, the eyes, the skin, the kidneys and the heart in 1 in 10,000 births (Gomez 1988; Kwiatkowski and Short 1994; Short et al. 1995; Crino and Henske 1999; Clinical Case 10.5). The characteristic brain lesions with a potato-like or root-like (therefore tubers) consistency were first described by Bourneville (1880). TSC lesions are characterized as hamartomas, i.e. benign tumours composed of cellular elements normally present in a tissue. The CNS manifestations of TSC include tubers in the cerebral cortex and subependymal nodules and giant cell astrocytomas protruding into the ventricular system. Tubers are regions of cortical dysplasia that likely result from an aberrant neuronal migration during corticogenesis. They are static lesions, directly related to the major neurological manifestations observed, including epilepsy, mental retardation and autism. These symptoms are highly variable in age of onset and severity. Two *TSC* genes have been identified,

TSC1 and *TSC2* (Consortium ECTS 1993; van Slegtenhorst et al. 1997). Both familial and sporadic TSC cases occur. Approximately 50% of TSC families show genetic linkage to *TSC1* and another 50% to *TSC2* (Povey et al. 1994). The *TSC1* (chromosome 9) and *TSC2* (chromosome 16) genes encode hamartin and tuberin, respectively, which are widely expressed in the brain (Guttmann et al. 2000; Kyin et al. 2001), and may interact as part of a cascade that modulates cellular differentiation, tumour suppression and intracellular signalling (Crino and Henske 1999). Focal cortical dysplasias may represent a 'forme fruste' of tuberous sclerosis (Andermann et al. 1987).

Hemimegalencephaly is a rare hamartomatous malformation of the brain, characterized by extreme asymmetry. It can occur isolated or associated with several neurocutaneous syndromes such as neurofibromatosis (Robain et al. 1988; Robain and Gelot 1996; Flores-Sarnat 2002). MRI examination reveals an overall increased size of the involved hemisphere, ventriculomegaly, colpocephaly (selective dispropor-
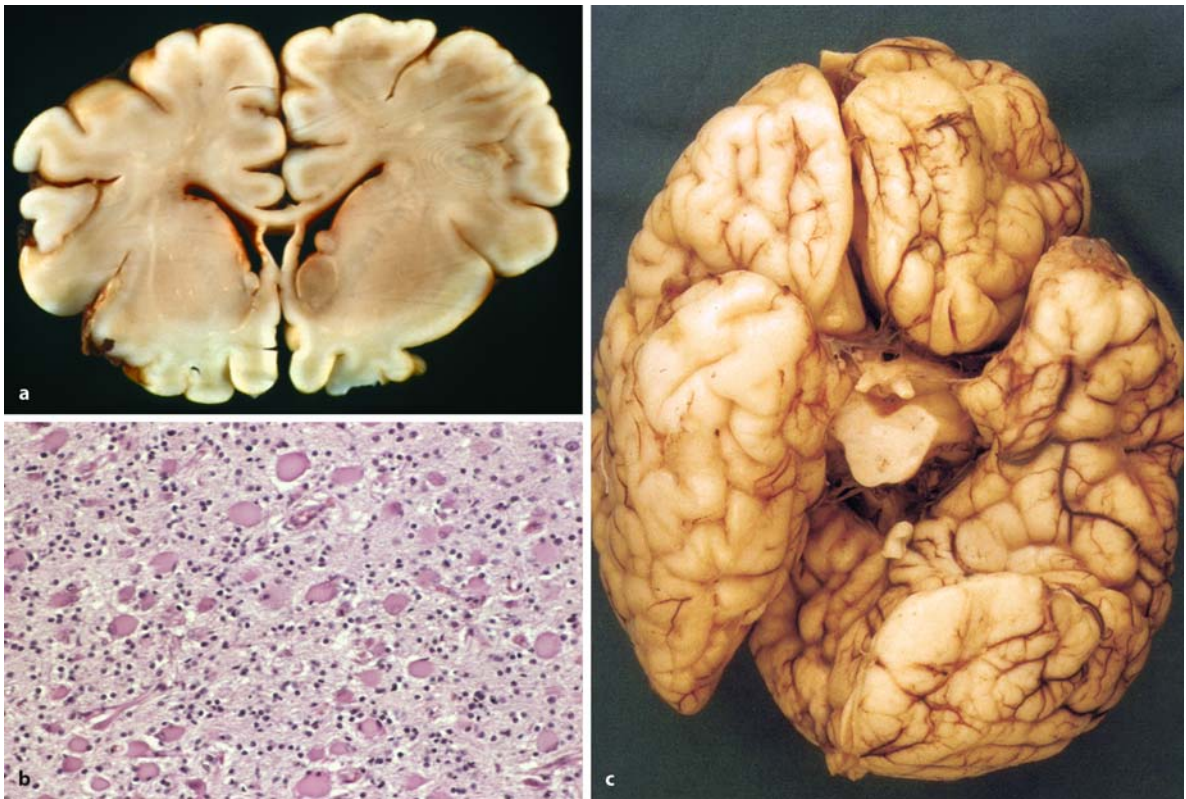
Fig. 10.44 a, **b** Tuberous sclerosis in a 5-day-old girl: tubers along the lateral ventricle (**a**) and large, ballooning cells (**b**) in such a tuber, and **c** ventral view of a hemimegalencephalic, male neonatal brain (**a**, **b** courtesy Akira Hori, Toyohashi; **c** courtesy Pieter Wesseling, Nijmegen).

Clinical Case 10.5
Tuberous Sclerosis Complex

The ***tuberous sclerosis complex*** (***TSC***) is a multisystem, autosomal dominant syndrome that usually affects the brain, eye, skin, kidneys and heart in 1 in 10,000 births (Short et al. 1995; Roach et al. 1998; Crino and Henske 1999). The CNS lesions of TSC include tubers in the cerebral cortex and subependymal nodules and subependymal giant cell astrocytomas along the ventricular system (Fig. 10.41a, b). The subependymal nodules extend into the ventricles and are asymptomatic. If these nodules enlarge and cause hydrocephalus, they are referred to as subependymal giant cell astrocytomas. Tubers are regions of cortical dysplasia most likely due to aberrant neuronal migration during corticogenesis, and are static lesions directly related to the neuropsychiatric manifestations of TSC such as epilepsy, mental retardation and autism. These symptoms are highly variable in age of onset and severity. The diagnosis of TSC should be considered in paediatric and adult patients with epilepsy, mental retardation or autism.

Case Report. The first pregnancy of a 26-year-old mother was complicated by the development of polyhydramnios around 27 weeks of gestation. Ultrasound examination showed an enlarged heart and hardly developed lungs. After a few days intrauterine death of the fetus was recognized. A boy with a body weight of 1,920 g and a crown–heel length of 38.5 cm was born spontaneously. At autopsy, the weight was 1,630 g, the difference of 300 g being due to loss of fluid from the polyhydramnios. Although rather low, weight and length were in line with those expected for 28 weeks of gestation. The heart weighed 47 g (normal 10 g), the lungs 16.4 g (normal 27 g), and the liver and spleen were strongly congested and enlarged. The strongly enlarged heart showed a large protrusion at its apex (Fig. 10.45a). On cross section, most of the volume of the heart was

Fig. 10.45 Tuberous sclerosis in a male fetus of 28 gestational weeks: **a** strongly enlarged heart with an apical protrusion; **b** irregular and angulated contours of the cerebral cortex; **c**, **d** coarse glial hyperplasia in haematoxylin–eosin-stained (**c**) and GFAP-stained (**d**) sections of the cerebral cortex (kindly provided by Gerard van Noort, Enschede)

taken by a large tumour of about 4 cm in diameter, arising from the ventricular septum. Only at the periphery a thin layer of more or less normal myocard was present. Microscopically, the tumour was identified as a rhabdomyoma. Brain weight was 165 g, in line with the gestational age. The gyral pattern of the cerebrum may be somewhat more developed for that age. The 'contours' of the gyri were angulated and irregular (Fig. 10.45b). After sectioning, some brain areas with a rather vast consistency could be palpated cortically. Such areas were also found along the ventricular system. Microscopically, the normal cortical lamination was replaced by a coarse glial hyperplasia with astrocyte-like cells. There were also large abnormal cells, some with two or more nuclei. With glial fibrillary acidic protein staining the so-called 'sheaf of wheat' configuration was prominent (Fig. 10.45 c, d). Periventricularly, large cells characteristic for tuberous sclerosis were present.

This case was kindly provided by Gerard van Noort (Laboratory for Pathology East-Netherlands, Enschede, The Netherlands).

References

Crino P, Henske EP (1999) New developments in the neurobiology of the tuberous sclerosis complex. Neurology 53:1384–1390

Roach ES, Gomez MR, Northrup H (1998) Tuberous sclerosis complex consensus conference: Revised clinical diagnostic criteria. J Child Neurol 13:624–628

Short MP, Richardson EP, Haines J, Kwiatkowski DJ (1995) Clinical, neuropathological, and genetic aspects of the tuberous sclerosis complex. Brain Pathol 5:173–179

Hemimegalencephaly may occur isolated or as part of neurocutaneous disorders (Flores-Sarnat 2002). It is a major but rare hamartomatous congenital malformation of the brain, remarkable for the often extreme asymmetry of the brain. An isolated case as well as one due to neurofibromatosis will be discussed (see Case Report).

Case Report. The first, isolated case concerns a girl, the first child of non-consanguineous healthy parents. Pregnancy and birth were normal. Three days after birth, asymmetric tonic convulsions

occurred. There was no fever or sepsis. No metabolic abnormalities were found and the CSF was normal. On examination, megalocephaly, hypotonia and a mild asymmetric posture were observed. Ultrasound examination revealed a dilated right lateral ventricle. The EEG showed a normal pattern over the left hemisphere, but theta–delta waves and epileptic discharges over the right hemisphere (Fig. 10.63). The unilateral hydrocephalus was treated by a ventriculo-peritoneal drain (Fig. 10.46 b). MRI at the age of 6 months revealed an undifferentiated fetal aspect of the cerebral cortex with heterotopia, lack of myelination of the right hemisphere, and partial pachygyria and poor myelination for that age of the left hemisphere (Fig. 10.46 a, b). Callosotomy at the age of 6 months resulted in a reduction of seizure frequency,
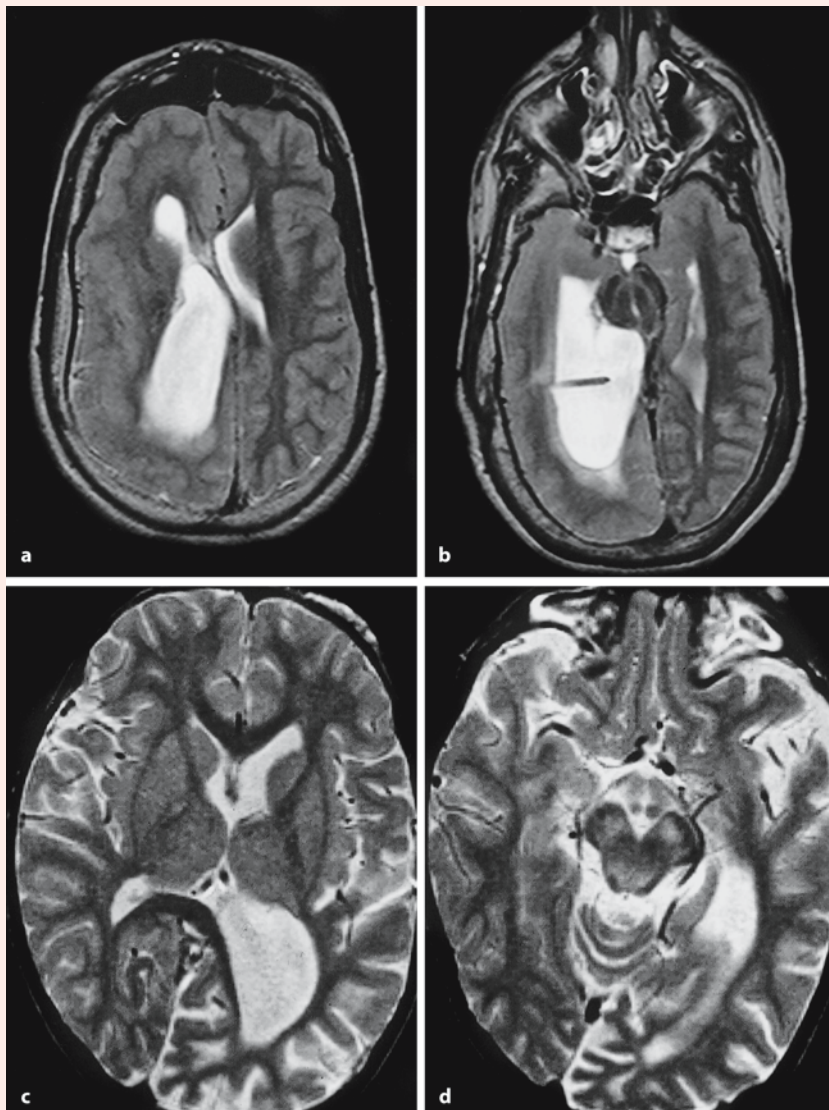
Fig. 10.46 Axial MRI showing hemimegalencephaly in two cases: **a, b** a case of non-familiar megalocephaly with a unilateral smooth cortex, an enlarged lateral ventricle and heterotopia; state after callosotomy to relieve seizures; **c, d** a case of neurofibromatosis with a unilaterally enlarged lateral ventricle and multiple hamartomas in the basal ganglia and brain stem (courtesy Willy Renier, Nijmegen)

but not in seizure freedom. At the age of 1 year, she was severely retarded, had uncontrolled movements and intractable tonic seizures weekly. This condition persisted during childhood. A spontaneous amelioration of the epilepsy occurred at puberty. At the age of 18 years, she could make non-verbal contact. Her epilepsy was stable with one tonic–clonic seizure a month, although continuous spike-wave discharges over the right frontocentral region remained present on the EEG.

The second hemimegalencephalic case concerns another girl, born after an uncomplicated pregnancy and delivery, who presented with bilateral congenital glaucoma. Her father had neurofibromatosis. Within a few months, the child also developed café-au-lait spots. During the following years, other skin lesions characteristic for neurofibromatosis appeared, such as freckling and plexiform neurofibromas. At the age of 5 years, an unexpected accelerated growth of the occipitofrontal circumference was noted. Photopho-

bia and a horizontal nystagmus were present. MRI revealed an asymmetric brain (Fig. 10.46 c, d), hypoplasia of the sphenoid, bitemporal encephaloceles, multiple hamartomas in subcortical structures such as the basal ganglia, the midbrain and the dentate nuclei, and white matter abnormalities in the centrum semiovale and the brain stem. The optic nerves and the chiasm were not involved and the EEG was normal. At the age of 10 years, cognitive development was subnormal and visual acuity was severely reduced. The right eye was replaced by a prosthesis, whereas vision of the left eye was reduced to 8 %. A cyst was found in the upper part of the mandible.

Reference

Flores-Sarnat L (2002) Hemimegalencephaly: Part 1. Genetic, clinical, and imaging aspects. J Child Neurol 17:373–384

tionate dilatation of the occipital horn of the lateral ventricle) and abnormal gyration. In Clinical Case 10.6, two examples of hemimegalencephaly are shown.

10.7.2   Malformations due to Abnormal Cortical Migration

This rather heterogeneous group of cortical malformations has been much more studied than the other groups of disorders of cortical development. Analysis of spontaneous and engineered mouse mutants (Table 10.1) has given a great impetus to our knowledge of human NMDs. The NMDs can be subdivided into the lissencephaly/SBH spectrum, the cobblestone complex and various forms of heterotopia (Table 10.4), and are characterized by the presence of mental retardation and epilepsy. From a pathogenetic point of view, human NMDs, together with spontaneous and engineered mouse mutants, define at least four distinct steps in cortical neuronal migration (Evrard et al. 1992; Copp and Harding 1999; Gleeson and Walsh 2000; Lammens 2000; Barkovich et al. 2001; Ross and Walsh 2001; Pilz et al. 2002; Figs. 10.47–10.50): (1) disorders at the onset of neuronal migration (nodular heterotopia); (2) disorders of the ongoing process of migration (classic, type 1 lissencephaly, double cortex syndrome); (3) problems in the penetration of the subplate (*reeler* mouse; human lissencephaly with cerebellar hypoplasia, LCH); and (4) disruption of the architecture of the developing cerebral wall, leading to an overmigration

of neurons (cobblestone, type 2 lissencephaly). Neuronal migration also depends on intact peroxisomal function (Janssen et al. 2003). Disorders of peroxisome biosynthesis result in the phenotypes of *Zellweger syndrome* and related syndromes (Clinical Case 3.6).

Disorders at the start of migration result in *nodular heterotopia*. *Bilateral periventricular nodular heterotopia* (*BPNH*) are X-linked disorders, in which cortical neurons are unable to leave their position in the ventricular zone (Fig. 10.41 c, d) owing to the absence of *Filamin 1* (*FLN1*). Boys with BPNH usually die before birth (Dubeau et al. 1995), whereas in normally intelligent girls a large proportion of patients suffer from seizures that begin in the second or third decade of life (Barkovich and Kjos 1992a; Huttenlocher et al. 1994; Raymond et al. 1994; Ekşioğlu et al. 1996; Cho et al. 1999; Poussaint et al. 2000). Linkage analysis mapped BPNH to chromosome Xq28 (Ekşioğlu et al. 1996), and the gene has subsequently been identified as the *FLN1* gene (Fox et al. 1998). The encoded protein, FLN1, is also known as actin-binding protein 280 (Hartwig et al. 1980; Gorlin et al. 1990), which is known to play a critical role in the control of cell shape, migration (Nagano et al. 2004), filapodia formation and chemotaxis. BPNH caused by *FLN1* mutations has a wide clinical spectrum and is caused by different genetic mechanisms, including somatic mosaicism (Leventer and Dobyns 2003; Guerrini et al. 2004). Kakita et al. (2002) studied an autopsy case of a woman with BPNH, due to a novel exon 11 mutation of the *FLN1* gene (Clinical Case 10.7).
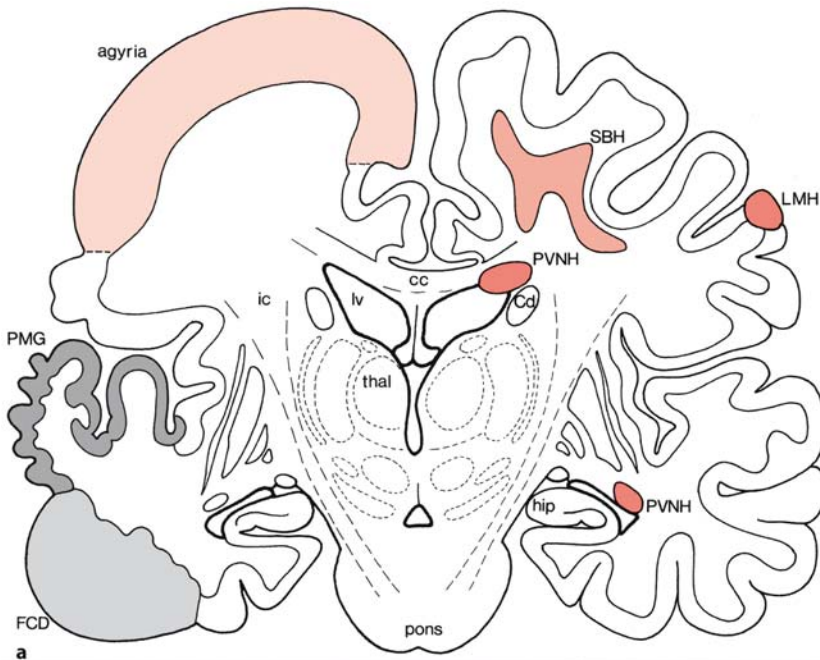
Fig. 10.47　a Overview of neuronal migration disorders and **b** frontal section of a fetal brain with extensive subependymal nodular heterotopia, obtained after spontaneous abortion at about the 16th gestational week. *cc* corpus callosum, *Cd* caudate nucleus, *FCD* focal cortical dysplasia, *hip* hippocampus, *ic* internal capsule, *LMH* leptomeningeal heterotopia, *lv* lateral ventricle, *PMG* polymicrogyria, *PVNH* periventricular nodular heterotopia, *SBH* subcortical band heterotopia, *thal* thalamus. (**a** after Copp and Harding; **b** from the Department of Neuropathology, Medizinische Hochschule Hannover; courtesy Akira Hori)
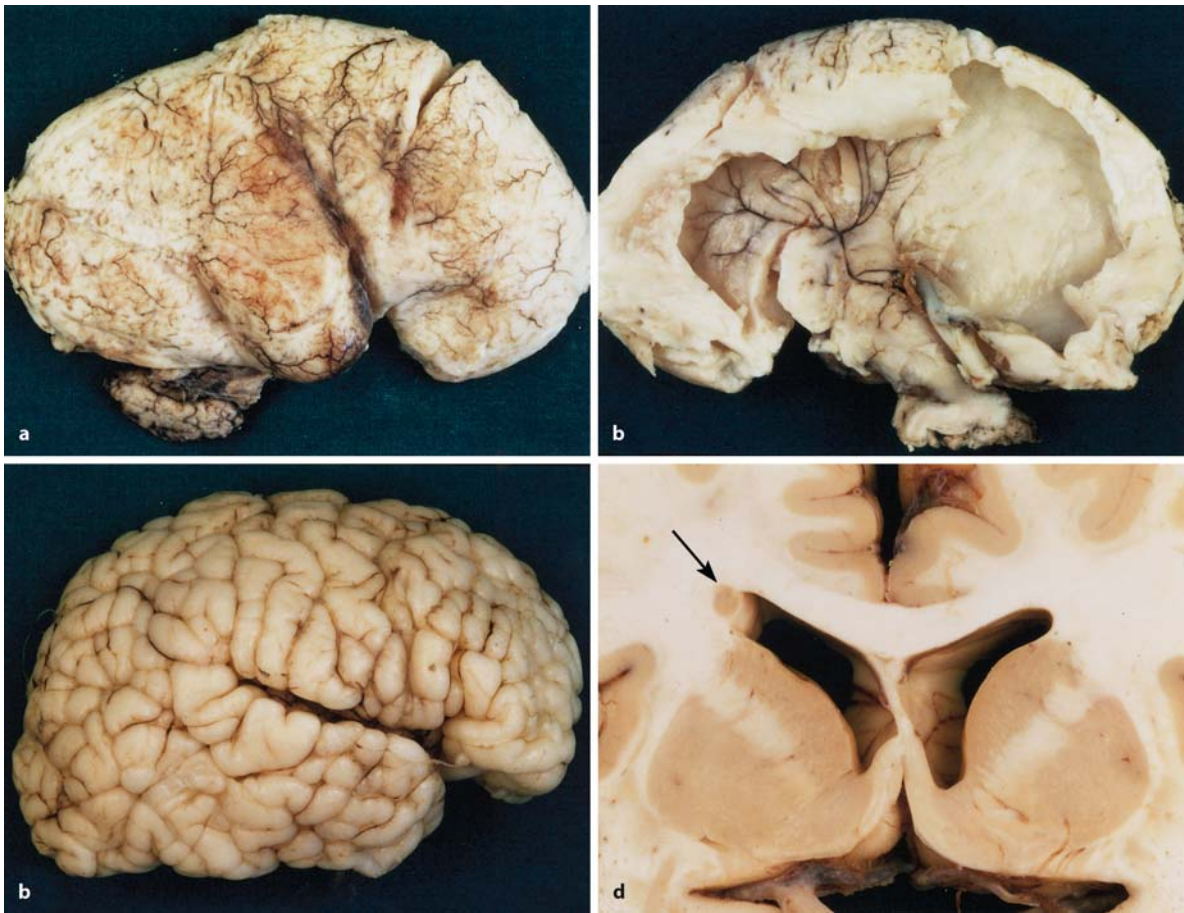
Fig. 10.48 Some examples of neuronal migration disorders: **a**, **b** Walker–Warburg syndrome with diffuse agyria (**a**) and severe hydrocephalus (**b**); **c** polymicrogyria; **d** a small periventricular heterotopia (*arrow*) at the dorsolateral corner of the left lateral ventricle (courtesy Pieter Wesseling, Nijmegen)
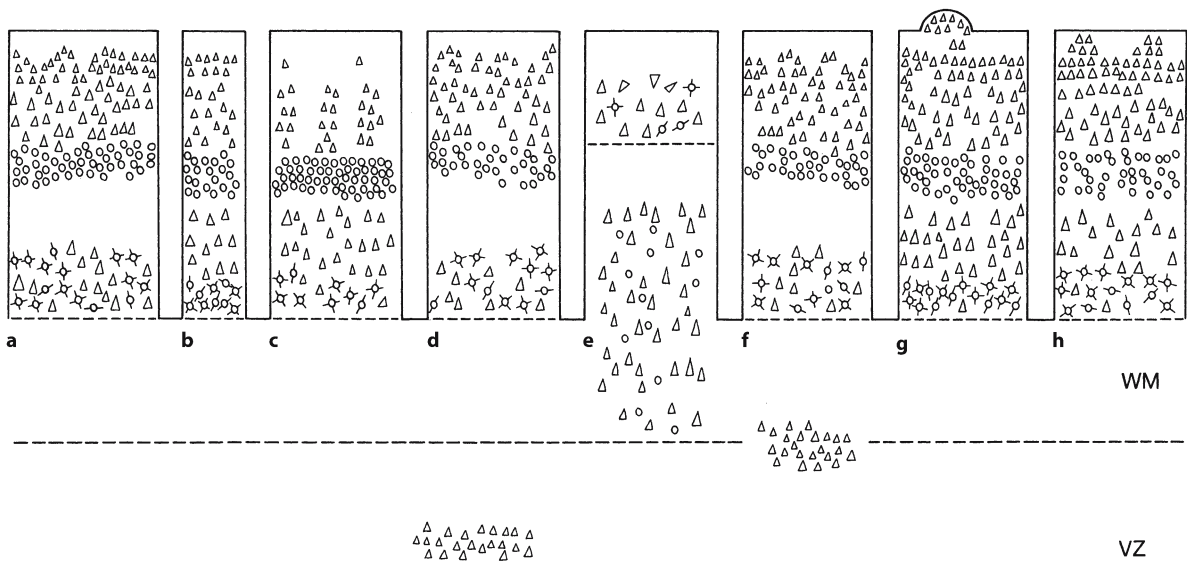
Fig. 10.49 Summary of the cortical organization in various neuronal migration disorders: **a** normal structure; **b** normal structure in a 'radial microbrain'; **c** microcephalia vera; **d** periventricular nodular heterotopia; **e** type I lissencephaly; **f** subcortical band heterotopia; **g** atypical microdysgenesis with leptomeningeal heterotopia; **h** polymicrogyria. *VZ* ventricular zone, *WM* white matter. (After Evrard et al. 1992)

Table 10.4 Classification of the lissencephalies (after Barkovich et al. 2001)

A. Lissencephaly and subcortical band heterotopia spectrum	1. Classic lissencephalies and SBH	a) Miller–Dieker syndrome with deletions of *LIS1* b) Lissencephaly or SBH with *LIS1* mutations c) Lissencephaly or SBH with *DCX* (*XLIS*) mutations d) Other lissencephaly and SBH loci
	2. Lissencephalies with agenesis of the corpus callosum	a) Lissencephaly/agenesis corpus callosum with neonatal death b) Lissencephaly/agenesis corpus callosum c) X-linked lissencephaly/agenesis corpus callosum with abnormal genitalia
	3. LCH	a) LCH identical to classic lissencephaly except moderate vermis hypoplasia b) LCH with anteroposterior gradient, malformed hippocampus and globular cerebellum: with *RELN* mutation or other loci c) LCH with severe brain stem and cerebellar hypoplasia, and neonatal death d) LCH with brain stem and cerebellar hypoplasia e) LCH with abrupt anteroposterior gradient f) LCH with agenesis of corpus callosum, brain stem and cerebellar hypoplasia
	4. Lissencephalies, not otherwise classified	
B. Cobblestone complex	1. Congenital muscular dystrophy syndromes	a) Walker–Warburg syndrome b) Muscle–eye–brain disease c) Fukuyama congenital muscular dystrophy
	2. Syndromes without muscular involvement	a) Cobblestone complex/muscle–eye–brain pattern with normal eyes and muscle b) Cobblestone complex diffuse with normal eyes and muscle

LCH lissencephalies with cerebellar hypoplasia
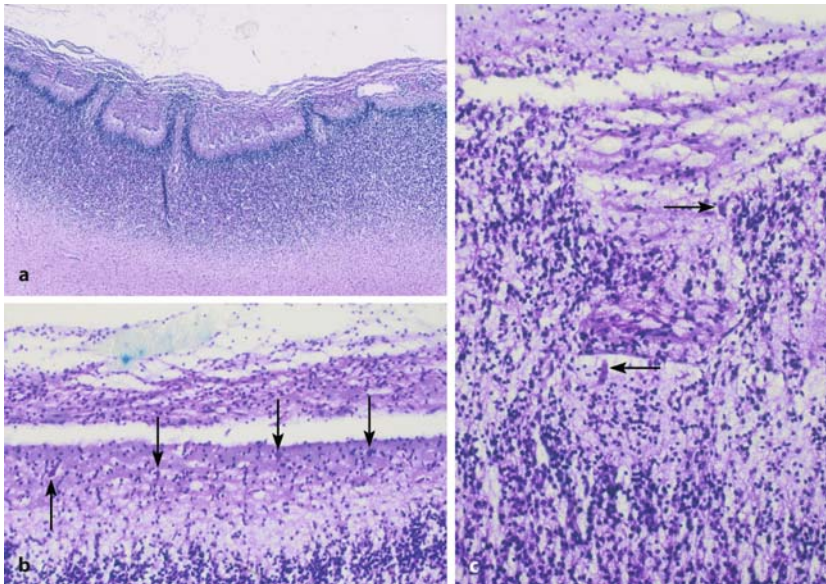
Fig. 10.50 a Gliomesenchymal dysgenesis with 'overshoot' of neuronal migration in a 27-gestational-week-old female fetus. **b** There were sufficient Cajal–Retzius cells (*arrows*) where the cortex appeared intact but they were reduced in number at the site of dysgenesis. **c** The thickening of the leptomeninges is visible at the site of overmigration through the broken glial limiting membrane (reproduced with permission from Hori 1999, *No Shinkei Geka* 27:969–985, copyright 1999, Igaku Shoin Ltd.)

The brain in the ***classic, type 1 lissencephaly*** ('smooth brain') has a macroscopically smooth surface and a thick, usually four-layered cortex (Fig. 10.52). In the ***Miller–Dieker syndrome*** characteristic facial dysmorphology, including microcephaly with bitemporal narrowing, high forehead, prominent occiput, broad nasal bridge, long philtrum and a promi-

nent upper lip, is present. If this striking facial appearance is missing, the term ***isolated lissencephaly sequence*** is used (Dobyns et al. 1984). Patients with the isolated lissencephaly syndrome tend to have a less severe grade of lissencephaly. Classic lissencephaly (Clinical Case 10.8) is characterized by severe mental retardation, epilepsy, feeding problems

Clinical Case 10.7
Bilateral Periventricular Nodular Heterotopia

Bilateral periventricular nodular heterotopia (**BPNH**) is a neuronal migration disorder that is characterized by subependymal grey matter nodules. The X-linked dominant inheritance pattern for BPNH is one of the best characterized syndromes, where the majority of patients are female. Most males with the underlying gene mutations die during early embryogenesis. The phenotype consists of epilepsy with normal or near normal intelligence. Age of seizure onset is variable but is usually in early adulthood (Battaglia et al. 1997). MRI usually shows thick and contiguous nodular heterotopia along the lateral ventricles, the frontal and occipital horns in particular (Fig. 10.41 c, d). Linkage analysis for BPNH mapped this order to Xq28, and the gene was subsequently identified as the *Filamin 1* gene. BPNH may occur in combination with Ehlers–Danlos syndrome, with mental retardation, with gastrointestinal dysmotility, with congenital nephrosis and with frontonasal dysplasia (Leventer and Dobyns 2003). Kakita et al. (2002) described the histopathological features of an autopsy case of BPNH with widespread glomeruloid microvascular anomalies and dysplastic cytoarchitecture in the cerebral cortex, due to a novel exon 11 *Filamin 1* mutation (see Case Report).

Case Report. The patient, a Japanese woman, was born at term with a patent ductus arteriosus that was surgically corrected at the age of 14 years. Her first seizure was noted at 16 years of age and was followed by frequent simple and complex partial seizures, despite treatment with antiepileptic drugs. Brain MRI showed heterotopic grey matter lining the walls of the lateral ventricles (Fig. 10.51a) and hypoplasia of the corpus callosum. She was judged as mildly mentally retarded. At the age of 48 years, she was unfortunately struck by a motorbike and died 3 days later. At autopsy, the fresh brain weighed 1,540 g and showed severe swelling with uncal and tonsillar herniations. Fresh ischemic changes were observed throughout the brain. The cause of her death appeared to be fat embolism. After the usual fixation, the cerebral hemispheres were sectioned coronally, and the brain stem, cerebellum and spinal cord transversely. Periventricular nodules were observed in the cerebrum (Fig. 10.51b). Within the periventricular nodules, well-differentiated pyramidal neurons were randomly oriented. A small proportion of neurons were immunolabelled for calbindin proteins. With the carbocyanine dye 1,1'-dioctadecyl-3,3,3',3'-tetramethylindocarbocyanine perchlorate (DiI) the connectivity of the nodules was studied. Fibres originating in the nodules extended into the surrounding white matter, adjacent nodules and the cerebral cortex. In the cerebral cortex, small closely packed vessels ran in a parallel fashion throughout all of the cortical layers. Astrocyte processes, labelled with an antibody against glial fibrillary acidic protein, invaded these vascular channels. Ultrastructurally, a network of basal lamina-like material lined with endothelial cells was evident. The cytoarchitecture of the cerebral cortex was disturbed, in that the columnar neuronal arrangement was distorted around the malformed vessels. This case represents an example of BPNH manifesting widespread developmental anomalies within the

Fig. 10.51 Bilateral periventricular nodular heterotopia: **a** T1-weighted axial MRI, showing multiple nodules lining the walls of both lateral ventricles; **b** coronal section of the right hemisphere, showing heterotopic nodules at the lateral angle of the lateral ventricle above the caudate nucleus (Klüver–Barrera stain) (from Kakita et al. 2002, with permission; courtesy Akiyoshi Kakita, Niigata)
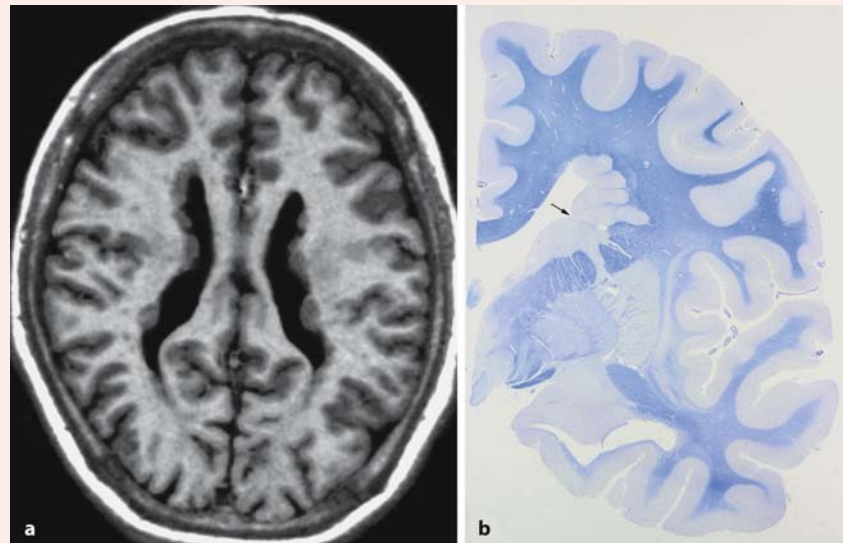
blood vessels and the cortical cytoarchitecture in the cerebrum.

This case was kindly provided by Akiyoshi Kakita (Department of Pathology, Brain Research Institute, Niigata University, Niigata, Japan).

References

Battaglia G, Granata T, Farina L, D'Incerti L, Franceschetti S, Avanzini G (1997) Periventricular nodular heterotopia: Epileptogenic findings. Epilepsia 38:1173–1182

Kakita A, Hayashi S, Moro F, Guerrini R, Ozawa T, Ono K, Kameyama S, Walsh CA, Takahashi H (2002) Bilateral periventricular nodular heterotopia due to filamin 1 gene mutation: Widespread glomeruloid microvascular anomaly and dysplastic cytoarchitecture in the cerebral cortex. Acta Neuropathol (Berl) 104:649–657

Leventer RJ, Dobyns WB (2003) Periventricular gray matter heterotopias: A heterogeneous group of malformations of cortical development. In: Barth PG (ed) Disorders of Neuronal Migration. Mac Keith, London, pp 72–82
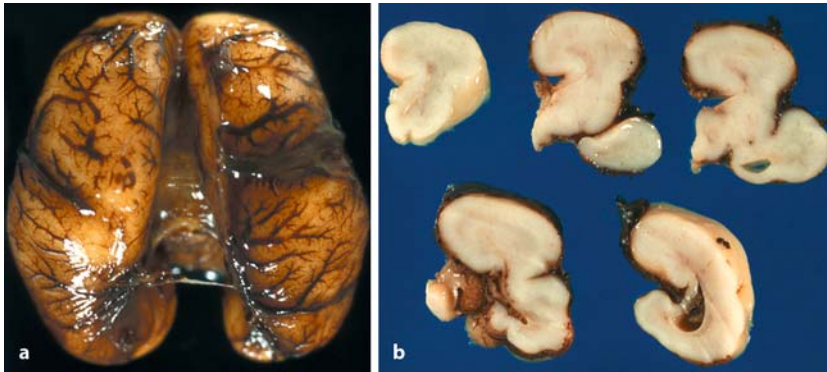
Fig. 10.52 Lissencephaly type I in a male newborn at the 32nd week of gestation. The 31-year-old mother had diabetes mellitus type I but already had a healthy daughter. After birth, the boy showed no movement and CT imaging revealed agyria with agenesis of the corpus callosum. He died on the second day. **a** Dorsal view of the lissencephalic brain. **b** A series of unstained coronal sections. (From the Department of Neuropathology, Medizinische Hochschule Hannover; courtesy Akira Hori)

and a shortened life span. For cases with severe microcephaly the term microlissencephaly is used (Sect. 10.7.1). In most cases of Miller–Dieker syndrome, a deletion of band 17p13.3 on the short arm of chromosome 17 is found, whereas in isolated cases of lissencephaly in 37–44% of cases microdeletions of this band are found (Dobyns and Truwit 1995). Mutations in the *Lissencephaly-1 gene* (*LIS1*) can be detected prenatally using fluorescent in situ hybridization (FISH) and fragment restriction length polymorphism (FRLP) techniques after chorionic villus biopsy sampling (Chap. 3).

A second, *X-linked form* of *lissencephaly* (*XLIS*) is expressed in different ways in males and females (Dobyns et al. 1996, 1999; D'Agostino et al. 2002). In boys, the phenotype is comparable to that of classic lissencephaly, but with a different location: in cases with *LIS1* mutations the malformations are predominantly expressed in the parietal and occipital lobes, whereas in the *XLIS* forms the frontal lobes are more involved (Pilz et al. 1998; Dobyns et al. 1999). Girls with the *XLIS* form of lissencephaly are less retarded

and have less severe epilepsy. They show ***subcortical band heterotopia*** (***SBH***) in which below the cerebral cortex a second cortex is found (Clinical Case 10.9). The causative gene for XLIS, *Doublecortin* (*DCX*), is located on the long arm of the X chromosome (des Portes et al. 1998; Gleeson et al. 1998; Gleeson 2000). The assumed mechanism for this different expression is the normal and random X-inactivation that occurs in females. When the chromosome carrying a mutated copy of *DCX* is inactivated, that neuron will presumably behave normally and migrate to the cortical plate. On the other hand, if the chromosome with a normal copy of *DCX* is inactivated, only the mutant allele will be expressed. Therefore, two populations of neurons exist in the ventricular zone, one expressing a normal copy of *DCX* and giving rise to the cortical plate, the other expressing the mutant *DCX* copy and forming a band of heterotopic neurons in the white matter. Despite its epileptogenic activity, SBH seems to be responsible for part of the functional activity of the brain, as was shown with functional MRI in a 12-year-old boy with epilepsy and SBH

Clinical Case 10.8
Miller–Dieker Syndrome

Miller (1963) and Dieker et al. (1969) described the first cases of lissencephaly occurring in siblings. Pregnancy may be complicated by polyhydramnios or decreased fetal movements. Neurological abnormalities include marked hypotonia, poor feeding, microcephaly and major seizures. The infants gradually become severely spastic. Death usually occurs before the end of the second year of life. In some cases characteristic facial abnormalities are found, including microcephaly with bitemporal narrowing, a high forehead and a prominent occiput, a broad nasal bridge with epicanthic folds, an upturned nose, malpositioned or malformed ears, micrognathia, a long philtrum and a prominent upper lip. There is late eruption of primary teeth and usually prominent palatal ridges can be seen. When this characteristic facial dysmorphology is present, the term Miller–Dieker syndrome is used and, when absent, the term isolated lissencephaly sequence is used (Dobyns et al. 1984). The neuropathology characteristic for Miller–Dieker syndrome will be discussed (see Case Report).

Case Report. The brain in patients with Miller–Dieker syndrome is usually smaller than normal. The cerebral hemispheres are smooth (Fig. 10.53 a). There is a spectrum from complete agyria to the presence of some ten sulci on the whole brain. The frontal and temporal opercula do not develop in the most severe cases. The lateral ventricles are relatively large (colpocephaly). The corpus callosum and the pyramidal tracts are smaller than normal. Microscopical examination shows a thick, usually four-layered cerebral cortex (Fig. 10.53 b). In the classic four-layered cortex a molecular layer overlies a thin superficial neuronal layer, a sparsely populated cellular layer and a thick neuronal layer. The cortex overlies a thin periventricular rim of white matter. In the white matter numerous grey matter heterotopia may be found. In most cases, heterotopia of the inferior olives (Fig. 8.27) and hypoplasia of the pyramidal tracts are associated findings, whereas dentate dysplasia, cerebellar heterotopia and granule cell heterotopia are occasional findings. The basal ganglia are normal.
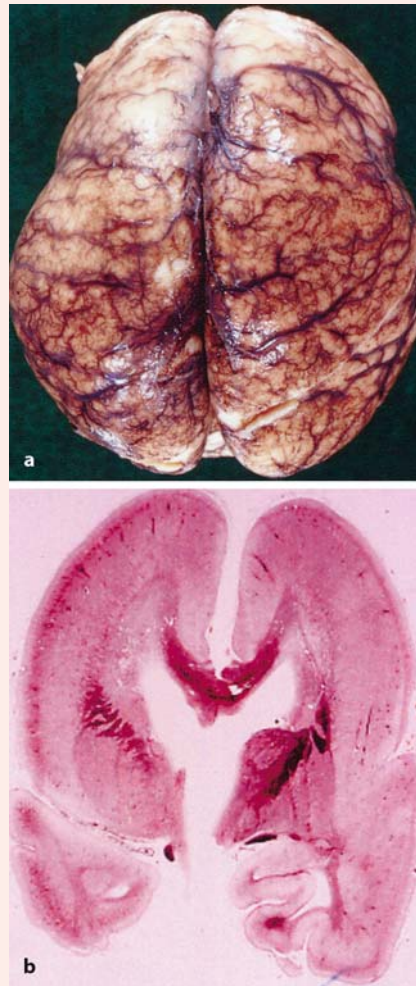
Fig. 10.53 Miller–Dieker case: **a** dorsal view of the lissencephalic brain; **b** coronal section, showing the thick cerebral cortex (courtesy Martin Lammens, Nijmegen)

References

Dieker H, Edwards RH, zu Rhein G, Cou SM, Hartman HA, Opitz JH (1969) The lissencephaly syndrome. Birth Defects Orig Artic Ser 5:53–64
Dobyns WB, Stratton RF, Greenberg F (1984) Syndromes with lissencephaly. I: Miller-Dieker and Norman-Roberts syndromes and isolated lissencephaly. Am J Med Genet 18:509–526
Miller JQ (1963) Lissencephaly in 2 siblings. Neurology 13:841–850

(Pinard et al. 2000). Finger tapping produced activation of a contralateral restricted frontal cortical area, both in the SBH and in the overlying cortex. An interesting rodent model for SBH is the *tish* rat (Lee et al. 1997, 1998; Schottler et al. 1998). A single preplate is formed, after which two cortical plates are formed: one in a normotypic position and a second in a heterotopic position in the intermediate zone. Heterotopic neurons in the *tish* cerebral cortex exhibit similar subcortical connections as normotypic neurons, and establish reciprocal connections with the thalamus. Therefore, primary sensory-motor information is represented in a parallel manner.

Clinical Case 10.9
Subcortical Band Heterotopia

Subcortical laminar or *band heterotopia* (*SBH*) is a neuronal migration disorder in which a band of heterotopic grey matter, a *double cortex*, runs parallel to the normal cerebral cortex separated by a thin layer of white matter (Fig. 10.41e). Most patients are female, and about half of them are heterozygotes for a loss-of-function mutation in the *DCX* (*XLIS*) gene encoded in chromosome Xq22.3-q23. Rare male cases may be caused by a mutation in either the *DCX* or the *LIS1* gene, the latter being encoded in chromosome 17p13.3. In the remaining patients, the causative mutation is unknown. Expression of the *DCX* gene product, doublecortin, is high in fetal CNS neurons but declines postnatally (Mizuguchi et al. 1999). Although it is presumed that the expression of doublecortin is reduced in the brain of many SBH patients, pathological evidence for this is scarce because it is extremely difficult to obtain brain tissue of this rare, non-fatal anomaly in the fetal period when expression of doublecortin is maximal. Mizuguchi et al. (2002) had the opportunity to examine the brain of a female fetus of 22 gestational weeks with SBH without a demonstrable *DCX* gene mutation. In their case, doublecortin immunoreactivity in the cortical plate was comparable to that of age-matched control fetuses, but it was severely reduced in the subcortical grey matter (see Case Report).

Case Report. The fetus was of the first pregnancy of a 27-year-old mother without a family history of neurological disorders. Ultrasound examination showed severe hydrocephalus of the fetus at the 22nd gestational week. Labour was induced and a female fetus with a crown–heel length of 290 mm and a head circumference of 205 mm was delivered. At autopsy, herniation of the pancreas, spleen, part of the left lobe of the liver, small intestine and part of the colon was found into the thorax owing to a large diaphragmatic hernia, resulting in a hypoplastic left lung and shifting of the mediastinum to the right. Neuropathological examination of the brain showed the presence of an undulating band of heterotopic grey matter underlying the entire neocortex, enlarged ventricles, absence of the corpus callosum, hypoplasia of the hippocampal formation, absence of the left caudate nucleus and fusion of the thalami (Fig. 10.54). Expression of doublecortin in the cerebral hemispheres was compared with that of two control fetuses of 26 weeks of gestation. In the SBH case, the cortical plate and ventricular zone showed strong immunoreactivity for doublecortin, which was comparable to that of control fetuses. The subcortical heterotopia, however, showed little immunoreactivity, as did the intermediate zone of controls. Immunostaining for doublecortin in the frontal neocortex of this SBH case and controls is shown in Fig. 10.55. A marked loss of doublecortin was found in neurons comprising the SBH.

This case was kindly provided by Masashi Mizuguchi (Department of Pediatrics, Tokyo University School of Medicine, Japan).
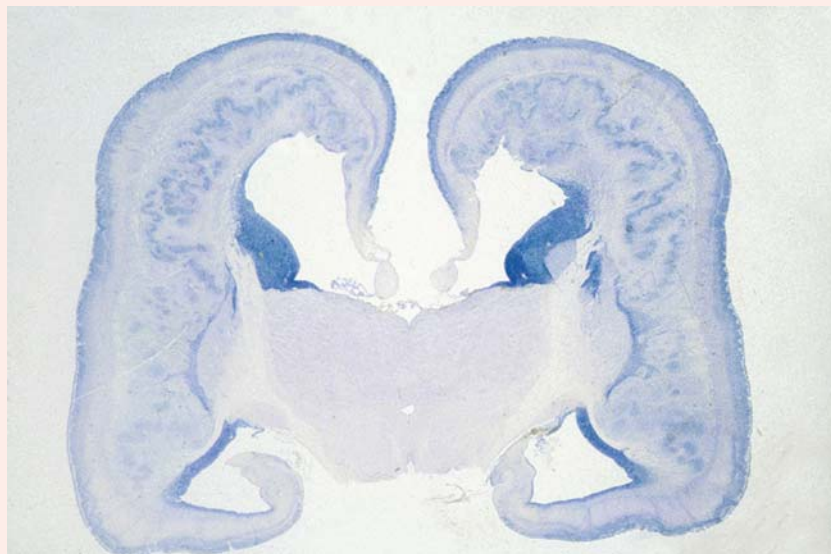
Fig. 10.54 Subcortical band heterotopia found in a 22-gestational-week-old female fetus with severe hydrocephalus. Note the extensive subcortical band of laminar heterotopia ('double cortex') and the absence of the corpus callosum and the left caudate nucleus. (Reproduced with permission from Hori 1999, *No Shinkei Geka* 27:969–985; copyright 1999, Igaku Shoin Ltd.)
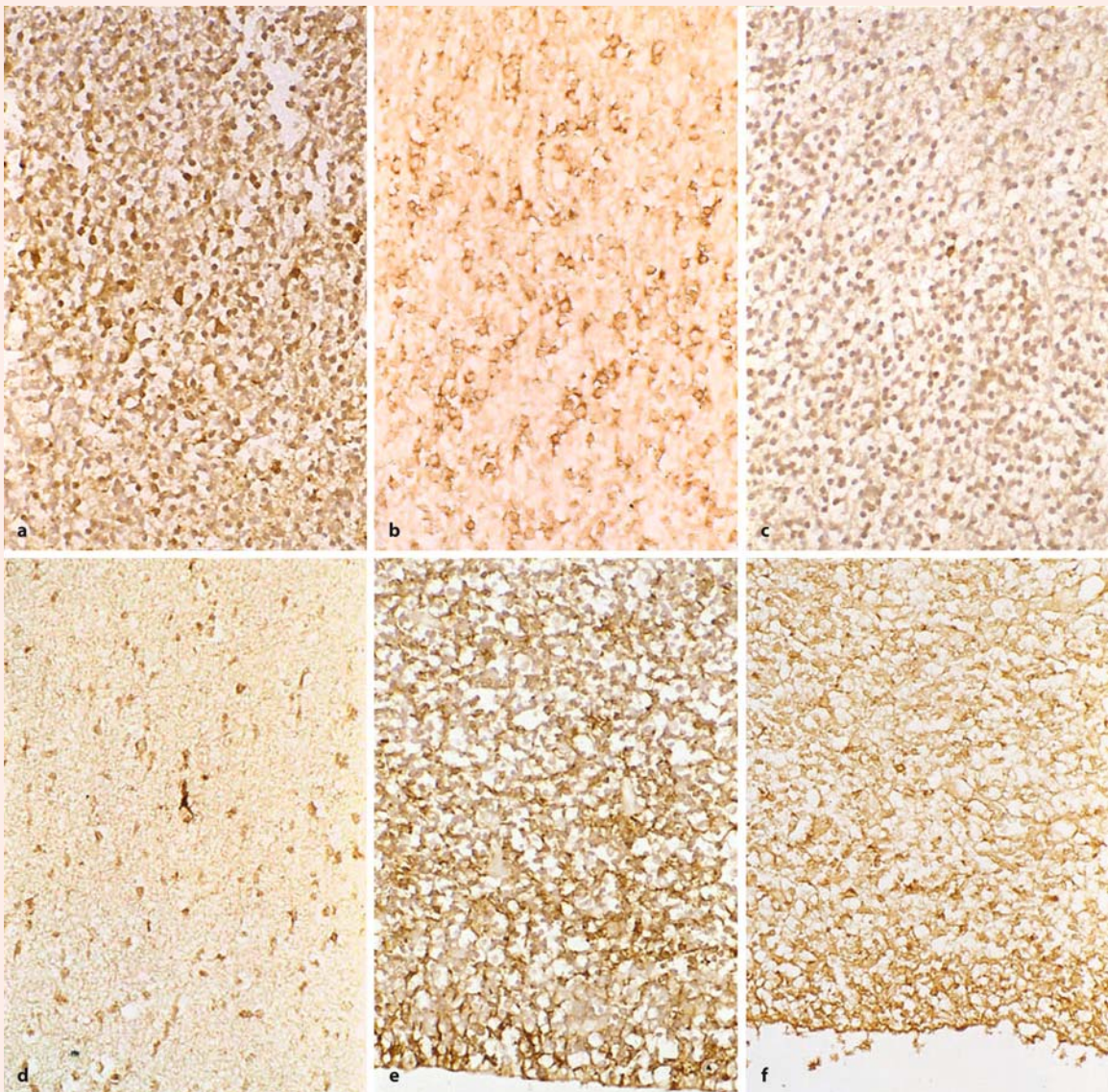
Fig. 10.55 Immunostaining for doublecortin of the frontal cortex of the subcortical band heterotopia case (**a**, **c**, **e**) and of a control fetus (**b**, **d**, **f**) at 26 weeks of gestation: high-power views of the cortical plate (**a**, **b**), heterotopic grey matter (**c**), the intermediate zone (**d**) and the ventricular zone (**e**, **f**). In both the patient and the control case, doublecortin immunoreactivity was positive in many of the cortical neurons (**a**, **b**) and ventricular cells (**e**, **f**). In the heterotopia (**c**) and the intermediate zone (**d**), however, most of the cells were negative except for some rare neurons. (From Mizuguchi et al. 2002, with permission; courtesy Masashi Mizuguchi, Tokyo)

References

Mizuguchi M, Qin J, Yamada M, Ikeda K, Takashima S (1999) High expression of doublecortin and KIAA0369 protein in fetal brain suggests their specific role in neuronal migration. Am J Pathol 155:1713–1721

Mizuguchi M, Takashima S, Ikeda K, Kato M, Hori A (2002) Loss of doublecortin in heterotopic gray matter of a fetus with subcortical laminar heterotopia. Neurology 59:143–144

**Lissencephaly
with Cerebellar Hypoplasia**

Agyria/pachygyria associated with cerebellar hypoplasia has recently been recognized as a heterogeneous group of neuronal migration disorders, described as *lissencephaly with cerebellar hypoplasia* or *LCH* (Barkovich et al. 2001; Ross et al. 2001). It occurs in families and is presumably inherited as an autosomal trait, some traits being due to *RELN* slicing mutations (Hong et al. 2000). Lissencephaly with agenesis of the corpus callosum and rudimentary dysplastic cerebellum may represent a subset of LCH of unknown aetiology, distinct from other types. Miyata et al. (2004) presented a detailed neuropathological description of a 7-day-old neonate, born at 38 gestational weeks, with such a malformation (see Case Report).

Case Report. At 27 weeks of gestation, ultrasound examination of the fetus of the third pregnancy of a 27-year-old mother (one normal baby, two spontaneous abortions) revealed dilatation of the fourth ventricle and absence of the cerebellum. Subsequent ultrasound examination at 30 and 36 weeks of gestation showed no further fetal growth and a Dandy–Walker malformation with hydrocephalus. Delivery was induced at 38 weeks of gestation. The male infant was intubated because of respiratory insufficiency. His birth weight was 2,100 g. The head was microcephalic (head circumference 27 cm) with small anterior and posterior fontanelles and closed sutures. There was mild hypertelorism and low-set ears. The baby moved all extremities with a normal muscle tone but showed diminished tendon reflexes. Chromosomal analysis revealed a normal male karyotype (46,XY), and fluorescent in situ hybridization analysis did not detect deletions in the DiGeorge and Miller–Dieker critical regions. Gene analysis of reelin (*RELN*) was not available. MRI made on the second day of life confirmed the severe brain malformations (Fig. 10.56 a, b). The infant died 7 days after birth.
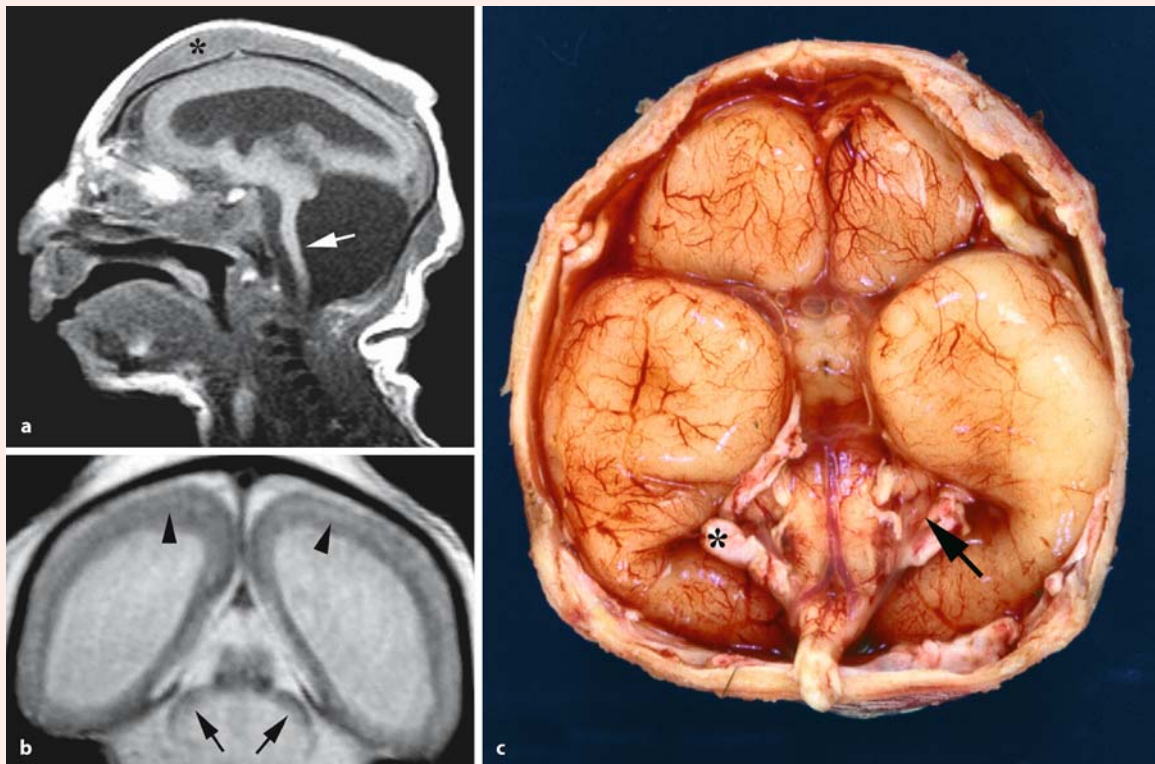
Fig. 10.56 A case of lissencephaly with a rudimentary dysplastic cerebellum: **a** Sagittal T1-weighted MRI, showing complete lack of gyral formation, a thick calvarium (*asterisk*), hypoplastic basal ganglia and thalamus, near total absence of the cerebellum with prominent cystic dilatation of the fourth ventricle and a hypoplastic brain stem (*arrow*). **b** T2-weighted MRI, showing the hypoplastic cerebellum (*arrows*) and a thin continuous zone of hypointensity in what seems to be the subcortical area (*arrowheads*). **c** Ventral view of the brain; note the hypoplastic brain stem and rudimentary cerebellum (*arrow*); the *asterisk* indicates the tentorium cerebelli.

At autopsy, the brain was very small for its gestational age, weighing 80 g after formalin fixation. The brain was severely hydrocephalic and totally agyric (Fig. 10.56 c–g). The corpus callosum was absent and bundles of Probst were not evident. The hippocampal formation was indistinct. The basal ganglia consisted of small masses of tissue that were continuous with the diencephalon. A rudimentary dysplastic cerebellum, dysplastic olivary nuclei and nearly complete absence of corticospinal tracts were also noted. Microscopically, the classic four-layered neocortical structure, characteristic for type 1 lissencephaly, and various types of dysplastic and malformative features were found throughout the brain. Unique features in this case were as follows: (1) bilateral periventricular undulating ribbon-like structures mimicking fused gyri and sulci, associated with aberrant reelin expression; (2) large dysplastic neocortical neurons positive for phosphorylated neurofilament, calbindin-D28K, tuberin, hamartin, doublecortin, LIS1, reelin and Dab1; (3) derangement of radial glial fibres; and (4) disorganized cerebellar cortex and heterotopic grey matter, composed exclusively of granule cells in the cerebellar deep white matter. Miyata et al. (2004) recommended the possible classification of this unique case among the LCH syndromes.

This case was kindly provided by Hajime Miyata (Department of Neuropathology, Institute of Neurological Sciences, Tottori University, Tottori, Japan).

References

Barkovich AJ, Kuzniecky RI, Jackson GD, Guerrini R, Dobyns WB (2001) Classification system for malformations of cortical development: Update 2001. Neurology 57:2168–2178

Hong SE, Shugart YY, Huang DT, Shahwan SA, Grant PE, Hourihane O, Martin ND, Walsh CA (2000) Autosomal recessive lissencephaly with cerebellar hypoplasia is associated with human RELN mutations. Nat Genet 26:93–96

Miyata H, Chute DJ, Fink J, Villablanca P, Vinters HV (2004) Lissencephaly with agenesis of corpus callosum and rudimentary dysplastic cerebellum: A subtype of lissencephaly with cerebellar hypoplasia. Acta Neuropathol (Berl) 107:69–81

Ross ME, Swanson K, Dobyns WB (2001) Lissencephaly with cerebellar hypoplasia (LCH): A heterogeneous group of cortical malformations. Neuropediatrics 32:256–263

Fig. 10.56 d Dorsal view of the brain, showing absence of gyri and sulci. **e**–**g**, Coronal sections of the cerebral hemispheres. Note the hypoplastic pallium with markedly enlarged ventricles, and an unusual undulation of the ependymal surface of the lateral ventricles (**f**). (From Miyata et al. 2004, with permission; courtesy Hajime Miyata, Tottori)

Clinical Case 10.11
Walker–Warburg Syndrome

Walker–Warburg syndrome is an autosomal recessive developmental disorder with a worldwide distribution, characterized by congenital muscular dystrophy, lissencephaly and eye malformations (Dobyns et al. 1989). The brain shows type 2 or cobblestone lissencephaly with absence of the corpus callosum, cerebellar hypoplasia and hydrocephalus. An encephalocele may be present. Two other autosomal recessive syndromes present with a similar combination of abnormalities: Fukuyama-type congenital muscular dystrophy (Clinical Case 10.12) and muscle–eye–brain disease. Through positional cloning, the genes for Walker–Warburg syndrome, Fukuyama-type congenital muscular dystrophy and muscle–eye–brain disease have been identified. Two cases from one family may illustrate the complex malformations found in Walker–Warburg syndrome (see Case Report).

Case Report. The first child of a 26-year-old mother died in utero and was born after 23 weeks of gestation. The immature fetus had a crown–heel length of 30.8 cm, a body weight of 532 g and a head circumference of 20 cm, within the range of 24 weeks of gestation. On X-ray examination, an immature skeleton was found without recognizable malformations. Hydrocephalus with cerebellar hypoplasia and dilatation of the fourth ventricle was present. At first inspection, no structural abnormalities were found in the cerebrum. Chromosomal analysis showed a normal 46,XY karyotype.

One year later, the second child also presented with hydrocephalus around 20 weeks of gestation. Labour was induced, and a male fetus with a body weight of 307 g and a crown–heel length of 25.5 cm was born. At autopsy, hydrocephalus, agyria with malformed cortex of the cerebrum and cerebellum, an encephalocele and strong hypoplasia of the vermis were found. This combination of malformations led to the diagnosis Walker–Warburg syndrome. At the level of the posterior fontanelle, a small protrusion with a diameter of about 1 cm was visible (Fig. 10.57a). After opening this cele, it appeared to be continuous with the posterior fossa. The tentorium and the cerebellum were in a high position. Brain weight was 48.3 g. The brain showed a very strong convex curvature and had a small length (Figs. 10.57 b, c, 10.58 a). The temporal and frontal poles were very close together, whereas the occipital pole was hardly developed. The connection of the occipital encephalocele with the brain was found on the dorsal side of the brain stem between the midbrain and the hindbrain. The hemispheres of the cerebellum, showing some fissures, were present, but a vermis was hardly visible (Fig. 10.57c). The cerebrum was agyric with a cobblestone aspect. After sectioning the brain, no corpus callosum was evident. The lateral ventricles were strongly enlarged, particularly the posterior horns. The cytoarchitecture of the cere-

Fig. 10.57 A fetal case of Walker–Warburg syndrome: **a** posterior view of the fetus, showing the site of the encephalocele; **b** dorsal view of the brain; **c** dorsal view of the brain stem and cerebellum (courtesy Gerard van Noort, Enschede)

bral cortex was strongly malformed throughout (Fig. 10.58 c, d). On its surface, the leptomeninges were thickened with an increase of mesenchymal and glial tissue. Extensive vascularization was found in the superficial part of the cerebral cortex. The tortuous vessels were surrounded by glial tissue. Roughly halfway between the pial surface and the ventricular zone, a border was found as far as which neurons had migrated and formed nodules. The superficial layers of both frontal lobes appeared to be fused. Basal nuclei were present as well as a capsula interna. Around the brain stem, the leptomeninges were also thickened, corresponding with the picture of the cerebral hemispheres. On the cerebellar surface, the thickened leptomeninges filled the space between the folia. A

Purkinje cell layer had not formed. At the level of the medulla, corticospinal tracts could not be clearly recognized. Re-examination of the brain of the first child showed brain malformations that also fit in with Walker–Warburg syndrome.

This case report was kindly provided by Gerard van Noort (Laboratory for Pathology East-Netherlands, Enschede, The Netherlands).

Reference

Dobyns WB, Pagon RA, Armstrong D, Curry CJ, Greenberg F, Grix A, Holmes LB, Laxova R, Michels VV, Robinow M (1989) Diagnostic criteria for Walker-Warburg syndrome. Am J Med Genet 32:195–210
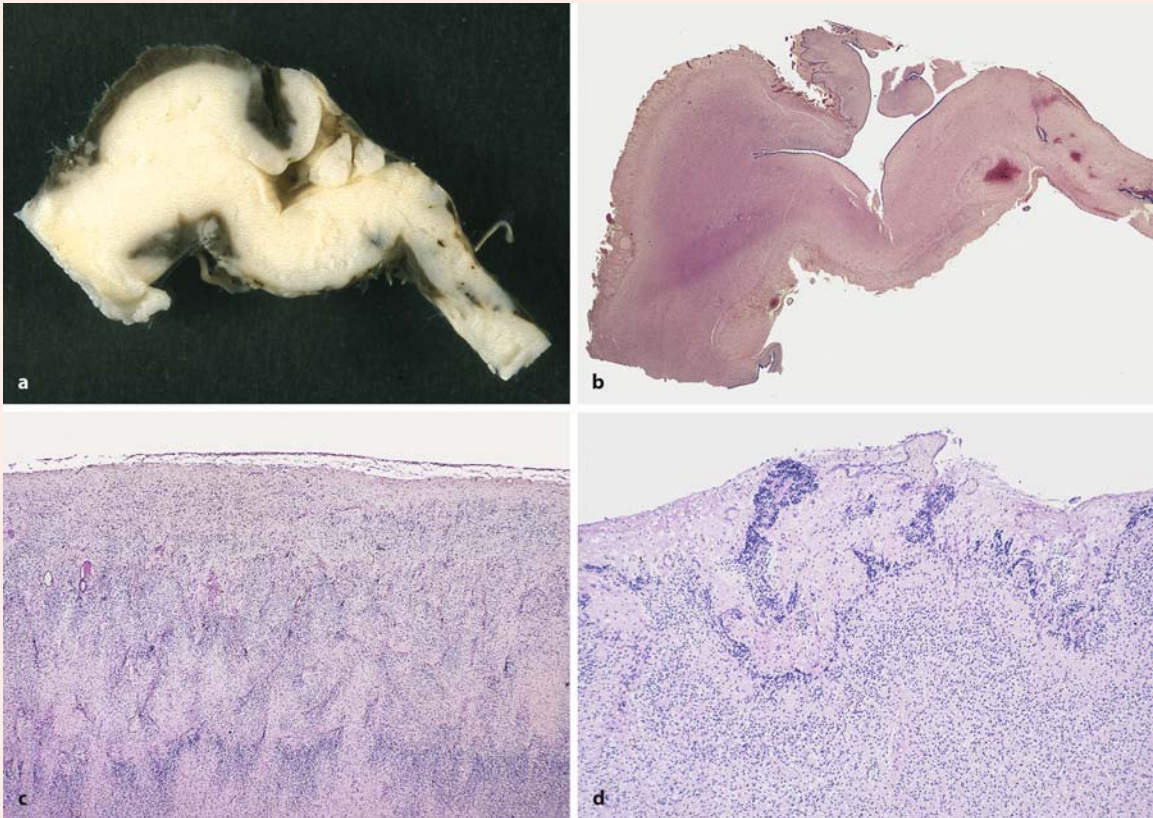
Fig. 10.58 A fetal case of Walker–Warburg syndrome: **a**, **b** unstained and stained sections of the brain, showing the very strong convex curvature; **c** the malformed cytoarchitecture of the cerebral cortex; **d** detail of thickened leptomeninges, covering cobblestone cortex (courtesy Gerard van Noort, Enschede)

Fukuyama-Type Congenital Muscular Dystrophy

Fukuyama-type congenital muscular dystrophy (*FCMD*) is a relatively common autosomal recessive disorder in Japan, and is characterized by congenital muscular dystrophy in combination with cortical dysgenesis and ocular abnormality (Fukuyama et al. 1981). FCMD patients usually survive beyond infancy, and ocular manifestations are rare and usually mild. It is the second most common form of childhood muscular dystrophy in Japan after Duchenne muscular dystrophy. Based on an incidence of 3 in 100,000, one person in about 90 persons could be a heterozygous carrier in Japan (Toda et al. 2003). Patients with FCMD present weakness of facial and limb muscles, and general hypotonia that usually appears before 9 months of age. The joints of affected individuals usually become contractive early and functional disability is more severe than in Duchenne muscular dystrophy. Most FCMD patients are never able to walk. Facial muscle involvement is characteristic. Patients usually become bedridden before they are 10 years old owing to generalized muscle atrophy and joint contracture, and most of them die by 20 years of age (Fukuyama et al. 1981). Severe mental retardation (IQ scores between 30 and 50) is found in all FCMD cases, and seizures occur in nearly half of the cases. Eye malformations include myopia, cataract, abnormal eye movements, a pale optic disc, and retinal lesions and detachment (Osawa et al. 1997). Brain MRI always shows pachygyria of the cerebral cortex, transient T2-weighed high intensity in the white matter and sometimes hypoplasia of the pons and cerebellar cysts (see Case Reports). The high intensity in the white matter is
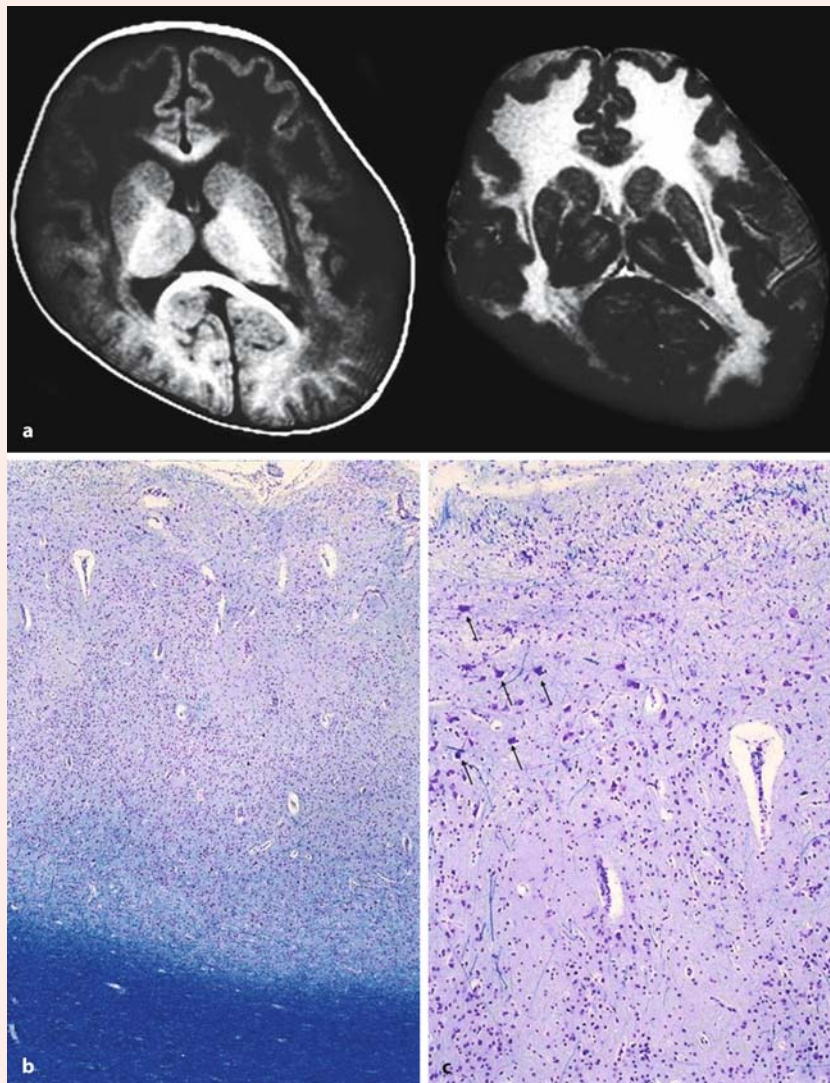
Fig. 10.59 Fukuyama type of congenital muscular dystrophy: **a** MRI showing pachygyria of the cerebral cortex; **b** Klüver–Barrera-stained section of cerebral cortex, showing lack of normal six-layered structure; **c** detail, showing thickened leptomeninges and breaks of glia limitans; *arrows* indicate Cajal–Retzius-like cells (courtesy Mieko Yoshioka, Kobe)

thought to be caused by delayed myelination (Osawa et al. 1997).

Case Report. The most common CNS malformations in FCMD are micropolygyria, pachygyria and agyria of the cerebral cortex (*cobblestone cortex*), in which a normal six-layered structure is lacking (Fig. 10.59). Focal interhemispheric fusion, thickened leptomeninges, mild to moderate ventricular dilatation, and hypoplasia of the corticospinal tracts have also been observed. Microscopically, frequent breaks in the glia limitans and basement membrane are present, leading to overmigration of neurons (Nakano et al. 1996). Disruption of the basal lamina in FCMD muscles has also been found (Ishii et al. 1997). In skeletal muscle, there is a prominent necrotic and regenerating process, with dense fibrosis from early infancy.

A second case, from a 15-year-old boy, is illustrated in Fig. 10.60. Since his birth he was hypotonic and constantly weakly crying. At 7 months of age, a stable head position was present. A muscle biopsy at the age of 1 year revealed FCMD. At 1.5 years of age, he could sit and began to speak some words. At 10 years, he was at his best for mobility; after that age there was continuous regression and he was not able to sit anymore. At the age of 15, he died of cardiac insufficiency due to cardiac hypertrophy, complicated by pneumonia. At autopsy, pneumonia, muscular dystrophy and lissencephaly type 2 were found (Fig. 10.60).

The first case was kindly provided by Mieko Yoshioka (Centre for Child Health and Development, Kobe), the second case by Dr. Sachio Takashima (International University of Health and Welfare, Fukuoka, Japan).

Fig. 10.60 Fukuyama type of congenital muscular dystrophy in a 15-year-old boy: **a** lateral view of the brain showing the cobblestone aspect of the cerebral gyri; **b** coronal section of the brain; note the rather simple gyration and the irregular surface of the cortex, corresponding to the gross appearance of the cobblestone gyri; **c** cortical dysgenesis in the cerebellum; note disorganized molecular and granular cell layers; **d** Klüver–Barrera-stained section of the left cerebral hemisphere, showing pachygyric appearance, a very irregular surface and a simple subcortical white matter organization; **e** detail of cerebral cortex, showing the irregular surface of the molecular layer, gliomesenchymal dysgenesis and sparse and irregularly structured cortical layers (courtesy Sachio Takashima, Fukuoka)
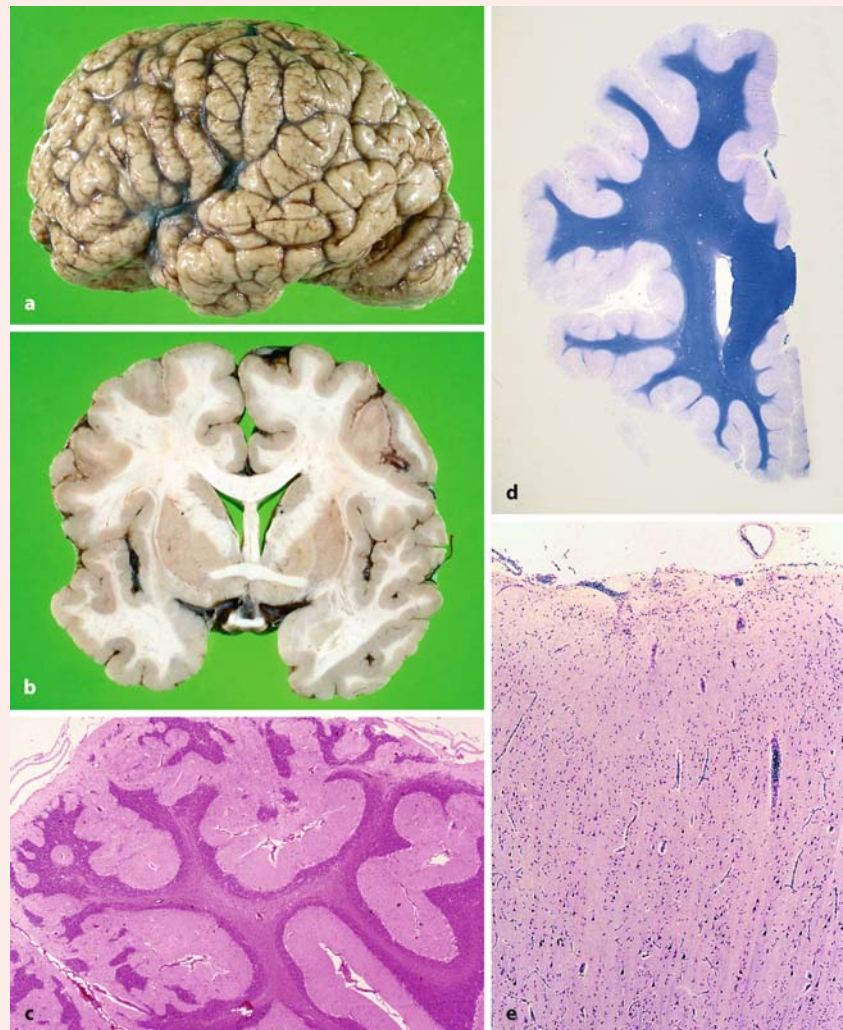
References

Fukuyama Y, Osawa M, Suzuki H (1981) Congenital progressive muscular dystrophy of the Fukuyama type – clinical, genetic and pathological considerations. Brain Dev 3:1–29

Ishii H, Hayashi YK, Nonaka I, Arahata K (1997) Electron microscopic examination of basal lamina in Fukuyama congenital muscle dystrophy. Neuromusc Disord 7:191–197

Nakano I, Funahashi M, Takada K, Toda T (1996) Are breaches in the glia limitans the primary cause of the micropolygyria in Fukuyama-type congenital muscular dystrophy (FCMD)? Pathological study of the cerebral cortex of an FCMD fetus. Acta Neuropathol (Berl) 91:313–321

Osawa M, Sumida S, Suzuki N, Arai Y, Ikenaka H, Murasugi H, Shishikura K, Suzuki H, Saito K, Fukuyama Y (1997) Fukuyama type congenital progressive muscular dystrophy. In: Fukuyama Y, Osawa M, Saito K (eds) Congenital Muscular Dystrophies. Elsevier, Amsterdam, pp 31–68

Toda T, Kobayashi K, Takeda S, Sasaki J, Kurahashi H, Kano H, Tachikawa M, Nagai Y, Taniguchi K, Sunada Y, et al. (2003) Fukuyama-type congenital muscular dystrophy (FCMD) and α-dystroglycanopathy. Cong Anom 43:97–104

Several other syndromes with lissencephaly as a component have been identified (Table 10.4). The best characterized of these is *lissencephaly with cerebellar hypoplasia* (*LCH*; Clinical Case 10.10 on pages 482 and 483), occurring in families and presumably inherited as an autosomal recessive trait (Hourihane et al. 1993; Farah et al. 1997; Kerner et al. 1999; Ross et al. 2001), some of which are due to *RELN* slicing mutations (Hong et al. 2000). Other genes in the *RELN* pathway may be involved, however, since LCH did not occur in a patient with a known *RELN* mutation (Pilz et al. 2002). Several groups of LCH can be defined (Ross et al. 2001; Miyata et al. 2004). On the basis of phenotypic features of 34 affected children, Ross et al. (2001) distinguished six subtypes of LCH. Two were associated with mutations in the *LIS1*, *DCX* and *RELN* genes, respectively. Gene mutations of the other four types remain to be determined. The phenotypic features used included small head circumference, cortical malformations ranging from agyria to a simplified gyral pattern and from near normal cortical thickness to marked thickening of the cortical grey matter. Cerebellar manifestations ranged from midline hypoplasia to diffuse reduction and disturbed foliation.

Type 2 or *cobblestone lissencephaly* is a complex malformation of the brain that consists of cobblestone cortex, abnormal white matter, enlarged ventricles, a small brain stem and a small cerebellum with cerebellar polymicrogyria. The cobblestone cortex is chaotically organized by a combination of agyria, pachygyria and polymicrogyria with a pebbled surface ('cobblestones'), and largely without lamination. The pathogenesis of cobblestone lissencephaly may be overmigration. Disruption of the pial–glial limiting membrane results in cells migrating past the cortical plate and into the leptomeninges (Fig. 10.58). Cobblestone lissencephaly is usually associated with ocular malformations and muscular dystrophy, and occurs in various forms. The *Walker–Warburg syndrome* (Walker 1942; Clinical Case 10.11 on pages 484 and 485) is characterized by diffuse agyria, hydrocephalus, eye malformations and cerebellar anomalies. It is an autosomal recessive disorder with a worldwide distribution (Williams et al. 1984; Dobyns et al. 1985, 1989; Barkovich et al. 1992a). Recently, Beltrán-Valero de Bernabé et al. (2002) found mutations in the *O*-mannosyltransferase gene *POMT1*. Related disorders are muscle–eye–brain disease (MEB), only found in Finland (Santavuori et al. 1989), and Fukuyama-type congenital muscular dystrophy (FCMD; Clinical Case 10.12 on pages 486 and 487), almost restricted to the Japanese (Fukuyama et al. 1981; Saito et al. 2003; Toda et al. 2003). The causative genes for FCMD (*Fukutin*) and MEB (*POMGnT1*) have been cloned (Kobayashi et al. 1998; Yoshida et al. 2001; Toda et al. 2003). In the brain of fetal FCMD patients, decreased expression of fukutin may provoke the disruption of the glia limitans (Yamamoto et al. 2002).

10.7.3 Malformations due to Abnormal Cortical Organization and Late Migration

This group of cortical malformations includes the polymicrogyrias and schizencephalies. Schizencephaly is usually accompanied by polymicrogyria. Barkovich and co-workers (1995, 1999, 2001) suggested that polymicrogyria (Fig. 10.48 c) results from a developmental disorder or injury that occurs towards the end of the period of neuronal migration and the early phase of cortical organization. In addition to the bilateral perisylvian form of Kuzniecky et al. (1993; Guerrini et al. 2000b), several other types have been described, such as a bilateral parieto-occipital type (Guerrini et al. 1997), bilateral frontal polymicrogyria (Guerrini et al. 2000a), and a generalized form (Chang et al. 2004). Polymicrogyria or schizencephaly may also occur in association with other brain malformations or as part of several multiple congenital anomaly–mental retardation syndromes. Polymicrogyria and schizencephaly thus appear to be common malformations of the cerebral cortex.
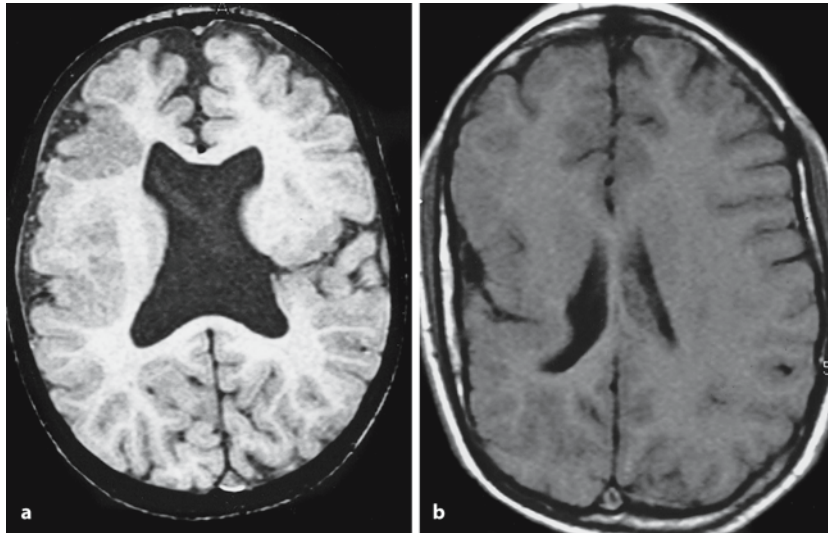
Fig. 10.61 Axial T1-weighted MRI of two cases of schizencephaly. **a** 'Open-lip' schizencephaly in a 3-year-old girl with right-sided hemiparesis since birth; a complete cleft extends from the pial surface to the lateral ventricle of the left hemisphere; the cleft is lined with grey matter. **b** 'Closed-lip' schizencephaly in a 16-year-old adolescent with left-sided hemiparesis, seizures and developmental delay. Irregular grey matter extends from the cortical surface to the lateral ventricle near the central gyrus. The walls of the cleft are apposed to each other. A dimple on the ventricular surface corresponds to the opening of the cleft into the lateral ventricle. (Courtesy Berit Verbist, Leiden)

Schizencephaly represents a cleft, unilateral or bilateral, extending from the pial surface of the cortex to the ventricular surface (Barkovich and Kjos 1992b). The term is used more commonly in neuroradiology (Fig. 10.61) than in neuropathology, where the term porencephaly is frequently used to indicate the absence of cortex where cortex should be (Friede 1989; Norman et al. 1995). Typically, the sides of the cleft are lined with polymicrogyric cortex. Schizencephaly/porencephaly is quite variable and causally heterogeneous. Some cases show an otherwise fairly normal cortex and mild clinical symptoms, usually seizures or cognitive difficulties, whereas in other cases there exists generalized malformation of the cortex with severe mental retardation and seizures (Barkovich and Kjos 1992b). Schizencephaly is classically viewed as a vascular lesion (Friede 1989); however, Brunelli et al. (1996; Granata et al. 1997) observed mutations in the *EMX2* gene in cases with clinically severe schizencephaly. *EMX2* mutations have not been observed so far in other cases of schizencephaly (Barkovich et al. 2001).

10.7.4   Disorders of Cortical Development and Epilepsy

NMDs occur in 20–40% of the refractory cases of epilepsy (Mischel et al. 1995; Sisodiya 2000; Guerrini et al. 2003). Hemimegalencephaly can present as early-onset severe epileptic encephalopathy or as partial epilepsy. Patients with focal cortical dysplasia (Palmini et al. 2004), characterized by focal cortical thickening and a simplified gyral pattern, have drug-resistant, often early-onset epilepsy. In tuberous sclerosis, 60% of patients have epilepsy and about 50% present with infantile spasms (Clinical Case 10.13). Most BPNH patients have partial epilepsy. In lissencephaly, usually severe epilepsy is found. In polymicrogyria, early-onset epileptic encephalopathy is common. Microscopical cortical malformations (microdysgenesis) may also act as a substrate for seizures in some patients with generalized epilepsy (Meencke 2000). The pathogenesis of epilepsy associated with developmental abnormalities in general is poorly understood, but there is extensive evidence for the intrinsic epileptogenicity of such lesions (Palmini et al. 1995). Histological studies of such cases (Battaglia et al. 1996; Spreafico et al. 1998; Ying et al. 1998; Hannan et al. 1999; Crino et al. 2002) showed many abnormalities at various levels of the part of the brain involved, including changes in cell structure, neuronal distribution, a decrease in the number of inhibitory GABAergic local circuit neurons and alterations in glutamate receptor subtype in dysplastic neurons. These studies suggest that a network imbalance of glutamatergic excitation and GABAergic inhibition may be fundamental to epileptogenesis.

Clinical Case 10.13
Neuronal Migration Disorders and Epilepsy

Many disorders of cortical development are associated with severe and often intractable epilepsy (see Case Report).

Case Report. The first case concerns a boy, born after 42 weeks of gestation by induced labour. Pregnancy was complicated by maternal hypertension. After 4 weeks, subtle seizures were observed by the parents, which 1 month later were followed by infantile spasms. The EEG showed a large hypofunctional and epileptogenic region at the right centrotemporal region. Computerized tomography and MRI clearly demonstrated the typical tubers found in the lateral wall of the lateral ventricles in tuberous sclerosis. Moreover, a large piece of abnor-

mal tissue was found around the central sulcus. There were also small tumours in both cardiac ventricles without haemodynamic obstruction and small cysts of the kidney without renal insufficiency. The child developed a mild left-sided hemiparesis, intractable epilepsy (generalized spasms, tonic and atonic seizures, myoclonic seizures, focal and generalized tonic–clonic seizures), severe mental retardation and autistic behaviour. At the age of 10 years, a left-sided intraventricular giant cell astrocytoma was detected. The EEG at that time showed continuously generalized epileptic discharges (Fig. 10.62).

The second case concerns the first girl with hemimegalencephaly discussed in Clinical case 10.6. An asymmetric EEG pattern and more epileptiform discharges over the right hemisphere than over the left hemisphere were found (Fig. 10.63).

The EEGs were made by Yvonne van den Bogaard (Department of Clinical Neurophysiology, Radboud University Nijmegen Medical Centre).

Fig. 10.62 EEG in a case of tuberous sclerosis, showing focal (*circles*) and generalized (*vertical column*) slow-spike and wave discharges (Lennox-like traces) as well as slow-background trace

Fig. 10.63 EEG in a case of hemimegalencephaly, showing asymmetric EEG pattern (*circles*) with higher voltages and more epileptiform discharges over the right (*R*) than over the left (*L*) hemisphere. Background trace is irregular and too slow for age

Some **rodent models** for **epilepsy** will be briefly discussed. Prenatal treatment of rats with methylazoxymethanol resulted in heterotopia in the CA1 subfield of the hippocampus (Chevassus-au-Louis et al. 1998). Heterotopic cells were phenotypically similar to neocortical supragranular neurons and exhibited similar patterns of neurogenesis and migration. They did not express molecular characteristics of CA1 neurons such as the limbic-associated membrane protein. Functional studies suggested that the neocortical heterotopia in CA1 were integrated in both the hippocampal and the neocortical circuitry. Freeze-lesioning of newborn rat neocortex leads to epileptiform activity in the neocortex of adult rats (Luhmann et al. 1998). The dysplastic cortex was characterized by the formation of a small sulcus and a three-to-four-layered architecture. Receptor autoradiography showed an imbalance between excitatory and inhibitory receptors which may cause the hyperexcitability (Zilles et al. 1998). Early GABA-mediated signalling is involved in many aspects of brain development (Ben-Ari 2001, 2002; Owens and Kriegstein 2002). Surprisingly, mice with null mutations in key genes of the GABAergic pathway show relatively few developmental malformations in the CNS. Fetal brains of mice lacking both GABA-synthesizing enzymes, GAD65 and GAD67, have only 0.02% of the normal content of GABA (Ji et al. 1999). These mice die at birth, but they show no obvious structural brain abnormalities. Many GABA-deficient mutant mice and mice with targeted deletion of GABA$_A$ receptor subunits have a lower seizure threshold or spontaneous seizures (Asada et al. 1996; Homanics et al. 1997; Kash et al. 1997), but again no major structural brain malformations were observed. Mice with non-functional GABA$_B$ receptors develop spontaneous epilepsy, hyperalgesia and impaired memory, but their brain morphology appears to be grossly normal (Schuler et al. 2001).

In cases of polymicrogyria and in Ammon's horn sclerosis, the normally disappearing reelin-expressing Cajal–Retzius cells persist (Eriksson et al. 2001; Blümcke et al. 2002; Thom et al. 2002). Microdysgenesis with relatively minor abnormalities such as the presence of neurons in the molecular layer or in the white matter has been found in patients with tempo-

Table 10.5 Various forms of epilepsy occurring in disorders of cortical development (after Porter et al. 2002)

Disorder	Cortical abnormalities	Clinical symptoms	Seizure types	EEG data
Lissencephaly	Smooth brain, lacking gyri and sulci; poorly organized, 4-layered cortex	Mental retardation, motor delay with axial hypotonia, seizures	Infantile spasms, myoclonic seizures, tonic	High amplitude, generalized fast activity
Heterotopia (periventricular, subcortical)	Misplaced collection(s) of neurons and glia; otherwise normal cells	Wide range of cognitive abilities, seizures	Complex partial seizures, generalized tonic–clonic seizures, simple partial seizures, infantile spasms, absences	Unilateral or bilateral sharps or spikes, frequent temporal discharges
Polymicrogyria	Multiple thin small gyri; loss of layer V pyramidal cells	Paresis, mental retardation, seizures	Complex partial seizures, myoclonic seizures, hemimyoclonic seizures, infantile spasms	Sharps and slowing in the region of the polymicrogyria
Cortical dysplasia	Normal, thickened cortex with loss of cortical layers; abnormal, large, immature neurons	Wide range of cognitive abilities, seizures	Complex partial seizures, infantile spasms, generalized tonic–clonic seizures	Focal rhythmic sharp discharges

ral lobe epilepsy (Meencke 2000; Thom et al. 2001). Aberrant activity of inhibitory GABAergic neurons may be associated with epilepsy. In cases of heterotopia in children, Hannan et al. (1999) showed abnormal immaturity of GABA networks within nodules in resected material. This could produce an excess of excitatory over inhibitory neuronal circuitry, thus inducing pathological activity. Moreover, with carbocyanine tracing they identified connections between neurons in different nodules and with other regions of the brain. Such aberrant neural circuits may communicate epileptogenicity in the cerebral cortex (Duchowny et al. 2000). Regional hyperexcitability in certain NMDs may also result from enhanced numbers of glutaminergic excitatory neurons as shown in cortical dysplasias and tuberous sclerosis (Crino et al. 2001, 2002; White et al. 2001). Therefore, there may be important differences in epileptogenesis between the various NMDs (Copp and Harding 1999; Porter et al. 2002; Table 10.5).

Ammon's horn sclerosis is the most common pathological substrate for temporal lobe eiplepsy with a characteristic pattern of loss of pyramidal neurons primarily in CA1 and hilar subfields, granule cell dispersion, cytoskeletal abnormalities in remaining hilar cells and reactive gliosis (Blümcke et al. 1999, 2002; Thom et al. 2002). Thom et al. (2002) studied a series of 183 hippocampectomies from adults with intractable epilepsy, and found hippocampal sclerosis in 90 % of cases, granule cell disorganization or severe dispersion in 40 % of cases and cytoskeletal abnormalities in hilar cells in 55 % of cases. The severity of granule cell disorganization correlated closely with the degree of hippocampal cell loss but not with the age of first seizure. These findings suggest that granule cell disorganization is closely linked with the progression of hippocampal sclerosis rather than a hallmark of impaired hippocampal maturation. In areas of maximal dispersion the number of granule cells was increased, suggesting enhanced neurogenesis of these cells. No correlation was found between the number of reelin-postive and calretinin-positive Cajal–Retzius cells in the molecular layer of the dentate gyrus and the severity of granule cell dispersion. The persistence of Cajal–Retzius cells points towards an early insult and an altered Reelin-signalling pathway (Blümcke et al. 2002).

Cellular pathology of hilar neurons in **Ammon's horn sclerosis** (Clinical Case 10.14) is characterized by altered axonal, dendritic and synaptic morphology (Blümcke et al. 1999). Such changes may develop during cellular reorganization in the epileptogenic hippocampus and will contribute to the development of temporal lobe epilepsy. Sprouting of mossy-fibre axons from dentate granule cells may play part in epileptogenesis (Parent and Lowenstein 1997; Chang and Lowenstein 2003). Newly sprouted mossy fibres from dentate granule cells can synapse on dendrites of neighbouring granule cells, resulting in a recurrent excitatory circuit. They may also sprout on inhibitory GABAergic interneurons. Excitatory interneurons, which normally innervate inhibitory interneurons, may be selectively vulnerable. Moreover, newly formed dentate granule cells may contribute to abnormal circuits.

10.7.5   Vascular Disorders

The vulnerability of the developing human brain to perinatal asphyxia and circulatory disturbances is discussed in Chap. 3. Marín-Padilla (1996, 1997, 1999)

Clinical Case 10.14
Ammon's Horn Sclerosis

Case Report. This boy was the second child of unrelated parents. The first child, a girl, was completely normal. The boy was born after an uneventful pregnancy. During the first year, psychomotor retardation became evident. From the first months generalized epilepsy was observed, and was difficult to control. MRI showed bilateral cortical dysgenesis. Because of the progressive deteriorating neurological status a metabolic disease was suspected. Intensive metabolic screening could not demonstrate any major underlying metabolic disorder. At 2 years of age, he was again admitted to the hospital because of status epilepticus. He developed an enterovirus infection. There was an episode of reversible liver failure. MRI revealed important ischemic cortical brain lesions. He finally died of acute bronchopneumonia.

At autopsy, no major congenital malformations were found apart from a slight syndactyly of the second and third toes of both feet. The brain weighed 1,070 g. There was bilateral polymicrogyria in the insular and occipital regions (Fig. 10.64). Furthermore, there was pseudolaminar necrosis of the frontal cortex. The hippocampus showed important gliosis and
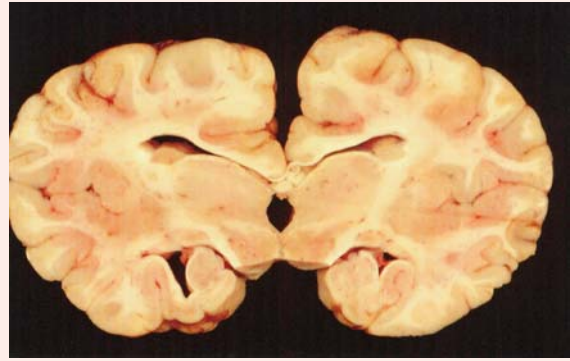
Fig. 10.64 Polymicrogyria in the insular region in a case of Ammon's horn sclerosis. Note the malformed hippocampi. (Courtesy Martin Lammens, Nijmegen)

sclerosis especially of areas CA1 and CA3 (Fig. 10.65), and to a lesser degree also of area CA2. In retrospect, the bilateral polymicrogyria was most probably the cause of the epilepsy, which led to secondary ischemic changes such as hippocampal sclerosis and pseudolaminar cortical necrosis, and to the deteriorating neurological state.

Fig. 10.65 Ammon's horn sclerosis: **a** section of the irregularly shaped hippocampal formation with sclerosis of the *CA1* field in particular; **b**, **c** details of the CA1 and CA2 fields, respectively (courtesy Martin Lammens, Nijmegen)
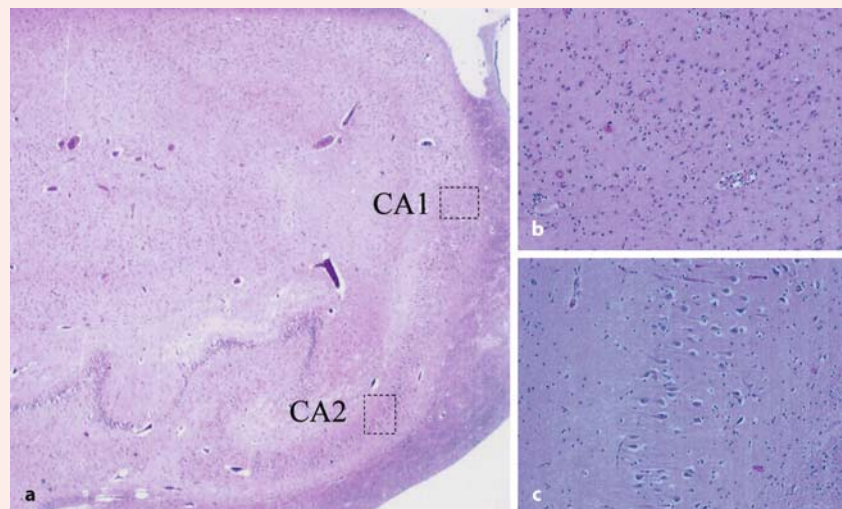
studied the consequences of such perinatal acquired encephalopathies on the developing neocortex. His extensive Golgi studies can be summarized as follows. The undamaged cortex adjacent to a perinatally acquired lesion survives, retains its intrinsic vasculature and is able to continue developing. However, its postinjury structural and functional differentiation is invariably and progressively altered. The grey matter overlying white matter lesions, despite partial deprivation of its input and inability to reach functional targets, survives, retains its intrinsic vasularization and undergoes progressive postinjury reorganization. The postinjury reorganization is characterized by neuronal transformations including atrophy, hy-

pertrophy, synaptic changes and reactive gliosis. Some axotomized projection neurons overlying white matter lesions, despite the loss of their functional targets, survive, develop new intracortical axonic profiles and become progressively transformed into local-circuit neurons. Comparable transformations were found for dendrotomized pyramidal neurons and intrinsic neurons. Some Cajal–Retzius cells survive, even in severe grey matter lesions. Surviving myelinated fibres in primarily undamaged cortical regions may be capable of interconnecting the dysplastic cortex with other cortical and subcortical regions and of carrying normal as well as abnormal (epileptic) impulses from it (Sect. 10.7.4). These postinjury neuronal, synaptic and fibrillar alterations are not static but are ongoing processes that will continue to affect the structural and functional development of the neocortex and influence the neurological and cognitive maturation of affected children.

10.7.6   Disorders of Cortical Connectivity

Disorders of cortical connectivity can easily be observed on MRI of the corpus callosum. Major malformations of the corticofugal projections are also evident on imaging by reduction of the cerebral peduncles. Pyramidal tract malformations are, however, more clearly visible on gross inspection of the brain stem during autopsy. Anomalies of other main fibre tracts such as the fornix are occasionally reported. *Malformations* of the *pyramidal tracts* may occur at various stages of development and, in general, are part of extensive malformations of the brain (ten Donkelaar et al. 1999, 2004). They may be found in malformations due to induction defects (anencephaly, encephaloceles, holoprosencephaly), abnormal cell proliferation (severe microcephaly, microlissencephaly), abnormal neuronal migration (the lissencephalies), abnormal axon guidance mechanisms, secondarily acquired injury leading to destructive lesions, in malformations leading to anomalies of decussation, and in disorders of myelination. Some examples of aplasia of the pyramidal tracts are discussed in Chap. 6.

Malformations of the *corpus callosum* are much more numerous than those of the long corticofugal systems (Aicardi et al. 1987; Barkovich et al. 1992b; Barkovich 2003). If normal development of the corpus callosum is disturbed, it may be completely absent (agenetic), partially formed (hypogenetic), formed in a defective way (dysgenetic) or contain too few axons (hypoplastic). Callosal agenesis may be due to lack of development of the commissural plate, agenesis or destruction of layer III cortical neurons, or severe white matter injury in the mid-second trimester (Barkovich 2003). A series of MRIs showing

callosal malformations are illustrated in Fig. 10.66. Abnormalities of the hippocampal commissure and the anterior commissure may accompany callosal anomalies (Raybaud and Girard 1998; Barkovich 2003). All three commissures are formed in the commissural plate, and all three may be involved in '*disorders of cerebral commissuration*' (Raybaud and Girard 1999). The hippocampal commissure is nearly always absent in patients with complete callosal agenesis, but may occasionally be present (Fig. 10.66c, d) and should not be mistaken for an isolated splenium which may be present in cases of holoprosencephaly (Barkovich 1990, 2003). The anterior commissure, connecting the middle and inferior temporal gyri of both hemispheres, is absent in about 40% of patients with complete callosal agenesis and is hypoplastic in another 25% (Utsunomiya et al. 1997; Raybaud and Girard 1998). Raybaud and Girard (1998, 1999) suggested the following classification for malformations of the telencephalic commissures: (1) *total absence of commissuration*; (2) *posterior absence of commissuration*: the anterior commissure is present, but not the corpus callosum and hippocampal commissure; (3) *posterior segmental calloso-hippocampal agenesis*: the anterior commissure and the rostral part of the corpus callosum are present; (4) *missing corpus callosum*: the anterior and hippocampal commissures are present; (5) *missing psalterium*: the corpus callosum is present throughout its extent but the two laminae of the septum are not apposed; this condition is usually described as persisting cavum septi pellucidi or cavum Vergae (Fig. 10.39); (6) *two different commissural beds*, one dorsal for the corpus callosum and one ventral for the psalterium; this situation corresponds to that in cysts of the cavum septi pellucidi or as cavum Vergae; (7) *septo-optic dysplasia*, characterized by a normal corpus callosum, a normal psalterium but no septal leaves laterally, and abnormalities of the optic nerves and the hypothalamopituitary system (Chap. 9); and (8) the *posterior 'splenium-like' commissure*, described by Oba and Barkovich (1995) in holoprosencephaly (Chap. 9). Normal and abnormal relationships of the corpus callosum to the septum pellucidum are shown in Fig. 10.67.

Callosal anomalies are frequent in trisomies (Clinical Case 10.15) and may be observed in various malformations of cortical development, including the lissencephalies (Barkovich et al. 1991; Dobyns and Truwit 1995; van der Knaap et al. 1997; Barkovich 1998), polymicrogyria and schizencephaly, heterotopia (Barkovich and Kjos 1992b; Raybaud and Girard 1998; Barkovich and Kuzniecky 2000), and interhemispheric cysts (Lena et al. 1995; Raybaud and Girard 1998; Barkovich 2003) as well as part of many complex syndromes, most frequently Aicardi syndrome (Aicardi et al. 1965, 1969; Ferrier et al. 1986; Billette de Villemeur et al. 1992l Aicardi 1996).

Fig. 10.66 MRI of callosal malformations. **a** Sagittal T1-weighted image of a 1-year-old girl with callosal hypoplasia; note the absence of the bulbous enlargements of the genu and the splenium, normally present at this age. **b** Sagittal T1-weighted image of partial absence of the corpus callosum; the genu is present, but the body and splenium are absent. **c, d** Sagittal and coronal T1-weighted images of a 2-year-old boy. An enlarged hippocampal commissure connects the fornices but not the hemisphere and mimicks the splenium of the corpus callosum on the sagittal image. The radial pattern of gyration of the medial cortex is due to the absence of the corpus callosum. (Courtesy Berit Verbist, Leiden)
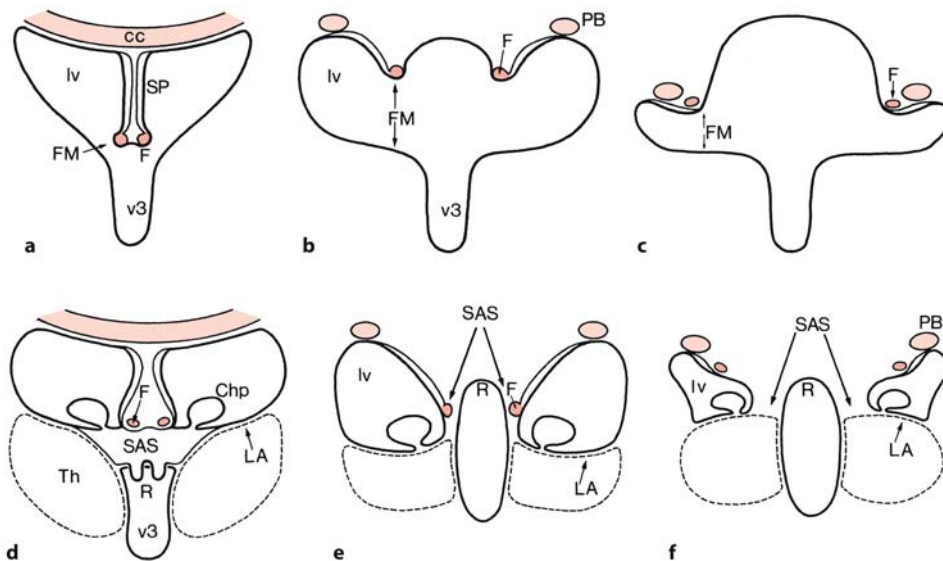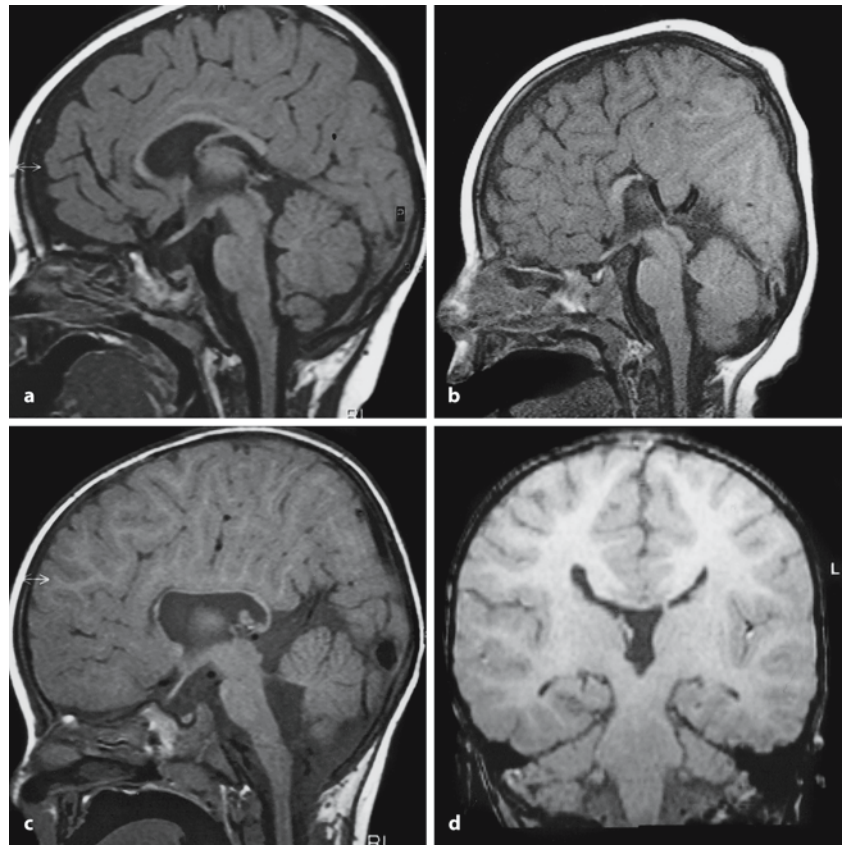
Fig. 10.67 Normal and abnormal relationships of the septum pellucidum to the foramen of Monro and the bundle of Probst: **a** normal relationship at the foramen of Monro (*FM*); **b, c** agenesis of the corpus callosum at the foramen of Monro; **d** normal relationship posterior to the foramen of Monro; **e** agenesis of the corpus callosum with the presence of two septa pellucidi; **f** agenesis of the corpus callosum without a septum pellucidum. *cc* corpus callosum, *Chp* choroid plexus of lateral ventricle, *F* fornix, *LA* lamina affixa, *lv* lateral ventricle, *PB* bundle of Probst, *R* roof of third ventricle, *SAS* subarachnoidal space, *SP* septum pellucidum, *Th* thalamus, *v3* third ventricle. (After Loeser and Alvord 1968)

Clinical Case 10.15
Callosal Agenesis

Agenesis of the *corpus callosum* may be observed in various malformations of cortical development. Two neonatal cases with multiple congenital malformations will be discussed (see Case Report).

Case Report. The first case concerns a prematurely (30 weeks of pregnancy) born boy who died shortly after birth. It was the fourth pregnancy of his 42-year-old mother. Birth weight was 1,520 g and crown–heel length was 39 cm. There were multiple congenital malformations, including facial dysmorphology with micrognathia, cataract, camptodactyly, malformations of the kidneys and severe hypoplasia

of the penis. Moreover, hyaline membrane disease and cardiomyopathy were found. The karyogram was normal 46,XY. Brain weight was 153 g, normal for the duration of the pregnancy. The corpus callosum was absent (Fig. 10.69) and the sparse sulci on the medial side of the cerebral hemisphere showed a radial arrangement. The second case comes from a boy, born after over 42 weeks of pregnancy, known with trisomy 18, found via amniocentesis at 39 weeks of pregnancy. It was the fourth pregnancy of a 39-year-old mother. The first three ended as spontaneous abortions. The baby died durante partu. Birth weight was 2,200 g and crown–heel length was 45.5 cm. Multiple congenital malformations were found characteristic for trisomy 18, such as facial dysmorphology with micrognathia, low implantation of the ears, crossed fingers II/III, pes varus, a ventricular septal defect,
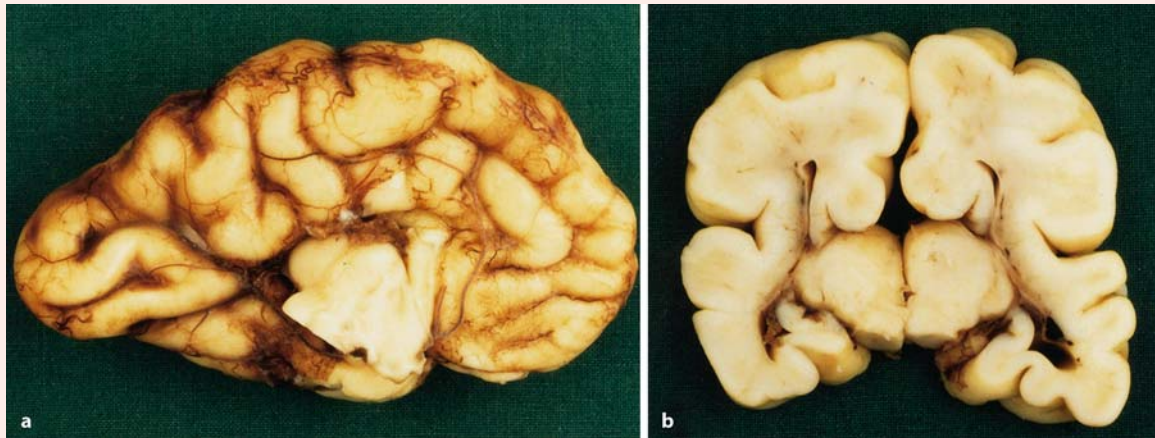
Fig. 10.68　Fetal case of callosal agenesis: **a** medial view of the brain; note radial arrangement of gyri; **b** coronal section of the brain (courtesy Pieter Wesseling, Nijmegen)

10.7.7　Mental Retardation

Mental retardation is a developmental disorder, characterized by global deficiency in cognitive and social abilities and onset during childhood. The most widely used definition (DSMMD 1994) comprises three criteria: (1) significantly subaverage intellectual functioning (IQ≤70); (2) significant limitations in adaptive functioning in skill areas such as communication, self-care, ability to live independently, and social and interpersonal skills; and (3) onset before the age of 18 years. Mental retardation is subdivided into several classes on the basis of the IQ present. The

WHO (1980) classification distinguishes profound (IQ<20), severe (IQ=20–35), moderate (IQ=35–50), mild (IQ=50–70) and borderline (IQ=70–85) classes. The prevalence of mental retardation is close to 3%, with a prevalence of 0.5% for those with an IQ≤50 (Hamel 1999; Chiurazzi and Oostra 2000).

In the majority of cases the cause of mental retardation is unknown, especially in 'mild' cases with an IQ>50 (Table 10.6). In this group interaction between genetic and environmental factors is thought to play the most important role, whereas in 'severe' mental retardation (IQ≤50) more often a single recognizable factor is present which is of genetic origin in at least

malrotation of the intestines and a very large scrotal hernia which contained large part of the intestines. Extensive interstitial bleeding was found in both lungs. The corpus callosum was completely absent (Fig. 10.70).

These cases were kindly provided by Pieter Wesseling (Department of Pathology, Radboud University Nijmegen Medical Centre) and Gerard van Noort (Laboratory for Pathology East-Netherlands, Enschede, The Netherlands), respectively.
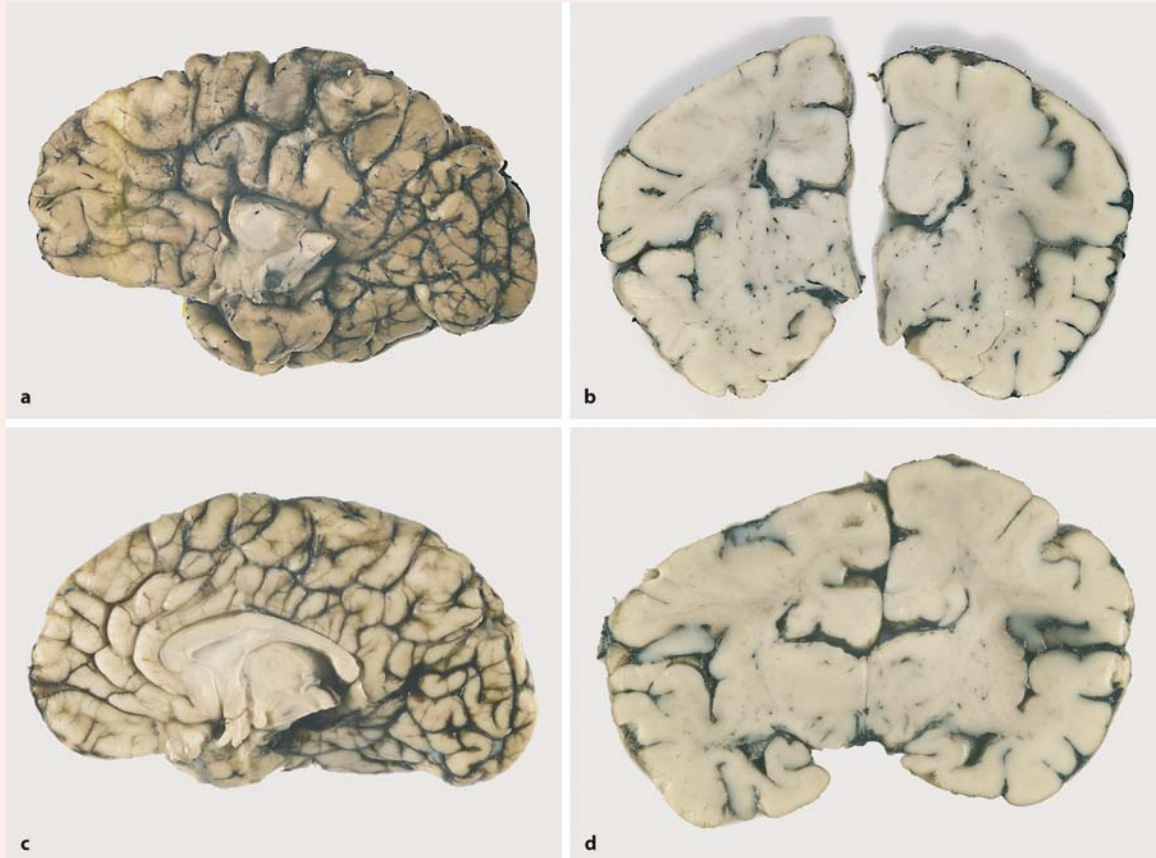
Fig. 10.69 Callosal agenesis in a trisomy 18 case: **a** medial view of the brain; **b** control case with normal corpus callosum; **c**, **d** two sections of the trisomy 18 brain. Note the bundles of Probst above the fornices. (Courtesy Gerard van Noort, Enschede)

50 % of cases (Flint and Wilkie 1996; Chiurazzi and Oostra 2000). Mental retardation can be part of a clinical syndrome (syndromic mental retardation) in which various congenital malformations such as body and brain malformations, neurological, neuroendocrine, psychiatric and metabolic defects may occur. More often, in non-syndromic mental retardation, no other functional or morphological abnormalities are observed, and a low IQ is the only detectable deficit. Among the environmental factors involved are maternal malnutrition, fetal alcohol exposure, fetal infections, premature birth, anoxia and hypothyroidy. Genetic causes of mental retardation range from chromosomal abnormalities, which are often, but not necessarily associated with severe mental retardation, to single-gene mutations and polygenic predisposition, which underlie milder forms. Among patients with mental retardation, males outnumber females. This male excess of mental retardation is partially explained by the existence of mutations in X-linked genes, causing *X-linked mental retardation* (*XLMR*; Lehrke 1972, 1974). In males, two syndromes are the most common causes of mental retardation: Down syndrome (trisomy 21; Chap. 3) and the fragile X syndrome, a single gene deficit. In females, Down and Rett syndromes are the

Table 10.6 Aetiologic classification of mental retardation

Disorders	Severe mental retardation (IQ<50) (%)	Mild mental retardation (IQ>50) (%)
Chromosomal abnormalities	15	5–10
Monogenic disorders, including fragile-X syndrome	20–25	5–10
CNS malformations with mental retardation	10	5
Acquired disorders (prenatal, perinatal, postnatal)	30–35	15
Unknown	20	60–65

leading causes of mental retardation. Many other syndromes are rare and may occur in single families. Mental retardation is associated with abnormalities in dendritic branching and spines (Purpura 1974, 1975a, b; Marín-Padilla 1972, 1976; Huttenlocher 1970, 1974, 1975, 1991; Scott et al. 1983; Kaufmann and Moser 2000; Ramakers 2002; Benavides-Piccione et al. 2004).

XLMR includes syndromic and non-specific/non-syndromic forms. Herbst and Miller (1980) estimated the prevalence of XLMR as 1.8 per 1,000 males with a carrier frequency of 2.4 per 1,000 females. Approximately one third of these patients have syndromic forms of XLMR in which mental retardation is associated with recognizable features on physical examination, laboratory investigations and imaging. The underlying gene defect has been identified in about 66 of the more than 140 syndromic forms, comprising about 45 genes and showing extensive allelism. For non-syndromic XLMR so far 20 genes are known allowing detection of the underlying defect in 26 of the 81 published families. Of all these genes, eight are involved in both syndromic and non-syndromic XLMR, underlining the – at least molecularly – vanishing boundaries between the two forms. Presently, it is estimated that about 10–13 % of all male mental retardation is due to mutations in X-linked genes (Ropers and Hamel 2005). Mental retardation with fragile X syndrome (FRAXA), the most common form of XLMR, and originally described as non-syndromic, is now also considered to be syndromic, although especially in young children features may be rather subtle.

The *fragile X syndrome* is characterized by cognitive impairment, postpubertal macro-orchidism (enlarged testes) and behavioural abnormalities such as hyperactivity and autistiform features (Hagerman 2002; Fig. 10.70). In most cases, the fragile X syndrome is due to the methylation-induced transcriptional silencing of the *fragile X mental retardation 1* (*FMR1*) gene that occurs as a result of the expansion of a CGG repeat in the 5' untranslated region of the gene and leads to the loss of its protein product fragile X mental retardation protein (FMRP; reviewed in Bardoni and Mandel 2002; Brown 2002; O'Donnell

Fig. 10.70 A young patient with fragile X syndrome. Note the subtle facial dysmorphisms like prognathia and a long face. Gaze avoidance is also visible. (Courtesy Ben Hamel, Nijmegen)

and Warren 2002). In humans without the syndrome, there are five to about 50 repeats, but in the great majority of fragile X patients the CGG repeat region is expanded to more than 200 repeats. Individuals with 55/56–200 repeats are carriers of a so-called premutation that is inherited unstably, particularly in the maternal line (Hagerman and Hagerman 2002; Kooy 2003). However, the premutation alleles predispose to premature ovarian failure among female carriers and a new tremor/ataxia syndrome (FXTAS) among older male – and to a lesser degree female – carriers (Hagerman et al. 2001; Hagerman and Hagerman

Table 10.7 Microdeletion syndromes leading to mental retardation

Syndrome	Locus	Gene	Main features
Wolf–Hirschhorn	4p16		Greek helmet face, hypertelorism, microcephaly, epilepsy
Cri-du-chat	5p16		Cat-like cry, microcephaly
Williams	7q11.23	*Elastin, LIM kinase*	Full lips, long philtrum, periorbital fullness, friendly character, hypercalcemia, supravalvular aortic stenosis
Langer–Giedion	8q24	*TRP1, EXT1*	Bulbous nose, sparse hair, cone-shaped epiphyses, exostoses
Wilms tumour, aniridia, genitourinary anomalies and mental retardation	11q13	*WT1*	Wilms tumour, aniridia, ambiguous genitalia, growth retardation
Prader–Willi	15q12	*SNPRN, Needin*	Hypotonia, obesity, small hands and feet
Angelman	15q12	*UBE3A*	No speech, ataxia, epilepsy, microcephaly, broad mouth, inappropriate laughter
Rubinstein–Taybi	16p13.3	*CREBBP*	Broad thumbs/big toes, beaked nose, down-slanting palpebral fissures
Miller–Dieker	17p13.3	*LIS1*	Lissencephaly
Smith–Magenis	17p11.2	*RAI1*	Coarse face, behavioural problems
DeGeorge/velocardiofacial dysmorphisms	22q11.2	*TBX1*	Cleft palate, conotruncal heart defect, facial

2002). Pathological studies from the brains of fragile X patients (Rudelli et al. 1985; Hinton et al. 1991; Wisniewski et al. 1991; Kaufmann and Moser 2000) and from *Fmr1* knockout mice (Comery et al. 1997; Nimchinski et al. 2001) showed abnormal dendritic spines implicating FMRP in synapse formation and function. Reyniers et al. (1999) studied the brains of two fragile X brothers with an *FMR1* full mutation. No evidence for specific abnormalities relevant to the fragile X syndrome were found. Cerebellar hypoplasia (posterior vermis hypoplasia), as suggested by human MRI studies (Reiss et al. 1991a, b; Mostofsky et al. 1998), was not evident in either patient. In fragile X knockout mice no size alterations of the brain were found in an in vivo high-resolution MRI study (Kooy et al. 1999). Fragile X syndrome may be caused by mild dysfunction of multiple regions in the brain, rather than by failure of a single brain region (Kooy 2003). Recently, with quantitative MRI effects of pre-mutation X-chromosomal CGG trinucleotide repeats on brain morphology were found (Moore et al. 2004). Male premutation carriers of FraX, compared with matched controls, showed significantly less voxel density in several brain regions, including the cerebellum, the amygdalo-hippocampal complex and the thalamus.

Non-syndromic XLMR is more prevalent than syndromic XLMR and is genetically highly heterogeneous (Toniolo and D'Adamo 2000; Ropers et al. 2003). So far, 20 genes have been identified in non-syndromic linked and possible XLMR cases, and an even smaller percentage of unselected male mental retardation cases. Through a thorough meta-analysis of all known linkage and gene data, Xp11 was found to be an attractive region to look at for XLMR genes (Ropers et al. 2003). Eight out of these 20 genes are involved in both syndromic and non-syndromic XLMR (Ropers and Hamel 2005). Much less is known of **autosomal mental retardation**, though given the fact that about 50% of all genes are expressed in the brain, thousands of autosomal genes may contribute to brain formation and/or functioning. The classic **microdeletion syndromes**, leading to mental retardation, are summarized in Table 10.7.

Rett syndrome (Rett 1966) is one of the leading causes of mental retardation and autistic behaviour in girls, affecting 1 in 10,000 to 1 in 15,000 females (Hagberg et al. 1983; Hagberg and Hagberg 1997), and is caused in at least 76% of cases by mutations in the X-linked gene *MECP2*, encoding methyl-CpG-binding protein 2 (Amir et al. 1999; 2000; Van der Veyver and Zoghbi 2000; Shahbazian and Zoghbi 2002; Armstrong et al. 2003). Gene-expressing profiling in the brain of *Mecp2* mutant mice has shown that MECP2 is not a global repressor of transcription, as previously thought, but that it has a specific role in the regulation of neuronal genes. The brain-derived neurotrophic factor (BDNF) and the *Hairy2a* gene have been identified as specific MECP2 targets, pointing to a role of MECP2 in neural plasticity, learning, memory and neurogenesis. X-inactivation studies in mice showed that MECP2 is important for neuronal survival and its expression is required beyond the developmental period (Chen et al. 2003).

The classic form of Rett syndrome, found almost exclusively in females, follows a distinct developmen-

Fig. 10.71 Rett syndrome. Note the alert, but introverted facial expression and the typical position of the hands. (Courtesy Belgian Society of Rett Patients)

tal course (Fig. 10.71). After apparently normal development until 6–18 months of age, they undergo a period of rapid regression with loss of purposeful hand use, deceleration of head growth, onset of repetitive, stereotyped hand movements, development of gait ataxia, apraxia, autistic features, seizures, respiratory dysfunction and show decreased somatic growth (Hagberg et al. 1983; Naidu 1997; Naidu et al. 2003). This period of rapid deterioration is followed by a stagnation phase, which lasts throughout adulthood. Volumetric MRI studies show an overall decrease in brain volume, affecting grey matter more than white matter, with the caudate nucleus and the frontal cortex presenting the largest reduction in volume (Reiss et al. 1993; Subramaniam et al. 1997). In postmortem studies a selective decrease in brain size was found (Jellinger and Seitelberger 1986; Armstrong 1992; Armstrong et al. 1999). Rett syndrome was first con-

Clinical Case 10.16
Male Rett Syndrome

Rett syndrome is a neurodevelopmental disorder, almost exclusively confined to females, due to mutations in the X-linked methyl-CpG-binding protein 2 (*MECP2*) gene. It is characterized by profound psychomotor retardation, typical hand movements, regression of speech, breathing abnormalities, epilepsy, dyskinesia and gait abnormalities. Rett syndrome was thought to be lethal in males. *MECP2* mutations do occur, however, in boys with a broad phenotypic spectrum, ranging from severe neonatal encephalopathy (Villard et al. 2000; Geerdink et al. 2002; see Case Report) to non-specific, moderate mental retardation.

Case Report. A boy was born as the third child of unrelated healthy parents. One sister was mentally retarded with autistic features and was not able to speak or walk. Rett syndrome was diagnosed when her brother was 8 months old. Another sister was not affected. The boy was born at term after an uneventful pregnancy. Apgar scores were 6 and 8 after 1 and 5 min, respectively. Birth weight was 3,100 g. Soon after birth, he showed respiratory insufficiency with apneas. Except for a high palate, no dysmorphic features were seen. Neurological examination revealed little spontaneous movement, little reaction to external stimuli, some spontaneous dyskinetic movements, axial hypotonia, hyperextension and rigidity of the limbs, and exaggerated deep tendon reflexes. Poor sucking and swallowing made nasogastric tube

feeding necessary. After a respiratory tract infection at the age of 4 months, he developed multifocal seizures which were difficult to control. He made no developmental progress, he did not reach for objects, his head control remained poor because of more prominent hypotonia, and dyskinetic movements became more obvious. MRI of the brain revealed bilateral pachygyria in the Sylvian region. At the age of 1 year, he had experienced two episodes of severe respiratory failure caused by aspiration and apneas. He died at the age of 13 months after a respiratory arrest.

At autopsy, brain weight was 568 g (925 g would have been normal). Inspection of the brain revealed a thick and more complex perisylvian gyral pattern, whereas the brain stem, cerebellum and spinal cord were normal. Coronal sections demonstrated bilateral complex gyri in the perisylvian area, especially of the deep insular gyri and part of the postcentral, superior and inferior parietal, and superior temporal gyri (Fig. 10.72 a). Microscopic examination of the malformed cerebral cortex revealed unlayered polymicrogyria with extensive fusion of the molecular layers (Fig. 10.72 b). There was an abrupt change to adjacent normally six-layered cortex. A few leptomeningeal glioneuronal ectopia were found. Other cortical regions, the basal ganglia, the cerebellum and the brain stem were normal. *MECP2*-mutation analysis revealed a 488–489 deletion as was found in the affected sister.

This case was kindly provided by Jan Rotteveel (Department of Child Neurology, Radboud University Nijmegen Medical Centre, Nijmegen, The Netherlands).
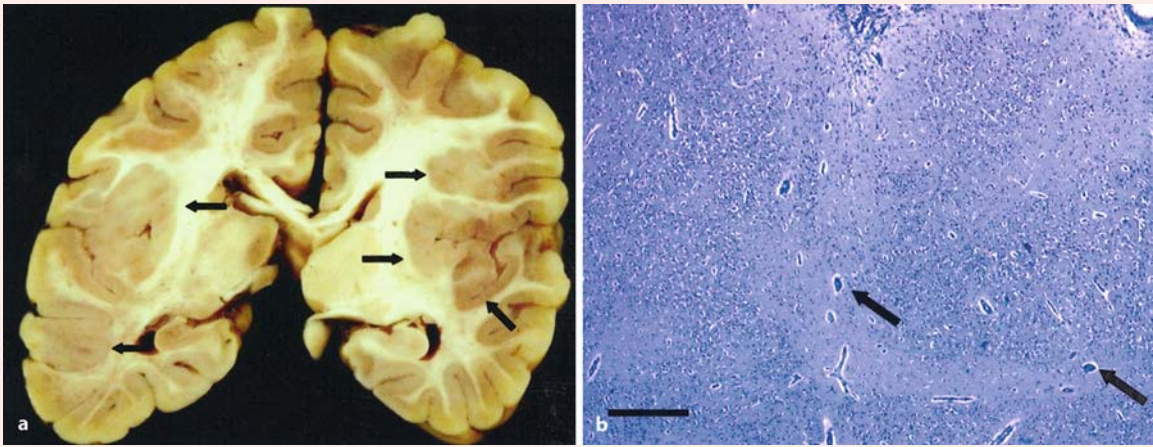
Fig. 10.72 Male Rett syndrome: **a** frontal section showing bilateral complex thick gyri in the perisylvian region, especially in the deep insular regions, more extensive on the right side than on the left side; **b** cresyl violet stained section through the insular region showing unlayered polymicrogyria; The *arrows* indicate meningeal vessels in fused molecular layers. (From Geerdink et al. 2002, with permission)

References

Geerdink N, Rotteveel JJ, Lammens M, Sistermans EA, Heikens GT, Gabreëls FJM, Mullaart RA, Hamel BCJ (2002) MECP2 mutation in a boy with severe neonatal encephalopathy: Clinical, neuropathological and molecular findings. Neuropediatrics 33:33–36

Villard L, Kpebe A, Cardoso C, Chelly J, Tardieu M, Fontes M (2000) Two affected boys in a Rett syndrome family: Clinical and molecular findings. Neurology 55:1188–1193

sidered to be a neurodegenerative disease, but the majority of neuropathological findings suggest that it is a disorder of arrested neuronal development (Armstrong 2001). Neurons of the cerebral cortex, basal ganglia, thalamus, hippocampus, amygdala and substantia nigra were smaller and more densely packed than in control subjects (Bauman et al. 1995). The dendrites of cortical neurons are reduced in length and complexity and have a reduced number of spines (Belichenko et al. 1994; Armstrong et al. 1995; see also Johnston et al. 2003).

For a long time, it was thought that Rett syndrome was lethal in males. However, it was found that practically all mutations occurred on the paternal X-chromosome. *MECP2* mutations in males have been found in a wide variety of phenotypes. Males with clinical Rett syndrome have either an XXY karyotype or are mosaics. Boys born in Rett syndrome families with severe and lethal neonatal encephalopathy were found to carry the same *MECP2* mutations as their female Rett syndrome relatives (Schanen et al. 1998; Geerdink et al. 2001; Clinical Case 10.16).

Dendritic abnormalities are the most consistent disorders associated with mental retardation (Kaufmann and Moser 2000). The earliest descriptions included dendritic spine dysgenesis, which was first associated with unclassified mental retardation, but can also be found in syndromic forms of mental retardation (Fig. 10.73). Genetic disorders with well-defined dendritic anomalies involving branches and/or spines include Down, Rett and fragile-X syndromes. Cytoarchitectonic analyses also suggest dendritic pathology in Williams and Rubinstein-Taybi syndromes (Kaufmann and Moser 2000). Dendritic abnormalities appear to have syndrome-specific pathogenesis and evolution, which correlate to some extent with their cognitive profile.

10.7.8 Neurobehavioural Disorders

Data from family, twin and adoption studies of psychiatric disorders such as schizophrenia, bipolar disorder, autism, attention-deficit hyperactivity disorder and addiction have indicated that genetics plays a major role in their pathogenesis (Inoue and Lupski 2003). For such disorders, multiple genetic and environmental factors may influence the susceptibility to the development of a phenotype. Rare families in which behavioural phenotypes segregate as Mendelian traits have been described. A positional cloning study in a large Dutch family with mild intel-
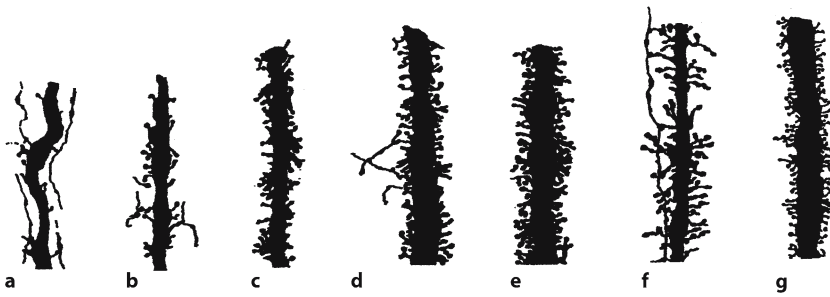
Fig. 10.73 Dendritic malformations in Patau and Down syndromes shown in drawings of Golgi preparations, depicting comparable segments of apical dendrites for layer V pyramidal neurons in the motor cortex: **a**–**e** different developmental stages in normal subjects in the fifth (**a**) and seventh (**b**) gestational months, in a neonate (**c**), and in the second (**d**) and eighth (**e**) postnatal months; **f** a newborn with trisomy 13–15 (Patau syndrome); **g** an 18-month-old infant with trisomy 21. Note the progressive increase in spine density, associated with a reduction in spine length, during normal development. Spines in Patau syndrome are not only sparse, but are also longer than expected for a neonate. The infant with Down syndrome had shorter and thinner rather than long spines. (After Marín-Padilla 1972)

lectual impairment and aggressive antisocial behaviour, segregating as an X-linked trait, identified a mutation in the monoamine oxidase A (*MAOA*) gene (Brunner et al. 1993 a, b). Mice lacking *Maoa* display aggressive behaviour (Cases et al. 1995). Caspi et al. (2002) demonstrated a significant effect of functional *MAOA* polymorphisms on antisocial behaviour in maltreated children. Several other genes have been linked to abnormal behavioural traits, including schizophrenia, speech and language disorders, and autism.

Recent studies suggest that altered interneuron development may underlie at least part of the pathophysiological process of neurobehavioural disorders (Buxhoeveden and Casanova 2002; Powell et al. 2003; Levitt et al. 2004). In mice with a targeted mutation of the gene encoding urokinase plasminogen activator receptor (uPAR), genetic disruption of cortical interneuron development caused region-specific and GABAergic cell-type-specific deficits, epilepsy and behavioural dysfunction (Powell et al. 2003). A 50% reduction of GABAergic interneurons was found in the anterior cingulate and parietal cortices, but interneuron numbers in the piriform and visual cortices did not differ from those of normal mice. A near complete loss of the parvalbumin subtype of GABAergic neurons was found, whereas other subclasses remained intact. Selectivity in interneuron disruption appears to be one of the neuroanatomical hallmarks of prefrontal cortical circuitry in individuals with schizophrenia (Woo et al. 1998; Lewis and Levitt 2002; Winterer and Weinberger 2004). The numerical density of synapses arising from parvalbumin-containing interneurons on pyramidal cells was reduced, but calretinin- and somatostatin-containing interneurons were spared (Woo et al. 1998). The developmental pathophysiology of autism is far less
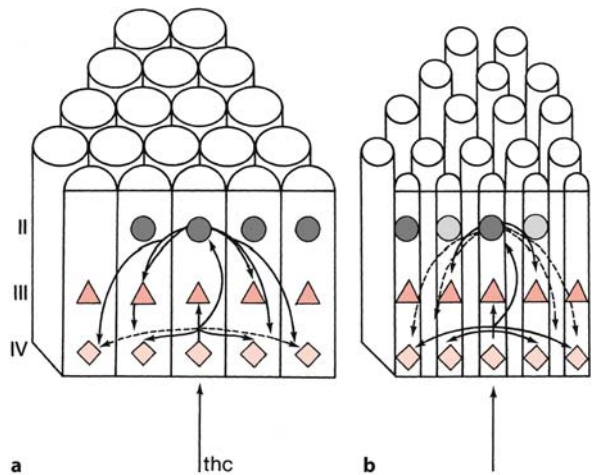
Fig. 10.74 Possible changes in minicolumn organization in autism. The neuronal relationships postulated to occur in normal cortical minicolumns (**a**) and minicolumn pathology reported in postmortem cortical tissue from individuals with autism (**b**). Each minicolumn forms a discrete functional unit with excitatory pyramidal cells (*red*) in layer *III* and spiny-stellate cells (*light red*) in layer *IV*, and inhibitory GABAergic interneurons (*dark grey*) in layer *II*, interconnected with each other. The minicolumns receive thalamocortical (*thc*) input. It was proposed that in autism the number or activity of GABAergic neurons is altered (*light-grey cells*), resulting in an altered circuitry. (After Levitt et al. 2004)

understood than that of schizophrenia, but recent data also point to a regional disruption of interneuron development. Minicolumn development (Fig. 10.74) showed similar changes as in schizophrenia, opposite to those in dyslexia (Casanova 1997; Casanova et al. 2002 a, b). Postmortem studies sug-

gest that the number of GABAergic interneurons is significantly reduced (Benes et al. 2000; Benes and Berretta 2001). Moreover, postnatal development of specific GABAergic neuron populations may be particularly vulnerable in schizophrenia and autism. The brains of individuals with autism initially are larger than normal (Brambilla et al. 2003; Courchesne et al. 2003), possibly owing to changes in the patterns of neuropil maturation and white matter development. Most autistic children exhibit abnormal EEG and sleep–wake patterns, suggesting that the balance between excitation and inhibition is disturbed (Thirumalai et al. 2002; Tuchman and Rapin 2002). The likelihood of altered interneuron development is also supported by the location of several genes involved in interneuron development, such as those of the *Dlx* family, at autism-susceptibility loci (Gutknecht 2001; Levitt et al. 2004).

Schizophrenia is the most common 'functional psychosis' and affects approximately 1 % of the world population. The hypothesis that schizophrenia results from a developmental, multifactorial, as opposed to a degenerative, process affecting the cerebral cortex has become popular over the last 20 years. Various factors may play a role, such as 22q11 deletion, which is associated with an increased risk of developing schizophrenia (Chow et al. 2002; Liu et al. 2002; Chap. 5). Moreover, catechol-*O*-methyl transferase gene polymorphism was found to influence the susceptibility to schizophrenia in a Japanese family (Weinberger et al. 2001). The *neurodevelopmental hypothesis* of schizophrenia suggests that subtle anomalous brain development occurs in utero and reveals itself symptomatically, years later as the heterogeneous symptoms of schizophrenia (Weinberger 1987, Kotrla et al. 1997; Raedler et al. 1998; Lewis and Levitt 2002). In schizophrenia, an abnormal cortical dopamine D1-to-D2 receptor activation ratio – in concert with, and in part related to, altered GABA and glutamate transmission – appears to interfere crucially with the stability of cortical representations of external and internal stimuli (Winterer and Weinberger 2004).

Classic observations include an increased frequency of obstetrical complications and prenatal exposure to infectious agents or toxins, and subtle physical, neurological and neuropsychological abnormalities (Cannon et al. 2002), which are present before the onset of florid symptoms in many patients with schizophrenia. A slight, quantitative increase in the size of the cerebral ventricles and cortical sulci, which is present in first-episode patients and is stable at subsequent assessments, may imply a subtle hypoplastic process affecting the forebrain (Raedler et al. 1998). In postmortem histological studies, morphometric abnormalities of the cerebral vesicles and of cortical areas (especially medial temporal lobe

structures) have been confirmed (Bogerts et al. 1985, 1993). Volumes of the hippocampus, amygdala and caudate nucleus were bilaterally significantly reduced, the internal pallidum showed a trend towards smaller volumes, whereas brain weight, putamen, accumbens and external pallidum were unchanged (Bogerts et al. 1993). Schizophrenia may involve cortical, limbic and subcortical structures as well as various neurotransmitter systems (Mai et al. 1993; Powers 1999). The heteromodal association neocortex is believed to be a major site of involvement in schizophrenia (Ross and Pearlson 1996). CT and MRI revealed a higher proportion of midline cerebral malformations in schizophrenia such as cavum septi pellucidi and cavum Vergae (Scott et al. 1993; Fukuzako and Kodamo 1998; Kwon et al. 1998; Nopoulos et al. 1998; Rajarethinan et al. 2001) and isolated absence of the septum pellucidum (Supprian et al. 1999; Filipovi et al. 2004).

Infantile autism is characterized by disordered language and cognitive skills, impaired social interactions, abnormal responses to sensory stimuli, events and objects, poor eye contact, an insistence on sameness, an unusual capacity for rote memorization, repetitive and stereotypic behaviour, and a normal physical appearance (Kanner 1943; DSMMD 1994). Affected boys outnumber girls by about 4:1 and approximately 75–85 % of these children function at a retarded level (van Karnebeek et al. 2002). A number of possible sites of brain abnormalities have been suggested, such as the limbic system (Darby 1976; Damasio and Maurer 1978; Courchesne 1997; Kemper and Bauman 1998), the cholinergic basal forebrain nuclei (Bauman and Kemper 1985; Bauman 1991), the brain stem (Courchesne 1997) and the cerebellar vermis (Courchesne 1997). MRI studies have reported abnormalities of the cerebellar vermis, but the results have not been uniformly replicated (Bauman et al. 1997). Saitoh et al. (2001) found MRI evidence for a smaller dentate area in autism. Brain overgrowth has been reported in the first year of life in autism (Brambilla et al. 2003; Courchesne et al. 2003). In a neuropathological study of nine brains of autistic individuals, Kemper and Bauman (1998) found that forebrain abnormalities were confined to the limbic system. Recently, Palmen et al. (2004) summarized the neuropathological findings on autism in the literature.

Williams syndrome is a rare sporadic disorder with a typical behavioural phenotype, characterized by a dissociation between language and face processing and spatial cognition, and overly social behaviour that is opposite to that seen in autism (Bellugi et al. 1999). It is due to a deletion on chromosome band 7q11.23. Williams syndrome is associated with specific morphological and physiological profiles: proportional sparing of frontal, limbic and neocerebellar

structures is seen on MRI; and abnormal functional organization of the neural systems that underlie language and face processing is found in event-related potential studies. In four autopsy brains of individuals with Williams syndrome, Galaburda et al. (1994b) found microcephaly and the relative curtailment of the occipital and posterior-parietal areas in three of the brains. One of the four brains showed a marked reduction in the size of the parietal, posterior-temporal and occipital regions in comparison with the rostral part of the brain. These abrupt and dramatic reductions led to the brain appearing as though a band had constricted its posterior portions. In an MRI study, Galaburda et al. (2001) found anomalies in the dorsal part of the cerebral cortex. The central sulci are separated by unusual gyral convolutions. The corpus callosum in Williams syndrome is more convex than that of controls, with an overall smaller volume, particularly of the splenium (Schmitt et al. 2001; Tomaiuolo et al. 2002).

Developmental dyslexia, a specific impairment of reading ability despite adequate intelligence and educational opportunity, is one of the most frequent childhood disorders (Habib 2000; Fisher and DeFries 2002; Voeller 2004). It has become increasingly apparent that the reading problems of people with dyslexia form part of a heritable neurobiological syndrome with a complex genetic basis (Ramus et al. 2003; Ramus 2004), making the isolation of genetic risk factors difficult. Nevertheless, several recent studies have reported the localization of genes that influence dyslexia and other language-related traits. Various hypotheses have been given to explain the neurobiological basis of dyslexia, including auditory (Galaburda et al. 1994a), magnocellular deficit (Stein and Walsh 1997; Demb et al. 1998), cerebellar deficit (Nicolson et al. 2001) and multilevel (Galaburda 1999) hypotheses. Anomalies of cell migration, such as molecular layer ectopia and focal polymicrogyri, have been observed by Galaburda and co-workers (Galaburda and Kemper 1979; Galaburda et al. 1985; Humphreys et al. 1990) in the perisylvian cortex of dyslexic brains, predominantly in the left hemisphere, and with a much greater prevalence than in control brains (Kaufmann and Galaburda 1989). Ectopia consisted of 50–100 cells that have overmigrated into the molecular layer. Cytoarchitectonic anomalies have also been found in the lateral geniculate nucleus (Livingstone et al. 1991), particularly in its magnocellular layers, and in the left medial geniculate nucleus of dyslexics (Galaburda et al. 1994a). Galaburda (1999) suggested that these thalamic anomalies may be the corollary of cortical anomalies (Ramus et al. 2003; Ramus 2004). Regional reductions of grey matter volume have been observed in familial dyslexia (Brambati et al. 2004).

References

Aicardi J (1996) Aicardi syndrome. In: Guerrini R, Andermann F, Canapicchi R, Roger J, Zifkin BG, Pfanner P (eds) Dysplasias of Cerebral Cortex and Epilepsy. Lippincott-Raven, Philadelphia, PA, pp 211–216

Aicardi J (1998) Diseases of The Nervous System in Childhood, 2nd ed. Mac Keith, London

Aicardi J, Lefebvre J, Lerique-Koechlin A (1965) A new syndrome: Spasms in flexion, callosal agenesis, ocular abnormalities. Electroencephalogr Clin Neurophysiol 19:609–610

Aicardi J, Chevrie JJ, Rousselie F (1969) Le syndrome spasmes en flexion, agénésie calleuse, anomalies choriorétiniennes. Arch Franc Pédiatr 26:1103–1120

Aicardi J, Chevrie J-J, Baraton J (1987) Agenesis of the corpus callosum. Handb Clin Neurol 50:149–173

Alcantara S, Ferrer I, Soriano E (1988) Postnatal development of parvalbumin and calbindin D28K immunoreactivities in the cerebral cortex of the rat. Anat Embryol (Berl) 188:63–73

Allendoerfer KL, Shatz CJ (1994) The subplate, a transient neocortical structure: Its role in the development of connections between the thalamus and the cortex. Annu Rev Neurosci 17:185–218

Amaral DG, Insausti R (1990) Hippocampal formation. In: Paxinos G (ed) The Human Nervous System. Academic, San Diego, CA, pp 711–755

Amir RE, Van den Veyver IB, Wan M, Tran CQ, Francke U, Zoghbi HY (1999) Rett syndrome is caused by mutations in X-linked *MECP2*, encoding methyl-CpG-binding protein 2. Nat Genet 23:185–188

Amir RE, Van den Veyver IB, Schultz R, Malicki DM, Tran CQ, Dahle EJ, Philippi A, Timar L, Percy AK, Motil KJ, et al. (2000) Influence of mutation type and X chromosome inactivation on Rett syndrome phenotypes. Ann Neurol 47:670–679

Amunts K, Schleicher A, Bürgel U, Mohlberg H, Uylings HBM, Zilles K (1999) Broca's region revisited: Cytoarchitecture and inter-subject variability. J Comp Neurol 412:319–341

Andermann F, Olivier A, Melanson D, Robitaille Y (1987) Epilepsy due to focal cortical dysplasia with microgyria and the forme fruste of tuberous sclerosis: A study of fifteen patients. Adv Epilepsy 16:35–38

Anderson SA, Mione M, Yun K, Rubinstein JLR (1999) Differential origins of neocortical projection and local circuit neurons: Role of Dlx genes in neocortical interneuronogenesis. Cereb Cortex 9:646–654

Anderson SA, Marín O, Horn C, Jennings K, Rubinstein JLR (2001) Distinct cortical migrations from the medial and lateral ganglionic eminences. Development 128:353–363

Andres C (2002) Molecular genetics and animal models in autistic disorder. Brain Res Bull 57:109–119

Ang ES Jr, Haydar TF, Gluncic V, Rakic P (2003) Four-dimensional migratory coordinates of GABAergic interneurons in the developing mouse cortex. J Neurosci 23:5805–5815

Angevine JB Jr (1965) Time of neuron origin in the hippocampal region. Exp Neurol 2(Suppl):1–70

Angevine JB Jr, Sidman RL (1961) Autoradiographic study of cell migration during histogenesis of cerebral cortex in the mouse. Nature 192:766–768

Armand J (1982) The origin, course and termination of corticospinal fibers in various mammals. Prog Brain Res 57:329–360

Armstrong DD (1992) The neuropathology of the Rett syndrome. Brain Dev 14(Suppl):S89–S98

Armstrong DD (2001) Rett syndrome neuropathology review 2000. Brain Dev 23(Suppl 1):S72–S76

Armstrong DD, Dunn JK, Antalffy B, Trivedi R (1995) Selective dendritic alterations in the cortex of Rett syndrome. J Neuropathol Exp Neurol 54:195–201

Armstrong DD, Dunn JK, Schultz RJ, Herbert DA, Glaze DG, Motil KJ (1999) Organ growth in Rett syndrome: A postmortem examination analysis. Pediatr Neurol 20:125–129

Armstrong DD, Deguchi K, Antalffy B (2003) Survey of MeCP2 in the Rett syndrome and the non-Rett syndrome brain. J Child Neurol 18:683–687

Armstrong E, Schleicher A, Omran H, Curtis M, Zilles K (1995) The ontogeny of human gyrification. Cereb Cortex 1:56–63

Arnold SE, Trojanowski JQ (1996a) Human fetal hippocampal development. I. Cytoarchitecture, myeloarchitecture, and neuronal morphologic features. J Comp Neurol 367:274–292

Arnold SE, Trojanowski JQ (1996b) Human fetal hippocampal development. II. The neuronal cytoskeleton. J Comp Neurol 367:293–307

Asada H, Kawamura K, Kume H, Ding R, Yi FY, Kanbara N, Kuzume H, Sanbo M, Yagi T, Obata K (1996) Mice lacking the 65kDa isoform of glutamic acid decarboxylase (GAD65) maintain normal levels of GAD67 and GABA in their brains but are susceptible to seizures. Biochem Biophys Res Commun 229:891–895

Bailey P, von Bonin G (1951) The Isocortex of Man. University of Illinois Press, Urbana, IL

Bar I, Lambert de Rouvroit C, Royaux I, Kritzman DB, Dernoncourt C, Ruelle D, Beckers MC, Goffinet AM (1995) A YAC contig containing the reeler locus with preliminary characterization of candidate gene fragments. Genomics 26:543–549

Bardoni B, Mandel J-L (2002) Advances in understanding of fragile X pathogenesis and FMRP function, and in identification of X-linked mental retardation genes. Curr Opin Genet Dev 12:284–293

Barkovich AJ (1990) Apparent atypical callosal dysgenesis: Analysis of MR findings in six cases and their relationship to holoprosencephaly. AJNR Am J Neuroradiol 11:333–340

Barkovich AJ (1998) Neuroimaging manifestations and classification of congenital muscular dystrophies. AJNR Am J Neuroradiol 19:1389–1396

Barkovich AJ (2000) Pediatric Neuroimaging, 3rd ed. Lippincott, Philadelphia, PA

Barkovich AJ (2003) Anomalies of the corpus callosum and cortical malformations. In: Barth PG (ed) Disorders of Neuronal Migration. Mac Keith, London, pp 83–103

Barkovich AJ, Kjos BO (1992a) Gray matter heterotopias: MR characteristics and correlation with developmental and neurologic manifestations. Radiology 182:493–499

Barkovich AJ, Kjos BO (1992b) Schizencephaly: Correlation of clinical findings with MR characteristics. AJNR Am J Neuroradiol 13:85–94

Barkovich AJ, Kuzniecky RI (2000) Gray matter heterotopia. Neurology 55:1603–1608

Barkovich AJ, Koch TK, Carroll CL (1991) The spectrum of lissencephaly: Report of ten cases analyzed by magnetic resonance imaging. Ann Neurol 30:139–146

Barkovich AJ, Gressens P, Evrard P (1992a) Formation, maturation, and disorders of brain neocortex. AJNR Am J Neuroradiol 13:423–446

Barkovich AJ, Lyon G, Evrard P (1992b) Formation, maturation, and disorders of white matter. AJNR Am J Neuroradiol 13:447–461

Barkovich AJ, Rowley H, Boller A (1995) Correlation of prenatal events with the development of polymicrogyria. AJNR Am J Neuroradiol 16:822–827

Barkovich AJ, Ferreiro DM, Barr RM, Gressens P, Dobyns WB, Truwit CL, Evrard P (1998) Microlissencephaly: A heterogeneous malformation of cortical development. Neuropediatrics 29:113–119

Barkovich AJ, Hevner R, Guerrini R (1999) Syndromes of bilateral symmetrical polymicrogyria. AJNR Am J Neuroradiol 20:1814–1821

Barkovich AJ, Kuzniecky RI, Jackson GD, Guerrini R, Dobyns WB (2001) Classification system for malformations of cortical development. Update 2001. Neurology 57:2168–2178

Barth PG (1987) Disorders of neuronal migration. Can J Neurol Sci 14:1–16

Battaglia G, Arcelli P, Granata T, Selvaggio M, Andermann F, Dubeau F, Olivier A, Tampieri D, Villemure JG, Avoli M, et al. (1996) Neuronal migration disorders and epilepsy: A morphological analysis of three surgically treated patients. Epilepsy Res 26:49–58

Bauman ML (1991) Microscopic neuroanatomic abnormalities in autism. Pediatrics 87:791–796

Bauman ML, Kemper TL (1985) Histoanatomic observations of the brain in early infantile autism. Neurology 35:866–874

Bauman ML, Kemper TL, Arin DM (1995) Pervasive neuroanatomic abnormalities of the brain in three cases of Rett's syndrome. Neurology 45:1581–1586

Bauman ML, Filipek PA, Kemper TL (1997) Early infantile autism. Int Rev Neurobiol 41:367–386

Bayer SA (1980a) Development of the hippocampal region in the rat. I. Neurogenesis examined with ^{3}H-thymidine autoradiography. J Comp Neurol 190:87–114

Bayer SA (1980b) Development of the hippocampal region in the rat. II. Morphogenesis during embryonic and early postnatal life. J Comp Neurol 190:115–134

Bayer SA, Altman J (1990) Development of layer I and subplate in the rat neocortex. Exp Neurol 107:48–62

Bayer SA, Altman J (1991) Neocortical Development. Raven, New York

Belichenko PV, Oldfors A, Hagberg B, Dahlström A (1994) Rett syndrome: 3-D confocal microscopy of cortical pyramidal dendrites and afferents. Neuroreport 5:1509–1513

Bellugi U, Lichtenberger L, Mills D, Galaburda A, Korenberg JR (1999) Bridging cognition, the brain and molecular genetics: Evidence from Williams syndrome. Trends Neurosci 22:197–209

Beltrán-Valero de Bernabé D, Currier S, Steinbrecher A, Celli J, van Beusekom E, van der Zwaag B, Kayserili H, Merlini L, Chitayat D, Dobyns WB, et al. (2002) Mutations in the O-mannosyltransferase gene POMT1 give rise to the severe neuronal migration disorder Walker-Warburg syndrome. Am J Hum Genet 71:1033–1043

Ben-Ari Y (2001) Developing networks play a similar melody. Trends Neurosci 24:353–360

Ben-Ari Y (2002) Excitatory actions of GABA during development: The nature of the nurture. Nat Rev Neurosci 3:728–739

Benavides-Piccione R, Ballesteros-Yáñez I, Martínez de Lagrán M, Elston G, Estivill X, Fillat C, De Felipe J, Dierssen M (2004) On dendrites in Down syndrome and DS murine models: A spiny way to learn. Prog Neurobiol 74:111–126

Benes FM, Berretta S (2001) GABAergic interneurons: Implications for understanding schizophrenia and bipolar disorder. Neuropsychopharmacol 25:1–27

Benes FM, Taylor JB, Cunningham MC (2000) Convergence and plasticity of monoaminergic systems in the medial prefrontal cortex during the postnatal period: Implications for the development of psychopathology. Cereb Cortex 10:1014–1027

Berger B, Alvarez C (1996) Neurochemical development of the hippocampal region in the fetal rhesus monkey. III. Calbindin D28k, calretinin and parvalbumin with special mention of Cajal-Retzius cells and the retrosplenial cortex. J Comp Neurol 366:674–699

Berger B, Alvarez C, Goldman-Rakic P (1993) Neurochemical development of the hippocampal region in the fetal rhesus monkey. I. Early appearance of peptides, calcium-binding proteins, DARPP-32, and the monoamine innervation in the entorhinal cortex during the first half of gestation (E47 to E90). Hippocampus 3:279–305

Berry M, Rogers AW (1965) The migration of neuroblasts in the developing cerebral cortex. J Anat (Lond) 99:691–709

Billette de Villemeur T, Chiron C, Robain O (1992) Unlayered polymicrogyria and agenesis of the corpus callosum: A relevant association? Acta Neuropathol (Berl) 83:265–270

Blaschke AJ, Staley K, Chun J (1996) Widespread programmed cell death in proliferative and postmitotic regions of the fetal cerebral cortex. Development 122:1165–1174

Blaschke AJ, Weiner JA, Chun J (1998) Programmed cell death is a universal feature of embryonic and postnatal neuroproliferative regions throughout the central nervous system. J Comp Neurol 396:39–50

Blümcke I, Zuschratter W, Schewe J-C, Suter B, Lie AA, Riederer BM, Meyer B, Schramm J, Elger CE, Wiestler OD (1999) Cellular pathology of hilar neurons in Ammon's horn sclerosis. J Comp Neurol 414:437–453

Blümcke I, Thom M, Wiestler OD (2002) Ammon's horn sclerosis: A maldevelopmental disorder associated with temporal lobe epilepsy. Brain Pathol 12:199–211

Bodensteiner JB, Schaefer GB, Craft JM (1998) Cavum septum pellucidi and cavum Vergae in normal and developmentally delayed populations. J Child Neurol 13:120–121

Bogerts B, Meertz E, Schönfeld-Bausch R (1985) Basal ganglia and limbic system pathology in schizophrenia. A morphometric study of brain volume and shrinkage. Arch Gen Psychiatry 42:784–791

Bogerts B, Falkai P, Greve B, Schneider T, Pfeiffer U (1993) The neuropathology of schizophrenia: Past and present. J Hirnforsch 34:193–205

Bourneville DM (1880) Contributions à l'étude de l'idiotie. III. Sclérose tubéreuse des circonvolutions cérébrales. Arch Int Neurol 1:81–91

Braak H (1976) A primitive gigantopyramidal field buried in the depth of the cingulate sulcus of the human brain. Brain Res 109:219–233

Braak H (1979) Pigment architecture of the human telencephalic cortex. V. Regio anterogenualis. Cell Tissue Res 204:441–451

Braak H (1980) Architectonics of the Human Telencephalic Cortex. Springer, BerlinHeidelberg New York

Braak H, Braak E (1992) The human entorhinal cortex: Normal morphology and lamina-specific pathology in various diseases. Neuroscience Res 15:6–31

Braak H, Braak E, Yilmazer D, Bohl J (1996) Functional anatomy of human hippocampal formation and related structures. J Child Neurol 11:265–275

Brambati SM, Termine C, Ruffino M, Stella G, Fazio F, Cappa S, Perani D (2004) Regional reductions of gray matter volume in familial dyslexia. Neurology 63:742–745

Brambilla P, Hardan, Ucelli di Nemi, Perez, Soares, Barale (2003) Brain anatomy and development in autism: Review of structural MRI studies. Brain Res Bull 61:557–569

Brazel CY, Romanenko MJ, Rothstein RP, Levison SW (2003) Roles of the mammalian subventricular zone in brain development. Prog Neurobiol 69:49–69

Brinks H, Conrad S, Vogt J, Oldekamp J, Sierra A, Deitinghoff L, Bechmann I, Alvarez-Bolado G, Heimrich B, Monnier PP, et al. (2004) The repulsive guidance molecule RGMa is involved in the formation of afferent connections in the dentate gyrus. J Neurosci 24:3862–3869

Broca P (1878) Anatomie comparée des circonvolutions cérébrales. Le grand lobe limbique et la scissure limbique dans la série des mammifères. Rev Antropol 1:385–498

Brodmann K (1909) Vergleichende Lokalisationslehre der Grosshirnrinde in ihren Prinzipien dargestellt auf Grund des Zellenbaues. Barth, Leipzig; English translation by LJ Garey (1999) Brodmann's 'Localisation in the Cerebral Cortex'. Imperial College Press, London

Brown WT (2002) The molecular biology of the fragile X mutation. In: Hagerman RJ, Hagerman PJ (eds) Fragile X Syndrome: Diagnosis, treatment and research, 3rd ed. Johns Hopkins University Press, Baltimore, MD, pp 110–135

Brun A (1965) The subpial granular layer of the foetal cerebral cortex in man. Its ontogeny and significance in congenital cortical malformations. Acta Pathol Microbiol Scand 179(Suppl):1–98

Brunelli S, Faiella A, Capra V, Nigro V, Simeone A, Cama A, Boncinelli E (1996) Germline mutations in the homeobox gene EMX2 in patients with schizencephaly. Nat Genet 12:94–96

Brunner HG, Nelen MR, Breakefield XO, Ropers H-H, van Oost BA (1993a) Abnormal behavior associated with a point mutation in the structural gene for monoamine oxidase A. Science 262:578–586

Brunner HG, Nelen MR, van Zandvoort P, Abeling NG, van Gennip AH, Wolters EC, Kuiper MA, Ropers H-H, van Oost BA (1993b) X-linked borderline mental retardation with prominent behavioral disturbance: Phenotype, genetic localization, and evidence for disturbed monoamine metabolism. Am J Hum Genet 52:1032–1039

Bruyn GW (1977) Agenesis septi pellucidi, cavum septi pellucidi, and cavum Vergae, and cavum veli interpositi. Handb Clin Neurol 30:299–336

Buxhoeveden DP, Casanova MF (2002) The minicolumn hypothesis in neuroscience. Brain 125:935–951

Cameron HE, McKay RDG (2001) Adult neurogenesis produces a large pool of new granule cells in the dentate gyrus. J Comp Neurol 435:406–417

Cannon M, Jones PB, Murray RM (2002) Obstetric complications and schizophrenia: Historical and meta-analytic review. Am J Psychiatry 159:1080–1092

Cao QL, Yan XX, Luo XG, Garey LJ (1996) Prenatal development of parvalbumin immunoreactivity in the human striate cortex. Cereb Cortex 6:620–630

Casanova MF (1997) Functional and anatomical aspects of prefrontal pathology and schizophrenia. Schizophr Bull 23:517–519

Casanova MF, Buxhoeveden DP, Switala AE, Roy EL (2002a) Minicolumnar pathology in autism. Neurology 58:428–432

Casanova MF, Buxhoeveden DP, Cohen M, Switala AE, Roy EL (2002b) Minicolumnar pathology in dyslexia. Ann Neurol 52:108–110

Cases O, Seif I, Grimsby J, Gaspar P, Chen K, Pournin S, Muller U, Aquet M, Babinet C, Shih JC, et al. (1995) Agressive behavior and altered amounts of brain serotonin and norepinephrine in mice lacking MAOA. Science 268:1763–1776

Caspi A, McClay J, Moffitt TE, Mill J, Martin J, Craig IW, Taylor A, Poulton R (2002) Role of genotype in the cycle of violence in maltreated children. Science 297:851–854

Caviness VS Jr (1973) Time of neuron origin in the hippocampus and dentate gyrus of normal and reeler mutant mice: An autoradiographic analysis. J Comp Neurol 151:113–120

Caviness VS Jr (1982) Neocortical histogenesis in normal and reeler mice: A developmental study based upon [³H]thymidine autoradiography. Dev Brain Res 4:293–302

Caviness VS Jr, Sidman RL (1973) Time of origin of corresponding cell classes in the cerebral cortex of normal and reeler mutant mice: An autoradiographic analysis. J Comp Neurol 170:449–460

Caviness VS Jr, Crandall JE, Edwards MA (1988) The *reeler* malformation, implications for neocortical histogenesis. In: Jones EG, Peters A (eds) The Cerebral Cortex, Vol 7. Plenum, New York, pp 489–499

Caviness VS Jr, Takahashi T, Nowakowski RS (1995) Numbers, time and neocortical neurogenesis: A general developmental and evolutionary model. Trends Neurosci 18:379–393

Caviness VS Jr, Takahashi T, Nowakowski RS (2000) Neurogenesis and the early events of neocortical histogenesis. In: Goffinet AM, Rakic P (eds) Mouse Brain Development. Springer, Berlin Heidelberg New York, pp 107–143

Caviness VS Jr, Takahashi T, Nowakowski RS (2003) Morphogenesis of the human cerebral cortex. In: Barth PG (ed) Disorders of Neuronal Migration. Mac Keith, London, pp 1–23

Cecchi C, Boncinelli E (2000) *Emx* homeogenes and mouse brain development. Trends Neurosci 23:347–352

Chae T, Kwon YT, Bronson R, Dikkes P, Li E, Tsai L-H (1997) Mice lacking p35, a neuronal specific activator of cdk5, display cortical lamination defects, seizures and adult lethality. Neuron 18:29–42

Chan WY, Kostović I, Takashima S, Feldhaus C, Stoltenburg-Didinger G, Verney C, Yew D, Ulfig N (2002) Normal and abnormal development of the human cerebral cortex. Neuroembryology 1:78–90

Chang BS, Lowenstein DH (2003) Mechanisms of disease: Epilepsy. N Engl J Med 349:1257–1266

Chang BS, Piao X, Giannini C, Cascino GD, Scheffer I, Wood CG, Topcu M, Terzan K, Bodell A, Leventer RJ (2004) Bilateral generalised polymicrogyria (BGP): A distinct syndrome of cortical malformation. Neurology 62:1722–1728

Chédotal A, Del Rio JA, Ruiz M, He Z, Borrell V, de Castro F, Ezan F, Goodman CS, Tessier-Lavigne M, Sotelo C, Soriano E (1998) Semaphorins III and IV repel hippocampal axons via two distinct receptors. Development 125:4313–4323

Chen H, Bagri A, Zupicich JA, Zou Y, Stoeckli E, Pleasure SJ, Lowenstein DH, Skarnes WC, Chédotal A, Tessier-Lavigne M (2000) Neuropilin-2 regulates the development of selective cranial and sensory nerves and hippocampal mossy fiber projections. Neuron 25:43–56

Chen H, Cheng Q, Lin Y, Meissner A, West AE, Griffith EC, Jaenisch R, Greenberg ME (2003) Depression of BDNF transcription involves calcium-dependent phosphorylation of MeCP2. Science 302:885–889

Chenn A, McConnell SK (1995) Cleavage orientation and the asymmetric inheritance of Notch1 immunoreactivity in mammalian neurogenesis. Cell 82:631–641

Chenn A, Braisted JE, McConnell SK, O'Leary DDM (1997) Development of the cerebral cortex: Mechanisms controlling cell fate, laminar and areal patterning, and axonal connectivity. In: Cowan WM, Jessell TM, Zipursky SL (eds) Molecular and Cellular Approach to Neural Development. Oxford University Press, New York, pp 440–473

Chevassus-au-Loius N, Rafiki A, Jorquera I, Ben-Ari Y, Represa A (1998) Neocortex in the hippocampus: An anatomical and functional study of CA1 heterotopias after prenatal treatment with methylazoxymethanol in rats. J Comp Neurol 394:520–536

Chi JG, Dooling EC, Gilles FH (1977) Gyral development of the human brain. Ann Neurol 1:86–93

Chiurazzi P, Oostra BA (2000) Genetics of mental retardation. Curr Opin Pediatr 12:529–535

Cho WH, Seidenwurm D, Barkovich AJ (1999) Adult-onset neurologic dysfunction associated with cortical malformations. AJNR Am J Neuroradiol 20:1037–1043

Chow EWC, Zipursky RB, Mikulis DJ, Bassett AS (2002) Structural brain abnormalities in patients with schizophrenia and 22q11 deletion syndrome. Biol Psychiatry 51:208–215

Comery TA, Harris JB, Willems PJ, Oostra BA, Irwin SA, Weiler IJ, Greenough WT (1997) Abnormal dendritic spines in fragile X knockout mice: Maturation and pruning deficits. Proc Natl Acad Sci USA 94:5401–5404

Condé F, Lund JS, Lewis DA (1996) The hierarchical development of monkey visual cortical regions as revealed by the maturation of parvalbumin-immunoreactive neurons. Dev Brain Res 96:261–276

Conel JL (1939) The Postnatal Development of the Human Cerebral Cortex. I. The cortex of the Newborn. Harvard University Press, Cambridge, MA

Conel JL (1941) The Postnatal Development of the Human Cerebral Cortex. II. The Cortex of the One-Month Infant. Harvard University Press, Cambridge, MA

Conel JL (1947) The Postnatal Development of the Human Cerebral Cortex. III. The Cortex of the Three-Month Infant. Harvard University Press, Cambridge, MA

Conel JL (1951) The Postnatal Development of the Human Cerebral Cortex. IV. The Cortex of the Six-Month Infant. Harvard University Press, Cambridge, MA

Conel JL (1955) The Postnatal Development of the Human Cerebral Cortex. V. The Cortex of the Fifteen-Month Infant. Harvard University Press, Cambridge, MA

Conel JL (1959) The Postnatal Development of the Human Cerebral Cortex. VI. The Cortex of the Twenty-Four-Month Infant. Harvard University Press, Cambridge, MA

Conel JL (1963) The Postnatal Development of the Human Cerebral Cortex. VII. The Cortex of the Four-Year Child. Harvard University Press, Cambridge, MA

Conel JL (1967) The Postnatal Development of the Human Cerebral Cortex. VIII. The Cortex of the Six-Year Child. Harvard University Press, Cambridge, MA

Consortium ECTS (1993) Identification and characterization of the tuberous sclerosis gene on chromosome 16. Cell 75:1305–1315

Copp AJ, Harding BN (1999) Neuronal migration disorders in humans and in mouse models – An overview. Epilepsy Res 36:133–141

Costa E, Davis J, Pesold C, Tueting P, Guidotti A (2002) The heterozygote reeler *mouse* as a model for the development of a new generation of antipsychotics. Curr Opin Pharmacol 2:56–62

Courchesne E (1997) Brainstem, cerebellum and limbic neuroanatomical abnormalities in autism. Curr Opin Neurobiol 7:269–278

Courchesne E, Carper R, Akshoomoff N (2003) Evidence of brain overgrowth in the first year of life in autism. JAMA 290:337–344

Crino PB, Henske EP (1999) New developments in the neurobiology of the tuberous sclerosis complex. Neurology 53:1384–1390

Crino PB, Duhaime A-C, Baltuch G, White R (2001) Differential expression of glutamate and GABA-A receptor subunit mRNA in cortical dysplasia. Neurology 56:906–913

Crino PB, Miyata H, Vinters HV (2002) Neurodevelopmental disorders as a cause of seizures: Neuropathologic, genetic, and mechanistic considerations. Brain Pathol 12:212–233

D'Agostino MD, Bernasconi A, Das S, Bastos A, Valerio RM, Palmini A, Costa da Costa J, Scheffer IE, Berkovic S, Guerrini R, et al. (2002) Subcortical band heterotopia (SBH) in males: Clinical, imaging and genetic findings in comparison with females. Brain 125:2507–2522

Damasio AR, Maurer RG (1978) A neurological model for childhood autism. Arch Neurol 35:777–786

Darby JH (1976) Neuropathological aspects of psychosis in childhood. J Autism Childhood Schizophrenia 6:339–352

D'Arcangelo G, Miao GG, Chen S-C, Soares HD, Morgan JI, Curran T (1995) A protein related to extracellular matrix proteins deleted in the mouse mutant *reeler*. Nature 374:719–723

D'Arcangelo G, Nakajima K, Miyata T, Ogawa M, Mikoshiba K, Curran T (1997) Reelin is a secreted glycoprotein recognized by the CR-50 monoclonal antibody. J Neurosci 17:23–31

deAzevedo LC, Hedin-Pereira C, Leht R (1997) Callosal neurons in the cingulate cortical plate and subplate of human fetuses. J Comp Neurol 386:60–70

Deguchi K, Inoue K, Avila WE, Lopez-Terrada D, Antalffy BA, Quattrocchi CC, Sheldon M, Mikoshiba K, D'Arcangelo G, Armstrong DL (2003) Reelin and disabled-1 expression in developing and mature human cortical neurons. J Neuropathol Exp Neurol 62:676–684

de Lacoste MC, Kirkpatrick JB, Ross ED (1985) Topography of the human corpus callosum. J Neuropathol Exp Neurol 44:578–591

Demb JB, Boynton GM, Heeger DJ (1998) Functional magnetic resonance imaging of early visual pathways in dyslexia. J Neurosci 18:6939–6951

Deng J, Elberger AJ (2001) The role of pioneer neurons in the development of mouse visual cortex and corpus callosum. Anat Embryol (Berl) 204:437–453

des Portes V, Pinard JM, Billuart P, Vinet MC, Koulakoff A, Carrié A, Gelot A, Dupuis E, Motte J, Berwald-Netter Y, et al. (1998) A novel gene required for neuronal migration and involved in X-linked subcortical laminar heterotopia and lissencephaly syndrome. Cell 92:51–61

Di Virgilio G, Clarke S (1997) Direct interhemispheric visual input to human speech areas. Hum Brain Mapping 5:347–354

Dobyns WB, Truwit CL (1995) Lissencephaly and other malformations of cortical development: 1995 An update. Neuropediatrics 26:132–147

Dobyns WB, Stratton RF, Greenberg F (1984) Syndromes with lissencephaly. I. Miller-Dieker and Norman-Roberts syndromes and isolated lissencephaly. Am J Med Genet 18:509–526

Dobyns WB, Kirkpatrick JB, Hittner HM, Roberts RM, Kretzer FL (1985) Syndromes with lissencephaly. II. Walker-Warburg and cerebro-oculo-muscular syndromes and a new syndrome with type II lissencephaly. Am J Med Genet 22:157–195

Dobyns WB, Pagon RA, Armstrong D, Curry CJ, Greenberg F, Grix A, Holmes LB, Laxova R, Michels VV, Robinow M (1989) Diagnostic criteria for Walker-Warburg syndrome. Am J Med Genet 32:195–210

Dobyns WB, Andermann E, Andermann F, Czapansky-Beilman D, Dubeau F, Dulac O, Guerrini R, Hirsch B, Ledbetter DH, Lee NS, et al. (1996) X-linked malformations of neuronal migration. Neurology 47:331–339

Dobyns WB, Truwit CL, Ross ME, Matsumoto N, Pilz DT, Ledbetter DH, Gleeson JG, Walsh CA, Barkovich AJ (1999) Differences in the gyral pattern distinguish chromosome 17-linked and X-linked lissencephaly. Neurology 53:270–277

Dooling EC, Chi JG, Gilles FH (1983) Telencephalic development: Changing gyral patterns. In: Gilles FH, Leviton A, Dooling EC (eds) The Developing Human Brain. Wright, Bristol, pp 94–104

DSMMD (1994) Diagnostic and Statistical Manual of Mental Disorders, IV. American Psychiatric Association, Washington, DC

Dubeau F, Tampieri D, Lee N, Andermann E, Carpenter S, Leblanc R, Olivier A, Radtke R, Villemure JG, Andermann F (1995) Periventricular and subcortical nodular heterotopia. A study of 33 patients. Brain 118:1273–1287

Duchowny M, Jayakar P, Levin B (2000) Aberrant neural circuits in malformations of cortical development and focal epilepsy. Neurology 55:423–428

Dum RP, Strick PL (1996) Spinal cord terminations of the medial motor areas in macaque monkeys. J Neurosci 15:6513–6525

Duvernoy HM (1992) Le cerveau humain. Surface, coupes sériée tridimensionelles et IRM. Springer, Berlin Heidelberg New York

Duvernoy HM (1998) The Human Hippocampus. Functional anatomy, vascularization and serial sections with MRI, 2nd ed. Springer, Berlin Heidelberg New York

Ekşioğlu YZ, Scheffer IE, Cardenas P, Knoll J, DiMario F, Ramsby G, Berg M, Kamuro K, Berkovic SF, Duyk GM, et al. (1996) Periventricular heterotopia: An X-linked dominant epilepsy locus causing aberrant cerebral cortical development. Neuron 16:77–87

Elliot Smith G (1897) The morphology of the indusium griseum and striae Lancisii. Anat Anz 13:23–27

Eriksson PS, Perfilieva E, Björk-Eriksson T, Alborn AM, Nordborg C, Peterson DA, Gage FH (1998) Neurogenesis in the adult human hippocampus. Nat Med 4:1313–1317

Eriksson SH, Thom M, Hefferman J, Lin WR, Harding BN, Squier MV, Sisodiya SM (2001) Persistent reelin-expressing Cajal-Retzius cells in polymicrogyria. Brain 124:1350–1361

Evrard P, Miladi N, Bonnier C, Gressens P (1992) Normal and abnormal development of the brain. In: Rapin I, Segalowitz SJ (eds) Child Neuropsychology. Elsevier, Amsterdam, pp 11–44

Eyre JA, Miller S, Clowry GJ, Conway EA, Watts C (2000) Functionally corticospinal projections are established prenatally in the human foetus permitting involvement in the development of spinal motor centres. Brain 123:51–64

Falconer DS (1951) Two new mutants, "trembler" and "reeler", with neurological actions in the house mouse (Mus musculus L). J Genet 50:192–201

Farah S, Sabry MA, Khuraibet A, Khaffagi S, Rudwan M, Hassan M, Haseeb N, Abulhassan S, Abdel-Rasool MA, Elgamal S, et al. (1997) Lissencephaly associated with cerebellar hypoplasia and myoclonic epilepsy in a Bedouin kindred: A new syndrome? Clin Genet 51:326–330

Fatemi SH (2002) The role of Reelin in the pathology of autism. Mol Psychiatry 7:919–920

Feess-Higgins A, Larroche J-C (1987) Le développement du cerveau foetal humain. Atlas anatomique. Masson, Paris

Ferrer I, Cusi MV, Liarte A, Campistol JC (1986) A Golgi study of the polymicrogyric cortex in Aicardi syndrome. Brain Dev 8:518–525

Filipovi B, Prostran M, Ilankovi N, Filipovi B (2004) Predictive potential of cavum septi pellucidi (CSP) in schizophrenics, alcoholics and persons with past head trauma. A postmortem study. Eur Arch Psychiatry Clin Neurosci 254:228–230

Fink GR, Frackowiak RSJ, Pietrzyk U, Passingham RF (1997) Multiple nonprimary motor areas in the human cortex. J Neurophysiol 77:2164–2174

Fisher SE, DeFries JC (2002) Developmental dyslexia: Genetic dissection of a complex cognitive trait. Nat Rev Neurosci 3:767–780

Flint J, Wilkie AOM (1996) The genetics of mental retardation. Br Med Bull 52:453-464

Flores-Sarnat L (2002) Hemimegalencephaly: Part 1. Genetic, clinical, and imaging aspects. J Child Neurol 17:373–384

Fox JW, Lamperti ED, Ekşioğlu YZ, Hong SE, Feng Y, Graham DA, Scheffer IE, Dobyns WB, Hirsch BA, Radtke RA, et al. (1998) Mutations in *filamin 1* prevent migration of cerebral cortical neurons in human periventricular heterotopia. Neuron 21: 1315–1325

Friede RL (1989) Developmental Neuropathology, 2nd ed. Springer, Berlin Heidelberg New York

Frotscher M (1997) Dual role of Cajal-Retzius cells and reelin in cortical development. Cell Tissue Res 290:315–322

Frotscher M (1998) Cajal-Retzius cells, Reelin, and the formation of layers. Curr Opin Neurobiol 8:570–575

Fukuyama Y, Osawa M, Suzuki H (1981) Congenital progressive muscular dystrophy of the Fukuyama tyoe – clinical, genetic and pathological considerations. Brain Dev 3:1–29

Fukuzako H, Kodama S (1998) Cavum septum pellucidum in schizophrenia. Biol Psychiatry 43:466–469

Gadisseux J-F, Goffinet AM, Lyon G, Evrard P (1992) The human transient subpial granular layer: An optical, immunohisto-chemical, and ultrastructural analysis. J Comp Neurol 324:94–114

Galaburda AM (1999) Developmental dyslexia: A multilevel syndrome. Dyslexia 5:183–191

Galaburda AM, Kemper TL (1979) Cytoarchitectonic abnormalities in developmental dyslexia: A case study. Ann Neurol 6:94–100

Galaburda AM, Sherman GF, Rosen GD, Aboitiz F, Geschwind N (1985) Developmental dyslexia: Four consecutive patients with cortical anomalies. Ann Neurol 18:222–233

Galaburda AM, Menard MT, Rosen GD (1994a) Evidence for aber-rant auditory anatomy in developmental dyslexia. Proc Natl Acad Sci USA 91:8010–8013

Galaburda AM, Wang PP, Bellugi U, Rossen M (1994b) Cytoarchitec-tonic anomalies in a genetically based disorder: Williams syndrome. Neuroreport 5:753–757

Galaburda AM, Schmitt JE, Atlas SW, Eliez S, Bellugi U (2001) Dorsal forebrain anomaly in Williams syndrome. Arch Neurol 58:1865–1869

Garel C (2004) MRI of the Fetal Brain. Normal development and cerebral pathologies. Springer, Berlin Heidelberg New York

Geerdink N, Rotteveel JJ, Lammens M, Sistermans EA, Heikens GT, Gabreëls FJM, Mullaart RA, Hamel BCJ (2002) MECP2 mutation in a boy with severe neonatal encephalopathy: Clinical, neuropathological and molecular findings. Neuropediatrics 33:33–36

Geyer S, Matelli M, Luppino G, Zilles K (2000) Functional neu-roanatomy of the primate isocortical motor system. Anat Embryol (Berl) 202:443–474

Giedd JN, Blumenthal J, Jeffries NO, Castellanos FX, Liu H, Zijden-bos A, Paus T, Evans AC, Rapoport JL (1999) Brain development during childhood and adolescence: A longitudinal MRI study. Nat Neurosci 2:861–863

Gleeson JG (2000) Classical lissencephaly and double cortex (sub-cortical band heterotopia): LIS1 and doublecortin. Curr Opin Neurol 13:121–125

Gleeson JG, Walsh CA (2000) Neuronal migration disorders: From genetic diseases to developmental mechanisms. Trends Neu-rosci 23:352–359

Gleeson JG, Allen KM, Fox JW, Lamperti ED, Berkovic SF, Scheffer IE, Cooper EC, Dobyns WB, Minnerath SR, Ross ME, Walsh CA (1998) *doublecortin*, a brain-specific gene mutated in human X-linked lissencephaly and double cortex syndrome, encodes a putative signaling protein. Cell 92:63–72

Goffinet AM (1979) An early developmental defect in the cerebral cortex of the *reeler* mouse. Anat Embryol (Berl) 157:205–216

Goffinet AM (1984) Events governing organization of postmigra-tory neurons: Studies on brain development in normal and *reeler* mice. Brain Res Rev 7:291–296

Goldowitz D, Cushing RC, Laywell E, D'Arcangelo G, Sheldon M, Sweet H, Davisson M, Steindler D, Curran T (1997) Cerebellar disorganization characteristic of reeler in scrambler mutant mice despite presence of Reelin. J Neurosci 17:8767–8777

Gomez MR (1988) Tuberous Sclerosis. Raven, New York

González JL, Russo CJ, Goldowitz D, Sweet HO, Davisson MT, Walsh CA (1997) Birthdate and cell marker analysis of scrambler: A novel mutation affecting cortical development with a reeler-like phenotype. J Neurosci 17:9204–9211

Gorlin J, Yamin R, Egan S, Stewart M, Sossel T, Kwiatkowski D, Hartwig J (1990) Human endothelial actin-binding protein (ABP-280, nonmuscle filamin): A molecular leaf spring. J Cell Biol 111:1089–1105

Gorman DG, Unützer J (1993) Brodmann's "missing" numbers. Neurology 43:226–227

Götz M, Bolz J (1994) Differentiation of transmitter phenotypes in rat cerebral cortex. Eur J Neurosci 6:18–32

Gould E, Reeves AJ, Fallah M, Tanapat P, Gross CG, Fuchs E (1999) Hippocampal neurogenesis in adult Old World primates. Proc Natl Acad Sci USA 96:5263–5267

Granata T, Farina L, Faiella A, Cardini R, D'Incerti L, Boncinelli E, Battaglia G (1997) Familial schizencephaly associated with *EMX2* mutation. Neurology 48:1403–1406

Grove EA, Tole S (1999) Patterning events and specification signals in the developing hippocampus. Cereb Cortex 9:551–561

Guerrini R, Dubeau F, Dulac O, Barkovich AJ, Kuzniecky R, Fett C, Jones-Gotman M, Canapicchi R, Cross H, Fish D, et al. (1997) Bi-lateral parasagittal parietooccipital polymicrogyria and epilepsy. Ann Neurol 41:65–73

Guerrini R, Barkovich AJ, Sztriha L, Dobyns WB (2000a) Bilateral frontal polymicrogyria: A newly recognized malformation syn-drome. Neurology 54:909–913

Guerrini R, Andermann E, Guerrini R, Dobyns WB, Kuzniecky R, Silver K, Van Bogaert P, Gillain C, David P, Ambrosetto G, et al. (2000b) Familial perisylvian polymicrogyria: A new familial syndrome of cortical maldevelopment. Ann Neurol 48:39–48

Guerrini R, Sicca F, Parmeggiani L (2003) Epilepsy and malforma-tions of the cerebral cortex. Epileptic Disord 9(Suppl 2):S9–S26

Guerrini R, Mei D, Sisodiya S, Sicca F, Harding B, Takahashi Y, Dorn T, Yoshida A, Campistol J, Krämer G, et al. (2004) Germline and mosaic mutations of *FLN1* in men with periventricular hetero-topia. Neurology 63:51–56

Gutknecht L (2001) Full-genomic scans with autistic disorder: A review. Behav Genet 31:113–123

Gutmann DH, Zhang Y, Hasbani MJ, Goldberg MP, Plank TL, Henske EP (2000) Expression of the tuberous sclerosis complex gene products hamartin and tuberin in central nervous system tissues. Acta Neuropathol (Berl) 99:223–230

Habib M (2000) The neurological basis of developmental dyslexia: An overview and working hypothesis. Brain 123:2373–2399

Hagberg B, Hagberg G (1997) Rett syndrome: Epidemiology and geographical variability. Eur Child Adolesc Psychiatry 6:5–7

Hagberg B, Aicardi J, Dias K, Ramos O (1983) A progressive syn-drome of autism, dementia, ataxia, and loss of purposeful hand use in girls: Rett's syndrome: Report of 35 cases. Ann Neurol 14:471–479

Hagerman RJ (2002) Physical and behavioral phenotype. In: Hagerman RJ, Hagerman PJ (eds) Fragile X Syndrome: Diagno-sis, treatment and research, 3rd ed. Johns Hopkins University Press, Baltimore, MD

Hagerman RJ, Hagerman PJ, eds (2002) Fragile X Syndrome: Diagnosis, treatment and research, 3rd ed. Johns Hopkins University Press, Baltimore, MD

Hagerman RJ, Leehey M, Heinrichs W, Tassone F, Wilson R, Hills J, Grigsby J, Gage B, Hagerman PJ (2001) Intention tremor, parkinsonism, and generalized brain atrophy in male carriers of fragile X. Neurology 57:127–130

Hamel BCJ (1999) X-Linked Mental Retardation – A clinical and molecular study. Thesis, University of Nijmegen

Hannan AJ, Servotte S, Katsnelson A, Sisodiya S, Blakemore C, Squier M, Molnár Z (1999) Characterization of nodular neuronal heterotopia in children. Brain 122:219–238

Hartmann D, De Strooper B, Saftig P (1999) Presenilin-1 deficiency leads to loss of Cajal-Retzius neurons and cortical dysplasia similar to human type 2 lissencephaly. Curr Biol 9:719–727

Hartwig J, Tyler J, Stossel T (1980) Actin-binding protein promotes the bipolar and perpendicular branching of actin filaments. J Cell Biol 87:841–848

Haslam RHA (1987) Microcephaly. Handb Clin Neurol 50:7–284

Hatanaka Y, Jones EG (1999) Novel genes expressed in the developing medial cortex. Cereb Cortex 9:577–585

Haydar TF, Kuan C-Y, Flavell RA, Rakic P (1999) The role of cell death in regulating the size and shape of the mammalian forebrain. Cereb Cortex 9:621–626

He S-Q, Dum RP, Strick PL (1993) Topographic organization of corticospinal projections from the frontal lobe: Motor areas on the lateral surface of the hemisphere. J Neurosci 13:952–980

He S-Q, Dum RP, Strick PL (1995) Topographic organization of corticospinal projections from the frontal lobe: Motor areas on the medial surface of the hemisphere. J Neurosci 14:3284–3306

Heimrich B, Vogt J, Simbürger E, Skutella T, Glumm R (2002) Axon guidance and the formation of specific connections in the hippocampus. Neuroembryology 1:154–160

Hennou S, Khalilov I, Diabira D, Ben-Ari Y, Gozlan H (2002) Early sequential formation of functional GABA$_A$ and glutamatergic synapses in CA1 interneurons of the rat foetal hippocampus. Eur J Neurosci 16:197–208

Herbst DS, Miller JR (1980) Non-specific X-linked mental retardation. II. The frequency in British Columbia. Am J Med Genet 7:461–469

Hevner RF, Kinney HC (1996) Reciprocal entorhinal-hippocampal connections established by human fetal midgestation. J Comp Neurol 372:384–394

Hewitt W (1961) The development of the human internal capsule and lentiform nucleus. J Anat (Lond) 95:191–199

Hinton VJ, Brown WT, Wisniewski K, Rudelli RD (1991) Analysis of neocortex in three males with the fragile X syndrome. Am J Med Genet 41:289–294

Hirotsune S, Takahara T, Sasaki N, Hirose K, Yoshiki A, Ohashi T, Kusakabe M, Murakami Y, Murumatsu M, Watanabe S, et al. (1995) The reeler gene encodes a protein with an EGF-like motif expressed by pioneer neurons. Nat Genet 10:77–83

His W (1904) Die Entwicklung des menschlichen Gehirns während der ersten Monate. Hirzel, Leipzig

Hochstetter F (1919) Beiträge zur Entwicklungsgeschichte des menschlichen Gehirns, I. Teil. Deuticke, Wien, Leipzig

Homanics GE, DeLorey TM, Firestone LL, Quinlan JJ, Handforth D, Harrison NL, Krasowski MD, Rick CEM, Korpi ER, Mäkelä R, et al. (1997) Mice devoid of γ-aminobutyrate type A receptor β3 subunit have epilepsy, cleft palate, and hypersensitive behavior. Proc Natl Acad Sci USA 94:4143–4148

Homayouni R, Curran T (2000) Cortical development: Cdk5 gets into sticky situations. Curr Biol 10:331–334

Hong SE, Shugart YY, Huang DT, Al Shahwan S, Grant PE, Hourihane JO, Martin NDT, Walsh CA (2000) Autosomal recessive lissencephaly with cerebellar hypoplasia is associated with human *RELN* mutations. Nat Genet 26:93–96

Honig LS, Herrmann K, Shatz CJ (1996) Developmental changes revealed by immunohistochemical markers in human cerebral cortex. Cereb Cortex 6:794–806

Hori A (1996) Precocious cerebral development associated with agenesis of the corpus callosum in mid-fetal life: A transient syndrome? Acta Neuropathol (Berl) 91:120–125

Hori A (1997) Anatomical variants of brain structure: Confused spatial relationship of the fornix to the corpus callosum and anterior commissure. Ann Anat 179:545–547

Hori A (1999) Morphology of brain malformations: beyond the classification, towards the integration. No Shinkei Geka (Neurol Surg) 27:969–985 (in Japanese)

Hori A, Stan AC (2004) Supracallosal longitudinal fiber bundle: Heterotopic cingulum, dorsal fornix or Probst bundle? Neuropathology 24:56–59

Hori A, Friede RL, Fischer G (1983) Ventricular diverticles with localized dysgenesis of the temporal lobe in cloverleaf skull anomaly. Acta Neuropathol (Berl) 60:132–136

Hourihane JO, Bennett CP, Chaudhuri R, Robb SA, Martin ND (1993) A sibship with a neuronal migration defect, cerebellar hypoplasia and congenital lymphedema. Neuropediatrics 24:43–46

Howell BW, Hawkes R, Soriano P, Cooper JA (1997a) Neuronal position in the developing brain is regulated by mouse disabled-1. Nature 389:733–737

Howell BW, Herrick TM, Cooper JA (1997b) Reelin-induced tyrosine phosphorylation of disabled 1 during neuronal positioning. Genes Dev 13:643–648

Hubel DH, Wiesel TN (1962) Receptive fields, binocular interaction and functional architecture in the cat's visual cortex. J Physiol (Lond) 160:106–154

Hubel DH, Wiesel TN (1977) Functional architecture of macaque monkey visual cortex. Proc R Soc Lond B 198:1–59

Hubel DH, Wiesel TN, Stryker MP (1978) Anatomical demonstration of orientation columns in macaque monkey. J Comp Neurol 177:361–379

Humphrey T (1960) The development of the pyramidal tracts in human fetuses, correlated with cortical differentiation. In: Tower DB, Schadé JP (eds) Structure and Function of the Cerebral Cortex. Elsevier, Amsterdam, pp 93–103

Humphrey T (1966a) The development of the human hippocampal formation correlated with some aspects of its phylogenetic history. In: Hassler R, Stephan H (eds) Evolution of the Forebrain. Thieme, Stuttgart, pp 104–116

Humphrey T (1966b) Correlations between the development of the hippocampal formation and the differentiation of the olfactory bulbs. Alab J Med Sci 3:235–269

Humphreys P, Kaufmann WE, Galaburda AM (1990) Developmental dyslexia in women: Neuropathological findings in three patients. Ann Neurol 28:727–738

Huttenlocher PR (1970) Dendritic development and mental defect. Neurology 20:381

Huttenlocher PR (1974) Dendritic development in neocortex of children with mental defect and infantile spasms. Neurology 24:203–210

Huttenlocher PR (1975) Synaptic and dendritic development and mental defect. In: Buchwald NA, Brazier MAB (eds) Brain Mechanisms in Mental Retardation. Academic, New York pp 123–140

Huttenlocher PR (1991) Dendritic and synaptic pathology in mental retrdation. Pediatr Neurol 7:79–85

Huttenlocher PR, Taravath S, Mojtahedi S (1994) Periventricular heterotopia and epilepsy. Neurology 44:51–55

Ikeda Y, Terashima T (1997) Corticospinal tract neurons are radially malpositioned in the sensory-motor cortex of the *shaking rat Kawasaki*. J Comp Neurol 383:370–380

Innocenti GM (1994) Some new trends in the study of the corpus callosum. Behav Brain Res 64:1–8

Inoue K, Lupski JR (2003) Genetics and genomics of behavioral and psychiatric disorders. Curr Opin Genet Dev 13:303–309

Insausti R, Amaral DG, Cowan WM (1987) The entorhinal cortex of the monkey: II. Cortical afferents. J Comp Neurol 264:356–395

Insausti R, Tuñón T, Sobreviela T, Insausti AM, Gonzalo LM (1995) The human entorhinal cortex: A cytoarchitectonic analysis. J Comp Neurol 355:171–198

Janssen A, Gressens P, Grabenbauer M, Baumgart E, Schad A, Vanhorebeek I, Brouwers A, Declercq PE, Fahime D, Evrard P, et al. (2003) Neuronal migration depends on intact peroxisomal function in brain and in extraneuronal tissues. J Neurosci 23:9732–9741

Jellinger K, Rett A (1976) Agyria-pachygyria (lissencephaly syndrome). Neuropediatrie 7:66–91

Jellinger K, Seitelberger F (1986) Neuropathology of Rett syndrome. Am J Med Genet Suppl 1(1986):259–288

Ji F, Kanbara N, Obata K (1999) GABA and histogenesis in fetal and neonatal mouse brain lacking both the isoforms of glutamic acid decarboxylase. Neurosci Res 33:187–194

Johnston MV, Mullaney B, Blue ME (2003) Neurobiology of Rett syndrome. J Child Neurol 18:688–692

Kahle W (1969) Die Entwicklung der menschlichen Grosshirnhemisphäre. Schriftenr Neurol 1:1–116

Kakita A, Hayashi S, Moro F, Guerrini R, Ozawa T, Ono K, Kameyama S, Walsh CA, Takahashi H (2002) Bilateral periventricular nodular heterotopia due to *filamin 1* gene mutation: Widespread glomeruloid microvascular anomaly and dysplastic cytoarchitecture in the cerebral cortex. Acta Neuropathol (Berl) 104: 649–657

Kandel ER, Schwartz JH, Jessell TM, eds (1991) Principles of Neural Science, 3rd ed. Elsevier, New York

Kanner L (1943) Autistic disturbances of affective contact. Nervous Child 2:217–250

Kash SF, Johnson RS, Tecott LH, Noebels JL, Mayfield RD, Hanahan D, Baelheshov S (1997) Epilepsy in mice deficient in the 65-kDa isoform of glutamic acid decarboxylase. Proc Natl Acad Sci USA 94:14060–14065

Kaufmann WE, Galaburda AM (1989) Cerebrocortical microdysgenesis in neurologically normal subjects: A histopathological study. Neurology 39:238–244

Kaufmann WE, Moser HW (2000) Dendritic anomalies associated with mental retardation. Cereb Cortex 10:981–991

Keibel F, Mall FP, Hrsg (1911) Handbuch der Entwicklungsgeschichte des Menschen. Hirzel, Leipzig

Keibel F, Mall FP, eds (1912) Manual of Human Embryology. Lippincott, Philadelphia, PA

Kemper TL, Bauman M (1998) Neuropathology of infantile autism. J Neuropathol Exp Neurol 57:645–652

Kempermann G, Jessberger S, Steiner B, Kronenberg G (2004) Milestones of neuronal development in the adult hippocampus. Trends Neurosci 27:447–452

Kerner B, Graham JM Jr, Golden JA, Pepkowitz SH, Dobyns WB (1999) Familial lissencephaly with cleft palate and severe cerebellar hypoplasia. Am J Med Genet 87:440–445

Khazipov R, Esclaper M, Caillard O, Bernard C, Khalilov I, Tyzio R, Hirsch J, Drhala V, Berger B, Ben-Ari Y (2001) Early development of neuronal activity in the primate hippocampus *in utero*. J Neurosci 21:9770–9781

Kilb W, Hartmann D, Saftig P, Luhmann HJ (2004) Altered morphological and electrophysiological properties of Cajal-Retzius cells in cerebral cortex of embryonic Presenilin-1 knockout mice. Eur J Neurosci 20:2749–2756

Klingler J (1948) Die makroskopische Anatomie der Ammonsformation. Denkschriften der Schweizerischen Naturforschenden Gesellschaft, Vol 78. Fretz, Zurich

Kobayashi K, Nakahori Y, Miyake M, Matsumura K, Kondo-Iida E, Nomura Y, Segawa M, Yoshioka M, Saito K, Osawa M, et al. (1998) An ancient retrotransposal insertion causes Fukuyama-type congenital muscular dystrophy. Nature 394:388–392

Koenderink MJT, Uylings HBM (1995) Postnatal maturation of layer V pyramidal neurons in the human prefrontal cortex. A quantitative Golgi analysis. Brain Res 678:233–243

Koenderink MJT, Uylings HBM, Mrzljak L (1994) Postnatal maturation of the layer III pyramidal neurons in the human prefrontal cortex: A quantitative Golgi analysis. Brain Res 653:173–182

Koester SE, O'Leary DDM (1994) Axons of early generating neurons in cingulate cortex pioneer the corpus callosum. J Neurosci 14:6608–6620

Kooy RF (2003) Of mice and the fragile X syndrome. Trends Genet 19:148–154

Kooy RF, Reyniers E, Verhoye M, Sijbers J, Bakker CE, Oostra BA, Willems PJ, Van Der Linden A (1999) Neuroanatomy of the fragile X knockout mouse brain studied using *in vivo* high resolution magnetic resonance imaging. Eur J Hum Genet 7:526–532

Kornack DR, Rakic P (1995) Radial and horizontal development of clonally related cells in the primate neocortex: Relationship to distinct mitotic lineages. Neuron 15:311–321

Kostović I (1990a) Zentralnervensystem. In: Hinrichsen KV (Hrsg) Humanembryologie. Lehrbuch und Atlas der vorgeburtlichen Entwicklung des Menschen. Springer, Berlin Heidelberg New York, pp 381–448

Kostović I (1990b) Structural and histochemical reorganization of the human prefrontal cortex during prenatal and postnatal life. Prog Brain Res 85:223–240

Kostović I, Goldman-Rakic PS (1983) Transient cholinesterase staining in the mediodorsal nucleus of the thalamus and its connectivity in the developing human and monkey brain. J Comp Neurol 219:431–447

Kostović I, Judáš M (2002) The role of the subplate zone in the structural plasticity of the developing human cerebral cortex. Neuroembryology 1:145–153

Kostović I, Rakic P (1990) Developmental history of the transient subplate in the visual and somatosensory cortex of the macaque monkey and human brain. J Comp Neurol 297:441–470

Kostović I, Lukinovic N, Judáš M, Bogdanovich N, Mrzljak L, Zecevic N, Kubat M (1989) Structural basis of the developmental plasticity in the human cerebral cortex: The role of the transient subplate zone. Metab Brain Dis 4:17–23

Kotrla KJ, Sater AM, Weinberger DR (1997) Neuropathology, neurodevelopment and schizophrenia. In: Keshavan MS, Murray RM (eds) Neurodevelopment & Adult Psychopathology. Cambridge University Press, Cambridge, pp 187–198

Kriegstein AR, Noctor SC (2004) Patterns of neuronal migration in the embryonic cortex/ Trends Neurosci 27:393–399

Kuypers HGJM (1981) Anatomy of the descending pathways. In: Brooks VB, Brookhart JM, Mountcastle VB (eds) Handbook of Physiology – The Nervous System, Vol 2: Motor Systems. American Physiological Society, Bethesda, MD, pp 597–666

Kuzniecky R, Andermann F, Guerrini R (1993) Congenital bilateral perisylvian syndrome: A study of 31 patients. The Congenital Bilateral Perisylvian Syndrome Multicenter Collaborative Study. Lancet 1993 (i):608–612

Kwiatkowski DJ, Short MP (1994) Tuberous sclerosis. Arch Dermatol 130:348–354

Kwon JS, Shenton ME, Hirayasu Y, Salisbury DF, Fischer IA, Dickey CC, Yurgelun-Todd D, Tohen M, Kikinis R, Jolesz FA, McCarley RW (1998) MRI study of cavum septi pellicidi in schizophrenia, affective disorders, and schizotypal personality disorders. Am J Psychiatry 15:509–515

Kwon YT, Tsai L-H (1998) A novel disruption of cortical development in *p35*–/– mice distinct from *reeler*. J Comp Neurol 395:510–522

Kyin R, Hua Y, Baybis M, Scheithauer B, Kolson D, Uhlmann E, Gutmann D, Crino PB (2001) Differential cellular expression of neurotrophins in cortical tubers of the tuberous sclerosis complex. Am J Pathol 159:1541–1554

Lamantia AS, Rakic P (1990a) Axon overproduction and elimination in the corpus callosum of the developing rhesus monkey. J Neurosci 10:2165–2175

Lamantia AS, Rakic P (1990b) Cytological and quantitative characteristics of four cerebral commissures in the rhesus monkey. J Comp Neurol 291:520–537

Lambert de Rouvroit C, Goffinet AM (1998) The reeler mouse as a model of brain development. Adv Anat Embryol Cell Biol 150:1–108

Lammens M (2000) Neuronal migration disorders in man. Eur J Morphol 38:327–333

Lammens M, Hiel JAP, Gabreëls FJM, van Engelen BGM, van den Heuvel LPWJ, Weemaes CMR (2003) Nijmegen breakage syndrome: A neuropathological study. Neuropediatrics 34:189–193

Lavdas AA, Grigoriou M, Pachnis V, Parnavelas JG (1999) The medial ganglionic eminence gives rise to a population of early neurons in the developing cerebral cortex. J Neurosci 19:7881–7888

Laxova R, Ohara PT, Timothy JAD (1972) A further example of a lethal autosomal recessive condition in sibs. J Ment Defic Res 16:139–143

Lee KS, Schottler F, Collins JL, Lanzino G, Couture D, Rao A, Hiramatsu K, Goto Y, Hong S-C, Caner H, et al. (1997) A genetic animal model of human neocortical heterotopia associated with seizures. J Neurosci 17:6236–6242

Lee KS, Collins JL, Anzivino MJ, Frankel EA, Schottler F (1998) Heterotopic neurogenesis in a rat with cortical heterotopia. J Neurosci 18:9365–9375

Lehrke R (1972) A theory of X-linkage of major intellectual traits. Am J Ment Defic 76:611–619

Lehrke R (1974) X-linked mental retardation and mental disability. Birth Defects 10:1–100

Lemire RJ, Loeser JJ, Leech RW, Alvord EC Jr (1975) Normal and Abnormal Development of the Human Nervous System. Harper & Row, Hagerstown, Maryland, MD

Lena G, van Calenberg F, Genitori L, Choux M (1995) Supratentorial interhemispheric cysts associated with callosal agenesis: Surgical treatment and outcome in 16 children. Child's Nerv Syst 11:568–573

Letinic K, Zoncu R, Rakic P (2002) Origin of GABAergic neurons in the human neocortex. Nature 417:645–649

Leventer RJ, Dobyns WB (2003) Periventricular gray matter heterotopias: A heterogeneous group of malformations of cortical development. In: Barth PG (ed) Disorders of Neuronal Migration. Mac Keith, London, pp 72–82

Levine D, Barnes PD (1999) Cortical maturation in normal and abnormal fetuses as assessed with prenatal MR imaging. Radiology 210:751–758

Levitt P, Eagleson KL, Powell EM (2004) Regulation of neocortical interneuron development and the implications for neurodevelopmental disorders. Trends Neurosci 27:400–406

Lewis DA, Levitt P (2002) Schizophrenia as a disorder of neurodevelopment. Annu Rev Neuroscio 25:409–432

Ligon KL, Echelard Y, Assimacopoulos S, Danielian PS, Kaing S, Grove EA, McMahon AP, Rowitch DH (2003) Loss of *Emx* function leads to ectopic expression of *Wnt1* in the developing telencephalon and cortical dysplasia. Development 130:2275–2287

Liu H, Abecasis GR, Heath SC, Knowles A, Demars S, Chen YJ, Roos JL, Rapoport JL, Gogos JA, Karayiorgou M (2002) Genetic variation in the 22q11 locus and susceptibility to schizophrenia. Proc Natl Acad Sci USA 99:16859–16864

Livingstone MS, Rosen GD, Drislane FW, Galaburda AM (1991) Physiological and anatomical evidence for a magnocellular defect in developmental dyslexia. Proc Natl Acad Sci USA 88:7943–7947

Loeser JD, Alvord EC Jr (1968) Agenesis of the corpus callosum. Brain 91:553–570

López-Bendito G, Molnár Z (2003) Thalamocortical development: How are we going to get there? Nature Rev Neurosci 4:276–289

Luhmann HJ, Raabe K, Qü M, Zilles K (1998) Characterization of neuronal migration disorders in neocortical structures: Extracellular *in vitro* recording. Eur J Neurosci 10:3085–3094

Lund JS, Angelucci A, Bressloff PC (2003) Anatomical substrates for functional columns in macaque monkey primary visual cortex. Cereb Cortex 13:15–24

Luskin MB, Pearlman AL, Sanes JR (1988) Cell lineage in the cerebral cortex of the mouse studied in vivo and in vitro with a recombinant retrovirus. Neuron 1:635–647

Mai JK, Berger K, Sofroniew MV (1993) Morphometric evaluation of neurophysin-immunoreactivity in the human brain: Pronounced inter-individual variability and evidence for altered staining patterns in schizophrenia. J Hirnforsch 34:133–154

Mallamaci A, Mercurio S, Muzio L, Cecchi C, Pardini CL, Gruss P, Boncinelli E (2000) The lack of *Emx2* causes impairment of *Reelin* signaling and defects of neuronal migration in the developing cerebral cortex. J Neurosci 20:1109–1118

Marín O, Rubinstein JLR (2001) A long, remarkable journey: Tangential migration in the telencephalon. Nat Rev Neurosci 2:780–790

Marín-Padilla M (1971) Early prenatal ontogenesis of the cerebral cortex (neocortex) of the cat (Felis domestica): a Golgi study. I. The primordial neocortical organization. Z Anat Entw Gesch 134:117–145

Marín-Padilla M (1972) Structural abnormalities of the cerebral cortex in human chromosomal aberrations. A Golgi study. Brain Res 44:625–629

Marin-Padilla M (1976) Pyramidal cell abnormalities in the motor cortex of a child with Down's syndrome. A Golgi study. J Comp Neurol 167:63–82

Marín-Padilla M (1978) The dual origin of the mammalian neocortex and evolution of the cortical plate. Anat Embryol 152:109–126

Marín-Padilla M (1990) Origin, formation, and prenatal maturation of the human cerebral cortex: An overview. J Craniofac Genet Dev Biol 10:137–146

Marín-Padilla M (1992) Ontogenesis of the pyramidal cell of the mammalian neocortex and developmental cytoarchitectonics: A unifying theory. J Comp Neurol 321:223–240

Marín-Padilla M (1996) Developmental neuropathology and impact of perinatal brain damage. I. Hemorrhagic lesions of neocortex. J Neuropathol Exp Neurol 55:758–773

Marín-Padilla M (1997) Developmental neuropathology and impact of perinatal brain damage. II. White matter lesions of neocortex. J Neuropathol Exp Neurol 56:219–235

Marín-Padilla M (1998) Cajal-Retzius cells and the development of the neocortex. Trends Neurosci 21:64–71

Marín-Padilla M (1999) Developmental neuropathology and impact of perinatal brain damage. III. Gray matter lesions of the neocortex. J Neuropathol Exp Neurol 58:407–429

McConnell SK, Kaznowski CE (1991) Cell cycle dependence of laminar determination in developing cerebral cortex. Science 254:282–285

McConnell SK, Ghosh A, Shatz CJ (1989) Subplate neurons pioneer the first axon pathway from the cerebral cortex. Science 245:978–982

McConnell SK, Ghosh A, Shatz CJ (1994) Subplate pioneers and the formation of descending connections from cerebral cortex. J Neurosci 14:1892–1907

Meencke H-J. (2000) Diagnosis of cortical and subcortical dysplasias in epilepsy. In: Schmidt D, Schachter SC (eds) Epilepsy – Problemsolving in clinical practice. Dunitz, London, pp 95–109

Mesulam M-M (1985) Patterns in behavioral neuroanatomy: Association areas, the limbic system, and hemispheric specialization. In: Mesulam M-M (ed) Principles of Behavioral Neurology. Davis, Philadelphia, PA, pp 1–70

Meyer G, Goffinet AM (1998) Prenatal development of reelin-immunoreactive neurons in the human neocortex. J Comp Neurol 397:29–40

Meyer G, Gonzalez-Hernandez T (1993) Developmental changes in layer I of the human neocortex during prenatal life: A DiI-tracing and AChE and NADPH-d histochemical study. J Comp Neurol 338:317–336

Meyer G, Wahle P (1999) The paleocortical ventricle is the origin of reelin-expressing neurons in the marginal zone of the foetal human neocortex. Eur J Neurosci 11:3937–3944

Meyer G, Soria JM, Martínez-Galán JR, Martín-Clemente B, Fairén A (1998) Different origins and developmental histories of transient neurons in the marginal zone of the fetal and neonatal rat cortex. J Comp Neurol 397:493–518

Meyer G, Goffinet AM, Fairén A (1999) What is a Cajal-Retzius cell? A reassessment of a classical cell type based on recent observations in the developing neocortex. Cereb Cortex 9:765–775

Meyer G, Castro R, Soria JM, Fairén A (2000a) The subpial granular layer in the developing cerebral cortex of rodents. In: Goffinet AM, Rakic P (eds) Mouse Brain Development. Springer, Berlin Heidelberg New York, pp 277–291

Meyer G, Schaaps JP, Moreau L, Goffinet AM (2000b) Embryonic and early fetal development of the human neocortex. J Neurosci 20:1858–1868

Meyer G, Lambert de Rouvroit C, Goffinet AM, Wahle P (2003) Disabled-1 mRNA and protein expression in developing human cortex. Eur J Neurosci 17:517–525

Mione MC, Cavanagh JFR, Harris B, Parnavelas JG (1997) Cell fate specification and symmetrical/asymmetrical divisions in the developing cerebral cortex. J Neurosci 17:2018–2029

Mischel PS, Nguyen LP, Vinters HV (1995) Cerebral cortical dysplasias associated with pediatric epilepsy. Review of neuropathological features and proposal for a grading system. J Neuropathol Exp Neurol 54:137–153

Miyata H, Chute DJ, Fink J, Villablanca P, Vinters HV (2004) Lissencephaly with agenesis of corpus callosum and rudimentary dysplastic cerebellum: A subtype of lissencephaly with cerebellar hypoplasia. Acta Neuropathol (Berl) 107:69–81

Mochida GH, Walsh CA (2001) Molecular genetics of human microcephaly. Curr Opin Neurobiol 14:151–156

Molnár Z, Adams R, Goffinet AM, Blakemore C (1998) The role of the first postmitotic cortical cells in the development of thalamocortical innervation in the *reeler* mouse. J Neurosci 18:5746–5765

Moore CJ, Daly EM, Tassone F, Tysoe C, Schmitz N, Ng V, Chitnis X, McGuire P, Suckling J, Davies KE, et al. (2004) The effect of premutation of X chromosome CGG trinucleotide repeats on brain anatomy. Brain 127:2672–2681

Mostofsky SH, Mazzocco MMM, Aakalu G, Warsofsky IS, Denckla MB, Reiss AL (1998) Decreased cerebellar posterior vermis size in fragile X syndrome. Correlation with neurocognitive performance. Neurology 50:121–130

Mountcastle VB (1957) Modality and topographic properties of single neurons of cat's somatic sensory cortex. J Neurophysiol 20:408–434

Mountcastle VB (1997) The columnar organization of the neocortex. Brain 120:701–722

Mrzljak L, Uylings HBM, Kostović I, van Eden CG (1988) Prenatal development of neurons in the human prefrontal cortex. I. A qualitative Golgi study. J Comp Neurol 271:355–386

Mrzljak L, Uylings HBM, van Eden CG, Judáš M (1990) Neuronal development in human prefrontal cortex in prenatal and postnatal stages. Prog Brain Res 85:185–222

Nadarajah B, Brunstrom JE, Grutzendler J, Wong ROL, Pearlman AL (2001) Two modes of radial migration in early development of the cerebral cortex. Nat Neurosci 4:143–150

Nagano T, Morikubo S, Sato M (2004) Filamin A and FILIP (Filamin A-interacting protein) regulate cell polarity and motility in neocortical subventricular and intermediate zones during radial migration. J Neurosci 24:9648–9657

Naidu S (1997) Rett syndrome: A disorder affecting early brain growth. Ann Neurol 42:3–10

Naidu S, Bibat G, Kratz L, Kelley RI, Pevsner J, Hoffman E, Cuffari C, Rohde C, Blue ME, Johnston MV (2003) Clinical variability in Rett syndrome. J Child Neurol 18:662–668

Nance MA, Berry SA (1992) Cockayne syndrome: Review of 140 cases. Am J Med Genet 42:68–84

Nathan PW, Smith MC, Deacon P (1990) The corticospinal tracts in man. Course and location of fibres at different segmental levels. Brain 113:303–324

Neu RL, Kajii T, Gardner LI, Nagyfy SF, King S (1971) A lethal syndrome of microcephaly with multiple congenital anomalies in three siblings. Pediatrics 47:610–612

Nguyen Ba-Charvet KT, Brose K, Marillat V, Kidd T, Goodman CS, Tessier-Lavigne M, Sotelo C, Chédotal A (1999) Slit2-mediated chemorepulsion and collapse of developing forebrain axons. Neuron 22:463–473

Nicolson RI, Fawcett AJ, Dean P (2001) A TINS debate – Hindbrain versus the forebrain: A case for cerebellar deficit in developmental dyslexia. Trends Neurosci 24:508–516

Nieuwenhuys R (1994) The neocortex. An overview of its evolutionary development, structural organization and synaptology. Anat Embryol (Berl) 190:307–337

Nieuwenhuys R (1996) The greater limbic system, the emotional motor system and the brain. Prog Brain Res 107:551–580

Nikolic M, Dudek YT, Kwon YT, Ramos YFM, Tsai L-H (1996) The cdk5/p35 kinase is essential for neurite outgrowth during neuronal differentiation. Genes Dev 7:816–825

Nimchinski EA, Oberlander AM, Svoboda K (2001) Abnormal development of dendritic spines in FMR1 knock-out mice. J Neurosci 21:5139–5146

Nopoulos PC, Giedd JN, Andreasen NC, Rapoport JL (1998) Frequency and severity of enlarged cavum septi pellucidi in childhood and schizophrenia. Am J Psychiatry 155:1074–1079

Norman MG, McGillivray BC, Kalousek DK, Hill A, Poskitt KJ (1995) Congenital Malformations of the Brain. Pathological, embryological, clinical, radiological and genetic aspects. Oxford University Press, New York

Nudo RJ, Masterton RB (1990) Descending pathways to the spinal cord. III. Sites of origin of the corticospinal tract. J Comp Neurol 296:559–583

Oba H, Barkovich AJ (1995) Holoprosencephaly: An analysis of callosal formation and its relation to development of the interhemispheric fissure. AJNR Am J Neuroradiol 16:453–456

O'Donnell WT, Warren ST (2002) A decade of molecular studies of fragile X syndrome. Annu Rev Neurosci 25:315–338

Ogawa M, Miyata T, Nakajima K, Yagyu K, Seike M, Ikenaka K, Yamamoto H, Mikoshiba K (1995) The reeler gene-associated antigen on Cajal-Retzius neurons is a crucial molecule for laminar organization of cortical neurons. Neuron 14:899–912

Ohshima T, Ward JM, Huh CG, Longenecker G, Veeranna XX, Pant HC, Brady RO, Martin LJ, Kulkarni AB (1996) Targeted disruption of the cyclin-dependent kinase 5 gene results in abnormal corticogenesis, neuronal pathology and perinatal death. Proc Natl Acad Sci USA 93:11173–11178

O'Leary DDM (1989) Do cortical areas emerge from a protocortex? Trends Neurosci 12:400–406

O'Leary DDM, Koester SE (1993) Development of projection neuron types, axon pathways, and patterned connections of the mammalian cortex. Neuron 10:991–1006

O'Leary DDM, Nakagawa Y (2002) Patterning centers, regulatory genes and extrinsic mechanisms controlling arealization of the neocortex. Curr Opin Neurobiol 12:14–25

Ono M, Kubik S, Abermathey CD (1990) Atlas of the Cerebral Sulci. Thieme, Stuttgart

O'Rahilly R, Müller F (1999) The Embryonic Human Brain. An atlas of developmental stages, 2nd ed. Wiley, New York

O'Rourke NA, Chenn A, McConnell SK (1997) Postmitotic neurons migrate tangentially in the cortical ventricular zone. Development 124:997–1005

Owens DF, Kriegstein AR (2002) Is there more to GABA than synaptic inhibition? Nat Rev Neurosci 3:715–727

Palmen SJMC, van Engeland H, Hof PR, Schmitz C (2004) Neuropathological findings in autism. Brain 127:2572–2583

Palmini A, Gambardella A, Andermann F, Dubeau F, da Costa JC, Olivier A, Tampieri D, Gloor P, Quesney F, Andermann E (1995) Intrinsic epileptogenicity of human dysplastic cortex as suggested by corticography and surgical results. Ann Neurol 37:476–487

Palmini A, Najm I, Avanzini G, Babb T, Guerrini R, Foldvary-Schaefer N, Jackson G, Lüders HO, Prayson R, Spreafico R, Vinters HV (2004) Terminology and classification of the cortical dysplasias. Neurology 62:S2–S8

Pandya DN, Karol EA, Heilbronn D (1971) The topographical distribution of interhemispheric projections in the corpus callosum of the rhesus monkey. Brain Res 32:31–43

Parent JM, Lowenstein DH (1997) Mossy fiber reorganization in the epileptic hippocampus. Curr Opin Neurol 10:103–109

Parnavelas JG (2000) The origin and migration of cortical neurones: New vistas. Trends Neurosci 23:126–131

Parnavelas JG, Barfield JA, Franke E, Luskin MB (1991) Separate progenitor cells give rise to pyramidal and nonpyramidal neurons in the rat telencephalon. Cereb Cortex 1:463–468

Pena SDJ, Shokeir MHK (1974) Autosomal recessive cerebro-oculo-facio-skeletal (COFS) syndrome. Clin Genet 5:285–293

Pilz DT, Matsumoto N, Minnerath S, Mills P, Gleeson JG, Allen KM, Walsh CA, Barkovich AJ, Dobyns WB, Ledbetter DH, Ross ME (1998) *LIS1* and *XLIS* (*DCX*) mutations cause most classical lissencephaly, but different patterns of malformation. Hum Mol Genet 13:2029–2037

Pilz D, Stoodley N, Golden JA (2002) Neuronal migration, cerebral cortical development, and cerebral cortical anomalies. J Neuropathol Exp Neurol 61:1–11

Pinard J-M, Feydy A, Carlier R, Perez N, Pierot L, Burnod Y (2000) Functional MRI in double cortex: Functionality of heterotopia. Neurology 54:1531–1533

Poliakov GI (1949) Structural organisation of the human cerebral cortex during ontogenetic development. In: Sarkissov SA, Filimonoff IN, Preobraschenskaja SN (eds) Cytoarchitectonics of the Cerebral Cortex in Man. Medgiz, Moscow, pp 33–92 (in Russian)

Poliakov GI (1959) Progressive neuron differentiation of the human cerebral cortex in ontogenesis. In: Sarkissov SA, Preobraschenskaja SN (eds) Development of the Central Nervous System. Medgiz, Moscow, pp 11–26 (in Russian)

Poliakov GI (1965) Development of the cerebral neocortex during the first half of intrauterine life. In: Sarkissov SA (ed) Development of the Child's Brain. Medicina, St. Petersburg, pp 22–52 (in Russian)

Porter BE, Brooks-Kayal A, Golden JA (2002) Disorders of cortical development and epilepsy. Arch Neurol 59:361-365

Porter R, Lemon R (1993) Corticospinal Function and Voluntary Movements. Monographs of the Physiological Society, Vol 45. Clarendon Press, Oxford

Poussaint TY, Fox JW, Dobyns WB, Radtke R, Scheffer IE, Berkovic SF, Barnes PD, Huttenlocher PR, Walsh CA (2000) Periventricular nodular heterotopia in a patiënt with filamin-1 gene mutation: Neuroimaging findings. Pediatr Radiol 30:748–755

Povey S, Burley M, Attwood J, Benham F, Hunt D, Jeremiah SJ, Franklin D, Gillett G, Melas S, Robson EB, et al. (1994) Two loci for tuberous sclerosis: One on 9q34 and one on 16p13. Ann Hum Genet 58:107–127

Powell EM, Campbell DB, Stanwood GD, Davis C, Noebels JL, Levitt P (2003) Genetic disruption of cortical interneuron development causes region- and GABA cell type-specific deficits, epilepsy, and behavioral dysfunction. J Neurosci 23:622–631

Powers RE (1999) The neuropathology of schizophrenia. J Neuropathol Exp Neurol 58:679–690

Price DJ, Thurlow L (1988) Cell lineage in the rat cerebral cortex: A study using retroviral-mediated gene transfer. Development 104:473–482

Price DJ, Willshaw DJ (2000) Mechanisms of Cortical Development. Monographs of the Physiological Society, Vol 48. Oxford University Press, Oxford

Price DJ, Aslam S, Tasker L, Gillies K (1997) The fates of the earliest generated cells in the developing murine neocortex. J Comp Neurol 377:414–422

Probst M (1901) Ueber den Bau des vollständig balkenlosen Grosshirnes sowie über Mikrogyrie und Heterotopie der grauen Substanz. Arch Psychiatr 34:709–786

Purpura DP (1974) Dendritic spine 'dysgenesis' and mental retardation. Science 186:1126–1128

Purpura DP (1975a) Dendritic differentiation in human cerebral cortex: Normal and aberrant developmental patterns. Adv Neurol 12:91–116

Purpura DP (1975b) Normal and aberrant neuronal development in the cerebral cortex of human fetus and young infant. In: Buchwald NA, Brazier MAB (eds) Brain Mechanisms and Mental Retatdation. Academic, New York, pp 141–169

Rademacher J, Caviness VS Jr, Steinmetz H, Galaburda AM (1993) Topographical variation of the human primary cortices: Implications for neuroimaging, brain mapping, and neurobiology. Cereb Cortex 3:313–329

Rademacher J, Bürgel U, Geyer S, Schormann T, Schleicher A, Freund H-J, Zilles K (2001) Variability and asymmetry in the human precentral motor system. A cytoarchitectonic and myeloarchitectonic brain mapping study. Brain 124:2232–2258

Raedler E, Raedler A (1978) Autoradiographic study of early neurogenesis in rat neocortex. Anat Embryol (Berl) 154:267–284

Raedler TJ, Knable MB, Weinberger DR (1998) Schizophrenia as a developmental disorder of the cerebral cortex. Curr Opin Neurobiol 8:157–161

Ragsdale CW, Grove EA (2001) Patterning the mammalian cerebral cortex. Curr Opin Neurobiol 11:50–58

Rajarethinam R, Miedler J, De Quardo J, Smet CI, Brunberg J, Kirbat R, Tandon R (2001) Prevalence of cavum septum pellucidum in schizophrenics studied with MRI. Schizophr Res 48:201–205

Rakic P (1974) Neurons in rhesus monkey visual cortex: Systemic relation between time of origin and eventual disposition. Science 183:425–427

Rakic P (1988) Specification of cerebral cortical areas. Science 241:170–176

Rakic P (1995) A small step for the cell, a giant leap for mankind: A hypothesis of neocortical expansion during evolution. Trends Neurosci 18:383–388

Rakic P, Yakovlev PI (1968) Development of the corpus callosum and cavum septi in man. J Comp Neurol 132:45–72

Ramakers GJA (2002) Rho proteins, mental retardation and the cellular basis of cognition. Trends Neurosci 25:191–199

Ramón y Cajal S (1891) Sur la structure de l'écorce cérébrale de quelques mammifères. La Cellule 7:123–176

Ramus F (2004) Neurobiology of dyslexia: A reinterpretation of the data. Trends Neurosci 27:720–726

Ramus F, Rosen S, Dakin SC, Day BL, Castellotto JM, White S, Frith U (2003) Theories of developmental dyslexia: Insights from a multiple case study of dyslexic adults. Brain 126:841–865

Ranke G (1910) Beiträge zur Kenntnis der normalen und pathologischen Hirnrindenbildung. Ziegl Beitr Path Anat 47:51–125

Ranson SW, Clark SL (1959) The Anatomy of the Nervous System. Its development and function. Saunders, Philadelphia, PA

Raybaud CA, Girard N (1998) Étude anatomique par IRM des agénésies et dysplasies commissurales télencéphaliques. Neurochirurgie 44(Suppl 1):38–60

Raybaud CA, Girard N (1999) The developmental disorders of the commissural plate of the telencephalon: MR imaging study and morphologic classification. Nerv Syst Child 24:348–357

Raymond AA, Fish DR, Stevens JM, Sisodiya SM, Alsanjari N, Shorvon SD (1994) Subependymal heterotopia: A distinct neuronal migration disorder associated with epilepsy. J Neurol Neurosurg Psychiatry 57:1195–1202

Reid CB, Liang I, Walsh C (1995) Systematic widespread clonal organization in cerebral cortex. Neuron 15:299–310

Reiss AL, Aylward E, Freund LS, Joshi PK, Bryan RN (1991a) Neuroanatomy of fragile X syndrome: The posterior fossa. Ann Neurol 29:26–32

Reiss AL, Freund L, Tseng JE, Joshi PK (1991b) Neuroanatomy in fragile X females: The posterior fossa. Am J Hum Genet 49:279–288

Reiss AL, Faruque F, Naidu S, Abrams M, Beaty T, Bryan RN, Moser H (1993) Neuroanatomy of Rett syndrome: A volumetric imaging study. Ann Neurol 34:227–234

Rett A (1966) Über ein zerebral-atrophisches Syndrom bei Hyperammonemie. Wien Med Wochenschr 116:723–726

Retzius G (1893) Die Cajal'schen Zellen der Grosshirnrinde beim Menschen und bei Säugetieren. Biol Unters Neue Folge 5:1–8

Retzius G (1894) Weitere Beiträge zur Kenntnis der Cajal'schen Zellen der Grosshirnrinde des Menschen. Biol Unters Neue Folge 6:29–36

Reyniers E, Martin J-J, Cras P, Van Marck E, Handig I, Jorens HRJ, Oostra BA, Kooy RF, Willems PJ (1999) Postmortem examination of two fragile X brothers with an *FMR1* full mutation. Am J Med Genet 84:245–249

Rice DS, Curran T (2001) Role of the reelin signaling pathway in central nervous system development. Annu Rev Neurosci 24:1005–1039

Richter W (1980) Neurohistologische und morphometrische Untersuchungen der Ontogenese der Regio cingularis mesoneocorticalis der Ratte. J Hirnforsch 21:53–87

Richter W, Kranz D (1978) Autoradiographische Untersuchungen zur Neurogenese und Morphogenese der Regio cingularis der Ratte. I. Proliferationsmuster in verschiedenen prae- und postnatale Stadien. Z Mikrosk-Anat Forsch 92:222–240

Richter W, Kranz D (1979a) Autoradiographische Untersuchungen zur Neurogenese und Morphogenese der Regio cingularis der Ratte. II. Proliferationskinetik in der Area praecentralis agranularis. J Hirnforsch 20:391–412

Richter W, Kranz D (1979b) Autoradiographische Untersuchungen zur Neurogenese und Morphogenese der Regio cingularis der Ratte. III. Migration und Lamination in den Regionen der cingulären Rinde und inder Area postcentralis. J Hirnforsch 20:475–505

Richter W, Kranz D (1979c) Autoradiographische Untersuchungen zur Neurogenese und Morphogenese der Regio cingularis der Ratte. IV. Quantitative Untersuchungen zue Ermittlung der Zellursprungszeiten der Cortexschichten. J Hirnforsch 20:581–629

Richter W, Kranz D (1980) Autoradiographische Untersuchungen zur Neurogenese und Morphogenese der Regio cingularis der Ratte. V. Quantitative Untersuchungen des Ablaufs der Migrationsvorgänge. J Hirnforsch 21:11–37

Rickmann M, Chronwall BM, Wolff JR (1977) On the development of non-pyramidal neurons and axons outside the cortical plate: The early marginal zone as a pallial anlage. Anat Embryol (Berl) 151:285–307

Robain O, Gelot A (1996) Neuropathology of hemimegalencephaly. In: Guerrini R, Andermann F, Canapicchi R, Roger J, Zifkin BG, Pfanner P (eds) Dysplasia of Cerebral Cortex and Epilepsy. Lippincott-Raven, Philadelphia, PA, pp 89–92

Robain O, Floquet J, Heldt N, Rozemberg F (1988) Hemimegalencephaly: A clinicopathological study of four cases. Neuropathol Appl Neurobiol 14:125–135

Roland PE, Zilles K (1996) Functions and structures of the motor cortices in humans. Curr Opin Neurobiol 6:773–781

Ropers H-H, Hamel B (2005) XLMR. Nat Rev Genet 6:46-58

Ropers H-H, Hoeltzenbein M, Kalscheuer V, Yntema H, Hamel B, Fryns J-P, Chelly J, Partington M, Gecz J, Moraine C (2003) Nonsyndromic X-linked mental retardation: Where are the missing mutations? Trends Genet 19:316–320

Rose M (1927a) Der Allocortex bei Tier und Mensch. I. Teil. J Psychol Neurol 34:1–111

Rose M (1927b) Die sog. Riechrinde beim Menschen und beim Affen. II. Teil des "Allocortex bei Tier und Mensch". J Psychol Neurol 34:261–401

Ross CA, Pearlson GD (1996) Schizophrenia, the heteromodal association neocortex and development: Potential for a neurogenetic approach. Trends Neurosci 19:171–176

Ross ME, Walsh CA (2001) Human brain malformations and their lessons for neuronal migration. Annu Rev Neurosci 24:1041–1070

Ross ME, Swanson K, Dobyns WB (2001) Lissencephaly with cerebellar hypoplasia (LCH): A heterogeneous group of cortical malformation. Neuropediatrics 32:256–263

Rubinstein JLR, Anderson S, Shi L, Miyashita-Lin E, Bulfone A, Hevner R (1999) Genetic control of cortical regionalization and connectivity. Cereb Cortex 9:524–532

Rudelli RD, Brown WT, Wisniewski K, Jenkins EC, Laure-Kamionowska M, Connell F, Wisniewski HM (1985) Adult fragile X syndrome. Clinico-neuropathologic findings. Acta Neuropathol (Berl) 67:289–295

Ruoss K, Lövblad K, Schroth G, Moessinger AC, Fusch C (2001) Brain development (sulci and gyri) as assessed by early postnatal MR imaging in preterm and term newborn infants. Neuropediatrics 32:69–74

Saito Y, Kobayashi M, Itoh M, Saito K, Mizuguchi M, Sasaki H, Arima K, Yamamoto T, Takashima S, Sasaki M, et al. (2003) Aberrant neuronal migration in the brainstem of Fukuyama-type congenital muscular dystrophy. J Neuropathol Exp Neurol 62: 497–508

Saitoh O, Karns CM, Courchesne E (2001) Development of the hippocampal formation from 2 to 42 years. MRI evidence of smaller area dentata in autism. Brain 124:1317–1324

Sanchez MP, Frassoni C, Alvarez-Bolado G, Spreafico R, Fairén A (1992) Distribution of calbindin and parvalbumin in the developing somatosensory cortex and its primordium in the rat: An immunocytochemical study. J Neurocytol 21:717–736

Sanes JR, Yamagata M (1999) Formation of lamina-specific synaptic connections. Curr Opin Neurobiol 9:79–97

Santavuori P, Somer H, Sainio K, Rapola J, Kruus S, Nikitin T, Ketonen L, Leisti J (1989) Muscle-eye-brain disease (MEB). Brain Dev 11:147–153

Sarkissov SA, Filimonoff IN, Kononowa EP, Preobraschenskaja SN, Kukuew LA (1955) Atlas of the Cytoarchitecture of the Human Cerebral Cortex. Medgiz, Moscow

Sarwar M (1989) The septum pellucidum: Normal and abnormal. Am J Neuroradiol 10:989–1005

Schaefer GB, Bodensteiner JB, Thompson JN (1994) Subtle anomalies of the septum pellucidum and neurodevelopmental deficits. Dev Med Child Neurol 36:554–559

Schanen NC, Kurczynski TW, Brunelle D, Woodcock MM, Dure LS, Percy AK (1998) Neonatal encephalopathy in two boys in families with recurrent Rett syndrome. J Child Neurol 13:229–231

Schmitt JE, Eliez S, Bellugi U, Reiss AL (2001) Analysis of cerebral shape in Williams syndrome. Arch Neurol 58:283–287

Schottler F, Couture D, Rao A, Kahn H, Lee KS (1998) Subcortical connections of normotopic and heterotopic neurons in sensory and motor cortices of the *tish* mutant rat. J Comp Neurol 395:29–42

Schuler V, Lüscher C, Blanchet C, Klix N, Sansig G, Klebs K, Schmutz M, Heid J, Genvry C, Urban L, et al. (2001) Epilepsy, hyperalgesia, impaired memory, and loss of pre- and postsynaptic GABA$_B$ responses in mice lacking GABA$_{B1}$. Neuron 31:47–58

Scott BS, Becker LE, Petit TL (1983) Neurobiology of Down's syndrome. Prog Neurobiol 21:199–237

Scott TF, Price TRP, George MS, Brillman J, Rothfus W (1993) Midline cerebral malformation and schizophrenia. J Neuropsychiatry Clin Neurosci 5:287–293

Seress L, Ábrahám H, Tornóczky T, Kosztolányi G (2001) Cell formation in the human hippocampal formation from mid-gestation to the late postnatal period. Neuroscience 105:831–843

Shahbazian MD, Zoghbi HY (2002) Rett syndrome and MeCP2: Linking epigenetics and neuronal function. Am J Hum Genet 71:1259–1272

Shaw CM, Alvord EC Jr (1969) Cava septi pellucidi et Vergae: Their normal and pathological states. Brain 92:213–224

Sheldon M, Rice DS, D'Arcangelo G, Yoneshima H, Nakajima K, Mikoshiba K, Howell BW, Cooper JA, Goldowitz D, Curran T (1997) Scrambler and yotari disrupt the disabled gene and produce a reeler-like phenotype in mice. Nature 389:730–733

Shinozaki K, Miyagi T, Yoshida M, Miyata T, Ogawa M, Aizawa S, Suda Y (2002) Absence of Cajal-Retzius cells and subplate neurons associated with defects of tangential cell migration from ganglionic eminence in *Emx1/2* double mutant cerebral cortex. Development 129:3479–3492

Short MP, Richardson EP, Haines J, Kwiatkowski DJ (1995) Clinical, neuropathological, and genetic aspects of the tuberous sclerosis complex. Brain Pathol 5:173–179

Shu T, Butz KG, Pachez C, Gronostajski RM, Richards LJ (2003a) Abnormal development of forebrain midline glia and commissural projections in *Nfia* knock-out mice. J Neurosci 23:203–212

Shu T, Li Y, Keller A, Richards LJ (2003b) The glial sling is a migratory population of developing neurons. Development 130: 2929–2937

Sidman RL, Rakic P (1982) Development of the human central nervous system. In: Haymaker W, Adams RD (eds) Histology and Histopathology of the Nervous System. Thomas, Springfield, IL, pp 3–145

Silver J, Lorenz S, Wahlsten D, Coughlin J (1982) Axonal guidance during development of the great commissures: Descriptive and experimental studies, in vivo, on the role of preformed glial pathways. J Comp Neurol 210:10–29

Sisodiya SM (2000) Surgery for malformations of cortical development causing epilepsy. Brain 123:1075–1091

Skutella I, Nitsch R (2001) New molecules for hippocampal development. Trends Neurosci 24:107–113

Smart IHM, McSherry GM (1982) Growth patterns in the lateral wall of the mouse telencephalon. II. Histological changes during and subsequent to the period of isocortical neuron production. J Anat (Lond) 134:415–442

Solodkin A, Van Hoesen GW (1996) Entorhinal cortex modules of the human brain. J Comp Neurol 365:610–627

Sommer W (1880) Erkrankung des Ammonshorns als aetiologisches Moment der Epilepsie. Arch Psychiatr 10:631–675

Soriano E, Cobas A, Fairén A (1989) Neurogenesis of glutamic acid decarboxylase immunoreactive cells in the hippocampus of the mouse. I: Regio superior and regio inferior. J Comp Neurol 281:586–602

Soriano E, Del Rio JA, Martinez A, Supèr H (1994) Organization of the embryonic and early postnatal murine hippocampus. I. Immunocytochemical characteristics of neuronal populations in the subplate and marginal zone. J Comp Neurol 340:1–25

Spreafico R, Frassoni C, Arcelli P, Selvaggio M, De Biasi S (1995) In situ labeling of apoptotic cell death in the cerebral cortex and thalamus of rats during development. J Comp Neurol 363: 281–295

Spreafico R, Pasquier B, Minotti L, Garbelli R, Kahane P, Grand S, Benabid AL, Tassi L, Avanzini G, Battaglia G, Munari C (1998) Immunocytochemical investigation on dysplastic human tissue from epileptic patients. Epilepsy Res 32:34–48

Spreafico R, Arcelli P, Frassoni C, Canetti P, Giaccone G, Rizzuti T, Mastrangelo M, Bentivoglio M (1999) Development of layer I of the human cerebral cortex after midgestation: Architectonic findings, immunocytochemical identification of neurons and glia, and in situ labeling of apoptotic cells. J Comp Neurol 410:126–142

Stein E, Savashan NE, Ninnemann O, Nitsch R, Zhou R, Skutella T (1999) A role for the Eph ligand ephrin A3 in entorhino-hippocampal axon targeting. J Neurosci 19:8885–8893

Stein J, Walsh V (1997) To see but not to read; the magnocellular theory of dyslexia. Trends Neurosci 20:147–152

Stephan H (1975) Allocortex. Handbuch der mikroskopischen Anatomie des Menschen, Vol 4, Teil 9. Springer, Berlin Heidelberg New York

Steup A, Lohrum M, Hamsho N, Savashan NE, Ninnemann O, Nitsch R, Fujisawa H, Püschel AW, Skutella T (2000) Semaphorin 3C and netrin-1 differentially affect axon growth in the hippocampal formation. Mol Cell Neurosci 15:141–155

Subramaniam B, Naidu S, Reiss AL (1997) Neuroanatomy in Rett syndrome: Cerebral cortex and posterior fossa. Neurology 48:399–407

Sunderland S (1940) The distribution of commissural fibers in the corpus callosum in the macaque monkey. J Neurol Psychiatr 3:9–18

Supèr H, Soriano E (1994) The organization of the embryonic and early postnatal murine hippocampus. II. Development of entorhinal, commissural, and septal connections studied with the lipophilic tracer DiI. J Comp Neurol 344:101–120

Supèr H, Uylings HBM (2001) The early differentiation of the neocortex: A hypothesis on neocortical evolution. Cereb Cortex 11:1101–1109

Supèr H, Martínez A, Del Rio JA, Soriano E (1998a) Involvement of distinct pioneer neurons in the formation of layer-specific connections in the hippocampus. J Neurosci 18:4616–4626

Supèr H, Soriano E, Uylings HBM (1998b) The functions of the preplate in development and evolution of the neocortex and hippocampus. Brain Res Rev 27:40–64

Supprian T, Sian J, Heils A, Hoffmann E, Warmuth-Metz M, Solymosi L (1999) Isolated absence of the septum pellucidum. Neuroradiology 41:563–566

Suzuki WA, Amaral DG (2003) Where are the perirhinal and parahippocampal cortices? A historical overview of the nomenclature and boundaries applied to the primate medial temporal lobe. Neuroscience 120:893–906

Sweet HO, Bronson RT, Johnson KR, Cook SA, Davisson MT (1996) Scrambler, a new neurological mutation of the mouse with abnormalities of neuronal migration. Mamm Genome 7:798–802

Takahashi T, Nowakowski RS, Caviness VS Jr (1995a) The cell cycle of the pseudostratified ventricular epithelium of the murine cerebral wall. J Neurosci 15:6046–6057

Takahashi T, Nowakowski RS, Caviness VS Jr (1995b) Early ontogeny of the secondary proliferative population of the embryonic murine cerebral wall. J Neurosci 15:6058–6068

Takiguchi-Hayashi K, Sekiguchi M, Ashigaki S, Takamatsu M, Hasegawa H, Suzuki-Migishima R, Yokoyama M, Nakanishi S, Tanabe Y (2004) Generation of reelin-positive marginal zone cells from the caudomedial wall of telencephalic vesicles. J Neurosci 24:2286–2295

Tan S-S, Kalloniatis M, Sturm K, Tam PPL, Reese BE, Faulkner-Jones B (1998) Separate progenitors for radial and tangential cell dispersion during development of the cerebral neocortex. Neuron 21:295–304

Tanaka D, Nakaya Y, Yanagawa Y, Obata K, Murakami F (2003) Multimodal tangential migration of neocortical GABAergic neurons independent of GPI-anchored proteins. Development 130:5803–5813

ten Donkelaar HJ (2000) Development and regenerative capacity of descending supraspinal pathways in tetrapods: A comparative approach. Adv Anat Embryol Cell Biol 154:1–145

ten Donkelaar HJ, Wesseling P, Semmekrot BA, Liem KD, Tuerlings J, Cruysberg JRM, de Wit PEJ (1999) Severe, non X-linked congenital microcephaly with absence of the pyramidal tracts in two saiblings. Acta Neuropathol (Berl) 98:203–211

ten Donkelaar HJ, Lammens M, Wesseling P, Hori A, Keyser A, Rotteveel J (2004) Development and malformations of the human pyramidal tract. J Neurol 251:1429–1442

Terashima T (1995) Anatomy, development and lesion-induced plasticity of rodent corticospinal tract. Neurosci Res 22:139–161

Thirumalai SS, Shubin RA, Robinson R (2002) Rapid eye movement sleep behavior disorder in children with autism. J Child Neurol 17:173–178

Thom M, Sisodiya SM, Harkness W, Scaravilli F (2001) Microdysgenesis in temporal lobe epilepsy. A quantitative and immunohistochemical study of white matter neurones. Brain 124:2299–2309

Thom M, Sisodiya SM, Beckett A, Martinian L, Lin W-R, Harkness W, Mitchell TN, Craig J, Duncan J, Scaravilli F (2002) Cytoachitectural abnormalities in hippocampal sclerosis. J Neuropathol Exp Neurol 61:510–519

Thomaidou D, Mione MC, Cavanagh JFR, Parnavelas JG (1997) Apoptosis and its relation to the cell cycle in the developing cerebral cortex. J Neurosci 17:1075–1085

Tissir F, Goffinet AM (2003) Reelin and brain development. Nat Rev Neurosci 4:496–505

Toda T, Kobayashi K, Takeda S, Sasaki J, Kurahashi H, Kano H, Tachikawa M, Nagay Y, Taniguchi K, Sunada Y, et al. (2003) Fukuyama-type congenital muscular dystrophy (FCMD) and α-dystroglycanopathy. Cong Anom 43:97–104

Tomaiuolo F, Di Paola M, Caravale B, Vicari S, Petrides M, Caltagirone C (2002) Morphology and morphometry of the corpus callosum in Williams syndrome: A T1-weighted MRI study. Neuroreport 13:2281–2284

Toniolo D, D'Adamo P (2000) X-linked non-specific mental retardation. Curr Opin Genet Dev 10:280–285

Trommsdorff M, Gotthardt M, Hiesberger T, Sheldon J, Stockinger W, Nimpf J, Hammer RE, Richardson JA, Herz J (1999) Reeler/disabled-like disruption of neuronal migration in knockout mice lacking the VLDL receptor and ApoE receptor 2. Cell 97:689–701

Tuchman R, Rapin I (2002) Epilepsy in autism. Lancet Neurol 1:352–358

Tyzio R, Represa A, Jorquera I, Ben-Ari Y, Hozlan H, Aniksztteyn L (1999) The establishment of GABAergic and glutaminergic synapses on CA1 pyramidal neurons is sequential and correlates with the development of the apical dendrite. J Neurosci 19:10372–10382

Ulfig N, Chan WY (2002) Axonal patterns in the prosencephalon of the human developing brain. Neuroembryology 1:4–16

Ulfig N, Szabo A, Bohl J (2001) Effects of fetal hydrocephalus on the distribution patterns of calcium-binding proteins in the human occipital cortex. Pediatr Neurosurg 34:20–32

Utsunomiya H, Ogasawara T, Hayashi T, Hashimoto T, Okazaki M (1997) Dysgenesis of the corpus callosum and associated telencephalic anomalies: MRI. Neuroradiology 39:302–310

Uylings HBM (2001) The human cerebral cortex in development. In: Kalverboer AF, Gramsbergen A (eds) Handbook of Brain and Behaviour in Human Development. Kluwer, Dordrecht, pp 63–80

Uylings HBM, Delalle I, Petanjek Z, Koenderink MJT (2002) Structural and immunocytochemical differentiation of neurons in prenatal and postnatal human prefrontal cortex. Neuroembryology 1:176–186

Van den Veyver IB, Zoghbi HY (2000) Methyl-CpG-binding protein 2 mutations in Rett syndrome. Curr Opin Genet Dev 10:275–279

van der Knaap MS, van Wezel-Meijler G, Barth PG, Barkhof F, Ader HJ, Valk J (1996) Normal gyration and sulcation in preterm and term neonates: Appearances on MR images. Radiology 200:389–396

van der Knaap MS, Smit LME, Barth PG, Catsman-Berrevoets CE, Brouwer OF, Begeer JH, de Coo IFM (1997) MRI in classification of congenital muscular dystrophies with brain abnormalities. Ann Neurol 42:50–59

van Eden CG, Mrzljak L, Voorn P, Uylings HBM (1989) Prenatal development of GABAergic neurons in the neocortex of the rat. J Comp Neurol 289:213–227

van Karnebeek CDM, van Gelderen I, Nijhoff GJ, Abeling NG, Vreken P, Rederer EJ, van Eeghen AM, Hoovers JMN, Hennekam RCM (2002) Am aetiological study of 25 mentally retarded adults with autism. J Med Genet 39:205–214

van Slegtenhorst M, de Hoogt R, Hermans C, Nellitt M, Janssen B, Verhoef S, Lindhorst D, van der Ouweland A, Halley D, Young J, et al. (1997) Identification of the tuberous sclerosis gene TSC1 on chromosome 9q34. Science 277:805–808

Verga A (1851) Sul ventriculo della volta e tre pilastri. Gazz Med Lombarda 2: Series 3, No 7 (quoted from Bruyn 1977)

Voeller KKS (2004) Dyslexia. J Child Neurol 19:740–744

Vogt BA, Nimchinsky EA, Vogt LJ, Hof PR (1995) Human cingulate cortex: Surface features, flat maps, and cytoarchitecture. J Comp Neurol 359:490–506

Vogt C, Vogt O (1919) Allgemeinere Ergebnisse unserer Hirn-forschung. J Psychol Neurol 25:279–461

von Economo C, Koskinas GN (1925) Die Cytoarchitektonik der Hirnrinde des erwachsenen Menschen. Springer, Berlin Heidel-berg New York

Walker AE (1942) Lissencephaly. Arch Neurol Psychiatry 48:13–29

Walsh CA (1999) Genetic malformations of the human cerebral cortex. Neuron 23:19–29

Walsh CA, Cepko CL (1988) Clonally related cortical cells show sev-eral migration patterns. Science 241:1342–1345

Walsh CA, Cepko CL (1992) Widespread dispersion of neuronal clones across functional regions of the cerebral cortex. Science 255:434–440

Ware ML, Fox JW, González JL, Davis NM, Lambert de Rouvroit C, Russo CJ, Chua Sc, Goffinet AM, Walsh CA (1997) Aberrant splic-ing of a mouse *disabled* homologue, *mdab1*, in the scrambler mouse. Neuron 19:239–249

Weinberger DR (1987) Implications of normal brain development for the pathogenesis of schizophrenia. Arch Gen Psychiatry 44:660–669

Weinberger DR, Egan MF, Bertolino A, Callicott JH, Mattay VS, Lipska BK, Berman KF, Goldberg TE (2001) Prefrontal neurons and the genetics of schizophrenia. Biol Psychiatry 50:825–844

White B, Hua Y, Scheithauer B, Lynch DR, Henske EP, Crino PB (2001) Selective alterations in glutamate and GABA receptor subunit mRNA expression in dysplastic neurons and giant cells in cor-tical tubers. Ann Neurol 49:6–78

Whitford KL, Dijkhuizen P, Polleux F, Ghosh A (2002) Molecular con-trol of cortical dendrite development. Annu Rev Neurosci 25:127–149

WHO (1980) International Classification of Impairments, Disabili-ties and Handicaps. World Health Organization, Geneva

Williams RS, Swisher CN, Jennings M, Ambler M, Caviness VS Jr (1984) Cerebro-ocular dysgenesis (Walker-Warburg syn-drome): Neuropathologic and etiologic analysis. Neurology 34:1531–1541

Winterer G, Weinberger DR (2004) Genes, dopamine and cortical signal-to-noise ratio in schizophrenia. Trends Neurosci 27:683–690

Wisniewski KE, Segan SM, Miezejeski CM, Sersen EA, Rudelli RD (1991) The Fra(X) syndrome: Neurological, electrophysiologi-cal, and neuropathological abnormalities. Am J Med Genet 38:476–480

Witter MP, Amaral DG (1991) Entorhinal cortex of the monkey: V. Projections to the dentate gyrus, hippocampus, and subicu-lar complex. J Comp Neurol 307:437–459

Witter MP, Van Hoesen GW, Amaral DG (1989) Topographical orga-nization of the entorhinal projection to the dentate gyrus of the monkey. J Neurosci 9:216–228

Woo TU, Whitehead RE, Melchitzky DS, Lewis DA (1998) A subclass of prefrontal gamma-aminobutyric acid axon terminals are selectively altered in schizophrenia. Proc Natl Acad Sci USA 95:5341–5346

Xu Q, Cobos I, De La Cruz E, Rubinstein JL, Anderson SA (2004) Ori-gins of cortical interneuron subtypes. J Neurosci 24:2612–2622

Yakovlev PI. Lecours A (1967) The myelogenetic cycles of regional maturation of the brain. In: Minkowski A (ed) Regional Devel-opment of the Brain in Early Life. Blackwell, Oxford, pp 3–70

Yamadori T (1965) Die Entwicklung der Thalamuskerne mit ihren ersten Fasersystemen bei menschlichen Embryonen. J Hirn-forsch 7:393–413

Yamamoto T, Kato Y, Karita M, Takeiri H, Muramatsu F, Kobayashi M, Saito K, Osawa M (2002) Fukutin expression in glial cells and neurons: Implication in the brain lesions of Fukuyama congen-ital muscular dystrophy. Acta Neuropathol (Berl) 104:217–224

Ying Z, Babb TL, Comair YG, Bingaman W, Bushey M, Touhalisky K (1998) Induced expression of NMDAR2 proteins and differen-tial expression of NMDAR1 splice variants in dysplastic neu-rons of human epileptic neocortex. J Neuropathol Exp Neurol 57:47–62

Yoshida A, Kobayashi K, Manya H, Taniguchi K, Kano H, Mizuno M, Izanu T, Mitsuhashi H, Takahashi S, Takeuchi M, et al. (2001) Muscular dystrophy and neuronal migration disorder caused by mutations in a glycosyltransferase, POMGnT1. Dev Cell 1:717–724

Yuste R, Bonhoeffer T (2004) Genesis of dendritic spines: Insights from ultrastructural and imaging studies. Nat Rev Neurosci 5:24–34

Zecevic N, Milosevic A, Rakic S, Marín-Padilla M (1999) Early devel-opment and composition of the human primordial plexiform layer: An immunohistochemical study. J Comp Neurol 412:241–254

Zaki PA, Quinn JC, Price DJ (2003) Mouse models of telencephalic development. Curr Opin Genet Dev 13:423–437

Zeki S (1993) A Vision of the Brain. Blackwell, Oxford

Zilles K (1990) Cortex. In: Paxinos G (ed) The Human Nervous Sys-tem. Academic, San Diego, CA, pp 757-802

Zilles K (2004) Architecture of the human cerebral cortex. In: Paxinos G, Mai JK (eds) The Human Nervous System, 2nd ed. Elsevier, Amsterdam, pp 997–1055

Zilles K, Qü M, Schleicher A, Luhmann HJ (1998) Characterization of neuronal migration disorders in neocortical structures: Quantitative receptor autoradiography of ionotropic glutama-ta GABA$_A$ and GABA$_B$ receptors. Eur J Neurosci 10:3095–3106

Zuckerkandl E (1901) Zur Entwicklung des Balkens und des Gewölbes. Sitzber Akad Wissensch Wien Math-Naturw Classe 110:233–307

Subject Index

I

R

T

W

Y

Z